European Operational Oceanography: Present and Future

Proceedings of the Fourth International Conference on EuroGOOS
6–9 June 2005, Brest, France

Edited by

H. Dahlin, EuroGOOS Office, Norrköping, Sweden

N.C. Flemming, UK

P. Marchand, Ifremer, Brest, France

S.E. Petersson, EuroGOOS Office, Norrköping, Sweden

Published by

EuroGOOS Office
SMHI
601 76 Norrköping
Sweden

Tel: +46 11 495 8030
Fax: +46 11 495 8001
Email: eurogoos@smhi.se
Internet: www.eurogoos.org

and

European Commission
Research Directorate-General
RTD.I.1.1. Earth Observation
21, rue du Champ de Mars - CDMA 3/187
B–1049 Brussels
Belgium

Tel: +32 2 296 1799
Fax: +32 2 299 4249

Photographs: Patrick Gorringe and Siân Petersson

Acknowledgements: EuroGOOS would like to thank Philippe Marchand from Ifremer for successfully taking on the challenge of organising the conference and Gilles Ollier at the European Commission for enabling these proceedings to be published.

First published 2006

Cataloguing data can be found at the end of this publication.

Luxembourg: Office for Official Publications of the European Communities, 2006

ISBN 92-894-9788-2

Printed in Belgium

PRINTED ON WHITE CHLORINE-FREE PAPER

Conference Organisers

Organising Committee

Philippe Marchand	Ifremer, France (Conference Chair)
Jacques Legrand	Ifremer, France
Hans Dahlin	EuroGOOS
Siân Petersson	EuroGOOS
Pierre Bahurel	Mercator Ocean, France
François Gérard	Météo-France, France

Scientific Steering Committee

Hans Dahlin	EuroGOOS Director
Peter Ryder	EuroGOOS Chair
Ola M. Johannessen	NERSC, Norway
Jan H. Stel	NWO ALW, Netherlands
Philippe Marchand	Ifremer, France
Jacques Legrand	Ifremer, France
Sylvie Pouliquen	Ifremer, France
Kostas Nittis	HCMR, Greece
Bertil Håkansson	SMHI, Sweden
Jon Turton	Met Office, UK
Sukru Besiktepe	Black Sea GOOS, IMR, Turkey
Erik Buch	BOOS, DMI, Denmark
Martin Holt	NOOS, Met Office, UK

International Advisory Committee

Jean-François Minster	CNRS, France
Enrique Alvarez Fanjul	PE, Spain
Kees Borst	RIKZ, Netherlands
Hannu Grönvall	FIMR, Finland
Trevor Guymer	NERC, UK
Bruce Hackett	met.no, Norway
Peter Koltermann	BSH, Germany
Wlodzimierz Krzyminski	IMWM, Poland
Charlotte Lang	RDANH, Denmark
Harald Loeng	IMR, Norway
Giuseppe Manzella	ENEA, Italy
Valery Martyschenko	Roshydromet, Russia
J.P. van der Meulen	KNMI, Netherlands
Glenn Nolan	Marine Institute, Ireland
David Palmer	EA, UK
Gregorio Parrilla	IEO, Spain
Georges Pichot	MUMM, Belgium
Jan Piechura	PAS, Poland
Kazimierz Szefler	MIG, Poland
Christos Tziavos	HCMR, Greece
Silvana Vallerga	MedGOOS, CNR, Italy
George Zodiatis	University of Cyprus

Ifremer Executive Organising Group

Alphonse Carlier
Monique Chapon
Jean-Bernard Donou
Alain Lagrange
Geneviève Le Grand
Véronique Le Guen
Brigitte Millet

Preface

The EuroGOOS conference has become a key event on the agenda of Oceanographic Research. The very successful 4th EuroGOOS conference, which took place in Brest from 6 to 9 June 2005, had the title "European Operational Oceanography: Present and Future". The conference reviewed the progress of operational oceanography during the past three years at both the European and global scales, identifying gaps in the current observing and forecasting capacity and contributing to the plans for the next steps towards efficient marine environmental predictions.

The EuroGOOS conference is now a well-established event taking place every three years, which has received the support of the European Commission since its early editions. The 4th EuroGOOS conference followed EuroGOOS conferences held in The Hague (1996), Rome (1999), and Athens (2002). The 4th EuroGOOS conference brought together over 300 scientists, engineers, policy makers and representatives of private companies concerned with operational oceanography. Representatives from the user communities were invited to present their views and their needs for operational marine services.

The Conference was organised at a time when major Earth Observation and Monitoring initiatives relevant to Operational Oceanography in which Europe is heavily involved are gaining momentum. These include GEOSS (Global Earth Observation System of Systems), GMES (Global Monitoring for Environment and Security), and INSPIRE (Infrastructure for Spatial Information in Europe). Indeed operational oceanography, including its relevant activities of systematic and long-term routine measurements of the oceans, together with coastal zones and atmosphere, and the rapid interpretation and dissemination of results and products, implies accessing a global set of Oceanographic Data that could be facilitated through GEOSS, thereby delivering services for the monitoring of the marine environment through GMES, and benefiting from a better data policy through INSPIRE. Many of the discussions which took place at the conference are situated at the crossroads of the above three initiatives and the conference helped the community of operational oceanographers to clarify their involvement versus these initiatives.

The Conference took place after the mid term of the European Community 6th Framework Programme and the end of many European Community 5th Framework Programme projects that have supported large integrated efforts towards developing a European Research Area. It provided a forum to report on major projects in operational oceanography and to prepare efficient planning of the contribution of the marine science community to the 7th Framework Programme. Since the last conference in Athens in December 2002, excellent progress has been made, in oceanographic research, in demonstrated capabilities, in effective services and in the opportunities to move forward to a more sustained future. Developments in modelling and data management are at the forefront of this work, due in part to increased computing capacity. There has also been steady growth in deployed technological capability, in the form of Argo floats and Ferry Box systems for example. The Glider technology has been reported for the first time, and

all these development are paving the way for an efficient monitoring and forecasting of the marine environment.

The above progress has been made possible thanks to the integrating and federating effort made by the European countries and the European Union working together in collaboration with EuroGOOS, which plays a key role in identifying European priorities for operational oceanography, promoting the development of the scientific, technology and computer systems for operational oceanography, and its implementation, assessing the economic and social benefits from operational oceanography, contributing to international planning and implementation of GOOS and promoting it at national, European and global level. EuroGOOS was also very successful in establishing Regional Task Teams for the Baltic, North West Shelf Seas, the Mediterranean and the Black Sea. Additionally Task Teams are working on the observations and modelling required in the adjacent Oceans, the Atlantic and Arctic. Collectively it results in a pattern of organisations and groups working very efficiently at the scales needed for nested modelling.

Now the community of operational oceanographers is reaching a critical time, when a major turn has to be made from science products to operational services. The recent launching of the GMES fast track marine core services, in which the EuroGOOS members are involved, should contribute to solving key issues for the successful implementation of Marine Core Services, such as the identification and organisation of potential service operators, the definition of their mandates, and the starting of a service level agreement elaboration process and the identification of resources at all levels: European, national, regional and institutional, including structural funds, based on consolidated cost estimates.

Beside the operational aspects, and upstream of it, the European research on oceanographic processes has to continue in order to make available more robust models describing the functioning of the oceanic systems. These conference proceedings represent an excellent review of the state of the art in the domain of operational oceanography in Europe today and can be utilised when shaping future research programmes in this domain. The robustness of the models describing the ocean processes often depends on the availability of appropriate data (in particular long time-series and adequate geographic coverage). Initiatives like GEOSS, which aims at achieving a high degree of convergence at the global level between existing observing systems, will contribute to consolidating the set of existing data and hence the quality of the models. The Commission proposal for the 7th Framework Programme specifically refers to research activities on marine systems under the Environment priority.

In closing, I would like to express my thanks to the EuroGOOS members for having associated the European Commission to the work and debates which took place during the 4th EuroGOOS conference.

P. Valette
Acting Director
Brest, 8 June 2005

Table of Contents

In situ and Remote Sensing Measurements

Data Management and User Needs

Regional Systems 2

In situ and Remote Sensing Measurements 2

EU Models 1

GMES-Oriented Projects

Regional Systems 3

EU Models 2

Coastal Zone

Data, Technology and Users

Index

Operational Oceanography: An Overview

Operational issues associated with practical observing and forecasting systems

Ralph Rayner*

Fugro GEOS/Ocean Numerics, Wallingford, UK

Abstract

Successful implementation of ocean observing and forecasting systems delivering data and information for practical customer applications requires close attention to a wide range of operational issues. Key issues are:

- Properly understanding customer needs
- Tailoring products to meet these needs
- Demonstrating fitness for purpose
- Providing adequate delivery mechanisms and customer support
- Legal liability aspects.

Keywords: Operational oceanography, observing systems, forecasting systems, verification.

1. Introduction

The end-user requirements for operational ocean observation and forecasting fall into three broad categories (Summerhayes and Rayner, 2002):

- Public good end-uses
  - Understanding global change
  - Predicting climate variability
  - Protecting and managing marine ecosystems
  - Protecting life and property on the coast and at sea
  - Human health
  - Security (environmental and military)
  - Sustainable utilisation of ocean resources
- Scientific end-use
  - Understanding the oceans and the Earth system
- Commercial end-use
  - Sale of operational information for a variety of commercial applications.

The demand for data and information to satisfy public good requirements is the most important socioeconomic driver for development of a Global Ocean Observing System (GOOS).

* Corresponding author, email: Ralph@RalphRayner.com

Commercial customers for ocean information represent a relatively small but important potential secondary end-user of the products of GOOS. It is these secondary commercial uses that form the main focus of this paper although some of the issues discussed are equally applicable to public good and scientific applications.

2. Users, end-users and customers

It is important to make a clear distinction between users, end-users and customers.

In the public good case the ultimate end-user is the tax payer. Through governments, tax payers support public good end-uses (maritime safety, security, environmental protection health, etc.) which are mostly delivered by public sector organisations (e.g. Navies, Environment Agencies, Meteorological Services, etc.).

Commercial customers are private sector organisations that buy oceanographic services because a knowledge of ocean behaviour has some impact on their business activities (optimised design of structures, reduced operating costs, etc.) or where there is a mandatory obligation to do so (meeting environmental protection legislation, mandatory safety issues, etc.).

There are usually intermediate users engaged in satisfying specific commercial customer needs.

3. End-user/customer needs

Public good end-user needs are extremely difficult to quantify and prioritise on an objective basis as it is often very difficult to relate levels of expenditure to resulting public benefit. However, in areas such as understanding and predicting climate change there is an implicit and almost certainly valid assumption that the benefits of public expenditure on GOOS are far in excess of the cost of implementing and operating the system.

Public expenditure priorities are often distorted by single events rather than being set through a systematic assessment of risk and return. For example, a major oil spill or a large tsunami event can quickly change the priorities of individual nations or groups of nations.

In contrast, paying commercial customers usually have very specific requirements and a good appreciation of the cost/benefit relationship — they will not buy an ocean information deliverable unless it provides a benefit substantially in excess of its cost.

The range of requirements for ocean information is small compared to environmental information in support of land-based commercial activities. This is because the bulk of commercial activity takes place on land and the human population lives on land, only venturing to sea in search of resources, to transport goods or to spend leisure time.

The main commercial markets for operational oceanographic information are largely confined to the oil and gas industry, the shipping industry, the coastal management sector, fisheries and the leisure industry.

Generally the potential customers in these sectors have little or no expertise or direct interest in oceanography. However, each sector has specialised requirements for oceanographic information specifically tailored to minimising their costs, ensuring that their

operations are carried out safely and ensuring that their activities have no unacceptable impact on the marine environment.

To achieve these objectives these industry sectors procure a range of marine information products under commercial contracts.

It is usually the case that these markets are discretionary; there is generally no mandatory requirement for the customer to obtain or use ocean information. It follows that new information products can usually only be sold on the basis of their demonstrable incremental benefit over existing services, or through meeting customer needs at lower cost than existing services which they then replace.

Customer requirements vary by geography as well as sector of application. For example, an oil and gas operator in the South China Sea has very different requirements to an operator in the Barents Sea because of the marked differences in the oceanographic regime of these two regions.

Responding to these niche markets with something which is genuinely useful, and hence valuable to a customer, requires a very detailed knowledge of relevant aspects of the customer's maritime activities.

As a result, the commercial market is generally served by highly-focused small businesses or small commercial arms of government agencies able to work closely with particular customer groups. Through working closely with a particular sector these intermediate users are able to identify and understand customer needs which can be satisfied through the development of specific tailored information products.

4. Tailoring products to customer needs

In some cases customer needs can be satisfied through the development of stand-alone private observing systems dedicated to specific customer requirements. As an example, some oil and gas companies procure the design, installation and operation of private observing networks to satisfy their needs for information to support safe vessel, subsea and helicopter operations around major offshore structures. Given their high cost there are few such systems in only the major offshore oil and gas basins where environmental conditions are a significant constraint on operations (for example, the North Sea).

The majority of the oceanographic information needs of commercial customers are met through secondary use of data collected for public good or scientific use, sometimes augmented by location specific measurements.

Increasingly, the remote sensed, *in situ* and model data and information being created through implementation of GOOS provide an input to this process.

Generally, the outputs from GOOS are unsuited to direct use by commercial end customers. Intermediate users take GOOS products and add value to them by customising them for particular applications.

At its simplest level this customisation may only involve changing the presentation of information to a form more readily utilised by the customer. More usually, the intermediate user will add substantial value through extensive processing of the data or through combining oceanographic data with other data types.

5. Fitness for purpose

In formal quality assurance systems, 'quality' is generally defined as 'fitness for purpose', ensuring that a product satisfies the defined needs of the customer.

For established oceanographic information products, fitness for purpose is often assumed through satisfactory long term usage. However, to successfully introduce new products a service provider will usually need to demonstrate fitness for purpose through achieving compliance with a defined customer expectation.

Intermediate users of GOOS data and information must therefore be able to demonstrate that a given information product is of sufficient utility to be of economic value to a customer.

At first sight this would appear to be a relatively straightforward process. First, understand the customer requirement, then build a service to deliver a suitable information product which is derived from observations or measurements of the environmental variable affecting the customers' activities. Where measured data is sparse make use of numerical modelling techniques to create a suitable information product.

In practise this has always been difficult to achieve. Sensitivity of the customer's marine operations to environmental conditions is invariably most acute at the extremes of the variable in question (greatest wave height, highest storm surge, strongest current, highest/lowest seawater temperature, etc.). Observations of the extremes are usually very limited. It is also at the extremes where numerical models (and sometimes observing systems) are operating at the limits of their validity.

As an example many of the early attempts to utilise hindcasting techniques to determine the statistics of the ocean's physical environment were found to underestimate extremes — but only after some lengthy and sometimes heated debates about whether the models or the measurements were in error!

The most likely new application area to be successfully developed based on GOOS products is commercial use of ocean forecast data. Here the problems of adequate verification are considerable. Unlike many of the public good and scientific applications of ocean forecasts, most commercial applications require accurate and reliable forecasting of oceanographic conditions at fixed points (e.g. an offshore structure). In the case of a sharply defined oceanographic feature (such as an eddy of a front) the commercial customer's requirement is a forecast of the absolute position of the feature relative to his location of operation.

Building model systems capable of doing this to an acceptable accuracy, and verifying the accuracy achieved remains a significant challenge. For example, determining the synoptic location and characteristics of large scale ocean features such as eddies is currently a challenge at the limit of present remote sensed and *in situ* observations.

6. Delivery mechanisms

Where an oceanographic information product is being used for operational purposes the reliability of delivery mechanisms becomes paramount. An extreme example is the 'floatover' operation illustrated in Figure 1. Failure of supply of 'real time' oceanographic information vital to planning and conducting the delicate positioning of the gas

production facilities over a pre-installed subsurface structure could have very costly consequences.

Operational data delivery systems must therefore be designed in such a way as to minimise the risk of failing to deliver the product and with levels of redundancy and backup appropriate to the intended use.

While the internet provides an in many ways ideal means of delivery, care should be taken to avoid over-dependence on this delivery route in business or safety critical applications, as internet outages can be relatively common offshore. Some form of backup path for at least limited delivery should also be considered.

However robust the delivery system is there is always a risk of failure, especially given that much of the data delivery chain is often outside the service provider's direct control. This is especially the case where data feeds are being taken passively from public good sources such as ftp download sites. This might be a non-critical component of the public good application and therefore not necessarily sufficiently robust for the intended secondary application.

Figure 1 'Floatover' of a gas production facility in the South China Sea.

7. Legal aspects

The potential for failure to deliver information vital to business or safety critical operations raises the issue of legal liabilities.

Supply of oceanographic information by an intermediate service provider for a fee places the provider in a legal contract with the customer with all the liability obligations that a binding contractual relationship implies.

It is entirely possible to limit the legal liabilities under such a contract but this does not necessarily protect the service provider especially in the event of negligent service provision resulting in substantial economic loss or loss of life or property. It is therefore wise (and in most cases contractually obligatory) that the service provider carries substantial professional indemnity insurance.

8. Conclusion

Many of the public good applications of GOOS are currently operating in an experimental mode and there is therefore no guarantee of their long-term sustainability. It is essential that more work is done on systematic evaluation of the socioeconomic benefits of such applications in order to solicit long-term operational funding. Hopefully, this will form a part of the result of work on the development of the marine components of GMES. The proposed European Marine Strategy can then provide a framework for systematic and sustained marine observations and forecasts.

If the outputs from the resulting public good services are made freely available for secondary use, intermediate users will build on this information to create and provide new bespoke value added services into niche commercial markets.

References

Summerhayes, C. and R.F. Rayner (2002). Operational Oceanography, in Oceans 2020: Science, Trends, and the Challenge of Sustainability, Eds Field, Hempel and Summerhayes, Island Press, August 2002.

Regional Systems 1

A new version of the operational oil drift forecasting system Seatrack Web

Cecilia Ambjörn*[1] and Johan Mattsson[2]

[1]*Swedish Meteorological and Hydrological Institute (SMHI), Sweden*
[2]*Royal Danish Administration of Navigation and Hydrography (RDANH), Denmark*

Abstract

Seatrack Web is an operational oil drift forecasting system covering the Baltic Sea and the eastern part of the North Sea. Seatrack Web is available over the internet using a client-server web application, which enables users to start an oil drift simulation and have the results presented in their web browser on demand. The server hosting the oil drift simulation code has access to the most recent weather and ocean forecasts, thus giving the user the "best possible" decision tool in an oil combating situation.

The drift model calculates the three-dimensional movements of substances or objects at sea, including sinking, stranding and turbulent dispersion. For oils the evaporation, emulsification and wave-induced vertical dispersion are also calculated. Floating objects can also be forecasted, in which case the direct influence of the wind may be included. Drift trajectories can also be run in backtracking mode, indicating the source of an object or spill. The results are displayed as particle trajectories on a map in a full-featured GIS interface. The trajectories may be animated, traced, zoomed and displayed in many ways. Oil properties, drift velocities, etc. are presented in tables. Other relevant information such as surface current vectors, sensitive areas, cities and so on can also be displayed. Seatrack Web is the HELCOM system for forecasting of oil drift, and the primary users are oil combating authorities in the countries surrounding the Baltic Sea. It has been in operation since the early 90s, and a lot of experience in its use has been gathered among users and developers. Together with new and changed demands this has led to a major upgrade of the system resulting in Seatrack Web 2.0. The presentation will give an overview of the system with focus on the new features and components.

Keywords: Seatrack Web, operational, oil spill, forecast, drift, spreading, weathering, HIROMB.

1. Introduction and background

Seatrack Web is an oil drift forecasting system covering the Baltic Sea and the eastern part of the North Sea. It is a tool developed mainly for oil spill combating authorities around the Baltic Sea to predict the fate and drift of oil spills. It is also used to identify illegal polluters, by calculating backwards from an existing spill detected in the sea. The Seatrack Web system is user friendly and fully operational, and is accessible over the internet. Its drift forecasts are based on the latest wind and current forecasts from operational weather service models.

* Corresponding author, email: cecilia.ambjorn@smhi.se

Seatrack Web was developed following HELCOM Recommendation 12/6 of 20 February 1991, and is regarded as the common HELCOM oil and chemical modelling and drift forecasting system. At the HELCOM Response meeting of October 2002 it was recognised that the system at this time needed upgrading to meet the requirements of a new HELCOM recommendation 24/7, addressing further development and use of drift forecasting for oils and other harmful substances in the Baltic. In addition, users of Seatrack Web had particular requests. Giving some examples, the Swedish Coast Guard wanted to include other oils relevant for the Baltic Sea area. They also needed predictions of viscosity changes, to be used during clean-up operations. The Finnish Environment Institute was interested in the interaction between oil and ice and also the possibility to see the ice cover and spreading simulations simultaneously. The Centre of Marine Research in Lithuania needed current forecasts in the Curonian Lagoon to be able to predict oil spill drift inside the lagoon. The Admiral Danish Fleet, responsible in Denmark for oil spill combating, wanted extended GIS functionality. Together with further suggestions for improvements from meetings, other users and from the expert group developing the system, an extensive specification for a new version of Seatrack Web could be established. The upgrading of the system started in 2004 and has now resulted in a new version, Seatrack Web 2.0.

2. Seatrack Web system overview

The Seatrack Web system has three parts. The first is the operational weather and ocean forecasting system, which provides the necessary wind and current fields. Presently Seatrack Web uses wind from the weather model HIRLAM (High Resolution Limited Area Model) and currents from the 3-dimensional baroclinic circulation model HIROMB (High Resolution Operational Model for the Baltic Sea), both run at SMHI (the Swedish Meteorological and Hydrological Institute). HIROMB is run twice a day using forcing fields from HIRLAM and produces 48-hour forecasts of currents, sea level, temperature, salinity and ice conditions for the North Sea−Baltic Sea area. The forecasts are post-processed to a format suitable for Seatrack Web, in which forecast fields 2 days ahead and 10 days back in time are accessible. HIROMB calculates current velocities in a regular grid with a horizontal resolution of one nautical mile and a vertical resolution in the range of 4−60 m with increasing resolution towards the surface. A detailed description of the HIROMB model is given by Wilhelmsson (2002).

The second part of the system is the drift, spreading and weathering model. The drift model in Seatrack Web is based on the Lagrangian particle tracking technique to model the drift and spreading of oil spills. The particles are advected in a three-dimensional velocity field, which is discretised in space and time. The spreading is mainly performed by gravitational spreading of buoyant oil at the sea surface, together with vertical shear spreading, see e.g. Reed *et al.* (1999) and Delvigne and Sweeney (1988). Weathering processes included are evaporation and emulsification, which cause changes in viscosity and oil density (Fingas, 1999; Lehr, 2001).

The third part is a client/server web application. It handles communication and comprises of a graphical user interface (GUI) on the client side and a Java Servlet on the server side. Any drift simulation is started on demand by an end-user, who enters simulation parameters through the user interface. The parameters are passed over the

internet, and a drift calculation is executed on the server, which has access to the wind and current forecasts. After completion the simulation results are returned to the client computer, where they are presented. To display maps and other relevant geographic information, an open source Java library for map applications OpenMap™ (BBN Technologies) is used. The results of a simulation are typically available within less than a minute, but the response time varies from seconds to several minutes depending on the type of calculation. The drift model and the Java Servlet are at present installed at SMHI and RDANH (the Royal Danish Administration of Navigation and Hydrography).

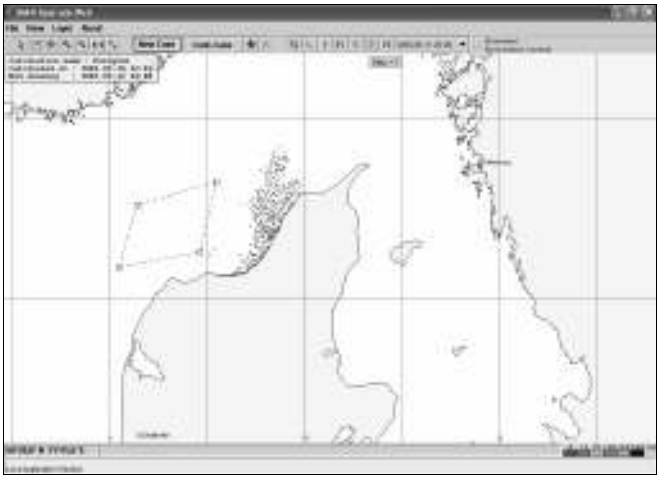

Figure 1 A particle cloud approaching the west coast of Denmark following an area outlet simulation.

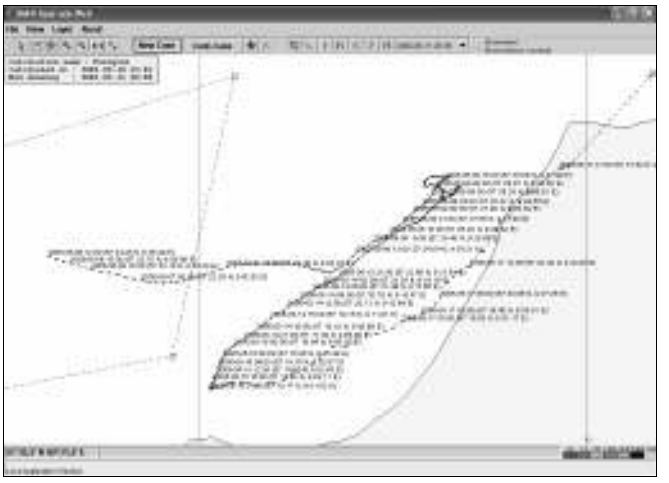

Figure 2 The trajectory for the same simulation as in Figure 1.

3. Using Seatrack Web

It is easy to set up a drift calculation in Seatrack Web. Via the graphical user interface the user provides information to the system. By varying the input a large number of different simulations can be performed. Essentially the user has to provide input in four groups. In **Time and position** the user can choose the time period of the calculation together with the position (latitude and longitude) and depth of the spill outlet. The spill can be released at a single point, along a straight line or inside a polygon. The user also decides whether the calculation should proceed forward or backward in time. Under **Substance type** the user selects kind of substance, in particular what oil type to use. In the third group, the user specifies the discharge conditions as an instantaneous spill of a given amount of oil or a continuous spill at a given discharge rate and duration. Finally, in the fourth group the user can set some current options for the calculation. The default choice is to read the forecasted currents from HIROMB every third hour. Alternatively, the user can set the current speed and direction manually, which makes user-defined scenario calculations possible.

The results of a calculation can be presented in many ways, and with various kind of additional information. The particles are either shown as particle clouds, colour coded to show the individual depth of the particles, or as trajectories where hourly centre positions of the cloud are shown. The particle clouds can be animated, traced and zoomed. Oil properties, drift velocities, etc. are presented in tables and plotted in graphs. Other relevant information such as surface current vectors, sensitive areas, cities and so on can also be displayed. Examples of how the results of a calculation are shown in the GUI are given in Figure 1–Figure 4.

Another factor of importance to user friendliness is the availability. During the years there have been very few failures in the availability of the system. Updates are also very easily distributed. When the user clicks the start link the version of the GUI is checked against the server version and an update is downloaded if necessary. Otherwise a cached version of the GUI is executed.

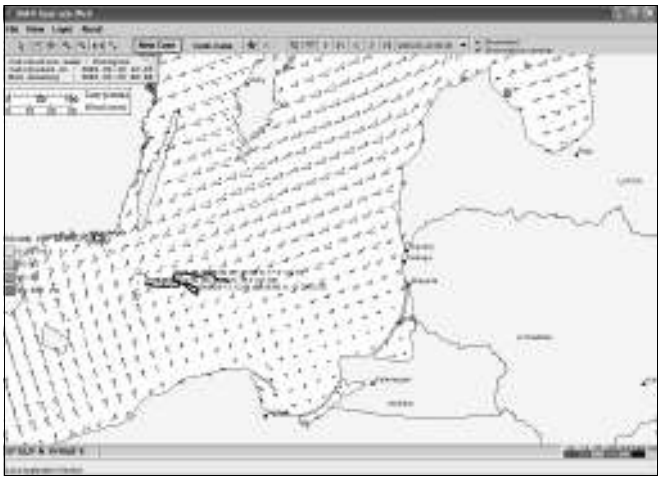

Figure 3 An example showing a trajectory together with wind and current arrows.

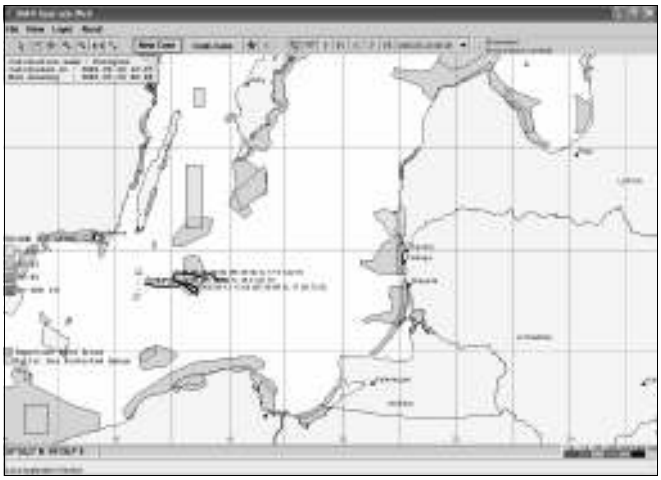

Figure 4 Same as Figure 3, but with an GIS layer showing sensitive areas being active.

4. Some new features in the system

Compared to the previous version of Seatrack Web there are some important improvements in the new version. The current field is now available in a one nautical mile resolution, compared to three nautical miles previously. Together with an improved turbulence scheme and the use of data assimilation in the latest version of HIROMB, this gives improved current fields to be used for drift simulations. The coastline in the calculation is now the 'real' coastline. Previously the coastline of the HIROMB grid was used, resulting in not so realistic simulations close to the coast.

There have been many changes in the GUI. There are now extensive GIS possibilities, including the possibility to easily add GIS layers. For instance, economic zones, sensitive areas and other interesting features can be shown. The outlet area can be introduced as an area consisting of 4 corners and the corner positions can be adjusted after they are chosen. Oil properties are shown directly in a graph where the time development is drawn. A view of the forecast can be sent directly as an e-mail.

Interaction between oil and ice is introduced in the new version, as well as a GIS layer showing the ice cover. There are also new oil types in the substance list, and improved oil weathering algorithms. A new drift and spreading code has been developed based on object oriented programming. This has increased the flexibility of the code and facilitates maintenance and further development.

5. Further development

There are many suggestions for further development on the system. There is a large user group in the countries surrounding the Baltic Sea which gives excellent feed-back, with new ideas and comments on the existing version. It gives the advantage of continuously improving the system, and developing it further, as a result of user experience. At present, the plans for improvement include using wave data from wave forecast models in the dispersion algorithm for oil. Then it will also be easy to show the wave heights on

the map. Also the prognostic turbulence parameters from the circulation model will be used, replacing the parametrised turbulence used today. Wind and current scenarios, designed by the user, together with extended outlet possibilities will be implemented, to show alternative developments of an oil spill. This is valuable in showing the risk of oil spills, to make plans for oil accidents that might happen and in learning about the oil's behaviour in water.

Acknowledgements

The financial support of the Swedish Coast Guard, the Swedish Rescue Service Agency, the Finnish Environment Institute and HELCOM are gratefully acknowledged.

References

BBN Technologies' OpenMap™ homepage, http://www.openmap.org

Delvigne, G.A.L. and C.E. Sweeney (1988). Natural dispersion of oil. Oil & Chemical Pollution, 4 281–310.

Fingas, M. (1999). The evaporation of oil spills: development and implementation of new prediction methodology. Proceedings of the 1999 Oil Spill Conference, pp 281–287.

Lehr, W.J. (2001). Review of modelling procedures for oil spill weathering behaviour. In: Oil Spill Modelling and Processes, (Brebbia, C.A., ed), pp 51–90, WIT Press, Southampton, UK.

Reed, M., Ø. Johansen, P.J. Brandvik, P. Daling, A. Lewis, R. Fiocco, D. Mackay and R. Prentki (1999). Oil spill modeling towards the close of the 20th century: Overview of the state of the art. Spill Science and Technology Bulletin, 1 (2) 3–16.

Wilhelmsson, T. (2002). Parallelization of the HIROMB ocean model. Licentiate thesis. Department of Numerical Analysis and Computer Science, Royal Institute of Technology, Stockholm.

The POL Coastal Observatory — the early years

Andrew Lane*[1], John Howarth[1], Roger Proctor[1], Philip Knight[1] and David Mills[2]

[1]*Proudman Oceanographic Laboratory, UK*
[2]*Centre for Environment, Fisheries and Aquaculture Science, UK*

Abstract

A pilot Coastal Observatory has been established in Liverpool Bay. It integrates (near) real-time measurements with coupled models in a pre-operational prediction system, and displays the results on the Web. We aim to understand how a coastal sea responds to natural and man-made forcing. The time series allow us to define seasonal cycles and their inter-annual variability, and to quantify the importance of events relative to mean conditions. Applications include eutrophication and shoreline management (coastal flooding and beach erosion/accretion), as well as understanding present conditions, to predict the impacts of climate change.

Integrated measurements cover a range of space and time scales, focusing on horizontal and vertical gradients. They include an *in situ* site (started in August 2002), monthly regional CTD surveys, an instrumented ferry and a HF radar system measuring surface currents and waves.

A suite of nested 3-D hydrodynamic and ecosystem models is run daily, centred on the Observatory area, covering the ocean/shelf of northwest Europe (at 12-km resolution), the Irish Sea (at 1.8 km) and Liverpool Bay (200-m resolution). The measurements will test the models against events as they happen in a truly 3-D context.

All measurements and model outputs are displayed on the Coastal Observatory website (http://coastobs.pol.ac.uk) for an audience of researchers, coastal managers and the public. Results from the first two years' operations are presented.

Keywords: Monitoring, operational model forecasting, Irish Sea, Liverpool Bay

1. Introduction

The Coastal Observatory, coordinated by the Proudman Oceanographic Laboratory, has been active in the Liverpool Bay area of the eastern Irish Sea for the past two and a half years (Proctor *et al.*, 2004). We aim to understand how a coastal sea responds to natural forcing, and the consequences of human activity, so we can use and manage resources better. The Observatory integrates real-time monitoring and forecasting, and is therefore a practical research tool. Data and model results are accessible via the Internet.

Descriptions of the components of (pre-operational) observations and modelling follow the project's rationale. Examples are given of the data and model results that are freely available on the project's web site. Finally, there is an outline of future directions.

* Corresponding author, email: A.Lane@pol.ac.uk

2. Rationale

2.1 Vision

The oceans are an essential component of the Earth System. To understand how our planet works and to predict the impacts of human activities and natural change, an Earth System approach linking ocean, land and atmosphere is necessary. Sustained, systematic observations of the ocean and continental shelf seas, at appropriate time and space scales allied to numerical models, are the key to their understanding and prediction. In shelf seas these observations address issues as fundamental as the effects of climate change, biological productivity and diversity, sustainable management, pollution and public health, safety at sea and extreme events.

Advancing understanding of coastal processes, to use and manage resources better, mitigate risks and explore for new phenomena, is challenging. Important controlling processes occur over a broad range of spatial and temporal scales which cannot be simultaneously studied solely with ship-based platforms.

The stimulus is both scientific curiosity and also the desire to improve the underpinning knowledge required for sound management decisions concerning the quality and sustainability of the seas.

2.2 Guiding principles

The present Coastal Observatory, focusing on the Irish Sea between Great Britain and Ireland, runs from 2001 to 2007, with a subsequent phase until 2012. It is an evolving pre-operational system making near real-time measurements to test forecast models.

The Observatory provides a framework which anyone is welcome to augment; with open access to basic data and model outputs. The British Oceanographic Data Centre is managing the collected data. We encourage our audience of researchers, managers and the public to actively use results from the Observatory, and to give us their feedback.

2.3 Location of the study area

The eastern Irish Sea is affected by all shelf-sea and coastal sea processes, making it an excellent study area. Processes exist on a range of space and time scales — both vertical and horizontal gradients are important, requiring corresponding sampling frequency and duration; detecting trends entails long-term time series. Estuarine inflow influences nearshore physical and biogeochemical processes (the region receives significant levels of nutrient inputs). Therefore, a multi-disciplinary approach is adopted in making measurements and formulating models.

3. Results from observations

3.1 Moored instruments

Three moorings are located close to the Mersey Bar lightship at 53° 32' N 3° 21.8' W, where the water depth is 22 m with a tidal range of ±4 m at spring tides (see Figure 1a).

1. An acoustic Doppler current profiler (ADCP) is attached to a sea bed frame together with a temperature and salinity sensor, pressure recorder, transmissometer and an acoustic modem for near real-time data telemetry via a surface buoy.

2. A directional wave buoy measures significant wave height and peak period.
3. Nutrient concentrations are measured on the SmartBuoy (maintained as part of the CEFAS network) also including temperature, salinity, pressure, chlorophyll, turbidity and downwelling PAR (photosynthetically active radiation).

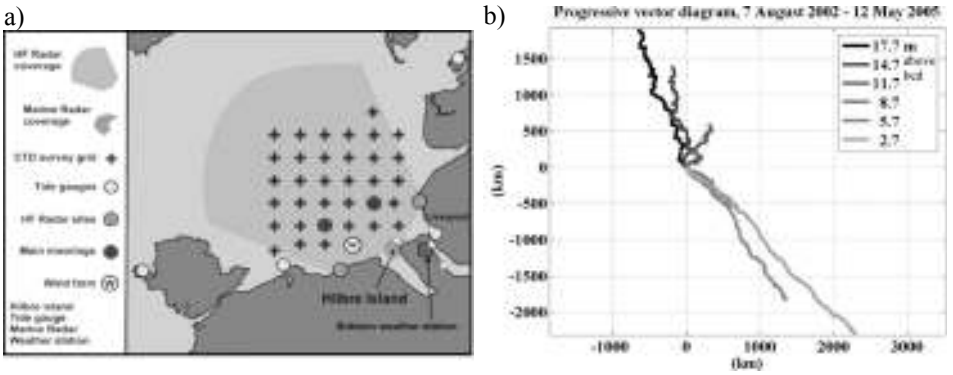

Figure 1 a) Location map showing measurements, b) progressive vector diagram, 7 August 2002 to 12 May 2005.

Harmonic analyses of current profiles from the ADCP, between August 2002 and May 2005, show the dominance of the semi-diurnal tidal constituents; currents are mostly rectilinear (in a nearly E–W direction). The amplitude of M_2 is largest (0.57 ms^{-1} at the sea surface), followed by S_2 (0.20 ms^{-1}) and N_2 (0.11 ms^{-1}). Other tidal constituents are about an order of magnitude smaller, with a distinctive shape for the mean component. Residual currents move northwards near the surface (2.5 cms^{-1} away from the coast) and south-eastwards near the bed (4 cms^{-1} towards the coast), with a minimum excursion at between 9 and 12 m above the bed, Figure 1b. This long-term feature results from the horizontal density gradient.

The sensor package on the CEFAS SmartBuoy continuously measures nitrate at the sea surface (NAS, *in situ* nitrate analyser, every two hours) and these measurements are combined with water samples automatically collected at daily intervals for later laboratory analysis (and for calibrations). Nutrient concentrations are then derived (in terms of the total oxidisable nitrogen) — the time series is shown in Figure 4 of Greenwood *et al.* (2005). Concentrations from the water samples collected on the ship-based survey are also plotted. This diagram represents one and a half years' results, highlighting the winter maxima ('hyper-nutrified conditions') and summer minima. NAS results have proved valuable as they reveal some high frequency variations in nutrient concentrations (attributed to freshwater inputs) that are not present in the water samples or the ship survey data.

3.2 Ship surveys

A survey is performed every six weeks (or four weeks in summer) onboard the RV Prince Madog, as well as servicing the mooring sites. There have been 26 surveys up to May 2005 which follow a fixed track (subject to the weather situation), measuring CTD (conductivity and temperature through depth) at each station visited. Additionally, water samples are taken near the surface and bed to determine concentrations of suspended

sediments and nutrients (processed by the University of Wales Bangor and the Southampton Oceanography Centre, respectively). At selected stations, water samples are analysed for nutrients, chlorophyll, phytoplankton and zooplankton (by CEFAS).

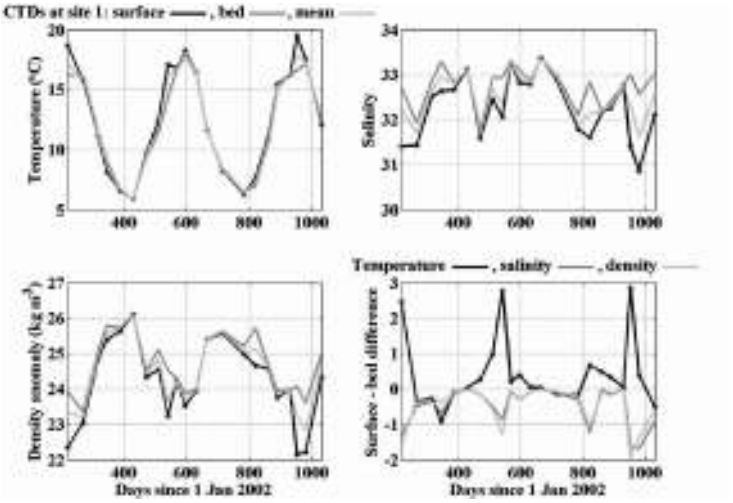

Figure 2 Surface and bed temperature, salinity and density from August 2002 to January 2005.

Time series of measurements at the main mooring site were obtained from the CTD surveys spanning the past two years. Surface, bed and depth-averaged temperature data exhibit a clear seasonal cycle (with slight stratification during early summer). The picture for salinity is less clear: the effects of freshwater inflows are evident when the water column stratifies. The density is dominated by the temperature signal, but the salinity strongly influences inter-annual variability and stratification. Surface-bed temperature differences are greatest in early summer; stably stratified conditions persist even when surface temperatures are at times cooler (but sufficiently less dense) than the bed during winter, Figure 2.

3.3 Instrumented ferry

Between Birkenhead and Belfast, FerryBox instruments fitted to the Liverpool Viking measure the conductivity, temperature, turbidity and fluorescence of water from 3 m below the surface. The underway data and the ferry's position are transmitted back to POL every 15 minutes via the Orbcomm satellite system.

The temperatures and salinities recorded during 2004 are compared with outputs from the Irish Sea model (IRS), a 1.8 km resolution model run operationally at the Met Office. Model temperatures are close to the measurements in winter, but are warmer in the western Irish Sea in summer, Figure 3. The model results match the observations more closely for salinity — especially the fresher water in the Liverpool Bay region. Although the model is driven by climatic mean value, there is some correlation with river flows.

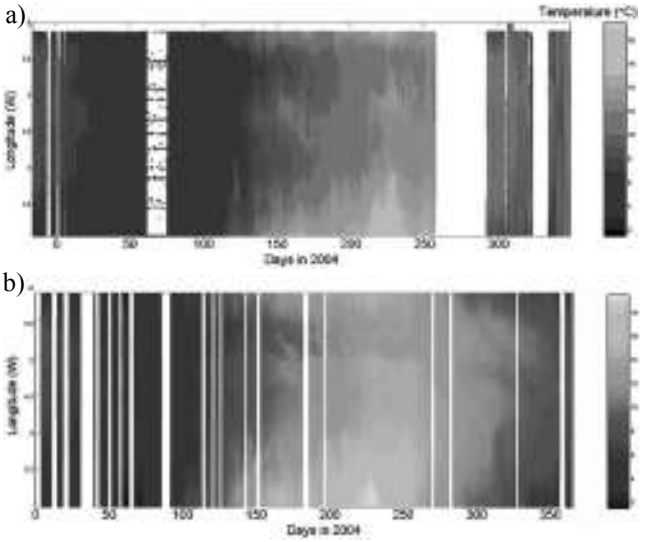

Figure 3 a) Observed, b) modelled surface temperature between Birkenhead and Belfast.

3.4 Land-based monitoring

The data returns of HF radar measurements of surface currents and waves between March and December 2004 are above 75% in nearshore regions, but fall off quickly with distance (greater than about 20 km) from the HF radar sites. Comparing the HF radar's M_2 maximum sea surface current amplitudes with the Irish Sea model shows the differences are smallest close to the coast. The model and HF radar currents appear to be offset by 5 cms^{-1}. At the mooring site, the M_2 current ellipse maximum and minimum amplitudes measured by the HF radar are consistent with ADCP current profiles, and corresponding M_2 phases differ by –4° and 2° respectively. An intended use of the HF radar is to obtain significant wave heights from recorded Doppler spectra, and these can be compared with Waverider data. (See Lane *et al.*, 1999, for a short description of a HF radar system.)

3.5 Satellite remote sensing

Composites of one week's remote sensing images of sea surface properties are useful for comparing with models and data to aid their interpretation. Sea surface temperatures have been routinely calculated from the infrared channels of the AVHRR series of sensors, operated by NOAA (the USA National Oceanic and Atmospheric Administration). SeaWiFS, launched in 1997, is a multi-channel (visible and infra-red) instrument used for studying ocean colour; chlorophyll *a* and suspended sediment concentrations can be derived after calibrating images against coincident *in situ* data.

4. Operational models

4.1 From the Atlantic to Liverpool Bay

The ocean Forecasting Ocean-Atmosphere Model (FOAM) at 1/9° resolution (approximately 12 km) predicts the temperature, salinity, water elevation and heat fluxes.

Together with meteorological forecasts (at 12-km resolution), these then force the Atlantic Margin Model (AMM) at 12-km resolution, which in turn provides inputs for the Medium-Resolution Continental Shelf model (MRCS) at 7 km. Daily forecasts are made for tides, waves, temperature and salinity. Models at higher resolution are the Irish Sea model (IRS, 1.8 km), and the Liverpool Bay model (LB at 200 m). With the exception of LB, these operational models are run routinely by the Met Office.

4.2 Linking MRCS and ERSEM

MRCS, based on the POL Coastal-Ocean Modelling System (POLCOMS), has been coupled with the European Regional Seas Ecology Model (ERSEM) to provide estimates of a range of parameters to aid coastal zone managers (eutrophication indicators). These include sea surface and bed temperatures, chlorophyll *a* and zooplankton, as well as mesozooplankton, NO_3, and N:P ratio.

4.3 Liverpool Bay: tides and suspended sediments

The 3-D Liverpool Bay model is also based on POLCOMS, and has been set up to provide tidal elevations and currents for simulating suspended sediments with a Lagrangian random-walk particle tracking module. Results for suspended and settled sediments in the Dee estuary show sediments enter and leave the estuary mostly through the Hilbre Channel on the east side. Sediment on the bed accumulates on the eastern shore, consistent with historical evidence.

5. The Coastal Observatory website

The website (http://coastobs.pol.ac.uk) is an important part of the Coastal Observatory project. Users have round-the-clock access to observations and up to 48 hour forecast model outputs without the need to register. However, free-of-charge registration allows users to retrieve (unverified) numerical data as it becomes available. Of the 500+ registrations so far, the general public represents 55%, researchers 20%, coastal managers 10%, teachers 10% and others 5%.

5.1 Observations

Up-to-date observations are from the coastal tide gauges, meteorological station, web camera, ferry measurements, HF radar results, river flows, satellite images, fixed moorings and CTD survey data.

5.2 Forecasts

Model outputs predicting up to 48 hours ahead include: mean currents, elevation, sea temperature and salinity, swell waves and wind waves, air temperature, wind speed and direction, cloud cover and rainfall.

6. Future directions

A second mooring site started in April 2005. The FerryBox suite of instruments will be installed on other ferry routes, and will include the monitoring of nutrients. Continued effort is required to ensure data quality, to analyse the streams of data being acquired and to synthesis these with the numerical models.

Funding is being sought for the next phase of the project in 2007–2012, and we will seek to enhance collaboration with European and International Coastal Observatory partners. The ultimate goal is to convert what is presently a research tool into an operational one.

References

Greenwood, N., D.K. Mills, M.J. Howarth, R. Proctor, D.J. Pearce, D.B. Sivyer, S.J. Cutchey and O. Andres (2005). High frequency monitoring in Liverpool Bay; variability of suspended matter, nutrients and phytoplankton. This volume, page 413.

Lane, A., P.J. Knight and R.J. Player (1999). Current measurement technology for nearshore waters. Coastal Engineering, 37, 343–368.

Proctor, R., M.J. Howarth, P.J. Knight and D.K. Mills (2004). The POL Coastal Observatory — Methodology and some first results. Proc. Estuarine & Coastal Modelling Conf., 3–5 November 2003, ASCE, pp 273–287.

High resolution monitoring of harmful algal blooms and oceanographic conditions in the Skagerrak

B. Karlson*

Oceanographic services, Swedish Meteorological and Hydrological Institute, Göteborg, Sweden

Abstract

Real time monitoring of harmful algal blooms with the necessary vertical resolution for detection of thin layers of phytoplankton is now possible. The Skagerrak is an area influenced by water from the Baltic and the North Sea. Harmful algal blooms (HABs) are a major concern in the area for aquaculture and the whole marine ecosystem. The water is mostly stratified and harmful algal blooms sometimes occur in thin layers in the water column. To monitor the development and advection of blooms a mooring with a profiling multi-parameter device is used. The system also consists of a surface buoy with sensors at 1 m depth and a sea floor mounted acoustic doppler profiler for measurement of current speed and direction as well as waves. The profiling device moves vertically through buoyancy control with a speed of around 30 cms^{-1}. It is fitted with sensors for chlorophyll *a* fluorescence, turbidity, oxygen, salinity, temperature and nitrate. The sampling frequency is normally set to 1 Hz giving a vertical resolution of about 30 cm. Data is transmitted every three hours using the GSM mobile phone system and will be presented on the internet in near real time. The mooring will be deployed at ca. 50 m depth close to the Swedish west coast at Måseskär, position N 58° 05.5', E11° 17.0'. The location of the mooring was chosen to catch the Baltic current, the Jutland current as well as deep Skagerrak water. The system is expected to be operational in summer 2005.

Keywords: Buoy, measurement platform, harmful algal blooms, vertical profiles, chlorophyll *a* fluorescence, oxygen, nitrate, turbidity, real time, currents, waves, salinity, temperature, Skagerrak, thin layers, phytoplankton.

1. Introduction

This paper presents an innovative profiling system for monitoring Harmful Algal Blooms (HABs) and coastal oceanographic conditions in the sea. HABs are a major concern in the Skagerrak–Kattegat area which is situated between the North Sea and the Baltic (Figure 1). The area is characterised by very small tidal amplitude (ca. 30 cm) and by mixing of several different water masses with typically large salinity differences, and stratification is often strong (e.g. Figure 2). Aquaculture along the coasts of Norway, Sweden and Denmark includes mussel farms (*Mytilus edulis*) and fish farms (e.g. *Salmo salar*). Low biomass blooms of phytoplankton genera such as *Dinophysis* and *Alexandrium* causing diarrhetic and paralytic shellfish poisoning respectively are common phenomena that at present require water sampling and microscopy for monitoring.

* Corresponding author, email: bengt.karlson@smhi.se

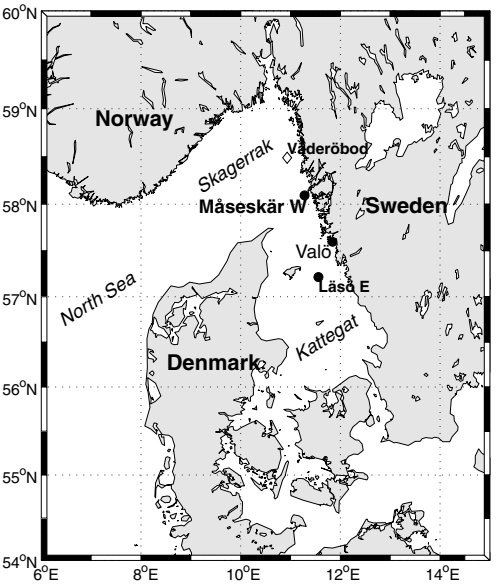

Figure 1 Map showing the locations of the Swedish oceanographic buoys in the Skagerrak–Kattegat. The profiling multiparameter system Måseskär W is planned to be deployed in late summer 2005. The mooring at Läsö E is a multiparameter buoy measuring meteorological parameters, waves, currents, salinity, temperature, salinity and chlorophyll *a* fluorescence at up to 10 different depths. Väderöbod measures surface temperature, wave height and direction. The Valö station, from which data is presented in Figure 2, is also indicated.

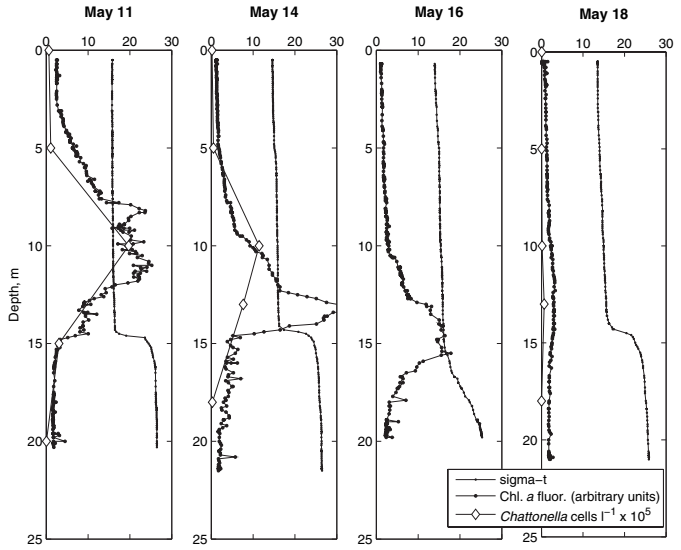

Figure 2 During the *Chattonella* bloom in 1998 sampling was made every three days at Valö close to Göteborg. Data is shown to illustrate the short term dynamics of harmful algal blooms in the area. The thin layers of phytoplankton detected as chlorophyll *a* fluorescence are sometimes, but not always, connected to a pycnocline.

High biomass blooms having effects on the entire ecosystem or causing fish kills such as those of *Chrysochromulina polylepis* in 1988 and *Chattonella* sp. in 1998, 2000 and 2001 respectively may be monitored using a combination of automatic and manual techniques. Remote sensing from air and space using for example the MERIS sensor on ENVISAT is used for monitoring the uppermost part of the ocean. An estimate of total phytoplankton biomass as chlorophyll *a* is obtained when suspended sediments or dissolved coloured material does not hamper the algorithms. However, clouds are a major problem in the area for remote sensing applications. Another technique used successfully is FerryBox systems on ships of opportunity. From ferries, total phytoplankton biomass data measured as chlorophyll *a* fluorescence is obtained in real time. Also ferries can be used for automatic sampling for later microscopic analysis on shore. One limitation is that only one depth, usually around 4 m, is sampled. Harmful algal blooms often occur in subsurface maxima (Figure 2), often in thin layers. Thus a system for obtaining profiles of phytoplankton biomass is desirable for HAB monitoring. Such a system is presented in this paper.

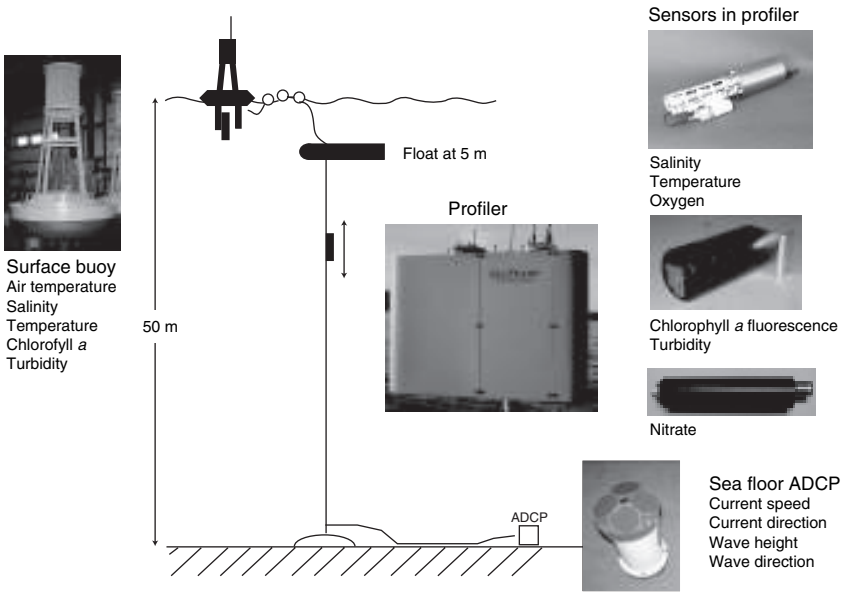

Figure 3 The system to be deployed at Måseskär W consists of a sea floor mounted ADCP, a multiparameter profiling device and a surface buoy with sensors at 1 m. Measurement profiles are made every three hours and data is transmitted in near real time to be published on the Web.

2. Technical description of system

The heart of the system (Figure 3) is a profiling device that moves up and down through the water column every three hours using buoyancy control. On this device several different types of sensors are mounted. They communicate with a processor in the profiler through standard protocols (RS232). Sampling at 1 Hz and a vertical velocity of ca. 20–30 cms^{-1} results in a vertical resolution of about 20–30 cm. A torpedo shaped float at 4 m tightens an inductive wire fastened to a bottom weight at 50 m depth. The

profiler moves along the wire between the sea floor and 5 m depth. A second set of sensors is mounted on the surface buoy at 1 m. Inductive modems connected to the sea floor mounted ADCP (Acoustic Doppler Current Profiler) and the profiler is used for communication with the surface buoy where a processor handles the data. Transmission to shore is accomplished using a GSM mobile phone modem. Satellite communication is possible but not needed close to shore. At the SMHI offices the data will be stored and automatically processed for publication on the Web. Special care has been used when designing the system to avoid biofouling. The sensors on the profiler rest on the sea floor most of the time. Optical windows are covered by copper shutters or cages. The sensors on the surface buoy will be affected most by biofouling but are also easiest to access for cleaning. Service intervals for cleaning and battery replacement are expected to be around 60 days in March–October and around 90 days in winter. Biofouling is expected to be the limiting factor for the time between service intervals.

3. Discussion

3.1 General discussion

The system presented solves several of the problems of monitoring the oceanographic conditions in the area. It is to the author's knowledge a unique combination of real time measurements of physical, chemical and biological variables with a high vertical and temporal resolution. Similar profiling systems have been used before (Arneborg *et al.*, 2004) but without real-time communication. Systems measuring at one or several depths also exist (e.g. Mills *et al.*, 2003) and work excellently in well mixed areas. Being able to observe thin layers of phytoplankton while sitting at a computer connected to the internet makes it possible to plan shipborne sampling effectively. Turbidity measurements are made to detect suspended sediments and to give extra information about other particles such as phytoplankton. Measurements of current speed and direction facilitate prediction of bloom advection. Basic measurements of salinity and temperature with a high vertical resolution are important to detect density gradients. The oxygen measurements close to the sea floor will produce early warnings of oxygen deficiency. Oxygen measurements closer to the surface indicate where primary production is high. The nitrate measurements use a method based on nitrate absorption in the UV-light region and has a lower detection limit than those based on wet chemical methods. The nitrate data will anyway provide interesting data on the nutrient dynamics. Wave data is essentially a bonus from a modern ADCP mounted at relatively shallow (50 m) site.

The system will be deployed on a site in the Baltic current which moves northward along the Swedish West Coast. Water from the Jutland current originating in the southern North Sea will most often be mixed into the Baltic current before the water reaches the buoy. Thus for warning purposes the data from the buoy is likely to be most useful for the northern part of the Swedish West Coast and the Southern coast of Norway. Ideally a buoy like the one presented should be part of an integrated network of buoys and other systems for monitoring the sea. There are several positions of interest for buoys in the area including one or two in the Jutland current.

3.2 Benefits with profiling systems

The most obvious benefit is of course the high vertical resolution of the data produced. Another advantage is that only one or two sets of sensors need to be purchased and calibrated. To obtain a vertical resolution of 5 m the traditional way in 50 m water depth would require 10 sets of sensors. Also biofouling is reduced because the profiler spends most of its time in the deep water where biofouling is much reduced compared to the productive zone. The system is also smaller and light which means that relatively small vessels can be used for service. All these factors result in increased cost efficiency.

3.3 Limitations with the presented system

A system like the one presented only monitors the total biomass of phytoplankton. Sensors discriminating between different groups, genera or species are not included. However, progress in optical oceanography as well as in molecular biological techniques for estimating biomass of HAB species may soon change this situation. In areas where cyanobacteria is a problem, e.g. the Baltic, sensors for phycocyanin fluorescence can be used to discriminate HABs from phytoplankton blooms in general. Other possibilities include *in situ* flow cytometers and microscopes for species or group recognition. It is of course also possible to mount sampling devices on the mooring but in this case samples must be collected and analysed in the laboratory.

Acknowledgements

This work is supported by the EU-funded project Forum Skagerrak II, Interreg IIIB North Sea and the Swedish Environmental Protection Agency. Bertil Håkansson and Henrik Lindh at SMHI and Sverker Skoglund at Ocean Origo AB have contributed to this paper.

References

Arneborg, L., C.P. Erlandsson, B. Liljebladh, and A. Stigebrandt (2004). The rate of inflow and mixing during deep-water renewal in a sill fjord. Limnol. Oceanogr., 49, 768–777.

Mills, D., R.W.P.M. Laane, J.M. Rees, M. Rutgers van der Loeff, J.M. Suylen, D.J. Pearce, D.B. Sivyer, C. Heins, K. Platt, and M. Rawlinson (2003). Smartbuoy: A marine environmental monitoring with a difference. In: H. Dahlin, N.C. Flemming, K. Nittis, and S.E. Petersson (eds), Building the European Capacity in Operational Oceanography, Proceedings of 3rd EuroGOOS Conference. Elsevier Oceanography Series. Elsevier, Amsterdam, pp. 311–316.

Recent developments in ocean forecasting at the Norwegian Meteorological Institute (met.no)

B. Hackett*, H. Engedahl and J. Albretsen

Norwegian Meteorological Institute (met.no)

Abstract

met.no offers a range of marine forecasting services based on a coupled model system, including operational models for the atmosphere, ocean circulation, waves, sea ice, ecosystem, drifting objects and oil spill fate. Development is carried out with the primary aim of improving the accuracy of forecasts out to +10 days. Priority areas of development are: increased spatial resolution, coupling to global ocean forecast data at open boundaries, coupling of process models, improving representation of freshwater runoff, better exploitation of observations in validation and assimilation, and ensemble forecasting.

Keywords: ocean forecasting, ocean modelling, maritime safety, marine environment

1. Introduction

The Norwegian Meteorological Institute (**met.no**) is tasked with the national responsibility for monitoring and forecasting meteorological and oceanographic phenomena that impact maritime activities in Norwegian waters. To this end, **met.no** maintains a suite of operational numerical forecasting models for the atmosphere, waves, ocean, sea-ice and marine ecosystem, in addition to a selection of operational satellite and *in situ* observations. Observational and forecast information is served to a broad range of public users, from expert maritime managers to the general public.

This paper offers first an overview of the ocean forecasting services at **met.no** and thereafter a description of the most important developments being pursued. The aim is to show how one small national forecasting agency approaches the challenge of serving prognostic oceanographic information to a broad range of maritime activities.

2. Ocean forecasting services

met.no's ocean services are focused on forecast times up to +10 days. They include three main types of service: daily forecasts of the "ocean weather", derived prognoses for drifting matter and daily forecasts of algal blooming in southern Norway. The numerical models and data streams involved are schematised in Figure 1.

2.1 "Ocean weather" forecasting

The backbone of the forecast system is the numerical weather prediction (NWP) models for Europe and the Arctic. The HIRLAM (hirlam.knmi.nl) code is run at 20 km resolution, using boundary conditions from the ECMWF; it provides 60 hour forecasts

* Corresponding author, email: Bruce.Hackett@met.no

four times daily. For high resolution applications, the Met Office's Unified Model (UM) and the MM5 model are run on nested local domains. The NWP models supply atmospheric forcing to the ocean models.

- For ocean waves, the WAM code is run on a 45 km grid for the northern seas, using boundary conditions from the ECMWF WAM, and a nested 8 km grid for the North Sea. Forecasts out to +60 h are issued twice daily.
- For storm surge water level, MI-POM, **met.no**'s version of the POM model (Blumberg and Mellor, 1987; Engedahl, 1995), is run in 3D homogeneous mode on a 20 km grid to forecast out to +60 hr.
- For ocean circulation (currents, temperature, salinity), the same model code is also run in 3D baroclinic mode on a suite of nested grids. A 4 km grid of the northern seas is standard ("Nordic4"), from which daily forecasts to +60 hours are issued. Monthly climatological data are used on the lateral boundaries.
- For Arctic sea ice forecasting, MI-POM is run in 3D baroclinic mode coupled with an ice model (MI-IM) on a 20 km grid of the northern seas and Arctic Ocean ("Arctic20"). ECMWF atmospheric forcing is used to give forecasts out to +240 hrs.

Data assimilation is used to a limited extent. For WAM, ENVISAT altimeter data are assimilated using a modified successive corrections scheme. The MI-POM circulation models assimilate SST and sea ice concentration from the EUMETSAT Ocean and Sea Ice Satellite Application Facility (OSI-SAF) using a nudging scheme (Albretsen and Burud, 2005).

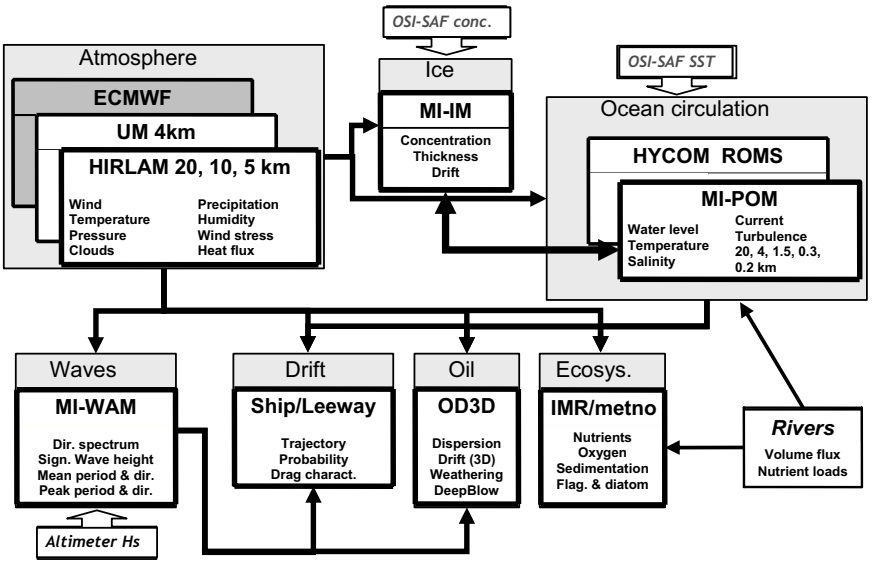

Figure 1 Schematic of the **met.no** operational model system for marine forecasting. Model codes, prognostic variables and resolutions are indicated. Arrows indicate coupling between models. Drift and Oil models are stand-by models; all others are run 1–4 times daily.

2.2 Support for maritime safety

met.no supports national services for maritime safety, specifically drifting objects, including ship drift and search and rescue (SAR), and oil spill combat. In both cases, **met.no** maintains standby models that are driven by the operational models for atmosphere, ocean circulation and waves.

- Drifting objects. The Leeway model, developed in cooperation with the U.S. Coast Guard, is applied to provide drift forecasts for a wide range of floating objects. Forecasts are run on demand using a web-based ordering and delivery system.
- Ship drift. A specific drift model for large vessels has been developed in cooperation with Det Norske Veritas. It is run at the request of the Norwegian Coastal Authority.
- Oil spill fate. A model for oil weathering, developed by SINTEF, is coupled to an advection-diffusion model to determine the fate of a marine oil spill. Forecasts are supplied on demand using a web-based ordering and delivery system.

For all the drift models, considerable effort has gone into selecting the best available forcing data from the suite of model data available.

2.3 Environmental monitoring

In cooperation with the Institute of Marine Research (IMR), MI-POM has been coupled to IMR's model for nutrients and algae (NORWECOM; Skogen, 1993). The coupled model system is run daily on a nested 20-4 km grid of the northern North Sea and Skagerrak ("Bio4") to give forecasts to +120 hrs. The forecasts are used primarily to predict algal blooms, but are also used in monitoring eutrophication indicators.

3. Current and future developments

3.1 Higher spatial resolution

met.no is continually moving models towards higher resolution grids. There are two reasons to do so:

1. The ocean mesoscale, as expressed by the Rossby radius of deformation, is of the order of 5–15 km in Norwegian waters. Baroclinic models need a grid spacing of a fraction of the deformation radius in order to replicate the mesoscale features, i.e., grids of 1–4 km are required.
2. Users of ocean forecasts are mostly near the coast, e.g., most SAR operations are within 5 km of the coast. The coast zone of Norway is extremely complicated, with thousands of islands and long, deep fjords. Resolving the coastal topography is a major challenge requiring model grids of even higher resolution than that dictated by the ocean mesoscale. A similar challenge is faced by NWP models confronted with steep and irregular terrain.

As a consequence, **met.no** is running pre-operationally MI-POM on a nested 1.5 km grid for the northern North Sea, together with a nested 300 m grid for the Oslofjord and a 200 m grid for the Bergen region. A primary aim is to provide fine-scale current forecasts for the heavily trafficked waters off southern Norway, especially recreational use (Oslofjord) and military use (Bergen region), see Figure 2.

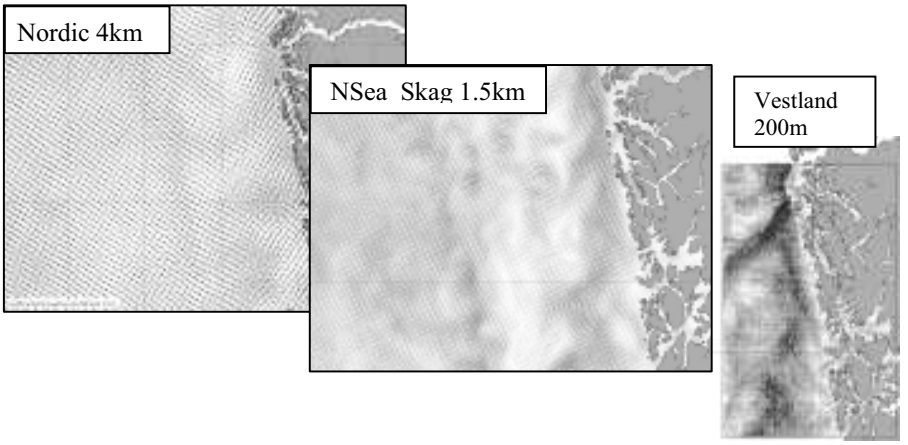

Figure 2 The effect of horizontal model resolution (grid spacing indicated) on current simulation off western Norway. The plots show current vectors, which are not legible, but the resultant shading effect shows the fine-scale current structure produced. Decreasing grid spacing yields more fine-scale structure as well as better definition of the complicated coastal topography. The two smaller models are nested into their neighbour to the left.

These shelf/coastal models will benefit from a suite of high-resolution NWP models, currently pre-operational, for forcing. The hydrostatic HIRLAM code is being run on grids of 10 and 5 km for Norway as candidate replacements for the current 20 km standard. The UM is being run non-hydrostatically on a 4 km grid, while the non-hydrostatic MM5 is run for air quality in the major urban areas. The ability of the non-hydrostatic models to replicate features like sea-breeze and orographic steering in fjords is particularly important for fine-scale coastal ocean models (Figure 3).

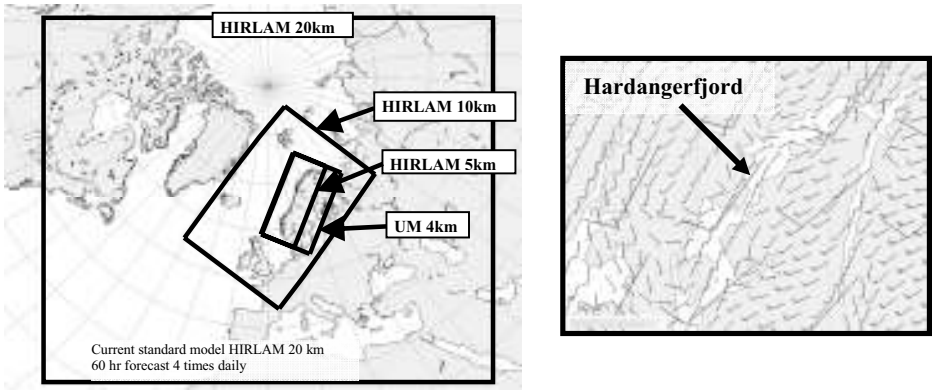

Figure 3 Left: NWP model grids currently run at **met.no** supplying forcing data to ocean models. ECMWF global model data are also used in some cases. Right: comparison of winds from HIRLAM 20 km (large wind vectors) and the nested UM 4 km (small wind vectors) for the Hardangerfjord near Bergen. Note that, over the fjord, the winds in the two models are oppositely directed (SSW for HIRLAM and NNE for UM). UM is run in non-hydrostatic mode.

3.2 Coupling to global ocean forecasts

There is also user interest for the deep ocean in Norwegian waters. In particular, the offshore industry is moving to exploration and production beyond the continental shelf, at depths in excess of 400 m. Currents along the Norwegian continental slope are strong and only partly influenced by local forcing. **met.no**'s local models have validated poorly for volume transport in the Norwegian Atlantic Current, which is very sensitive to specified lateral boundary conditions. In addition to currents, interannual variability in temperature and salinity has been lacking due to the use of climatological boundary conditions. Obtaining boundary data from assimilating global ocean models has been identified as a promising solution to these shortcomings. As part of the Mersea Strand 1 project (www.nersc.no/~mersea/), operational boundary forcing data from the Met Office FOAM model (Bell *et al.*, 2000) have been tested with a NI-POM/NORWECOM of the North Sea, giving daily forecasts to +108 hrs since 2003 (Figure 4). This operation continues in the Mersea Integrated Project (www.ifremer.fr/merseaip/), supplemented with a parallel run using data from the TOPAZ model (topaz.nersc.no/index.html); similar use of data from the Mercator system (www.mercator-ocean.fr/), including biochemical and sea ice variables, is also planned.

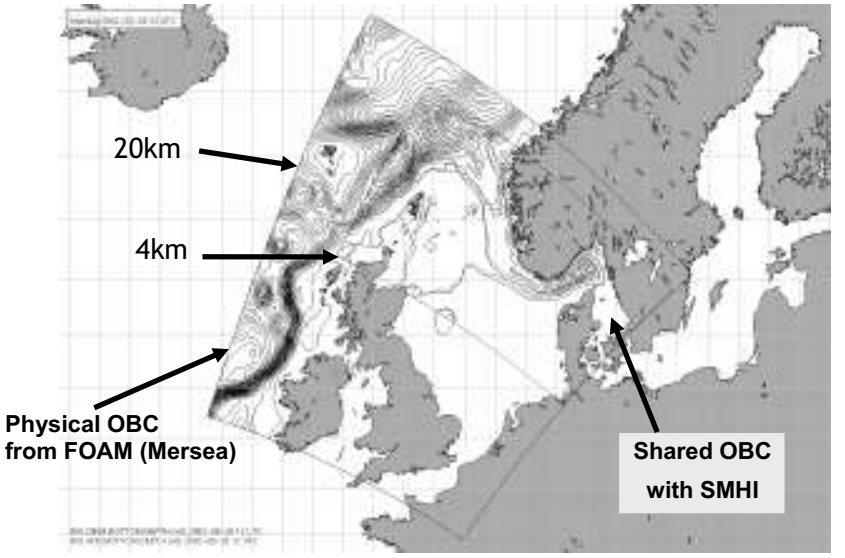

Figure 4 Use of lateral boundary data in test versions of the **met.no**/IMR ecosystem forecast model. The model system is a nested 20-4 km grid, run daily. Physical open boundary condition data at the open ocean boundary are supplied by the Met Office FOAM 1/9 North Atlantic model. For the exchange between the Baltic and North Sea, model data on a subgrid covering the Kattegat are traded between **met.no** and SMHI, both for physical and biochemical parameters.

Complementing the global ocean data applied at the open ocean boundaries is the interface to the Baltic, which is not modelled explicitly at **met.no**. A solution in which model data in the Kattegat are exchanged between **met.no** and SMHI (Sweden) has been under testing in daily routine since 2003 (Figure 4).

3.3 Coupling of models

The aim of fully coupling models for marine geophysics is to improve the representation of the processes at the interfaces between those models, specifically the fluxes at the air-sea-ice interfaces, and thereby improve forecast accuracy. Much of this development has been carried out in climate modelling studies (see for example RegClim, regclim.met.no/index_en.html), but adaptations to medium-range forecasting are required. The coupled hydrodynamic/ice model MI-POM/MI-IM has been in pre-operational service since 2003, running on the 20 km grid of northern waters. The coupled model is now being tested for fine-scale application (4 km grid) looking toward implementation in the Nordic4 model.

The next step is establishing a fully parallelised, relocatable coupled system consisting of hydrodynamics (MI-POM), sea ice (MI-IM) and ecosystem (NORWECOM), to be completed in 2005.

Implementation of coupled atmosphere and ocean models for operational forecasting is a further aim, but is being approached piecemeal. Tests carried with a coupled NWP/wave model (ECMWF/WAM) to calculate the momentum flux to MI-POM have shown an improvement in forecast skill for storm surge (Sætra *et al.*, 2005). Prognostic currents from MI-POM have been implemented in WAM (one-way coupling) in order to improve wave forecasts used in ship routing applications (Mersea IP activity). A coupled atmosphere/ocean/ice model system has been developed for climate studies, and will serve as the methodology for coupling arbitrary component models in a future forecasting system.

3.4 Freshwater runoff

With ever greater focus on coastal and ecosystem processes, the role of freshwater runoff has become more important for medium range forecasting. The current operational practise is to use monthly climatological values of volume flux and "typical" values of nutrient loads. Recent efforts have gone into assessing the sensitivity of the Skagerrak hydrodynamics to runoff (Albretsen and Røed, 2005) and obtaining near-real-time observations of volume fluxes from the major Norwegian rivers. Complementing this, **met.no** has initiated a survey of potentially operational river data within the Northwest Shelf Operational Oceanography System (NOOS; www.noos.cc). The ultimate aim of this effort is to obtain near-real-time observations of freshwater fluxes to the model domains, along with observations/estimates of nutrient loads and prognostic values from hydrological models.

3.5 Validation and assimilation

The utilisation of observations, both for validation of and assimilation in operational ocean models, has been weak at **met.no**. This is partly due to the sparseness of real-time observations in the shelf/coastal zone which is the main focus. A number of validation studies have been carried out in hindcast, but only recently have daily updated validation products been implemented. The latter are considered a vital tool for improving forecast skill. A performance evaluation programme has been started in which validation products will be implemented for key forecast parameters and assessment meetings are held bi-annually.

Developments in assimilation include:

1. implementing estimates of swell spectra from synthetic aperture radar in WAM
2. replacing nudging of OSI-SAF SST and sea ice concentration data in MI-POM/MI-IM with a multivariate error sub-space Kalman filter scheme (Albretsen and Burud, 2005)
3. preparing for imminent observing systems such as gliders, shallow water ARGO and HF coastal radar.

3.6 Ensemble forecasting

A recurring criticism of ocean forecast products is the lack of error bars. NWP is attempting to meet the same type of criticism through ensemble forecasts, where the spread of the ensemble is interpreted as a measure of uncertainty. This appears to be a fruitful approach also for a number of ocean forecast products. At **met.no**, products from the ECMWF Ensemble Prediction System (EPS) are routinely used for marine weather forecasting and for wave forecasting. A more recent initiative is downscaling the EPS atmospheric fields for the Norwegian area to provide more spatial detail. Building on this, the oceanography group have used the downscaled fields to run an ensemble of storm surge forecasts (Figure 5). The ensemble forecasts are currently under assessment, but are expected to become an important tool for water level forecasting. In addition, the system will pave the way for other ocean parameters, such as wave height, surface currents and algal blooming.

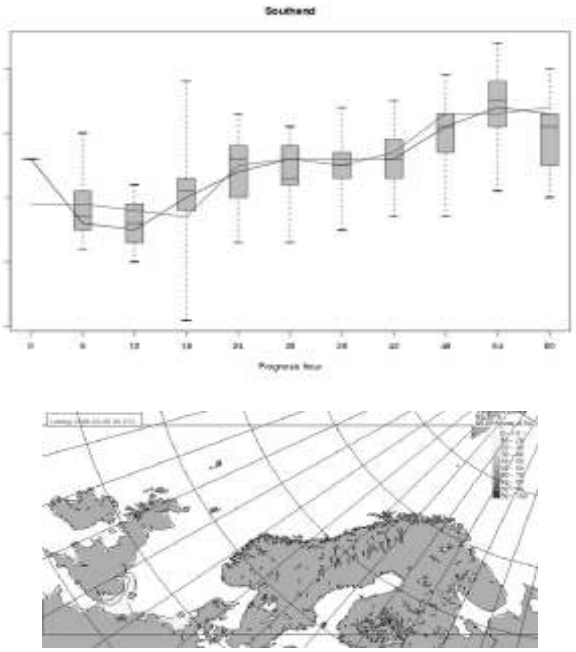

Figure 5 Example of ensemble water level forecast. Top: time series for Southend, where box-and-whisker plots represent the spread of the ensemble members, and the solid lines show the control member and operational prognosis; horizontal axis is prognosis time, vertical axis is sea

level anomaly. Bottom: field representation showing probability for exceeding 0.5 m water level at forecast time +60 hrs; note region of higher probability off SE England.

References

Albretsen, J. and I. Burud (2005). Assimilation of sea surface temperature and sea ice concentration in a coupled sea ice and ocean model. This volume, page 661.

Albretsen, J. and L.P. Røed (2005). Sensitivity of Skagerrak dynamics to freshwater discharges: insight from a numerical model. This volume, page 771.

Bell, M.J., R.M. Forbes and A. Hines (2000). Assessment of the FOAM global data assimilation system for real-time operational ocean forecasting. J. Mar. Sys., 25, 1–22.

Blumberg, A.F., and G.L. Mellor (1987). A description of a three-dimensional coastal ocean circulation model. In: Three-Dimensional Coastal Ocean Models, ed. N.S. Heaps, AGU Coastal and Estuarine Ser., 4, American Geophysical Union, Washington D.C.

Engedahl, H., (1995). Implementation of the Princeton Ocean Model (POM/ECOM3D) at the Norwegian Meteorological Institute (DNMI). Research Rep. No. 5, Norwegian Meteorological Institute, Oslo, Norway, 40 pp.

Skogen, M., (1993). A User's Guide to NORWECOM, The Norwegian Ecological Model System. Report No. 6, Institute of Marine Research, Bergen, Norway.

Sætra, Ø., J. Albretsen and P. Janssen (2005). Sea state dependent momentum fluxes for ocean modelling. In preparation.

Can Operational Oceanography support decision-making in the coastal zones?

F.M. Santoro*[1] and J.H. Stel[2]

[1]*Interdepartmental Centre IDEAS, University Ca' Foscari of Venice, Italy*
[2]*International Centre for Integrative Studies, University Maastricht, The Netherlands*

Abstract

The coastal zone is the place of the highest ecosystem goods and services (Costanza *et al.*, 1997). Coastal zones are under threat from both natural and anthropogenic forcing which limit the capacity of these ecosystems to support the coastal goods and services. There is an urgent need for a better understanding of natural and human induced processes to develop and underpin informed decision-making in the coastal zones. This will involve insights and know-how from a multitude of decision-makers and disciplines. Various countries have signed a large number of international and multinational agreements calling for safety at sea and sustainable use and management of marine resources. To respond to this call we have to monitor and forecast processes and changes in the ocean space. This is the rapidly emerging field of operational oceanography. Integration of *in situ* data and observation from space together with advanced modelling should serve as input to a decision support system that can be used for scenario development and as a management tool for coastal development. It goes without saying that stakeholders and end-users should be involved in the design process of these systems.

This paper presents the preliminary results of a questionnaire sent to relevant stakeholders to investigate the role of operational oceanography in the decision-making process of the coastal zones.

Keywords: Operational oceanography, decision-making, decision support system, participatory processes, coastal zones, integrated coastal management.

1. Introduction

The coastal areas are among the most important and productive environments; they support the production of goods and services with an estimated value of 12.5 trillion USD per year (Costanza *et al.*, 1997). The capacity of these systems to support the goods and services is declining because of a variety of phenomena inducing changes in characteristics and processes typical of these ecosystems. Although the phenomena of interest tend to be local in scale, they are globally ubiquitous with a pattern that suggests they are, more often than not, local expressions of larger scale forcing of natural origin, anthropogenic origin, or both (UNESCO, 2003).

The driving forces that are the principal causes of these changes are, in the coastal zones, mainly related to the multiple and, often conflicting activities that can take place along the world coastlines.

* Corresponding author, email: fsantoro@unive.it

In this context we definitely need to monitor and observe the system in order to achieve a better understanding of processes, changes and possible cause-effect relationships at the origin of the changes. The capability of managing the coastal areas in an integrated manner and the goal of sustainable use of the oceans and coastal resources depend crucially on the scientific knowledge of the marine system variability, particularly on our capability to forecast at the relevant space and NRT (near real time) scales. (Zodiatis *et al.*, 2003).

2. Decision-making in the coastal zones

There is a necessary chain of logical transformations to support decision-makers and policy-makers, as well as all the relevant actors involved in the management of coastal zones, to produce better informed decision-making especially when dealing with complex systems and issues like those present in the coastal zones environments.

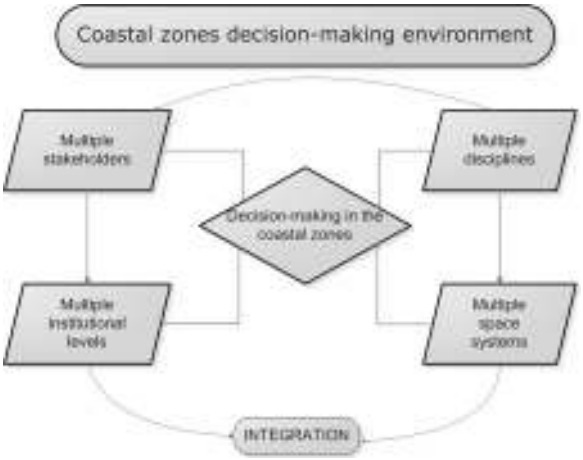

Figure 1 The decision-making environment in the coastal zones.

There is still a gap between the collection of data and the use of them; the question is how to translate the results of modelling and observing systems in a way that decision-makers and policy-makers could understand. One powerful tool is offered by a category of computerised systems called Decision Support Systems (DSS). Traditionally models have been developed for just one discipline or for just one topic, but the main aim of DSS is to have a tool able to integrate different models and different analytical and visual tools and to offer users the possibility of exploring effects and impacts of different strategies and policies.

The elements of a DSS are basically the data and the knowledge base, which contains all the data to be input in the inference engine, and the inference engine itself which can have an integration of multiple disciplines models, able to produce a number of indicators, criteria and alternatives. For example a coastal management problem would use indicators such as population growth, land-base pollution, and waste water treatment levels. The system would develop alternatives or scenarios and also through the use of

evaluation techniques, would enable users to evaluate alternatives according to the criteria produced during the inference phase.

Despite great effort over the last few years for developing several examples of DSS, and in particular for coastal and river management, there are few examples of the use of these systems in reality. There are many reasons for this lack of success of decision support systems. One reason could be that the users find the system too detailed, time consuming and costly to use. Other reasons are related to the general complexity of the systems, while still other reasons are related to the uncertainty of the model output and on the appropriateness for solving the decision question. Many authors state that the limited involvement of users in the development phase can lead to unsuccessful DSS (Uran and Janssen, 2003).

One simple answer to these questions is that the developers of a DSS should involve the users in the first phases of the process. It is of fundamental importance that the different stakeholders are able to participate and interact with the developers and among themselves to have a precise idea of the real needs and the responses required from such a system.

3. Participatory processes

Participatory processes are increasingly seen as one of the most effective ways to achieve the goal of a rational and sustainable management of natural resources. For example, within Agenda 21, it is asserted, "one of the fundamental prerequisites for the achievement of sustainable development is broad public participation in decision-making" (UNCED, 1992).

3.1 The Integrated Coastal Zone Management questionnaire

Among the most widely used methods for stakeholder consultation are questionnaires. In this paper we present some preliminary results from a questionnaire developed for a wide consultation of potential users of marine monitoring and forecasting systems, mainly to investigate the potential links between those systems and the coastal zone management process. The questionnaire is available on-line (www.santoro.free.fr/questionnaire/questionnaire.html) and has been sent to different categories of stakeholders.

These categories encompass environmental protection agencies, port authorities, governmental institutions at local, national and international levels, as well as universities and research institutes.

The questionnaire is composed of four different sections:

1. general information of the respondent
2. coastal issues, with questions on the most important environmental problems, economic activities and governance issues in the coastal zones
3. monitoring and forecasting systems, to investigate which are the most important needs of these potential users paying particular attention to the most important parameters to monitor and forecast.
4. decision-making processes in the coastal zones, to identify the role of numerical modelling and *in situ* measurements for the coastal zone planning process as well as

the link between the dissemination and the communication of data and results coming from operational oceanography systems on the involvement of end-users and potential stakeholders.

Figure 2 The ICZM questionnaire (http://www.santoro.free.fr/questionnaire/questionnaire.html).

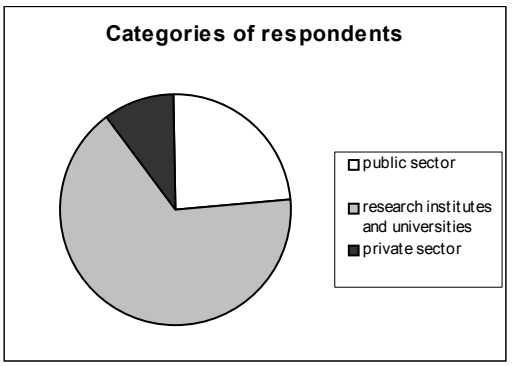

Figure 3 The percentages of different categories of respondents (52 responses in total).

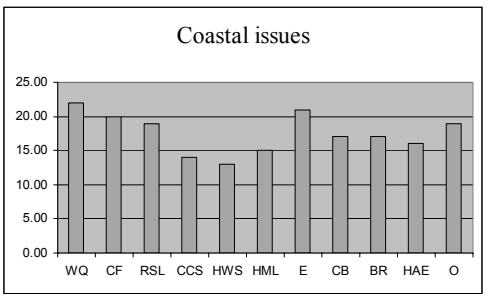

Figure 4 The most important coastal environmental issues according to the results of the questionnaire. WQ: Sea state, CF: Coastal flooding, RSL: Rising Sea Level, CCS: Chemical contamination of seafood, HWS: Human pathogens in water and shellfish, HML: Habitat modification and loss, E: Eutrophication, CB: Changes in species biodiversity, BR: Biological responses to pollutants, HAE: Harmful algal events, O: Overexploitation of fish stocks.

Some preliminary results of the questionnaire are shown in Figure 4. The answers requiring a ranking exercise have been processed using the Borda method, for each person's rankings, the Borda function awards n–1 points to the highest ranked alternative, n–2 points to the next highest ranked alternative, and so on, where n represents the number of alternatives under consideration. The coastal issues for the graph in Figure 4 represent the alternatives. From the answers already analysed the most important coastal issues are water quality and eutrophication.

The most frequently mentioned parameters to monitor are sea level, temperature, primary production and particulate carbon and nitrogen.

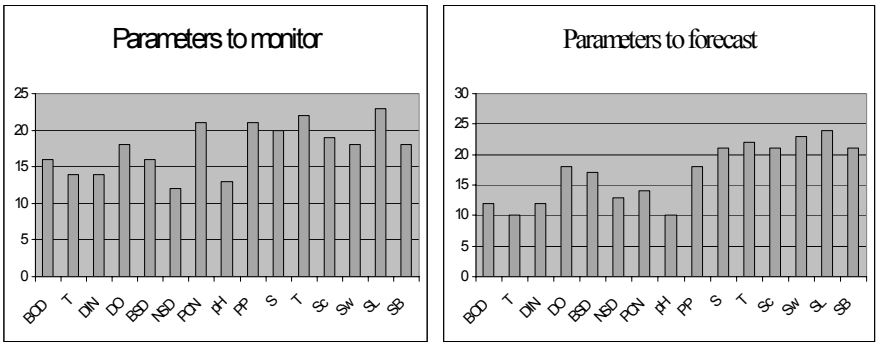

Figure 5 A rank of the most important parameters to monitor and forecast according to the results of the questionnaire. BOD: biological oxygen demand, T: transparency, DIN: dissolved inorganic nutrients, DO: dissolved oxygen, BSD: benthic species diversity, NSD: nekton species diversity, PCN: particulate organic carbon and nitrogen, pH: pH, PP: primary production, S: salinity, T: temperature, Sc: surface currents, Sw: surface waves, SL: sea level, Sb: sediment budget.

The most frequently mentioned parameters to forecast are sea level, sea waves, temperature and salinity.

4. Conclusions and future developments

A reliable knowledge of natural and human-induced changes in the coastal zones for decision-makers is of paramount importance due to the emergence of risks and environmental problems in these areas. Operational oceanography can offer an important contribution to the development of a more knowledge-based decision-making. Tools like decision and planning support systems can be very powerful in finding a way to translate the observed and modelled data into useful information for all the relevant coastal stakeholders.

Public participation processes are one of the possible ways for creating this missing link between scientists and the possible end-users of operational oceanography products.

The questionnaire presented in this paper is an example of these kinds of processes. The results will be used for identifying the most important issues for different stakeholders and to design a decision support system able to respond to their needs.

Acknowledgements

Part of this work was done during a Marie Curie fellowship in ICIS in the context of the SENSE Research Network.

We would also like to thank Nadia Pinardi and Sergio Castellari for their support, and Mita Patel and Bas Amelung for reviewing the contents of the questionnaire.

References

Antunes, P. and R. Santos (1999). Integrated environmental management of the oceans, Ecological Economics 31: 215–226.

Boesch, D.F. (1999). The role of science in ocean governance, Ecological Economics 31: 189–198.

Buanes, A., S. Jentoft, *et al.* (2004). In whose interest? An exploratory analysis of stakeholders in Norwegian coastal zone planning, Ocean & Coastal Management 47: 207–233.

Costanza, R., F. Andrade, *et al.* (1999). Ecological Economics and sustainable governance of the oceans, Ecological Economics 31: 171–187.

Costanza, R., R. d'Arge, *et al.* (1997). The value of the world's ecosystem services and natural capital, Nature 387: 253–260.

Davos, C.A. (1999). On determining the social relevance of oceanography, Progress in Oceanography 44: 457–468.

Edwards, S.D., P.J.S. Jones, *et al.* (1997). Participation in coastal zone management initiatives: a review and analysis of examples from the UK, Ocean & Coastal Management 36: 143–165.

Fabbri, K.P. (1998). A methodology for supporting decision making for integrated coastal zone management, Ocean & Coastal Management 39: 51–62.

Fedra, K. and E. Feoli (1998). GIS technology and spatial analysis in the coastal zone management, EEZ Technology Ed.3: 171–179.

UNESCO (2003). The Integrated Strategic Design Plan for Coastal Ocean Observation Module of the Global Ocean Observing System. GOOS Report No 125, IOC Information Document Series No 1183.

Uran, O. and Janssen, R. (2003). Why are spatial decision support systems not used? Some experiences from the Netherlands, Computer, Environments and Urban Systems 27: 511–526.

Zodiatis, G., R. Lardner, G. Georgiou, E. Demirov, N. Pinardi and G. Manzella (2003). The Cyprus Coastal Ocean Forecasting System, Sea Technology 44: 10–16.

Limited area weather forecasting for the MFSTEP activities: sensitivity and performance analysis

G. Kallos*[1], I. Pytharoulis[1], P. Katsafados[1], P. Louka[1] and G. Galanis[2]

[1]*University of Athens, School of Physics, Atmospheric Modelling and Weather Forecasting Group, Greece*
[2]*Naval Academy of Greece, Section of Mathematics, Greece*

Abstract

The Atmospheric Modelling and Weather Forecasting Group (AM&WFG) operates the SKIRON/Eta system for the Mediterranean Region at mesoscale resolution and forecasting horizon of five days for the purpose of the MFSTEP project. The predicted fields are used to drive various resolutions of oceanographic and wave model configurations operated at various institutes. The system has been in operational use since January 2003 by utilising GFS global analysis and forecasts on daily basis, while for the operational needs of MFSTEP it utilised Météo-France data. Additionally, series of sensitivity tests with various sets of SSTs and evaluation procedures have been carried out. It is concluded that the atmosphere does not always respond to spatial resolution of SSTs in a significant way. The evaluation procedures showed that the system is consistent in its basic characteristics and the forecast skill maintenance throughout the forecasts is remarkable.

Keywords: nonhydrostatic SKIRON/Eta, MFSTEP, SST, bias, RMSE, statistical analysis

1. Introduction

Limited area weather forecasting is necessary for a large number of applications in research and operational mode. The NWP outputs are commonly implemented off-line in a wide range of modelling systems, such as photochemical models, ocean general circulation models and wave models. The usual forecast horizon of these products is up to three days and their skill ranges between 80−90%. Nowadays, there is a requirement for accurate predictions that maintain their skill for periods longer than 3 days.

In the framework of the EU MFSTEP (Mediterranean Forecasting System: Toward Environmental Predictions) project, the two well-known regional atmospheric models SKIRON/Eta and Aladin are integrated operationally in the Mediterranean region providing 5-day weather forecasts. A number of model outputs are disseminated to the ocean modellers at high spatiotemporal resolution in order to force their regional, shelf and wave models. The role of AM&WFG is: a) to provide atmospheric forecast and hindcast fields to various ocean, wave and mesoscale atmospheric models by utilising the SKIRON/Eta modelling system and b) to perform a series of sensitivity experiments.

The atmospheric model forecasts usually contain errors which are associated with factors such as the model resolution and the initial conditions. The horizontal resolution is a

* Corresponding author, email: kallos@mg.uoa.gr http://forecast.uoa.gr

crucial parameter in areas with high variability in the physiographic characteristics (Mass *et al.*, 2002) such as the Mediterranean region. High horizontal resolution of about 10 km was employed by the regional atmospheric models during MFSTEP.

The initial conditions and particularly the SSTs exert a significant influence on medium-range and seasonal atmospheric forecasts (e.g. Pytharoulis, 1999; Katsafados *et al.*, 2005). Certainly, one must bear in mind that convection is very insensitive to changing SSTs in the absence of large-scale flow (Tompkins and Craig, 1999). Future work needs to focus on the Mediterranean region in order to understand the effects of SSTs on atmospheric forecasts in the basin.

The aims of this paper are to describe the configuration and the performance of the SKIRON/Eta modelling system and to study its sensitivity to changes in the SST field. Section 2 will present the characteristics and the setup of SKIRON/Eta, while the performance of the model and its sensitivity to SSTs will be investigated in section 3.

2. SKIRON/Eta modelling system

The SKIRON/Eta modelling system has been developed for operational use by the AM&WFG. It consists of various modules for pre- and post-processing together with a version of the model appropriately coded to run on any parallel computer platform utilizing any number of processors. The SKIRON/Eta system is based on the Eta/NCEP model (Janjic, 1994). A detailed description of its characteristics and configurations can be found in Kallos (1997) and Papadopoulos *et al.* (2002).

SKIRON/Eta is a full physics atmospheric model with several unique capabilities that make it appropriate for regional/mesoscale simulations in regions with varying physiographic characteristics. It has the unique capability to use the "step-mountain" Eta vertical coordinate and it includes the option to use nonhydrostatic dynamics. The nonhydrostatic model appears to be computationally robust at all resolutions and efficient in NWP applications (Janjic *et al.*, 2001). Sophisticated parametrisations are utilised in order to represent the various physical processes such as radiation, convection, grid-scale precipitation and clouds, boundary layer and soil processes.

The hydrostatic version of the system has been successfully used operationally in the University of Athens since 1997. It has also been successfully applied to a large number of different regions and for long forecasting periods (e.g. Papadopoulos *et al.*, 2002; Katsafados *et al.*, 2005). The nonhydrostatic SKIRON/Eta has been in operational use since January 2003 utilising NCEP/GFS global analyses and forecasts at a resolution of 1°×1° on a daily basis and producing 5-day forecasts (http://forecast.uoa.gr). In the framework of MFSTEP, the analyses and 3-hourly forecasts of the ARPEGE model (Météo-France) at a resolution of 0.25°×0.25° are used to drive the system (http://forecast.uoa.gr/mfstep).

Finally, the model domain covers the entire Mediterranean region with a horizontal increment of 0.1°×0.1° (Figure 1), while 38 Eta levels are used in the vertical. The computational domain was chosen through sensitivity experiments taking into account the computer time which is a key parameter in operational operations.

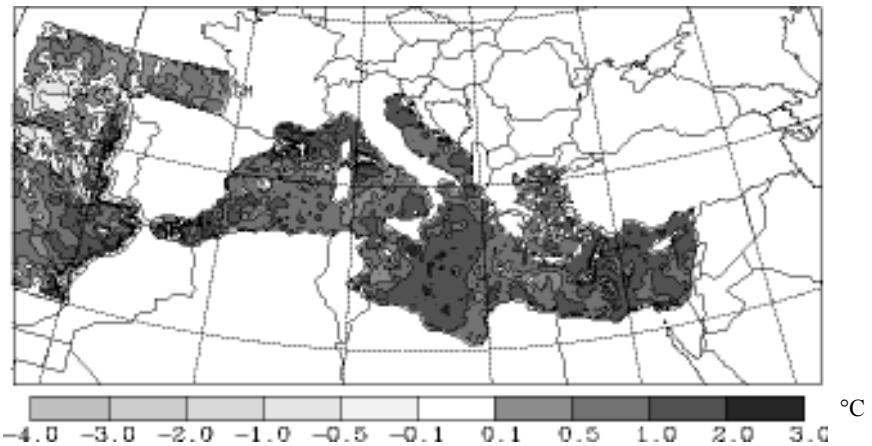

Figure 1 Horizontal plot of the difference between the high-resolution (1/16°×1/16°) and the NCEP (0.5°×0.5°) SSTs on the SKIRON/Eta grid on 13 October 2004. Units: °C. Dark shading corresponds to positive differences.

3. Sensitivity to SSTs and performance analysis

The sensitivity of the atmospheric forecasts on SSTs and the model performance were investigated through a series of experiments with different SSTs. The two datasets which are utilised in this study became available by NCEP and CNR-Rome for the 8-month period June 2004–January 2005. The long period of data allowed their intercomparison and the performance of simulations under various meteorological conditions.

The SKIRON/Eta modelling system operationally uses the daily global NCEP SSTs at a resolution of 0.5°×0.5°. Thiebaux *et al.* (2003) showed that the use of the high resolution SSTs by the ETA model resulted to improved forecasts of storm track and precipitation over Eastern US. A high-resolution satellite SST dataset is produced operationally by CNR-Rome and it became available in order to be implemented in SKIRON/Eta. The horizontal resolution of this dataset is 1/16°×1/16° (longitude-latitude), while its domain extends from 18.125°W to 36.25°E and from 30.25°N to 46°N. These SSTs were expected to represent the spatial variability of the sea-surface temperatures in the Mediterranean Sea more accurately than the 0.5°×0.5° NCEP SSTs.

3.1 SST intercomparison

The SST intercomparison was performed on a common grid using monthly mean fields and well-known statistical tests. Both SSTs were interpolated into the 0.1°×0.1° E-grid of the operational SKIRON/Eta domain and the statistical methods were applied on the grid-points at which both datasets were valid. A total of 15556 sea grid-points were used.

The two datasets generally exhibited small differences in the Mediterranean sea with values less than 0.5°C (Table 1). The high-resolution satellite dataset provided colder SSTs than the NCEP set in June, July, December 2004 and January 2005, while warmer values were estimated from August to November 2004. Larger differences appeared only locally and they were mainly located close to the coastline, probably due to the fact that the high-resolution set could better resolve local features. Examination of mean monthly

charts of absolute SST difference showed that the differences were generally smaller than 0.8–1°C, while their area-average value did not exceed 0.6°C (Table 1). Also, the two datasets exhibited significant similarities in their monthly variability. Table 1 shows that the difference in the monthly mean standard deviation between the two SSTs was less than 0.1°C.

Table 1 The monthly mean differences, absolute differences and standard deviation of the high-resolution and the NCEP SSTs from June 2004 to January 2005, averaged over the SKIRON/Eta grid-points that were valid for both datasets. Positive differences indicate warmer SSTs in the high-resolution satellite dataset. Units: °C.

Month	Days with valid data	Mean Difference	Mean Absolute Difference	Mean Standard Deviation	High-resolution NCEP
Jun 2004	29	–0.333	0.587	1.394	1.313
Jul 2004	29	–0.222	0.566	0.777	0.753
Aug 2004	31	0.029	0.489	0.626	0.556
Sep 2004	28	0.097	0.504	0.641	0.697
Oct 2004	30	0.336	0.552	0.71	0.729
Nov 2004	28	0.242	0.54	1.089	1.047
Dec 2004	31	–0.167	0.388	0.654	0.637
Jan 2005	31	–0.13	0.375	0.499	0.536

3.2 Experimental setup

The SST intercomparison and day-by-day analysis showed that the high-resolution and the NCEP SSTs do not differ significantly. A limited number of days with significant differences were identified and they were selected for sensitivity experiments.

The main criteria for selecting these cases were the existence of important SST differences between the two datasets and the occurrence of significant weather in the basin. Following these criteria, seven cases were chosen with positive and negative anomalies appearing between the two sets. The initial time (and the duration) of these runs was at 0000 UTC on 14/07/04 (120 hrs), 21/07/04 (120 hrs), 13/10/04 (72 hrs), 03/11/04 (72 hrs), 17/11/04 (120 hrs), 05/01/05 (120 hrs) and 19/01/05 (120 hrs). The weather conditions during these periods covered the typical weather types that prevail in the Mediterranean basin from June to January.

Two simulations were performed for each selected case. In the one run the model was integrated using the NCEP SSTs. In the other run, the model utilised the high-resolution SSTs, with the NCEP SSTs being used in data void regions. This is necessary because the NWP models require full meteorological fields in the initial conditions. Subjective analysis and special algorithms did not allow the use of cases with unrealistically sharp gradients in regions where both datasets were used. In all other aspects the two simulations were identical and their only difference was the SSTs. ARPEGE analyses and forecasts were used as initial and lateral boundary conditions, respectively.

3.3 Case study

A frontal zone was located over western Greece on 13–14 October 2004 and it was associated with heavy rain, thunderstorm activity and strong winds. In this period the

high-resolution SSTs were up to about 1.5°C warmer than the NCEP ones in the region west of Greece (Figure 1).

The forecasts at selected meteorological stations of western Greece that were affected by the frontal zone (Corfu and Aktio) were analysed. The outputs of the two simulations were similar in most aspects and significant differences appeared in the precipitation. The use of different SSTs induced spatiotemporal differences in the distribution of precipitation in the basin (Figure 2) due to modulation of the transition speed of the rainbands, with the precipitation amounts remaining nearly the same. However, the case study did not indicate any clear improvement due to the use of the high-resolution SSTs.

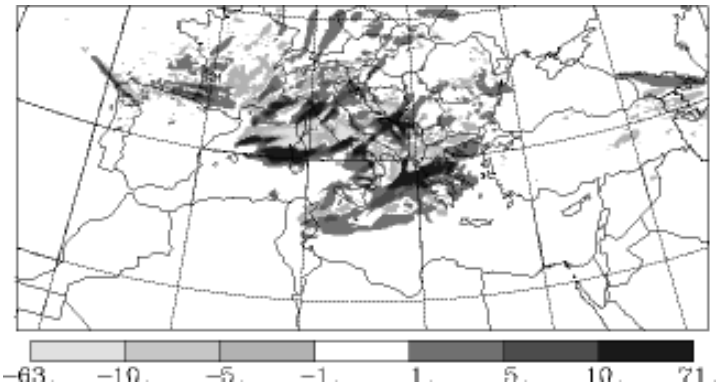

Figure 2 The differences of the 72-hour accumulated precipitation (mm) between the runs with the high-resolution and the NCEP SSTs. Initial time at 0000 UTC 13 October 2004. Dark shading corresponds to positive differences.

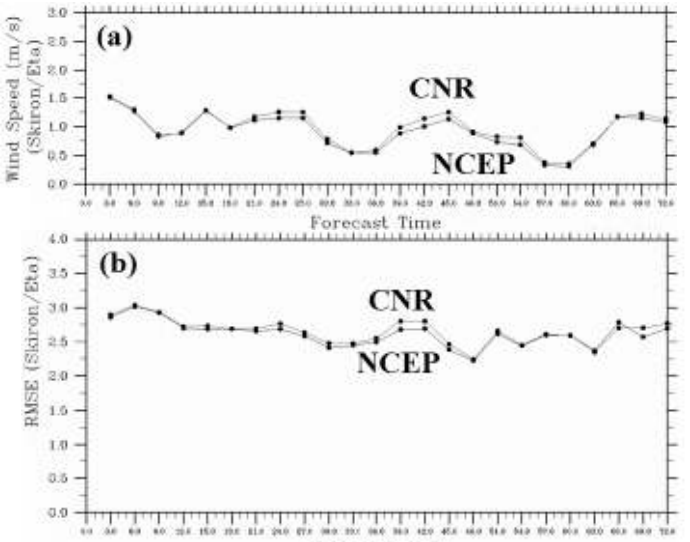

Figure 3 a) Bias and b) RMSE scores of the 10 m wind speed versus forecast time for the runs forced by NCEP SSTs and high-resolution SSTs (CNR).

3.4 Statistical analysis

The assessment of the influence of the high-resolution SSTs on limited area forecasting in the Mediterranean was investigated further through statistical analysis. In this task the maximum available near-shore surface observations (METAR and SYNOP) were used.

Bias and root mean square errors (RMSE) of 10 m wind speed (Figure 3) and 2 m air temperature (Figure 4) indicated that the changes in the lower boundary forcing did not significantly affect the forecasting capabilities of the model. A slight difference between the two runs was mainly detected on the second day of the simulations (Figure 3), but it did not exceed 0.25 ms^{-1}. In general, the model output showed an overestimation of the 10 m wind speed with the RMSE varying between 2.2 and 3 ms^{-1}. Regarding the 2 m air temperature, an improvement in both bias and RMSE scores appeared in the simulations with the high-resolution SSTs (Figure 4). The reduction of RMSE was systematic affecting the whole period of forecast (72 hours). In both sets of experiments, there is a slight underestimation (overestimation) of the maximum (minimum) 2 m temperature. However, the most interesting result of the statistical analysis is the significant consistency of bias and RMSE for the whole 72-hour forecast period.

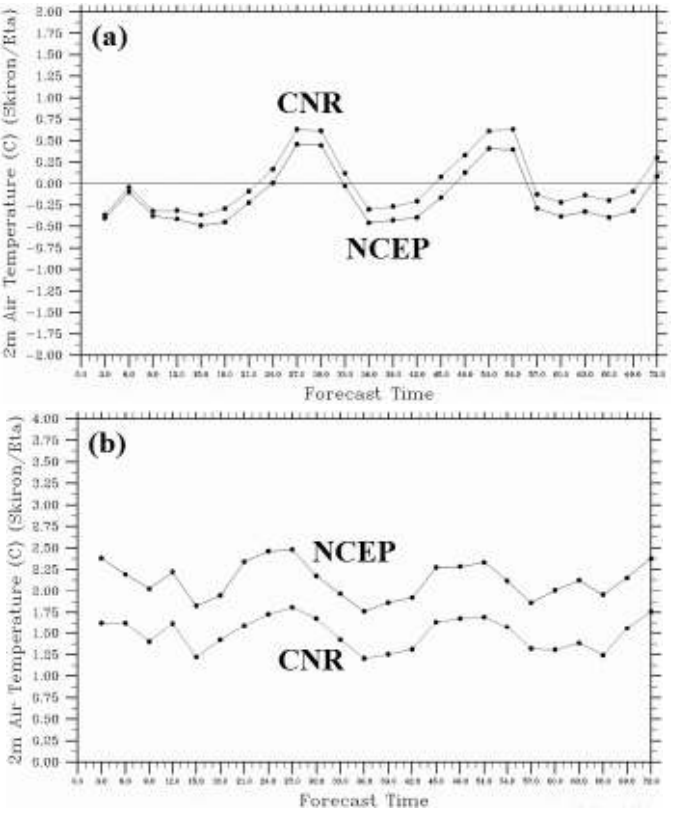

Figure 4 a) Bias and b) RMSE scores of the 2 m air temperature versus forecast time for the runs forced by NCEP SSTs and high-resolution SSTs (CNR).

Finally, the statistical analysis of the 6-hour accumulated precipitation showed that in the selected stations the predicted precipitation is generally not strongly influenced by the SSTs. However, a rather important sensitivity was indicated in the intense precipitation events with rates stronger than 16 mm per 6 hours (not shown).

4. Conclusions

The AM&WFG provides high-resolution limited area weather forecasts and hindcasts to various ocean and atmospheric models by utilising the SKIRON/Eta system. The short to medium range forecasts are sensitive, in local scales, to changes in the underlying SSTs in the presence of significant weather. The prediction skill did not always seem to improve due to the use of high-resolution satellite SSTs. The impact of the high-resolution SST forcing in SKIRON/Eta appears to be more pronounced in the 2 m air temperature and negligible in the 10 m wind speed. Regarding the precipitation, there are spatiotemporal differences in its distribution due to the use of the CNR and NCEP SSTs, but the amounts remain nearly the same. Finally, it is very important to note that the SKIRON/Eta forecast skill was maintained throughout the runs.

Acknowledgements

We would like to thank Dr. R. Santoleri for providing the high-resolution satellite SSTs. This study was funded by the EU project MFSTEP (Contract: EVK3−CT−2002−00075).

References

Janjic, Z.I. (1994). The step-mountain Eta Coordinate Model: Further Developments of the Convection, Viscous Sublayer and Turbulence Closure Schemes. Mon.Wea.Rev., 122, 927−945.

Janjic, Z.I., J.P. Gerrity and S. Nickovic (2001). An alternative approach to nonhydrostatic modelling. Mon.Wea.Rev., 129, 1164−129.

Kallos, G. (1997). The regional weather forecasting system SKIRON. Proceedings of the Symposium on Regional Weather Prediction on Parallel Computer Environments, 15−17 October 1997, Athens, Greece.

Katsafados, P., A. Paparopoulos and G. Kallos (2005). Regional atmospheric response to tropical Pacific SST perturbations. GRL, 32, L04806.

Mass, C.F., D. Ovens, K. Westrick and B.A. Colle (2002). Does increasing horizontal resolution produce more skilful forecasts? Bull. Amer. Meteor. Soc., 83, 407−430.

Papadopoulos, A., G. Kallos, P. Katsafados and S. Nickovic (2002). The weather forecasting system for POSEIDON—An overview. GAOS, 8, 219−237.

Pytharoulis, I. (1999). African Easterly Waves and their transformation into tropical cyclones in north Atlantic. Ph.D. Thesis, Univ. of Reading, UK. pp 196.

Thiebaux, J., E. Rogers, W. Wang and B. Katz (2003). A new high-resolution blended real-time global sea surface temperature analysis. Bull. Amer. Meteor. Soc., 84, 645−656.

Tompkins, A. and G.C. Craig (1999). Sensitivity of tropical convection to SST in the absence of large-scale flow. J.Climate, 12, 462−476.

Marine weather forecasting in a regional meteorological agency (MeteoGalicia)

P. Montero*[1], P. Carracedo[1], M. Barreiro[1], S. Torres[1], M. Ruiz-Villarreal[2], M. Gómez[3], J. Carlos[3] and V. Pérez-Muñuzuri[3]

[1]MeteoGalicia, Consellería de Medio Ambiente, Santiago de Compostela, Spain
[2]Instituto Español de Oceanografía, A Coruña, Spain
[3]Ente Público de Puertos del Estado, Spain

Abstract

In November 2002, the Prestige oil tanker sank and produces one the worst oil spills recorded in Galicia, showing the necessity of developing operational oceanography in the area. To that end, MeteoGalicia (the regional weather forecasting agency) have recently implemented wave and hydrodynamic models which run operationally coupled to the meteorological model ARPS. At this moment, MeteoGalicia is running two operational wave models (WaveWatch III and SWAN) to forecast the marine weather and a 3D primitive equations model (MOHID) to describe the coastal currents. In the future, this 3D model will be coupled to a global model in order to get realistic boundary conditions (Project ESEOO) in collaboration with other institutions trying to develop a Spanish oceanographic operational system. MeteoGalicia aims to achieve a high-quality marine dynamics forecast within a scale of several hundred metres in order to satisfactorily describe the Galician Rias dynamic. All the outputs of this system are used daily by MeteoGalicia forecasters and are available on the MeteoGalicia web page (http://www.meteogalicia.es).

Keywords: Meteorology, models, Galicia, weather forecast, oil spill.

1. Introduction

The Galician coast (NW Spain) is one of the most productive estuarine regions in the world. Located at the north-western Iberian margin, it is under the influence of seasonal upwelling events, so fisheries and aquaculture industries are among the main sources of income in the region. Besides that, a lot of tanker tracks cross Galician waters. Around 800 million tons of oil can pass near the Galician coast. Moreover, environmental protection of the region and sustainable development of other economical activities (e.g. tourism, sport fishing, sailing) are becoming more important, so a regional strategy of marine weather forecast is demanded by society in order to respond these issues.

MeteoGalicia is the Regional Meteorological Service of Galicia. The main aims of MeteoGalicia are: a) meteorological and climate observation of Galician weather, b) weather forecast, downscaling for the purpose of Galician people, c) Research, on atmospheric and oceanological sciences. In addition, in order to answer requests, MeteoGalicia has developed a special marine forecast to add to the daily main weather forecast. This paper shows the advanced tools used to achieve this objective.

* Corresponding author, email: pedro.montero@meteogalicia.es

2. Marine Forecast System

2.1 Setup

Two atmospheric numerical models (ARPS & MM5) (Souto *et al.*, 2003; Dudhia, 1993) run twice daily for a coarse and fine grid centred in Galicia. These models are fed by the NCEP/NOAA GFS model. They are validated every day against data from the Galician net of meteorological stations. The marine weather forecasters use numerical outputs of winds, temperature, precipitation, etc. Moreover, ARPS' wind output is used to run wave models. Two models are used: WaveWatchIII runs once a day in order to forecast sea surface waves in the ocean and the SWAN model is run for nearshore forecast. These models are validated against buoy measurements from the public agency Puertos del Estado, (Carracedo *et al.*, 2005).

A radiative transfer model, FASTR, is fed every day by GFS stratospheric ozone output in order to forecast UV Index for Galician region. A validation of this numerical forecast can be found in Petazzi *et al.* (2004).

In order to obtain a tidal currents forecast, a hydrodynamic model MOHID2000 (Ruiz-Villarreal *et al.*, 2002; Montero *et al.*, 2003) is run every day for the Galician area and four nested grids. The objective of this system is to support the coupling with spill models to be used in emergency plans needing a fast response. Further work will introduce atmospheric pressure and wind forcing in the system. Calibration and validation of this modelling system can be found in Torres-López *et al.* (2005).

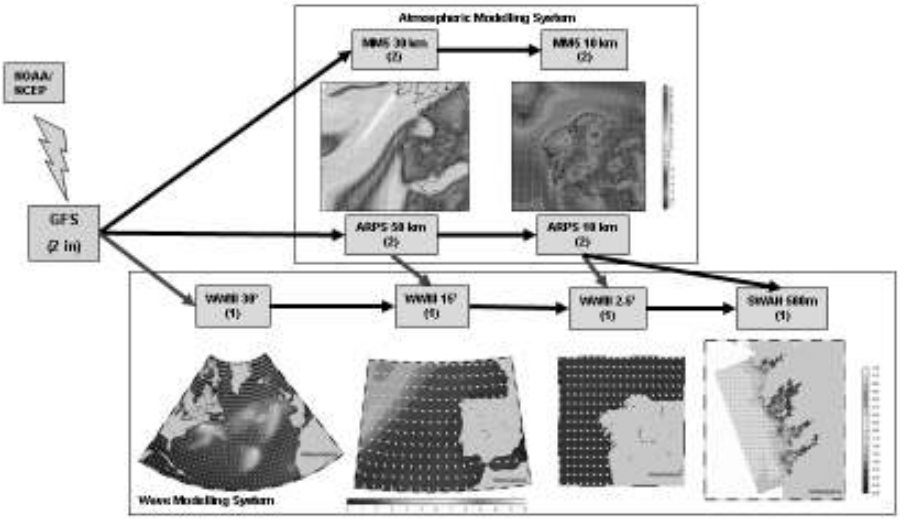

Figure 1 Set up of atmospheric and wave models. Arrows show the forcements between models. Numbers in brackets indicate the number of times each model is run in a day.

2.2 Daily Products

Every day, forecasters use numerical models to make two marine weather forecasts (one in the morning and another in the afternoon).

Wind, waves, swell, temperature and other weather conditions are forecasted for two periods of the day and for coastal zones. The scope of this forecasting is three days. All of this information is published on the MeteoGalicia web site (www.meteogalicia.es) and is spread to regional television, radio as well as the press. All of the forecast information is inserted in a database and validated against *in situ* measurements.

2.3 Non-daily products

In order to respond in an emergency situation, like an oilspill, Lagrangian models are coupled to hydrodynamical models. Moreover, weather forecast information is updated as often as necessary during crises.

3. Conclusions

A marine weather forecast system was set up in MeteoGalicia, the Galician Meteorologic Agency. The main objectives of this system are to help forecasters in their daily reports and to be used by the oil spill management office of the Galician government.

Further work will include wind and baroclinic forcings in order to obtain a full 3D baroclinic picture of the Galician currents running every day in MeteoGalicia. Coordination with national projects like ESEOO is a fundamental task to obtain this objective. Special efforts will be made to connect the model outputs with forecasters and the persons in charge for a fast response to an oil spill.

Acknowledgements

The authors would like to thank to MARETEC–IST for MOHID model support. This paper is a contribution to the ESEOO project (ref. VEM2003–20577C14–12) financed by CICYT and the Platerias project (ref. PGIDIT03TAM60401PR) financed by Xunta de Galicia.

References

Carracedo, P., M. Barreiro, S. Torres, P. Montero, M. Ruiz-Villarreal, M Gomez, J.C. Carretero and V. Perez-Muñuzuri (2005). High resolution wave forecasting at the Galician coast. This volume, page 362.

Dudhia, J. (1993). A Nonhydrostatic Version of the Penn State/NCAR Mesoscale Model: Validation Tests and Simulation of an Atlantic Cyclone and Cold Front. The Monthly Weather Review, 121, 1493–1513.

Montero, P., J. Blanco, J.M. Cabanas, J. Maneiro, Y. Pazos, A. Moroño, C.F. Balseiro, P. Carracedo, B. Gómez, E. Penabad, V. Pérez-Muñuzuri, F. Braunschweig, R. Fernades, P.C. Leitão and R. Neves (2003). Oil Spill Monitoring and Forecasting on the Prestige-Nassau accident. Proceedings 26th Arctic and Marine Oilspill Program (AMOP) Technical Seminar, 2, 1013–1029.

Pettazzi, A., P. Montero, C.Balseiro, J.A. Souto and V. Pérez Muñuzuri (2004). Evaluation of a radiative transfer model for ultraviolet index operational forecast in Galicia (Spain). Proceedings of the 1st General Assembly of the European Geosciences Union. Nice, April 25–30, 2004. Geophysical Research Abstracts, Vol.6, EGU04–A–00196.

Ruiz-Villarreal, M., P. Montero, J.J. Taboada, R. Prego, P.C. Leitão and V. Pérez-Villar (2002). Hydrodynamic Model Study of the Ria de Pontevedra under estuarine conditions. Estuarine, Coastal and Shelf Science, 56. 101–103.

Souto, M.J., C.F. Balseiro, V. Pérez-Muñuzuri, M. Xue and K. Brewster (2003). Impact of Cloud Analysis on Numerical Weather Prediction in the Galician Region of Spain. Journal of Applied Meteorology 42, 129–140.

Torres Lopez, S., M. Barreiro, P. Carracedo, P. Montero, M. Ruiz Villarreal, and V. Perez-Muñuzuri (2005). Tide forecast on the Galician Coast. This volume, page 59.

Turning the tides

Marc E. Philippart*[1] and Jan-Rolf Hendriks[2]

[1]*Rijkswaterstaat – North Sea Directorate, Rijswijk, The Netherlands*
[2]*Rijkswaterstaat – Zeeland Directorate, Middelburg, The Netherlands*

Abstract

At Rijkswaterstaat a forecasting system for water level, currents and salinity has been set up in the past years. The components have been developed by the National Institute for Coastal and Marine Management of Rijkswaterstaat. This system contains the numerical models from large scale continental shelves to small-scale 3D coastal zones, extended with data assimilation tools. The introduction of this system took place side by side with applications already in existence, data streams, and operational products, which need extra attention so as not to be disturbed. The existing needs are supported and extended and new ways to use more benefits are explored. The main goal is to distribute this data to existing and new users and prove the validity of this forecasting system in safety and economic activities all around the North Sea, nationally and internationally.

Keywords: operational forecasting, storm surge, models, shipping guidance, North Sea, oil spill management, data distribution

1. Introduction

In the Netherlands several tasks of Rijkswaterstaat are supported by the two Hydro Meteo centres. One of them is situated in the south (Middelburg) and covers the Zeeland region including the route to Antwerp. The other is situated near The Hague (Rijswijk) and covers the rest of the tidal waters including the entire North Sea. The main tasks are to warrant safe and economic optimal shipping guidance to the ports of Antwerp, Rotterdam and Amsterdam; safety aspects like closing storm surge barriers and predicting the state of the sea for all kind of off-shore activities. Further the information can support operational water management, cleaning up oil spills and efficient and precise determination of the reduction level for bathymetric soundings.

Figure 1 Berge Stahl (365000 dwt) on her way to Rotterdam; Measlant stormsurge barrier; Prestige on her way down.

* Corresponding author, email: M.E.Philippart@dnz.rws.minvenw.nl

Recently we accomplished operationalisation of a whole new suite of models to satisfy these needs. This action was a tough and exciting voyage. We would like to report on this journey by presenting the problems we met, the "blisters" that occurred but also some of the nice views we saw on the way.

2. Models

The models and data assimilation tools are developed by the National Institute for Coastal and Marine Management of Rijkswaterstaat. In the project Nautilus a whole suite of models were set up that form a perfect match for each other.

The large scale continental shelf model (DCSM98) has a grid size of about 8 kilometres and is driven by 11 astronomical components and wind and pressure fields from the KNMI-Hirlam meteorological model (Philippart, 1997). This model is extensively calibrated with the use of adjoint modelling. A large set of observations, *in situ* as well as satellite altimeter data, is used in this calibration (Philippart, 2002). Operationally a Kalman filter is used to perform data assimilation of 5 locations along the British east coast and 3 along the Dutch coast. These observations give a good clue about the wind effects on the North Sea. The impact of the assimilation gives an improvement of the forecast until 12 hours from the last used observation. This continental shelf model is also used at the KNMI for storm surge forecasting.

In the DCSM98 model the Southern North Sea model is nested. The boundaries are nested with a grid step of 1/3th of the coarser model and stretch from Bournemouth to Cherbourg and from Aberdeen to Hanstholm. It is a curvilinear grid with mesh size from 6 to 1 kilometres. It is also used in combination with Kalman filtering.

In the southern North Sea model the model of the Dutch Coastal zone is nested with a grid refinement of factor three. The model follows the coast in a zone of 70 kilometres and has a good description of the estuaries. For optimal boundary conditions a special version of the Kalman filter is used: the Kalman smoother. Measurements of coastal locations are use to correct the boundary 100 minutes earlier, which is the travel time of the tide from boundary to the coast. After this correction the model is re-run with the new forcing (Brummelhuis, 1990).

Again nested with factor three there are detailed models of the Schelde Estuary, the Zeedelta model with the Rotterdam area including the rivers halfway across the Netherlands (barriers Tiel, Megen and Lith) and one around the IJmuiden area.

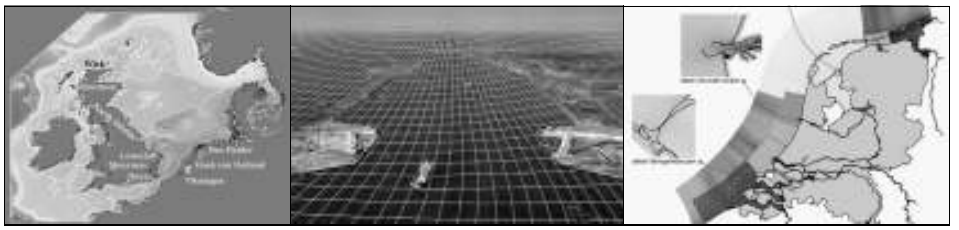

Figure 2 Continental Shelf model; grid definitions; detailed models.

All these models are used in a 2-dimensional version. A 3-dimensional version of Zeedelta and IJmuiden has been prepared and is waiting for extended computer

resources. The models are nested successively, where the 3 most detailed models can run at the same time. The models can run in parallel on several computers. The ultimate situation of running them as just one model with areas of different refinement of grids is now technically prepared.

3. Making the models operational

The process of making the models from institute tools to real operational services is often underestimated. Input for the models to run has to be gathered from different sources and must be automatised in a robust way. Wind and pressure fields from KNMI must be sent to our computers as soon they are available. Measurements of water level and river discharge are continuously monitored and sent to our database. Further a prediction of river flow and sluice operations must be available. Once gathered, all the data streams must be secured with enough redundancy and stored in the operational database. Especially when using data assimilation a good quality control of the information is needed. Also a check of the output is needed to be sure the data, which is used more and more in automatised processes, is not corrupt. All these actions need to be scripted with occasional intervention from the operational team. They check the input, fill gaps and extrapolate discharges. Further they kick-off the models and after a while check the output produced.

Setting up the hardware and software to launch an operational service contains a lot of work. It is like climbing a mountain without a map. The main route is more or less clear but a lot of sidetracks appear during this route. Like lots of projects the budget and manpower are limiting components. Also the changing surroundings in policy, computer hardware and client needs have to be taken into account on the way up. An extra problem was the fact that the introduction of this system took place side by side with already existing applications, data streams and operational products. Step by step we reached the top and have the main applications running for our goals.

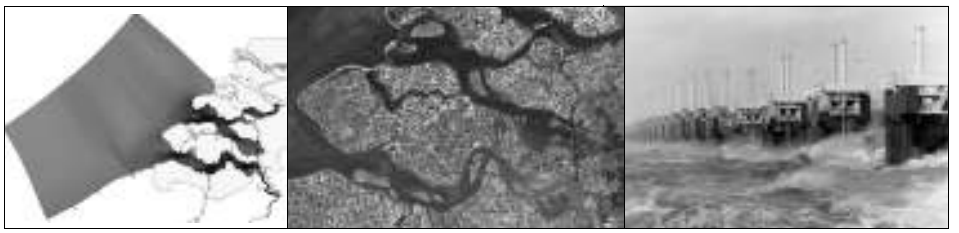

Figure 3 The Scheldes model area; dynamic area seen from space; the Oosterschelde storm surge barrier.

3.1 On the first mountain

Now the time has come to really enjoy the views! An enormous amount of information in time (until 48 hours ahead) and space (the whole North Sea) is available now. We rewrote several applications to use the data. Instead of giving the pilots to Rotterdam a forecast based on a single location neural network, the water level and current along the whole Euro-Maasgeul is given. Dedicated forecasts are distributed for a whole range of customers, some direct and some through our website. Several quality checks are performed on the results of the models. Where available these data are compared with

measurements. For blind spots we made extra water level observations with pressure gauges. Although we have one of the most extended monitoring networks, the availability of current measurements are still rare (2 fixed ADCPs at sea near the entrance of Rotterdam and IJmuiden).

4. Next mountain

The next mountain to climb is to disseminate this data to our existing and new users and prove the validity of this forecasting system in safety and economic activities all around the North Sea.

In exploring the new possibilities we made a database containing the model data for the whole grid. A specific format, based on XML, is used to obtain interpolated data in the users' own coordinate system. The next step is to make a webtool for this data stream where every user can get the information needed for their own purpose. We use this already for precise determination of the reduction level for bathymetric soundings. The track of the monitoring vessel is put into a webtool and the water level data of the model is interpolated in time and space on this track. The output can be directly used to transform soundings to bathymetry, relative to a fixed reference plane.

Some of our new interests are using the data for oil spill movement (clean up operations and prosecution) and for search and rescue. Besides all the economic and safety benefits, saving one extra person will justify the work we have done.

Figure 4 Cross current at harbour entrance; current atlas Southern North Sea; Search and Rescue.

Acknowledgements

We want to thank the staff at the National Institute for Coastal and Marine Management (Nautilus project team) for their innovative skills and the way they have incorporated these skills into the models. Also the operators of the Hydro Meteo centres for taking over the models and using them operationally 4 times daily. We also want to thank Regien Brouwer for making the scripts where all the handling of input and output takes place.

References

Philippart, M.E. and A. Gebraad (1997). A new storm surge forecasting system. J.H. Stel, H.W.A. Behrens, J.C. Borst, L.J. Droppert, J.P. van der Meulen (eds.) Operational Oceanography, The challenge for European co-operation, Proceedings of 1st EuroGOOS Conference, Elsevier Oceanography Series.

Philippart, M.E. and A. Gebraad (2002). Assimilating satellite altimeter data in operational sea level and storm surge forecasting. N.C. Flemming, S. Vallerga, N. Pinardi,

H.W.A. Behrens, G. Manzella, D. Prandle, J.H. Stel (eds.). Operational Oceanography, Implementation at the European and Regional scales, Proceedings of 2nd EuroGOOS Conference, Elsevier Oceanography Series.

Brummelhuis, P.G.J. ten and A.W. Heemink (1990). Parameter identification in tidal models with uncertain boundary conditions. Stochastic Hydrology and Hydraulics, Vol. 4, No. 4, pp. 193–208.

Verlaan, M. (1998). Efficient Kalman filtering algorithms for hydrodynamic models. Phd. Thesis TU Delft.

Tide forecast on the Galician Coast

S. Torres-López*[1], P. Carracedo[1], P. Montero[1], M. Barreiro[1], S. Torres[1], M. Ruiz-Villarreal[2] and V. Pérez-Muñuzuri[3]

[1]MeteoGalicia, Consellería de Medio Ambiente, Santiago de Compostela, Spain
[2]Instituto Español de Oceanografía, A Coruña, Spain
[3]Ente Público de Puertos del Estado, Spain

Abstract

A 3-D circulation model of the Eastern North Atlantic is used to determine tidal dynamics along the Galician coast. Results are compared with tidal gauge data and harmonic constants provided by Puertos del Estado-Clima Marítimo (PE) and ellipse parameters from moorings in the Galician shelf and in the Ria de Vigo. The model reproduces tidal amplitude quite well. Phase lags are similar to findings of previous works. Modelled and measured tidal current intensity are also in good agreement. Higher resolution grids nested in the main domain notably improve predicted ellipse parameters.

Keywords: Tidal dynamics, hydrodynamic models, Galician Coast

1. Introduction

This work is part of the development of a regional oceanographic forecast system in the Galician coast (NW of Spain) by MeteoGalicia (regional meteorological agency). The MOHID model is going to be used in this system as a circulation model. So, although several tidal models have been applied previously in this region (Vincent and Le Provost, 1988; Le Cann, 1990; Alvárez-Fanjul *et al.*, 1997) providing a very complete picture of tidal dynamics, the MOHID model is validated here in order to test the quality of the tidal predictions.

2. Model Description and simulation conditions

The MOHID model has been developed by MARETEC−IST (www.mohid.com). It is a volume-difference, baroclinic primitive-equation model with a high order advection scheme (TVD), and many choices of turbulence closure including the k-e scheme used in the GOTM (Burchard *et al.*, 1999).

The domain (Figure 1) covers an area extending from 32º to 48º N in latitude and from 0.50º W to 15º W in longitude. The domain has a constant resolution of 0.05º (consistent with the ESEOO project) and 42 layers identical to that used by MERCATOR system. A nesting experiment have been made in the Ria de Vigo in order to increase spatial resolution up to 500 m. In this work, we show results using tidal forcing only, although the response of the model to river flow and upwelling-downwelling cycles, including density driven circulations, is also investigated. Tidal forcing is specified as a harmonic component from the FES95 global model at the open boundary of the grid. All the simulations were run for a period of one month in barotropic conditions.

* Corresponding author, email: silvia.torres@meteogalicia.es

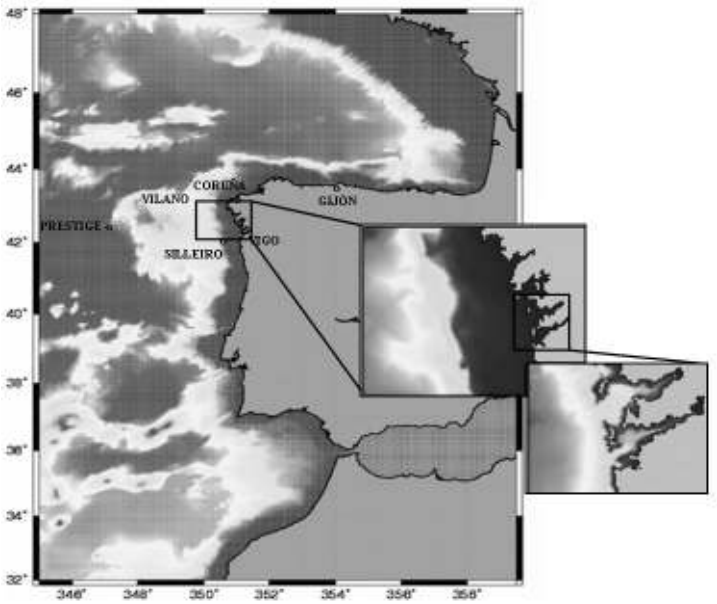

Figure 1 Domain of computation and topography. The labels represent tidal gauges (Gijón, A Coruña, Vilagarcia and Vigo) and mooring points (Prestige, Silleiro and Ría de Vigo moorings and Vilano and Silleiro surface current meters).

3. Results

3.1 Tidal amplitude validation

The general patterns associated with the propagation of the tidal wave are correctly reproduced (Figure 2 and Figure 3), but some differences can be found. The percentage errors of the semidiurnal components are lower than 3.5% except for S2 (<6.6%). Semidiurnal phase lags are lower than 8 minutes regarding September 2002 tidal gauge data. Semidiurnal phases (especially S2) agree quite badly with nine-year phases computed by PE. Diurnal component percentage errors (Table 1) are larger in most of the harbours, which must be due to the small absolute values of the diurnal components, making altimeter based determination more difficult and increasing the inaccuracy of the open boundary condition. Larger discrepancies are present in diurnal phase values too.

3.2 Tidal current validation

In order to validate the simulated tidal circulation, M2 MOHID tidal ellipses were compared with those obtained from three mooring places at the Prestige sinking location — Silleiro Cape and Ría de Vigo — and with surface currentmeter data from PE buoys (Table 2). The Prestige mooring consists of a set of seven mechanical current-meters distributed throughout the water column, while Silleiro and Ría de Vigo consists of Doppler current meters. Data has been integrated in depth to obtain barotropic tide and compare easily with modelled data. Ria de Vigo grid 500 m tidal ellipse parameters correspond to the three levels nested where the inner domain is 500 m grid size.

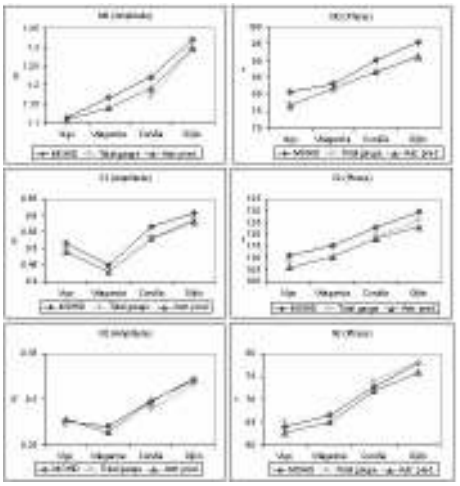

Figure 2 MOHID main semidiurnal harmonics amplitudes (left column) and phases (right column) compared with September 2002 tidal gauge constants and with nine years harmonic analysis at Vigo, Vilagarcia, Coruña and Gijón.

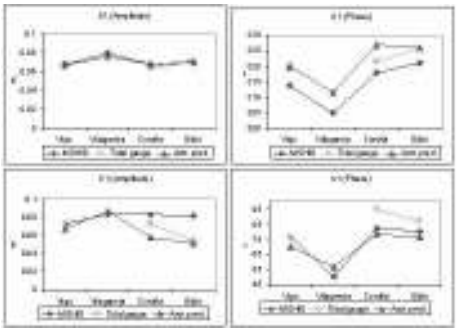

Figure 3 MOHID main diurnal harmonics amplitudes (left column) and phases (right column) compared with September 2002 tidal gauge constants and with nine years harmonic analysis at Vigo, Vilagarcia, Coruña and Gijón.

Table 1 Top: Amplitude percentage errors and phase lags (minutes) between MOHID results and tidal gauge data during September 2002. Bottom: Amplitude percentage errors and phase lags between MOHID results and astronomic constants computed by PE for nine year tidal gauge series.

SEPTEMBER 2002 TIDAL GAUGE ERROR										
	M2		**S2**		**N2**		**O1**		**K1**	
	Am(%)	**Ph(')**	**Am(%)**	**Ph(')**	**Am(%)**	**Ph(')**	**Am(%)**	**Ph(')**	**Am(%)**	**Ph(')**
Vigo	1.1	7.3	4.0	4.7	1.5	–2.2	6.3	–10.6	1.4	0.3
Coru	3.5	7.8	6.2	8.0	3.1	–2.8	7.9	–7.4	13.7	–26.5
Gijón	1.8	8.0	3.4	7.0	1.6	–0.4	2.8	–9.7	50.0	–14.5
ASTRONOMIC PREDICTION ERROR										
	M2		**S2**		**N2**		**O1**		**K1**	
	Am(m)	**Ph(')**	**Am(m)**	**Ph(')**	**Am(m)**	**Ph(')**	**Am(m)**	**Ph(')**	**Am(m)**	**Ph(')**
Vigo	0.3	8.4	4.9	10.2	0.7	2.9	1.5	–13.1	7.5	13.3
Vilag	2.4	2.4	4.6	9.5	2.5	3.1	5.5	–13.8	3.5	–13.7
Coru	2.5	7.4	6.6	10.1	0.4	1.4	0.0	–18.4	43.6	7.6
Gijón	1.7	9.1	4.6	13.0	0.3	4.2	1.4	–10.2	58.8	7.2

Table 2 M2 MOHID ellipse parameters from different resolution domains (GRID 5 km, GRID 500 m) compared to M2 ellipse parameters obtained from depth integrated velocity time series (MOOR(DI)) and from surface currentmeter records of PE buoys.

	major	emaj	minor	emin	inc	einc	pha	epha
Prestige Sinking Location								
GRID 5 KM	0.034	0.002	0.009	0	82.16	1.32	63.55	2.79
mooring	0.037	–	0.007	–	71.03	–	79.24	10.5
Silleiro Cape								
GRID 5 KM	0.05	0.002	0.01	0	80.07	0.97	32.64	2.05
mooring	0.056	0.002	0.001	0	2	3.64	5	8.66
PE BUOY	0.032	–	0.015	–	135.4	–	119	–
Ría Vigo								
GRID 5KM	0.28	0.06	0.03	0.03	16.05	6.77	3.97	15.01
GRID 500 M	0.13	0.021	0.01	0.01	25.24	4.05	353.2	6.61
Mooring	0.101	1.8	0.014	1.21	25.08	6.73	358.2	9.22
Vilano								
GRID 5 KM	0.123	0.006	–0.005	0	153.3	2.01	189	2.55
PE BUOY	0.117	0.075	–	0	130.3	–	110	–

Not enough measurements are available to validate tidal currents properly. However, ellipses axes of simulated currents are quite similar to those of measured data, describing the same spatial pattern: The minimum semi-major axis (0.03 ms^{-1}) can be found for M2 at the Prestige mooring location, increasing up to 0.12 ms^{-1} at Vilano Cape. The simulated ellipses are rotating clockwise, with an orientation following the model bathymetry lines. Differences for orientation angles, in a wide range between 0.2º and 80º, can be explained by the small resolution of the domain. The most precise values correspond to the highest resolution domain (Ria de Vigo) and to the outer location (Prestige mooring), less influenced by the topography.

4. Conclusions

According to previous works (Le Cann *et al.*, 1990; Fanjul *et al.*, 1997), the amplitude and phase of both observed and simulated constituents show the expected Kelvin wave behaviour, with largest amplitudes and phase lags towards the Atlantic northern coast. Tidal level average errors are less than 0.07 m and RMS are around 0.10 m. Differences between modelled M2 amplitude constants and those derived from tidal gauge data are no larger than 5% at all the harbours.

The employed grid size does not permit obtaining a satisfactory description of the currents close to the coast. Orientation, semi-major and semi-minor axis differences decrease notably when a nested domain with higher resolution is used (i.e. Ria de Vigo results). Further studies should be carried out to find a compromise solution between the time simulation and the improvement of the results as a consequence of the increase of resolution and nesting, in order to maintain the operational value of the system.

Acknowledgements

The authors would like to thank Puertos del Estado for providing tidal constants and tide gauge series by means of its site web (www.puertos.es) and MARETEC–IST for MOHID model support. Useful comments and data were obtained from S. Piedracoba and J. Herrera-Cortijo. Thanks to I.F. Rodil for allowing us to use the background photography and to C. Garcia-Prado for helpful suggestions.

This paper is a contribution to the ESEOO project (ref. VEM2003–20577C14–12) financed by CICYT and the Platerias project (ref. PGIDIT03TAM60401PR) financed by Xunta de Galicia.

References

Burchard, H. (1999). Recalculation of surface slopes as forcing for numerical water column models of tidal flow. App. Math. Modelling, 23:737−755.

Fanjul, E.A., I. Rodríguez and B. Pérez (1997). A description of the tides in the Eastern North Atlantic. Progress in oceanography. Progress in Oceanography, Vol. 40 pp 217−244.

Le Cann *et al.* (1990). Barotropic Tidal dynamics of the Bay of Biscay Shelf: observations, numerical modelling and physical interpretation. Continental Shelf Research, Vol. 10, 723−758.

Vincent, P. and C. Le Provost (1988). Semidiurnal tides in the Eastern Atlantic from a finite element numerical model. JGR, Vol. 93, Nº C1, pp543−555.

Near-operational system of Black Sea circulation

G.K. Korotaev, V.L. Dorofeyev* and U.B. Ratner

Marine Hydrophysical Institute NAS, Sevastopol, Ukraine

Abstract

This paper presents a near-operational system permitting continuous monitoring of the circulation and stratification of the Black Sea. The system is based on the primitive equation model of the Black Sea circulation with a 5 km grid step. External forces are provided by NCEP reanalysis. An important part of the near-operational system is assimilation of space remote sensing data including sea surface anomalies, providing in a near real time mode by AVISO/Altimetry a multi-satellite data active archive centre dedicated to space oceanography (France) and surface temperature (via direct reception of Advanced Very High Resolution Radiometer (AVHRR)).

The output of the system is a time series of three dimensional hydrophysical fields (temperature, salinity, current velocities). The data from surface drifting buoys and deep profiling floats are used for validation of the model output. Surface drifting buoys provide data for validation of surface current velocity and sea surface temperature. Three profiling floats deployed at parking depths of 200, 750 and 1550 m are used for validation of weekly mean velocity and temperature and salinity profiles. The resulting statistics form the model validation and show that the near-real time operational system is capable of nowcasting and forecasting hydrographic fields with reasonable accuracy.

1. Introduction

The satellite remote sensing systems enable the study of a wide range of processes developing in seas and oceans. However, remote sensing data can provide only surface parameters of the sea, and it is important to describe the three-dimensional structure of the hydrological fields. For more efficient use of the remote sensing information a concept of satellite monitoring of the ocean has been offered (Nelepo, 1984). The main idea of satellite monitoring is to extrapolate measurements from the surface into the depth with the help of a numerical model. Active inclusion of models allows not only the gaps in the satellite measurements to be filled but also enable forecasting of the change of the sea state.

One of the fundamental elements of the concept is the ability to determine the surface conditions, which are needed for numerical integration of the model equations. In particular, satellite measurements of the sea surface temperature and near surface wind allow users to determine surface boundary conditions for equations of balance of heat and momentum. The satellite remote sensing data can also solve the problem of initialisation, that is, determination of the initial conditions for integration of the hydrodynamics equations. Modern altimeters are one of the most efficient instruments for ocean monitoring, as the altimetric measurements of the surface topography enable the variability of sea currents to be studied from large scales to meso-scales.

* Corresponding author, email: otdp@alpha.mhi.iuf.net

Reconstruction of the currents can be carried out by means of assimilation of the altimetry data in the numerical models of seas. As the topography of the sea surface reflects deep processes, regular assimilation of these data allows the model to get to the state where influence of the initial conditions becomes unimportant. Thus, assimilation of altimetry allows first nowcasting of the currents and then forecasting. On the basis of the conception of satellite monitoring a system of nowcasting of the Black Sea circulation was developed. The system worked in a near operational regime. The results obtained by this system were validated by means of comparison with independent measurements of drifting buoys (drifters) and PALACE profiling floats.

2. Description of the system

2.1 Hydrodynamical model

The main part of the system is the hydrodynamical model of the Black sea circulation. The model is based on traditional primitive equations (Demyshev and Korotaev, 1992). Finite-difference discretisation of the model equations is done on the C-grid. The model has 35 non-uniformly spaced levels more frequent near the surface and near the bottom. The horizontal resolution is uniform with a 5 km grid step. External forces are provided by NCEP reanalysis. The Rossby radius of the internal mode for the deep part of the Black Sea is equal to 25 km. Therefore the horizontal resolution of the model can enable the mesoscale variability of the Black Sea to be resolved (Dorofeyev and Korotaev, 2004a).

2.2 Altimetric data

The important part of the system is an assimilation block of satellite altimeter data. The system uses satellite data from ERS, TOPEX/Poseidon, GFO, Jason and EnviSat altimeters. The altimetric measurements are available from Toulouse space centre through the AVISO project. (The altimeter product produced by the CLS Space Oceanography Division with support from CNES, published by AVISO/Altimetry a multi-satellite data active archive centre dedicated to space oceanography and supported by CNES, the French space agency).

Preprocessing of data sets includes correction of the data for influence of atmosphere refraction, surface waves, atmospheric pressure and the geoid. As a result these data contain anomalies of sea surface height with respect to mean sea surface topography. The mean sea surface topography includes a geoid height and mean dynamical sea level. Unfortunately, the accuracy of the geoid model for the Black Sea is not sufficient, so we need additional information to obtain the mean dynamical sea level. For these purposes we use annual mean climatic sea level (Korotaev *et al.*, 2000), obtained by means of assimilation of all available hydrographic data in the numerical model. These fields of sea level are interpolated to the position of each track and added to the surface anomaly retrieved from the altimeter data to obtain the absolute dynamical sea level. The climatic changes of the sea level are also applied to exclude a strong seasonal variability of the Black Sea level due to the river discharge and annual cycle of precipitation and evaporation (Korotaev *et al.*, 1998).

2.3 Data assimilation procedure

The data assimilation procedure is based on the Kalman filter theory. Full application of the three-dimensional Kalman filter demands solution of a system of differential equations in six-dimensional space and is too expansive. To simplify the procedure the following assumptions were made:

- error statistics of the predicted fields are stationary in time, horizontally uniform and isotropic
- cross-correlation between salinity (and temperature) and sea level is presented as a product of two functions depending on horizontal and vertical coordinates
- error statistics of the predicted fields is proportional to the natural statistics for the same fields.

According to these assumptions auto-correlation and cross-correlation functions were estimated from observations and used in the simulations. In addition to altimetry the model assimilates satellite images of the sea surface. These are images of Very High Resolution Radiometer (AVHRR), NOAA satellites. The data are received and processed at the Marine Hydrophysical Institute. The final product has a space resolution of about one kilometre.

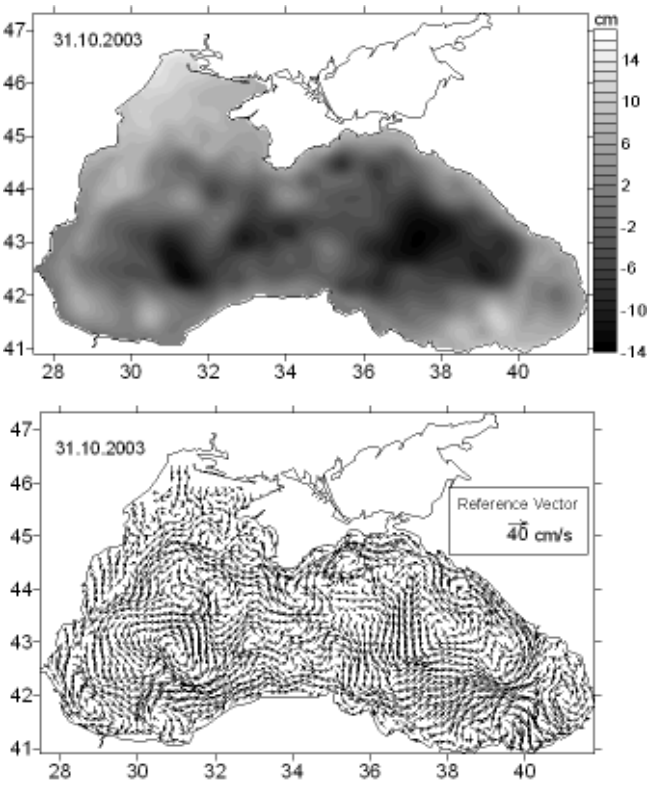

Figure 1 Maps of sea surface topography (upper) and surface currents as a result of assimilation of satellite and AVHRR-SST data in the model.

3. Validation of the results

The output of the system is the set of three dimensional hydrographic fields for the Black sea region. An example of these fields is presented in Figure 1.

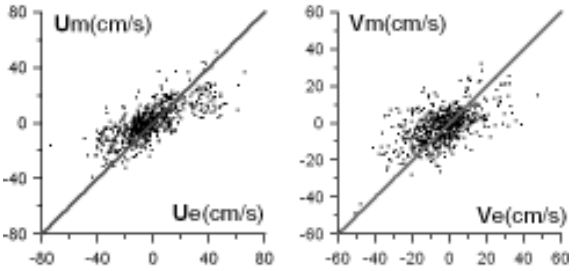

Figure 2 Comparison of drifters velocities (x axis) and appropriate simulated velocities (y axis). Left: zonal component, right: meridional component.

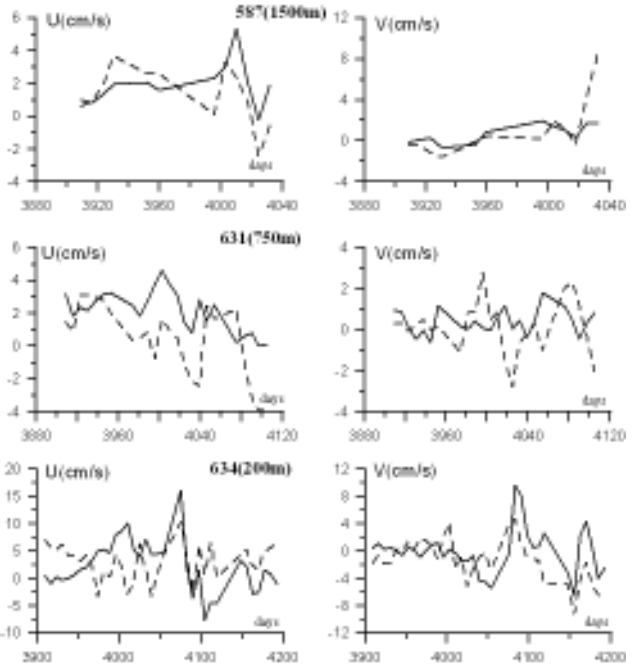

Figure 3 Comparison of float velocities (PALACE profiling floats) and appropriate simulated velocities (observed–solid line, simulated–dotted line) as a function of time.

To validate the results we use measurements from drifters. There are surface drifting buoys and profiling floats. The Black Sea drifter experiment was started in 1999 as part of a complex scientific study of the Black Sea ecosystem and the shelf–deep basin interactions provided by Russian oceanographers from the P.P. Shirshov Institute of Oceanology (Moscow), Marine Hydrophysical Institute, Ukrainian National Academy of Sciences (Sebastopol), and Department of Oceanography, Naval Postgraduate School

(Monterey, USA). Since then 60 drifters have been deployed in the Black Sea, some of them equipped with thermistors.

The Black Sea profiling buoy project was initiated in 2002. The floats were deployed by Turkish research vessel on 2 September on the section across the Bosphorus Strait. Float 587 is deployed to the parking depth 1550 m, float 631 is at a parking depth 750 m and float 634 at depth 200 m. All floats provide profiling from 1550 m depth. The data are recovered from the floats via the Argos system. The floats spend 7 to 8 hours transmitting on the surface with one message transmitted every 46 to 54 seconds. Data are transmitted weekly.

The temperature and salinity profiles via pressure and T–S relations together with float trajectories are presented in near-real time on http://flux.ocean.washington.edu/metu. The validation experiments show that temperature, salinity and current velocity fields may be re-constructed efficiently and precisely by data assimilation tools in the presence of fairly dense coverage of observations within the basin (Dorofeyev and Korotaev, 2004b). As an example, comparison of the simulated velocities and appropriate velocities from surface drifters and PALACE profiling floats is presented in Figure 2 and Figure 3.

Acknowledgements

This work is supported in part by the EU project ARENA and CRDF Grant CGP2003 UG2–2536–SE–03.

References

Nelepo, B.A. (1984). Satellite monitoring of the ocean climate. Meteorology and hydrology, N8, p.12–24.

Dorofeyev, V.L. and G.K. Korotaev (2004a). Assimilation of satellite altimetry data in the eddy-resolving model of the Black Sea circulation, Marine Hydrophysical Journal, N1, p. 52–68.

Dorofeyev, V.L. and G.K. Korotaev (2004b). Validation of the results of modelling the Black Sea circulation based on the data of profiling floats. In: Ecological safety of coastal and shelf area and complex use of the shelf resources. Remote sensing of marine ecosystem. MHI, IGN, OB IBSS, Sevastopol, pp 63–74.

Korotaev, G.K., S.G. Demyshev and V.V. Knysh (2000). Three-dimensional climate of the Black Sea. 2000 In: Black Sea Ecosystem Processes and Forecasting/Operational Database Management System. Report of the Workshop and Project Evaluation Meeting. Istanbul, 15–18 May 2000.

Korotaev, G.K., O.A. Saenko, C.H. Koblinsky, S.G. Demyshev and V.V. Knysh (1998). An accuracy, methodology and some results of the assimilation of the TOPEX–POSEIDON altimetry data into model of the Black Sea general circulation (in Russian), J. Earth Res. Space, 3, p.35–51.

Korotaev, G.K., V.L. Dorofeyev and T.Yu. Smirnova (2004). Accuracy of the nowcast of surface currents in the system of the Black Sea satellite monitoring. In: Ecological safety of coastal and shelf area and complex use of the shelf resources. Remote sensing of marine ecosystem. MHI, IGN, OB IBSS, Sevastopol, pp 75–92.

A technical overview of the POSEIDON II system

D. Ballas*, A. Mallios and P. Pagonis

Hellenic Centre for Marine Research, Greece

Abstract

The Ionian Sea, Aegean Sea and the Levantine basin represent areas of scientific, economic and social importance. Current scientific research indicates that these areas play an important role in the dynamic physical processes of the entire Central-Eastern Mediterranean. Moreover, these areas are of major economic and social significance, since they are intensively used for tourism and recreation, fishing and fish-farming, offshore and coastal installations, etc. In addition, the surrounding coastal marine environment is one of the highest qualities in the Mediterranean, deserving special care and attention. With these ideas in mind, an advanced POSEIDON II monitoring system was designed for the Eastern Mediterranean Sea in order to support the requirements of the ecological modelling and to provide environmental information for integrated marine ecosystem management and maritime safety on a national and regional scale. The system will upgrade the existing POSEIDON I buoy network to improve its functionality, operational capabilities and observing capacity, including new biochemical and deep sea observations instruments. Furthermore it will be enriched with new buoys covering the Ionian and NW Levantine Seas, except the Aegean Sea.

Keywords: Monitoring, buoys

1. Introduction

POSEIDON-I, the ancestor of the POSEIDON-II project, was developed during 1997–2000 and is an integrated ocean monitoring, forecasting and information system for the Hellenic Seas. The project was co-financed by the EEA–EFTA Mechanism (85%) and the Greek Ministry of National Economy (15%). It consists of a monitoring network based on 11 oceanographic buoys, a two-way communication system and the data analysis and numerical forecasting system.

The monitoring network is configured to acquire data every three hours, which is a balanced compromise between frequent measurements and saving energy and communication costs. The parameters that are measured are wind speed and direction, wave height and direction, current speed and direction, air temperature and pressure, chlorophyll *a* concentration, dissolved oxygen, sea conductivity and temperature at depths of 3–50 m, light attenuation, and radioactivity.

The communication system is based on Inmarsat-C modems, which have been proven a reliable solution. GSM modems have been used independently as a more cost effective solution when the coverage of the GSM network has permitted their use.

The forecasting component of the POSEIDON system includes three separate numerical models that had the following characteristics when delivered in 2000:

* Corresponding author, email: dballas@ath.hcmr.gr

1.1 Weather forecasting model

The model produces weather forecasts for the next 72 hours on a daily basis. The model is implemented in 1/10° horizontal resolution over Greece, and 1/4° resolution over the wider Mediterranean area while it downscales the global analysis produced by the NCEP (USA).

1.2 Offshore wind wave forecasting model

The model is able to forecast the wave conditions in the Aegean and Ionian Sea for the next 48 hours. The horizontal resolution of the numerical simulation is 5 km, which is adequate in order to better describe the complex coastline of the Aegean Sea. The main outputs are the significant wave height, period and direction.

1.3 General circulation forecasting model

The model is able to forecast the current field in the Aegean and Ionian Seas in the whole water column (including surface) as well as the temperature, salinity and density for the next 72 hours. The horizontal resolution of the model is 5 km (see Soukissian *et al.*, 2000, for a complete description of the system).

1.4 Other models that can be used upon request

An oil drift model can be used in case of accidental oil release in the marine environment and uses as input the meteo, waves and currents forecasts. This model has been recently upgraded towards a complete oil spill detection and forecasting service for the Aegean Sea (Perivoliotis *et al.*, 2005).

A near-shore wave model is capable of extending the information from the open-sea wave model and buoy measurements, to the coastal areas. One main output of this model is the near bottom velocity, which can be used for calculation of sediment transport.

2. The Poseidon II project

2.1 The project objectives

During the five years of operation of the POSEIDON system a number of problems have been encountered. The weaknesses of the project and proposals for the improvement in performance of the system have been registered. New ideas about the operation of the system have been evaluated. The Poseidon II project gave the opportunity to implement these proposals.

The principal objectives for Poseidon II project can be summarised to the following:

1. Development of operational marine forecasting system providing ocean and meteorological information for the entire Eastern Mediterranean Sea.
2. Fulfilment of national obligations to international agreements like MEDGOOS, initiatives like GMES, EuroOCEANS, etc.
3. Upgrading of the existing possibilities of the Operational Centre by adding remote sensing techniques in the system.
4. building of a homogeneous buoy network covering the Ionian and Aegean Seas and the Cretan Passage.

5. Integration of the latest technological advances in ocean monitoring and extending the area of surveillance in the entire water column.
6. Extension of the sensor calibration capabilities in order to improve data quality.

2.2 Limiting factors of the existing system and the proposed improvements to support POSEIDON II activities

The energy adequacy of the buoys is a very important factor for the overall system performance. The maintenance surveys comprise a great part of the total expenses. The reduction of necessary visits for maintenance presupposes a robust power supply system. Furthermore the expansion of the system in the Ionian Sea enforces a necessity for larger power capacity.

The current power supply system is based on six solar panels and accumulators with a total capacity of 240 Ah. The energy balance provided by the described power supply system cannot ensure continuous operation especially after a long period without sunshine. On the other hand the energy consumption is increasing mainly because the demand for multi parametric monitoring systems is increasing. New applications under development, such as warning systems, demand a higher sampling rate and data transmission which is also energy consuming. The extension of the system in the Ionian Sea enforces a reconstruction of the power supply system.

An important part of the POSEIDON II project is the upgrade of the existing buoys. Reconstruction of the power supply system has first priority. The combination of more powerful solar panels and a wind generator will ensure the energy adequacy of a system with increasing energy needs. Re-arrangement of the batteries compartment will enable installation of additional batteries, increasing the total energy capacity of the buoy. Separating the battery compartment from the electronics compartment will improve the security of the system and a new charger-controller will increase the lifetime and efficiency of the batteries. A wind generator has been planned to be installed on the buoy so that a sun-independent energy source will provide the necessary energy surplus.

One weak point of the monitoring stations was that the acquisition unit could only interface with specific sensors. In a couple of cases the manufacturers of these sensors went out of business so the sensors could neither be repaired nor replaced. The necessity for a system with open architecture, in which the user will have the possibility of adding different sensors without hardware changes in the system, became obvious.

A new generation processor with acquisition software based on a real time operating system with powerful debugging features and remote access utilities has been requested from the system vendor for the POSEIDON II project. Data from additional sensors that will describe the system status (i.e. internal pressure, leakage detector, current consumption/production and flashlights monitoring) are included in the system specifications. The idea behind these new features is an early stage convenient diagnosis of problems that can lead to avoidance of greater system damage.

The capability of the existing system to measure oceanographic parameters was restricted to 3 m depth with the exception of a CTD string whose operational depth was at a maximum of 45 m. The new physical parameters that have been introduced and the need for deeper observations made our current system out of date. To solve the problem the Conductivity–Temperature string will be replaced with another string, which uses an

inductive modem as interface to the acquisition unit. The same cable is also used as a mooring line. This structure permits deep-sea measurements at a depth of 1000 m. However the most important issue is that this way we have the flexibility to install any type of sensor having RS-232 communication interface to arbitrary depths.

Biofouling is a limiting factor for the level of quality of the data a sensor produces, especially for optical sensors. In the POSEIDON I case, the data from the dissolved oxygen, chlorophyll *a* and light attenuation sensors became useless three weeks after the deployment. To confront the biofouling problem we have chosen a new sensor type whose measurement principles permit reliable operation in a eutrophic environment. The new dissolved oxygen sensor's measurement principle is based on the effect of dynamic luminescence quenching by molecular oxygen. Another methodology used to confront the biofouling is to equip the sensors with bio shutters or pumps. The sea water only flows through the sensors during measurement, reducing the biofouling effects.

Regarding the sensor measurement drift — a factor that reduces the data quality — the Poseidon personnel perform calibration to a set of sensors on board, just before deployment. One reason for this is that if we calibrate at the on-shore laboratory we would need twice the number of sensors (not possible for financial reasons). Another reason is that analog sensors should be calibrated together with the A/D converter unit. Moreover some circuits in the acquisition unit include amplifiers, making the calibration procedure of a sensor dependent on the buoy it will be installed on.

New calibration equipment has been ordered so that personnel can themselves perform level one calibration. Care has been taken, so that any new sensor that will be provided will have a built-in digital converter. The advantage of using this type of sensor is that they are interchangeable between the buoys and the calibration can be performed with the facilities of the on-shore laboratory environment at the operational centre.

The POSEIDON I upgrade also includes five new oceanographic buoys that will be added to the existing monitoring network, and are compatible with the existing buoys. However some of their features like their greater buoyancy make them suitable for deployment in deep-sea with a large number of sensors installed on them. Included in the set of new sensors to be installed on the buoys are an acoustic rain gauge, a nutrient analyser, a hyper spectra radiometer and an ADCP. The combined cable-mooring line permits the adoption of one or more sensors at arbitrary depths.

In addition to the inductive interface an acoustic modem interface will be installed on the buoys. The purpose of this acoustic link is to make the buoy act as a relay station for deep-sea oceanographic platforms. Part of the project is to produce an autonomous deep ocean station to be ready to accept installation of various sensors. In this part of the project the main target is to provide a sensor platform at the sea bottom to measure at least pressure and transmit data acoustically to the surface buoy. This facility should comply with the principles of the Tsunami warning system developed by NOAA as a deep ocean system for an early warning of Tsunami waves. A critical part of this task is to decide how to operate this deep ocean platform, and the limitations in terms of power consumption, service, maintenance and acoustic transmission. Furthermore there is a need to investigate the potential of installing additional instruments. Here in particular the service intervals, data transmission rate and power consumption consequences should be thoroughly investigated.

The communication system has proved to be working satisfactorily. Nevertheless minor modifications of the system were necessary because the existing Inmarsat-C modems are not supported any more by the manufacturer. New generation low consumption modems will be integrated to the system. The policy of transferring the data to an Inmarsat-C modem in the operation centre, although reliable, resulted in a doubling of communications fees. It has been proposed to transfer the data to an earth station and fetch the data using Internet from the Inmarsat provider. This will reduce the communication fees by 50%. Because the Inmarsat-C is not a real-time on-line system, an additional satellite communication system (iridium) will be installed in the buoys to ensure the implementation of remote access utilities in areas without GSM coverage.

3. Conclusions

The objectives of the POSEIDON II project will extend the monitoring activities to an even wider geographic region and for the entire water column. Moreover the investigation of new physical and chemical parameters as well as pilot applications, such as the deep-sea platform, created a necessity for acquiring new buoys while upgrading the existing ones. The experience gained over the last 5 years, from the operation of the POSEIDON I system, helped considerably in finding the proper solutions while locating the system malfunctions and inefficiencies.

References

Zervakis, V., E. Krassakopoulou, G. Assimakopoulou, P. Renieris, A. Ballas, A. Mallios, and E. Papageorgiou (2003). *In situ* calibrations of biofouling-prone oceanographic sensors in the framework of the POSEIDON project. Building the European Capacity in Operational Oceanography, Proceedings of 3rd International Conference on EuroGOOS, 3–6 December 2002, Athens, Elsevier Oceanography Series, pp. 373–375.

G. Triantafyllou, G. Petihakis, K. Dounas and A. Theodorou (2001). Assessing marine ecosystem response to nutrient inputs. Marine Pollution Bulletin, 43(7–12):175–186.

Soukissian, T.H. and G.Th. Chronis (2000). POSEIDON: A marine environmental monitoring, forecasting and information system for Greek Seas. Mediterranean Marine sciences, 1, 1, pp. 71–78.

Soukissian T.H., G.T. Chronis and K. Nittis (1999). POSEIDON: Operational marine monitoring system for Greek seas, SEA TECHNOL 40 (7).

Nittis K., V. Zervakis, L. Perivoliotis *et al.* (2001). Operational monitoring and forecasting in the Aegean Sea: System limitations and forecasting skill evaluation, MAR POLLUT BULL 43 (7–12): 154–163.

Perivoliotis, L., K. Nittis, A. Charissi, G. Gemelli (2005). An integrated service for oil spill detection and forecasting in the marine environment. This volume page 381.

Irish seabed mapping operations, bathymetric data and implications for oceanographic modelling

Jonathan White*[1], Kieran Lyons[1], Sheena Fennell[1], Pauline Ní Fhlatharta[1], Sean Cullen[2], Eibhlin Doyle[2] and Fiona Fitzpatrick[1]

[1]*Marine Institute, Ireland*
[2]*Geological Survey of Ireland*

Abstract

The Geological Survey of Ireland began surveying the Irish EEZ in 1999. Since then, in strategic partnership with the Marine Institute, as the Irish National Seabed Survey (INSS), 413 760 km^2 of Irish waters between the 200 m and 4 500 m contours have been surveyed. Prior to collection of these data, much of the Irish coastal area was last surveyed between 1840 and 1935 using leadline, with deeper waters surveyed using only single beam echo sounders with low coverage and data extrapolated to full coverage (UKHO, 2003).

Data from the INSS assist National policy and obligations to international agreements, support sustainable development of marine activities, renewable and non-renewable resources, enable habitat mapping (MESH, 2005) and further research by the academic and technological communities. The Marine Institute use XYZ data in the creation of bathymetric grids for oceanographic modelling. The extent of discrepancies encountered between INSS data and historic soundings, currently being used for much of the oceanographic modelling of the area and implications are highlighted here.

Keywords: Bathymetry, oceanographic modelling, seabed surveying, Northeast Atlantic

1. Introduction

As highlighted by Holt *et al.* (2004) there has been rapid increase in both resolution and run lengths of shelf sea models over recent years, attributable to improvements in high performance computing, enabling representation of marine processes occurring at much finer resolution. This has been paralleled by increasing availability of physical oceanographic data through heightened demand by the oceanographic and forecasting community for new data collection, and notably through opening up of the community at large to data exchange, owing to development, acceptance and respect of data policies. This is a significant and continuing progression in European oceanography, permeated by International and National data policies such as those of EuroGOOS (2000), the IOC (2003), and the Marine Institute's Data Policy (2004).

Model developments over the Northeast Atlantic domain include the North Atlantic models of Mercator (2003) — resolution of 0.06° (5–7 km); Proudman Oceanographic Laboratories Coastal Ocean Modelling System — horizontal resolution of 1.8 km and the UK Met Office's specific wave models — European resolution of 0.25° (N–S): 0.4° (E–

* Corresponding author, email: jonathan.white@marine.ie

W) and UK resolution of 0.16° (N–S): 0.11° (E–W) (Weaver *et al.*, 2002). All are dependent upon historic bathymetric data, which while collected with the utmost precision available at the time, is nonetheless, questionable for application in oceanographic modelling.

Potential inaccuracies in available bathymetry are twofold: firstly, much data originates from the UK Hydrographic Office, developed for navigation and as such is given as shoal bias to provide mariners with minimal anticipated clearance (Pepper, pers. comm.); secondly, much of the data for the region originates from surveys with sporadic coverage — the majority of the west European bathymetric data were collected with "incomplete coverage echo sounder" or "leadline between 1840 and 1935" (UKHO, 1997). These techniques are highly accurate in horizontal positioning, however, they tend to miss seabed features below the scale of the survey grid.

Quality controlled XYZ data from multibeam echo sounders of the INSS, gridded at 0.005°, became available to the Marine Institute in the autumn of 2004 and provided extensive coverage off the west coast of Ireland (Figure 1).

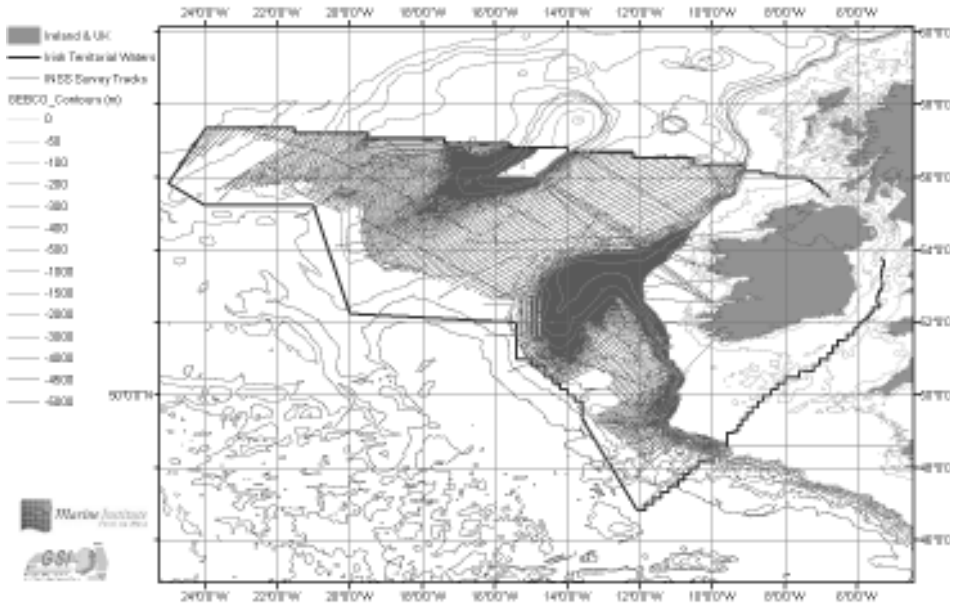

Figure 1 Irish National Seabed Survey tracklines indicating coverage of processed bathymetry data for oceanographic modelling.

2. Discussion

Comparison of GEBCO (General Bathymetric Chart of the Oceans, 2003) 1 minute (Figure 2) and INSS bathymetry (Figure 3; 0.005° regridded to 1 minute) as proportional difference shows good agreement for the vast majority of the territory. Areas of over- and under-estimates in reported GEBCO depths are also apparent (Figure 4). Discrepancies are most evident along the Irish shelf slope, running north of the Porcupine Bank and inshore to its east. In these areas GEBCO reports shoaler, in the ranges of 1:0.75 to

1:0.90, peaking in certain areas between 1:0.50 to 1:0.75. Similar instances are observed to the west of The Rockall Bank, in the Hatton–Rockall Basin and to the southwest of this area. On the Porcupine Bank GEBCO reports deeper than the INSS, between 1:1.10 and 1:1.75. Differences are also evident along the Goban Spur, where both positive and negative discrepancies range in the order of 1:1.75 to 1:0.75. GEBCO report areas over the Porcupine Bank (~300 m in depth) deeper than INSS data up to 150 m, while GEBCO depths on the shelf edge at ~1400 m are coincidental with INSS depths of 1050 m, a discrepancy of 350 m.

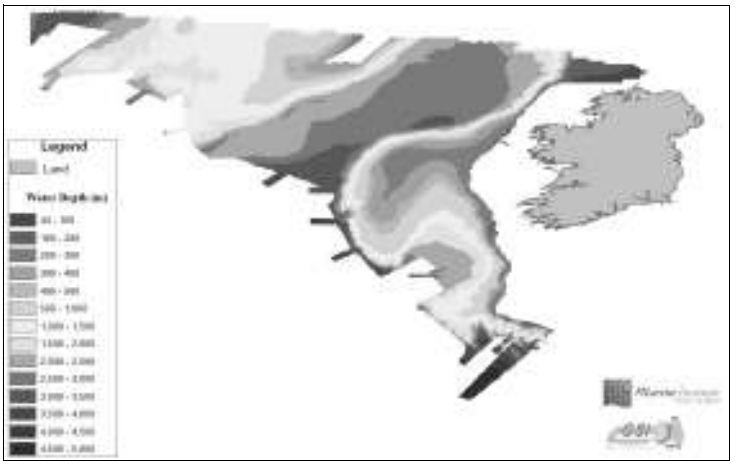

Figure 2 GEBCO 1 minute resolution.

Figure 3 Irish National Seabed Survey 1 minute resolution.

The value of accurate bathymetry for oceanographic modelling in the North Sea — an area with much better coverage and anticipated improvement through NOOS (North West Shelf Operational Oceanographic System) — are noted by Zijderveld and Verlaan (2004). Available data sets in this area are identified as GEBCO (1 minute resolution)

and ETOPO (2 minute resolution), acknowledged as being 20 years old, yet relatively modern compared to coverage west of Ireland. The rapid increase in computing power and availability of oceanographic data for model initiation and validation is increasing the resolution of events which can be resolved (Holt *et al.*, 2004); however, in the current climate and in line with results of these comparisons it appears that more significant inaccuracies in models are going to arise from inaccurate bathymetric data. EuroGOOS instigated development of non-shoal biased gridded bathymetric data for hydrographic modelling in European waters in association with the UKHO (Nic Flemming, pers. comm.). To date, this is still in development and with the evident improvement in soundings gathered by the INSS, there is clearly much progress to be made in data licensing, agreements and amalgamation. The improved oceanographic modelling work will be developed by the Marine Institute over the foreseeable future using INSS data, and comparable work is being done by other European National and International agencies. The requirements of European programmes such as GMES for high accuracy modelled forecasts in this geographic area, should inspire and progress National and International justification for continuation and development of seabed mapping in the North Eastern European waters, Irish waters and indeed across Europe.

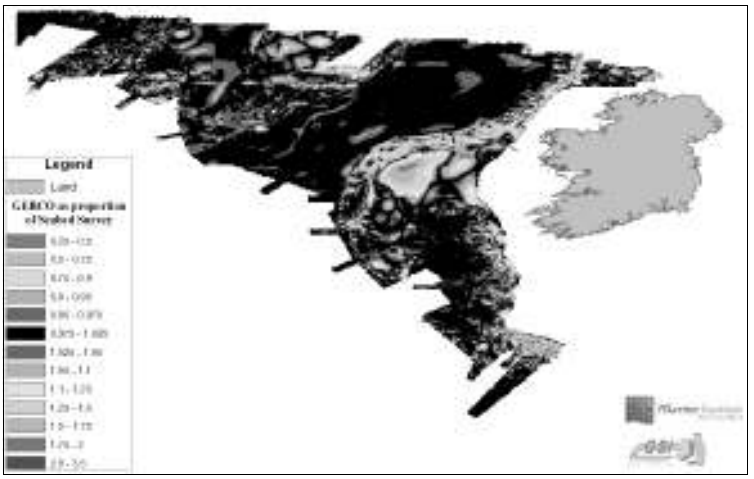

Figure 4 GEBCO bathymetry as a proportion of INSS bathymetry.

Acknowledgements

The authors would like to thank all individuals who have worked on the Irish National Seabed Survey.

References

EuroGOOS (2000). EuroGOOS Data Policy: Policy and practice for EuroGOOS for exchange of oceanographic and related data and products including guidelines on relationships in commercial oceanographic activities. EG99.37.

GEBCO (2003). General Bathymetric Chart of the Oceans Centenary Edition. British Oceanographic Data Centre, UK.

Holt, J.T., E.F. Young, R. Proctor and S.L. Wakelin (2004). High resolution hydrodynamic model-observation comparisons on the shelf west of Great Britain. Geophysical Research Abstracts, Vol. 6. 03813.

IOC Oceanographic Data Exchange Policy (Res. IOC−XXII−6, 2003). The Intergovernmental Oceanographic Commission.

Marine Institute (2004). Data Policy Version 1.0. Marine Institute, Ireland.

Mercator (2003). www.mercator-ocean.fr

MESH (2005). Development of a framework for Mapping European Seabed Habitats. www.searchmesh.net

UKHO (2003). United Kingdom and Republic of Ireland Continental Shelf Admiralty Surveys including contract Surveys to Admiralty Specifications to 31st March, 2003, United Kingdom.

Weaver, N., A. Saulter and M. Holt (2002). Developments in operational wave forecasting at the Met Office. British Wind Energy Association 24th Annual Conference.

Zijderveld, A. and M. Verlaan. (2004). Towards a new gridded bathymetry for storm surge forecasting in the North Sea. Geophysical Research Abstracts, Vol. 6. 05177.

The ICES annual ocean climate status summary 2004

Sarah L. Hughes*[1] and Alicia Lavín[2]

[1]*Fisheries Research Services (FRS) Marine Laboratory, Aberdeen, UK*
[2]*Instituto Español de Oceanografía, Laboratorio de Santander, Spain*

Abstract

The ICES Annual Ocean Climate Status Summary is prepared each year by the ICES Working Group on Oceanic Hydrography (WGOH). The IAOCSS is an ICES contribution to GOOS, summarising a large and complex dataset in a timely manner and in an accessible format. Ocean climate data from 15 regions around the North Atlantic are brought together by WGOH members and summarised in the report. This paper presents a summary of the results from the 2004 IAOCSS report. In almost all areas of both eastern and western North Atlantic during 2004, temperature and salinity in the upper layers remained higher than the long term average, with new records set in numerous regions. There was isolated cooling off the eastern North American coast. In most areas the trend over the last decade (1994–2004) has been one of warming.

Keywords: Climate change, North Atlantic, temperature, salinity, timeseries data.

1. Introduction

Ocean climate data from fifteen regions around the North Atlantic are described in the ICES Annual Ocean Climate Status Summary (IAOCSS); data from the 2004 report are summarised here. The IAOCSS report is prepared by the ICES Working Group on Oceanic Hydrography (WGOH), and represents an ICES contribution to the GOOS programme. The IAOCSS report summarises a large and complex dataset just a few months after the year of collection and presents the data in a clear and accessible format. Observations from one year are compared to the average conditions and the longer-term trends in each dataset. The data have usually been collected as part of a standard oceanographic section, repeated annually or more frequently. From a large dataset at each location, summary timeseries are created as indicators of conditions in that particular area.

Data are presented as anomalies in order to show how the values compare to the average or 'normal' conditions. Normal conditions refer to the long-term average of each parameter during the period 1971–2000. For datasets that do not extend as far back as 1971, the normal conditions have been calculated from the start of the dataset up to 2000. Where necessary, the seasonal cycle has been removed from each dataset, either by calculating the average seasonal cycle over the period 1971–2000, or drawing on other sources such as regional climatological datasets. The anomalies have also been normalised with respect to the standard deviation of the annual data over the base period.

* Corresponding author, email: S.Hughes@marlab.ac.uk

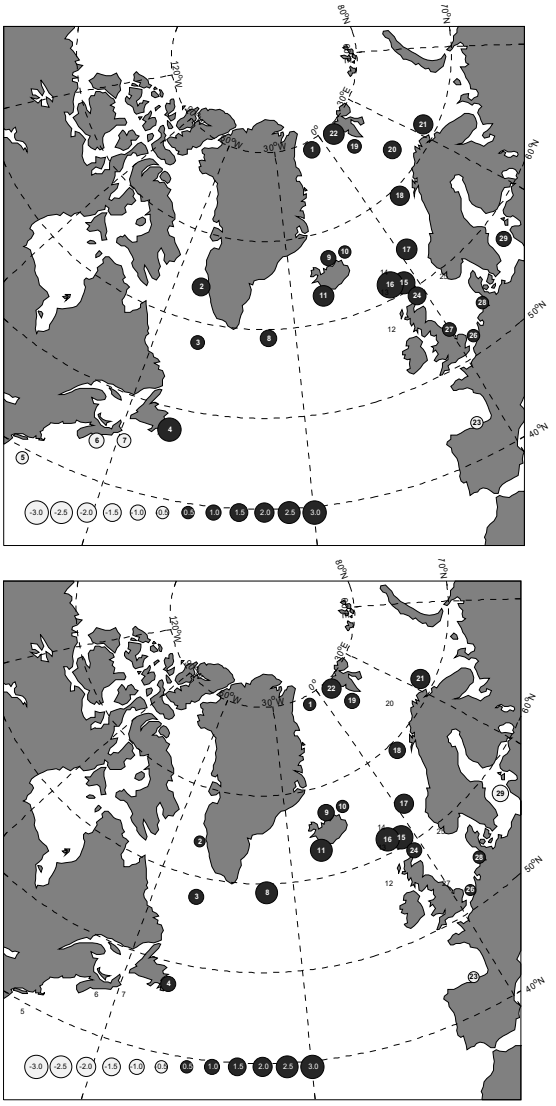

Figure 1 Annual average upper layer anomalies from WGOH *in situ* data, (top: temperature, bottom: salinity). The anomalies are normalised with respect to the standard deviation, e.g. a value of +2 indicates that the data (temperature or salinity) for that year was 2 standard deviations above normal. Normal conditions are the mean values calculated from all data available in the base period 1971–2000; note that some timeseries are shorter than others. An index number with no circle indicates that there was no data available for 2004 at the time of publication.

2. Conditions in 2004

Figure 1 (top) shows temperature anomalies during 2004 for all areas of the North Atlantic. In most areas the annual average temperatures were between 1 and 2 standard deviations above normal conditions. The highest values in 2004 were observed in the

Faroe–Shetland Channel (Index number 16, Figure 1) where the temperature was 3.75 standard deviations above normal. In a number of other areas (4: Newfoundland Shelf, 11: South East Iceland, 18: Southern Norwegian Sea) values were also very high, more than 2 standard deviations above normal. A notable exception was the eastern North American Coast, where temperatures during 2004 were around 1 standard deviation below normal. Salinities in the upper layers were also higher than normal following a similar pattern to that of temperature (Figure 1, bottom). The Baltic Sea (29) is the only region with a strong negative salinity anomaly, and in fact salinities at this site have been steadily decreasing since 1978 (ICES, 2005).

In 2004 the ICES WGOH added some supplementary data to the IAOCSS, namely a gridded sea-surface temperature (SST) dataset for the North Atlantic extracted from the Optimum Interpolation SSTv2 dataset, provided by the NOAA–CIRES Climate Diagnostics Center in the USA. Figure 2 shows the SST anomaly for 2004 calculated from this gridded dataset. Although there is some question about the accuracy of the data in high latitudes where *in situ* data is sparse and satellite data are hindered by cloud cover, the pattern of SST anomaly for 2004 is very similar to that seen in the WGOH temperature data (Figure 1, left). From this figure we can see a large band of positive anomalies stretching across both sides of the North Atlantic ocean. The area of negative anomalies on the eastern North American coast is also very clear.

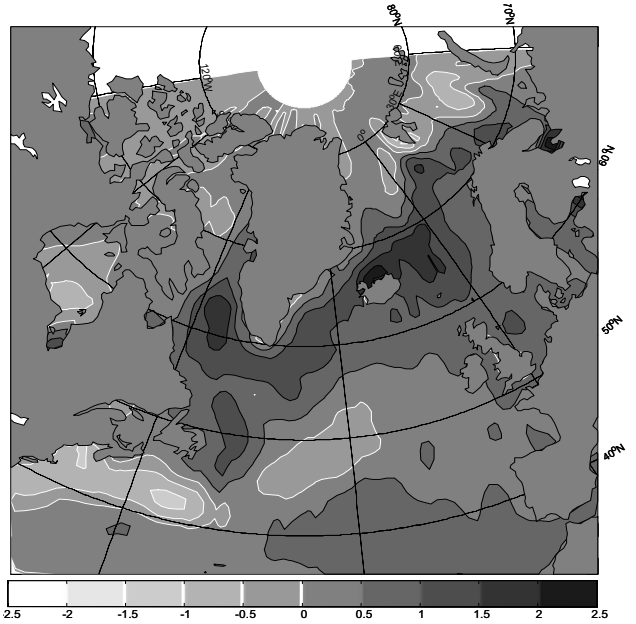

Figure 2 Annual Average Sea Surface Temperature Anomaly (°C) for 2004 from the NOAA Optimum Interpolation SSTV2 dataset, provided by the NOAA–CIRES Climate Diagnostics Center, USA. The anomaly is calculated with respect to normal conditions for the period 1971–2000. The data are produced on a one-degree grid from a combination of satellite and *in situ* temperature data. Dark grey shading indicates a positive anomaly, lighter grey shading highlighted with a white border indicates a negative anomaly.

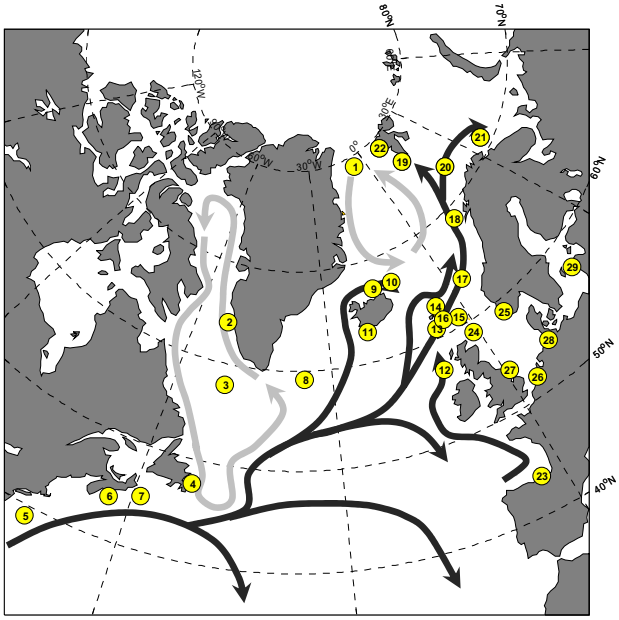

Figure 3 Map showing the location of each of the timeseries along with a schematic of the surface circulation of the North Atlantic. Light grey arrows show the cooler waters of the sub-polar gyre. Dark grey arrows indicate the movement of warmer waters in the sub-tropical gyre.

3. Long Term Trends

The general pattern of oceanic circulation in the upper layers of the North Atlantic in relation to the areas described in the IAOCSS report is shown in the schematic of Figure 3. In most areas the trend over the last decade (1994–2004) has been one of warming. This warming has been particularly evident in the northwest European shelf region where record high values have been observed in 2003 and 2004 (Figure 4c) and in the North Sea (Figure 4f). The rising trend in temperature over the last decade can be clearly seen in Atlantic waters flowing further north towards the Arctic (Figure 4d) and also in the cooler waters of the sub-polar gyre (Figure 4a). A notable exception to this trend are the waters on the eastern North American coast (Figure 4b), in which the temperatures have decreased to lower than normal levels over the last five years (1999–2004).

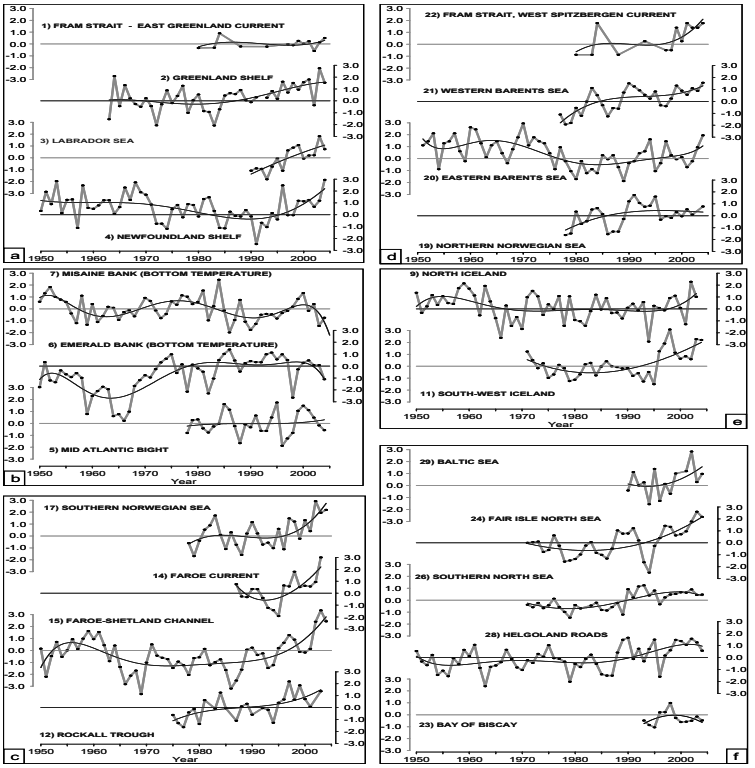

Figure 4 Timeseries of temperature anomaly from selected WGOH *in situ* data for the period 1950–2000. Thick lines with dots indicate annual average anomalies. Thin lines show the decadal scale trend in the data, derived from a polynomial fit. The anomalies are normalised with respect to the standard deviation, e.g a value of +2 indicates that the data was 2 standard deviations above normal. Normal conditions are the mean values calculated from all data available in the base period 1971–2000.

Acknowledgements

All of the data presented in this paper and the ICES Annual Climate Status Report are contributed by members of the ICES Working Group on Oceanic Hydrography. This paper would not be possible without the commitment made by these members, their institutes and the funding bodies to the continuation of these valuable oceanic timeseries.

References

ICES (2005). The Annual ICES Ocean Climate Status Summary 2004/2005, Hughes, S.L. and A. Lavín (eds.) ICES Cooperative Research Report, No 275, 37pp.

The scales of the surface temperature and salinity fields in the southern Aegean Sea as derived from FerryBox space-series measurements

Harilaos Kontoyiannis* and Dionysios Ballas

Hellenic Centre for Marine Research

Abstract

The spatial scales of the surface temperature and salinity fields in the Aegean Sea are examined from space-series measurements obtained from a flow-through system installed on a ship of opportunity that travels daily between Athens and Crete. The first eight months of the operation of this system yielded space-series measurements that span a continuous record of ~60 days during the winter period 2003–2004 and on monthly continuous records in late autumn 2003 and late spring 2004.

A north–south gradient, with values increasing towards the south characterises the salinity and temperature records. This change varies from trend-like (smooth and continuous) to abrupt (front-like). Higher variability exists in the northern half of the route during all seasons. The space-series were de-meaned and the dominant scales of the temperature and salinity eddy fields were examined based on the zero-crossing of the autocorrelation functions. Separate calculations were carried out for the northern half of the route, over depths not exceeding 800 m, and for the southern half of the route which is into the Cretan Sea over depths 1000–1500 m.

All dominant scales are higher (~50 km) during the winter homogenisation period and lower (~20 km) during late fall and late spring. However the temperature records in the Cretan Sea indicate an opposite tendency in the de-meaned records, because in these records the mesoscale temperature variability is superimposed on a long-scale north–south transition to higher temperatures which determines the shape of the autocorrelation functions. The purely mesoscale variability, however, preserves the basic characteristic of higher scales in winter, lower in summer.

Keywords: hydrography, eddy fields, spatial scales, ships of opportunity, FerryBox, flow-through systems

1. Introduction

In November 2003, a flow-through system (Figure 1) was installed on board the ferry KRHTH II that travels every night between Piraeus near Athens and Heraklion in Crete (Figure 3 top) returning to each port every other day. This system provides very dense (600-metre averaged) surface measurements of temperature, salinity, fluorescence and turbidity of sea-water that is pumped into the ship from a depth of 5 m and is used for cooling of the air-conditioning motors of the ship.

* Corresponding author, email: hk@hcmr.ath.gr

Figure 1 The flow through system.

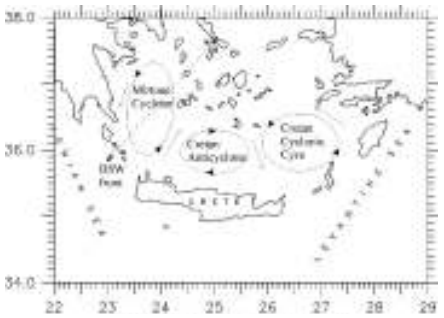

Figure 2 Sketch of dynamic structures in areas of ferry-box route. The Black Sea Water (BSW) front is approximately along the SW–NE line.

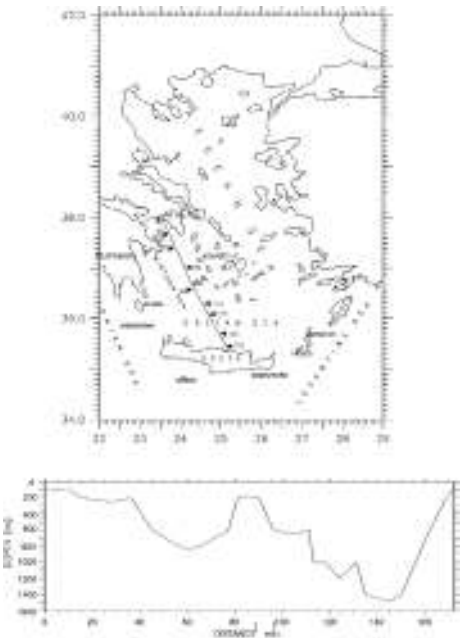

Figure 3 top: ferry route; bottom: along-route bathymetry.

The area of this 'ferry-box' route is associated with highly variable and not very well-known dynamic structures in the northern part, in which the depths do not exceed 800 m (Figure 3 bottom) and by the typical mesoscale structures of the Cretan Sea over depths exceeding 1000 m (Figure 2), which themselves exhibit variability (Theocharis *et al.*, 1999) but are less influenced by nearby islands or coastal areas as in the northern half of the route.

2. Results

The first eight months of operation of this ferry box system yielded, among a series of problems (www.poseidon.ncmr.gr/ferrybox), space-series measurements of surface temperature and salinity which span a continuous record of nearly 60 days during the winter mixing period (January 2004 to March 2004), and monthly continuous records in late autumn 2003 and late spring 2004, characterised as periods of correspondingly progressive breakdown and development of the seasonal thermocline.

Figure 4–Figure 6 show characteristic examples of variability in the salinity and temperature space-series records that is exhibited during seven-day (synoptic) periods in late autumn 2003, winter and late spring 2004. A north–south gradient exists in these records. Occasionally this gradient is smooth as in winter and spring (Figure 5 and Figure 6) and other times is abrupt as in the late-autumn salinity series and resembles a

frontal structure (Figure 4). It should be noted that the sharp salinity gradients in the northern 80 miles of the route are expected to be influenced by the spreading of the Black Sea water plume which presents a strong seasonal signal during late autumn in the southwestern Aegean Sea (Figure 2).

To examine the dominant spatial scales in the salinity and temperature eddy fields, the auto-correlation functions were computed from all space-series (Lumley and Panofsky, 1964). Separate calculations were carried out for the northern half of the route and for the part of the route into the Cretan Sea. Prior to computing the autocorrelation function the space series were de-meaned only; no special treatment such as filtering or de-tiding was applied to these space series, since the tidal signal is negligible. Figure 7 shows an example of correlation functions in November 2003, while Figure 8 shows the overall evolution in the dominant scales (expressed by the zero-crossing) through the available observations.

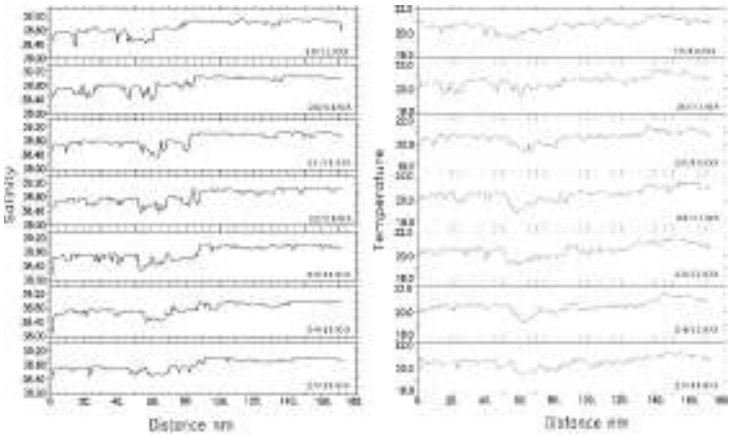

Figure 4 Salinity (left) and temperature (right) space-series records from 19–25 November 2003.

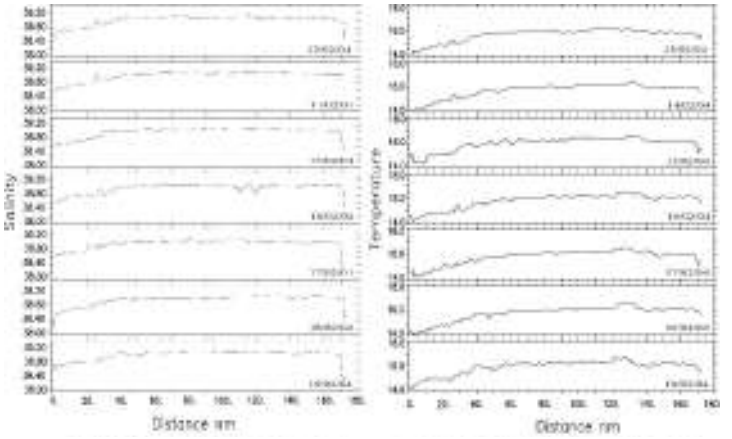

Figure 5 Salinity (left) and temperature (right) space-series records from 13–19 February 2004.

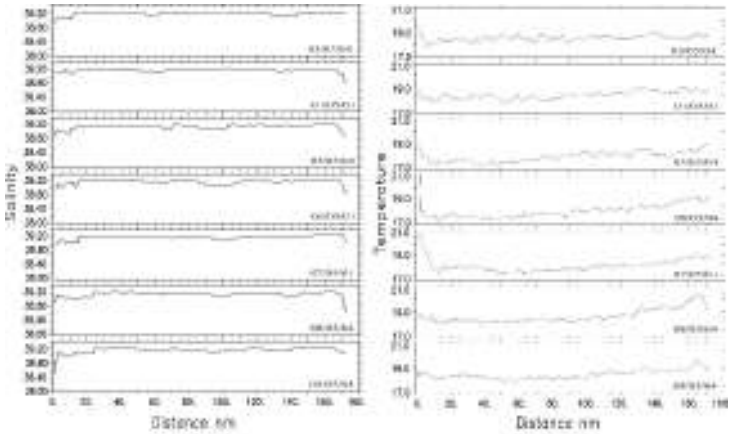

Figure 6 Salinity (left) and temperature (right) space-series records from 3–9 May 2004.

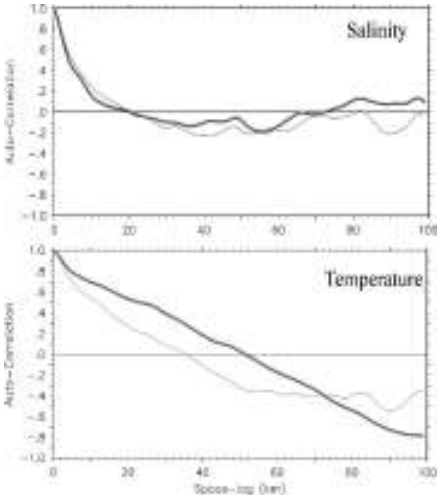

Figure 7 Seven-day averaged spatial auto-correlation functions of salinity and temperature during the period 19–26 November 2003. Thin lines are for the northern 80 miles of the route, while thick lines are for the remaining south part. Zero-crossing is the distance from the origin at which the correlation crosses the x axis. The dominant spatial scale is characterised by the zero crossing.

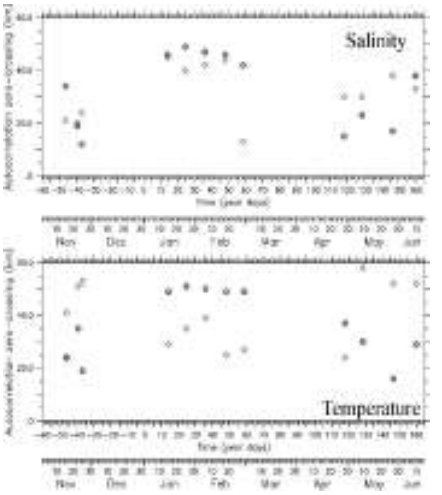

Figure 8 Time-evolution of the zero-crossing of the auto-correlation functions of salinity and temperature. The zero-crossing values are based on 10-day averages of corresponding auto-correlations. Thick circles are for the northern 80 miles of the ferry-box route, and thin diamonds for the southern part in the Cretan Sea.

3. Conclusions

In general, there is a tendency for all dominant scales to be higher in winter (~50 km) and lower (~20 km) in late autumn and late spring. However, the temperature records in the Cretan Sea indicate an opposite tendency in which higher eddy scales are detected in late

autumn and late spring and lower eddy scales in winter. This occurs because in late autumn and late spring there is a trend-like increase in temperature from route-mile ~100 to route-mile ~180 (Figure 4 and Figure 5). This long trend results in higher spatial scales. It is obvious that these observations are more sensible when they are combined with pictures of the concurrent dynamic structures along the route. This is associated with the need for the synergy of FerryBox and remote-sensing data.

Acknowledgements

The present work is funded by the European Commission FP5 contract EVK2–CT–2002–00144.

References

Theocharis A., E. Balopoulos, S. Kioroglou, H. Kontoyiannis, and A. Iona (1999). A synthesis of the circulation and hydrography of the South Aegean Sea and the Straits of the Cretan Arc (March 1994–January 1995), Progress in Oceanography, 44, 469–510.

Lumley J. and H. and Panofsky (1964). The structure of the Atmospheric Turbulence. John Wiley and Sons, New York

Multidisciplinary investigations at the deep-sea long-term station "Hausgarten" (Fram Strait, Arctic Ocean)

Thomas Soltwedel*, Eduard Bauerfeind, Melanie Bergmann, Karen von Juterzenka, Michael Klages, Jens Matthiessen, Eva-Maria Nöthig, Eberhard Sauter and Ingo Schewe

Alfred-Wegener-Institut für Polar- und Meeresforschung, Germany

Abstract

The deep-sea long-term observatory "Hausgarten" of the Alfred Wegener Institute for Polar and Marine Research, Germany, was established in summer 1999 in the eastern Fram Strait off Spitsbergen. Beside a central experimental area at 2500 m water depth, we defined 9 stations along a depth transect between 1000–5500 m, and an additional 6 stations along a latitudinal transect crossing the central "Hausgarten" station, which will be revisited yearly to analyse seasonal and interannual variations in biological, geochemical and sedimentological parameters.

Moorings carrying current meters and sedimentation traps are used to assess hydrographic conditions in the area and to characterise and quantify organic matter fluxes to the seafloor. The exchange of solutes between the sediments and the overlaying waters are studied to investigate major processes at the sediment-water-interface. Vertical gradients of nutrients, organic carbon contents, C/N ratios, porosity and other geochemical parameters are determined to characterise the geochemical milieu of the upper sediment layers. Biogenic sediment compounds are analysed to estimate activities and total biomass of the smallest sediment-inhabiting organisms. The quantification of benthic organisms from bacteria to megafauna is a major goal in biological investigations.

Keywords: Long-term investigations, multidisciplinary, deep sea, Arctic Ocean, global change

1. Introduction

The deep sea represents the largest ecosystem on earth. Due to its enormous dimensions and inaccessibility, the deep-sea realm is the world's least known habitat. To understand ecological ties, the assessment of temporal variabilities is essential. Only long-term investigations at selected sites, describing seasonal and interannual variations, can help to identify changes in environmental settings determining the structure, the complexity, and the development of deep-sea communities. The opportunity to measure processes at sufficient time scales will also help to differentiate between natural variabilities and environmental changes due to anthropogenic impacts.

Climate change comprises severe threats to mankind and there is a strong need for a long-term and large-scale commitment to the monitoring of global change. High latitudes are amongst the most sensitive environments with respect to climate change, a

* Corresponding author, email: tsoltwedel@awi-bremerhaven.de

fact urgently demanding the assessment of time series especially in polar regions. To detect and track environmental changes at a deep-sea site in the transition zone between the northern North Atlantic and the central Arctic Ocean, and to experimentally determine the factors controlling deep-sea biodiversity, the German Alfred Wegener Institute for Polar and Marine Research (AWI) established the deep-sea long-term observatory "Hausgarten", representing the first, and so far only open-ocean long-term station in a polar region.

Multidisciplinary long-term investigations at "Hausgarten" address the central issue of monitoring ocean margin environments and, hence, will help to identify disturbances of the ecosystem from a creeping or an episodic introduction of human impacts. By building up a sound database, our investigations will contribute to a better assessment of the status of benthic communities and the entire deep-sea ecosystem, thereby providing a baseline for future studies. Long-term data assessed at "Hausgarten" will help to distinguish between normal (natural) amplitudes of change and man-induced changes, and hence contribute to a sustainable management and a safer use of European continental margins.

2. "Hausgarten" observatory

"Hausgarten" consists of 15 permanent sampling sites along a depth transect from Vestnesa Ridge to the Molloy Deep (1000–5500 m) and along a latitudinal transect following the 2500 m isobath crossing the central "Hausgarten" site (Figure 1), which serves as an experimental area for long-term experiments at the deep seafloor.

Repeated sampling and the deployment of moorings and different long-term lander systems, which act as local observation platforms, has taken place since the beginning of the station in summer 1999. Frequent visual observations with towed photo/video systems allow the assessment of large-scale distribution patterns of bigger epibenthic organisms. At regular intervals, a work capable Remotely Operated Vehicle (ROV) is used for targeted sampling, the positioning and servicing of autonomous measuring instruments, and the performance of *in situ* experiments and geo-referenced video-footage. A 3000 m depth rated Autonomous Underwater Vehicle (AUV), will extend our sensing and sampling programmes in the near future; first scientific missions at "Hausgarten" are projected for autumn 2005.

Multidisciplinary research activities at "Hausgarten" observatory are carried out in close co-operation with Belgian, Polish and Russian colleagues, and cover almost all compartments of the marine ecosystem from the pelagic zone to the benthic realm, with some focus on benthic processes. Water column studies comprise the assessment of physical and chemical parameters as well as flux measurements of particulate organic matter to the deep seafloor. At the sediment-water interface, the measurement of pore-water oxygen profiles provides a suitable tool for the determination of C_{org} fluxes and of C_{org} remineralisation rates. Benthic investigations comprise biochemical analyses to estimate the input of organic matter from phytodetritus sedimentation and activities and biomasses of the small sediment-inhabiting biota as well as assessments of distribution patterns of benthic organisms (covering all size classes from bacteria to megafauna) and their temporal development.

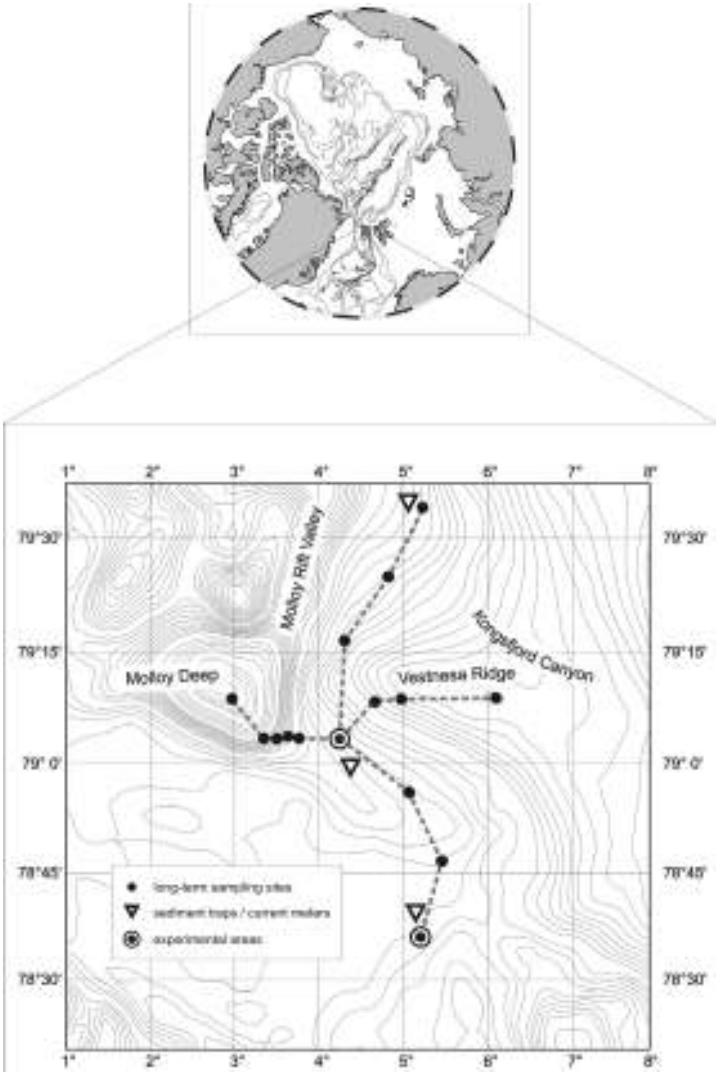

Figure 1 Deep-sea long-term station "Hausgarten" in the Fram Strait, Arctic Ocean.

3. First Results

Six years of investigations at "Hausgarten" are certainly too short to produce a sound database to evaluate ecosystem shifts in relation to environmental changes. Nevertheless, our data exhibit some interesting trends, but so far we do not know whether they indicate long-lasting alterations of the system or simply reflect natural variability on multi-year time-scales, e.g. in relation to variations in the Arctic Oscillation. Water temperatures in the Fram Strait have significantly increased over the last years. Between the summers of 2003 and 2004, a massive temperature increase of 0.6°C was observed within the upper 500–1000 m of the water column. Our own temperature records covering the years 2001 through 2004 exhibited not only small seasonal variations but also an overall slight

temperature increase even at 2500 m water depth at the central “Hausgarten”. Analyses of biogenic sediment compounds between the summers of 2000 and 2004 revealed a general decreasing input of phytodetritial matter to the seafloor, and subsequently, a decreasing trend in sediment-bound organic matter and “total microbial biomass” (estimated from phospholipid measurements) in the sediments. An ongoing trend in decreasing organic matter fluxes will certainly affect the entire deep-sea ecosystem.

4. Future Perspectives

The “Hausgarten” observatory is a long-term commitment of the Alfred Wegener Institute for Polar and Marine Research (AWI). At the same time, it represents the Arctic Node of the European Seafloor Observatory Network (ESONET) Initiative, a proposed sub-sea component of the European programme GMES (Global Monitoring for Environment and Security) to provide strategic long-term monitoring capability in geophysics, geotechnics, chemistry, biochemistry, oceanography, biology and fisheries. In this respect, “Hausgarten” will also play a vital role in a projected Arctic component of the “Global Ocean Observing System”, Arctic GOOS.

Acknowledgements

We gratefully thank the ships’ officers and crews of the German research-icebreaker POLARSTERN and the French RV L’ATALANTE for generously supporting us during numerous expeditions to “Hausgarten”. Experiments at the deep seafloor were not possible without the exceptional support of the Ifremer/Genavir ROV team from Toulon, France. We likewise thank our technical staff and students who have assisted in the collection and analysis of the material collected at “Hausgarten” observatory.

In situ and Remote Sensing Measurements

Development of the Irish National Tide Gauge Network

Guy Westbrook*[1], John Wallace[2] and Glenn Nolan[1]

[1]*Oceanographic services, Marine Institute, Ireland*
[2]*Marine Informatics Ltd., Ireland*

Abstract

Real time and predicted tidal data available in Ireland are generated from water level observations that are mostly undertaken in support of what is an effective integrated vessel traffic management system (VTMS). The resultant data often do not represent a true marine harmonic upon which future regional predictions can be accurately based. Maritime commerce, engineering and flood protection now require increased accuracy and resolution, and the Irish National Tide Gauge Network (INTGN) is a permanent infrastructure project that aims to build, over a number of phases, a full set of permanent, well-understood, tidal monitoring stations to fully resolve the situation around Ireland. The structure of the project is currently a private public partnership (PPP) between a state agency, the Marine Institute, and a high technology services provider, Marine Informatics. Phase 1 of the work is almost complete with 5 stations soon to be reporting data via GSM to a central location where an SQL database underlies a near real time web portal (www.irishtides.ie). During the development phase 'raw' data are reported for general information and interest to a growing potential user community, but the overall objective is to put these data to work and generate both a real time and predictive reporting capability. The work is being carried out through a number of strands where expertise and tools are being brought together to tackle the challenges of installation/ maintenance and quality assurance of these facilities. The robustness of the reporting capability and infrastructure will be tested through inter-comparison with state-of-the-art facilities currently in operation elsewhere.

Keywords: Ireland, tides, network, GSM, real time, operational, GLOSS, www.irishtides.ie, www.marine.ie/databuoy.

1. Introduction

In recent years a series of reports have detailed the infrastructure that exists within Ireland for monitoring coastal water levels (Sutton *et al.*, 1999; Murphy *et al.*, 2003). Copious evidence has been presented that the water level gauges are (1) often not in the correct place to fully resolve the tidal harmonic around the Irish coastline, (2) instrumentation is often not of sufficient quality to resolve the vertical movement to the <1 cm GLOSS standard, (3) predictions currently provided by third parties are, while very good considering model source data, not sufficiently accurate or precise and (4) there is no effective real time data reporting facility available.

* Corresponding author, email: guy.westbrook@marine.ie

This project serves to address these fundamental inadequacies and will provide a fully managed and quality assured reporting capability, i.e. a service that contributes to the quality of life of the population of Ireland; effectively resolve the Irish coastline (including seeking opportunities to include Northern Ireland); establish a permanent data acquisition infrastructure; instigate a planned maintenance system; establish a robust communications network; ensure data are effectively managed and disseminated within Ireland and beyond and make data available through agreement in national resource sharing activities.

2. Network Development

The project structure takes the form of a public private partnership bound by a simple contract allowing www.irishtides.ie to be adaptable as the final organisation of the network takes shape through a process of 'node' development. In this way discussion and negotiation may be ongoing with various parties at any instance in time, only becoming a fully interfaced node when all criterion are met and understood by all parties when a permanent arrangement can be established. Figure 1 shows a basic schematic of how a node can become part of the network. The process begins with local discussion to examine the business case for a site being established, this includes investigating local sources of funding for (1) capital purchase and (2) future current expenditure, e.g. maintenance and telecommunications. Once a position has been reached the node is assessed in terms of its usefulness to the national strategic monitoring framework and, if appropriate, capital monies are sought from various sources. At this point a new monitoring station is installed including a GSM enabled data logger, or this is added to existing infrastructure. Data from all nodes are reported to a central receiving station in Dublin which houses the Microsoft SQL web server and archiving system. In parallel with the data management structure are various efforts developing and reporting through a real time and predicative capability to harmonic analysis of the data sets as well as cross referencing, quality assurance and providing tailored data sets supporting the 'node sponsor'. Underlying these activities is a programme of work surveying and cross referencing data being recorded at each station — the 'node quality statement'. This will enable a full understanding of the quality of data being derived from each location and provide an understanding of the effort needed to be put into correcting any deficiencies.

2.1 Current status of the network

As of August 2005 the network has 5 stations interfaced and on-line (see Figure 2). All stations are reporting data which is transferred hourly (6 minute acquisition) to the central servers which underlie the web site www.irishtides.ie.

With respect to data quality, the information is of immediate use in harmonic analysis (in time) and determining real time information about the state of the diurnal and spring, neap cycle but more investigation and exhaustive cross comparison will be required to fully understand the nature of the data being reported relative to ordnance survey datum Malin Head. This is in hand and will continue as phase 2 of the network progresses.

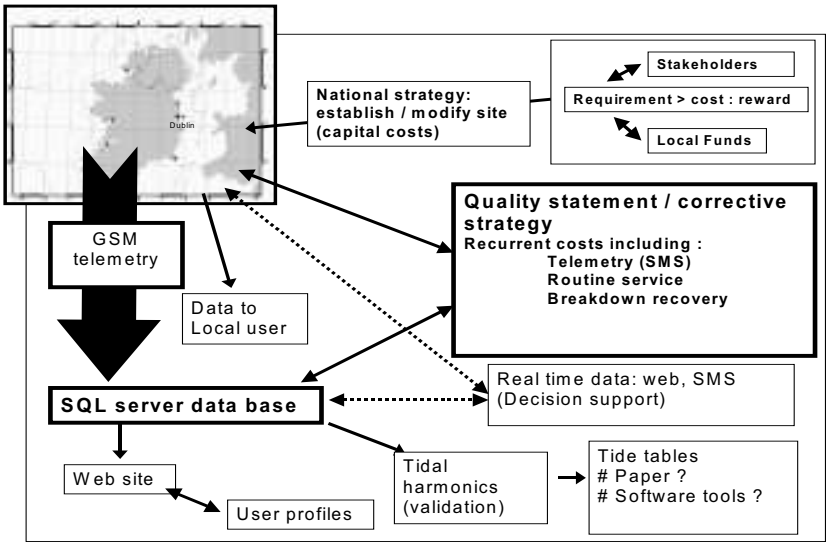

Figure 1 Schematic illustrating a high level view of 'node' development.

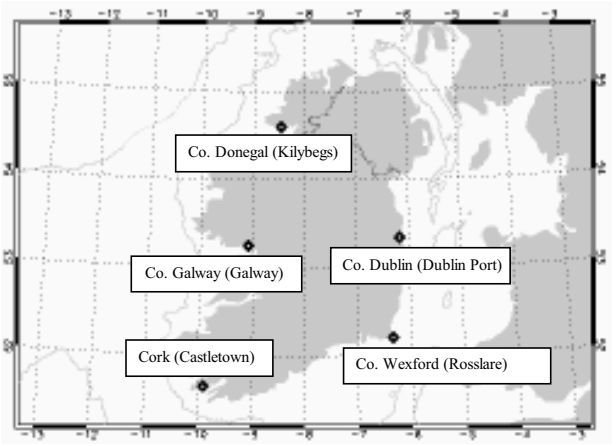

Figure 2 The August 2005 status of the developing network.

2.2 Case study

Phase 2 of the development includes a number of initiatives to both exploit existing requirements, as well as establish new stations to strategically expand the initial 5 stations to eventually resolve the southern Ireland coastline (in the first instance).

To illustrate the nature of the phase 2 development there follows a brief introduction to the work package being jointly implemented between the Irish national Tide Gauge Network and Dublin City Council (DCC).

Since a serious flooding event in February 2002, DCC have been involved in various engineering works to upgrade the flood defences in and around the Dublin area basin. Part of these works include the installation of a real time water level monitoring capacity

consisting of two river-mounted gauges to monitor two inter-tidal zone stations and one monitoring a marine harmonic (see Figure 3).

The infrastructure being deployed the INTGN is being established as a key system within the safety critical response capability, acting as a hub through which information is passed to the key decision makers in times of an imminent flooding emergency (see Figure 4). This serves to illustrate the scale of inter-organisational cooperation arising out of the work. It is anticipated that the system will be live and in use by the end of 2005.

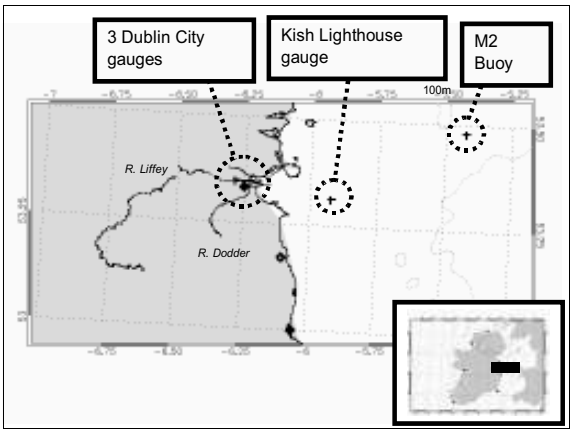

Figure 3 The location of the of the Dublin City sponsored nodes of the Irish National Tide Gauge Network.

2.3 'First cut' validation of data

A trial exercise was conducted to bring together two data sets: (1) data worked up by the Proudman Oceanographic Laboratory providing the Galway Harbour Company with a set of tide tables and (2) data collected by the new gauge installed in Galway Port (atmospheric pressure corrected). These data were cross referenced with the levelling datum (Ordnance Survey datum Malin Head) using equipment assembled for the purpose through contemporaneous measurements collected on site, see Figure 5A. Figure 5B illustrates preliminary results through a simple comparison between 'wl_irishtides.ie' (open squares) with the predictions 'wl_Galway Harbour Co.' (closed triangles) which show a significant difference in water level reported ranging from a minimum difference of 0.007 m to a maximum difference of 1.95 m, with an average of 1.07 m (n=106) over the 4 week period.

Although the results presented in Figure 5B show a similar general pattern, at this early stage it would only be appropriate to say that both the data sets are in some way incorrect when absolute accuracy is required, although generally speaking the two data sets correspond well in terms of phase with respect to time.

Knowledge of the site raises additional questions regarding the location as it is an area where regular and significant fresh water intrusion can and does have a significant affect on the physical structure of the tidal stream during the cycle. It is precisely this aspect of the inclusion of existing level monitoring stations that is, and will continue to be,

examined in great detail as the key component of the 'quality statements' discussed earlier (see Figure 1) progress, identifying the list of remedial actions required to obtain data of sufficient quality to report to the wider community.

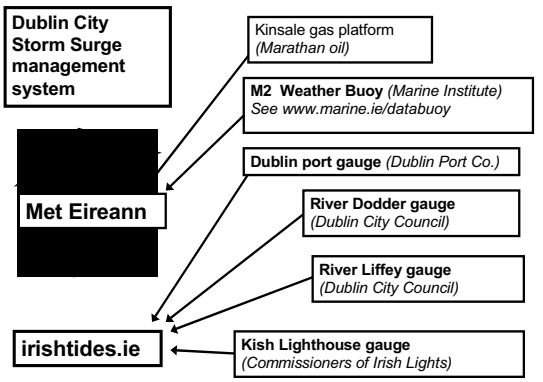

Figure 4 The role of the Irish National Tide Gauge Network within the Dublin area flooding emergency response system.

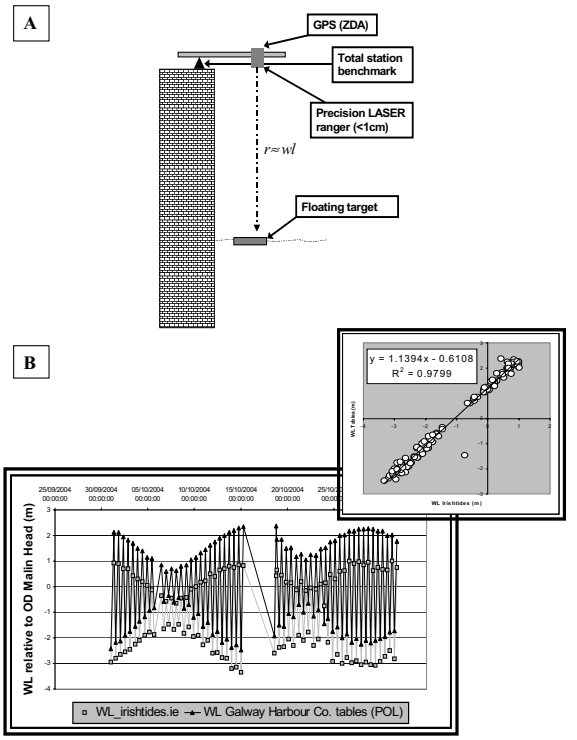

Figure 5 (A) A sketch of the equipment used to cross reference data collected on site with the survey datum and (B) an initial comparison between data provided to the Galway Harbour Company by the Proudman Oceanographic Laboratory.

3. Conclusions

The Irish national Tide Gauge Network is progressing at an acceptable pace, with the initial phase now complete. The structure of the network is in the form of a public private partnership, PPP, between an Irish Government state agency (the Marine Institute) and a small hi-technology service provider (Marine Informatics Limited). The partnership has proven adaptable to successfully allow for the inclusion of other parties in the structure of the organisation as it moves to phase 2 and roll out around the coast of Ireland. Whilst the primary objective is to establish a managed tidal monitoring network, at each stage that a new 'node' is under discussion the local need is considered first and solutions implemented as part of the work. Data policy is developing both centrally and in discussion with sponsors and will continue to do so in conjunction with various funding opportunities.

Through this network, Ireland will become self sufficient in the reporting of tidal data both in terms of a predictive and real time capacity to highly varied users across the private and public sector. Together with other national infrastructure initiatives (e.g. the Irish National Data Buoy Network, see www.marine.ie) this project makes a tangible and permanent contribution to the understanding and operational use of near-shore oceanography in the region. In time it will allow Irish specialists to contribute to and participate in the international monitoring networks and systems, building on existing Global Sea Level Observing System (GLOSS) monitoring efforts.

Acknowledgements

The authors wish to thank the following organisations for their time and effort thus far: The Marine Institute and their parent Irish Government Department: the Department of Communication, Marine and Natural Resources, The staff of Marine Informatics Limited, University College Cork, Irish Rail, Dublin Port Company, Dublin City Council, The Irish Association of Harbour Masters, the Environmental Protection Agency, Proudman Oceanographic Laboratory and the Galway Harbour Company.

References

Murphy, J., G.D. Sutton, C. O'Mahony and P. Woodworth (2003). Scoping Study To Assess the Status of Ireland's Tide Gauge Infrastructure and Outline Current and Future Requirements. Prepared for the Department of Communications, Marine and Natural Resources, University College Cork.

Sutton, G.D., A.J. Wheeler, J. Murphy and G. Nolan (1999). Scoping study to examine the feasibility of installing a national Tidal information archiving network. For Marine Institute (project leader in joint project with Hydraulic and Marine Research Centre, UCC, and Martin Ryan Institute, NUIG).

Bibliography

UNESCO (2002). Manual on Sea level measurement and Interpretation, Volume III — Reappraisals and Recommendations as of the year 2000. IOC Manuals and Guides No. 14, Volume III.

Comparison of eutrophication processes and effects in different European marine areas based on the results of the EU FP-5 FerryBox Project

D.J. Hydes*[1], C. P. Bargeron[1], B.A. Kelly-Gerreyn[1], H. Wehde[2], W. Petersen[2], S. Kaitala[3], V. Fleming[3], K. Sørensen[4], J. Magnusson[4], I. Lips[5] and U. Lips[5]

[1]*National Oceanography Centre, Southampton, UK*
[2]*GKSS, Germany*
[3]*FIMR, Finland*
[4]*NIVA, Norway*
[5]*EMI, Estonia*

Abstract

A key hypothesis of the EU FP-5 FerryBox Project is that the data from the FerryBoxes can be used to accurately and precisely determine the connection between environmentally significant processes such as eutrophication and their physical and biogeochemical driving processes. This is being tested by comparing evidence from the range of conditions sampled in the FerryBox project. An important development is a procedure for indexing the size and duration of blooms to facilitate comparisons between different years and areas. The results show the effectiveness of the data in linking the extent and duration of blooms to specific detectable physical features, such maximum concentrations of winter nutrients. Work on the measurement of dissolved oxygen suggests that these measurements provide important information to supplement that available from measurements of fluorescence particularly for the estimation of production.

Keywords: FerryBox, eutrophication, nutrients, numerical indicator, oxygen, fluorescence

1. Introduction

FerryBox is a European Union Science Framework project (FP5) funded to link the work of eleven groups with an interest in developing the use of ships of opportunity for scientific studies of marine systems. The structure of the project is described in this volume by Petersen *et al*. A key area of the work is developing the scientific application of the data sets collected. Eutrophication was chosen as a topic for study because of the wide concern around Europe about its extent and the possible consequences (C.E.C., 2000). Several examples of use of FerryBox are available for example investigations on abiotic factors controlling the potentially toxic cyanobacterial bloom occurrence (Lips, 2005), and the derived methods could be applied in for other areas. A key task of the FerryBox project was to establish procedures for the ready comparison of the data from the different systems and different areas where data was collected which range from the Baltic to the eastern Mediterranean Sea.

* Corresponding author, email: djh@noc.soton.ac.uk

The core FerryBox sensors used on all the routes are temperature, salinity chlorophyll-*a*-fluorescence and turbidity (Petersen *et al.*, this volume). The first stage of the comparison process is to provide a simple means of summarising the different data sets. Work by the NIVA team suggested that this could be done relatively simply on the basis of mean and variance in the data at different positions along each route over one year and then comparing one year with the next. The next stage is to test the idea that a numerical indicator (Baan and van Buuren, 2003) that has been derived from Baltic FerryBox data (Fleming and Kaitala, in press) can be used to compare conditions along other FerryBox routes. To test the relationship between the "spring bloom intensity index" and eutrophication, the index has to be compared with concentrations of dissolved nutrients driving the spring bloom. This requires that measurements of nutrients are made. In addition new methods are being tested in the project to see if they can enhance the information available from the standard set of sensors. On the Portsmouth–Bilbao route the discrete oxygen data has been used to derive estimates of organic carbon production as the relationship between oxygen and carbon is stoichiometrically constrained. This has the potential to produce continuous estimates of biological production when new sensors are used.

Due to the space restriction with this paper only data from the Portsmouth–Bilbao route operated by NOC and the FIMR route in the Baltic used to develop the plankton bloom indicator are presented.

2. Methods

2.1 Summary of annual data sets along FerryBox routes

To provide annual summaries of the data along the FerryBox route the data for each calendar year of operation is binned into an appropriate number of boxes for the particular route (for the Portsmouth–Bilbao route, this is was done at 0.1° latitude intervals). When different years are being compared, data is only binned from those periods when the system was in operation in each year. The mean and the variance in the data in each bin are then calculated.

2.2 Spring bloom intensity index

The procedure to be used is based on that developed by Fleming and Kaitala (in press). The running average was calculated from median chlorophyll *a* biomass per area per day. Missing day medians were substituted by interpolating adjacent medians. A chlorophyll *a* threshold level of 5 $\mu g l^{-1}$ was set to determine the beginning and end of the spring bloom. The threshold level was chosen by testing different values (c.f. Siegel *et al.*, 2002). 5 $\mu g l^{-1}$ was found to be suitable for the Baltic area. This value is low enough to detect the start of the bloom but high enough not to include fluctuations in the summer minimum as part of the bloom. The intensity index is calculated by an approximation of a time-intensity integral for the days where the chlorophyll *a* seven-day running average exceeded the threshold value of 5 $\mu g l^{-1}$. The length, peak and mean chlorophyll *a* level of the bloom are also calculated. If the chlorophyll *a* value descends below the threshold level in the middle of the bloom, the bloom is regarded as consisting of separate periods. Thus the intensity index and the length of the bloom are calculated using only the periods exceeding the threshold level. If the spring bloom did not exceed

the threshold level, the intensity index is zero, as are the length, peak and mean values. If the data did not cover the beginning of the bloom (i.e., data collection had started too late), the calculated intensity indexes are smaller than in reality and these years are flagged as such in the resulting data tables. A similar procedure of inspection was employed to determine the threshold value for the Portsmouth–Bilbao route. On this route because the determination is based on the continuous record of fluorescence measured on the ferry the threshold was found on the basis of the measured fluorescence. This was then converted to *in situ* chlorophyll *a* to make the index value comparable to values derived by Fleming and Kaitala (in press). This was done using data from monthly calibration crossings during which water samples were collected for the determination of *in situ* chlorophyll *a*. A fluorescence value of 3 $\mu g l^{-1}$ (apparent chlorophyll *a*) was found to give the best definition between the different areas along the route. This is about 50% higher than the median concentration (c.f., Siegel *et al.*, 2002), and is equivalent to 1–2 $\mu g l^{-1}$ *in situ* cellular chlorophyll *a*.

To compare the relationship between the spring bloom intensity index and nutrients Fleming and Kaitala (in press) used the geometric mean of the concentrations nitrate, phosphate and silicate, for the maximum observed concentrations prior to the bloom.

Table 1 Comparison of estimates of net community production ($g C m^{-2}$) over the spring summer period. See text for explanation of symbols and abbreviations.

Area	O2 W'92	O2 W&M'99	dNO3	dO2	dChl
CEC	80	38	19	9	18
WEC	63	33	19	15	19
Ush	119	60	24	17	9
SB	83	41	20	13	13
NBB	67	32	22	14	14
SBB	41	20	13	11	4

2.3 Use of dissolved oxygen measurements to estimate biological production

Between February and July 2004 measurements of dissolved oxygen were made on the monthly calibration crossings on the Portsmouth–Bilbao route. The difference between the observed oxygen concentration and the solubility of oxygen at the *in situ* temperature and salinity of the water sample (the oxygen anomaly) was calculated. The anomaly was used to determine the direction of the oxygen flux across the sea surface. It was then used with available wind speed data to estimate the oxygen flux across the sea surface. This gives a measure of net community production (Najjar and Keeling, 2000). For the data presented in Table 1, the estimates based on the two most commonly used parametrisations of the relationship between gas exchange and wind speed ("O2 W'92", Wanninkhof, 1992 and "O2 W&M'99", Wanninkhof and McGillis, 1999) are presented. These are compared to estimates of production based simply on changes between the sampling crossings in concentrations of the production related parameters nitrate (dNO3), oxygen (dO2) and chlorophyll *a* (dChl). To assess the link between hydrography and production the route was divided into different hydrographic regions. CEC (central English Channel) — shallow and tidally well mixed year round; WEC (western English Channel) — seasonally stratified; Ush (Ushant frontal area) — subject to varying

stratification and upwelling; SB Shelf break region of steep shelf with occasional upwelling; NBB (northern Bay of Biscay) — deep water seasonally stratified and influenced by river water; SBB (southern Bay of Biscay) — seasonally intensely stratified and oligotrophic in summer (Pingree and Griffiths, 1978; Lavin *et al.*, in press).

3. Results and discussion

3.1 Summary of annual data sets along FerryBox routes

Figure 1 shows summary plots comparing the mean salinity and temperature between Portsmouth and Bilbao in 2003 and 2004. The value of these plots is that key features appear above any noise in the data. With respect to temperature the relatively hot summer in 2003 is seen clearly in the data south of 47°N. Water temperatures in the southern Bay of Biscay were the highest recorded in the last ten years (Lavin, pers comm.). The feature results from intensification of the seasonal pycnocline resulting from the trapping of fresh waters from the Spanish and French coast above the thermocline once the seasonal thermocline begins to form. The FerryBox data provides the first insight into the fact that this feature can extend from the Iberian coast to the shelf break on the northern side of the Bay. Interestingly overall salinities in the Bay of Biscay were similar in 2003 and 2004. What is seen in the salinity plot is the effect of different wind fields on the movement of fresh water from the Loire and Gironde. Winds were more northerly in 2004 producing the salinity minimum seen at 47.5°N in 2004. The feature is discussed in more detail in Kelly-Gerreyn *et al.* (this volume).

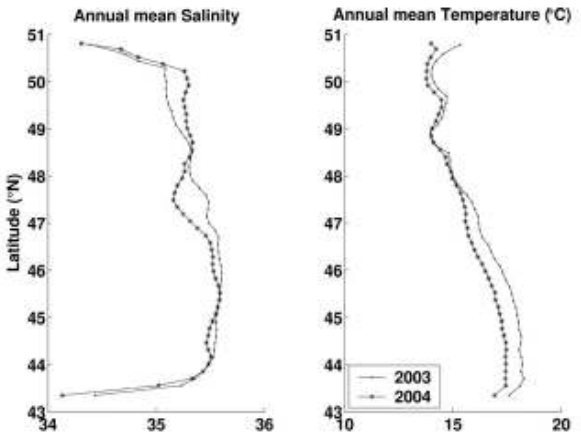

Figure 1 Comparison of mean values of salinity and temperature along the Portsmouth–Bilbao route in 2003 and 2004.

3.2 Spring bloom intensity index

In Figure 2 the data assembled by Fleming and Kaitala (in press) from the Baltic is compared to values of the phytoplankton spring bloom plankton index and nutrient concentration from the outer western European margin water sampled by the Portsmouth–Bilbao FerryBox. The plot contains data from the Baltic collected between 1992 and 2004. These are divided into data from different regions of the Baltic with

progressively higher concentrations of nutrients. In the data from the Portsmouth–Bilbao route the points represent the data divided into 1° latitude bands and the data from 2003 and 2004 are distinguished. The plot shows that there is a relationship between the bloom index and the concentration of nutrients that holds across the spectrum of environments.

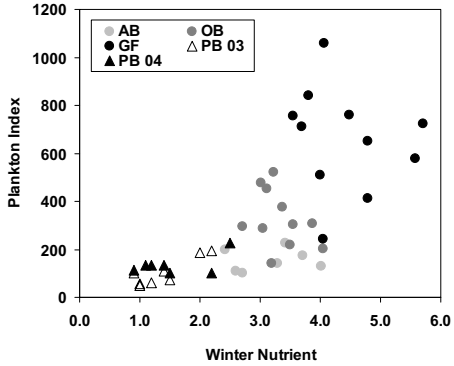

Figure 2 Plot of the spring phytoplankton bloom index against the geometric mean of the maximum winter nutrient concentrations, for results from the Baltic (GF: Gulf of Finland, OB: Open Baltic and AB: Arkona Basin) in 1992–2004, and Portsmouth to Bilbao in 2003 (PB 03) and 2004 (PB 04).

3.3 Use of dissolved oxygen measurements to estimate biological production

In Table 1 the results of the comparison of the estimates of net community production show that only estimates of production based on calculation of the oxygen flux produce results that are in line with existing direct measurements of productivity in these regions, which are in the range 25–90 gCm^{-2} (Joint *et al.*, 2001). In Table 1 the Ushant area shows up clearly as the region of highest productivity; this is in line with the known higher productivity of frontal regions (Pingree and Griffiths, 1978).

4. Findings

The simple summary of the data from the FerryBox lines based on taking the means of the annual data sets provides an effective way of summarising the data from the different lines and detecting major changes between years in the different regions being studied. As part of the process of summarising the data from all the FerryBox project routes plots like this are being prepared for each route.

Similarly the phytoplankton spring bloom index appears to have potential for comparing data from the different regions and giving an indication of the extent to which eutrophication can be related to concentrations of nutrients. The data already available from the Baltic shows how widely the index and its relationship to concentrations of nutrients can vary from year to year. This provides a challenge, to extend the analysis now to see if the reasons for these variations can be found in the available data sets. It also suggests that a degree of caution should be observed when trying to make judgements on the basis of data from a single year. The next stage in this evaluation is to include data from the other FerryBox routes when it becomes available.

The work with measurements of oxygen on the Portsmouth–Bilbao route has demonstrated the potential of oxygen measurements for providing estimates of productivity which are potentially more reliable than those which can be obtained from measurements of chlorophyll *a* fluorescence. Continuous measurements of oxygen using the Aanderaa Optode® are now being tested on the Cuxhaven–Harwich and the Portsmouth–Bilbao routes. Maps of oxygen data and fluorescence data have been compared from the Cuxhaven and Harwich route. They show a good correspondence between increases in both parameters during the spring bloom. Subsequently concentrations of oxygen are seen to be relatively high in surface waters when the biological production is below the surface and below the sampling depth of the ferry so the productivity is not detected in the fluorescence signal but is in the oxygen signal. This is because the oxygen produced by biological growth diffuses towards the surface and demonstrates an added advantage of oxygen measurements in that they allow subsurface production to be detected and estimated.

Acknowledgements

We are very grateful for the assistance of the different ferry companies whose ships we use (Color Line, DFDS, P&O Ferries, Silja Line, Tallink). Without them the work would not be possible. This work was supported within the Fifth Framework Program "Energy, Environment and Sustainable Development Programme", Contract no. EVK2–CT–2002–00144.

5. References

Baan, P.J.A. and J.T. van Buuren (2003). Testing of indicators for the marine and coastal environment in Europe. Part 3. European Environment Agency Technical Report, 86, 65 pp.

C.E.C. (2000). Directive 2000/60/EC of the European Parliament and of the Council of 23 October 2000 establishing a framework for Community action in the field of water policy. Official Journal of the European Communities, L 327, 1–73.

Fleming, V. and S. Kaitala (In Press). Phytoplankton spring bloom intensity index for the Baltic Sea estimated for the years 1992 to 2004, Hydrobiologica.

Joint, I. and 26 others (2001). Pelagic production at the Celtic Sea shelf break — the OMEX I project. Deep-Sea Research II, 48, 3049–3081.

Kelly-Gerreyn, B.A., D.J. Hydes, L.J. Fernand, A.M. Jégou, P. Lazure and I. Puillat (2005). Linking French Atlantic rivers to low salinity intrusions in the western English Channel: highly resolved monitoring from the EU "FerryBox" project. This volume page 432.

Lavin, A., L. Valdes, F. Sanchez, P. Abaunza, A. Forest, J. Boucher, P. Lazure and A.M. Jegou (In Press) The Bay of Biscay: Chapter 24 pp 933–1001 In The Seas Vol. 14, (Eds Robinson and Brink) Harvard Press.

Lips, I. (2005). Abiotic factors controlling the cyanobacterial bloom occurrence in the Gulf of Finland. Dissert. Biol. Univ. Tartuensis, 108, 47 pp.

Najjar, R.G. and R.F. Keeling (2000). Mean annual cycle of the air-sea oxygen flux: A global view, Global Biogeochemical Cycles, 14, 573–584.

Petersen, W., F. Colijn, D.J. Hydes, S. Kaitala, H. Kontoyiannis, A. Lavin, I. Lips, J. Howarth, H. Ridderinkhof and K. Sørensen (2005). European FerryBox Project: From on-line oceanographic measurements to environmental information. This volume page 551.

Pingree, R.D. and D.K. Griffiths (1978). Tidal fronts on the shelf seas around the British Isles, Journal of Geophysical Research, 83, 4615–4622.

Siegel, D.A., S.C. Doney and J.A. Yoder (2002). The North Atlantic Spring Phytoplankton Bloom and Sverdrup's Critical Depth Hypothesis, Science, 296, 730–733.

Wanninkhof, R. and W.R. McGillis (1999). A cubic relationship between air-sea CO2 exchange and wind speed, Geophysical Research Letters, 26, 1889–1892.

Wanninkhof, R. (1992). Relationship between wind speed and gas exchange over the ocean, Journal of Geophysical Research, 97, 7373–7382.

High resolution operational monitoring of suspended matter distribution during harbour dredging

Tarmo Kõuts*, Liis Sipelgas and Urmas Raudsepp

Marine Systems Institute at Tallinn University of Technology, Estonia

Abstract

The marine environment of the Pakri Bay in the southern Gulf of Finland is under heavy anthropogenic stress due to development of two harbours in the area. Since 2002, the total amount of dredged sediments has reached 3.5 mil.m^3 in that coastal bay. A monitoring system for SPM transport and distribution that includes high resolution field measurements, satellite remote sensing and numerical modelling was introduced. The results from two case studies, one for qualitative comparison of three methods for monitoring of SPM distribution and the other for the assessment of environmental impact of SPM through the changes of underwater light conditions on macroalgae *Fucus vesiculosus* growth are presented. The results show qualitatively good agreement of SPM distribution (or other related parameter) obtained by three different methods. The worsening of underwater light intensity that reaches benthic macroalgae restrains the growth and causes decline of the biomass during dredging periods.

Keywords: suspended particulate matter, hydrodynamic modelling, remote sensing, Gulf of Finland, Baltic Sea.

1. Introduction

A significant amount of suspended particulate matter (SPM) is naturally discharged into coastal sea both from point sources such as rivers, as well as from resuspension caused by wave activity. Seawater in shallow coastal areas with open coastline belongs frequently to a highly turbid water class. In addition to natural sources, a considerable amount of SPM is washed into the water column by technological activities concerning shipping and harbour management, mainly by dredging. The actual amount of SPM added to the water depends mainly on the amount of dredged material, but also on the grain size and implemented dredging technology. The transport and fate of SPM depends on the physical properties of particles and local hydrodynamic conditions. The latter is to some extent controlled by the bathymetry of the particular water basin where the harbour is located. For instance, in sheltered and small bays the affected area could be small, but the environmental impact could be worse due to high local concentrations of SPM. At the open coast, SPM can spread over a larger sea area, but more dispersed. Resuspension of sediments is inevitable during dredging operations.

The main effect of increased SPM concentration in seawater on environmental conditions is the decrease of water transparency — less light penetrates to the marine biota and photosynthesis activity in the euphotic zone goes down. Another effect of dredging operations is that additional nutrients are added to the water column, which could cause

* Corresponding author, email: tarmo.kouts@sea.ee

eutrophication. Sedimentation could cover the benthos and cause lower productivity of fish stock during the spawning period. Also, heavy metals and other harmful substances may be washed into the water column during dredging.

Monitoring of SPM transport and distribution along with the estimation of dredging impact on the marine environment is crucial especially when sensitive and critical marine areas are close to the dredging site. In this paper, we present a system for monitoring the suspended matter distribution during harbour dredging, which is based on combined application of numerical modelling, satellite remote sensing and *in situ* measurements. The results from two case studies in Pakri Bay, the southern Gulf of Finland, are presented. The first example shows an application of the method for monitoring of SPM distribution focusing on validation of the system. The second example presents an attempt to estimate the effect of suspended sediments on benthic macroalgae growth. Two harbours are rapidly developing in the Pakri Bay — Paldiski North Harbour and Paldiski South Harbour (Figure 1). Dredging activity started in 2002 and is still ongoing, and a total of 3.5 mil m^3 has been dredged so far.

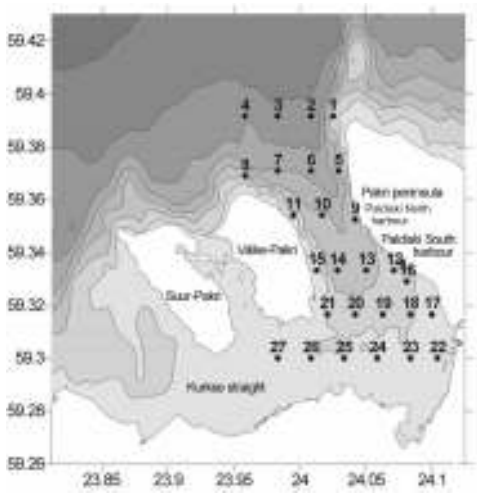

Figure 1 Bathymetry of Pakri Bay within the limits of hydrodynamic model domain. Darker colours show deeper water, max. depth 60 m on the map. Dots and numbers indicate the locations of visited sampling stations.

2. Monitoring methods

The monitoring system implemented in the Pakri Bay consists of three components — *in situ* measurements and laboratory analyses of water samples, remote sensing, and numerical modelling. Vertical profiles of temperature, salinity and turbidity were measured at sampling stations using a self-contained CTD probe SAIV204 equipped with a Seapoint turbidity sensor. The same probe was also used in mooring stations for measurements of time-series of turbidity together with currents at some fixed locations close to the harbours. The concentration of suspended matter from water samples was determined using the dry weight method (Lindell, 1999), and the concentration of chlorophyll *a* was calculated according to Lorenzen's (1967) formulae and the content of

dissolved organic matter was estimated using spectrophotometrical method (Højerslev, 1988). The concentrations of nutrients, heavy metals and other harmful substances were determined from a limited number of water samples. The underwater downward vector irradiance (E_d, $W m^{-2}$) was measured by lowering the radiance sensor LI-192 SA (LI-COR, inc. USA) with a 0.5-metre depth interval. Surveys of *in situ* spatial distribution of SPM in the Pakri Bay were performed by measuring light absorption and attenuation in the surface layer, and by using an Attenuation Meter AC-9 (WetLabs Inc.) optical instrument in the flow-through set-up.

Remote sensing images from a MODIS spectrometer installed on Terra and Aqua satellites were downloaded from the GES Distributed Active Archive Center (http://eosdata.gsfc.nasa.gov/data/datapool/). The sensors register the radiance signal backscattered from the atmosphere and sea surface. Level 1B MODIS images with spatial resolution of 250 m from two bands, 620–670 nm (band 1), 841–876 nm (band 2) were used in the analysis. The band 1 and band 2 scaled integer (SI) values were converted to remote sensing reflectance, by means of the calibration coefficients as follows:

$$Reflectance = Scale*(SI - Offset)$$

The values of *scale* and *offset* are given with each image by MODIS data support, and geocorrection is also applied. Reflectance data were corrected for the atmospheric effects in common practical levels recommended in Chavez (1988; 1996) in order to make images comparable with each other. This method requires estimation of a reference target on each image such as deep clear water pixels — a "dark object" — whereas deep clear water absorbs all light in the near infrared wavelength region. Thus the water-leaving signal should have brightness values close to zero (Gilabert *et al.*, 1994) and the detected signal is radiation backscattered from the atmosphere and water surface. The atmospheric normalising algorithm could be defined as:

$$L_{\text{out}}(i,j,k) = L_{\text{in}}(i,j,k) - L_{\text{corr}}$$

where $L_{\text{out}}(i,j,k)$ is the atmospherically corrected reflectance value of the output pixel at row i and column j of band k; $L_{\text{in}}(i,j,k)$ is the reflectance value of the input pixel at row i and column j of band k; and L_{corr} is the correction value independent of band. In our case the correction value was the value of the darkest pixel of band 2.

The numerical modelling system consists of hydrodynamic particle transport and a benthic macroalgae growth model. The hydrodynamic model applied in this study is a finite difference model based on non-linear shallow-water equations. The model covers the bay (Figure 1) with a uniform horizontal grid of 125×125 m. Radiation boundary conditions were implemented at the open boundaries. The currents were driven by wind measured at Pakri Bay. A Lagrangian particle transport model was used for calculation of SPM transport. Particles were released to the water column from single or multiple point sources, the intensity of which depends on actual dredging volume on a daily basis. The number of discharged particles was proportional to the dredging amount and followed the time schedule of particular dredging. In the water column, the particles were transported by pre-calculated currents from the hydrodynamic model and randomly dispersed.

A simple benthic macroalgea growth model was implemented for the estimation of the dredging impact on the changes of macroalgae biomass. The model takes into account

macroalgae production and respiration. Other biological processes such as exudation, natural mortality and grazing are neglected. In this model, the changes of macroalgae biomass depend on the existing biomass:

$$\frac{dB}{dt} = B(P_g - R)$$

where B ($\mathrm{gCm^{-2}}$) is macroalgae biomass, P_g ($\mathrm{h^{-1}}$) is gross production rate and R ($\mathrm{h^{-1}}$) is the respiration rate (Alvera-Azcarate *et al.*, 2003). Underwater light conditions were assumed to be the only limiting factor for macroalgae production, i.e.

$P_g = P_{g\max} f(I)$,

where $P_{g\max}$ is the maximum gross production rate and

$f(I) = \frac{I}{I_k + I}$ is the light limiting function,

where I ($\mathrm{Wm^{-2}}$) is the light intensity at macroalgae depth and I_k is the half-saturation light intensity.

3. Results

The first step in implementing the monitoring system is to achieve a qualitative comparison of SPM distribution (or another parameter that indirectly represents SPM concentration in water) from *in situ* measurements, remote sensing data and model simulation results. The period from 15 April to 22 May 2003 was selected for testing the monitoring system, as the existing database of measurements was most extensive for that period. Reflectance data from MODIS images provided information on qualitative spatial distribution of the surface water turbidity. Higher reflectance is an indicator of more turbid water. The linear regression obtained between SPM concentrations and atmospherically normalised reflectance was $SPM = 112.32 L_{\mathrm{out}} + 4.5812$ with correlation coefficient 0.71. The hydrodynamic part of the model system was validated by comparing two-week long time series of modelled and measured currents from a single location at 7 m depth at Paldiski North Harbour. A comparison showed that calculated and measured currents were in reasonable agreement (not shown). A qualitative comparison of MODIS reflectance images, simulated particle distribution and *in situ* measured Secchi depths also showed good agreement in most cases, and a sample comparison for 13 May 2003 is presented in Figure 2. It should be pointed out that a direct comparison between model simulated SPM concentrations and observations is difficult, because of uncertainties about the actual amount of resuspended sediments and also its actual granular consistence.

Water transparency was the poorest, less than 1 m, at the dredging site and the area of low water transparency (between 1 and 2 m) extends southward. A region of moderate water transparency (between 2 and 3 m) is located northward of the harbour. An unaffected region has water transparency in excess of 4 m at the eastern coast of Väike Pakri Island. The satellite image shows a similar reflectance distribution pattern. High reflectance is close to the harbour and at the southern coast of Pakri Bay. A moderately turbid area extends northwards from the harbour and a low turbid area is found at the Väike Pakri Island. A relatively clear water region penetrates the southern Pakri Bay

through the Kurkse Strait. Water transparency measurements and satellite images integrate the contribution from all optically active substances. SPM distribution from the numerical model results only include SPM from dredging. The calculated SPM distribution coincides with water transparency measurements and the satellite images. The highest SPM concentration is close to the Paldiski South Harbour and the area of increased SPM extends to the south and north. The southward spreading of SPM occurs in a narrow strip, while the northward spreading is wider, which is consistent with measurements and satellite images. Also the locations of "clear water" zones are simulated correctly.

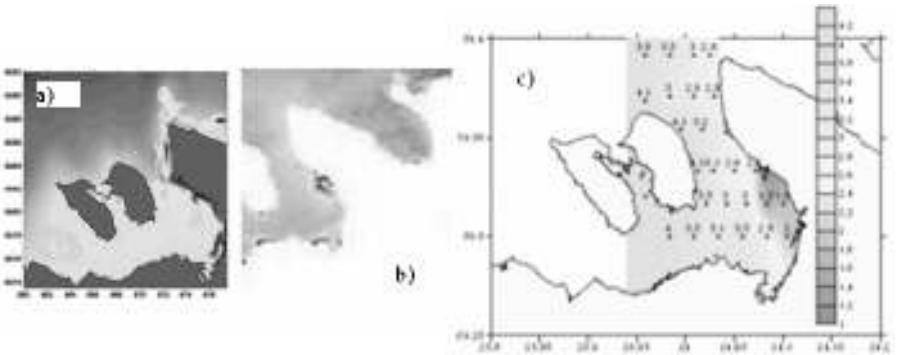

Figure 2 (a) Modelled SPM distribution; (b) MODIS reflectance image; (c) *in situ* measured Secchi depths; all for 13 May 2003. Darker colours correspond to more turbid water.

The dredging period from 20 June to 21 July 2004 at Paldiski South Harbour and a 10-day long post-dredging period were used for the estimation of the effect of resuspended sediments on the growth of benthic macroalgae *Fucus vesiculosus*. The dredged volume was 178000 m^3. SPM transport was calculated using the previously described hydrodynamic and particle transport model. Solar irradiance at the water surface was obtained from the closest appropriate weather station. To get light conditions at the depth of *Fucus vesiculosus*, the relationship between SPM concentration in the water column and the light attenuation coefficient was estimated. The downward vector irradiance (E_d, $W m^{-2}$) was measured along with water samples and SPM concentrations were determined in the laboratory. The diffuse attenuation coefficient (K_d) was calculated from the downward vector irradiance measurements using the following equation (Dera, 1992):

$$K_d(z) = -\frac{d}{dz}[\ln E_d(z)] = \frac{1}{E_d(z)} \cdot \frac{dE_d(z)}{dz}$$

For determining the contribution of suspended matter to light attenuation, the correlation between K_d and suspended matter was calculated. The relationship obtained between 25 simultaneous K_d and suspended matter measurements from different stations in Pakri Bay was $K_d = 0.0538 \cdot C_{SM} + 0.1712$ with determination factor $r^2 = 0.72$. Light attenuation with depth was calculated using Lambert-Beer's law assuming that SPM distribution is vertically uniform and the light attenuation coefficient is constant in the water column. A comparative test was run for a "clear water" case, i.e. assuming that the light attenuation coefficient is equal to 0.1712 m^{-1}.

The spatial distribution of light intensity relative to clear water cases that penetrate to the bottom integrated over the dredging period is presented in Figure 3. The coastal area between Paldiski South and North harbours is the most severely affected by dredging. Only 10–20% of light penetrates to the bottom in comparison with the "clear water" case. Light conditions are about 50% worse to the north from Paldiski North Harbour and in the central Pakri Bay. The southern part of the bay is almost unaffected. During the dredging, SPM was mainly transported northward from the dredging site due to prevailing winds from the southwest sector. The light conditions at the bottom changed by up to 15% 10 days after the dredging was finished (Figure 3). The light conditions became better in the areas which were the most affected during dredging. Between Paldiski South and North harbour, and at the coast of the Pakri peninsula to the north of Paldiski North harbour the recovery was up to 10% compared to the light conditions at the end of dredging. The light conditions became worse in the central Pakri Bay and to the south from the Paldiski South Harbour, which is the result of SPM redistribution in Pakri Bay. Winds from the north dominated during that period, which cause southward currents and SPM transport.

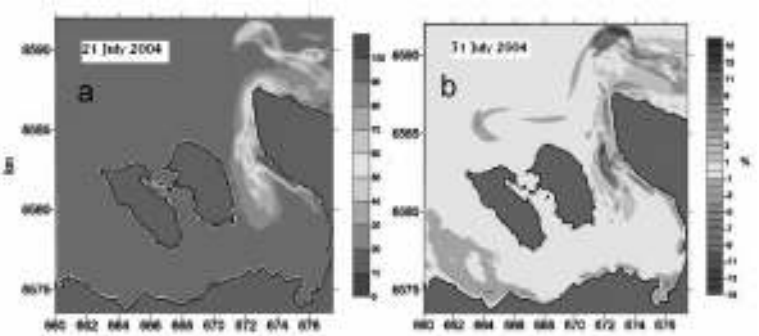

Figure 3 (a) Percentage of light intensity relative to the "clear water" case that reached the bottom of Pakri Bay at the end of dredging period. The dredging period was from 20 June to 21 July 2004. (b) Percentage of light intensity relative to the end of dredging that reached the bottom of Pakri Bay 10 days after the dredging was finished. Positive (negative) values indicate areas where light conditions have improved (worsened).

As a test, we considered relatively short-term impact of SPM on *Fucus vesiculosus* in Pakri Bay. SPM distribution severely affected light conditions at the bottom between the harbours and along the western coast of the Pakri peninsula during this dredging period. This area has suitable substrate for *Fucus vesiculosus* and this species has been found there. The initial distribution of *Fucus vesiculosus* is shown in Figure 4. It was compiled by monitoring the benthic vegetation taking into account observed coverage and height of the species. The following coefficients were used in model simulation:

$P_{g\max} = 2.5\times10^{-3}h^{-1}$, $R = 3.5\times10^{-4}h^{-1}$ and $I_k = 50\ \mathrm{Wm}^{-2}$

To take into account the integrated effect on the *Fucus vesiculosus* community the spatially integrated biomass was calculated. In general, the biomass of *Fucus vesiculosus* increased in Pakri Bay during the dredging period (Figure 4). There was no difference between the biomass in the first three days, as the SPM due to dredging did not reach the area of *Fucus vesiculosus* growth. From the fourth day the biomass values start to

separate from each other. By the end of dredging period the difference between biomasses was about 12%. The disparity between biomasses increased after the dredging, and reached about 16% in 10 days. Although the entire biomass of *Fucus vesiculosus* increased in Pakri Bay, the *Fucus vesiculosus* biomass has become lower that the initial value between Paldiski South and North harbours.

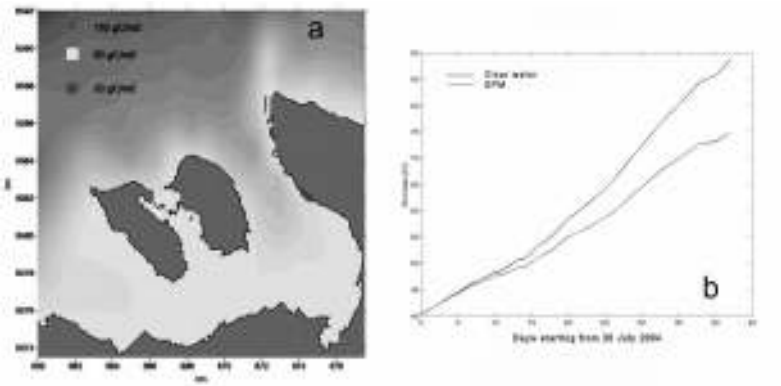

Figure 4 Initial distribution of *Fucus vesiculosus* biomass (a) in Pakri Bay, used as initial conditions for numerical model. (b) Time series of spatially integrated *Fucus vesiculosus* biomass in Pakri Bay in case of dredging (upper line) and "clear water" (lower line) during the one month long dredging period. Day 0 corresponds to the beginning of dredging on 20 June 2004.

4. Conclusions

A high-resolution monitoring system for monitoring of SPM concentration during dredging operations based on a combination of *in situ* measurements, remote sensing and numerical modelling was introduced, implemented and tested. The system was used for two case studies during harbour dredging in Pakri Bay, the southern Gulf of Finland. Results from the first case study show reasonable qualitative agreement of SPM distribution when the methods were applied separately from each other. In combination, *in situ* measurements accompanied by laboratory analyses of water samples enable calibration of MODIS images of satellite remote sensing. The latter then provides SPM distribution maps during cloud free days. Both *in situ* measurements and satellite remote sensing can be used for the validation of numerical models including particle transport models, and provide input data for the data assimilation procedure, if necessary. The second case study shows an example of how to estimate the impact of dredging on the growth of perennial macroalgae *Fucus vesiculosus*. The increased SPM concentration worsens underwater light conditions, which is usually the main limiting factor for the growth of benthic macroalgea in shallow water. Rough estimates show a considerable decrease in light intensity at the bottom in the coastal area in the vicinity of the dredging site, which results in the decline of benthic macroalgea biomass. Due to considerable spatial variability of water quality parameters (water transparency and turbidity, suspended particulate matter distribution, underwater light conditions) during dredging operations, a high-resolution monitoring system is recommended for estimation of the environmental impact in the coastal sea.

Acknowledgements

This study was partially supported by research grant 5596 from the Estonian Science Foundation.

References

Alvera-Azcarate, A., J.G. Ferreira and J.P. Nunes (2003). Modelling eutrophication in mesotidal and macrotidal estuaries. The role of intertidal seaweeds. Estuarine, Coastal and Shelf Science, 57, 715–724.

Chavez, P.S. Jr. (1988). An improved dark-object subtraction technique for atmospheric scattering correction of multispectral data. Remote Sensing of Environment, 24 (3), 459–479.

Chavez, P.S. Jr. (1996). Image-based atmospheric corrections-revisited and improved. Photogammetric Engineering and Remote Sensing, 62, 1025–1036.

Dera, J. (1992). Marine physics. PWN-Polish Scientific Publishers, Warszawa.

Gilabert, M.A., C. Conese and F. Maselli (1994). An atmospheric correction method for the automatic retrieval of surface reflectances from TM images. International Journal of Remote Sensing, 15, 2065–2086.

Højerslev, N.K. (1980). On the origin of yellow substance in the marine environment. Oceanogr. Rep., Univ. Copenhagen. Inst. Phys. 42: 1–35.

Lindell, T., D. Pierson, G. Premazzi and E. Zilioli (eds). (1999). Manual for monitoring European lakes using remote sensing techniques. Luxembourg. European Communities. ISBN 92–828–5390–X.

Lorenzen, C.J. (1967). Determination of chlorophyll and phaetopigments; spectrophotometric equations. Limnol. Oceanogr. 12: 343–346.

Phytoplankton community succession during the summers 2001 and 2002 in the Baltic Sea

Seppo Kaitala*, Vivi Fleming and Seija Hällfors

Finnish Institute of Marine Research, Finland

Abstract

Phytoplankton communities of the Baltic Sea are characterised by high seasonal variability. The ordination analysis has been applied for the phytoplankton community development during the summer of the years 2001 and 2002.

Detrended correspondence analysis (DCA) reveals clear succession phases with different patterns for the Southern and Central Baltic Sea and the Gulf of Finland. The data was obtained by automatic flow-through measurements and water sampling on board the commercial ferry Finnpartner travelling across the Baltic Sea from Helsinki to Travemünde within the Alg@line monitoring programme. Data analyses indicated that the community succession repeated a similar pattern during the both years. The most stable community was found in the Southern Baltic Sea. An analysis of the time series of the parameters suggests a strong coupling between external and biological factors.

Keywords: phytoplankton succession, community ordination

1. Introduction

Phytoplankton monitoring of the Baltic Sea has a long tradition dating a hundred years back (Hensen, 1887). The phytoplankton communities of the Baltic Sea are characterised by high seasonal variability. Also in modern taxonomical studies, phytoplankton species are characterised by occurrence in different parts of the Baltic Sea (Hällfors, 2004). To reveal similar plant communities in terrestrial ecology, ordination methods have been widely used (Jongman *et al.*, 1987) and ordination methods have been applied to differentiate diatom communities from the sediments of Baltic Sea (Kaitala *et al.*, 1991). This study aims to reveal the development patterns of the phytoplankton communities in different regions of the Baltic Sea.

2. Methodology

The data was obtained by automatic flow-through measurements and water sampling on board the commercial ferry Finnpartner travelling across the Baltic Sea from Helsinki to Travemünde within the monitoring programme Alg@line. 24 water samples were collected from approximately 5 metre depth on one transect every 1 to 3 weeks, starting in February/March and lasting to October/November. Semi-quantitative phytoplankton analyses were made from the water samples according to Rantajärvi *et al.* (1998). The semi-quantitative amount is an integer between 1 and 5, estimated according to the relative abundance of the species in each water sample. Missing species were given the

* Corresponding author, email: Seppo.Kaitala@fimr.fi

value 0. The Alg@line sampling and analyses are described in Leppänen and Rantajärvi (1995) and Ruokanen *et al.* (2003).

Table 1 Phytoplankton species ordered by DCA

Species	Site group							
	G1		G2		G3		G4	
	01	02	01	02	01	02	01	02
Gymnodinium spp. (autotroph)	X							X
Prorocentrum minimum		X						
Paraphysomonas spp.	X							X
Chaetoceros danicus	X							X
Chaetoceros sp.		X						
Coscinodiscus granii		X						
Cylindrotheca closterium		X						
Dactyliosolen fragilissimus	X	X						
Eupodiscales spp.	X	X						
Skeletonema costatum	X	X						
Anabaena lemmermannii				X				
Aphanizomenon flos-aquae			X	X				
Aphanocapsa delicatissima			X	X				
Coelomoron pusillus				X				
Cyanodictyon planctonicum				X				
Synechococcus spp.				X			X	
Dinophysis acuminata			X	X				
Glenodinium spp.			X	X				
Heterocapsa rotundata			X					X
Dinobryon faculiferum				X			X	
Eutreptiella gymnastica				X			X	
Dictyosphaerium subsolitarium			X					
Monoraphidium contortum			X	X				
Planctonema lauterbornii			X	X				
Ebria tripartita			X					X
Katablepharis remigera			X	X				
Planktolyngbya spp.					X			
Hemiselmis virescens					X	X		
Plagioselmis prolonga					X	X		
Teleaulax acuta					X	X		
Teleaulax amphioxeia					X	X		
Gymnodinium spp. (heterotroph)						X	X	
Heterocapsa triquetra					X			
Pseudopedinella tricostata						X	X	
Oocystis lacustris					X			X
Leucocryptos marina					X	X		
Nodularia spumigena							X	X
Prochlorotrix spp.							X	X
Chrysocromulina spp.							X	X
Pseudopedinella elastica			X			X		
Actinocyclus octonarius		X			X			
Cyclotella choctawhatcheeana		X			X			
Nitzchia paleacea								X
Mesodium rubrum			X			X		

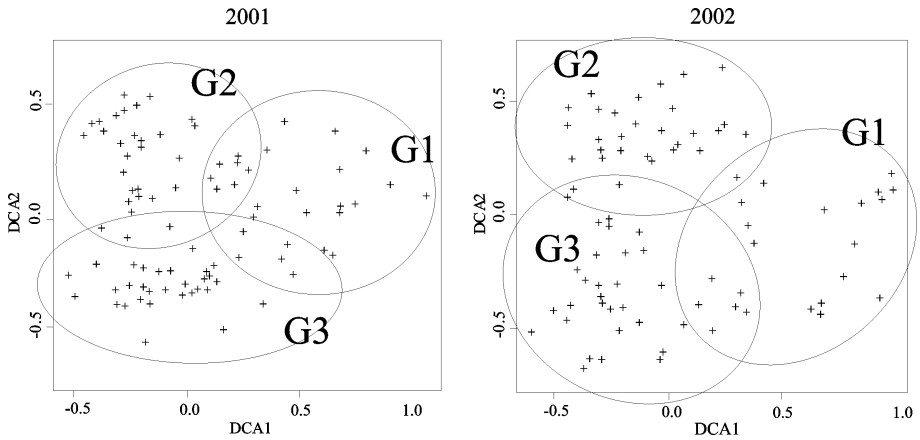

Figure 1 DCA biplots for phytoplankton sampling sites. G1, G2 and G3 ellipsoids marked as site groups determined by DCA analysis. The sites occurring in overlapping areas of the ellipsoids are determined to form group G4.

The study period was defined to last from May to August. The commonness of each species was determined separately for both years by calculating the mean of the semi-quantitative abundance. Species with mean abundance less than 0.5 were dropped from the statistical analyses. Biplots of phytoplankton species and sampling sites were constructed using detrended correspondence analysis (DCA). From the biplots of the DCA axis 1 and 2 the sites were grouped according to their location in the biplot (Figure 1). These groups could be considered as different types of species communities. The species determining the community groups are shown in the Table 1. The sites were then plotted on maps transect by transect and corresponding sample points are marked with ellipsoids according to their community group.

3. Phytoplankton species ordered by DCA

The community group G1 is characterised by diatoms, partly by small centric species (*Thalassiosira* spp., *Cyclotella choctawhatcheeana*), partly by chain forming centric species (*Skeletonema costatum*, *Chaetoceros* spp.) and by the large centric species *Coscinodiscus granii*, which has its main occurrence during the autumn. Most observations of *Dactyliosolen fragilissimus* are restricted to southern parts of the Baltic Sea like those of the dinoflagellate *Prorocentrum minimum* during summer months.

The community group G2 consists of the filamentous blue-green alga *Aphanizomenon flos-aquae*, small colonial blue-green algae (*Aphanocapsa* sp., *Coelomoron pusillus*, *Cyanodictyon* spp.), dinoflagellates of different sizes (*Dinophysis* spp., *Glenodinium* spp.) and the green algae *Monoraphidium contortum* and *Planctonema lauterbornii*. Also the blue-green alga *Anabaena lemmermannii*, the euglenophycean *Eutreptiella gymnastica* and the heterotrophic flagellate *Katablepharis remigera* seem to belong mainly to this community.

The community group G3 consists mainly of nanoflagellates. The cryptophycean flagellates (*Hemiselmis virescens*, *Plagioselmis prolonga*, *Teleaulax* spp.) are characteristic.

The green algae *Oocystis* spp., the dinoflagellate *Heterocapsa triquetra* and the heterotrophic flagellate *Leucocryptos marina* belong to this community.

4. Discussion and conclusions

The analysis of the phytoplankton community succession enables the characteristic communities to be distinguished. Detrended correspondence analysis (DCA) reveals clear succession phases with different patterns for the Southern and Central Baltic Sea and the Gulf of Finland. Data analyses indicated that the community succession repeated a similar pattern during both years. The spring community succession started from the south and proceeded towards the north. In the summer the most stable community was found in the Southern Baltic Sea. Analysis of time series of the parameters suggests a strong coupling between external and biological factors. The community succession analysis can be used in evaluation of eutrophication status and in observations of harmful algae. Characteristic communities may also be useful for satellite image analysis.

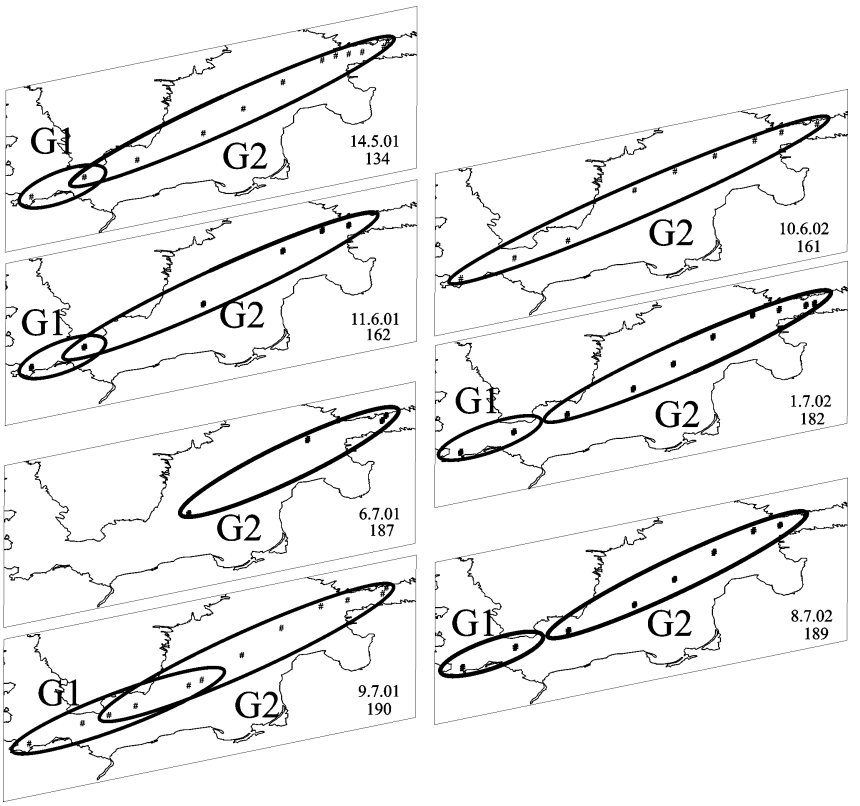

Figure 2 Phytoplankton communities in May, June and beginning of July during the years 2001 and 2002 according to DCA analysis.

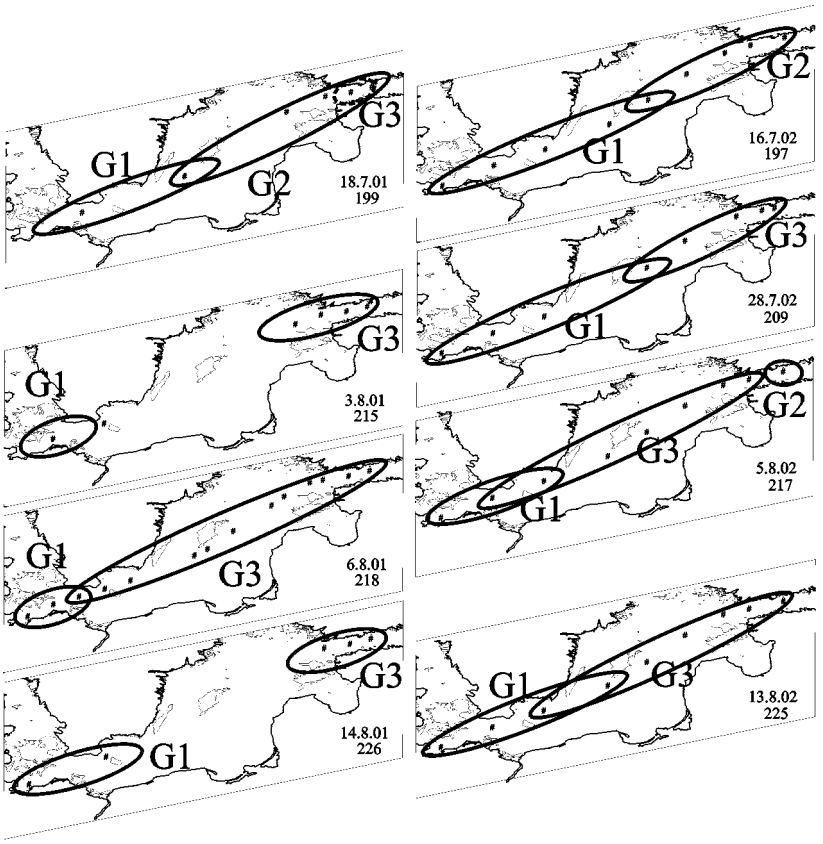

Figure 3 Phytoplankton communities in July and August during the years 2001 and 2002 according to DCA analysis.

Acknowledgements

The work was partially financed by the EU project FerryBox: From on-line oceanographic observations to environmental information (5th Framework Programme of the European Commission CN:EVK2200200144, 2002–2005).

References

Hensen, V. (1887). Über die Bestimmung des Planktons oder des im Meere treibenden Materials an Pflanzen und Thieren; nebst Anhang. 5. Bericht d. Kommission zur Wissen. Unters. d. Deutsch. Meere. Berlin, 1–108.

Jongman, R.H.G., C.J.F. ter Braak and O.F.R. van Togeren (1987). Data analysis in community and landscape ecology. Pudoc, Wageningen, 299 pp.

Hällfors, G. (2004). Checklist of Baltic Sea Phytoplankton Species including some heterotrophic protistan groups. Baltic Sea Environment Proceedings Series No 95. 208 pp.

Ruokanen, L., S. Kaitala, V. Fleming and P. Maunula (2003). Algaline: joint operational unattended phytoplankton monitoring system in the Baltic Sea. In: Dahlin, H., N.C.

Flemming, K. Nittis, and S.E. Petersson (eds.) (2003). Building the European Capacity in Operational Oceanography, Proceedings of 3rd EuroGOOS Conference, Elsevier Oceanography Series. 69: 519–522.

Kaitala, S., V.N. Maximov and Å. Niemi (1991). A simple approach to estimate similarity in ecosystem analysis. Vegetatio 96: 101–112.

Leppänen, J.-M. and E. Rantajärvi (1995). Unattended recording of phytoplankton and supplemental parameters on board merchant ships — an alternative to the conventional algal monitoring programmes in the Baltic Sea. In: Lassus, P., Arzul, G., Erard-Le Denn, E., Gentien, P. and Marcaillou-Le Baut, C. (eds), Harmful marine algal blooms, Lavoisier, Paris: 719–724.

Rantajärvi, E., V. Gran, S. Hällfors and R. Olsonen (1998). Effects of environmental factors on the phytoplankton community in the Gulf of Finland: unattended high frequency measurements and multivariate analyses. In: Tamminen, T. and Kuosa, H. (eds), Eutrophication in planktonic ecosystems: Food web dynamics and elemental cycling; Developments in hydrobiology (127). Hydrobiologia 363:127–139.

Assessment of global and regional ocean sea surface chlorophyll *a*

S. Djavidnia*, F. Mélin and N. Hoepffner

EC–Joint Research Centre, Institute for Environment & Sustainability, lnland & Marine Waters Unit, Italy

Abstract

Ocean colour provides information on the biological state of the oceans, and therefore represents an essential element for assessing environmental issues and fostering sustainable exploitation of marine resources. An accurate assessment of the differences between the available ocean colour data sets is necessary to develop appropriate algorithms to merge concurrent products, as well as to ensure the consistency of the overall time series. This study compares standard ocean colour products of sea surface chlorophyll *a* concentration obtained concurrently from different sensors and algorithms (SeaWiFS, MODIS-AQUA, MERIS and POLDER-2) at global and regional scales.

Keywords: Ocean colour, chlorophyll, MERSEA, global and regional evaluation, remote sensing

1. Introduction

Ocean colour provides information on the biological state of the oceans, and therefore represents an essential element for assessing environmental issues and fostering sustainable exploitation of the marine resources. The analysis of its derived products also supports a better understanding of the marine biogeochemical cycles.

The ocean colour data record will be more valuable as longer times-series become available. However, this necessarily relies on a suite of subsequent (and in some cases overlapping) ocean colour missions, whose differences in terms of sensor characteristics, calibration or even algorithms make the creation of a high quality consistent long-term data stream a challenge. The assessment of the differences between existing data sets is a first step in addressing this question. It also gives an insight into the uncertainties affecting these products and helps in the development of appropriate techniques to merge concurrent products.

This study compares standard ocean colour products of sea surface chlorophyll *a* (Chl-*a*) concentration obtained concurrently from different sensors and algorithms at both global and regional scales. For the regional scales, 3 representative regions are selected for illustration.

2. Sea spectral reflectance and chlorophyll *a*

The Chl-*a* concentration is derived from the signal reaching the satellite sensor in a two-step approach: first the water leaving radiance (L_w) is calculated from the calibrated top-

* Corresponding author, email: samuel.djavidnia@jrc.it

of-atmosphere radiance recorded by the sensor, through a process of atmospheric correction; then the spectrum of L_w can be used to derive the concentration of the optically significant constituents, either via a semi-analytical or an empirical method. For the global ocean, such a constituent is the chlorophyll *a* pigment, which is a proxy for phytoplankton biomass.

3. Satellite sensors and data

Table 1 shows the characteristics of the different space sensors that have measured sea surface reflectance on a global scale since 1997 and that are used in our study.

Table 1 Ocean colour sensor characteristics.

Sensor	Agency	Life-time	Swath (km)	Resolution (km)	No. of bands	Spectral Coverage (nm)
SeaWiFS	NASA	01/08/97–	2800	1.1[1]	8	402–885
MERIS	ESA	01/03/02–	1150	0.3/1.2	15	412–1050
MODIS-A	NASA	04/05/02–	2330	1	36	405–14385
POLDER-2	CNES	14/12/02–14/09/03	2400	6	15	443–910

[1] *in Local Area Coverage Mode*

All the analyses have been conducted using monthly means of Standard Mapped Image Level 3 data of approximately 9 km grid cells. A suite of different algorithms has been used to derive the Chl-*a* concentration, all of them based on an empirical band ratio inversion method (O'Reilly *et al.*, 1998; Carder *et al.*, 1999; Morel and Antoine, 2000; Loisel *et al.*, 2002).

4. Analysis methods

All Chl-*a* data were logarithmically transformed before comparison, since the natural distribution of ocean chlorophyll usually observed is log-normal (Campbell, 1995). The comparative statistical analysis was performed between pairs of sensors on co-located pixels with a valid Chl-*a* value ranging from a minimum of 0.01 $mg\,m^{-3}$ to a maximum of 20.0 $mg\,m^{-3}$.

The quantitative comparison of two products illustrated in this study relies on the calculation of a signed mean relative difference (SRD) between the two sensors, the evaluation of the frequency distribution functions as well as the calculation of the areal mean, mode and standard deviation.

These calculations were performed for the entire globe as well as for all the biogeochemical provinces described by Longhurst (1998). The results focus on the year 2003 where the four sensors presented were active at the same time (note that POLDER-2 was lost in October 2003 due to the failure the ADEOS 2 satellite platform).

5. Global assessment

Figure 1 shows the global Chl-*a* monthly mean values for 2003 for the four sensors. Note that values from SeaWiFS (S) and MODIS-Aqua (A) are very close, while MERIS (M) and POLDER-2 (P) have concentrations which are considerably lower. The histograms in Figure 2 show the difference in distribution between MERIS, MODIS, SeaWiFS and POLDER-2 on the entire globe for the month of March 2003. It is interesting to note the larger variance of MERIS and especially the presence of lower values.

Figure 1 Chl-*a* global mean values. See text for definition of symbols.

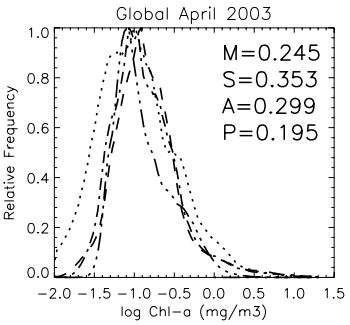

Figure 2 Chl-*a* global distribution functions and corresponding mean values (in mgm^{-3}).

On a global scale, the SRD in Chl-*a* concentration between MODIS and SeaWiFS is rather small (less than 5%) all year round. For a specific temporal and spatial instance the difference can be more accentuated: for instance, in the spring and autumn months at high latitudes in the North Atlantic, the signal from SeaWiFS can reach values which are almost 50% greater than MODIS.

Monthly mean SRD's in Chl-*a* concentration between MERIS and both MODIS and SeaWiFS are instead more marked. In the northern hemisphere (e.g. North Atlantic Tropical Gyre (NATR) and North Pacific Tropical Gyre (NPTG) provinces), the signal of the latter two sensors is always greater than the one from MERIS, and in some winter months this difference can reach values up to 50%. In the southern hemisphere, MODIS and SeaWiFS are systematically greater than MERIS, with SRD's being greater (reaching up to 75%) in the autumn and winter months for the southern Pacific, southern Atlantic and southern Indian gyres.

6. Regional assessment

This section focuses on three provinces: South Atlantic Gyral (SATL), a southern hemisphere oligotrophic region; Mediterranean Sea (MED), a generally oligotrophic northern hemisphere region but with a very large range of Chl-*a* values; and Benguela Current Coastal (BENG), an upwelling southern hemisphere region with very high productivity.

The monthly mean Chl-*a* values for the SATL province (Figure 3) show that POLDER-2 exhibits the highest values, this being a clear departure from the global result, while MODIS and SeaWiFS have very similar signals and MERIS is somewhat lower. These lower values are clearly visible from the distribution functions of MERIS, MODIS, and SeaWiFS for May 2003 (Figure 4).

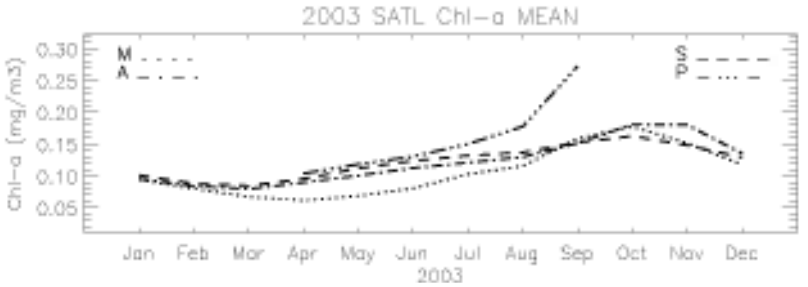

Figure 3 Chl-*a* South Atlantic Gyral province mean values.

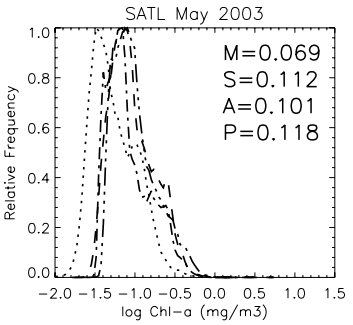

Figure 4 Chl *a* South Atlantic Gyral province distribution functions and corresponding mean values (in mgm^{-3}).

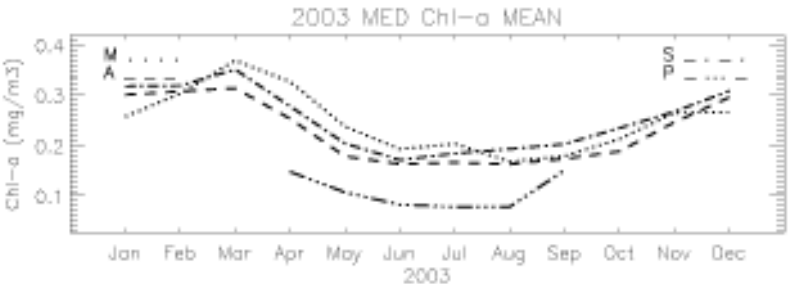

Figure 5 Chl *a* Mediterranean Sea province mean values.

The monthly mean Chl-*a* values for the MED province (Figure 5) show that MERIS values are systematically greater than MODIS and SeaWiFS during the spring and early summer months. If we concentrate on the summer month of July (Figure 6), the difference in distribution and the shift to higher values for MERIS is very clear.

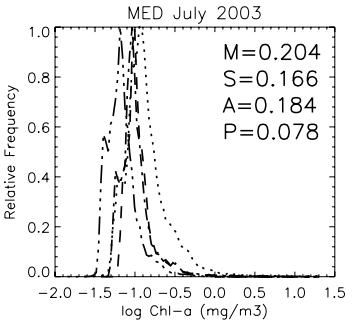

Figure 6 Chl-*a* Mediterranean Sea province distribution functions and corresponding mean values (in mgm^{-3}).

On the other hand in the BENG province, the MODIS Chl-*a* monthly mean values are consistently higher than the ones from the other sensors (Figure 7). From the distribution functions (Figure 8), we can see that the median and variance are fairly similar for MODIS and SeaWiFS, while for MERIS there is both a shift in the mode and an increase in the variance.

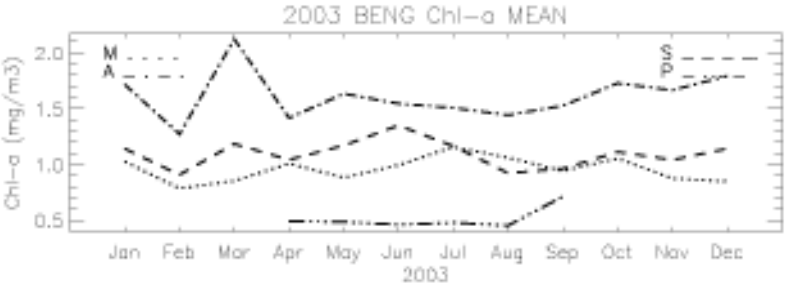

Figure 7 Chl *a* Benguela Current Coastal province mean values.

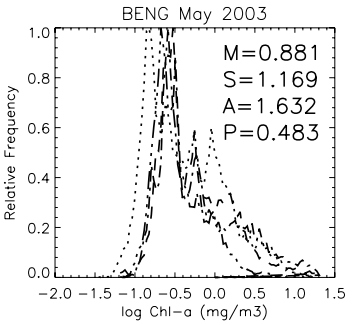

Figure 8 Chl *a* Benguela Current Coastal province distribution functions and corresponding mean values (in mgm^{-3}).

7. Conclusion

Differences in Chl-*a* estimation by different sensors are to be expected, however it is interesting to analyse how these are distributed both temporally and spatially. SeaWiFS and MODIS are globally in good agreement. This is favoured by several factors, including the use of a similar processing chain (atmospheric correction and inversion algorithm), as well as the constant inter-calibration activity being conducted between the two sensors. By contrast MERIS has a larger variance and globally lower median values, similarly to POLDER-2 (note that MERIS data is a preliminary demonstration product only, complete reprocessing and delivery of the whole dataset is foreseen in the near future).

This study also underlines the importance of conducting comparisons on appropriate time and space scales, which seem to reveal more differences than global values. This activity is now being completed by a comparison of the satellite products with field measurements.

Acknowledgements

This work was supported by the MERSEA (Marine Environment and Security for the European Area) FP6 Integrated Project, in the framework of the Ocean and Marine services element of GMES (Global Monitoring for Environment and Security).

References

Campbell, J.W. (1995). The lognormal distribution as a model for bio-optical variability in the sea. Journal of Geophysical Research, 100(C7), 13237–13254.

Carder, K.L, F.R. Chen, J.P. Cannizzaro, J.W. Campbell and B.G. Mitchell (2004). Performance of the MODIS semi-analytical ocean color algorithm for chlorophyll *a*. Advances in Space Research, 33, 1152–1159.

Loisel, H., P.-Y. Deschamps, J.M. Nicolas and C. Moulin (2002). Polder-2 / Ocean Colour / Bio-optical algorithms. LOA ATBD, 1–9.

Longhurst, A. (1998). Ecological Geography of the Sea, pp 338. San Diego: Academic Press.

Morel, A. and D. Antoine (2000). ATBD 2.9. Pigment index retrieval in case 1 waters. ESA ATBD, Issue 4 Rev: 2, 1–26.

O'Reilly, J.E., S. Maritorena, B.G. Mitchell, D.A. Siegel, K.L. Carder, S.A. Garver, M. Kahru and C. McClain (1998). Ocean color chlorophyll algorithms for SeaWiFS. Journal of Geophysical Research, 103(C), 24937–24953.

Monitoring the chlorophyll concentration in coastal waters using *in situ* measurements and remote sensing data

Francis Gohin*, Karine Laffont and Marie-Madeleine Daniélou

Centre IFREMER de Brest, France

Abstract

Since the launch of SeaWiFS in September 1997 a large amount of ocean colour measurements have been collected and processed for a better knowledge of the temporal and spatial variability of the primary productivity. Empirical algorithms provide an estimation of the chlorophyll concentration with sufficient accuracy for monitoring the biological environment of the English Channel waters, including the turbid plume of the river Seine. These data, only available when there is cloud-free sky, can be combined with observations collected by conventional *in situ* networks, located along the shore, to provide a more regular service for surveillance. Most of the *in situ* measurements, obtained from the IFREMER/REPHY or INSU/SOMLIT networks, are acquired close to the shore while 1 km resolution satellite data are mostly available offshore. There is a statistical challenge to handle these different kinds of data which appear nevertheless to be complementary in several ways. For this purpose, the geostatistical tools and the kriging interpolator have been used. *In situ* data can be considered as a reference measurement for assessing the long term evolution of the ecological status of the waters while satellite data are more suited for mapping the biological features over the continental shelf and for validating biogeochemical models.

Keywords: satellite, coastal, chlorophyll, geostatistics

1. Introduction

The monitoring of chlorophyll concentrations at the coast is required for different purposes including a better knowledge of the food chain, conditioning the growth of fish larvae and shellfish, the surveillance of harmful phytoplankton population, the evaluation of the eutrophication risk, and to check the effect of new environmental laws and policy. This surveillance is based on *in situ* measurements which enable a long-term observation of the variability due to natural or man-induced processes.

However, the spatial extent of the coastal observations is very restrictive for many applications and the use of satellite data is required to enlarge our view of the primary productivity observed through the chlorophyll concentration. Satellite data are also particularly suited for validation and, in the near future, assimilation in biogeochemical models (Druon *et al.*, 2004). Satellites like SeaWiFS or MODIS, and also MERIS though its smaller swath width, give us a daily coverage (for cloud-free sky). Designed for the observation of the chlorophyll concentration in open sea, where the optical constituents of the medium are pure water and phytoplankton whose quantity can be related to the

* Corresponding author, email: Francis.Gohin@ifremer.fr

phytoplankton pigment, SeaWiFS can also provide very useful data in coastal waters when local algorithms (neuronal, empirical or semi-analytical) are used. For seven years, since the launch of SeaWiFS, from the end of 1997 to the end of 2004, IFREMER has used SeaWiFS for monitoring the chlorophyll concentration over the continental shelf of the eastern Bay of Biscay and the English Channel. Satellite-derived chlorophyll has proven to be unbiased, for instance without overestimation, and thus reliable even in areas where the load in suspended or resuspended sediment is high (river plumes, coastal waters after winter storms). Therefore, satellite-derived chlorophyll can be used as a complement to *in situ* measurements which are acquired and processed in coastal laboratories using different instruments and are themselves likely to show large errors as well. This no-bias in satellite-derived estimation enables a common management of the different data sets, obtained *in situ* or from remote sensing.

2. The *in situ* network

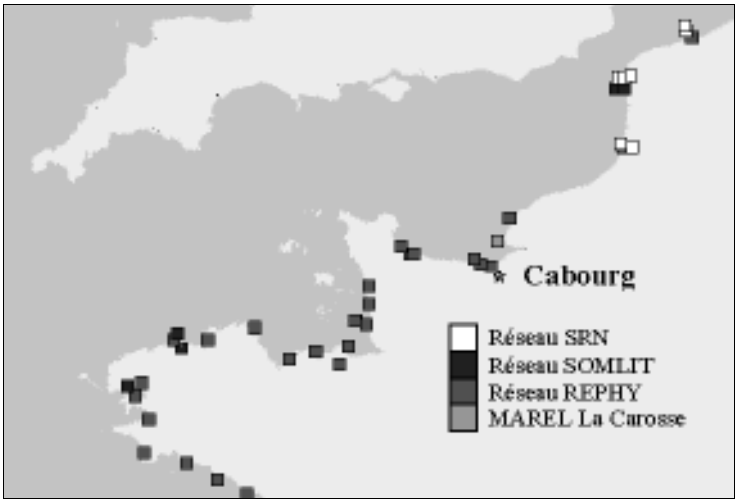

Figure 1 The *in situ* networks (the location of Cabourg, the station in the vicinity of the Seine plume, is indicated on the map).

The SOMLIT network has been developed by INSU (Institut National des Sciences de l'Univers) with a double aim:

- to monitor a set of locations for assessing the mean effect of the climatic and anthropogenic forcing on the long-term evolution of the coastal environment
- to build a minimum reference set of environmental data (including chlorophyll) for each location without excluding additional measurements for specific-site research.

The Phytoplankton and Phytotoxin Network (REPHY) monitors phytoplankton species, particularly those which are toxic to humans or marine organisms. This national network, carried out by IFREMER, also measures the Chl-*a* concentration for assessing the phytoplankton biomass.

Other local networks, linked to these national networks, are also shown in Figure 1. A new network, Réseau Hydrologique du Littoral Normand (RHLN), reinforces the surveillance of the water quality along the shores of Normandy. The station of Cabourg, located in relatively clear and rich waters, may show very high levels of chlorophyll concentration (See Figure 2 for August 2002). Another interesting feature on the graphs shown in Figure 2 is the early bloom in April 2003, compared to 2002. The question arising is how the satellite is able to reproduce and complete these series?

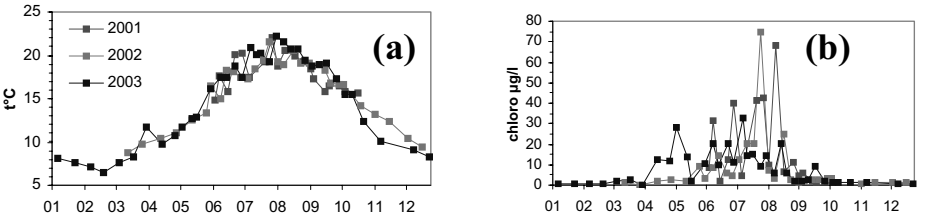

Figure 2 Time series of (a) temperature and (b) chlorophyll concentration measured at Cabourg from 2001 to 2003. See Figure 1 for the location of Cabourg.

3. Satellite-derived chlorophyll

Despite their well-known limitations in coastal waters, the ocean colour sensors provide a unique means for observing the phytoplankton distribution over the continental shelf. However, optical techniques from space platforms are hampered by clouds. The chlorophyll concentration in the English Channel has been routinely estimated since the launch of SeaWiFS in August 1997 by using a look-up table described in Gohin *et al*. (2002). The SeaWiFS reflectance, or the normalised water leaving radiance from which it is derived, is used to retrieve Chl and mineral SPM (Suspended Particulate Matter).

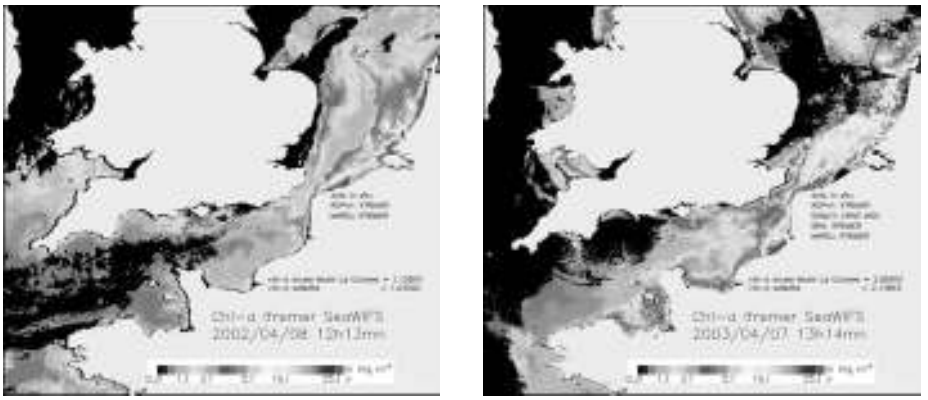

Figure 3 Satellite-derived concentrations for the beginning of April 2002 (left) and 2003 (right).

The chlorophyll maps of Figure 3, observed on 2002/04/08 (left) and 2003/04/07 (right) show two contrasting situations at the beginning of the production season. Early phytoplankton growth has been observed in spring 2003 as shown on the field measurement graphs at Cabourg (Figure 2).

4. Synthetic maps

4.1 The kriging method used for merging the data

The kriging method is based on the assumption that the underlying process (chlorophyll concentration) is a continuous random variable in space and time, which can be described in terms of the mean and (auto-)covariance function. The kriging system is obtained from minimising the variance of the error estimation E(Zo* – Zo) where Zo* is an estimator of Zo. In ordinary kriging, Zo* is searched as a linear combination of the observations available in the neighbourhood of the location where the estimation is carried out. The kriging estimator, within the geostatistical hypotheses, is unbiased and of minimum variance. For a better inference of the covariance, the structural analysis and the kriging is applied to the anomaly (defined as the difference between the daily chlorophyll concentration and the 7 year average on the same day).

Before kriging, another assumption is made on the satellite error. The error is expanded into two terms. The first one refers to the instrument noise, independent from one pixel to another, and the second to the result of the uncertainty in the quality of the atmospheric correction. This last term, which can be partially related to the geometry of the satellite-sea-sun optical path, locally affects a group of pixels in a similar manner and we consider it as a correlated error.

In our case, the auto-correlation is defined locally from a relationship between the local variance, as observed on the images, and the parameters of the covariance. This can also be related to the "proportional effect" resulting from an apparent relationship between the local variance and the square of the average.

4.2 Searching points in the neighbourhood before kriging

Before proceeding to kriging, searching for an appropriate neighbourhood is the first task. The points, chosen around the location where the estimation is to be carried out, have to be selected in such a manner that they build a well-balanced set of data in space and time. A minimum number of 16 data is imposed for kriging, with a search area centred on the day of the estimation and extending up to 4 days in time.

4.3 Illustration of the method for May 1st 2002

Figure 4 shows the different products involved in estimating the chlorophyll concentration on a given day, here 1 May 2002. First, anomaly maps are built by subtracting the daily seven-year average to the chlorophyll concentration maps of the closest days. The same transformation is applied to *in situ* data.

Next, a new anomaly map is calculated by kriging and, after adding the average concentration of the day, the estimated image is proposed as the synthesis image. The variance of the estimation error is also derived from the kriging system. The error appears greater in Figure 4 in the areas where the variability, expressed through local variograms, is higher (the plume of the river Seine, along the Northern coast, etc.)

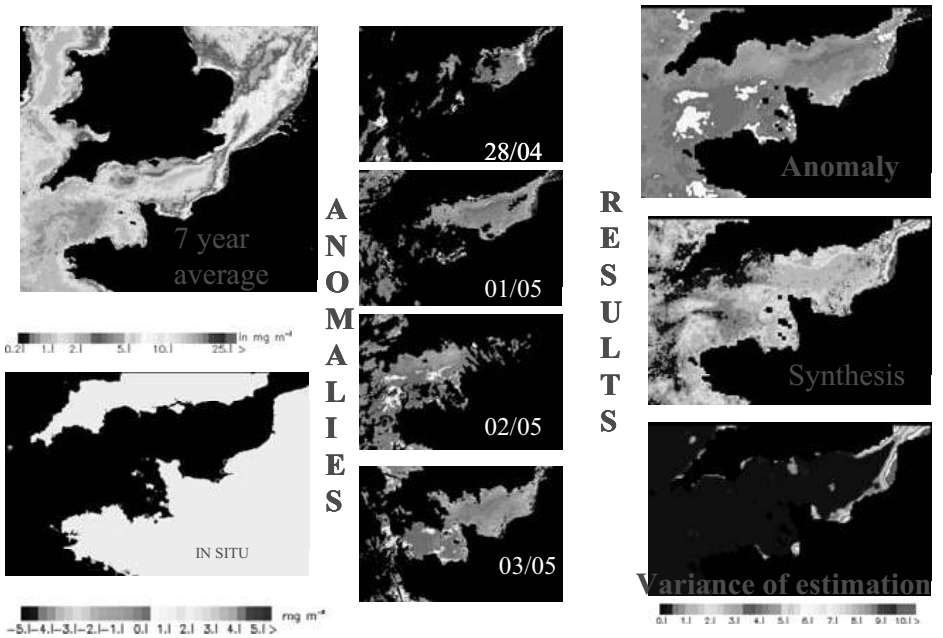

Figure 4 Kriging the chlorophyll concentration on 1 May 2005.

5. Comments on the sat-situ series at Cabourg and discussion

We can now consider the time series of the chlorophyll concentrations available for the emblematic location of Cabourg. Does the satellite-derived series reproduce the variability observed on the *in situ* measurements shown on Figure 2? Does the satellite series in some way complete the *in situ* series? The answer is clearly yes. Figure 5 shows, for the years 2002 (left) and 2003 (right) the satellite chlorophyll concentration at Cabourg before kriging (a) the interpolated chlorophyll concentration and (b) the "co-kriged" series where *in situ* data are added to satellite data into the kriging neighbourhood. By comparing (a) and (b), we observe that the interpolation has generated many new points in the temporal series, making it much more appropriate for further analysis. Satellite-derived and *in situ* series in (b) have the same characteristics. Early production in April 2003 is well-observed in both sets of data. The high peak at the beginning of August 2002, observed on a single *in situ* data, is shown during a longer period on the interpolated images (c), which results from merging by co-kriging, gives a coherent representation of both series, with a strong participation of the satellite data. This seven-year experience from SeaWiFS data shows that there is no technical opposition for using *in situ* and satellite data, not only side by side but also in a merging service, allowing better surveillance of the coastal environment.

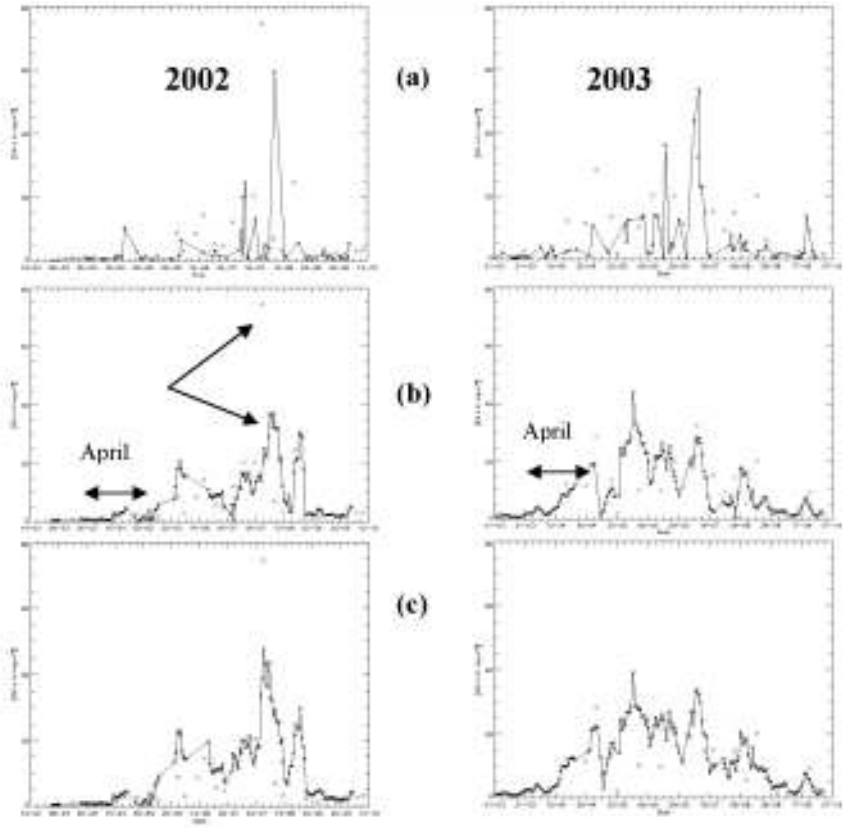

Figure 5 The time series of chlorophyll concentration from *in situ* (stars) or remote sensing (continuous line) origins at Cabourg in 2002 (15/02 to 12/10 on the left) and 2003 (01/03 to 07/10 on the right). (a) before kriging (cloud-free days), (b) after kriging satellite data, (c) after co-kriging and merging both types of data.
The main characteristics of the 2002 and 2003 years (chlorophyll concentration in April and a strong peak in August 2002) are similarly shown on the graphs, whatever the origin of the data.

Acknowledgements

The authors are very grateful to the SeaWiFS Project and the Distributed Active Archive Center, at the Goddard Space Flight Center.

References

Druon, J.N., W. Schrimpf, S. Dobricic and A. Stips (2004). Comparative Assessment of Large-Scale Marine Eutrophication: North Sea Area and Adriatic Sea as Case Studies. Marine Ecology Progress Series, Vol. 272 1–23.

Gohin, F., J.N. Druon and L. Lampert (2002). A five channel chlorophyll concentration algorithm applied to SeaWiFS data processed by SeaDAS in coastal waters, International Journal of Remote Sensing, 23, 1639–1661.

Satellite monitoring of cyanobacterial blooms in the Baltic Sea — The Baltic Algal Watch System

Martin Hansson*, Bertil Håkansson and Bengt Karlson

Oceanographic Unit, Swedish Meteorological and Hydrological Institute, Sweden

Abstract

The summer blooms of nitrogen-fixing cyanobacteria are regular phenomena in the Baltic Sea but the past years' strong and widespread blooms have caused major environmental concern both to the public and authorities due to their toxicity and the increased nitrogen input. One of the most abundant toxic species *Nodularia spumigena* can pose a threat to animals and children. The Baltic Algae Watch System (BAWS) at SMHI has been operational since 2002 and provides information both to the public and to the Information Offices for Skagerrak/Kattegat, the Baltic Proper and the Bothnian Bay. The main source of information is the satellite sensor AVHRR (Advanced Very High Resolution Radiometer).

Keywords: Cyanobacterial blooms, Baltic Sea, algal blooms, satellite monitoring, *Nodularia*.

1. Introduction

Summer blooms of cyanobacteria usually dominated by *Nodularia spumigena* and *Aphanizomenon baltica* (*flos-aquae*)[1] are regular phenomena in the Baltic Sea and nearly as old as the present brackish water phase, starting as far back as ~7000 years ago (Bianchi, 2000). Most cyanobacteria e.g. *Nodularia* use dissolved molecular nitrogen (N_2) as an additional nutrient source, which allows them to bloom in the summer when the growth of other phytoplankton is limited by nitrogen (Wheeler *et al.*, 1986; Fonselius, 1995). At some stage of the bloom the algae lose their buoyancy control and the algae aggregate at the surface. These accumulations of blooming algae have a distinct character (see Figure 1) and can be seen as meandering shapes on the surface formed by wind and currents. (Degerholm, 2002; Finni *et al.*, 2001; Kahru *et al.*, 1994).

Although mass blooms of cyanobacteria have been know since the 19th century, it has been debated whether the area extent and intensity of the blooms have increased because of anthropogenic sources of eutrophication (Kahru *et al.*, 1994; Kahru, 1997; Bianchi, 2000; Finni, 2001; Kononen, 2001). Studies of pigments in sediment cores (Poutanen and Nikkilä, 2001) suggest that the occurrence and intensity of blooms in the Baltic Sea have increased since the 1960s. The increase seems to have peaked during the 1970s but returned and stabilised during the 1980s to slightly increased levels. These sediment

1 The taxonomic position of *Aphanizomenon flos-aquae* in the Baltic Sea is uncertain. The name *Aphanizomenon baltica* is commonly used by e.g. HELCOM

* Corresponding author, email: Martin.Hansson@smhi.se

analyses are difficult to perform in recent sediments, but during 1997–2004 there have been at least four years with massive blooms in vast areas of the Baltic Sea (Andersson and Karlson, 2004; Hansson, 2004, SMHI, unpublished results). In recent years there has also been an increased interest from both the public and authorities since the peak of the bloom usually coincides with the summer holidays. The occurrence of blooms is a nuisance, especially when thick surface accumulations aggregate along the coast, releasing bad odours and preventing swimming. At worst, the release of toxic substances from *Nodularia* may kill dogs and cattle that drink the water. Humans and especially children who get in contact with contaminated water usually suffer from skin irritation, stomach problems and flu-like symptoms (Degerholm, 2002; Edler *et al.*, 1995).

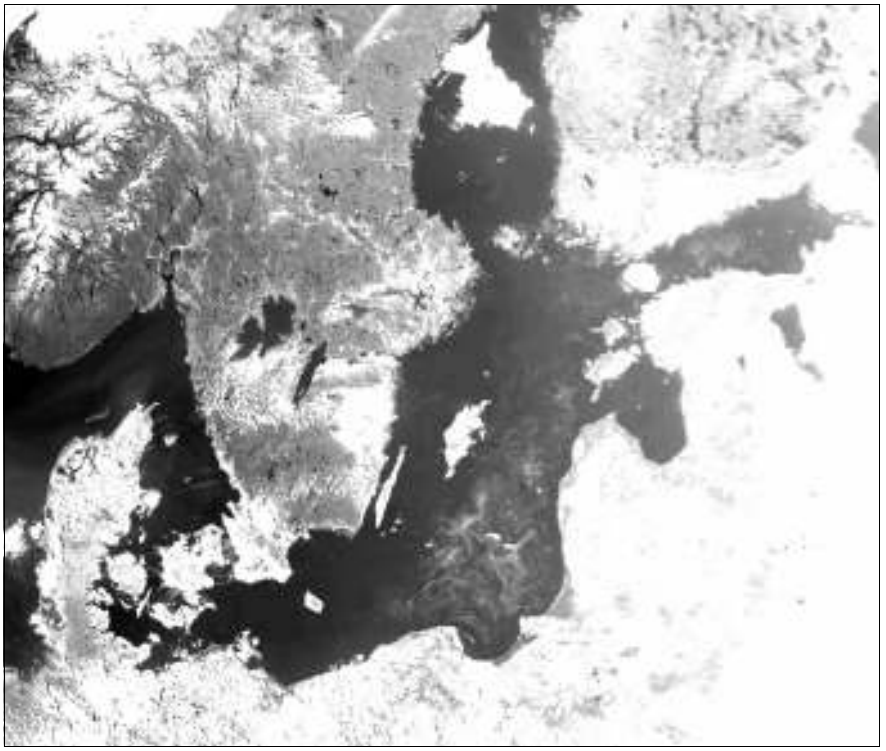

Figure 1 NOAA–AVHRR image (visual channel 1) of the Baltic region. Cyanobacterial blooms can be seen as meandering shapes on the ocean surface, in the eastern Baltic Proper and in the Gulf of Finland.

However, due to the high spatial and temporal variability and the scarcity of data from the open sea, long-term changes in the extent of cyanobacterial blooms are very difficult to investigate using conventional ship-borne monitoring. Hence there is a need to use other forms of data and methods that enable near real-time (NRT) monitoring over vast areas on a regular basis. Collecting data using satellite-based sensors has many advantages. The NOAA–AVHRR (Advanced Very High Resolution Radiometer) sensors give a synoptic view of the Earth's surface covering large areas on a regular basis. The repeat cycle is high; 2–4 useful images per day. Data delivery is fast, and images can be

provided within an hour of an overpass. The main disadvantage is that the sensor cannot "see" through clouds, which limits the monitoring ability at these high latitudes where there is a high presence of clouds. The satellite data is also limited to the top metres of the ocean surface; blooms at greater depths are invisible (Gordon *et al.*, 1999).

Cyanobacteria blooms were first detected in satellite imagery by LANDSAT 1 and 2 in the early 1970s. However, it took another 15 years before it was noted that the AVHRR sensor was suitable for detection of cyanobacterial blooms (Håkansson, 2000). A compiled time series of bloom observations based on AVHRR data was produced by Kahru *et al.* (1994) and Kahru (1997) showing the area extent of the blooms between 1982 and 1997. The results did not indicate any clear trend of increasing bloom events but the data showed large-scale inter-annual variability and new areas were found to host cyanobacteria blooms (Håkansson, 2000).

2. Material and method

The method used to process NOAA–AVHRR data to detect cyanobacteria blooms in the Baltic Sea was developed by M. Kahru and O. Rud at the University of Stockholm (Karhu, 1997). The method is basically a supervised classification algorithm (See Figure 2) that relies on multiple thresholding and difference in visible, near infrared and thermal channels to distinguish cyanobacteria accumulations from other common features such as land, clear water, clouds, haze, sun glint and error pixels. The method includes manual interpretation and correction of each satellite scene. Areas with surface accumulation of cyanobacteria have an increased reflectance in the visible band. Usually such areas possess an albedo varying between 2.3–4.0% whereas lower and higher values are recognised as water or clouds respectively. The method also included a calculation of spatial texture in 3×3 pixel windows in the visible band 1. This step is not included, because it usually fails to recognise blooms, resulting in extensive manual corrections. The near-infrared band 2 and the two thermal bands 4 and 5 are used to screen clouds, haze, land or errors. Pixels with band 2 albedo exceeding the corresponding band 1 albedo by 0.1% are classified as land or errors. Band 4 temperatures lower than a certain varying threshold and with a band 4 and band 5 difference greater than 2 °C are classified as clouds or haze (Karhu, 1997).

A common problem when using AVHRR data is the relatively coarse pixel size (~1 km^2), which make detection of blooms impossible near the coast. Hence, this method can only be applied for monitoring offshore blooms. It is also of great importance to be able to screen clouds when monitoring cyanobacterial blooms, to get an estimate of cloud-free observations in relation to bloom and cloud observations. The method described above was easily adjusted to screen the cloud cover of the Baltic Sea. Cloud analyses are made on all scenes that are processed.

The results from the daily satellite monitoring have been compared with *in situ* measurements of algae concentrations and temperature profiles (offshore *in situ* data from SMHI and Stockholm Marine Research Centre (SMF)). The biological data consist of measurements of *Nodularia* and *Aphanizomenon* taken with tubes from 0–10 m depth, giving an integrated estimate of the algae concentration.

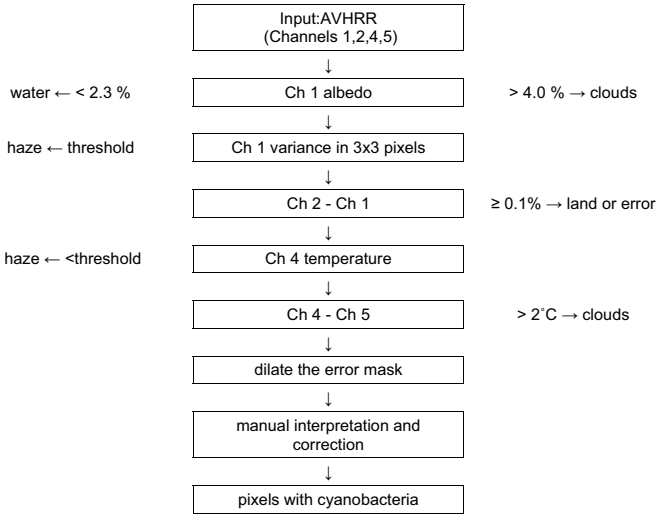

Figure 2 Flowchart of the algorithm for detecting cyanobacteria accumulations in NOAA–AVHRR imagery, from Karhu (1997).

2.1 The algal monitoring system

The monitoring system BAWS was developed in early 2002 to provide information to the public and the three Marine Information Offices in Sweden (The Skagerrak and Kattegat, the Baltic Proper and the Gulf of Bothnia). A restricted web site was created to assemble information that can be useful for monitoring and prediction of the blooms' movements and development. The system is available to marine environmental managers and scientists all around the Baltic region and is operational from June–September (contact the author for access). The Baltic Algal Watch System includes:

- Daily monitoring of cyanobacterial blooms using satellite imagery
- NRT Sea Surface Temperature (SST)
- NRT information from coastal observations and weather stations
- *In situ* measurements; Hydrographic profiles and phytoplankton analyses
- Annual summaries that show the number of bloom and cloud observations in each pixel
- Other information about large-scale ocean phenomena
- Seatrack web, forecast and dispersion calculations of oil spill and chemicals, but also for surface accumulations of cyanobacterial blooms
- Model results (3–48 hours):
  - HIROMB; currents, temperature, salinity
  - HYPNE; wave height
  - HIRLAM; wind direction and speed.
- Incoming solar radiation, the STRÅNG model, providing photosynethic photon density from the last 24 hours.

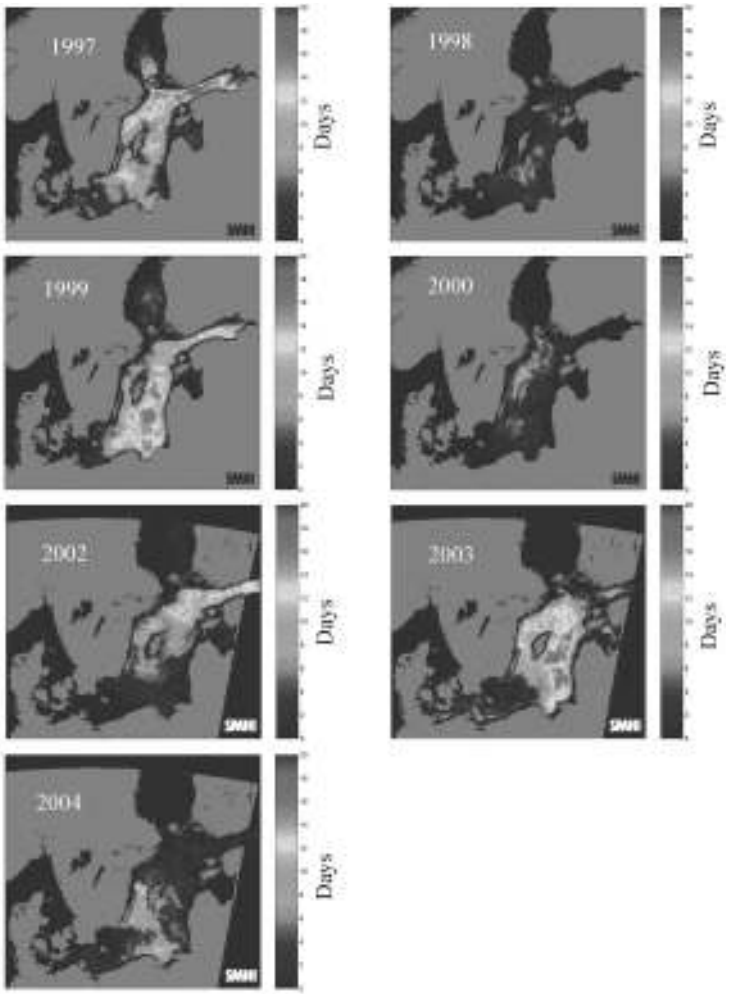

Figure 3 Annual estimates of the number of days with observed blooms in each pixel, based on daily satellite monitoring. Results from BAWS 2002–2004 and the EU project HABES (Harmful Algal Bloom Expert System) 1997–2000. Year 2001 is missing due to satellite antenna problems.

3. Results

3.1 Surface accumulations of cyanobacteria observed from satellite

The daily observations of blooms have been stacked to produce yearly maps of all satellite observations. The maps in Figure 3 present the geographical locations of the blooms and number of days of bloom observations in each pixel. Similarly, cloud cover maps were produced presenting the number of days with cloud cover in each pixel during the main bloom season in July and August.

To account for the cloud cover a test was made to calculate the "expected" number of days with blooms using the ratio between the observed number of blooms and the total

number of cloud-free observations (including bloom observations). The ratio was then multiplied by the total length of the "surface accumulation season" (defined as the time period between the first and the last satellite observation of blooms) during each year to get an estimate of the "expected" number of days with blooms. The overall mean difference between observed and "expected" were only between 1 and 3 days during the seven years analysed. The maximal difference was up to 7–10 days at some locations.

4. Discussion

4.1 Dynamics of cyanobacterial blooms

The environmental factors that regulate the intensity of the blooms and the conditions causing the inverted sedimentation are only vaguely understood. Obvious candidates for the initiation of a bloom are: high incoming solar radiation, strong near-surface stratification, suitable surface temperatures, low winds and sufficient amounts of biological available phosphorus. If one or more of the factors named above is absent there is a good chance that the bloom is less intense or never appears. Figure 4 presents all *in situ* measurements of *Nodularia* and *Aphanizomenon* versus temperature and month at BY31 during the period 1990–2002. Hence the water temperature should exceed 13.5–14.0 °C. This temperature is valid for *Nodularia* and *Aphanizomenon* even though the latter seems to be able to initiate blooms even at lower temperatures, 12–13 °C.

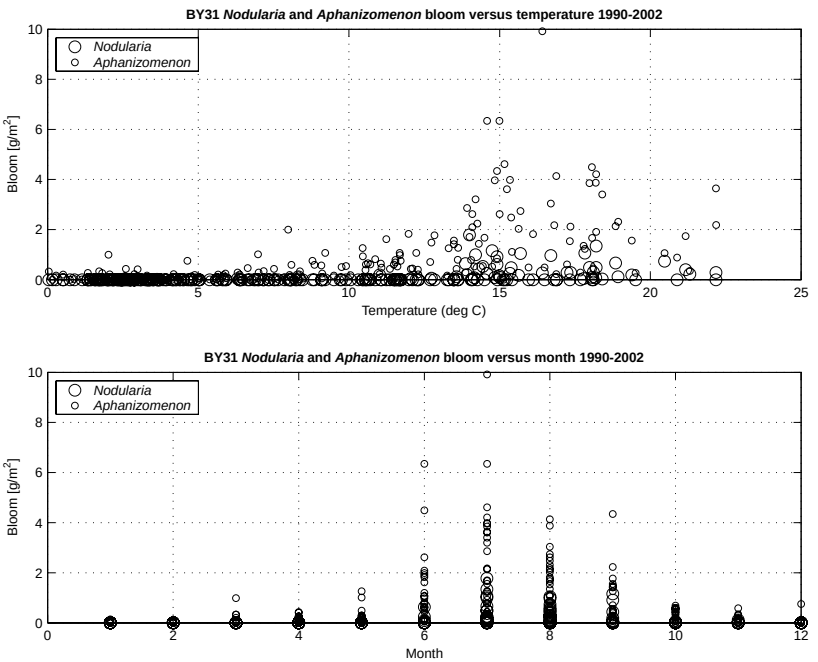

Figure 4 *Nodularia* and *Aphanizomenon* concentrations versus surface temperature and month at station BY31, 1997–2002.

Regarding the inverted sedimentation, it is well known that accumulations appear on the surface in calm and sunny weather. During periods of strong heating and low winds, the wind-driven mixing is insufficient to stir the solar heat absorbed near the surface throughout the depth of the early morning mixed layer. As solar heating proceeds, a permanent or diurnal stratification is generated and heat becomes trapped at a progressively shallower stratified layer. High solar radiation and the associated strong near-surface stratification may be one of the factors that cause the surface trapped algae to lose their buoyancy regulation, which results in inverted sedimentation. As the surface accumulation further increases the heating and the stratification by absorbing more light through their pigments, a positive feedback loop is generated that results in further surface accumulations. Although strong winds can quickly break the stratification and redistribute the algae into deeper layers and make the accumulation disappear from the surface, Karhu *et al.* (1993) showed that dense accumulations remain clearly detectable the following day even at wind speeds of 8 $m s^{-1}$.

5. Summary and conclusion

The Baltic Algal Watch System, which has been operational since 2002 has shown that the combination of satellite imagery, model results and *in situ* measurements, assembled at one location, is a powerful tool for monitoring and prediction of cyanobacterial blooms in the Baltic Sea. The system has been appreciated and frequently used by authorities, environmental managers, media and the public. The results from the monitoring have also made scientific contributions.

The main conclusions from this study can be summarised as follows:

- The cyanobacterial blooms show large inter-annual variability. Years with massive blooms can be followed by years with only minor blooms. The first surface accumulation is usually observed in early July and proceeds to the end of August. It is obvious that cyanobacteria are initially present in the water column before becoming visible in satellite imagery. The time elapsed between the start of the bloom in the water column and the first observations of surface accumulations depends strongly on weather conditions and stratification of the water column. The mean for the period studied is 9 days.
- Cloud cover, which is a major problem when using NOAA–AVHRR data, can be accounted for. The mean difference between the observed and "expected" number of days with cyanobacteria in each pixel is 1–3 days.
- The increase of the blooms both in area extent and intensity that have been debated is very difficult to prove. Satellite data has been available for about 3 decades, and this period is too short to show trends or natural variability of the phenomena. Hence it is of great importance to add data to the relatively long NOAA–AVHRR time-series so that long term changes and trends can be detected in the future.
- Future work will focus on introducing other NRT satellite data such as MERIS or MODIS and obtaining homogenous data sets of the mapping procedure using different sensors, and further evaluating the impact of clouds on the mapping procedure.

Acknowledgements

The authors would like to acknowledge the MISTRA (Swedish Foundation for Strategic Environmental Research) research programme RESE (REmote Sensing for the Environment) for making this possible, Pia Andersson and Patrick Gorringe (SMHI) for assistance with the operational monitoring and Svante Nyberg (SMF) for the CTD data.

References

Andersson, P. and B. Karlson (2004). Pilot study Baltic Sea. In: Blauw, A.N. (Eds.). Harmful Algal Blooms Expert System, final report. p. 8–1–8–66. Delft Hydraulics, Delft. www.habes.net

Bianchi, T.S., E. Engelhaupt, P. Westman, T. Andren, C. Rolff and R. Elmgren (2000). Cyanobacterial blooms in the Baltic Sea: Natural or human-induced? Limnol. Oceanogr., 45(3), 716–726.

Degerholm, J. (2002). Ecophysiological characteristics of the Baltic Sea N2-fixing cyanobacteria Aphanizomenon and Nodularia, Doctoral thesis, Department of Botany, University of Stockholm.

Edler, L., E. Willén, T. Willén and G. Ahlgren (1995). Skadliga alger i sjöar och hav, Naturvårdsverkets rapport 4447.

Finni, T., K. Kononen, R. Olsonen and K. Wallström (2001). The History of Cyanobacterial Blooms in the Baltic Sea. Ambio Vol. 30 No.4–5.

Gordon, J., M. Antoine, C. Francois, M. Calatuyud, V. Barale, H.M. Snaith, O. Rud, M. Ishii, M. Gade, J.M. Redondo and A. Platinov (1999). The Clean Seas Project — Final report. Produced with the support of DG XII/D of the European Commission under contract number: ENV4–CT96–0334.

Fonselius, S. (1995). Västerhavets och Östersjöns Oceanografi, SMHI Oceanografi rapport. ISBN 91–87996–07–3.

Håkansson, B. (2000). Satellite remote sensing of coastal oceans: water quality and algae blooms. Seas at the millenium: An Environmental evaluation (edited by C. Sheppard). Elsevier Science Ltd. Vol.3, 293–302.

Kahru, M. (1997). Using Satellites to Monitor Large-Scale Environmental Change: A case study of the Cyanobacteria Blooms in the Baltic Sea. Monitoring algal blooms: New techniques for detecting large-scale environmental change. Landes Bioscience.

Kahru, M., U. Horstmann and O. Rud (1994). Satellite Detection of Increased Cyanobacteria Blooms in the Baltic Sea: Natural Fluctuation or Ecosystem change? Ambio Vol. 23 No. 8.

Kahru, M., J.-M. Leppänen and O. Rud (1993). Cyanobacterial blooms cause heating of the sea surface, Mar. Ecol. Prog. Ser., Vol. 101: 1–7.

Kononen, K. (2001). Eutrophication, Harmful Algal Blooms and Species Diversity in Phytoplankton Communities Examples from the Baltic Sea. Ambio, vol. 30 No. 4–5.

Poutanen, E.-L. and K. Nikkilä (2001). Carotenoid pigments and tracers of cyanobacterial blooms in recent and postglacial sediments in the Baltic Sea. Ambio, vol. 30, No. 4–5.

Wheeler, P.A. and D.L. Kirchman (1986). Utilization of inorganic and organic nitrogen by bacteria in marine systems, Limnology and Oceanography, 31(5), 998–1009.

GOSUD: Global Ocean Surface Underway Data Project

Loïc Petit de la Villéon*[1], Thierry Delcroix[2], Robert Keeley[3], Thierry Carval[1] and Catherine Maillard[1]

[1]*Ifremer Centre de Brest, France*
[2]*IRD / Legos Toulouse, France*
[3]*MEDS Ottawa, Canada*

Abstract

Ocean salinity is one of the key variables for monitoring and modelling ocean circulation. Therefore the initial focus for the project has been on salinity observations collected by thermosalinograph, although other variables are under active consideration.

The goal of GOSUD is to develop and implement a data system for ocean surface data, to acquire and manage these data and to provide a mechanism to integrate these data with other types of data collected in the world oceans. The data concerned are those collected as a platform is underway from the ocean surface down to about 15 m depth.

The objective of GOSUD is to organise the surface underway data that are now collected and to work with data collectors to improve present practices to try to meet the benchmarks of spatial, temporal sampling and data accuracy required to meet GOOS objectives and operational oceanography requirements.

Keywords: Sea surface salinity, sea surface temperature, thermosalinometer

1. Introduction

The Global Ocean Surface Underway Data (GOSUD) Project is an Intergovernmental Oceanographic Commission (IOC) programme designed as an end-to-end system for data collected by ships at sea. The goal of the GOSUD Project is to develop and implement a data system for surface ocean data, to acquire and manage these data and to provide a mechanism to integrate these data with other types of data collected in the world oceans. For the purposes of this project, the data concerned are those collected as a platform is underway and from the ocean surface down to about 15 m depth.

2. Operations

2.1 Data management

Everything begins with the platforms at sea that make routine, underway measurements. Participants are encouraged to send the data ashore as quickly as possible. It is the desire of the GOSUD project that these data be available as soon after collection as possible (hours to days) although meeting this target may be difficult for certain kinds of data. The data received in each country are expected to pass through quality control procedures standardised for the project and carried out by each participant or another person

* Corresponding author, email: Loic.Petit.De.La.Villeon@ifremer.fr

acting on their behalf. It is expected that some of these procedures will be automated and sufficiently robust to remove the most serious errors in the data. After such procedures, participants send the data immediately to a global data server set up for the project. It is from this global server that GOSUD provides users with data. GOSUD participants are also encouraged to send the data to the GTS, either in the existing TRACKOB code form, or in BUFR format, since some potential users may still wish to use the GTS as a source of data.

The GOSUD project does not intend to manage any data extracted from the GTS unless this is the only source available. Instead there is a monitoring function carried out to compare data appearing on the GTS to data received at the global server. This function occurs routinely, and identifies differences between the two data streams. Where data are found to appear on the GTS but not on the global server, the originators are contacted and encouraged to become part of the project. Where data appear on the global server but not on the GTS, originators are encouraged to make the data available on the GTS so that traditional GTS users will have access to the data from this distribution system.

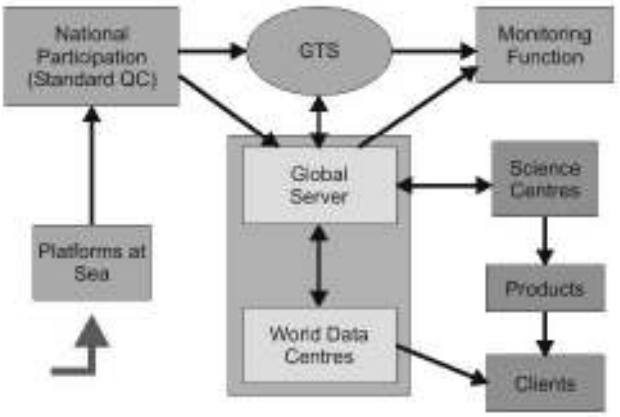

Figure 1 GOSUD Project data flow.

2.2 Data access

The global server is the central hub of the project. Its job is to act as the archive for such data, and to interface to the World Data Centres that also hold historical underway data. The global server provides data and products to users, and works in collaboration with project participants to monitor the state of the data system. The global server verifies the integrity of the data being provided, and reconciles early data received with the same data received at a later time and with more extensive quality assurance procedures having been employed.

The linkage between the global server and the World Data Centres is very important. The two parties share the long term archive responsibilities to ensure the ongoing safekeeping of the data. They also share the responsibilities of providing data and products from the start of the GOSUD project into holdings from the historical past.

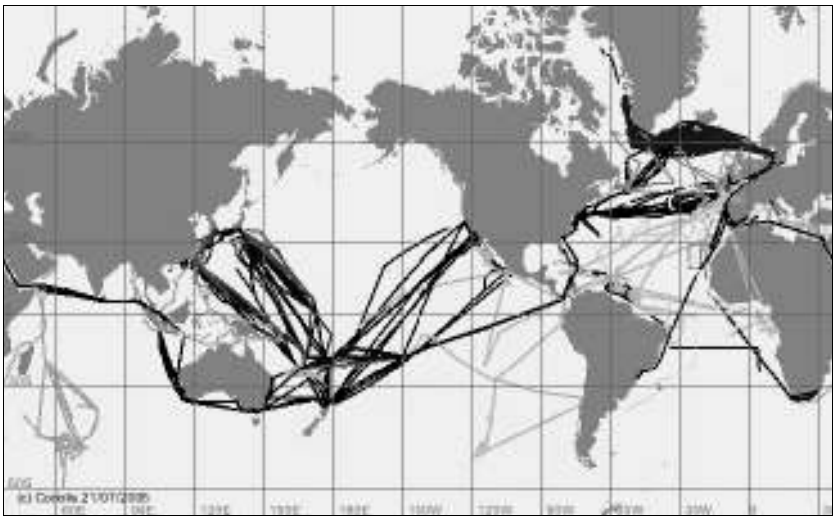

Figure 2 Data residing on the GOSUD ftp server with observation dates from early 2000 to mid-July 2005. The different track colours indicate different sources of the data.

2.3 Products

It is very important for the global server to collaborate with one or more science centres in defining, developing and disseminating scientific products from the project. It is through these products that the project will be known and some of its success measured.

A substantial amount of work has been done with the TSG data collected in different oceans with a lead role being played by IRD, France. Figure 3 and Figure 4 below are examples of mean conditions calculated by a combination of TSG and surface observations from profiles. These maps are generated at a 1×1 degree resolution in position, both monthly and as an annual mean.

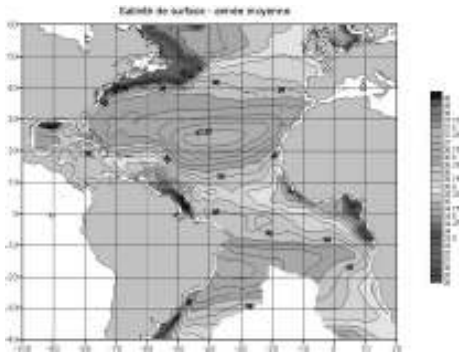

Figure 3 Annual mean surface salinity in the Atlantic Ocean (from IRD).

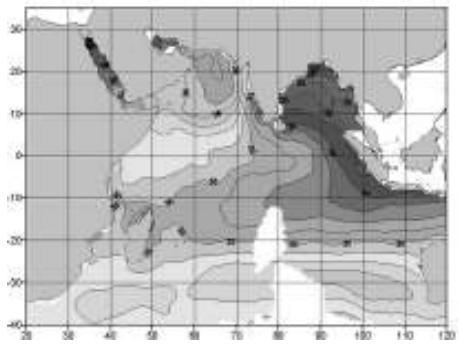

Figure 4 Annual mean surface salinity in the Indian Ocean (from IRD).

Web data access can also be considered as a derived product. The GOSUD Global Server, hosted by the Coriolis data centre, provides an interactive web interface where data can be selected and downloaded. Figure 5 shows this interface and provides infor-

mation on the 17 vessels (either research or merchant) which have provided data to the project during the past 12 months.

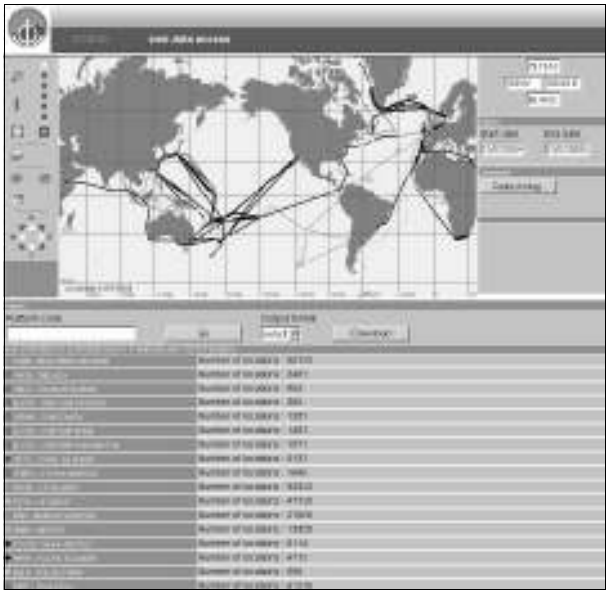

Figure 5 GOSUD data web access.

3. Conclusion

More information on the project can be found on www.gosud.org. The project is looking actively for volunteer ships — either commercial or research vessels — which would like to join the project by transmitting their data.

Acknowledgements

The GOSUD project is a project of the IOC International Oceanographic Commission and is supported by IODE International Oceanographic Data Exchange. We acknowledge the support they provide to the project.

We are also very grateful to the ship operators and marine researchers who contribute to the project by collecting and sharing their data.

Operations and developments in the Irish Weather Buoy Network

Sheena Fennell*, Guy Westbrook, Glenn Nolan and Kieran Lyons

Marine Institute, Galway, Ireland

Abstract

In 2005 the Irish Weather Buoy Network accomplished the initial remit to deploy five marine meteorological platforms in Irish coastal waters. These platforms have been deployed to increase the accuracy of forecasts around the Irish coastline and thereby increase safety at sea. In 2004 self-logging high accuracy temperature and conductivity sensors (SBE 16+) were added to each platform to begin a baseline data set of the coastal waters around Ireland. There are plans over the next few years to replace the acquisition system subject to available funding and a suitable acquisition system. It is planned that the replacement system will accommodate more sensors, have two-way communications system to allow flexibility in sample rates and enhance trouble-shooting capabilities.

Keywords: Operational oceanography, meteorology, weather buoys, Ireland.

1. Introduction

The Irish Weather Buoy Network consists of five operational platforms around the coast of Ireland (Figure 1). These provide near real time hourly information on wind speed and direction, significant wave height and period, air and sea temperature, atmospheric pressure and humidity. The data is transmitted through the Meteosat system to Germany and then uploaded onto the GTS (Global Telecommunications System) where it is downloaded by the UKMO and Met Eireann and forwarded onto the Marine Institute via e-mail. It is then uploaded onto the website www.marine.ie/databuoy.

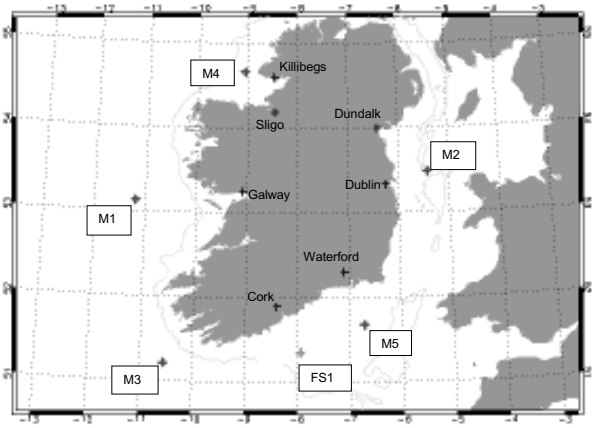

Figure 1 The location of the Irish Weather Buoy Network.

* Corresponding author, email: sheena.fennell@marine.ie

The project was established after a report in 1996 called for an increase in the accuracy of marine forecasting around the Irish coastline to minimise the number of lives being lost at sea. At present Ireland's maritime industry is worth well in excess of €3bn and employs in the region of 44000 people (Marine Institute, 2005). The project was set up as a collaboration between the Irish Department of Communications, Marine and Natural Resources (DCMNR), Marine Institute (MI), UK Met Office (UKMO) and Met Eireann (ME).

Since the first deployment in 2000 a new buoy has been deployed each year and in 2003 Marathon Oil added the weather station they maintain on the Kinsale Gas platform to the data set (FS1).

Table 1 Location of the Irish weather buoys.

Year	Buoy	Latitude	Longitude
2000	M1	53° 07' 36"N	11° 12' 00"W
2001	M2	53° 28' 08"N	05° 25' 05"W
2002	M3	51° 13' 00"N	10° 33' 00"W
2003	M4	54° 40' 00"N	09° 04' 00"W
2003	FS1	51° 22' 25"N	07° 56' 07"W
2004	M5	51° 41' 24"N	06° 42' 24"W

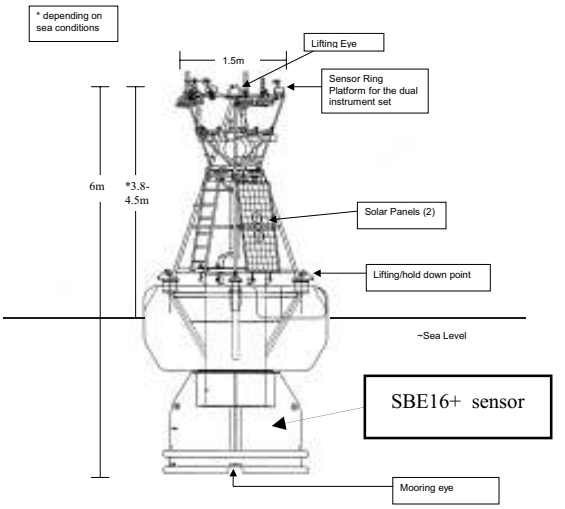

Figure 2 Buoy structure.

2. Observational extremities

The buoy hulls are designed to withstand conditions in the North Atlantic and are made of a closed cell structure and then covered with elastomer. The moorings are a combination of open link chain and dynema rope. Each platform and the moorings are serviced annually and more frequently if problems arise.

Since the first deployment in 2000 off the west coast there have been a number of intense depressions that have passed through the coastal waters. In particular in January 2005 the M1 buoy on the west coast experienced some of the most severe weather since its deployment in 2000. Atmospheric pressure dropped from 1006 to 986 millibars over a 10-hour period (see Figure 3). Wave height rose sharply after the drop in atmospheric pressure and reached 11.9 m at 16:00 hrs on 11 January (see Figure 4). From Figure 5 it can be seen that max gusts reached 68 knots at 12:00 midday on 11 January. All sensors survived including the cup anemometers and wind vanes. This type of near real time acquisition of data can be used for input into storm surge models and also allows for more accurate coastal reports.

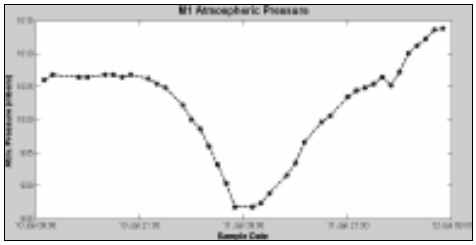

Figure 3 M1 atmospheric pressure.

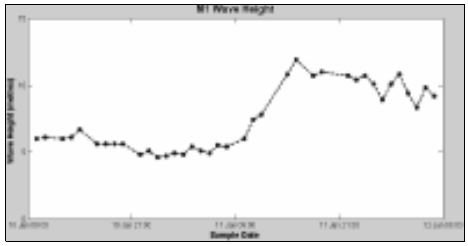

Figure 4 M1 wave height.

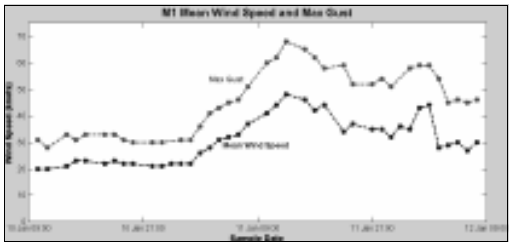

Figure 5 M1 mean wind speed and max gusts.

3. Addition of oceanographic instruments

In 2004 SBE 16+ sensors were added to all five platforms (Figure 2) to establish a temperature and salinity database for the waters surrounding Ireland. The instrument is self-powered and self-logging with a sample interval of 30 minutes. Data has been successfully recovered from the service visits to date during 2005. Data quality is good with very little biofouling occurring on the sensors. An ADCP was also deployed on M1 on the west coast during 2004. It was placed in line within the mooring with a cage manufactured in-house. This deployment was treated as a trial to establish recovery and deployment procedures and also to determine what type of motion the sensor itself experiences and whether this type of deployment is acceptable.

4. Future of the network

Currently the project is aiming to move towards acquiring a new Data Acquisition System. The system currently on the buoys was developed by the UKMO, which is a reliable system and has performed well. The project would now like to move to an acqui-

sition system that is capable of integrating a new communications system, additional sensors such as ultrasonic wind sensors and also to have remote configuration abilities from a land base. Maintenance of the existing five platforms will continue on a regular basis.

Acknowledgements

The authors would like to thank the Irish Department of Communications, Marine and Natural Resources, UK Met Office, Met Eireann, The Marine Institute and Marathon Oil.

References

Report to the Minister of the Marine (1996). Report of the Fishing Vessel Safety Review Group, Government Publications, 95 pp.

Douglas-Westwood Limited (2005). Marine Industries Global Market Analysis, Marine Foresight Series No.1, 128 pp.

Marine Institute (2005). Ireland Ocean Economy and Resources. Unpublished.

A new modular marine free-fall CPT

S. Stegmann[1], A. Kopf[1] and H. Villinger[2]

[1]Research Centre Ocean Margins, University of Bremen, Germany
[2]Department of Geoscience, University of Bremen, Germany

Abstract

Cone Penetration Tests (CPT) are a standard method for the *in situ* characterisation of shallow subseafloor sediments. Hence we have developed an easy-to-use, lightweight free-fall CPT (FFCPT) lance for shallow marine application (200 m water depth). The lance consists of an industrial 15 cm^2 piezocone measuring pore pressure, temperature, tilt, tip resistance and sleeve friction. The lance may be optionally equipped with extension rods (0.5–6.5 m total length) to control penetration depth. A pressure case (200 m) hosts a microprocessor, volatile memory, battery, and accelerometer, and may be loaded with additional weights (up to 90 kg) for tests in indurated sediment.

Initial deployments have been successfully carried out in muddy to coarse-grained sediments. The results attest similar friction ratios as in standard CPT tests, with the maximum penetration having exceeded 4 m sub-seafloor depth (as a function of the weight added). Our main focus was pore pressure, which generally rises during impact (between 10 and 50 kPa in excess of hydrostatic pressure). However, even medium-grained sediments often show rapid decays towards ambient values during dissipation tests (30 minutes to 5 hours).

Keywords: Cone penetration test, pore pressure, friction, sediment, *in situ* measurement

1. Introduction

Since the early 1920s, CPT measurements have become a widely accepted means to characterise the geomechanical properties of soft to indurated sediments in onshore and offshore settings. The principle of the testing procedure is vertical profiling using a lance equipped with a standard cone (usually 10 or 15 cm^2 in diameter), which is pushed into the sediment at a constant rate of 2 $cm\,s^{-1}$ (e.g. Lunne *et al.*, 1997). The cone can be equipped with various sensors, most often measuring tip and sleeve resistance (as a function of sediment stiffness), pore pressure (to be monitored in different positions, u1–u3), temperature and tilt. The two parameters of major interest are friction ratio (i.e. the ration between sleeve friction and tip resistance) and pore pressure, since both of them control sediment strength and effective stress state. As a consequence, CPTs are efficient devices in tasks such as cable or pipeline laying, slope stability concerns, navigability of harbours/estuaries, or ground-truthing of geophysical data.

One of the most difficult environments in standard CPT sediment characterisation is the marine realm because the penetration force is not easily provided. In shallow water, pontoons may be used to host onshore devices (CPTs mounted on trucks, etc.), however,

* Corresponding author, email: stegmann@uni-bremen.de

in deeper water, heavy rigs have to be lowered to the seafloor in order to provide an inert abutment to push the lance-shaped device into the sediment. For this purpose, an easy-to-handle, lightweight CPT free-fall device was designed, which offers the possibility of cost- and time-effective *in situ* measurement in quasi undisturbed sediments, as there is no need for rigs put down on the sea floor.

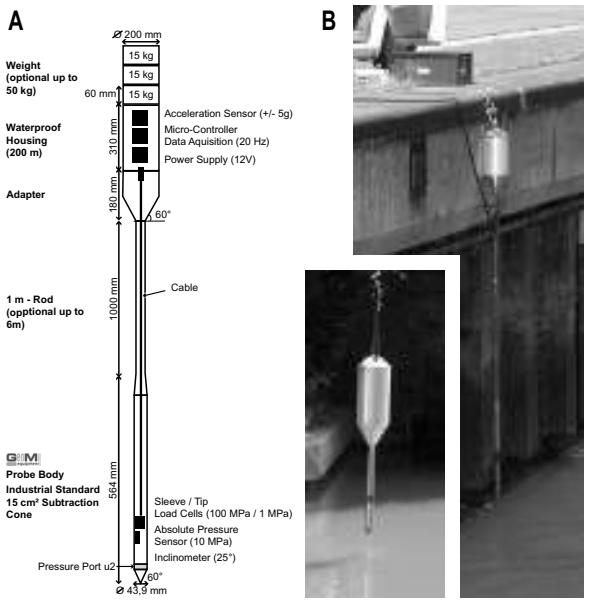

Figure 1 A) Schematic diagram of FFCPT; B) Photographs of FFCPT in the longer (5 m) and shorter (no extension rod; see inset) configuration prior to deployment.

2. Instrument design and method

The free-fall instrument developed at RCOM Bremen is characterised by its modular design concerning length and weight (see Figure 1A). It therefore can be handled by two people from very small platforms, but could also be used on large vessels using a winch. The lance consists of an industrial 15 cm^2 piezocone (with pore pressure in u2 position, temperature, tilt sensors, as well as the capability to measure tip and sleeve resistance) and a pressure case containing a microprocessor, volatile memory, battery, and accelerometer. As a result, the device works completely autonomous. Data are sampled and recorded at variable frequency, the upper limit being 20 Hz. The FFCPT may be optionally equipped with additional weights (up to 90 kg) and extension rods (0.5–6.5 m total length; see Figure 1B) to control penetration depth. The modular design allows us *in situ* profiling of sediments by repeated testing at the same site. Each added weight increases penetration by a couple of cm to dm, so that each horizon can be monitored regarding its frictional response, temperature, and — most importantly — pore pressure decay after insertion of the probe. Penetration depth is further controlled by the speed the probe enters the sediment (namely controlled rate using a winch vs. free fall). Our initial results indicate that the device is a worthwhile cost- and time-efficient alternative to conventional CPT systems.

3. Results and discussion

Initial FFCPT measurements focused on pore pressure response of the sediment rather than sediment profiling or mechanical resistance. The data presented here represent preliminary results of our initial measurements at sites located in marine to brackish settings at the North German coast and adjacent estuaries/streams. In those settings, water depth varied between 1 m and 12 m. They include the ports of Bremerhaven, Wilhelmshaven, and Kuhgraben near Bremen. In addition to CPT tests with various total lengths and weights of the lance, sediment samples were taken for laboratory analyses such as density, porosity, and grain size distribution. A more complete data set, showing detailed analyses of data quality and temporal/spatial resolution during penetration, is given in Stegmann *et al.* (2006).

3.1 Sediment strength and composition

Shear strength *sensu stricto* is not measured directly with a CPT, but estimated from the resistance of the tip and sleeve of the device during penetration. Our main goal was not only to relate the FFCPT data to the sediment itself, but to standard (i.e. pushed) CPT tests published in the literature (see summary in Lunne *et al.*, 1997).

In the uppermost decimetres, the tip resistance was found to reach values up to 1 MPa, which is higher than what is known from standard tests. This result was most pronounced when inserting in free-fall mode and can be attributed to the high force upon insertion. Below ca. 50 cm, the absolute insertion pressures agree well with those in pushed tests (see compilation by Lunne *et al.*, 1997, and references therein). However, if we regard the friction ratio (i.e. tip resistance being normalised against sleeve friction), our data are in good agreement with standard CPT tests. Friction ratio ranges from 1 to 9%, with the lower values typically corresponding to sands and their high tip resistance. This assumption was confirmed by grain size analyses using a Beckman Coulter LS200 laser particle size analyser. The Kuhgraben samples are dominated by sand (ca. 62%) and with clay contents around 5%, while the mud from the other sites comprise clayey silt with sand contents of 20% and 32% respectively.

In principle, the resistance of the sediment upon penetration can be combined with maximum sampling frequency (20 Hz) and known terminating depth, so that sediment profiling is possible by integration of the acceleration data. In practice, however, a more appropriate way is coring near the testing location to recover sediment for laboratory testing.

3.2 Pore pressure measurements

The pressure of the fluid between sediment particles has a profound effect on the stress state, and hence stability of the material. Its transient increase due to tides, geodynamics (e.g. tectonic loading, rapid sedimentation) and human construction is an important factor in hazard research. Generally, fine-grained sediments show high fluid pressures owing to their low permeability and poor drainage (Maltman, 1994; Strout and Tjelta, 2005). As a consequence, pore pressure monitoring was our main objective during the FFCPT deployments. Figure 2 shows pore pressure records from four tests with variable duration (0.5–6 hours). It can be seen that even in the finer grained settings (clayey silt; see previous section), the induced pore pressure decreases significantly within hours. In

the Wilhelmshaven test (Figure 2A), this decay is overprinted during rising tide during the Bremerhaven test. The absolute initial pore pressures (assuming the harbour sediments to exhibit hydrostatic stress state) measured range between 30–50 kPa. In contrast, the initial pore pressure peak in the silty sands of Kuhgraben was ca. 10 kPa in excess of hydrostatic (see Figure 2B). Moreover, the sands show a more rapid pressure decay due to their higher permeability as well as a lower water head.

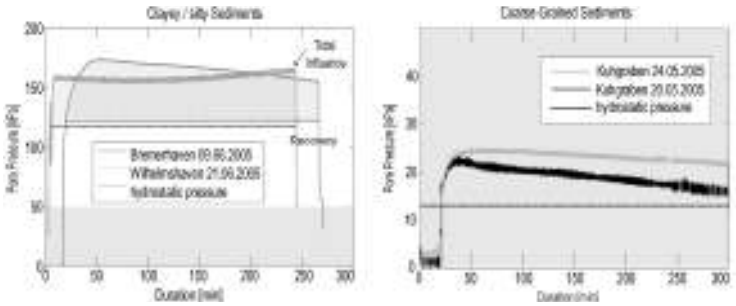

Figure 2 Pore pressure data from various FFCPT deployments with hydrostatic pressure at the seafloor for reference (dashed lines). Left: Fine-grained sediments; Right: Coarse-grained sediments. Note different scale of y-axes!

In conclusion, we present data from our first successful multiple deployments of a new FFCPT in unconsolidated sediments of variable grain size. *In situ* friction measurements agree with those from standard CPT tests in the literature (Lunne *et al.*, 1997). Pore pressure curves indicate moderately fast decay rates of induced pore pressure, shedding light on the possible stress response of those sediments. Our device is time- and cost-efficient, and — in its lightweight configuration — may be used from small platforms and without a winch or crane.

Acknowledgements

M. Lange is acknowledged for valuable suggestions and immense help with construction, programming, and testing of the FFCPT. Our colleagues V. Berhorst, B. Heesemann, N. Kaul, and T. Mörz provided valuable discussion. S. Potthoff is also thanked for supporting the Wilhelmshaven tests. Funding for this research was provided by the German Science Foundation (DFG) to the Research Centre Ocean Margins. This is RCOM publication # 0323.

References

Lunne, T., P.K. Robertson and J.J.M. Powell (1997). Cone Penetrating Testing In Geotechnical Practice, Spon Press, pp. 312.

Maltman, A. (ed.) (1994). The Geological Deformation of Sediments, Champman & Hall, London, pp. 362.

Stegmann, S., H. Villinger and A. Kopf (2006). Concept and Design of a modular, marine Free-fall CPT system — A time- and cost-efficient device for *in situ* geotechnical characterisation of marine sediments, Sea Technology, in press.

Strout, J.M. and T.I. Tjeta (2005). "*In situ* pore pressures: What is their significance and how can they be reliably measured?" Marine and Petroleum Geology 22, 275–285.

Towards an assimilation of MODIS-derived Sea Surface Temperature (SST) by the Optos_nos model

Virginie Pison* and Bouchra Nechad

MUMM RBINS, Brussels, Belgium

Abstract

Aiming to use the MODIS-derived SST to improve the surface forcing of the Optos_nos model, our first task consists of a cross-comparison between satellite data, model results and *in situ* measurements. We note that the accuracy of the model must be improved close to the coast and that the procedure of flagging clouds must be improved before the satellite data can be used as forcing.

Keywords: SST, North Sea, MODIS, Coherens, validation

1. Introduction

The objective of this study is to assess the capability of MODIS-derived SST to improve the quality of the SST Optos_nos model results.

Comparisons between satellite and Optos_nos modelled SST are carried out to address the weaknesses of the model which may be corrected by the satellite data and/or to determine places where the available satellite data are too sparse or of too bad quality. Satellite and modelled SST are then compared with *in situ* measurements.

This preliminary work shows that, at this stage, the satellite derived SST must be improved to avoid disturbing the model instead of improving it.

2. Description of the data sources

Our study focuses on the year 2004. Our zone of interest is the North Sea. This study mainly consists of a global cross-comparison between satellite-derived SST, modelled SST and *in situ* data. Each source is described hereafter.

2.1 Satellite-derived SST

The MODerate resolution Imaging Spectro-radiometer (MODIS) onboard the two satellites EOS AQUA and EOS TERRA retrieve the Sea Surface Temperature (SST) from the radiance measured at 2 infrared bands centred around 11 μm and 12 μm — hereafter called 11 μm SST for daytime SST — plus a 4 μm night-time SST generated from radiances measured in 2 mid-infrared narrow bands centred around 3.9 μm and 4.0 μm. The 4 μm SST algorithm is not used for daytime products because the measured radiance at short wave infrared wavelength is contaminated by reflected sun radiation.

Daily products of SST are generated using the calibrated algorithm of Brown and Minnett (1999) and Minnett *et al.* (2003) for daytime and night-time SST:

$$\mathrm{SST} = c1 + c2 \times T_{11} + c3 \times (T_{11} - T_{12}) \times T_{\mathrm{src}} + c4 \times (\sec\theta - 1) \times (T_{11} - T_{12})$$

* Corresponding author, email: V.Pison@mumm.ac.be

where T_{11} (resp. T_{12}) is the brightness from channel 11 μm (resp. 12 μm), θ is the satellite zenith angle and T_{src} is an estimate of the SST, generated using the MultiChannel Linear (MCSST) algorithm of McClain *et al.* (1985).

For night-time SST, the 4 μm algorithm is used:

$$SST4 = c1 + c2 \times T_{3.9} + c3 \times (T_{3.4} - T_{4.0}) + c4 \times (\sec\theta - 1)$$

Daily products of mean SST and related Quality Level (QL) data with 4 km resolution covering the North Sea area during the year 2004 were downloaded from the Goddard Earth Science Distributed Active Archive Center (GES DAAC) Online FTP website (http://disc.gsfc.nasa.gov/data/datapool/). The level of processing of SST is level 3, which refers to atmospherically corrected, re-projected and 4 km averaged data. QL data provide an indication of the level of confidence we may give to SST product, ranging from 0 (= good quality) to 3 (= bad quality). QL 2 refers to clouded pixels. These products are available in HDF format.

The downloaded SST and QL data were read and further processed using the ENVI software. SST data have been filtered using QL products keeping only good quality flagged pixels for each map. Data have then been re-projected to match the model grid (1/12° intervals for longitude and 1/24° intervals for latitude).

2.2 Model

The Optos_nos model is the operational implementation of the Coherens code (Luyten *et al.*, 1999) on the North Sea from 4°W up to 10°E and from 48.5°N up to 57°N. The horizontal resolution is about 5 km (1/12° in longitude, 1/24° in latitude). The vertical component is represented by 20 sigma layers.

At the open boundaries, currents and elevation are provided by a 2D model covering the whole continental shelf. Salinity is fixed at 35 along the western boundary and at 34.9 along the northern boundary in inflow conditions. A zero gradient is imposed for the temperature and in outflow conditions for the salinity.

At the river boundaries, discharge based on a climatological mean is imposed. Salinity is set to zero. For the temperature, a zero-gradient is imposed.

At the surface, the UKMO forecasts for wind, atmospheric pressure, cloud cover, rain, humidity and air temperature at 10 m above the sea surface are used to estimate the wind stress and the heat flux.

2.3 *In situ* measurements

Various sources of *in situ* data are available for the validation of the SST in the zone of interest: the observations from the R.V. Belgica (available since 2004 on the web site www.mumm.ac.be/EN/Monitoring/Belgica/campaigns.php); the hourly SST at three fixed stations in the Channel (see www.metoffice.com/research/ocean/goos/maws.html); the SST maps from the Bundesamt für Seeschifffahrt und Hydrographie (Loewe, 2003) interpolated from ship and station data, also using AVHRR satellite data (see www.bsh.de/en/Marine_data/Observations/Sea_surface_temperatures) and the observations from the Monitoring Network Flemish Banks (see www.vliz.be/Nl/coast/mvb).

3. Results

Figure 1 shows, for all satellite pictures, averaged values of SST over the whole domain derived from MODIS and computed with the Optos_nos model. Figure 2 gives time series of SST from satellite, from the model and measured *in situ* in the Belgian coastal zone (Westhinder station).

On Figure 3 and Figure 4, the weekly average difference (and the standard deviation of this difference) of SST between the model and respectively the satellite data and the BSH maps is shown. Only grid points with at least one non zero MODIS value over the week are taken into consideration.

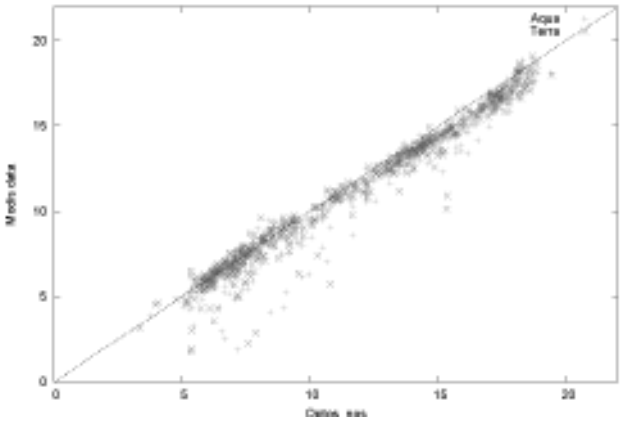

Figure 1 Mean SST (in °C) obtained by the Optos_nos model (x axis) and by Aqua and Terra (y axis).

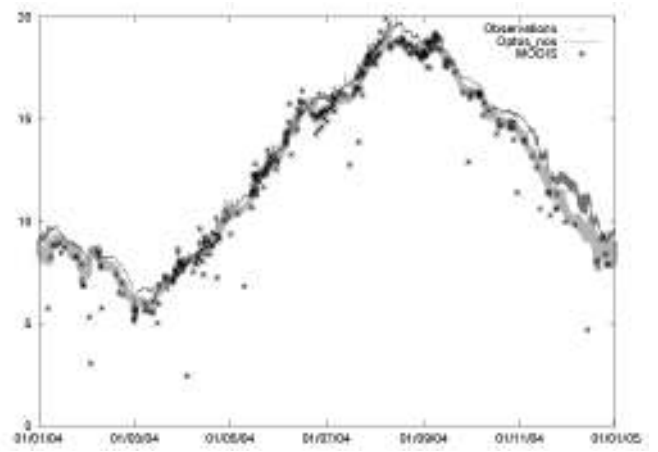

Figure 2 SST (in °C) observed, computed by Optos_nos and derived from Modis at the Westhinder station (51.38°N, 2.44°E).

4. Discussion

The spatial averaged SST (Figure 1) computed by the Optos_nos model and obtained by Modis, shows the same trend. We have observed that the greater differences corresponded to satellite pictures with less valid values (i.e. with more clouds). Globally, the mean difference of SST is 0.55° (0.65° in absolute value).

At Westhinder station (Figure 2) and Sandettie station (not shown here), there is a good fit between the observations, the model results and the satellite data. The Optos_nos simulations are less good (too hot) for late summer and the end of the year. Some of the daytime values of the satellite are clearly underestimated. All Modis SST "outlier" values come from pixels located in the vicinity of clouds. These pixels are actually contaminated by clouds or cloud shadow but have been missed during the quality control.

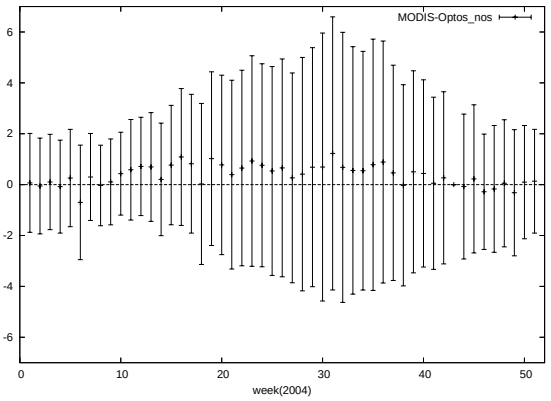

Figure 3 Weekly averaged difference and standard deviation of the difference of SST (°C) between Modis and Optos_nos.

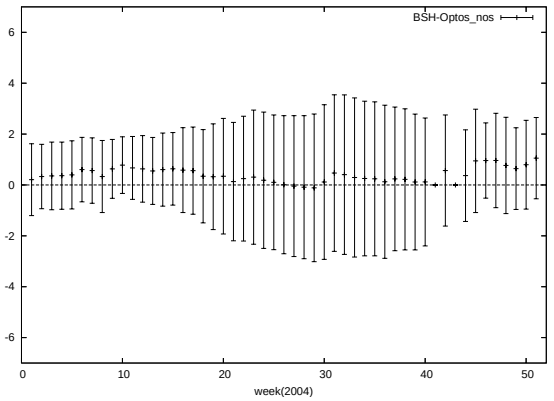

Figure 4 Weekly averaged difference and standard deviation of the difference of SST (°C) between BSH maps and Optos_nos.

The weekly mean difference between the model and the other sources of information is always less that 1.22 °C. We notice that the standard variation is higher in the summer and that the model is closer to the BSH maps (maximum 3.13 °C) than to the MODIS values (maximum 5.36 °C).

Spatial repartition of the difference of SST (not shown here) permits us to detect a problem near to the coast for the model and near to the clouds for the satellite.

5. Conclusion

In summary, MODIS SST products (mean SST and related QL data) could help the model to accurately forecast the SST field provided that the QL is improved over cloud contaminated pixels. A spatial filter may also be used to roughly eliminate any abrupt spatial variation of SST which can disturb the model. This confirms the SST validation made by the MODIS processing team which pointed out the necessity to improve the procedure of flagging cirrus and low level clouds or fogs (Evans, 1999).

In the next steps, the observations of the FerryBox project will be used to determine the source of the differences of SST. The algorithm for detection of clouds will be improved. The Optos_nos model will be improved near to the coasts. Finally the impact of the use of the Modis-derived SST as forcing of the Optos_nos model will be tested.

Acknowledgements

NOOS partners, especially G. Dumon (head of Hydrografie and Hydrometeo, Afdeling Waterwegen Kust) and M. Holt (Manager Operational Ocean Modelling, UK Met Office), are thanked for giving us access to *in situ* data.

References

Brown, O.B. and P.J. Minnet (1999). MODIS Infrared Sea Surface Temperature Algorithm. Algorithm Theoretical Basis Document, University of Miami.

Evans, R.H. (1999). Processing Framework and Match-up Database MODIS algorithm (V3) http://modis.gsfc.nasa.gov/data/atbd/atbd_mod26.pdf, University of Miami.

Loewe, P. (2003). Weekly North Sea SST Analysis since 1968. Original digital archive held by Bundesamt für Seeschifffahrt und Hydrographie, D–20305 Hamburg, P.O. Box 301220, Germany.

Luyten P.J., J.E. Jones, R. Proctor, A. Tabor, P. Tett and K. Wild-Allen (1999). COHERENS — A Coupled Hydrodynamical-Ecological Model for Regional and Shelf Seas: User Documentation. MUMM report, Management Unit of the Mathematical Models of the North Sea, 914 pp. [Available on CD-ROM at www.mumm.ac.be/coherens].

McClain, E.P., W.G. Pichel and C.C. Walton (1985). Comparative performance of AVHRR-based multichannel sea surface temperatures. Journal of Geophysical Research, 90 pp 11589–11601.

Minnett, P.J., R. Evans and O.B. Brown (2003). MODIS Terra sea surface temperature thermal (SST) and mid-infrared (SST4) data quality summary.

Development and applications of wave-piercing underwater vehicles for gathering data

Hugh W. Young* and Stephen J. Phillips

Autonomous Surface Vehicles Ltd., UK

Abstract

Autonomous wave-piercing vehicles combine many of the advantages of ASVs and AUVs. They have the endurance, economy, speed, communications and positioning of ASVs combined with the stability and most of the covertness of AUVs to give a new, adaptable mobile instrumentation platform. If they are also stable at slow and zero speeds they can deploy sensors to depth either from a winch or from a daughter ROV or AUV.

The Survey Autonomous Semi-Submersible (SASS) is just such a vehicle. SASS technology permits small, unmanned platforms to deploy sensors and other equipment above or below the sea away from a ship or from the shore. It floats at operating depth, and so remains stable at slow to zero speeds.

Keywords Data gathering, mobile buoy, ocean survey, bathymetry, marine biology, autonomous vehicle, stable platform, EEZ Governance, remote sensing, fisheries research, pollution monitoring, air/sea interface, personnel safety.

1. Introduction

Wave-piercing vehicles, in common with other surface vehicles, have the advantage of communicating and sensing over long ranges with high bandwidths by radio, accurate positioning by GPS, and reliable, well-developed and low cost propulsion systems breathing air. Unlike other surface vehicles, however, wave-piercing vehicles have improved stability, efficiency and reduced vessel motion due to the waves.

Fully submerged unmanned vehicles (UUVs) on the other hand have limited communication and sensor range and bandwidth, difficulty in accurate positioning and are generally short of power. The former can be overcome to some extent by interrupting the mission and surfacing, but the latter remains a serious disadvantage. Unmanned wave-piercing vehicles (UWVs) bridge the gap between fully submerged UUVs and unmanned surface vehicles (USVs). They can also be regarded as an economical substitute for surface ships for data gathering, carrying their sensors to considerable ranges and transmitting the data back in real time.

UWVs were developed to overcome the disadvantages of unmanned surface vehicles. These vehicles are comparatively inexpensive, and behave adequately in calm water, but are of limited value in a seaway due to their unstable motion at survey sensor speeds.

* Corresponding author, email: hugh@asv.org.uk

2. Initial development of SASS

Briefly, the SASS technology involves a submerged torpedo-like body running just below wave depth with a ballasted keel for stability, and a strong upright fared strut or spar, integral with the body, protruding through the water surface. The spar provides the buoyancy to float at the correct depth with the mean water-line half way up the spar. It allows the use of air for conventional prime movers and radio frequency coverage for communications and GPS or DGPS positioning. It also provides a stable structural component above water essential for launch, recovery and refuelling, see Figure 1.

As an autonomous wave-piercing vehicle a SASS vehicle has the attraction of being able to use low cost propulsion, control and positioning equipment. As a semi-submersible a SASS vehicle floats at operating depth and does not rely on forward speed for depth control. Thus it permits stable hovering at slow or zero speeds, while being able to use the power and endurance of an air-breathing engine. A diagrammatic representation is shown in Figure 1.

After computer simulation, theoretical studies and tank testing, a demonstrator model was built. Both calm water and rough water tests were undertaken, see Figure 2. The demonstrator was shown to be directionally and vertically stable in slow and high speed runs in calm water; it also performed well in rough water, particularly in head sea conditions. In particular the ability of the semi submersible vehicle to perform at low speeds, which constitutes much of the novel technology, was proven without doubt.

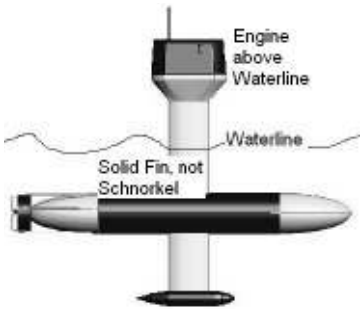

Figure 1 Diagrammatic representation of a SASS.

Figure 2 SASS demonstrator trials.

3. Prototype SASS vehicle

To develop a marketable product required the building of a prototype vehicle, command and control system, and a launch and recovery system. A prototype vehicle, 5.5 metres in length, has been constructed and trialled in the Solent. The vehicle is shown in Figure 3–Figure 5.

3.1 Vehicle characteristics

The propulsion system for this vehicle consists of a diesel engine driving the propeller via a gearbox. For stowage the spar is capable of folding forward when recovered as shown in Figure 4.

Figure 3 SASS prototype ready for launch.

Figure 4 SASS prototype stowed for transit.

Figure 5 SASS prototype under test.

Figure 6 SASS prototype basin trials.

3.2 Launch and recovery

One of the main criticisms of autonomous vehicles from operators is the difficulty of launching and recovering them. The SASS project has two approaches; avoid recovery whenever possible by use of the "Take Station" mode, and use the stable, rigid spar, which is an integral part of the structure and which penetrates the water surface, to ease the recovery task when this is unavoidable.

4. Prototype trials

4.1 Basin trials

The prototype SASS vehicle was launched at the Southampton Oceanography Centre in March 2004, and initial trials were successful.

4.2 Sea trials

Sea trials were carried out in the Solent in August 2004. Greater radio ranges and speeds were achieved, and stability at zero and slow speeds, as well as in turns, were amply demonstrated, as well as confidence in the vehicle's behaviour over more extended periods.

4.3 Video trials

Trials to demonstrate the ability of a SASS vehicle to give detailed visual information at a distance compared with an RIB (Rigid Inflatable Boat) were carried out in early April 2005. Figure 7 shows the vehicle at sea with the camera mounted on the engine cowling. This type of information could be useful in identifying suspect contacts at a distance for EEZ control, or for wave observations.

4.4 Acoustic trials

Further trials were carried out in April 2005 with a synthetic aperture sonar. The sonar was mounted in a specially designed substitute keel which replaced the normal keel. High resolution demonstration surveys were carried out in Weymouth Bay. The normal keel was then replaced and trials are well advanced to install a swath bathymetry sonar in the nosecone to be carried out at Southampton Water in September 2005, and later in Weymouth Bay.

Figure 7 SASS prototype with camera as sea.

Figure 8 Drawing of SASS + ROV.

5. Daughter vehicle programme

Because SASS vehicles can remain stable while stationary — they can deploy small imaging ROVs and relay the images via the umbilical by telemetry to shore or a mother ship. A schematic drawing of the arrangement is shown in Figure 8.

Extending the idea of SASS vehicles as mother ship substitutes leads to the concept of a daughter AUV. The SASS prototype vehicle is not itself capable of carrying AUVs, but the basic SASS technology is flexible and concept studies are planned to develop suitable vehicles for deploying Remus and Gavia sized AUVs, possibly in pairs so that one can be on station while the other is recharged.

However the SASS vehicle need not carry the AUV. It can carry out another function of a mother ship by escorting the AUV, updating its inertial navigation system (INS) and checking that the sensor instrumentation is working without requiring it to interrupt its task and come to the surface. This combination can provide subsea data profiles of all types at long radio ranges.

6. Mobile buoy concept

The UWV technology permits a vehicle to remain stable while remaining in one position determined by GPS. It can therefore act a mobile buoy, able to take or change station on command and without ground tackle. This permits positioning in deep water where ground tackle would be impossible, and for long missions. The vehicle can also be used as a drifting buoy, reporting its position by GPS. In this mode it can deploy a thermistor chain or other instrumentation to gather data or samples from depth.

7. Applications

The SASS technology is capable of a wide range of data-gathering applications, many of which are particularly relevant to EuroGOOS.

Swath bathymetry can be combined with above-water video surveillance. This applies to EEZ survey and control. Bathymetry is also useful for studying the seabed topology in areas of interest for tidal studies or where the sea bed is rapidly changing.

The ability of the SASS type of vehicle to hover and act as a mobile buoy has many applications, for example fish and oceanographic studies. Pollution can be monitored using similar techniques.

Data for air/sea interface studies can also be acquired including the study of waves. Above-water or underwater information from coastal areas, particularly those which are dangerous or difficult to access, can be obtained for ecological, tidal, bathymetric or pollution studies. Surveying archipelagos can be difficult and dangerous, and the problem can be eased by UWVs.

8. Conclusions and acknowledgements

The SASS wave-piercing vehicle has been developed to satisfy these requirements. Furthermore the early computer simulations of the SASS vehicles showed that the design could be varied in length and hull diameter without detriment to performance and thus specialised vehicles can be designed for particular purposes.

A 5.5 metre prototype SASS vehicle has been built and has undergone successful trials. The development of the SASS prototype has put in place a key link for the evolution of systems capable of delivering high-resolution sub-sea data at considerable range.

The authors gratefully acknowledge the support of a grant from the UK NERC/DTI “SeaSense” programme and from the DTI for the grant of a SMART award.

Improvements in continuous, systematic monitoring of phytoplankton growth using a FerryBox

M.C. Hartman*, S.E. Hartman and D.J. Hydes

National Oceanography Centre, Southampton, UK

Abstract

The Solent Southampton Water system is a temperate latitude estuary with high nutrient loadings. A FerryBox system has been operated there since 1999. The suite of sensors measure temperature, salinity, fluorescence, turbidity and position. In 2004 the FerryBox methods were improved to reduce the effects of bio-fouling on the sensors. The sensors were systematically cleaned and calibrated during weekly ferry crossings. Possible shifts in calibration of the fluorescence sensor were monitored using solid fluorescent Perspex blocks. The sensor was found to be stable and this systematic approach quantifies the degree of fouling that can occur in a productive estuary. Continuous monitoring allows us to pinpoint the timings of phytoplankton bloom initiation and duration. Comparison of the fluorescence and data for measurements of *in situ* chlorophyll demonstrate the large (5 fold) variability in the ratio of fluorescence to chlorophyll throughout the estuary with the time of year.

Keywords: FerryBox, Southampton Water, phytoplankton, bio-fouling, fluorescence

1. Introduction

Southampton Water and the Solent are a relatively well-studied estuarine system (e.g. Iriarte and Purdie, 2004). The extra value of continuous monitoring using FerryBox systems has been demonstrated in recent years (Holley and Hydes, 2002). FerryBox work in Southampton Water contributes to the activities of the EU−FP6 Environment FerryBox project and is a test area for the development of a marine information system in EU IST project iMARQ IST−2001−34039 (Information System for Marine Aquatic Resource Quality). The core FerryBox suite of sensors operated on all the routes of the project measures salinity, temperature, fluorescence and turbidity. A key activity of the project (Petersen *et al.*, 2005) is the determination of best practice for operation of such systems. The iMARQ project also required not only data for validation of its models but like "FerryBox" needed data of known accuracy. A major problem with autonomous systems is fouling of the sensor heads, especially for optical sensors such as fluorimeters. In 2004, to improve our knowledge of sensor performance, a regular programme of maintenance and calibration was carried out on a weekly basis. This included first tests of new solid state calibration reference materials for the fluorimeter and turbidity sensors which were provided by the manufacturer Chelsea Technology Group (CTG). Fluorescence measurements are used to estimate *in situ* concentrations of chlorophyll *a* and hence of total phytoplankton biomass. To do this a link must be established between *in*

* Corresponding author, email: mch@noc.soton.ac.uk

situ fluorescence and water sample chlorophyll concentrations. This paper will concentrate on our work on the stability of fluorescence measurements.

2. Method

In 2004 the FerryBox system on the "Red Falcon" ferry (Holley and Hydes, 2002) was replaced by a new system similar to that described in Hydes *et al.* (2003). This uses a CTG MiniPack CTD-F (conductivity, temperature, pressure and chlorophyll *a* fluorescence) in line with a CTG MiniTracka Turbidity sensor. These are in circuit parallel to the ferry's cooling water supply. The data collected in the engine room are merged with data from a GPS system mounted on the bridge. The ferry travels the length of the estuary up to 16 times a day and data are recorded at 1 Hz frequency. Subsequent processing was done with data binned into one minute intervals.

At approximately weekly intervals over the period of operation of the system in 2004, between May and October, two people worked on the ferry during 17 of the 3 hour round trips. Firstly the sensors were removed from their housings. The reading from the "dirty" fluorimeter was recorded in air in the dark and then in the dark with the solid state reference block placed in the light path. The sensor heads were then cleaned using tap water and Decon 90 solution. The readings from the fluorimeter were then again recorded in air in the dark with and without the reference block in place. Use of the calibration blocked was introduced from crossing 7 onwards.

Water samples were then collected at about 10 minute intervals while the ferry was underway for calibration of the conductivity, fluorescence (filtered immediately) turbidity sensor (filtered and weighed on shore). The loaded chlorophyll filters were placed immediately into test tubes containing 90% acetone and analysed on return to the laboratory using the method of Welschmeyer (1994). Qurban *et al.* (2004) provides evidence for the need for rapid processing of extracted chlorophyll *a* samples.

3. Results

3.1 Fluorimeter stability

The results obtained from the fluorimeter readings when it was removed from the flow housing before and after cleaning are shown in Table 1. Columns 2 and 3 shows comparisons between the dirty and clean readings obtained when it was in the dark with no reference block in place. They show that the dirty windows of the fluorimeter carry a variable degree of fluorescent fouling which is removed by cleaning. When the reference block is in place the readings from the dirty fluorimeter would be expected to be lower than with clean windows because of obscuration of the lens which is the case. However the output is also lower than the readings from the dirty window in air because light is probably collimated by the block sufficiently to reduce the amount of light striking and exciting the fluorescent material attached to the dirty detector window. The clean results (column 5) with the reference block in place indicate sensitivity of the fluorimeter is stable over the 10 week period of these tests.

Table 1 Results from use of fluorimeter reference blocks (units are apparent gl^{-1} chlorophyll based on a calibration of the instrument with a standard solution of chlorophyll *a* in acetone).

	No block		Block in place	
Crossing	**dirty**	**clean**	**dirty**	**clean**
7	85	2	23	47
8	139	2	25	47
9	157	1	20	47
10	91	2	17	46
11	33		28	45
12	158	3	24	48
13	128	1	20	45
14			31	45
15	41	2	23	44
17	125	5	36	45

3.2 Change in chlorophyll/fluorescence ratio

It is known that the fluorescence to chlorophyll ratio is variable due to changes in the both the dominant planktonic organisms and their photo-physiological state (Falkowski and Raven, 1997). However the degree of change in a system like Southampton Water is poorly documented. It is important that more information is made available because of the need to derive reliable indicators of the eutrophication status of different environments linking nutrient input to biomass production. In Figure 1 all the data from the measurements of chlorophyll *a* extracted into acetone are compared with the fluorimeter values recorded at the time of sampling. For biological sampling the regression of these two data sets shows a relatively high R^2 value of 0.85. However from the ratio of chlorophyll *a* to fluorescence calculated for the individual crossings it can be seen plotted in Figure 2 that the value of the ratio increases by a factor of about 5 over the period of sampling.

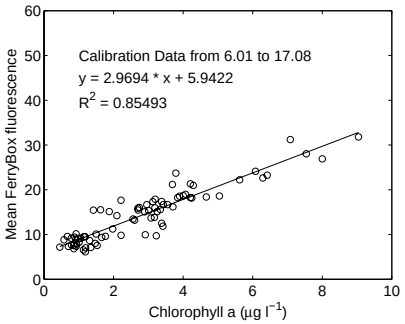

Figure 1 Fluorescence to chlorophyll relationship 2004.

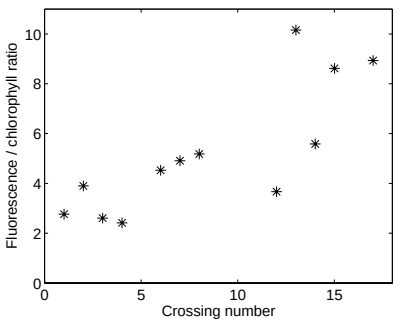

Figure 2 Variation in the fluorescence to chlorophyll ratio for each calibration crossing.

4. Adjusting for bio-fouling

The upper plot in Figure 3 shows all the fluorimeter data recorded over a typical week during 2004. On day 243 a cleaning and calibration crossing was done. The effect of this can be seen in the data as a sudden decrease in the fluorimeter signal. The variability in the degree and rate of bio-fouling during the year can be judged from the rate of change in the base line. This is based on the experience that the blooms are localised in the estuary (Iriate and Purdie, 2004) and areas of minimum fluorescence with little plankton activity should be identifiable on each individual ferry crossing and the minimum value should change very little. After the cleaning event on day 243, although the amount of fluorescent material was relatively low compared to earlier in the week the onset of bio-fouling starts within 3 days of the cleaning event, whereas after the preceding cleaning event fouling had occurred less quickly.

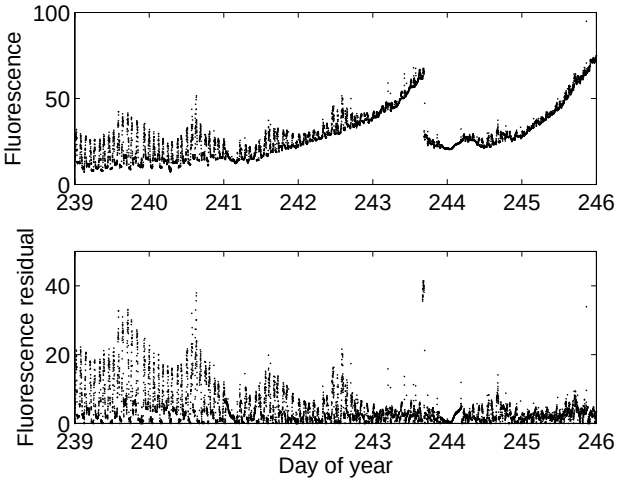

Figure 3 Fluorescence data before and after baseline correction

To reduce the effect of bio-fouling on our ability to detect true plankton bloom events, changes in the baseline measurement due to sensor bio-fouling can be removed at the data processing stage. The procedure was to identify the minimum value for each crossing and subtract that value from all the values measured during that particular crossing. The resulting fluorescence reading after this correction was renamed the fluorescence residual. The corrected data for the week are shown in the lower part of Figure 3. In this plot it is easier to recognise the diurnal variation in bloom intensity and the progressive waning of the bloom as conditions in the estuary become more turbulent with transition from neap to spring tide conditions.

5. Conclusions

The measurements from the use of the fluorescence reference block showed the sensor output to be stable when clean (Table 1). They also indicate that bio-fouling results in both the attachment of fluorescent material to the lens and as would be expected obscuration of the lenses.

The variation in the observed ratio of chlorophyll to fluorescence is large and suggests that any monitoring system based on fluorescence measurements must be used in conjunction with *in situ* measurements of chlorophyll *a*, if it is being used in a regulatory framework which uses a concentration of chlorophyll *a* to define a water quality standard.

A simple procedure of adjusting the data on the basis of the minimum value observed during a crossing improves the presentation of the data for assessing the timing of bloom occurrence.

Acknowledgements

This work would not have been possible without the much appreciated help and cooperation of Red Funnel Ferries Ltd. The work reported here was supported by the EU–FP6 projects "FerryBox" and "iMARQ" and the UK NERC CSP project "BICEP". The system was implemented with considerable support from Jon Campbell of OED-NOC, Southampton and John Elliott of CTG designed and made the solid state fluorimeter standard.

References

Falkowski, P.G. and J. Raven (1997). Aquatic Photosynthesis, Blackwell, Oxford 375 pp.

Holley, S.E. and D.J. Hydes (2002). FerryBoxes and data stations for improved monitoring and resolution of eutrophication-related processes: application in Southampton Water UK, a temperate latitude hypernutrified estuary, Hydrobiologica, 475/476, 99–110.

Hydes, D.J., S.E. Hartman, B.A. Kelly-Gerreyn, J. Dodgson, J.M. Campbell, N.A. Crisp, M. Edwards, B. Dupee, A.M. Lavin and C.M. González-Pola (2003). Use of a Ferrybox system to look at shelf sea and ocean margin process pp 297–303 In Building the European Capacity in Operational Oceanography, (H. Dahlin, N.C. Flemming, K. Nittis and S.E. Petersson, eds) Elsevier Oceanography Series, 69.

Iriarte, A. and D.A. Purdie (2004). Factors controlling the timing of major spring bloom events in a UK south coast estuary. Est. Coastal Shelf Sci., 61, 679–690.

Petersen, W., F. Colijn, D.J. Hydes, S. Kaitala, H. Kontoyiannis, A. Lavin, I. Lips, J. Howarth, H. Ridderinkhof and K. Sørensen (2005). European FerryBox Project: From online oceanographic measurements to environmental information. This volume, page 551.

Qurban, M.A., D.J. Hydes, A.M. Lavin, C.M. González-Pola, B.A. Kelly-Gerreyn and P. Miller (2004). Sustained "Ferry-Box" Ship of Opportunity observations of physical and biogeochemical conditions across the Bay of Biscay ICES Annual Science Conference Vigo Spain 2004, paper no. CM 2004/N:09 19pp CD ROM publication.

Welschmeyer, N.A. (1994). Fluorometric analysis of chlorophyll a in the presence of chlorophyll b and phaeopigments, Limnol. Oceanogr., 39, 1985–1992.

FerryBox observations in the Southern North Sea — application of numerical models for improving the significance of the FerryBox data

Henning Wehde*[1], Friedhelm Schroeder[1], Franciscus Colijn[1], Ulrich Callies[1], Susanne Reinke[1], Wilhelm Petersen[1], Corinna Schrum[2], Andreas Plüß[3] and David Mills[4]

[1]*GKSS Research Centre Geesthacht GmbH, Geesthacht, Germany*
[2]*Danish Institute for Fisheries Research, Copenhagen, Denmark*
[3]*Bundesanstalt für Wasserbau, Hamburg, Germany*
[4]*CEFAS, Suffolk, UK*

Abstract

Within the framework of the EU-supported FerryBox project a measuring system (FerryBox) is operated onboard a ship of opportunity on the route from Cuxhaven (Germany) to Harwich (United Kingdom). While running more or less the same track each transect the spatial and temporal resolution of observations is very high along the route. However, the temporal and spatial information beside the ferry route is only limited. To improve the significance of the FerryBox data for the southern North Sea, numerical models were applied to get deeper insight into the fate of water parcels measured by the FerryBox system. Consideration of tracer advection as well as primary production served as the explanation for deviations between buoy data and FerryBox observations.

Keywords: FerryBox, *in situ* measurements, numerical modelling

1. Introduction

Within the framework of the EU supported FerryBox project several ferries operating in different European waters were equipped with automatic measuring systems, so called FerryBoxes (Petersen *et al.*, this volume). A key question addressed within the project is the investigation of the potential of FerryBox data to precisely determine the connection between environmental significant processes and their physical and biogeochemical driving processes. Using calculated indices like the spring bloom intensity index, different regional regimes were successfully characterised based on the FerryBox data (Hydes *et al.*, this volume). Since FerryBox data sets are limited to the specific tracks of the ferries, additional information beside the routes from for example fixed monitoring stations are needed to resolve environmental characteristics with a broader spatial extension. However, the simple comparison between the FerryBox data and those from fixed stations by using the nearest geographical data points often fails, because of the predominant circulation pattern of the surrounding water masses.

The present study therefore focuses on methodical aspects to resolve and display the fate of water measured with a FerryBox. To derive more realistic comparisons between data

* Corresponding author, email: Henning.Wehde@gkss.de

from FerryBoxes and those from fixed monitoring stations, numerical models and Langrangian tracer methods were employed as examples for the Southern North Sea.

2. Materials and methods

2.1 Observations

Two different observational data sets were used within this study, measurements from the German FerryBox system installed on the Cuxhaven–Harwich ship of opportunity (Petersen *et al.*, 2003; Wehde *et al.*, 2003) and a spatially fixed buoy data set from the CEFAS Gabbard Buoy (Mills *et al.*, 2003). The latter forms part of the National Marine Monitoring Programme (NMMP) of the UK. The measured parameters available from the FerryBox are temperature, salinity, pH, oxygen, turbidity, fluorescence, ammonium, nitrate, o-phosphate and silicate, whereas the buoy data comprises phytoplankton concentration, conductivity, temperature, suspended sediment concentration, light penetration and nutrients. The position of the Gabbard Buoy as well as the track of the FerryBox route is displayed in Figure 1. For the present study the time window of spring/ summer in 2002 is used as an example and salinity as well as chlorophyll fluorescence are compared to buoy data.

2.2 The numerical model

The models applied for the present study consists of a general circulation model (GCM), a Lagrangian Tracer model and a primary production module. The two-dimensional GCM uses an unstructured triangular grid and is forced with variable wind, tides and Coriolis force. A coupled nesting is applied for the estuary regions with highest resolution of the model in the southern German Bight (80 m) and lowest resolution of the model in the northern North Sea (3 km) (Plüß, 1999). Water parcels measured with the German FerryBox were introduced as Lagrangian Tracers into the GCM in order to simulate the geographical displacement. To simulate the temporal development of non-conservative tracers like chlorophyll a primary production module (Wehde *et al.*, 2001) is implemented for each of the tracers.

3. Results and discussion

A direct comparison between FerryBox and Gabbard Buoy data illustrates well the spatial heterogeneity in the Southern Bight, and provides the motivation for more detailed numerical investigations (Figure 2). Inclusion of the drift signal by implementation of Lagrangian tracers significantly improved the overlap between buoy data and drifted FerryBox data (Figure 3). The main characteristics of the different datasets are now in good agreement. The softened salinity anomaly observed in the FerryBox data set can be explained by entrainment of surrounding water masses on the way from the Gabbard buoy up to the FerryBox line. The travel time the water parcels need coming from the Gabbard buoy to the ferry line is displayed in Figure 4. It is obvious that beginning with relatively long travel times during the early spring the travel times decrease until the second half of May (~ day 140). With the start of the building of a seasonal thermocline the transport velocity decreases again and the water needs more time to be transported from the Gabbard buoy up to the ferry line for the rest of the period.

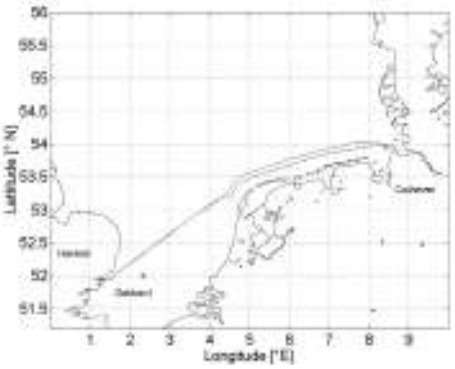

Figure 1 FerryBox route from Cuxhaven to Harwich and location of Cefas' Gabbard Buoy.

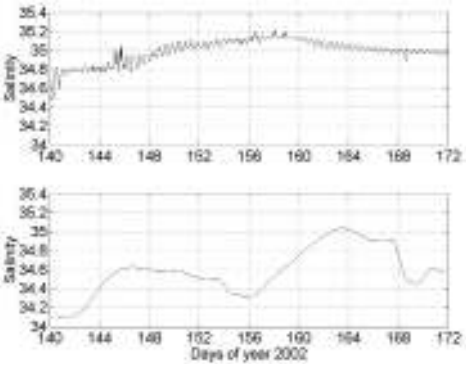

Figure 2 Comparison between salinity data from Cefas' Gabbard Buoy (upper panel) and FerryBox (lower panel) using data from the nearest geographical point of the route to Gabbard station.

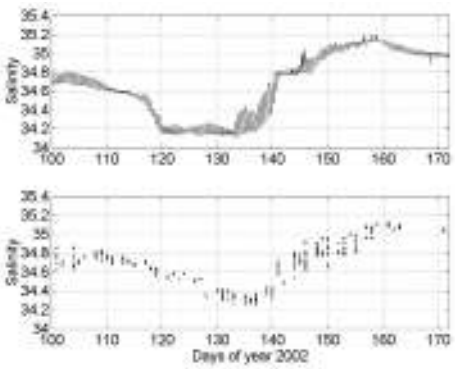

Figure 3 Comparison of salinity data measured at Cefas Gabbard buoy (upper panel) with salinity data from passive tracers, observed with the FerryBox and transported within the GCM (lower panel).

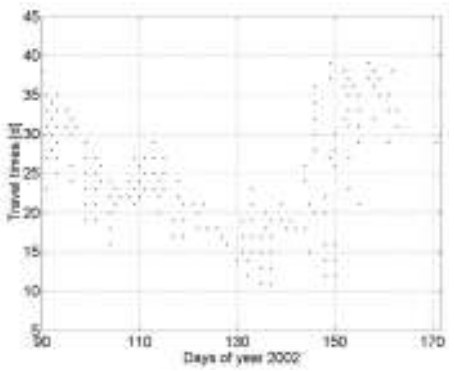

Figure 4 Travel times the water parcels need for the distance FerryLine−Gabbard station.

While the results for salinity are strongly improved with the help of the implemented Lagrangian tracers, the comparisons for non-conservative parameters like chlorophyll fluorescence remain unsatisfactory (Figure 5). Although the data displayed are thought to be the same water mass, as concluded from salinity comparison, the results with respect to its chlorophyll content are very different. None of the characteristics of the Gabbard buoy data set are described within the simulated FerryBox data set.

By applying the chlorophyll module for the Lagrangian tracers, taking the measurements from the Gabbard buoy as initial values and forcing the simulations by realistic light conditions and measured nutrient distribution at the Gabbard buoy, the results for the non-conservative parameter chlorophyll fluorescence are strongly improved (Figure 6). All the characteristics of the different data sets are now estimated to be in good

agreement. The bloom feature observed at the Gabbard buoy in May (~ day 150) decreases on the way up to the ferry line, due to the lack of sufficient nutrient concentrations as indicated by the nutrient data of the Gabbard buoy. Applying the coupled Lagrangian-plankton module the bloom observed by the FerryBox could be developed from the initially low chlorophyll values observed at the monitoring station.

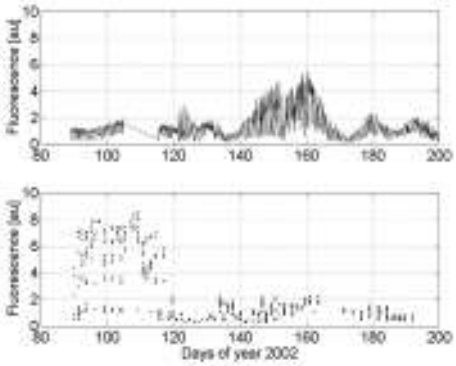

Figure 5 Chlorophyll fluorescence observed at Cefas' Gabbard buoy (upper panel) and chlorophyll fluorescence of water passively transported within the GCM (lower panel).

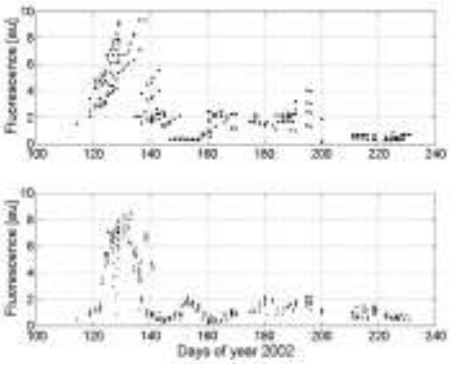

Figure 6 Comparison between observed FerryBox Chl Fluorescence (lower panel) and estimated chlorophyll for tracers starting from Gabbard and drifting to the FerryBox route (upper panel).

4. Conclusion

In our study, we have presented an example of an application of the use of numerical models to explain deviations in different observational data sets and it was shown that models are a valuable instrument to improve the significance of observational data that is obtained from FerryBoxes. In future, these tools will be applied to provide estimations of the variability of conservative and non-conservative parameters in the southern North Sea.

Acknowledgements

We are grateful for the great help of the Crew of the "Admiral of Scandinavia". This study was supported within the Fifth Framework Programme of the European Union under Contract Number EVK2−CT−2002−00144.

References

Hydes, D.J., C.P. Bargeron, B.A. Kelly-Gerreyn, H. Wehde, W. Petersen, S. Kaitala, V. Flemming, K. Sørensen, J. Magnusson, I. Lips and U. Lips (2005). Comparison of eutrophication processes and effects in different European marine areas based on the results of the EU FP5 FerryBox Project. This volume page 101.

Mills, D.K., R.W.P.M. Laane, J.M. Rees, M. Rutgers van der Loeff, J.M. Suylen, D.J. Pearce, D.B. Sivyer, C. Heins, K. Platt and M. Rawlinson (2003). Smartbuoy: A marine environmental monitoring buoy with a difference. in: H. Dahlin, N.C.

Flemming, K. Nittis and S.E. Petersson: Building the European Capacity in Operational Oceanography, Proc. Third International Conference on EuroGOOS, Elsevier Oceanography Series Publication series 19, 311–316.

Petersen, W., F. Colijn, D.J. Hydes, S. Kaitala, H. Kontoyiannis, A. Lavin, I. Lips, J. Howarth, H. Ridderinkhof and K. Sørensen (2005). European FerryBox Project: From online oceanographic measurements to environmental information. This volume page 551.

Petersen, W., M. Petschatnikov, Schroeder, F. and F. Colijn (2003). FerryBox Systems for Monitoring Coastal Waters. in: H. Dahlin, N.C. Flemming, K. Nittis and S.E. Petersson: Building the European Capacity in Operational Oceanography, Proc. Third International Conference on EuroGOOS, Elsevier Oceanography Series Publication series 19, 325–333.

Plüß (1999). Nordseemodell der BAW-AK, Berechnung der Tidedynamik in der Nordsee und der Deutschen Bucht, Report Bundesanstalt für Wasserbau, in German.

Wehde, H, J.O. Backhaus and E.N. Hegseth (2001). The influence of oceanic convection on primary production, Ecol Mod 138, 115–126.

Wehde, H., W. Petersen, M. Petschatnikov, F. Schroeder and F. Colijn (2003). Development and distribution of plankton observed with a FerryBox system for monitoring coastal waters. ICES ASC 2003, Tallinn, Estonia.

The stationary FerryBox Helgoland: supporting the Helgoland Roads time-series

C.J. Engelke*[1,2], K.H. Wiltshire[1], F. Colijn[2,3], K.-J. Hesse[2] and F. Schroeder[3]

[1]*Alfred-Wegener-Institute for Polar and Marine Research, Biologische Anstalt Helgoland, Germany*
[2]*Research and Technology Centre Westcoast of the Christian-Albrecht-University at Kiel, Germany*
[3]*GKSS Research Centre, Institute for Coastal Research, Germany*

Abstract

The Helgoland Roads time-series is a unique long-term data set, sampled five times a week, since 1962. This data set is of great importance for the investigation of long-term changes in the German Bight and the North Sea. To support this time-series an automated, autonomous measuring station with FerryBox technology was established on the island of Helgoland. This increases the parameters measured and facilitates high resolution observations of rapid environmental changes. We demonstrate the good agreement of physical data (temperature, salinity) between the Helgoland Roads time-series and the automated measuring station, supporting the basic assumption that the same body of water is sampled and hence fulfilling a basic requirement for mutual support and continuity.

Keywords: phytoplankton, nutrients, temporal high resolution, automated measurements, North Sea

1. Introduction

There is a growing requirement for long-term high-resolution data of physical, chemical and biological parameters to evaluate the effects of global change on the marine environment. These are needed for the interdisciplinary description of processes and events, and to create an understanding of the interactions in European coastal systems. Furthermore, long-term time-series of nutrient and algal dynamics will play a major role in supporting the European Directives, such as the Nitrate Directive, the Urban Wastewater Treatment Directive and the Water Framework Directive, and for Integrated Coastal Zone Management. Despite their great importance for the monitoring of long-term effects of climatic, oceanographic and direct human changes in coastal waters, oceanographic time-series in Europe are rare. Most time-series are limited in duration and temporal resolution.

The longest continuous time-series covering oceanographic, chemical and biological parameters in the North Sea is the Helgoland Roads time-series (Wiltshire 2004). Since 1962, samples have been taken daily at 54°11.3'N, 07°54.0'E (Figure 1). Parameters determined include Secci depth, sea surface temperature and salinity, inorganic nutrient concentrations (phosphate, silicate, ammonia, nitrate, nitrite), and microscopic phyto-

* Corresponding author, email: cengelke@awi-bremerhaven.de

plankton composition and biomass (Hickel *et al.*, 1993; Wiltshire and Dürselen, 2004). The use of this unique data set has been recently summarised (Franke *et al.*, 2004).

Work load generally restricts time-series duration and its temporal resolution, as well as data analysis, quality control and data dissemination. The idea of using ships-of-opportunity and ferries as carriers of scientific payloads has led to the development of an automated, autonomous measuring system, the FerryBox, which can sample at high frequencies and operates unattended for weeks (Hydes *et al.*, 2002). Under the 5th Framework Programme the European FerryBox Project was established and FerryBoxes were operated on nine ferry lines in the Baltic, North and Mediterranean Sea (European FerryBox Project, www.ferrybox.org). A stationary automated measuring system based on FerryBox technology was installed on Helgoland to augment the long-term time-series. It measures temperature, conductivity, pH, dissolved oxygen, turbidity and fluorescence several times per minute, algal spectral classes every three minutes and inorganic nutrients — silicate, phosphate, ammonium, nitrite and nitrate — every two hours. The increased sampling frequency allows for better observation of the results of highly dynamic processes, e.g. storm events, daily algal oxygen production and freshwater effects at Helgoland.

Two positions on Helgoland have been used for the stationary FerryBox system. The initial placing of the FerryBox in the basement of the Helgoland Aquarium was influenced by long piping and air bubbles. Therefore the system was moved in May 2004 to a pumping station directly in the breakwater wall in the north-east quay. Both positions are just a few hundred metres from the station of the Helgoland Roads time-series (Figure 1).

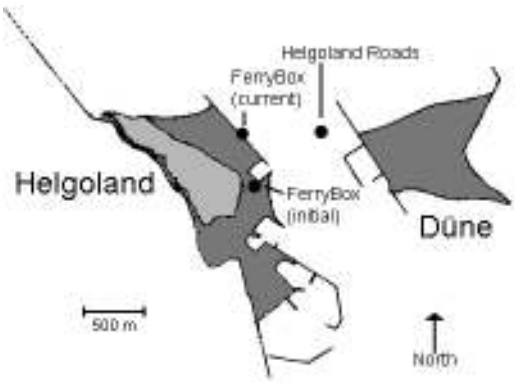

Figure 1 Sampling station for the Helgoland Roads time-series (54°11.3' N, 07°54.0' E), and initial and current position of the stationary, automated FerryBox measuring station. (Map: German Federal Maritime and Hydrographic Agency (BSH), modified).

2. Comparability of Helgoland Roads and FerryBox

In order to use the automated measuring station to support the Helgoland Roads time-series it was necessary to show that both measuring series sample the same body of water. It is generally assumed that tidal currents mix the water in the shallow (5–8 m) passage between Helgoland and Düne (Greve *et al.*, 1996).

Temperature and salinity data from the Helgoland Roads time-series are presented from January 2003 to April 2005, and are complemented by data from the stationary FerryBox starting in July 2003 (Figure 2). Correlation analysis was performed on Helgoland Roads temperature and salinity data and the corresponding FerryBox measurement from the same times (± 25 minutes). The correlation of temperature measured at Helgoland Roads and by the FerryBox for the whole time period supplies an excellent R^2-value of 0.9448 (Figure 3a). Only a small improvement of the correlation can be observed when data from the new breakwater wall position was considered exclusively ($R^2 = 0.9639$). There is a larger effect of the new FerryBox position with respect to the correlation of the salinity data. While the R^2-value is only 0.632 for data from the initial position (Figure 3b), the correlation improves much at the breakwater wall ($R^2 = 0.7816$) (Figure 3c).

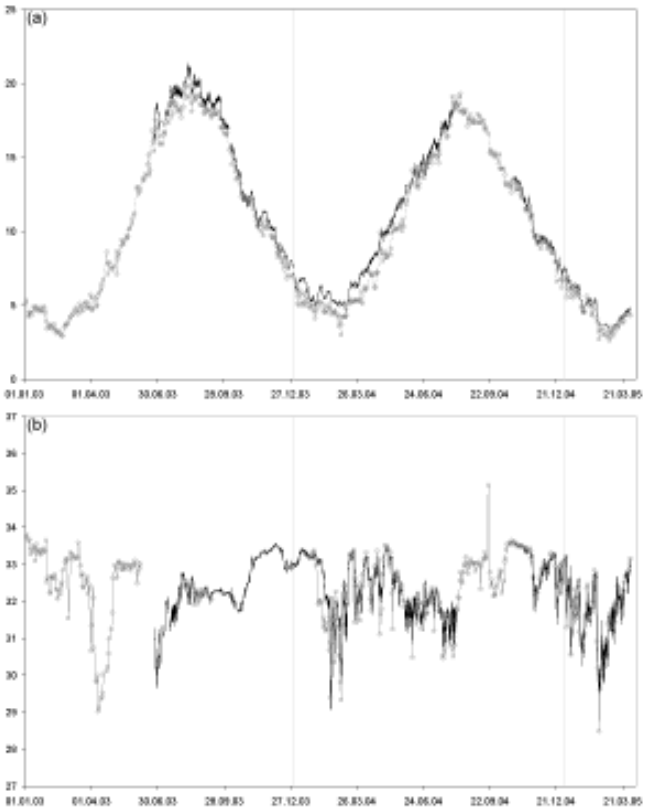

Figure 2 Data from the Helgoland Roads time-series (grey with circles) from January 2003 to March 2005, and from the stationary FerryBox system Helgoland (black) from July 2003 to March 2005 for (a) temperature and (b) salinity.

3. Conclusions

From the good agreement of the two data sets we conclude, that the same body of water is sampled by the Helgoland Roads time-series and the stationary FerryBox, and therefore one main prerequisite for the support of the time-series is fulfilled. The

FerryBox also demonstrated its ability to measure additional parameters (dissolved oxygen, pH), and the increased measurement frequency allows the observation of rapid, so far under-represented changes in the aquatic environment around the island of Helgoland. The results from the FerryBox will also facilitate new interpretations of the long-term data set of the Helgoland Roads time series.

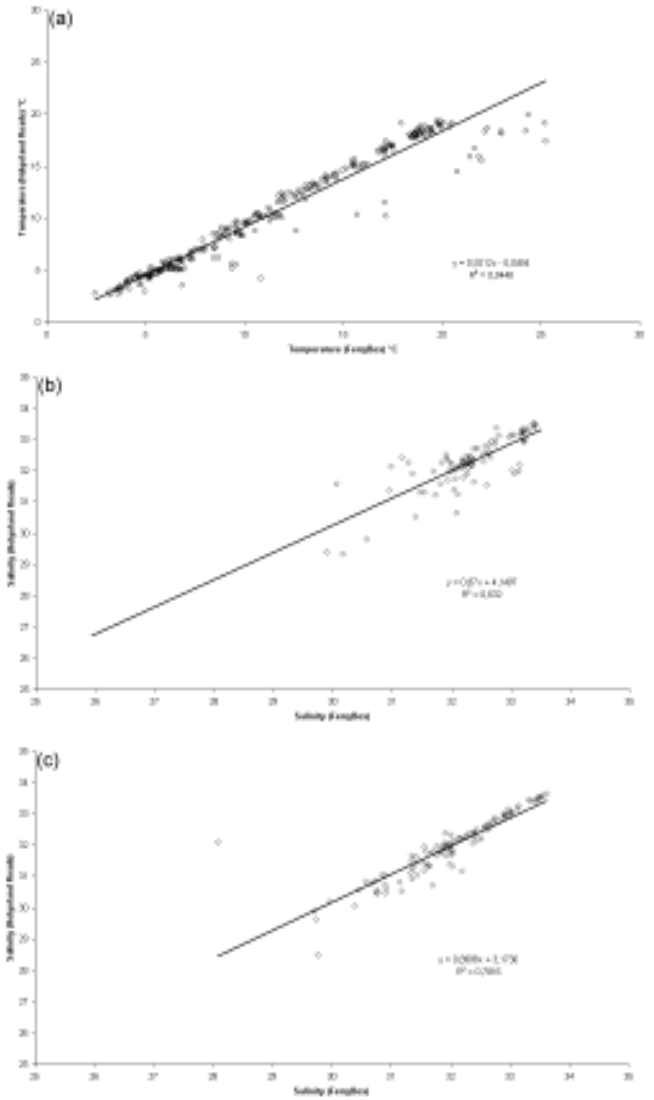

Figure 3 Correlation analysis of Helgoland Roads and FerryBox system data for (a) temperature July 2003 to April 2005, and salinity (b) at the initial site and (c) at the new position.

References

Franke, H.-D., F. Buchholz and K.H. Wiltshire (2004). Ecological long-term research at Helgoland (German Bight, North Sea): retrospect and prospect — an introduction. Helgoland Marine Research 58, 223–229.

Greve, W., F. Reiners and J. Nast (1996). Biocoenotic changes of the zooplankton in the German Bight: the possible effects of eutrophication and climate. ICES Journal of Marine Science 53, 951–956.

Hickel, W., P. Mangelsdorf and J. Berg (1993). The human impact in the German Bight: Eutrophication during three decades (1962–1991). Helgoland Marine Research 47, 243–263.

Hydes, D., A. Yool, J.M. Campbell, N.A. Crisp, J. Dodgson, B. Dupee, M. Edwards, S. E. Hartman, B.A. Kelly-Gerreyn, A.M. Lavin, C.M. González-Pola and P. Miller (2002). Use of a Ferry-Box system to look at shelf sea and ocean margin processes. 3rd International Conference on EuroGOOS, Athens, Greece, Elsevier, 297–303.

Wiltshire, K.H. (2004). Editorial. Helgoland Marine Research 58, 221–222.

Wiltshire, K.H. and C.-D. Dürselen (2004). Revision and quality analyses of the Helgoland Reede long-term phytoplankton data archive. Helgoland Marine Research 58, 252–268.

Technological development of the Polish Marine Observational Network

Włodzimierz Krzymiński*[1], Marzenna Sztobryn[1], Magdalena Kaminska[1], Waldemar Stepko[1], Roman Skapski[2] and Bogusz Piliczewski[1]

[1]*Institute of Meteorology and Water Management, Maritime Branch in Gdynia, Poland*
[2]*Institute of Meteorology and Water Management, Head Office, Warszawa, Poland*

Abstract

It is necessary for well-established and organised services to operate sustained and up-to-date observational networks. In Poland, the whole marine operational activity at the Institute of Meteorology and Water Management is based on the network of permanent coastal (both onshore and offshore) and open sea stations.

Significant technological improvement of that network was achieved thanks to financial support from different national and international projects during the last few years. As a result, the Hydrological and Meteorological Monitoring, Forecasting and Protection System was built. It consists of the following measuring and observational parts: meteorological and hydrological network, weather radar system and lightning monitoring system. All modules have been connected with central and regional databases as well as different forecasting models by means of modern structured telecommunication network.

Modern autonomous meteorological measuring stations were installed along the Polish coastline in the framework of the World Bank, among others. Besides that, the four modern transmission systems for sea level measurements were installed in as part of the 5th Framework Programme activity. Two new water level stations were upgraded in the EC funded ESEAS-RI project, while the two others were upgraded in the EC funded PAPA project. In both cases the almost real time data are presented for the end users, and enable registered users to download the data directly from the data server. It is planned to use these stations as the part of the Baltic Sea level stations network for data assimilation in hydrodynamical models as part of the BOOS collaboration.

In combination with sea level measurements, the system for oceanographic data transmission from the research vessel "Baltica" is also under development.

Keywords: Baltic Sea, coastal hydrology, marine services, measuring systems

1. Introduction

The Polish marine observational and measuring network was originally established along the Polish coast line of the Baltic Sea in the 1950s. Since the 60s, measurements at coastal stations have been followed by intensive measurements during research cruises (Dziadziuszko, 1996; Krzymiński and Dziadziuszko, 1997).

For the whole time the network itself and the measurements maintained good agreement with international standards as well as data quality control in general. However, the

* Corresponding author, email: Wlodzimierz.Krzyminski@imgw.pl

occurrence of a 1000 year flood in 1997 caused a sudden increase of awareness among politicians of the need of significant technological improvement of the anti-flood protection system and a hydro-meteorological network to better protect citizens against natural hazards. As a result, measures to upgrade the system were undertaken in the national project SMOK which was supported by the World Bank and guaranteed by the Polish Government. This enterprise was financed within the B2 component. Moreover, it was decided to upgrade the coastal water level stations and also to improve the protection system against storm surges occurring along Polish coast. Additionally, the research projects ESEAS and PAPA in the 5th Framework Programme gave added value to the existing infrastructure, in particular in the form of an upgrade of communication means for better data exchange and use.

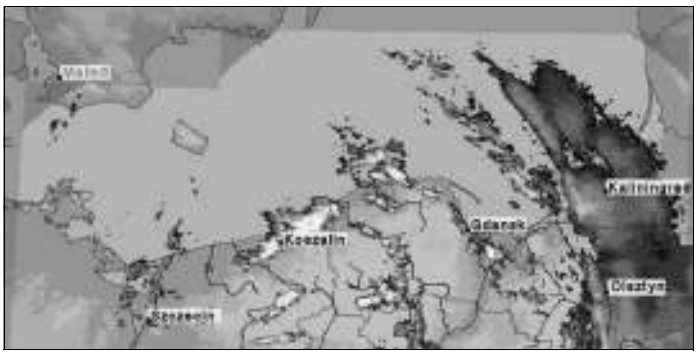

Figure 1 Polish meteorological radars' composite image. The light grey area indicates Baltic Sea coverage by the radars.

Figure 2 Location of regular and automatic sea level gauges along the Polish coast of the Baltic.

In the first stage of the SMOK project, the meteorological radar network was improved leading to the coverage of the whole of Poland and the Polish Exclusive Economical Zone of The Baltic Sea (Figure 1). Three of the existing radars were upgraded and five new ones were built in 2002–2004. The final one started operating in December 2004.

In parallel, four autonomous sea level gauges with automatic data transmission were installed along the Polish coast: in Darlowo, Ustka, Wladyslawowo and the Gdansk harbour (Figure 2) in 2004. The station in Wladyslawowo was selected to be a 1st class ESEAS sea level station. It is equipped with a sea level sensor, SST, CGPS and gravity sensor. Some other stations were supplied with new pressure and water temperature sensors and GPRS modems.

Also, a marine data transmission system was installed on board the r/v Baltica in 2004. At the beginning of 2005, the system was successfully used for temperature and salinity raw data transfer to the operational database of the Department of Oceanography and Baltic Monitoring in Gdynia.

2. Technical description

Data from eight meteorological radars are collected in operational mode, combined together and presented in graphical form. Weather forecast offices use maps of precipitation (including intensity and cloudiness) refreshed every 5 minutes, while for public presentations on internet (via a web page through IMWM's SOK — Client Oriented Service) maps are refreshed only every hour.

Sea level stations are equipped with pressure and water temperature sensors OTT PS 1 located in existing pipes of mechanical gauges. Data are registered in a Logosens2® data logger with sufficient memory capacity for the data collected during 2 years. Data stored in the data logger can be read directly by the operator as many times as is necessary. In the case of a power cut the data can be stored in the data logger for up to 5 years.

These stations use two different communication modules, either GSM or GPRS. In the case of stations in Wladyslawowo and Darlowo, data are recorded every 10 minutes and once an hour the set of the data is sent to the server in Gdynia. The system generates SMS messages which are sent automatically by Wavecom GPRS (General Packet Radio Service) Fasttrack modem as an e-mail. Furthermore data messages are forwarded to the ESEAS server and are available through www.eseas.org (Sztobryn *et al.*, 2005).

In the case of the Ustka and Gdansk stations, data transmission is performed automatically every hour via the GPRS packet data transmission system using the Wavecom GPRS Fasttrack module. A spare transmission system using GSM modem MC35 operates for servicing. It can be used for transmission of the different data types as voice, fax, numerical data and SMS. Communication with the GSM modem terminal is provided using standard AT commands from a remote operator.

The systems described above differ from each other regarding sea level data presentation. This can be static or dynamic. As soon as an SMS message is received by the server from Wladyslawowo or Darlowo the static graphs of sea level and water temperature are created and presented on IMWM's web page www.imgw.pl/wl/internet/zz/baltyk/wladyslawowo.html (Sztobryn *et al.*, 2005). In contrast to this solution data from Ustka and Gdansk are read by an external service provider and then forwarded to IMWM's operational database (Krzymiński, and Kaminska, 2004). To reduce costs of connection, energy consumption and to ensure stability of connection during data transmission, two GPRS channels are used. The installed software switches automatically between channels during the data transmission process. Stored data are managed by

Hydras3® software. It makes automation of certain tasks possible: reading data from the measuring devices, receiving alarms from stations, exporting data from the HYDRAS3 database and others (Wilczewski and Penar, 2004). Data stored in the local operational database every hour are presented on an interactive web page pomiary.imgw.gdynia.pl. It allows for the selection of different locations, time periods of the presentation and also downloading data in tabular form to the registered client computers (Figure 3).

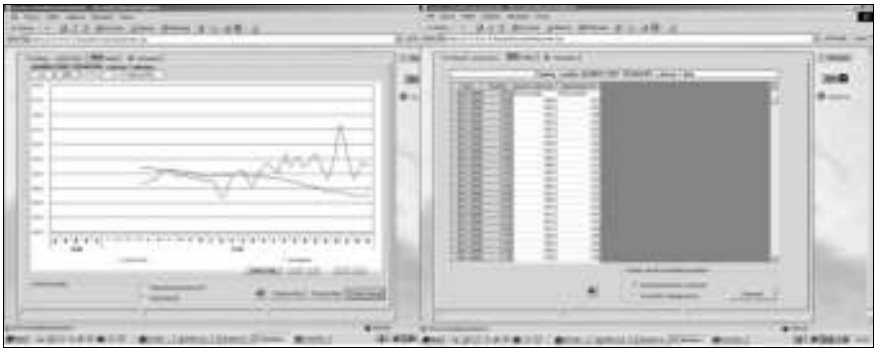

Figure 3 Graphical presentations of sea level data from coastal stations (left panel) and tabular presentations (right panel) on the interactive web site.

Meteorological and sea level real-time and near-real time data are very important in daily routine operational work of meteorological and hydrological forecast offices. Real-time validation of sea level forecasts as well as hydrological and hydrodynamical models could be performed thanks to incorporation of real-time data into validation procedures. The frequency of sea level forecasts obtained from models is lower than operational data — they are received every hour. Some meteorological data are received every hour and some every 3 hours. Sea level data, as mentioned above, are stored with a time step of 10 minutes. These data can be retrieved directly from the station by the operator when a hydrological situation is dangerous, for example during a storm surge. Thanks to the described technical development, operational services at IMWM have modern tools for their activities.

Technical development has also covered raw data transfer in near-real time from research vessels (SOOP) operating within the Polish zone of the Baltic Sea. In parallel to the improvement of the sea level measurements transmission, the system for oceanographic data transmission from the research vessel has been developed. Installation of a new satellite communication system Inmarsat MiniM on board the r/v Baltica made it possible to transmit vertical temperature and salinity measurements collected during research cruises. Despite some weaknesses of Inmarsat MiniM (it is not a very fast device), it is sufficient for transmission of small data sets such as vertical TS profiles. A satellite terminal was installed on board r/v Baltica at the end of 2004 and was successfully used during the first oceanographic cruises of 2005 for transmission of some oceanographic data (salinity and temperature) from the sea directly to the onshore server. As soon as data sets are received they are available on the Internet Monitoring Service web page baltyk.imgw.gdynia.pl/oroma. The tabular data sets are available for registered users as well (Figure 4) (Krzymiński and Piliczewski, 2005). After a cruise, chemical

(nutrients) and biological (chlorophyll *a*) data are entered into an operational database, and are available through the web page.

The Internet Monitoring Service was financed with funds of two EU 5th Framework Programme activities: the OROMA and SEA-SEARCH projects with financial support from the Polish Chief Inspectorate for Environmental Protection.

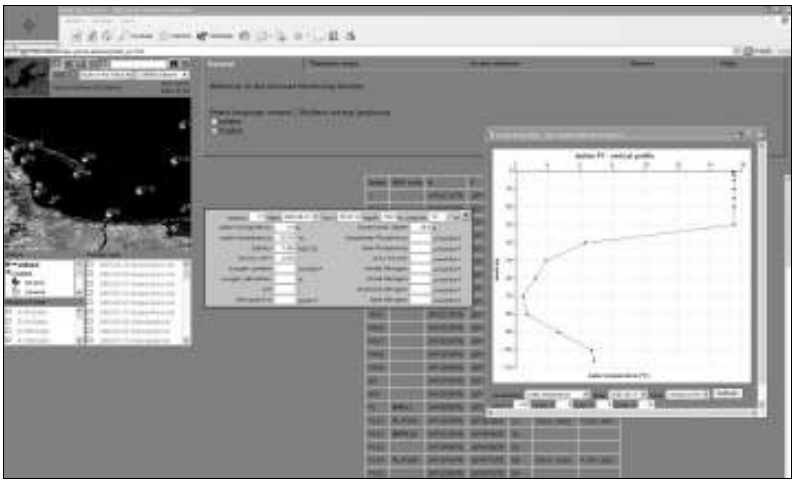

Figure 4 An example of IMWM's Internet Monitoring Service page presenting data in tabular and graphical forms.

References

Dziadziuszko, Z. (1996). Seventy Five Years of Activity of the Institute of Meteorology and Water Management — Maritime Branch, Wiad. Inst. Met. Gosp. Wodnej., XIX, No. 3.

Krzymiński, W. and Z. Dziadziuszko (1997). Polish Oceanographic Service — present status and prerequisites to join EuroGOOS. In: Operational Oceanography, The Challenge for European Co-operation, Proceedings of the First International Conference on EuroGOOS, The Hague, The Netherlands, Elsevier, 351–357.

Krzymiński, W. and M. Kaminska (2004). Instrumentation upgrade at IMWM, PAPA 2nd Annual Meeting, Koge, Denmark, 29–30.11.2004, oral presentation.

Krzymiński, W. and B. Piliczewski (2005). The Internet Monitoring Service — a step forward dissemination and distribution of the polish marine monitoring data, IMDIS conference, 1–3.06.2005, Brest, France, poster presentation.

Sztobryn, M., W. Stepko, R. Zdunek and B. Kowalska (2005). Quality Analysis of Sea Level Data from Polish Coastal Zone, conference "Methods of Quality Control for the Polish Hydrological and Meteorological Service", Warszawa 2005, pp. 230–237, (in Polish).

Wilczewski, P. and W. Penar (2004). Automated measurements of water level and temperature — technical documentation (in Polish).

Development of new technologies for the high variability phenomena data acquisition in the MFSTEP–VOS project

Marco Marcelli*[1], Antonia Di Maio[2], Viviana Piermattei[1], Giuseppe Zappalà[3] and Giuseppe Manzella[4]

[1]*Department DECOS, Tuscia University, Italy*
[2]*AQSmare, Roma, Italy*
[3]*CNR IAMC sez. Messina, Italy*
[4]*ENEA CLIM Forte S. Teresa, Italy*

Abstract

Physical and biological processes of the marine ecosystem have a high spatial and temporal variability, whose study is possible only through high resolution and synoptic observations. For this reason a new sliding vehicle (SAVE) was designed, in order to collect physical and optical profiles in the upper 200 m of the water column. SAVE slides along a cable between the surface and a depressor, that is towed at a fixed depth, and is composed of an underwater unit, an on board unit and a data transmission system. A prototype was realised in the framework of the EC funded project MFSTEP. Many tests have been performed by using the R/V 'Luigi Sanzo' of the CNR IAMC — Section of Messina:

- SAVE depressor navigational behaviour
- Pitch, roll and depth stability
- Data acquisition from trim control.

The depressor was manufactured from PVC and was deployed at different depths to test the behaviour in the water. A cylinder pressure vessel was installed on the SAVE depressor containing a miniature pressure transducer and a biaxial inclinometer sensor.

A test version of the sliding vehicle was made in PVC, containing a CTD probe, fluorimeter and PAR sensors. SAVE was connected to the depressor cable through a sliding system of teflon, and acquired physical-chemical and biological parameters in the water from surface to the depressor depth.

Keywords: SAVE, towed vehicle, MFSTEP, USV, depressor

1. Introduction

The main problem faced by experimental oceanographers is the development of technologies that can resolve the spatial and temporal scales of the physical, chemical and biological phenomena at sea. In operational oceanography, this problem is even more demanding, since the observations must often be gathered from for example ships of opportunity or other platforms where any kind of technical maintenance is impossible. Furthermore systems need to be simple and cheap, in order to allow easy operational use.

* Corresponding author, email: marcomarcell@tin.it

Ships of opportunity have traditionally provided cost-effective measurements of the upper thermocline temperature. Many technologies have been developed during the last decades, for a more effective observation of the marine environment. The ARGO programme is now providing a fruitful combination of observations over the world ocean and the Mediterranean. Other new technologies, such as gliders, have demonstrated their valuable contribution to operational oceanography.

The marine monitoring systems are making more and more use of autonomous vehicles, capable of acquiring and transmitting data without human intervention. The monitoring programme based on ships of opportunities needs to be strongly revised. There are some clear advantages in the use of commercial ships (e.g. repetitive tracks, high return of data), however the number of parameters collected operationally by the majority of the ships is very limited (normally temperature profiles). Some important technological developments and new sampling strategies can enhance the contribution of commercial ships to important programmes aiming to acquire long-term information on the marine ecosystem variability and changes (e.g. Agenda 21).

2. The SAVE project

In order to have a more effective and multidisciplinary data collection system from ships of opportunities, and avoid the use of expendable probes, as much as possible, a new towed sliding vehicle was designed called SAVE (Sliding Advanced VEhicle), able to provide quasi-synoptic measurements in deep sea as well as in shallow waters.

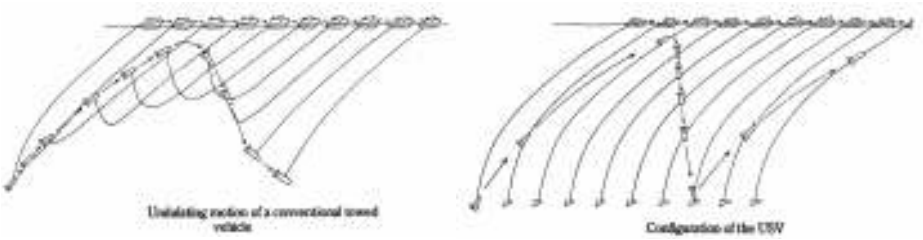

Figure 1 The different approaches (from Nomoto *et al.*).

Two approaches can be selected for the collection of profiles from a ship (see Figure 1):

- Towed undulating system, where the vehicle slides along a cable stretched by a depressor (USV = Undulating Sliding Vehicle)
- "yo-yo" approach where the cable follows the vehicle.

One of the main problems in designing a profiling system is the need to reduce the hydrodynamic forces which are accompanied by the changes of the tow cable position. This problem can be resolved by adopting a USV system, composed of two elements:

- a depressor, towed at fixed depth
- a measuring vehicle (the SAVE), that slides along the cable.

As the magnitude of the hydrodynamic forces necessary for undulation increases with undulation amplitude, large wings are needed for a large undulation amplitude. In the towed vehicles the hydrodynamic drag of the tow cable also resists the fast undulating motion through the sea water.

The USV configuration is favourable because it doesn't need to change the position of the cable during the undulating motion.

In synthesis SAVE has a reduced drag of the cable allowing:

- a fast undulating motion through the water column
- large undulating amplitude through the water column
- no fairings (important for using ships of opportunity).

The SAVE general architecture is shown in Figure 2. An on-board unit consists of:

- Power system
- Data reception system
- Software
- GPS
- Winch

A underwater units consists of:

- a depressor and the SAVE vehicle
- an electronic module to manage the system (installed either on depressors or on the fish)
- a wings' control system — data transmission system
- firmware for data and probes management. The instrumental payload is the control probes (pitch, roll, stability, deep) (installed either on depressors or on the fish)
- measurement probes (CTD, PAR, Fluorimeter) installed on the SAVE vehicle.

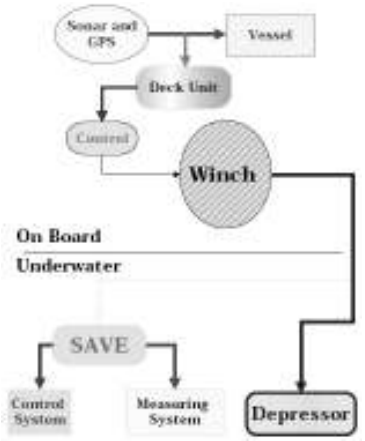

Figure 2 SAVE general architecture

The first tests were carried out during two different cruises, on 26 and 28 May 2004, on board the 'Luigi Sanzo' of the CNR IAMC, section of Messina.

The design of the depressor has to consider the strain on the cable with a speed varying between 2 and 10 knots. The maximum operative depth at those speeds with a steel cable of 6 mm is 200 m. This final wing design will be realised in plastic with internal steel

arms. The first depressor was designed to test the behaviour in the water at different depths; for this reason the cylinder pressure vessel was installed on the SAVE depressor to acquire data to trim control. Figure 3 shows the stability of roll and pitch.

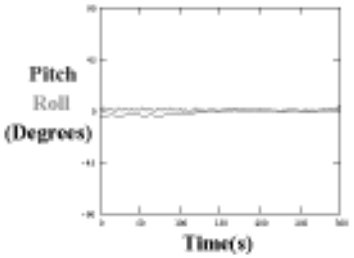

Figure 3 Stability of roll and pitch.

Figure 4 The field test of the depressor unit. On the wing the steel cylinder with the Falmouth sensors is visible (see text) and on the cable the first prototype (the white vessel) of the SAVE.

The conductivity and temperature sensors to be installed on the SAVE (Falmouth OEM) and their electronic control system were assembled in a steel pressure cylinder installed on the depressor (Figure 4). The first prototype of the vehicle comprised a simulation of the SAVE (manufactured in white PVC) containing an Idronaut probe for CTD, fluorimetric and PAR measurers, and was connected to the depressor cable through a sliding system of teflon, enabling acquisition of the physical-chemical and biological parameters of the water, to the depressor depth (Figure 4).

Acknowledgements

This work was partially supported by the EC MFSTEP and CNR SAM projects.

References

Nomoto, M., Y. Tsuji, A. Misumi and T. Emura (1986). An Advanced underwater towed vehicle for oceanographic measurements. Advances in underwater technology, ocean science and offshore engineering, vol. 6, pp 70–88, 1986.

An automatic multiple launcher for expendable probes

Giuseppe Zappalà*[1] and Giuseppe M.R. Manzella[2]

[1]*CNR-IAMC Section of Messina, Italy*
[2]*ENEA CLIM La Spezia and IMC Oristano, Italy*

Abstract

A Voluntary Observing Ship programme has been running in the Mediterranean from September 1999. During these years, the data collection and transmission methodology has been improved with new technologies, aiming at the improvement of the cost effectiveness of the data collection system. This paper describes an automatic multiple launcher for expendable probes designed to be used on Voluntary Observing Ships.

Keywords: Voluntary Observing Ships, data collection, expendable probes, automatic launcher

1. Introduction

The use of expendable probes, launched from dedicated ships as well as from commercial vessels, is one of the most effective ways to collect profiles of parameters characterising sea water (usually temperature, sometimes also conductivity). The Voluntary Observing Ship (VOS) programme in the Mediterranean uses XBTs with the main objective of providing data for forecast models (Pinardi *et al.*, 2003).

The Mediterranean VOS has been running since September 1999 and was implemented as a component of the Mediterranean Forecasting System (MFS), a project divided into different phases, the first of which (pilot project) was financially supported by the EC in the framework of the MAST programme (Fusco *et al.*, 2003). MFS−VOS has continued as part of other European and Italian projects.

Data are actually acquired by means of a Sippican system, composed of a hand launcher, MK12 or MK21 card and a computer. The launching procedures and the control of the profiles on the computer screen require a lot of effort from the technicians engaged in data collection. At the end of the MFS pilot project, the analysis of the VOS system indicated a need to develop new transmission systems and more automated data acquisition systems.

A multiple launcher has been developed aiming to facilitate the management of the data collection by ship personnel and reduce the personnel costs. It was designed and built in the framework of the EU funded research programme "Mediterranean Forecasting System Towards Environmental Prediction" (MFSTEP).

* Corresponding author, email: giuseppe.zappala@iamc.cnr.it

2. The mechanical hardware

The heart of the system is a launch tube, built from AISI 316 steel, in which the probe is fitted with its envelope. An upper cap, holding the electrical connections of the probe, closes the launch tube; opening the lower door releases the probe which falls into the water.

Two pneumatic cylinders control the door: a small one keeps it closed, a bigger one moves it.

In the actual MFS−VOS design, the system assembles eight launch tubes on a frame with their pneumatic actuators; two watertight boxes host respectively the electro-pneumatic valves feeding the cylinders and the computerised control system (Figure 1).

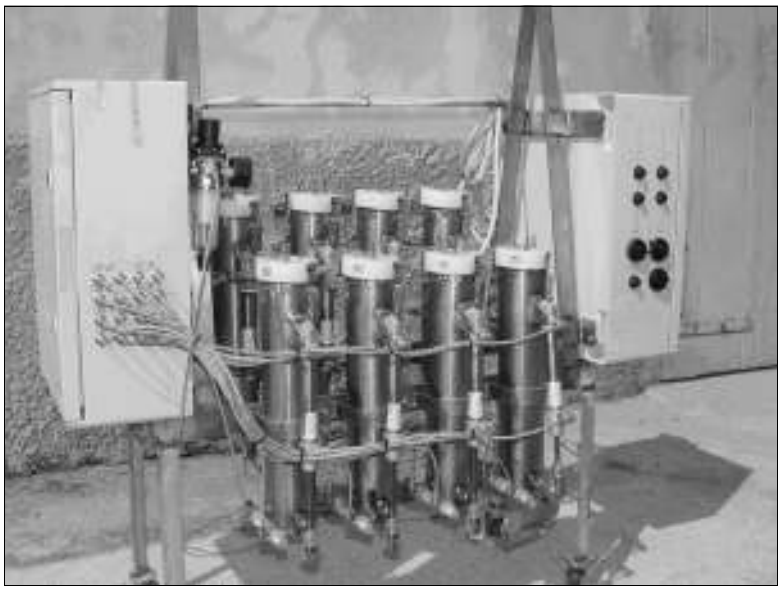

Figure 1 The multiple launcher with the electro-valves box (left) and the electronics box (right).

3. The control computer hardware and software

3.1 The electronic hardware

All operations are coordinated by an industrial grade computer, based on IEEE 696 compliant boards, interfaced with GPS, data acquisition and communication devices. Both analogue and digital interfaces are available to collect data coming from different devices (passive and active expendable probes, meteo sensors, etc.).

Remote communications are performed using a GPRS modem with an embedded TCP-IP stack; a serial port is available to connect other communication devices (e.g. satellite modems), but other communications systems could also be used (e.g. satellite phones).

A balanced source circuit (Figure 2) was designed to interface standard passive temperature probes with 12 or 16 bit Analog to Digital Converters.

Two equal currents are injected in both the wires coming from the probe and the potentials V_A and V_B are measured; the circuit is closed by the sea water; the switch SW1 (a relay contact) enables testing of the continuity of the probe circuit.

To avoid perturbation to the measurements, a multiple stage amplifier is used to adapt the signal coming from the probe to the need of the ADC; the circuit was built using high quality precision instrumentation amplifier ICs.

The first stage uses unity gain configuration, having high input and low output impedance; the second stage is a differential amplifier with gain = 2; the third stage is a low output impedance low-pass filter with gain = 1 and ft = 40 Hz. Ten times a second, the mean of 16 (V_B–V_A) measurements is calculated; the resistance of the thermistor is obtained using Ohm's law, and hence the measured temperature using the standard formula.

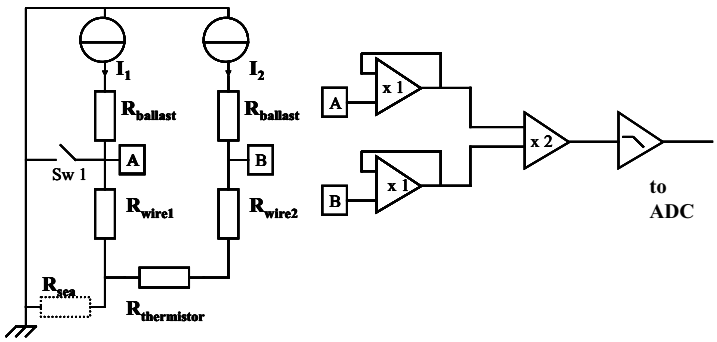

Figure 2 The schematics of the probe interface board.

3.2 The software

Two software sets were developed, able to manage 96 launch events and 96 alarms:

- A local control program, written in Microsoft Compiled Basic v. 7.1 with routines in Assembly Language, running in Datalight DOS environment
- A remote control program, written in Microsoft Visual Basic v. 6.0, running in Windows environment.

Launch options are:

- northern than
- southern than
- eastern than
- western than
- far from
- at GPS time
- at PC time

The collected data are locally stored and can be transmitted as e-mails.

Data coming from the GPS are continuously compared with the programmed launch–alarm positions.

Every hour, a "sequence manager" starts a macro-command sequence, that can be different for each time and is remotely reprogrammable; new releases of the software and of the sequences are uploadable to the station without suspending normal activity. The macro-commands enable management of the data acquisition and transmission, the mission programming, the station hardware and the measuring instruments.

Acknowledgements

This activity is funded in the framework of the MFSTEP project, 5th EU FP. The authors acknowledge the support provided by N. Pinardi and G. Coppini. The work of technicians during these years have provided the necessary information for the design. We wish to thank A. Baldi and F. Conte. A special acknowledgment to F. Reseghetti who provided a careful analysis of the Sippican system.

References

Fusco, G., G.M.R. Manzella, A. Cruzado, M. Gacic, G.P. Gasprini, V. Kovacevic, C. Millot, C. Tziavos, Z. Velasquez, A. Walne, V. Zervakis and G. Zodiatis (2003). Variability of mesoscale features in the Mediterranean Sea from XBT data analysis. Annales Geophysicae, 21, 21–32.

Georgi, D.T., J.P. Dean and J.A. Chase (1980). Temperature calibration of expendable bathythermographs, Ocean Eng., 7, 491–499.

Pinardi N., I. Allen, E. Demirov, P. DeMey, G. Korres, A. Lascaratos, P.Y. LeTraon, C. Maillard, G. Manzella and C. Tziavos (2003). The Mediterranean ocean Forecasting System: first phase of implementation (1998–2001). Annales Geophysicae, 21, 3–20.

Roemmich, D. and B. Cornuelle (1987). Digitisation and calibration of the expendable Bathythermograph, Deep Sea Research, 34, 299–307.

Reseghetti, F., M. Borghini and G.M.R. Manzella, Analysis of T4/T6/DB XBT performances and comparison with CTD temperature measurements in Western Mediterranean Sea, Deep Sea Research, submitted.

Data Management and User Needs

Delayed mode quality control on Argo floats at the Coriolis Data Centre

C. Coatanoan* and T. Loubrieu

Ifremer, IDM, France

Abstract

Recalibrations of ARGO floats cannot be easily performed. A remote calibration method is required to correct salinity sensor drifts by using hydrographic reference databases. At the Coriolis data centre, the Wong *et al.* method, adapted by Böhme and Send, has been applied to the North Atlantic environment to produce the delayed mode dataset for the Gyroscope project. Within the European project Gyroscope, each float has been scrutinised for the delayed mode QC following the steps defined by Argo; a large coordination effort has taken place between the PI and the data centre to study the results of the method.

Since this application has been carried out on some floats older than two years, it appears that some of them show offsets or drifts, at least for the latest cycles. Most of them can be easily corrected from the DMQC method, but from this first experience, we can mention that when a float shows irregular behaviour, especially when a significant drift appears, we need to apply specific procedures. To calculate these corrections, for each float, a sliding window has been implemented to take into account neighbouring profiles. However, when a drift or jump is observed, the float series have to be split so as not to contaminate the stable segment. Complementary diagnostic plots have been developed at the Coriolis Data Centre to compare DMQC results with temperature and salinity residuals and fields of climatology.

Most of the Gyroscope floats have been processed in delayed mode. For these floats, the delayed mode data have been integrated into the database and can be downloaded from the Coriolis Data Centre.

To be able to properly apply the Wong−Böhme method, a relevant reference dataset is needed, which should be supplied by the CTD carried out during the float deployment. This may be also the base of the ARGO Regional DAC (Data Assembly Centre).

Keywords: Delayed mode, quality control, Argo, profiling float, salinity sensor

1. Introduction

Recalibration is generally not possible due to the moving nature of floats, so float datasets are usually checked in an indirect way. A method based on mapping a set of calibrated data by objective analysing to the float profile position has been developed. The method applied at the Coriolis Data Centre is the method of Wong *et al.* (2003) adapted to the North Atlantic environment by Böhme and Send (2005) to produce the delayed mode data for the Gyroscope project for the first time.

* Corresponding author, email: Christine.Coatanoan@ifremer.fr

Recalibration is set up to correct sensor drifts by using historical hydrographic data. The objective mapping method used takes into account the high spatial and temporal variabilities of the North Atlantic. Assuming that a conductivity offset changes slowly over time, the float measurements are fitted linearly to the mapped salinities in potential conductivity space by weighted least-squares. The result is a set of calibrated salinity data with corresponding uncertainties.

2. The delayed mode QC method

The method uses the two main state variables temperature θ and salinity *S*. Mean θ-*S* relationships can be used to estimate salinity from measurements of temperature and pressure. The CTD measurements (WOD01 and others) are interpolated on 2 dbar levels to store all information but with a reduced amount of data. To provide an acceptable vertical coverage the deepest measurement for each station must be below 1000 m.

The horizontal data selection is based on a spatial distance *D* and fractional distance in potential vorticity *F*. The vertical data selection selects 10 float measurements for each profile (top and bottom measurements (525–2000 dbar), minimum and maximum of *T* and *S*, two with tightest *P*-*T* definition and two with highest *P*-*S* definition). A temporal distance *t* is also taken into account.

The final objective estimate at the float profile location is the sum of two stages of mapping: the first calculates the basin-wide mean, in the second the residuals are mapped to the float profile location using a covariance function of the temporal and small spatial separation. All measurements are converted to potential conductivity to eliminate differences in pressures between historical and float data. Then the potential conductivities of the float are fitted to the mapped potential conductivities.

The delayed mode QC process relies on the available CTD reference database. If we do not have enough reference data, the DMQC method can not work, so it is very important to collect all the CTD data from all the oceanographic cruises. Special effort is put into encouraging scientists to make all their hydrographic datasets more easily available.

3. Analysis of ARGO floats

3.1 Results of the DMQC method

Some diagnostic plots allow the behaviour of the float to be followed in order to understand the correction computed from the DMQC method for the calibration.

Salinity anomalies on isotherms allow detection of whether a physical or technical event is the cause of the detected drift/offset of the sensor. Figure 1 shows a drift at the end of the float time-series, where the plot of the float location shows the used reference dataset; the circles are the cycles of the studied float, and the diamonds are the selected data from the reference database to run the objective mapping.

A weighted least-squares fit is made for a time-varying slope of the correction term to smooth out outliers (Figure 2).

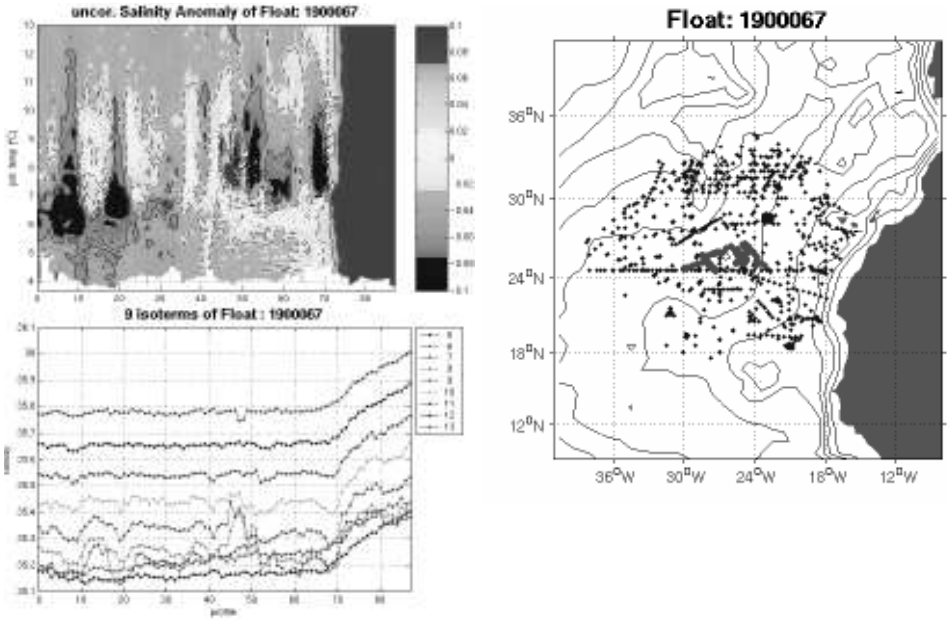

Figure 1 Examples of diagnostic plots provided by the DMQC method. Left: salinity anomalies and salinity on deepest isotherms versus float cycles; Right: float location and reference data.

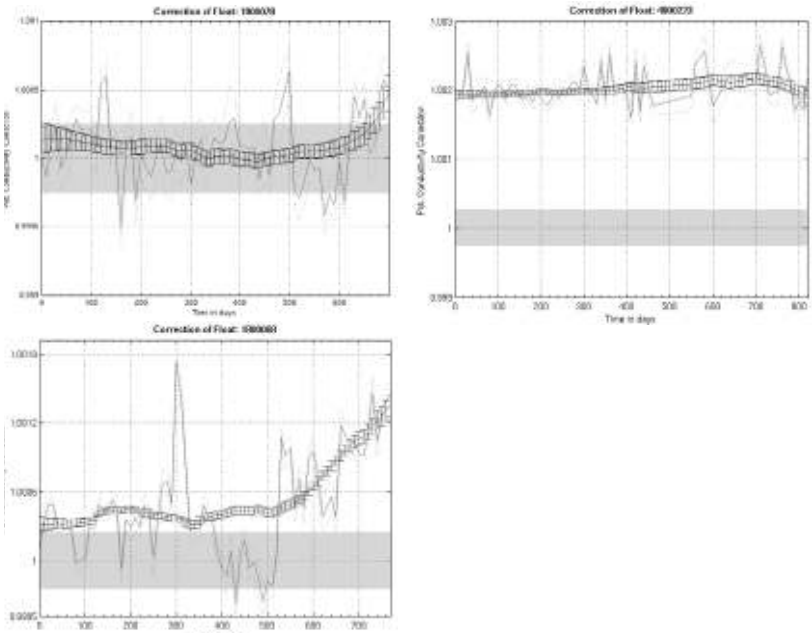

Figure 2 Examples of results of the DMQC method. The individual corrections are represented by the noised curve and the smoothed corrections (with a sliding window of ±6 months) are the curves associated with the error bars corresponding to two times the standard deviation of the fit. The box corresponds to an accuracy of ±0.01 psu.

When the correction and associated error bars intersect the grey box in Figure 2, the correction is not significant. When an offset is observed, it has been shown that using the tank error reduced this offset. A positive drift is consistent with fouling of the conductivity cell. Specific procedures have to be applied when a drift or jump is observed, and the float series have to be split so as not to contaminate the stable segment.

A plot also shows θ-*S* diagrams before and after the correction: in this case (Figure 3) the results of the recalibration allow a significant correction of the observed drift.

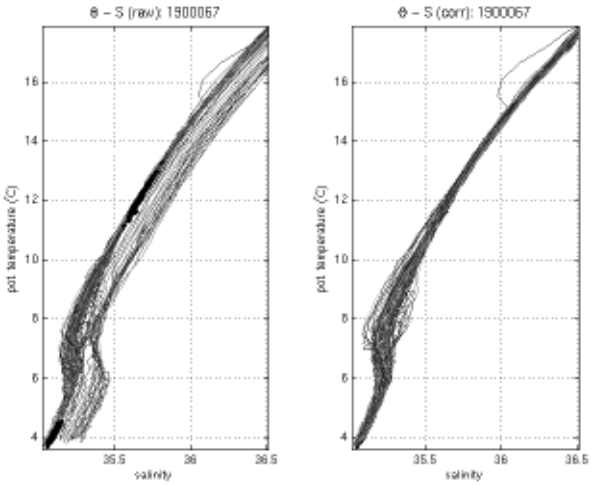

Figure 3 TS diagram plot before and after the calibration correction. The drift observed in the deep water in the raw data has been corrected by application of the DMQC correction.

3.2 Complementary tools

In parallel, a data analysis system based on optimal estimation methods has been developed and implemented at the Coriolis data centre. The method of the differences is used to make comparisons between measurement points and objective analysis fields: using the temporal closer objective analysis, getting grid points around the float, making horizontal and vertical interpolations and differences with the measurement point. Plots for some levels (Figure 4) present differences for all measurement points and means, cycle by cycle.

The residual values allow possible drifts or offsets to be followed for some levels. The comparison with the climatology enables determination of whether the detected drift or offset is artificial.

Other work on pressure offset and battery voltage is also in progress to understand whether the detected offset and drift are correlated with a technical problem.

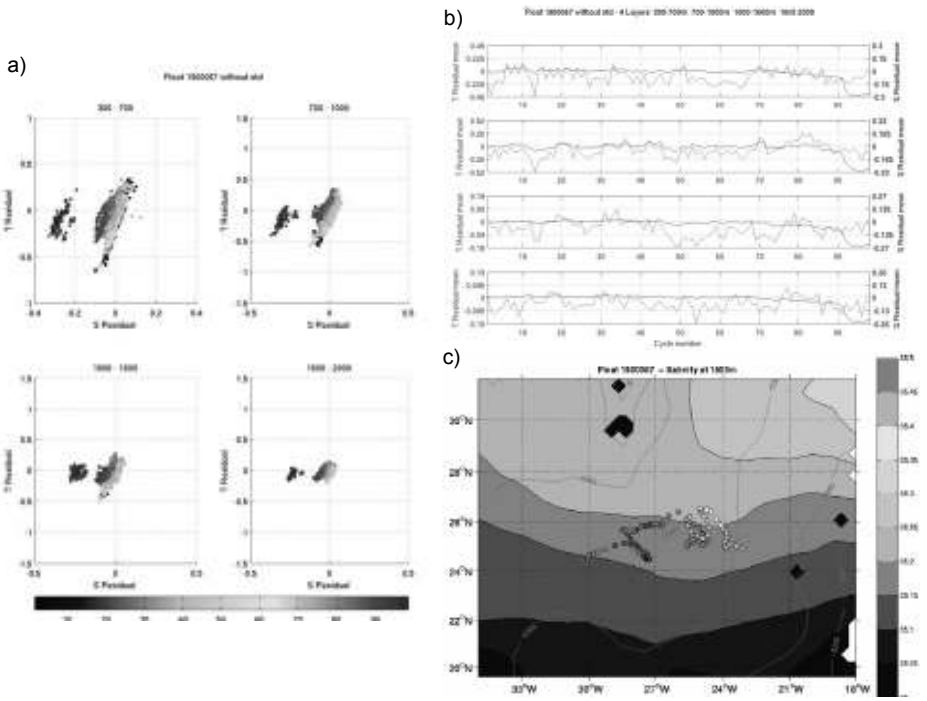

Figure 4 Examples showing a drift for the salinity sensor. a) Temperature residuals versus salinity residuals at different levels range according to the cycle number of the float; b) temperature and salinity residuals versus cycle numbers; c) comparison of the float salinity (or temperature) value with the climatology computed from the objective analysis.

4. Conclusion

The analysis of the float time series has shown that the salinity measurements can drift slowly over time. Due to the drift and offset observed on the salinity sensor, it is necessary to recalibrate float data in delayed mode.

Offsets and drifts are detectable in the Gyroscope floats of the North Atlantic and a corresponding correction is supplied using the objective mapping method. The result is a set of calibrated salinity data with corresponding statistical uncertainties. Seabird sensors seem more stable than FSI sensors.

To help to determine the correction, complementary tools have been developed, using the residuals and fields of an objective analysis taking into accounts all type of data available in the Coriolis database (profilers, xbt, ctd, moorings). Argo delayed-mode procedures are mainly based on reference databases. Historical hydrographic datasets used to select 'best' profiles for the mapping to the float profile are insufficient in some oceanic areas and need to be updated with recent cruise data.

Acknowledgements

We would like to thank Philippe Galaup, Virginie Thierry and Emmanuelle Autret from Ifremer for providing help in processing steps of the DMQC method and developing complementary tools. This work is a contribution to the Argo project.

References

Böhme, L. and U. Send (2005). Objective analyses of hydrographic data for referencing profiling float salinities in highly variable environments. Deep-Sea Res. II, 52, 651–664.

Wong, A.P.S., G.C. Johnson and W.B. Owens (2003). Delayed-Mode Calibration of Autonomous CTD profiling Float Salinity Data by θ-S Climatology. Journal of Atmospheric and Oceanic Technology, 20, 308–318.

Climatology and interannual variability of the North Atlantic based on the Coriolis analysis system

F. Gaillard*[1], E. Autret[1], A. Keziou[1] and T. Loubrieu[2]

[1]*Laboratoire de Physique des Océans, Ifremer, France*
[2]*IDM-ISI, Ifremer, France*

Abstract

The Coriolis real time analysis system started operating in 2000 over the North Atlantic. The dataset collected in real time and delayed mode during this 5-year period has been revisited and a re-analysis has been produced with the same analysis system. Temperature and salinity fields have been reconstructed on a 1/3 degree grid, on more than 50 levels from the surface down to 2000 m. From these fields, associated errors and datasets, a new climatology representative of the 2000–2004 period has been computed, along with updated elementary statistics. The use of those basic products is wide, ranging from automatic quality control to the tuning of numerical models. The seasonal to interannual variability of the various regions of the basin has been examined, and it appears that a long term signal can be detected. Given the current observing system, these products could easily be updated on an annual basis and extended to the world ocean. The dataset also allows for estimation of higher order statistics. The large scale horizontal structure of the variability is extracted with principal component analysis while the more homogenous meso-scales are described by the usual horizontal covariances.

Keywords: Ocean interannual variability, ocean data analysis system

1. Introduction

Since the beginning of the ARGO programme, which plans to deploy 3000 profiling CTD floats over the world ocean, the amount of data (in particular salinity) for the 0–2000 m depth range has increased considerably. The Coriolis data centre, acting as one of the ARGO GDACs, collects and distributes these data in real time. It also gathers *in situ* observations of temperature and salinity from a large variety of other instruments (XBT, XCTD and CTD, moorings). One of the main concerns of Coriolis has been to define a system for real-time data quality control that is at the same time efficient — able to process an increasingly large number of data, and reliable — in order to ensure the detection of outliers but preventing excessive false alarms. The need for data based on high level products such as gridded fields of temperature and salinity expressed by various scientific communities was another requirement.

We have developed an analysis system that answers both demands. It is based on optimal estimation techniques and combines Coriolis data with *a priori* information derived from the climatology and elementary statistics. Diagnostic tools applied to the daily analysis residuals allow detection of outliers and triggers an alarm. The results are inspected by

* Corresponding author, email: Fabienne.Gaillard@ifremer.fr

an operator and the quality flags are manually confirmed. Once a week, a second pass analysis is performed on the cleaned database to produce the gridded fields which are made available on the Coriolis Web site.

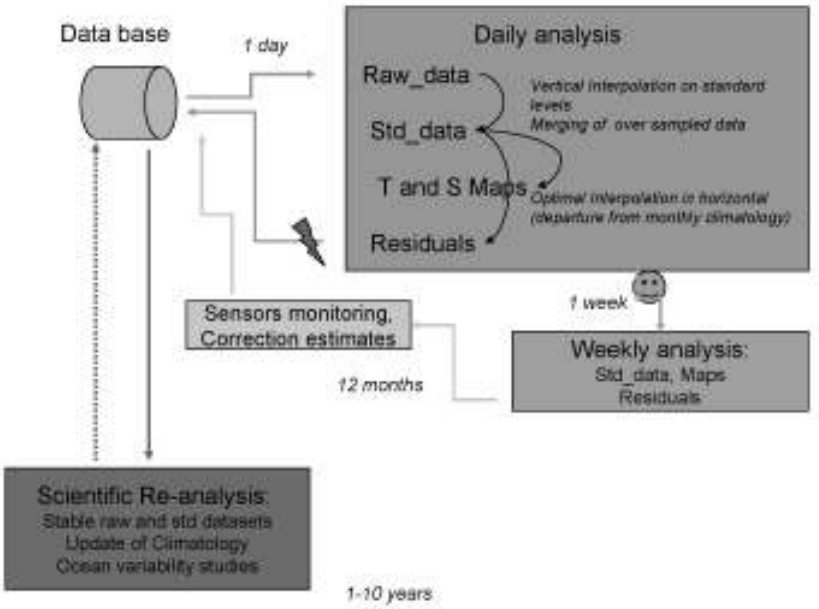

Figure 1 Coriolis analysis system.

In order to validate the system, we have performed a re-analysis of the Atlantic basin for the period 2000−2004 with the exact operational real-time configuration. The only difference with the weekly real time analysis lies in the dataset used: in our case we have access to the data transmitted to Coriolis after the analysis date. The re-analyses are then 'centred', while the real-time analyses are slightly biased backward in time. The first results of this analysis are:

1. an inventory of the database
2. an overview of the profilers' long term drift
3. a new 'climatology' representing recent years.

This last point is presented here. We will proceed with a study of the time and space variability.

2. Coriolis analysis system

The analysis is derived from optimal estimation methods as exposed by Bretherton *et al.* (1976). In order to permit the data quality control, temperature and salinity are analysed separately, on horizontal levels. The solution is searched as an anomaly relative to a monthly climatology (Reynaud *et al.*, 1998). For each analysis date, all data closer than 3 weeks in time are collected and converted to anomalies relative to the climatology to build the data vector (d). The covariance matrices involved in the solution:

$$x^a = x^f + C_{ao}(C_o + R)^{-1} d$$

are constructed using the Gaussian structure functions in time and space defined for the area considered and the data noise. The variances are deduced from the full dataset. We produce analysed fields on 59 levels between 5 and 2000 m. The grid spacing is 1/3°.

The system is run in 3 different modes as shown in Figure 1. In the case of our re-analysis, the dataset was extracted from the database at once, and included all data available at that time. This dataset had been quality controlled with the 'daily loop', so that bad data had been flagged, but no corrections on instrument drift had been applied.

3. An updated climatology

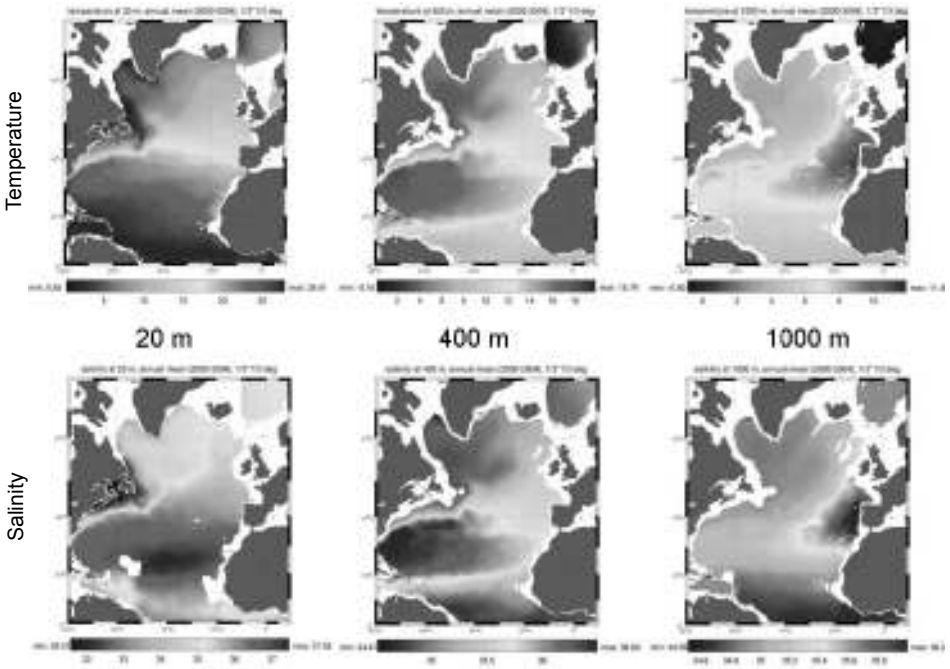

Figure 2 Annual mean temperature (top) and salinity (bottom) over the period 2000–2004, at three levels (from left to right).

3.1 Building the climatology

The 2000–2004 period corresponds to the setting up of the ARGO array over the Atlantic, starting mostly in the Northern hemisphere, so our analysis is limited to this basin. The number of data available each month at each level shallower than 800 m rose from 200 in 2000 to 1200 in 2004. The first goal of the analysis is to extract a mean seasonal cycle representing the year range 2000–2004. To construct each month of the cycle, all weekly analyses relative to this month and above an error threshold have been averaged. The annual mean fields were obtained by averaging the monthly means. Providing a sufficiently low error level on each month, this mean is unbiased relative to the season. Figure 2 shows the mean field obtained for different levels.

3.2 Annual mean anomaly

This new climatology can be compared to similar products obtained from previous data. The first comparison is done with our reference climatology (Reynaud *et al.*, 1998). This climatology was computed by objective analysis on pressure levels from a dataset strongly weighted toward the years 1970–1980. Near the surface, we observe a global warming except around Newfoundland and over the mid-Atlantic ridge just north of 50°N. At 400 m the Northern seas appear cooler, starting from the Norwegian sea, the Greenland sea and reaching most of the Labrador sea. A cold anomaly is observed along the path of the North Atlantic current. Despite differences in the small scale amplitudes, the large scale structure of the anomalies are similar when computed relative to Hydrobase 2 (Produced by WHOI).

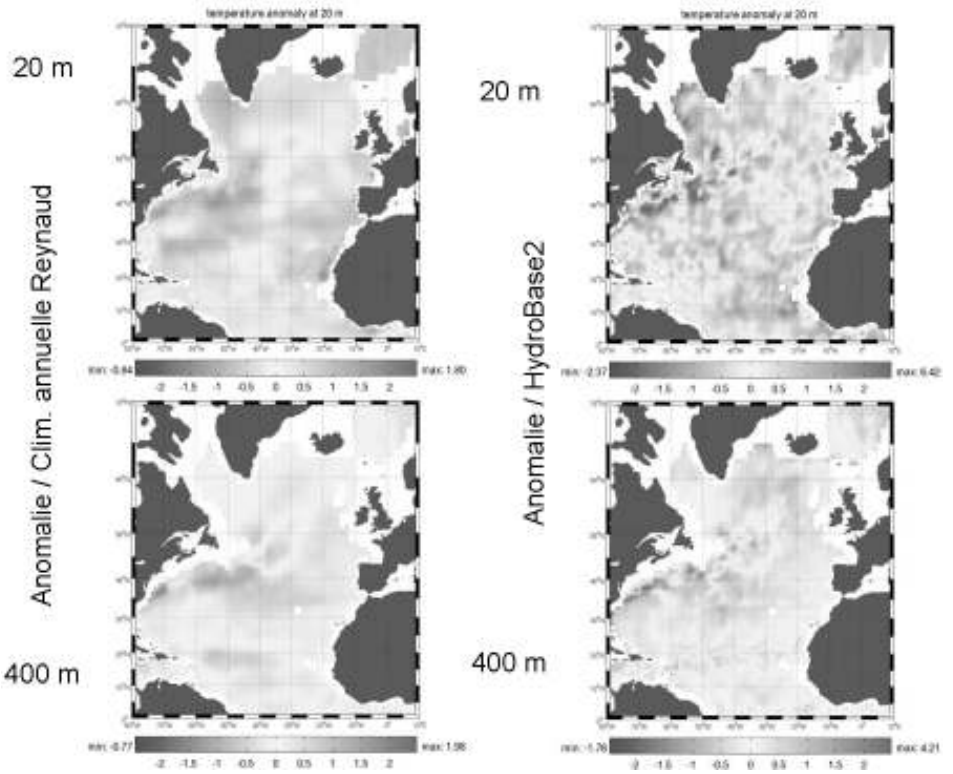

Figure 3 Temperature anomalies relative to previous climatologies. Left: anomaly relative to our reference (Reynaud, 1998); Right: anomaly to Hydrobase 2. This climatology was computed on density levels.

3.3 Seasonal cycle

To determine whether the mean warming observed over most of the basin in the upper layer was evenly distributed over the year, we analysed the seasonal cycle at different test points. To obtain more representative series, we averaged the time series over a 4 degree square area surrounding the points. The time series at four test points in the northern part of the basin are presented in Figure 4. At all test points we notice that our

curve is above the previous climatologies. It appears more regular than Hydrobase2 in winter with a well-defined minimum in February−March.

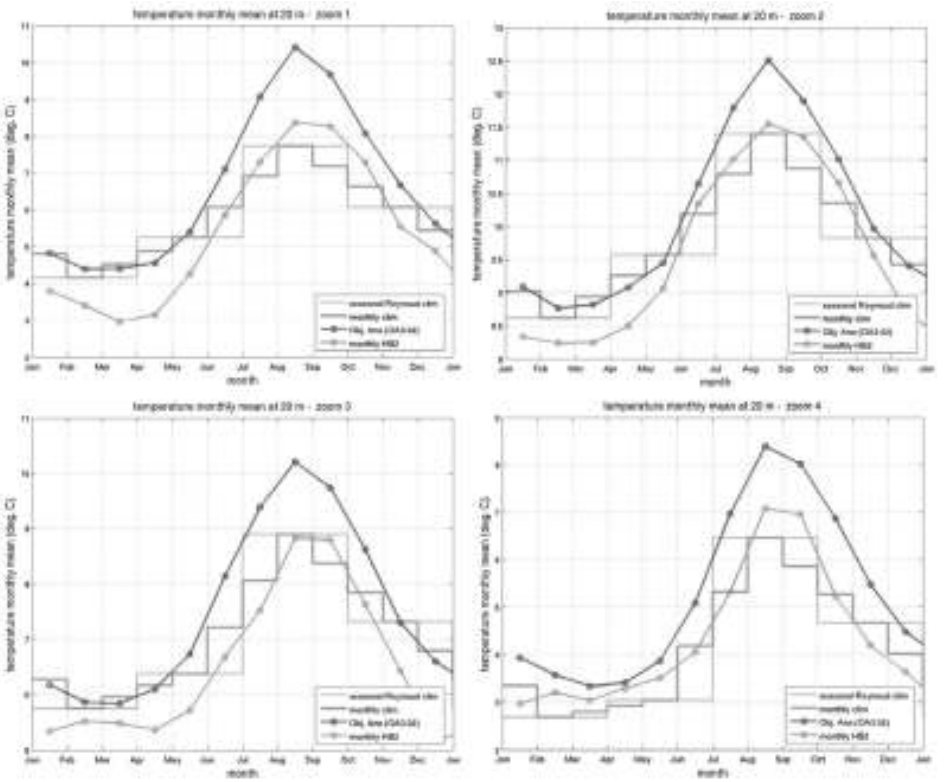

Figure 4 Seasonal cycle for temperature at 20 m for the Northern test points (top left: Norwegian sea, top right: Iceland basin, bottom left: Irminger basin, bottom right: Labrador sea). Dark grey curve: our mean monthly annual cycle, light grey curve: Hydrobase2 monthly annual cycle, in grey, Renaud98 seasonal cycle, and the monthly interpolation used as reference for the analysis.

3.4 Interannual variability

To study the spatial structure of the variability, empirical orthogonal functions of the anomaly relative to the annual cycle have been computed. The time series of the leading mode at 100 m shows a clear tendency over the 5 years of the analysis. We are presently analysing the correlation with the sea-surface variability and trying to extract the vertical propagation.

4. Conclusion

Although this work is still in progress, some conclusions can already be drawn. The analysis tool developed for Coriolis is simple, efficient and robust. Some improvements are already planned, in particular the use of continuous covariances that take into account the bathymetry (as done by Böhme *et al.*, 2005).

The Argo database is impressive and a high quality climatology has been obtained already over most of the North Atlantic. The remaining gaps should be filled by the end of 2005. Changes relative to previous climatologies are clear and this data set gives access to the interannual variability in many areas.

Acknowledgements

We would like to thank the technical staff involved in all aspects of the Argo profiler deployments, as well as the Coriolis data centre for providing this high quality, easy to use data set.

References

Böhme, L. and U. Send (2005). Objective analysis of hydrographic data for referencing profiling float salinities in highly variable environments, Deep Sea Research II, 52, 651–664.

Bretherton, F.P., R.E. Davis, *et al.* (1976). A technique for objective analysis and design of oceanographic experiments applied to MODE-73. Deep-Sea Research 23: 559–582.

Reynaud, T., P. Le Grand, *et al.* (1998). A new analysis of hydrographic data in the Atlantic and its application to inverse modeling. WOCE Newsletter 32: 29–31.

Economics of sustained marine measurements

Ece Ozdemiroglu*[1] and Ian Townend[2]

[1]*Economics for the Environment Consultancy Ltd. (eftec), UK*
[2]*ABP Marine Environmental Research Ltd., UK*

Abstract

This paper summarises the research commissioned by the UK Inter-Agency Committee on Marine Science and Technology (IACMST) and undertaken by eftec. The focus of the work is to recommend a methodology to quantify the economic benefits of marine measurements.

The benefit assessment framework developed for the study involves:

1. making a qualitative case
2. making a quantitative case (e.g. expert derived weights or scores, types of activities that use the data, etc.)
3. quantifying the benefits of sustained marine measurements in monetary terms by: market price paid for marine measurement data, proxies to market price, and willingness to pay of users to purchase marine measurement data (especially if data are currently provided for free).

Assessing the benefits of marine measurements is the focus of this paper since this is where the current practice is the weakest. However, the paper also seeks to answer the following questions:

1. What are the types of marine measurements of concern?
2. What are the objectives or purposes of using marine measurements?
3. Who uses or directly benefits from these measurements?
4. What are the benefits they derive from their use of marine measurements?
5. How much does it cost to collect the marine measurements of concern?
6. Are the benefits of data use worth the cost of collection?

Benefits to direct users of data are relatively straightforward to measure. There are also environmental and social benefits, which could partially be captured by the (economic) benefits to direct users of data. The methodology is illustrated by application to the Jason-2 altimetry satellite and to Liverpool Bay Coastal Observatory Monitoring.

Keywords: Marine measurements, economic benefits, economic valuation, cost benefit analysis

1. Introduction

This paper is based on a study commissioned by the Global Ocean Observing System Action Group (GOOSAG) of the UK Inter-Agency Committee on Marine Science and

* Corresponding author, email: ece@eftec.co.uk

Technology (IACMST). The study entitled "The Economics of Sustained Marine Measurements" aimed to establish a method for evaluating the benefits of the UK's long-term marine monitoring programme (IACMST, 2004).

While the benefits of a well co-ordinated programme of marine measurements[1] are widely accepted, the ability to demonstrate or quantify these benefits is more limited. The methodology recommended for this involves estimating the economic benefit of activities that use marine measurement data and assessing how this benefit would change with changes in data. When aggregated across all activities, this provides us with an estimate of the economic benefit of the information itself. The term 'benefit' is used in its widest meaning and includes:

- economic benefits to the users of marine measurement data such as reduced operational costs, precautionary spending and avoided damage from weather events and waves
- environmental benefits such as reduced environmental damage from oil spills due to improved spill management using better marine data
- social benefits such as better understanding of the marine environment through more informed documentaries, articles, books, etc.

Since the term economic benefit in economics terminology refers to all benefits that improve human welfare, all of the above benefits could be referred to as 'economic benefits'. Moreover, all benefit categories have efficiency implications — as all require spending on data collection and analysis and allocating this spending in the most efficient way. The above classification will be used subsequently since what is conventionally referred to as 'economic' or 'commercial' is relatively easier to quantify and express in monetary terms.

Some of the benefits extend beyond those received by a single public or private entity and as a result are not included in any price paid for the data (if there is such a price at all as most data are provided for free). These wider benefits to the economy and society are derived by making better decisions with the help of better information and are known as *external* benefits. Precisely because of the existence of these external benefits, there is no real incentive for any one entity (public or private) to pay for the creation of the system. Provision of such external benefits is one of the characteristics of a public good, others being non-rivalry (consumption of the good by one party does not decrease the consumption opportunity of other parties) and non-excludability (it is not possible to exclude parties from the use of the good by, for example, pricing). Marine measurements, thus, fit this definition and are public goods. NOAA *et al.* (2000) go a step further and refer to these benefits as *network externalities* to emphasise the fact that the value of an integrated, sustained and comprehensive system is many times that of the value of its parts. The existence of network externalities mean that while many parties benefit from marine measurements, no one party has the incentive to invest in it. This points to the

1 These include observations of the physical, chemical and biological parameters of the marine environment taken for research, emergency response and monitoring purposes.

requirement for **sustained** marine measurements and collaborative or public funding for them.

This paper introduces the concept of economic value for marine measurements (Section 2) and the recommended methodology (Section 3). Further detail on these issues, application to two case studies and a stand-alone guidance document can be found in IACMST (2004).

2. Economic benefits of sustained marine measurements

Why do we need marine measurements? The short answer is that they increase our understanding of the marine environment. Such improved understanding, in turn, is beneficial so long as it contributes to more efficient use and protection of the marine environment. 'Efficient use and protection' in this context involves sectors such as fishing, oil and gas exploration, navigation as well as marine conservation and effects of changes in the marine environment (e.g. due to climate change or our exploitation of the marine resources) on the ecology and the human use of marine and coastal environments.

The marine environment is an asset providing a flow of goods and services (physical, aesthetic, intrinsic and moral). To account for this multitude of goods and services and their benefits, a taxonomy of values (or benefits) has been developed, the components of which add up to 'total economic value' (TEV). TEV is made up of use benefits and non-use benefits. Use benefits are derived from the actual direct and indirect use of a good or service. These also include potential future use (option value). The term 'non-use benefits' is used to signify the benefits derived from knowing that others (altruistic value) and future generations (bequest value) have access to a sufficient amount of goods and services and simply that the marine environment exists (existence value).

TEV is measured by preferences of individuals: their willingness to pay (WTP) to secure benefits or to avoid their loss (or costs) and their willingness to accept (WTA) to forgo benefits or to tolerate costs. When goods and services are provided in actual markets, people express their preferences via their purchasing behaviour. In other words, the market price is a minimum reflection of how much they are willing to pay for the benefits they derive from consuming that good or service[2].

Most environmental resources (and generally information) generate 'non-market' or 'external' benefits since they are not traded in actual markets and hence there are no market price data for them. Instead, economists have developed alternative techniques to measure individuals' preferences and hence the TEV of the resource. These techniques use price data when they exist or create hypothetical markets for when such data do not exist. In either case, the unit of measurement for benefits is money which allows benefits to be compared with the costs of providing these benefits (e.g. the benefits of marine measurements compared to the cost of sustaining measurement programmes).

---

2 People may indeed be willing to pay an amount larger than the market price, in which case they get 'something for nothing' or, in economics, they are said to have a 'consumer surplus'. Note that when the market price is zero, the consumer surplus is at its highest and is equal to Willingness to Pay (WTP).

In order to use the TEV taxonomy in the context of this paper, we need to distinguish between the marine measurements and the improvements due to uses and protection of the marine environment as an output of better measurements. Marine measurements can be directly used by the maritime industry, scientists, oil and gas explorers, recreational users, coast guards, coastal defence units and others. Benefits may also accrue to indirect users such as book and newspaper readers and television and film audiences who benefit from the output of the direct users.

Improved uses and protection of the marine environment, in turn, benefit exploration, fishing and other extractive uses of the seas through reduced operational costs or increased revenue. Better information can also influence spending decisions such as improving the timing of precautionary spending for, say, coastal defence; preventing the occurrence, or reducing the impacts of oil spills, coastal erosion and so on.

Table 1 presents the taxonomy of total economic value of sustained marine measurements and protection of marine resources, which is an outcome of better information through marine measurements. Although it uses different terminology, Table 1 is simply another presentation of economic, environmental and social benefits mentioned in Section 1. This taxonomy is also recommended by the UK Government's Green Book (HM Treasury, 2003) which is the key guidance for all public sector spending projects. The Green Book advocates combining economic, financial, social and environmental costs and benefits of a policy, programme or project.

Table 1 Total economic value.

TEV components	Marine measurement information and data	Better use and protection of the marine environment through better information
Direct use	• Long term monitoring and forecasting • Scientific research • Day-to-day marine related operations • Precautionary spending • Other (cost of substitute data)	• Fisheries • Oil and gas exploration • Offshore renewables • Tourism and recreation • Conservation (cost savings or value added of data)
Indirect use	• book and newspaper readers • TV and film audiences	Functions of marine ecosystems as part of sustained life on earth
Option value	same examples as use value — but in future	Better protection of marine environment for future use by the individual
Altruistic value	Use of historic data (since a significant portion of analysis today depends on historic data the same would hold for future analysis). The information also has a value in and of itself as part of civilisation and human progress.	Better protection of marine environment for others to use
Bequest value		Better protection of environment for future generations to enjoy
Existence value		Better protection of marine habitats and species for the sake of their existence

3. Benefit assessment methodology

The benefit assessment methodology here suggests ways in which the economic benefits can be quantified in monetary terms. In doing this, the link between better data and better decisions is explored. Concrete evidence on this link is often lacking. The methodology recommended takes account of these uncertainties by relying on the judgment of experts

and data users. There are a number of questions that need to be answered in the process of assessing the benefits (and costs) of sustained marine measurements. These are:

1. What are the types of marine measurements of concern?
2. What are the objectives or purposes of using marine measurements?
3. Who uses or benefits from these measurements?
4. What are the benefits users derive from marine measurements and can these benefits be quantified?
5. How much does it cost to collect the marine measurements of concern?
6. Are the benefits of use worth the cost of collection?

To answer the first five questions, the recommended methodology follows the benefit assessment framework illustrated in Figure 1. It shows that we first need to identify what type of raw data we are dealing with. In order to identify the economic benefits we also need to establish what type of uses (products, services or applications) are made of the data for what purpose and by whom (benefits and beneficiaries). The most crucial point at this stage is to establish a link between data and the economic and other activities that use the data. To what extent these activities benefit from data is the main question to answer. NOAA and ONR (2000) makes the simplifying assumption of a 1% improvement in revenue or a 1% cost saving due to availability of marine measurements. While this assumption is useful and the only workable one in absence of any other evidence, in our study we have tried to get at more case-specific estimates of this assumption through consultations with direct and indirect users. Non-use values are even harder to estimate and our study did not explicitly attempt to do this. There are three levels of benefit assessment:

1. making a qualitative case for sustained marine measurements
2. making a quantitative case for sustained marine measurements (e.g. expert derived scores, types of activities that use the data, etc.)
3. quantifying the benefits of sustained marine measurements in monetary terms.

If the first (qualitative) level is sufficient to make a case for a particular marine measurement project, there may not be a need to proceed with the subsequent levels of assessment. Note that the methodology recommended here is in addition to any scientific, environmental or social arguments that can be made for sustaining marine measurements.

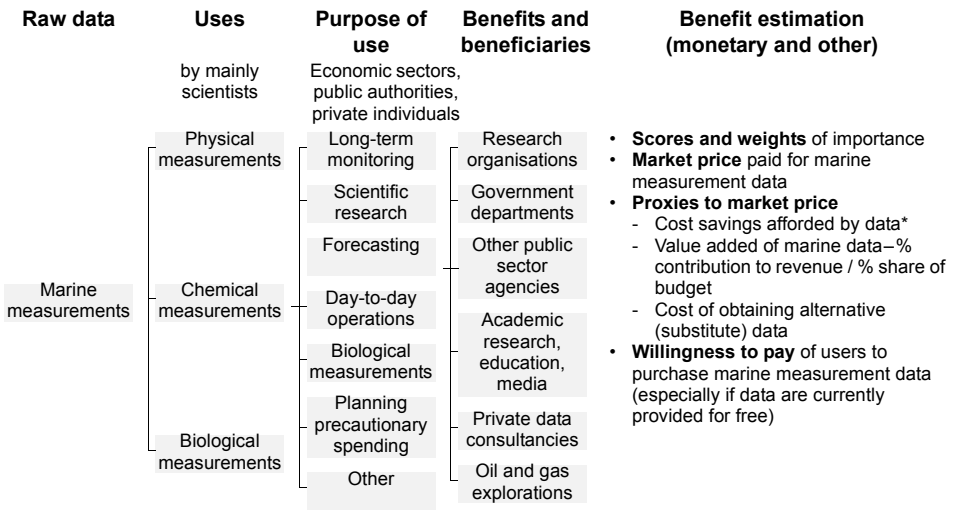

Figure 1 Benefit assessment framework.

When necessary, the second level of analysis involves an expert or user opinion based scoring system. The scores are allocated to identify the importance of the data as an input to wider scientific research, long-term monitoring, forecasting, day-to-day operations, planning precautionary spending and others. This approach was tested in our study by way of a stakeholder / user consultation exercise but can also be undertaken on the basis of expert judgment of a select group of users or published information.

The third level involves quantifying the benefits of sustained marine measurements in monetary terms. This is the most novel of the three approaches with limited previous application in the UK and elsewhere. However, if the approach can be implemented, it generates the only expression of benefits, which can be directly compared to the cost of collecting marine measurements. Therefore, the approach lends itself to cost benefit analysis.

Three measures can be used to express the benefits of sustained marine measurements in monetary terms:

1. Market price paid for marine measurement data
2. Proxies to market price
   - Cost savings (especially for day-to-day operations that use such data)
   - Value added by marine measurement data (% share of revenue)
   - Cost of obtaining alternative (substitute) data
3. Willingness to pay of users to purchase data (especially if data are currently free)

The above measures are different ways of looking at the benefits of marine measurement data. Therefore, they are complementary, with the exception of market price and willingness to pay. The case studies in the study report show that some work better for some types of users than others.

The first measure is the market price paid for marine measurements data. The market price paid for any good or service reflects the benefits derived by the buyers as mentioned in Section 1; it is a minimum measure of the benefits buyers receive. The limitation of this measure is that most marine measurements are publicly-funded and provided to users for free or at subsidised prices.

In the absence of a market or market price data, we could use proxies to market price. Since the information on market proxies (and, more importantly, quantitative evidence of the relationship between better marine data and better decision making) is not readily available, it is necessary to collect information through user consultation or expert judgment.

One proxy to market prices is cost savings afforded by data to capital investments and day-to-day operations. For example, better marine measurement data could improve ship routing leading to a reduction in journey times (cost savings). The economic value of this time saving (saved ship operating costs) would be an indication of the benefit of this particular use of marine measurements. The cost savings could also be experienced by improving the timing of precautionary spending for, say, coastal defence (either saved construction costs if spending is postponed or avoided damage if spending is brought forward). Another proxy to market prices is the value added afforded by marine measurements to economic activities. This approach views marine measurements as an input into the production of goods and services. A simple relationship can be assumed to exist between the use of marine measurements and the annual revenue or turnover of the process they are an input to.

Finally, cost of alternative data is another market proxy. This approach asks the question 'How would the absence of such data and applications impact the users? Would an alternative source of the same data (or alternative data that serves the same purpose) be used and if so what would this be and how much would it cost to obtain?' This is akin to identifying 'substitutes' and costing these. Sometimes there may not be a substitute for a particular marine measurement for a particular use.

The third measure is an alternative to the market price or its proxies. It involves eliciting individuals' preferences (their WTP or WTA) for marine measurements. Obtaining this measure means asking current or potential users of marine measurements what they would be willing to pay for these measurements (if they were not provided for free). The case studies show that this measure, though widely used in economics, does not work well for organisations where those who use the data and those who make the funding decisions are different individuals.

To summarise, if a market price exists for marine measurement data, the starting point for benefit assessment should be the market price. If market prices do not exist, cost savings afforded by better marine information should be used. If the necessary links between marine information and decision making which leads to cost savings cannot be made, the alternative of the 'value added' approach can be used. The value added approach requires the user to assess the importance of marine data as an input to their economic activities. Cost savings are likely to be subsumed within this value added.

We implemented the methodology outlined here to estimate the benefits to the UK from the launch of the Jason-2 altimetry satellite. Jason-2 is a joint project between NASA,

NOAA, CNES and EUMETSAT. It will allow the continuation of the altimetry measurements currently collected by Jason-1 and will also lead to improved coverage, if the new measurement technology proves to be successful. Without Jason-2, it is likely that global altimetry measurements will cease beyond 2007.

We covered benefits to research organisations, government departments, other public sector agencies like sea rescue, private consultancies who analyse the data for their own products, and the oil and gas exploration industry through email and telephone questionnaires which were applied to 36 current and potential users of satellite altimetry data, 23 of which responded. The results showed that users gave a score of 3.8 for the importance of satellite altimetry data[3]; the market price paid was around £500 000 per year by those respondents who had to pay for the data; cost savings afforded by the data was about £800 000 per year and those who could establish the link between data and their revenue suggested benefiting from the data to the tune of £3 million per year. Substitute data cost measures could not be used as users believed there was no substitute for satellite altimetry data for their purposes. A very few users were able to state a WTP over and above the cost of data, which was on average around £100 000 per year.

This case study (the more comprehensive of the two implemented) was not comprehensive by any means. However, it was sufficient for the purposes of the appraisal. Even the lowest estimates from this partial analysis revealed that the UK benefits of altimetry information to be produced by Jason-2 were in excess of the costs of the UK's sponsorship and this information was included in the business case for this sponsorship. In fact, the lowest (UK) benefit estimates at around £610 000 per year are about just under twice as much as the (UK) cost estimates of around £332 000 per year.

4. Conclusions

The scope for quantifying benefits and hence the effort expended to estimate costs and benefits are relevant concerns for all goods and services provided publicly. Specific questions to be considered include 'How much effort should be expended?', 'Which costs and benefits should be included?' and 'How sensitive will the results be to the scope of analysis and level of effort expended?'. The answers to these questions depend on the purpose of the benefit assessment.

If the objective is to demonstrate the benefit of marine measurements, a level of analysis that captures only some of the uses / users would be sufficient. If, however, the objective is to implement a full cost benefit analysis, then strictly all costs and all economic benefits to all users of information should be included as much as possible.

The findings of the Jason-2 case study[4] showed that even partial benefit assessments could help with making a better case for spending on marine measurements and is in line with the suggestion by the NOAA and ONR Panel (NOAA and ONR, 2000) that it is not necessary to know all the benefits or "the value of the economic benefits to the last dollar

3 Where a score of 0 meant "marine measurements had no effect on the success of the user's activities" and 5 meant "the user's activity would not exist without the marine measurements".

4 Jason-2 case study available at www.oceannet.org

before making a decision". Even without precise information, much can be said about the likely magnitude of the economic benefits of marine measurements.

Acknowledgements

The authors wish to thank the Steering Group of the study this paper is based on including Trevor Guymer and John Portmann of the Southampton Oceanographic Centre, University of Southampton and Jon Turton (UK Met Office) and the peer reviewer Professor Kerry Turner (University of East Anglia) as well as Mr. Allan Provins (eftec) who also contributed to the main study.

References

H M Treasury (2003). The Green Book: appraisal and evaluation in central government, Treasury Guidance, HM Treasury, London.

IACMST (2004). The Economics of Sustained Marine Measurements, report prepared by eftec (Economics for the Environment Consultancy), London (available from GOOSAG web site: www.oceannet.org, or hard copies available from saea@soc.soton.ac.uk).

NOAA and ONR (2000). The Economics of Sustained Ocean Observations: benefits and rationale for public funding, a joint publication of National Oceanic and Atmospheric Administration and the Office of Naval Research.

Needs for operational marine services: drift and waves

P. Daniel*, J.-M. Lefèvre, Ph. Dandin, S. Varlamov, K. Belleguic, H. Chatenet and F. Giroux

Météo-France, Toulouse, France

Abstract

There is currently an increasing demand for integrated marine meteorological and oceanographic data and services. Operational oceanography products can help improve the behaviour and quality of existing marine meteorological systems: marine pollution drift forecasts, search and rescue operations and sea states forecasts.

The use of products delivered from operational oceanography systems to oil spill and object drift applications is investigated. The evaluation is conducted with the French operational drift forecast system MOTHY and three operational oceanography systems, MERCATOR (Mercator-Océan, France), FOAM (Met Office, UK) and MFS (INGV, Italy).

The present work focuses on evaluating the effects of introducing large scale currents in the MOTHY system. This effect is investigated in the Bay of Biscay, the Caribbean Sea and in the Western part of the Mediterranean Sea. Preliminary results are very encouraging. Operational oceanography products do significantly improve the response capability in two different cases.

1. Introduction

Several European operational oceanography and data assimilation systems have been implemented over the last few years. All these systems use different operational capacities, data streams and expertise. Remote sensing and *in situ* data are acquired and assimilated in state-of-the-art ocean general circulation models to analyse and forecast the 3D state of the North Atlantic, adjacent European Shelf Seas, and the Mediterranean Sea. They aim to support a wide range of scientific and operational services and applications including oil spill monitoring, marine safety as well as the offshore oil industry.

The National Forecasting Centre, at Météo-France, runs an operational service to support the authorities in both oil spill response and search and rescue operations. French operational capacity in oil spill drift forecast is based on Météo-France and Cedre expertise. The core of the service is a trajectory model MOTHY. The system includes local area hydrodynamic coastal ocean models with tidal and real time atmospheric forcing from global meteorological models. Pollutants can be oil or floating objects. MOTHY has been extensively used during the Erika (December 1999) and Prestige (November 2002) crisis in the Bay of Biscay.

The system is also operated for search and rescue operations on demand from the Centres Régionaux Opérationnels de Surveillance et de Sauvetage (CROSS). The motion

* Corresponding author, email: pierre.daniel@meteo.fr

of a drifting object on the sea surface is the net result of a number of forces acting upon its surface (mainly water currents and atmospheric wind). There was a considerable increase in the requests these last years. The key issue in such a service is the rapidity of the response and the ability to use the drift system in any region of the world ocean.

The present work focuses on evaluating the effects of introducing large scale currents in the MOTHY system. This effect is investigated in the Bay of Biscay, the Caribbean Sea and in the Western part of the Mediterranean Sea with operational oceanography systems such as MERCATOR (Mercator-Océan, France), FOAM (Met Office, UK) and MFS (INGV, Italy).

2. Key features of the MOTHY model

The MOTHY model developed by Météo-France is used on an operational basis to predict the drift of pollutants on the ocean surface. It is based on a hierarchy of nested limited domain ocean models coupled to a pollutant dispersion model. The model is driven by tidal forcing specified at the open boundaries and by wind and pressure fields provided by atmosphere models. These atmosphere models can be the IFS model (European Centre for Medium-Range Weather Forecasts) or the ARPEGE model (Météo-France) (Courtier *et al.*, 1991). The system was designed specifically for drift forecasting. Currents are computed using a shallow water model coupled to an analytical turbulent viscosity model with a bilinear eddy viscosity profile (Poon and Madsen, 1991), so as to represent vertical current shear. This approach is particularly well-suited to areas where large-scale currents are negligible (such as in the English Channel or on the continental shelf in the Bay of Biscay). In seas affected by large-scale currents, the results must be reviewed by a forecaster. This is always the case in the Mediterranean Sea, for example, and sometimes necessary for the Spanish coastline in the Bay of Biscay, depending on the place, time, season and year.

The oil slick is modelled as a distribution of independent droplets that move in response to currents, turbulence and buoyancy. Turbulent diffusion is modelled with a three-dimensional random walk technique. The buoyancy force depends on the density and size of the oil droplets so that larger (more buoyant) droplets tend to remain in the surface layer whereas the smaller droplets are mixed downwards (Elliot, 1986). In general, about 65 to 70% of the droplets remain on the sea surface. If a droplet is moved on to land, then that droplet is considered beached and takes no further part in the simulation. A weathering module is also included (Comerma *et al.*, 2002).

The model was calibrated on a few well-documented pollution incidents such as Torrey Canyon, Amoco Cadiz and Tanio (Daniel, 1996). Operated since 1994 in the marine forecast section at Météo-France, it has been used extensively for the Erika (Daniel *et al.*, 2001, 2002) and the Prestige incidents (Daniel *et al.*, 2004). A meteorologist on duty is able to run the model on request. An average of ten interventions each month are conducted in real time.

3. Key features of MERCATOR, FOAM and MFS models

The MERCATOR formulation is based on the primitive equations for the temporal evolution of ocean speed, temperature and salinity in its three horizontal and vertical

dimensions. The version used here is the PSY2 prototype (Bahurel *et al.*, 2001). It marks the start of high resolution MERCATOR forecasting for European seas assimilating altimeter and *in situ* data, and then on the basis of this data, generates analyses and forecasts of the three-dimensional state of the ocean in these regions. The model resolution is 1/15 degree with 43 levels unevenly spaced in the vertical and is based on the OPA code (Madec *et al.*, 1998). The model is forced with atmospheric forecast field variables from ECMWF operational products.

FOAM is an ocean and sea-ice model and assimilation system that produces real-time daily analyses and forecasts of temperature, salinity, currents and sea-ice in the deep ocean, for up to five days ahead. A global version of FOAM on a latitude-longitude grid with 1° spacing and 20 levels has produced 5-day forecasts daily in the Met Office operational suite since 1997. A nested model covering the Atlantic and Arctic with a grid spacing of 35 km and 20 levels was introduced into the operational suite in January 2001. Five-day forecasts have been made daily by a nested model covering the North Atlantic with a 12 km grid since April 2002 (Bell *et al.*, 2000).

The Mediterranean Forecasting System (MFS) currently produces ten-day ocean forecasts for the whole Mediterranean Sea once a week (Pinardi *et al.*, 2003). The start day of the forecast is Tuesday at 12:00 each week. The relevant data sets — Sea Level Anomalies (SLA) from altimeters, Sea Surface Temperature (SST) from satellite radiometers, temperature profiles from Ship of Opportunity XBTs — are currently assimilated every week into the model with an intermittent Optimal Interpolation scheme. The model resolution is 1/8 degree with 31 levels unevenly spaced in the vertical and is based upon the Modular Ocean Model code (Pacanowski *et al.*, 1990). The model is forced with atmospheric forecast field variables from ECMWF operational products. Recently, the MOM code has been replaced by the OPA code (Madec *et al.*, 1998).

4. Bay of Biscay: Prestige incident

4.1 Prestige incident

On Wednesday, 13 November 2002, the single-hulled oil tanker Prestige, flying the Bahamas flag, sent a distress call offshore of the region of Cape Finisterre (Galicia, Spain). The tanker was carrying 77000 tons of heavy fuel oil loaded in St. Petersburg (Russia) and Ventspils (Latvia), and was heading to Singapore via Gibraltar. The vessel developed a reported 30 degrees starboard list during passage in heavy seas and strong wind. As the engine was damaged, the ship became out of control and drifted according to the weather conditions. An aerial observation revealed a fuel leak at sea. The ship sank on 19 November after being towed in various directions.

The first slicks reached the coasts of Galicia in the morning of 16 November between La Coruña and Cape Finisterre. Two other oil stranding flows followed in late November and in early December. During December, the northern coast of Spain was touched from Asturias to the Spanish Basque Country. The first slicks impacted the Gijon area (Asturias) on 4 December. Afterwards, stranding of thick, viscous balls, pancakes and various sized patches regularly hit the northern coast of Spain. At the beginning of January, the coast of Galicia was faced with a fourth massive pollutant flow whereas in

Asturias, Cantabria and Euskadi (the Spanish Basque country) these phenomena remained relatively moderate. The French coast was hit near St. Jean de Luz on 31 December. The stranding, at various densities hit Brittany in May and the coast of the Channel in September. In France roughly 2500 km has been affected, the last stranding occurring in October, 11 months after the wreckage.

4.2 Combining MOTHY with MERCATOR

In the Prestige area, MOTHY includes only the wind current. The French MERCATOR system (Mercator-Océan, France) is used here to provide long range currents to the MOTHY system.

For the Prestige shipwreck, we used daily current data from Mercator's high-resolution model. Coupling Mercator surface currents directly to the MOTHY module simulating the oil slick does not represent surface drift properly for two reasons. One is that the current in the model's upper level (3 metres) is much weaker than surface drift. A joint study by Ifremer and Météo-France (Jouan *et al.*, 2001) after the Erika oil spill showed that to use the current in the last level of a 3D model, it is necessary to refine the vertical grid size in the first few metres directly below the surface. The second reason is an operational one. The coupled model must be able to take into consideration rapid changes in the wind and keep constantly up to date. The chosen approach aims to extract from Mercator the information that MOTHY needs and feed it into the current system. It is necessary to take the low-frequency information that MOTHY does not resolve (the large-scale current) and the high-frequency information that Mercator does not reproduce properly (rapid changes in the wind) into account without any overlap.

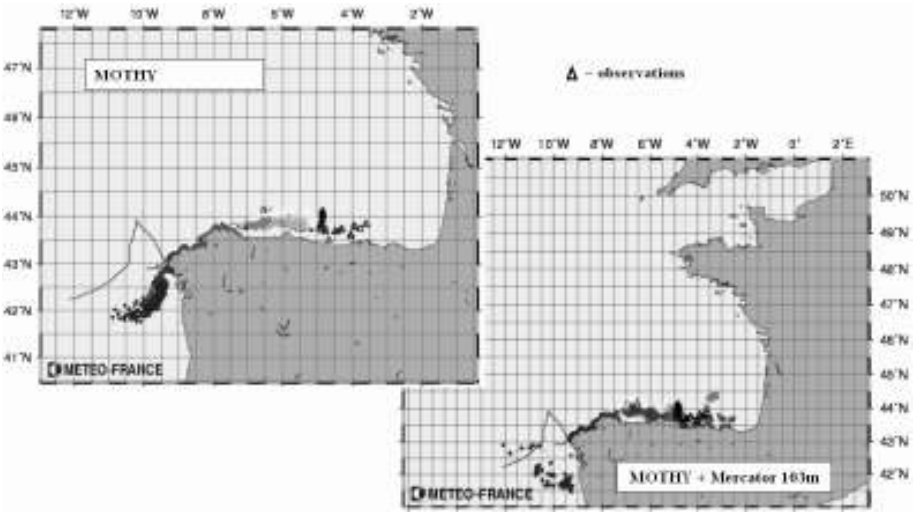

Figure 1 13 December 2002 at 12 UTC. Comparison between a model and *in situ* observation based on a constant leakage along the tanker's trajectory. The MOTHY simulation shows a drift which lags behind the observations. Adding a 103 m Mercator current distinctly improves its performance.

It was decided to use the Mercator current below the layer directly affected by the wind. The 103-metre current appears the most suitable for representing the missing information while remaining unaffected by surface effects. The drift current is thus the sum of the current computed by MOTHY and Mercator's 103-metre current. This first attempt at integrating Mercator currents in MOTHY was carried out during the Prestige disaster and will be enhanced in the future. It is nonetheless a solution that makes the most of national operational means and was used as such by French authorities.

The impact of adding the Mercator high-resolution model's 103 metre current to represent the large-scale current missing from MOTHY is unclear during the first few days of the spill (Daniel *et al.*, 2005) but becomes useful in the Bay of Biscay for longer simulations (Figure 1). Mercator's contribution is visible for long-term simulations in waters where large-scale circulation is negligible. This result is a major progress for oil spill planning since it allows the authorities to be provided with a more accurate view of the possible consequences for the coastline.

5. Caribbean Sea: Polmar trial

An antipollution Polmar exercise was organised on December 8, 2003, in the North-West of Martinique. Fire protection foam was spilled into the sea by the Maïto tug boat of the French Navy. Two drifting buoys provided by Cedre were dropped and the MOTHY model was activated. The two buoys drifted towards the west as far as the south of Jamaica before entering into the Gulf of Mexico (Figure 2), running approximately 2000 miles in three months. A major pollution offshore Martinique could thus be propagated into the entire Caribbean zone at a mean velocity of 1.5 knots.

The potential contribution of operational oceanography products was checked (Chatenet and Giroux, 2004). Adding either the MERCATOR or the FOAM currents to the MOTHY system improves the calculation of the drift, but significant differences exist between MERCATOR and FOAM in this area, in particular on the location of the eddies downwind of the Caribbean islands.

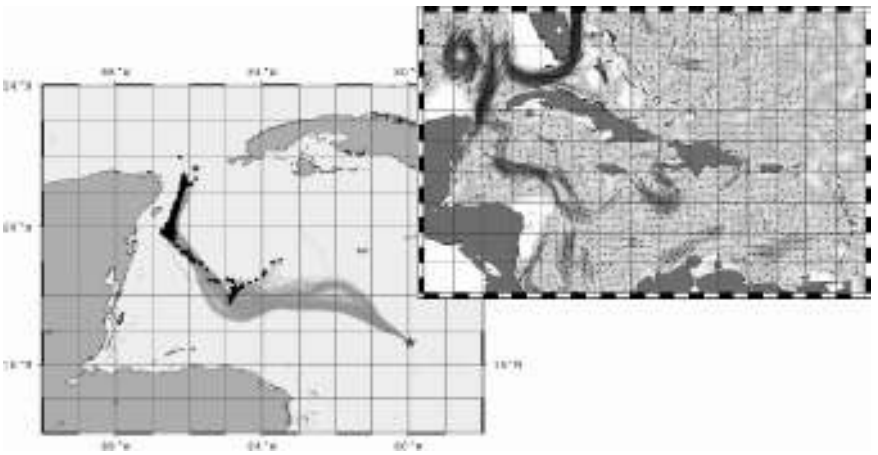

Figure 2 Oil slick drift simulation (trajectory in gray and black droplets) compared with the trajectory of a buoy. Mercator current at 100 m depth.

6. Western Mediterranean Sea

A preliminary study (Lyria incident, 1993) in the Mediterranean Sea based on monthly means from the MERCATOR prototype gave promising results (Daniel *et al.*, 2003). The MOTHY system was interfaced with MFS daily snapshots. The simulations (Daniel *et al.*, 2005) showed that the space-time variability of the currents is difficult to model and has a large impact on the drift.

On 14 December, 2004, a drifting buoy was released during the training exercise LIONMED'04. The buoy is supposed to drift at the same speed as an oil spill. The MOTHY system was interfaced with three operational oceanography systems (MERCATOR, FOAM and MFS) and compared with real measured data (Belleguic, 2005). Again, the three operational models show large differences in the area of interest. None of the combinations is able to reproduce the drift of the buoy (Figure 3).

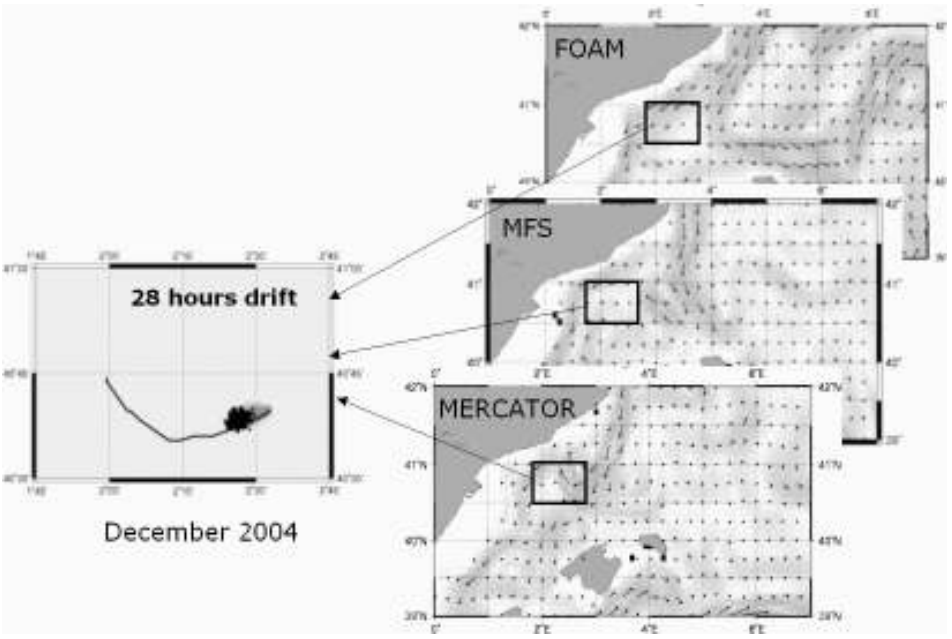

Figure 3 Left: oil slick drift simulation (trajectory in gray and black droplets) compared with the trajectory of the buoy (in black). Right: FOAM, MFS and MERCATOR current at 100 m depth.

7. Waves

Operational oceanography systems may improve wave forecasting through wave/current interaction.

The model system will be interfaced to the real time global and regional MERSEA forecast products, and used to demonstrate the benefit of using forecast products for wave forecasting. In a specific application to the European Seas, areas of discrepancy between observed and predicted waves, as provided by satellite altimeters and sea-state models respectively will be identified. Results will be correlated with surface currents from MERSEA estimates. In a further step, the evaluation of the impact of currents on

the sea-state will be performed for a few cases and will be based on sea-state model hindcasts.

8. Conclusion

The reported results are very encouraging. They validate the efforts undertaken by organisations investing in the construction of oceanography systems. This work will be continued as part of the French contribution to Europe's operational oceanography project, MERSEA (Marine EnviRonment and Security for the European Area). It will very likely be crucial to defining specific fields and processing, computing information during the simulation of ocean models, and assessing different filters and combinations prior to supplying these products on an operational basis.

Acknowledgments

This work was supported by Météo-France with the help of a large number of individuals. We would particularly like to thank P. Bahurel and Eric Greiner (Mercator-Océan, France), M. Bell and M. Holt (Met Office, UK), N. Pinardi and C. Fratianni (INGV, Italy), and M. Espino and E. Comerma (LIM-UPC, Spain).

References

Bahurel, P., P. De Mey, T. De Prada, E. Dombrowsky, P. Josse, C. Le Provost, P.-Y. Le Traon, A. Piacentini and L. Siefridt (2001). MERCATOR, forecasting global ocean, AVISO Altimetry Newsletter, No. 8, October 2001, CNES, Toulouse, France, p. 14–16.

Bell, M.J., R.M. Forbes and A. Hines (2000). Assessment of the FOAM global data assimilation system for real-time operational ocean forecasting. J. Mar. Sys, 25, 1–22.

Belleguic, K. (2005). Modélisation de dérive d'objets en mer, Rapport de stage de fin d'études no. 990, ENM, 92 pp.

Chatenet, H. and F. Giroux (2004). Prise en compte des courants issus de l'océanographie opérationnelle dans le modèle MOTHY, Rapport de stage de fin d'étude no. 976a et 976b, ENM, 64 pp. et 31 pp.

Comerma, E., M. Espino, P. Daniel, A. Doré and F. Cabioch (2002). An update of an oil spill model and its application in the bay of Biscay: the weathering process, Oil and Hydrocarbon Spills III, Modelling, Analysis and Control, WIT Press, pp. 13–22.

Courtier, P., C. Freydier, J.F. Geleyn, F. Rabier and M. Rochas (1991). The ARPEGE Project at Météo-France, ECMWF workshop, European Center for Medium-Range Weather Forecast, Reading, England.

Daniel, P. (1996). Operational forecasting of oil spill drift at Météo-France, Spill Science & Technology Bulletin. Vol. 3, No. 1/2, pp. 53–64.

Daniel, P., P. Josse, P. Dandin, V. Gouriou, M. Marchand and C. Tiercelin (2001). Forecasting the Erika oil spills, Proceedings of the 2001 International Oil Spill Conference, American Petroleum Institute, Washington, D.C, pp 649–655.

Daniel, P., P. Dandin, P. Josse, C. Skandrani, R. Benshila, C. Tiercelin and F. Cabioch (2002). Towards better forecasting of oil slick movement at sea based on information from the Erika, 3nd R&D forum on high-density oil spill response, IMO, 10 pp.

Daniel, P., F. Marty, P. Josse, C. Skandrani and R. Benshila (2003). Improvement of drift calculation in MOTHY operational oil spill prediction system, Proceedings of the 2003 International Oil Spill Conference, American Petroleum Institute, Washington, D.C.

Daniel, P., P. Josse, P. Dandin, J.-M. Lefevre, G. Lery, F. Cabioch and V. Gouriou (2004). Forecasting the Prestige Oil Spills, Proceedings of the Interspill 2004 conference, Trondheim, Norway.

Daniel, P. and Ph. Dandin (2005). Benefits and use of operational oceanography systems for drift forecasts, Proceedings of the 2005 International Oil Spill Conference, American Petroleum Institute, Washington, D.C.

Daniel, P., P. Josse and Ph. Dandin (2005). Further improvement of drift forecast at sea based on operational oceanography systems, Coastal Engineering VII, Modelling, Measurements, Engineering and Management of Seas and Coastal Regions, WIT Press, pp 13–22.

Elliott, A.J. (1986). Shear diffusion and the spread of oil in the surface layers of the north sea. Deutsche Hydrographische Zeitschrift 39(3), 113–137.

Jouan, M., P. Lazure, P. Daniel and P. Josse (2001). Evaluation du potentiel de MARS3D pour la prévision de dérive d'hydrocarbures. Comparaison avec MOTHY dans le cas de l'Erika., Rapport Liteau, Ifremer, Météo-France, 32 pp.

Madec, G., P. Delecluse, M. Imbard and C. Lévy (1998). OPA 8.1 Ocean General Circulation Model reference manual. Note du Pôle de modélisation, Institut Pierre-Simon Laplace, no. 11, pp 91.

Pacanowski, R.C., K. Dixon, and A. Rosati (1990). Readme file for GFDL-MOM 1.0, Geophys. Fluid Dyn. Lab., Princeton, N. J.

Pinardi N., I. Allen, E. Demirov, P. De Mey, G. Korres, A. Lascaratos, P.-Y. Le Traon, C. Maillard, G. Manzella and C. Tziavos (2003). The Mediterranean ocean Forecasting System: first phase of implementation (1998–2001). Annales Geophysicae, 21: 3–20.

Poon, Y.K. and O.S. Madsen (1991). A two layers wind-driven coastal circulation model. J. Geophys. Res.,vol 96, C2, 2535–2548.

Sonar range estimation using MREA-04 operational ocean modelling

Frans-Peter A. Lam*

TNO Defence, Security and Safety, Underwater Technology Dept., The Netherlands

Abstract

Naval operations in coastal waters are a huge challenge for modelling support in several disciplines. For example, any decision dependent on sonar performance could be dependant on a proper translation of input from a reliable oceanographic model, that itself relies on reliable input from a meteorological model. Obviously many things can go wrong, and it is not surprising that there are not many examples for the complete information chain; from scratch or climatology to final operational interpretation and decision.

During the MREA-04 exercise near Lisbon, in an attempt to complete the abovementioned chain, sonar range forecasts were provided based on the oceanographic fields provided by the Harvard Ocean Prediction System (HOPS). These fields are four-dimensional (xyz-t), or, in terms of operational sonar modelling: at any time, in any direction, providing range-dependent sound velocity profiles. This was used to model performance of a low frequency active sonar (LFAS) system, common in Anti-Submarine Warfare (ASW). At three hypothetical ship positions, the (simplified) sonar performance was provided in near real-time. This procedure can easily be extended to the track of any ship.

Keywords: operational oceanography, sonar performance, acoustic propagation, ocean modelling

1. Introduction: range dependent sonar performance modelling

Figure 1 Personnel of the Snellius expedition (1929–1930) in Indonesian waters (right), and portraits of Willebrord van Roijen Snell (Snellius, 1580–1626; left) and J.L.H. Luymes, head of the Hydrographic Service of the Royal Netherlands Navy from 1914 to 1934.

* Corresponding author, email: frans-peter.lam@tno.nl

1.1 Historical prelude

In the past, the Royal Netherlands Navy (RNLN) has played an important role in Dutch meteorological and oceanographic research (e.g. Van Bennekom and Otto, 2003). It was LCDR M.H. Jansen who made the link to M.F. Maury ("father of physical oceanography") in the USA. Jansen was the Dutch delegate at the Brussels Maritime conference in 1852 (organised by Maury), and he helped professor Buys-Ballot in founding the Royal Netherlands Meteorological Institute in January 1854 (Van Everdingen, 1953; Otto, 2003; Van Lunteren, 2003). Later, the RNLN provided the "research" vessel (HMS Siboga) for the first Dutch oceanographic expedition in 1899–1900 in Indonesian waters. The focus of the research was on (descriptive) biology, supervised by Prof. M.W.C. Weber. The commanding officer was LCDR G.F. Tydeman.

In 1929 and 1930, the Snellius expedition took place, also in Indonesian waters. Geology and physical oceanography were now receiving more attention, with P.M. Van Riel as scientific leader and LCDR F. Pinke as commanding officer of the HMS Willebrord Snellius. This famous expedition would not have been organised without the support of J.L.H. Luymes. Recently, in 2003 and 2004, the RNLN has commissioned two new hydrographic survey vessels, with the names HNLMS Snellius (A802) and HNLMS Luymes (A803).

1.2 Oceanography and sonar

The importance of oceanographic modelling for sonar support is best illustrated by so-called range-dependent scenarios, here focusing on applications for ASW. In oceanographic terms, long range sonar performance is mainly affected by eddies, fronts, internal tides/waves and high-frequency fluctuations. Apart from the effects in the water column, the sea-bed also has a significant effect on sound propagation and scattering, but this effect is excluded in the present study. Here we present an example from literature to demonstrate the range-dependent effects.

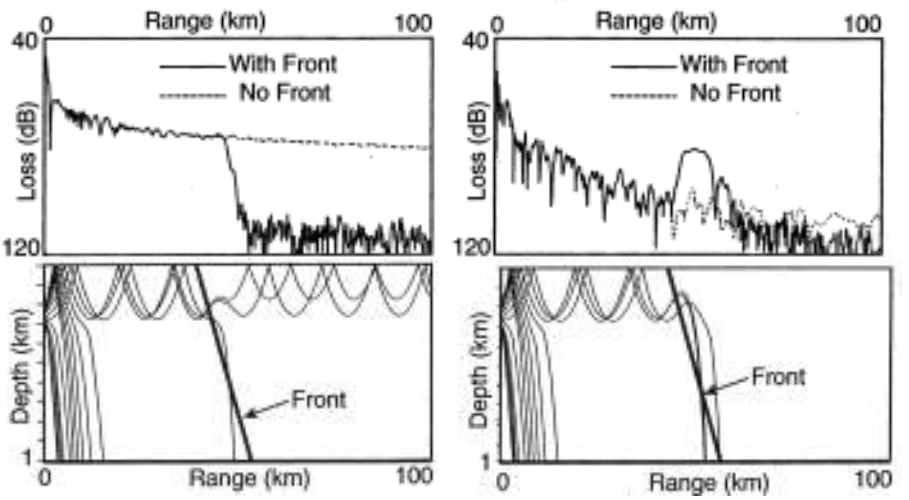

Figure 2 Sound propagation through a front. Top: propagation loss for a receiver depth at 100 m (left) and at 300 m (right). Bottom: sound ray diagram for source at 40 km (left) and at 42.5 km from front. Pictures taken from Robins and Harrison (1994).

1.3 Sound propagation through a front

Propagation through a front is addressed in Robins and Harrison (1994), see Figure 2. In this figure, examples are given for two receiver depths, and for two source positions (frequency is 100 Hz). The pictures show that the presence of a front is not just a slight modification of the sound propagation. Instead, the propagation can change dramatically, and is dependant on parameters such as sonar depth or position.

Similar examples for the impact of the presence of high frequency internal waves on sound propagation can be given (Lam, 2005; Elliot and Jackson, 1998; Munk, 1981). Note that internal (tidal) waves were already measured during the earlier mentioned Snellius expedition (Lek, 1938; Defant, 1960, p.545).

2. Sonar products for MREA-04

The NL contribution for MREA-04 is best characterised by what it is NOT aiming for:

- It is not extending any existing oceanographic modelling
- It is not extending any existing acoustic modelling

It is rather combining two existing components: the HOPS regional model provided by Harvard University (HOPS-MREA04 website), and the active sonar module (REACT) of the sonar performance model ALMOST (ALMOST website). The HOPS model/ system is forced by meteorological forecasts, in this case the NOGAPS model, and actual (CTD) measurements were assimilated. The output for sonar performance is presented (summarised) in simple graphs for maximum sonar range. In this procedure the following data chain was thus completed:

Meteo model → ocean model → sonar model → operational product.

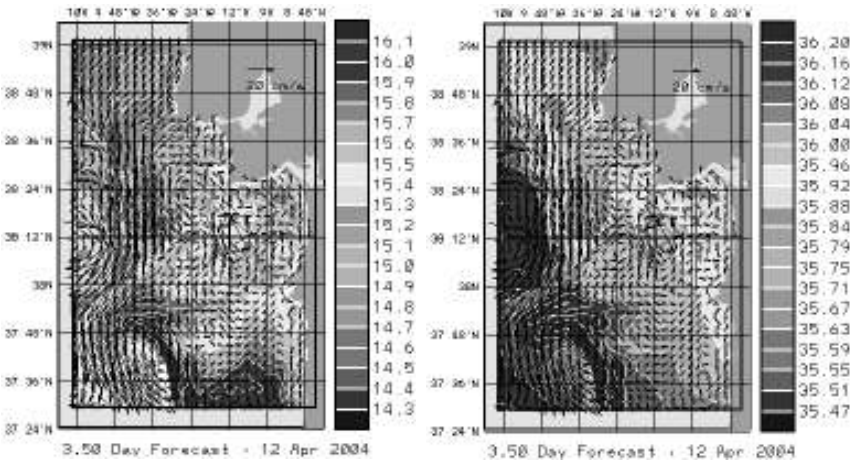

Figure 3 An example of output fields (including current vectors) of the regional HOPS model for temperature (left) and salinity (right) at the sea surface near the coast of SW Iberia.

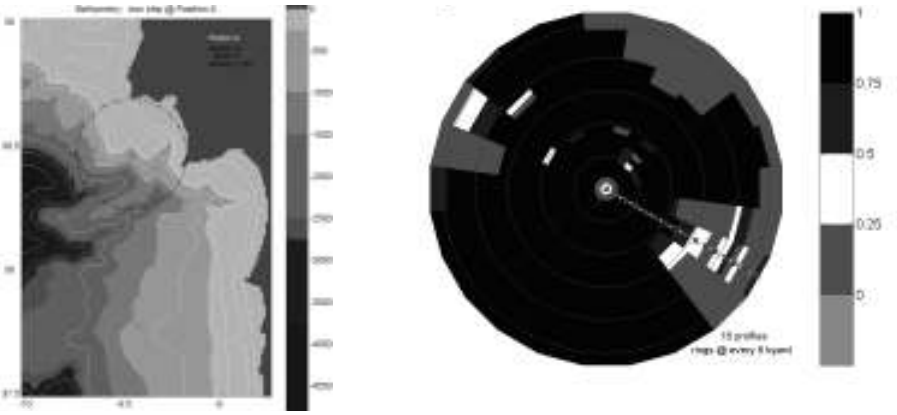

Figure 4 Left: ship position A used for sonar performance prediction. Ship's heading is 120°. Positions B and C (headings 170 and 190 respectively), further south along the coast are not shown here. Right: Simplified graph used to present sonar performance for 24 directions (bearings) for the first 25 km. Probability of detection for a possible target is roughly indicated by three grey-scales. The dark grey is used for cases where no calculation could be performed. In the direction of the heading of the ship (here 120°), the sampling of bottom depth (plus symbols) and sound speed (crosses) is given. In this example 32 bottom segments and 16 sound speed profiles are used for the sonar performance calculation.

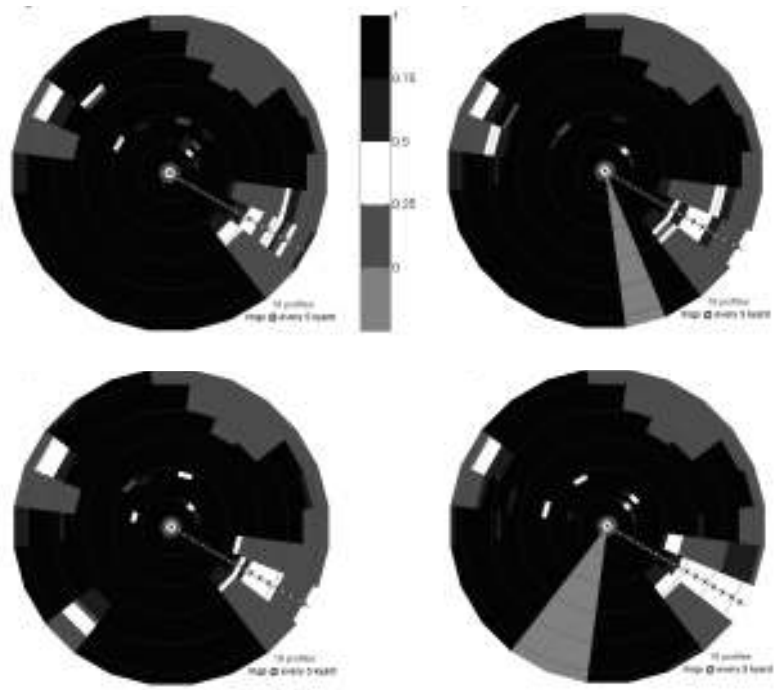

Figure 5 Sonar performance for position A, based on forecasts of 10 April 2004 after 00, 12, 24 and 84 hours.

Based on daily forecasts (Figure 3) of 3D-fields of temperature and salinity, the three dimensional sound speed is calculated at all (forecasted) times. In this "predicted" environment, sonar performance is calculated for the hypothetical positions of three ships: A, B and C. These positions (see Figure 4, left, for position A) more or less simulate a survey along the Portuguese coast south of Lisbon, and crossing the Setubal canyon. Quite arbitrarily, three different sediment types (coarse sand, muddy sand and mud, respectively) are used in the calculations for these three locations.

Sonar performance for each position is summarised with a simple graph, see Figure 4 (right), for an example. These graphs are actually displaying probability of detection for a target given. Detailed sonar parameters and target assumptions can be found in Lam (2005b). More examples for different forecasts are given for positions A and C in Figure 5 and Figure 6, respectively. An (arbitrary) comparison between range dependent and single profile (at x=0; i.e. range independent) sonar performance calculations is given in Figure 7 for position B. All examples are for forecasts of the last day modelled for MREA-04: 10 April 2004.

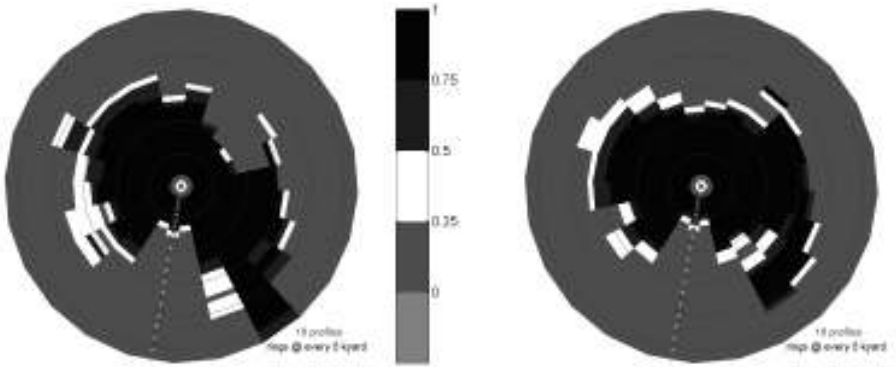

Figure 6 Sonar performance for position C, based on forecasts of 10 April 2004 after 00 and 84 hours. The overall performance at this position is worse, because a muddy seafloor is assumed here (coarse sand at position A).

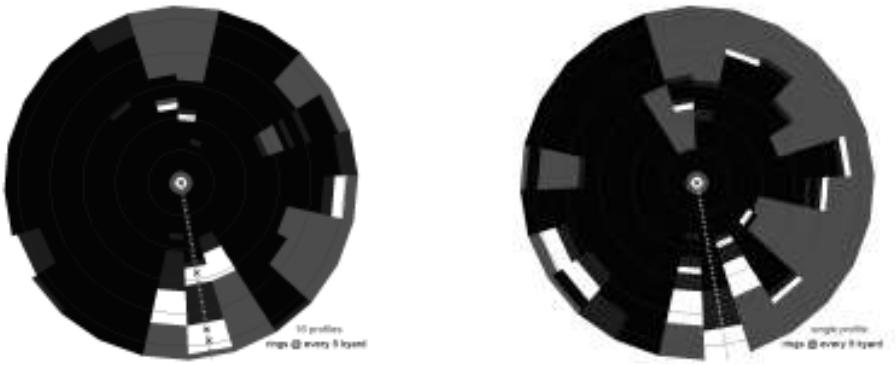

Figure 7 Sonar performance for position B, based on forecast of 10 April 2004 after 48 hours. Here range dependent sonar modelling (left) is compared with sonar modelling based on a single sound speed profile (range independent, right). Note that this single (forecasted) profile is probably still much better than the profile taken from any historical database.

3. Conclusions

Sonar range calculations are performed in near real time, as an extension to available ocean modelling. After the receipt of the ocean fields (HOPS regional forecasts), sonar ranges were available for the GEOS-server within an hour. These sonar ranges were delivered daily on board NRV Alliance from 6 to 10 April 2004.

The sonar ranges provided were quite arbitrary examples, and could be modified for any other ship's position, heading and sonar/target specifications. Also, specific sound propagation conditions, like interactions with fronts and eddies, are not explored. As stated in the previous section, no effort has been made to validate the range dependent modelling, which is far from trivial. No realistic bottom sediment database was incorporated in the modelling.

In the examples shown, variability is relatively small, but significant. This is also the result of the automated (and quite arbitrary) procedure followed. Probably more extreme differences in the sonar range forecasts can be found. Differences for sonar ranges as calculated by a single profile from an historical database, although this has not been tried, are expected to be large. Finally, by incorporating realistic sea floor input more variability in the sonar ranges is expected.

Acknowledgements

The HOPS regional model output data was provided by the HOPS-Harvard team of Prof. A.R. Robinson. During the work on board support was provided by Emanuel Coelho, Michel Rixen and Andrea Cavanna (webmaster). We thank the Captain and crew of NRV Alliance for the pleasant atmosphere on board during MREA-04. Acoustic modelling support was provided by the following TNO colleagues: Pieter Schippers, Frank Benders, Michael Ainslie, Wilco Boek and Hans Groen. This work is carried out within the OcMod project, as part of the Acoustic Environment Programme of Prof. Dr. Dick Simons. The work is funded by the Royal Netherlands Navy, and was (is) supervised by LCDR Frans Jansen (LCDR René Dekeling). An extended version of this paper can be found in Lam (2005b).

Websites

HOPS-MREA04: http://people.deas.harvard.edu/~leslie/BP04
ALMOST: http://www.tno.nl (search for "ALMOST" and "sonar")

References

Defant, A. (1960). Physical oceanography. Vol.II, Pergamon.

Elliot, A.J. and J.F.E. Jackson (1998). Internal waves and acoustic variability. OCEANS'98 conference proceedings, 10–14.

Lam, F.P.A. (2005). Analysing the (internal) tides with MREA-04 NCOM data. MREA workshop proceedings.

Lam, F.P.A. (2005b.) Sonar range estimation using MREA-04 operational modelling. UDT Europe, Amsterdam 21–23 June 2005, Conference Proceedings.

Lam, F.P.A. *et al.* (2005). Analysing the internal tides with an operational oceanographic model. MREA special issue J.Marine Systems (in preparation).

Lek, L. (1938). Die ergebnisse der strom- und serienmessungen. The Snellius-expedition in the eastern part of the Netherlands East Indies 1929–1930. Vol.II, part 3, Brill, Leiden. 169pp.

Munk, W. (1981). Internal waves and small-scale processes. In: B.A. Warren and C. Wunsch (Eds), Evolution of physical oceanography. 264–291.

Otto, L. (2003). Marin Henri Jansen, his activities in connection with the Brussels maritime conference and his ideas with respect to marine research. VII International Congress on the History of Oceanography, Kaliningrad, September 8–12, 2003; http://vitiaz.ru/congress/en/index.html.

Robins and Harrison (1994). ECUA conference proceedings, 487–493.

Van Bennekom and L. Otto (2003). Oceanography in the Netherlands and the Dutch navy. VII International Congress on the History of Oceanography, Kaliningrad, September 8–12, 2003; http://vitiaz.ru/congress/en/index.html.

Van Lunteren, F.H. (2003). Buys Ballot en het KNMI. (in Dutch) Ned.Tijdschrift voor Natuurkunde 69(5), 152–155.

Van Everdingen, E. (1953). C.H.D. Buys Ballot, 1817–1890. (in Dutch), Daamen, The Hague.

Aviso Altimetry Products: take your pick!

Vinca Rosmorduc*

CLS, France

Abstract

Since the launch of Topex/Poseidon, more than 12 years ago, satellite altimetry has evolved in parallel with the user community and oceanography. As a result of this evolution, we now have:

- A bigger choice of products, more and more easy-to-use, spanning complete GDRs to pre-computed sea level anomalies and gridded datasets
- a mature approach, combining altimetric data from various satellites and merging data acquired using different observation techniques, including altimetry, to give us a global view of the ocean
- data available in real or near-real time for operational use.

Aviso have been distributing Topex/Poseidon and ERS altimetric data worldwide since 1992, and Jason-1 and Envisat since 2002. Integration of all those missions is one of the keys to global modelling of the ocean for assimilation in GODAE.

An overview of available products, describing their applications and features, is presented.

Keywords: Data distribution, satellite altimetry, high-level products

1. Introduction

Aviso stands for Archiving, Validation and Interpretation of Satellite Oceanographic data. It has been set up in 1992 to process, archive and distribute data from the NASA/ CNES ocean radar altimetry satellite Topex/Poseidon (T/P). Now, twelve years later, Aviso user service activities encompass:

- Operational distribution of Topex/Poseidon, Jason-1 and Envisat GDRs
- Distribution of high-level altimetry products, including operational distribution of Ssalto/Duacs multimission near-real time products
- A catalogue of altimetry, orbit determination and precise location products
- Outreach of ocean altimetry, orbit determination and precise location activities.

The Aviso user service is open 52 weeks a year, on working days. Mails are centralised, with a unique email address (aviso@cls.fr), and answered within five working days. Expert advice is requested whenever useful, with the whole panel of expertise available to us, from instruments to oceanography, geodesy, including Calval and processing expertise.

* Corresponding author, email: vinca.rosmorduc@cls.fr

All information, whether on data or outreach are updated on the Aviso website www.aviso.oceanobs.com, in both French and English (a Spanish section is also available, for basic information).

2. Data users and uses

Aviso users have evolved over the years: the first users were PIs/Co-Is of the T/P mission, i.e. mostly altimetry experts or at least physical oceanographers with a working knowledge of altimetry; new users now are mostly neophytes (Rosmorduc and Picot, 2004). There has also been a change from programmers, i.e. people able to write themselves a program in Fortran or C, to largely software users. Another change is that even physical oceanographers are no longer specialised in a specific observation technique. They now use every available observation system and also model outputs to observe and study a class of phenomena. Thus they do not wish to delve too deeply into characteristics of each technique, and expect to benefit from a "standardised" dataset format, highly processed data, and clear, to-the-point, information. Moreover, users are no longer only physical oceanographers: we are reaching a much wider audience, including biologists, chemical oceanographers, climatologists, meteorologists, end-users, students and even school children! The origin of users is also diversified, with more and more developing countries joining the altimetry users. With the broader audience came the need for more and more "basic" information, easy-to-use data and tools, since the new laboratories getting involved do not always have the background in altimetry data processing that previous users had.

One element to take into account in defining and distributing data is "what for?": no dataset can be used for all purposes. If Waveforms or even GDRs contain, by definition, all the possibilities of the other, higher-level datasets, they may not be practical to users. Some uses imply non-standard processing (ice, land applications, hydrology to a certain extent): thus we need to decide whether to send the Waveforms for those applications, or to deliver specific data for those uses. All in all, one of the main activities of the user service is to advise potential users on the product most adapted for their needs, computer skills and altimetry literacy.

3. Datasets

When Aviso first released its data in 1993, those were "only" Geophysical data records, from Topex and Poseidon-1, distributed on CD-ROMs. Now things are both much more complicated, and much easier. More complicated, since there are today several different datasets, available either in delayed and/or in near-real time, and on different media, for different satellites (see Figure 1). And much easier, because data, their format and the tools to use them are simpler now.

Two main types of datasets are available:

- "monomission" data, mainly from the Ssalto "basic" ground processing segment, CMA (Centre Multi-mission altimétrique). This includes:
  - Wind/Wave data and Operational Sensor Data Records (OSDR, along-track data)
  - (Interim) Geophysical Data Records ((I)GDR, along-track data)

- Waveforms: Sensor Geophysical Data Records (SGDR, along-track data)
- Maps of Wind/Wave data (NRT-MWind and NRT-MSWH, gridded data)
- Monomission sea level anomalies (DT-SLA, along-track data)
- Monomission corrected sea surface heights (DT-CorSSH, along-track data), including corrections

• "Ssalto/Duacs" multi-mission altimeter data, which involves post-processing, homogenisation, etc. This includes:

- Maps of Sea Level Anomalies (DT- and NRT-MSLA, gridded data)
- Maps of Absolute Dynamic Topography (NRT-MADT, gridded data)
- Sea Level Anomalies (DT- and NRT-SLA, along-track data)
- Absolute Dynamic Topography (NRT-ADT, along-track data)

where DT (delayed time) means that data used to compute the product were processed using precise orbit and NRT (near-real time) means that data use Diode onboard navigator orbit (for OSDR), or preliminary orbit (produced in 2 or 3 days).

From the CD-ROMs of 1993, data distribution media have evolved. With internet, and high bandwidth, on-line dissemination is possible even for large files. Moreover, interactive techniques have been developed, so that now only minimum computer skills are needed to plot a map from altimetry data.

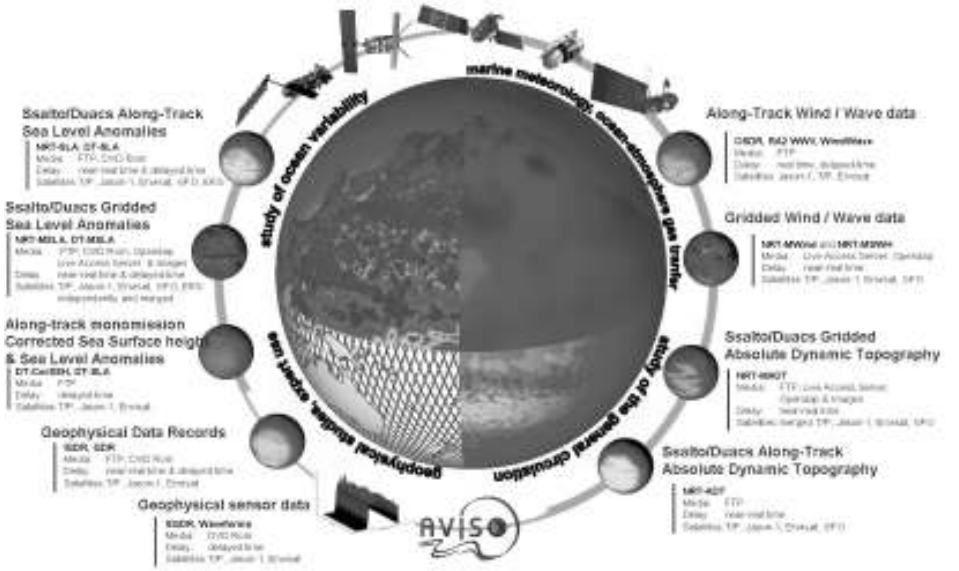

Figure 1 A whole constellation of data products from ocean altimetry satellites, including multi-mission products, available along-track and gridded, in delayed and near-real time, for different uses (oceanography, geophysics, meteorology, operational, etc.), for different users (from experts to newcomers), and on different media (DVD, FTP, web interactive interfaces, etc.)

- CD/DVD-ROM: Aviso delayed-time data are now mostly distributed on DVD-ROM (DVD-R) rather than CD-ROM. Jason-1 + T/P GDR are thus sent on DVD every 2 months (6 cycles of both missions) to registered users
- FTP: anonymous FTP, except for Near-Real Time Ssalto/Duacs data of less than 30 days (those need the signature of a license agreement to be accessed)
- Live Access Server: interactive on-line visualisation tool, allows the plotting of gridded data over the whole earth or on selected regions, as a map, Hovmoller diagram or along-time evolution curve. Some statistical functions are also available (temporal and geographical averages, variance)
- Opendap enables access to remote data sets through familiar data analysis and visualisation packages (e.g. Matlab, IDL, Ferret, ncBrowse, Live Access Server), just as if they reside locally on the user's machine. Opendap handles transport, translation and subsetting of data
- Images are maps plotted with some of the data.

4. Perspectives

Over more than twelve years, Aviso has gained real experience in the field. During the same time, applications — both scientific and practical — have diversified, some expected, some completely unexpected. One of the challenges is to continue serving the broadest community possible, by implementing new tools (especially interactive ones), developing dedicated datasets, and keeping in mind standardisation and easiness of use.

However, even the most easy-to-use, interactively accessible and self-explanatory data shouldn't be distributed if there is nobody to answer the users' questions. So, having people connected with data processing to answer users must continue.

At the very time when altimetry has found its place among the ocean data, and multi-mission altimetry demonstrated its importance, the future is still insecure, due to questions of system sustainability (with a high risk of a gap in mission over the next few years) and consistency with the past.

References

Aviso web site: http://www.aviso.oceanobs.com.

Aviso Live Access Server: http://las.aviso.oceanobs.com.

Rosmorduc, V. and N. Picot (2004). Twelve years of user services for ocean topography users: Aviso experience and lessons learned, Ensuring the Long-Term Preservation and Adding Value to the Scientific and Technical Data (PV) 2004, ESA/ESRIN, Frascati, Italy.

Ocean-observing systems meta-data management: EDIOS results in the Central and Western Mediterranean region

Alessandra Giorgetti* and Renzo Mosetti

Istituto Nazionale di Oceanografia e di Geofisica Sperimentale–OGS, Trieste, Italy

Abstract

The Web-based European DIrectory of Ocean-observing Systems contains comprehensive and validated information of all ocean monitoring sites operating in Europe in a routine and repeated way. A classification system as well as a global and updated survey of spatial, temporal and parameter distribution of all platforms or devices continuously operating in the Central and Western Mediterranean region are possible for the first time. The analysis of EDIOS information can provide crucial elements for the development and the improvement of harmonised, unduplicated and cost effective Global Ocean-Observing Systems on different scales according to the different strategic plans.

Keywords: Database, operational oceanography, monitoring systems, *in situ*, routine

1. Introduction

The European DIrectory of Ocean-observing Systems (EU-EDIOS) has been developed as an initiative of EuroGOOS, to provide information on systematic and long-term routine ocean-observing, measuring and monitoring systems operating in Europe (Verduin and Fischer, 2003). Detailed metadata on 366 fixed observing points (meteorological and meteo-oceanographic platforms, tide gauge and wave-rider buoys) and 1008 hydrological stations (STD/CTD, XBT and bottle casts) related to different areas of the Central and Western Mediterranean region (and the Spanish coast on the Atlantic slope) can be found within EDIOS, as shown in Figure 1. The wide range of information includes a technical specification on data collection methods, on the measured parameters, on their spatio/temporal characteristics, on the responsible organisation, with links to the data-holding centres, and were acquired thanks to the contribution of 29 institutes from Italy, Spain, Malta, Slovenia, Croatia, Albania and Yugoslavia, listed in Table 1.

2. The ocean-observing systems classification

The ocean-observing systems have been classified within EDIOS into three broad categories indicating the ease and freedom of access, degree of automatic data delivery and support, and the commitments towards international programmes and applications. This information is of particular interest in the strategic plan design of different Global Ocean Observing System components (UNESCO, 2000; UNESCO 2001). Almost half of the ocean-observing systems listed in the Central and Western Mediterranean region (21 of 47) have been classified as generating operational data open to all users (fully available to both GOOS and the GRAs), grade class A, one fifth have been classified as

* Corresponding author, email: agiorgetti@ogs.trieste.it

generating data available at Regional level (in principle available to EuroGOOS and MedGOOS), grade class B, while the remaining (17 over 47) have been classified as local stations, generating data not accessible by external users, a waste of operational data to EuroGOOS, grade class C. Nevertheless, the 15 different indicators, used in EDIOS classification and listed in Table 2, can help to identify whether the ocean-observing systems could be upgraded to a more accessible status, and whether this could be of major value to operational oceanography in Europe.

Table 1 Institutes contributing to EDIOS in the Central and Western Mediterranean region.

Institute of Oceanography and Fisheries, Split, Croatia
Agenzia per la Protezione dell'Ambiente e per i servizi Tecnici (APAT), Roma, Italy
APAT, ARPAV–Osservatorio Regionale Acque, Padova, Italy
ARPA Emilia-Romagna–Struttura Oceanografica Daphne, Cesenatico, Forlì, Italy
CNR, Istituto di Scienze Marine, ISMAR/Biologia del Mare, Venezia, Italy
CNR, Istituto di Scienze Marine, ISMAR/Sezione di Trieste, Trieste, Italy
CNR, ISMAR/Sezione Studi Marini e Costieri, Sezione di Venezia, Italy
CNR, ISMAR/Istituto per l'Ambiente Marino Costiero, Sezione di Messina, Italy
CNR, Istituto Studi sui Sistemi Intelligenti per l'Automazione, Sezione di Genova, Italy
CNR, IAMC International Marine Center–Sezione di Oristano, Sardinia, Italy
Comune di Venezia–Centro Previsioni e Segnalazioni Maree, Venezia, Italy
CORILA, Consortium for Coordination of Research Activities concerning the Venice Lagoon System, Venezia, Italy
ENEA, Centro Ricerche Ambiente Marino, La Spezia, Italy
General Office for Air Force Meteorology, Roma, Italy
Istituto Nazionale di Oceanografia e di Geofisica Sperimentale–OGS, Trieste, Italy
National Center for Meteorology and Aeronautical Climatology, Pomezia, Roma, Italy
ARPA-FVG/OSMER, Osservatorio Meteorologico Regionale, Cervignano, Udine, Italy
Provincia di Sassari, Sassari, Italy
Venice Water Authority–Consorzio Venezia Nuova, Venezia, Italy
Department of Public Health, Civic Centre, Zabbar, Malta
Environment Protection Directorate, Environmental Officer, Floriana, Malta
IOI-Malta Operational Centre, University of Malta, Valletta, Malta
National Institute of Biology, Marine Biology Station, Piran, Slovenia
Ente Público Puertos del Estado–State Ports Authority, Madrid, Spain
ICM-CSIC, Institut de Ciències del Mar, Barcelona, Spain
Instituto Español de Oceanografía–Sede Central, Madrid, Spain
Instituto Geográfico Nacional, Ministerio de Fomento, Madrid, Spain
Universitat Politècnica Catalunya/Laboratori d'Enginyeria Marítima, Barcelona, Spain
Institute for Marine Biology, Kotor, Montenegro, Yugoslavia

Table 2 Classification of all EDIOS entries in the Central and Western region.

MIF Identifier	NODC	No restrictions	Real time data	Open archive	IOC data policy	3-year plus	Global programme	QA/QC	EuroGOOS, WMO, ICES, etc. data policy	GRA programme	Real time in GRA	Real time data contact	Regional programme	GRA data only	National programme	Notes	GRADE CLASS
Croatia Jurana	Y	N	Y	N	–		N	Y	N	N	N	Y	N	N	Y		C
Croatia Veli Rat	Y	N	Y	N	–		N	Y	N	N	N	Y	Y	N	Y	Started EACE	C
Croatia Ship	Y	N	Y	N	–		N	Y	N	N	N	Y	N	N	Y		C
Italy Adricosm	Y	Y	Y	Y	–		Y	Y	Y	Y	Y	Y	Y	N	N		A
Italy 5Terre	N	Y	Y	N	–	2004	N	Y	N	N	N	Y	N	N	Y		C
Italy CO2	Y	Y	N	N	–		Y	Y	WMO	N	N	N	N	N	N	CCL Scripps	B
Italy VOS	Y	Y	Y	Y	–		Y	Y	Y	Y	Y	Y	Y	N	N		A
Italy Evoline	Y	Y	Y	Y	–		N	Y	N	N	N	Y	N	N	Y		A
Italy Mambo	Y	Y	Y	Y	–		N	Y	N	N	N	Y	N	N	Y		A
Italy Odas1	N	N	N	N	–		N	Y	N	N	N	N	Y	N	N		C
Italy Arpa FvG	N	Y	Y	Y	–		N	Y	N	N	N	Y	N	N	Y	On request	A
Italy SIMN_RMN	Y	Y	Y	Y	–		Y	Y	Y	N	N	Y	N	N	Y	WMO	A
Italy SIMN_RON	Y	Y	Y	Y	–		Y	Y	Y	N	N	Y	N	N	Y	GTS—WMO	A
Italy IBMbuoy	N	Y	N	Y	–		N	Y	N	N	N	N	Y	Y	Y		B
Italy IBMmeteo	N	Y	Y	Y	–		N	Y	N	N	N	Y	N	N	N		A
Italy ITTtide	Y	Y	N	Y	–		N	Y	N	N	N	N	N	N	N	PSMSL	A
Italy Dolcevita	N	N	Y	N	–	2004	N	Y	N	N	N	Y	Y	N	N		C
Italy APAT	N	Y	N	Y	–		Y	Y	EEA	N	N	N	N	N	Y	Eionet EEA	A
Italy CNRbuoy	N	N	Y	N	–	N	Y	Y	Y	Y	N	N	Y	N	N	MedGOOS	C
Italy IMCbuoy	N	N	Y	N	–	2004	Y	Y	Y	Y	Y	N	Y	Y	N	MedGOOS	B
Italy IMCctd	N	N	N	N	–	2003	N	N	N	N	N	N	N	N	Y		C
Italy Corila	N	N	Y	N	–	2004	N	Y	N	N	N	Y	N	N	Y		C
Italy VeComune	Y	Y	Y	Y	–		N	Y	N	N	N	Y	N	N	Y		A
Italy VeIdrografico	N	Y	N	Y	–		N	?	N	N	N	N	N	N	Y		C
Italy VeMagistrato	N	?	N	N	–		N	?	N	N	N	N	N	N	Y		C
Italy MeteoAM	Y	Y	Y	N	–		N	Y	N	N	N	Y	N	N	Y	WMO	A
Italy ArpaVeneto	Y	Y	Y	N	–		N	Y	N	N	N	Y	N	N	Y	WMO	A
Italy ArpaEmRo	Y	Y	Y	N	–		N	Y	N	N	N	Y	N	N	Y	WMO	A
Italy Daphne	N	Y	N	N	–		N	Y	N	N	N	Y	N	N	Y		B
Italy Sassari	N	N	N	N	–	2008	N	Y	N	N	N	N	N	N	Y		C
Italy AcquaAlta	N	Y	N	Y	–		N	Y	N	N	N	N	N	N	N		C
Italy Messina	N	Y	Y	N	–		N	Y	N	N	N	Y	Y	N	Y		B
Malta 1	N	N	N	N	–		N	N	N	N	N	N	N	N	Y		C
Malta 2	N	N	N	N	–		N	N	N	N	N	N	N	N	Y		C
Slovenia MBS-NIB	Y	Y	Y	N	–		N	Y	N	N	N	Y	N	N	N		B
Spain PdEcoastal	Y	Y	Y	Y	–		N	Y	N	N	N	Y	N	N	Y		A
Spain PdEdeepr	Y	Y	Y	Y	–		N	Y	N	N	N	Y	N	N	Y		A
Spain PdEmeteo	Y	Y	Y	Y	–		N	Y	N	N	N	Y	N	N	Y		A
Spain PdEtide	Y	Y	Y	Y	–		N	Y	N	N	N	Y	N	N	Y		A
Spain PdEcurrent	Y	N	N	N	–		N	Y	N	N	N	N	N	N	Y		C
Spain CSIC	Y	Y	Y	Y	–		N	N	N	N	N	Y	N	N	N		A
Spain IEObuoy	Y	N	N	N	–		N	Y	N	N	N	N	N	N	Y		B
Spain IGNbuoy	Y	Y	N	N	–		Y	Y	GLOSS	N	N	N	N	N	Y	RIMA	B
Spain XIOM	Y	Y	Y	Y	–		N	Y	N	N	N	Y	N	N	Y		A
Spain IEOctd	Y	N	N	N	–		N	Y	N	N	N	N	Y	N	Y		B
Yugoslavia	N	N	N	N	–		N	N	N	N	N	N	N	N	Y		C

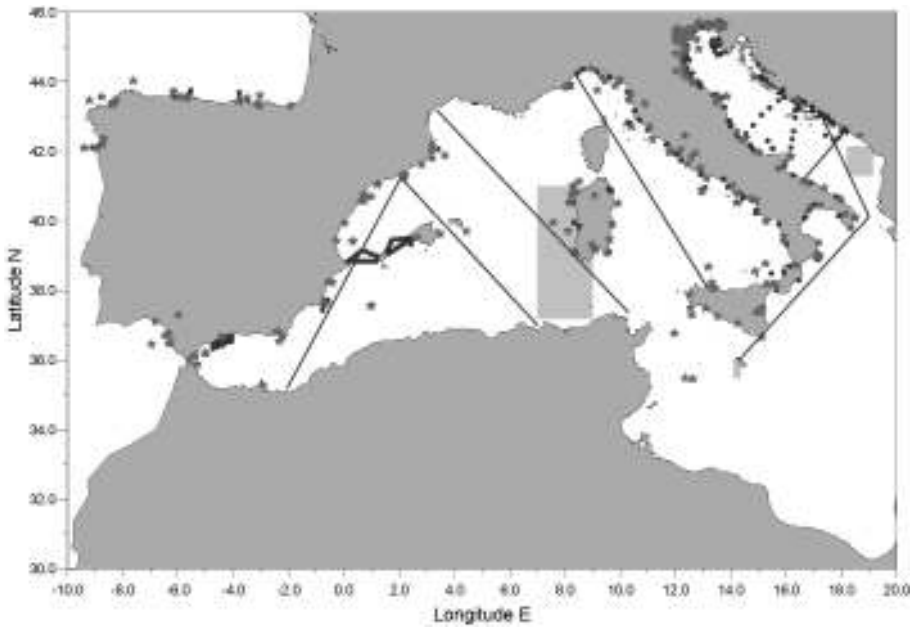

Figure 1 Spatial coverage of ocean-observing systems in the Central and Western Mediterranean.

3. The ocean-observing systems distribution

The global analysis of the spatial distribution of *in situ* ocean-observing systems in the Central and Western Mediterranean region, as shown in Figure 1, shows a homogeneous and continuous coverage in coastal environmental monitoring, gathered with physical and bio-geochemical surveys, sea-level, waves and meteorological buoy networks, maintained by national agencies (Agenzia per la Protezione dell'Ambiente e per i servizi Tecnici in Italy, Puerto del Estado in Spain, etc.). These coastal networks, aiming to observe, measure and forecast the main atmospheric and marine coastal processes for civil and marine environmental protection, generate operational data fully available to GOOS (following EDIOS classification). The spatial distribution of multiparametric buoys shows a wide dispersion in their geographical displacement (from open-sea to coastal areas) as well as in data availability (from Global, European to local scale following EDIOS classification).

The temporal distribution analysis, as indicated in Table 3, shows the longest time series of observations for sea-level, waves and meteorological parameters. Physical and bio-geo-chemical coastal survey parameters have been monitored on a continuous basis since the beginning of the 1980s and assimilated into operational oceanography competence. Ocean *in situ* monitoring with multiparametric automated buoys, widely used to evaluate the accuracy of numerical models simulations, against independent measurements, as well as of remote sensing information, shows the best temporal coverage (in terms of accuracy and frequency of observations).

Table 3 Temporal distribution of ocean-observing systems in the Central and Western Mediterranean

Parameters	Start	# sites	Min. Frequency	Average Frequency
METEO	1960/1984*	273	1 min	1 h
WAVE	1989/1982*	50	30 min	1 h
SLEV	1968/1943*	150	1 min	15 min
CURRENT	1990	135	5 min	10 min
TEMP, PSAL	1978/1969	41+965	10 min	15 d
BIO-GEO-CHEMICAL	1978/1987*	5+854	7 d	30 d

*Starting date of Italian and Spanish National Coastal Monitoring Networks, respectively

4. Conclusion

The European DIrectory of Ocean-observing Systems provides a global overview of all systematic and long-term *in situ* ocean-monitoring systems, which is and will be updated in the coming years within Sea-Search, SeaDataNet, EuroGOOS and IODE networks. Local basin-scale products, as presented in Iona *et al.* (2005) have been made available to the user community to ensure the most effective distribution of validated end updated information. The analysis of EDIOS information can provide crucial elements to reach a harmonised marine research, with reduced duplication of monitoring efforts, sharing and exchanging of observation and human resources at an international level.

Acknowledgements

This work was not possible without the efficient and collaborative contribution of the above mentioned institutes from Italy, Spain, Malta, Slovenia, Croatia, Albania and Yugoslavia as well as the financial support of the European Union Concerted Action Contract No. ENV1−CT−2001−20005.

References

Iona, A., A. Lykiardopoulos, I. Dokos, P. Gotsis, E. Balopoulos, C. Maillard and A. Giorgetti (2005). A database on ocean observing and monitoring systems of the Mediterranean and Black Sea. This volume, page 248.

UNESCO (2000). Strategic Design Plan for the Coastal Component of the Global Ocean Observing System (GOOS), GOOS Report no. 90, IOC/INF-1146, 160 pp.

UNESCO (2001). Strategic Design Plan for the IOC-WMO-UNEP-ICSU-FAO Living Marine Resources Panel of the Global Ocean Observing System (GOOS), GOOS Report no. 94, IOC/INF-1150, 88 pp.

Verduin, J. and J. Fischer (2003). EDIOS: European Directory of the Initial Ocean Observing System in H. Dahlin, N.C. Flemming, K. Nittis, and S.E. Petersson, Building the European Capacity in Operational Oceanography, Proceedings 3rd EuroGOOS Conference, Elsevier Oceanography Series 69, 265−271.

Black Sea operational database for ARENA project

I. Bolgov and E. Nesterov*

Hydrometeorological Research Centre of Russia

Abstract

This paper describes an operational database, as part of the operational section of the Black Sea database for the ARENA project. The database contains information in SHIP and BUOY code forms from Global Telecommunication System (GTS) over the Black Sea during period 2000–2004.

Keywords: Black Sea, database, code forms, SHIP, BUOY.

1. Introduction

An operational database, as part of the operational section of the Black Sea database for the ARENA project has been created at the Hydrometeorological Research Centre of Russia (HRCR). The database contains information in SHIP and BUOY code forms from GTS for the Black Sea during the period 2000–2004: sea surface temperature, air temperature, sea level pressure, wind speed, wind direction, dew point temperature, visibility, cloudiness, wave height and period, swell height and period. The database includes some additional parameters for ships and buoys.

2. Relational database organisation

The non-relational databases serve as basic sources of oceanographic data at HRCR. Creation and use of these databases has sufficient history and is basically focused on operational use. In addition, the data of observations stored in these databases are updated cyclically. Obviously, it is meaningful to keep the information, including oceanographic data, not only in archives, but also in relational databases.

A complex set of programs for inquiry, reception of the information from the database, checking procedures, selection of duplicated telegrams and loading into other databases has been created. For loading into the ORACLE database, there is a selection of duplications, carried out on a unique compound key. The loaded data are located in a non-normalised table, with each record containing one observation element. In non-normalised tables the data are stored for several days for removal of duplications. After that the data are stored in the normalised tables.

3. Black Sea database information

Black Sea data in SHIP and BUOY code forms are sparse. The period 2000–2004 includes data from approximately 500 ships and 50 buoys. The main source of buoy data is the international pilot drifter experiment in the Black Sea which was operated in 1999–2003. One of the basic goals of the experiment was the investigation of the possi-

* Corresponding author, email: nesterov@mecom.ru

bilities for creation of a long-life drifter network in the Black Sea for operational oceanography and hydrometeorology. A total of 49 meteorological drifters were deployed from October 2001 to April 2003 (Figure 1).

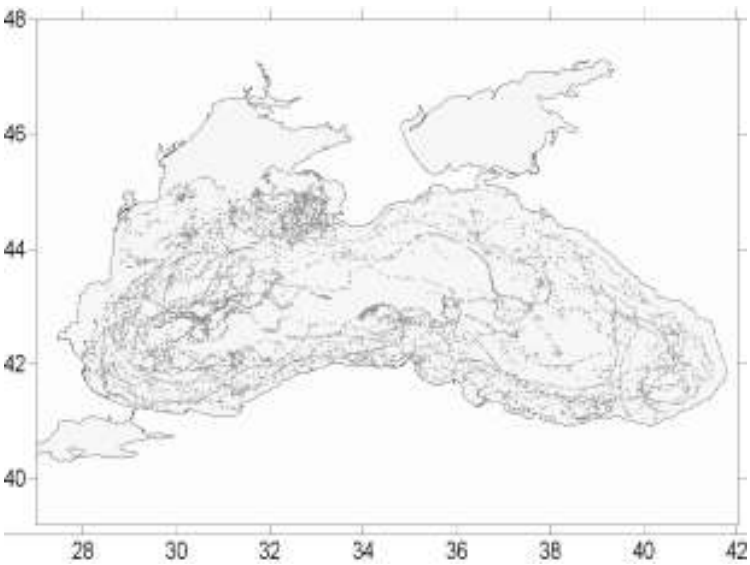

Figure 1 Trajectories of 45 drifting buoys from GTS October 2000–January 2004.

The lifetime of these 45 drifting buoys varies from 50 to 700 days.

The information in the Black Sea operational database may be used as input for initialisation of models and for assimilation in model simulation processes.

The MONCOZE Pilot Ocean Monitoring System (POMS); a tool for marine environmental monitoring

B. Hackett*[1], J. Albretsen[1], L.P. Røed[1], J.A. Johannessen[2] and E. Svendsen[3]

[1]*Norwegian Meteorological Institute (met.no)*
[2]*Nansen Environmental and Remote Sensing Center (NERSC), Norway*
[3]*Institute of Marine Research (IMR), Norway*

Keywords: ocean monitoring, models, ecosystem

1. Introduction

The national development project MONCOZE (Monitoring the Norwegian Coastal Zone Environment; www.nersc.no/MONCOZE/) aims to provide tools and knowledge for managing the marine coastal environment of southern Norway. It is a collaboration between oceanographic researchers at the Institute of Marine Research (IMR), met.no and the Nansen Environmental and Remote Sensing Center (NERSC). A fuller description of the project is given by Johannessen *et al.* (2005). One pillar of MONCOZE is the Pilot Ocean Monitoring System (POMS), which is the technical solution to making relevant information available to users.

POMS is a response to recent developments in ocean observing systems, primarily the availability of operational and pre-operational data products from diverse observations and numerical models. At the start of the project (2001), a range of observations — both from satellites and *in situ* — and numerical model results were already available for Norwegian coastal and shelf waters, some operational and some ready for operational implementation. However, the data were (and still are) produced and managed by different providers. The challenge for MONCOZE was to integrate the available information into a form readily available for users. In order to do so, two issues needed to be addressed at the outset:

1. defining the target users and their needs
2. ensuring access to the relevant information products.

User requirements have been a major theme in EuroGOOS since its inception, and a broad range of users and user needs have been identified (Fischer and Flemming, 1999). In MONCOZE, the focus is narrowed to coastal and shelf seas ecosystem management, where public fisheries and water quality authorities are the prime stakeholders. These users are scientifically knowledgeable and well-versed in interpreting diverse environmental information. MONCOZE has sought close involvement with users, primarily through consultation with fisheries management at IMR. Access to relevant information content has to a large degree been ensured, since the three partner institutions are providers of a majority of the required data. IMR is the main provider of *in situ* observations in Norwegian oceanic waters; NERSC and met.no are providers of satellite data; all three have strong modelling groups. In addition, met.no supplies an established infrastructure for handling and dissemination of data products.

* Corresponding author, email: Bruce.Hackett@met.no

On this basis, POMS is designed to meet the following general requirements:

- Encompass operational observations, operational model results, off-line products
- Bring together specified monitoring and forecast products in a consistent presentation framework
- Ensure timely updating of products
- Facilitate timely acquisition and dissemination of data products for partners, management, scientists and value-added users
- Tailor presentation framework for efficient routine analysis tasks
- Facilitate interactive analysis and commentary.

Notably lacking from this list is public outreach, which is of secondary importance for a management tool.

MONCOZE is a 5-year project with demonstration periods in 2004 and 2005. POMS is developed in two phases: a version 1 aimed to demonstrate proof of concept and serve the mid-term demonstration period; a version 2 based on the lessons learned in operating a POMS, possibly exploiting recent advances in technology and serving the final demonstration period. POMS is implemented at met.no and is operated within the operational ICT service.

2. POMS version 1

The scheme for version 1 (hereafter POMS1) is shown in Figure 1. Data providers are the MONCOZE partners and all information is disseminated to users via the POMS server. POMS1 consists of a product repository (ftp server) and a web presentation server. In order to get a service up and running in a fairly short time, POMS1 is kept fairly simple. Nearly all products delivered by the providers are in the form of graphics files. In order to meet the requirements for consistent presentation, "standards" were defined for plotting data, e.g. map boundaries, variable units, depths, etc. Thus, production of presentation graphics is located at the data providers and it is their task to follow the agreed standards; POMS1 is essentially a picture viewer.

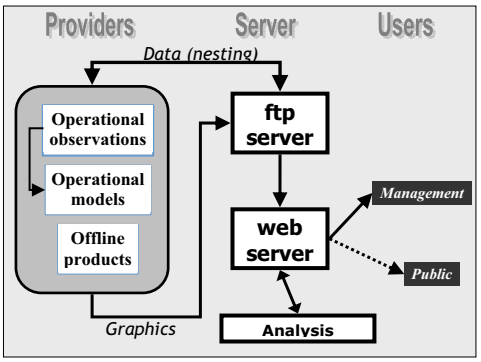

Figure 1 POMS1 architecture.

The main task for POMS1 is organising sets of graphics files and maintaining a corresponding web page menu system. The ftp server is checked continuously, and newly

arrived files are moved to a dedicated repository directory. Organisation of the files is determined by a file naming convention that ensures uniqueness of each file arriving on the ftp server. The contents of the repository are re-scanned hourly and all menus on the web server are updated accordingly. Any file arriving on the ftp server that follows the naming convention will then automatically appear on the web server. Over time, the number of files in the repository grows, disk capacity is filled and response time to the user suffers. Therefore, the repository is divided into three main sub-directories:

1. Recent data, containing only the most recently arriving operational products. The number of files is small enough for the response time for updating the menus to be kept short. In practice, the definition of "recent" varies by product type. For example, satellite images (5–10 per day) for the last three days are retained here. On the other hand, operational model products (which are relatively numerous) are only kept for the latest model run (daily or weekly, depending on the model). After the preset time age limit, selected files are moved to the Archive subdirectory.
2. Archive data, consisting of files up to a longer age limit, say, 30 days old. Response time for accessing these products is considerably slower, but still acceptable. Note that this response time is independent of bandwidth for the network. Files older than the age limit are deleted.
3. Background data, containing static products, e.g. depictions of climatology. So far, the number of data files has been small enough that response time is not an issue.

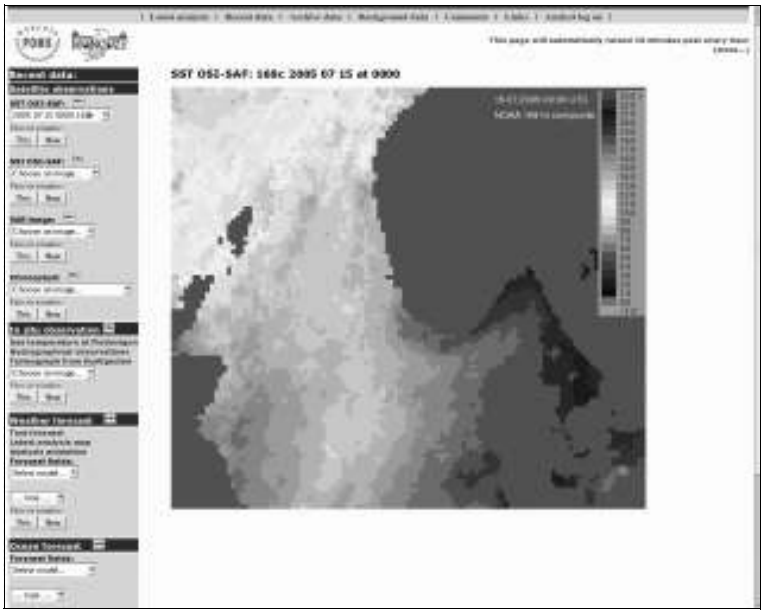

Figure 2 Screenshot of POMS1. At top is the main menu. In this view, "Recent data" has been selected, giving the product-selection menus shown at left (view is truncated at bottom). A product from the SST OSI-SAF menu has been selected for viewing in the main window (a satellite SST 7-day composite). Note: colour scheme has been converted to gray-tone for publication purposes; see moncoze.met.no for to view full colour rendition.

The layout of the web pages (see Figure 2) reflects the repository structure. The main menu line at the top contains pathway buttons to each of the data sub-directories, presenting their contents by means of pull-down menus in the left panel. Take the "Recent data" page (Figure 2) as an example. The left panel contains main sections for satellite observations, *in situ* observations and model forecasts. Under each section, buttons and pull-down menus show the available products. To facilitate comparison of products, the user may choose to display the specified product in the main window ("This") or in a pop-up window ("New"). Information on each product is available via buttons on each pull-down menu.

POMS1 also includes an analysis module (Figure 1) to publish an expert assessment of current conditions based on available information. It is found in the web pages via the "Latest analysis" button in the top menu. Note also the "Comments" and "Analyst logon" buttons, which are password-protected pages for comments by users and a designated analyst, respectively.

POMS is reached through moncoze.met.no, which shows a welcome page containing a selection of operational products showing the current situation in the MONCOZE area. Users may log on to access the full selection of available products.

3. Lessons learned

POMS1 came on-line in the spring of 2003 and has been continuously available since then. The initial selection of products was heavily biased towards operational ocean models, since these were readily accessible and easy to plot. Ocean (including ecosystem), wave and atmospheric model fields from met.no's operational suite, as well as pre-operational ocean models from NERSC and met.no, formed the backbone. Satellite SST fields from the EUMETSAT OSI-SAF provided by met.no were the main observations, later supplemented by SeaWIFS and MERIS ocean colour imagery provided by NERSC and by surface current fields from a coastal HF radar system on the west coast. More recently, daily surface solar irradiance fields derived from AVHRR (also from OSI-SAF) have been added, as well as sample SAR imagery from ENVISAT and RADARSAT1. Obtaining *in situ* observations in near-real time (NRT) has proven more difficult.

Users have pointed out both the usefulness of the information and the shortcomings of the service. Feedback has been received since the opening of POMS1, and was particularly requested during the first demonstration period in spring 2004. More recently (May 2005), POMS was heavily utilised during a dedicated research cruise in the Norwegian Coastal Current. The operational products were used to direct the observation programme underway. Among the lessons learned are:

- There are too few *in situ* observation products. The available observations are chiefly from satellite radiometers, which are degraded by cloud cover
- Attempts to get all providers to conform to uniform plotting formats (map projection, colour coding, etc.) were not entirely successful. The differences are often large enough to hinder comparison
- Users request more flexibility in selecting views into model data (depths, contour intervals, etc.)

- Users request the ability to zoom in and out on graphical presentations
- Storage capacity for graphics files is a limiting factor
- Response time to a ship using satellite communications is acceptable, as long as the link is maintained
- There are some unresolved issues about permission for displaying satellite products in an operational service
- Users request access to the underlying data
- Users request default values in the pull-down menus.

4. POMS version 2

POMS2 attempts to address the problems encountered by:

- More active pursuit of *in situ* data sets for inclusion. A major step forward is the NRT delivery of CTD data from research vessels run by IMR. This supplements other NRT observations already available at met.no, but not yet displayed in POMS1: tide gauge data for Norway, Denmark and UK; ARGO profile data, synoptic marine meteorological observations (from the meteorological GTS); discharge observations for Norwegian rivers (from The Norwegian Water Resources and Energy Directorate).
- Reorganising the POMS architecture. In the new architecture (Figure 3), all graphical production is moved to the web-server; providers supply data files to the ftp server from which they are pre-processed to facilitate graphical rendering using a single graphics engine. Storage of graphics files is replaced by storage of data files. The graphics engine used is DIANA, met.no's tool for DIgital ANAlysis (to be available under open source license from 2006). A benefit of this approach is that several of the interactive capabilities of DIANA may be exploited, e.g. a user may seed drifting objects in a current field at arbitrary locations.
- Introducing a new web presentation system. The web presentation system is a web map server (WMS), compliant with Open Geospatial Consortium standards (www.opengeospatial.org). WMS facilitates not only interactive presentation in a GIS-like web site, but also exchange of information layers with compliant third party servers. The latter facility allows dissemination of information without breaching constraints on data security. Adoption of this technology results in part from experience with the EU-funded project DISMAR (www.nersc.no/Projects/dismar/). The use of open standards is deemed important for operational robustness and to ensure exchange of information layers. The basic page and menu design is similar to POMS1.

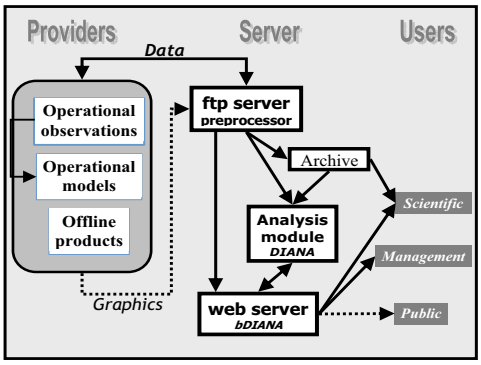

Figure 3 POMS2 architecture.

POMS2 will replace version 1 by the end of 2005. Issues concerning access to data sets and display of certain satellite data have not been fully addressed yet. MONCOZE is a development project. If and when POMS is moved to sustained operations, these issues will need to be resolved.

Acknowledgements

The MONCOZE project (2001–2005) is supported by the Research Council of Norway under contract 143559/431. Many thanks to Anette Lauen Borg (POMS1), Trond Michelsen and Arild Burud (POMS2) for carrying out the technical implementation. The comments and encouragement of colleagues and public users are gratefully acknowledged.

References

Fischer, J. and N.C. Flemming, (1999). Operational Oceanography: Data Requirements Survey, EuroGOOS Publication No. 12, Southampton Oceanography Centre, Southampton. ISBN 0–904175–36–7.

Johannessen, J.A., B. Hackett, E. Svendsen, H. Søiland, L.P. Røed, N. Winther, L. Pettersen, J. Albretsen and M. Skogen (2005). Monitoring the Norwegian Coastal Zone Environment — the MONCOZE approach. This volume, page 809.

Meta-data management structures for ocean observing systems in the Eastern Mediterranean and the Black Sea

A. Iona*, E. Papageorgiou, A. Lykiardopoulos, P. Karagevrekis and E. Balopoulos

Hellenic Centre for Marine Research, Anavyssos, Greece

Abstract

The meta-data management carried out by the Hellenic National Oceanographic Data Centre within the EC EDIOS Project for the Eastern Mediterranean and Black Sea is presented. The collected meta-data information for the observing systems that operate in routine and repeatedly in the region is described. An Internet accessible meta-database was developed and made available to the user community as a CD-ROM.

Keywords: Eastern Mediterranean, observing systems, meta-database

1. Introduction

A significant part of world economic activity and a wide range of services, amenities and social benefits depend on the wise use of the sea. These activities are subject to uncertainty, loss of efficiency, and direct costs and damage caused by various alterations of the marine environment. This is in particular true for the Mediterranean and the Black sea basins, where there is outstanding evidence that they are both undergoing naturally and anthropogenically induced changes on a multitude of time-scales. Therefore, information on ocean observing, measuring and monitoring systems operating in the above mentioned basins is of vital importance for a great variety of operational data users. Such information, for example, is useful for operational researchers, who need real time data to calibrate their models, as well as for supporting the global projects that study the environmental changes and the weather forecasting programmes. Likewise, the above information facilitates public authorities and policy makers to reach the right decisions and adopt resolutions for better management of the existing knowledge and for formulating the basis of predictions and strategies for the rational exploitation, effective management and protection of the marine environment and its resources.

2. Regional data centre assembling

2.1 Meta-data acquisition

In 2001 an initiative was undertaken by EuroGOOS for the development a European DIrectory of Ocean-observing Systems (EDIOS). The project gathered information on ocean observing, measuring and monitoring systems in the seas and oceans surrounding Europe. This information is considered a powerful tool and a prerequisite for the full implementation of EuroGOOS, by allowing for the first time an analysis of the continuously available data for operational models in Europe.

* Corresponding author, email: sissy@hnodc.ncmr.gr

The Hellenic National Oceanographic Data Centre, [which operates in the Hellenic Centre for Marine Research (HCMR/HNODC)], as a Regional Meta-data Sampling Centre of the EU/EDIOS Project, for the Eastern Mediterranean and the Black Sea, established contacts with 25 institutes from 9 countries in the region (Bulgaria, Cyprus, Georgia, Greece, Israel, Lebanon, Romania, Turkey and Ukraine). Detailed Meta-data Information Forms (MIFs) for 2103 points (hydrological, chemical, biological, meteorological data, multiparameter buoys, tide gauges), 12 areas (hydrological, satellite data) and 146 tracks (hydrological, biological data), were collected through a wide joint cooperation of the countries of the above regions. These provide information related to the geographical position of the observations, the type and sampling frequency of measurements, the instruments and devices used, as well as the research programmes and the responsible institutes along with their correspondent links. The geographical distribution of the "Ocean Observing Platforms" as well as the "Satellite data" is shown in Figure 1 and Figure 2 respectively.

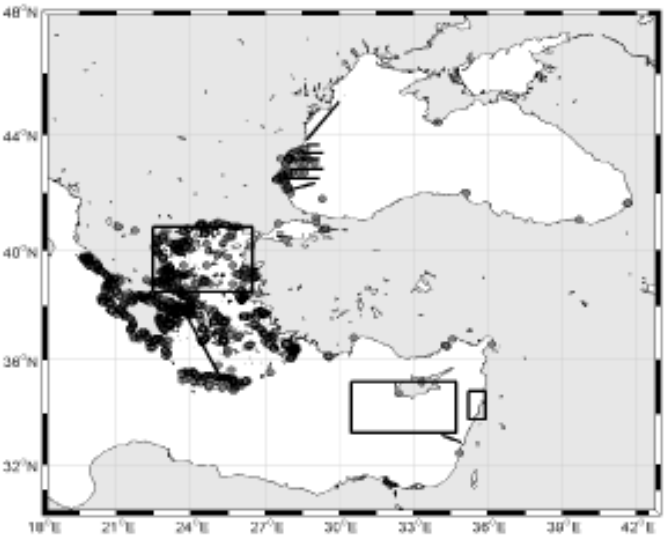

Figure 1 Geographical distribution of the Ocean Observing Stations.

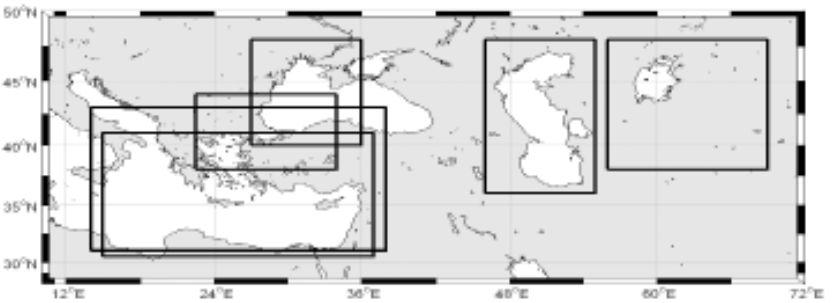

Figure 2 Satellite data coverage.

2.2 Dissemination of meta-data information and products

A regional web site for the Eastern Mediterranean and the Black Sea was developed by HNODC in order to facilitate the dissemination of the project results and promote the project in the region (http://hnodc.ncmr.gr/edios). The system provides all the related information and allows on-line submission of the completed MIFs. The collected meta-data have been organised in a regional database accessible from the web site. The tools that were used for the development of the database are MySQL relational database, PHP scripting language and Javascript. The database enables the users to retrieve and download all the meta-data information connected with the observing stations, using multiple selection criteria, such as geographical coordinates, platform type, parameter and instrument type, station type and country.

Furthermore, a CD-ROM with the meta-data related database was produced and made available to the scientific community. The CD-ROM included the meta-data of the rest of the Mediterranean Sea collected from the French Data Centre (IFREMER/SISMER) and the Italian Data Centre (OGS) for the western and central region respectively. The software was developed by HCMR/HNODC using Borland's "Delphi" Object Oriented Developers Platform and ESRI's "Map Objects" Mapping and GIS components. It consists of an interactive map and selection criteria in the upper part of the window while the query results are shown in the lower part. The interface is shown in Figure 3.

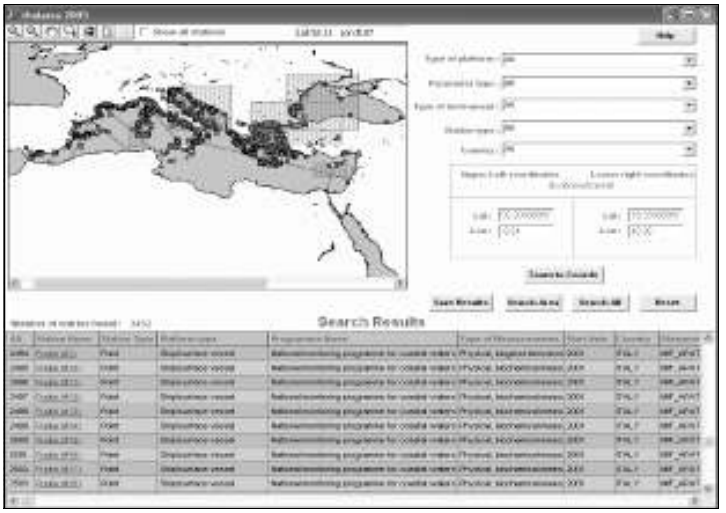

Figure 3 Application interface of the CD-ROM "Thalassa 2005".

The database of the Mediterranean and the Black Sea will be maintained and regularly updated in the future and the updates will be available at HNODC/EDIOS website.

Acknowledgements

This work has been done within the framework of the EC EDIOS Project. It was financially supported by the Environment Programme of the European Union (EU Concerted Action Contract No. ENV1−CT−2001−20005). We acknowledge the support of the EC, HCMR/HNODC, IFREMER/SISMER, OGS.

Regional Systems 2

Implementing the Coastal Module of GOOS

Thomas C. Malone*[1] and Anthony Knap[2]

[1]*US Office for Integrated and Sustained Ocean Observations, USA*
[2]*Bermuda Biological Station for Research, Inc., USA*

Abstract

Coastal nations worldwide are experiencing changes in their coastal marine and estuarine systems that jeopardise sustainable development, human health and safety, and the capacity of marine ecosystems to support products and services valued by society. Because these changes and their causes often transcend national borders, national concerns over their impacts have led to numerous international agreements that require sustained, timely, routine and reliable assessments of the condition of coastal marine and estuarine systems and timely predictions of the effects of natural hazards, climate change and human activities on them. Implementation of the coastal module of the Global Ocean Observing System (GOOS) will provide data and information required to achieve these objectives. To these ends, the Coastal Ocean Observation Panel (COOP) has completed a strategic implementation plan that presents recommendations for the phased development of a Global Coastal Network (GCN) through the establishment and networking of GOOS Regional Alliances (GRAs), National GOOS programmes, and existing global programmes. This presentation summarises recommended high priority actions for

1. Implementing the observing, data management, and modelling elements of the GCN
2. Capacity building on a global scale
3. Pilot projects critical to establishing the GCN
4. The implementation of performance metrics needed to improve the GCN over time.

1. Introduction

In 2003, over thirty nations agreed to a declaration at the Earth Observing Summit affirming the need "to monitor continuously the state of the Earth, to increase understanding of dynamic Earth processes, to enhance prediction of the Earth system, and to further implement our international environmental treaty obligations", and, thus the need for "timely, quality, long-term, global information as the basis for sound decision making." A 10-year implementation plan for establishing a Global Earth Observing System of Systems (GEOSS) was completed in February, 2005. The Global Ocean Observing System (GOOS) is the oceans and coasts component of the GEOSS.

GOOS is developing as a global network that systematically acquires and disseminates data and information based on requirements specified by groups that use, depend on, manage or study marine and estuarine systems (UNESCO, 1998). The observing system consists of two related and convergent modules:

* Corresponding author, email: t.malone@ocean.us

1. An open ocean module concerned primarily with detecting and predicting natural hazards and changes in the ocean-climate system and their effects on marine operations and services
2. A coastal module concerned primarily with effects of human activities, natural hazards and climate change on public health risks, the condition of coastal marine and estuarine ecosystems, and the living resources they support (Malone *et al.*, 2005).

Together, these modules are being designed and implemented to provide data and information needed to achieve six related societal goals:

- Improve predictions of weather variability and climate change
- Improve the safety and efficiency of marine operations
- Mitigate the effects of extreme weather (e.g. tropical storms) more effectively
- Reduce public health risks
- Protect and restore healthy ecosystems more effectively
- Sustain living marine resources.

Table 1 Examples of the drivers of change (forcings) and associated phenomena of interest in coastal marine ecosystems that are the subject of coastal GOOS (UNESCO, 2003).

	FORCINGS OF INTEREST
"Natural"	• Global warming, sea level rise • Natural hazards (extreme weather, seismic events) • Currents, waves, tides and storm surges • River and groundwater discharges, sediment inputs
Anthropogenic	• Alteration of hydrological and nutrient cycles • Inputs of chemical contaminants and human pathogens • Harvesting natural resources (living and non-living) • Physical alterations of the environment • Introductions of non-native species
	PHENOMENA OF INTEREST
Climate & weather	• Variations in sea surface temperature; surface fluxes of momentum, heat and fresh water; sources and sinks of carbon; sea ice
Marine operations	• Variations in water level, bathymetry, surface winds, currents and waves; sea ice; susceptibility to natural hazards
Natural hazards	• Storm surge and coastal flooding; coastal erosion; susceptibility to natural hazards; public safety and property loss
Public health	• Risk of exposure to human pathogens, chemical contaminants, and biotoxins (contact with water, aerosols, seafood consumption)
Healthy Ecosystems	• Habitat modification, loss of biodiversity, cultural eutrophication, harmful algal events, invasive species, chemical contamination, diseases in and mass mortalities of marine organisms
Living marine resources	• Fluctuations in spawning stock size, recruitment and natural mortality; changes in areal extent and condition of essential habitat; food availability • Aquaculture production and water quality

Achieving these goals depends on the capacity to rapidly detect and provide timely predictions of a broad spectrum of coastal phenomena of interest (Table 1).

During the decade since UNCED in 1992, substantial progress has been made in the design and implementation of the open ocean module (UNESCO, 1999; Koblinsky and Smith, 2001). In contrast, although a high priority of the international community, development of the coastal module has been slow. This is due in part to two related limitations:

1. The lack of capacity to rapidly and routinely detect changes in those phenomena of interest that require measurements of biological and chemical variables
2. The lack of operational models required to predict the occurrence of or changes in phenomena of interest relevant to human health, ecosystem health, and living marine resources.

Thus, improving operational capabilities of GOOS in these areas depends on major advances on at least three research fronts:

- Development of integrated data communications and management systems that provide rapid access to diverse data from many sources
- Development of *in situ* and remote sensing techniques for near real-time provision of data on key biological and chemical variables
- Development of data assimilation techniques and coupled physical-ecological models that can be run in an operational mode.

As recently approved by the Intergovernmental Committee on GOOS (I-GOOS), the Implementation Strategy for the Coastal Module of GOOS recognises these challenges and recommends procedures for addressing them (UNESCO, 2005).

2. Design of the Coastal Module

Key design considerations include the following:

1. Although each goal given above has unique requirements, they have many common requirements for observations, data management, and modelling
2. Phenomena of interest are often local expressions of larger scale changes in the ocean basins and coastal drainage basins
3. The observing system must efficiently link observations and models via data management and communications and it must deliver data and information in forms and at rates required by groups that use, depend on, manage and/or study marine and estuarine systems
4. The system must be multidisciplinary
5. Priorities, requirements and capabilities for observations and data analysis vary among countries and regions
6. Many of the elements needed to build the observing system are in place
7. Operational capabilities for improving marine operations and services and mitigating the impacts of natural hazards are more advanced than those for ecosystem-based management of public health risks, water quality, and living marine resources
8. The observing system will be implemented by nations and regional bodies.

To address these considerations, the Integrated Strategic Design Plan for the Coastal Module of GOOS (UNESCO, 2003) calls for the implementation of regional coastal ocean observing systems (RCOOSs) and the networking of these systems globally to form a Global Coastal Network (GCN). GOOS Regional Alliances (GRAs) and national GOOS programmes (Figure 1) are in the process of establishing RCOOSs through the engagement of stakeholders and partnerships with existing regional programmes (e.g. LME programmes, Regional Seas Conventions and Regional Fishery Bodies).

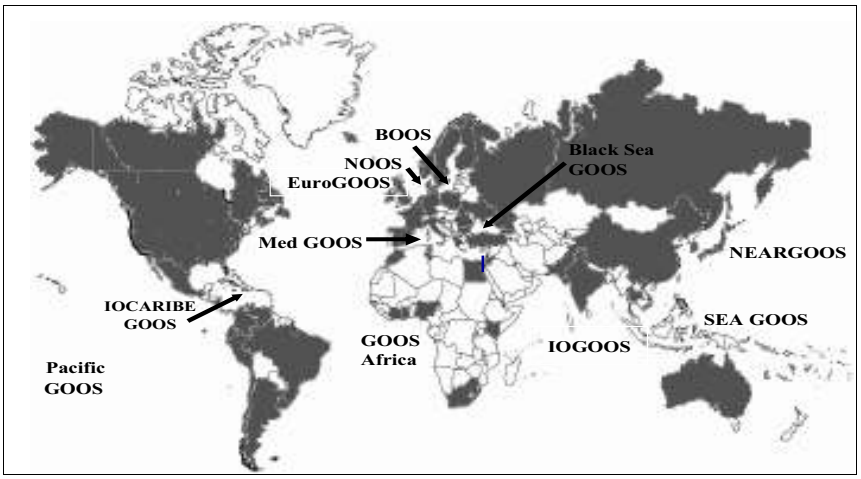

Figure 1 GOOS Regional Alliances (GRAs) and National GOOS Programmes (dark grey).

Although elements of the GCN are in place, they are not linked and integrated. Observational elements that are to be linked to form an integrated system of observations include

1. Coastal networks for near shore observations (e.g. the global network of coastal tide gauges, GLOSS)
2. Fixed platforms, moorings, drifters, and underwater vehicles for *in situ* measurements
3. Research and survey vessels, volunteer observing ships
4. Airborne, space-based and land-based remote sensing remote sensing from satellites and aircraft; research and survey ships.

The GCN will

1. Measure, manage and analyse common variables needed by all or most coastal nations and regions
2. Establish a sparse network of sentinel and reference stations for early detection of the effects of land-based inputs (e.g. freshwater, sediments, dust, and nutrients) and basin scale variability (e.g. the El Niño-Southern Oscillation, North Atlantic Oscillation, Pacific Decadal Oscillation)
3. Apply internationally accepted standards and protocols for measurements, data telemetry, data management and modelling.

The provisional common variables include geophysical variables (temperature, salinity, currents, waves, sea level, shoreline position, bathymetry, sediment grain size), chemical variables (dissolved inorganic nutrients, dissolved oxygen, sediment organic content), biological variables (faecal indicators, phytoplankton biomass, benthic biomass), and biophysical variables (optical properties). Depending on national and regional priorities, GRAs may increase the resolution at which the common variables are measured, supplement common variables with the measurement of additional variables and provide data and information products that are tailored to the requirements of stakeholders in the respective regions.

3. Implementing the Coastal Module of GOOS

The Implementation Strategy for the Coastal Module of GOOS presents the COOP recommendations for developing the coastal module in six related areas:

1. The measurement subsystem (regional development, establishing the global coastal network, and data telemetry)
2. The data management subsystem (general requirements and design; establishing common standards and protocols; national, regional and global data organisations; challenges, current capabilities and plans for improvement)
3. The modelling and analysis subsystem (community-based modelling, developing and improving regional modelling capabilities)
4. Developing and improving capacity (capacity building in the developing world, improving operational capabilities of the coastal module through research)
5. Developing the coastal module through pilot projects (building capacity in the developing world, improving operational capabilities)
6. Performance evaluation (indicators of performance, phased implementation of performance evaluations, immediate actions needed to evaluate the performance of subsystems).

The over 50 recommendations made by the COOP cannot be reviewed here, so recommendations the Panel believes are immediate priorities for global development of the coastal module are highlighted here.

3.1 The Global Coastal Network

Given current operational capabilities and the socio-economic impacts of coastal flooding worldwide, a high immediate priority is the development of multi-hazard forecasting capabilities to mitigate more effectively the impacts of coastal flooding on coastal communities, ecosystems and living marine resources. As a minimum, a multi-hazard system should be developed as part of the GCN to manage and mitigate the impacts of coastal flooding caused by tsunamis, tropical storms, and extra-tropical storms.

Observing subsystem

- Review and update the recommended set of common variables
- Determine requirements for observations and establish internationally accepted standards and protocols for *in situ* measurements

- Periodically review the quality and utility of coastal satellite products in light of remote sensing requirements recommended by the IGOS Coastal Theme Team
- Determine optimal locations for stations and transects that will provide early warnings of the effects of basin scale events and land-based sources on coastal systems.

Data management and communications

The Data Management System (DMS) should be a distributed, web-based system that provides rapid access to diverse data from many sources. Key recommendations include the following:

- Establish nested networks on national, regional and global scales for managing non-geophysical variables that employ common metadata standards, enable data discovery and access, develop web services, and establish archives
- Explore the ability of JCOMM–IODE to manage biogeochemical data streams.

Modelling

Development of operational modelling capabilities is critical to establishing a user-driven system in which data requirements for models drive the development of the DMS and observational subsystems. The key to achieving this operational objective and improving operational capabilities is the development of community modelling networks.

- Establish community modelling networks to develop ensemble modelling capabilities for predicting the time-space extent and impacts of coastal flooding, for predicting coastal erosion, and for ecosystem-based management of public health risks, water quality and living marine resources.

3.2 Pilot projects

Current operational capabilities of the GOOS are most advanced for those goals that require meteorological and physical oceanographic data (safe and efficient marine operations, forecasting extreme weather and associated phenomena such as storm surge flooding) and least advanced for those goals that require chemical, biological and ecological data. Operational services for physical variables already exist at the local and regional level for coastal regions in Europe, USA, Japan, SE Asia, Australia, and in offshore oil and gas sectors globally. Developing a coastal module of GOOS that provides data and information needed to achieve all six societal goals will require research and efficient use of new technologies and knowledge to improve operational capabilities of the coastal module. Pilot projects are critical to this process, and the COOP strategy recommends a set of high priority pilot projects that will build capacity to enable developing countries to participate in and benefit from GOOS and improve operational capabilities. Four of these are highlighted here as high priorities:

1. **Global Storm Surges and Flooding Risk**: Coastal flooding is an ever present threat to many low-lying, coastal regions. Storm surge models are now run operationally for many coastal regions and can provide very useful short term forecasts (lead times of hours to days) of coastal flooding. The main objective of this project would be to construct a storm surge modelling system with global coverage that can provide short-term forecasts and decadal-scale hindcasts, and also be used for climate change

scenarios. The development of such a system would also provide a good opportunity for capacity building and allow the surge modelling community to clearly define the required accuracy and resolution of coastal wind and air pressure forecasts and reanalyses. A community-based modelling approach should be employed.

2. **Development of coastal ocean colour products**: Spatially synoptic assessments of phytoplankton on the scales of coastal marine and estuarine ecosystems are possible only from remote sensing of ocean colour. In addition to phytoplankton pigments, concentrations of coloured organic matter and suspended sediments can be extracted from space-based measurements of ocean colour. However, the optical complexity of most coastal waters and problems in removing the effects of land and the atmosphere from the signal detected from space lead to substantial uncertainties in estimates. For delivery of ocean colour data-products on global scales of known quality, pilot projects are needed to establish standard procedures for developing, evaluating and improving ocean colour algorithms for translating ocean colour into useful products, e.g. comparable estimates of surface fields of chlorophyll *a*, CDOM, turbidity, and water clarity from different regions.
3. **Couple shelf and deep ocean models to increase the skill of coastal circulation models**: Quantify the increase in predictability of physical and biogeochemical conditions on the shelf that result from using open boundary conditions generated by deep ocean forecast systems such as those being developed by GODAE. It will be advantageous to conduct pilot projects in contrasting regions (e.g. narrow versus wide shelves, eastern versus western boundaries of ocean basins). It will also be important to supplement shelf modelling with an active shelf observation programme to calibrate and validate coastal models.
4. **Develop coastal data assimilation experiments patterned after GODAE**: Real-time assessments of changes in surface current fields and directional wave spectra are needed to address all six societal goals of the coastal module. Thus, the COOP recommends that coastal GODAE projects (CODAE) be implemented that integrate data streams from land-based remote sensing (HF radar), *in situ* measurements (ADCP current meters) and space-based remote sensing (SAR, scatterometry, sea surface height) to provide near real-time, high resolution maps of sea surface currents and waves for coastal regions.

3.3 Implementing mechanisms

The global ocean-climate component of GOOS is in the process of being implemented under the oversight of the Joint Commission for Oceanography and Marine Meteorology (JCOMM) which has established programme areas for observations, data management, products and services and capacity building. Currently, there is no equivalent body to oversee implementation of the coastal module on a global scale.

The GCN will develop by incorporating existing global programmes (e.g. space-based remote sensing, GLOSS, GCRMN) and by networking or scaling up of elements developed for RCOOSs (e.g. capacity to down-link and interpret data streams from space-based sensors, CPR). To achieve this, a global body is needed to coordinate global development of a GCN that meets national and regional needs, ensures interoperability and enables effective capacity building. Thus, the COOP recommends the establishment

of a Global Body of GRAs to represent the interests of participating countries and to coordinate the development of a GCN that meets the common data and information needs of all regions (Figure 2).

To begin this process, the COOP recommends the formation of an *ad hoc* JCOMM–GSSC Task Team to work with GRAs to address two immediate issues:

1. Agree on a mechanism or mechanisms to coordinate global implementation
2. If needed, begin the process of establishing expert teams corresponding to the JCOMM Programme Areas.

   Priorities for global implementation include

   - establishing multi-national partnerships for building capacity in the developing world through GRAs, especially in the southern hemisphere and the western Pacific
   - funding pilot projects for building capacity and improving operational capabilities.

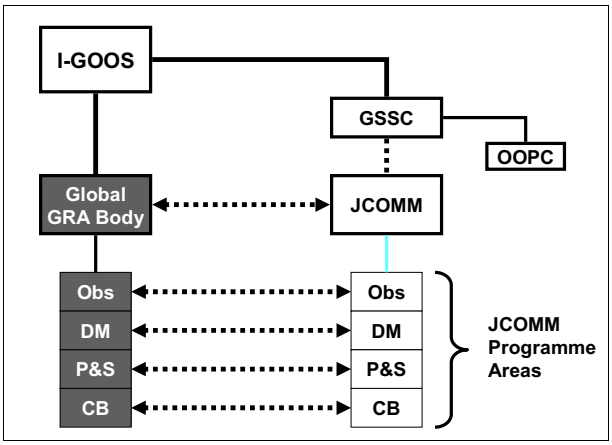

Figure 2 GOOS is developing under the auspices of the Intergovernmental Committee on GOOS (I-GOOS). The GOOS Scientific Steering Committee (GSSC) provides scientific and technical advice to ensure the development of a scientifically sound system. The JCOMM oversees operational development of the global ocean-climate module of GOOS in four programme areas. The COOP recommends a parallel structure for overseeing the development of the coastal module. Solid lines represent formal lines of communication. Dashed lines represent coordination and collaboration.

References

Koblinsky, C. and N.R. Smith (eds) (2001). Observing the Oceans in the 21st Century. GODAE Project Office, Bureau of Meteorology, Melbourne, Australia, 604 pp.

Malone, T.C., A. Knap and M. Fogarty (2005). Overview of science requirements. In The Global Coastal Ocean: Multiscale Interdisciplinary Processes. The Sea, Robinson, A.R., Brink, K.H. (eds) 13: 757–784.

United Nations Educational, Scientific and Cultural Organization (UNESCO) (1998). The GOOS 1998. GOOS Publication No. 42, IOC, Paris, 144 pp.

UNESCO (1999). Global physical ocean observations for GOOS/GCOS: an action plan for existing bodies and mechanisms. GOOS Rpt. No. 66, 50 pp.

UNESCO (2003). The Integrated Strategic Design Plan for the Coastal Ocean Observations Module of the Global Ocean Observing System. GOOS Publication 125, IOC, Paris, 190 pp.

UNESCO (2005). Strategic Implementation Plan for the Coastal Module of the Global Ocean Observing System. IOC, Paris, (in press).

Linking the coastal zone to GOOS

Silvana Vallerga*[1] and Aldo Drago[2]

[1] CNR, Istituto Ambiente Marino e Costiero, c/o IMC, Oristano, Italy
[2]IOI–Malta Operational Centre, University of Malta

Abstract

The EC project GRAND aims at supporting the GOOS Regional Alliances (GRAs) to improve local operations in coastal waters by using products from the Global Ocean Observing System. The GRAs link over 100 institutions from 83 countries all around the world. They have begun to co-ordinate their efforts to maximise the benefits of GOOS for operational oceanography. EuroGOOS is leading the way. In GRAND the GRAs have identified two key technical problems that must be overcome to link the coastal zone to GOOS:

1. Bridging the gap in scales between global observations and local needs
2. adding ecosystem information.

GRAND is designing a regional strategy to address these problems by using advanced technologies and methods. It will start by adapting two state-of-the-art European modelling technologies using unstructured adaptive meshes and Lagrangian Ensemble ecology. These technologies will then be integrated into a prototype What-If? Prediction system. GRAND is also assessing the status of assets and needs of each regional system. These activities lie in the mainstream policy of the IOC/UNESCO Inter-governmental Committee for GOOS.

Keywords: GOOS, I-GOOS, GRAND, GRAs, GRC, operational oceanography, regional strategy, nowcast, forecast, what-if? prediction.

1. Introduction

1.1 Operational oceanography

Operational oceanography provides information and predictions about aspects of the sea to address a range of customer needs such as water quality, port and off-shore installation design, fisheries and aquaculture, tourism, transportation, exploitation of resources and coastal development. Operational oceanographers use tools developed to explore the sea and modelling methods that oceanographers have developed to understand what they discover. The classical techniques of observation and prediction by induction assume that the system is linear and stationary. They have been successful in solving many problems. But a new framework, no longer stationary and linear, is emerging because of the pressure of population growth on natural resources, the legacy of non-sustainable exploitation, and the response of the biosphere to changes in pollution and radiative forcing. Inadequate simulation of ecology and lack of data at the regional scale are limiting coastal operational oceanography.

* Corresponding author, email: vallerga@ge.cnr.it

1.2 The role of GOOS in operational oceanography

WOCE successfully tested the use of global observations to describe coherent structures in the marine environment. This led John Woods to launch, at the Second World Climate Conference in 1990, a Global Ocean Observing System to enable permanent observation of seas and oceans and prediction of future change (Woods 1991, 1992, 1993). In 1992 the UNCED endorsed this global system of ocean observations and the IOC formally initiated the GOOS, later joined by WMO, UNEP and ICSU. It is steered by I-GOOS, the Inter-Governmental Committee for GOOS.

GOOS is a global system designed to produce global-scale products with the potential to improve operational oceanography at local level. It also provides the marine data needed for the Global Climate Observing System, proposed to WMO soon after GOOS was launched. Climate has since become the major driver for GOOS products. GODAE is the first global trial. It will assess the products obtainable from a prototype GOOS array, mainly of satellite altimeters and ARGO floats.

However, the great majority of customers for operational oceanography, and therefore for GOOS, are concerned with processes in the coastal zone that are important even when the climate is stationary. So the IOC has strongly supported the development of a coastal strategy for GOOS, and the coastal states have focused the I-GOOS goals in 2002–2005 on coastal customers. The I-GOOS goals are:

1. transfer prototypes from research into operations
2. learn from the regions
3. empower the regions
4. address operations in EEZs.

Specific initiatives were taken to support each goal. The EC project GRAND supports these I-GOOS goals.

1.3 The regional approach and GRAND

I-GOOS recognises that creating an effective GOOS will depend critically on the co-ordinated development of regional activities. Thus I-GOOS is supporting the GOOS Regional Alliances, each of which is grouping major institutions from countries with a shared interest in a specific area of the marine environment. The GOOS Regional Forum, initiated by I-GOOS, facilitates the sharing of best practice. The GOOS Regional Council (GRC), formed by the heads of the GRAs, provides a decision-making body for the regions acting collectively. The GRC provides a coherent voice expressing the needs of coastal customers in GOOS. In so doing it balances the Climate Convention which expresses the needs of climate customers in GOOS.

I-GOOS and MedGOOS proposed GRAND to the EC to empower the regions to link their coastal zones to GOOS. The partners of the project are eleven GRAs (Figure 1): MedGOOS, Africa GOOS, Black Sea GOOS, EuroGOOS, GOOS Regional Alliance of South Pacific, Indian Ocean GOOS, IOCaribe GOOS, North East Asia GOOS, OceAtlan, Pacific Islands GOOS, and South East Asia GOOS. The advanced technologies are being developed by Imperial College London.

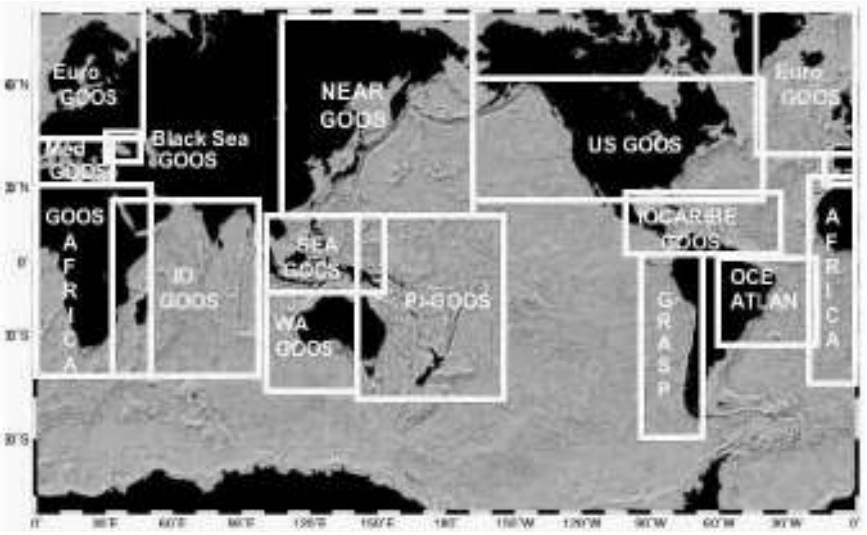

Figure 1 The GRAs in 2005. Their boundaries are indicative. From www.grandproject.org.

2. The challenge of GRAND

The main challenge for GRAND is to design a regional strategy to extract local benefits from the global scale products of GOOS. This is supported by identification of essential technologies, a survey of regional assets and needs, advanced training workshops and publications. GRAND strongly supports the participation of developing countries in GOOS and GEOSS, while promoting the European contribution to the global observing systems, GMES. To derive maximum benefit from GOOS for coastal communities the GRAs require action in two broad areas: technical — data, science and technology; organisational — co-ordination, skilled people and funds. GRAND is helping the GRAs to address this challenge of linking the coastal zone to GOOS.

2.1 Data

The work done in GRAND has shown that considerable capability already exists throughout the GRAs to collect data at the length and timescales necessary to solve local problems. The GOOS is designed to collect data at the global scale. There is a gap in the spectrum of data collection at a regional level between the local and global ocean scale. Field trials are needed to assess the impact of this gap on local services and to design an effective way forward. They will extend the work of GODAE.

2.2 Science and technology

The GRAs have identified two key technical barriers to linking coastal needs to GOOS products:

1. gap in scales
2. lack of ecosystem information.

Predictive techniques and modelling are a particular weakness. The traditional method of nesting models within models can lead to errors. An important goal is to introduce modelling techniques that permit an error-free transition between scales.

Many problems in coastal areas are related to chemical and ecological factors rather than just the physics of the marine environment. Yet the majority of marine models are physical. Simulating the ecosystem better in operational models is a high priority. Biofeedback in ecosystem models produces non-linearity that cannot be addressed effectively by the method of induction used in operational oceanography.

3. The GOOS gap

Coastal communities should benefit from the large investment in GOOS, but concentration of effort has so far been on physical properties of the ocean, and there is a lack of capability to address ecosystem response. The Climate Convention has developed a strong customer-pull for a clearly-defined problem. The GOOS observations are at the appropriate scale for that problem. The Coastal Scientific Community has not developed a similar customer-pull because the problems are diverse, the observation length and time scales are different, and there are technical and scientific problems with the transition between global and local scales, and of ecology. Before the founding of the GRC there was no clear organisational structure that could co-ordinate a coherent input to GOOS from the multitude of local end-users. This has resulted in a "GOOS Gap" illustrated schematically in Figure 2.

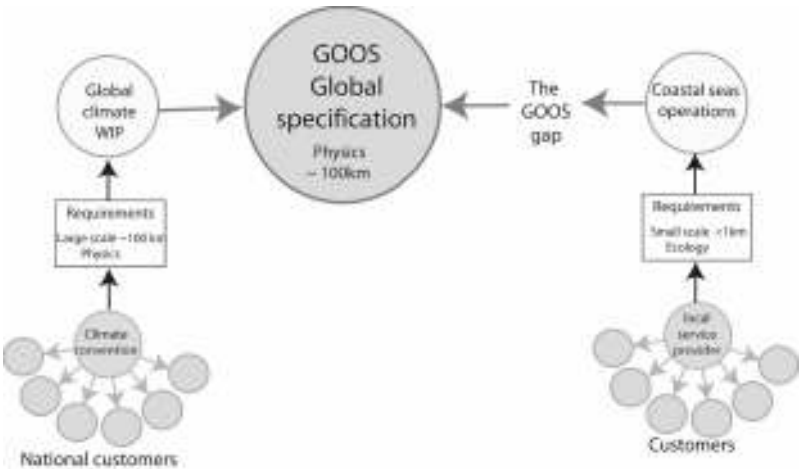

Figure 2 The GOOS Gap (Woods and Morrice, 2006).

4. New technology

A significant element of the "GOOS Gap" arises from deficiencies in three areas:

1. modelling error generation
2. What-if? predictive capability
3. addressing ecosystem response.

The capacity building in GRAND focuses on the transfer of new technologies to close that gap, plus the training and support necessary to exploit these technologies within the regions.

4.1 Ocean circulation modelling

Closing the GOOS gap has top priority for service providers seeking to use GOOS global-scale products to improve their products for coastal customers. The classical solution, nested models, is known to produce errors. Those errors can be avoided by adaptive mesh modelling, developed at Imperial College London (Ford *et al.*, 2004). This technology permits much more realistic representation of bathymetry (Figure 3) and ocean circulation by automatically providing enhanced resolution wherever it is needed, for example to describe flow interaction with bathymetry, or transient jets and fronts. Such very high resolution is computationally affordable because it is only provided where needed. Adaptive mesh technology is incorporated in the Imperial College Ocean Model (ICOM), which also features non-hydrostatic dynamics and advanced data assimilation. ICOM was presented at the GRAND Workshops. The effectiveness of ICOM is being demonstrated by simulating the interaction between circulation in a coastal lagoon and the open Mediterranean Sea.

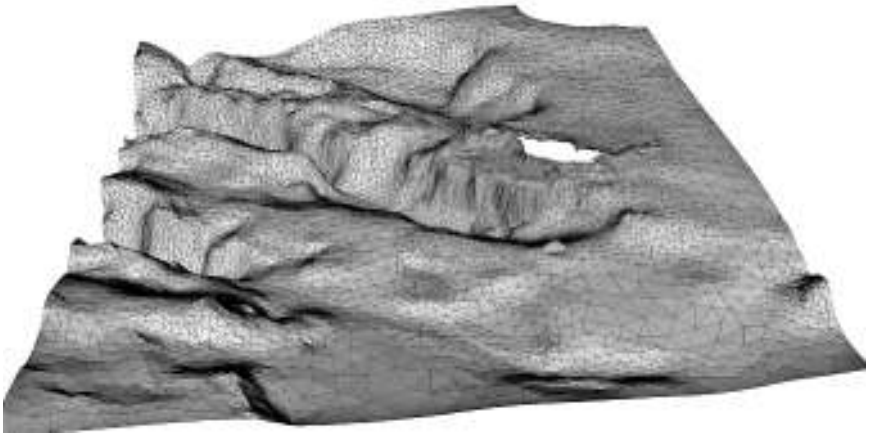

Figure 3 Unstructured mesh bathymetry around Malta produced for MAMA (Gorman, 2005).

4.2 Ecology

Many of the customer needs for operational oceanography, such as fisheries, pollution, toxic blooms and cholera epidemics require the model to incorporate ecosystem processes. It is necessary to adopt an ecosystem metamodel that guarantees global stability and therefore reliable predictions under a wide range of conditions. Popova *et al.* (1997) have shown that the Eulerian metamodel widely used in research on biological oceanography (e.g. in ERSEM) is not globally stable. However Woods *et al.* (2005) have demonstrated that the Lagrangian Ensemble metamodel (Woods, 2005) is globally stable. LE modelling underpins the new science of Virtual Ecology, which promises useful predictability for operational oceanography, especially for What-If? Prediction in support of planning (Woods, 2006). The Virtual Ecology Workbench (VEW), which

automates the creation and analysis of Virtual Ecosystems was demonstrated in the GRAND Workshops. The VEW training manual is one of the GRAND publications.

5. The GRAND publications

5.1 The GOOS Regional Prospectus

The GOOS Regional Prospectus gathers all the ideas and data generated by GRAND into a self-contained publication that will be used by the GRAs to explain the strategy they are adopting to improve coastal operational oceanography by exploiting the global-scale products of GOOS. The chapters address: Operational oceanography; The challenge; Global Ocean Observing System; New technology; A regional approach; Regional funding opportunities, A regional strategy. The GOOS Regional Prospectus is being written by John Woods and Alex Morrice with input from all GRAND members. The follow-up project GRACE will (if funded) produce a detailed implementation plan.

5.2 The VEW Training Manual

The VEW (Virtual Ecology Workbench) is a powerful and flexible software tool for creating virtual ecosystems without the need for programming. Its graphical user interface helps the user to specify the model, the scenario for forcing by exogenous processes, and the environmental events that are the subject of What-If? Prediction. GRAND is funding the preparation of the VEW training manual.

Acknowledgements

GRAND is funded by the EC FP6. We thank John Woods and Alex Morrice for excerpts from the GOOS Regional Prospectus, and MAMA and the ICOM research group for providing the Malta unstructured mesh high definition bathymetry.

References

Ford, R., C.C. Pain, M.D. Piggott, A.J.H. Goddard, C.R.E. de Oliveira and A.P. Umpleby (2004a and b). A non-hydrostatic finite-element model for three-dimensional stratified oceanic flows. Part I: Model formulation & Part II Model validation. Monthly Weather Review 132 (12), 2816–2831 and 2832–2844.

Gorman, G.J. (2005). Small to large scale gridding and meshing for ocean modelling: Malta in the Mediterranean. EC MAMA final report.

Malone, T. and A. Knap (2005). Implementing the Coastal Module of GOOS. This volume, page 262.

Popova, E.E., M.J.R. Fasham, A.V. Osipov and V.A. Ryabchenko (1997). Chaotic behaviour of an ocean ecosystem model under seasonal external forcing. J. Plankton Res., 19(10), 1495–1515.

UNESCO (2003). GOOS Report 125.

Vallerga, S. (1998). Operational Ocean Forecasting: Why and How. Mare Amico. Anno II, n. 2, pp. 17–26.

Woods, J.D. (1991). Oceanography on a global scale: the new challenge. Phys. Ed 26, 159–163, 168.

Woods, J.D. (1992). Monitoring the ocean. In B. Cartledge ed. "Monitoring the environment" Oxford University Press 123–156.
Woods, J.D. (1993). The case for GOOS IOC /INF–915, Paris.
Woods, J.D., H. Dahlin, L. Droppert, M. Glass, S. Vallerga, and N.C. Flemming (1996). The Strategy for EuroGOOS. EuroGOOS Publication 1, Southampton Oceanography Centre, Southampton. ISBN 0904175227.
Woods, J.D. (2005). The Lagrangian Ensemble metamodel for simulating plankton ecosystems. Progress in Oceanography (in press).
Woods, J.D., W. Barkmann and A. Perilli (2005). Stability and predictability of a Virtual Plankton Ecosystem created by an individual-based model. Progress in Oceanography (in press).
Woods, J.D. and A. Morrice (2006). The GOOS Regional Prospectus. GRAND Publ. 1 (in press).
Woods, J.D. (2006). Forecasting a Large Marine Ecosystem Ch. 18 in V. Shannon, G. Hempel, C. Moloney, P. Rizzoli and J.D. Woods (eds.) Benguela: Predicting a Large Marine Ecosystem, Elsevier (in press).

Acronyms and URLs

ARGO		www.argo.ucsd.edu/
EC	European Commission	www.europa.eu.int
ERSEM	European Regional Seas Ecosystem Model	www.pml.ac.uk/ecomodels/ersem.htm
FP6	Sixth Framework Programme	www.europa.eu.int
GEOSS	Global Earth Observation System of Systems	earthobservations.org
GOOS	Global Ocean Observing System	www.ioc.unesco.org/goos
GRA	GOOS Regional Alliances	www.grandproject.org
GRACE	GOOS Regional Alliances Collaboration for Empowerment	
GRC	GOOS Regional Council	
GMES	Global Monitoring for Environment and Security	www.gmes.info
GRAND	GOOS Regional Alliances Network Development	www.grandproject.org
GODA E	Global Ocean Data Assimilation Experiment	www.USGODAE.org
I-GOOS	Inter-Governmental Committee for GOOS	www.ioc.unesco.org/goos
ICOM	Imperial College Ocean Model	http://amcg.ese.ic.ac.uk/cgi-bin/index.pl?page=home.htm
ICSU	International Council for Science	www.icsu.org
IOC	Intergovernmental Oceanographic Commission	www.ioc.unesco.org
MAMA	Mediterranean network to Assess and upgrade Monitoring Forecasting Activity in the basin	www.mama-net.org
MedGOOS	Mediterranean GRA	www.medgoos.org
UNEP	United Nations Environment Programme	www.unep.org
VEW	Virtual Ecology Workbench	www.ic.ac.uk/ese/research/cosmic
WMO	World Meteorological Organization	www.wmo.org
WOCE	World Ocean Circulation Experiment	www.woce.org

Near-operational Black Sea nowcasting/forecasting system

G. Korotaev*[1], E. Cordoneanu[2], V. Dorofeyev[1], V. Fomin[3], A. Grigoriev[4], A. Kordzadze[5], A. Kubryakov[1], T. Oguz[6], Yu. Ratner[1], D. Trukhchev[7] and H. Slabakov[7]

[1]*Marine Hydrophysical Institute, Ukraine*
[2]*National Meteorological Administration, Romania*
[3]*Marine Branch of Hydrometeorological Institute, Ukraine*
[4]*State Oceanographic Institute, Russia*
[5]*Institute of Geophysics, Georgia*
[6]*Institute of Marine Sciences, Turkey*
[7]*Institute of Oceanology, Bulgaria*

Abstract

This paper presents a near-operational system enabling continuous monitoring of the circulation and stratification of the Black Sea. The system is based on the regional atmospheric model with a 24 km grid step, a primitive equation model of the Black Sea circulation with a 5 km grid step, a nine-compartment basin-scale ecosystem model with the same spatial resolution and a set of local circulation models with a resolution of 0.5–1.2 km nested near the coast of the riparian countries. The basin-scale circulation model assimilates sea surface anomalies, provided in near real time by AVISO (France) and surface temperature (via direct reception of AVHRR). The output of the system includes near surface meteorology, three-dimensional hydrography and surface chlorophyll concentration. Surface drifting buoys provide data for validation of surface current velocity and sea surface temperature. Profiling floats are used for validation of a weekly mean velocity, temperature and salinity profiles.

Keywords: numerical modelling, operational oceanography, assimilation, ecosystem model.

1. Introduction

The EC project ARENA started in 2003. One of the project goals is to establish a pilot nowcasting/forecasting system in collaboration with Black Sea GOOS and other international projects being carried out in the basin. The general structure of the regional nowcasting/forecasting system was designed during the first year of the project. It was arranged that the minimal nowcasting/forecasting system of the Black Sea basin should have a regional weather prediction model, basin-scale circulation and ecosystem models and high-resolution circulation models for coastal regions which are most important for potential users. It was also evident that basin-scale models should have a data assimilation capacity to achieve relevant accuracy of nowcasted and forecasted fields. The assessment of the available resources in the region has shown that the development of

* Corresponding author, email: ipdop@ukrcom.sebastopol.ua

the Black Sea nowcasting/forecasting system could be made by means of careful coordination of the ongoing national modelling activities. On the other hand it was evident that the Black Sea countries are not themselves able to provide the data for assimilation into models. Therefore the Black Sea nowcasting/forecasting system development is based on the available resources in the region with broad international collaboration.

2. Initial observing system

The initial Black Sea observing system consists of three components. The most important is the remote sensing component combining data from several space missions. Data from space altimeter missions are processed by both the NASA Ocean Pathfinder project and the AVISO service and adjusted to the Black Sea basin by Korotaev *et al.* (2001). The output of the altimeter data preprocessing is the dynamical topography of the Black Sea surface. Korotaev *et al.* (2001) and Korotaev *et al.* (2003) have shown that a broad range of the basin variability is reproduced well, starting from mesoscales. Data from the IR scanner AVHRR are available in the Black Sea region through direct reception by HRPT receiving stations in Turkey and Ukraine. MHI–NASU regularly processes this data to retrieve and map the Black Sea surface temperature. Ground truth validation of IR SST against *in situ* data shows its rms accuracy to be around 0.5–0.7° (Ratner *et al.*, 2004).

Modern satellite multi-spectral devices observing sea surface in the visible range, such as SeaWiFS and MODIS, are considered to be the basic source of information about ecological and biochemical processes taking place in the Black Sea. Standard NASA sea colour data are mainly used in the Black Sea region. However there is a difference in real atmospheric aerosol and bio-optical properties in the Black Sea region from standard models recommended by NASA. Application of the regionally adjusted algorithms improves accuracy of the surface chlorophyll determination.

Free-drifting platforms are another important component of the Black Sea observing system. The most intense international project "Experimental monitoring of the Black Sea for operational meteorology and oceanography using surface drifting buoys" with the participation of Ukraine, Russia, USA, France and partial support from Turkey, Romania, Bulgaria and Georgia has made it possible to launch 5–10 surface drifting buoys per year in the Black Sea starting in 2000 (Eremeev *et al.*, 2002). Drifting buoys deployed in the Black Sea have a sail at a depth of 15 m. The positioning of buoys by the Argos system enables determination of the velocity of surface currents. Sensors displaced on drifting buoys measure atmospheric pressure and sea surface temperature. Surface drifting buoys with a thermistor chain — a new efficient tool for the study of the Black Sea upper layer — were elaborated by MHI–NASU within the framework of the project "Remote Sensing of Marine Ecological System" project (Tolstosheev *et al.*, 2004) at the Science and Technology Centre in Ukraine. Six such buoys were launched starting from the end of August 2004 and have shown good potential for continuous observations of the upper mixed layer dynamics. Five profiling floats were launched in the Black Sea in the framework of the project "Observing the Black Sea with Profiling Floats" which is funded by the NICOP programme. Project participants are Turkey, Ukraine and USA. Three PALACE profiling floats elaborated by the group of School of Oceanography, University of Washington were deployed in the Black Sea in September

2002. Two more floats were launched in spring 2005. All floats are deployed in the Western part of the basin at depths between 100 m and 1600 m to monitor the surface and intermediate-depth characteristics of the flow fields and water mass structures. The data are transmitted weekly via the Argos system. The temperature and salinity profiles against pressure and the T−S relation together with float trajectories are presented in near-real time on the web site http://flux.ocean.washington.edu/metu.

3. Basin-scale nowcasting/forecasting system

The Black Sea nowcasting/forecasting system is being developed by the consortium of the riparian countries. Black Sea GOOS and ARENA projects coordinate ongoing national activities and some other international programmes sponsoring investigations of the Black Sea. The Black Sea nowcasting/forecasting system now includes regional high-resolution atmospheric forecasting, basin-scale nowcasting and forecasting of marine dynamics and ecosystem and forecast of high-resolution near-coastal circulation and stratification. The pilot real-time operation of the system was carried out in July 2005 during five days (http://arena.mhi.net.ua).

3.1 Regional atmospheric model

A new high resolution (24×24 km) regional atmospheric model developed and supported by NMA of Romania became available to the Black Sea community last year. The model belongs to the ALADIN family and is integrated with open boundary conditions which are presented operationally by the global model of Météo-France. The Romanian regional atmospheric model provides not only reanalysis but also two days' forecast both in GRIB and ASCII formats. Forecasted fields over the Black Sea include 10 m wind components, latent and sensible heat flux, cumulated solar and thermal radiation flux, instantaneous flux of solar and thermal radiation, evaporation, large scale and convective precipitation of rain and snow fall.

3.2 Circulation model and data assimilation

The Black Sea circulation model elaborated by the MHI group (Demyshev and Korotaev, 1992) is used as the core of the nowcasting/forecasting system. The model has 33 non-uniformly spaced levels, which are more frequent near the surface and near the bottom of the basin. The horizontal resolution is uniform with a 5 km grid step whereas the Rossby radius is equal to 25 km in the deep part of the Black Sea basin. Therefore the horizontal resolution of the model and selected viscosity and diffusion coefficients can resolve mesoscale variability of the Black Sea (Dorofeyev *et al.*, 2001). The circulation model operates with upper boundary conditions following from the regional atmospheric model and climatic data about river runoff and water and salt exchange through the Bosphorus Strait. The model assimilates altimetry and sea surface temperature. The assimilation procedure is based on the optimal interpolation of the sea level for the correction of both temperature and salinity fields. A hindcast of the Black Sea circulation with assimilation of the altimeter sea level is carried out for the period from spring 1992. The assimilation of sea surface temperature derived from AVHRR scanners is carried out by replacing simulated temperature within the upper mixed layer by the observations. The development of Black Sea basin-scale nowcasting with assimilation of remote sensing data in near-real time began in July 2003 in the framework of the project

"Remote Sensing of Marine Ecosystem" sponsored by EC and Canada through the Science and Technology Centre in Ukraine (http://odop.mhi.net.ua/).

3.3 Ecosystem model

The coupled circulation and ecosystem model based on the MHI basin-scale three-dimensional model is the part of the Black Sea nowcasting/forecasting system. The ecosystem module is an extended version of the one-dimensional bio-geo-chemical model, described by Prof. T. Oguz in the set of publications (Oguz *et al.*, 1999a,b; 2001a,b). It is shown that the model is able to reproduce seasonal variability of the Black Sea ecosystem with relevant accuracy during the eutrophication stage and invader pressure. However the current state of the Black Sea ecosystem is relatively healthy which permits us to avoid unnecessary complication of the trophic structure. Therefore the three-dimensional ecosystem model includes nine compartments, namely diatom and flagellete presenting phytoplankton, micro and meso zooplankton, bacteria, dissolved nitrogen, particulate nitrogen, nitrates and ammonium. The three-dimensional Black Sea circulation model was developed jointly by IMS (Turkey), MHI (Ukraine) and MIT (USA) in the framework of the collaborative project of Civilian Research and Development Foundation "Interdisciplinary Modelling Studies for the Black Sea Circulation and Ecosystem". The model runs with a 5 km grid step providing realistic distribution of surface phytoplankton and other components on meso and seasonal scales.

3.4 Validation of the model outputs

Independent data from surface drifting buoys and profiling floats are used to validate simulated currents, salinity and temperature distributions. It is shown that the drifting buoy trajectories correspond well with the current structure predicted by the model. The evolution of current velocity along the trajectory of a drifting buoy also demonstrates good reproduction of the low-frequency flow variability by the model (Dorofeyev *et al.*, 2004). Data from profiling floats allows evaluation of the weekly averaged deep velocity accuracy. Weekly mean currents even at a depth of 1550 m measured by profiling floats and simulated by the model are in good agreement (Dorofeyev and Korotaev, 2004a). Accuracy of SST simulation by the model was estimated by comparison with the data from surface drifters. Ratner and Bayankina (2004) show that the rms error lies in the range 0.5–0.7°, i.e. in the same limit as the accuracy of SST retrieval from AVHRR data. An error of temperature or salinity simulation varies with depth approximately repeating the profile of mean temperature or salinity gradients. However topography of isosurfaces is in rather good agreement with observations as shown by (Dorofeyev and Korotaev, 2004b) by comparing simulations with COMSBlack hydrographic surveys.

4. Regional nesting models

Regional weather prediction carried out by NMA in Romania with a marine basin-scale nowcasting/forecasting system provides a good basis for the development of operational nowcast and forecast of coastal dynamics with high spatial resolution. Ongoing national initiatives concerning oceanographic modelling of the most important regions along the Black Sea coast were considered as the base of the nesting strategy development. Regional models of Burgas Bay (Bulgaria), Poti region (Georgia), Danube mouth (Romania), Novorossiysk region (Russia), Kalamita Bay and the North-Western shelf of

the Black Sea (Ukraine) were nested in the basin-scale circulation model of MHI. These models have a better resolution than the basin-scale model and are an important tool for human activity support in the coastal area. All models are based on the primitive equations. Each model is able to specify open boundary conditions from the basin-scale circulation model of MHI.

5. Pilot operation of the Black Sea nowcasting/forecasting system

The initial observing system developed by the Black Sea GOOS community and the circulation model running in data assimilation mode enables nowcasting and forecasting of the Black Sea circulation in near-real time mode. Pilot operation of the Black Sea nowcasting/forecasting system was carried out during five days in July 2005. Each morning NMA of Romania provided an analysis and two-day forecast of atmospheric fluxes on the sea surface. Then the Marine Hydrophysical Institute of National Academy of Sciences of Ukraine downloaded atmospheric data, data from PALACE profiling floats and available space altimetry data from the AVISO service in Toulouse (France), via Internet. In parallel, the processing of AVHRR imagery was carried out by MHI Remote Sensing Department to derive SST for cloud free regions. Then the basin-scale circulation model was integrated for three days. The previous day's analysis of currents, temperature and salinity was used as the initial conditions. The one-day run of the basin-scale circulation model with sea surface boundary conditions specified by the atmospheric model analysis until the current day and the assimilation of all available data enabled nowcasting of currents, temperature, salinity, phytoplankton and other biochemical fields. The two-day run of the model with predicted atmospheric forcing provided forecasts of marine dynamics and ecosystem. Nowcasted currents, temperature and salinity were then interpolated on the grid of every nested model and used as initial conditions for the regional high resolution forecast. Open sea boundary conditions for every nested region were prepared, based on the basin-scale model forecast. Initial and boundary conditions were then placed on the MHI server and were available for every nested region. Each responsible group integrated their local model for two days providing high-resolution prediction of currents, temperature and salinity. Results of the forecast were displayed on the MHI server (http://arena.mhi.net.ua). A pilot operation of the initial Black Sea nowcasting/forecasting system has shown that the Black Sea community is able to realise routine nowcasting/forecasting of marine dynamics and ecosystem for practical needs based on the internal resources and participation of international data exchange.

Acknowledgements

The authors are grateful to the EC ARENA project for the support of the collaborative efforts on the coordination of the nowcasting and forecasting activities. The MHI authors were partially supported by the STCU project 2241 "Remote Sensing of Marine Ecosystem" and the CRDF grant UG2−2536−SE−03 "Interdisciplinary Modelling Studies for the Black Sea Circulation and Ecosystem".

References

Demyshev, S.G. and G.K. Korotaev (1992). Numerical energy-balanced model of baroclinic currents in the ocean with bottom topography on the C-grid. In: Numerical models and results of intercalibration simulations in the Atlantic ocean. Moscow, pp. 163–231 (in Russian).

Dorofeyev, V.L. and G.K. Korotaev (2004a). Validation of the results of modelling the Black Sea circulation based on the data of floating buoys. In: "Ecological Security of Coastal and Shelf Zone and Complex use of Shelf Resources" V.11 Sevastopol pp. 63–74 (in Russian).

Dorofeyev, V.L. and G.K. Korotaev (2004b). Assimilation of the satellite altimetry data in the eddy-resolving model of the Black Sea circulation, Marine Hydrophys. Journ. N1 pp52–68 (in Russian).

Dorofeyev, V.L., S.G. Demyshev and G.K. Korotaev (2001). Eddy-resolving model of the Black Sea circulation. In "Ecological Security of Coastal and Shelf Zone and Complex use of Shelf Resources" (A.I. Felzenbaum memorial volume), Sevastopol, p.71–82. (in Russian).

Eremeev, V.N., E. Horton, S.V. Motyzhev, P.-M. Poulain, S.G. Poyarkov, D.M. Soloviev, S.V. Stanichny and A.G. Zatsepin (2002). Studies of Black Sea macro- and mesoscale circulation with application of SVP and SVP-B drifters. Present results and future plans. Development in Buoy Technology, Communications and Data Applications, UNESCO DBCP CD ROM Technical Document Series, No. 21–2002. Article No.8, P.1–9.

Korotaev, G.K., O.A. Saenko and C.J. Koblinsky (2001). Satellite altimetry observations of the Black Sea level. Journ. Geoph. Res. V.106 N C1 pp 917–933.

Korotaev, G.K., T. Oguz, A.A. Nikiforov and C.J. Koblinsky (2003). Seasonal, interannual and mesoscale variability of the Black Sea upper layer circulation derived from altimeter data. Journ. Geoph. Res. Vol. 108 N C4.

Korotaev, G.K., V.L. Dorofeyev and T.Yu. Smirnova (2004). Accuracy of the diagnosis of surface currents in the system of the Black Sea satellite monitoring. In: "Ecological Security of Coastal and Shelf Zone and Complex use of Shelf Resources" V.11 Sevastopol 2004 pp. 75–92 (in Russian).

Oguz, T., H. Ducklow, P. Malanotte-Rizzoli, J.W. Murray, V.I. Vedernikov and U. Unluata (1999a). A physical-biochemical model of plankton productivity and nitrogen cycling in the Black Sea. Deep Sea Research, I, 46, 597–636.

Oguz, T., U. Unluata, H.W. Ducklow and P. Malanotte-Rizzoli (1999b). Modelling the Black Sea pelagic ecosystem and biogeochemical structure: A synthesis of recent studies. In: "Environmental Degradation of the Black Sea: Challenges and Remedies", S. Besiktepe, U. Unluata and A. Bologa (Eds). NATO ASI Series, i 2–56, Kluwer Academic Publishers, 197–224.

Oguz, T., J.W. Murray and A. Callahan (2001a). Simulation of Suboxic–Anoxic interface zone structure in the Black Sea. Deep Sea Research I, 48, 761–787.

Oguz, T., H.W. Ducklow, J.E. Purcell and P. Malanotte-Rizzoli (2001b). Simulation of recent changes in the Black Sea pelagic food web structure due to top-down control by gelatinous carnivores. J. Geophys. Res,., 106, 4543–4564.

Ratner, Yu.B., S.V. Stanichny and D.M. Solov'ev (2004). Comparison of the values of the Black Sea surface temperature obtained from the data of the NOAA AVHRR–3 equipment and SVP-drifters in March–August 2003. In: Ecological Security of Coastal and Shelf Zone and Complex use of Shelf Resources V.11 Sevastopol pp. 155–173 (in Russian).

Ratner, Yu.B. and T.M. Bayankina (2004). Comparison of the surface temperature values obtained from the model of the Black Sea dynamics and the data of SVP-drifters in March–August 2003. In: "Ecological Security of Coastal and Shelf Zone and Complex use of Shelf Resources" V.11 Sevastopol pp. 51–62 (in Russian).

Tolstosheev, A.P., E.G. Lunev, G.K. Korotaev and S.V. Motyzhev (2004). Thermoprofiling drifting buoy. In: "Ecological Security of Coastal and Shelf Zone and Complex use of Shelf Resources" V.11 Sevastopol pp. 143–154 (in Russian).

Present status of the Baltic Operational Oceanographic System

BOOS Steering Group: E. Buch*[1], J. Elken[2], J. Gajewski[3], B. Håkansson[4], K. Kahma[5] and K. Soetje[6]

[1]*DMI, Denmark*
[2]*Marine Systems Institute, Tallin Technical University, Estonia*
[3]*Maritime Institute Gdansk, Poland*
[4]*SMHI, Sweden*
[5]*FIMR, Finland*
[6]*BSH, Germany*

1. Introduction

BOOS is a formal association of institutes from Sweden, Finland, Russia, Estonia, Latvia, Lithuania, Poland, Germany and Denmark taking national responsibility for operational oceanographic services, which will support the protection of lives and properties and the promotion of the development of society. BOOS was officially formed in 2001 when the members signed a Memorandum of Understanding, but the planning and cooperation was initiated several years earlier and the first BOOS strategy was formulated in 1999 (Buch and Dahlin, 2000).

BOOS is based on existing national observation programmes, which are already extensive, but can be made more operational. At present the physical oceanographic observations such as water level, temperature, salinity, waves, currents and sea ice are the most operational in the sense that real-time or near real-time data delivery is implemented by most BOOS member organisations. BOOS is therefore in its present stage of development primarily focusing on the production of services related to physical parameters.

The key word in the BOOS Strategy 2004–2010 is the further integration of the operational oceanography activities in the Baltic Sea, so that by the end of the period BOOS will be able to provide an integrated service to marine users and policy makers in support of safe and efficient off-shore activities, environmental management, security, and sustainable use of marine resources. The strategy involves all elements of an operational oceanographic system:

- Observations including real-time data exchange, quality control and analysis
- Forecast modelling ranging from Baltic scale to local scale with high resolution. The modelling activities will further include assimilation of observations, coupling of models, and a multi-model based prediction system for ensemble forecasting
- Dissemination of products, services and information, primarily via the BOOS homepage, which in the future will be a central portal for marine information for the Baltic Sea.

* Corresponding author, email: ebu@dmi.dk, www.boos.org

A substantial part of the developments of BOOS over the past 2–3 years has been accomplished through the EU-funded project PAPA, resulting in:

- A detailed overview of the observation network (real time and delayed mode). This work has been accomplished in cooperation with the EU-funded project EDIOS
- Fully developed data exchange via ftp boxes (data delivered by all members) with a specially developed exchange software
- New water level stations available on the internet through an upgrading program
- Mapping of QA procedures
- Production of daily maps of SST
- An optimal observation network is under design. This work in being done in close cooperation with the EU-funded research project ODON
- A status report on various existing operational forecasting models and plans for developments
- Implementation of a training and education programme for colleagues from the eastern Baltic countries
- National awareness meetings on operational oceanography.

2. BOOS data exchange

In order to build a regional operational oceanographic system based on contributions from all partners it is necessary to have a well-functioning operational data exchange system. BOOS has built a simple but effective ftp box system to exchange data.

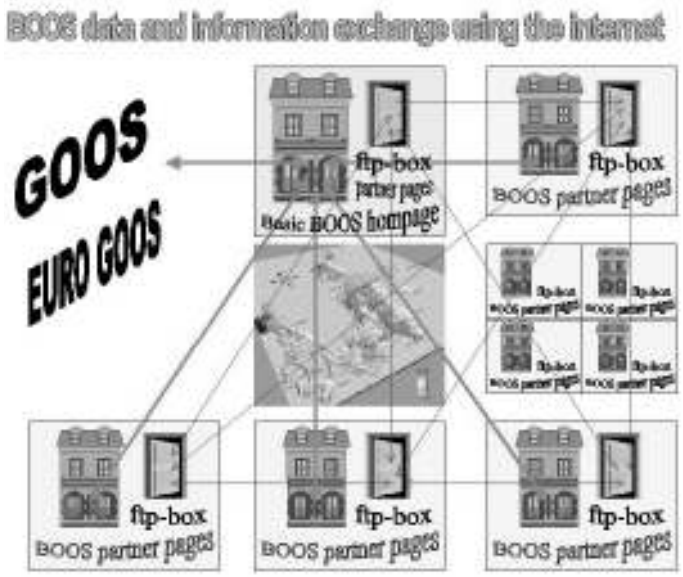

Figure 1 Members of the BOOS co-operation exchange data using a system of ftp boxes. Each member institution puts the data it wants to exchange with the other members in its own ftp box, where it can be collected by the other partners. The system is protected by usernames and passwords.

The experience of BOOS is however that the most severe problem in establishing a data exchange system has not been the technical set-up but institutional and national rules and regulation regarding exchange and release of data. All the legal aspects concerning data exchange, i.e. the right to use data for institutional and commercial purposes, is addressed with great care in the EuroGOOS data policy, which the members have agreed to follow. Despite this agreement it has not been an easy task and it took a long time for some of the individual BOOS members to attain the necessary permission to exchange their data in real-time. Through the PAPA project most of the problems have been solved and the ftp box system has been fully developed.

3. BOOS products

The BOOS web page www.boos.org was first established in 1999, and today presents a number of operational oceanographic products produced using information from all BOOS partners as well as links to the partner product dissemination web pages. Hereby a wealth of operational oceanographic information is available through the BOOS web page.

The first common BOOS product was a display of real-time observations of water levels from selected water level stations in the Baltic. At the start in 1999 only Danish and Swedish observations were available, but since then every country has started to deliver data.

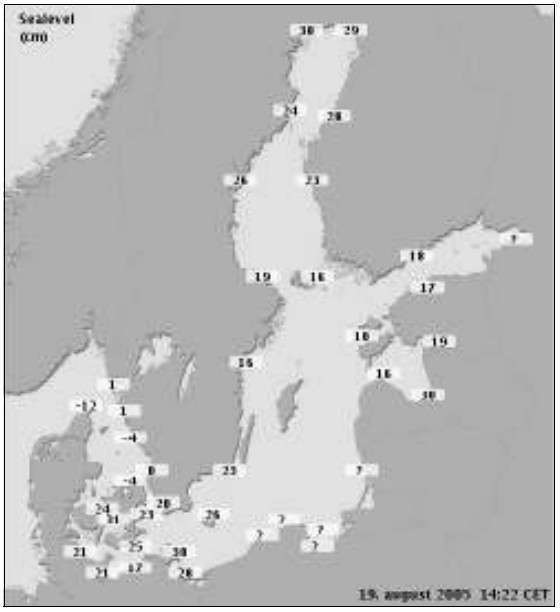

Figure 2 Presentation of real-time observations of water level in the Baltic Sea as presented on www.boos.org.

Sea surface temperature (SST) has been produced on a weekly basis for the Baltic and North Sea for several years by our German colleagues at Bundesamt für Seeschifffahrt und Hydrographie (BSH), but a daily product has been high on the agenda because SST

can change rapidly on a local scale in the Baltic Sea. Therefore daily updates are of importance as information by itself but also for assimilation into meteorological and oceanographic forecasting models. Through the ODON project an operational productions system for a daily SST product for the North Sea–Baltic Sea system has been established based on satellite observations and optimal interpolation technology (Høyer and She, 2004).

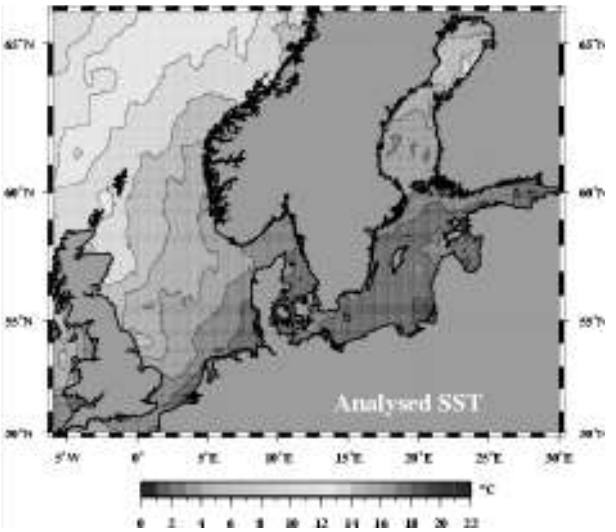

Figure 3 Example (from 9 August 2005) of an SST map produced on a daily basis.

Other real-time observational products produced by a united BOOS effort are waves and harmful algae. Additionally several of the BOOS partners run a suite of operational forecasting models producing forecasts of water level (storm surge warnings), waves, horizontal and vertical distribution of temperature, salinity and currents, transports and drift of passive material such as oil drift. These forecasts are available on the national/institutional web pages linked from the BOOS page. Common BOOS forecasting products are in the development phase.

4. A success story

During 7–9 January 2005, northern Europe was hit by the hurricane Edwin/Gudrun which caused severe property damage in northern Europe and killed at least 17 people. In the Baltic Sea the hurricane caused storm surges and in some regions record high water levels were recorded; for example Pärnu, Estonia observed 275 cm over mean sea level. Also extreme wave heights were experienced in the open Baltic area during this event. No direct observations were available but detailed analyses performed by BOOS members (Soomere *et al.*, 2005) indicate wave heights of the order of 10–11 m, which are exceptional in this region.

The hurricane was predicted by the national meteorological agencies well in advance and within the BOOS community forecasts of water level and waves were exchanged. This exchange of forecasts was of great value to the countries in the eastern Baltic which had

a storm surge warning system operational at the time. Estonia, which was right in the centre of the hurricane track, especially benefited from this information exchange and the information was broadcasted through the media and used in preparedness operations, thereby contributing to the saving of lives and property.

The Estonian government have subsequently established a more formal storm surge preparedness organisation, which relies on the established BOOS cooperation for the operational forecasting part.

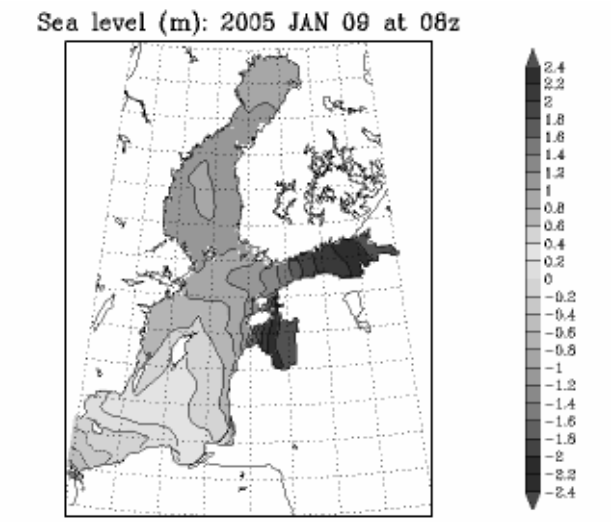

Figure 4 Water level forecast for 9 January 2005 0800 as produced on 7 January 2005 1200.

References

Buch, E. and H. Dahlin (2000). BOOS Plan. Baltic Operational Oceanographic System 1999–2003. EuroGOOS publication no. 14.

Høyer J.L. and J. She (2004). Validation of satellite SST products for the North Sea and Baltic Sea region. Technical Report 04–11, Danish Meteorological Institute.

Soomere, T, A. Behrens, L. Tuomi and J.W. Nielsen (2005). Unusual wave conditions in the Baltic Proper and in the Gulf of Finland during windstorm Gudrun. Boreal Environment Research (Submitted).

Operational Oceanography for the North West European Shelf Seas NOOS 2002–2005

M.W. Holt*

Met Office, UK

Abstract

Arising from the EuroGOOS NW Shelf task team, the NW Shelf Operational Oceanographic System NOOS was established in September 2002, with national agencies signing a Memorandum of Understanding. Membership of NOOS has now grown to twelve agencies, with responsibilities ranging from monitoring to forecast modelling, and there are three associate research institutes. Members of NOOS routinely provide a range of services to their national governments, and some are also demonstrating this through participation in ESA GMES service element projects. NOOS works through networking to establish collaborative, incremental developments to the day-to-day business of the member agencies. Thus NOOS activities are truly sustainable. Where available, individual member agencies gain project funding from national or EC Framework Programme research projects.

NOOS activities include data exchange for sea level observations and storm surge forecasts, co-operation on development of 3D forecast modelling, contribution to the ICES–EuroGOOS North Sea pilot project for an ecosystem-based approach to fisheries management, exchange of calculated model transports, and bi-lateral developments to provide robust and resilient backup for storm surge forecast modelling.

Keywords: Operational oceanography, shelf seas, modelling, marine ecosystem, monitoring, GMES services, storm surge forecasting

1. Introduction

Developing from the EuroGOOS NW Shelf Task Team, NOOS was formed in September 2002 following the operational agencies signing a Memorandum of Understanding. This paper gives an overview of the resources provided by the NOOS partners, describes the services provided by the NOOS partners, and describes the voluntary co-operation activities undertaken by NOOS.

2. NOOS: Partners and resources

2.1 NOOS partners

Full membership of NOOS is open to those national agencies providing operational oceanographic services to government. Associate membership is open to research institutes and non-governmental or other multi-national organisations with aims and objectives consistent with those of NOOS. In June 2005 there were twelve full partners and three associate members. These represent Norway, Sweden, Denmark, Germany, the

* Corresponding author, email: martin.holt@metoffice.gov.uk

Netherlands, Belgium, United Kingdom and Ireland, covering the entire coastline of the North Sea and Irish Sea. Full details are given on the NOOS website www.noos.cc.

2.2 NOOS resources

The funding available to NOOS member institutes comes primarily from the national governments, with some support for research and development projects provided by the European Commission (DG Research). The approximate proportions of the available annual budget are shown in Figure 1, which covers the staff and *in situ* monitoring costs across a range of agencies. This does not include ship time, national contributions to remote sensing costs, or the cost of provision of supercomputing facilities. By far the bulk of the annual budget of NOOS partners is concerned with operating and maintaining monitoring networks. In addition to the resources outlined in Figure 1, NOOS partners operate a range of research vessels or have access to ship time, and several NOOS partners run ferryboxes.

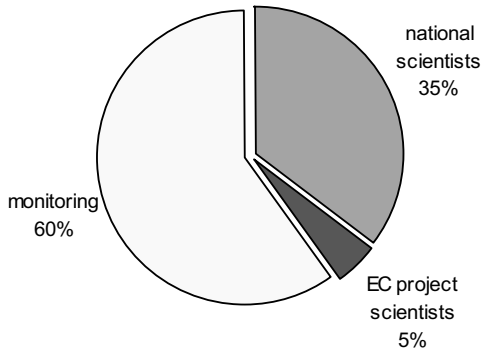

Figure 1 The approximate distribution of the relevant annual budgets of NOOS members, showing the breakdown between costs of *in situ* monitoring, scientists on nationally funded activities and research supported by European Commission Framework Programme projects.

3. NOOS: providing services

NOOS members provide a range of services to their national and regional governments and to industry. These include coastal flood forecasting (waves, storm surges), search and rescue forecast modelling, oil spill or marine pollution drift forecasts, met-ocean forecasts for offshore oil and gas operations, forecasts for shipping transport including services contributing to safety of life at sea, sea ice forecasting and monitoring, harmful algal bloom monitoring and warning, fisheries management assessments, forecasts for defence and naval operations, and monitoring and forecasting in coastal waters for tourism and leisure.

A summary of the key services is presented in Table 1. An in-depth evaluation of these and other developing services for the NW Shelf is being carried out by the NOOS steering group during 2005. These services are provided as national contributions to intergovernmental agreements such as JCOMM, MPERSS, GMDSS and OSPAR. In addition to those listed in Table 1, some of the northern members of NOOS also provide services for sea-ice forecasting.

Table 1 Summary of key services.

Service	Present capability	Gaps and required developments	User groups
Storm surge forecast	2D surge models, nested high resolution models for local coastlines. Met forcing updated four times daily. NOOS exchange of selected point forecasts.	Quantification of risk: Ensemble forecasts. Data assimilation. Estuary scale modelling.	National protection agencies, local authorities. Shipping ports and harbours.
Oil spill drift prediction	Some models are tide only. Some can use forecast winds and currents. Some are 3D (for seabed blowout modelling). Some use web interface.	Web interface as required for all users. Improved use of forecast currents, including 3D. Validation.	National protection agencies MPERSS
Water quality and HAB forecast	Ferry box monitoring, *in situ* monitoring, remote sensing. 1D or box ecosystem modelling. Demonstrations of 3D nowcast modelling.	Full 3D marine ecosystem nowcast-forecast modelling. Additional monitoring.	National protection agencies, public, local authorities.
Waves and sea state	High resolution regional 2nd and 3rd generation wave models, updated four times daily with latest regional weather prediction forcing. "Rogue wave" risk index. Forecast wave energy spectra.	Nested higher resolution near local coastlines, use of spectral nearshore transfor-mation models.	Ship routing, including commercial companies, coastal flood forecasting.

4. NOOS: making a difference

The first activity to develop under NOOS was the exchange of storm surge forecasts at selected points around the North Sea coastline. Each day the participants prepare timeseries datasets and place them in "ftp boxes" for retrieval by the others. Some of the agencies have developed display and decision aid tools to present the different forecasts. This "poor man's multi-model ensemble" helps to quantify the error in the predicted timing and amplitude of a surge event. In addition the data exchange provides important resilience in the event of the failure of any of the individual forecast systems. A web-based display system "MATROOS" is under development at RIKZ, and may be later made available to all participants.

For validation of the surge forecasts, an exchange of water level (tide gauge) data has been established, and these data are also displayed on the NOOS website. Since the EuroGOOS conference 2002 (Holt, 2003), this has extended to include the full North Sea coastline. Using the exchanged data, a storm surge forecast validation study was carried out by RIKZ, and presented at the EGS 2004 meeting. In this way all participants have gained further information and understanding from the exchange activity, with the workload shared.

Other work in NOOS seeks to develop a 3D forecast modelling infrastructure, with provision of boundary data for nested local 3D models of the North Sea. Part of this work is supported by MERSEA. NOOS partners are sharing information on river flow rates and inputs to the NW Shelf, and there is also collaboration on provision of

boundary data for modelling the Norwegian Sea. A new project is the exchange and intercomparison of modelled transports.

As the former SEANET project agency partners are now in NOOS, a new NOOS activity will be defined during 2005, to address shared development and operation of NW Shelf monitoring networks.

NOOS partner participation in European Commission research projects includes FP5 EDIOS, ODON, FerryBox, MERSEA, Sea-Search, MAXWAVE, DISMAR, and FP6 MERSEA IP. NOOS partners make the transition from research to operations.

MUMM, Met Office, BSH, POL, IMR and met.no are contributing to the ICES–EuroGOOS North Sea pilot project, providing recent climate status assessments of the North Sea for use in an ecosystem based approach to fisheries management. This project is also demonstrating a fisheries application for nowcast coupled physical-ecosystem modelling (Figure 2).

4.1 National activities

A broad range of nationally funded activities take forward capability and service development within NOOS, and experience from these projects is shared. These activities include the POL Irish Sea Coastal observatory, the Norwegian MONCOZE, the UK and Norwegian application of nowcast-forecast marine ecosystem 3D modelling, and the NIVA ColorLine ferrybox (Figure 3) (www.ferrybox.no).

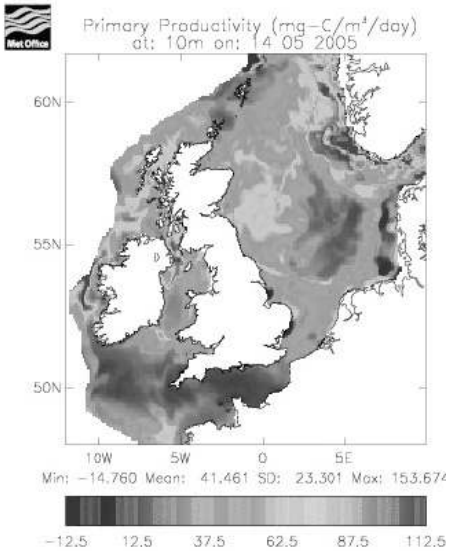

Figure 2 Model estimate of primary production, from the Met Office nowcast of the POLCOMS_ERSEM model.

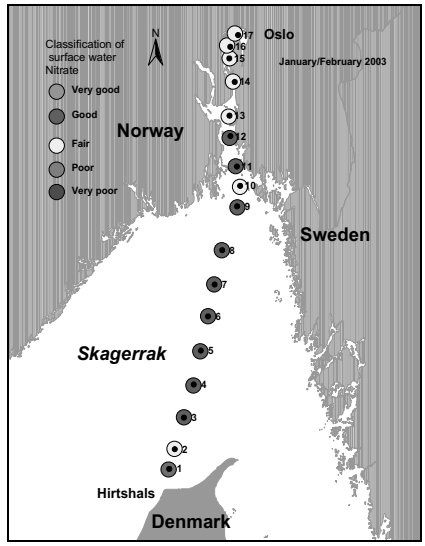

Figure 3 Example of classification (Eutrophication) of surface water according to the Norwegian classification system (Oslo–Hirtshals) (courtesy of NIVA).

5. NOOS challenges: 2008 and beyond

The aim of NOOS is to achieve efficient shared development and production of ocean monitoring and forecasting services for the European NW Shelf. The challenge facing NOOS partners is to do that within the constraints of existing national and European budgets, and within the developing framework of GMES and GEO. An important task here is to provide inputs to the SEPRISE project, and to provide effective demonstration of a "networked" capability for monitoring and forecasting for the NW European shelf seas.

NOOS builds on the day-to-day business of the operational agencies, so NOOS is sustainable. Many of the anticipated sustainable services of GMES will be provided by NOOS member agencies.

Acknowledgements

Information, figures and material provided by the NOOS partners and the NOOS steering group members are gratefully acknowledged.

References

Holt, M.W. (2003). Towards NOOS — the EuroGOOS NW Shelf task team 1996–2002 in Dahlin, H., N.C. Flemming, K. Nittis, and S.E. Petersson (eds.) (2003). Building the European Capacity in Operational Oceanography, Proceedings of 3rd EuroGOOS Conference, Elsevier Oceanography Series. pp 461–465.

Mediterranean Forecasting System Toward Environmental Prediction (MFSTEP): status of implementation

Nadia Pinardi[1], Mario Adani, Alessandro Bonazzi, Alessandro Coluccelli, Giovanni Coppini*[1], Srdjan Dobricic, Vicente Fernandez Lopez, Claudia Fratianni, Sara Lunghi, Francesca Marzocchi, Paolo Oddo, Marina Tonani and MFSTEP partners

[1]*Istituto Nazionale di Geofisica e Vulcanologia–INGV, Bologna, Italy*

Abstract

The main elements of the Mediterranean Forecasting System (EuroGOOS Publication No. 11, 1998) are now upgraded and developed by the EU project "Mediterranean ocean Forecasting System: Toward Environmental Predictions" (MFSTEP) that started 1 March 2003 and will end in February 2006.

MFS is based on the demonstration of the real time functioning of an integrated system composed of:

- the near real time observing system
- a numerical forecasting systems at basin scale and for sub-regional areas
- a product dissemination/exploitation system.

The MFSTEP Targeted Operational Period started in September 2004 and the project has produced basin scale (6.5 km resolution) and sub-regional forecasts up to 3 km resolution in several open ocean and shelf areas. Forecast production is ongoing and forecasts are produced once a week at the basin scale for 10 days and at the sub-regional scale for 5 days, using Limited Area Model high resolution weather forecasts. The observing system is also working in real time and all data (satellite and *in situ*) are assimilated into the basin scale model. The forecasts and analysis data are available in real time to both an internal and external community of users. The latter is composed of governmental and military agencies, environmental protection agencies, research institutes and private companies.

The system has also developed biochemical models for future predictions of algal blooms in different shelf areas. End-user applications involve oil spill forecasting, contaminant dispersion in coastal areas, a real time observing and modelling system for fish management, search and rescue forecasts and Rapid Environmental Assessment modelling. Finally, a study of the forecast economic value and impact is being carried out.

The operational functioning of the MFS is demonstrated through the MFSTEP web site: http://www.bo.ingv.it/mfstep/.

Keywords: Operational oceanography, forecasting system, Mediterranean Sea.

* Corresponding author, email: coppini@bo.ingv.it

1. Introduction

1.1 Current status of the Mediterranean Forecasting System

The main elements of the Mediterranean Forecasting System are now upgraded and developed by the EU project MFSTEP that will last 3 years, ending in February 2006.

The Mediterranean Forecasting System that has been developed, demonstrated and made operational is composed of:

- A near real time observing system
- A numerical forecasting system at basin scale and with downscaling in sub-regional and shelf areas
- A product dissemination/exploitation system.

The MFSTEP Targeted Operational Period (TOP) started in September 2004 and ended in March 2005, collecting a large amount of data for assimilation and model verification. Part of the deployed observing platforms are still active and observations will continue to be collected for the next year.

During TOP, eight forecasting centres have started to produce forecasts in real time at the basin scale (6.5 km of resolution) (Figure 1), at four sub-regional areas with a resolution up to 3 km and in four shelf areas with a resolution of 1.5 km. Forecasts are produced once a week at the basin scale for 10 days and at the sub-regional scale for 5 days, using Limited Area Model (LAM) high resolution weather forecasts.

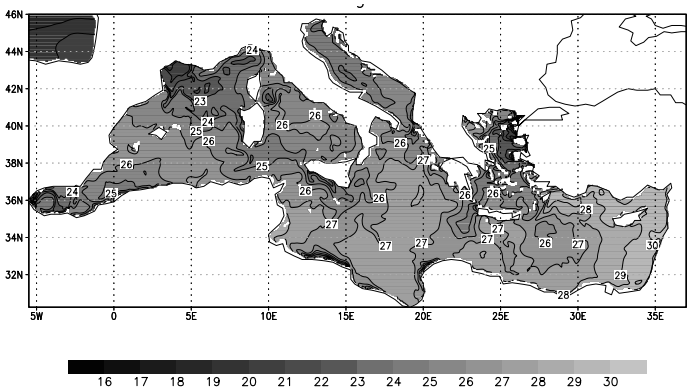

Figure 1 Surface temperature forecasted for 30 August 2005 by the large scale model upgraded in MFSTEP.

MFSTEP has also organised a downloading and viewing service (following the INSPIRE nomenclature), i.e. data are displayed operationally through a Web service and products are also downloadable by the interested community using ftp with password. The end-user community is composed of governmental and military agencies, private companies, environmental protection agencies and research institutes.

MFSTEP has also developed a new biochemical model (so-called BFM) that is constructed to be easily interfaced with operational hydrodynamic models for future predictions of algal blooms in different shelf areas.

End-user applications involve oil spill forecasting, contaminant dispersion in coastal areas, real time observing and modelling systems for fish management coupled to ocean forecasting, search and rescue forecasts and Rapid Environmental Assessment modelling. Finally the study of the forecast economic value and impact is being carried out.

This paper gives an overview of the products and results for the five components of MFSTEP:

a) The real time observing system

b) The numerical forecasting systems

c) The ecosystem modelling and data assimilation

d) The viewing and downloading MFS CORE service

e) The end-user applications and services.

2. The real time observing system

The observing system components running operationally progressively since summer 2004 are:

1. Voluntary Observing Ship (VOS) programme composed of 9 tracks with 12 nautical miles resolution (Figure 2) and full profile transmission (Manzella *et al.*, 2003). As part of the technological improvements, a multiple launcher for XBT has been constructed and will be tried operationally. Furthermore a new prototype expandable instrument (T-FLAP) has been constructed that can collect temperature and fluorescence data from VOS as well as a new tethered instrument for multidisciplinary upper thermocline monitoring (SAVE) also from VOS.
2. A network of Mediterranean Multidisciplinary Moored Array (M3A) stations with real time collection and dissemination of data (E1–M3A in the Cretan Sea, E2–M3A in the Southern Adriatic Sea, W1–M3A in the Ligurian Sea) (Nittis *et al.*, 2003). Figure 3 shows time-series of chlorophyll *a* at different depths from the E1–M3A buoy. The calibrated values (Figure 3 right) are able to capture the well-known structure of the summer–autumn period with the chlorophyll maximum at ~110 m depth.
3. 23 MEDARGO floats deployed from VOS, with 350 m parking depth, 700 m profiles and a 5-day cycle (every 5 cycles a 2000 m profile is also collected) (Figure 4).
4. An altimeter near real time data analysis system using four available altimeter sensors for sea surface elevation anomalies.
5. A real time analysis of satellite radiometric measurements (AVHRR) that produces daily SST fields from night time passes (Buongiorno Nardelli *et al.*, 2003).
6. A near real time analysis of scatterometer winds producing daily optimal estimates of surface winds.
7. A glider autonomous vehicle experiment in the Ionian Sea (a coastal glider sampling down to 200 m depth and a deep glider sampling down to 950 m depth) (Figure 5).

The real time data dissemination network works properly on a weekly time scale.

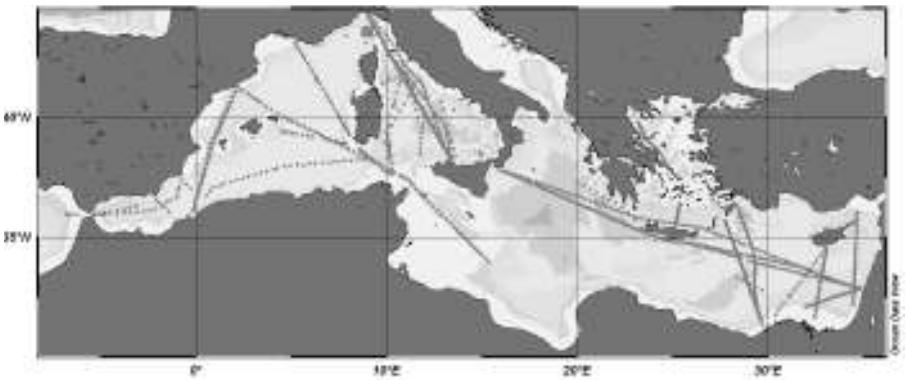

Figure 2 XBT drops from May 2004 to April 2005 within the MFSTEP project showing bathymetry.

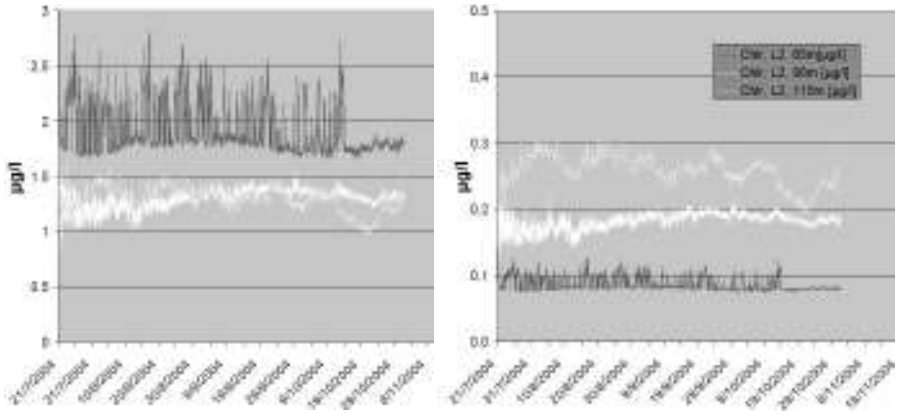

Figure 3 Time-series of chlorophyll *a* at different depths from the E1–M3A site in the Aegean Sea. The calibrated values (right) are able to capture the well-known structure of the summer–autumn period with the chlorophyll maximum at ~110 m depth.

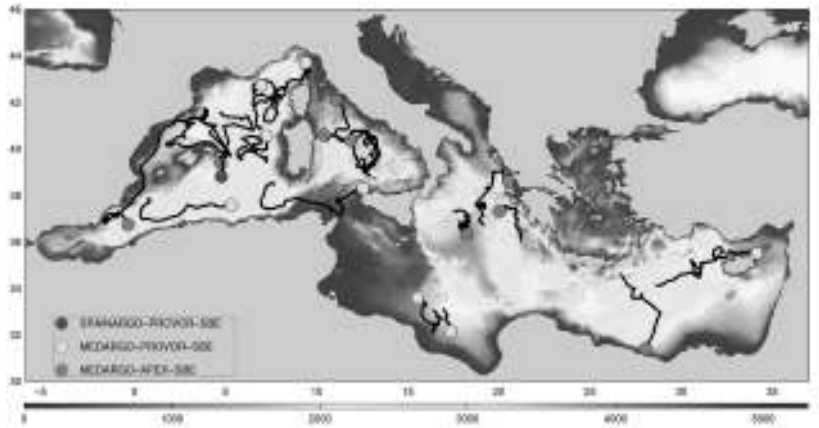

Figure 4 Tracks and positions of the MEDARGO floats.

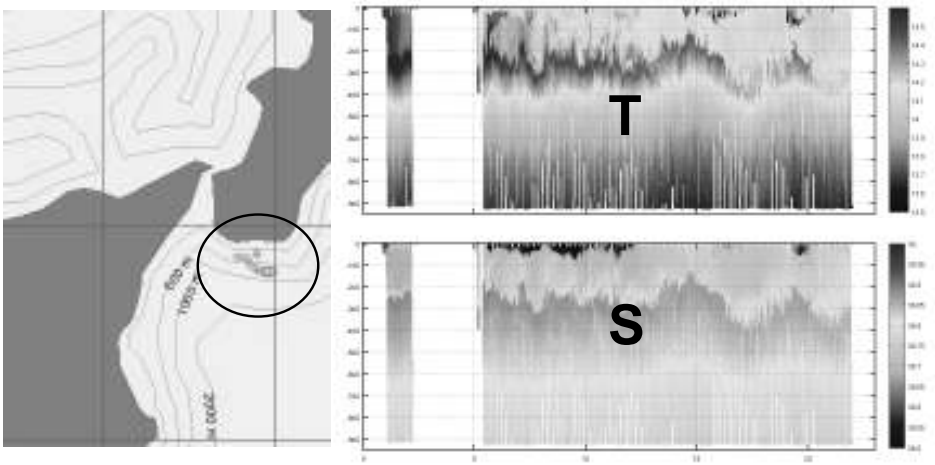

Figure 5 Glider temperature data in virtual mooring mode south of Calabria (1–25 February 2005 ~500 km).

The sampling strategy in the Mediterranean is assessed by the Observing System Simulation Experiment (OSSE) activities. The OSSE experiments have shown the complementarities of the first three elements of the observing system listed above and the final results will show the optimal sampling scheme for the Mediterranean basin scale circulation. Innovative assimilation of float trajectories from MEDARGO is being completed.

3. The numerical forecasting system component

The operational numerical forecasting system component is now composed of:

1. A 10-day basin scale forecasting model at 6.5 km resolution and 71 levels. The forecasts have been available in real time for the whole of the Targeted Operational Period–TOP (Figure 6).
2. Four regional forecasting models at 3 km resolution in four regions nested in the basin scale model. The regions are the North-Western Mediterranean, the Sicily Strait, the Adriatic Sea (Figure 7) and the Aegean-Levantine Sea. Forecasts are produced weekly and for five days in the future.
3. Four shelf forecasting models at 1.5 km resolution in four regions nested in the regional scale models. The shelf area systems are: CYCOFOS, for the Eastern Levantine and Cyprus shelf, the GULF OF LION shelf area, the MALTA shelf area, the South-Eastern Levantine shelf area. Other shelf models have been implemented but they are not operational.
4. Operational weather forecasts at 10 km resolution are produced to force the regional and shelf nested models with the SKYRON–Athens (Kallos, 1997) and the Météo-France–Czech Republic LAM systems (Radnoti *et al.*, 1995; Horanyi *et al.*, 1996).
5. Several new schemes for data assimilation at the basin scale and for the nested models have been developed. An upgraded Reduced Order Optimal Interpolation

Scheme for the basin scale model is now assimilating with a daily cycle sea level anomalies, XBT profiles, ARGO profiles and satellite composites of sea surface temperature. Data assimilation tools developed for shelf models are:

- A variational initialisation scheme for nested models
- A multivariate variational initialisation and assimilation scheme that allows the coarser scale model outputs and the local observations to be considered at the same time.

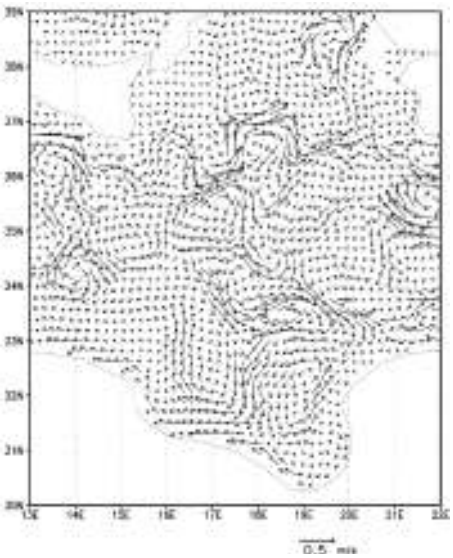

Figure 6 Surface currents (1 m) forecasted for 30 August 2005 by the large scale model upgraded in MFSTEP.

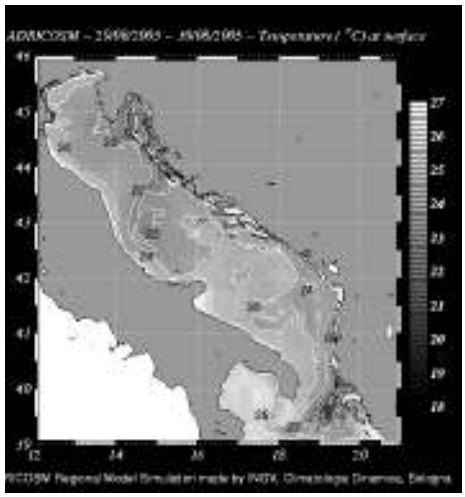

Figure 7 Sea surface temperature forecasted for 29 August 2005 by ADRICOSM.

Forecasting bulletins are produced and data can be accessed on the local web sites:

1. ADRICOSM forecasting system for the Adriatic Sea: http://www.bo.ingv.it/adricosm
2. ALERMO forecasting system for the Levantine and Aegean Sea: http://pelagos.oc.phys.uoa.gr/mfstep/bulletin
3. North Western Mediterranean Sea forecasting system: http://www.noveltis.net/mfstep-wp9/interface/english/NWMED_bulletin.php
4. SICILY CHANNEL forecasting system: http://www.imc-it.org/progetti/mfstep/Forecast/bulletin.htm
5. CYCOFOS: http://www.ucy.ac.cy/cyocean/cycofos/bulletin.php
6. GULF OF LION forecasting system: http://www.noveltis.net/mfstep-wp9/interface/english/GL_bulletin.php
7. MALTA forecasting system: http://www.capemalta.net/MFSTEP/results.html

4. The ecosystem modelling sub-component

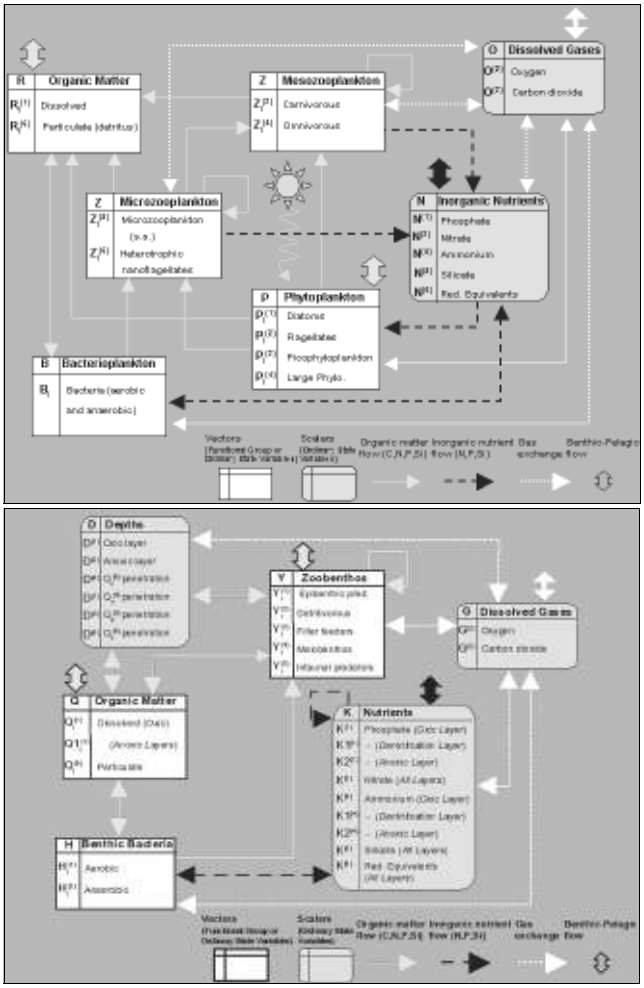

Figure 8 Top: Schematic of the BFM pelagic component structure; Bottom: Schematic of the BFM benthic component structure.

In MFSTEP one new numerical model for the marine food web has been developed and disseminated. It is called the Biochemical Flux Model (BFM) and is the evolution of the previous ERSEM code, developed in the third EU–FP under the MAST theme. The BFM is still based upon a biomass and functional group representation of the marine food web (Figure 8) but it now considers more processes in the bacterial compartment including variable carbon to chlorophyll ratio, allowing for phytoplankton adaptation to light in the open ocean areas. The code has been constructed to be easily coupled to any hydrodynamic model, via a coupling interface that is now left free to the user to specify. The code is written in F90 and is implemented in the Adriatic Sea and the Levantine and Aegean Seas.

In addition to the BFM, the Singular Evolutive Extended Kalman filter (SEEK) has been coupled to the biochemical flux model and disseminated in order to start experiments on the assimilation of surface chlorophyll data from satellites.

5. The viewing and downloading CORE service

MFSTEP has developed a CORE service for ocean currents in the Mediterranean Sea. This CORE service consists mainly of making available several gridded model data sets integrating the observations and the model output via data assimilation.

The products disseminated by this CORE service are essentially the basic hydrodynamic state variables such as sea level, tri-dimensional currents, tri-dimensional temperature, salinity and density fields. Some ancillary fields are also considered such as the heat fluxes, the surface stresses and the water flux.

Two different CORE services are implemented:

1. A **viewing service** that provides a Web-based access to images that represent graphically the products. This service is useful for the general public, for far-reaching discovery purposes, and for educational purposes.
2. A **downloading service** that provides an ftp-based data transmission system between the basin scale models and the sub-regional/shelf scale forecasting centres, between the different forecasting models and some of the end-users applications.

This part of MFSTEP developed in a rapid way before the TOP and it has been the basic means for accessing both images and numerical information from the forecasting centres by commercial users and other end-users such as fishermen.

6. The end-user and application services

The end-users component that exploit the nowcasting/forecasting products made available from the CORE service is composed of:

- Oil spill forecasting models
- Floating objects forecasting models
- Contaminants fate prediction models
- Relocatable models for fast emergency intervention at sea
- Combination of hydrodynamic field state variables and pelagic fish data sets for stock assessment and management in the open sea and Adriatic shelf areas.

MFSTEP applications have been designed to meet the needs of international conventions and agreements in the Mediterranean Sea. In particular, MFSTEP will contribute to organising the response to oil and other contaminant pollution in the Mediterranean Sea as defined by the Barcelona Convention. Furthermore, it will help to develop new strategies for sustainable fisheries by providing new and solid observational and modelling evidence of the coupling between hydrodynamics and fish stock biomass variables.

7. Conclusions

A short term forecasting system for the Mediterranean basin scale and the coastal areas has been developed that provides continuous monitoring of the flow field evolution and

its changes. Such a system is the backbone for more environmentally oriented systems that will provide forecasts in the near future of coastal algal biomass variability, pollutant dispersion and indicators of ecosystem health and change.

The concept is that dynamic downscaling is required in order to reach the necessary resolution for the appropriate simulation of transport and coastal processes and for coupling with biochemical tracers. This paper demonstrates that forecasting from the basin scales to the shelf areas is practical with present day technology and that MFS can be used to set up support warning systems for some environmental hazards.

This system also provides the means to improve our understanding, and our capability to accurately model the physical processes with an incremental approach and the optimal usage of all information.

Acknowledgements

This work has been funded by MFSTEP, a project supported by the European Community, V Framework Programme — Energy, Environment and Sustainable Development; Contract no. EVK3–CT–2002–00075. All the partners of the project are thanked for their contribution to the material of this document.

References

Buongiorno Nardelli, B., G. Larnicol, E. D'acunzo, R. Santoleri, S. Marullo and P.Y. Le Traon (2003). Near Real Time SLA and SST products during 2 years of MFS pilot project: processing, analysis of the variability and of the coupled patterns. Annales Geophysicae 21 (1), 103–121.

Kallos, G. (1997). The Regional weather forecasting system SKIRON. Proceedings of the Symposium on Regional Weather Prediction on Parallel Computer Environments, 15–17 October 1997, Athens, Greece. 1–9.

Manzella, G.M.R., E. Scoccimarro, N. Pinardi and M. Tonani (2003). Improved near real-time data management procedures for the Mediterranean ocean Forecasting System — Voluntary Observing Ship program. Annales Geophysicae 21 (1), 49–62.

Nittis, K., C. Tziavos, I. Thanos, P. Drakopoulos, V. Cardin, M. Gacic, G. Petihakis and R. Basana (2003). The Mediterranean Moored Multi-sensor Array (M3A): system development and initial results. Annales Geophysicae 21 (1), 75–87.

Pinardi, N. and N. Flemming (1998). The Mediterranean Forecasting System Science Plan. EuroGOOS Publication No. 11, Southampton Oceanography Centre.

Radnoti, G., R. Ajjaji, R. Bubnova, M. Caian, E. Cordoneanu, K. Von Der Emde, J.D. Gril, J. Hoffman, A. Horanyi, S. Issara, V. Ivanovici, M. Janousek, A. Joly, P. Le Moigne and S. Malardel (1995). The spectral limited area model ARPEGE/ALADIN. PWPR Report Series no. 7, WMO-TD no. 699, 111–117.

IBI–roos: Coordination of an operational oceanography system in the Iberia–Biscay–Irish (IBI) area

Alicia Lavín*[1] and Sylvie Pouliquen[2]

[1]*IEO, Santander, Spain*
[2]*Ifremer, Brest, France*

Abstract

A large number of human sea-related activities such as fishing, maritime transport, aquaculture, security and rescue, and toxic events warming are of high economic and social importance in the Iberia–Biscay–Irish area and are the main motivation for establishing and coordinating an Operational Oceanography System.

The overall objective of the IBI–roos Task Team in partnership with the international communities and agencies is to develop and implement an Iberian, Biscay, Irish regional observation system for optimal and sustainable monitoring and forecasting in this marine region using state-of-the-art remote-sensing, *in situ* measurements, numerical modelling, data assimilation and dissemination techniques. The IBI–roos region comprises almost the entire Celtic Sea, the whole of the Bay of Biscay, the western Iberian margin, and the Gulf of Cadiz.

IBI–roos constitutes a close co-operation between national governmental marine laboratories and agencies in the countries surrounding the area responsible for collection of observations, model operations and production of forecasts, services and information for the industry, the public and other end users. A number of institutions and agencies of Portugal, Spain, France, UK and Ireland are willing to collaborate and Moroccan institutions have been invited to join the Task Team.

The collected data should fulfil operational needs as well as temporary and long-term demands from scientific research and the national policy on sustainable use of coastal regions and calamity prevention (e.g. Erika and Prestige). IBI–roos is being built on existing monitoring programmes and activities at sea and at the coastline sustained by the countries bordering the area. Many of these oceanographic observatories are based on long term projects addressing assessment of practical needs such as fisheries management, sea health or secure transportation.

Many marine-related industries and services can substantially benefit from an ocean observing system based on the operational oceanography concept. The observing and forecasting of harmful algae blooms, fish stocks, pollution, water quality, sea level and waves are of a great importance, not only to the (potential) users whose activities are carried out in the IBI–roos region, but also to a larger Atlantic community.

Keywords: Operational Oceanography, Iberia–Biscay–Irish area, monitoring, modelling

* Corresponding author, email: alicia.lavin@st.ieo.es

1. Introduction

IBI–roos constitutes a close co-operation between national governmental marine laboratories and agencies in the countries surrounding the Bay of Biscay and adjacent seas responsible for collection of observations, model operations and production of forecasts, services and information for the industry, the public and other end users.

The IBI–roos is planned to co-ordinate, strengthen and harmonise the national and international efforts to assess and predict the marine environment and thus effectively improve operational oceanography, defined as the activity of systematic and long-term routine monitoring of the seas, their interpretation, and the rapid dissemination of products (typically forecasts, but also assessments to politicians, and mobilisation of resources to face unexpected events such as the recent Prestige oil spill).

IBI–roos is based on a family of programmes, projects and modules that already exist, which are financed and operated by different institutions and marine laboratories in the Bay of Biscay. The existing ocean observing systems in the Bay of Biscay and adjacent seas have been developed and maintained to meet their own purposes.

The existing observation systems should adapt and integrate new technologies to make observations more complete, more effective and more affordable, and the data infrastructure and management system should be complementary to existing systems and attuned to multiple sources of data and their multiple uses. Ocean observations in the Bay of Biscay and adjacent seas require more effective co-ordination among institutions and countries.

The establishment of an oceanographic operational observing system in the Bay of Biscay will also be relevant for the work of intergovernmental councils such as the Intergovernmental Oceanographic Commission (IOC), the International Council for the Exploration of the Sea (ICES), the convention for the protection of the marine environment of the North-East Atlantic (OSPAR), the International Hydrographic Organization (IHO), the International Maritime Organization (IMO) and the World Meteorological Organization (WMO).

2. Objectives

The overall objective of the IBI Task Team in partnership with the international communities and agencies, is to develop and implement a sustainable system for optimal monitoring and forecasting in the Irish–Biscay–Iberian marine region using state-of-the-art remote-sensing, *in situ* measurements, numerical modelling, data assimilation and dissemination techniques.

In order to meet these objectives there is a need to

- Improve efficiency and reducing redundancy by sharing data, tools and products between the groups
- Encourage networking amongst scientists to improve and share know-how on techniques
- Further develop the observing system network for operational monitoring and forecasting of ocean parameters
- Provide biological data to protect the marine ecosystem and conserve biodiversity

- Improve exploitation and dissemination of data for the existing observing systems, both *in situ* and remote sensing
- Further validate and improve existing modelling systems
- Integrate scales and processes by improving downscaling, nesting techniques and coupling between bio-physical models
- Develop provider services to process and disseminate data and products for the different users
- Improve and provide new services for fisheries, HAB, water quality, sea-level and waves, pollution, etc.

The potential users we plan to reach are:

- Transport
- Harbour operation and design
- Fisheries
- Aquaculture
- Construction and engineering
- Energy production
- Coastal protection
- Environmental protection and preservation
- Recreation
- The scientific community
- Management, administration, and the public.

3. State-of-the-art in the area

The rationales for setting up an IBI–roos Task Team are numerous and can be summarised as follows:

- Physical circulation is well known at the North Atlantic scale, but less at regional level. Interaction between the open ocean and shelf seas is less well-known. The impact of seasonal variability on ecosystems still needs some adjustments.
- Several ocean circulation modelling activities are handled at national level but the coupling of large scale to local scale models is still an emerging activity. Additional validation activities are required.
- Several national services are available for sea level and wave forecasting but with very little collaboration between groups.
- Several experiments have started on coupling between hydrodynamic and biogeochemical models but they still need improvement to reach operational needs.
- A lot of observing systems exist in the area, but are developed at national level, often not coordinated between countries, and not developed enough to be able to efficiently monitor the complete area.

- A lot of satellite data are available but only a few groups use them operationally especially near the coast. Improvement of satellite products and merged satellite/*in situ* products should be made for a better service to users.
- Data management activities are spread among institutions and improvement of data processing and exchange (format, quality control, easy access) should help the use of the data in the community. Synergy with international and EuroGOOS groups is important.

Figure 1 The IBI–roos area in the Eastern North Atlantic, showing bathymetry.

4. Oceanographic characteristic of the area

The IBI-roos region comprises almost the entire Celtic Sea, the whole of the Bay of Biscay, the European sector of the Gulf of Cadiz and the western Iberian margin (Figure 1). The western limit is defined by 10° W and the eastern limit by the continent. The northern limit roughly corresponds to southern Ireland and the southern with Gibraltar.

The hydrodynamics of the region are dominated by the following features:

- A weak anticyclonic circulation in the oceanic part of the Bay of Biscay with mesoscale features such as anticyclonic eddies, a poleward-flowing slope current, a coastal upwelling particularly evident along the western Iberian coast, a northward flow of Mediterranean Water particularly relevant to the (bottom-trapped) shallow and upper cores, and the generation and displacement of eddies carrying MW out of the IBI-roos region.
- A shelf circulation governed by the combined effects of tides (which are particularly important over the Armorican shelf and the southern Celtic Sea), buoyancy (coastal currents induced by run-off from the main rivers) and wind, and river plume fluctuations and lower salinity lenses that sustain the Cold pool called the “Bourrelet froid” (Vincent and Kurc, 1969) isolated in the middle part of the French shelf.

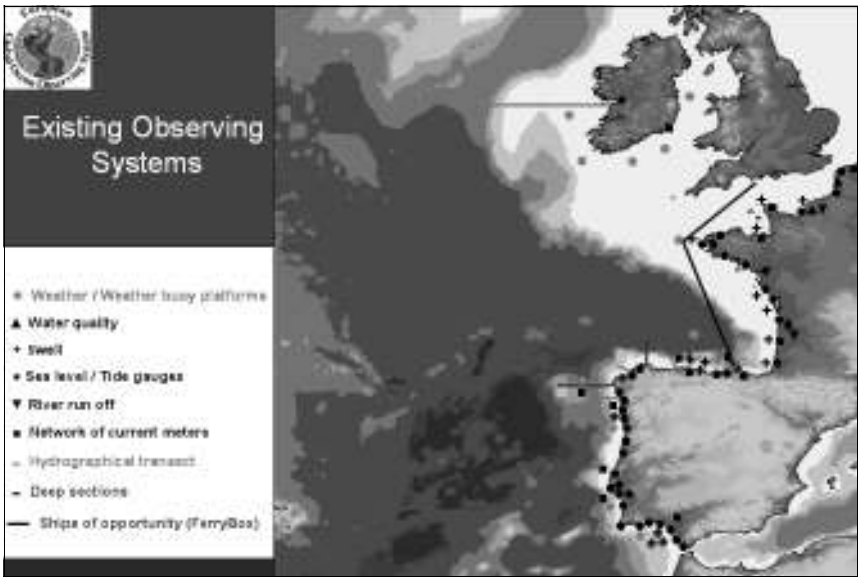

Figure 2 Existing systems in the IBI−roos area.

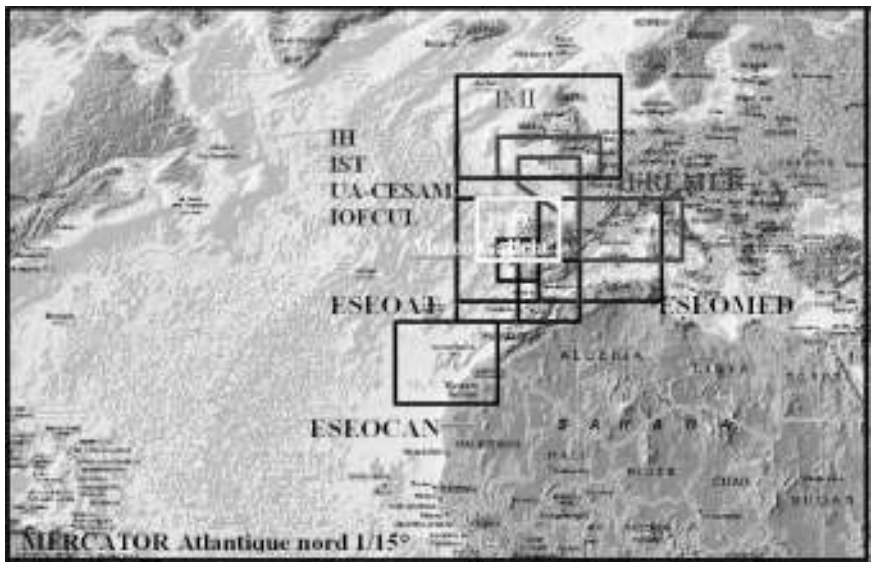

Figure 3 Existing models in the IBI−roos area.

5. Existing systems in the area

IBI−roos is being built on existing monitoring programmes and activities at sea and along the coastline sustained by the countries bordering the Bay of Biscay and adjacent seas. Many of these oceanographic observatories are based on long term projects addressing the assessment of practical needs such as fisheries management, sea health or secure transportation.

Most physical parameters can be measured accurately with sensors from research and commercial vessels, fixed platforms, profilers and floating buoys. Although all these systems lack synopticity, remote sensing systems can resolve the spatial variability for some parameters and therefore support operational products offered in near real time.

Biological measurements are still at earlier stages of technical development and real-time data, temporal coverage and spatial resolution of processes are bottlenecks that limit the generation of operational products. The creation and introduction of new technology regarding biological measurements should be considered as a challenge to IBI–roos in itself.

Despite the fact there is no common action yet, several institutes in South-Western Europe are actively working on developing modelling and assimilation in the area of the Irish, Biscay and Iberian shelves and slopes going from large scale (basin and regional scales) to small scale (coastal and even local scales). It is obvious that networking activities between the different model teams will benefit the community in terms of providing better forecasts in the IBI area.

6. Strategic plan

6.1 Observation needs

A long list of needs according to the strategic plan has been elaborated after review of existing monitoring systems: river runoff necessities, synoptic T/S information of the water column, lagrangian T/S profilers, monitoring by vessels of opportunity (VOP), improved links between remote sensing and *in situ* data, improves bottom topography, development of new systems as gliders, etc.

6.2 Model from regional to coastal

The main effort planned by the IBI–roos modelling team will be based on the downscaling from global to regional, coastal and local scales. Techniques for downscaling, nesting and coupling will be improved, validation of the different systems will be completed at all scales and the complete system will be a ‘best effort’ as well as operational.

6.3 Providing services/users

The main services have been identified but more detailed plans need to be elaborated in the following areas: fisheries, harmful algal bloom, pollution, sea level and waves, and water quality.

6.4 Data management and exchanges

A number of systems for data management, archiving, and data distribution already exist in the enlarged Bay of Biscay area but they are handled at national or institution level with poor coordination between institutes, especially for coastal and real-time applications. Moreover *in situ*, satellite and model data are often processed, archived and distributed through separate means, which does not help development of value-added applications.

IBI–roos will take advantage of theses systems to build a ‘system of systems’ which will provide oceanographic and environmental information to a wide range of users. This

'system of systems' will consist of existing components and networks; it will be based on the MERSEA project and the SEADATANET initiative funded in the framework of the EC's 6th Framework Programme. The aim is to enable users to access information stored at different locations from a 'one-stop' shopping point, which will also make the link with global networks.

The plan would ease data sharing between the different contributors, extending existing services and leading to an integrated data and product service for the IBI–roos community. For this we plan to build the IBI–roos box shown in Figure 4 that will make the link between the global system, under construction within MERSEA Integrated Project, and existing local/coastal systems that are in direct connection with the coastal application users at governmental and commercial level.

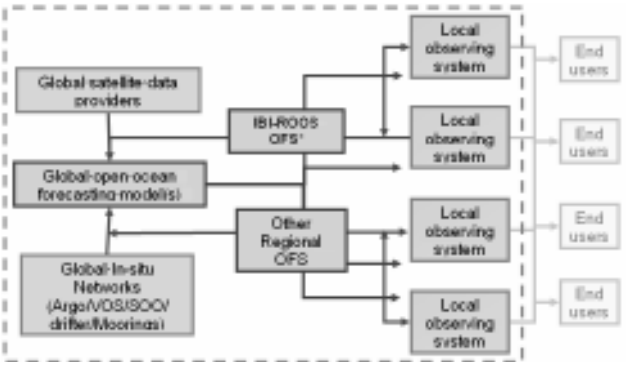

Figure 4 Data sharing with IBI–roos.

Table 1 Institutes that have participated in one or several of the three IBI–roos meetings and could be members of the IBI–roos Task Team

EuroGOOS members	Non EuroGOOS members
IFREMER (France)	IST (Portugal)
IEO (Spain)	NOC (GB)
Puertos del Estado (Spain)	Meteo Galicia (Spain)
Météo-France	IIM–CSIC (Spain)
IMR (Ireland)	IRD (France)
Mercator-Ocean (France)	Ipimar (Portugal)
	Fundacion AZTI (Spain)
	Universidade de Lisboa (Portugal)
	Instituto Hidrografico (Portugal)

References

Dahlin, H., N.C. Flemming, K. Nittis, and S.E. Petersson (eds.) (2003). Building the European Capacity in Operational Oceanography, Proceedings of 3rd EuroGOOS Conference, Elsevier Oceanography Series.

Sandven, S. (2005). The Arctic Ocean and the Need for an Arctic GOOS, EuroGOOS Publication no. 22, EuroGOOS Office, 31–33.

Governance of Europe's Exclusive Economic Zones: a vision

Jan H. Stel*

University Maastricht, The Netherlands

Abstract

Society and as a consequence policy and decision making has become increasingly complex. In dealing with this complexity, governance will be a key concept in policy making for the coming decades. The concept is highly normative, value loaded, and subject to many interpretations. Yet, the various definitions have in common that they emphasise the need to address human activities and development as well as economic and environmental imperatives simultaneously. As such, the issue requires an integrated approach.

In this paper the interrelation between ocean space and human activities is discussed with a focus on the Exclusive Economic Zones (EEZ) for which countries by international law have a responsibility towards both sustainable use of its resources and marine protection. The EEZ notion has dramatically changed the world map, making France the largest Ocean State of the world.

The European Union Member States' EEZs, Blue Europe, form a priceless asset. They contribute significantly to Europe's prosperity and overall quality of life. However, our understanding of the full social-economic value of this vast resource is far from complete. A healthy EEZ — covering oceanic and near-shore systems — provides for example renewable food supplies, transportation highways, fossil and renewable energy, tourism opportunities, and biotechnology supermarkets.

Governance of Europe's EEZ needs new concepts that build on the characteristics and behaviour of the system itself. Ecosystem management, building on economic efficiency and sustainability, is basic to modern policy making with respect to the marine environment. Yet, such an approach needs marine information as provided by EuroGOOS that is also transferred into dedicated decision support systems to underpin the highly complex policy making. This paper discusses some innovative concepts, in which stakeholder participation is a central theme.

Keywords: GOOS, EuroGOOS, Exclusive Economic Zone, governance, transition management, integrated assessment

1. Introduction

At 06.58.50 local time an earthquake with force nine on the Richter scale took place off Atjeh in Indonesia. The tsunami that was the result of these forces of nature caused havoc, especially in the coastal zones around the Indian Ocean. Despite early warnings to 26 Indian Ocean rim countries including Indonesia and Thailand by the Tsunami

* Corresponding author, email: jh.stel@icis.unimaas.nl

Warning Center on Hawaii, most authorities and people were not able to take the right decisions. The estimated economic cost is still unknown but is reaching billions of US$ while the final death toll is an estimated 280000 people, making the 2004 tsunami the deadliest in recorded history. In contrast with inhabitants of the Pacific regions, people in the Indian Ocean region are unfamiliar with tsunamis and did not read the signs properly.

Human activity is dependent on and part of the ecosystems we live in. Yet human activity has changed ecosystems during the past fifty years more rapidly and intensively than ever before. This process alone will increase during the coming decades due to population growth and the linked economic growth to increase human welfare. This will lead to a growing demand for ecosystem functions and services for food, water and energy. The draft Millennium Ecosystem Assessment (2005) reiterates the strong and in some aspects wrong message of the Club of Rome that leads to the notion of sustainable development. This assessment also advocates the new realisation that expansion of human activities can lead to sudden changes or discontinuities (Van Notten, 2005; Kemp, 2005), which form a serious thread to humankind. Examples are new diseases in farming and aquaculture, changes in regional climate and the collapse of different fisheries.

The United Nations Conference on the Law of the Sea (UNCLOS) came into force in November 1994. It introduced the notion of the 200 nautical miles of the Exclusive Economic Zone (EEZ) that brings some 37% of ocean space (Stel, 2002) under national jurisdiction. This is the largest enclosure in human history. In Europe, Portugal became the largest Ocean State with a marine territory of 1.6 million km^2. Yet, the dimension of the EEZ of the European Union is not known in detail. Integrated management of Europe's EEZ is lacking but urgently needed as was demonstrated by the chaos during the sinking of the Prestige in the Spanish EEZ (Stel, 2003). The present European policy towards the EEZ is sectorial with a focus on transport, fishery and protection. In the EEZ each State has the right to explore, exploit, manage and conserve the natural resources as well as having an obligation to protect them.

Another innovative aspect of UNCLOS was the introduction of the notion of the 'common heritage of mankind' by Arvid Pardo in 1967. In this notion all resources of the seabed beyond national jurisdiction are seen as a common heritage that should be used for peaceful purposes and managed in the interest of all, including future generations. This notion was strongly opposed by technologically more advanced nations having state-of-the-art marine capabilities. It is basically a non-ownership arrangement in which user rights but no ownership rights of a common property resource can be obtained (Mann Borgese, 1998). The High Seas part of ocean space still is, like the atmosphere, outer space and Antarctica a global common area (Buck, 1998), without any national ownership. A challenge for the future is to experiment with and develop new management concepts for good and just governance of this part of ocean space (Ostrom *et al.*, 2000).

2. Integration

Integrated assessment is a relatively new paradigm for sustainable development of the EEZ. It is a multidisciplinary process of structuring knowledge elements from various scientific disciplines and stakeholders in such a way that all relevant aspects of a

complex societal problem are considered in their mutual coherence for the benefit of decision making (Rotmans, 2001). Integrated assessment can be seen as a particular form of decision support. Basically bits and pieces from different knowledge domains are combined to gain insights for decision making that go beyond the reach of a separate discipline. The integrated assessment toolkit combines the use of disciplinary knowledge with integration tools such as IA models, participatory methods and scenarios, to foster tacit knowledge.

In the SCENE model the three pillars of sustainability are applied in a system-type approach of thinking, in terms of flows and stocks. The basic rationale is to consider the EEZ (which includes the legal zone of the Continental Shelf) as a complex system that consists of a number interrelated stocks (economic, ecological and social-cultural) and flows. Stocks are described quantitatively and qualitatively; flows make all exchanges within and between the stocks explicit. These flows are both tangible and related to physical or financial flows, or intangible and related to for instance information or knowledge flows. In the SCENE model (Figure 1) three forms of capital are distinguished:

- Social-cultural capital relates to the quality and quantity of the population or to social and cultural provisions such as demographic structure, knowledge structure, cultural heritage, etc.
- Ecological capital relates to the quality and quantity of natural stock e.g. minerals, fish, water quality, biodiversity and shipping lanes.
- Economic capital relates to the quality and quantity of the economic infrastructure such as resources and materials, labour structure, transport infrastructure (ports), etc.

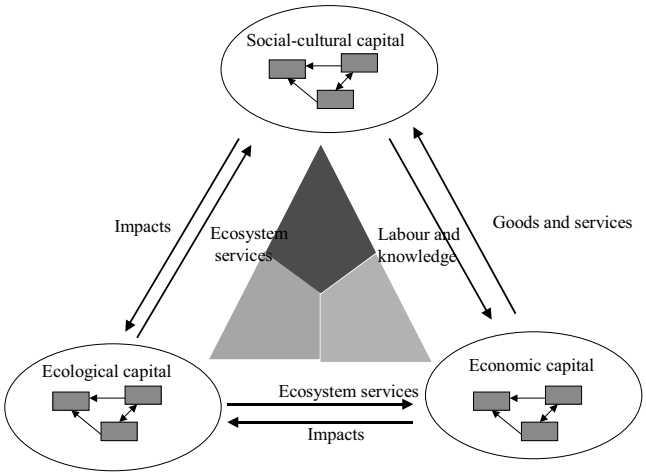

Figure 1 SCENE model developed by ICIS.

Human activities affect the stocks in these forms of capital. This influences both the amount as well as the quality of the stocks. Short-term changes are expressed in terms of flows, being intraflows for flows within a capital form and interflows for exchanges between different capital forms. Long-term changes are expressed by the stocks, which

have a number of properties: quantity, quality, spatial claim and function. The status of any stock is based upon these four properties. Moreover, renewable and non-renewable stocks, as well as stocks that can be directly or indirectly influenced or can be influenced in the short or long term should be taken into account. If we consider a system such as an EEZ as a combination of stocks and flows, then its condition can be judged in a similar way to the position of a company, assessed in term of a balance sheet (stocks) and a statement of profits and losses (flow).

Plurality is part of integrated assessment as uncertainty legitimates different perspectives such as disciplinary perspectives, different actor or stakeholder perspectives and different worldviews. Despite thousands years of trading, Indian Ocean societies viewed the sea as a source of imported goods. Although the ocean was a presence in social life, it was seen as a special place of trade, outside society and social processes. Ocean space was considered as an area to be crossed as quickly as possible; not as territory for control, influence or social power (Steinberg, 2001). European societies, however, viewed the ocean in terms of ownership. It is this difference in attitude that has finally led to the Western domination of ocean space.

Van Asselt (2000) defined a perspective as 'a coherent and consistent description of the perceptual screen through which people or groups of people interpret the world and its social dimensions, and which guides them in actions.' As a consequence a perception involves both how people interpret the world (worldview) and how they react upon it (management style). In the Cultural Theory (Thompson *et al.*, 1990) a typology of perspectives is given to express pluralism. In this theory that is based on anthropological research, five perspectives are distinguished: hierarchist or controllist, egalitarian or environmental individualist or market-optimist, fatalist, and hermit (Figure 2). The first three are active perspectives as they share an action-oriented worldview and management style. They differ fundamentally, however, with regard to the type of action and the effectiveness of these actions.

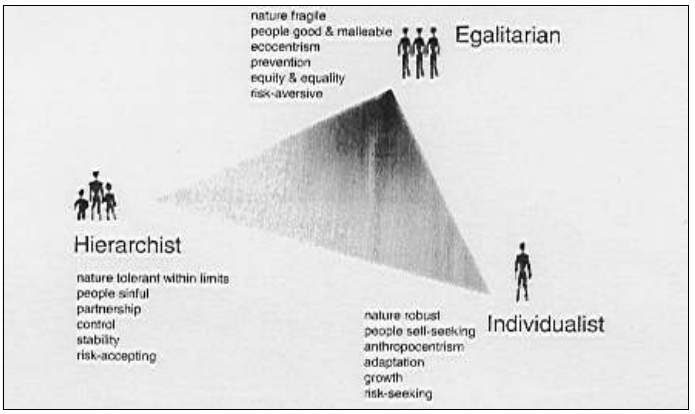

Figure 2 Main features of perspectives.

Uncertainty is a fact of our daily life and is not only related to the future; it also colours for instance our interpretation of ancient history and past climates (Pollock, 2003). Uncertainty is fundamental to scientific research. Climate change for instance is vested

with uncertainties. The main reason for this is on the one hand the variability of the climate system as given by the geological record and on the other hand our limited knowledge of the most important feedback mechanisms. For instance, ocean space, the most important component of the climate system, is hardly known and observed and shows non-linear behaviour. As a consequence small changes can have large effects (butterfly principle). Another source of uncertainty relates to social uncertainty, as human behaviour is not predictable. Therefore the behaviour of social actors, society and its policy are uncertain too. Van Asselt (2000) developed a typology of the sources of uncertainty to facilitate the distinction between for instance highly uncertain and less uncertain issues and, by this, to increase the quality of strategic planning and policy advice.

3. Transition management

Transitions are well known from the geological record, but the notion of a transition has its roots in biology and population dynamics. The transition concept is currently also used as a heuristic to describe and explain the complexity of social changes. A transition can be defined as a long term process of change during which a society or a subsystem of society fundamentally changes (Rotmans *et al.*, 2000) that are often related to changes in worldview or in paradigms. It consists of a set of interconnected changes, which reinforce each other but take place in different areas, such as technology, economy, ecology, culture, institutions, behaviour and belief systems. Like sustainable development, transitions require a long time period, at least a generation (25−50 years), because existing structures, institutions and mental frames have to be broken down and new ones have to be developed. A transition is a spiral that reinforces itself, gaining speed to the point of irreversibility. Multiple causalities and co-evolutionary processes mark possible development pathways and drive transitions. The direction and pace are often randomly influenced by policies and actions of all societal actors.

Transitions require system innovations: organisation-exceeding, qualitative innovations which are realised by a variety of participants within the system, and which fundamentally change both the structure of the system and the relation between the participants. System innovations transcend the level of an individual, an individual firm or individual organisation or institution. They take place at the level of a sector, a branch, city or region. This involves innovation of production and consumption processes, technological, institutional and political-governmental innovation. Within these system innovations, individual-level innovations occur, in terms of product, process and project innovations. An example is a possible future energy transition to biomass, which will involve system innovations in transport (bio fuels), electricity generation (co-combustion, gasification of biomass), agriculture (bio crops), but also in policy (integral biomass policy regarding energy, biodiversity, space use, agriculture and transport) and culture (surmount barriers among the public against alternative energy carriers).

Four different phases in terms of time can be distinguished in the S-curve of any transition:

- A predevelopment phase where there is very little visible change at the system-level but a great deal of experimentation at the individual level

- A take-off phase where the process of change starts to build up and the state of the system begins to shift because of different reinforcing innovations or surprises
- An acceleration phase in which structural changes occur in a visible way through an accumulation and implementation of socio-cultural, economic, ecological and institutional changes
- A stabilisation phase where the speed of societal change decreases and a new dynamic equilibrium is reached.

All transitions contain periods of slow and fast development, caused by processes of positive and negative feedback. A transition can be accelerated by one-time events, such as a war or large accident (Prestige) or a crisis (oil crisis) but is not caused by such events.

When analysing transitions, it is useful to use the multilevel scheme of Geels and Kemp (2000). This scheme (Figure 3) makes a distinction between niches, regimes and the socio-technical landscape at three interfering scale levels — the micro-, meso- and macro-level. At the macro level the societal landscape is determined by changes in macro economy, political culture, demography, natural environment, worldviews and paradigms. This level responds to relatively slow trends and developments. At the meso-level, social norms, interests, rules and belief systems operate that underlie strategies of companies, organisations and institutions and policies of political institutions. At the micro or niche-level individual actors, technologies and local practices are addressed. At this level, variations to and deviations from the status quo can occur as a result of new ideas and new initiatives such as new techniques, alternative technologies and social practices.

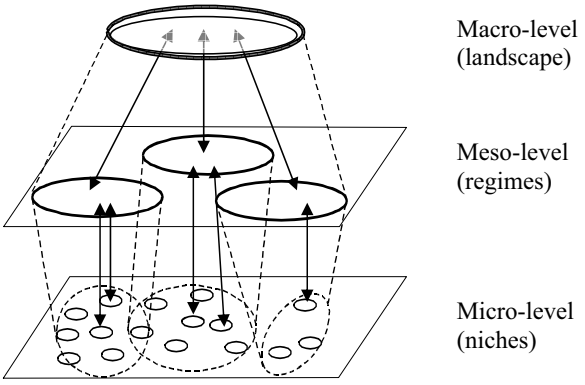

Figure 3 Interaction of innovation processes between different scale levels.

The concept of transition management is rooted in fields as multi-level governance and adaptive management (Rotmans *et al.*, 2000). This concept indicates that, although transitions cannot be managed in terms of command and control, they can be managed in terms of influencing and adjusting: a more subtle, evolutionary way of steering. So, the direction and pace of transitions can be influenced. The basic underlying rationale is that structural and institutional changes influencing the market, innovation and political-administrative systems and vice versa, lead to transitions. Transition management aims

to better organise and coordinate this process at a societal level and tries to govern it into a sustainable direction.

Key elements of transition management are:

- Systems-thinking in terms of more than one domain (multi-domain) and different actors (multi-actor) at different scale levels (multi-level); how developments in one domain or level gel with developments in other domains or levels; trying to change the strategic orientation of regime actors
- Long-term thinking (at least 25 years) as a framework for shaping short-term policy
- Hind- and forecasting: the setting of short-term and longer-term goals based on long-term sustainability visions, scenario studies, trend analyses and short-term possibilities
- A focus on learning and the use of a special learning philosophy of learning-by-doing and doing-by-learning
- An orientation towards system innovation and experimentation
- Learning about a variety of options (which requires a wide playing field)
- Participation from and interaction between stakeholders.

Transition management can be organised in transition arenas (Loorbach, 2002) that are small multi-actor networks of innovators, experts, strategic and/or original thinkers. Within transition arenas a systemic analysis of a complex problem (based on a SCENE-analysis) in a participatory manner leads to a shared problem perception on a systems-level. This common ground will provide the basis for the development of shared visions on the desired future state of the system and leads to a joint transition agenda that contains common problem perceptions, goals, action points, projects and instruments. The latter are used here in the broad sense: from tax measures to public-private arrangements, and new instruments. So, the transition-agenda forms a compass for the transition arena participants, which they can follow straightforwardly during their transition journey.

4. Conclusions

Perceptions colour our view towards resource use of ocean space and especially the EEZ. Indian Ocean societies and China viewed the sea as a special place of trade, outside society and social processes. It was considered as an area to be crossed as quickly as possible; not as territory for control, influence or social power (Steinberg, 2001).This view is comparable to the present view of Western societies when one plans a holiday by car in France. Planning the route to take, the highways to use, only focuses on how to reach the destination; not on ownership of the highways used. Western societies, however, view ocean resources and ocean space in terms of ownership through the notion of the 'freedom of the seas'. During the last century this view lead to the largest enclosure in human history: the EEZ. Nowadays, each State has the right to explore, to exploit, to manage and to conserve its natural marine resources as well as the obligation of protecting them.

After World War II a transition in our relation with the sea took place from a technologically balanced use of ocean resources to a non-sustainable use of ocean space through

pollution from land-based human activities and unrestricted use of this common resource. Since the Industrial Revolution, human activity in the coastal zone is increasingly affected by a host of poorly planned and badly regulated activities, from the explosive growth of coastal cities and towns to the increase in tourism, from industrialisation to the expansion of fish farming, from the development of ports to measures to control flooding and related spatial planning.

There is an urgent need for integrated marine policies towards ocean space and its EEZs, for a marine policy at for instance the European level in which the different human activities and use of ocean space is regulated holistically instead of sectorially. During the last decade EuroGOOS successfully laid the foundations for a European marine information capability that is expressed in sub-regional entities such as the Baltic Operational Oceanographic System, the North West Shelf Operational Oceanographic System and the Mediterranean Global Ocean Observing System. Yet, linking these marine information systems with decision support systems and applying modern techniques to involve stakeholders in a participatory way as well as exploring new and innovative concepts such as transition management for a sustainable use and protection of Europe's EEZs will be the next step to support governance of the Europe Union as an Ocean State.

References

Buck, S.J. (1998). The global commons: an introduction. Island Press, Washington.

Geels, F.W. (2002). Understanding the Dynamics of Technological Transitions, A co-evolutionary and socio-technical analysis. Thesis, Enschede, Twente University Press.

Geels, F. and R. Kemp (2000). Transities vanuit sociotechnisch perspectief (Transitions from a socio-technical perspective), background report to the study "Transitions and transition management" by ICIS and MERIT for the NMP-4, November 2000, UT, Enschede en MERIT, Maastricht, the Netherlands.

Kemp, M. (2005). Science in culture: Inventing an icon, Schellnhuber's map of global 'tipping points' in climate change. Nature 437, 1238-1238 (27 Oct. 2005)

Loorbach, D. (2002). Transition management: governance for sustainability. Paper presented at the International Conference on Governance and Sustainability, 30/09–01/10, Berlin.

Loorbach, D. and J. Rotmans, in press. Managing transitions for Sustainable Development. Transformation Research, Kluwer, Amsterdam.

Mann Borgese, E. (1998). The oceanic circle, governing the seas as a global resource. United Nations Press, Tokyo, Japan.

Millenium Ecosystem Assessment, draft (2005). Living Beyond Our Means: Natural Assets and Human Well-being. http://www.millenniumassessment.org/en/products.aspx

Ostrom, E., Th. Dietz, N. Dolsak, P.C. Stern, S. Stonich and E.U. Weber (2000). The drama of the commons. National Academy Press, Washington D.C., USA.

Pollack, H.N. (2003). Uncertain science…uncertain world. Cambridge University Press, United Kingdom.

Rotmans, J. (2001). Integrated assessment: a bird's eye view. In: Van Asselt, M.B.A., J. Rotmans and S.C.H. Greeuw, A provisional handbook for integrated assessment, ICIS: 20–68.

Rotmans, J., R. Kemp, M.B.A. van Asselt, F.W. Geels, G. Verbong and K. Molendijk (2000). Transitions and Transition Management: the case of an emission-poor energy supply. (in Dutch), ICIS, Maastricht, the Netherlands.

Rotmans, J., R. Kemp and M.B.A. van Asselt (2001). More Evolution than Revolution. Transition Management in Public Policy. Foresight 3, 1: 15–31.

Stel, J.H. (2002). Mare Nostrum–Mare Liberum–Mare sit Aeternum, duurzaam gebruik van de oceanische ruimte. Oratie, Universiteit Maastricht: 1–34 (in Dutch).

Stel, J.H. (2003). Society and sustainable use of the Exclusive Economic Zones. In: Dahlin, H., N.C. Flemming, K. Nittis and S.E. Petersson (Eds), Building the European capacity in operational oceanography. Proceedings of the third international conference on EuroGOOS. Elsevier oceanography series, 69: 592–597.

Steinberg, Ph.E. (2001). The social construction of the ocean. Cambridge Studies in International Relations 78. Cambridge University Press, United Kingdom.

Teisman, G. (1992). Complexe besluitvorming (Complex Decision-making). Elsevier, The Hague, the Netherlands.

Thompson, M., R. Ellis and A. Wildavsky (1990). Cultural theory. Westview Press, Oxford, UK.

Van Asselt, M.B.A. (2000). Perspectives on Uncertainty and Risk: The PRIMA approach to decision support, Kluwer, Dordrecht, the Netherlands.

Van Notten, M.B.A. (2005). Writing on the wall: scenario development in times of discontinuity. Thesis University Maastricht, the Netherlands.

Coriolis, a French project for operational oceanography

S. Pouliquen*[1], T. Carval*[1], L. Petit de la Villéon*[1], L. Gourmelen*[2] and Y. Gouriou*[3]

[1]*Ifremer Brest, France*
[2]*Shom Brest, France*
[3]*IRD Brest, France*

Abstract

The seven French agencies concerned with ocean research are together developing a strong capability in operational oceanography based on a triad including satellite altimetry (JASON), numerical modelling with assimilation (Mercator), and *in situ* data (**Coriolis**).

The **Coriolis** project aims to build a pre-operational structure to collect, validate and distribute ocean data (temperature/salinity profiles and currents) to the scientific community and modellers.

The four goals of **Coriolis** are:

- To build up a data management centre, part of the Argo network for the GODAE experiment, able to provide quality-controlled data in real time and delay modes
- To contribute to deployment of Argo floats mainly in the Atlantic with about 300 floats during the 2001–2005 period
- To develop and improve the technology of the profiling Provor floats as a contribution to Argo
- To integrate into **Coriolis** other data presently collected at sea by French agencies from surface drifting buoys, PIRATA deep sea moorings, and oceanographic research vessels (XBT, thermosalinograph and ADCP transmitted on a daily basis).

By the end of 2005, recommendations will be given to transform the **Coriolis** activity into a permanent, routine contribution to ocean measurement, in accordance with international plans that will follow the Argo/GODAE experiment.

Keywords: *In situ*, operational oceanography, Argo, data exchange, Mersea

1. Introduction

The Earth's climate is determined by the atmosphere and the ocean which transport and exchange huge amounts of heat and water. Within the climate system, the interactions are numerous and complex. The atmosphere is a transient and temperamental partner. The ocean, which reacts slowly, is the memory of the system. According to annual cycles

* Corresponding authors, email: sylvie.pouliquen@ifremer.fr, thierry.carval@ifremer.fr petit@ifremer.fr, gourmel@shom.fr, yves.gouriou@ird.fr

and geographical areas, it can absorb or accumulate huge amounts of heat, water and carbon, transport it over large distances, and subsequently release it in the atmosphere.

Understanding, monitoring and forecasting ocean-circulation variability require a combination of theoretical studies, *in situ* measurements and numerical models. Today it has become possible, because of scientific expertise, increased computer capabilities, numerical modelling, observation capability from space and *in situ* measurements. It is the challenge of operational oceanography for which France has established a research programme including three complementary projects:

- JASON which will provide altimetric data following Topex/Poseidon mission
- Ocean modelling with Mercator which assimilates satellite and *in situ* data
- *In situ* measurements and data distribution with **Coriolis**.

These projects contribute to the international programmes GODAE (Global Ocean Data Assimilation Experiment) for modelling aspects and to Argo for *in situ* measurements. Both of them will be operational during the 2004–2005 period.

2. What is Coriolis?

Coriolis is a pilot project, resulting from a study conducted by the seven French organisations involved in ocean research (CNES, CNRS, IFRTP, IRD, Météo-France, SHOM and Ifremer). It is setting up a complete structure for acquisition, validation and distribution, in real and delayed modes, of *in situ* data over the world ocean: mainly physical parameters such as temperature, salinity and currents (profiles or sections with high vertical or horizontal resolution and time series).

Coriolis has three phases:

- A Preparation phase (2000–2002) synchronised with the Mercator demonstration phase, to set up the system
- A Demonstration phase (2003–2005) during which **Coriolis** will operate in an operational mode
- An Evaluation phase (2004–2005), which will provide recommendations for a sustainable operational structure, based on the experience gained.

The **Coriolis** project is organised into four sub-projects:

1. Development of the **Coriolis** data centre
2. French contribution to Argo
3. Development of profiling floats
4. Integration of national activities related to *in situ* measurements.

There is also a transversal component, which provides scientific support to the other projects.

3. Development of the Coriolis data centre

3.1 Real time

Built on 20 years of experience from the Ifremer oceanographical data centre SISMER the **Coriolis** data centre has been set up progressively to collect, control, and distribute

physical oceanography *in situ* data, initially temperature and salinity profiles. The core of this centre is located in Brest. It handles *in situ* data available in near real time coming from the GTS (Global Transmission System of meteorological data whose French partner is Météo-France) and also from other sources including French floats, buoys, and research vessels (Figure 1). 6500 profiles are now provided to Mercator on a weekly basis. These data are assimilated by Mercator and are also used in real-time by other customers, such as the Hydrographic Service of the French navy (SHOM), Météo-France and other GODAE modellers.

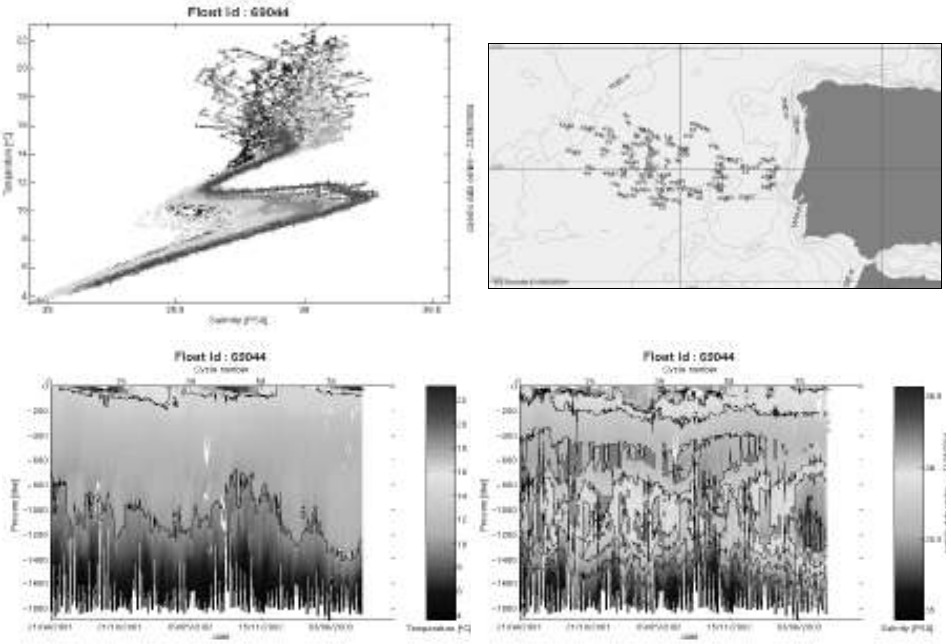

Figure 1 T/S diagram, T and S sections for a nearly 3 year lifetime of a Provor float offshore Spain (www.coriolis.eu.org).

The **Coriolis** data centre also operates in delayed mode for:

- Instruments and sensors monitoring for the estimation of sensor drifts
- Re-analysis and data synthesis: gridded fields in different areas.

3.2 Weekly analysis

Coriolis has developed an analysis system able to serve both the validation needs and the production of weekly gridded fields. This system based on an objective analysis (Bretherton *et al.*, 1975) is operated by the data centre in real time. It allows detection of outliers and provides weekly T and S fields. It is used for sensor drifts monitoring within a time scale of 6–12 months. Finally, multi-year analyses are produced for climatological studies (Figure 2).

For more information see Gaillard and Autret (2005).

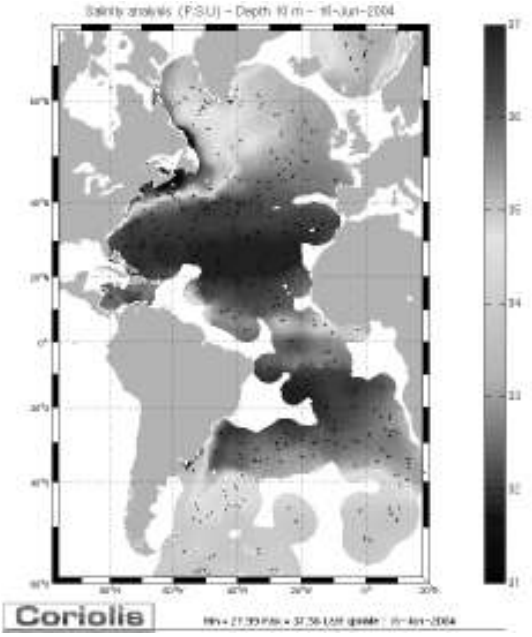

Figure 2 Weekly salinity analysis at 10 m depth for the Atlantic Ocean available through a LAS server www.coriolis.eu.org/cdc/ObjectivesAnalysis/global_atlantic.htm.

3.3 Delayed mode quality control

For 2 years the Argo Science team has been working on defining salinity delayed-mode procedures designed to specifically check artificial drifts and offsets.

The free-moving nature of profiling floats means that most float salinity measurements are without accompanying *in situ* "ground truth" values for absolute calibration (such as those afforded by shipboard CTD measurements). Therefore Argo delayed-mode procedures for salinity rely on reference databases and statistical methods for detecting artificial drifts and offsets. However, since the ocean has inherent spatial and temporal variabilities, these drift and offset adjustments are subject to statistical uncertainties. That is why corrections are provided together with an estimation of the error to users.

For more information see Coatanoan (2005).

4. French contribution to Argo

Coriolis contributes to the Argo programme (A global array of profiling floats). By 2007, the Argo programme should have deployed 3000 profiling floats according to a regular grid in the world ocean. The float displacement gives information on the fields speed. Such a network will provide a low-resolution sampling, at a 10-day frequency. Argo is placed in the context of international programmes on the ocean monitoring (GODAE) and on climatic variability studies (CLIVAR), and under the auspices of several agencies, such as the World Organization of the Meteorology (WMO) and the Intergovernmental Oceanographical Commission (IOC) of UNESCO (www.argo.ucsd.edu).

France has first focused its deployments in the Atlantic Ocean, gradually from North to the South. It will supply 300 profiling floats (2001–2005); this contribution includes 55 floats funded by the European Commission for the demonstration project "Gyroscope" and the Integrated project Mersea co-ordinated by Ifremer.

The **Coriolis** data centre (www.coriolis.eu.org) has also volunteered to be one of the two Argo Global Data Centres together with the US GODAE centre, providing a unique access to all the Argo data acquired over the entire globe. These centres are fed by various national data centres which validate the data provided by the floats they deployed, using the same quality control procedures as defined by the "Argo data management team".

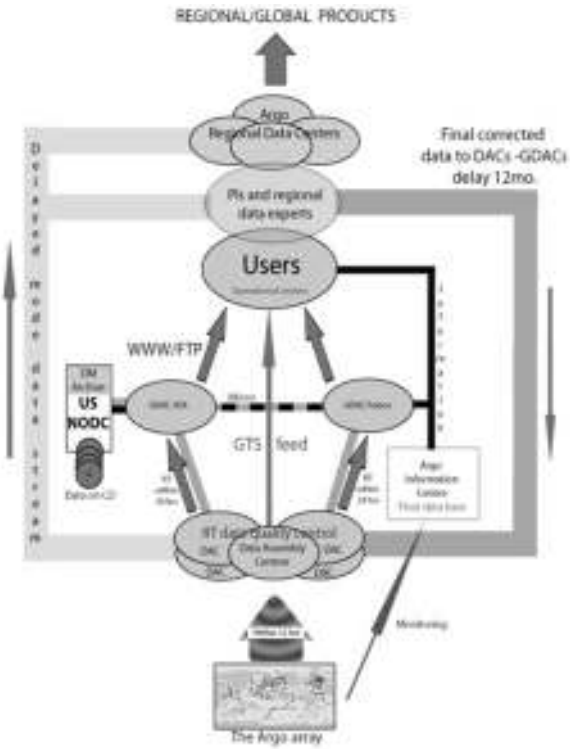

Figure 3 Argo data management network.

5. Profiling floats development: The French Provor float

Within the **Coriolis** framework, through an industrial partnership with the Martec company, Ifremer has developed a free-drifting hydrographic profiler named Provor based on Marvor technology (which doesn't need any ballasting operation before launch).

Temperature and salinity measurements are performed during the ascent and/or descent, and at drift; the sampling strategy is set before launching and parametrised for at least two user-defined layers. A coastal version of Provor, named Pagode, is under devel-

opment. Also studies to add new sensors such as oxygen and carbon are conducted by Ifremer (See Marchand and Loaec, 2005).

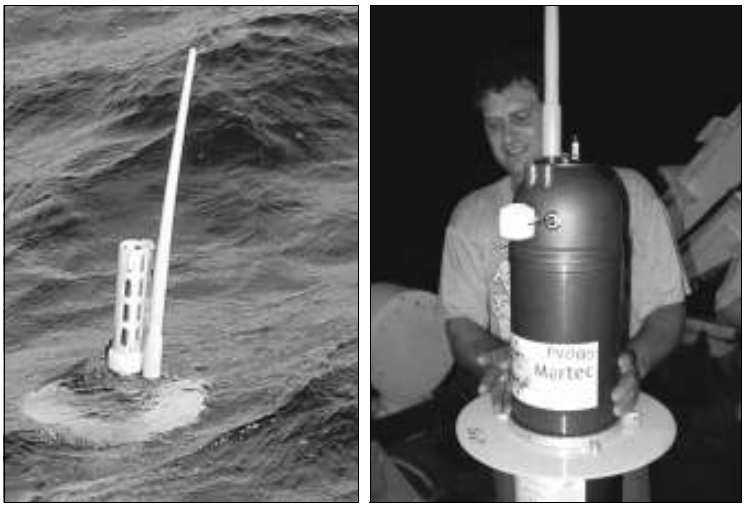

Figure 4 Profiling float Provor equipped with Seabird sensor (left) and FSI (right).

6. Integration of national activities related to *in situ* measurements

Many *in situ* measurements necessary for operational oceanography are made regularly by the French agencies involved in **Coriolis**: SHOM (XBT, hydrographic cruises), Ifremer (4 large research vessels), IPEV (one large research vessel cruising in Indian and Antarctic oceans), IRD (WOCE lines, XBT lines and thermosalinometers), Météo-France (drifters and several moorings), CNRS (floats). Unfortunately, data are not always transmitted in real time to data centres.

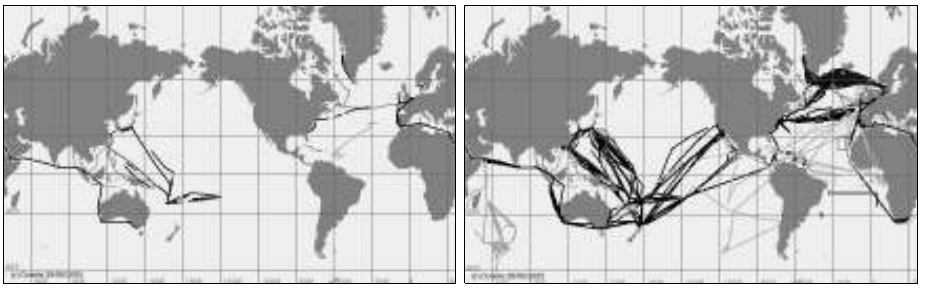

Figure 5 Left: Sea surface salinity data acquired from French research vessels and transmitted in real time to the **Coriolis** data centre in 2005. Right: Sea surface salinity acquired since 2000 on VOS within the French Observatory ORE-SSS. Both of them represent the French contribution to GOSUD (Global Ocean Surface Underway Data) under the IOC umbrella.

Coriolis aims to organise the systematic collection in real time of *in situ* measurements made either as routine or within the framework of specific research activities, in order to

meet the operational oceanography needs. It harmonises reduction, control and calibration processes to cope with operational constraints (see Petit de la Villéon, 2005).

7. Prospects

The **Coriolis** project implementation by the French agencies in charge of oceanography will contribute to the ocean observing system, providing world coverage of the oceans in real time. **Coriolis**, a multi-disciplinary pilot project, is involved in new autonomous instrument development with up-to-date transmission capability, in float deployment in the Atlantic Ocean (then the world) and in data collection, processing and distribution to users (public authorities, scientific community, and industry sector). Within the Mersea Integrated Project, the **Coriolis** data centre will be extended to serve the European ocean forecasting systems: for this it will integrate data coming from other European research vessels, start distributing biochemical data coming from moorings and gliders as well as improving climatology over the Atlantic ocean.

It aims to be continued when the world programmes, to which it relates, will have drawn their assessment for the coming years. We will then witness an evolution similar to the one observed in meteorology field twenty years ago: deep-sea oceanography will go from science to operational for the benefit of the world population on a sustainable base. Nevertheless it will then be necessary to assume the recurring cost of such a programme.

References

Gaillard, F. and E. Autret (2005). Climatology and interannual variability of the North Atlantic from Coriolis re-analysis, this volume page 201.

Coatanoan, C. (2005). Delayed Mode Quality Control on Argo floats at the Coriolis Data Centre, this volume page 195.

Marchand, P. and G. Loaec (2005). *In situ* monitoring of the ocean: present and future technologies available for operational oceanography. This volume, page 822.

Petit de la Villéon, L. (2005) GOSUD: Global Ocean Surface Underway Data Project, this volume page 311.

E-SURFMAR: an operational Surface Marine Observation Programme in the North Atlantic and adjacent seas

Pierre Blouch*

Météo-France

Abstract

E-SURFMAR is an optional programme of the ground-based EUMETNET Composite Observing System (EUCOS). EUMETNET is the Conference of European National Meteorological Services.

In 2005, 15 European Meteorological Services out of the 20 EUMETNET members have been participating in the E-SURFMAR programme. The objective of this programme is to co-ordinate, optimise and progressively integrate the activities for surface observations over the sea within the EUCOS operational framework.

E-SURFMAR includes Voluntary Observing Ships (VOS) operated by participating members as well as data buoys which have been co-ordinated by the European Group on Ocean Stations (EGOS) for many years. Each of the components is fitted with a Technical Advisory Group who helps the Programme Manager to conduct the programme.

One of the main objectives of EUCOS is to optimise the ground observing system to improve short range forecasting over Europe. In this context, a suitable network of surface marine observations has been proposed by E-SURFMAR to meet WMO requirements of surface marine data for regional Numerical Weather Prediction (NWP) as a complement to the data provided by satellite remote sensing. The proposition includes an increase of the density of air pressure measurements carried out north of 30°N in the North Atlantic and in the Mediterranean Sea, as well as the use of a few moored buoys for the calibration and the validation of wind and wave satellite data.

Keywords: EUMETNET, EUCOS, SURFMAR, NWP, weather prediction, VOS, data buoys

1. Introduction

E-SURFMAR is an optional programme of the ground based EUMETNET Composite Observing System (EUCOS). EUMETNET is the Conference of European National Meteorological Services.

The E-SURFMAR objectives are to co-ordinate, optimise and progressively integrate the activities for surface observations over the sea within the EUCOS operational framework. The main objective of EUCOS is to optimise the ground observing system to improve short range forecasts over Europe.

* Corresponding author, email: Pierre.Blouch@meteo.fr

In 2005, 15 European Met Services out of the 20 EUMETNET members have been participating in the E-SURFMAR programme: Belgium, Denmark, Finland, France, Germany, Greece, Iceland, Ireland, Italy, Netherlands, Norway, Portugal, Spain, Sweden and United Kingdom.

E-SURFMAR is funded through the contributions of its participating members (720 k€ in 2006). Members contribute to the programme according to the Global National Income (GNI) of their respective countries.

The programme started on 1 April 2003. It has been initially defined with a duration of 4 years divided into two stages of two years each: design study during stage 1, then implementation during stage 2. Météo-France is responsible for the programme.

E-SURFMAR includes:

- Voluntary Observing Ships (VOS) operated by EUMETNET members: 650 ships reporting human observations every month plus 60 shipborne Automated Weather Stations (AWS). E-SURFMAR actively participates in the works of the VOS Panel of WMO (JCOMM/SOT)
- Data buoys previously co-ordinated by the European Group on Ocean Stations (EGOS): a permanent network of about 50 drifting buoys plus a few offshore moored buoys. E-SURFMAR is a regional action group of the Data Buoy Co-operation Panel (JCOMM/DBCP).

Each of the components is fitted with a Technical Advisory Group who helps the Programme Manager to conduct the programme.

2. Phase I — Network design study (2003–2004)

The main question was: "which *in situ* surface marine data are presently the most sensitive to improve Numerical Weather Predictions (NWP) as a complement to the satellite data?" The study, carried out in 2004, answered:

- Air pressure (MSLP) for direct assimilation into weather models. Pressure observations are essential to anchor the surface pressure field in analyses but these observations are still too sparse over the sea. According to ECMWF studies, surface winds, provided for instance by satellites and assimilated in isolation, can have a detrimental impact on Numerical Weather Predictions.
- Sea surface temperature (SST), wind and waves for the validation and the calibration of satellite data.

Although the EUCOS area of interest is bounded by 90°N–10°N; 70°W–40°E, the study showed that the most sensitive area for MSLP is north of 30°N.

The study then made an inventory of the existing systems providing these parameters and their distribution over the North Atlantic and the Mediterranean Sea. It noticed a significant decrease in the number of ships reporting "manual observations" and the necessity to speed up the deployment of shipborne AWS systems. A recommendation was therefore made to increase the number of hourly MSLP observations north of 30°N through the use of more drifting buoys and more shipborne AWS systems than are used at present. A target of 175 drifting buoys deployed each year and 45 new AWS systems has been proposed.

The design study also recommended consideration of four existing moored buoys for the calibration and the validation of wind and waves satellite data. The existing surface marine observing systems already provide *in situ* SST measurements for the calibration of satellite data. The new (recommended) systems will strengthen this.

3. Phase II — Programme implementation (2005–2006)

3.1 Drifting buoys

So far, 50 drifting buoys have been procured each year by EGOS members on a voluntarily basis (Figure 1). In 2005, the drifting buoys were funded by E-SURFMAR. From 2006, the communication costs for these buoys will be also funded by E-SURFMAR. By this time, the European operational drifting buoys will have been fully integrated within EUCOS.

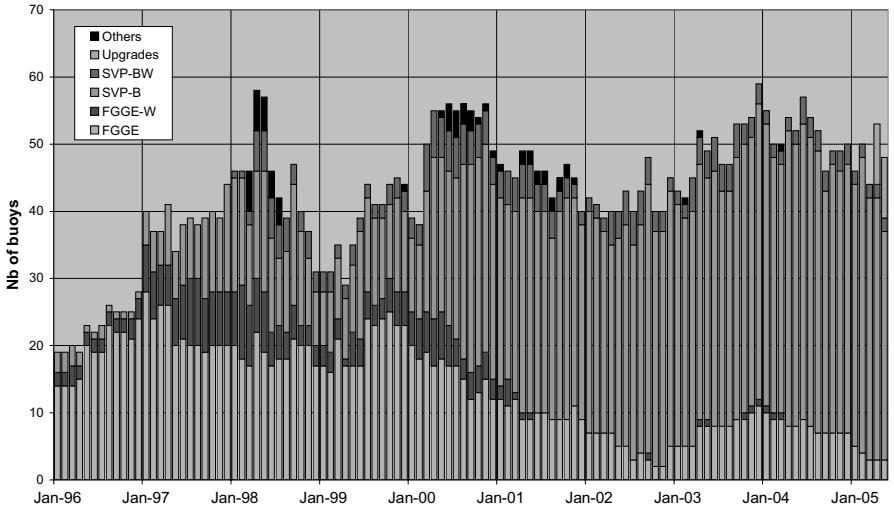

Figure 1 Number of operational drifting buoys operated by EGOS later E-SURFMAR in the North Atlantic according to their type.

For a few months, a fruitful co-operation with NOAA/AOML has enabled E-SURFMAR to fund barometer upgrades on surface drifters deployed in the North Atlantic. 20 SVP-B drifters upgraded by E-SURFMAR were deployed in 2005.

The number of drifting buoys deployed each year into the sensitive area should increase in the future, accordingly to the programme budget and the continuation of the co-operation with NOAA.

3.2 Voluntary Observing Ships (VOS)

A procedure has been settled to compensate the participants who operate a fleet of VOS. Compensation is paid according to the volume of observations carried out by each member and reported onto the Global Telecommunication System of the WMO (GTS).

E-SURFMAR is very concerned by VOS communication costs. Savings are sought through a better use of satellite links commonly used by VOS (e.g. Inmarsat-C) or the use of alternative ones (e.g. Iridium and Globalstar).

Since 2005, E-SURFMAR plans to fund a few shipborne AWS systems every year. These systems, called BATOS, have been developed by Météo-France. In order to speed up their deployment aboard European ships, participants are invited to purchase additional systems at their own expense. They will be compensated for their use.

Figure 2 The BATOS shipborne AWS system

Figure 3 K-pattern buoy

3.3 Moored buoys

In January 2005, E-SURFMAR took over the data buoy activities previously carried out by the EGOS group. EGOS had been concerned with two moored buoy networks: the K-pattern buoys operated by the UK, France and Ireland and the Spanish deep water network.

Following the recommendations of the E-SURFMAR design study, four moored buoys out of these two networks have been considered as EUCOS moored buoys. Compensation is paid for the operation of these buoys. Plans exist to upgrade the three K-pattern buoys to enable them to provide directional wave spectra. One buoy would need to be relocated in a more suitable position.

3.4 Networks monitoring

Observing systems are monitored every day and actions are taken as appropriate when problems occur with the data they report, for example drifting buoys running ashore, biased air pressure observations due to an uncorrected barometer height, etc. Quality control tools, including graphs of comparisons between observations and weather model outputs and blacklists of platforms reporting dubious values, are available to operators on the Internet.

3.5 Performance evaluation

The performance of the E-SURFMAR networks are regularly evaluated: data availability on the GTS, data timeliness and data quality. For EUCOS objectives, it is essential to have a maximum of reliable data transmitted onto the GTS with the shortest delays.

The performances differ from one component to another. For instance, the timeliness of shipborne AWS and moored buoys is better than for conventional VOS and drifting

buoys. The quality of air pressure measurements is currently lower for conventional VOS than for the other components.

4. The future (2007–)

It is strongly desirable for E-SURFMAR to become a core programme of EUCOS in 2007 just like E-ASAP and E-AMDAR which already have this status. By then, EUMETNET will probably have 28 members i.e. the 25 EC countries plus Iceland, Norway and Switzerland.

An increase in the density of air pressure measurements carried out in the North Atlantic and in the Mediterranean Sea will be made through optimisation of the existing observing systems (savings) and an expected increase of the E-SURFMAR budget. Ship observations and moored buoys will be better compensated.

However, even in the best case, the targets proposed by the design study will not be reached for many years.

5. Conclusion

E-SURFMAR is now on track. It is an *in situ* operational programme. For the meteorological community, this implies data transmission onto the GTS in "real-time". Funded by 15 European meteorological services according to the country GNIs, its existence is more reliable than if it was only funded by fewer participants on voluntary contributions.

E-SURFMAR is surrounded by several advisory groups — two technical ones (VOS and Data Buoys) and one scientific (EUCOS Scientific Advisory Team), with representatives from its participant members. It progressively integrates the European surface marine observation activities for weather forecast.

The CIESM observational network for understanding long-term hydrological changes in the Mediterranean Sea

Jean-Luc Fuda*[1], Claude Millot[2] and the CIESM[3] group

[1]*CNRS–Centre d'Océanologie de Marseille (Service d'Observation), France*
[2]*CNRS–Laboratoire d'Océanographie et de Biogéochimie, France*
[3]*Commission Internationale pour l'Exploration Scientifique de la mer Méditerranée*

Abstract

Most hydrological data sets come from scattered CTD casts that only allow calculation of linear trends over years or decades. The information is thus relatively poor as data significance cannot be estimated, relationships with other data sets cannot be computed, trend values cannot be compared between places (since data is generally available over different periods), and new data sets have low added value.

Following a CIESM (Commission Internationale pour l'Exploration Scientifique de la mer Méditerranée) dedicated workshop held in 2002, a programme has been developed (www.ciesm.org/marine/programs/hydrochanges.htm) for collecting hydrological time series with autonomous CTDs permanently operated in key places in the Mediterranean Sea (e.g. the strait of Gibraltar and other passages, and dense water formation zones) and maintained locally by the institutes that are partners of the project.

This strategy has already been validated by the first 15-month hourly time series collected at Gibraltar in 2003–2004, revealing dramatic changes to the Mediterranean outflow composition.

Keywords: Mediterranean Sea, long term changes, hydrology

1. Introduction

In the last decade, warming and increasing salinity trends have been reported for surface, intermediate and deep waters of the Mediterranean Sea. Some results are presented in Table 1, in the form of trend values evaluated by several authors over different periods and time durations.

It should firstly be specified that the mechanisms that were put forward for explaining such trends are still being debated; it is obviously beyond the scope of this paper to analyse such mechanisms that are generally discussed in detail in the cited works.

Even though knowledge of long-term hydrological variations in the Mediterranean is highly valuable, it was inferred mainly from ship-handled CTDs operated in various locations with typical (and generally irregular) sampling intervals ranging from weeks to months and even years. In some rare cases, the reported trend values were obtained from data recorded at fixed stations in the framework of systematic observing programmes such as the one conducted by J. Pascual offshore Barcelona in Spain (Pascual *et al.*,

* Corresponding author, email: fuda@com.univ-mrs.fr

1995). This means that only linear trends over years to decades (reported in Table 1 as °C/yr and psu/yr) can be calculated because of the low number of data values. Such data sets do not allow scales of major importance to be resolved, such as the mesoscale, and the calculated trends can hardly be compared from place to place since they generally correspond to different periods. It is not possible in practice to sample regularly a point at a high rate with a ship-handled CTDs, except during short-term dedicated experiments. This is illustrated in Figure 1 for larger scales, which shows slow general increasing trends but also smooth month-scale variations (e.g. in late 1999) recorded at ~3500 m in the Tyrrhenian. Characterizing the latter properly with ship-handled CTDs would demand a huge effort in term of logistics, while an autonomous instrument able to record samples hourly during a couple of years without maintenance will resolve all scales at the lowest cost.

Moreover, linear trends compiled from data collected during independent cruises spreading over years and decades are potentially doubtful because of the mixing of data of heterogeneous quality, the irregular temporal distribution of samples (i.e. data "clusters" at the time of the cruises, separated by long empty periods) and the more or less subjective and/or arbitrary choices of horizontal and vertical boundaries for selecting CTD data entering in trend computations. In addition, ship-handled CTDs do not allow the correct sampling of any along-slope vein at intermediate and greater depths (Sammari and Millot, 2000). From a practical point of view, it is clear that maintaining a permanent (i.e. over several decades) weekly to even monthly hydrological monitoring with ship-handled CTDs is extremely demanding in terms of ship-time and manpower availability for a coastal area, as it is totally unrealistic for an open ocean one.

Table 1 Hydrological trends for some Mediterranean water masses: AW (Atlantic Water), LIW (Levantine Intermediate Water), WMDW (Western Mediterranean Deep Water), EMDW (Eastern Mediterranean Deep Water). See (CIESM, 2001) for an exhaustive review of Mediterranean water masses and related acronyms.

Concerned water mass/ sub-basin	Depth (m)	Period	T trend (10^{-3} °C/yr)	S trend (10^{-3} psu/yr)	Authors
AW / offshore Barcelona (Spain)	0	1973–1994	+35	NA	Pascual *et al.*, 1995
	80	1973–1994	+20	NA	
AW / Liguro-Provençal	NA	1960–1995	0	+4.3	Krahmann and Schott, 1998
LIW / whole western Med	[250 500]	1960–1995	0	0	
LIW / Tyrrhenian	[600 1500]	1973–1992	+19	+5.0	Zodiatis and Gasparini, 1996
WMDW / Algero-Provençal	2000	1909–1955	+0.82	+0.3	Rohling and Bryden, 1992
	2000	1955–1989	+1.6	+0.94	
WMDW / Algero-Provençal	2000	1960–1995	+1.6	+0.8	Krahmann and Schott, 1998
WMDW / Provençal	2000	1959–1996	+3.5	+1.1	Béthoux and Gentili, 1999
EMDW / Ionian	3000	1960–1991	+2.1	NA	Tsimplis and Baker, 2000
EMDW / Levantine	3000	1960–1991	+1.2	NA	

2. The CIESM Network: history of creation and present status

From 1996 to 2002, the abyssal surroundings of Ustica island (in the southern Tyrrhenian sub-basin) were surveyed as complementary investigations to the deployment of a long-term multi-parametric deep-sea observatory, the european Geophysical and Oceanographic STation for Abyssal Research — GEOSTAR (Beranzoli *et al.*, 2000). In 1999–2000 and 2000–2001, high-quality autonomous CTDs and temperature loggers (SBE37/SBE16 and SBE39 from SEA-BIRD) and specially temperature-calibrated AANDERAA current meters with enhanced resolution (~0.002°C) on short (~10 and ~100 m) moorings, were deployed at the bottom (~3500 m). Unexpectedly, the recorded hourly temperature and salinity time series (Figure 1) have revealed large monthly variations superimposed on monotonic increases found to be one order of magnitude greater than all the trends reported up to now for the deep waters of all other Mediterranean sub-basins (see Table 1). Moreover, comparison with historical data extracted from the MEDATLAS database (MEDATLAS group, 1997) have revealed an important acceleration of hydrological trends occurred since the mid 1990s (Fuda *et al.*, 2002). Besides their intrinsic scientific interest (Fuda *et al.*, 2002), these time series have also definitely convinced us that autonomous CTDs deployed at fixed selected locations were much more relevant and cheaper than ship-handled CTDs for efficient monitoring of hydrological changes on the long-term.

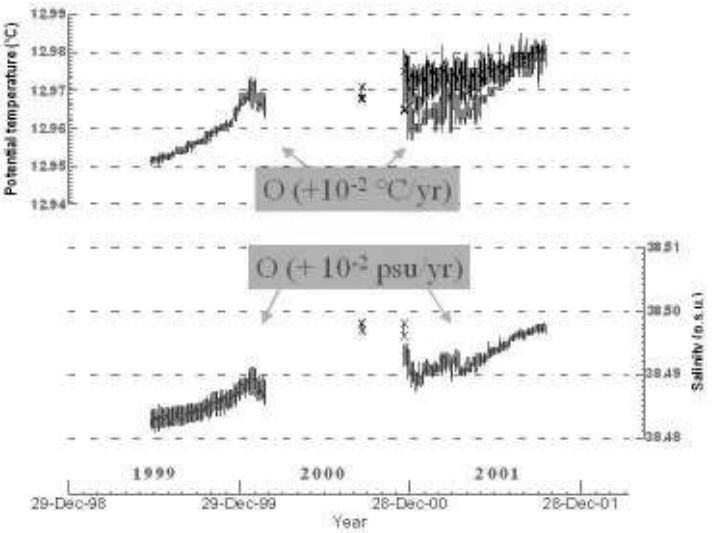

Figure 1 Temperature and salinity time series at ~3500 m, ~20 nautical miles NE from Ustica island.

The 2000–2001 temperature time series values were collected with several instruments (SBE37, SBE39 and Aanderaa current meters [resolution: 0.002°C]) evenly distributed between 3400 and 3500 m.

In April 2002, the CIESM (Commission Internationale pour l'Exploration Scientifique de la mer Méditerranée) organised a dedicated workshop during which several physical oceanographers (mainly) from the riparian countries developed a realistic monitoring

strategy to describe and understand long-term hydrological changes in the Mediterranean Sea (CIESM, 2002). This workshop has led to the setting up of a network aimed at collecting hydrological time series with autonomous CTDs permanently operated in key places (e.g. the strait of Gibraltar, other passages, dense water formation zones) and managed locally by the project partners (Figure 2). These CTDs are set on 10-m moorings recovered (by acoustic release) and immediately re-deployed every 1–2 years, which requires ~1-day ship-time only. Among the CTDs presently in operation, most are Sea-Bird SBE37 (accuracy: few 10^{-3} °C/10^{-4} Sm^{-1}, resolution: few 10^{-4} °C/10^{-5} Sm^{-1} and stability per month: few 10^{-4} °C/10^{-4} Sm^{-1}) that allow 1-hour time series to be collected during up to ~6 years.

This programme is placed under the patronage of the CIESM and is coordinated by the Observation Service of the Centre d'Océanologie de Marseille (COM). It is presently fully operational at numerous key sites (Figure 2). Institutes actually conducting operations are SHOMAR (Morocco), INSTM (Tunisia), CNR and OGS (Italy), COM-LOB (France) and CSIC and IEO (Spain). Additional moorings will be deployed in the forthcoming months/years offshore Algeria, Egypt and Crete, and managed respectively by ISMAL, AUDO/NIOF and HCMR. Up to now, equipment has been provided by the institutes themselves and by the CIESM that is willing to involve as many southern countries as possible.

Figure 2 Map of the CIESM network. Labels indicate the involved partners.

3. First results and conclusion

The strait of Gibraltar, a key location, was the first passage to be instrumented by the SHOMAR in collaboration with the COM in order to permanently monitor both the Atlantic Water surface inflow (at ~80 m on the Moroccan side) and the Mediterranean Water deep outflow (at ~270m on a small plateau, only ~1 km away from the deepest part of the V-shaped sill).

Figure 3 displays the very first 15-month (January 2003 to April 2004) hourly temperature and salinity time series of the outflow's characteristics. The most evident feature is the fortnightly tidal period that appears on both records. The lowest temperatures and highest salinities characterise the less-modified Mediterranean Water and its variations on each semidiurnal cycle. Any 2-week zoom (not shown) of these records matches the description made more than 20 years ago (Bryden and Stommel, 1982), namely the fact that MW is always more or less modified during spring tides while "pure" MW flows out during neap tides.

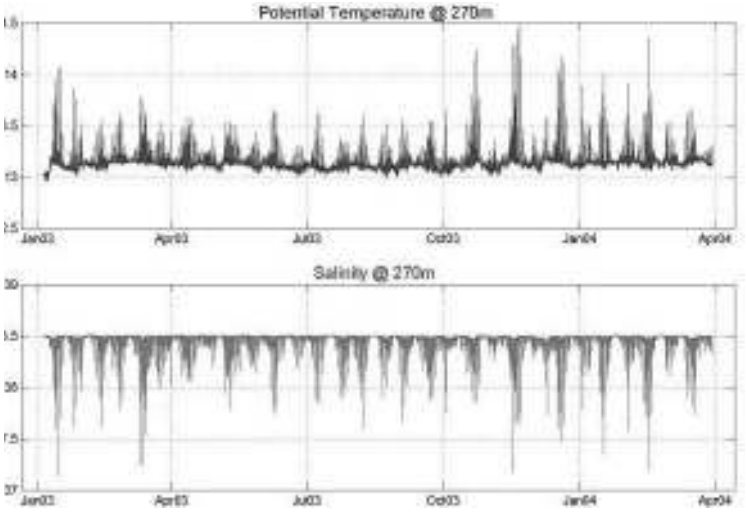

Figure 3 The network's very first 15-month temperature and salinity time series collected at 270 m in the deeper part of the strait of Gibraltar.

Apart from these expected features, these data have first of all revealed dramatic changes in the Mediterranean outflow's composition. Consistently with older time series, we have indeed demonstrated (Millot *et al.*, 2005) that the densest waters outflowing since the mid 90s in the deeper part of the strait no longer originate mainly from the western basin (as shown in the past by 1960s–1980s historical data and which is generally still believed today) but from the eastern basin, leading to an outflow that is much warmer (~0.3°C) and saltier (~0.06) than ~20 years ago. These changes cannot be attributed to the WMDW decadal trends that are ~10 times less (see Table 1). In the submitted paper, this was linked with the dramatic Eastern Mediterranean Transient (Roether *et al.*, 1996) that caused exceptionally dense waters to be formed in the southern Aegean to replace (and uplift) older bottom deep waters generated in the southern Adriatic.

Considering that the Mediterranean outflow sinks and spreads into the northern Atlantic where it participates in the North Atlantic Deep Water formation (e.g. Levitus *et al.*, 2000), it is obvious that monitoring the Mediterranean Sea in as many key sites as possible is crucial also at a global scale. We are thus convinced that the CIESM network will represent a fundamental tool to monitor and understand the Mediterranean long-term hydrological changes, as well as their impact on the Atlantic and even global functioning.

Acknowledgements

We thank the CIESM Director-General F. Briand for the support given to this programme. Special thanks are due to the Royal Navy of Morocco and its crews, as well as to the SHOMAR's engineers for their kind and efficient help in the deployment of the very first moorings of the network in the strait of Gibraltar.

References

Beranzoli, L., T. Braun, M. Calcara, D. Calore, R. Campaci, J.M. Coudeville, A. De Santis, G. Etiope, P. Favali, F. Frugoni, J.L. Fuda, F. Gamberi, F. Gasparoni, H. Gerber, M. Marani, J. Marvaldi, C. Millot, P. Palongio, G. Romeo and G. Smriglio (2000). European Seafloor Observatory offers new possibilities for deep sea studies. EOS, 81, 5, 45–49.

Béthoux, J.P. and B. Gentili (1999). Functioning of the Mediterranean Sea, past and present changes related to freshwater input and climate evolutions. J. Mar. Sys., 19, 33–47.

Bryden, H. and H. Stommel (1982). Origin of the Mediterranean outflow. J. Mar. Res., 40 (suppl.), 55–71.

CIESM (2001). document on the Mediterranean Water Mass Acronyms, www.ciesm.org/catalog/WaterMassAcronyms.pdf, 3p.

CIESM (2002). Tracking long-term hydrological change in the Mediterranean Sea. CIESM workshop series, no.16, 134 pages, Monaco. www.ciesm.org/online/monographs/Monaco02.html.

Fuda, J.L., G. Etiope, C. Millot, P. Favali, M. Calcara and E. Boschi (2002). Warming, salting and origin of the Tyrrhenian Deep Water. Geophys. Res. Letters, 29, 1886, doi:10.1029/2001GL014072.

Krahmann, G. and F. Schott (1998). Long-term increases in Western Mediterranean salinities and temperatures: Anthropogenic and climatic sources. Geophys. Res. Lett., 25, 4209–4212.

Levitus, S. *et al.* (2000). Warming of the World Ocean. Science 287, 2225–2229.

MEDATLAS group (1997). A Mediterranean hydrographic atlas from a composite quality checked temperature and salinity data, IFREMER Ed. (3 CD-ROM).

Millot, C., J. Candela, J.-L. Fuda and Y. Tber (2005). Large warming and salting of the Mediterranean outflow due to changes in its composition. Submitted Deep-Sea Res.

Pascual, J., J. Salat and M. Palau (1995). Evolucion de la temperatura del mar entre1973 y 1994 cerca de la costa catalana. In: Proceedings of the International Colloquium "The Mediterranean Sea in the 21st century: Who for?", 23–29, Montpellier, France.

Roether, W., B.B. Manca, B. Klein, D. Bregant, D. Georgopoulos, V. Beitzel, V. Kovacevic and A. Luchetta (1996). Recent changes in Eastern Mediterranean Deep Waters. Science, 271, 333–335.

Rohling, E.J. and H. Bryden (1992). Man-induced salinity and temperature increases in Mediterranean Deep Water. J. Geophys. Res., 97, 11191–11198.

Sammari C. and C. Millot (2000). Hydrological variability in the Channel of Sicily. In "The Eastern Mediterranean climatic transient: its origin, evolution and impact on the ecosystem", CIESM Workshop series no. 10, 65–69.

Zodiatis, G., and G.P. Gasparini (1996). Thermohaline staircase formations in the Tyrrhenian Sea. Deep-Sea Res., 43, 655–678.

The EUMETSAT Ocean and Sea Ice SAF

Guenole Guevel*

Météo-France, Centre de Météorologie Spatiale, Lannion, France

Abstract

In order to complement its Central Facilities capability in Darmstadt and benefit more from expertise in Member States, EUMETSAT created Satellite Application Facilities (SAFs) — specialised development and processing centres based on co-operation between several institutes and hosted by a National Meteorological Service.

The O&SI SAF is an answer to the common requirements of meteorology and oceanography for a comprehensive information on the ocean–atmosphere interface. These requirements come primarily from National Meteorological Services (NMSs), as well as oceanic and climate research agencies. The OSI SAF also aims at satisfying the needs of the operational oceanography (MERCATOR, MERSEA, MEDSPIRATION, GHRSST, etc.) and the economic actors exercising their activities on or in the ocean.

After its development phase conducted by EUMETSAT, the National Meteorological Services of France, Denmark, the Netherlands, Norway and Sweden, and Ifremer, the O&SI SAF is now in its Initial Operations phase (IOP) which is planned to last till February 2007. The IOP consortium is constituted by Météo-France, met.no, DMI, KNMI, and SMHI.

The first scope of the O&SI SAF IOP is to produce and distribute operationally in near real-time products:

- Related to the following parameters: Sea Ice characteristics, Wind^{+}, Sea Surface Temperature (SST) and radiative fluxes (Short wave and long wave) (
- Using combined satellite data derived from GOES-E, NOAA, DMSP/SSMI, METEOSAT-08, SeaWinds^{+}, and Metop (from 2007 onwards)
- Covering defined areas (High Latitudes, Global, Atlantic or Regional).

$^{+}$The Wind product, derived currently from SeaWinds, will stay under pre-operational status till 2007. Other products have been set operational in 2004)

Another important scope of the OSI SAF IOP is to conduct R&D activities for enhancing the current products or creating new products: A global Sea Ice will be operational in 2005, and a global SST is being developed, which is planned to be operational in 2008. The OSI SAF Web site (www.osi-saf.org) offers general information on the production and the project, and quick looks at the products. Moreover, registered users benefit from user support and have free access to the products via the ftp servers.

Keywords: OSI,O&SI (Ocean and Sea Ice), SAF (Satellite Application facility).

* Corresponding author, email: guenole.guevel@meteo.fr

1. Overview on the products

One of the main targets of the OSI SAF is to provide users in near-real-time with quality controlled products. Complete information on each product is provided in the relevant Product User Manual available on the Web site www.osi-saf.org, under "documentation". The main characteristics of the product are summarised in Table 1.

Table 1 Product characteristics.

Product	Format	Projection & horizontal resolution	Unit	Input satellite data	Time-liness	Central Time or frequency	Access
GLB Wind	BUFR	satellite swath, 25 km	ms^{-1}	SeaWinds, ASCAT	10 min	N/A	KNMI ftp server
LML SST	GRIB, HDF, NetCDF	isolat, isolon 0.1°	°C	GOES-E + MSG	2 h	8-daily	M-F ftp server, IFREMER ftp server, EUMETCAST
LML SSI and DLI		isolat, isolon 0.1°	Wm^{-2}	GOES-E + MSG	2 h	8-daily	
MAP SST		isolat, isolon 0.1°	°C	GOES-E + MSG + NOAA	2 h	00, 12 UTC	
MAP SSI and DLI		isolat, isolon 0.1°	Wm^{-2}	GOES-E + MSG + NOAA	2 h	12 UTC	
NAR SST		polar stereo-graphic 2 km	°C	NOAA AVHRR	2 h	4-daily	
HL Sea Ice *	GRIB, HDF	polar stereo-graphic 10 km		DMS/SSMI, SeaWinds, ASCAT, AVHRR	2 h	12 UTC	Met.no ftp server, EUMETCAST

* HL Sea Ice is being extended to Global coverage.

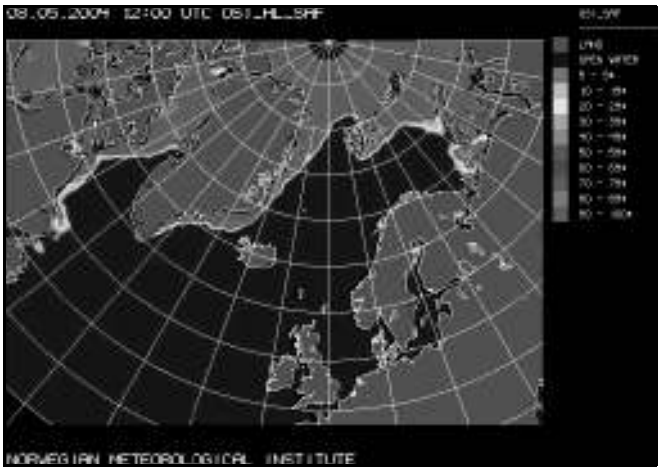

Figure 1 Sea Ice concentration. The product under met.no responsibility with DMI co-operation, is composed of 3 fields (Sea Ice Edge, Sea Ice concentration, Sea Ice Type) with the associated quality flags. It is a multisensor product obtained by using a Bayesian approach.

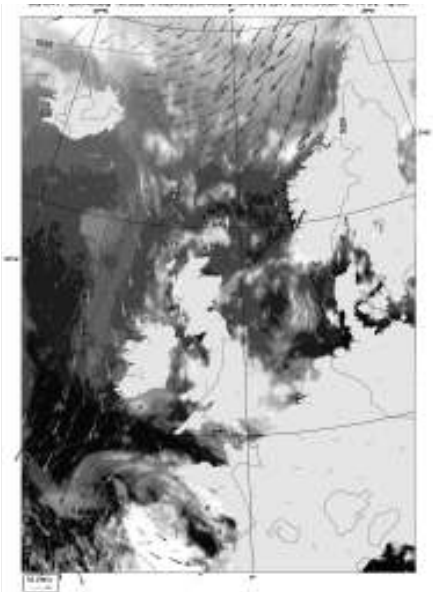

Figure 2 Example of SeaWinds Wind, compared here with HIRLAM output. The horizontal resolution is planned to be improved from 100 km to 25 km. The Global Wind is currently produced on a pre-operational basis by KNMI, and will be replaced by an operational product derived from Metop/ASCAT when satellite is available.

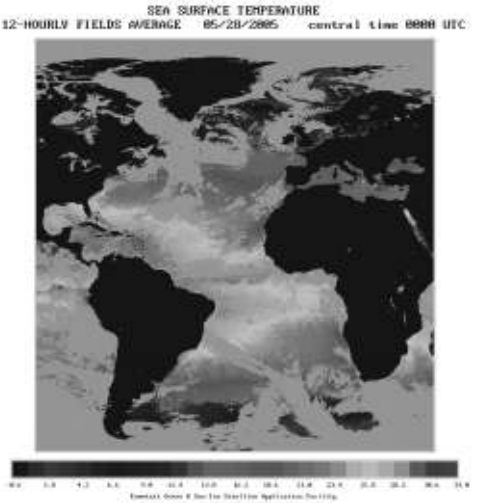

Figure 3 The LML SST derived from Met-08 + GOES-E is a 3-hourly product. The daily merging with NOAA 16/17 results in the MAP SST (shown here). All SST algorithms are currently based on a split window. The LML area covers from 100°W to 45°E, and from 60°S to 60°N. MAP area reaches North Pole, thanks to NOAA SST (also true for Fluxes) processed at met.no and DMI.

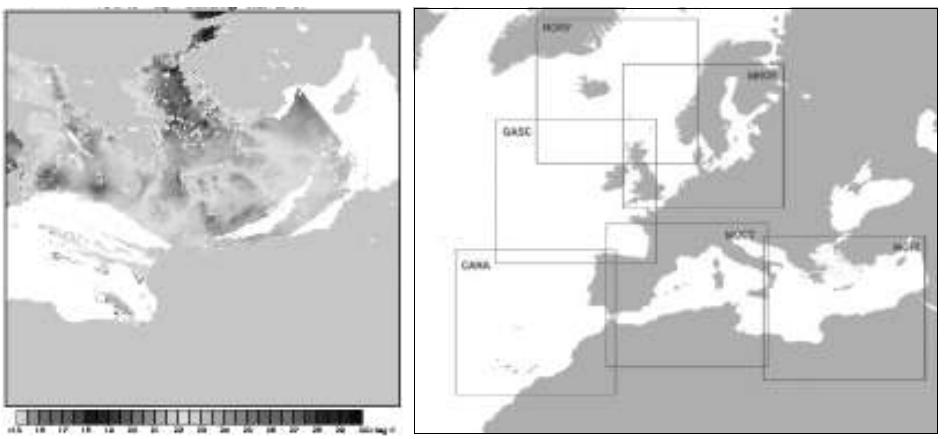

Figure 4 Example of NAR SST product on the Eastern Mediterranean Sea area, derived from NOAA-16 AVHRR. Note: All SST products are composed of 3 fields: SST, time, and quality index. The NAR SST is produced 4 times a day over 7 pre-defined areas.

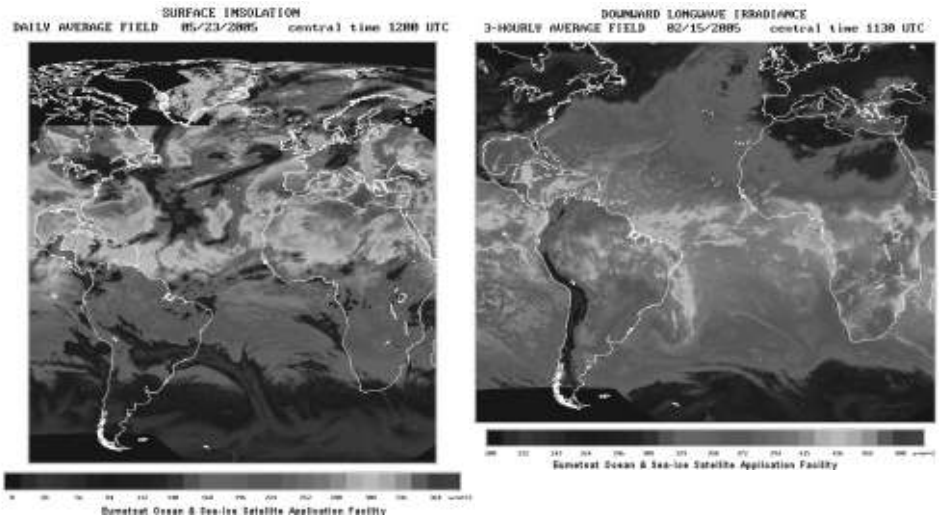

Figure 5 Left: Example of MAP SSI Flux, daily merged product derived from GOES-E, MET-08 and NOAA 16/17 AVHRR. Right: Example of LML DLI Flux, 3-hourly product derived from GOES-E and MET-08 AVHRR.

The physical method **inputs** for Figure 5 (left) are visible data (0.6 μm), cloud types (NWC SAF) and model output (h2o:Arpege). Note that LML and MAP are pre-defined areas for SST and fluxes.

The bulk parametrisation **inputs** for Figure 5 (right) are cloud types (NWC SAF), model outputs (Ta, hu), SSI. Note that SSI and DLI products are composed of a SSI (resp. DLI) field, and a quality index field.

2. Product quality results

The products are continuously validated against *in situ* measurements. See also "Validation Results" on the web site, and the statistics in the Quarterly Reports issued 4 times a year and available in the documentation section on the website. Some results are given here. The maximum allowed values are shown as thick lines.

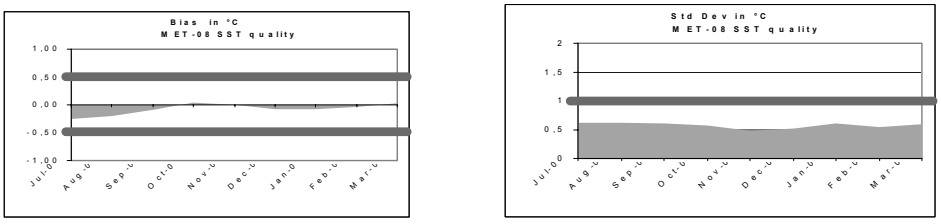

Figure 6 MET-08 SST Quality results over the period July 2004−March 2005.

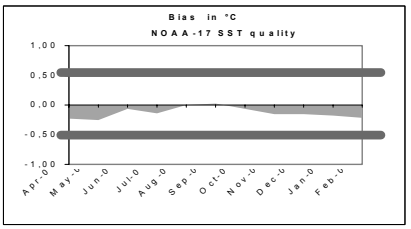

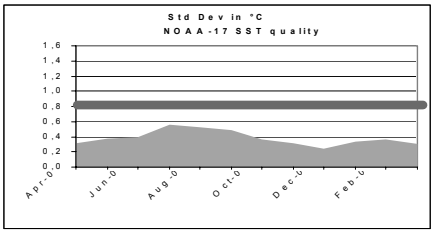

Figure 7 NOAA-17 NAR SST Quality results over the period April 2004–March 2005.

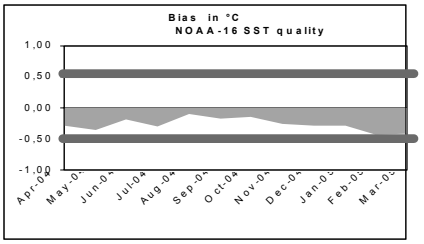

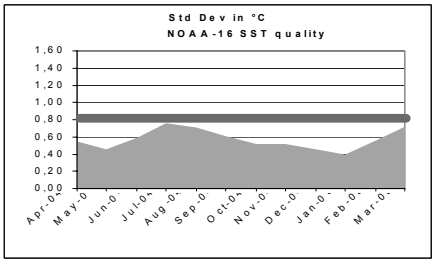

Figure 8 NOAA-16 NAR SST Quality results over the period April 2004–March 2005. The results show the bad impact of a recurrent technical problem onboard the satellite.

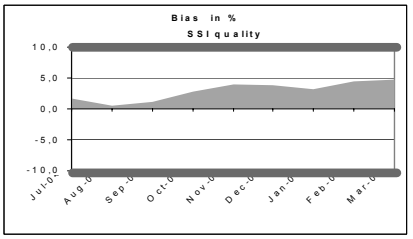

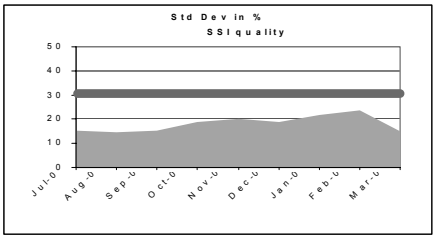

Figure 9 SSI Quality results over the period April 2004–March 2005. Most of the pyranometer stations are located in Europe, but there are also some in Northern America.

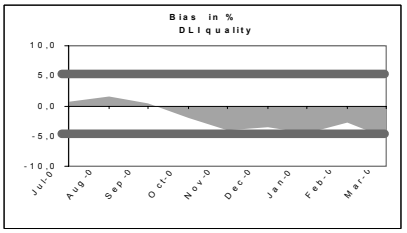

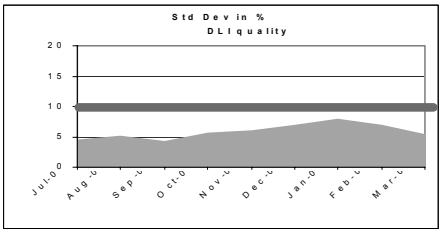

Figure 10 DLI Quality results over the period April 2004–March 2005. Very few pyrgeometer stations are available, and a longer period is needed for full validation.

3. Access to the products and archive

Near-real-time access to the products is shown in Table 1. Statistics on the products availability, as shown here in Figure 11, are provided in the Quarterly Reports, available on the web site. The archive is made locally and accessible to users on request.

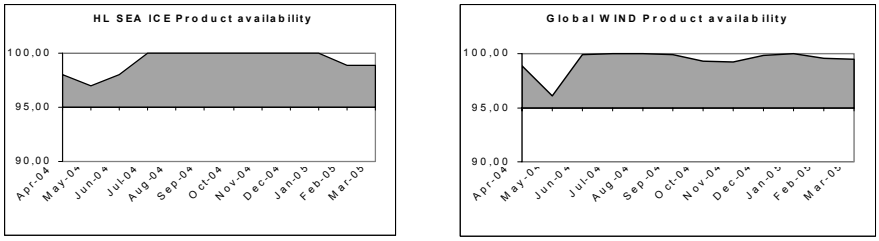

Figure 11 HL Sea Ice and SeaWinds Wind availability. OSI SAF Products are required to be available for distribution within the specified time in more than 95% of the cases where input satellite data are nominal (on a monthly basis).

4. Interaction with users

The most appropriate way for interactions with the users, apart from workshops and conferences, is the helpdesk available to the users registered on www.osi-saf.org.

5. The future

The Metop/AVHRR Global SST, currently under development, is planned to be operational in 2008. It will be produced twice daily in NetCDF and GRIB 2 format, with a 0.1° lat-lon resolution and 12 h timeliness.

For the next phase, which will cover 2007 to 2012, both temporal and spatial resolution of the existing products will be improved in general, and new products are likely to be produced, i.e. Ocean Colour and Sea Ice Drift, taking benefit from new satellites, like NPOES. The implementation of a user friendly distribution tool is planned in order to allow users to extract and re-map sub-areas from the products processed at full resolution and satellite projection.

The usage of the OSI SAF products should be consolidated, particularly by taking into account user requests expressed via the web site user support, bearing in mind the requirements coming from GCOS, GOOS and GMES, which are already taken into account by the OSI SAF in the framework of MEDSPIRATION, GHRSST, MERSEA, ICEMON.

List of acronyms

ATL	Atlantic
DLI	Downward Long wave Irradiance
DMI	Danish Meteorological Institute
GBL	Global
HL	High Latitude
IOP	Initial Operational Phase
KNMI	Koninklijk Nederlands Meteorologisch Instituut
LML	Low and Mid Latitude
MAP	Merged Atlantic Product
NRT	Near-real-time
M-F/CMS	Météo-France / Centre de Météorologie Spatiale
NAR	Northern Atlantic and Regional
OSI,O&SI	Ocean and Sea Ice
SAF	Satellite Application facility
SMHI	Swedish Meteorological and Hydrological Institute
SSI	Surface Short wave Irradiance
SST	Surface Solar Irradiance

Identification of the capabilities and gaps in the existing observational systems in the Black Sea region

Hristo Slabakov*[1], Kakhaber Bilashvili[2], Yuriy Ilyin[3], Alexander Postnov[4], Sergey Motyzhov[5], Sergey Stanichny[5] and Nikolay Valchev[1]

[1]*Institute of Oceanology–Bulgarian Academy of Sciences, Bulgaria*
[2]*Iv. Javakhishvili Tbilisi State University, Georgia*
[3]*Marine Branch of Ukrainian Hydrometeorological Institute, Ukraine*
[4]*State Oceanographic Institute, Russia*
[5]*Marine Hydrophysical Institute–NASU, Ukraine*

Abstract

ARENA (A REgional capacity building and Networking programme to upgrade monitoring and forecasting Activity in the Black Sea basin) is the first project of the Black Sea GOOS. It is the regional initiative of the GOOS and its mission is to foster development of the means whereby the information needed by governments, industry, science and the general public to deal with marine related issues is supported by a global network to systematically acquire, integrate and distribute oceanic observations, and to generate analyses, forecasts and other useful products. ARENA is an EC FP5 project and aims at building capacity on operational services and integration of the Black Sea region into GOOS. This paper acquaints a wide spectrum of interested parties with the impact and goals of Black Sea GOOS as well as showing the benefits of operational oceanographic services. Furthermore, attention is focused on identification of capabilities and gaps in the existing observational systems in the region. Finally, an overview of potential end-users of the ARENA products and their needs is given.

Keywords: Black Sea GOOS, operational oceanography, observing systems, gaps, end users

1. Introduction

The ARENA project fulfils the Black Sea GOOS mission complying with the objectives set out in the Black Sea GOOS Strategic Action and Implementation Plan (2003):

- To contribute to international planning and implementation of GOOS and promote it at national, regional and global level
- To develop regionally, enabling riparian countries to sustain GOOS activities
- To promote the development of science, technology and computer systems for operational oceanography
- To provide high quality data and time series for a better understanding and improvement of the Black Sea ecosystem

* Corresponding author, email: arena@io-bas.bg

- To find means to ensure the most effective use of existing technologies related to operational oceanography and marine meteorology.

ARENA aims to plan and design the major precursors of a regional operational system, including setting up a network between the relevant institutions and establishing links for dissemination of marine data and services, developing an integrated Black Sea forecasting system to serve end-user needs, raising public awareness and building an efficient DBMS to enable understanding of the determinant processes and facilitate decision making. The project is targeted towards various user groups and the operational capabilities fostered by ARENA will create economic benefits via optimum/efficient environmental management in agencies, regulatory authorities, and in industrial undertakings. Thus, ARENA has strategic political and economical value for both the EU and the riparian countries.

The ARENA project aims to promote studies and evaluation of the economic and social benefits generated by operational oceanography. As mentioned earlier, ARENA is a joint effort of all Black Sea bordering countries — Bulgaria, Romania, Ukraine, Russia, Georgia and Turkey — which will set the basis for the monitoring, modelling and forecasting. This implies improvement and better utilisation of the natural and human (scientific) resources as well as existing capacity. To this end a proper evaluation of the observing systems as well as identification of gaps and needs is required. The following section provides an overview of this assessment.

2. Resources of regional observational systems

2.1 Shore-based stations

The network of coastal stations — synoptic, climatic, sea level, hydrochemical, etc. — shown in Figure 1, is supported to provide data on a wide spectrum of variables to define the Black Sea boundary conditions.

Figure 1 Network of shore-based stations.

The number of operating stations is about 85, but some of them are not supplied appropriately. Some facilities are outdated, for example a number of tide and wave gauges and current meters were manufactured in the 60s or 70s; and other equipment like CTD-probes are used only during research cruises. While feasible hydro-meteorological data are still collected, acquisition of biogeochemical data has been limited to an inappropriate level. In general, oceanographic and hydrometeorological systems and corresponding research and scientific resources (Figure 2) still exist in valuable quality and quantity. Attention should be paid to the relatively small number of young scientists and operators involved in this sphere. ARENA deals with this problem by trying to create a group of interested young people through relevant training activities.

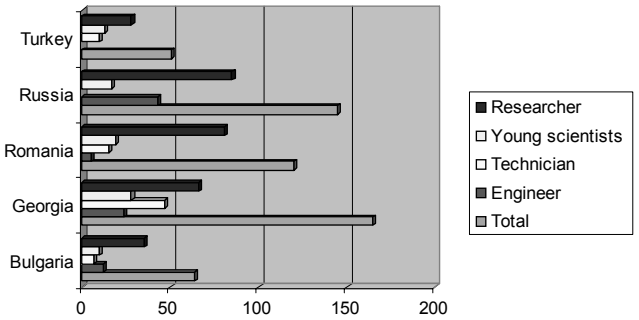

Figure 2 Distribution of human resources among partner countries.

2.2 Ship services

Partner institutions have a number of available research vessels used to implement monitoring programmes or national and international scientific and commercial cruises. The r/v "Akademik" of the Institute of Oceanology (Bulgaria) is a well-equipped and efficient multi purpose research vessel with 1225 t displacement. It is the only one of its class operating in the basin and has been employed in a number of scientific cruises funded by GEF, NATO, etc. The Shirshov Institute of Oceanology (Russia) operates r/v "Akvanavt", NIMRD (Romania) — r/v "Steaua de mare", IMS (Turkey) — r/vs "Bilim", "Erdemli" and "Lamas", MHI (Ukraine) — r/v "Striz".

There is also some existing experience with respect to ships-of-opportunity. However, the potential of regular ferry boat lines is not fully realised. Therefore, suitable conditions for organisation of an efficient VOS programme are at hand.

2.3 Satellite observations

Most of participating institutions are experienced in utilisation of satellite observations and data processing. Generally, the information comes from conventional sources and is available via Internet. Scatterometer data by QUIKSCAT provide daily sea surface wind with 20 km spatial resolution. Altimeter data of TOPEX/POSEIDON, ERS, JASON and GEOSAT missions give along-track measurements of the sea height surface anomaly. The set of products such as sea surface chlorophyll concentration, spectral reflectance, atmospheric optical depth, etc. are also available.

The MHI–NASU has an operational 1.7 GHz HRPT receiving station with a 2 m dish antenna. Data archives contain AVHRR raw data from NOAA-17 and previous NOAA

satellites that have been processed since 1996 to derive the SST field (see Figure 3). SeaWiFS data are processed using SeaDAS software for chlorophyll estimation.

IMS–METU also have access to the HRPT Antenna Server System which acquires, archives, processes, and displays real-time data from the AVHRR sensor on the NOAA TIROS-N series satellites. This system provides SeaWiFS data as well. A METEOSAT SDUS receiver (1.2 m dish antenna) is operational since 1992 and receives SDUS WEFAX data transmitted by EUMETSAT through Meteosat-5.

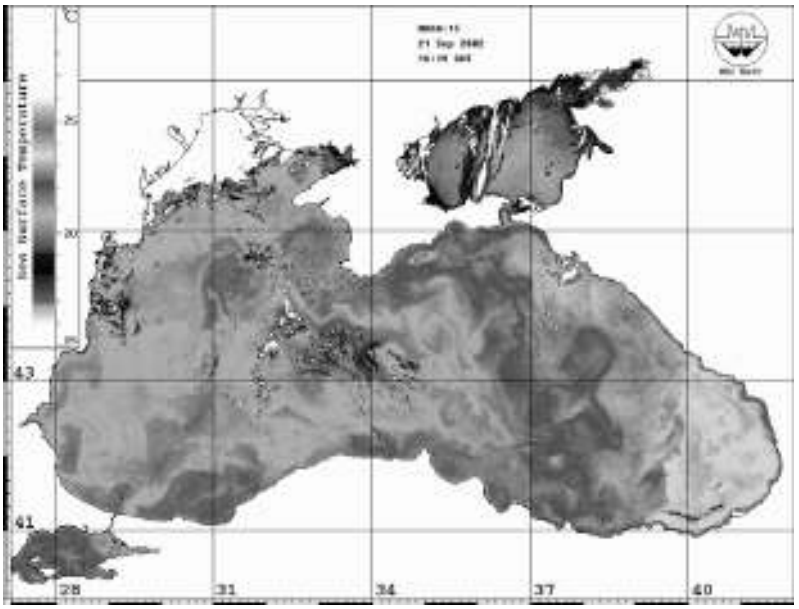

Figure 3 Capacity of observational systems: example of AVHRR SST map.

The "Planeta" Scientific and Research Centre on space hydrometeorology is the leading organisation for exploitation and development of Russian space observation systems. It operates a space data receiving and processing complex and consists of three divisions located in Obninsk, Novosibirsk and Khabarovsk. The SRC "Planeta" is equipped with a number of modern receiving and transmitting facilities supporting the different missions and serving many satellite systems, including SPOT and RESOURS.

2.4 Drifters

The Black Sea pilot drifter experiment started in 1999 and continued during the period of 2001–2003 in the framework of WMO–IOC's DBCP programme. One of the basic goals of the experiment is to investigate the possibilities for operational drifter network development in the Black Sea. Three types of buoy have been used since 1999: SVP, SVP-B (mainly employed), and XAN-3 drifters. A total of 49 Lagrangian meteorological drifters produced by Navoceano (USA) and Marlin-Yug (Ukraine) were deployed from October 2001 to April 2003. They have WMO numbers and the data obtained are distributed via ARGOS and GTS among the users all over the world.

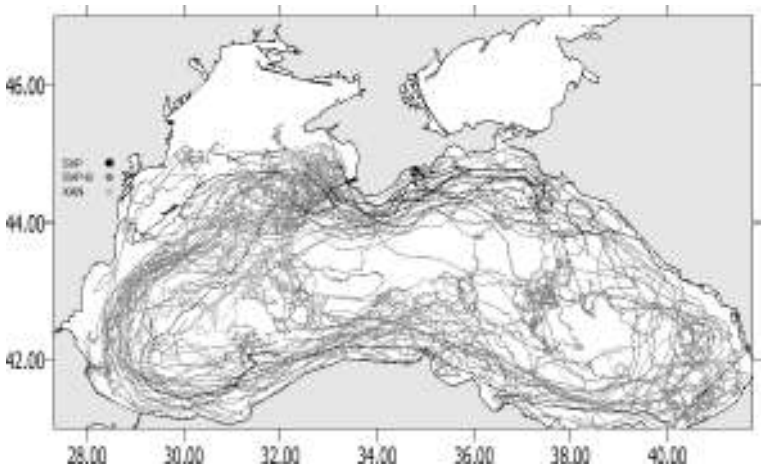

Figure 4 Tracks of buoys deployed in the Black Sea.

Figure 4 illustrates all drifter tracks deployed during the period mentioned. Another 16 SVP-B drifters were set up in 2003 and 6 SVP-B additionally equipped with temperature sensors were deployed during March–April 2004. The results allow technology to be developed for supporting the optimal drifter network density in the Black Sea.

2.5 Numerical modelling

The development of the Black Sea nowcasting/forecasting system assumes the extension of the regional atmospheric models supported by the Hydro-Meteorological Services of Bulgaria and Romania in the framework of the Météo-France ALADIN project for the entire Black Sea area and an improvement of the ecosystem model of IMS–METU into a three-dimensional model operating in near-real time mode. The use of a high-resolution regional atmospheric model makes medium-range forecasting of the Black Sea circulation possible. Special efforts are put into accurate forecasting of circulation in the coastal zone. A set of regional models will be nested in the basin-scale ones. Two types of thematic models are also planned to be coupled with the basin-scale circulation model: wave and oil spill surveillance models (see Korotaev *et al.* (2005) and Kubryakov *et al.* (2005) in this volume).

3. Identification of end-user needs

One of the main guiding targets of ARENA is the identification of end-user groups of operational marine data and forecasts. The effectiveness of ARENA strongly depends on close collaboration between the scientific community and end-users. Five general classes of users for data and information are specified:

1. Operational users that analyse the collected data and produce different forecasts serving to impose regulation measures
2. Authorities and managers of large-scale projects needing timely oceanographic information, including statistics and climatic trends
3. Industrial enterprises that work with safety of structures and avoidance of pollution

4. Tourism and recreation related users aiming to protect human health
5. Scientists, engineers, and economists carrying out special research, strategic design studies, and other investigations to advance the application of marine data.

The analysis of information received during the extensive inquiry among all potential end users reveals a variety of data and information needs encompassing physical, chemical, biological and hydrometeorological observation. Nevertheless, the common requirement concerns development of forecasting systems to provide accurate real-time or near-real time information supporting decision making and environmental management. The end-user distribution according to their needs is presented in Figure 5.

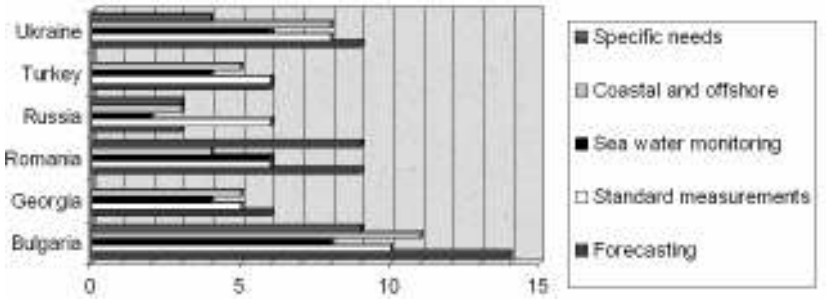

Figure 5 End-users distribution according to user needs.

4. Conclusion: problems and benefits

In order to meet challenges in marine operational observational systems as well as to improve the ongoing basin-wide activities it is necessary to identify the gaps and needs of the Black Sea countries. This is carried out through analysis of deliverables information available through ARENA and taking into account the main priority of the operational oceanographic system, namely to work in the near-real time or real time mode as well as comparing and trying to equalise the capabilities of partner countries. It is concluded that the current situation in the field of operational oceanography varies with a rather wide range. Nevertheless, common problems exist, for example the fact that operational systems continually suffer from inadequacy of corresponding financial support at the national level. Other major problems are:

- Absence of modern automatic sampling equipment both in the fields of hydrometeorology and oceanography
- No continuous automatic measurements exist
- Sparse observations in the open sea after a dramatic decrease during the 90s
- Communication network: upgraded within ARENA but still needs to be developed to satisfy operational data flow needs
- The sea forecast models are still operating in delayed or near-real time mode; they are still to be tested and sustained in real time mode
- Due to low salaries the number of young scientists contributing to development of the Black Sea operational system is rather limited.

Another set of more crucial problems consists of:

- Absence of a coordinated system for Black Sea monitoring, which is considered the main gap
- The currently existing Black Sea GOOS should but does not include oceanographic cruises, as they are not supported by national funds
- The system of direct observations is currently limited to a small number of poorly coordinated national and international projects and small programmes, which do not provide a comprehensive description of the current Black Sea ecosystem state.

A reviewed description of present capabilities of the Black Sea region and assessment of further needs is expected to contribute to the development of a basin-scale sustained observation and forecasting system providing valuable information and products to a variety of end users. This will contribute to implementation of the Black Sea Environmental Programme which applies the Bucharest Convention for protection of the Black Sea against pollution. This effort will serve also for:

- Planning and implementation of GOOS and promoting it at a regional and national level
- Identification of regional priorities for operational oceanography
- Finding means to ensure the most efficient use of existing national technologies and scientific resources related to operational oceanography and marine meteorology.

It is also very important to stress the economic and social benefit of the ARENA project, assisting integration, elaborating on existing oceanographic data products and services for regional and basin-wide decision-making purposes.

Acknowledgements

This paper is considered as a contribution to the EC FP5 ARENA Project, Contract No. EVK3−CT−2002−80011.

References

ARENA Deliverables. /www.arena-blacksea.net/

Black Sea GOOS Strategic Action and Implementation Plan. IOC/INF No.1176, UNESCO, 1993.

Korotaev, G., E. Cordoneanu, V. Dorofeyev, V. Fomin, A. Grigoriev, A. Kordzadze, A. Kubryakov, T. Oguz, Yu. Ratner, D. Trukhchev and H. Slabakov (2005). Near-operational Black Sea nowcasting/forecasting system. This volume page 269.

Kubryakov, A., A. Grigoriev, A. Kordzadze, G. Korotaev, S. Stefanescu, D. Trukhchev and V. Fomin (2005). Nowcasting/Forecasting subsystem of the circulation in the Black Sea nearshore regions. This volume page 605.

Strategic Plan and Principles for Global Ocean Observing System (GOOS). GOOS Report No.41, IOC/INF−1091, UNESCO, 1998.

Towards Operational Oceanography: the Global Ocean Observing System (GOOS). IOC/INF−1028, UNESCO, 1996.

Circulation in Galicia-Southern Bay of Biscay: reanalysis of the circulation influencing the Prestige oil spill

M. Ruiz-Villarreal*[1], C. Gonzalez-Pola[2], P. Otero[1], G. Diaz del Rio[1], A. Lavin[3] and J.M. Cabanas[4]

[1]*Instituto Español de Oceanografía, CO A Coruña, Spain*
[2]*Instituto Español de Oceanografía, CO Gijón, Spain*
[3]*Instituto Español de Oceanografía, CO Santander, Spain*
[4]*Instituto Español de Oceanografía, CO Vigo, Spain*

Abstract

A summary of the oceanographic conditions during the period of the Prestige oil spill (November 2002) and the following spring is presented based on hydrographical data and on model results. The implications of this experience for operational oil spill forecasting are discussed.

Keywords: Prestige oil spill, operational forecasts of circulation, slope current, river plumes, mesoscale activity

1. Introduction

On 13 November 2002, the Prestige oil tanker containing 77000 tonnes of heavy oil reported it was in trouble near Cape Finisterre (NW Iberian coast). The ship approached the coast on 14 November and afterwards was towed on a route first northwards and then southwestwards while at the same time leaking oil. The ship finally sank on the south-western flank of the Galician Bank, an offshore seamount 200 km from the coast. More than 60000 tonnes of oil sank with the tanker, which were released and drifted toward the coast driven mainly by the dominant winds. Oil from this second spill stranded on the Galician coast at the end of November and in early December. The northern Spanish coast was affected by stranding of oil slicks from early December onwards. Slicks were also reported in French Atlantic coastal areas during the following months. For other discussions on the Prestige event in the present volume see Daniel *et al*. (2005).

Operational oil spill models used to predict the drift of pollutants have wind as the main forcing and currently they only take into account the effect of barotropic currents, but not of large scale currents (Daniel *et al.*, 2004). Several attempts at simulating the Prestige oil spill have been performed at the time of the spill and afterwards (Montero *et al.*, 2003; Hackett, 2004; Daniel *et al.*, 2004). These exercises put forward the influence of forcing the drift model with large scale currents in the prediction of stranding places. In recent years, results from large scale operational systems are becoming routinely available. However, large differences appear in predicted currents and thermohaline fields between systems (see for example the intercomparison exercise in MERSEA strand 1, http://strand1.mersea.eu.org/html/strand1/intercomparison.html). As shown by

* Corresponding author, email: manuel.ruiz@co.ieo.es

Hackett (2004), MERCATOR and FOAM surface current fields at the time of the Prestige oil spill are quite different and stranding predictions vary depending on the current field used in forcing the drift model. An analysis of circulation and its comparison with the forecasts is therefore necessary.

The analysis of the circulation in the area is also crucial for evaluating the impact of the oil spill in the ecosystem. In contrast with the situation for other oil spills, there are biological time series in the area (see references in Ruiz-Villarreal *et al.*, 2005), but the strong interannual variability can mask effects and makes it difficult to ascribe observed deviations to the impact of oil spill. In this sense, a study of oceanographic conditions in this particular year in comparison to other years and especially of the conditions during the following spring, an important biological event after the accident, is a requisite for any study of the response of the ecosystem.

2. Impact of circulation in the oil spill

The area affected by the oil spill is located in an Eastern Boundary Current System and is affected by seasonal upwelling during spring and summer. This seasonality is only a first order description of the system and event variability is dominant. The conclusions of this chapter are based on the analysis of a hydrographic data set that comprises data from routine hydrographic lines and cruises and from multi-disciplinary cruises organised to provide information about different aspects of the impact of the spill. Further details about the data set and about the impact of circulation on the Prestige oil spill are given in Ruiz-Villarreal *et al.* (2005). In the present contribution, the conclusions are complemented with results of the PSY2 MERCATOR prototype in the area and with simulations performed with the ROMS model.

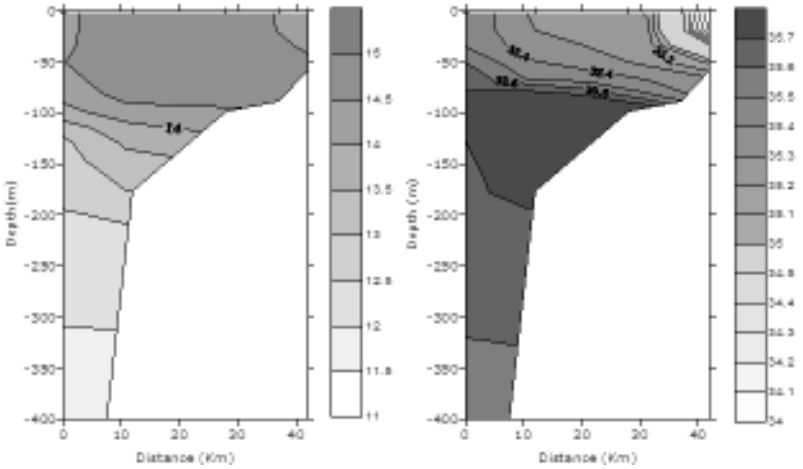

Figure 1 Temperature (°C) and salinity (psu) radial transect on the Galician west coast performed during cruise Prestige-Plataforma 1202 (December 2002).

2.1 Conditions during the oil spill

The oil spill took place in the downwelling season. Wind transport was mainly towards the coast and explained the drift of oil spill released at the time of sinking towards the

coast. A cruise performed on December 2002 during downwelling conditions similar to those during towage and spill can be used to illustrate the main features of coastal circulation at the time of the accident (Figure 1). Coastal circulation was characterised by the presence of freshwater plumes and the presence of the poleward current (carrying warmer and saltier waters) on the slope.

As we mentioned in the introduction, the impact of coastal circulation in the spill was inferred from the different behaviour of drift simulations with or without currents from a circulation model. It is not straightforward to include currents in oil drift models, especially if they already include barotropic currents (Daniel *et al.*, 2004). Further uncertainties are associated with the temporal availability of model output, usually daily from large-scale operational systems (Hackett, 2004), and with the level of realism of the physics considered in the model: Hackett (2004) and Daniel *et al.* (2004) used models with open-ocean physics and Montero *et al.* (2003) considered a seasonal poleward current. The main spill was stopped at the shelf in front of Galician Rias without stranding on them (Montero *et al.*, 2003), and river plumes could have played a role. However, the response of the coupled system plume-poleward current to wind events is not precisely known and variability is not fully resolved by the models used in the reviewed drift prediction exercises. Work is currently being carried out to perform simulations with ROMS with realistic forcing (tides, freshwater run-off from all rivers and high resolution meteorological forcing) to assess the response of plumes to wind events and further details of this will be given in a forthcoming paper.

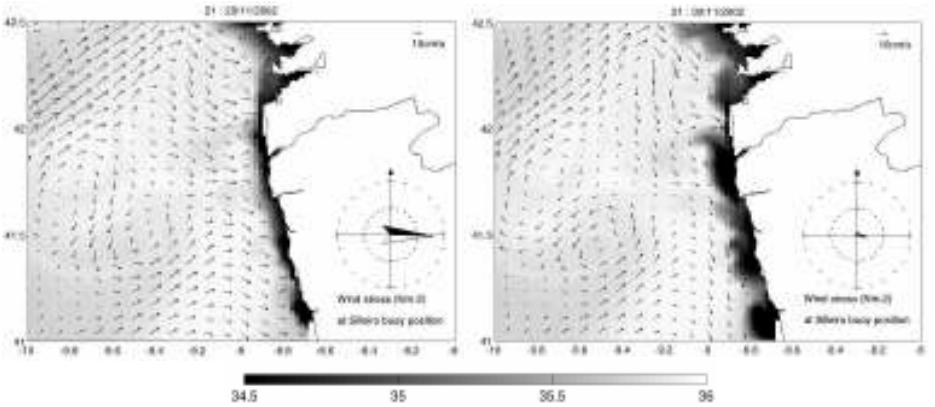

Figure 2 Simulated surface velocity and salinity for days 29 and 30 November, before stranding of the main oil spill. Grey-scale tint indicates salinity (psu) and the 10 cms^{-1} current vector is shown at top right.

Figure 2 shows surface velocities and salinity for 29 and 30 November, before the stranding of the second oil spill. On previous days, downwelling conditions prevailed. From 29 to 30, a relaxation of the wind occurred, followed by upwelling favourable winds. Figure 2 illustrates the response of the plume to wind changes: during downwelling conditions it is confined to the coast, while when the wind relaxes or turns upwelling favourable, an offshore extension of this plume is induced. This response, with a time scale of hours, is likely to affect the stranding points of the oil spill, not only through the change in wind or in coastal circulation, but possibly also through the

enhanced dispersion associated with the dynamic response of plumes to wind and its interaction with the poleward current domain. In this sense, our simulations show meanders and eddy activity in the frontal area.

2.2 Drift to the Cantabrian Sea

From early December, slicks drifted into the Cantabrian Sea. Although wind is the dominant factor in driving the oil slicks, some studies (Garcia-Soto, 2004) claim that the poleward current or Navidad helped in dispersing the oil. The poleward slope current is detected in the Cantabrian Sea from December on, although the penetration shows strong interannual variability. Warmer SST in December and January satellite imagery is considered a signature of the penetration of the poleward current, and years with a clear signal are called Navidad years. However, the clearest evidence is the presence of a subsurface intrusion of saltier and warmer waters on Cantabrian slopes. Routine IEO monthly hydrographical transects in the Cantabrian Sea do not detect an intrusion in winter–spring 2003, in contrast to other years, including the precedent winter 2002 and other Navidad years like 1996 and 1998.

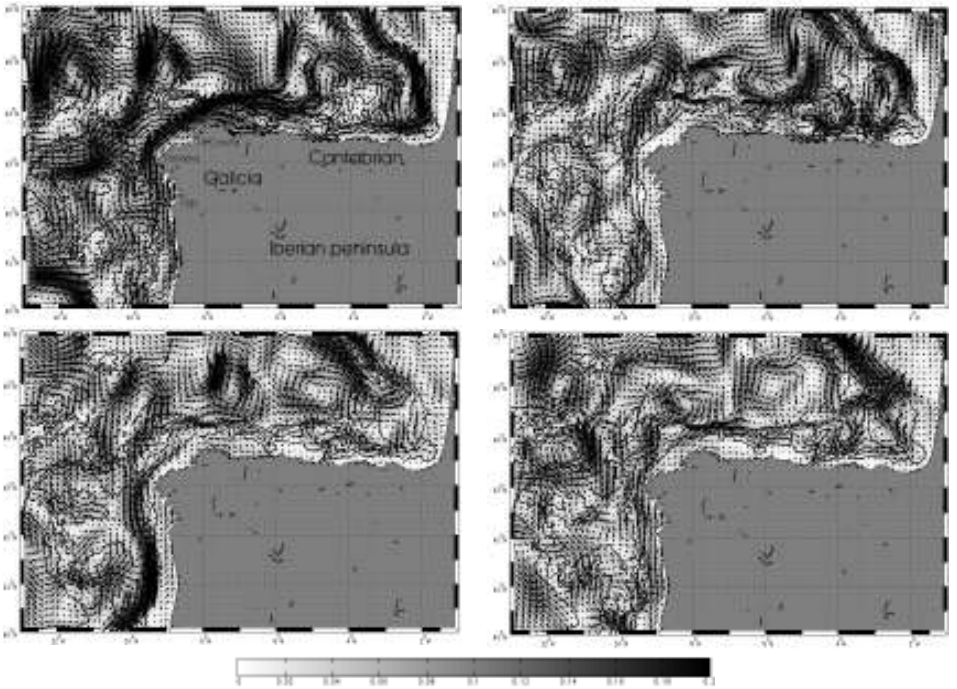

Figure 3 Monthly mean surface velocity ($cm s^{-1}$) from MERCATOR PSY2 model for December, January, February and March. The grey-scale tint indicates velocity.

Inspection of monthly mean currents from the MERCATOR model (Figure 3) combined with the analysis of wind can help in understanding the circulation pattern. A surface poleward current is clear in December in the Cantabrian Sea, and is not present in the following months, which could explain the lack of hydrographical signs of the intrusion. Analysing wind averages in the Cantabrian Sea (Figure 4) from NCEP (Daily Global

Analyses, www.cdc.noaa.gov) for the period 1996–2003, it appears that 2003 was the only year with a northwestward net wind component in the Bay of Biscay for the winter–spring period. Although wind forcing is not the main factor in generating the poleward slope current, it might be an important factor in its penetration in the Cantabrian Sea. Consequently, the unusual wind conditions in the winter–spring transition are likely to have affected the observed circulation, apart from influencing the drift of oil slicks.

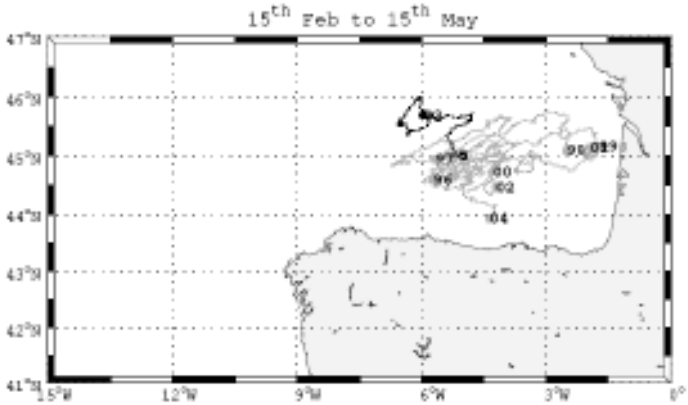

Figure 4 NCEP Accumulated Wind Stress for the Prestige oil spill influence area for the winter–spring transition of the year of the accident (2003, black line), compared to years from 1996 to the present (grey).

2.3 Spring transition

During this year, some cruises were performed during spring, a transition season marked by the change to dominance of upwelling favourable winds. The spring transition is gradually driven by upwelling pulses. There is evidence of interannual variability in ecological parameters associated with the presence or not of freshwater fronts and of the poleward current on the slope. The analysis of the data set and the comparison with the autumn cruises suggests that during upwelling pulses in spring (the first spring one in Galicia was the end of March), the slope poleward current weakened and was exported offshore. Also noticeable is the presence of slope water eddies in the area, which have been reported in winter and related to instabilities of the poleward current. In the Cantabrian Sea, wind data and hydrographic data indicate that spring, defined as the season of dominance of NE winds, and consequently of upwelling, appeared early in 2003. Spring conditions were different in Galicia in contrast with the Cantabrian Sea, with earlier upwelling and no poleward slope current last spring. This has to be taken into account when studying oil spill impacts on the ecosystem. Furthermore, these conditions are also relevant for understanding the fate of oil slicks in the Bay of Biscay during spring.

2.4 Galicia Bank

The ship sank in one of the flanks of the Galicia Bank, an offshore seamount. Although there are literature references on the impact of the bank in larger scale circulation in the NE Atlantic, not much information is available about the local dynamics associated with the bank. Hydrographic surveys have been carried out in the vicinity and a mooring line

was established from April to September 2003 near the wreck position. The analysis of this data set reveals the tidal distortion associated with the bank and especially a strong mesoscale activity in its vicinity at different levels, including Mediterranean Water, where signatures of meddies have been detected.

3. Implications for operational oil spill forecasting

We have briefly reviewed circulation in the area during the time of the Prestige crisis and the following spring and we have summarised information relevant for the analysis of the oil spill drift and its impact on the ecosystem. From an operational point of view, our results indicate that the use of operational circulation models to provide information on circulation to oil drift models needs more development:

- The predictive skill of circulation models has not been fully assessed. In this sense, it is remarkable that adjustments to the forecast systems have been performed after the Prestige time and predictions have been improved (see e.g. Mercator-Ocean Newsletter 12) and we have used best hindcast of the improved products. Interesting advances in this area are being achieved through system intercomparison exercises like MERSEA. Useful initiatives that complement this are the reanalysis of situations of interest like the Prestige time and the dissemination of forecasts to local experts.
- The existing operational systems do not resolve important details of coastal circulation. The spill affected a seasonal upwelling system in an end autumn–winter situation characterised by intense shelf and slope circulation. This is not fully resolved by the existing operational systems mainly based on model assumptions suited to open ocean physics which use forcing fields of not enough temporal or spatial resolution. The existing initiatives towards coastal ocean forecasts coupled to existing operational systems must be supported to improve our capacity of operational oil spill forecasting.
- The impact of circulation on pollutant drift is not clear. Wind seems the dominant driving agent, but it does not suffice for adequate predictions of drift and stranding in areas of strong circulation. Considering the effect of currents is not straightforward: apart from the effect of mean currents, mesoscale activity might have an impact in dispersion in the offshore area (as suggested by Hackett, 2004 results), but also near the coast through enhanced dispersion in frontal structures. Evaluation of operational systems in terms of their predictions of mesoscale activity at different scales is likely to open a way for improvements on oil spill forecasting.

Acknowledgements

MRV is supported by a Ramon y Cajal fellowship (MCyT and FEDER). This paper is a contribution to projects PLATERIAS (PGIDIT03TAM60401PR), ESEOO (VEM2003–20577–C14–02) and VACLAN (REN2003–08193–C03–01 / MAR).

References

Daniel, P., P. Josse, P. Dandin, J. M. Lefevre, G. Lery, F. Cabioch and V. Gouriou, (2004). Forecasting the Prestige oil spills. Proceedings of the Interspill 2004 conference, Trondheim, Norway.

Daniel, P., J.-M. Lefevre, Ph. Dandin, S. Varlamov, K. Belleguic, H. Chatenet and F. Giroux (2005). Needs for operational marine services: drift and waves. This volume page 216.

Garcia-Soto, C. (2004). 'Prestige' oil spill and Navidad flow, Journal of the Marine Biological Association of the United Kingdom, 84(2), 297–300.

Hackett, B. (2004). The impact of global ocean model forcing data on oil spill fate prediction: a comparative study of the 'Prestige' accident, Report No. 13–2004, Norwegian Meteorological Institute, Oslo, Norway, 26 pp.

Montero, P., J. Blanco, J.M. Cabanas, J. Maneiro, Y. Pazos, A. Moroño, C.F. Balseiro, P. Carracedo, B.P. Gomez, E. Penabad, V. Perez Muñuzuri, F. Braumschweig, R. Fernandes, P.C. Leitao, and R.J.J. Neves (2003). Oil spill monitoring and forecasting on the Prestige-Nassau accident, Proceedings 26th Arctic and Marine Oil Spill Program (AMOP) Technical Seminar. Environment Canada, Ottawa, Canada, 2, 1013–1029.

Ruiz-Villarreal, M., C. Gonzalez-Pola, G. Diaz del Rio, A. Lavin, P. Otero, S. Piedracoba and J.M. Cabanas (2005). Oceanographic conditions in Galicia and the Southern Bay of Biscay and their impact on the Prestige oil spill, Marine Pollution Bulletin, Prestige special issue, Marine Pollution Bulletin.

Sea ice monitoring and modelling in a small bay

Tarmo Kõuts*[1], Liis Sipelgas[1] and Keguang Wang[2]

[1]Marine Systems Institute at Tallinn University of Technology, Estonia
[2]Helsinki University, Finland

Abstract

An increased occurrence of mild winters when ice cover is only formed in coastal sea and is unstable and dependent on the local wind regime is an increasing trend in the Baltic sea. Operative monitoring of ice cover is realised by applying MODIS (Moderate Resolution Imaging Spectrometer) images. A method of ice type classification from satellite information is developed and maps of ice conditions in the entire Gulf of Riga with a spatial resolution of 500 metres are produced. The classified sea ice maps were verified by repeated field surveys at different stages of ice development.

Development of ice conditions in the Gulf of Riga (sub basin of the Baltic Sea) and Pärnu bay (shallow basin in NE part of the Gulf of Riga) are simulated, both in hind- and forecast mode using an ice dynamic model based on the conservation laws of ice and momentum with a three-level ice state and a viscous-plastic rheology. The model parameters have been estimated by comparing the model outcome with a database of ice charts and satellite images.

A drastic sea ice dynamic event in the Pärnu Bay in April 2003 was selected for detailed analysis and modelling. Sea ice during the event was driven about 45 km southwestward in three days and the entire Pärnu bay became ice-free. A fine resolution ice model with parameters similar to those for the whole Baltic Sea reproduced well the dynamic events in the small bay.

Keywords: sea ice dynamics, model, ice thickness distribution, remote sensing, Gulf of Riga, Baltic Sea.

1. Introduction

The length of the ice season in the Baltic Sea is 5–7 months. The Gulf of Riga is a relatively closed brackish water basin in the eastern part of the Baltic Sea, with a size of 14×110 km and a mean depth of 26 m (Figure 1). Pärnu Bay is located in the northeast corner of the Gulf of Riga, where the harbour town of Pärnu is situated. Pärnu Bay can be divided into an inner and outer basin. The inner part can be defined as a basin located north of the Liu-Tahkuranna line (Figure 1), measuring approximately 13×14 km, with an area of about 180 km^2 and maximum depth 7.6 m. The outer part extends down to the southern tip of Kihnu Island, forming an area of about 25×25 km, 500 km^2 with a maximum depth of about 15 m.

Ice forms annually in the Gulf of Riga. The length of the ice season is 3–6 months, and in mild winters only Pärnu Bay freezes. Usually the ice thickness in the Pärnu Bay is large enough (more than 15 cm) to form fast ice, and winter navigation is comparably easy, as

* Corresponding author, email: tarmo.kouts@sea.ee

a stable ship channel can be broken in. In mild winters thin ice cover (also melting ice in the spring period) is broken by winds and driven into movement causing very variable ice conditions in the area, which strongly influence the ship traffic into the Pärnu harbour.

Winter navigation restrictions for shipping are settled every year in the Gulf of Riga, both by Estonian and Latvian authorities, announcement of which should occur at least 1 week in advance, therefore there is a great need for exact operative knowledge of ice conditions as well as forecasts in the Gulf of Riga and Pärnu Bay. Remote sensing data of ice distribution combined with modelling the ice dynamics in a fine spatial scale is therefore needed to support winter navigation as well as port management in the region.

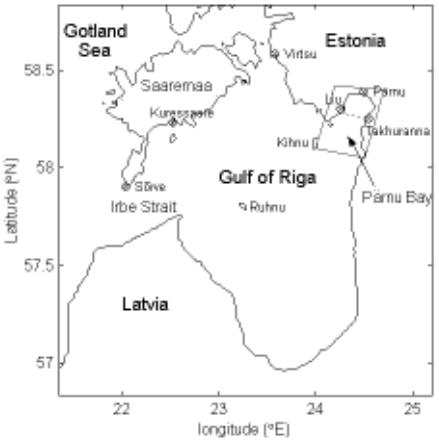

Figure 1 Morphometry of the Gulf of Riga and the Pärnu Bay.

2. Methods

For monitoring ice conditions we used MODIS channels with a spatial resolution of 250 metres placed in the wavelength region of 620–670 nm (band 1), and 841–876 nm (band 2). This enabled us to determine ice extent, openings, leads and also some dynamic properties of drift ice in the Gulf of Riga with very fine spatial and temporal scale. Ice type classification was applied using spectral differences of ice types (Figure 2) and a SAM (Spectral Angle Mapper) tool in ENVI software (Environment for Visualising Images). Classification was applied on MODIS 500 metre reflectance images and maps with ice type classification were obtained with a 500 m resolution, as shown in Figure 2. Near real time MODIS data was download form the GES Distributed Active Archive Center (http://eosdata.gsfc.nasa.gov/data/datapool/).

An ice dynamic model of the Gulf of Riga (Wang *et al.*, 2003) is used to hindcast and forecast the ice conditions. The model represents drift ice as a granular, compressible, two-dimensional medium. The "grains" are individual ice floes, which form drift ice particles, and the resulting medium is approximated by a continuum. The necessary condition is that the length scales d, D and L_G of ice floes, drift ice particles, and gradients of drift ice properties, respectively, satisfy $d<<D<<L_G$ (Leppäranta, 1998). The motion of drift ice is calculated from the conservation laws of ice and momentum. Winds

and currents drive the ice, and the response of the ice to the forcing comes from the internal stress and the adjustment of the ice mass distribution. High-resolution models for the sub-basins in the Baltic Sea, with a grid length of 5 km and 1.852 km, have produced realistic results down to length scales of L_G about 100–200 km (Wang *et al.*, 2003; Zhang, 2000). The purpose of this study is to investigate the applicability of this continuum model in fine resolution for a very small basin such as Pärnu Bay, with $L_G \approx$ 15 km and $D < 500$ m. The study shows that when the ice is thin and the floe size is small, the continuum approximation is still feasible.

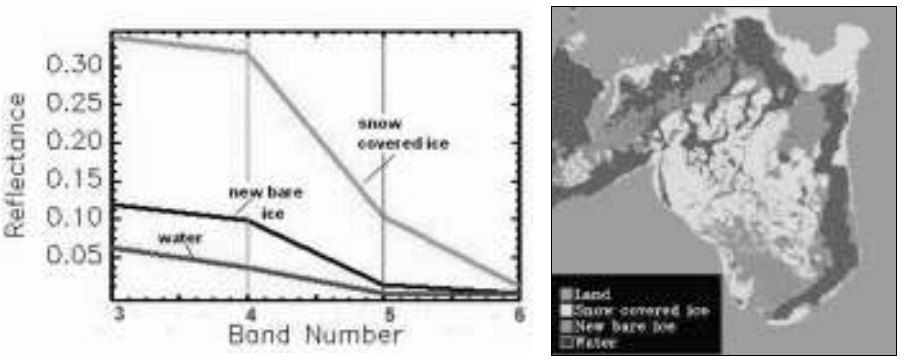

Figure 2 Left: Spectral shape of snow covered ice, new bare ice and water. Right: Ice types in Gulf of Riga on 11 March 2003.

3. Results and discussion

A major ice dynamic event in the beginning of April 2003 occurred and is hereby analysed in more detail. The ice condition in winter 2002/2003 for the overall Baltic Sea had an average maximum ice extent. However, a very special situation for this winter was that it had a longer ice period with thicker ice. Sea ice first appeared in the Gulf of Riga on 4 December 2002 and the whole Gulf was ice-covered as early as 3 January 2003. The drift ice thickness in the open Gulf of Riga during the whole winter was between 10 and 40 cm and the stable fast ice thickness was generally about 40–60 cm, but quite exceptional and special measurements for this winter were made in some locations in the Pärnu bay showing a fast ice thickness of up to 80 cm. The same kind of features are also reported for the 2002/2003 winter from the small coastal bays in the Gulf of Finland (Ari Seinä, Finnish Ice Service, personal communication).

Ice conditions on 4 and 7 April 2003 derived from MODIS satellite data are illustrated in Figure 3. Comparison of the two images shows the entire ice field drifting south-westward.

Short-range (3–5 days) model simulations of ice dynamics are performed using initial ice thickness and concentration data obtained both from *in situ* measurements and satellite images. Since ice was immobile during most of the time, our attention was focused on identifying the critical point when ice began to move and ridge. Typical values of the drift ice thickness were chosen as 10 cm for the compacted ice and 30 cm for the fast ice region. Fast ice does not move in the model and new ice and open ice were ignored.

For wind forcing the surface wind measured at Pärnu (Figure 1) was used, with a time interval of 5 minutes. The current velocity beneath the layer of frictional influence of the ice was set to zero. The grid size in Pärnu bay is 463 m (for the entire Gulf of Riga it is 1852 m) with a time step of 5 minutes. The other parameters used in the standard simulation are the same as those in Wang *et al.* (2003). Drift ice thickness was chosen to be 30 cm and its concentration 0.8, fast ice thickness was set to 50 cm and concentration 1. The measured wind speed and direction at Pärnu (see Figure 1) during the period, recorded every 5 minutes, is taken as forcing data to model runs. A notable characteristic of the wind is that it seldom exceeded 10 $m s^{-1}$, and during 6–7 April, it was only about a moderate 5 $m s^{-1}$.

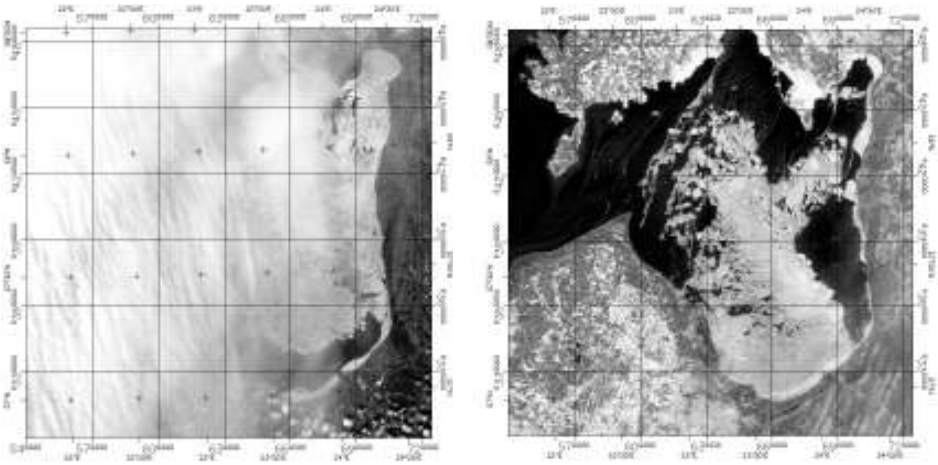

Figure 3 Ice coverage on 4 April (left, partially covered by cloud) and on 7 April 2003 (right) in the Gulf of Riga, colour composites of MODIS reflectance images.

Close inspection of the ice image of 4 April (Figure 3a) shows cracks and leads along the coastline in the Pärnu Bay and the ship channel is also visible. Winds from the SW on 4 April pushed water into the Pärnu Bay, raising all the ice cover, and the following N–NE wind together with a lower water level destroyed comparatively thick fast ice so that it drifted out from the Bay. This is probably the main reason why up to 80 cm thick fast ice was broken and transported out from entire bay, during a single dynamic event.

4. Conclusions

High-resolution monitoring and modelling of a small bay has been presented, based on the conservation laws of ice mass and momentum with a three-level ice state (open water, undeformed ice, and deformed ice) and a viscous-plastic rheology. An extreme ice dynamic event in 2003 was analysed in Pärnu Bay. The model was capable of reproducing the main characteristics of a dynamic drift ice event. It is surprising to find that the ice strength parameter P* is again optimised as $P^* = 3.0 \times 10^5$ $N m^{-2}$, which is very close to those of the Gulf of Riga (Wang *et al.*, 2003), the whole Baltic Sea (Haapala and Leppäranta, 1996), and polar oceans (Hibler and Walsh, 1982; Hibler and Ackley, 1983). MODIS near real time data and the ice classification procedure that was developed enabled detailed monitoring of ice cover properties during winters of 2002–2005.

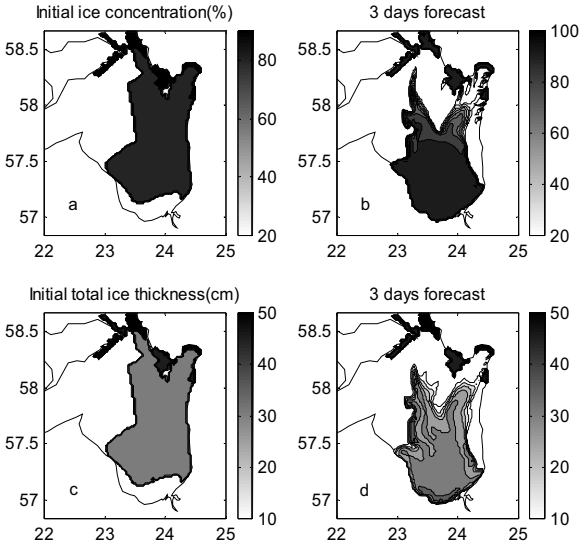

Figure 4 Standard simulation of ice field from 4 April 2003.

Acknowledgements

The authors gratefully acknowledge the Academy of Finland, the Natural Science Foundation of China (grant No. 40230082) and the Estonian Science Foundation (grant No. 4171) for financial support.

References

Haapala, J. and M. Leppäranta (1996). Simulations of the ice season in the Baltic Sea. Tellus, 48A, 622–643.

Hibler III, W.D. (1979). A dynamic and thermodynamic sea ice model. J. Phys. Oceanogr., 9, 815–846.

Sandven, S. (2005). The Arctic Ocean and the Need for an Arctic GOOS, EuroGOOS Publication no. 22, EuroGOOS Office, 31–33.

Hibler III, W.D. and J. Walsh (1982). On modelling seasonal and interannual fluctuations of Arctic sea ice. J. Phys. Oceanogr., 12, 1514–1523.

Hibler III, W.D. and S.F. Ackley (1983). Numerical simulation of the Weddell Sea pack ice. J. Geophys. Res., 88, 2873–2887.

Leppäranta, M. (1998). The dynamics of sea ice. In M. Leppäranta (ed.). Physics of Ice-Covered Seas, Vol. 1, pp. 305–342. Helsinki University Press.

Leppäranta, M., Y. Sun and J. Haapala (1998). Comparisons of sea-ice velocity fields from ERS-1 SAR and a dynamic model. J. Glaciol., 44, 248–262.

Wang K., M. Leppäranta, and T. Kõuts (2003). A sea ice dynamics model for the Gulf of Riga. Proc. Estonian Acad. Sci. Engineering, 9, 107–125.

Zhang, Z.H. (2000). Comparisons between observed and simulated ice motion in the northern Baltic Sea. Geophysica, 36, 111–126.

Zhang, Z.H. and M. Leppäranta (1995). Modeling the influence of ice on sea level variations in the Baltic Sea. Geophysica, 31(2), 31–46.

Adjustment of forcing inputs in a regional forecasting system by means of optimisation methods

E. Comerma*[1,2], M. Espino[2], F.J. Menéndez[3], J. Gómez[2], A.S.-Arcilla[2] and M. Salazar[2]

[1]*Ocean Engineering, University of Rhode Island, USA*
[2]*Maritime Eng. Lab (LIM/UPC), Barcelona, Spain*
[3]*Centro Jovellanos de Salvamento Marítimo (Sasemar), Gijón, Spain*

Abstract

During two training exercises of virtual spill carried out by the Spanish Maritime Safety and Rescue Agency (SASEMAR) in the NW-Mediterranean Sea, a preliminary forecasting system against marine pollution has been tested. Operational oceanography Met-ocean products have been used, integrated and provided to managers. Several PTR-drifting buoys were released during both exercises in order to simulate a virtual surface spill. Their successive positions were collected by satellite in near-real-time, leading to a comparison between observation and drift forecast. The exercises aimed to demonstrate the usefulness of existing met-ocean products to forecast the drift of the buoys. Hence the main effort was focused on the optimisation of the drifting factors, i.e. the adjustment of the direct stress into the floater. Outputs of several models working at different spatial and temporal resolution were available, leading to a comparison between their results.

Keywords: Maritime drill exercises, forcing optimisation, surface drift

1. Introduction

This paper aims to summarise on-going activities related to the implementation of a Regional Forecasting System to combat marine pollution in the Catalan coastal waters. The so-called CAMCAT System is intended to help Catalan Authorities during pollution emergencies. This system will be based (nested) to existing larger forecasting projects, integrating coastal observational data.

Some questions arose during the set-up of this project:

- Nowadays, which centres/projects/systems provide met-ocean forecasts on a regular basis in the Western Mediterranean Sea?
- Which are the characteristics and limitations of the products that they provide? (i.e. temporal and spatial resolution)
- Using these met-ocean results as forcing inputs for the pollutant transport module, how can we improve the accuracy of the surface drift predictions?
- What will be the consequences / impact of errors in the forcing fields over the forecasts? (Jordà *et al.*, 2005).

This project is being developed within the framework of the on-going Operational Oceanographic projects MFSTEP (Mediterranean Forecasting System Toward Environ-

* Corresponding author, email: eric.comerma@upc.edu

mental Predictions) and ESEOO (Development of a Spanish System of Operational Oceanography). The modelling component of the CAMCAT system, called ARLEQUIN, is charged with integrating all the met-ocean data and evaluating the best relationship of forcing inputs through previous optimisation analysis.

2. Maritime exercises and feedback into modelling

2.1 Description of Sasemar maritime training exercises

In order to test and improve response capabilities, two maritime crisis exercises were carried out by the Spanish Maritime Safety and Rescue Agency (Sasemar) in the North-Western Mediterranean Sea:

1. LIONMED, December 2004. A surface drifting PRT-buoy was released half way between Barcelona and Palma of Mallorca. The buoy drifted for several days (14–26) before landing on Menorca Island (Figure 1).
2. MED05, May 2005. Several drifting buoys were released near Palma of Mallorca. These buoys were also tracked via Argos.

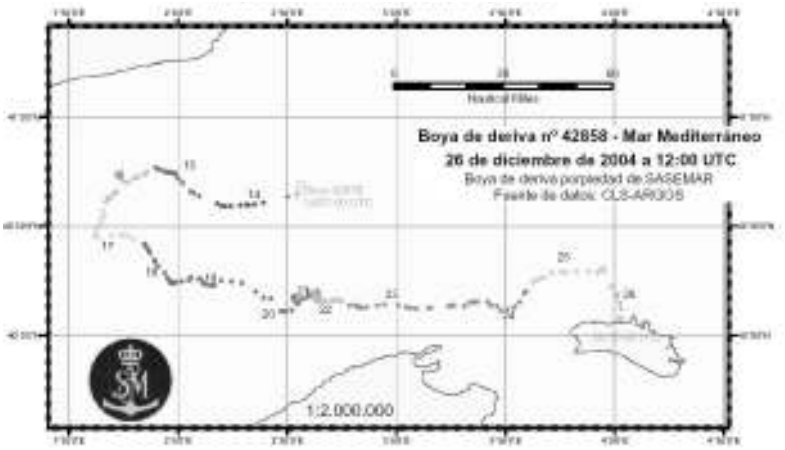

Figure 1 Surface drift of buoy released during the LIONMED exercise (14–26 December 2004).

For both exercises, a "Monitoring and Forecasting" unit called USYP was established to assist the management team, handling all available met-ocean information and providing drift forecasts. Despite the accuracy of the predictions issued by that team, it was the first time that such a scientific team was integrated in the decision-making chain. Feedback from LIONMED was transferred to MED05, improving data integration within a GIS framework.

2.2 Operational oceanography framework

Several forecasting models were already operational at the time of the drill exercises. Therefore, outputs from the following models have been used to force the drift module of ARLEQUIN: winds from ALADIN (0.1º resolution, Météo-France), HIRLAM (0.2º res., INM-Spanish MetOffice) and MASS (5' res., SMC-Catalan MetOffice) and hydrodynamics from SYMPHONIE (3 km res., POC/Noveltis), MFS1671 (1/16º res., MFSTEP

project) and PSY2V1R1 (~1/16º res., Mercator project). It is worth mentioning that SYMPHONIE is forced with ALADIN, so more coherent results can be expected using that coupling that any other combination of models.

Observed met-ocean data corresponding to the period of exercises are also available from the coastal buoys of Puertos del Estado (Spanish Harbours Authority) and XIOM (Catalan Net of MetOcean Measurement Buoys).

3. Reanalysis of surface drifts

3.1 Forcing terms: Wind-induced drift and surface currents

In case of a marine emergency, operational forecasting systems should predict the transport of objects and pollutants in the upper layer of the water column as accurately as possible. However, operational hydrodynamic models are not yet able to describe the vertical profile of horizontal velocities with enough accuracy, neither spatial nor temporally. Therefore, when using winds and currents model outputs, it is necessary to avoid counting twice the effect of wind stress in modelling the drift of an object in the water surface. For that reason, an additional/analytic term may be added to the hydrodynamics in the upper water layer, in order to attain the wind stress forcing (Comerma, 2004).

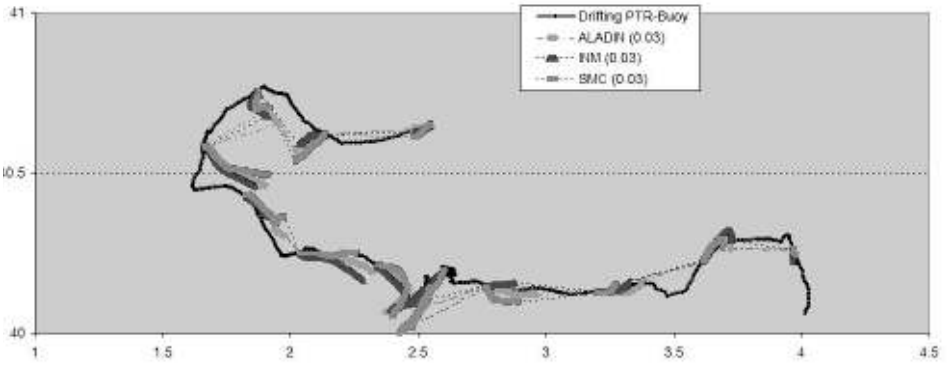

Figure 2 Lionmed drift re-analysis using 3% of ALADIN, INM and SMC winds (at 24 h spans).

In order to assess the optimal combination and weighting of forcing inputs, wind and current models outputs have been compared, between them and against observed data, corresponding to the LIONMED exercise. Some expected results have been:

- Forecasted wind fields from different models are quite similar, in time, space, speed and direction, leading to a similar wind-driven prediction (Figure 2). They widely agree with coastal buoy observations. Fewer differences appear mainly in open sea (where there are no measurements).
- Forecasted and analysed current fields differ greatly from model to model (sometimes giving opposite directions). It should be noted that only daily averaged values could be compared. Consequently, drift forecasts forced only with currents (without an additional wind stress term) are highly sensitive to hydrodynamic output.

3.2 Forcing optimisation: Methodology

All along the LIONMED buoy drift, successive positions are interpolated (discretised) in regular spans of 30 minutes (continuous line in Figure 2). Then forcing fields are interpolated at each position, enabling comparison of speed and direction of buoy velocity, currents and winds. During some episodes, buoy drift can be clearly correlated with the winds and/or currents; in others, the velocity of the buoy is unexpectedly great compared to the forcing. The aim of forcing optimisation is to obtain an averaged relationship (weighting) of the buoy movement and forcing inputs, i.e. to be able to define a wind and currents factor in the calculation of the buoy drift.

At each position, two deflection angles are defined as the difference in directions between 'buoy drift & wind' and 'buoy drift & currents'. For example, Figure 3 plots the relationship between wind speed and the wind drift factor required to reproduce the corresponding buoy drift speed, for only episodes when the 'buoy-wind' deflection is less than 45º (i.e. closer to the Ekman surface drift). Paying attention to winds greater than 5 ms^{-1}, we obtain a parabolic relationship that will be used in future runs of the drifting model. This parabolic function gives an average drift factor of 5%.

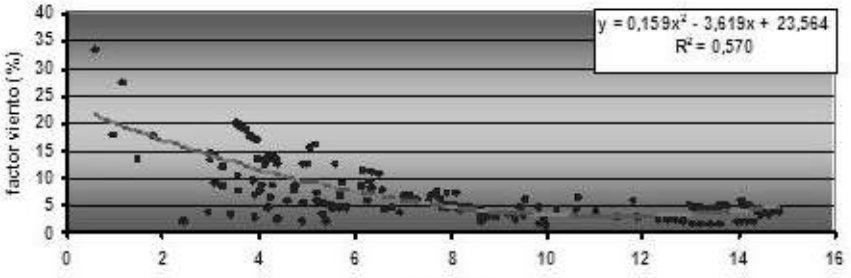

Figure 3 Adjustment of drift factor against wind speed (for deflection < 45º)

References

Comerma, E. (2004). Numerical Modelling of the drift and weathering hydrocarbons spilled at sea. Operational Application to combat black tides. 301 pp. (in Spanish), PhD Thesis, Polytechnic University of Catalonia (UPC).

Jordà, G., E. Comerma, R. Bolaños and M. Espino (2005). Impact of forcing errors in the CAMCAT oil spill forecasting system. A sensitivity study. J. of Mar. Systems, in press.

Real-time forecast modelling for the NW European Shelf Seas

M.W. Holt*, J.P. Osborne, J.R. Siddorn, P. Hyder and E. O'Dea

Met Office, UK

Abstract

The Met Office has run a 3-D circulation model of the NW European shelf seas in the daily suite of operational forecast models since June 2000, using the POLCOMS system implemented on a ~12 km grid, providing a nowcast and 48-hour forecast. It is forced by surface hourly winds and pressures, and 6-hourly heat fluxes from the Met Office Numerical Weather Prediction model. Open boundaries of elevation and barotropic currents are derived from tidal harmonics; and those of temperature, salinity and elevation are from the Atlantic FOAM deep ocean model. Comparison with moored buoy and AVHRR satellite observations shows that the model represents well the evolution of sea surface temperature (SST) in the North Sea. Nested regional models of the Irish Sea region, at one nautical mile resolution, and the Medium Resolution Continental Shelf (MRCS) region, a ~6 km resolution model covering the NW European Shelf to the 200 m contour, were introduced in 2003 and early 2005. The MRCS model includes a basic representation of sediment transport. In addition, a coupled physical-ecological model on the MRCS domain using the POLCOMS-ERSEM system is running pre-operationally in near real time. A quasi-barotropic relocatable model can also be applied in high resolution to any region of the shelf seas.

Data from the models are available either via the Met Office Data and Products Distribution Service for operational purposes, or from patrick.hyder@metoffice.gov.uk on request for research collaborations. They are currently provided to several oceanographic research centres (e.g. POL, MUMM, SAMS, NOCS and DMI) through national and international projects (e.g. NOOS and NORSEPP). Modelled surface currents and winds have been used to force the VISAR Search and Rescue package developed by the University of Wales, Bangor.

Keywords: Operational ocean forecasting, currents, drift forecasts, coastal observatory.

1. Introduction

The shelf seas group is a component of the National Centre for Ocean Forecasting (NCOF) in the UK Met Office (www.ncof.gov.uk). NCOF operationally runs various configurations of the Forecast Ocean Assimilation Model (FOAM) for global deep ocean regions; global and UK wave models; and the shelf seas suite of models. The shelf seas group runs several 3-D hydrodynamic models in the NW European Shelf region using the POLCOMS 3-D hydrodynamic modelling system (www.pol.ac.uk). In addition the POLCOMS-ERSEM system is used for a near-operational ecosystem model of the NW

* Corresponding author, email: martin.holt@metoffice.gov.uk

European Shelf. Model output is provided to various institutes through national and international projects, and is also used for search and rescue and oil spill simulations; for forecasts of harmful algal blooms; and for forecasts of visibility and turbulent kinetic energy parameters.

2. The models

1. The Atlantic Margin Model (AMM) is a ~12 km (1/9°×1/6°) resolution physical model, extending from approximately 40° N to 65° N and 20° W to 13° E, nested into 1/3° Atlantic FOAM (Holt and James, 2001). The model has 32 vertical levels defined using the s coordinate system. It includes freshwater input from rivers and from the Baltic. Information about the model domain can be found at: www.metoffice.gov.uk/research/ncof/shelf/amm.html.
2. The Irish Sea Model (ISM) is a ~1 nm (1/60°×1/40°) resolution model, extending from approximately 51.0° N to 56.0° N and from 7.0° W to 2.7° W, nested into the AMM model. The model has 18 vertical levels. More information can be found on: www.metoffice.gov.uk/research/ncof/shelf/irishsea.html. Data from the model are provided to the POL Coastal Observatory http://cobs.pol.ac.uk/.
3. The relocatable Model is a quasi-barotropic model which can be applied to any region at the required resolution. It uses the POLCOMS modelling system but is initialised with constant temperature and salinity and, hence, does not simulate baroclinic processes. It uses the Grenoble FES99 tidal harmonics at the boundary and is usually implemented in nested models from large scale (12 km) to high resolution (1 nm and, if required, to 200 m). Winds and pressure surface forcing can be applied and several vertical levels with bottom friction are usually simulated. This model has been applied in a variety of locations, such as the Solent, and can be run without wind and pressure forcing long periods in advance of the required date.
4. The Medium Resolution Continental Shelf Model (MRCS) is a 6 km (1/15°×1/10°) resolution model of the continental shelf, extending from approximately 48° N to 62° N and 12° W to 13° E, nested into the AMM model. The model has 18 vertical s-levels, includes a basic representation of sediment transport and is run operationally on a daily basis. Further information can be found at: www.metoffice.gov.uk/research/ncof/mrcs/index.html.

The POLCOMS-ERSEM MRCS is a coupled physical and ecosystem model of the MRCS domain (Siddorn *et al.*, 2005). ERSEM is a generic model that describes both the pelagic and benthic ecosystems and the coupling between them in terms of the significant bio-geo-chemical processes affecting the flow of carbon, nitrogen, phosphorus and silicon. It uses a 'functional group' approach to describe the ecosystem, whereby biota are grouped according to their trophic level and sub-divided according to size and feeding method. A hindcast has been completed for 2002–2004. This model is run in near real time with weekly updates. It simulates all the principal biogeochemical components including nutrients (nitrates, phosphates and silicates), phytoplankton (flagellates, dinoflagellates, diatoms and picoplankton) and zooplankton (heterotrophic flagellates, mesozooplankton (copepods) and microzooplankton).

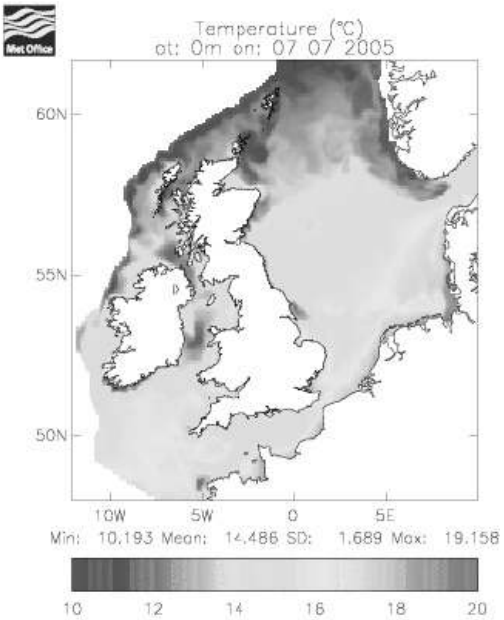

Figure 1 Daily mean sea surface temperature on 7 July 2005 at 00:00 GMT simulated by the MRCS model.

3. Model applications

Some examples of model applications include:

1. Harmful algal blooms. The prediction of the onset of harmful algal blooms, through computational modelling or otherwise, is a complex task. Many species of algae can give rise to harmful blooms. We do not attempt to explicitly model individual harmful species but rely on a fuzzy logic-type approach. The functional group information from the POLCOMS-ERSEM model is used in combination with biogeochemical and physical output from the model to map risk of bloom incidence.
2. Search and rescue (SAR) and Oil drift. Currents and winds from Met Office models have been used as forcing for the VISAR search and rescue package developed by the University of Wales, Bangor. Grib format currents and winds from the Met Office models can also be used as input for the BMT SARIS/OSIS search and rescue, and oil drift models.

4. Future work

Planned developments for Met Office shelf seas models include:

1. POLCOMS-WAM: A coupled wave-hydrodynamic model for UK waters will be assessed.
2. NEMO: The Forecast Ocean Assimilation Model (FOAM) group of the UK Met Office (with help from others) is in the process of transitioning to the NEMO ocean modelling framework. The development of NEMO is now a collaborative European

effort (www.lodyc.jussieu.fr/opa/NEMO). The NEMO modelling framework will be further developed for shelf-wide application.

3. HRCS: A 1 nautical mile resolution POLCOMS model of the NW European shelf to the 200 m contour (MRCS domain) will be evaluated.

5. Discussion

Data from these models are available for use through collaborative international and national projects. For example, through a project of the NW shelf Operational Oceanographic System (NOOS, Holt 2003), data are provided to MUMM and to DMI to assist in the development of local 3D circulation forecast modelling of the North Sea.

Acknowledgements

The POLCOMS system is developed by Proudman Oceanographic Laboratory (POL). The POLCOMS-ERSEM system is developed by POL and Plymouth Marine Laboratories, and applied at the Met Office under the UK National Met. Programme with support from the MERSEA integrated project.

References

Holt, J.T. and I.D. James (2001). An s coordinate density evolving model of the northwest European continental shelf: 1, Model description and density structure. Journal of Geophysical Research, 106, 14015–14034.

Holt, M., Z. Li and J. Osborne (2003). Real-time forecast modelling for the NW European Shelf Seas. In Dahlin, H., N.C. Flemming, K. Nittis, and S.E. Petersson (eds.) (2003). Building the European Capacity in Operational Oceanography, Proceedings of the Third International Conference on EuroGOOS, 2002, Athens, Greece, Elsevier Oceanography Series. 484–489.

Holt, M.W. (2003). Towards NOOS — the EuroGOOS NW Shelf task team 1996–2002 in Dahlin, H., N.C. Flemming, K. Nittis, and S.E. Petersson (eds.) (2003). Building the European Capacity in Operational Oceanography, Proceedings of the Third International Conference on EuroGOOS, 2002, Athens, Greece, Elsevier Oceanography Series. pp 461–465.

Siddorn, J.R., J.I. Allen, J.C. Blackford, F.J. Gilbert, J.T. Holt, M.W. Holt, J.P. Osborne, R. Proctor and D.K. Mills, (Submitted). Modelling the hydrodynamics and ecosystem of the North-West European continental shelf for operational oceanography. Journal of Marine Systems (Special Issue proceedings of Liege Colloquium 2004).

High resolution wave forecasting at the Galician coast

P. Carracedo*[1], M. Barreiro[1], S. Torres[1], P. Montero[1], M. Ruiz-Villarreal[2], Marta Gómez[3], Juan Carlos Carretero[3] and V. Pérez-Muñuzuri[1]

[1]*MeteoGalicia, CMA-USC, Santiago de Compostela, Spain*
[2]*Instituto Español de Oceanografía, A Coruña, Spain*
[3]*Ente Público de Puertos del Estado, Spain*

Abstract

Galician Rias Baixas is one of the most productive ecosystems present at NW Iberian coast. Especially after the Prestige disaster, the Galician government realised the sensitivity of this region. In this sense, several models for tidal dynamics and wind currents as well as numerical models for wave forecasting are currently being improved and validated inside this region by MeteoGalicia.

Keywords: Coastal wave forecast, wave modelling, Rias Baixas

1. Introduction

The wave forecasting system being tested consists of a three level WaveWatch III nesting coupled to a high resolution (500 m) level implemented using the SWAN model. Real time wind forcing comes from the ARPS model, used by MeteoGalicia to perform a daily forecast. The low resolution three level nested model based on WaveWatchIII has been tested during last year, and high resolution nesting based on SWAN is been tested. The prototype implemented includes Rias Baixas, which is one of the most important regions from an economical point of view.

2. Modelling system

The modelling strategy is based on two wave models. A low resolution forecast is achieved with the 3rd generation model WaveWatch III, originally developed by Marine Modelling and Analysis Branch (MMAB) of National Centers for Environmental Prediction (NCEP). The SWAN model (Simulating Waves Nearshore), developed by Delft University of Technology, is used for high resolution wave forecasting at Galician Rias Baixas. Both models solve wave action spectra propagation, although some additional source/sink terms have been added to SWAN, i.e. SWAN is specifically designed for coastal applications.

In order to solve North Atlantic swell, wave production and propagation is calculated using global NCEP/NOAA GFS 10-m wind as input. Two one-way nestings propagate swell from the deep North Atlantic to coastal regions achieving the necessary resolution down to 2.5' for the Galician region. The local wind dynamic is solved using ARPS output from daily forecasts at MeteoGalicia.

* Corresponding author, email: pablo.carracedo@meteogalicia.es

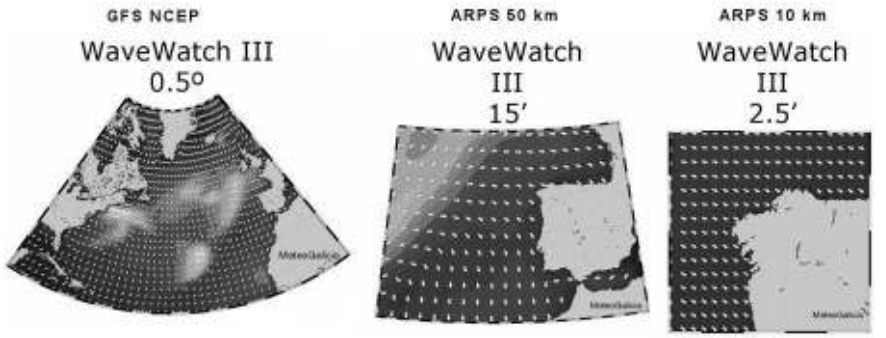

Figure 1 Low resolution system set-up. Snapshot of significant wave height (background tint) and mean wave direction (arrows) for three nested models. The North Atlantic model grid covers 90º W to 5º E and 15º N to 75º N which is enough to solve swell generation and propagation. GFS 10 m wind forcing is used for this task and also as a boundary condition for the ARPS 50 km model. ARPS 50 km 10 m wind forcing is introduced into the 15' model grid covering 24º W to 0º W and from 33º N to 48º N, in addition to spectral boundary condition from the 0.5' coarser grid. This procedure is updated using ARPS 10 km nested 10 m wind forcing and the 2.5' model grid, covering 10.75º W to 6º W and 41º N to 44.75º N.

3. Results

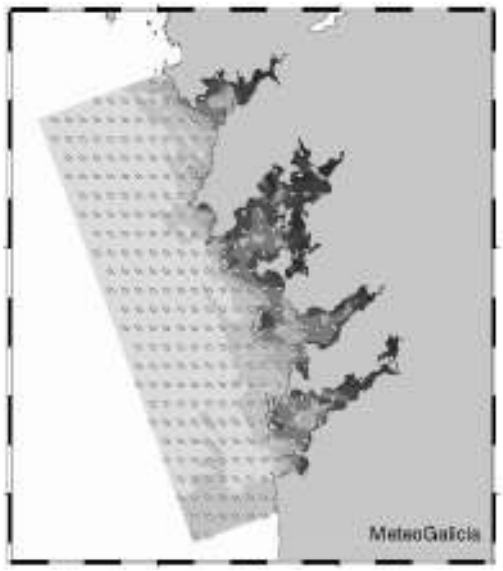

Figure 2 Plot of significant wave height (background tint) and mean wave direction (arrows) for Rias Baixas model grid.

3.1 High resolution model

Spectral data from the 2.5' Wavewatch model and ARPS 10 km 10 m wind are reprojected to a UTM grid to obtain a 500 m high resolution wave prediction. Wave prediction goes into Rias Baixas which is a difficult coastal structure for wave modelling.

A rotated grid of 104×170 grid points is used in order to represent the natural orientation of Rias Baixas. With this particular orientation we achieve the maximum sea/land point ratio.

3.2 Model validation

Data from the WaveWatchIII model are validated against field data which are available from Puertos del Estado−Clima Marítimo's deep water buoys network.

Table 1 Location of Puertos del Estado buoys.

Estaca de Bares	44º 3.6' N 7º 37.2' W
Cabo Vilano	43º 29.4' N 9º 12.6' W
Cabo Silleiro	42º 7.2' N 9º 24.0' W

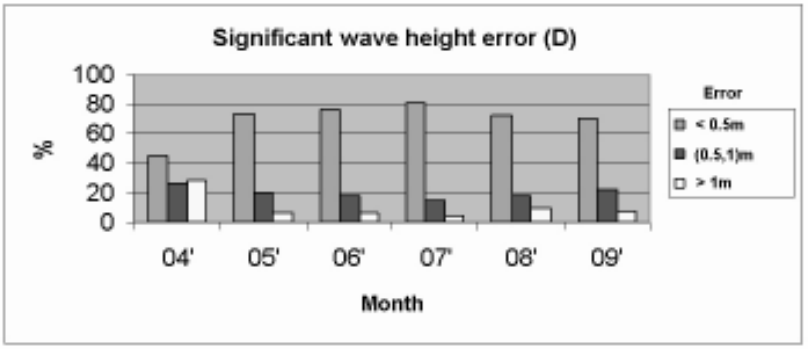

Figure 3 Six months statistic (2004) of classified significant wave height at Estaca de Bares model grid point.

4. Conclusions and future work

A wave forecasting system from North Atlantic to regional scale has been presented. Model validation efforts are becoming operational to generate monthly statistics. Algorithms for sea and swell separation are being implemented to be used in daily forecast.

We are currently studying coupling to a 2D tidal currents model based on MOHID developed by MARETEC Group (IST, Lisbon) and used in a daily forecast of tidal water level and water currents.

Some new implementations of the SWAN model covering new coastal regions are planned.

Acknowledgements

The authors would like to thank Marta Gomez and Juan Carlos Carretero from Puertos del Estado (www.puertos.es) for their help and support during the implementation of SWAN.

References

Tolman, H.L. (1991). A third-generation model for wind waves on slowly varying, unsteady and inhomogeneous depth and currents, Journal of Physical Oceanography, Vol. 21, pp 782–797.

Booij, N., R.C. Ris and L.H. Holthuijsen (1999). A third-generation wave model for coastal regions, Journal of Geophysical Research, Vol. 104, C4, 7649–7666.

Balseiro, C.F. *et al.* (2003). Tracking the 'Prestige' oil spill. An operational experience in simulation at MeteoGalicia, Weather, Vol. 58.

Taboada, J.J. *et al.* (1998). Evaluation of the Seasonal Variations in the Residual Patterns in the Ría de Vigo (NW Spain) by means of a 3D Baroclinic Model, Estuarine, Coastal and Shelf Science, Vol. 47, No. 5, pp. 661–670.

Desert dust deposition over the Mediterranean Sea estimated with the SKIRON/Eta

G. Kallos*[1], P. Katsafados[1], C. Spyrou[1] and A. Papadopoulos[2]

[1]*University of Athens, School of Physics, Atmospheric Modelling and Weather Forecasting Group, Greece*
[2]*Hellenic Centre for Marine Research, Greece*

Abstract

As presented in the previous EuroGOOS conference, the model-estimated annual amounts of Saharan dust deposited over the Mediterranean waters is of the order of 107 tn/year. This paper illustrates and briefly describes a database of model-derived seasonal amounts of dust deposited on Mediterranean waters and European land, using the SKIRON/Eta system, fully coupled with a desert dust module. Our study focuses mainly on the years 2003 and 2004 when the system was upgraded by using four particle size bins for the simulation of the desert dust cycle. It was found that the model can be a reliable tool for studying the spatio temporal variability of the desert dust cycle.

1. Introduction

Mineral dust, produced by wind erosion over arid and semi-arid areas of North Africa may, under favourable weather conditions, blow on the winds to the Middle East, Mediterranean, Europe, and even across the Atlantic Ocean. Dust particles have profound effects at a variety of scales, exerting many influences on the earth's environment and climate, as well as on human health. By scattering and absorbing solar radiation dust modifies the planetary albedo and reduces the amount of radiation reaching the surface (direct effect of aerosols, Charlson *et al.*, 1991). Secondly, aerosols act as CCN thereby modifying the microphysical, microchemical and hence optical and radiative properties of clouds (indirect effect of aerosols, Jones *et al.*, 1994). Dust particles also affect the climate through their influence on marine primary productivity (Jickells *et al.*, 1998) and there is even evidence that dust may cause ocean cooling (Schollaert and Merrill, 1998).

The dust amounts deposited on the surface are in direct proportion to the seasonal variability of the dust cycle in the atmosphere. Analyses of ground- and satellite-based observations and model simulations can lead to useful results in relation to the spatio-temporal variability of dust deposition. To have a feeling of the magnitude and the spatio-temporal distribution of dust deposition on ground surfaces the use of a credible numerical model is considered essential. In this study the SKIRON/Eta weather forecasting system fully coupled with a dust cycle module was used (Nickovic *et al.*, 2001; Papadopoulos *et al.*, 2002; Kallos *et al.*, 2005). The dust module was developed at the University of Athens and incorporates several state-of-the-art parametrisations for the simulation of the production, transport and deposition of desert dust particles.

* Corresponding author, email: kallos@mg.uoa.gr

2. Calculation of dust amounts deposited on the surface and seabed

In order to derive the seasonal amounts of Saharan dust deposited on the Mediterranean basin and Europe the system was integrated over a domain covering North Africa, Mediterranean and a large part of Europe and the Middle East. 32 vertical levels were used stretching from the ground to the model top (15 800 m), while a horizontal resolution of $0.24° \times 0.24°$ was applied. At each model grid point the dry and wet depositions were estimated assuming them as an average of the sub-area around each one.

By utilising the first 24 hours from the SKIRON/Eta forecasts, the geographical distribution of the total dust mass deposited on surface has been calculated on a monthly basis for the period January 2000 to December 2004 (60 months). Since the model has the capability to calculate dry and wet deposition separately it was possible to derive the geographical distribution of these two components of the total dust deposition, for each month of the five-year period. Since January 2003 calculations have been performed using four particle size bins (Table 1).

Table 1 Features of typical dust particles (Nickovic *et al.*, 2001).

K	Type	Centred particle radius (μm)
1	Clay	0.73
2	Silt, small	6.10
3	Silt, large	18.00
4	Sand	38.00

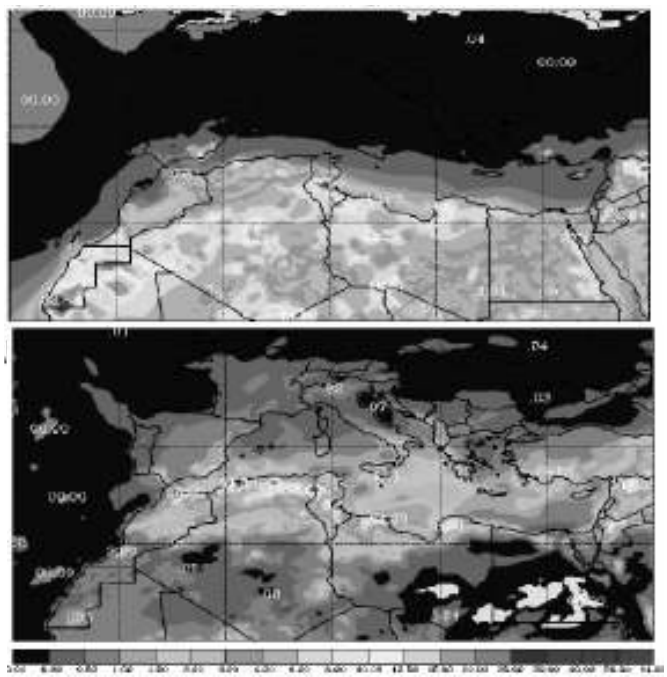

Figure 1 Annual dust deposition (top: dry and bottom: wet) for 2003 using 4 particle size bins. The unit of deposition is gm^{-2}.

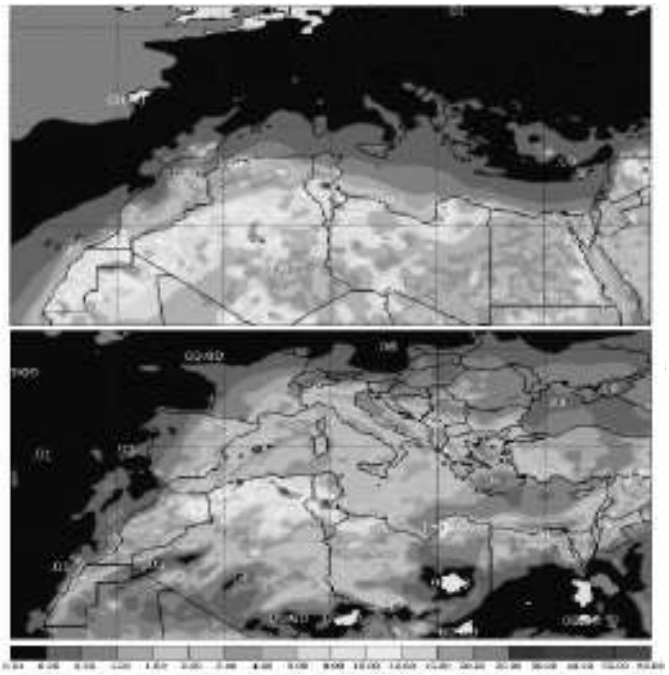

Figure 2 Annual dust deposition (top: dry and bottom: wet) for 2004 using 4 particle size bins. The unit of deposition is gm^{-2}.

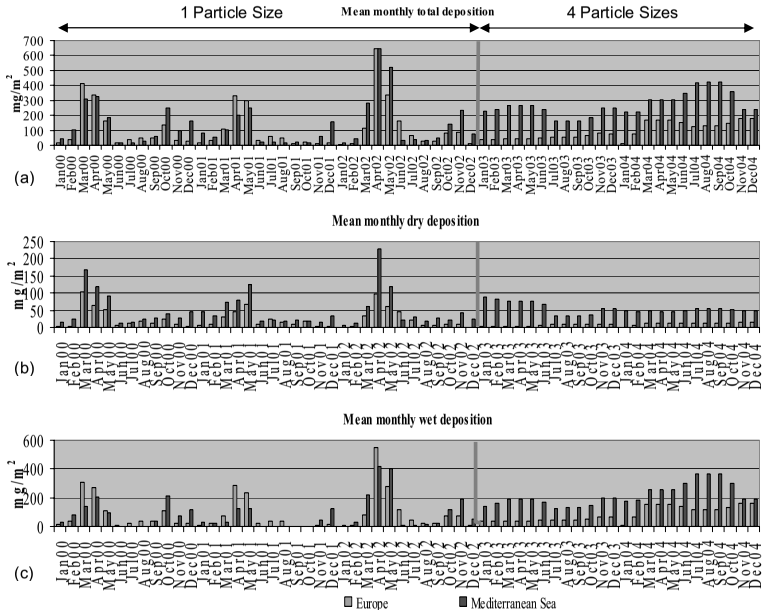

Figure 3 Mean Monthly Deposition (top: total, centre: dry and bottom: wet) for 2000–2004 for Europe and the Mediterranean. The transition from 1 particle size to 4 is indicated by the bold vertical line.

The dry and wet deposition (in $g m^{-2}$) for the year 2003 are depicted in Figure 1 and for the year 2004 in Figure 2. Figure 3 shows the monthly distribution of dust deposited on the Mediterranean Sea and Europe for the years 2000–2004.

During winter and spring the Mediterranean region is affected by two upper air jet streams: the polar front jet stream, originally located over Europe, and the subtropical jet stream which is typically located over northern Africa. The combined effects of these westerly jets in winter and spring support the propagation of extra-tropical cyclones towards the East and Southeast, resulting in dust plume intrusion in the Mediterranean. Moreover during spring and autumn the sea waters are relatively cool and the convective activities associated with rain are not significant enough to washout the dust.

During summer and autumn, due to differential heating between the land of Northern Africa, Southern Europe and the Mediterranean a southern flow is created that reduces the transported amounts of dust towards the Mediterranean basin.

For the years 2003 and 2004 the simulations were performed using 4 particle size bins. According to this classification the lighter particles can now be transported towards the Mediterranean waters and be deposited over Europe.

By utilising the estimated monthly dust deposition, the total annual amount of dust deposited on the Mediterranean Sea and Europe has been calculated. These quantities are presented in Table 2.

Table 2 Total annual dust deposition (in 10^3 tons) on the Mediterranean Sea and Europe

	Europe			Mediterranean Sea		
	Total	**Dry**	**Wet**	**Total**	**Dry**	**Wet**
2000	3914	936	2978	3962	1541	2421
2001	2909	725	2184	2500	1255	1245
2002	4723	883	3840	5132	1546	3586
2003	1999	256	1743	6752	1828	4924
2004	4933	398	4535	9306	1504	7802

The model-derived values presented above are in reasonable agreement with existing observations (e.g. Guerzoni *et al.*, 1999), especially for the years that 4 particle sizes were used for the simulation of the desert dust cycle. However a series of evaluation tests using actual measurements need to be conducted in order to have a clear picture of the upgraded systems capabilities.

3. Conclusions

The dust cycle in the atmosphere is considered important due to several implications such as climate, urban air quality, ecosystems, regional/mesoscale weather and rain. With the use of the SKIRON/Eta modelling system, fully coupled with a desert dust cycle module, a database of model-derived seasonal amounts of dust deposited on the Mediterranean Sea and Europe has been created. The transport and deposition patterns of the Saharan dust in the Mediterranean Basin can vary significantly according to the climatic and general circulation patterns, as the amount of Saharan dust deposited on

Europe and Mediterranean waters exhibits significant seasonal and inter-annual variability. The strength and frequency of occurrence of the Saharan dust episodes define the annual deposition amounts and patterns to a high degree, as in some cases the mass deposited through a single episode, in a certain location, can change significantly the local deposited quantities on a monthly and annual basis.

In conclusion the SKIRON/Eta system is capable not only for the prediction of Saharan dust episodes in an accurate way, but can be used for deriving dust climatology as well.

References

Charlson, R.J., J. Langner, H. Rodhe, C. Leovt and S. Warren (1991). Perturbation of the Northern Hemisphere radiative balance by backscattering from anthropogenic sulfate aerosols. Tellus, 43AB, 152–163.

Guerzoni, S., R. Chester, F. Dulac, B. Herut, M.-D. Loye-Pilot, C. Measures, C. Migon, E. Molinaroli, C. Moulin, P. Rossini, C. Saydam, A. Soudine and P. Ziveri (1999). The role of atmosphere deposition in the biogeochemistry of the Mediterranean Sea, Prog. Oceanogr. 44:147–190.

Goudie, A.S. and N.J. Middleton (2001). Saharan dust storms: nature and consequences. Earth-Science Reviews, 56, 179–204.

Hatzianastassiou, N., B. Katsoulis and I. Vardavas (2004). Global distribution of aerosol direct radiative forcing in the ultraviolet and visible arising under clear skies. Tellus, 56B, 51–71.

Jickells, T.D., S. Dorling, W.G. Deuser, T.M. Church, R. Arimoto and J.M. Prospero (1998). Air-borne dust fluxes to a deep water sediment trap in the Sargasso Sea. Global Biogeochemical Cycles 12, 311–320.

Jones, A., D.L. Roberts and A. Slingo (1994). A climate model study of the indirect radiative forcing by anthropogenic sulfate aerosols. Nature, 370, 450–453.

Kallos, G., S. Nickovic, A. Papadopoulos, D. Jovic, O. Kakaliagou, N. Misirlis, L. Boukas, N. Mimikou, G. Sakellaridis, J. Papageorgiou, E. Anadranistakis and M. Manousakis (1997). The regional weather forecasting system SKIRON: An overview, in: Proceedings of the International Symposium on Regional Weather Prediction on Parallel Computer Environments, G. Kallos, V. Kotroni, and K. Lagouvardos, ed., ISBN: 960–8468–22–1, University of Athens, Greece, pp. 109–122.

Kallos, G., A. Papadopoulos, P. Katsafados and S. Nickovic (2005). Trans-Atlantic Saharan dust transport: Model simulation and results, Submitted to Journal of Geophysical Research.

Nickovic, S., G. Kallos, A. Papadopoulos and O. Kakaliagou (2001). A model for prediction of desert dust cycle in the atmosphere, J. Geophys. Res. 106:18113–18129.

Papadopoulos A., G. Kallos, P. Katsafados and S. Nickovic (2002). The Poseidon weather forecasting system: An overview, GAOS 8:219–237.

Schollaert, S.E. and J.T. Merill (1998). Cooler sea surface west of the Sahara Desert correlated to dust events. Geophysical Research Letters 25, 3529–3532.

In situ and Remote Sensing Measurements 2

On radar imaging of mesoscale eddies and fronts

J.A. Johannessen*[1,2], V. Kudryavtsev[3,4], D. Akimov[4], T. Eldevik[1,5], N. Winther[1] and B. Chapron[6]

[1]*Nansen Environmental and Remote Sensing Center, Bergen, Norway*
[2]*Geophysical Institute, University of Bergen, Norway*
[3]*Nansen International Environmental and Remote Sensing Center, St.Petersburg, Russia*
[4]*Marine Hydrophysical Institute, Sebastopol, Ukraine*
[5]*Bjerknes Center for Climate Research, Bergen, Norway*
[6]*Institute Français de Recherche pour I'Exploitation de la Mer, Plouzané, France*

Abstract

The surface signatures of meandering fronts and eddies have been regularly observed and documented in SAR images. Wave-current interactions, the suppression of short wind waves by natural film and the varying wind field resulting from atmospheric boundary layer changes across an oceanic temperature front all contribute to the radar image manifestation of such mesoscale features. The corresponding imaging mechanisms are quantitatively explored using a new radar imaging model (Kudryavtsev *et al.*, 2005) that solves the energy balance equation where wind forcing, viscous and wave breaking dissipation, wave-wave interactions and generation of short waves by breaking waves are taken into account. SAR image expressions of current fronts and eddies are then simulated based on oceanic fields derived from two numerical ocean models. The comparison of simulated images with ERS SAR and Envisat ASAR images is favourable. The new radar imaging model therefore provides a promising tool for advancing the quantitative interpretation of current features manifested in SAR images.

Keywords: Fronts, eddies, radar imaging model, ocean modelling.

1. Introduction

The ocean is rich in mesoscale dynamics. Examples are meandering currents and eddy generation with distinct sea surface temperature fronts, the sporadic occurrence of filaments and jets, and wind-driven coastal upwelling and downwelling. Due to a general lack of sufficient high quality *in situ* observations, the understanding of how these features contribute to the complicated surface roughness modulation pattern often manifested in SAR images is incomplete. In turn, our ability to interpret and quantify surface current features imaged by SAR has not been adequately developed. The systematic use of SAR image observations for quantitative studies of the mesoscale ocean features has thus been hampered.

The fundamental equations for SAR imaging of surface current features have nevertheless gradually become better known (Alpers and Hennings, 1984; Lyzenga and Bennett, 1988; Apel, 1994; Romeiser and Alpers, 1997; Romeiser *et al.*, 2001; Kudryavtsev *et al.*, 2005) and can now be applied to simulate SAR image expressions.

* Corresponding author, email: johnny.johannessen@nersc.no

Figure 1 schematically outlines the main steps of the new radar imaging model (RIM) by Kudryavtsev *et al.* (2005). Based on a detailed quantitative characterisation of the surface current, the near-surface wind field, and the presence of surfactants, the conservation of wave action (i.e. energy balance) is invoked to consistently describe the surface roughness modulations. The roughness is partitioned into larger scale waves and small scale Bragg waves. The mean square slope (mss) of larger scale waves contributes directly to specular reflection (sp), but also to Bragg (br) scattering by means of the tilting of shorter waves. In addition, wave breaking (wb) of larger scale waves alters the surface roughness and generates smaller scale Bragg waves. In turn, the total surface scattering properties can be quantified and used to simulate the normalised radar cross-section (NRCS) given by:

$$\sigma_0^p = (\sigma_{br}^p + \sigma_{sp})(1-q) + \sigma_{wb} q$$

where q is the fraction of the sea surface covered by breaking waves and p is polarisation.

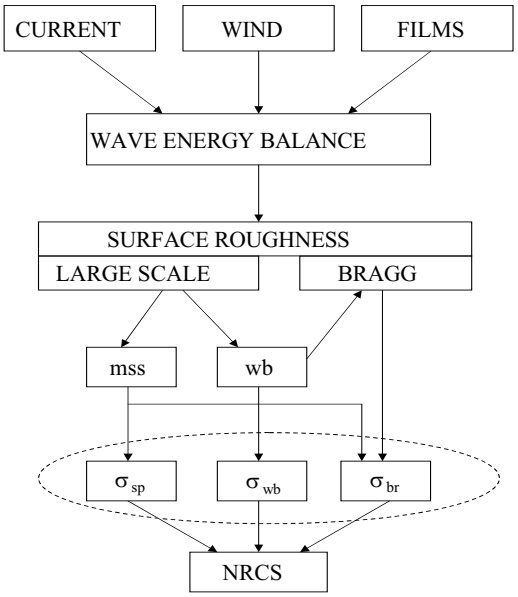

Figure 1 Schematic illustration of the main radar imaging model assumptions and principles. Note that the sea surface roughness is an integral from the large scale tilt that determines mean square slope (mss) and breaking waves (wb) to the small scale Bragg (br) wavelengths. The three terms that contribute to the normalised radar cross-section (NRCS) are quasi-specular contribution, impact from breaking waves and Bragg scattering, respectively denoted σ_{sp}, σ_{wb}, σ_{br}.

The general demand for high quality *in situ* validation data is bypassed by the alternative use of surface fields of temperature and current derived from numerical ocean models. The models are a high resolution process model (Eldevik and Dysthe, 2002) and a model of the Norwegian Coastal Current (NCC) (Winther and Evensen, 2005). The model data are fed into the RIM of Kudryavtsev *et al.* (2005).

2. Frontal eddies

As discussed and highlighted in Kudryavtsev *et al.* (2005) the RIM provides consistent insight into the physics responsible for the image manifestation of surface current features. To illustrate and quantify these different SAR imaging effects, a series of basic RIM simulations for C-band radars are conducted for simple current fields (for more details see Johannessen *et al.*, 2005). In order to account for the effect of changes in the marine atmospheric boundary layer (MABL) on the radar imaging, the simulation is also expanded to include an accompanying change in the sea surface temperature. A step-like temperature front with a drop of 3 °C is considered with neutral stratification on the up-wind side of the front. The model simulations reveal in this case surface roughness changes from the combined effect of varying wind stress in the MABL (induced by the sea surface temperature front) and surface current convergence and divergence (induced by the meandering current). The results are plotted in Figure 2. The overall characteristics of these results clearly reveal the importance of wave breaking in the vicinity of surface convergence, combined with a drop in wind stress at the down-wind cold and stable side of the front. Hence, the joint delta- and step-like change in NRCS is resulting from the enhanced wave breaking combined with the changes in the wind stress.

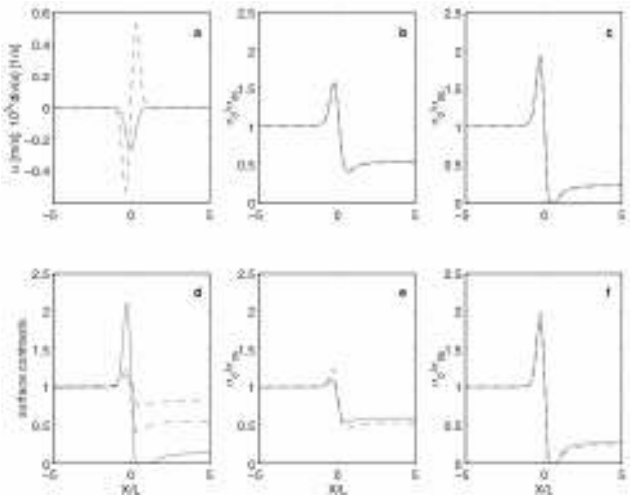

Figure 2 Model response for the meandering shear current front accompanied by a sea surface temperature front. a) Current velocity component perpendicular to the front (solid line); current divergence (dashed line); b) NRCS contrasts for C-band at 20° incidence angle, VV (solid) and HH (dashed) polarisations for down-wind radar look direction; c) Same as (b) but for cross-wind radar look direction; d) Relative contribution to the contrasts for white caps coverage (solid), mean square slope (dashed) and Bragg waves spectrum (dotted-dashed); e) Same as for (b) but for 40° incidence angle; f) Same as (e) but for cross-wind radar look direction.

Building on these results the capability of the RIM to simulate the 2-D imaging of frontal eddies and coastal current features is examined. The background data of sea surface current, surface temperature and wind speed to be fed into the RIM are entirely taken from 3-D numerical ocean models, sidestepping the problem of lacking *in situ* data. In cases where no damping film material is present, the eddy features are expressed as a

bright radar modulation along the converging front. An example of such a SAR image expression of a 10 km in diameter cyclonic eddy in the Norwegian Coastal Current is shown in Figure 3a that generally depicts the eddy boundary with a bright NRCS anomaly exceeding the background by up to 2–3 dB (Johannessen *et al.*, 2005).

Eldevik and Dysthe (2002) recently put forward a conceptual model for the generation and evolution of "spiral eddies" (Munk *et al.*, 2000). As an unstable current front evolves, there is both sharpening of horizontal gradients and nonlinear windup of the front to produce cyclones. Eldevik and Dysthe (2002) suggest that buoyant geostrophic jets in the upper ocean are prone to producing unstable fronts with wavelengths and growth rates consistent with the spirals. An example of the simulated surface flow pattern from their fine resolution (650 m horizontally, 5 m vertically) numerical experiments is shown in Figure 3b. Both modelled and observed spiral eddies are associated with streaks of strong cyclonic shear and convergence. Due to the convergence, the passive surface floating material accumulates to delineate the model eddies of Figure 3b.

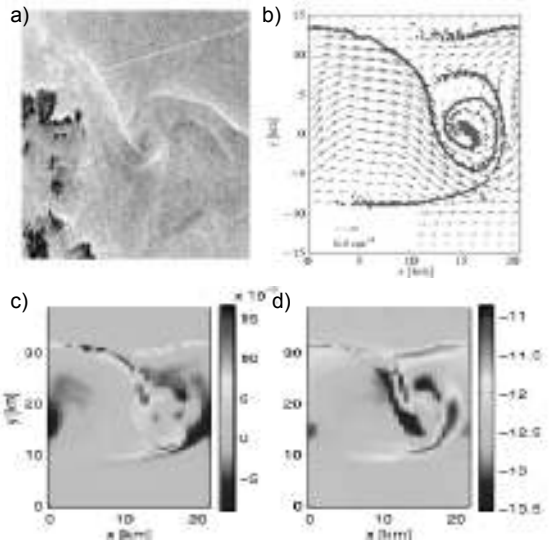

Figure 3 a) ERS-1 SAR image expression of 10 km cyclonic eddy feature in the Norwegian Coastal Current; b) modelled spiral eddies as traced out by passive floats and the surface velocity field; c) corresponding surface divergence field; d) simulated radar cross section using the modelled current field with b as input.

The surface current field (Figure 3b) with its zones of convergence and divergence (Figure 3c) obtaining a strength of about $10^{-4}\,s^{-1}$ are used in the RIM to produce the NRCS field shown in Figure 3d. For a near surface wind speed of 5 ms^{-1} from southwest (between cross-wind and downwind radar look direction) the NRCS contrasts along the eddy boundary reach up to 2 dB. The enhanced wave breaking of intermediate waves in the vicinity of the zones of surface current convergence is the dominant source for the radar cross-section modulation and subsequent SAR image manifestation. This is confirmed by comparing the NRCS plot (Figure 3d) with the surface current divergence field (Figure 3c) as well as the distribution of the passive floating material (Figure 3b).

3. Mesoscale variability

Capitalising on this result we proceed with an examination of how well the Envisat ASAR image expression of the Norwegian Coastal Current (NCC) off the southwest coast of Norway obtained on 9 May 2003 (Figure 4a) can be interpreted using the RIM. The HYCOM (Bleck, 2002; Winther and Evensen, 2005) realisation of the meandering surface current and surface temperature distribution at 2−4 km spatial resolution, displaying a nearly 2°C thermal front (Figure 4b), and the divergence field (Figure 4c) for the same day is shown. The model is forced with atmospheric fields provided by the European Center for Medium-range Weather Forecasting (ECMWF). The corresponding simulated NRCS for a 5 ms^{-1} wind normal to the radar look direction is shown in Figure 4d.

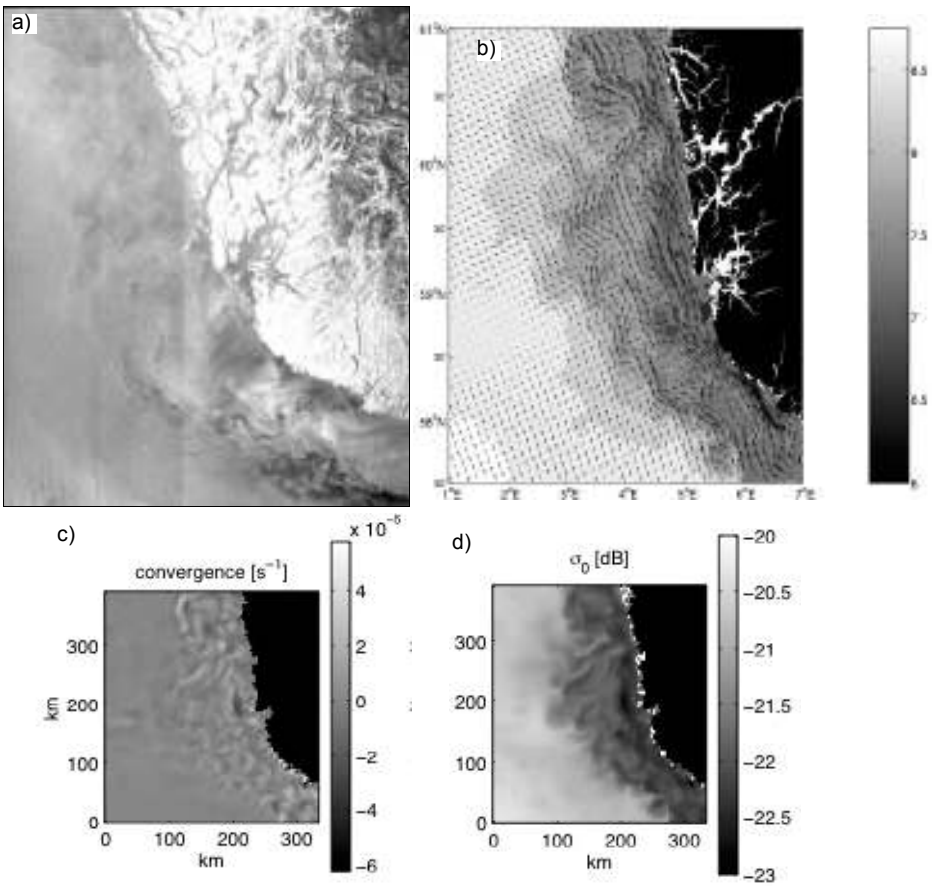

Figure 4 a) ASAR image of the Norwegian Coastal Current off southwest coast of Norway on 9 May 2003; b) The corresponding simulated surface current vector map (max. 0.6 ms^{-1}) and temperature pattern (°C, values indicated in grey scale bar); c) divergence map; d) simulated NRCS (HH). The ASAR image is oriented along the descending flight track of the satellite and thus slightly skewed versus the model north−south orientation.

The ASAR image expression (not corrected for the antenna pattern) is fairly complicated with bands of bright and dark NRCS predominantly confined within the area occupied by the NCC (Figure 4a, b). The dominant wavelength of the modulation pattern is about 20–30 km with peak-to-background NRCS contrast ranging from 1–3 dB. In comparison the mesoscale variability of the surface current within the NCC (Figure 4b) also attains a dominant length scale of 30 km. The current strength associated with these features ranges from 0.4–0.6 ms^{-1}. The divergence field (Figure 4c) reveals an abundance of zones of current convergence and divergence with magnitudes of up to $2\times10^{-5}s^{-1}$. This is an order of magnitude less than for the spiral eddies discussed in Section 2. In turn, the simulated NRCS obtains rather weak modulation depths up to 1 dB (Figure 4d). The structure and orientation of the modulations, on the other hand, agrees very well with the dominant pattern in the convergence and divergence field. The distinct drop in the level of simulated NRCS within the NCC arises from the transformation of the MABL over the colder coastal surface water. This expression is not pronounced in the ASAR image and may be attributed to the real MABL regime (different wind speed and sea surface temperature) and hence wind stress as suggested by the weaker thermal front of about 1.3°C found in a simultaneous, but partly cloud covered satellite Advanced Very-High Resolution Radiometer (AVHRR) thermal infrared image (not shown).

Overall, this approach to interpreting SAR image expressions in the context of surface current convergence and divergence zones seems very promising. Combining numerical ocean models and the RIM thus appears as a powerful tool to either validate ocean models or quantify SAR images expressions of mesoscale current features as there is rarely sufficient quality and coverage by *in situ* data.

4. Summary

By combining the new RIM with surface current fields from state-of-the-art ocean models, the 2-D radar image manifestations of mesoscale fronts and eddies have been simulated (for full details see Johannessen *et al.*, 2005). The comparison with ERS–1 SAR and Envisat ASAR images for the case of eddies and meanders from the NCC is very promising. In particular, it is concluded that:

- The forward simulations consistently emphasise the crucial role of current convergence and divergence that occur along meandering fronts and eddies
- In the case of convergence, the surface roughness modulation comes from the (direct and indirect) effects of the breaking of intermediate scale waves that takes place within the converging zone due to wave-current interaction.

Hence, the RIM apparently includes the dominant interactive processes and their subsequent modulations of the sea surface roughness. More evaluations are certainly needed to consolidate these results. However, the consistent approach in the RIM can potentially enable the use of multiple sources of surface information, including 3D ocean models, atmospheric forcing fields, different satellite sensor wavelength and polarisation characteristics, as well as *in situ* devices (such as HF radars). Note also that a growing number of experimental SAR satellites are planned to be launched within the next few years (e.g. TerraSAR X, COSMO-Skymed) that will complement the currently operating C-band

Radarsat and Envisat ASAR. Future work will also be directed towards the combination of this approach with the Doppler centroid information retrieved in SAR systems (e.g. Chapron *et al.*, 2005). Overall, we therefore conclude that these promising results will open new opportunities for more systematic studies of mesoscale ocean variability based on SAR in the coming years.

Acknowledgement

Core support for this study was provided by the EU funded 5th Framework Programme (FP5) project MARSAIS (contract no. EVG1−CT−2000−00029), the SARMIS project financed under the bilateral EU−Russia support agreement (INTAS contract no. 00−598), and the MONCOZE and ProClim projects funded by the Norwegian Research Council (contract no. 143559/431 and 155923/700). Moreover, the Norwegian Space Centre has supported the work under the contract JOP.8.3.3.06.01.1. In addition the authors also acknowledge the support of ESA under the ESA−IAF project on "GMES Networking with Russia and Ukraine".

References

Alpers, W., and I. Hennings (1984). A theory of the imaging mechanism of underwater bottom topography by real and synthetic aperture radar, J. Geophys. Res., 89(C6), 10,529−10,546.

Apel, J.R. (1994). An improved model of the ocean surface wave vector spectrum and its effects on radar backscatter, J. Geophys. Res., 99(C8), 16,269−16,291.

Bleck, R. (2002). An oceanic general circulation model framed in hybrid isopycnic-cartesian coordinates, Ocean Modelling, 4, 55−88.

Chapron, B., F. Collard and F. Ardhuin (2005). Direct measurements of ocean surface velocity from space: Interpretation and validation, J. Geophys. Res., 110, C07008, doi:10.1029/2004JC002809.

Eldevik, T. and K.B. Dysthe (2002). Spiral eddies. J. Phys. Oceanogr., 32, 851−869.

Johannessen, J.A., V. Kudryavtsev, D. Akimov, T. Eldevik, N. Winther, O.M. Johannessen and B. Chapron (2005). On radar imaging of current features: 2. Mesoscale eddy and current front detection, J. Geophys. Res., 110, C07017, doi:10.1029/2004JC002802.

Johannessen, J., R. Shuchman, G. Digranes, D. Lyzenga, W. Wackerman, O. Johannessen and P. Vachon (1996). Coastal ocean fronts and eddies imaged with ERS−1 synthetic aperture radar, J. Geophys. Res., 101, 6651−6667.

Kudryavtsev, V., D. Akimov, J.A. Johannessen and B. Chapron (2005). On radar imaging of current features: 1. Model and comparison with observations, J. Geophys. Res., 110, C07016, doi:10.1029/2004JC002505.

Lyzenga, D.R. and J.R. Bennett (1988). Full-spectrum modeling of synthetic aperture radar internal wave signature, J. Geophys. Res., 93(C10), 12,345−12,354.

Munk, W., L. Armi, K. Fischer and F. Zachariasen (2000). Spirals on the sea. Proc. Roy. Soc. London A, 456, 1217−1280.

Romeiser, R. and W. Alpers (1997). An improved composite surface model for the radar backscattering cross section of the ocean surface. 2. Model response to surface

roughness variations and the radar imaging of underwater bottom topography, J. Geophys. Res., 102(C11), 25,251–25,267.

Romeiser, R., S. Ufermann and W. Alpers (2001). Remote sensing of oceanic current features by synthetic aperture radar-achievements and perspectives, Annales of Telecommunications, no. 11/12, November–December, pp. 661–671, 2001.

An integrated service for oil spill detection and forecasting in the marine environment

Leonidas Perivoliotis*[1], Kostas Nittis[1] and Anna Charissi[2]

[1]*Institute of Oceanography, Hellenic Centre for Marine Research, Athens, Greece*
[2]*Dept. of Informatics and Telecommunications, University of Athens, Greece*

Abstract

In the framework of the ROSES (Real-Time Ocean Services for Environment and Security) project funded by ESA under the GMES initiative, an integrated service for oil spill detection and forecasting was developed and tested in a pilot phase. The service was implemented in the Central and South Aegean Sea (Greece) and combined the information from SAR image analysis together with state-of-the-art numerical models in order to provide a complete picture of the detection and the evolution of an oil spill in the marine environment. Complete reports for both detection and forecasting processes were available through a dedicated web site to the Greek marine authorities in near real time. The pilot operational phase of the service was between April and September 2004.

Keywords: Oil spills, SAR image analysis, detection, forecasting, numerical modelling

1. Introduction

The European action known as GMES (Global Monitoring for Environment and Security) aims to deliver a decision-support system for use by the public and policy-makers, with the capability of acquiring, processing, interpreting and distributing information related to environment, risk management and natural resources. This effort is co-funding by the European Space Agency (ESA) and the European Commission (EC). Under this umbrella of coordinated actions, the ROSES (Real-Time Ocean Services for Environment and Security) project was funded by ESA in order to plan and deliver an operational and autonomous European capacity and services for global monitoring for marine environment and safety. As an ESA project, it was mainly focused on the use of Earth Observation (EO) data in the design of the relevant marine services. According to its implementation plan, during its first phase (2003–2004) the main goal was to initialise an operational use of the precursor systems while in the longer term (up to 2008) the main goal was to set ROSES as the reference for Ocean Services.

During the first period of the project, a complete service for oil spill monitoring and forecasting was delivered in a pilot phase. The service was an integration of the oil spill detection processes that were applied on satellite-based SAR images together with state-of-the-art numerical models that were able to forecast the oil spill evolution in the marine environment. The deployment of the service was a joint effort of Telespazio (Rome, Italy), which received and analysed the SAR images, and the Hellenic Centre for Marine Research, which implemented the numerical models to predict the fate of the oil in the

* Corresponding author, email: lperiv@ath.hcmr.gr

sea. The service was designed to deliver, within few a hours after the satellite data acquisition, a synthetic and comprehensive web-based report concerning the oil spill detection and forecast of its fate. The geographical implementation area was the Central and South Aegean Sea (22–27°E, 35–39°N, Figure 1) in Greece, while the reports were sent to the responsible authorities i.e. the Greek Ministry of Mercantile Marine (MMM) and the General Secretariat of Civil Protection (GSCP). One of the main objectives of the project was to demonstrate that the use of EO data and numerical models has reached a mature level and could be used for the production of real time operational services.

The service application area (Central and South Aegean) belongs to the Mediterranean Sea (Figure 1) which has been characterised as a "Special Area" by the MARPOL 73/78 convention and is protected by the Barcelona convention against illicit vessel discharges. But, as the transportation of the oil from the Black Sea countries to Europe and US is expected to significantly increase during the forthcoming years, the need for an effective surveillance and forecasting tool is more than obvious. Furthermore, the POSEIDON operational oceanography system (Soukissian *et al.*, 2000; Nittis *et al.*, 2005) that has been installed and operates in the Aegean Sea since 1999 provides all the necessary background information for realistic forecasting products.

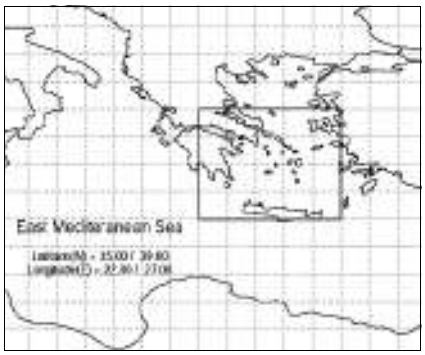

Figure 1 Service implementation area.

Figure 2 Typical ERS2 cycle over Aegean Sea.

2. Service components

The oil spill pilot service developed for the Aegean Sea has the following components:

- **Monitoring part**: Routine acquisition and analysis of SAR images taken by the ERS–2 satellite over the predefined area. This process was realised by Telespazio
- **Forecasting part**: The oil spill weathering and drift model of HCMR was used. The basic background information for the oil spill forecasts (wind, waves and 3-D currents) was taken from the daily forecasting products of the POSEIDON system (Soukissian *et al.*, 2000).
- **Dissemination part**: A dedicated web page (http://roses.ncmr.gr) was created to host the detailed information about the oil spill detection and forecasting. Access to this page was restricted to registered users only.

2.1 Monitoring part

The monitoring and detection part of the service was performed at the Matera Ground Station in Italy. The images that can be acquired by this ground station are relevant to Europe and North Africa. In Figure 2, a typical ERS cycle over the Aegean Sea is illustrated together with all the possible SAR image acquisitions in the surveillance area.

The oil spill detection process that follows the SAR image acquisition is based on the principle that the presence of oil films is very effective in damping wind-generated gravity-capillary short waves on the sea surface, resulting in a dark appearance against a brighter background. The applied Oil Spill Detection Algorithm (OSAD) chain was composed of the following steps:

- Generation, just after the SAR data acquisition, of a very low spatial resolution product with a pixel spacing of 200 m, with a ground coverage of 100 km in width and up to 4000 km in length
- Quick inspection of the imaged areas for identification of features suspected to be oil slicks and processing in high resolution mode, Precision Image format (PRI), of "suspected" images only
- Radiometric calibration, correction for the incidence angle and correction to compensate for the sea angle backscattering variation, land masking, manual or automatic oil spill detection and report generation.

In cases where the detection method was manual, the operator inspected the images, selected those portions of the image that might contain slicks and executed a predefined set of measurements. In the automatic mode the system selected the areas of low backscatter and then performed the measurements: the algorithm used was based on a statistical approach with a classifier based on known values from verified slicks.

2.2 Forecasting part

The forecasting application was based on an oil-spill weathering and drift model that simulates the dispersion of oil droplets and their chemical transformations, using the necessary background information (wind, waves, currents and diffusivities) provided by the POSEIDON's numerical modelling infrastructure.

The oil-spill dispersion and weathering model

The model is based on the PARCEL model (Pollani *et al.*, 2001) which is able to simulate not only the drift of the oil but also the chemical transformations under the specific environmental conditions. The oil slick is represented as "parcels" with time-dependent chemical and physical characteristics. The 3-D position of each parcel is calculated using advection and diffusion estimates while additional information such as wind and wave conditions and hydrological characteristics are requested for the simulation of the varying physicochemical properties.

The basic processes simulated by the oil-spill model are evaporation, emulsification, beaching and sedimentation:

- The evaporation process (transfer of oil from the sea surface to the atmosphere) mainly influences the lighter fractions of the hydrocarbons and can result in a 20–40% loss of oil in the first few hours. It is affected by the surface area and thickness of the spill, the vapour pressure, the wind speed and the temperature. The method

used to characterise the evaporation of the oil has been suggested by Stiver and MacKay (1984) and Stiver *et al.* (1989).

- The emulsification process describes the mixing of water in the heavier fractions of the hydrocarbons and is affected by the wind and wave conditions as well as by temperature and spill characteristics (local thickness, degree of weathering, etc.). The numerical approach of the emulsification process that is used in the oil spill model has been proposed by Riemsdijk van Eldik *et al.* (1986).
- The sedimentation process describes the trapping of oil particles that reach the sea bottom while the beaching process addresses the trapping of oil along the coast depending on the type of coastline (rocky cliff, tidal flats, etc.). For beaching and sedimentation processes the model uses the Gundlach approach (1987).

The POSEIDON system forecasting models

The necessary background information for the oil spill simulations was provided by the three operational models of the POSEIDON system:

- The meteorological forecasting model which is based on the ETA Limited Area Model (Janjic, 1994; Papadopoulos *et al.*, 2002) and downscales the global NCEP or ECMWF forecasts over the Mediterranean Sea (0.24° grid) with a high resolution nesting over the Aegean Sea (0.1° grid). This model provides air-sea boundary conditions to the ocean models.
- The wind wave model which is based on the WAM model (The WAMDI group, 1998) and provides wave height and direction information for estimates of Stoke's drift.
- The 3-D hydrodynamic model based on the Princeton Ocean Model — POM (Blumberg and Mellor, 1987) and provides the three components of the current field as well as horizontal and vertical diffusivities.

3. Service operation

Whenever an oil spill was detected through the routine SAR image analysis by Telespazio, a complete report was sent to HCMR. This report was in HTML format, ready to be uploaded to the web server, and contained information on date and time of the acquisition, the central coordinates (in latitude and longitude) of the SAR image, the number of the oil spills detected in the image and for each oil spill, the barycentre (in latitude and longitude), the area (in km^2) covered by the oil, the perimeter of the oil spill and the probability score.

After the receipt of the report by the Operational Center of HCMR, the detection data were used by the oil model to produce forecasts. The forecasting report consisted of sequential graphs showing the oil spill evolution every hour for the next 72 hours after the time of the event. Additionally, each graph contained information about the volume of the oil that evaporated, emulsificated, reached the sea floor or the nearest beach.

Upon completion of the forecasting part of the service, both the detection and forecasting report were available through the dedicated web site. The registered end-users were informed by e-mail to visit the web site and get the necessary information about the recorded event.

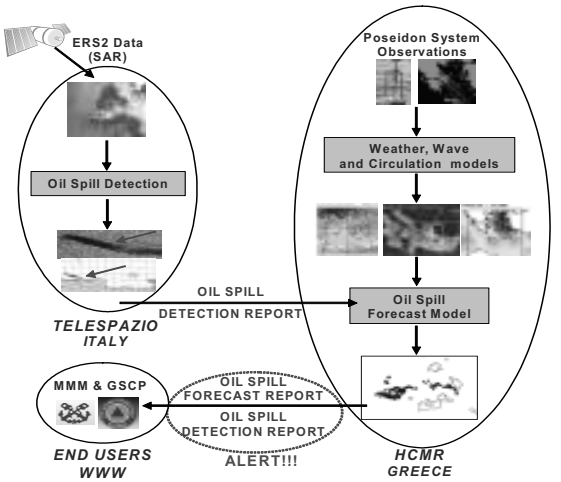

Figure 3 Service overview.

An overview of the service operation is illustrated in Figure 3. The service trial period was initially planned to last for about 3 months, from 26 April to the end of July 2004, but during this period it was decided by the ROSES consortium to extend the trial period by one more month (27/8/04–29/9/04) and the final pilot phase lasted about 4 months. The time delay between the satellite data acquisition and the notification of the end users was an average of around 4.5 hours: Telespazio needed about 4 hours to complete the detection process while HCMR needed about 30 minutes to produce the oil forecasts. Figure 4 and Figure 5 present typical oil spill detection and forecasting reports in the form available to end users.

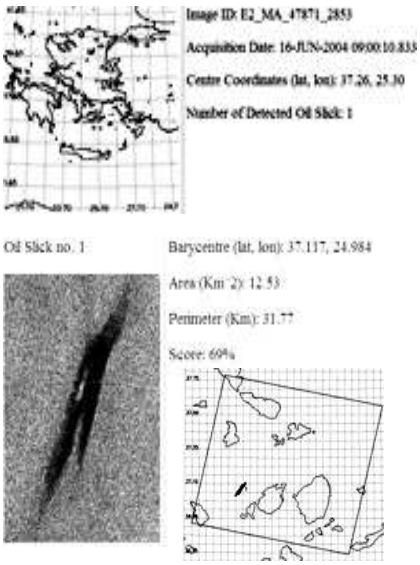

Figure 4 Oil Spill Detection report.

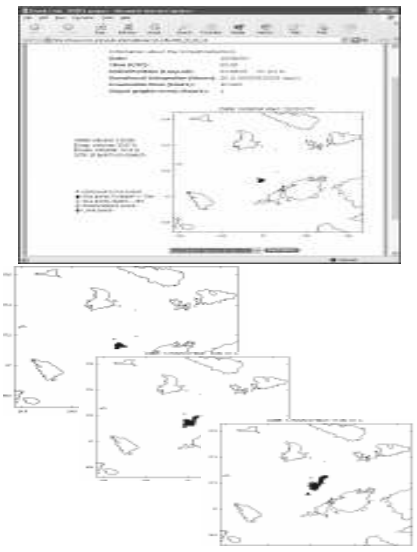

Figure 5 Oil Spill Forecast report.

For technical reasons, during the service trial phase, only the ERS−2 data in descending orbits were analysed. According to the ERS−2 schedule, in the four-month period of the service, 24 descending passes were realised over the Aegean. For two of them no valid SAR data were available while from the remaining 22 passes, 105 images were collected and analysed (an average of five valid frames per passage were available).

The analysis of the 105 SAR images resulted in 34 oil spill detections on 16 images (more than one spill was detected in the most cases). Accordingly, 32 warning emails were sent to the end users. The corresponding responsible authority, the Hellenic Coast Guard, used the reports mainly for informational reasons and in very few cases tried to verify the detection results. Even in these cases, this was done almost one day after the notification and in all cases there was nothing to be reported. This is expected, especially in cases of light oils discharges which are characterised by high evaporation rates.

4. Comments and future plans

The general comments of the users of the service can be summarised as "useful but complementary at this stage". Three main points have been identified as critical to the service performance:

- The 4−5 hour delay between satellite acquisition and end-user notification was considered to be too long for any kind of operational use of the supplied information. It should be limited to one hour or less.
- The SAR data should be available in much more frequent time scales in order to provide support for monitoring activities. During the trial period, the satellite revisiting time over the area exceeded 7 days.
- Possible application of ship detection on the SAR images would provide significant help to the identification of the polluters, in combination with Vessel Traffic Management System (VTMS) data.

For implementation of the next phase, the European Space Agency (ESA) based on users' comments, outlines the real-time operational mode and the significant improvement of the service quality as the major requirement for the scaling up of the effort. In more details, the service components should comply with the following requirements:

- The satellite revisiting time should be limited to one day or less (this can be achieved in many geographical areas by the combined use of all available satellites)
- The probability of detection should be better than 80% for minor spills and better than 90% for major spills
- The spatial accuracy of the detection should be better than 150 m
- The delivery time should be limited to 30 minutes from the satellite overpass and definitely not longer than 60 minutes
- The forecast products should be delivered in a 5×5 km resolution for the complete area and in a 1×1 km resolution for inshore areas of interest
- The delivery of forecasts should be realised within 3 hours of a slick detection.

The above requirements are expected to be fulfilled in the next three years, transforming the oil spill service into a valuable tool for operational surveillance and crisis management and a successful component of GMES.

Acknowledgements

This work was carried out in the framework of the ROSES project, funded by ESA and coordinated by Alcatel Space, contract number: 393136296.

The authors would like to thank Dr. Giovanni Gemeli form Telespazio, Rome, Italy for his input on the monitoring component of the service.

References

Blumberg, A.F. and G.L. Mellor (1987). A description of a three-dimensional coastal ocean circulation model. In Three-Dimensional Coastal Ocean Circulation Models, Coastal Estuarine Sci., 4, pp 1–16, AGU, Washington D.C. 1987.

Gundlach, E.R. (1987). Oil holding capacities and removal coefficients for different shoreline types to compute simulate spills in coastal waters, Proc. Oil Spill Conf., 1987, pp. 451–457.

Janjic, Z.I. (1994). The Step-mountain Eta Coordinate Model: Further Developments of the Convection, Viscous Sublayer and Turbulence Closure Schemes. Monthly Weather Review, 122, 927–945.

Nittis, K. L. Perivoliotis, D. Ballas, G. Korres, T. Soukissian, A. Papadopoulos, A. Mallios, G. Triantafyllou, A. Pollani, V. Zervakis, D. Georgopoulos, V. Papathanassiou and G. Chronis (2005). POSEIDON II: A second generation monitoring and forecasting system for the Eastern Mediterranean Sea. This volume page 585.

Papadopoulos, A., G. Kallos, P. Katsafados, and S. Nickovic (2002). The Poseidon weather forecasting system: An overview. The Global Atmosphere and Ocean Systems, 8, No 2–3, 219–237.

Pollani, A., G. Triantafyllou, G. Petihakis, K. Nittis, K. Dounas and C. Koutitas (2001). The POSEIDON Operational Tool for the Prediction of Floating Pollutant Transport, Marine Pollution Bulletin, Vol. 43/7–12, pp 270–278.

Riemsdijk van Eldik, J., R.J. Ogilvie and W.W. Massie (1986). MS4: Marine spill simulation software set. Process descriptions. Dept. Civil Engineering, Delft Univ. of Technology, Delft, The Netherlands, 74p.

Stiver, W. and D. Mackay (1984). Evaporation rate of spills of hydrocarbons and petroleum mixtures, Envir. Sci. Technology, 18, No 11.

Stiver, W., W. Shiu and D. Mackay (1989). Evaporation times and rates of specific hydrocarbons in oil spills, Envir. Sci. Technology, 23, 101–105.

Soukissian, T., G. Chronis and the Poseidon Group (D. Ballas, D. Vlahos, K. Nittis, Ch. Diamanti, L. Perivoliotis, E. Papageorgiou, S. Barbetseas and A. Mallios) (2000). Poseidon: a marine environmental monitoring, forecasting and information system for the Greek Seas. Mediterranean Marine Science, 1/1, 71–78.

The WAMDI Group, 1998. The WAM model — A third generation ocean wave prediction model. J. Phys. Oceanogr., 18(12), 1775.

Global analysis of sea surface salinity variability from satellite data

S. Michel*, B. Chapron, J. Tournadre and N. Reul

Laboratoire d'Océanographie Spatiale, Ifremer, Brest, France

Abstract

An integral model of the oceanic mixed layer is used to estimate the Sea Surface Salinity anomalies caused by atmospheric heat fluxes, evaporation-precipitation budget, wind friction and geostrophic circulation. Input parameters are air-sea fluxes, wind stress, sea surface temperature from a meteorological model and geostrophic velocity derived from several altimeter measurements. The model is tested using daily climatological forcing fields, in terms of amplitude and spatial distribution of the salinity response. The horizontal transport variations are the first cause of salinity variability, but the fresh water flux or the deep mixing can dominate locally.

Keywords: Sea surface salinity, ocean mixed layer, satellite data, salt budget

1. Introduction

Sea Surface Salinity (SSS) is a key parameter to estimate the influence of oceans on climate. Unlike temperature, it has no direct effect on air/sea exchanges, but it determines the convection and re-emergence of water masses, which are crucial for seasonal to interannual variability of the global system. Unfortunately, SSS measurements are expensive and very heterogeneously distributed, so spatial distribution and time variability are still poorly known over most of the ocean surface. Thus there were approximately 20 times more temperature than salinity measurements during the WOCE period in the 1990s. Some recent studies took advantage of *in situ* data in well-sampled areas (Delcroix, 2004; Reverdin, 2005) and other authors analysed the SSS variability using ocean general circulation models (Furevik, 2002; Mignot, 2003), but at present, no SSS global analysis has ever been performed and very few studies have attempted to evaluate its variability at frequencies higher than seasonal.

The most classical way to overcome the lack of salinity data is based on temperature-salinity correlations, due to density conservation in a given water mass (Emery, 1976). Unfortunately, T/S relationships are far from universal and become very uncertain at the surface, because of air-sea exchanges. A more sophisticated way consists of combining temperature profiles and sea level anomalies from altimeters (Maes, 2000), through the steric effect which relates the total height and the density anomalies of a water column. This requires knowledge of the vertical structures of temperature and salinity variability. On the other hand, general circulation models can produce very interesting results, including global scale and high frequencies. Some of them already assimilate SLA and/or SST (Vossepoel, 2002) to correct the model biases in the upper layer, but most models need a relaxation of SSS toward climatological data, otherwise it would drift to unreal-

* Corresponding author, email: smichel@ifremer.fr

istic values and corrupt the whole circulation. Therefore, such models are hardly helpful in studying the natural fluctuations of salinity at the ocean surface.

Hereafter we propose an alternative method, intermediary between vertical 1D mixed layer models and 3D general circulation models: the Slab Mixed Layer model. It is described in the following section, along with the forcing data which are used to run the simulations. The third section explains how the mixed layer depth is estimated, using SST data. Then in the fourth section, the global salinity budget is addressed and the variability is compared to *in situ* data. Finally, in the last section, the conclusions are summarised and some perspectives are presented.

2. Model and forcing data

2.1 Slab Mixed Layer model

A horizontal 2D model of the mixed layer (described in Mignot, 2003) was designed to simulate the air-sea interactions and the upper ocean internal processes. It is a quasi-geostrophic, 1½ layer model, as the mixed layer is actively forced, while the deeper layer is passively fixed to a climatological cycle. The upper layer is characterised by its depth h and a vertically homogenous salinity S and temperature T. This layer is affected by heat and moisture exchanges with the atmosphere, wind-induced divergence and transport, horizontal geostrophic advection, vertical mixing with the underlying water and lateral diffusion (Figure 1). The time-evolution of T and S at any grid point is then:

$$\frac{\partial T}{\partial t} = \vec{u} \cdot \vec{\nabla} T - \frac{\Gamma(w_e)(T - T_d)}{h} + \frac{Q_{net}}{c_p \rho_0 h} + \kappa \nabla^2 T \tag{1}$$

$$\frac{\partial S}{\partial t} = \vec{u} \cdot \vec{\nabla} S - \frac{\Gamma(w_e)(S - S_d)}{h} + \frac{(E - P - R)S}{h} + \kappa \nabla^2 S \tag{2}$$

where $\vec{u}$ is the horizontal current, h the mixed layer depth, w_e the vertical entrainment velocity, T_d and S_d the lower layer temperature and salinity, Q_{net} the net heat flux and (E–P–R) the net freshwater flux. The constant values are the seawater specific heat c_p=4200 J.kg^{-1}K^{-1}, its volumic mass ρ_0=1020 kgm^{-3} and the lateral diffusivity κ=2000 m^{2}s^{-1} (consistent with the horizontal resolution). In both equations, the first term on the right-hand side represents horizontal advection (of heat or salt). The horizontal current is the resultant of Ekman (u_E) and geostrophic (u_g) velocities:

$$\vec{u} = \vec{u_E} + \vec{u_g} = \frac{1}{\rho h l f} \vec{\tau} \wedge \vec{k} + \frac{g}{f} \vec{\nabla} \eta \wedge \vec{k} \tag{3}$$

where $\vec{\tau}$ is the wind stress vector, ρ the mixed layer density, f the Coriolis parameter, l the transport integration length (i.e the mesh-size) and η the surface elevation.

The second term on the right-hand side of equation (3) represents the vertical entrainment. It only contributes if the entrainment velocity w_e is positive, so the Γ function is defined as: $\Gamma(x)=0$ if $x<0$, $\Gamma(x)=x$ if $x<0$. The entrainment velocity is the

sum of the Ekman pumping w_E (due to wind stress curl) and the deepening rate of the mixed layer w_m (representing diapycnal mixing through the layer base):

$$w_e = w_E + w_m = \frac{1}{\rho}\left|\vec{\nabla} \wedge \frac{\vec{\tau}}{f}\right| + \frac{\partial h}{\partial t} \tag{4}$$

The third term represents the air-sea exchange of heat or moisture. Note that the atmospheric heat flux is related to SST (through its latent, sensible and radiative components), whereas the freshwater flux is not directly linked to SSS. Thus a feedback exists between temperature and thermal flux, but not between salinity and haline flux. The fourth term represents the horizontal diffusion, corresponding to small-scale processes which can not be simulated explicitly because of the model resolution.

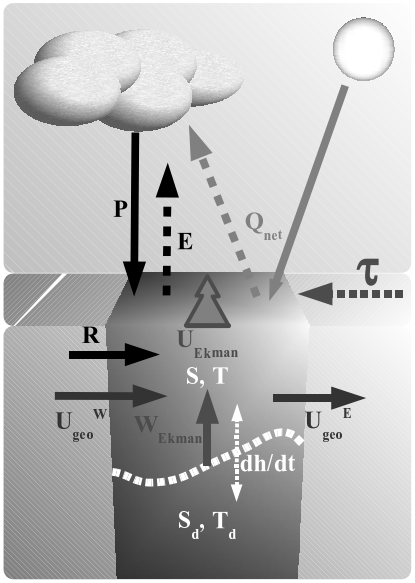

Figure 1 Schematic of the Slab Mixed Layer model.

2.2 Configuration and input datasets

The Slab Mixed Layer model is used to estimate the contribution of each term to the salinity budget. To focus on the daily to seasonal variability of the SSS, the model is forced with daily climatological data. The World Ocean Atlas 2001 monthly climatology is used to initialise the model and to set the hydrological parameters of the deeper layer at all time-steps.

To force the model at the surface, a daily climatology was computed from the ERA40 reanalysis of ECMWF's meteorological model (SST, wind stress, heat and freshwater net fluxes). Only the last 12 years were used (1990–2001), because this period benefited from the assimilation of many satellite measurements.

Geostrophic velocities are obtained from the Absolute Dynamic Topography of the SSALTO–DUACS project, which combines measurements from the 5 simultaneous

altimetric missions: TOPEX–Poseidon, ERS–2, GFO, Jason and ENVISAT. A climatology was computed from the 3 available years (2002–2004). Unrealistically high values were eliminated ($u_g > 2.0$ m s^{-1} and $v_g > 1.5$ m s^{-1}) and velocities were set to zero where the ocean is too shallow for the geostrophic balance to be achieved ($z < 200$ m).

The spatial grid is the same as the ECMWF model, with a 1.125° isotropic resolution. Finally, a 30-day running mean was applied to each climatological field, in order to filter out the fluctuations which are too fast for the mixed layer to adjust. Therefore, the space and time scales which can be simulated are similar to the scales of the future salinity measurement from satellites (100 km and 10 days for an optimal accuracy).

3. Mixed Layer Depth

This model requires a prior evaluation of the Mixed Layer Depth (MLD) to quantify the impact of the vertical processes. This depth can be estimated in many different ways from *in situ* profiles, but no universal criterion can be defined. So, a global MLD climatology was derived from SST satellite measurements, which led to estimation of an "effective depth", adapted to our simplified representation of the superficial ocean. This is achieved by integrating the model to invert the temperature equation (1.1), using inputs of surface fluxes and SST.

The MLD distribution computed from the model is compared to *in situ* estimates, based on millions of individual profiles (Figure 2). It exhibits a peak around 25 m, while De Boyer Montégut (2004) obtained a peak value at 35 m for the thermocline and 15 m for the pycnocline. This value also ranges between the averages of the seasonal (15 m) and permanent pycnocline (60 m) from the WOA climatology. Note that 34% of the daily values from the model are negative and 9% are higher than 1000 m. Such extreme values correspond to situations or areas where the model does not properly simulate the dominant physical processes, or where the forcing data uncertainty is too high.

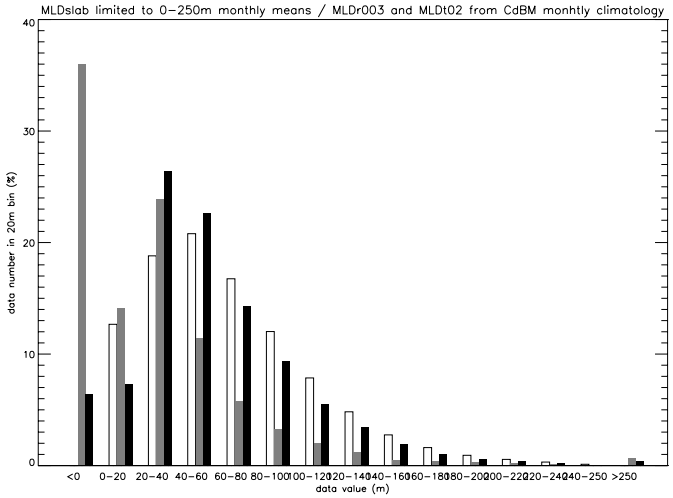

Figure 2 Histogram of MLD in 20 metre bins, obtained from the model (white) and from the pycnocline (grey) or thermocline (black) of De Boyer Montégut.

To construct our daily climatology of MLD, we kept values in the range 1–500 m (51% of the results), exhibiting the best time-correlation with the thermocline depth from *in situ* data. A 30-day running mean and a 3×3-point smoothing was then applied, in order to filter out the smallest scales. The time correlation of the resulting field with the observed thermocline depth is satisfying over most of the global ocean (Figure 3). The correlation is higher than 0.8 over the whole northern hemisphere, except in the tropical band, and greater than 0.6 over the major part of the southern subtropical and subpolar areas. Note that the lowest correlations are obtained where *in situ* measurements are rare (especially in the Southern Ocean).

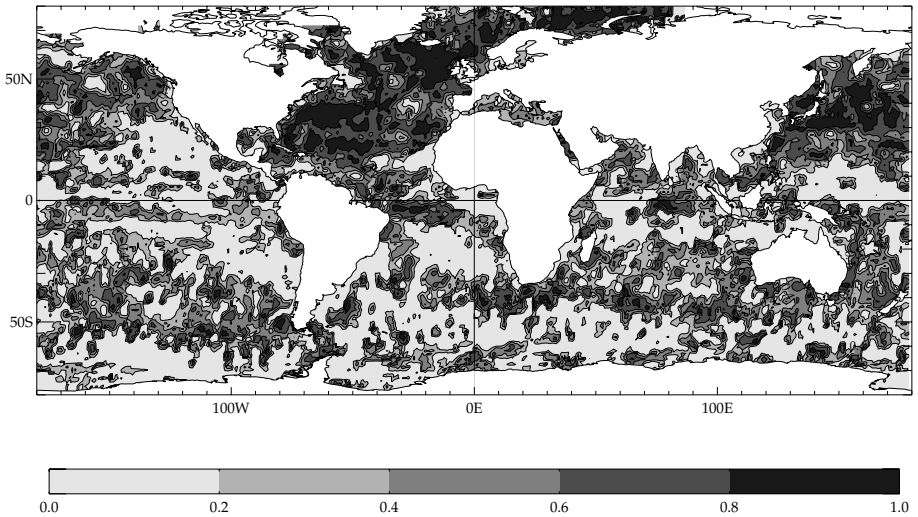

Figure 3 Time correlation of the MLD from the model (after filtering and smoothing) and the thermocline depth from De Boyer Montégut monthly climatology.

4. Salinity budget

The "effective" MLD, together with the other forcing fields, is used to simulate the temperature and salinity variations during a climatological year. The SST budget was analysed to validate the model results and the effectiveness of the MLD inversion. Consistently with previous studies, the dominant term is generally found to be air-sea heat flux. Ekman and geostrophic advections play a secondary role. The effects of vertical entrainment and diapycnal diffusion are only large locally.

The mean variation rate of each term during a seasonal cycle is presented (Figure 4). Ekman transport is significant in tropical regions with strong salinity gradients. It tends to increase the SSS just north of the equatorial divergence (because the salinity minimum is shifted northward) and to decrease it in other wind-driven currents. The geostrophic advection is found to have a higher impact and exhibits structures at smaller scales. It transports fresher water in western boundary currents and saltier water into central tropical basins. The Ekman vertical entrainment is secondary, but can induce a strong local salinisation in near-equatorial areas and coastal upwelling regions. The vertical mixing at the base of the mixed layer plays a major role in areas with strong stratifi-

cation. It counteracts the desalinisation due to advection near river mouths and over continental shelves, as well as the salinisation due to evaporation in subtropical gyres. The atmospheric freshwater flux reduces the salinity in Inter-Tropical Convergence Zones and increases it in subtropical areas. Lastly, the lateral diffusion cannot be uniformly neglected. It has a considerable impact in regions with intense horizontal gradients, where it exhibits bipolar structures. It is particularly strong offshore major rivers and in frontal zones, i.e. edges of boundary currents and the Sub-Antarctic Front.

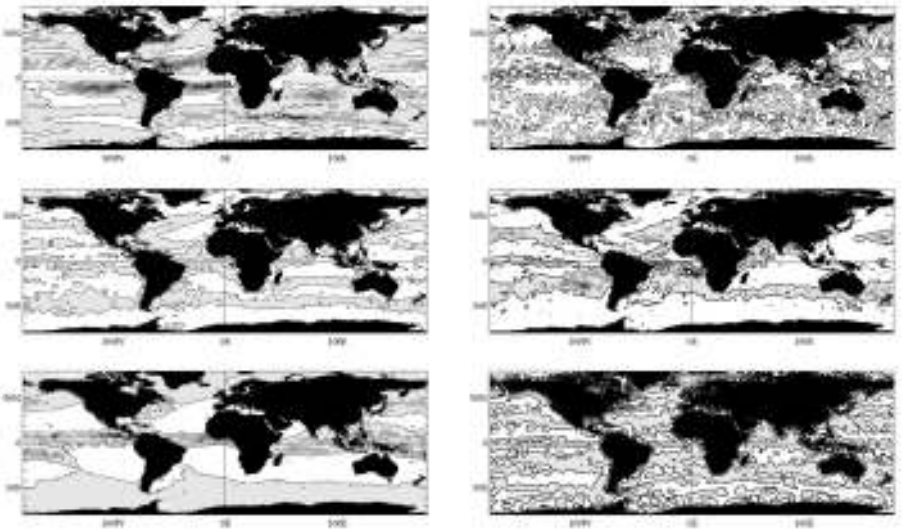

Figure 4 Annual mean of the SSS variation rates from the 6 terms of the salinity equation (contour interval: 10^{-3} psu/day, negative values in grey, positive values in white).

Table 1 Annual global statistics of the salinity balance in the mixed layer: mean value and local extrema, mean amplitude (all in 10^{-3} psu/day) and contribution to the total amplitude (in %). The equatorial band (3°S–3°N) was suppressed for Ekman terms, as well as the continental shelf (depth less than 200 m) for geostrophic advection and sea-ice covered areas for all terms.

Physical process	Min.	Mean	Max.	Amplitude	Percentage
Ekman advection	–230	–0.36	+34	0.88	11.7
Geostrophic advection	–342	–0.16	+125	3.53	37.2
Ekman entrainment	–8	+0.13	+37	0.27	2.4
Diapycnal mixing	–10	+0.77	+65	1.37	19.0
Atmospheric flux	–113	+0.08	+6	0.99	17.5
Horizontal diffusion	–97	–0.06	+124	1.03	11.6
Total variation	–496	+0.40	+241	4.80	100.0

The global average of each term (Table 1) reveals that horizontal advection tends to decrease the salinity of the mixed layer (-0.5×10^{-3} psu/day), by transporting fresher waters from the highest latitudes, and the Ekman component plays the major role in this desalinisation. In contrast, the vertical entrainment tends to increase the SSS ($+0.9\times10^{-3}$

psu/day) by bringing saltier waters from the deeper layer, mainly through diapycnal mixing. Air-sea freshwater fluxes and lateral diffusion have an almost neutral effect in this planetary balance ($\pm 0.1 \times 10^{-3}$ psu/day). The total variation rate would lead to a slight salinisation of the mixed layer ($+0.4 \times 10^{-3}$ psu/day, equivalent to +0.15 psu/year), which is similar to the SSS drift in many general circulation models. This bias would be reduced with realistic runoffs and a finer treatment of sea-ice.

In terms of amplitude, geostrophic advection appears 3 times as strong as Ekman transport. Thus total advection represents almost half (49%) of the SSS fluctuations. Vertical entrainment comes in second position (21%), essentially because of diapycnal mixing. Atmospheric flux also plays a considerable role (18%), slightly greater than horizontal diffusion (12%). Therefore, none of the physical processes embedded in the model seem negligible in the salinity budget, in contrast to the temperature case, which is dominated by surface heat flux and advection.

The global distribution of the dominant term indicates that various types of balances exist (Figure 5). Geostrophic advection dominates over a larger area than Ekman transport, which rules only in zones corresponding to the strongest Trade winds. Diapycnal mixing has the second widest geographical extent, concentrated in small tropical areas and in large subpolar areas. Air-sea flux comes next, dominating along both southern and northern subtropical bands, where there is a lot of evaporation and weak advection ("ocean deserts"). Lateral diffusion can dominate in some coastal fringes, along the strongest fronts and in the sea-ice areas. Ekman pumping is a very marginal process, mainly contributing in the most intense upwelling spots.

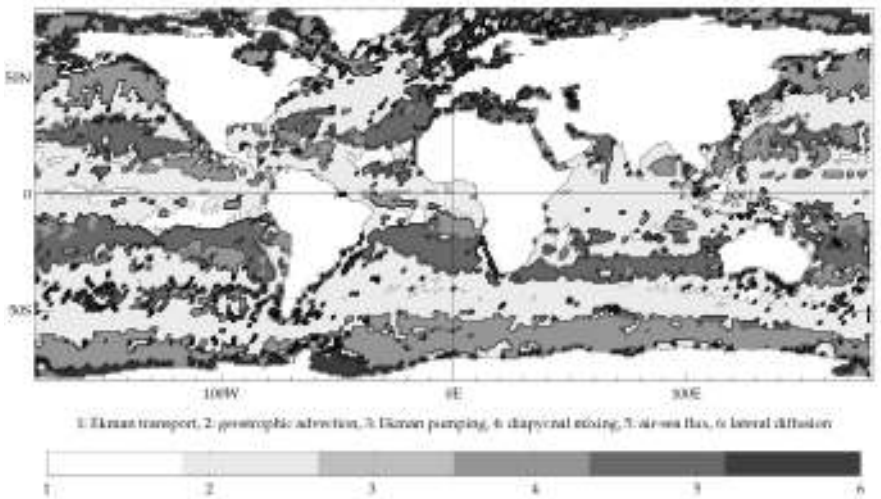

Figure 5 Dominant term in the SSS time-evolution, at each point of the global ocean (numbered from 1 to 6).

The sum of these effects leads to the total SSS variation rate. Simulated SSS variance compares well with observations (Figure 6). The variability is extreme near the mouths of major rivers and high in western boundary currents, ITCZs, seasonally ice-covered areas and part of the Sub-Antarctic Front. The model appears to be well suited to the

principal mechanisms affecting salinity in the surface layer and succeeds in capturing the SSS variability at seasonal scale.

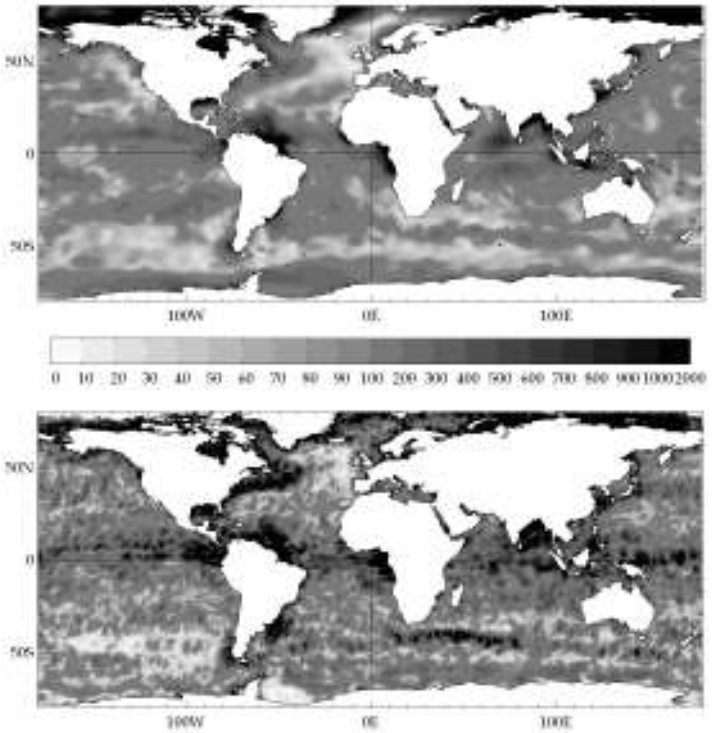

Figure 6 Top: observed SSS variance from the World Ocean Atlas 2001 monthly climatology. Bottom: simulated SSS daily variance (in 10^{-3} psu).

5. Conclusions and perspectives

A simple 2D-model of the oceanic mixed layer was developed, forced by atmospheric fluxes and surface topography, with prognostic variables temperature, salinity and depth. It was integrated over the global ocean, during a climatological year and with a daily frequency, in order to determine the main variability mechanisms of SST and SSS at scales of a few days to a season.

Using SST as input data, the model produces a MLD in agreement with the best estimates from *in situ* measurements. This output field must be carefully filtered to eliminate out-of-range values, which are caused by local inadequacy of the model or critical noise in the forcing data. It reveals a precise picture of the mixed layer, with spatial and temporal resolutions that can not be reached using present *in situ* observations.

This MLD is then used jointly with the forcing fields, to simulate the evolution of SST and SSS. This helps to quantify the impact of each physical process. The thermal contributions are in agreement with previous studies. Geostrophic horizontal transport generally dominates SSS variations. The impact of Ekman transport is slightly lower,

except in regions with strong permanent winds. Freshwater flux can be the main source of variability at the centre of subtropical gyres. The vertical entrainment term dominates in many areas, not only in coastal upwelling regions. The contribution of the lateral mixing remains weaker, apart from very strong haline fronts.

The SSS variations simulated with this simple model reflect quite well the spatial distribution of observed variability. Therefore, this method should be able to produce accurate SSS anomalies in quasi-real time, from satellite measurements of wind, surface elevation, rain and evaporation flux. These results should be useful for calibrating, and even improving, the salinity products from SMOS and Aquarius future space missions.

Acknowledgements

The authors would like to thank the European Centre for Medium Weather-range Forecasts and Météo-France for providing the ERA40 reanalysis, the AVISO centre for the Absolute Dynamic Topography and the National Oceanographic Data Center for the WOA climatology.

References

Delcroix, T., A. Dessier, Y. Gourriou and M. McPhaden (2004). Time and space scales for sea surface salinity in the tropical oceans, Deep Sea Res., in press.

Reverdin, G., E. Kestenare, C. Frankignoul and T. Delcroix (2005). *In situ* surface salinity and subtropical Atlantic Ocean. Part 1: Large scale variability, Prog. Ocean., submitted.

Furevik, T., M. Bentsen, H. Drange, J.A. Johanessen and A. Korablev (2002). Temporal and spatial variability of the sea surface salinity in the Nordic Seas, J. Geophy. Res.-Oceans, 107 (C12), 109–124.

Mignot, J. and C. Frankignoul (2003). Interannual to interdecadal variability of sea surface salinity in the Atlantic and its link to the atmosphere in a coupled model, J. Geophys. Res.-Oceans, 109 (C4), 1–14.

Emery W.J. and R.T. Wert (1976). Temperature–Salinity Curves in the Pacific and their Application to Dynamic Height Computation, J. Phys. Ocean., 6, 613–617.

Maes, C. and D. Behringer (2000). Using satellite-derived sea level and temperature profiles for determining the salinity variability: a new approach, J. Geophys. Res., 105, 8537–8547.

Vossepoel, F.C., G. Burgers and P.J. Van Leeuwen (2002). Effects of correcting salinity with altimeter measurements in an equatorial Pacific ocean model, J. Geophys. Res.-Oceans, 107 (C12), 8001.

De Boyer Montégut, C., G. Madec, A.S. Fischer, A. Lazar and D. Iudicone (2004). Mixed layer depth over the global ocean: an examination of profile data and a profile-based climatology, J. Geophys. Res.-Oceans, 109 (C12), 52–71.

Biofouling prevention by local chlorination for *in situ* measuring systems

L. Delauney*, C. Compere, M. LeHaitre, V. Lepage and Y. Faijan

IFREMER Brest, ERT/IC, Interfaces et Capteurs, France

Abstract

This paper presents the results obtained in laboratory and at sea, with various instruments, protected from biofouling by a localised chlorine generation system. The sensors involved are based on electrode, optical and optode technologies. These results are quite promising and demonstrate the efficiency of a localised chlorine generation biofouling protection method and its adaptability to various oceanographic instruments.

Keywords: Biofouling, prevention, sensors, *in situ*, monitoring, oceanography

1. Introduction

These days, many marine autonomous environment monitoring networks are set up around the world. These systems take advantage of existing superstructures such as offshore platforms, lightships, piers, breakwaters, or are placed on specially designed buoys. The networks commonly use various sensors such as dissolved oxygen, turbidity, conductivity, pH or fluorescence units. Emphasis has to be placed on the long term quality of measurements which may face very short term biofouling effects. The biofouling can disrupt the quality measurement sometimes in less than a week.

Many techniques to prevent biofouling on instrumentation are actually listed and studied by researchers and manufacturers. Some of them have begun to be implemented on instruments. However very few of them have been tested *in situ* for medium term deployment. A convenient method consists of localised chlorine generation.

The tests were carried out on various *in situ* places and during long term periods from 56 days up to 190 days. Experiments were performed mostly in summer in order to take advantage of the high level fouling rate from March to October.

2. Method

The local chlorination technique was applied to three instrument technologies, optic (turbidity and fluorescence), electrodes (conductivity) and optode (oxygen). This document shows the results on conductivity, oxygen and fluorescence sensors.

For each test, in the laboratory or at sea, two sensors were placed simultaneously, one unprotected and one protected by the local chlorination device. The measurements were internally recorded or when possible recorded by a laptop for real time data analysis. When possible some water sampling and reference analyses were performed in order to follow the drift of the protected sensor in real time.

* Corresponding author, email: Laurent.Delauney@ifremer.fr

2.1 Local chlorination hardware

Figure 1 and Figure 2 show the local chlorination device on various instruments.

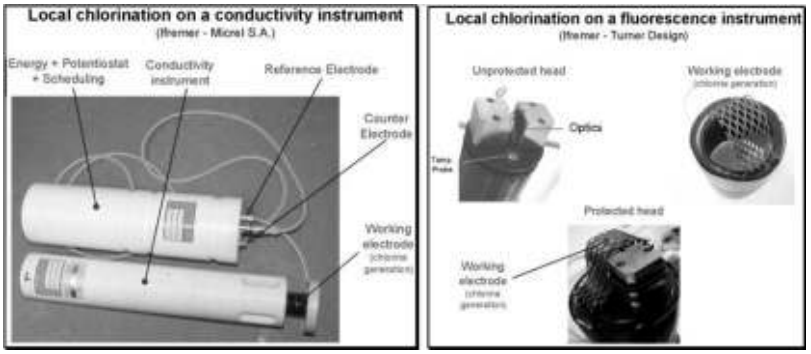

Figure 1 Local chlorination on conductivity sensor (left) and on fluorometer (right).

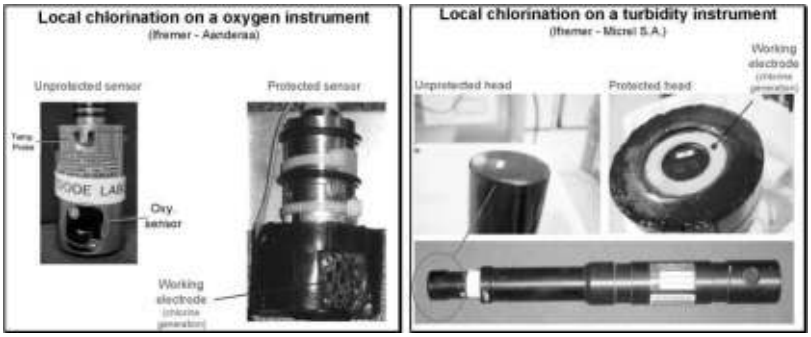

Figure 2 Local chlorination on oxygen optode (left) and on turbidity sensor (right).

The system is based on a potentiostat which applies a fixed potential between a working electrode and a reference electrode. Thus a very weak current is driven between the counter electrode and the working electrode. Chlorine is produced at the working electrode due to electrolysis of sea water. The working electrode needs to be adapted to the geometry of the sensor. Nevertheless this was not a problem for the tested sensors but the adverse effect on the measurement must be checked in the laboratory before the first deployment.

The actual electronic pack uses one D cell and is equipped with a scheduler in order to program the chlorination period on and off. This enables energy to be saved and leaves chlorine-free periods for proper sensor measurement. The system is completely autonomous (energy), allows chlorination sequencing and for studying purposes allows potential and current recording.

2.2 Adverse effect laboratory check

In order to implement the system on the instruments it is necessary to check the adverse effect on the measurement. Electrodes in the vicinity of a sensor may perturb measurements. Consequently a “Laboratory check” and a “specific calibration” is necessary. In the same way Biocide molecules can interfere with membranes or induce local water

property modifications; this effect must be studied even if it can be overcome by "Chlorination scheduling".

Every instrument has been tested in the laboratory with standard solutions or standard analytical methods in order to calibrate the signal of a protected instrument versus an unprotected one. According to the parameter measured the following standard methods were used: Oxygen: Winkler titration. Fluorescence: Ifremer Fluorescein protocol. Conductivity: Natural seawater sampling and a Reference Guildline salinometer.

The adverse effect laboratory check consists of comparing the responses of two instruments with one of them equipped with the local chlorination device. Two steps are performed. The first step determines the adverse effect of the local chlorination hardware which will be possible to overcome by specific calibration. The second step determines the adverse effect of the chlorine generation which will be possible to overcome by a scheduling of the chlorination generation.

3. Results — Adverse effect laboratory check

3.1 Conductivity — Micrel TPS 35

Step 1: Adverse effect of the local chlorination device: The two instruments are placed in a temperature-controlled sea water bath. None of them are equipped with the local chlorination device. The two instruments show an initial difference of 0.4 PSU which can be overcome by calibration adjustment. The local chlorination device was then installed on one of the two instruments. The graph in Figure 3 shows that the original 0.4 PSU shift remains unchanged.

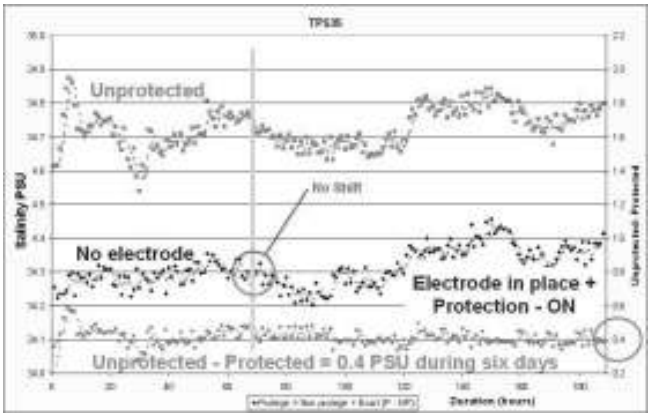

Figure 3 Adverse effect on a conductivity sensor. The top curve gives the signal of the unprotected instrument during the six days of experiment. The middle curve gives the signal of the protected instrument. The lower curve gives the difference between the two signals. Apart from an original shift of 0.4 PSU due to instrument calibration, no perturbation due to the biofouling protection device could be measured.

Step 2: Adverse effect of chlorine generation: During the experiment the chlorination has been powered on in order to detect the effect of chlorine. Again no effect could be observed as shown by the middle curve in Figure 3.

Conclusion: Conductivity seems not to be affected by chlorine generation and the TPS 35 Micrel conductivity sensor is not sensitive to the local chlorination device and chlorine generation. Apparently no special care needs to be taken in order to use the local chlorination protection system with this equipment.

3.2 Oxygen — Aanderaa optode

Step 1: Adverse effect of the local chlorination device: The two instruments are placed in a sea water bath. One of them is equipped with the local chlorination device (optode #1). The two instruments show an initial difference of 0.22 mgL^{-1} which will be overcome by calibration adjustment (Figure 4). The local chlorination device was then switched from one instrument to the other (from optode #1 to optode #2). The graph in Figure 4 shows that the original 0.22 mgL^{-1} shift remains unchanged.

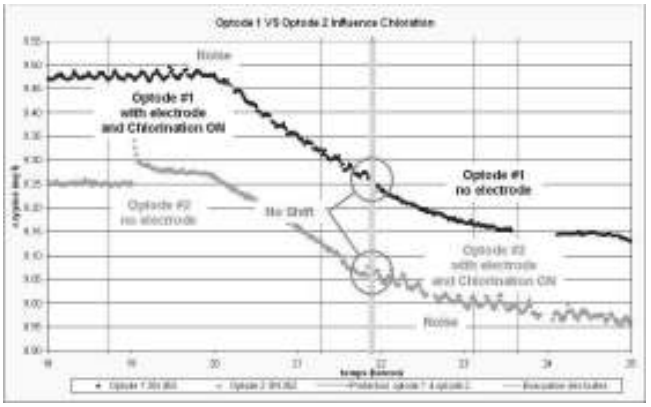

Figure 4 Adverse effect on an optode oxygen sensor. The top curve gives the signal of optode #1. The lower curve gives the signal of optode #2. Apart from an original shift of 0.22 mgL^{-1} due to instrument calibration, no perturbation due to the biofouling protection device could be measured.

Step 2: Adverse effect of chlorine generation: Both signals show a small perturbation when chlorination is turned on. The noise observed is less than 0.05 mgL^{-1} of oxygen. This value is two time less than the Winkler titration accuracy. The adverse effect appears as a noise due to the scheduling of the chlorination.

Conclusion: The local chlorination device does not affect the optode oxygen reading.

The chlorine produced is seen by the optode as an oxygen signal. In this case the chlorination scheduling keeps the amplitude of the perturbation negligible. Consequently it is imperative to schedule the chlorination with the optode sensor.

4. Results — *In situ* test

4.1 Conductivity — Micrel TPS 35

A local chlorination protection device was tested on the conductivity instrument at St Anne du Portzic Brest in France. Two instruments were placed on site, one protected and one unprotected. The local chlorination scheduler was adjusted in order to last for 3 months with no maintenance.

The graph in Figure 5 shows the measurement obtained during the field test in St Anne du Portzic Brest in France.

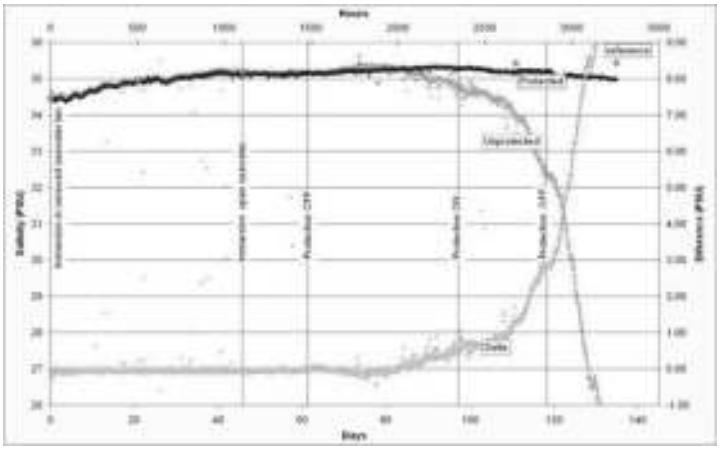

Figure 5 Conductivity sensor *in situ* results, 133 days 03 June–16 October 2003, Brest.The top curve shows measurement from protected instrument. The upper curve that then drops shows measurement from the unprotected instrument. The bottom curve shows the difference between the two signals. The drift started after 80 days, it remains linear up to the 110th day and became exponential until the end (133 days).

The reference measurements obtained by water sampling and Guildline Salinometer conductivity analysis (dots on Figure 5) show a slight shift of the protected instrument (0.5 PSU). This drift is probably due to a stop in the chlorination process after the 120th day due to a lack of energy (battery worn out).

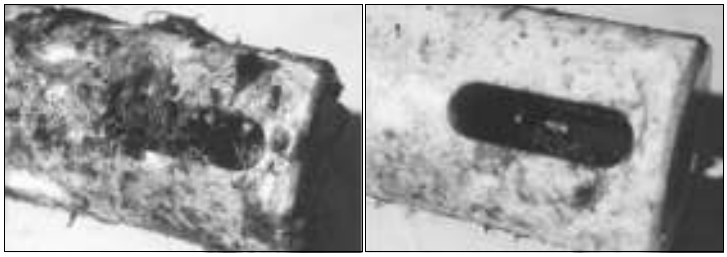

Figure 6 TPS 35 Micrel conductivity sensor unprotected (left), protected (right)

Figure 6 compares the unprotected conductivity sensor with the protected one after the 133 days deployment. Visually we can appreciate the efficiency of the biofouling protection. It is surprising that the local chlorination system placed inside the white probe housing has protected the outside.

It can be concluded that the local chlorination biofouling protection for the TPS 35 Micrel conductivity sensor is efficient and was clearly proven during the St Anne du Portzic Brest test for a 133-day continuous period. The drift of the unprotected instrument started after 80 days in August.

4.2 Oxygen — Aanderaa optode

A local chlorination protection device was tested on the oxygen instrument at St Anne du Portzic Brest, France. Two instruments were placed on site, one protected and one unprotected. The local chlorination scheduler is adjusted in order to last for 3 months with no maintenance.

The graph in Figure 7 shows the measurement obtained from day 110 to day 140 during the field test in St Anne du Portzic Brest.

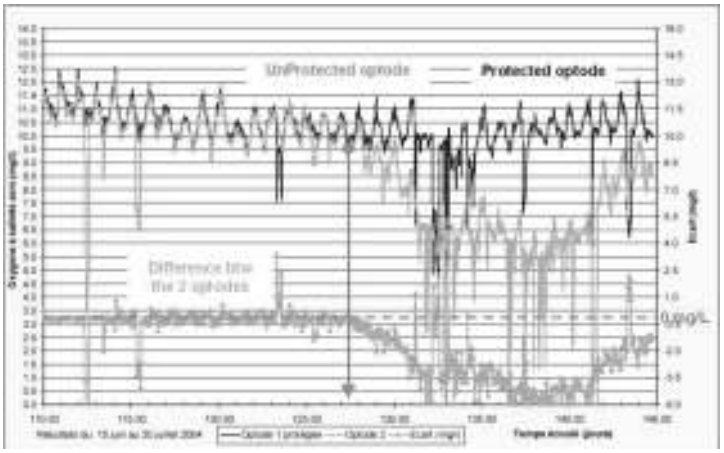

Figure 7 Oxygen optode sensor *in situ* results for 190 days duration January–July 2004, Brest.The top curve shows measurements from protected instruments. The upper curve that then drops shows measurements from the unprotected instrument. The lower curve shows the difference between the two signals. The drift started after 127 days. The protected optode signal is very good up to the 160th day. The Winkler analyses which were realised up to the 160th day confirm this result.

After the 160th day we cannot confirm that the protected sensor is still better than ±0.2 $mg\,L^{-1}$. It seems that the protected sensor shows a temporary failure between the 160th and 170th days.

It can be concluded that the local chlorination biofouling protection for the oxygen optode sensor is efficient and was clearly proven during the St Anne du Portzic Brest test for a 160 days continuous period. The drift started after 130 days, in April.

4.3 Fluorescence — Scufa Turner Designs

A local chlorination protection device was tested on the fluorescence instrument at Millport island, Scotland for 100 days. Two instruments were placed on site, one protected and one unprotected. The local chlorination scheduler is adjusted in order to last for 3 months with no maintenance. The graph in Figure 8 shows the measurement obtained during the field test at Millport island.

The protected instrument signal (lighter curve) is very good up to the 70th day. After day 70 the real time acquisition system failed and the chlorinator batteries wore out. When the system recovered ten day later, the protected instrument signal shows a slight drift which is probably due to a small biofouling development during the chlorination failure period.

It can be concluded that the local chlorination biofouling protection for the fluorometer sensor is efficient and was clearly proven during the Millport Island test for a continuous period of 70 days. After 70 days, the drift observed is mainly due to the failure of the chlorinator battery.

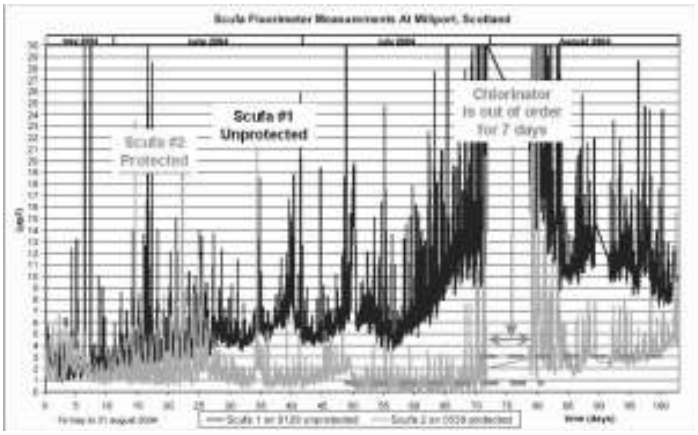

Figure 8 Fluorescence sensor *in situ* results. 100 days duration May–August 2004, Millport Island. The upper curve shows measurements from the unprotected instrument. The lower curve shows measurement from the protected instrument. The drift started after 10 days.

5. General conclusion

A local chlorination biofouling prevention system has been tested on many oceanographic instruments for coastal monitoring. Very encouraging results have been obtained for the parameters commonly used for marine coastal monitoring. Each deployment has been a success for a duration of up to 160 days. Various types of biofouling have been prevented: biofilm, algae, barnacles, etc. The system can be adapted to many kinds of instrument quite easily. The energy need is compatible with autonomous monitoring (One D cell for 3 months).

Special care should be taken for some sensitive parameters like oxygen or fluorescence, as the chlorination period must be scheduled in order to leave a free time interval to perform the measurements with the protected sensor. Future work needs to be performed in order to integrate the hardware system inside the sensors in order to improve compacity.

The system is now used by Ifremer for autonomous coastal monitoring enabling a reasonable maintenance frequency of 3 months with high quality measurements obtained.

Acknowledgements

Ifremer would like to thank Phil Cowie from UMBS, Millport, Scotland, for very good work taking care of the SCUFA Fluorometer experiment in Millport. This work is part of the European Project BRIMOM (Biofouling Resistant Infrastructure for Measuring, Observing and Monitoring), Project number EVR1–CT–2002–40023. www.brimom.org.

An automated system for high frequency monitoring of coastal waters

Michel Repecaud*, Patrice Woerther, Yannik Aoustin, Michel Hamon, Christian Bonnet, Olivier Gontier, Laurent Delauney, Jean-François Rolin and Jacques Legrand

Ifremer, France

Abstract

The Marel system now offers the possibility of a real network for high frequency monitoring for coastal sea waters. Ten years experience of managing such networks makes the long term coastal sea survey a reality.

Firstly, the technological innovation implemented inside the measuring cell on top of the system enables continuous cleaning of the sensors, while injection of chlorinated ions in the circuit prevents biological clogging.

Secondly, specific sensors for temperature, salinity, oxygen, fluorescence, turbidity and pH have been qualified to guarantee measurement precision over a 3-month period without any intervention. All these sensors measure their parameters every twenty minutes and data transmission is done only twice a day. Alarms and remote controls are also transmitted in real time to the data centre on land.

Thirdly, this operational network is now working in different coastal sites all around the the French coast and offers the possibility of information on the sea water directly on internet.

Keywords: High frequency monitoring, operational sea coastal survey, *in situ* sea water analysis.

1. Introduction

Since 1995 the TSI department of Ifremer has been developing a large range of Marel systems adapted for different types of locations around the French coast. These ten years of work on new parameters and new locations permit the constitution of a large expertise on high frequency data collection, and operational maintenance.

2. Marel main functionalities

The basis of the Marel system is the circulation of water with production of chlorine which ensures full control of measuring conditions.

3. Major achievements

During the last ten years Ifremer has designed, managed and maintained a large panel of stations functional all around the French coast from the north to the south.

* Corresponding author, email: Michel.Repecaud@ifremer.fr

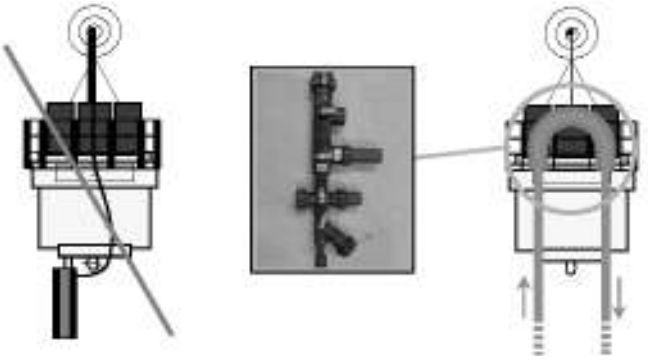

Figure 1 Working process of the Marel system.

Figure 2 The most important types of site.

4. Measured parameters

Table 1 Physico-chemical parameters.

Parameters	Range	Accuracy
Water temperature	–5 to +30°C	0.1°C
Conductivity	0 to 70 $mScm^{-1}$	0.3 $mScm^{-1}$
Dissolved Oxygen	0 to 20 mgl^{-1}	0.2 mgl^{-1}
pH	6.5 to 8.5 upH	0.2 upH
Turbidity	0 to 4000 NTU	10%
Chlorophyll	0 to 50 FFU	10%

Table 2 Additional parameters

Parameters	Range	Accuracy
Nitrates	0.1 to 100 $\mu mol l^{-1}$	5%
Silicates	0.1 to 100 $\mu mol l^{-1}$	5%
Phosphates	0.1 to 100 $\mu mol l^{-1}$	5%
Ammonium	0.05 to 100 $\mu mol l^{-1}$	5%
p CO_2	200 to 1000 μatm	1 μatm

Table 3 Meteorological parameters

Parameters	Range	Accuracy
Air temperature	–20 to +30°C	0.1°C
Air pressure	900 to 1100 Hpa	0.3 Hpa
P.A.R.	0 to 3000 $\mu mol s^{-1} m^2$	10 $\mu mol s^{-1} m^2$
Hygrometry	0–100%	2%
Wind speed	0 to 40 $m s^{-1}$	1 $m s^{-1}$
Wind direction	0 to 360°	10°

5. Operational organisation

"On site" maintenance: Theses networks need an operational organisation to control and maintain the stations. Ifremer now has a break-down team to repair the possible problems, to organise network supervision and also for preventive maintenance.

Meteorology under quality assurance: All follow-up devices, sensor calibration and each action on the stations are carried out following quality assurance procedures in order to guarantee the quality of the results.

National database constitution: The quality and homogeneity of all the measured parameters enable the creation of a national database. This database contains the results of all the national networks, making a coastal water survey possible.

6. Data management

All the French networks are organised under the **ROSLIT** project. This project gives cohesion between all sites, and has been working since 2005, so validation and data dissemination are made on the same central basis.

7. Data processing

All data are treated and flagged under well-known standards which are described below:

Raw data are available in "real-time", flagged **Q0.5**, and transferred from the station to land only every 12 hours because of the communication cost, but data transmission can be forced in the case of an environmental hazard.

Data processing "first step": The **Q1** data processing level is reached after a weekly manual expert data validation.

Data processing "second step": The **Q2** data processing level is reached after the sensors check (three months). Over this ultimate data level, the data are qualified and flagged under an international standard of quality.

8. Examples of long term series

The high frequency data acquisition has long term series, exemplified by the Marel Iroise network. Figure 3 shows the comparison between a weekly network (SOMLIT) and the hourly network of Marel-Iroise.

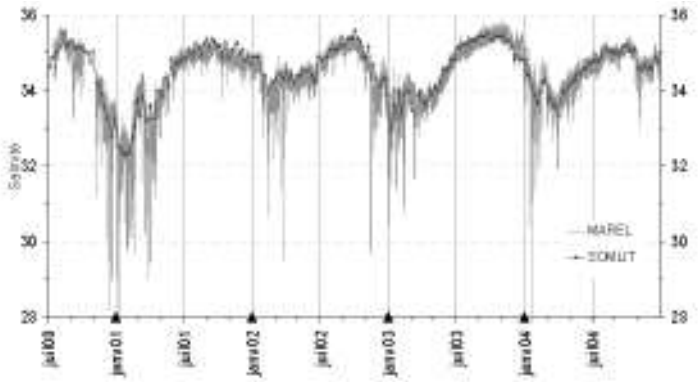

Figure 3 Marel-Iroise: 2000–2005.

The longest data series was obtained at the Honfleur station (Marel Baie de Seine network) working since 1997, see Figure 4. Data are available at www.ifremer.fr/difMarelSeine/

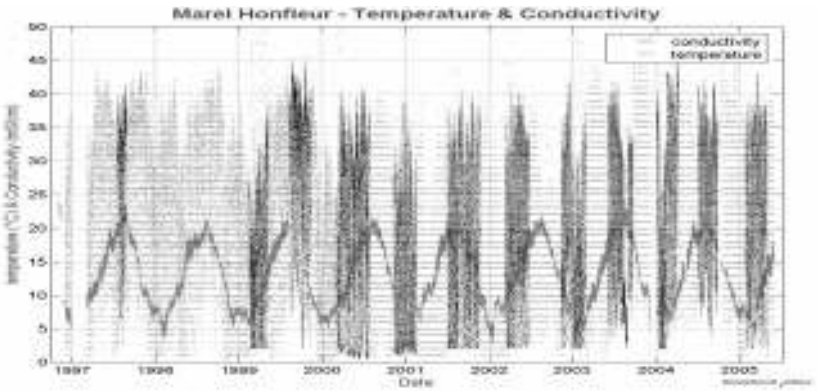

Figure 4 Marel Honfleur 1997–2005.

The most recent local network installed was the Pauillac (Gironde network) which has 4 stations with high frequency capabilities.

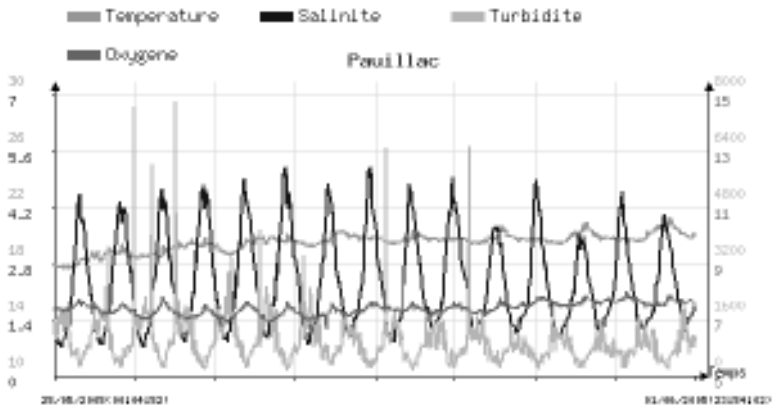

Figure 5 Marel-Pauillac 6 days results.

9. Marel new developments

In parallel Ifremer is developing some station models that take into account several conditions such as price, electrical power, and transportability: the **CHEMINI** (a miniaturised ammonium analyser) and the **Marel-Estran** new portable system.

10. Conclusion

All the networks are administered under the ROSILT project, now implementing a fully operational sea coastal survey all along the French coast. The high frequency long-term data acquisition forms a platform for surveys and studies for the global database which is being built continuously. All the data can be accessed directly by anybody directly on the web!

Ocean observing system instrument network infrastructure

Duane R. Edgington and Daniel Davis*

Monterey Bay Aquarium Research Institute (MBARI), USA

Abstract

This paper summarises results of a workshop on Instrument Software Infrastructure held at MBARI, Moss Landing, California USA on 13−15 September 2004, jointly sponsored by the National Science Foundation (NSF) and Ocean Research Interactive Observatory Networks (ORION) program. The workshop included over fifty participants, including international participants from Germany, Canada, and Japan. This was one of the first technical workshops in the development of a series of ocean observatories under the US Ocean Observatory Initiative (OOI) being managed under the ORION program. The specific focus of this workshop was to define the standard requirements to be met by software infrastructure for sensors, instruments and platforms for observing systems in the ORION program. These requirements include the issues of configuring, interfacing, and managing devices, including sensors and actuators, to a network based observing system as well as managing the resources necessary to support such devices. The topics include the capability of supporting plug-and-work instrumentation using a service oriented network architecture. A major issue addressed is the observatory infrastructure requirements necessary for managing data and metadata coming from sensors and instruments of the observatory in support of an integrated data management system.

Keywords: ocean observatory, infrastructure, plug-and-work, sensor network, data management

1. Introduction

Developments in network technology over the past several decades have led to the dominance of web-based interfaces to information and databases for the earth sciences. More recently the development of 'smart sensor networks' (O'Reilly, 2001) has led to web-based access to real-time sensor array networks in the astronomical and seismological communities. These web-based services communicate with sensor networks through 'infrastructure middleware', a layer of software between the user and the sensors.

The instrument network infrastructure challenge for ocean sciences is to develop and apply these sensor network technologies for application to ocean observatories where the problems of deploying, configuring, managing, and accessing sensors, instruments and their platforms are compounded by the hostile conditions and remoteness of the ocean environment.

In September 2004, over fifty participants attended an ORION and NSF-sponsored three day international Workshop on instrument network infrastructure for ocean observa-

* Corresponding author, email: dada@mbari.org

tories at the Monterey Bay Aquarium Research Institute (MBARI) on Monterey Bay in California. The purpose of the workshop was to identify, analyse, and discuss the issues and requirements for developing a standard approach to instrument network infrastructure for ocean observatories. The purpose of this presentation is to summarise the issues and results discussed at this workshop.

2. The ORION project

The Ocean Research Interactive Observatory Networks (ORION) program is a US−NSF program to define, plan, implement and develop ocean observing systems for the US Ocean Observing Systems Initiative (OOI) (Isern, 2004). A major ORION Workshop was held in San Juan, Puerto Rico in January 2004 to establish the science initiatives and requirements for defining and planning the observatories under this program (Schofield, 2005). Three observatory efforts have been identified for the ORION program: relocatable deep sea moored buoys, a regional scale cable-based network observatory, and a network of coastal observatories. The first major observatory to be implemented will be a cable-based regional scale observatory in the North East Pacific coast of the US. A prototype for this system is being deployed by the Monterey Bay Aquarium Research Institute (MBARI) in autumn this year, called the Monterey Accelerated Research System (MARS).

3. Instrument network infrastructure requirements

Scientific requirements for US ocean observatories are fully discussed in both the SCOTS and ORION Workshop Reports (Dickey, 2003; Schofield, 2005). A complete discussion of the instrument infrastructure requirements summarised here may be found in the NSF SENSORS Workshop Report at the SENSORS Project website.

Requirements for instrument software infrastructure are divided into five basic areas:

Design requirements: This section includes requirements for scalability, extensibility, and interoperability of instruments and data. The architecture for the infrastructure must take into account the need for observatories to expand, and ensure that system behaviour scales appropriately as the number of instruments increase. Moreover, instruments should be interoperable with a minimum of configuration in any observing system in the ORION program, and the data from any particular system in the ORION program should be usable with data from any other ORION system.

Observatory resource management: This includes the requirements for managing system level resources: power, bandwidth, data storage and buffering, and environmental effects. Environmental effects are how the use of system elements, including instruments, platforms or sensors may affect measurements and the usefulness of other elements in the system. This means that physical space, acoustic noise, chemical effects, and electromagnetic effects should be properly characterised and managed.

Observatory monitoring and operation: This category includes the requirements for operational monitoring, safety, security, fault tolerance and detection, diagnostics and recovery. The scientific effectiveness of an observatory requires that it be reliably and efficiently operated and maintained on a 24/7 basis.

Instrument management: Efficient use of large numbers of diverse instruments (Daley, 2004) requires a life cycle approach to instrument management, including instrument configuration to the system, portability, scalability, remote service and calibration. It also includes time distribution or synchronisation, plug and work (automated service discovery) and event response requirements. To achieve interoperability of instruments the configuration and interfacing of instruments must not only be standardised, but must be as simple as possible to facilitate the widest possible use.

Data and metadata management: Data is the primary product of observatories. Metadata is the data required to make the primary data meaningful. User requirements for data management have been addressed elsewhere (DMAC Report, 2005). The infrastructure requirements include provisions for data packet types as well as all data delivery and control services: acquiring data, sampling control, data time stamping, latency, and quality control requirements as well as metadata requirements for data, instruments and platforms. To achieve data interoperability, as well as to facilitate data storage and access by users, there needs to be a uniform conceptual approach to data and metadata, including the 'system metadata' required to describe the observing system and to manage it reliably.

4. Observatory levels

In addition to an identification of the primary areas into which requirements for ocean observatories can be grouped, the workshop participants recognised a need to place requirements into hierarchical levels based on the capabilities that the requirements address. Although the intent is not to suggest that observatories necessarily be developed according to the levels below, the workshop participants recognised the need for an iterative, incremental approach to the development of infrastructure middleware. The levels below provide one such road map.

Level 0: Prototype Observatory: These operational observatories are not truly member systems within the ORION program, but could be used as test beds for the development of instruments and/or capabilities for operational ORION level observatories. The requirements in this category area provide a level of capability sufficient to support their use as test beds.

Level I: Fundamental Observatory: This is a base level observatory that can support basic science experiments and implements a set of common capabilities shared by all systems at this level, including basic data and metadata interoperability. At this level science users will be able to deploy their instruments and reliably obtain their data but there will be little if any support for collaboration and coordination of instruments to support complex experiments by many scientists. Instruments may be interoperable between observatories at this level, but some configuration may be required by the user.

Level II: Collaborative Observatory: In addition to the capabilities of the prior levels, this level has instrument infrastructure to support the collaboration and coordination of instruments and their measurements which are distributed through the observing system. In addition the infrastructure supports ease of configuration of instruments as well as plug and work, or automated service discovery, capabilities.

Level III: Auto Adaptive Observatory: The qualification for an observatory at this level is that in addition to the capabilities of Level II, its infrastructure provides capabilities that support scientific experiments or ocean observations that require autonomous event detection and response, as well as a basic level of autonomous resource management for data storage, bandwidth, and power.

5. Conclusions

The NSF SENSORS Workshop on Instrument Software Infrastructure is an initial, but critical technical step towards applying the benefits of web based network technology to the development of ocean observatories. Participants also recognised that technical requirements may also be driven by general policies, some of which may need to be developed and articulated incrementally.

Acknowledgements

We wish to acknowledge our appreciation to the National Science Foundation, the ORION program office, and to the David and Lucille Packard Foundation for their generous support of research and development at MBARI, of which this effort is a part.

References

Daley, Kendra. L., R.H. Byrne, A.D. Dickson, S. Gallager, J.P. Perry and M. Tivey (2004). Chemical and Biological Sensors for Time-Series Research: Current Status and New Directions. Vol. 38, No. 2, Marine Technology Society Journal. pp. 121–142.

Dickey, T. and S. Glenn (2003). Scientific Cabled Observatories for Time Series (SCOTS) Report. National Science Foundation, Arlington, VA, 92pp.

DMAC Report, Ocean.US, NOAA, (March 2005). "Data Management and Communications Plan for Research and Operational Ocean Observing Systems. I. Interoperable Data Discovery, Access, and Archive", (http://dmac.ocean.us/dacsc/imp_plan.jsp).

Isern, A.R. and H.L. Clark (2004). The Ocean Observatories Initiative: A Continued Presence for Interactive Ocean Research. Vol. 37, No. 3, Marine Technology Society Journal. pp. 26–41.

Jahnke, R., L. Atkinson, J. Barth, F. Chavez, K. Daly, J. Edson, P. Franks, J.O'Donnell and O. Schofeld (2002). Coastal Ocean Processes and Observatories: Advancing Coastal Research. Skidaway Institute of Oceanography, Savannah, GA.

O'Reilly, T.C. *et al.* (2001). "Smart Network" Infrastructure for the MBARI Ocean Observing System, Proceedings of the IEEE OCEANS 2001 Meeting, Honolulu.

Schofield, O. and M. Tivey (2005). "ORION — Ocean Research Observatory Networks", ORION Workshop Report, January 4–8, San Juan, Puerto Rico.

Web sites

NSF SENSORS Workshop: www.mbari.org/rd/sensors/2004workshop.htm
MARS: www.mbari.org/mars/
ORION: www.orionocean.org
MBARI: www.mbari.org/

High frequency monitoring in Liverpool Bay; variability of suspended matter, nutrients and phytoplankton

N. Greenwood*[1], D.K. Mills[1], M.J. Howarth[2], R. Proctor[2], D.J. Pearce[1], D.B. Sivyer[1], S.J. Cutchey[1] and O. Andres[1]

[1]*Centre for Environment, Fisheries and Aquaculture Science (CEFAS), Lowestoft Laboratory, UK*
[2]*Proudman Oceanographic Laboratory, Liverpool, UK*

Abstract

Liverpool Bay receives substantial nutrient inputs and has been identified as a region which needs to be kept under surveillance through targeted monitoring. CEFAS has deployed a SmartBuoy in Liverpool Bay since November 2002, to provide high frequency measurements of physical, chemical and biological parameters which are telemetered back to the laboratory in near real time. The data are used to increase the evidence base and confidence when making formal assessments of eutrophication in the area. Time series data are presented for suspended load, nutrients and phytoplankton chlorophyll. Substantial temporal variability from hourly and daily through to annually is evident. A comparison of measured nutrient concentrations with OSPAR assessment criteria is made.

Keywords: SmartBuoy, *in situ* monitoring, eutrophication

1. Introduction

There is an increasing demand for robust data sets on which to base assessments of eutrophication required by an increasing range of international and European policy treaties and directives (e.g. OSPAR, Water Framework Directive, Urban Waste Water Treatment Directive, Nitrates Directive, Habitats Directive). Liverpool Bay is a turbid, shallow and tidally energetic coastal embayment of the Irish Sea that receives nutrient inputs from the estuarine area of the Mersey as well as from coastal sewage discharges. An assessment of the Irish Sea/Liverpool Bay region, carried out within the first application of the OSPAR Comprehensive Procedure (Malcolm *et al.*, 2003), revealed elevated nutrient enrichment.

Traditional ship-based surveys provide good spatial resolution but poor temporal resolution of the episodic changes occurring in this highly dynamic area. CEFAS has developed SmartBuoy, a moored platform to provide high frequency surface measurements of chemical, physical and biological parameters which are published in near real-time to the internet (Mills *et al.*, 2002, www.cefas.co.uk/monitoring). SmartBuoy has been operational in the North Sea since 2000 and a SmartBuoy has been deployed in Liverpool Bay since November 2002 as part of the Liverpool Bay Coastal Observatory Programme (Proctor *et al*., 2004, www.cobs.pol.ac.uk), co-ordinated by the Proudman

* Corresponding author, email: N.Grenwood@cefas.co.uk

Oceanographic Laboratory (POL). The high-frequency measurements provided by SmartBuoy in Liverpool Bay will better resolve the full scale of temporal variability and increase the evidence base and confidence when making formal assessments of eutrophication in the area.

2. Approach

The SmartBuoy payload and sampling frequency is summarised in Table 1. The SmartBuoy in Liverpool Bay is located in a grid of sampling stations (Figure 1). There are approximately nine cruises a year during which the mooring is serviced and water samples are collected at the grid stations for determination of salinity, suspended load, nutrients and chlorophyll.

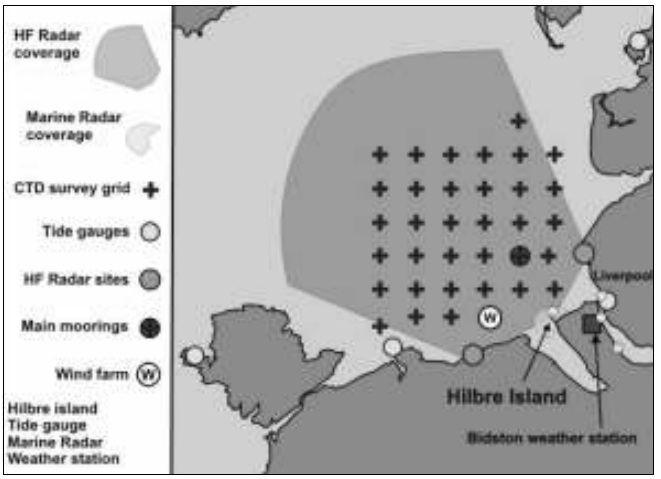

Figure 1 Location of SmartBuoy (main mooring) and sampling sites in the study area.

Table 1 Details of the SmartBuoy payload, variables measured and sampling frequency.

Instrument/Sensor	Variable	Sample frequency
Multi-channel logger and system controller with telemetry, interfaced with various sensors	Salinity Temperature Chlorophyll fluorescence Turbidity PAR irradiance at 1m and 2 m	1Hz in 2 x 10 minute bursts/hour
Aqua Monitor water sampler	TOxN (total oxidisable nitrogen) Dissolved silicate Suspended load Phytoplankton counts and composition	Up to daily
NAS-2E and NAS-3X *in situ* nitrate analyser	TOxN (total oxidisable nitrogen)	2 hourly

3. Results

Tidal, seasonal and inter-annual variability in the measured parameters is evident in the time series plots. Turbidity is generally highest and more variable in the winter months of October to April (Figure 2a). The OBS sensor is calibrated using the results from the gravimetric determination of suspended load from the Aqua Monitor samples. This reveals that suspended load concentrations reached a maximum of 140 mgl^{-1} in 2003 and 215 mgl^{-1} in 2004. The vertical attenuation coefficient calculated from downwelling PAR (Photosynthetically Active Radiation) measured at 1 m and 2 m, closely follow the turbidity results (Figure 2b). The major factor controlling *Kd* is the concentration of fine suspended minerogenic material; high suspended load leads to high attenuation and therefore low penetration of light into the water column.

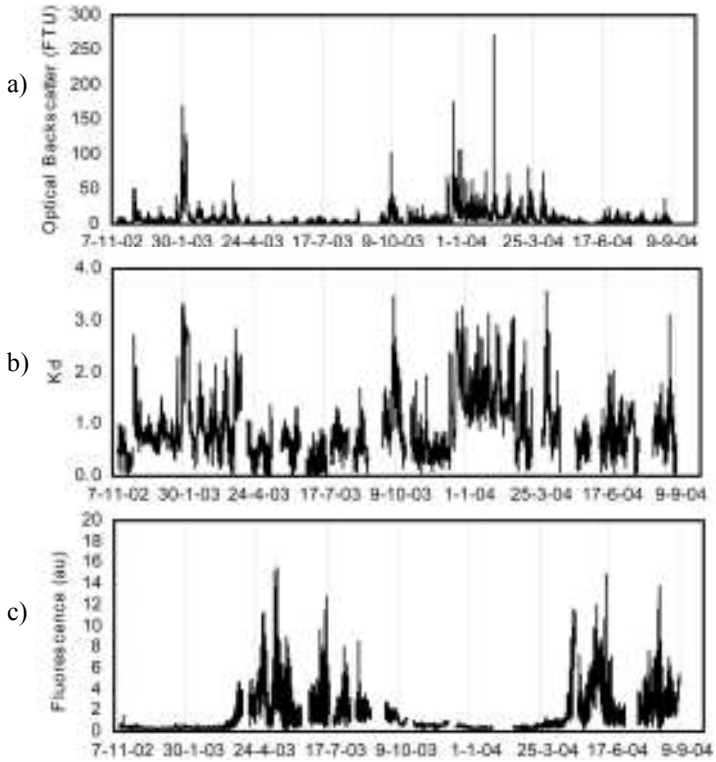

Figure 2 Time series of a) optical backscatter, b) vertical attenuation coefficient *Kd* and c) chlorophyll fluorescence measured at the surface in Liverpool Bay.

The spring bloom in 2003 started in mid-April but was later in 2004, starting at the beginning of May. Chlorophyll fluorescence values were similar in both years and decreased to over-winter levels during October (Figure 2c). Analysis of water samples for phytoplankton species composition revealed that diatoms dominated during the spring bloom in April 2003, with cell concentrations reaching 0.8×10^6 cells l^{-1} (Figure 3). The concentration of diatoms then decreased whilst flagellate cell numbers increased, reaching a maximum of over 1×10^6 cells l^{-1} at the end of August. Two harmful algal bloom species, *Dinophysis acuminata* and *D. Norvegica*, were found to be present.

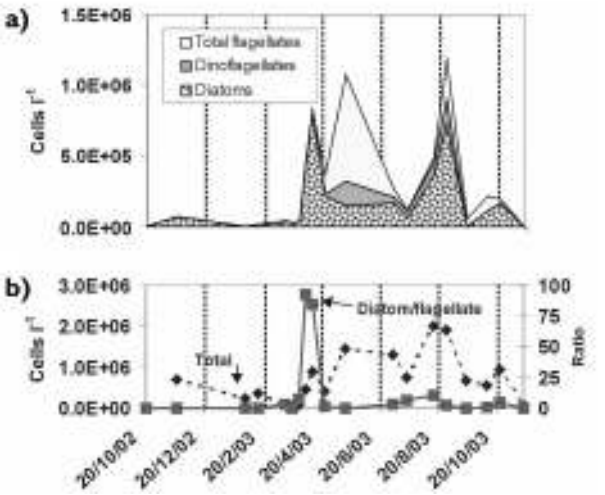

Figure 3 Time series of a) phytoplankton biomass as cell numbers for the major taxonomic groups and b) total cell numbers and the diatom to flagellate ratio in Liverpool Bay.

Winter maxima and summer minima of TOxN and silicate are evident at the SmartBuoy site (Figure 4). Liverpool Bay is hyper-nutrified during the winter; peak over-winter TOxN concentrations reached over 35 μM in 2002/3 and over 60 μM in 2003/4. Peak Si concentrations reached over 20 μM in the winter of both years. There is substantial short-term variability in the high frequency TOxN record obtained from the NAS, which is driven by freshwater inputs.

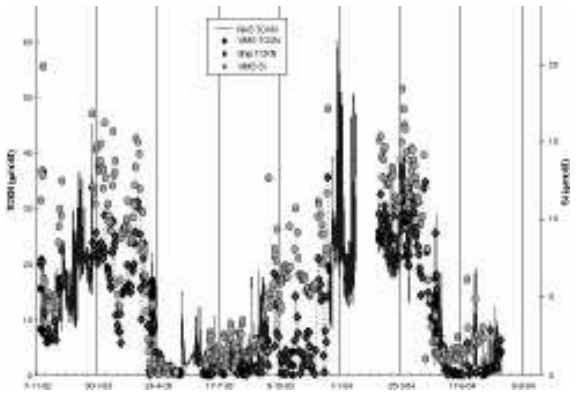

Figure 4 Plant nutrient concentrations measured at the surface in Liverpool Bay. Data shown are from the NAS, water sampler and discrete samples.

Winter nutrient data are of specific interest with regard to formal assessments of eutrophication for OSPAR. Data from the SmartBuoy have been compared to winter nutrient data collected using ship-based surveys (Figure 5a). The data from the SmartBuoy lie within the spread of historic ship-based data. However, results from the SmartBuoy in 2002 give a median and mean of 16 μM (Figure 5b) compared to a mean of 10 μM and a median of 12 μM for ship-based observations. Concentrations of TOxN measured by the

SmartBuoy in 2003 were greater than in 2002, with a mean and median of 22 μM. Concentrations of TOxN in both years therefore exceeded the OSPAR threshold of 10.8 μM.

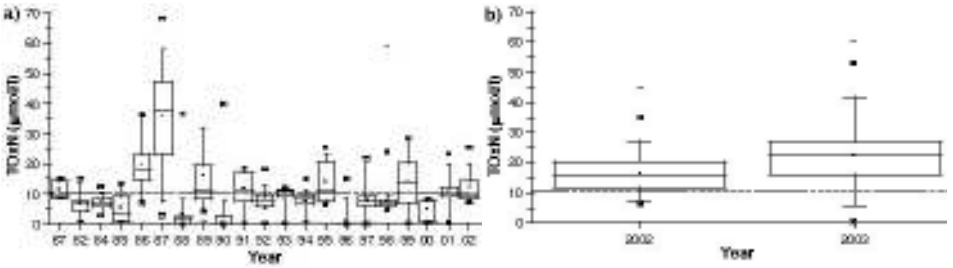

Figure 5 Box plots of winter TOxN concentrations in Liverpool Bay from a) ship-based measurements from a wide range of programmes and b) from the *in situ* analyser, water sampler and discrete samples. The dotted line is the t10.8 μM threshold TOxN concentration for the OSPAR region of Irish Sea/Liverpool Bay.

4. Discussion and conclusions

The data clearly demonstrate that there is substantial temporal variability, hourly, seasonally and annually, in the parameters measured. Suspended load concentrations reach a maximum over the winter, leading to high attenuation of light. During the same period, nutrient concentrations are elevated and in 2002 and 2003 concentrations of TOxN exceeded the OSPAR threshold. Nutrient concentrations fall in April/May associated with an increase in the concentration of phytoplankton. Diatoms dominate during the first month of the bloom after which flagellate cell numbers increase.

A second SmartBuoy is to be deployed in Liverpool Bay in May 2005. Data from both buoys will be compared to assess the spatial variability of the measured parameters.

Acknowledgements

This work is supported by the UK Department of Environment, Food and Rural Affairs (AE1228) as part of the Proudman Oceanographic Laboratory (POL) Coastal Observatory. The authors would like to thank the crew of the RV Prince Madog and staff at POL for their assistance with deployments of the SmartBuoy.

References

Malcolm, S., D. Nedwell, M. Devlin, A. Hanlon, S. Dare, R. Parker and D. Mills (2003). First Application of the OSPAR Comprehensive Procedure to waters around England and Wales.

Mills, D.K., R.W.P.M Laane, J.M. Rees, M. Rutgers van der Loeff, J.M. Suylen, D.J. Pearce, D.B. Sivyer, C. Heins, K. Platt and M. Rawlinson (2003). Smartbuoy: A marine environmental monitoring buoy with a difference. In: Building the European capacity in Operational Oceanography. Elsevier Oceanography Series, 69, 311–316.

Proctor, R., M.J. Howarth, P.J. Knight and D.K. Mills (2004). The POL Coastal Observatory — methodology and some first results. Proc. Eighth Int. Conf on Estuarine and Coastal Modeling, M.L. Spaulding (ed.). ASCE. pp 273–287.

Operational monitoring system of cyanobacterial pigment signals

M. Raateoja*, P. Ylöstalo, J. Seppälä, S. Kaitala and P. Maunula

Finnish Institute of Marine Research, Helsinki, Finland

Abstract

Harmful algal blooms in the Baltic Sea are typically dominated by the two cyanobacterial taxa, whose distribution can not be monitored with adequate precision with the *in vivo* fluorescence of Chlorophyll *a*. Here, we present the ship-of-opportunity system that records not only the *in vivo* fluorescence of Chlorophyll *a*, but also that of phycocyanin that is the light-harvesting pigment specific for cyanobacteria. We demonstrate this underway measurement system, its advantages, and the environmental value of the information it provides.

Keywords: operational oceanography, Baltic Sea, blue-green algae, cyanobacteria, phycocyanin, ship of opportunity, SOOP

1. Introduction

In the Baltic Sea (BS), harmful algal blooms (HABs) are usually linked to filamentous cyanobacteria, and more specifically, the taxa *Nodularia spumigena* and *Aphanizomenon flos-aquae*, the former being hepatotoxic. The mass occurrences of these taxa are a natural phenomenon of the BS, and have been occurring since long before the era of industrialisation. Still, these blooms have become a recurrent phenomenon especially during the latest decade, and to a large part their present extent and intensity are caused by man-made eutrophication. Due to their negative impact on the recreational and economic value of the BS, these blooms have received wide attention in the media, caused concern amongst the decision-makers, and have drawn attention to the eutrophication of the BS.

The alarmingly worsened environmental state of the BS has created the need for more up-to-date and accurate tools for assessing the state of the BS. The BS is covered by an extremely dense monitoring network in a global ocean scale, but the monitoring tools adopted do not provide all the information needed to properly monitor the undesired environmental trend of the BS. Especially critical is the need for a system capable of providing quantitative basin-wide information of the cyanobacterial distribution. This feature is made operational in the Alg@line ship-of-opportunity (SOOP) platform crossing the Baltic Proper as of June, 2005.

2. Cyanobacterial fluorescence signal

Traditionally, the estimate of phytoplankton standing stock in the field is obtained by Chlorophyll *a* (Chl *a*) concentration, either measured from the water samples by pigment extraction, or indirectly by the *in vivo* fluorescence of Chl *a* (IVF of Chl *a*) (Lorenzen,

* Corresponding author, email: mika.raateoja@fimr.fi

1966). Being rapid, reliable, and applicable for underway mappings, the IVF of Chl *a* has been adopted as the guideline for the SOOP-based assessment of the phytoplankton biomass distribution.

The conventional fluorometry employing bluish excitation (peak wavelength typically 430 to 440 nm) is directed to probe the IVF characteristics of Chl *a* that is the ubiquitous phytoplankton pigment in the oceans, and has its absorption maximum (λ_{Amax}) at 436 nm. For the eukaryotic phytoplankton groups, Chl *a* is well represented in the photosystem II that is the origin of >90% of all the IVF leaving the cells (Büchel and Wilhelm, 1993). Consequently, the eukaryotic phytoplankton exhibit a strong fluorescence response to the bluish fluorometric excitation.

Cyanobacteria possess a unique pigment matrix in terms of pigment composition that hinders the applicability of the conventional fluorometry to efficient cyanobacterial mapping. In cyanobacteria, the light is harvested mainly by phycobiliproteins that absorb light at a distinctly longer waveband than the blue absorption band of Chl *a*. Hence, the bluish fluorometric light fails to excite the cyanobacterial photosynthetic apparatus in a similar manner to the eukaryotic one. Cyanobacteria do possess Chl *a*, but most of it is situated in the low-fluorescing photosystem I (Campbell *et al.*, 1998), leading to very low IVF for the conventional fluorometers to track.

This apparent inability of the conventional fluorometry to assess the cyanobacterial biomass with a similar reliability to that of the eukaryotic phytoplankton is well-known (Cunningham, 1996; Schubert *et al.*, 1989). In the BS, this feature is particularly problematic, as the ecologically most important bloom-forming phytoplankton taxa here are cyanobacteria. Fortunately, various manufacturers have introduced special optical set-ups that allow the conversion of a conventional fluorometer to one more suitable for the detection of cyanobacterial distribution as based on the IVF of phycocyanin (PC, λ_{Amax} at 620 nm). PC is the main light-harvesting pigment in the two cyanobacterial taxa mentioned. Notwithstanding this development the critical step to operational applications has been surprisingly hard to accomplish.

3. System set-up, calibrations, and Q/C

The Alg@line SOOP monitoring system has been described in detail by Rantajärvi (2003) and Ruokanen *et al.* (2003). As there has been some development since these summaries, the current Alg@line system on-board "Finnpartner" crossing the Baltic Proper on the route Helsinki–Travemünde is presented in Figure 1. A Turner Designs 10-AU bench-top fluorometer with a 10-096 PC optical kit of a 620 nm excitation filter, a 650 nm emission filter, and a reference filter >665 nm (Turner Designs, Inc.) is used for the detection of cyanobacterial pigment signal. A Turner Designs SCUFA fluorometer with a 460 nm excitation filter and a 685 nm emission filter (Turner Designs, Inc.) is used for the detection of the fluorescence traces of eukaryotic phytoplankton, i.e. of Chl *a*. This instrument also includes the turbidity channel. A fast repetition rate fluorometer FAST^{tracka} (Chelsea Technologies Group) monitors the efficiency of the photochemical processes linked to photosynthesis. Temperature and salinity are monitored with an Aanderaa 3210 salinity-temperature sensor and an Aanderaa 3444 external temperature sensor (Aanderaa Instruments).

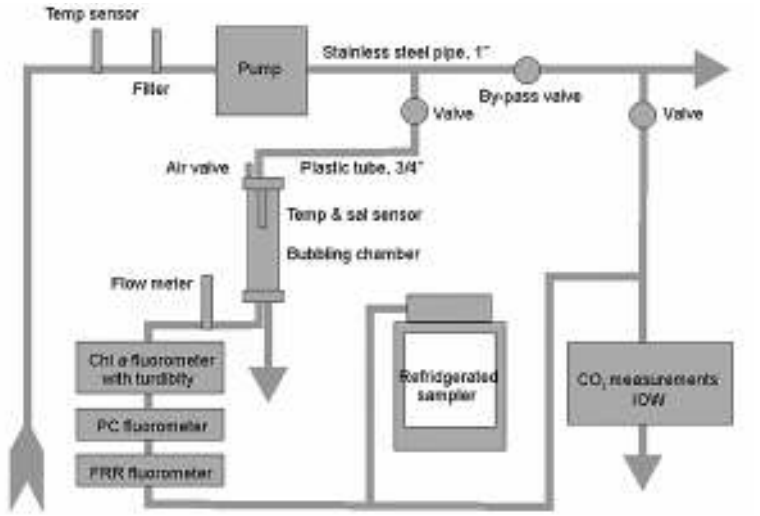

Figure 1 The underway surface water measuring system on-board "Finnpartner".

The IVF of Chl *a* that the SOOP-system provides is converted to Chl *a* concentration by addressing the relation between the IVF of Chl *a* and the actual Chl *a* concentration measured by pigment extraction from the water samples, and the results are reported in mass units of Chl *a* in a volume unit. This approach does not work with PC, because it can not be extracted completely from the cyanobacterial cells (Simis *et al.*, 2005). Furthermore, the PC content of cyanobacteria is variable, and thus, the IVF of PC can not be directly related to cyanobacterial biomass (Seppälä *et al.*, unpubl.). We assess the relation between the IVF of PC and that of pure C-PC of a known concentration. For the reference, we use the commercially available C-PC in phosphate buffer (Cyanotech, Inc.). The results are reported in IVF units equalling mass unit of pure C-PC in a volume unit. In the future, the IVF of PC will be scaled to the *in vivo* absorption of PC and to cyanobacterial cell numbers.

The consistency of the performances of the PC-tuned 10-AU and the regular SCUFA are checked using a 10-AU-904 and a 2000-901 solid secondary standards (Turner Desings, Inc.), respectively, every time the ship is visited, that is, approximately once per week. During every visit, the relation between the IVF of Chl *a* and actual Chl *a* concentration of the water samples is checked, and the impact of biofouling is minimised by cleaning the flow-through cuvette of the PC-tuned 10-AU and the optical windows and the flow-through cap of SCUFA.

The salinity and temperature sensors are calibrated annually, checked once every three months using salinity samples and waterpaths respectively, and cleaned monthly.

4. Results and discussion

There is a gap between the waveband of the bluish fluorometric excitation (430 to 500 nm) and that of the light the cyanobacteria can efficiently utilise (500 to 620 nm). Strictly speaking, cyanobacteria can absorb also bluish light by Chl *a* in the photosystem I, but as already mentioned, its impact on the IVF is minor. Another gap takes place

between the waveband of cyanobacterial fluorescence (570 to 650 nm) and the detection waveband of a conventional fluorometer (>680 nm). These features prevent the meaningful use of conventional fluorometry for cyanobacterial mapping. We tested the difference in the IVF of Chl *a* between one of the key cyanobacterial taxa in the BS (*Nodularia*) and a representative of a eukaryotic phytoplankton species (*Nannochloris* sp.) that as a chlorophyte phytoplankton harbouring Chl *a* and Chl *b* (Jeffrey and Vesk, 1997) responds sharply to the bluish excitation. As a regular fluorometer exciting bluish light we used a Turner Designs 10-AU with 10-037 Chl *a* optical kit of a 340–500 nm excitation filter, and a >665 nm reference filter (Turner Designs, Inc.). The ratio of the IVF of Chl *a* to the Chl *a* concentration for *Nannochloris* was 15 to 20-fold, as compared to *Nodularia* (data not shown). This result suggests that the biomass increase of *Nodularia*, e.g. in the context of late-summer bloom patches, has to be 15 to 20 times the biomass increase in the eukaryotic phytoplankton community to trigger a similar increase in the IVF of Chl *a*. These results have been corroborated by similar tests with other eukaryotic taxa (Seppälä and Ylöstalo, unpubl.). Thus, it is apparent that the conventional fluorometry provides an estimate of the cyanobacterial biomass that is far from the truth, if the estimate is based solely on the IVF of Chl *a*.

This drastic difference is explained by the adaptation of *Nodularia* to the optical light field of the BS. The BS is, for an oceanic environment, a highly turbid and humic environment, where the natural light milieu has shifted considerably towards the longer waveband, as compared to the oceans (Ferrari *et al.*, 2003; Raateoja *et al.*, 2004). To compensate for this optically unique environment, the ecologically most important bloom-forming cyanobacterial taxa in the BS, *Nodularia* and *Aphanizomenon*, most probably harbour phycoerythrocyanin (PEC, λ_{Amax} 570 to 595 nm) as the shortest wavelength absorbing pigment (Seppälä *et al.*, 2005). Thus, these taxa can not efficiently absorb the bluish light excited by the conventional fluorometry with their photosystem II pigment complexes, and their fluorescence response triggered by the bluish excitation remains equally low.

It is now clear that the conventional fluorometry can not be used for meaningful cyanobacterial monitoring in the BS, but will the PC-tuned approach perform any better? The operational monitoring of cyanobacteria using the set-up described was only started in June 2005 — at the time the growth of cyanobacteria was still slow mainly due to low water temperature. The more prominent cyanobacterial surface accumulations appear in the BS during the late-summer. Hence, the performance of the system on-board "Finnpartner" could not be demonstrated up to the time this article was submitted, but its capacity was proven during the test period on-board FIMR's research vessel "Aranda" in July, 2004. The simultaneous underway measurements of the IVF of Chl *a* and PC were carried out in the frontal area in the Gulf of Finland, BS (Figure 2). The study revealed the bloom patches of cyanobacteria exhibiting strong IVF of PC in the warm water side of the front, intermediate IVF of PC in the colder water mass, and low IVF of PC in the warmer water mass outside the front. The cross-frontal variation in the IVF of Chl *a* was only moderate, and the two fluorescence parameters were not directly related. Consequently up to 6-fold differences were observed in the ratio of the IVF of PC to the IVF of Chl *a* in the study area. The IVF of Chl *a* did not reveal the accumulation of cyanobacteria along the front, but the IVF of PC did, thus proving the potential of the system. The

biomass of *Aphanizomenon*, the dominant cyanophyte during the cruise, and the IVF of PC were linearly related (r^2=0.79, n=6, data not shown). The visual observations during the cruise corroborate the IVF of PC based view over the spatial cyanobacterial distribution (J. Seppälä, pers. comm.).

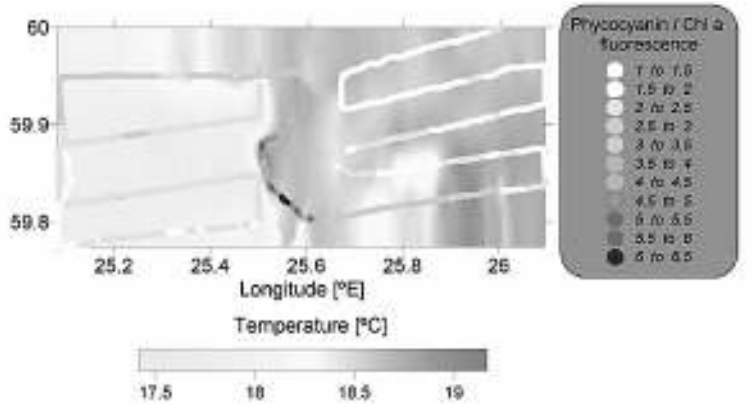

Figure 2 Variation in the ratio of *in vivo* fluorescence of PC to the *in vivo* fluorescence of Chl *a* in the Gulf of Finland during late summer 2004 overlaid by isotherms.

It may be reasonably argued that the unique optical characteristics of the BS, and the consequent light-harvesting characteristics of the dominant cyanobacterial taxa are just an exception to the rule in the global context. On a global scale, cyanobacteria do harbour pigments that harvest light in shorter wavelengths than PEC, or PC. *Phycoerythrin* (PE) is usually responsible for the harvesting of light of the shortest waveband in cyanobacteria. PE has its λ_{Amax} around 495 or 575 nm depending on its chromophores (Sidler, 1994). PE is responsible for an important part of the light-harvesting in for example the ubiquitous oceanic cyanobacteria *Synechococcus* spp. and *Trichodesmium* spp. (Subramaniam *et al.*, 1999; Wood *et al.*, 1998). Still, using a fluorometer with the excitation peak near to λ_{Amax} of Chl *a*, i.e. around 440 nm, the impact of PE on the resulting IVF should be quite minor.

The most important HAB species in the oceanic environment are dinoflagellates that are usually responsible for red tides and shellfish poisonings PSP, DSP, and NSP (Anderson, 1997; Horner *et al.*, 1997; Tester and Steidinger, 1997). Dinoflagellates as representatives of chromophyte phytoplankton harbour Chl *a* and Chl *c* (Jeffrey and Vesk 1997), and respond sharply to the bluish excitation. It might therefore be asked what the point is in developing monitoring strategies for a phytoplankton group that is not an important HAB group in the world ocean. Cyanobacteria are an important HAB group not only in the BS, but also in coastal areas and various fresh-water systems; lakes, reservoirs and estuaries. Amongst those, the reservoirs serving as water sources for human settlement and cattle are especially sensitive to cyanobacterial toxins (Sellner, 1997). Of the two dominant cyanobacterial taxa in the BS, *Nodularia* is hepatotoxic, and has been associated with poisonings of domestic animals around the world (Laamanen *et al.*, 2001). Concentrating on coastal areas and fresh-water systems, i.e. areas in the vicinity of human settlements, and directly experienced by man, toxic cyanobacteria pose a serious threat that is more immediate to the humans than the oceanic HABs.

Currently the fittest choice for the rapid environmental assessment over large oceanic provinces is earth observation (EO). The EO sensors targeted for ocean colour mapping regularly have channels corresponding to the blue absorption maximum of Chl *a* (e.g. MODIS, MERIS). Furthermore, the in-water Chl *a* algorithms for the EO products have already been developed for different oceanic provinces. Consequently, EO-based Chl *a* maps have become a routine output of environmental monitoring programmes. The BS is optically unique, though, and represents an extra challenge for the development of local in-water algorithms for Chl *a* (HELCOM, 2004), as the blue absorption peak of Chl *a* gets somewhat dampened by the absorption by chromophoric dissolved organic matter (CDOM). The situation is more problematic for the mapping of cyanobacterial distribution in the BS. The successful basinwide synoptic mapping of cyanobacteria requires a consistent source of suitable EO data, and a powerful ground-truthing source. The waveband corresponding to the absorption maximum of PC is currently included only in the sequence of bands of MERIS (Envisat/ESA) that is not widely commercially available. This information is available using multi-spectral approaches from other sensors such as MODIS (Aqua/Terra/NASA), even though MODIS does not provide data corresponding to the absorption maximum of PC *per se*. The ground-truthing of the EO-based PC products is another topical problem, as there is no easy way to estimate the amount of PC in a unit of sample volume (Simis *et al.*, 2005). Thus, a field data set of PC analogous to Chl *a* for EO data validation purposes is not available. This fact emphasises the value of the approach presented here that provides information of PC, if not in mass units of PC in a volume unit, at least in IVF units equalling the mass unit of PC in a volume unit. Basically, this development permits the ground-truthing of the EO-based products of PC distribution.

5. Conclusions

Like Chl *a* for water quality monitoring, the mapping of PC will have a solid contribution for the monitoring of cyanobacterial HABs. A combination of the prompt determination of PC, high-frequency underway sampling, and EO customer products is the best choice for the efficient cyanobacterial monitoring, because these blooms are very patchy in nature.

Today's aquatic environment, under heavy and continuous anthropogenic pressure, requires robust monitoring tools for the accurate assessment of its environmental state. The near-real-time approach is becoming more a requirement than a recommendation for environmental monitoring programmes. This trend is made in part possible by the recent development in telemetry and EO. The ground-truthing of the EO products is usually considered as the critical step simply because there has not been much development in the field measuring techniques, except the establishment of the SOOP-ideology. It is therefore recommended to fully utilise the capacity of this unattended but highly tailored approach to environmental monitoring.

Acknowledgements

The authors and the Alg@line consortium would like to thank the shipping company Finnlines for providing the platform and crew time, and Turner Designs, Inc. for their collaboration. This work was funded by the Finnish Institute of Marine Research for

M.R. and P.M., by Walter and Andrée de Nottbeck foundation and Academy of Finland for P.Y., by Maj and Tor Nessling foundation for J.S., and by the EU FerryBox project: From on-line oceanographic observations to environmental information (5th Framework Programme of the European Commission CN:EVK2–2002–00144) for S.K.

References

Anderson, D.M. (1997). Bloom dynamics of toxic *Alexandrium* species in the northeastern U.S., Limnology and Oceanography, Vol. 42, pp. 1009–1022.

Büchel, C. and C. Wilhelm (1993). *In vivo* analysis of slow chlorophyll fluorescence induction kinetics in algae: progress, problems and perspectives. Photochemistry and Photobiology 58.

Campbell, D., V. Hurry, A.K. Clarke, P. Gustafsson and G. Öquist (1998). Chlorophyll fluorescence analysis of cyanobacterial photosynthesis and acclimation, Microbiology and Molecular Biology Reviews, Vol. 62, pp. 667–683.

Cunningham, A. (1996). Variability of *in vivo* chlorophyll fluorescence and its implications for instrument development in bio-optical oceanography, Scientia Marina, Vol. 60, pp. 309–315.

Ferrari, G.M., F.G. Bo and M. Babin (2003). Geo-chemical and optical characterizations of suspended matter in European coastal regions, Estuarine Coastal and Shelf Science, Vol. 57, pp. 17–24.

HELCOM (2004). Thematic report on Validation of algorithms for Chlorophyll a retrieval from satellite data of the BS area, Vol. 94, Helsinki Commission.

Horner, R.A., D.L. Garrison, and F.G. Plumley (1997). Harmful algal blooms and red tide problems on the U.S. west coast, Limnology and Oceanography, Vol. 42, pp. 1076–1088.

Jeffrey, S.W. and M. Vesk (1997). Introduction to marine phytoplankton and their pigment signatures. In: Phytoplankton pigments in oceanography: guidelines to modern methods (eds. S.W. Jeffrey, R.F.C. Mantoura, and S.W. Wright), UNESCO publishing.

Laamanen, M.J., M.F. Gugger, J.M. Lehtimäki, K. Haukka and K. Sivonen (2001). Diversity of toxic and nontoxic *Nodularia* isolates (Cyanobacteria) and filaments from the BS, Applied and Environmental Microbiology, Vol. 67, pp. 4638–4647.

Lorenzen, C. (1966). A method for continuous measurement of *in vivo* chlorophyll concentration, Deep-Sea Research, Vol. 13, pp. 223–227.

Raateoja, M., J. Seppälä and P. Ylöstalo (2004). Fast repetition rate fluorometry is not applicable to studies of filamentous cyanobacteria from the BS, Limnology and Oceanography, Vol. 49, pp. 1006–1012.

Rantajärvi, E. (ed.) (2003). Alg@line in 2003: 10 years of innovative plankton monitoring and research and operational information service in the BS, Vol. 48, Finnish Institute of Marine Research.

Ruokanen, L., S. Kaitala, V. Fleming, and P. Maunula (2003). Alg@line — joint operational unattended phytoplankton monitoring in the BS. In: Building the European capacity in operational oceanography (eds. H. Dahlin, N.C. Flemming, K. Nittis, and S.E. Petersson), Elsevier Oceanography Series, Vol. 69. Elsevier.

Schubert, H., U. Schiewer and E. Tschirner (1989). Fluorescence characteristics of cyanobacteria (blue-green algae), Journal of Plankton Research, Vol. 11, pp. 353–359.

Sellner, K.G. (1997). Physiology, ecology, and toxic properties of marine cyanobacterial blooms, Limnology and Oceanography, Vol. 42, pp. 1089–1114.

Seppälä, J., P. Ylöstalo and H. Kuosa (2005). Spectral absorption and fluorescence characteristics of phytoplankton in different size fractions across a salinity gradient in the BS, International Journal of Remote Sensing, Vol. 26, pp. 387–414.

Sidler, W.A. (1994). Phycobilisome and phycobiliprotein structure. In: The molecular biology of cyanobacteria (ed. D.A. Bryant), Kluwer.

Simis, S.G.H., S.W.M. Peters and H.J. Gons (2005). Remote sensing of the cyanobacterial pigment phycocyanin in turbid inland water, Limnology and Oceanography, Vol. 50, pp. 237–245.

Subramaniam, A., E.J. Carpenter, D. Karentz and P.G. Falkowski (1999). Bio-optical properties of the marine diazotrophic cyanobacteria *Trichodesmium* spp. I. Absorption and photosynthetic action spectra, Limnology and Oceanography, Vol. 44, pp. 608–617.

Tester, P.A. and K.A. Steidinger (1997). *Gymnodinium breve* red tide blooms: initiation, transport, and consequences of surface circulation, Limnology and Oceanography, Vol. 42, pp. 1039–1051.

Wood, A.M., D.A. Phinney and C.A. Yentsch (1998). Water column transparency and the distribution of spectrally distinct forms of phycoerythrin-containing organisms, Marine Ecology Progress Series, Vol. 162, pp. 25–31.

A combinative assessment of oceanographic conditions using buoy and AVHRR measurements in the Southern Aegean Sea

D.G. Kalantzi*, Ch.T. Soukissian and K. Nittis

Hellenic Centre for Marine Research - Institute of Oceanography, Greece

Abstract

The aim of this work is the oceanographic assessment of the upper circulation patterns of the south Aegean Sea based on *in situ* and remote-sensed data for a period of 12 months (06/2000–06/2001). The *in situ* data include current speed and direction, wind and temperature time series obtained from three buoys which are part of the POSEIDON system, responsible for the real-time monitoring of the marine environmental conditions in the Aegean Sea. The remote-sensed data originate from the AVHRR installed on NOAA satellites. The partially-analysed data was provided from the on-line database of the German Aerospace Centre (DLR). Through this work the data were transformed into 12 SST (SST) imageries, each one referring to the mean monthly values of the surface temperature of the examined area. Furthermore, the quality of the two data-sets (*in situ* and remote-sensed data) was compared and evaluated (06/1999–05/2000) through the use of primary statistics and a local calibration (linear regression) equation for the AVHRR data was derived.

Keywords: AVHRR, Aegean Sea, calibration, POSEIDON system

1. Introduction

The first part of this work focuses on the general circulation of the south Aegean, which has been shown by previous studies to have prevailing multi-scale circulation patterns consisting of mesoscale cyclonic and anticyclonic features. These movements seem to control the local circulation while exhibiting a prominent seasonal variability. Both the surface patterns and the seasonal heating of the water are probably associated with the surface mixed-layer at the level of the seasonal thermocline. The second part deals with the direct statistical comparison of *in situ* and remote sensed data leading to the proposal of a new calibration equation for the SST referring to the south Aegean Sea.

2. Data processing and analysis

The data analysed in this paper correspond to 3 locations: Rhodes Island (Location 1), Dia Island (Location 2), and Avgo Island (Location 3), see Figure 1.

For the circulation study of the examined area, three different sets of time series (1 year) from location 3 were analysed (3 h interval): the first set refers to 6 sea-temperature time series at depths of 3, 10, 20, 30, 40, and 45 m. The second set refers to wind speed and direction and the third set refers to current speed and direction. For the statistical

* Corresponding author, email: yolanda@ath.hcmr.gr

comparison of *in situ* temperature and SST, one data set of mean daily temperature measurements at 3 m depth from each location 1 and 2 were processed and examined (B set). The remote sensed data comprise of 12 appropriately processed SST maps referring to the entire Aegean Sea region and 2 yearly time-series of daily SST point measurements corresponding to the coordinates of mooring sites 1 and 2 (S set).

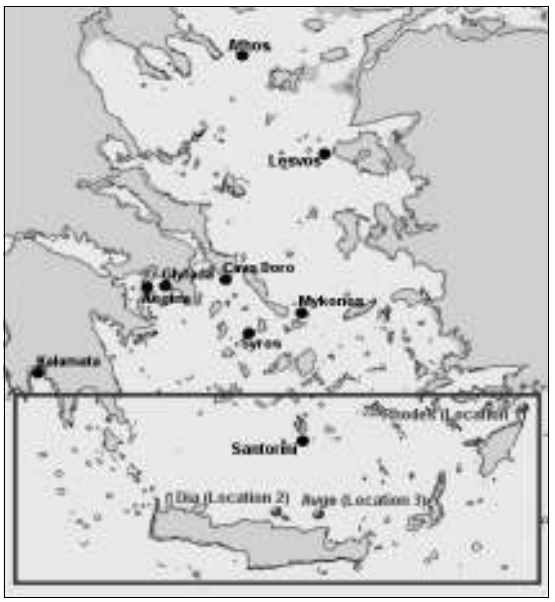

Figure 1 The POSEIDON network (grey dots designate the buoys used for this study).

See also Ballas *et al*. (2005) and Nittis *et al*. (2005) for more Poseidon papers.

3. Results

Through the study of the graphs and maps (of which a small sample is shown in Figure 2) we studied

1. The thermocline mechanism which divides the time period into 2 discrete parts: i) the stratification period and ii) the mixing period
2. The wind-sea surface interaction which induces mixing incidents even during stratification periods
3. We tracked possible upwelling and downwelling phenomena indissolubly connected with the formation of surface patterns.

In general, this methodology combining graphical representations of *in situ* sea parameters with successive monthly SST maps helped us to study the general mechanisms of the surface circulation as well as to elucidate their prominent seasonality. These results were in agreement with former studies describing the surface circulation of the Aegean such as Hopkins (1978), Georgopoulos *et al.* (1992), Theocharis *et al.* (1993), Zodiatis *et al.* (1993, 1994), Cardin *et al.* (2002), Nittis and Perivoliotis (2002) and Kourafalou and Barbopoulos (2003).

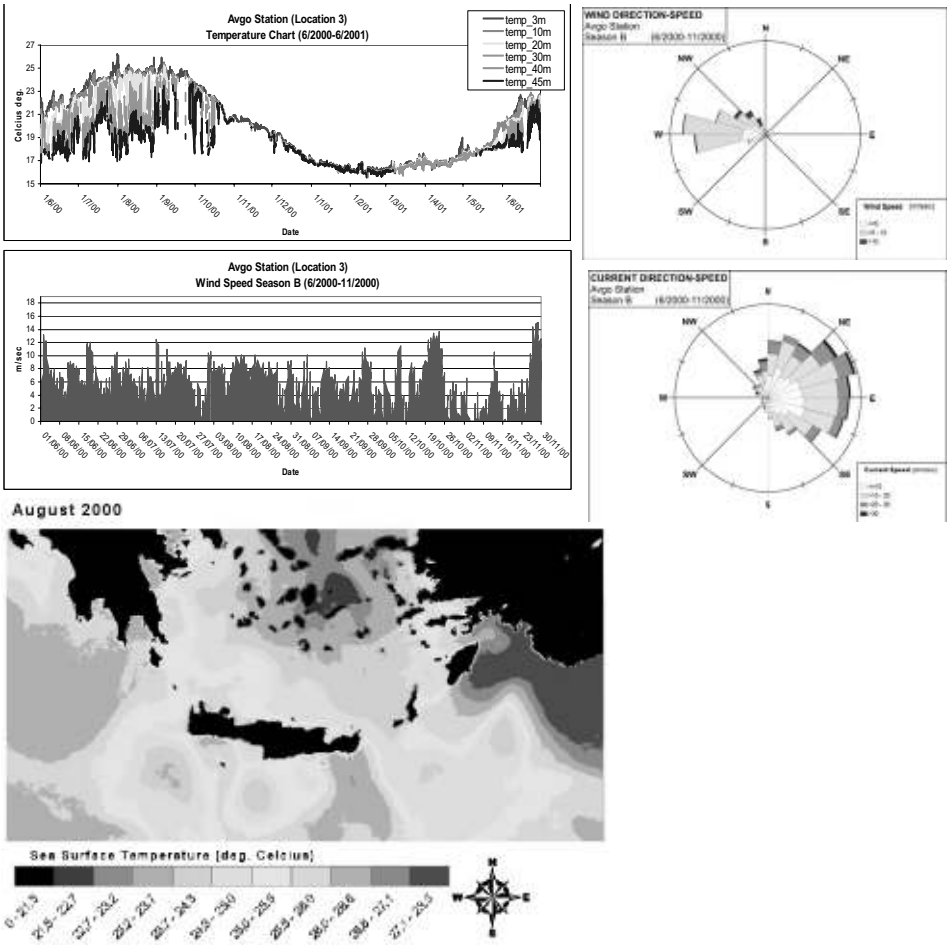

Figure 2 Representative graphs and SST map of this study.

4. A new calibration equation for South Aegean

General conditions: Using the method of ordinary least squares we estimate the parameters of the basic regression relation (Ryan, 1997) using the available collocated surface temperature data:

Table 1 Linear regression equation of $\hat{T}_{SAT}$ against T_B for locations 1 and 2 under general conditions (mixing conditions in parentheses).

	Adjusted coeff. of determination	Regression equation	
Location 1	$R^2 = 0.88158$, $(R^2 = 0.9764)$	$\hat{T}_{SAT} = 0.81499 + 0.959033\,T_B$	(1)
Location 2	$R^2 = 0.96502$, $(R^2 = 0.9894)$	$\hat{T}_{SAT} = -0.66359 + 1.02956\,T_B$	(2)

The regression equations after exclusion of outliers from further analysis (see the works of Cook, 1977; Draper and Smith, 1998, p. 75) are of the form:

Table 2 Linear regression equation of $\hat{T}_{SAT}$ against T_B for locations 1 and 2 under general conditions and mixing conditions (relationships in parentheses) after excluding outliers.

	Adjusted coeff. of determination	Regression equation	
Location 1	$R^2 = 0.96921$,	$\hat{T}_{SAT} = -0.52032 + 1.02442 T_B$	(3)
	$(R^2 = 0.98375)$	$(\hat{T}_{SAT} = 0.16814 + 0.9966 T_B)$	
Location 2	$R^2 = 0.98406$,	$\hat{T}_{SAT} = -0.80461 + 1.03705 T_B$	(4)
	$(R^2 = 0.99237)$	$\hat{T}_{SAT} = -0.43129 + 1.0203 T_B)$	

It is clear that the equations obtained have profound similarities suggesting that the calibration of SST data for the Aegean Sea can be performed in a unique way.

Mixing conditions: In order to examine the regression equation under mixing conditions in the sea surface layer, we take sub-samples of the entire population corresponding in days where the mean daily wind speed exceeds 7 $\mathrm{m s^{-1}}$. Strong wind fields enhance the dynamic convection towards both vertical and horizontal directions. Nevertheless, the AVHRR resolution is of the order of 1 km and so temperature homogeneity of wide surface areas suits the agreement of *in situ* and R-S SST measurements. In this case it is clear that there is a significant improvement in the value of R^2, indicating a much stronger linear relationship between $\hat{T}_{SAT}$ and T_B. The corresponding adjusted coefficients of determination are shown in parentheses in Table 1. By a similar outlier analysis we obtain the results shown in parentheses in Table 2. It is obvious that, in general, there is an improvement in the obtained values of the adjusted coefficient of determination. An almost perfect linear dependence between $\hat{T}_{SAT}$ and T_B holds for location 1 $(R^2 = 0.99237)$.

Inverse regression equation: Considering that T_B is the "correct" value of sea surface temperature and $\hat{T}_{SAT}$ is the value-under-calibration of temperature we can apply the inverse regression method, cf. Netter *et al.*, (1989), Ryan (1997, pp. 31–34), Draper and Smith (1998, pp. 83–86).

Table 3 Calibration equation of $\hat{T}_{SAT}$ against T_B for locations 1 and 2 under general conditions and mixing conditions (in parentheses).

Location 1	$\hat{T}'_{SAT} = 0.9761 + 0.5079 T_{SAT}$	(5)
	$(\hat{T}'_{SAT} = -0.1687 + 1.0034 T_{SAT})$	
Location 2	$\hat{T}'_{SAT} = 0.9642 + 0.7738 T_{SAT}$	(6)
	$(\hat{T}'_{SAT} = -0.4227 + 0.9801 T_B)$	

The inverse regression method actually suggests "solving" the obtained regression equations with respect to T_B for the purpose of predicting T_{SAT} for a given value of $\hat{T}_{SAT}$. Specifically, from the above equations we can easily obtain the results depicted in Table 4, where $\hat{T}'_{SAT}$ is the calibrated satellite sea surface temperature and T_{SAT} is the initial value of sea surface temperature obtained directly from the satellite. The similarity of the obtained calibration equations is evident.

Table 4 Simple calibration equations of SST for South Aegean Sea.

Strong mixing conditions		General conditions (mixing and non-mixing)	
$\hat{T}'_{SAT} \approx 0.13 + 0.99 T_{SAT}$	(7)	$\hat{T}'_{SAT} \approx 0.97 + 0.65 T_{SAT}$	(8)

References

Ballas, D., A. Mallios and P. Pagonis (2005). A technical overview of the POSEIDON II system. This volume page 69.

Brown, S.A., M. Folk, G. Goucher and R. Rew (1993). Software for portable scientific data management, Computers in Physics, Vol. 7, p(p). 304–308.

Cardin, V., M. Gacic, K. Nittis, V. Kovacevic and L. Perini (2002). Sub-inertial variability in the Cretan Sea from M3A buoy, Annales Geophysicae, Vol. 21, pp. 89–102.

Draper, R. and H. Smith (1998). Applied regression Analysis, Wiley–Interscience.

Georgopoulos, D., E. Salusti and A. Theocharis (1992). Dense water formation processes in the North Aegean sea (Eastern Mediterranean), Ocean Modeling, Vol. 95, pp. 4–6.

Cook, R.D. (1977). Detection of influential observations in linear regression, Technometrics, Vol. 19, pp. 15–18.

Hopkins, T.S. (1978). Physical processes in the Mediterranean basins, Estuarine transport processes, South Carolina, USA, B. Kjerfve (ed.), "University of South Carolina Press", p. 269–310.

Kourafalou, V.H. and K. Barbopoulos (2003). High resolution simulations on the North Aegean Sea seasonal circulation, Annales Geophysicae, Vol. 21, pp. 251–265.

Netter, J., W. Wasserman and M.H. Kutner (1989). Applied Linear Regression, Analysis of Variance and Experimental Designs, p(p). 271–275, Boston.

Nittis, K. and L. Perivoliotis (2002). Circulation and hydrological characteristics of the North Aegean Sea: a contribution from real-time buoy measurements, Mediterranean Marine Science, Vol. 3, No. 1, p(p). 21–31.

Nittis, K., L. Perivoliotis, D. Ballas, G. Korres, T. Soukissian, A. Papadopoulos, A. Mallios, G. Triantafyllou, A. Pollani, V. Zervakis, D. Georgopoulos, V. Papathanassiou and G. Chronis (2005). POSEIDON II: A second generation monitoring and forecasting system for the Eastern Mediterranean Sea. This volume page 585.

Ryan, P. (1996). Modern Regression Methods, Jossey–Bass.

Soukissian, T., G. Chronis and K. Nittis (1991). POSEIDON: Operational marine monitoring system for the Greek seas. Sea Technology, Vol. 40, No. 7, pp. 31–37.

Theocharis, A., D. Georgopoulos, A. Lascaratos and K. Nittis (1993). Water masses and circulation in the central region of the Eastern Mediterranean: Eastern Ionian, South

Aegean and Northwest Levantine, 1986–1987, Deep-Sea Research II, Vol. 40, No. 6, pp. 1121–1142.

Zodiatis, G. and E. Balopoulos (1993). Structure and characteristics of fronts in the North Aegean Sea, Bolletino in Oceanologica Theorica ed Applicata, Vol. XI, No. 2, pp. 113–124.

Zodiatis, G. (1994). Advection of the Black Sea water in the North Aegean Sea, Global Atmos, Ocean Syst., Vol. 2, No. 1, pp. 41–60.

Linking French Atlantic rivers to low salinity intrusions in the western English Channel: highly resolved monitoring from the EU "FerryBox" project

B.A. Kelly-Gerreyn*[1], D.J. Hydes[1], L.J. Fernand[2], A.M. Jégou[3], P. Lazure[3] and I. Puillat[4]

[1]*1National Oceanography Centre, Southampton, UK*
[2]*Centre for Environment, Fisheries and Aquaculture Sciences, Lowestoft, UK*
[3]*Ifremer, Direction de l'Environnement Littoral, Service Applications Opérationnelles, France*
[4]*LODYC/IRD, Laboratoire d'Océanographie Dynamique et Climatologie, Paris, France*

Abstract

Low salinity surface waters at the southern entrance (Ushant) to the western English Channel have been monitored from a near-continuous record of data collected on a ferry operating between Portsmouth (UK) and Bilbao (Spain) since April 2002. These fresh waters originate from poleward flowing plumes from French Atlantic rivers (e.g. Loire). Winter river outflows were above average in 2004 and 2003 and average in 2002 which is consistent with the minimum salinities observed near Ushant in late winter (33.68, 33.90, 34.53 in 2004, 2003, 2002, respectively). These surface water masses intrude into the western English Channel in all three years of monitoring, suggesting a frequent phenomena. The extent of the intrusion is linked to prevailing winds, with southerly winds favourable to intrusion. In contrast, northerly winds force the plume waters offshore. It is hypothesised that the more intense of these low salinity intrusions (in 2003) can enhance summer blooms of the red tide forming dinoflagellate *Karenia mikimotoi* through both increased stability of the upper water column and nutrient supply.

Keywords: low salinity intrusion, *Karenia mikimotoi*, ship of opportunity, FerryBox, wind, Loire, Gironde, western English Channel

1. Introduction

The English Channel has one of the longest histories in oceanographic research (e.g. Rennell, 1793) and yet a coherent understanding of some commonly observed features has not been fully established. Such features include the occurrence and fate of low salinity waters at the southern entrance to the western English Channel and the varying intensities in the regular summer blooms (sometimes >100 mg Chl m^{-3}) of the red-tide forming dinoflagellate *Karenia mikimotoi* (previously and mistakenly identified as *Gyrodinium aureolum*, Pingree *et al.*, 1977) in the central Channel.

A FerryBox system provides greatly enhanced detail in the seasonal dynamics (April 2002–August 2004) of salinity and chlorophyll-fluorescence along a ship's route operating year-round between Portsmouth (UK) and Bilbao (Spain). These FerryBox

* Corresponding author, email: bag@noc.soton.ac.uk

data are analysed alongside river and wind data from the French Atlantic coast allowing us to examine both the source and fate of the low salinity waters and the possible causes for differences in bloom intensity of *K. mikimotoi* among years in the western English Channel. This paper is closely aligned to two other papers in this volume (Hydes *et al.*, 2003; Qurban *et al.*, 2005).

2. Study area and data sources (FerryBox)

The main details of the study area and the sources of data can be found in Hydes *et al.* (2003). Operations began in April 2002 and are still ongoing. The ferry route (Figure 1) is that of the P&O European Ferries Ltd. ship "Pride of Bilbao" between Portsmouth (UK, 50.8°N, –1.1°E) and Bilbao (Spain, 43.4°N, –3.0°E). The distance is approximately 1000 km and the journey time is about 35 hours. Repeat rates are between 4 hours and 4 days depending on location. Measurements of temperature, conductivity and chlorophyll fluorescence (Chelsea Technologies Group MiniPack) are made at 1 Hz from samples taken from the ship's cooling water supply at 5 metres depth. In 2003 and 2004, manned monthly calibration crossings collected samples for salinity and acetone extracted chlorophyll as well as the nutrients nitrate, phosphate and silicate. We focus on the salinity and chlorophyll data in this paper.

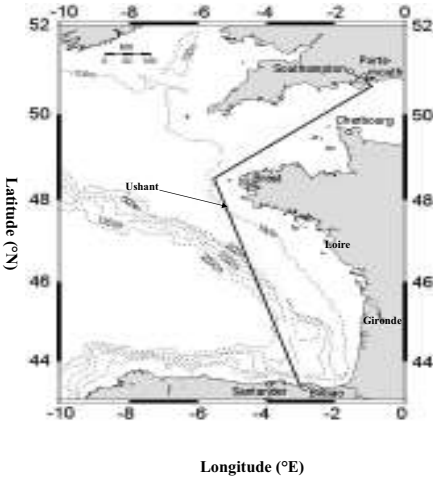

Figure 1 Map of ferry route and associated study area.

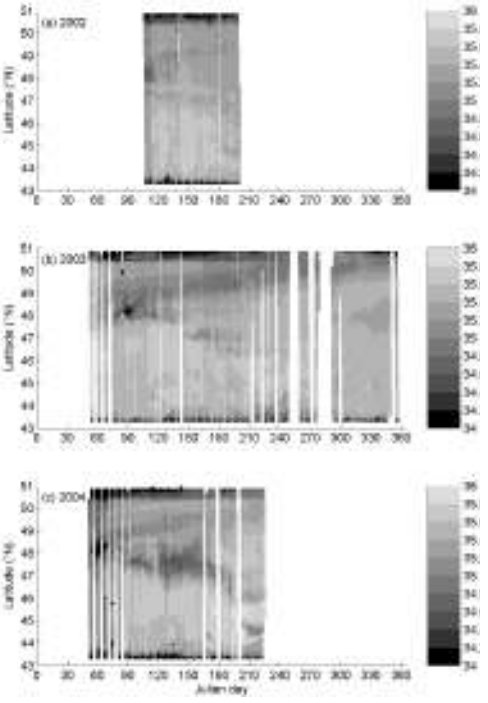

Figure 2 Salinity data along the route of the Pride of Bilbao (five-minute averaged data is posted) for a) 2002, b) 2003 and c) 2004.

3. Results

Sea surface salinities (5 minute averages) between Portsmouth and Bilbao are shown for the period 2002–2004 in Figure 2a–c. A salinity minimum was observed between March and mid-April in the vicinity of Ushant (48.5°N, 5.1°W) in all years (Figure 2a-c). The minimum salinity at this location in each year was 34.51 (19 April 2002), 33.90 (1 April 2003) and 33.68 (2 March 2004). This surface water feature moved northeastwards into the western English Channel in all years. Low salinity waters (< 35) entered the western English Channel in 2003, while higher salinity water (≥ 35) intruded in 2002 and 2004. The surface water mass moved furthest into the western English Channel in 2003 (Figure 2b). A persistent patch of low salinity water (< 34.6) between March (day 90) and June (day 180) was observed between 47°N and 48°N in 2004 (Figure 2c).

4. Discussion

4.1 Source and fate of the low salinity waters

Puillat *et al.* (2004) show that predominately southeasterly winds during winter enhance the poleward flow (due to the earth's rotation) of plumes from the Loire and Gironde, enabling waters with salinities < 34.5 to reach southern Brittany in some years. Mean river flows (data source: French National Database for Hydrometry and Hydrology-HYDRO) for the three months January to March (the period preceding the appearance of the low salinity waters near Ushant) were highest in 2004 (Loire = 2259 $m^3 s^{-1}$, Gironde = 1952 $m^3 s^{-1}$), next highest in 2003 (Loire = 1962 $m^3 s^{-1}$, Gironde = 1678 $m^3 s^{-1}$) and lowest in 2002 (Loire = 982 $m^3 s^{-1}$, Gironde = 597 $m^3 s^{-1}$). These interannual differences in river flows are consistent with the differences in the minimum recorded salinities near Ushant: 34.51 (2002), 33.90 (2003) and 33.68 (2004). Wind data (not shown, source: Météo-France) from the French Atlantic coast (station Chassiron, between the Loire and Gironde) show that the predominant winds were northeasterly in 2002 and 2004 and were a combination of northwesterly (counter to plume flow) and southeasterly (with plume flow) in 2003 in the time period between peak river flows and the arrival of low salinity waters near Ushant. The northwesterly winds were stronger (90% > 5.7 ms^{-1}) than the southeasterly winds (32% > 5.7 ms^{-1}) in 2003. These wind data help to explain the differences in the time taken for the peak river flow signal to reach Ushant (~80 days in 2003, ~40 days in 2002 and 2004).

The appearance of the low salinity water near Ushant in late winter in 2002 and 2004, coincided with the onset of predominantly northerly winds (station Ushant) for the next two months. Such winds force surface waters southwards across the shelf and cause upwelling along the French Atlantic coast to move the plume waters offshore. This helps to explain the position of low salinity waters on the shelf in 2004 (Figure 2c). The dispersion of the low salinity water (that is the lack of waters < 35 salinity) evident in 2002 is likely to result from the lower volume of plume waters combined with the tidally active region around Ushant. In contrast, the arrival of low salinity water near Ushant in 2003 coincided with predominately south westerly winds for the following month. These winds explain the intrusion of the low salinity water into the western English Channel in 2003 (Figure 2b). Hence, differences in both dominant winds and in river outflow between 2002 and 2004 appear to control the fate of the low salinity waters off Ushant.

4.2 Coincidence of low salinity waters and summer blooms

Time series of salinity and chlorophyll-fluorescence in the western English Channel (Figure 3) shows a coincidence in the timing of the arrival of the low salinity feature from Ushant and the timing of the peak chlorophyll-fluorescence in 2003. This peak in chlorophyll fluorescence was identified as a monospecific bloom of *K. mikimotoi* by microscopic identification of water samples taken on a manned crossing (section 2).

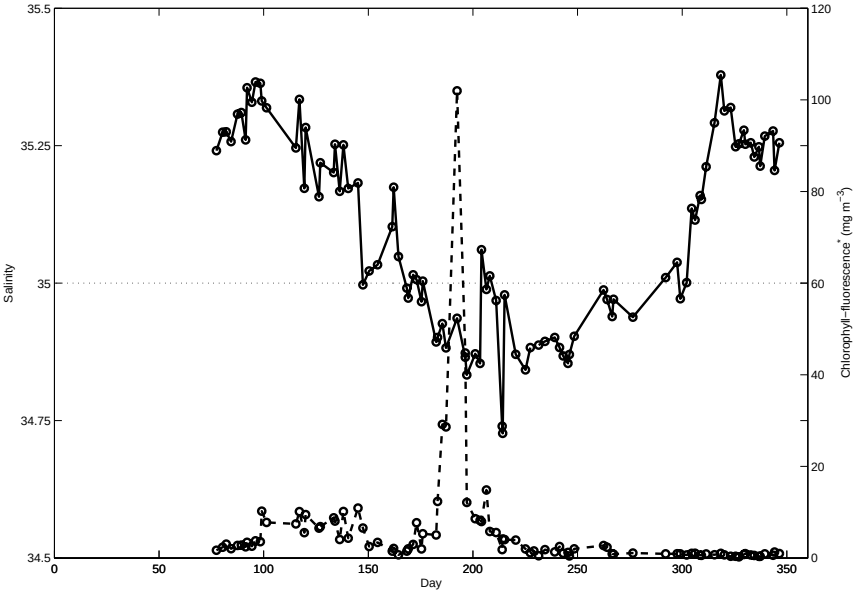

Figure 3 Time series of salinity and chlorophyll fluorescence in the western English Channel (49.8°N, 4°W) during 2003.

4.3 Possible mechanisms for enhancing summer blooms

The period during which the low salinity waters arrive near Ushant in 2003 is prior to the spring phytoplankton bloom. Data from the monthly manned calibration crossings (not shown) show that nutrient concentrations were at their maximum near Ushant (9 µM NO_3^-, 4.2 µM Si, 0.23 µM $PO_4^=$) in March 2003 while chlorophyll was still < 2 mg Chl m^{-3}. This agrees with the findings of Morin *et al.* (1991) who found that maximum nutrient concentrations occurred in March (1982) in the same region. It would therefore be expected that these low salinity waters would be a source of nutrients to the western English Channel.

It is reasonable to in part attribute differences in chlorophyll concentrations between years to the fact that surface water temperatures (not shown) were higher in the summer of 2003 (16.8°C, mean for bloom period 19 June–19 July) compared with 2002 (14.9°C) and 2004 (15.2°C). A link between well-established thermoclines and intense blooms of *K. mikimotoi* was suggested by Pingree *et al.* (1977). It is also reasonable to consider that the associated vertical density gradient will be enhanced by the presence of the low salinity intrusion and so promote the conditions favourable for an intense algal bloom as observed in 2003.

5. Conclusions

Low salinity water was observed originating close to Ushant between March and April in 2002, 2003 and 2004. These waters are linked to the river plumes of the Loire and Gironde which are known to make their way northward along the French Atlantic coast. Winter river outflows in 2003 and 2004 were higher than in 2002. Wind direction (south-westerly) was more favourable for transporting the river plumes into the western English Channel in 2003, whereas wind direction was predominately northerly, favouring the movement of plume waters across the shelf in 2004. The lower river flow in 2002 and the tidally active regime near Ushant act to disperse the low salinity water. It is hypothesised that the interannual variability in the intensity of the summer blooms of *Karenia mikimotoi* in the western English Channel is connected to the variability of the intrusion of low salinity water among years. It is suggested that the possible mechanisms by which blooms are enhanced are increased surface water buoyancy and nutrient delivery.

Acknowledgements

This work is part of the EU–FP5 project "FerryBox" (Contract no. EVK2–CT–2002–00144), and would not have been possible without the assistance of P&O Ferries Ltd.

References

Hydes, D.J., A. Yool, J.M. Campbell, N.A. Crisp, J. Dodgson, B. Dupee, M. Edwards, S.E. Hartman, B.A. Kelly-Gerreyn, A.M. Lavin, C.M. Gonzalez-Pola and P. Miller (2003). Use of a Ferry-Box system to look at shelf sea and ocean margin processes. Proceedings of the 3rd EuroGOOS Science Conference, Athens, December 2002, Elsevier, pp 297–303.

Morin, P., P. Le Corre, Y. Marty and S. L'Helguen (1991). Spring Evolution of Nutrients and Phytoplankton on the Armorican Shelf (North-West European Shelf). Oceanologica Acta 14, 263–279.

Pingree, R.D., P.M. Holligan and R.N. Head (1977). Survival of dinoflagellate blooms in the western English Channel. Nature 265, 266–269.

Puillat, I., P. Lazure, A.M. Jegou, L. Lampert and P. Miller (2004). Hydrographical variability on the French continental shelf in the Bay of Biscay, during the 1990s. Continental Shelf Research 24, 1143–1163.

Qurban, M.A., D.J. Hydes, B.A. Kelly-Gerreyn, P. Holligan and P. Miller (2005). Variations in phytoplankton speciation and growth due to hydrodynamic and chemical drivers between coastal and open ocean waters: use of data from a "FerryBox" ship of opportunity. This volume page 696.

Rennell, J. (1793). Observations on a current that often prevails to the westward of Scilly; endangering the safety of ships that approach the British Channel. Philosophical transactions of the Royal Society of London 83, 182–200.

Estimation of instantaneous stream-functions in the ocean from SST images

Jordi Isern-Fontanet*, Antonio Turiel, Emilio García-Ladona and Jordi Font

Institut de Ciències del Mar (CSIC), Barcelona, Spain

Abstract

This paper presents a new method for the estimation of surface currents from satellite images. This method is based on the multifractal singularity extraction technique, the Maximum Singular Stream-function Method (MSSM), which provides an approximation to the stream-function from experimental data in 2D turbulent systems. The essence of MSSM relies on statistical and geometrical properties associated with the energy cascade in flows; due to that association, the method provides an instantaneous velocity field and thus it does not require a sequence of images to evaluate velocities. The technique can be applied to images of different tracers; as an application, we show the results on AVHRR SST images.

Keywords: singularity analysis, surface velocities, sea surface temperature.

1. Introduction

A key problem in operational oceanography is to have a good estimation of the velocity field in real time. *In situ* data are often sparse and not synoptic which makes the use of oceanographic satellites almost essential. However, the estimation of surface velocities from satellite data is far from trivial. In principle, the simplest way is to apply the geostrophic approximation to altimetric measurements. Unfortunately, these measurements only allow estimation of one of the velocity components. To retrieve the complete 2D field some kind of interpolation is required (Le Traon *et al.*, 1998). An attractive alternative is to try to estimate surface velocities from Sea Surface Temperature (SST) images. In the past years some techniques, such as the maximum cross-correlation method (MCC) have been developed with these objectives (e.g. Bowen *et al.* 2002). However, this method has three main drawbacks, the final resolution of the velocity field is lower than the original, it needs a sequence of images and also very fine tuning. An alternative method that can potentially overcome these problems is the Maximum Singularity Stream-function Method (MSSM) that has been successfully applied to low (9 km) and medium (4 km) spatial resolution SST images (Turiel *et al.*, 2005; Isern-Fontanet *et al.*, 2005). In this paper we show the results of the method when applied to high resolution (1 km) SST images.

2. The Maximum Singularity Stream-function Method

This method can be decomposed into three steps (Turiel *et al.*, 2005):

Step 1 Singularity analysis: Let $s(\boldsymbol{x})$ be a multifractal signal in a planar flow (AVHRR SST in our case). It will be assumed that $s(\boldsymbol{x})$ is mainly advected by the flow, but not

* Corresponding author, email: jisern@icm.csic.es

necessarily conserved (even more, diffusive and/or reactive effects may be important). What is characteristic to multifractal signals is local power-law scaling. Such scaling is assessed using wavelet projections of $|\nabla s(\boldsymbol{x})|$ over an appropriate wavelet function Ψ, at each location $\boldsymbol{x}$ and variable scales r (denoted by $T_\Psi s(\boldsymbol{x},r)$). Then, the signal s will be multifractal if and only if

$$T_\Psi s(\boldsymbol{x}, r) \sim r^{h(\boldsymbol{x})}$$

Then, at each point $\boldsymbol{x}$ a singularity exponent $h(\boldsymbol{x})$ is assigned.

Step 2 Main streamlines identification: Once every point $\boldsymbol{x}$ is assigned a singularity exponent $h(\boldsymbol{x})$, it is possible to decompose the signal into different patterns (the fractal components). Then, we assume that the Most Singular Manifold (MSM), given by

$$F_\infty \equiv \{ h(\boldsymbol{x}) | h(\boldsymbol{x}) < h_0 \}$$

where h_0 is a given threshold value (h_0=0), represents streamlines. Thus we impose that velocities over this set (v_∞) have to be parallel to the MSM. As a first guess we take the modulus equal to 1 and the same sign as $\nabla s(\boldsymbol{x})$.

Step 3 Stream-function reconstruction: The Most Singular Stream-function φ_M is reconstructed using only the velocities over the MSM (v'_∞) through the convolution

$$\varphi_M = \boldsymbol{g} * (\boldsymbol{e}_z \times v'_\infty), \; T_F(\boldsymbol{g}) = \frac{i\boldsymbol{k}}{k^2}$$

where $T_F(\boldsymbol{g})$ is the Fourier expression of the vectorial kernel $\boldsymbol{g}$. This algorithm has been experimentally validated in different instances as image-processing (Turiel *et al.*, 2002) and analysis of meteorological images (Grazzini *et al.*, 2002), exhibiting a high performance.

3. Results and discussion

Figure 1 shows the original AVHRR SST image captured directly from the NOAA satellites, the MSM and the resulting stream-function (the MSS) for two images of an Algerian eddy. First it is important to notice that although Figure 1 shows a sequence, the MSS is computed from a single image. On the other hand, it is also important to realise that the final resolution is the same as the original image and in principle only one parameter has to be selected (h_0). As it is evident from Figure 1, the MSM outlines some of the streamlines of the flow. However, due to sensor limitations and numerical errors these streamlines may brake into pieces (Turiel *et al.*, 2005). Another aspect of the MSM is that they are relatively thick lines. In theory, the MSM should have been obtained as the set with a singularity exponent equal to the most singular exponent instead of applying a threshold value to get it but inhomogeneities of the flow necessitate the definition used here.

The stream-function has been constructed using only the information contained on the MSM and using the non-dimensional velocity defined previously (v'_∞). Previous studies (Turiel *et al.*, 2005; Isern-Fontanet *et al.*, 2005) have demonstrated that when compared with altimetry the MSM provides a better estimation of the stream-function than the SST. Unfortunately, since it is a geometrical method it is only able to identify some streamlines but not the sense and intensity of the velocities over these stream-lines. This

produces an indetermination in the stream-function that has to be solved using independent data such as altimetric measurements (Isern-Fontanet *et al.*, 2005).

Although there are some limitations with the problem of the estimation of velocity modulus and sense, this method has proven to be very robust and with an enormous potential for operational oceanography. In previous studies it has been shown that for global-scale velocity fields, using altimetry is a good choice for solving the indetermination of the method. On the other hand, for coastal and regional observing systems two strategies are possible. First, since the region is constrained, empirical models could be developed for the estimation of the velocity. Second, it could be combined with *in situ* measurements such as moored current meters.

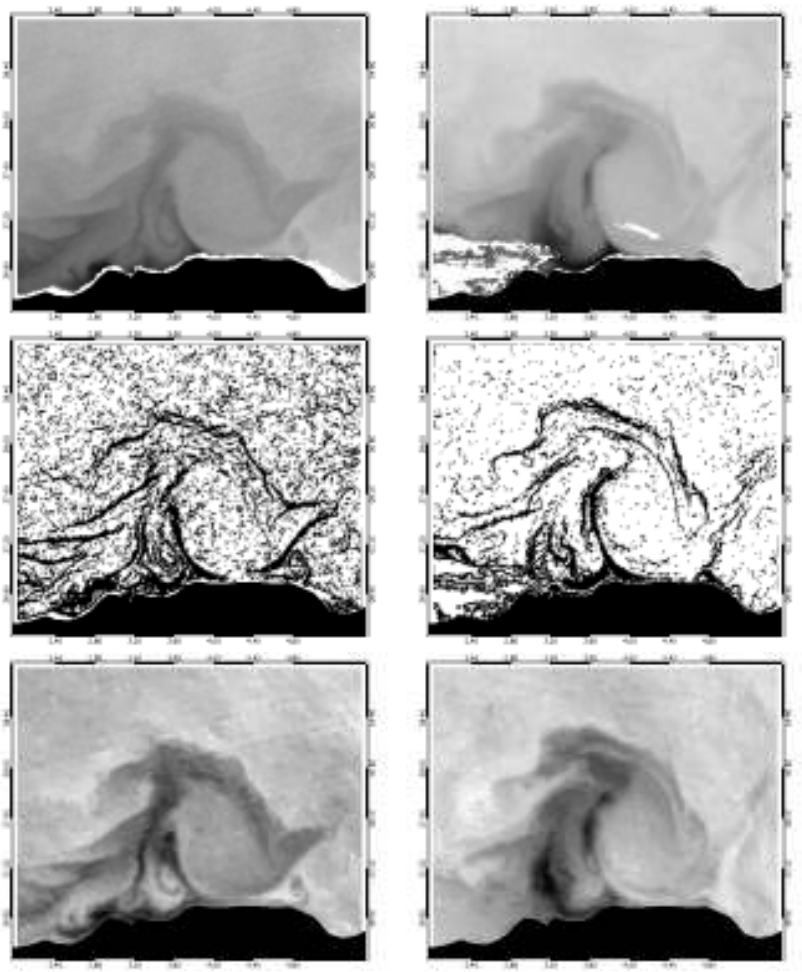

Figure 1 From top to bottom: SST image of an Algerian eddy (western Mediterranean sea), spatial distribution of the Most Singular Manifold (F_∞, MSM) and the Maximum Singular Stream-function (φ_M, MSS). These images correspond to 4 August 2003 (left, NOAA-16 satellite) and 7 August 2003 (right, NOAA-15 satellite).

Acknowledgements

This work is a contribution to the EU MERSEA project (AIP3−CT−2003−502885) and has also been partially supported by the MCyT project ESEOO (VEM2003−20577). A. Turiel is funded by a Ramon y Cajal fellowship from the Spanish Ministry of Education. The AVHRR SST images have been downloaded from http://ers.cmima.csic.es/saidin/ using the SAIDIN utility built with funding from the EU MAMA project (EVR1−CT−2001−20010).

References

Grazzini, J., A. Turiel and H. Yahia (2002). Entropy estimation and multiscale processing in meteorological satellite images, in Proc. of ICPR 2002, vol. 3, pp. 764−768.

Isern-Fontanet, J., A. Turiel, E. García-Ladona and F. Font (2005). Estimation of surface currents from moderate resolution Sea Surface Temperature images: The Maximum Singularity J. Atmos. Oceanic Technol., to be submitted.

Le Traon, P., F. Nadal and N. Ducet (1998). An improved mapping method of multisatellite altimeter data. J. Atmos. Oceanic Technol., 15:522−534.

Turiel, A. and A. del Pozo (2002). Reconstructing images from their most singular fractal manifold, IEEE Trans. on Im. Proc., 11, 345−350.

Turiel, A., J. Isern-Fontanet, E. García-Ladona and J. Font (2005). A multifractal method for the instantaneous evaluation of the stream-function in geophysical flows, accepted in Phys. Rev. Lett.

A new method to reduce noise on satellite sea surface temperature observations

Jacob Lorentsen Høyer* and Jun She

Danish Meteorological Institute, Denmark

Abstract

Statistical comparisons between coinciding satellite and *in situ* sea surface temperature (SST) observations show that satellite errors tend to be more spatially correlated than temporally. These findings have been used to perform tests where *in situ* observations of high quality (e.g. buoys) are utilised to perform a real time correction of the satellite observations over a large area. The method has been tested in the North Sea and the Danish Straits, where the improvements in the satellite errors can be up to 0.2 °C, based on one buoy. These findings open up the use of accurate real time buoy observations to reduce errors on operational satellite SST products.

Keywords: Satellite SST observations, error reduction, operational products, North Sea.

1. Introduction

Observations of sea surface temperature (SST) from passive infrared satellite observations have become one of the most widely used satellite products for oceanic and meteorological applications. The errors of the SST products are typically in the range of 0.5 °C in open ocean and about 0.7 °C for coastal applications. The two major error contributions — when the satellite observations are compared to *in situ* observations at a few metres depth — arise from the atmospheric correction and from the difference between the skin temperature at the very top of the surface (~10 μm) layer and at 1–2 metres depth. In the recent years, several methods have been presented to reduce the errors in the satellite observations and thus to make the satellite observations more representative of the *in situ* observations (e.g. Horrocks *et al.*, 2003; Castro *et al.*, 2003). In general the methods use auxiliary data such as wind and heat flux to correct the vertical temperature variations in the upper 1–2 metres. However, as the processes in the upper ocean are very complicated, the existing methods have not been able to fully account for the vertical temperature differences (Castro *et al.*, 2003).

This study proposes a new method of correcting the satellite SST observations. The method is based upon the findings that the differences between satellite an *in situ* observations are correlated in space over several hundred kilometres. By using a few accurate real time buoy observations, we are thus able to correct real time satellite observations over a much larger area. The method has been applied to the North Sea and the Danish Straits for the year 2001 because a large *in situ* dataset was available for validation through the ODON project.

* Corresponding author, email: jlh@dmi.dk

2. *In situ* and satellite observations

A large amount of *in situ* observations (~200 000) from the year 2001 have been gathered from the North Sea/Baltic Sea within the ODON project. The observation database comprises observations from fixed platforms, ships of opportunity, FerryBox and from scientific cruises.

Two different satellite products are used for this study. The first product is the Ocean and Sea Ice SAF (O&SI-SAF) product, MNOR, which has a resolution of 2 km in the North Sea/Baltic Sea region and provides data from the NOAA 16 and 17 (Brisson, 2001). The other satellite product is produced by BSH in Hamburg and provides data from the NOAA 12 satellite with resolutions of about 1.5 km (Loewe, 1996). Only night-time data are used in this study. See Høyer and She (2004, 2005) for details on the quality control and data processing of the observations.

3. Error correlations

Spatial and temporal correlations have been calculated from both *in situ* and satellite observations. The data set has been averaged into 10×10 km grids and one average per day prior to the calculation. The correlations have only been calculated from grid points where both *in situ* and satellite observations are available to make the results intercomparable and to exclude differences in the results due to sampling issues. The average spatial and temporal correlations are shown in Figure 1.

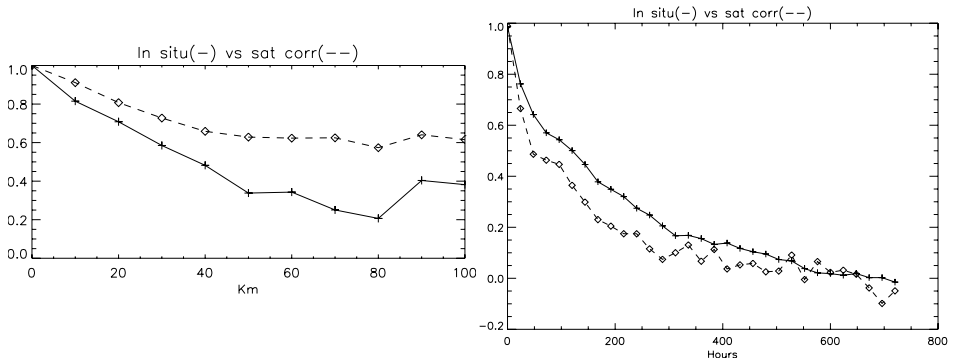

Figure 1 Spatial (left) and temporal (right) correlations calculated from satellite and *in situ* observations. All results are calculated from grid points where both satellite and *in situ* observations are available.

The higher spatial correlations of the satellite observations compared to the *in situ* observations indicate that the spatial noise on the satellite observations has a much larger scale than on the *in situ* observations. Conversely, the differences between the temporal satellite and *in situ* correlations indicate that the noise on the satellite observations — which is higher than on the *in situ* observations — is not very well correlated from one day to the next. These findings are essential for the construction of a method that uses real time *in situ* observations to reduce the differences between the satellite and the *in situ* observations. Note that several processes, such as atmospheric effects, cool skin

layer and diurnal thermoclines can account for these differences and that we only focus on the combined effect.

4. Correction method

Assuming that the real time buoy observations of SST are well calibrated, we use the difference between satellite SST and buoy SST in a local region to correct a much larger field. In this way we are able to correct for some of the spatially correlated errors on the satellite SSTs. The correction is performed as:

$$\tilde{T}_{\text{sat}}(x, y, t) = T_{\text{sat}}(x, y, t) - \Delta T(x_0, y_0, t)$$

$$\Delta T(x_0, y_0, t) = T_{\text{sat}}(x_0, y_0, t) - T_{\text{bouy}}(x_0, y_0, t)$$

where the tilde represents the corrected observations and the correction term is calculated using coinciding satellite and buoy observations at x_0 and y_0.

5. Results

The performance of the method to reduce noise on satellite observations was tested using data from the three buoys shown in Figure 2. *In situ* observations, not used for the corrections, were used to validate the satellite SST observations before and after the correction was applied. The RMS results are shown in Figure 3 for each buoy as a function of the radius of the correction area. All three figures show that there is a significant potential for reducing the errors on the satellite observations. The satellite RMS errors are consistently reduced for all the areas. The largest effect in reducing the RMS errors is seen when the EMS is being used for the correction, where the errors are reduced by up to 0.2 °C close to the buoy.

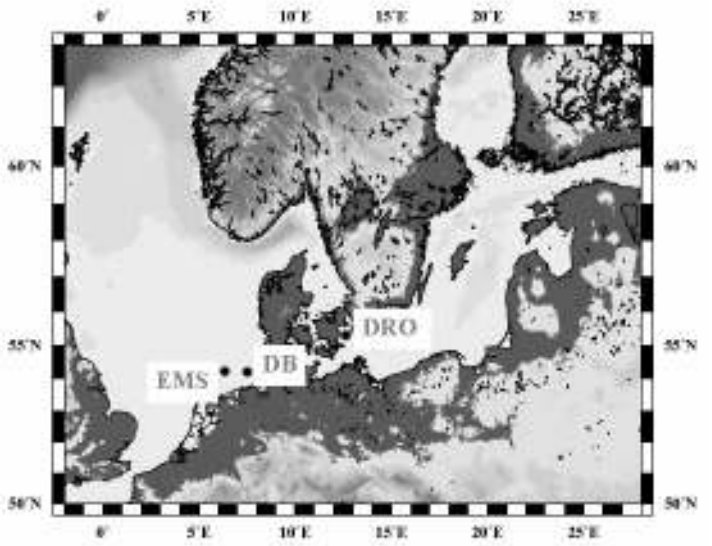

Figure 2 Positions of buoys used to test the correction method: Drogden (DRO), Deutsche Bucht (DB) and the EMS buoy.

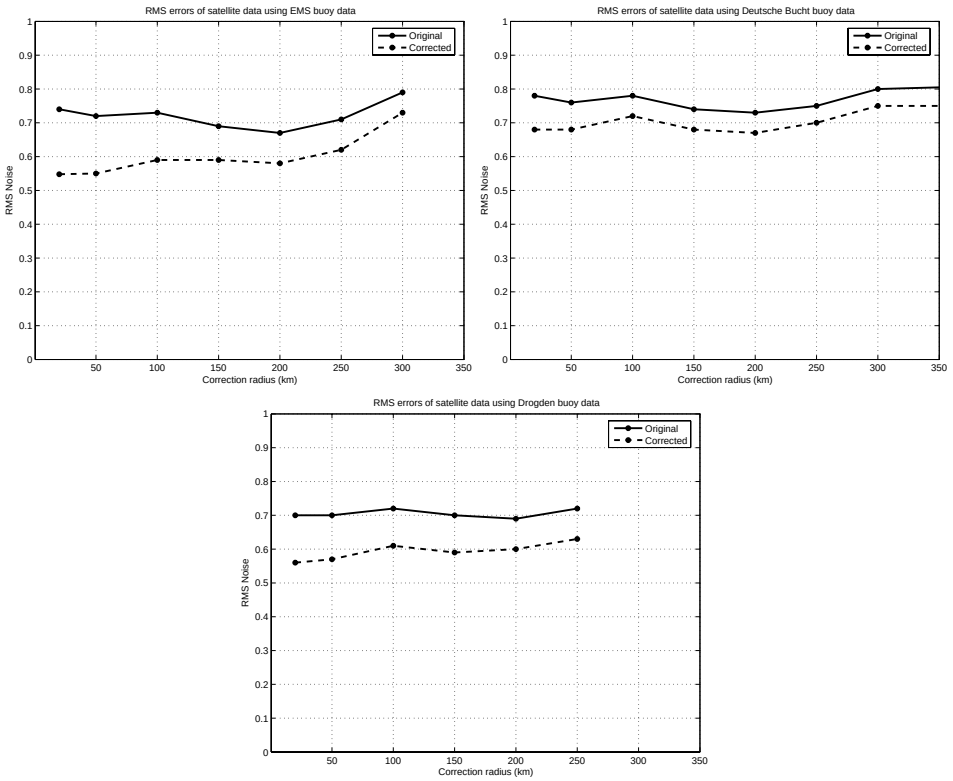

Figure 3 RMS errors of the satellite observations during the year 2001, as a function of distance from the buoy. The continuous line indicates the original satellite error and the dashed line shows the RMS errors of the corrected fields.

6. Conclusions

Comparisons of empirical correlations from satellite and *in situ* observations showed large spatial correlations of the noise on the satellite observations. This implies that satellite data over a large area can be corrected using a limited number of accurate *in situ* observations. Observations from 3 buoys in the North Sea and in the Danish Straits have been used to test the improvements of the method. The method reduced satellite RMS errors by up to 0.2°C over regions of several hundred kilometres, demonstrating the large potential for operational applications.

Ongoing and future work includes the application of this method to satellite observations all over the North Sea and to incorporate the spatial scale of the errors, to estimate corrections based upon a combination of several buoys.

Acknowledgements

This work is supported by the European Commission under the Fifth Framework Programme via the ODON project (Optimal Design of Observational Networks), Contract No. EVK3−2002−00082.

References

Brisson, A., P. Le Borgne and A. Marsouin (2001). Ocean & Sea Ice SAF, North Atlantic Regional Sea Surface Temperature, O&SI SAF Product Manual version 1.1. Météo-France/DP/CMS, France.

Castro, S.L., G.A. Wick and W.J. Emery (2003). Further refinements to models for the skin-bulk sea surface temperature difference, J. Geophys. Res., Vol. 108, C12, doi:10.1029/2002JC001641.

Horrocks, L.A., B. Candy, T.J. Nightingale, R.W. Saunders, A. O'Carroll and A.R. Harris (2003). Parametrisations of the ocean skin effect and implications for satellite-based measurements of sea surface temperature, J. Geophys. Res., Vol. 108, C3, doi:10.1029/2002JC001503.

Høyer, J.L. and J. She (2004). Validation of satellite SST products for the North Sea-Baltic Sea region. Technical Report 04−11, Danish Meteorological Institute.

Høyer, J.L. and J. She (2005). Optimal interpolation of sea surface temperature for the North Sea and Baltic Sea, J. Mar. Sys. in press, 2005.

Loewe, P. (1996). Surface temperatures of the North Sea in 1996, Dt. Hydrogr. Z., 48, 175−184.

EU Models 1

Mercator Ocean Monitoring and Forecasting System, a contribution to GMES

P. Bahurel*[1], E. Dombrowsky[2] and the Mercator project team

[1]*Mercator Ocean, Ramonville Saint-Agne, France*
[2]*CLS, Ramonville Saint Agne, France*

Abstract

The **Mercator** Ocean Monitoring and Forecasting System is routinely operated in near-real-time in Toulouse by the **Mercator** team since early 2001, and has been regularly upgraded, expanding the geographical coverage, improving models and assimilation schemes, adding new data and building new products. As part of GMES EC (MERSEA Strand 1, MERSEA IP) and ESA (ROSES) projects, **Mercator Ocean** has been regularly delivering operational estimates of the ocean circulation and thermodynamics at high resolution at regional and global scales, and progressively structuring the core of a GMES Ocean Service. This ocean monitoring and forecasting service is implemented using high resolution ocean general circulation models (OGCM), real-time processing of remotely sensed and *in situ* observations, and data assimilation techniques.

Different systems are running at global and regional (North Atlantic, Tropical Atlantic and Mediterranean Sea) scales, with different resolutions (global: 2° to ¼°; regional: 1/3° to 1/16°). **Mercator Ocean** forecasters provide weekly ocean bulletins, composed of a full 3D real-time depiction of the ocean physics, a 2-week forecast, and a set of validation results. Synthesis bulletins are also computed to describe feedbacks on extreme events or demonstration exercises. In the MERSEA project, **Mercator Ocean** is committed to developing the European high resolution (1/12°) Global Ocean physics prediction system, that will be run by the end of 2008 through the GMES operation phase. Products and services provided by **Mercator** are distributed to the scientific community, to public bodies such as met services and agencies dealing with the ocean and its environment, and also to private bodies that are directly linked with the customers operating in the marine environment. The ROSES GSE project demonstrated the role of this new kind of ocean information service in enhancing the quality of monitoring and forecasting in oil spill and harmful algal bloom (HAB) services.

Keywords: operational oceanography, ocean forecasting, GMES, Mersea, Mercator

1. Introduction

The **Mercator** project is the French initiative for operational ocean monitoring and forecasting.

The project was launched in 1995 by the six major French agencies involved in oceanography — Centre National d'Etudes Spatiales (CNES), Centre National de Recherche Scientifique (CNRS), Institut Français de Recherche pour l'Exploitation de la Mer (IFREMER), Institut de Recherche pour le Développement (IRD), Météo-France,

* Corresponding author, email: Pierre.Bahurel@mercator-ocean.fr www.mercator.eu.org

and Service Hydrographique et Océanographique de la Marine (SHOM), with involvement of their subsidiaries CLS and CERFACS.

The project is led by the **Mercator Ocean** public company, created in 2002 by these six Patron agencies for the purpose of establishing a joint operational capacity for global high resolution ocean monitoring and forecasting.

2. Mercator Ocean, quick overview

2.1 The Mercator Ocean ocean monitoring and forecasting system

The **Mercator** system provides a full 3D depiction of the ocean dynamics and thermo-haline circulation (T, S, currents, mixed layer depth, etc.), with priority given to high resolution (eddy resolving) scales. Near real time information is available on a routine basis, by providing weekly near-real-time analyses and 2-week forecasts, as well as multi-annual reanalyses with data assimilation.

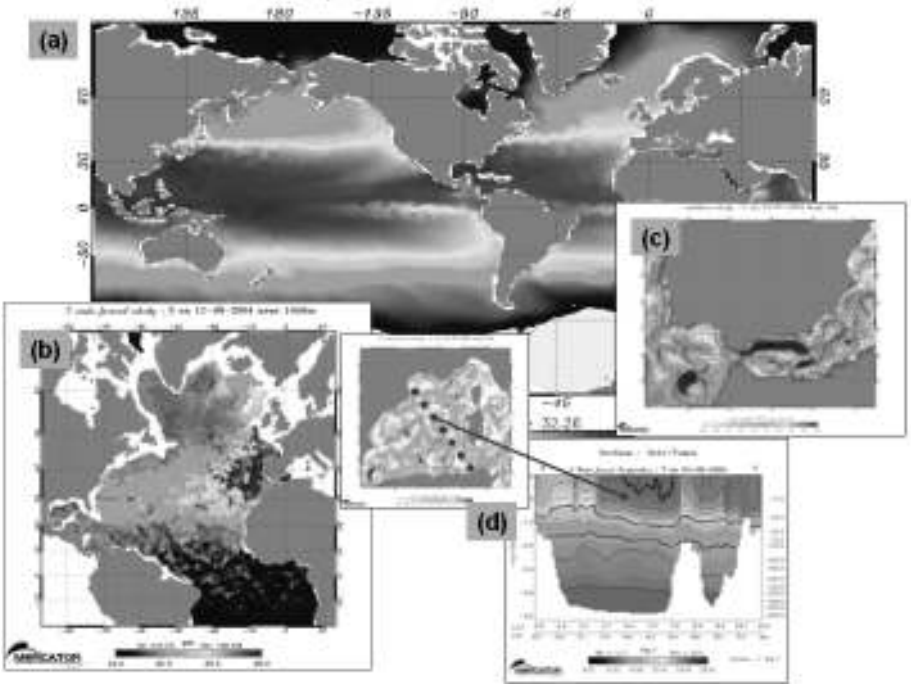

Figure 1 Examples of **Mercator Ocean** system outputs. (a) Global Ocean (2° model) sea surface temperature field, real-time analysis 28 July 2004 computed 28 July 2004; (b) North & Tropical Atlantic (1/3° model) 1000 m depth salinity, 2-week forecast 11 August 2004 computed 28 July 2004; (c) Gibraltar straight (5−7 km model, ~1/16°) surface currents; real-time analysis 21 July 2004 computed 21 July 2004; (d) Mediterranean sea (5−7 km model, 1/16°) Temperature vertical section between Sète and Tunis (and surface current map); 2-week forecast 4 August 2004 computed 21 July 2004.

Components

- **Model**: based on the OPA/NEMO z-coordinate primitive equation ocean code (Madec *et al.*, 1998). Four configurations are available and assessed: Global 2°, Global ¼°; North Atlantic 1/3°; coupled North Atlantic 1/15° and Med Sea 1/16°.
- **Assimilation**: based on the **Mercator** Assimilation Suite (SAM), where different implementations are possible. The implementation SAM1 is based on the multivariate optimal interpolation SOFA scheme developed by LEGOS (De Mey and Benkiran, 2001); SAM2 is based on the Singular Extended Evolutive Kalman (SEEK) filtering analysis method, developed in LEGI (Pham *et al.*, 1998; Testut *et al.*, 2003); and SAM3 which is based on variational methods. SAM1 is fully operational, SAM2 is used today for off-line studies and SAM3 is under development.
- **Input data**: **Mercator** relies on existing data assembly centres to collect, process and validate its input real time and delayed mode data. Input data include altimeter topography (from the SSALTO/DUACS centre), *in situ* temperature, salinity and currents observation (from the CORIOLIS centre), sea surface temperature (Global Reynolds SST products; Eumetsat SAF Ocean & Ice) and forcing fields (ECMWF).
- **Internal metrics**: **Mercator** has routinely provided its "technical bulletin" on the internet coupled to each weekly ocean bulletin since January 2001, providing internal diagnostics of assimilation. The system was upgraded in the framework of GODAE and the MERSEA Strand 1 GMES/EC project by the implementation of the standard metrics adopted by all MERSEA centres on North Atlantic and Med Sea.

A quarterly newsletter is edited and gives up-to-date **Mercator** system validation results and system descriptions.

2.2 A project, transitioned to an operational centre

By the end of 2005, **Mercator Ocean** will have fulfilled the initial project objectives defined in 1995, and gone far beyond:

- (*a trained team*) In the **Mercator Ocean** assimilation centre (near Toulouse, France), Research & Development (Modelisation, Assimilation, Data Handling), Development & Integration, Scientific Validation, Operation & Services (system operation, ocean bulletin production and dissemination) activities are conducted by a core team of around 40 people, composed of researchers, engineers, technical and administrative staff. By now, the team has been providing around 250 weekly ocean bulletins without any service interruption to a wide range of users.
- (*an advanced forecasting system*) A suite of ocean forecasting prototypes of growing complexity have been progressively implemented through 2001–2005, with three major releases and a continuous assessment activity. Three systems are currently running, delivering weekly ocean nowcasts on North and Tropical Atlantic, Med Sea, and Global Ocean. This enables a full capacity to hindcast (10–15 years behind), nowcast (real-time) and forecast (14 days) the four-dimensional physical state of the ocean at global, basin and regional scales.
- (*a close link with users*) Ocean products are disseminated to more than 150 referenced and regular users; they cover a wide spectrum of application areas, from research to operational, public to private market, marine to environment applications.

Close collaboration with the scientific community is in place with a Science Working Team gathering around 100 researchers.

- (*international and European partnerships*) **Mercator Ocean** is a core partner of major and leading initiatives in operational oceanography (see below).

Mercator Ocean patron agencies are now moving firmly to an operational centre, a core contribution to the GMES Ocean.

3. Mercator Ocean, a European mission

3.1 Partnerships for GMES

Mercator is the French contribution to the Global Ocean Data Assimilation Experiment (GODAE) — the international experiment for operational oceanography (see www.bom.gov.au/bmrc/ocean/GODAE), and has developed privileged collaborations with American, Japanese and Australian teams involved in ocean forecasting projects. **Mercator** is a member of the science working teams for space missions (e.g. OST for Jason altimetry) and involved as an active user in observation projects such as Argo (*in situ*) or GHRSST (surface temperature). Various bilateral partnerships to enhance operational oceanography developments at international and European level (e.g. MOON in the Mediterranean Sea, NEMO for the ocean code) are in place.

Mercator Ocean is member of EuroGOOS, the European component of the Global Ocean Observation System (GOOS) (see www.eurogoos.org).

Mercator Ocean is one of the core partners of the Marine component of the European GMES programme and is:

- an active partner of European Commission projects such as MERSEA Strand 1 (FP5) and MERSEA Integrated Project (FP6), to develop an integrated European capacity for ocean monitoring and forecasting, jointly with first ranking ocean forecasting centres in Europe (e.g. Exeter, Bergen, Bologna or Copenhagen).
- an active partner of European Space Agency projects, such as ROSES (and its full-scale extension MARCOAST, under discussion) for the consolidation of the link between core and downstream application services, or definition of the Sentinel-3 Ocean mission.
- involved in various initiatives to define and develop the GMES Ocean component.

The **Mercator Ocean** European Mission for the GMES implementation phase has been defined through these different initiatives, as a two-fold mission:

- (system operator) develop and operate the European High Resolution Global Ocean forecasting system
- (service provider) provide the reference “core” ocean information to the different downstream services serving the end-users.

3.2 Mercator Ocean, a “system operator” for Global Ocean

Mercator Ocean is presently running a 2° resolution global ocean system (low resolution for seasonal forecasting), and a 5–7 km North Atlantic and Mediterranean Sea

basin-scales system (mesoscale application). It is committed to developing the European High Resolution Global Ocean component.

Plan

As part of its European mission, **Mercator Ocean** will develop a full eddy-resolving capacity on Global Ocean physics, and ensure full integration with European seas systems and applications. The plan is to

- renew its forecasting chain to ensure full integration with regional and application systems
- start running a fast-track demonstrator with a ¼° global ocean capacity (step 1), with a refined grid at 1/12° on the North Atlantic and Mediterranean Sea (step 2) reaching full integration with other European systems and applications
- develop and run the 1/12° global ocean system (step 3).

A fast-track demonstrator

Version 1 of the fast-track demonstrator will be operated and fully assessed during the MERSEA Target Operational Period (October 2005−March 2006). Version 1 will combine a ¼° global ocean capacity (with the **Mercator** NEMO global configuration, and a univariate version of the SAM1 assimilation tool), and a 1/12° to 1/16° capacity of North Atlantic and Mediterranean Sea (with the **Mercator** NEMO mesoscale configuration, and the multivariate version of SAM1 to assimilate altimetry, SST and *in situ* profiles).

The system will be operated weekly on a pre-operational basis, to provide real-time nowcasts and 14-day forecasts. A first release is foreseen in 2006, to integrate the Mersea experiment feedbacks and improvements in modelling and assimilation.

The 1/12° global ocean system

The target system is currently under development, based on the **Mercator** technical and scientific background demonstrated in the various systems already running.

3.3 Mercator Ocean, a "service provider" for GMES Ocean

Developing this new generation of ocean service, able to provide a fruitful operational, 4D space and time consistent and accurate "general ocean information" to specialised ocean services, is the key objective of **Mercator** operational oceanography. It refers to a "core service", i.e. committed to building a consistent and generic 1D to 4D depiction of the ocean state for the direct use and benefit of the specialised downstream services.

Mercator Ocean has defined four service lines to fulfil this European Mission for the application sector.

Service Line 1: "ocean tools development and maintenance"

Mercator Ocean develops, maintains and provides ocean data handling and modelling/ assimilation tools to expert users.

It is one reference centre for the maintenance of the European OPA/NEMO ocean code. It will enhance its current capacity to develop and maintain ocean model configurations (e.g. the ORCA ¼° global ocean), assimilation tools with the **Mercator** Assimilation

Suite (SAM) with optimal interpolation, SEEK and variational versions, and model and observation data handling tools.

Service Line 2: "ocean data production"

Mercator Ocean provides and disseminates a 4D state of the global ocean physics in real time and reanalysis mode.

This service includes the elaboration of 3D model data (hindcast/nowcast/forecast) provided on a regular basis; the data provision consistent with format standards defined at international level (e.g. COARDS/CF) and tested under GODAE and Mersea experiments; with access through automated standard tools: ftp, opendap e-technologies (Mersea experience). **Mercator** will enhance this capacity by progressively (from regional to global) adding the prediction of ecosystem variables.

Service Line 3: "validation & assessment"

Mercator Ocean provides fully assessed information from the **Mercator Ocean** forecasting system, with full transparency towards users.

This service includes a real-time ocean validation bulletin, a delayed mode assessment study, references for an international "metrics" definition, shared by the GODAE community to assess systems, skill scores (model against data, analysis against forecast), and user case studies.

Service Line 4: "ocean information expertise"

Mercator Ocean provides a human expertise for model data production.

This service includes ocean bulletins (ocean forecasters) for real-time production, specific case studies reviewed on a hindcast mode, and indicator production with simplified and quick-look products for a specific application area.

4. Conclusion

The **Mercator Ocean** forecaster team has progressively developed an Ocean Service serving today more than 150 referenced users, from different application sectors (institutional to private sectors, operational to research, ocean maps to assessment), bringing ocean expertise and assimilation capacity.

Transition to an operational centre, built to play an active role in the GMES Ocean, is clearly committed and on its way.

Operational oceanography in Europe is at a turning point. An integrated and multi-scale ocean monitoring and forecasting capacity is challenging but doable. Long-term sustainability of the space and *in situ* observation effort and our joint modelling/assimilation core capacity is critically required.

Mercator Ocean, as a partner of the GMES Ocean group being built for example in Mersea, is ready and willing to fulfil its European mission for global ocean and contribute to GMES.

Acknowledgements

Mercator Patrons agencies: CNES, CNRS, Ifremer, IRD, Météo-France and SHOM.

GMES: EC/FP5 MERSEA Strand 1, EC/FP6 MERSEA IP, ESA/GSE ROSES.

References

De Mey, P., and M. Benkiran (2001). A multivariate reduced-order optimal interpolation method and its application to the Mediterranean basin-scale circulation. In: Ocean Forecasting: Conceptual basis and applications, N. Pinardi (Ed.), Springer-Verlag heidelberg, 472 pp.

Madec, G., P. Delecluse *et al.* (1998). OPA8.1 Ocean general circulation model reference manual. Paris, France, IPSL: 97.

Pham, D., J. Verron and M. Roubaud (1998). A Singular Evolutive Extended Kalman filter for data assimilation in oceanography. J. Mar. Syst., 16(3–4), 323–340.

Testut, C.E., P. Brasseur, H.M. Brankart and J. Verron (2003). Assimilation of sea surface temperature and altimetric observations during 1992–1993 into an eddy-permitting primitive equation model of the North Atlantic Ocean, J. Mar. Syst., 40–41 (April 2003), pp 291–316.

The TOPAZ monitoring and prediction system for the Atlantic

Laurent Bertino*, Knut-Arild Lisæter, François Counillon, Intissar Keghouche, Nina Winther and Soazig Parouty

Mohn-Sverdrup Center/Nansen Environmental and Remote Sensing Center, Norway

1. Introduction

The need for high quality predictions of marine parameters has been well identified. For example, during recent years, offshore oil-exploration activities have expanded off the continental shelves to deeper waters. Drilling and production of oil and gas at depths of 2000 metres or more are ongoing at several locations, and the Arctic Shelf contains considerable resources in ice-covered areas. This has introduced a need for real time forecasts of oceanic currents and sea-ice which in some cases may have severe impact on the safety related to drilling, production and critical operations. Sustainable exploitation of marine resources are becoming increasingly important, e.g. commercial fisheries and fish farming. In future fisheries management systems, information about marine parameters such as nutrient and plankton concentrations, and pollutants, will be increasingly important for accurate monitoring and prediction of fish stocks. Thus, there are needs for operational monitoring and prediction of both physical and biological marine parameters.

An operational ocean forecasting system will have to rely on integrated use of observations of physical, biological, and chemical variables and coupled physical and marine ecosystem models. This integration can best be done using data assimilation techniques. Thus, one will have to further develop and implement consistent data assimilation techniques for primitive equation models and also new suitable methods for assimilation of data into the models of the marine ecosystem that respect their non-Gaussian probability distribution. Further, the real time processing and flow of observational data must be developed and maintained.

The TOPAZ system is being developed to meet the needs from future users of marine parameters. It involves both the implementation and validation of state-of-the-art ocean circulation models and marine ecosystem models, and the development of novel data assimilation methodologies. System development has been supported by two previous European Commission funded projects — the DIADEM and TOPAZ projects — and current work is aimed at integration into the European MERSEA system within the MERSEA Integrated Project. By combining the expertise of major European groups, the challenges of operational oceanography (e.g. fitness for purpose, accuracy and data distribution) are more likely to be met in the near future.

* Corresponding author, email: laurent.bertino@nersc.no, http://topaz.nersc.no

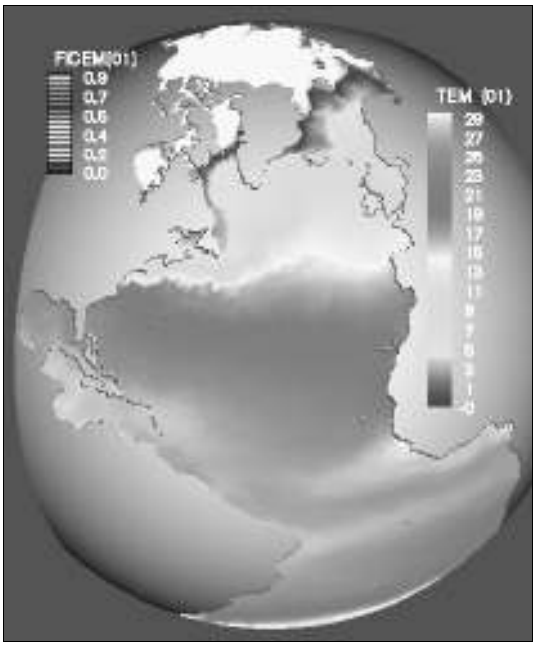

Figure 1 Model domain used for the TOPAZ prediction system. The plot shows a nowcast of sea surface temperature and ice concentration on 7 June 2005.

In contrast to other state-of-the-art forecasting systems, such as FOAM (www.ncof.gov.uk), Mercator (www.mercator.com.fr) and MFSTEP (www.bo.ingv.it/mfstep), the TOPAZ team has chosen to use an advanced data assimilation technique (the Ensemble Kalman Filter) and an ocean model based on hybrid vertical coordinate (HYCOM, Bleck, 2002). The other European systems use isopotential coordinate models and non-evolutive data assimilation methods, which on the other hand affords them higher horizontal resolution.

The model domain used for the TOPAZ prediction system is shown in Figure 1. The grid is created using a conformal mapping of the poles to two new locations using the algorithm outlined in Bentsen *et al.* (1999). The figure shows sea surface temperature and ice concentration. The resolution of the model varies from 20 km in the Arctic Ocean to 40 km near the Equator. To meet the end user needs it is necessary to introduce nested regional models with very high resolution in the target areas where mesoscale processes must be properly resolved. The nested models depend on the basin-scale model but not the inverse so that each nested system can be purposely tuned to satisfy one application without disturbing the globality of the system.

HYCOM has been coupled to a sea-ice model and a Carbon:Nitrogen Regulated Ecosystem Model (REcoM) with carbon and nitrogen being decoupled. A multi-category sea-ice model has recently been coupled to HYCOM and run with the ERA40 ECMWF reanalysis forcing fields. The coupled model reproduces well the observed distributions of ice thickness in the central Arctic and ice export through the Fram Strait (Lisæter, 2005).

With the inclusion of a nesting capability and the assimilation of both *in situ* data and data from a variety of satellite sensors, the TOPAZ system constitutes a state-of-the-art and flexible operational ocean prediction system. The model system has been designed to be easily extendible to other geographical areas including the global domain and it allows for nesting of an arbitrary number of regional high resolution models with arbitrary orientation and horizontal resolution.

2. Real time operation

Within the TOPAZ project the original MICOM ocean model has now been replaced with the new advanced Hybrid Coordinate Ocean Model (http://hycom.rsmas.miami.edu/). From January 2003, the real-time experiment has resumed with assimilation of sea level anomalies merged from three satellites (ERS2, Jason-1 and GEOSAT follow on) and improved SST (known as Reynolds SST). From September 2003, remotely sensed ice concentrations observations from SSM/I are also assimilated. The assimilation of all three data types is done by the Ensemble Kalman Filter. Further, we have developed an implementation for assimilation of real-time *in situ* observations of temperature and salinity. These will be integrated into the real time system at the beginning of 2006. Two regional high-resolution models covering the Gulf of Mexico and the North Sea currently receive boundary conditions from TOPAZ and run in real-time.

A regional system covering the Barents Sea is under development and will also be run in real time. On 1 January 2005, HYCOM has been upgraded by its latest version (v2.1) which has improved physics (better representation of the Montgomery potential). This upgrade has significantly improved the transport of North Atlantic Waters into the Nordic Seas and the Arctic. In June 2005, a fourth order numerical scheme for momentum advection was implemented, which has shown considerable advantages over the classical second order scheme for similar computer costs, especially at high resolution (Winther *et al.*, 2005).

One critical issue is the forecast reliability in case of incident (e.g. computer failure, missing input data). Due to the very nature of the Ensemble Kalman Filter, the computational burden is split between a hundred independent computer jobs. This has strong advantages in term of optimal use of the computer; it makes the system easy to restart in case of incident and imposes relatively low requirements on the computer facilities. The TOPAZ system has therefore only delayed the issue of a forecast three times since 2003 due to either computer failures, missing data, personnel on holidays or combinations of these.

Results are displayed on the project web page http://topaz.nersc.no as well as validation statistics against *in situ* data provided by the Coriolis center.

3. European integration

Data collection, model validation and upgrades of system components necessary to satisfy the user needs are some of the most time demanding activities. Fortunately some of these tasks can be put in common with other groups and some level of integration has already been achieved by the use of common sources of data (Coriolis, DUACS and ECMWF) and by the definition of metrics and file formats for assessing the quality of

the model output (that was initiated during the Mersea Strand-1 EC project). Such joint efforts ought to be pursued in the future as long as they do not level off the original initiatives where potential interest is backed by scientific evidence.

Future steps certainly included the set up of common file exchange formats and protocols for other regions than those considered in Mersea Strand-1, the definition of validation metrics and statistics useful for models having different vertical and horizontal coordinate systems, and pursuit of different types of delayed-mode validation data.

4. Summary

This paper has discussed the implementation and operation of an operational monitoring and prediction system for the Atlantic and the Arctic Basins. The system is based on sophisticated modelling and data assimilation tools and is set up for real time operation, and now assesses the impact of the remote sensing products on the predictions.

The real time operation of the system has proved to be feasible and relies on the availability of remote sensing products in near real time, and atmospheric forcing fields from the meteorological forecasting centres. The forecasts of eddies in the Gulf of Mexico have been presented to potential users in the offshore oil industry by Ocean Numerics Ltd. revealing their strong interest in the way the problem is tackled and providing useful feedback for future product developments.

Finally it should be stated that the TOPAZ system complies with and contributes to the plans of international programmes such as GODAE and GMES. The system developed has similarities with the other major initiatives in GODAE and will in many respects be complementary to these. Further, the system is one of the major initiatives contributing to the EuroGOOS task teams, in particular the Atlantic Task Team, by developing an assimilation system for predicting the ocean circulation in the Atlantic, and the Arctic Task Team by the focus on ice modelling and assimilation of ice variables in the Arctic.

References

Bentsen, M., G. Evensen, H. Drange and A.D. Jenkins (1999). Coordinate transformation on a sphere using a conformal mapping, Mon. Weather Rev., 127, 2733–2740.

Bleck, R. (2002). An oceanic general circulation model framed in hybrid isopycnic-Cartesian coordinates, Ocean Modelling, 4, 55–88.

Lisæter, K.A. (2005). A sea ice model describing the ice thickness distribution, Ocean Modelling, submitted.

Winther, N., Y. Morel and G. Evensen (2005). Efficiency of high order numerical schemes for momentum advection, Ocean Modelling, submitted.

A review on the progress and problems of modelling and data assimilation of biochemical variables in the Cretan Sea ecosystem

George Triantafyllou*
Institute of Marine Biology of Crete, Greece

Abstract

This paper presents a review of the progress made and problems existing in the application of ecosystem modelling and data assimilation in the Cretan Sea. In particular, issues are discussed pertaining to the use of different variants of the Singular Evolutive Extended Kalman filter (SEEK) in ecosystem modelling. The problems are analysed and there is a discussion of the assimilation results that show a continuous decrease in the estimation error and a clear improvement of the model's behaviour.

Editor's note: This paper was inadvertently omitted from the Proceedings of the 3rd EuroGOOS Conference held in Athens in December 2002, and is therefore published here.

Keywords: Ecosystem model, data assimilation, Cretan Sea.

1. Introduction

The Mediterranean Forecasting System Pilot Project (MFSPP) was a EuroGOOS Test Case for the Mediterranean. A major aim of the MFSPP was to develop robust ecosystem models and methodologies for the efficient integration of observations with hydrodynamic and biogeochemical models. Although the ultimate aim is to assimilate data in fully coupled biophysical ocean models, it is easier to begin with simpler ecosystem models and progressively build up an understanding of the issues involved in assimilating data into them. Despite their simplicity in relation to coupled models, these ecosystem models are nevertheless excellent for parameter tuning and customisation for a specific ecosystem. Towards these issues an existing generic model was tuned and validated for the Cretan Sea (Triantafyllou *et al.*, 2003b), one of the most oligotrophic regions of the world, the largest and deepest basin in the south Aegean Sea (2500 m). At a later stage it was used for the development of the fully 3D model presented by Petihakis *et al.*, (2002).

While data are useful to validate and improve the behaviour of the model, the assimilation of these is now recognised as the most efficient way to improve the consistency between data sets and model simulation. The extended Kalman filter is an extension of the Kalman filter to non-linear dynamic systems. However, its implementation in realistic ecosystems is not feasible because of its high computation cost. Different degraded forms of the extended Kalman filter have been proposed, which reduce the dimension of the system (n) through some kind of projection into a low dimensional sub-

* Corresponding author, email: gt@ath.hcmr.gr

space (Cane *et al.*, 1995; Fukumori and Malanotte-Rizzoli, 1995; Hoang *et al.*, 1997). The filters used for the Cretan Sea were based on the Singular Evolutive Extended Kalman (SEEK) proposed by Pham *et al.*, (1997). The filters approximate the model error covariance matrix by singular low rank (r) (r<<n), with the correction of the errors made only along certain directions, i.e. in a sub-space of dimension (r). The SEEK filter has been successfully implemented in different realistic ocean applications (Pham *et al.*, 1997; Verron *et al.*, 1998; Brasseur *et al.*, 1999; Hoteit *et al.*, 2001). Carmillet *et al.* (2001) used it with fixed directions of correction, assimilating ocean colour data into a simple 3D physical-biochemical model of the North Atlantic Ocean. In the case of the Cretan Sea, the SEEK filter was implemented with a 1D complex ecosystem model assimilating real observations of oxygen and nitrate, validating its performance with independent chlorophyll data (Hoteit *et al.*, 2003b). Furthermore, the filter was implemented in a fully 3D biophysical model of the Cretan Sea, using the standard twin experiment technique (Triantafyllou *et al.*, 2003a).

2. Ecosystem modelling

Even before discussion of assimilation techniques, we are faced with the first question: "what is the proper ecosystem model able to reasonably describe the functioning of a specific ecosystem?" The ecosystem of the Cretan Sea was described by two highly portable, on-line coupled models, the Princeton Ocean Model (POM) (Blumberg and Mellor, 1987), which provides the background physical information to the ecological model, and the European Regional Seas Ecosystem Model (ERSEM) (Baretta *et al.*, 1995), which describes the biogeochemical cycles. A detailed description of the trophic relations between the different groups of the model can be found in Petihakis *et al.* (2002).

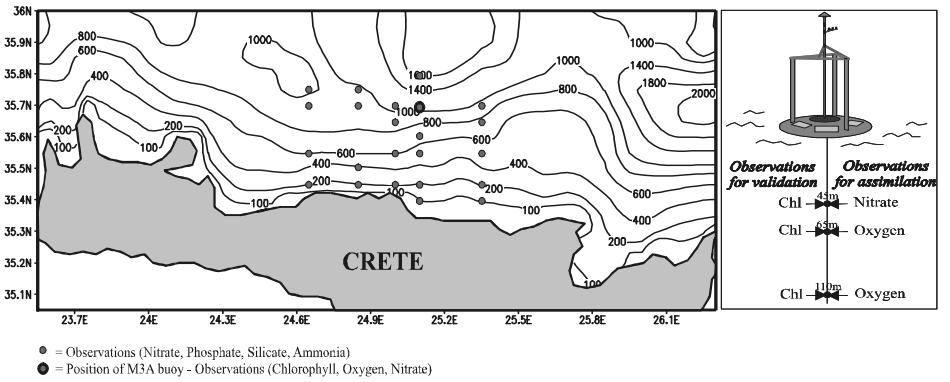

Figure 1 Simulation domain including the location of pseudo-observations and position and schematic representation of M3A buoy.

The Triantafyllou *et al.* (2003b) model was evaluated against *in situ* data collected from the M3A buoy deployed in the Cretan Sea (Figure 1) in the framework of the MFSPP. The model satisfactorily describes the functioning of the ecosystem in the upper part of the water column but underestimates the chlorophyll concentrations at the deep layers because of its one-dimensional nature. However, it provides a successful numerical base

for the development of the three-dimensional ecosystem model and implementation of data assimilation techniques.

The three-dimensional description of the Cretan Sea ecosystem is given in Petihakis *et al.* (2002), where model set-up initial and boundary conditions, and a detailed discussion on the model results can be found. The model covers the Cretan Sea shelf area between 23.55–26.3 E and 35.05–36.06 N with a lattice of 50×20 grid points (Figure 1). In the vertical there are 30 layers of variable thickness with logarithmic distribution near the surface for greater accuracy in the surface mixed layer. The model was based on the one-dimensional model of Triantafyllou *et al.* (2003b), which provided the initial conditions for the biochemical parameters.

For the validation of the model results, a cost function was used (Moll, 2000). This function enables the comparison of model results with *in situ* data by a non-dimensional value that indicates how successful the model is in comparison with the real data. The categories of the cost function results used were (<1=Very good, 1–2=Good, 2–5=Reasonable, >5=Poor). The implementation of the cost function showed that in the upper layer (0–150 m), 60% of the model results were very good, 30% good, 10% reasonable, and only one score was classified as poor. In the deeper layers (depth>150 m), 34% of the results were very good, 28% good, 36% reasonable, and 2% poor. These results indicate that the model exhibits a better behaviour at the surface layer, which is more biologically significant, and is less efficient at the deeper layers. In addition, modelling annual primary and bacterial productivity was found to be within the range of the data reported in the literature. An important outcome of this study showed that the biology in the Cretan Sea is significantly driven by the hydrodynamics. The model results show circulation features similar to those described by Theocharis *et al.*, (1993). A double gyre system consisting of an anticyclone to the west and a cyclone to the east interconnected by meandering currents was persistent in the region. The influence of this is depicted in the productivity of the Cretan Sea, where higher values are shown between the gyral dipole, and lower values at the centre of the anticyclone (Figure 2).

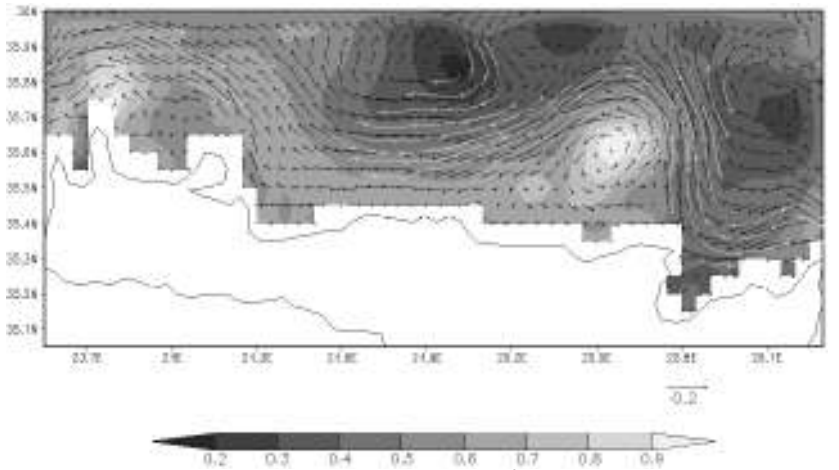

Figure 2 Annual chlorophyll concentrations (mg m^{-3}) and velocity field at 50 m.

3. Assimilation of biogeochemical data

The models described here consider the SEEK filter and two of its variants, the Singular Fixed Extended Kalman (SFEK) filter, assuming persistence of the error sub-space with time, and the Singular Extended Interpolated Kalman (SEIK) filter, in which the linearisation used in the SEEK filter is replaced by linear interpolation (Triantafyllou *et al.*, 2003a). Here, we briefly present the SEEK filter, adopting a notation proposed by Ide *et al.* (1997). A schematic diagram of the filter algorithm is illustrated in Figure 3.

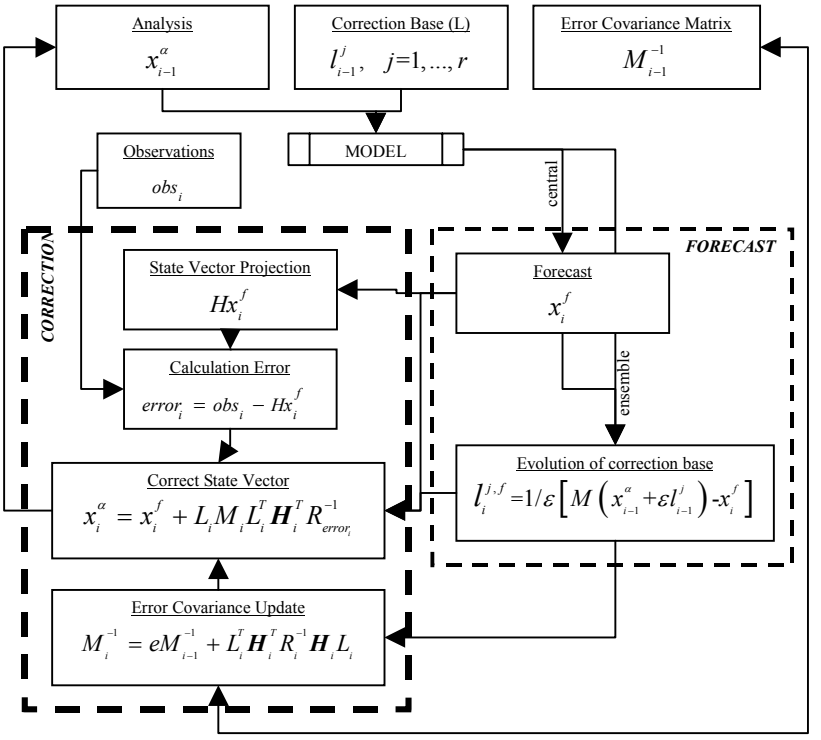

Figure 3 Schematic diagram of the assimilation cycle. In the forecast module the central state and the evolution of the correction base are integrated by the model dynamics (Equations (3) and (5)). In the correction module the forecast is corrected (Equation (6)) using available observations and the updated error covariance matrix (Equation (9)). See text for mode details and the description of the mathematical symbols.

A physical system is described by:

$$X^{t}(t_k) = M(t_k, t_{k-1}) X^{t}(t_{k-1}) + \eta_k \tag{1}$$

where $X^{t}(t_k)$ denotes the vector representing the true state at time t, $M(s,t)$ is an operator describing the system transition from time s to time t and η is the system noise vector. At each time t_k, it is observed that

$$Y_k^o = H_k X^t(t_k) + \varepsilon_k \tag{2}$$

where H_k is the observational operator and ε_k is the observational noise. The noises η_k and ε_k are assumed to be independent random vectors with mean zero and covariance matrices Q_k and R_k respectively. To initialise the filter, a long sequence of state vectors is generated by the model run $X^a(t_0)$, and is taken as the average of these vectors. The initial error covariance matrix of rank (r), $P^a(t_0)$, is obtained via an EOF analysis (according to Pham *et al.*, 1997).

In the forecast stage, at time t_{k-1}, we assumed an estimate $X^a(t_{k-1})$ of the system state and its corresponding error covariance matrix $P^a(t_{k-1})$, in the factorised form $L_{k-1}U_{k-1}L_{k-1}^T$, where L_{k-1} and U_{k-1} are of dimensions $n \times r$ and $r \times r$ respectively. The model (1) is used to forecast the state as:

$$X^f(t_k) = M(t_k, t_{k-1})X^a(t_{k-1}) \tag{3}$$

The corresponding forecast error covariance matrix can then be approximated by:

$$P^f(t_k) = L_k U_{k-1} L_k^T + Q_k \tag{4}$$

where

$$L_k = \mathbf{M}(t_k, t_{k-1})L_{k-1} \tag{5}$$

and $\mathbf{M}(t_k, t_{k-1})$ is the gradient of $M(t_k, t_{k-1})$ evaluated at $X^a(t_{k-1})$.

In the correction stage, the new observation Y_k^o at time t_k is used to correct the forecast according to:

$$X^a(t_k) = X^f(t_k) + L_k U_k L_k^T \mathbf{H}_k^T R_k^{-1} [Y_k^o - H_k X^f(t_k)] \tag{6}$$

with $\mathbf{H}_k$ the gradient of H_k evaluated at $X^f(t_k)$ and U_k computed from:

$$U_k^{-1} = [U_{k-1} + (L_k^T L_k)^{-1} L_k^T Q_k L_k (L_k^T L_k)^{-1}]^{-1} + L_k^T \mathbf{H}_k^T R_k^{-1} \mathbf{H}_k L_k \tag{7}$$

The corresponding filter error covariance matrix is then equal to:

$$P^a(t_k) = L_k U_k L_k^T \tag{8}$$

In order to treat the model errors, the approach described by Pham *et al.* (1997) was followed. Thus, a so-called compensation technique that amplifies the pre-existing error modes during the forecast is used to parametrise the model errors. The equation is then rewritten, by means of a forgetting factor ρ, as:

$$U_k^{-1} = \rho U_{k-1}^{-1} + L_k^T \mathbf{H}_k^T R_k^{-1} \mathbf{H}_k L_k \quad (9)$$

More details can be found in Pham *et al.* (1997) regarding the observation error.

Table 1 provides information regarding the configuration of the assimilation experiments and the variants of the SEEK filter (SFEK, SEIK) used in each case. More details can be found in Hoteit *et al.* (2003a, 2003b) and Triantafyllou *et al.* (2003a).

Table 1 Configuration of assimilation experiments.

Model	Initial period	Filter	Obs num	Data to assimilate[1]	Exper-iment, assim. period	Compens .Factor	Rank of corr basis
1D	Years:5 Vectors:600	SFEK	3	Nitrate, Oxygen	Twin, 3mo: 1/1–1/3/00	0.9	5, 10, 15, 20[2]
"	"	"	3	Chlorophyll	"	"	15 EOF[3]
"	"	"	5	Chlorophyll, Oxygen	"	"	"
"	"	"	4	Chlorophyll, Nitrate	"	"	"
"	"	"	3	Nitrate, Oxygen	"	"	"
"	"	"	3	"	Real, 3mo: 5/3–12/5/00	0.25, 0.5, 0.75	15 EOF[4]
3D	Years:2 Vectors:400	SFEK	23x30[5]	Nitrate, Phosphate, Silicate, Ammonia (in all grid[5])	Twin	0.9	10, 20, 30, 40[2]
"	"	SEIK	"	"	"	"	10

[1]Nitrate (at 45 m), Oxygen (at 65 and 115 m), Chlorophyll (at 45, 65 and 110 m).
[2]Sensitivity experiments for the models were run with progressively increasing modes of the error covariance matrix to check if the relative RMS is reaching a saturation value.
[3]Different combinations of pseudo data were assimilated into the 1D model to study the sensitivity of the assimilation system in relation to the observations.
[4]Sensitivity experiment using different forcing factors in the assimilation of *in situ* observations.
[5]23 stations x 30 layers

4. Summary and conclusions

The Cretan Sea has been monitored over an extended period of time providing valuable information and a unique opportunity for ecosystem modelling and data assimilation.

The SEEK filter was applied to a 1D ecosystem model of the Cretan Sea for the assimilation of pseudo and *in situ* data provided by the M3A buoy. Furthermore, the filter assimilated nitrate, phosphate, silicate, and ammonia pseudo-data from 23 stations into a complex 3D coupled physical-biogeochemical model. The twin experiments have demonstrated the pre-operational ability of the filter to efficiently control the evolution of the model state. This is in agreement with the multivariate character of the error subspace, which contains the dominant modes of the model's variability, and therefore, the cross correlations among different model variables. Additionally, in the 3D application the model exhibits sensitivity to the initial conditions performing better in eutrophic

areas. Application with real data over the period 5/3–8/5/2000 revealed a clear improvement in the model's behaviour in the upper part of the water column with respect to the reference simulation run. The model underestimates chlorophyll concentrations at 115 m failing to follow the observations. This might be attributed to the inconsistencies between EOFs and data.

It is clear that special care should be taken in the implementation of the assimilation schemes, and sensitivity experiments are suggested for the proper configuration of the assimilation algorithms. Variational methods based on the optimal control theory and sequential methods based on the Kalman filter have provided new tools to increase the predictive capability of the ecosystem models. It is critical that these new theories be applied with the utmost care otherwise we may destroy a theory that currently shows a great deal of promise.

Acknowledgements

The Mediterranean Forecasting System Pilot Project (MAS3–PL97–1608) has supported this work.

References

Baretta, J.W., W. Ebenhoh and P. Ruardij (1995). The European Regional Seas Ecosystem Model, a complex marine ecosystem model, Netherlands Journal of Sea Research, 33, 233–246.

Blumberg, A.F. and G.L. Mellor (1987). A description of a three-dimensional coastal ocean circulation model, In Heaps, N.S. (Ed.) Three-Dimensional Coastal Ocean Circulation Models, Coastal Estuarine Science, 4, AGU, Washington D.C., pp. 1–16.

Brasseur, P., J. Ballabrera-Poy and J. Verron (1999). Assimilation of altimetric observations in a primitive equation model of the Gulf Stream using a singular evolutive extended Kalman filter, Journal of Marine Systems, 22(4), 269–294.

Cane, M.A., A. Kaplan, R.N. Miller, B. Tang, E.C. Hackert and A.J. Busalacchi (1995). Mapping tropical Pacific sea level: data assimilation via a reduced state Kalman filter, Journal of Geophysical Research, 101(10), 599–617.

Carmillet, V., J.M. Brankart, P. Brasseur, H. Drange, G. Evensen and J. Verron (2001). A singular evolutive extended Kalman filter to assimilate ocean color data in a coupled physical-biochemical model of the North Atlantic ocean, Ocean Modelling, 3(3–4), 167–192.

Fukumori, I. and P. Malanotte-Rizzoli (1995). An approximate Kalman filter for ocean data assimilation: an example with an idealised Gulf Stream model, Journal of Geophysical Research, 100(C4), 6777–6793.

Hoang, H.S., P. De Mey, O. Tallagrand and R. Baraille (1997). Adaptive filtering: Application to satellite data assimilation in oceanography, Journal Dynamics of Atmospheres and Oceans, 27, 257–281.

Hoteit, I., D.T. Pham and J. Blum (2001). A semi-evolutive partially local filter for data assimilation, Marine Pollution Bulletin, 43, 164–174.

Hoteit, I., G. Triantafyllou and G. Petihakis (2003a). Towards a data assimilation system for the Cretan Sea ecosystem using a simplified Kalman filter, Journal of Marine Systems.

Hoteit, I., G. Triantafyllou, G. Petihakis and J.I Allen (2003b). A Singular Evolutive Extended Kalman filter to assimilate real *in situ* data in a 1-D marine ecosystem model, Annales Geophysicae, 21, 389–397.

Ide, K., A.F. Bennett, P. Courtier, M. Ghil and A.C. Lorenc (1997). Unified notation for data assimilation: operational, sequential and variational, Journal of Meteorological Society of Japan, 75(1B), 181–189.

Moll, A. (2000). Assessment of three-dimensional physical-biological ECOHAM1 simulations by quantified validation for the North Sea with ICES and ERSEM data, ICES Journal of Marine Science, 57, 1060–1068.

Petihakis, G., G. Triantafyllou, J.I. Allen, I. Hoteit and C. Dounas (2002). Modelling the Spatial and Temporal Variability of the Cretan Sea Ecosystem, Journal of Marine Systems, 36, 173–196.

Pham, D.T., J. Verron and M.C. Roubaud (1997). Singular evolutive Kalman filter with EOF initialization for data assimilation in oceanography, Journal of Marine Systems, 16, 323–340.

Theocharis, A., D. Georgopoulos, A. Lascaratos and K. Nittis (1993). Water masses and circulation in the central region of the Eastern Mediterranean: Eastern Ionian, South Aegean and Northwest Levantine, Deep-Sea Research II, 40(6), 1121–1142.

Triantafyllou, G., I. Hoteit and G. Petihakis (2003a). A singular evolutive interpolated Kalman filter for efficient data assimilation in a 3D complex physical-biogeo-chemical model of the Cretan Sea, Journal of Marine Systems, 40–41, 213–231.

Triantafyllou, G., G. Petihakis and J.I. Allen (2003b). Assessing the performance of the Cretan Sea ecosystem model with the use of high frequency M3A buoy data set, Annales Geophysicae, 21, 365–375.

Verron, J., L. Gourdeau, D.T. Pham, R. Murtugudde and A.J. Busalacchi (1998). An extended Kalman filter to assimilate satellite altimeter data into a nonlinear numerical model of the tropical Pacific: method and validation, Journal of Geophysical Research, 104(C3), 5441–5458.

Application of a Dual Kalman Filter in a complex ecosystem model

G. Triantafyllou*[1], G. Petihakis[1], G. Korres[1], I. Hoteit[2] and A. Pollani[1]

[1]*Hellenic Center for Marine Research, Anavyssos, Greece*
[2]*Scripps Institution of Oceanography, USA*

Abstract

Data assimilation into dynamic models is a necessity dictated by the increasing need for prognostic capabilities. In this work the performance of a Dual Assimilation Scheme in a complex ecosystem model applied in the oligotrophic environment of the Eastern Mediterranean is evaluated. Results indicate that by assimilating only sea surface height (SSH) in the physical submodel and chlorophyll *a* (chl *a*) in the ecological submodel the model error is significantly reduced in all important variables.

Keywords: Dual assimilation, ecosystem model

1. Introduction

During the last decade physical oceanography has actively moved to the area of forecasting with the development of very robust and efficient operational modelling tools. Marine ecosystem models on the other hand have been focusing mainly on concept testing and simple system structures, being limited by the complexity of aquatic systems and the available computer resources. Only during the last few years has the advancement in computers allowed the development of 3D complex ecosystem models, which are fully coupled with hydrodynamic models. Considering the prognostic capability of the latter there is an increasing need to develop quantitative ecosystem models where the focus is on prognostic capabilities. However, fitting ecological data into observations is often a difficult task, either due to poor knowledge of the system or due to model simplification (Vallino, 2000). The reductionism approach dictates the grouping of a number of organisms in a common compartment, making the estimation of parameters from direct measurements difficult.

Even though the model used in this study allows a number of parameters to vary within certain limits (variable C:N:P), there are fixed parameters adding errors in the simulations. In stable systems such errors might be small but they become very important in variable systems where conditions change dramatically in short time intervals. Another problem is the scarcity of field measurements for the biological variables — if they are available it is difficult to employ them for model improvement.

The above constraints can be overcome through the integration of models with field data known as data assimilation, a rather common practice in oceanography and meteorology. Assimilation in ecological models is challenging and much more difficult, since the system is highly complex, driven by the physics with significant spatial and temporal variability. Efforts focusing on the assimilation of biological variables only have shown

* Corresponding author, email: gt@ath.hcmr.gr

significant improvements in the model's behaviour (Triantafyllou *et al.*, 2003a). However even if the model is frequently updated, phenomena of "strange" biological responses such as hot spots of production are not rare, as the physical model might be diverging from the truth. Thus a dual assimilation scheme where the physical component is "corrected" or assimilated followed by the ecology seems a better approach. In this study a dual Kalman filter is presented and analysed while its efficiency is justified through different scenarios.

2. Assimilation scheme

2.1 Model

The coupled physical-biogeochemical model is composed of the Princeton Ocean Model (POM) (Blumberg and Mellor, 1987), which describes the hydrodynamics, and the European Regional Seas Ecosystem Model (ERSEM) (Baretta *et al.*, 1995). The two models are coupled on-line, with the former acting as the driver for the ecology. ERSEM is a generic model made evident by the variety of environment in which it has been applied (for a review see Petihakis, 2004). The prognostic variables for ERSEM are oxygen, carbon dioxide, phosphate, nitrate, silicate, ammonia, all the phytoplankton and zooplankton groups, particulate organic matter, dissolved organic matter, bacteria and benthic particulate organic matter, while the prognostic variables of the POM model are the sea surface elevation, the zonal and meridional components of velocity U,V (the vertical velocity is solved diagnostically) and their depth-averaged counterparts ($\overline{U}$, $\overline{V}$), potential temperature T, salinity S, the turbulent kinetic energy q^2 and the turbulent kinetic energy times the turbulent length scale q^2l. The model domain covers the Eastern Mediterranean basin with coordinates 30°.7N–41°.2N and 20°E–36°.4E and a resolution of 6 minutes and 24 sigma layers in the vertical.

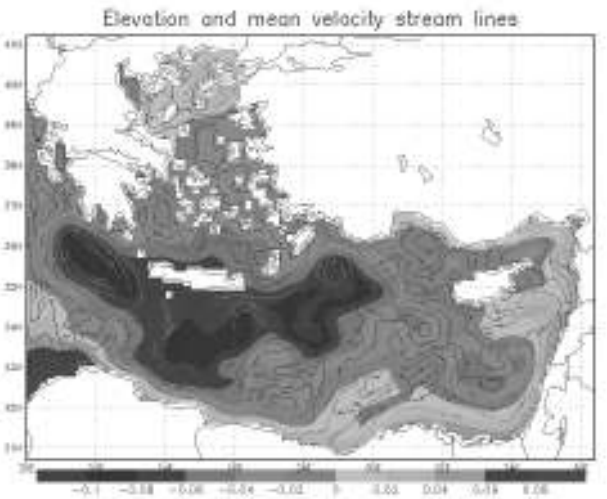

Figure 1 Model domain.

2.2 Description of the SEEK filter

Consider a physical system described by

$$X^t(t_k) = M(t_k, t_{k-1})X^t(t_{k-1}) + n(t_k) \quad (1)$$

where $X^t(t)$ denotes the vector representing the true state at time t, $M(t,s)$ an operator describing the system transition from time s to time t, and $n(t)$ the system noise vector. At each time t_k, one observes

$$X_k^o = H_k X^t(t_k) + \varepsilon_k \quad (2)$$

where H_k is the observational operator and ε_k is the observational noise. The noises $n(t_k)$ and ε_k are assumed to be independent random vectors with mean zero and covariance matrices Q_k and $\sigma^2 R_k$, respectively. Often R_k is assumed to be the identity matrix and then σ^2 represents the error covariance. The parameter σ^2 is introduced as the observation error matrix and may be known only up to a constant factor, and even if it is known, it is preferable to estimate σ^2 from the data, for reasons explained later.

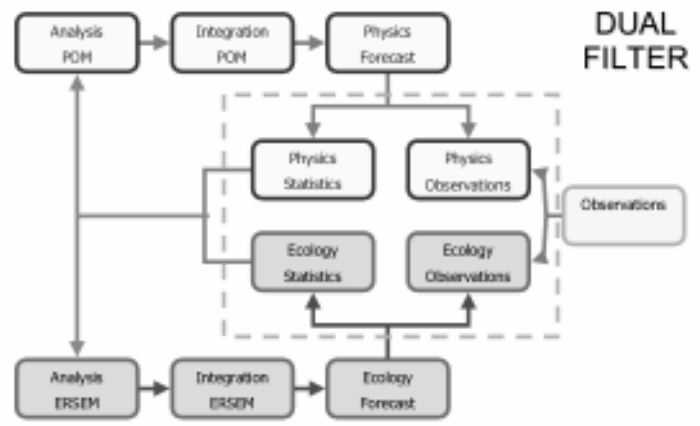

Figure 2 Dual assimilation filter.

The sequential data assimilation involves the estimation of the state of the system at each observation time, using only observations up to that time. In linear cases, this problem has been solved by the Kalman filter, while in the non-linear cases, the model is often linearised around the current estimated state vector, which directs to the so-called extended Kalman (EK) filter (see for example Ghil and Malanotte-Rizzoli, 1991, for details). The SEEK filter aims to reduce the prohibitive cost of the EK filter (in meteorology and oceanography applications), arising from the significant number (n) of the state variables. The main idea behind this is to view the error covariance matrix as singular with a low rank $r<<n$. This leads to a filter in which the error corrections are only made along certain directions parallel to a linear subspace of dimension r. These directions are those for which error is not sufficiently attenuated by the system dynamics.

This filter proceeds in two steps apart from an initialisation stage. To initialise the filter, a long sequence of state vectors is generated according to our model considering $X^a(t_0)$ as the average of these vectors and $P^a(t_0)$ as the rank r approximation to their sample covariance matrix, obtained via an EOF analysis (see Pham *et al.* 1997, for details).

Forecast stage

At time t_{k-1} an estimate $X^a(t_{k-1})$ of the system state and its corresponding error covariance matrix $P^a(t_{k-1})$, in the factorised form $\sigma^2 L_{k-1} U_{k-1} L_{k-1}^T$ where L_{k-1} and U_{k-1} are of dimension $n \times r$ and $r \times r$ respectively, are available. The model (1) is used to forecast the state as

$$X^f(t_k) = M(t_k, t_{k-1}) X^a(t_{k-1}).$$

The forecast error covariance matrix is given by

$P^f(t_k) = \sigma^2 L_k U_{k-1} L_k^T + Q_k$ where $L_k = \boldsymbol{M}(t_k, t_{k-1}) L_{k-1}$ and $\boldsymbol{M}(t_k, t_{k-1})$ is the gradient of $M(t_k, t_{k-1})$ evaluated at $X^a(t_{k-1})$.

Correction stage

The new observation Y_k^o at time t_k is used to correct the forecast according to

$X^a(t_k) = X^f(t_k) + G_k[Y_k^o - H_k X^f(t_k)]$ where G_k is the gain matrix given by

$G_k = L_k U_k L_k^T \boldsymbol{H}_k^T R_k^{-1}$ with $\boldsymbol{H}_k$ the gradient of H_k evaluated at $X^f(t_k)$ and U_k computed from

$$U_k^{-1} = [U_{k-1} + (L_k^T L_k)^{-1} L_k^T Q_k L_k (L_k^T L_k)^{-1}]^{-1} + L_k^T \boldsymbol{H}_k^T R_k^{-1} \boldsymbol{H}_k L_k.$$

The corresponding filter error covariance matrix is then equal to

$$P^a(t_k) = \sigma^2 L_k U_k L_k^T.$$

2.3 Experimental setup

The model spun up for four years to reach a quasi steady state and afterwards another integration of two years was carried out to generate a historical sequence for the calculation of the EOF basis. The filter was initialised by the mean of the historical data set, while for the assimilation experiments pseudo-observations of the sea surface height (SSH) and sea surface chlorophyll (CHL) were used. The total assimilation period was 120 days. In the assimilation experiments the 'POM filter' and the 'ERSEM filter' were initialised by error covariance matrices of ranks 40 and 10, which explain 90% and 91% of the total system variance respectively. In the presentation of the assimilation results the relative root mean square (RRMS) error was used (Triantafyllou *et al.*, 2003a).

3. Results and discussion

Model simulations start at the beginning of January integrating for the next 120 days. Figure 3 shows the RRMS error of the free run and the filter run for the four most important physical variables, sea surface height (SSH), temperature, salinity and velocity. In all cases the filter shows a very good behaviour, significantly better than the free run for most of the integration period. Only in the case of velocity does the error start to increase after 40 days although it remains well below the value of 1. This might be attributed to the phase-space regime that the filter evolves, in which strong non-linearities could become significant, reducing the performance of the assimilation scheme. It is

interesting that by only assimilating one variable, in this case SSH, the performance of the physical model is markedly improved.

Having mentioned that hydrodynamic models are much more robust with a higher degree of accuracy compared to the ecological ones, it is expected that the variables associated with the biological processes should exhibit higher error values (Figure 4). However, in all cases, the assimilation of only chlorophyll in conjunction with the assimilation of SSH efficiently constrains the model towards the true state of the system. The more detailed filter in both chemical and biological components enhances the prognostic capability of the model with error values always under 1.

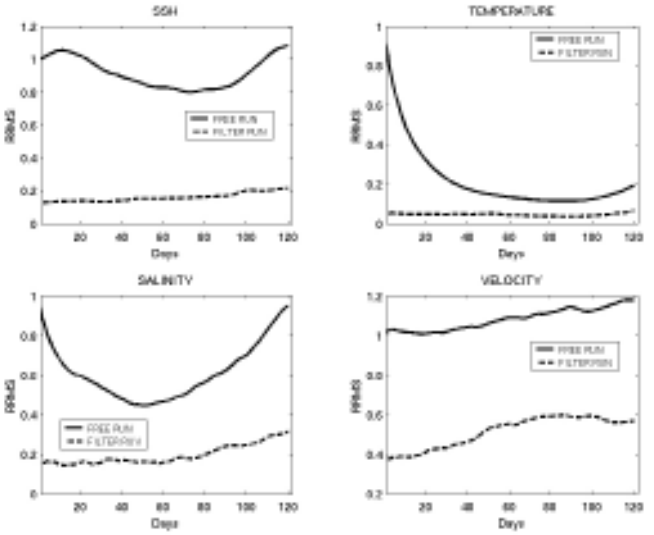

Figure 3 RRMS error for physical variables.

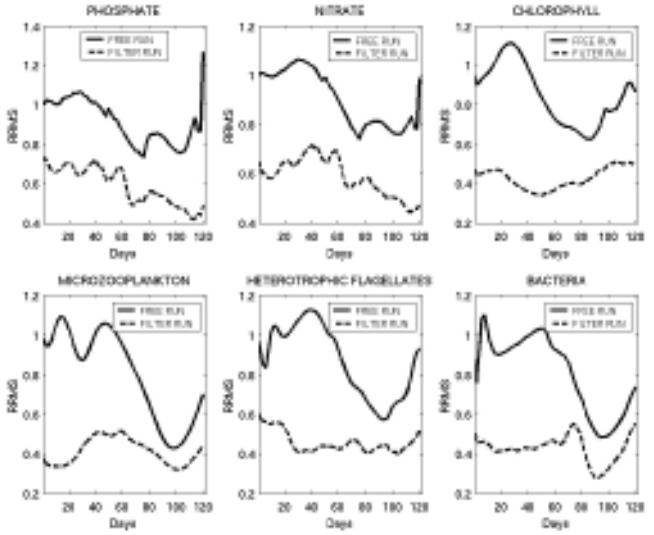

Figure 4 RRMS error for ecological variables.

The fact that both free and filter runs are improved (phosphate, nitrate and microzooplankton) after 60 days is attributed to the increased variability of the system during winter months (January–February). This variability is particularly evident in the concentrations of nutrients as mixing replenishes the euphotic zone from deeper layers and at the same time bacteria try to get advantage of this supply taking up inorganics.

As the system moves into spring the variability is moved towards the primary producers, with the initiation of the spring bloom and thus an expected increase in the error of chlorophyll. Looking at the microzooplankton error, from approximately 40 to 80 days of integration there is an increase, which is related to prey–predator dynamics, as during that period a shift in the diet takes place from bacteria to phytoplankton.

The experimental results indicate the efficiency of the dual assimilation scheme, which compared to simple single assimilation, is significantly higher, especially when the system under study is characterised by oligotrophic conditions where a strong coupling of physics with the biology is expected (Triantafyllou *et al.*, 2003b). Thus a dual assimilation of both model components (physical–biological) is important as shown by those variables mostly affected (nutrients).

Acknowledgements

This work has been supported by Mediterranean Ocean Forecasting System: Toward Environmental Predictions (MFSTEP) project.

References

Baretta, J.W., W. Ebenhoh and P. Ruardij (1995). The European Regional Seas Ecosystem Model, a complex marine ecosystem model. Netherlands Journal of Sea Research, 33: 233–246.

Blumberg, A.F. and G.L. Mellor (1987). A description of a three-dimensional coastal ocean circulation model. In: N.S. Heaps (Editor), Three-Dimensional Coastal Ocean Circulation Models. Coastal Estuarine Science. AGU, Washington, D.C., pp. 1–16.

Ghil, M. and P. Malanotte-Rizzoli (1991). Data assimilation in meteorology and oceanography. Adv. Geophys, 33: 141–266.

Petihakis, G. (2004). Hydrodynamic and Ecological Simulation of the Ecosystem of Pagasitikos Gulf. (In Greek) Thesis, University of Thessaly, Volos, 393 pp.

Pham, D.T., Verron, J. and M.C. Roubaud (1997). Singular evolutive Kalman filter with EOF initialization for data assimilation in oceanography. Journal of Marine Systems, 16: 323–340.

Triantafyllou, G., I. Hoteit and G. Petihakis (2003a). A singular evolutive interpolated Kalman filter for efficient data assimilation in a 3-D complex physical-biogeochemical model of the Cretan Sea. Journal of Marine Systems, 40–41: 213–231.

Triantafyllou, G., G. Korres, G. Petihakis, A. Pollani and A. Lascaratos (2003b). Assessing the phenomenology of the Cretan Sea shelf area using coupling modelling techniques. Annales Geophysicae, 21: 237–250.

Vallino, J.J. (2000). Improving marine ecosystem models: use of data assimilation and mesocosm experiments. Journal of Marine Research, 58: 117–164.

A new version of the European public domain code COHERENS

Patrick Luyten*[1], Isabel Andreu-Burillo[2], Alain Norro[1], Stéphanie Ponsar[1] and Roger Proctor[2]

[1]*Management Unit of the North Sea Mathematical Models, Belgium*
[2]*Proudman Oceanographic Laboratory, UK*

Abstract

COHERENS is an integrated three-dimensional model for coastal and shelf seas, previously developed in EU-MAST projects and available as a public domain code. Since its release in 2000, it has found several users within and outside the European Union. A brief description is given of the model and the user group. A complete upgrade is currently prepared in response to recent developments in numerical and data assimilation techniques, current evolutions in computing capacity and specific user requests. New options have been provided for applications on parallel machines, the Ensemble Kalman filter, nested grids, curvilinear and terrain-following coordinates and additional schemes. Applications of COHERENS in two ongoing FP5 programmes are further presented.

Keywords: integrated modelling, public domain code, user group

1. Introduction

COHERENS (COupled Hydrodynamical-Ecological model for REgioNal and Shelf seas) is a three-dimensional multi-purpose programme developed during the MAST projects PROFILE (1990–1996) and COHERENS (1997–1999). The code is composed of four major compartments:

- a physical core part for currents, elevations, temperature, salinity, turbulence and a module for wave–current interaction
- a simple biological module containing eight state variables including two types of nutrients
- a sediment model for the deposition and resuspension of particulate matter
- a Eulerian and a Lagrangian tracer module for the transport of dissolved matter.

A number of switches are installed within the code to select, depending on the user's needs, different types of processes or numerical schemes (turbulence closures, advection schemes, boundary conditions, etc.). Default options are provided for model switches and parameters so that the code can readily be applied for various purposes without major modifications or a detailed knowledge of the internal structure. An extensive user manual (Luyten *et al.*, 1999) is provided covering all aspects of model setup and descriptions of the scientific background. Simple test cases have been implemented to enable easy testing of the code's installation and portability on a specific computing platform and to illustrate a setup for a particular application.

* Corresponding author, email: P.Luyten@mumm.ac.be

2. User group

The source code of COHERENS, together with the documentation and test cases, is publicly available on CD-ROM for non-commercial applications, via electronic registration on the Internet (www.mumm.ac.be/coherens). Since the official release in April 2000, the number of registered users has grown continuously (Figure 1). In May 2005, the user list contained more than 700 world-wide registrations from 72 countries. A geographical distribution of users and a list of countries with the largest user groups is given in Table 1.

Table 1 Geographical distribution (%) of users and countries with the largest number of registrations in May 2005.

Continent		Country			
Europe	32	**USA**	108	**Spain**	28
N. America	17	**Korea**	64	**Brazil**	26
C/S America	9	**China**	63	**Germany**	22
Asia	35	**Indonesia**	52	**Belgium**	20
Africa	2	**UK**	37	**India**	20
Australia, New Zealand	5	**Australia**	30	**Italy**	19

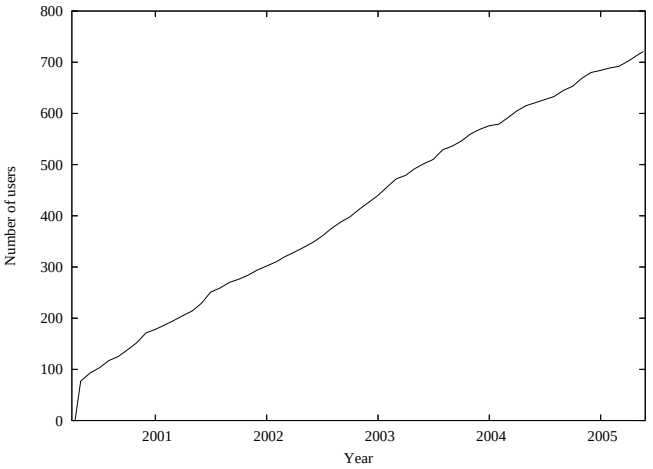

Figure 1 Evolution of the number of registered COHERENS users.

An important issue for developers of open codes is to know who is using the program and what the main intentions and type of applications are. The following can be deduced from the information given by the users on the registration log file:

- Most of the users are young scientists at a pre- or postdoctoral level who intend to make specific scientific studies, e.g. for preparing a PhD thesis. There is also interest from university lecturers who would like to use the code and the documentation as part of their teaching classes, environmental agencies for water quality studies and private companies.

- About 40% of the applicants mentioned specific applications, 15% showed an academic interest, 10% plan to compare COHERENS with other user or public domain codes. The remaining 35% expressed a general interest without providing details.
- The type and area of intended application vary widely from ecosystem, sediment and physical (circulation, tides) modelling to chemical pollution problems and particle tracking studies within shelf seas, coastal zones, lagoons, estuaries, lakes and reservoirs.

An electronic user group has been established for problem and bug reports, specific questions concerning model setup and suggestions for improvements. These comments proved to be useful for the upgrade of the model, further discussed below.

3. The new version

COHERENS was developed during the period 1990–1999 and can be considered as one of the first integrated models within the public domain. Since then, significant progress has been made in computing performance and in the development of more advanced numerical techniques. A complete update became necessary and has been undertaken as part of the FP5 project ODON. General objectives are:

- to take into account the improvements of recent years in computer hardware (parallel computing) and programming languages (FORTRAN 90)
- implementation of schemes for data assimilation
- extension of the model's applicability from the estuary and coastal zone to the ocean basin by the use of more flexible grids and nesting
- creation of optional user interfaces for model input or for the coupling with biological and sediment modules
- to respond to specific user requests.

Although the code has grown considerably in size, the new version remains compatible with the older one and can be used by individuals with a portable PC as well as by institutes with large computing facilities. The most important features of the new code are summarised below. They are mainly provided as options which can be selected by the user.

- The old FORTRAN 77 language is replaced by FORTRAN 90. Obvious advantages are a better management of internal memory (up to a factor of 3 to 4 compared to the previous version depending on the application) via dynamical array allocation, structured model setup and a more transparent structure of the code.
- An option is provided to run the program in parallel mode on distributed-memory machines via the installation of MPI (Version 1.1) public domain library. This offers the possibility of huge savings in CPU time and process memory.
- The σ-coordinates are replaced by the more flexible terrain-following s-coordinates (Song and Haidvogel, 1994), allowing simulations to be performed for areas with strong bathymetric slopes, such as a shelf edges.

- The model grid can be defined using orthogonal curvilinear coordinates in the horizontal so that coastlines, estuaries or other specific areas can be resolved with higher accuracy.
- Two schemes for data assimilation are provided. The first is a simple scheme for the assimilation of sea surface temperature (Annan and Hargreaves, 1999). The second, which is currently being tested, is the Ensemble Kalman Filter following Evensen (2003, 2004).
- Nested grids can be selected by the user. This permits creation of a hierarchy of sub-domains of increasing resolution, or focusing on selected coastal areas.
- Existing schemes have been improved and new ones added: turbulence closures (e.g. Canuto *et al.*, 2001), pressure gradient force, sponge layers and radiation conditions at open boundaries, astronomical tides, etc.
- A drying/wetting algorithm is now implemented.
- Model input/output can be provided via multiple files, each with their own time resolution, either in standard "COHERENS" format or via a user-defined interface. This makes it possible, in particular, to import data for assimilation from different sources (satellite data, buoys, CTD profiles, moving ships).

4. Applications in EU projects

4.1 DITTY project

COHERENS is currently applied in two FP5 programmes. The first is the DITTY project (Development of an Information Technology Tool for the Management of European Southern Lagoons under the influence of river-basin runoff). The main objective is the development of a Decision Support System (DSS) for the management of coastal lagoons. The DSS will contain a database, a geographical information system and a coupled river-basin-coastal lagoon model. COHERENS is taken for the physical part of the code and further coupled to models for the simulation of biochemical cycles (including clam farming) and the watershed (Marinov *et al.*, 2005b). Five test sites have been selected. Bench mark exercises and scenario analyses have been developed and an intercomparison exercise is currently performed with existing site models.

Figure 2 shows the circulation field in the Sacca di Goro lagoon in northern Italy at flood tide and easterly wind. Tides enter from the Adriatic Sea to the South. The aim of the simulation is to analyse the effect of a new sea connection created in August 1992 after a severe anoxic crisis. It is seen that the presence of the channel reduces the circulation in the western part and intensifies the anticyclonic eddy in the central part of the lagoon. Further studies have been made to study the impact on the biological cycle and clam production. For more details, see Marinov *et al.* (2005a,b).

Figure 3 displays the horizontal distribution of salinity and temperature in the Thau lagoon (French Mediterranean coast). The site is connected to the sea via a narrow channel at the city of Sète to the Southeast. The main input of fresh water is through the river Vène at the Northeast corner. Despite the limited size of the lagoon (~70 km^2) a strong variability in both parameters can be observed. Results of the simulation will be compared with the MARS-3D model developed at IFREMER.

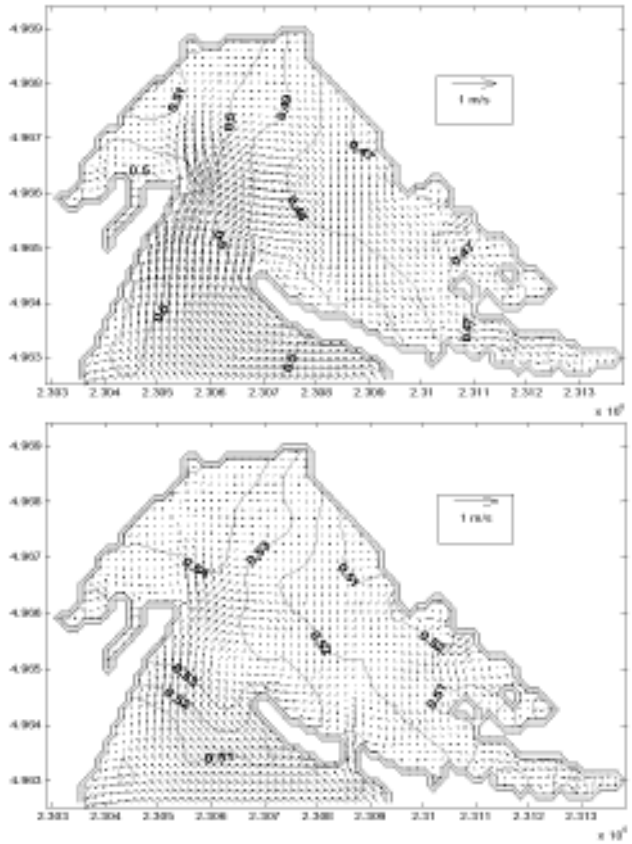

Figure 2 Circulation field and surface elevation (m) in the Sacca di Goro lagoon at flood tide for the original bathymetry (left) and after opening of the new connection to the Adriatic Sea (right).

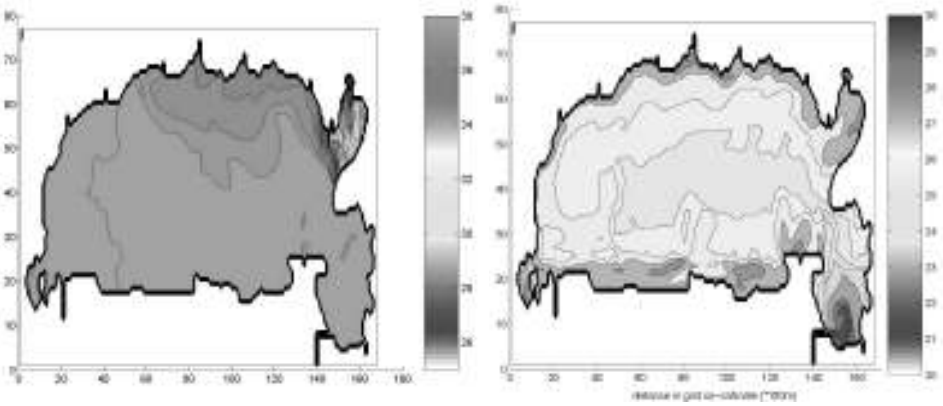

Figure 3 Salinity (left) and temperature (right) surface distribution in the Thau lagoon.

4.2 ODON project

The objective of ODON (Optimum Design of Observational Networks) is the development of methods for the design of observing systems in shelf seas and to test these techniques for sea surface temperature and temperature-salinity profiling networks in the Baltic and North Sea. Sample locations are selected from a proxy ocean, representing the "true" state, from simulated data obtained with a high resolution in model grid and boundary forcing. The quality of the sampling strategies will be tested by performing Observing System Simulation Experiments (OSSEs) via the implementation of data assimilation schemes.

The North Sea proxy run using forcing data for the year 2001 is conducted with the updated parallel version of COHERENS and a grid resolution of one nautical mile. Model area, river outflow locations and domain decomposition (for 96 processes) are given in Figure 4. Meteorological surface data at hourly intervals have been supplied by the Danish Meteorological Institute from the HIRLAM model. Tidal harmonics and daily profiles of currents, temperature and salinity are derived from simulations with the POLCOMS model (Proudman Oceanographic Laboratory) covering a larger area.

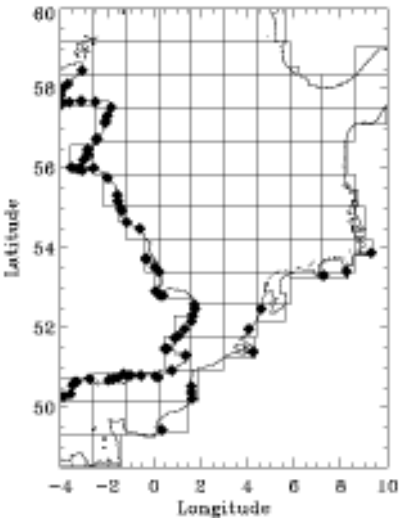

Figure 4 Model area, domain decomposition and locations of river output for the North Sea proxy run.

Baroclinic inflow/outflow conditions are imposed at the eastern boundary to include the exchange of water masses with the Baltic Sea.

Validation of the model data with satellite observations and comparison with a simulation performed using the SST assimilation scheme of Annan and Hargreaves (1999) are further discussed in Ponsar *et al.* (this volume). To illustrate the importance of high-resolution model numerical data, the simulation is repeated with the same forcing now using a coarser resolution of four nautical miles. Time series of temperature in September–October 2001 at 59°20' N, 1° E for the two runs are compared in Figure 5 with the thermistor data taken at the same location during the PROVESS campaigns (Howarth *et al.*, 2002) for the year 1998. The high vertical oscillations, driven by tidal-

inertial motions, are typical for the North Sea (Luyten *et al.*, 2003) and are clearly only realistically represented in the run with the highest resolution.

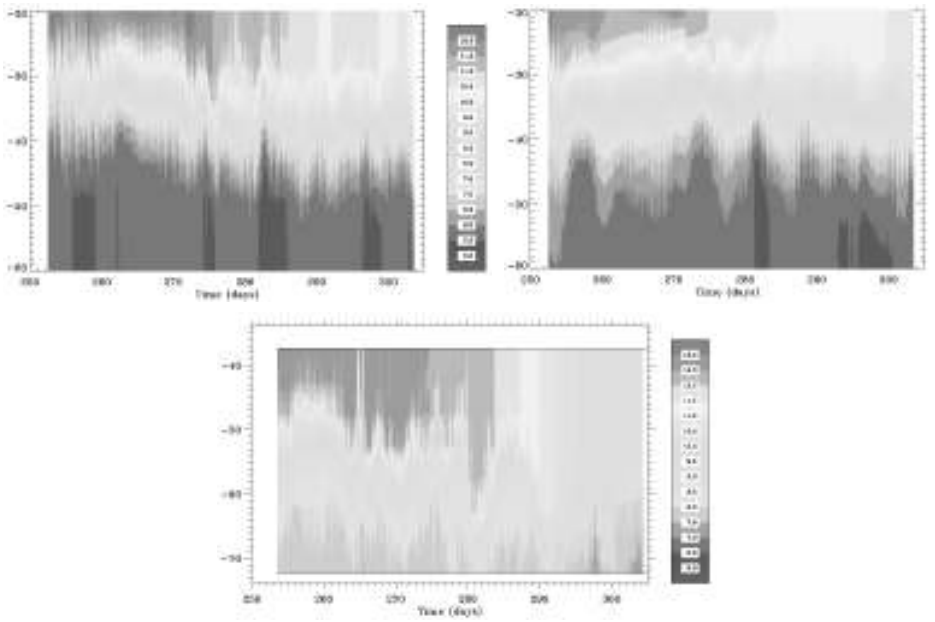

Figure 5 Time evolution of temperature profiles at the PROVESS station (59°20' N, 1° E) according to the model run with 1 n.m. resolution (top left), 4 n.m. resolution (top right) and the 1998 thermistor data of the PROVESS project.

5. Concluding remarks

The success of COHERENS as a public domain code and its world-wide distribution can be attributed to a combination of factors:

- Robustness: Until now, only one real bug had been reported by the user group.
- Portability: Once the code is properly installed and the correct setup has been made, the program should be running properly. Temporary problems may arise for the installation and compilation, but this seems unavoidable in view of the multiple operating systems and compilers available on the market.
- Documentation: A proper user documentation is essential since every instruction or each type of model setup must exactly match with the model's performance and vice versa. Secondly, it can prevent users from setting up the program incorrectly or from starting applications for which the model is not designed.
- Test cases: They are an indispensable tool since they allow users to perform trial runs, soon after installation, without any prior knowledge of the code.

The upgrade of COHERENS is still in progress. The MPI-installation has already been tested on different parallel machines. The Ensemble Kalman Filter will be validated as part of the ODON project. Experienced users of the old model code offered assistance for debugging and testing of the new one. Its final release is expected in the year 2006.

Acknowledgements

The DITTY and ODON projects are funded by the European Commission through contracts no. EVK−CT−2002−00084 and EVK3−CT−2002−00082. We wish to thank Dimitar Marinov (Joint Research Centre, Ispra, Italy) for providing the figures of the Sacca di Goro simulation.

References

Annan, J.D. and J.C. Hargreaves (1999). Sea surface temperature assimilation for a three-dimensional baroclinic model of shelf seas, Continental Shelf Research, 19, 1507−1520.

Canuto, V.M., A. Howard, Y. Cheng and M.S. Dubovikov (2001). Ocean turbulence. Part I: One-point closure model — Momentum and heat vertical diffusivities, Journal of Physical Oceanography, 31, 1413−1426.

Evensen, G. (2003). The Ensemble Kalman Filter: theoretical formulation and practical implementation, Ocean Dynamics, 53, 343−367.

Evensen, G. (2004). Sampling strategies and square root analysis schemes for the EnKF, Ocean Dynamics, 54, 539−560.

Howarth, M.J., J.H. Simpson, J. Sündermann and H. van Haren (2002). Processes of vertical exchange in shelf seas (PROVESS), Journal of Sea Research, 47, 199−208.

Luyten, P.J., J.E. Jones and R.Proctor (2003). A numerical study of the long- and short-term temperature variability and thermal circulation in the North Sea, Journal of Physical Oceanography, 33, 37−56.

Luyten, P.J., J.E. Jones, R. Proctor, A. Tabor, P. Tett and K. Wild-Allen (1999). COHERENS — A coupled hydrodynamical-ecological model for regional and shelf seas: User documentation, MUMM Report, 911 pp.

Marinov, D., A. Norro and J.M. Zaldivar (2005a). Application of COHERENS model for hydrodynamic investigation of Sacca di Goro coastal lagoon (Italian Adriatic shore), Ecological Modelling, submitted.

Marinov, D., J.M. Zaldivar, A. Norro, G. Giordani and P. Viarol (2005b). Integrated modelling in coastal lagoons. Part B: lagoon model Sacca di Goro case study (Italian Adriatic Sea shoreline), EUR Report no. 21558 EN.EC, Joint Research Centre, 90 pp.

Ponsar, S., I. Andreu-Burillo and P. Luyten, (2005). Sea surface temperature assimilation in a high resolution model of the North Sea. This volume page 719.

Song, Y. and D. Haidvogel (1994). A semi-implicit ocean circulation model using a generalised topography-following coordinate system. Journal of Computational Physics, 115, 228−244.

Towards forecast of the NW European Coastal Shelf: benchmarking model performance

J.I. Allen*[1], J.C. Blackford[1], J.T. Holt[2], M. Holt[3], R. Proctor[2] and J.R. Siddorn[3]

[1]*Plymouth Marine Laboratory, UK*
[2]*Proudman Oceanographic Laboratory, UK*
[3]*MetOffice, UK*

Abstract

Marine ecosystem models are becoming increasingly complex and sophisticated, and are being evaluated as short term forecast tools. Currently far too little attention has been, and is generally, paid to model errors and the extent to which model outputs actually relate to real-world processes. Analysing errors within highly multivariate model-outputs, and relating them to even more complex and multivariate observational data, is not a trivial task. Here we describe the application of summary error statistics, to a complex spatio-temporal model run for the period 1988–1989 in the southern North Sea, coinciding with the North Sea Project which collected a wealth of observational data. The techniques allow a simple assessment of model performance over the whole domain.

Keywords: Ecosystem model, ERSEM, POLCOMS, North Sea.

1. Introduction

We live in a rapidly changing environment, and perhaps the greatest challenge of our age is to understand and predict the consequences of changes in, *inter alia*, climate, biogeo-chemical cycles and human resource use, and mitigate the impacts. Ecosystems, by their very nature, are dynamic and change in space, time and composition over a range of scales. To manage human impacts on ecosystems successfully, we need to understand issues of scale and natural variability (Hardman-Mountford *et al.*, 2005). It is also essential to be able to separate anthropogenic impacts from natural fluctuations. Large-scale marine ecosystem models are tools with which we can potentially incorporate this range of variability and the reasons for it, into a management approach. However a systematic analysis of the performance of 153 biological models incorporating plankton demonstrated that the ambitious efforts over the last decade to increase the level of biological detail and spatial complexity and to use longer simulation periods, has not led to a systematic improvement in model performance (Arhionditsis and Brett, 2004). Arhionditsis and Brett (2004) found that only 47% of the models assessed had any validation and only 30% determined some measure of goodness of fit. Consequently, if we are to develop useful modelling tools for the marine environment we need to be able to understand and quantify the uncertainties inherent in the simulations.

The POLCOMS-ERSEM model system is a state-of-the-art coupled hydrodynamic-ecosystem model for shelf seas which has been applied to the North West European Continental Shelf on a 7 km grid. The model is currently being evaluated within an

* Corresponding author, email: JIA@pml.ac.uk

operational framework using operationally available high resolution atmospheric and lateral boundary forcing, allowing hindcast and near-real time nowcast simulations to be performed. In this paper we describe simple metrics which can be used to benchmark overall model performance.

2. Methods

Focusing on a subset of outputs from a model run for which we have appropriate comparative observations from the field, we apply a combination of error statistics, correlations and multivariate analyses in order to explore relationships between model outputs and observations, and the distribution of errors within the model.

2.1 Data sets—simulations and observations

The medium resolution continental shelf (MRCS) model is a hindcasting/forecasting system being developed by POL, PML and UK Met Office. It is based on a coupled 3D hydrodynamic and ecosystem model (POLCOMS-ERSEM; Allen *et al.*, 2001, Holt *et al.*, 2004), set up on a ~7 km grid with boundaries following the North-West European Continental Shelf break. Boundary forcing for temperature, salinity, currents and sea surface elevation are obtained from the 12 km Atlantic Margin Model, which is nested in the FOAM system (Bell, 2000). The model includes the density evolving physics of POLCOMS (Holt and James, 2001) and a size-fractionated SPM sub-model (Holt and James, 1999), coupled with the state-of-the-art biogeochemical processes of ERSEM (Blackford *et al.*, 2004; Baretta *et al.*, 1995).

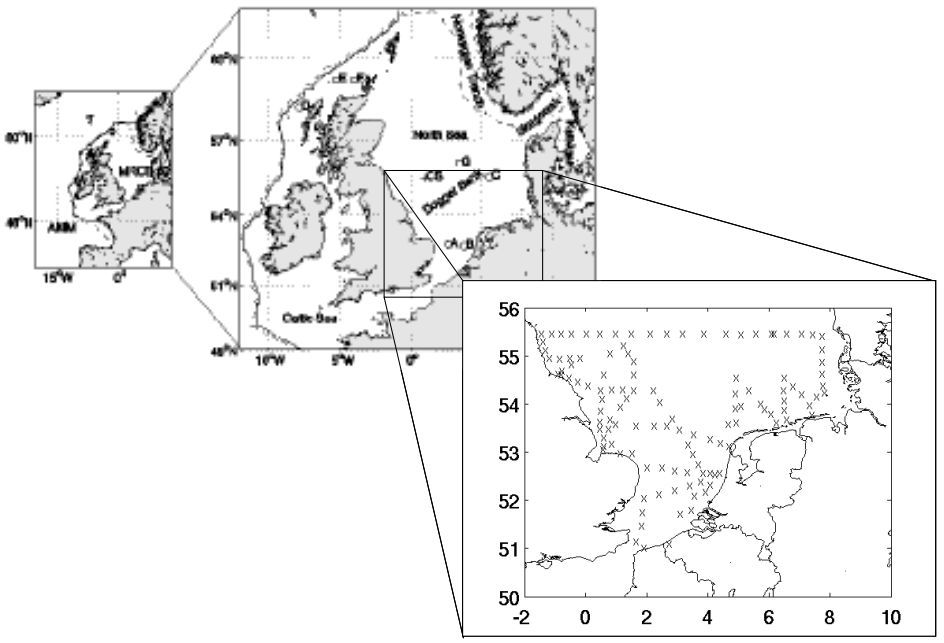

Figure 1 The Medium Resolution Continental Shelf (MRCS) model domain. Also shown is the sub-domain of the MRCS analysed using the SOM which includes the NSP survey stations.

The North Sea community project (NSP, Charnock *et al.*, 1994) collected a wealth of observational data from the southern North Sea in 1988 and 1989, and this is the period that we choose to simulate. The model domain and the area sampled during the NSP, on which our analyses focus, are shown in Figure 1. Further details of the simulations of 1988/89 analysed here are described in Holt *et al.* (2005). Data, including temperature, salinity, chlorophyll, nitrate, phosphate, ammonia, silicate and suspended sediment, were collected at ~120 CTD and water-sampling stations during each of 16 monthly NSP cruises between August 1988 and October 1989 (~1600 stations in total). Naturally, there are large variations in the quantity and quality of data for assessing the various model variables. However, there are data to verify many variables in the ecosystem model and all elements of the physics model, apart from the turbulence variables.

2.2 Error statistics

We consider the direct like-with-like comparison of model and data in space and time with conventional correlation statistics along with measures of model efficiency and bias. In the following D are the observational data, $\overline{D}$ the mean of the observational data and M the corresponding model estimates.

The Nash Sutcliffe Model Efficiency (*ME*) is a measure of the ratio of model error to variability in observational data. It is commonly used to assess the performance of river catchment models which have similar temporal variability characteristics (rapid increases and decreases) to phytoplankton. It is calculated as

$$ME = 1 - \frac{\sum (D - M)^2}{\sum (D - \overline{D})^2}$$

The squaring of the error rewards a good fit and punishes a poor fit. Performance levels are categorised as: >0.65 excellent; 0.65−0.5 very good; 0.5−0.2 good; <0.2 poor (Marechal and Holman 2004).

3. Results and discussion

Rigorous validation of these simulations has been reported for the hydrodynamics (Holt *et al.*, 2005), the biogeochemistry (Allen *et al.*, submitted) and zooplankton (Lewis *et al.*, in prep). They indicate that the model has short term hindcast skill for: temperature, salinity, currents, tidal components, potential energy anomaly, and nutrients. Additionally they suggest seasonal hindcast skill for chlorophyll and ability to capture the spatio-temporal variability of phytoplankton and zooplankton from the Continuous Plankton Survey. Consequently we have a large quantity of different type's validation information on the model, but no simple overall measure of model performance.

We have taken a direct model:data comparison in space and time for all the temperature, salinity, chlorophyll, nitrate, phosphate, ammonia, silicate and suspended sediment data in the NSP and used it to calculate simple metrics of model performance for each variable (square of the correlation coefficient (R^2) and the slope of the best fit line (S), model efficiency (*ME*) and ratio of standard deviation of the model and data (*RSD*). Plotting R^2 against S gives a simple representation of model performance (the closer R^2 and S are to 1 the better the fit; Figure 2). This clearly shows that the model has skill for

temperature, salinity, nitrate and phosphate, and is confirmed by the model efficiency values. Plotting *ME* against *RSD* (Figure 3) gives an alternative representation. *RSD* give a measure of whether the model matches the variance of the data and *ME* indicates whether the variability of the model data mismatch is smaller than the variability of the data, the ideal values being 1 in both cases. Once again it demonstrates that the model has skill for temperature, salinity, nitrate and phosphate. It also suggests that for SPM, silicate and chlorophyll the model:data mismatch is of the same order as data variability (*ME*), the bare minimum criteria for model performance. The model clearly underestimates the variance of chlorophyll and silicate, both of these are systematically underestimated in the coastal regions of the model due to poor representation of the optical environment in the model (Allen *et al.*, submitted) and underestimation of the freshwater silicate loads. The model clearly has no skill for ammonia suggesting the parametrisations of its biological production, nitrification and denitrification processes require further work.

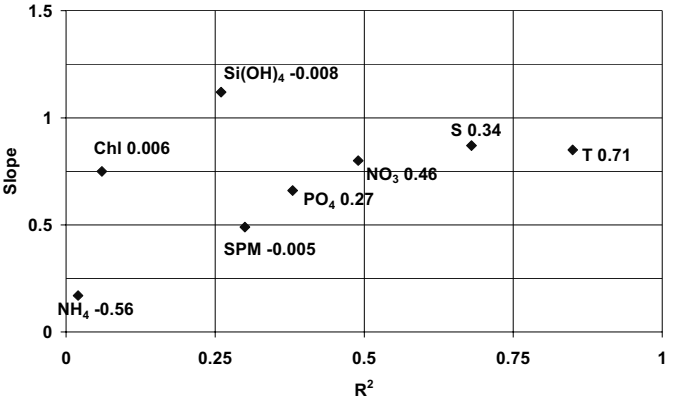

Figure 2 Summary diagram of overall model performance: Model efficiency plotted against the ratio of observed to modelled variance.

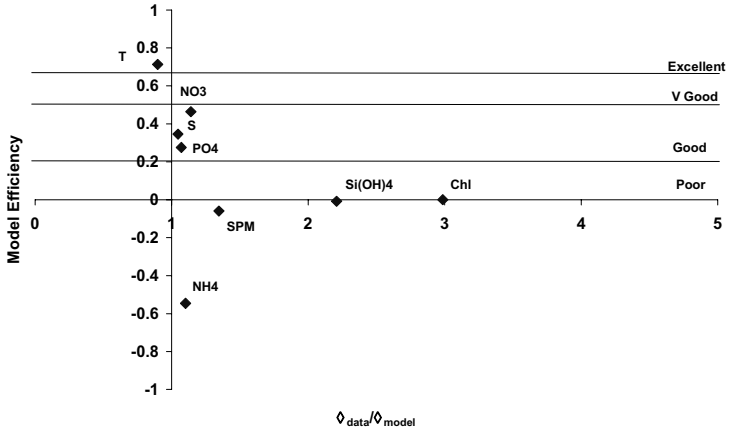

Figure 3 Summary diagram of overall model performance: Model efficiency plotted against the ratio of observed to modelled variance.

4. Conclusions

Clearly there is a need to define minimum performance levels for models, particularly those used in policy-relevant situations. Establishing natural levels of variability within and between marine ecosystems is a necessary prerequisite to rigorous model validation, and requires data collection which takes into account the issues of time, space and scale. Uncertain metrics need to be fit for purpose. These plots provide a simple overview of model performance and could be used as a benchmark to assess the success of alterations to the model. We should however caution that these metrics are a summary and not a substitute for the detailed analysis of model performance required to gain insight into process descriptions. In this study we have deliberately chosen to be unforgiving by making a direct model:data comparison in space and time, with no tolerance for errors in, for example, the time of a bloom or the depth of the thermocline. As these models are being evaluated for their short-term operational forecast potential this is the right thing to do, and the model does well in terms of hindcast performance for temperature, salinity, nitrate and phosphate.

Acknowledgements

This work was funded in part by the EC-MERSEA Integrated Project.

References

Allen, J.I., P.J. Somerfield and F.G. Gilbert (2005). On the quantification of uncertainty in high-resolution coupled hydrodynamic-ecosystem models. J. Mar. Sys. submitted.

Allen, J.I., J. Blackford, J. Holt, R. Proctor, M. Ashworth and J. Siddorn (2001). A highly spatially resolved ecosystem model for the North West European Continental Shelf. Sarsia 86: 423–440.

Arhonditsis, G.B. and M.T. Brett (2004). Evaluation of the current state of mechanistical aquatic biogeochemical modeling. Mar. Ecol.Prog. Ser. 271: 13–26.

Baretta, J.W., W. Ebenhöh and P. Ruardij (1995). The European Regional Seas Ecosystem Model, a complex marine ecosystem model. Neth. J. Sea Res. 33: 233–246.

Bell, M.J., R.M. Forbes and A. Hines (2000). Assessment of the FOAM global data assimilation system for real-time operational ocean forecasting. J. Mar. Sys., 25, 1–22.

Blackford, J.C., J.I. Allen and F.G. Gilbert (2004). Ecosystem dynamics at six contrasting sites: a generic modelling study. J. Mar. Sys. 52, 191–215.

Charnock, H., K.R. Dyer, J.M. Huthnance, P.S. Liss, J.H. Simpson and P.B. Tett (Eds) (1994). Understanding the North Sea System. The Royal Society, Chapman and Hall, London, 222 pp.

Hardman-Mountford, N.J., J.I. Allen, M.T. Frost, S.J. Hawkins, M.A. Kendall, N. Meiszkowska, K.A. Richardson and P.J. Somerfield (2005). Diagnostic monitoring of a changing environment: An alternative UK perspective. Mar. Poll. Bull. (in press).

Holt, J.T., R. Proctor, J.C. Blackford, J.I. Allen and M. Ashworth (2004). Advective controls on primary production in the stratified western Irish Sea: an eddy resolving model study. J. Geophys. Res. 109(C05024): doi: 10.1029/2003JJC001951.

Holt, J.T., J.I. Allen, R. Proctor and F.G. Gilbert (2005). Error quantification of a high resolution coupled hydrodynamic-ecosystem coastal ocean model: part 1 Model overview and hydrodynamics. J. Mar. Sys. (in press).

Holt, J.T. and I.D. James (2001). An s-coordinate model of the North West European Continental Shelf. Part 1 Model description and density structure. J. Geophys. Res. 106(C7): 14015–14034.

Holt, J.T. and I.D. James (1999). A Simulation of the Southern North Sea in comparison of measurements form the North Sea Project. Part 2: Suspended Particulate Matter. Cont. Shelf Res. 19: 1617–1642.

Lewis, K., J.I. Allen and A.J. Richardson (In preparation). On the use of CPR data for the validation of complex ecosystem models.

Maréchal, D. and I.P. Holman (2004). Regionalisation of a conceptual catchment-scale hydrological model for England and Wales. Hydrol. Process. Submitted.

MarineXML — Have we achieved pre-standardisation?

Keiran Millard*[1], Rob Atkinson[2], Andrew Woolf[3], Roy Lowry[4], Pieter Haaring[5], Francisco Hernandez[6], Torill Hamre[7], Dan Pillich[8], Holger Bothien[8], Ward Vanden Berghe[6], Ian Johnson[3], Brian Matthews[3], Hans Dahlin[9], Nic Flemming[9], Vladimir Vladymyrov[10], Bev Meckenzie[11], Alan Edwards[12], Willem van der Hoeven[5], Quillon Harphen[1] and Gill Ross[13]

[1]*HR Wallingford, UK*
[2]*Social Change Online, UK*
[3]*Central Laboratory of the Research Councils, UK*
[4]*British Oceanographic Data Centre, UK*
[5]*RIKZ, The Netherlands*
[6]*VLIZ, Belgium*
[7]*Nansen Environmental Remote Sensing Center, Norway*
[8]*Seven Cs, Germany*
[9]*EuroGOOS, Sweden*
[10]*IOC/IODE*
[11]*UK Marine Information Council*
[12]*European Commission, Belgium*
[13]*UK Met Office*

Abstract

The eXtensible Mark-Up Language (XML) developed by the World Wide Web Consortium can be used to develop a framework that improves the interoperability of data in support of marine observing systems. There have been several initiatives investigating how this can be achieved in practice, but to date there has been no strong direction that the marine community should take. This paper presents the findings of an international project tasked with providing such direction. In particular it provides 'pre-standardisation' advice and justification to the international marine community on the use of XML standards for data interoperability. Importantly this embraces the very broad extent of the marine community, covering the very many disciplines and domain areas that exist. This paper is a subset of a full position paper by the MarineXML initiative on the use of XML for marine data exchange. This paper can be downloaded from the MarineXML website (www.marineXML.net).

Keywords: XML, GML, ISO−TC211, marine data exchange

1. Introduction

The huge diversity of data formats, proprietary data management systems, analysis packages, numerical models and visualisation tools complicate the processing, management and accessibility of marine data. This diversity severely limits the multiple

* Corresponding author, email: k.millard@hrwallingford.co.uk

re-use of data and reduces our access to the data. Additionally the present complexity of accessing and integrating data makes it tedious, often labour-intensive, to generate knowledge of marine processes and risks associated with activities in the marine environment.

Today, the marine community is in a situation where large volumes of data are collected by an increasing number of agencies and scientists for an increasing number of purposes. The desire to build regional or global databases, aggregating data from multiple sources is also increasing. This is evident at the European level through the development of INSPIRE[1] and GMES[2] and at an international level through GEO[3] and GOOS[4]. The need for a common data framework to enable this integration has now become an essential component of building our knowledge of the marine environment. It has been considered that the eXtensible Mark-Up Language (XML) developed by the World Wide Web Consortium can be used to develop such a framework. This would build on the approaches that have been used in other domain areas such as the geospatial (Lake, 2004), chemistry, genetics and finance (Millard, 2003).

MarineXML is an initiative under the governance of the IOC/IODE[5] of UNESCO[6] to improve marine data exchange within the marine community. The European Commission has provided a funding contribution to this initiative as part of its 5th Framework Programme to undertake a 'pre-standardisation' task of identifying the approaches the marine community should adopt regarding XML technology to achieve improved data exchange. This project (MarineXML EC) ran from February 2003 to January 2005. This position paper reports on the findings of this project. Other projects have contributed to MarineXML in this timeframe including the Study Group on XML (SGXML) of ICES/IOC[7], the UK NERC Data Grid Project[8] and the UKHO S-57 GML project[9]. All these projects worked closely together to reach consensus on using XML for marine data exchange. The authors accordingly believe that they have been successful in providing a level of pre-standardisation to inform a route-map towards an extensible framework of standardisation for data exchange in the marine community based on the adoption of ISO[10] and OGC[11] standards.

---

1 www.ec-gis.org/inspire/
2 www.gmes.info
3 http://earthobservations.org
4 ioc.unesco.org/goos
5 International Oceanographic Data and Information Exchange Committee of the International Oceanographic Commission of UNESCO
6 United Nations Education, Scientific and Cultural Organisation
7 www.marineXML.net. ICES/IOC SGXML focused on the issue of parameter dictionaries
8 http://ndg.nerc.ac.uk
9 www.ukho.gov.uk/b2b_gml_home.asp
10 International Organisation for Standardisation (www.iso.org)
11 Open Geospatial Consortium (OGC) (www.opengis.org)

2. Principles for developing an XML framework for marine data exchange

From the research and analysis several principles for an XML-based framework for marine data exchange were established and these are presented in this section.

2.1 Principle 1 — marine data exchange based on ISO19136 (GML Feature Types)

The alignment between ISO and OGC on ISO19136 makes GML the clear (only) choice for developing an XML-based framework for marine data exchange. The adoption of this approach by significant organisations in the marine community such as IHO and WMO also reinforces this.

2.2 Principle 2 — there is no single 'Marine Feature Type'

From the standards review it is clear that it is not possible to have a single 'Marine Feature Type'. Given the diversity of the marine community, what is needed is a mechanism to represent what needs to be exchanged. This was a challenge to early views held by the project on how an XML-based exchange framework could work. Whilst it was accepted that some degree of modularity was required, it was perhaps not conceived how broad this modularity had to be to represent the whole of the marine community.

2.3 Principle 3 — different sub-communities take responsibility for their feature types

The breadth of the marine community means that it becomes wholly impractical for any single organisation, such as IOC, to manage and maintain all the Feature Types that the marine community could require. Different parts and operations of the marine community need to subscribe to their own data standards as these are integral to their operations. These standards are often highly specialised to meet the requirements of particular services, for example the highly specialised feature types for universal exchange of meteorological observations (SYNOPs, METARs, etc.). The definition of such specialised feature types is rightly the domain of international organisations such as the WMO.

2.4 Principle 4 — MarineXML feature type responsibilities

Through its MarineXML initiative, IOC/IODE should act as the authority (registry owner) for the specialist feature types that are central to the marine community and the general purpose feature types for exchange within the marine community (e.g. to enable 'cruise' and 'met observations' to be effectively combined). These general-purpose feature types should be developed in liaison with key organisations in the marine community such as IHO and WMO, not least to combine resources for standards maintenance and update.

2.5 Principle 5 — wrapper for legacy data

The XML based framework should not only encode text-based data as XML, but is also required to provide a wrapper to data that exists or is best delivered by binary encoded files.

3. General purpose feature types for the marine community

Taking account of the above principles, MarineXML looked to develop and test some general purpose Feature Types for data exchange within the marine community. To undertake this activity MarineXML collaborated with the NERC Data Grid Project. This project was investigating the Feature Types necessary for data exchange between the oceanographic and meteorological communities.

This timely collaboration enabled a very rigorous development and documentation of GML Application Schema to encode these Feature Types. The resultant schema at the time of the testbed was referred to as the 'NDG data model', although it is now released as Climate Science Mark-Up Language (CSML) (Woolf *et al.*, 2004a). In addition to modelling various climate science data types, CSML also provides a wrapper mechanism to encapsulate the representation of those data objects in file-based storage artefacts such as NetCDF and GRIBB.

Feature Types in the NDG Data Model are defined primarily on the basis of geometric and topologic structure, and not the semantics of the observable or measurand according to the following principles.

3.1 Offloading semantics onto coordinate reference system

If two features would 'look the same' structurally, apart from the underlying coordinate reference system, then they are modelled as the same feature, e.g. a vertical sounding radar is a sequence of profiles in time with a series of vertical heights as the spatial domain; a scanning radar is a sequence of sloping profiles (at fixed elevation) in time and in azimuth with a series of ranges as the spatial domain. These are modelled as the same feature type, just with a different underlying coordinate reference system.

3.2 Offloading semantics onto physical parameter type

If two features would 'look the same' structurally, apart from the physical parameter type, then they are modelled as the same feature, e.g. a vertical wind-profiler is plotted with wind barbs, while a temperature sounding is plotted as a line — these are regarded as the same feature type, distinguished only by the physical parameter type.

3.3 Sensible plotting as discriminant

A principle to suggest a workable minimum granularity of feature type definition is to use the requirement for 'sensible plotting' as a discriminant, i.e. there should be sufficient detail in, and sufficient difference between, feature types to enable unsupervised 'sensible plotting' by an appropriate piece of software. The Feature Types described by the CSML Model are presented in Table 1 and shown conceptually in Figure 1.

The feature types do not carry any explicit topologic descriptions. For instance, both a scanning radar and a vertical sounding radar are modelled with the same feature type (CSMLProfileSeries). The spatial geometry of the first may be modelled topologically as a series of curves connected at an origin node, while the second is a single curve. Similarly, the topological relationship between a series of marine CTD casts and the associated ship track is left implicit in the CSMLProfileSeries feature type. GML provides rich schemas for describing topology — a requirement may arise in the future to add this information to the CSML Data Model.

Table 1 CSML feature types[1]

CSML feature type	Description	Examples
TrajectoryFeature	Discrete path in time and space of a platform or instrument	Ship's cruise track, aircraft's flight path
PointFeature	Single point measurement	Raingauge measurement
ProfileFeature	Single 'profile' of some parameter along a directed line in space	Wind sounding, XBT, CTD, radio-sonde
GridFeature	Single time-snapshot of a gridded field	Gridded analysis field
PointSeriesFeature	Series of single datum measurements	Tidegauge, rainfall timeseries
ProfileSeriesFeature	Series of profile-type measurements	Vertical or scanning radar, shipborne ADCP, thermistor chain timeseries
GridSeriesFeature	Timeseries of gridded parameter fields	Numerical weather prediction model, ocean general circulation model

[1]From Woolf *et al.*, 2004b

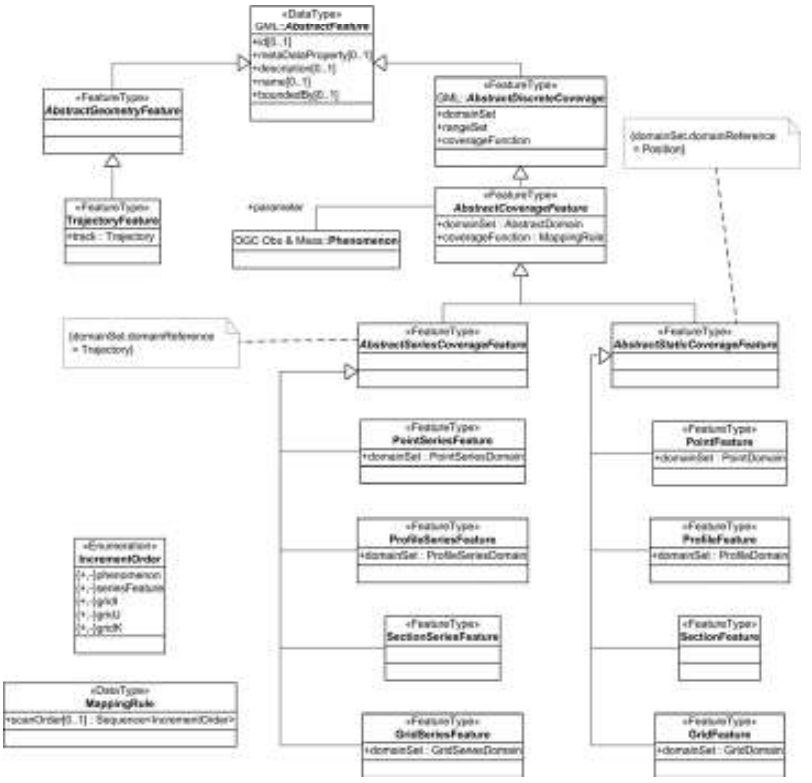

Figure 1 Conceptual model of CSML feature types.

Using CSML for marine data exchange was examined as part of a testbed and was found to both perform well and could easily be applied. This testbed looked at the interchange

of biological sampling data, gridded products from satellites, modelled hydrodynamics, measured hydrodynamics and hydrographic data in navigation charts. (Millard *et al.*, 2005; Pillich *et al.*, 2005).

4. Conclusions

MarineXML is an initiative of the IOC/IODE of UNESCO to improve data exchange within the marine community. The European Commission has provided a funding contribution to this initiative to undertake a 'pre-standardisation' project on the approaches the marine community should adopt regarding XML technology. We believe that the results from this project are sufficient to claim that this pre-standardisation has been achieved.

Firstly, the alignments between OGC (Open Geographic Consortium) and ISO on the development of a reference standard for feature type encoding using XML means that many communities in the broad marine domain are now considering the deployment of data standards based around Feature Type catalogues. This includes key communities such as the IHO and the WMO. Accordingly any deployment in the marine domain needs to be based on this model.

Secondly the project demonstrated how weakly-typed (i.e. generic) feature types represented as GML application schema can provide an effective interchange between the data formats used across the marine community. This includes the communities engaged in physical and biological oceanography, numerical modelling and remote sensing.

Taking this platform as point of departure, MarineXML has provided a number of next steps to be taken to ensure the wider adoption of open exchange standards for marine data and has identified resources to undertake them. Our continued aim is for the deployment of marine services that are not limited by the short-term technical considerations of users and providers.

References

Lake, R. (2004). Geography Mark-Up Language — Foundation for the Geo-Web, Wiley, ISBN 0–470–87154–7.

Millard, K. *et al.* (2003). MarineXML — using XML technology for marine data interoperability Proceedings of The Colour of Ocean Data, IOC Workshop Report No 188, VLIZ Special Publication No 16 Brussels, Belgium 25–27 November 2002 pp163–175.

Millard, K. *et al.* (2005). Using XML Technology for Marine Data Exchange. A Position Paper of the MarineXML Initiative. Download from www.marineXML.net.

Pillich, D, H. Bolthien, P. Haaring and Q. Harphen (2005). Testbed demonstration of marine data exchange through GML application schema. Deliverable D10 of the MarineXML project, www.marineXML.net, MarineXML_D10_Draft8.pdf, 11/04/05.

Woolf *et al.*, (2004a). Climate Science Modelling Language: Standards-Based Markup For Metocean Data, Proceedings of the American Met Society 85th annual meeting in San Diego 10–13 Jan. 2004.

Woolf, A. (2004b). Climate Science Mark-Up Language, Users Manual, v1.0, http://ndg.nerc.ac.uk/csml.

Modelling coastal dynamics in the Gulf of Lions: Effect of grid resolution

C. Langlais*[1,2], B. Barnier[1], J.M. Molines[1] and P. Fraunié[2]

[1]*LEGI, Université J.Fourier, Grenoble, France*
[2]*LSEET-LEPI, Université du Sud Toulon Var, La Garde, France*

Abstract

Fluxes across ocean shelves are dominated by complex coastal dynamics. In the Mediterranean Sea, the circulation is driven by a combination of factors operating at different but often related time scales. More precisely, in the Gulf of Lions, mixing and dispersion are dominated by interactions between freshwater dynamics associated with the large Rhône river discharge, coastal upwellings and the North Mediterranean shelf current. To find out how these processes operate and interact, a regional model of the Gulf has been integrated. The model is based on the primitive equation NEMO code, with two different resolutions: 1/16° (~5 km) and 1/64°(~1 km). Our analysis focuses on the mesoscale variability of the coastal circulation and especially on the North Current which acts either as a barrier when flowing along the shelf break or as an efficient flushing system when intruding the Gulf of Lions.

Keywords: Gulf of Lions, coastal dynamics, modelling

1. Introduction and method

The variability of the Mediterranean Sea has been studied intensively in the past twenty years and more recently projects focus on exchanges between coastal and open ocean. To know how coastal processes operate and interact, we use a model of the Gulf of Lions (GoL) based on the NEMO code (see section 2). The main objectives of the paper are to evaluate the modelling ability of the code in coastal areas and the relevance of the forcing used. The second section of this paper is a description of the main circulation features of the GoL and of the numerical model. The third section is an overview of the model representation of the physical processes in play in the GoL.

2. Gulf of Lions

2.1 Description

The GoL is an extended continental shelf located in the north western part of the Mediterranean Sea. Between Toulon (France) and Cap Creux (Spain), the shelf slope constitutes a long open boundary towards the deep adjacent basin and is broken by abrupt canyons (Figure 1). In a microtidal sea, the shelf circulation is mainly driven by the atmospheric forcing. Dominant winds are the strong north-western winds (Mistral and Tramontane channelled by the surrounding orography), and the southeastern offshore winds. The Rhône River discharge is the main fresh water input with a mean

* Corresponding author, email: clothilde.langlais@lseet.univ-tln.fr

flow rate of 1700 $m^3 s^{-1}$. On the shelf (Figure 1), due to the semicircular shape of the gulf and the coriolis force, the continental winds generate coastal upwellings, downwellings and inertial current. The general circulation is dominated by a cyclonic along slope current, the Northern Current (NC) (Millot, 1990). This strong geostrophic current forms the northern branch of the general circulation of the western Mediterranean Sea basin. In winter, there are also occasional events on the shelf: dense water formation which can be associated with cascading. In the GoL, mixing and dispersion of water masses are dominated by the interactions between these different processes.

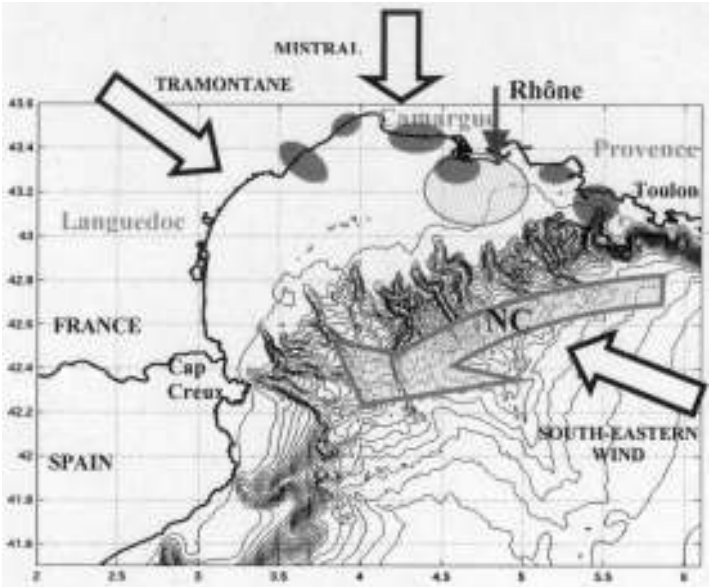

Figure 1 Gulf of Lions hydrodynamic processes: the North Mediterranean Current (NC, grey arrow), the freshwater Rhône river inflow (clear oval), coastal upwellings (dark ovals).

In this complex coastal area, the short-term variability is connected to the mesoscale and seasonal time-scales. The wind drives the high frequency coastal dynamics variability, acting at time scales of a few hours on the river plume dynamics and a few days on the upwelling/downwelling. Coastal hydrology and the NC structure are dominated by low frequency seasonal variability.

2.2 NEMO model

To know how the coastal processes operate and interact, a regional model of the GoL has been elaborated using the NEMO code (i.e. the most recent version of the OPA model, Madec *et al.*, 1998). It is a three-dimensional primitive equation model, with a free surface formulation and Z levels in the vertical. A turbulent kinetic energy equation is used for the turbulent closure. A leapfrog scheme is used for time stepping. In the coastal model, the free surface formulation is usually combined with a time-splitting method, but in NEMO an original filtering method of the barotropic gravity waves is used (Roullet and Madec, 2000), which is suited for microtidal seas. Generalised "terrain following" coordinate systems are often used in coastal areas. However, Z levels with

partial step topography can be a suitable alternative when a high number of vertical levels is used, and this alternative is explored here. A new formulation of the river inflow has been developed for NEMO which treats the freshwater inflow as an open boundary, specifying salinity, temperature and velocity. The frequency of the forcing is really significant in coastal areas. The atmospheric forcing is provided every 6 hours by ERA40 (ECMWF's most recent re-analysis at 1.125° resolution) and applied with bulk formulae. Conditions at the limits of the regional model are handled with radiative open boundary conditions. Boundary data are provided every 5 days by the global 1/16° Mediterranean Sea model of the operational oceanography centre MERCATOR-Ocean. Daily Rhône river inflow values have been obtained from the Companie National du Rhône.

2.3 Configurations

For the study, two configurations have been developed with two different horizontal and vertical resolutions. GDL16 has an horizontal resolution of 1/16° (5 km) and 36 vertical levels, and GDL64 1/64° (~1 km) and 130 vertical levels. The increase in horizontal resolution allows the representation of the bathymetry to be improved, especially the canyons and the shore line. An increase of the number of vertical levels from 36 to 130 gives a resolution of 1 metre at the surface and of no more than 30 metres near the bottom.

3. Results

3.1 Rhône river plume

The Rhône river freshwater input influences the sea surface dynamic relatively far away from the mouth. The few metres thickness of the plume and the complex front dynamics make the simulation of the river inflow a difficult challenge.

Figure 2 compares the outputs of the two configurations with the output of a 2D meso-scale hydrostatic model used by Arnoux (1998) and dedicated to plume modelling. A better resolution limits the numerical diffusion and improves the salinity gradients between the plume and the adjacent water. In particular the high vertical resolution significantly improves the vertical structure: the fresh layer is thinner and the shape of the south extent approaches the typical vertical isohaline structure associated with a more diffuse part at the bottom of the plume.

3.2 Wind-driven upwellings

Under north-western wind conditions, vertical pumping of cold water is generated and coastal upwellings appear along the coasts of Camargue and Provence. The phenomenon displays large spatial and temporal variability. The location of isolated upwelling cells is controlled by the shape of the coastline (Millot and Wald, 1980) and the temporal variability is controlled by the wind. In GDL16, the cold areas are too wide and homogeneous, whereas in GDL64 the phenomenon displays the observed spatial variability with source points and filaments. If we compare GDL64 upwelling events with the schematic representation of Millot (1990) (Figure 3), the surface circulation is correctly simulated, but the discrete distribution of cold waters is not always perfect.

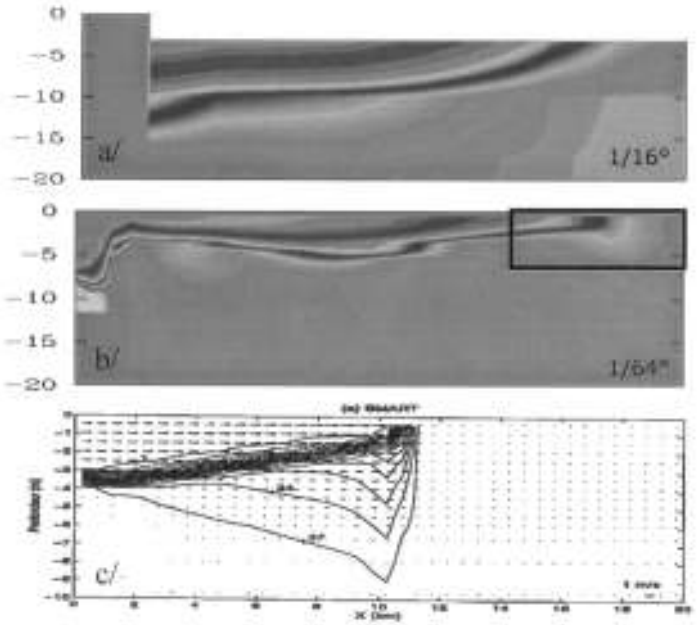

Figure 2 Vertical salinity section across the river plume: a) GDL16; b) GDL64; c) salinity and velocity field of a 2D plume obtained with a meso-scale hydrostatic model (Arnoux, 1998).

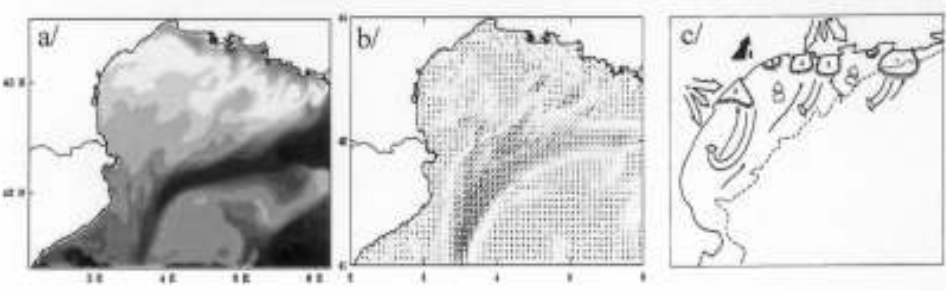

Figure 3 Upwelling event: a) surface temperature field, b) surface velocity field, c) schematic representation of Millot (1990).

Actually, upwellings along the north-eastern coast of the Gulf are influenced by the Mistral, and the upwelling south of Cap d'Agde is due to Tramontane. Because of the 1.125° resolution of the wind forcing, Mistral and Tramontane are not distinguishable from each other in ERA40. We compare in Figure 4 the ERA40 wind field (about 100 km resolution) with that from the ALADIN model (10 km resolution). Clearly ALADIN winds are able to separate the various wind patterns with more accuracy.

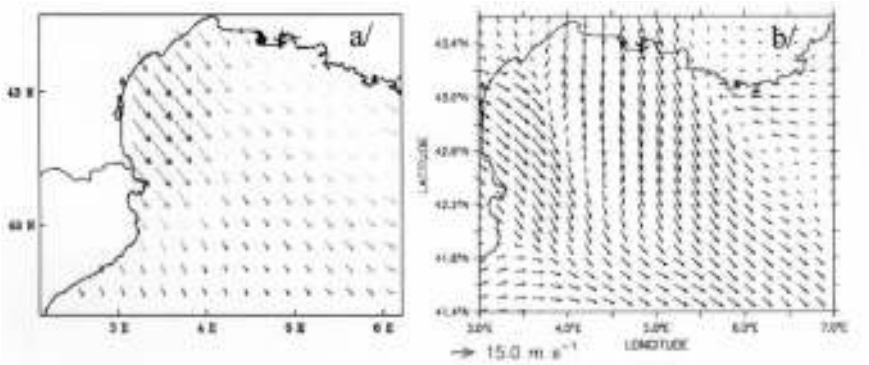

Figure 4 Continental wind field: a) ERA40 wind, b) ALADIN wind.

3.3 North Current mesoscale variability and intrusions

The NC is far from being a steady current, and its variability occurs over a wide range of scales, from a few weeks to seasonal and interannual. The analysis focuses here on the mesoscale variability. Mesoscale measurements are more frequent in winter when the NC is close to the coast (Petrenko, 2003) and feels the influence of the bottom topography. The unstable current generates meanders with an amplitude of 10–20 km and a wave length which varies widely (between a few tens to a few thousand km, Flexas, 2002). Their typical phase speed is about 10–20 km/day (Millot, 1999). GDL16 does not reproduce this variability (Figure 5a). In GDL64 the growth and propagation of meanders is observed (Figure 5b) with a mean amplitude of 13 km, and a wave length of about 50 km. We also observe anticyclonic eddies on the north side of the shelf current. The eddies are associated with large meanders, they grow near Marseille and the Grand Rhône canyon and drift in the main stream along the shelf break until the Lacase Duthiers canyon.

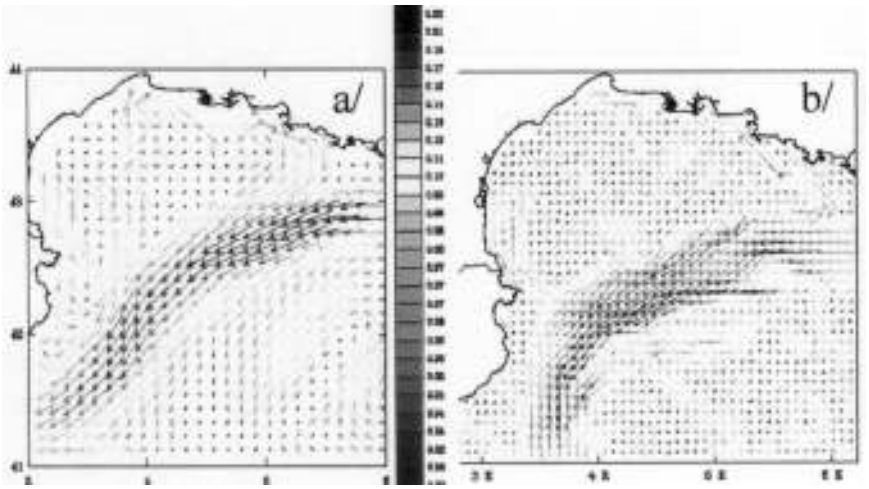

Figure 5 velocity field at 25 m: a) GDL16, b) GDL64.

Flowing along the continental slope, the NC sometimes splits in two branches, one of which enters the GoL to participate in the impoverishment of the Gulf ecosystem. This behaviour is still not well understood and occurs along the whole continental break: near the entrance of the Gulf, in the middle and near the Lacaze Duthier canyon. At the entrance, Millot and Wald (1980) explained it as a relaxation after a mistral event. More recently, Petrenko *et al.* (2003) observed intrusions during the MOOGLI cruises and explained them as bathymetric effects under stratified conditions. In GDL64, those intrusions have been observed, and we have classified then into two types depending on the atmospheric forcing: they occur under low wind conditions after a Mistral or Tramontane, or under East/Southeast wind conditions after a low wind condition. Those two wind situations create intrusions and contribute to on-shelf mixing, differently from the meanders generated near the Grand-Rhône canyon which just create local intrusions.

3.4 Discussion

The above analysis of the physical processes at work in the GoL allows numerical characteristics to be underlined, that are important for the simulation of the region. The 1 km horizontal resolution limits the diffusion, allowing the deformation radius to be solved. The 1 m vertical resolution is necessary for a fine representation of the thermocline and of the plume dynamic, and the Z coordinate system enables a 1 m resolution over the whole domain. The complex continental shelf circulation is influenced by the wind stress curl (Petrenko, 2003), and even if the GDL64 resolution allows the coastal upwelling development, the high spatio-temporal variability of the phenomenon is still not represented with ERA40 forcing fields due their coarse resolution. In the future, the atmospheric forcing will be provided by the REMO hourly re-analysis, which covers the period 1980–2000 at 18 km resolution.

4. Conclusions and perspectives

This work in a coastal area with the NEMO code is part of the MERCATOR project which is engaged in large European projects MERSEA and EuroGOOS. The objective is to study fluxes across the GoL shelves which are dominated by complex coastal dynamics. The first GDL64 results illustrate the ability of NEMO in this coastal area. We shall pursue the analysis of the different components of the coastal circulation, in particular the shelf circulation and the dense water formation on the shelf. The next stage will be to carry out 10 years of simulation (1990–2000) with the REMO meteorological forcing. Analyses of this simulation will aim to improve understanding of the effects of bathymetry, atmospheric forcing and stratification on the NC instabilities and analyse the interactions between the NC and the shelf circulation.

Acknowledgements

We acknowledge the support from the GMMC national programme and from the IDRIS national centre for computational resources.

5. References

Arnoux-Chiavassa, S. (1998). Modélisation d'écoulement côtiers stratifiés présentant des fronts: application au panache du Rhône. Thèse de doctorat de l'université de Toulon et du Var.

Flexas, M., X. Durrieu de Madron, M.A. Garcia, M. Canals and P. Arnau (2002). Flow variability in the Gulf of Lions during the MATER HFF Experiment (March–May 1997). J.Mar.Syst., 33–34 197–214.

Madec, G., P. Delecluse, M. Imbard and C. Lévy (1998). OPA 8.1 Ocean General Circulation Model, reference manual, Notes du Pôle de Modélisation 11, Institut Pierre Simon Laplace, Paris.

Millot, C. and L. Wald (1980). The effect of the Mistral wind on the Ligurian current near Provence. Oceanologica Acta, 3, 399–402.

Millot, C. (1990). The Gulf of Lions' hydrodynamics. Continental Shelf Research, 10 (9–11), 885–894.

Millot, C. (1999). Circulation in the Western Mediterranean Sea. Journal of Marine Systems, 20, 423–442.

Petrenko, A.A. (2003). Variability of circulation features in the gulf of Lion NW Mediterranean Sea. Importance of inertial currents. Oceanologica Acta 26 323–338.

Roullet, G and G. Madec (2000). Salt conservation, free surface and varying levels: a new formulation for ocean general circulation models. J. Geophys. Res., 105, 23,927–942.

Design, manufacture, servicing and usage of FerryBox systems

Justin Dunning* and Stephen Hand

Chelsea Technologies Group, UK

Abstract

FerryBox is a European funded project designed to gain better understanding of water quality over both temporal and spatial scales. In order to achieve this, sensors in flow-through systems have been fitted to eight routinely operating European ferries. The data sets obtained will provide a comprehensive source for assessment of long-term trends in coastal water systems and aid the development of operational and ecological models on water transport and environmental parameters. The Chelsea Technologies Group has been providing Ferrybox type equipment to both the military and civil markets for over 20 years and can demonstrate how these systems have evolved to meet both scientific and survey requirements, developing and utilising key technologies as they have become available.

Examples are presented of early systems which store data to local dataloggers, progressing to the latest systems available which provide data transmission from ship to shore. Servicing of these systems is a key issue to their successful operation, and methods adopted to reduce service intervals are discussed. Challenges such as biofouling of such systems are addressed, and a number of solutions which are currently being adopted are presented. Examples of different data presentation methods and styles along with their respective merits are discussed. Examples of Ferrybox data are presented, and their value to different stakeholders, including scientists, monitoring agencies, surveyors and educators are identified. It will be demonstrated how such data is directly addressing the needs of European Environmental legislation. Investment issues of such systems are also addressed, including how public outreach using the data generated can be used as a catalyst to contribute funding and goodwill from ferry companies.

Keywords: FerryBox, *in situ* monitoring, fluorimeter, biofouling, sea-surface monitoring system, ferry operators

1. Introduction

The Chelsea Technologies Group (CTG) are involved in the development of opto-electronic instrumentation mainly for environmental monitoring and Life Science applications, but also work in both the offshore and process engineering sectors. More recently expertise has been acquired in acoustic transducer design and a full range of hydrophones and projectors are now also offered.

CTG are generally more associated with *in situ* fluorimeters, offering a range of underwater fluorimeters mainly for the measurement of chl *a*, and more recently for the actual analysis of photosynthesis within water systems. The original Aquatracka was a devel-

* Corresponding author, email: jdunning@chelsea.co.uk

opment from joint work with what was formerly the Institute for Oceanographic Sciences (IOS), now the National Oceanography Centre, Southampton.

CTG are also associated with towed undulating vehicles, after working with IOS on the SeaSoar and with Plymouth Marine Laboratory on both the AquaShuttle and more recently the NuShuttle.

2. Past flow-through systems

In the past CTG have designed and supplied a number of flow-through water monitoring systems for both military and environmental monitoring applications. This included the Sea-Surface Monitoring System for the UK Ministry of Defence, which allowed the Subpack, a multisensor package designed for operation on the Navy's submarine fleet, to be operated on a surface vessel. The Sea-Surface Monitoring System (SSMS) (Figure 1) consisted of salinity, temperature, chl *a* fluorescence, hydrocarbon fluorescence, Gelbstoffe fluorescence, and bioluminescence sensors. The system also included a De-aeration System and Laminar Flow System, and was deployed successfully in many regions including Arctic and Mediterranean waters.

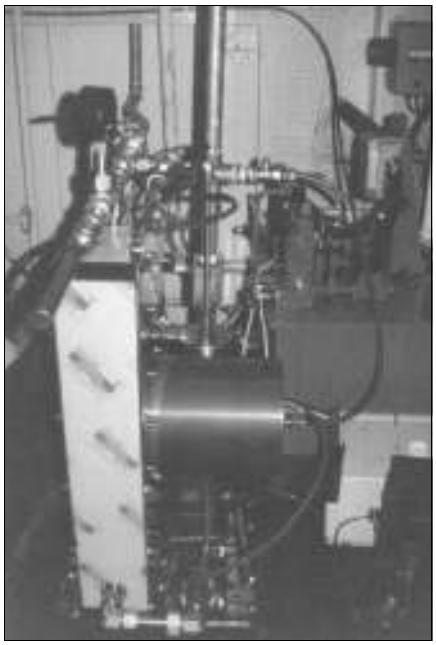

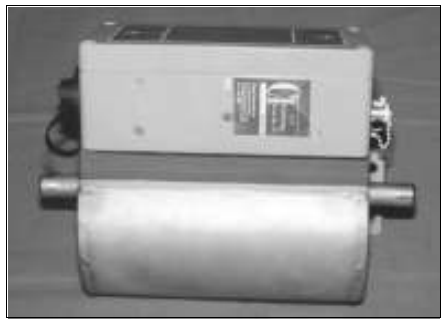

Figure 1 (left) The Sea-Surface Monitoring System. Developed for the UK MOD.

Figure 2 (above) The CT Flowcell. Operated on UK fisheries vessels.

A smaller system was also developed for what was the Ministry of Agriculture, Food and Fisheries (MAFF), now the Centre for Environment Fisheries and Aquaculture Science (CEFAS), which used conductivity and temperature sensors as used on what was the Chelsea AquaPack, an *in situ* conductivity, temperature, depth and fluorescence logging unit. The flow cell itself (Figure 2) was a titanium fabrication, which needed to avoid dead space where possible, yet be large enough for the titanium wall not to interfere with the inductive conductivity head. A number of these units were operated by MAFF on their own vessels for many years.

CTG had also developed a flow-through unit which accommodated the AquaPack CTD-F and other *in situ* instruments to allow these instruments to be easily fitted and removed, to provide deployment flexibility offering the user either *in situ* or flow-through mode. This system was supplied to the UK Environment Agency who operated this system on one of their coastal vessels.

3. Current FerryBox Instrumentation

The CTG range of *in situ* instruments had been updated with the arrival of the MiniPack CTD-F, the successor to the AquaPack CTD-F. The unit is small and offers high performance, and was considered at an early stage for adaptation into a flow-through system. It has the capability of accepting a large number (16) external analogue sensors and can be used as either a real time or internal recording device. The specification, although not WOCE, is still of a high standard and covers the demands of coastal and ocean monitoring. This unit takes the role of the hub of any other instrumentation system, and takes in a large number of other analogue sensors.

The onboard fluorimeter can be configured in factory to measure a variety of different fluorophors. Generally the on-board fluorimeter on the MiniPack is configured to detect chl *a*. If further fluorophors are required in a system, a Minitracka II can be supplied and connected.

There are certain benefits gained from adapting *in situ* sensors for flow-through operations. As they are designed for *in situ* operation, they are robust which is an advantage when they are to be fitted within engine rooms of commercial ferries. By careful design of flow manifolds, the heads of the sensors themselves can be easily exposed for checking and cleaning. They also do not have to be dedicated solely to flow-through operation, but can be used for *in situ* operation when required.

4. European Union FerryBox Programme

The EU Framework V funded programme FerryBox (2002–2005) covers three scientific fields: eutrophication, transport of sediments, and stability and transport of water masses. The scientific/technical objectives include cost-effective relevant information, provision of reliable monitoring and management system, and provision of real time data to improve accuracy of numerical models.

The various instrumented ferry routes within the consortium demonstrate that the main interest lies within the North sea and Baltic sea. Two of the ferry routes, the Portsmouth to Southampton P&O ferry and the Southampton to Cowes Red Funnel ferry have been in operation for a good number of years before the European programme.

Project activities involving CTG include

- Inter-calibrations and comparisons of available Ferrybox systems
- Deriving relevant information for monitoring, assessment and scientific understanding
- Providing end-user communities with relevant application information on these systems
- Public outreach presenting information in an informative way

- Offering possibilities to detect environmental impacts on large scales.

Other project activities include

- Collecting data, proving applicability, reliability and operability
- Producing easily acquired, quality controlled, inter-comparable datasets
- Providing validation and ground-truth measurements for remote sensing.

Work has been conducted with the National Oceanography Centre, Southampton on Ferrybox systems for a number of years prior to the commencement of the EU project in 2002. A flow-through manifold for the Minitracka II fluorimeter had been developed, which had mainly been adopted by the water supply companies, and they found these generally worked well. However, when addressing the requirements for the Isle of Wight FerryBox system, there was a clear requirement to try and reduce the dead volume within the flow cell, as this would avoid possibilities of sediment entrapment within the flowcell which would directly affect readings. There was also a requirement from the Ferry companies themselves to maintain a pressure integrity of 10 Bar, for safety reasons. Both these requirements were addressed in the design of a new flow-through manifold for the Minitracka II, and a similar but slightly larger manifold was designed for use with the MiniPack CTD-F.

The four core parameters being measured by all partners within the project include salinity (conductivity), temperature, chlorophyll *a* and turbidity. On the NOC operated Pride of Bilbao (P&O Ferries) vessel, these parameters are being measured by the MiniPack CTD-F and a Minitracka II, configured for measurement of turbidity.

For both these Ferries CTG had provided the instrumentation, and offered the data as a straightforward RS232 signal. NOC's technical team addressed the issues of data transmission from ship to shore, using ORBCOMM, and have also set up a web based system which presents the data in near real time.

One of the key requirements within the project is to offer systems that have relatively low costs of ownership, yet maintain certain standards when it comes to quality of the data itself. Biofouling is a critical issue in all aspects of environmental *in situ* monitoring, and remains a problem when it comes to Ferrybox systems. There are also problems of taking in highly turbid and sometimes contaminated waters within ports. CTG had already developed flush windows for the fluorimeter, both for Minitracka II and MiniPack CTD-F for flow-through systems. Previously, these windows were recessed within the window bezel, to assist in ambient light rejection for *in situ* applications, but this recess allowed sediment entrapment in this critical area. The flush window design has now overcome this, and also allows easier cleaning of the window during maintenance.

Tasks relating to biofouling prevention within the project include:

- Investigating with the view of implementing automatic cleaning systems which will automatically trigger when the ferry enters port
- Developing Secondary Solid Standards which can be easily offered to on board CTG fluorimeters to check levels of biofouling.

CTG are also partners within another EU Funded programme, BRIMON, which is specifically looking into techniques for combating biofouling. Work conducted under

this programme has now provided a number of alternative technologies that can be adopted in biofouling prevention.

5. Commercial FerryBox systems

Future commercial FerryBox systems will need to be flexible to address the many varieties of craft to which they may be fitted. There will also be differing requirements when it comes to such details as data handling. The approach which has been taken within the company is a modular one, not just for sensor selection but also for feature selection.

Some systems will need to offer basic features, where the client's data management requirement simply dictates that the data be recorded locally to memory for subsequent downloading. For example, a system that had been provided to the PNIRO in Murmansk, within the Russian Federation, is operated from a research vessel rather than an actual ferry, and therefore had no requirement for a passenger display. The system entailed the MiniPack CTD-F and Minitracka II, fitted to a standard FerryBox frame which included a flow-through system based on 12 mm bore tubing, with check valve, pressure gauge and isolation valves.

Other systems will require further features in relation to data handling. For systems to be fitted to commercial ferries, data transfer to remote stations is required to avoid regular visits to the system whilst in port. This can be achieved by use of either radio, GSM or satellite communications. FerryBox systems should be capable of simple integration to any of these systems. A recent system developed for the Marine Laboratory Aberdeen (MARLAB) stores the data to a local disk during passage. When the ferry comes into port, a base station receives all data in one transmission automatically. Such a system prevents excessive data transmission costs of continuous transmission during passage.

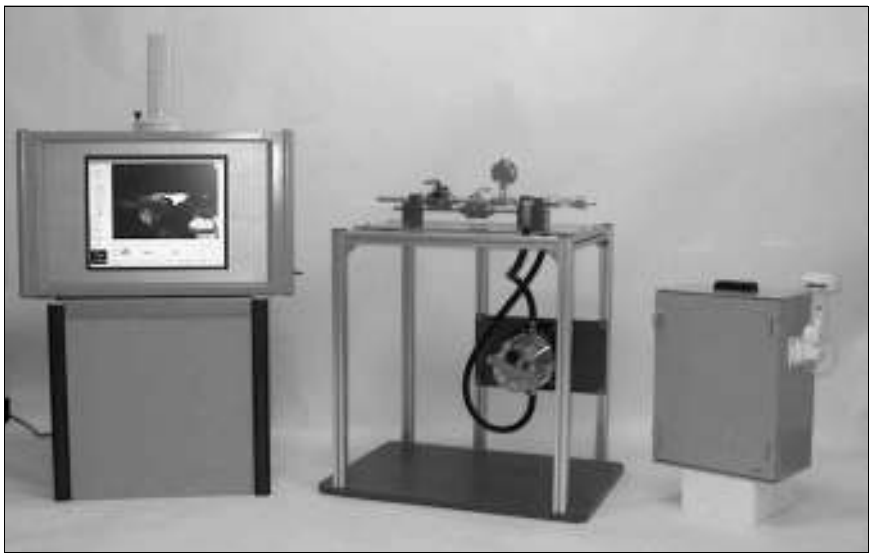

Figure 3 Ferrybox system as delivered to the Marine Laboratory, Aberdeen.

The MARLAB system (Figure 3) also includes a passenger display that shows the ferry passengers where they are on passage and also flicks to a display of oceanographic data taken in real time, and explains the relevance of the data. The exact ferry onto which this will be fitted is as yet to be confirmed, but it is envisaged that it will be from Aberdeen to the Hebrides, and possibly later to Norway.

6. Conclusion

Great interest in FerryBox systems has already been received via the Chelsea network of agents throughout the world, not just for fitment to commercial ferries, but also for fitment to cargo vessels, vacational cruise liners as well as inland waterway vessels. Experience has already shown that ferry companies are willing to work with such systems, providing their maintenance is not onerous and as long as passengers can clearly see the company's commitment to environmental concerns via such facilities as the passenger display. It is important that FerryBox operators continually discuss operations between themselves, as this will assist in further FerryBox routes to be taken up by sharing their experiences in ferry operator relationships. Chelsea Technologies see such systems as offering real value when it comes to costs of environmental monitoring and we plan in the coming months to promote such systems to monitoring authorities, scientists and ferry operators. Through the EU funded programme, we can demonstrate that costs of ownership are attractive against high demands from tight budgets from national governments. These systems offer an attractive solution to the demands now imposed by such drives as the Water Framework Directive and Clean Seas Directive.

Acknowledgements

Part of this work was supported by the Fifth Framework Programme "Energy, Environment and Sustainable Development Programme", Contract no. EVK2−CT−2002−00144. Gratitude is also expressed to Dr. David Hydes for his assistance and valuable feedback before and during the above programme.

References

Hydes, D.J., J. Campbell and J. Dunning (2004). Systematic Oceanographic Data Collected by FerryBox, Sea Technology Magazine.

Hydes, D.J. and J. Dunning (2005). FerryBox celebrates first year of data collection, The Marine Scientist. Issue No 10, 32−35.

Evaluation of the operational sea level forecast systems — the Gulf of Finland case

Maria Gästgifvars*[1], Kai Myrberg[2], Sylvin Müller-Navarra[3], Anette Jönsson[4] and Vibeke Huess[5]

[1]*Finnish Environment Institute (SYKE)*
[2]*Finnish Institute of Marine Research (FIMR)*
[3]*Bundesamt für Seeschifffahrt und Hydrographie (BSH), Germany*
[4]*Swedish Meteorological and Hydrological Institute (SMHI)*
[5]*Danish Meteorological Institute (DMI)*

Abstract

This paper is devoted to validation of sea level forecasts in the Gulf of Finland. Daily forecasts produced by operational Baltic Sea oceanographic models HIROMB and two set-ups of the BSHcmod are investigated. The forecast results have been analysed for the period November 2003 to January 2005, which includes two major winter storms. The hourly sea level observations are from three Finnish stations along the coast of the Gulf of Finland. Over 90% of the sea level forecasts were found within the range of 15 cm of the observed sea levels which can be stated as a good result. It can still be concluded that the quality of short-time meteorological forecasts used to force hydrodynamic models play an important role especially in the case of forecasting high sea level events that cause flooding.

Keywords: sea level, models, modelling, operational, Baltic Sea, Gulf of Finland

1. Introduction

Today, operational sea level forecast from 3D models is widely used in the Baltic Sea area in various countries and institutes. However, until recently not very many studies have been devoted to comparing the quality of the sea level results from 3D operational models. In this paper daily forecasts produced by the operational Baltic Sea oceanographic HIROMB model and by two set-ups of the BSHcmod are analysed. The HIROMB model is run daily by SMHI. The two different set-ups of BSHcmod are maintained by BSH and DMI. The main idea is to investigate the models' ability to reproduce sea levels observed on the Gulf of Finland (GoF) and to find reasons for the possible differences in between the results.

2. Material and methods

2.1 Hydrodynamic models

HIROMB and BSHcmod are operational Baltic Sea models (Table 1) that the three institutes SMHI, BSH and DMI are running in their daily routine services. The 3D hydrodynamic models originate from BSH but the model set-ups now run in the daily services

* Corresponding author, email: Maria.Gastgifvars@ymparisto.fi

have been further developed by different modelling groups and not all the same features have been implemented to all these versions. There are some differences e.g. in calculation of the wind stress and bottom friction between HIROMB and BSHcmod that might influence the sea level calculation. Ultimo 2004, a modified version of the BSHcmod code was implemented at DMI (modifications include a damping source added to a vertical mixing scheme and a decrease in the horizontal mixing). Before that there were no physical differences in DMI's and BSH's model versions, so any differences before December 2004 might only be due to differences in the meteorological forcing. Sea level observations are not assimilated in any of these operational forecast systems.

Table 1 Basic properties of the Baltic Sea hydrodynamic model set-ups.

	HIROMB	**BSHcmod**	**DMI's set-up of BSHcmod**
Meteorological forcing	HIRLAM–SMHI	GME/LM German weather service	HIRLAM–DMI
Horizontal grid resolution of the meteorological model	22 km		15 km before June 2004: 5 km after June 2004
Wind drag coefficient C_D	$c_D=(0.7+0.09W_{10})\,A10^{-3}$ (Wilhelmsson 2002)	$c_D=(0.63+0.066W_{10})\,A10^{-3}$ (Dick *et al.* 2001)	same as BSHcmod
Horizontal grid resolution	1 n.m. and 3 n.m.	6 n.m.	6 n.m.
Equilibrium tides	no	yes (Müller-Navarra, 2002)	no
Ice modelling	yes (Dick *et al.* 2001)	yes (Dick *et al.* 2001)	yes
Open boundary forcing	2D north-east Atlantic storm surge model		

2.2 Data

Sea level observations were collected at three mareographs: Hanko, Helsinki and Hamina (Figure 1). The data consist of 10991 hourly observations from each station during the period 1 November 2003–31 January 2005 and include the highest sea level ever recorded at these stations on 9 January 2005. Another high sea level event occurred in the GoF in December 2003 (Figure 1). Mean sea levels and standard deviations are presented in Table 2. As expected, the mean sea level as well as the sea level fluctuation increases in this elongated estuary from west to east.

Hourly sea level forecast data were collected from the following operational model set-ups: HIROMB 3 n.m. (N=9749, N=number of data), HIROMB 1 n.m. (N=9684), BSHcmod (N=10824) and DMI (N=10812). When compared to the observations (N=10991) it can be seen that quite a number of data are missing especially from the HIROMB forecasts. This is for technical reasons concerning data transfer and storage. The reader should note that the forecast time series produced with different models vary in respect to the forecast range. The DMI model set-up has a forecast range up to 6 h, HIROMB and BSHcmod up to 24 h and from BSHcmod forecasts between +24 h and +48 h are also analysed.

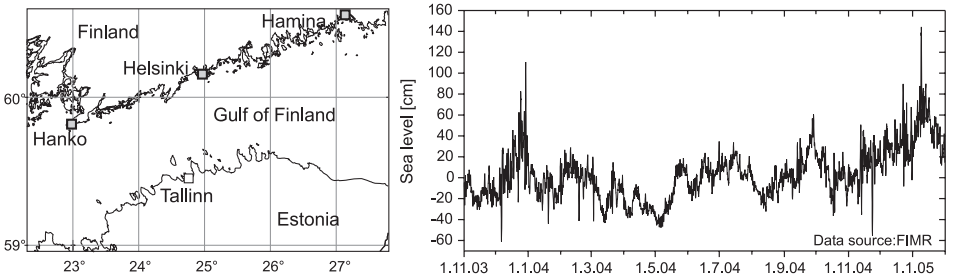

Figure 1 Sea level observation sites at the Finnish coast of the Gulf of Finland and the sea level in Helsinki from November 2003 to January 2005. Reference level: Finnish geodetical height system N60.

Table 2 Mean sea levels and standard deviations of observations and model results for the period November 2003–January 2005.

Data	Mean sea level [cm]			Std. deviation [cm]		
	Hanko	Helsinki	Hamina	Hanko	Helsinki	Hamina
Mareograph (Finnish geodetical N60-height)	1.4	2.8	9.1	22	24	28
HIROMB 1nm	2.6	4.3	6.9	19	21	25
HIROMB 3nm	–1.2	0.6	2.9	21	24	27
BSHcmod	2.0	4.6	7.8	23	26	31
DMI's set-up of BSHcmod	1.5	3.7	7.1	18	20	24

The reference level of the sea level observations is the Finnish geodetical N60-height system but the zero-level of the models vary. Hence the modelled values were fitted to the mean sea level of Hanko for the period November 2003–January 2005 by subtracting values 43, 48 and 41 cm from all simulated data of BSHcmod, HIROMB and DMI model set-ups respectively. This enables to us to compare several observation sites and models as the modelled mean sea levels are adjusted to the same reference level (Table 2). The change of mean sea level due to land uplift that is annually 1–2 mm along the GoF is not taken into account since the study period is short.

2.3 Analysis methods

Different methods including standard statistical methods as well as non-parametric skill tests are used to determine the system's ability to forecast sea level. The statistical measures comprise calculation of bias, the mean absolute error (MAE) of forecasts versus observations, root mean square error and standard deviation of error that reveals the spread of errors.

The US National Oceanic and Atmospheric Administration (NOAA) has developed for their purposes standards for evaluating operational hydrodynamic model systems (NOAA, 2003). According to these, central frequency (CF) is used in skill assessment of the models. CF indicates how large a percentage value of model errors is within acceptable limits. NOAA has defined these limits to be 15 cm in which case the target performance level is that over 90% of the forecast errors are found within the limits. The

Positive Outlier Frequency (POF) and the Negative Outlier Frequency (NOF) measure how often the forecasted sea level is significantly higher or lower than the actual sea level. The target value for POF and NOF is that less than 1% of the forecast errors are more than 30 cm. These limits are used for these statistical measures with target values that are the same as defined in the US standards (NOAA, 2003; Schmalz, 2004).

3. Results of the skill assessment of the model systems

From among the three monitoring stations the best sea level forecast results are achieved in Hanko. In case of each model set-up the statistical error values presented in Table 3 grow in the GoF towards the east due to the largest variations of sea level there and due to the maximum effect of seiches.

MAEs for the whole study period vary between 5–9 cm (Table 3). The variation is larger when the monthly mean absolute errors are assessed. In Helsinki the calculated monthly MAE values were 2–13 cm, in Hanko 2–12 cm and in Hamina 3–15 cm. Filinkova *et al.* (2002) analysed the performance of BSHcmod at a Russian station Shepelevo in the eastern GoF from November 2000 to June 2002. For that period they obtained MAE of 10 cm. During our study period BSHcmod performed slightly better than that in the Finnish stations.

Table 3 The sea level forecast analysis from November 2003 to January 2005.

Statistical Measure		Bias (forecast-obs.)			Mean absolute error, MAE			Std. dev. of error			RMSE		
Model		Hanko	Helsinki	Hamina	Hanko	Helsinki	Hamina	Hanko	Helsinki	Hamina	Hanko	Helsinki	Hamina
DMI	1–6 h	0.1	1.0	–2.0	4.6	5.2	6.0	5.8	6.5	7.5	5	6	7
HIROMB 1 nm	1–24 h	1.2	1.5	–2.2	6.8	7.5	8.0	8.5	9.1	10.3	8	9	10
HIROMB 3 nm	1–24 h	–2.6	–2.2	–6.2	5.4	6.0	8.0	6.8	7.6	8.9	6	7	8
BSHcmod	1–24 h	0.6	1.8	–1.3	5.6	6.4	7.2	7.2	8.2	9.9	7	8	10
BSHcmod	24–48 h	0.6	1.7	–1.3	5.9	7.0	8.5	7.6	9.3	12.8	8	9	13

Table 4 Frequencies of forecast errors.

Statistical Measure [Target Value]			Central Frequency % CF (15 cm) [> 90%]			Positive Outlier Frequency % POF (+30 cm) [< 1%]			Negative Outlier Frequency NOF (–30cm) [< 1%]		
Model, forecast range, N = number of data			Hanko	Helsinki	Hamina	Hanko	Helsinki	Hamina	Hanko	Helsinki	Hamina
DMI	1–6 h	N = 10 812	99.3	97.7	93.4	0.0	0.0	0.0	0.0	0.0	0.0
HIROMB 1 nm	1–24 h	N = 9684	90.9	88.9	86.8	0.0	0.0	0.1	0.1	0.2	0.7
HIROMB 3 nm	1–24 h	N = 9749	95.8	94.5	86.3	0.0	0.0	0.0	0.0	0.1	0.7
BSHcmod	1–24 h	N = 10824	97.3	94.4	89.8	0.1	0.3	0.5	0.1	0.1	0.5
BSHcmod	24–48 h	N = 10824	96.4	91.9	85.4	0.1	0.5	1.2	0.3	0.5	1.4

The average values of standard deviation of errors are 6–13 cm (Table 3). During 1997–2000, Dick *et al.* (2001) validated BSHcmod against three stations on the German Baltic coast and at those stations the annual standard deviation of errors had the same magnitude as they were 7–12 cm. On average the CF was 93% but some variation between the models can be seen in Table 4. Almost all POF and NOF values met the target value <1%.

4. Validation of extreme high sea level situations

Most important in operational sea level forecasting is that extreme high and low events are forecasted well in advance so that the public is informed of possible critical sea levels. Figure 2 and Table 4 present the performance of the models during two separate high sea level cases. The forecasted amplitudes were commonly lower that the observed ones during the case in December 2003. In an earlier HIROMB validation study covering a period of more than a month Kalas *et al.* (2001) also concluded that the amplitudes were under-predicted. Stanislawczyk (2002) validated the HIROMB model output related to an extreme hydrometeorological event off the Polish coast in December 1999 and found about 2–4 hours time lag and 15 cm underestimation of the peak value. The extreme high sea levels caused by the "Gudrun" storm in January 2005 were forecasted within quite acceptable error limits by DMI's model set-up and HIROMB. The performance of BSHcmod is discussed in the next section.

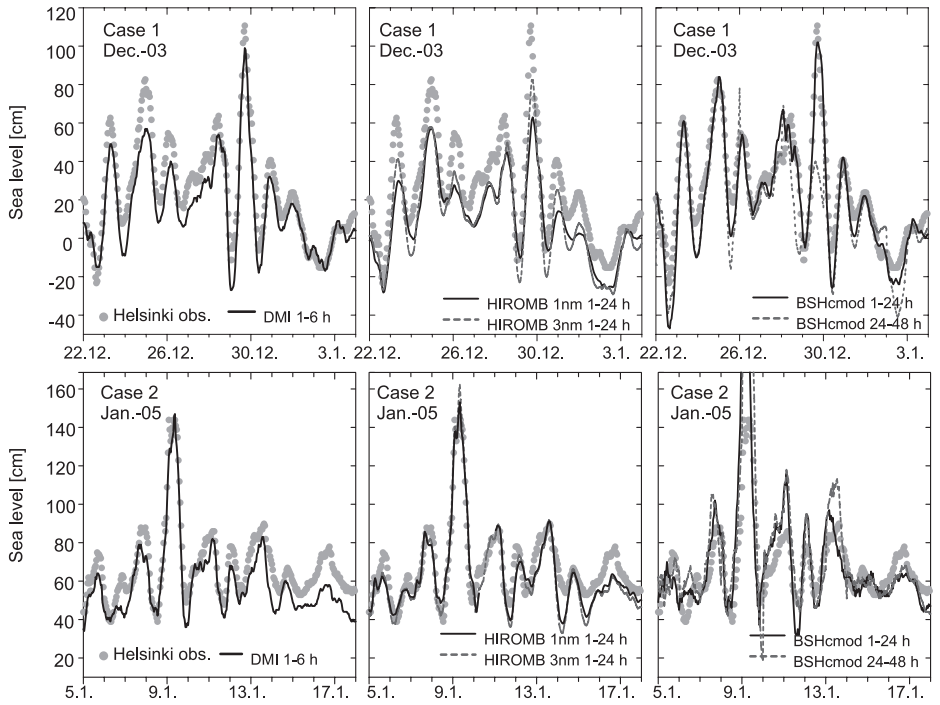

Figure 2 Time series of measured and forecasted high sea level events in Helsinki.

Table 5 Comparison of observed and forecasted sea levels during two high sea level cases.

Time	Mareograph/Model set-up		Max. sea level [cm] / Forecast Error [cm] / Time shift								
			Hanko			Helsinki			Hamina		
Case 1 29 Dec 2003	Mareograph (Finnish N60–height level)		80	–	–	111	–	–	149	–	–
	DMI	(1–6 h)	63	**–17**	–1 h	99	**–12**	0 h	132	**–17**	0 h
	HIROMB 1 nm	(1–24 h)	39	**–41**	+2 h	63	**–48**	+2 h	91	**–58**	+2 h
	HIROMB 3 nm	(1–24 h)	47	**–33**	+3 h	82	**–29**	+1 h	111	**–38**	0 h
	BSHcmod	(1–24 h)	76	**–4**	0 h	102	**–9**	0 h	165	**16**	0 h
	BSHcmod	(24–48 h)	29	**–51**	+4 h	40	**–71**	–2 h	64	**–85**	–6 h
Case 2 9 Jan 2005	Mareograph (Finnish N60–height level)		122	–	–	144	–	–	192	–	–
	DMI	(1–6 h)	117	**–5**	–1h	147	**3**	0 h	190	**–2**	–1 h
	HIROMB 1 nm	(1–24 h)	127	**5**	–2 h	153	**9**	–1 h	192	**0**	0 h
	HIROMB 3 nm	(1–24 h)	128	**6**	–2 h	162	**18**	–1 h	203	**11**	0 h
	BSHcmod	(1–24 h)	151	**29**	+4 h	225	**81**	–4 h	276	**84**	–6 h
	BSHcmod	(24–48 h)	153	**31**	–1 h	236	**92**	–4 h	358	**166**	–1 h

5. Discussion and conclusions

During the study period over 90% of the hourly water level forecasts produced with the different operational Baltic Sea model set-ups matched up to the actual water levels in Hanko and Helsinki within the range of 15 cm. This result meets one of the quality standards that NOAA has set for operational hydrodynamic models. In case of Hamina over 85% of the forecast were within acceptable error limits. Thus, the model's ability to forecast sea level variations is better in the western GoF than in the eastern part of the Gulf. One day forecasts of HIROMB and BSHcmod included less than 1% of values that differed more than 30 cm of the observed sea levels which can be considered a good performance.

The high sea level in December 2003 was commonly under-predicted by the models, as has been the case in some earlier studies. The "Gudrun" storm case in January 2005 was well-captured by the HIROMB and DMI model set-ups. HIROMB performed notably better than in the earlier high sea level case. The BSHcmod substantially over-predicted the amplitude due to a hidden data transfer problem between the German weather service and BSH, which considerably influenced the sea level forecasts during weather periods with rapid changes in air pressure and wind velocities. A hindcasts calculation with corrected meteorological data gave far better results. All the models forecasted the timing of the flood cases sufficiently enough while the time-shift of the forecasted sea level peaks compared to the observations was a few hours.

Comparison of the BSHcmod forecasts, one and two days ahead, reveal that the quality of the shorter forecasts is better. The most notable difference between the 1–24 h and 24–48 h forecasts was observed during the high sea level in December 2003. Longer forecasts, two to three days ahead, produced by the operational Baltic Sea models should be validated more carefully and preferably establish a continuous validation system

based on information from several models while long and accurate enough forecasts provide early information that can be used by authorities for preparation of protection measures to minimise the losses caused by flooding.

References

Dick, S., E. Kleine, S.H. Müller-Navarra, H. Klein and H. Komo (2001). The Operational circulation model of BSH (BSHcmod)-model description and validation. Bundesamt für Seeschifffahrt und Hydrographie No. 29/2001, 49 pp.

Filinkova, O., G. Ivanov, K. Klevanny and S. Müller-Navarra (2002). Comparison of observed water levels and BSHcmod model forecasts in the eastern Gulf of Finland, Environmental and Chemical Physics 24 (4) 198–205.

Kalas, M., A. Staskiewicz and K. Szefler (2001). Water level forecast for the Pomerian bay from the HIROMB model. Oceanological Studies 30 (3–4) 39–57.

Müller-Navarra, S.H. (2002). Implementation of the equilibrium tide in a shelf sea model. Environmental and Chemical Physics 24, 127–132.

NOAA (2003). NOS Standards for evaluating operational nowcast and forecast hydrodynamic model systems. NOAA Technical Report NOS CS 17. U.S. Department of Commerce, National Ocean Service, Coastal Survey Development Laboratory. 47 pp.

Schmalz, R.A. (2004). Development of the NOS Galveston Bay operational Nowcast/ Forecast system. In proceedings of IMEMS 2004, the Seventh International Marine Environmental Modeling Seminar. Washington D.C.

Stanislawczyk, I. (2002). Validation of HIROMB model using an extreme hydrometeorological event. Environmental and Chemical Physics 24 (3) 168–170.

The importance of atmospheric forcing versus topographic forcing on oceanic eddies generation by islands

Bárbara Jiménez*[1] and Pablo Sangrà[2]

[1]*ForWind-Center for Wind Energy Research, Institute of Physics, University of Oldenburg, Germany*
[2]*Faculty of Marine Sciences, Department of Physical Oceanography, University of Las Palmas de Gran Canaria, Spain*

Abstract

A quasi-geostrophic numerical model has been developed with the aim of studying the relative importance of atmospheric and topographic forcing on oceanic eddy generation by isolated islands. The model was forced with three different incident wind speeds corresponding to weak, medium and strong wind intensities, and four different incident currents with weak, medium, intense, and very intense speeds. Results show that in periods where the incident wind speed is in the medium-strong range and the incident current speed is slow (low Reynolds number), the atmospheric forcing is the trigger mechanism for oceanic eddy generation. Eddies are then spun off from the island for low Reynolds number (Re) of the oceanic flow (Re<20). However, when the current speed is very intense (high Reynolds number) the vorticity input by the wind is quickly advected by oceanic flow and does not contribute to the generation of oceanic eddies.

When solely atmospheric forcing is considered, only two stationary eddies are generated at the island wake. In this case, eddies of opposite sign are not sequentially spun off by the island and a Von Kármán-like eddy street is not developed downstream of the island. Therefore, the main mechanism responsible for the development of an eddy street is the topographic perturbation of the oceanic flow by the island flanks. The wind at the island wake acts only as an additional source of vorticity promoting the generation of an eddy street to lower intensity of the impinging oceanic flow, but is not capable of generating an eddy street without the topographic forcing.

Keywords: oceanic eddies, islands, topographic forcing, atmospheric forcing, quasi-geostrophic numerical model.

1. Introduction

In some periods of the year the velocity of the Canary Current has enough intensity for topographic oceanic eddy generation by the Gran Canaria Island (Navarro-Pérez y Barton, 2001). Other mechanisms such as atmospheric forcing can be viewed as supplementary mechanisms for eddy generation. Atmospheric vorticity is injected to the ocean through the Ekman pumping mechanism at the island's wake. This mechanism has been already suggested by Barton *et al.* (2000) for the Gran Canaria Island, and Patzert (1969), Flament (1994) and Lumpkin (1998) for Hawaii.

* Corresponding author, email: barbara.jimenez@forwind.de

A quasi-geostrophic numerical model has been developed with the aim of studying the relative importance of atmospheric and topographic forcing on oceanic eddy generation by Gran Canaria Island. The model was forced with three different wind speeds which correspond to weak, medium and strong wind intensities, and four different currents with weak, medium, intense, and very intense speeds.

2. Numerical experiments

2.1 Atmospheric forcing

The wind field is calculated via the numerical integration of the following vorticity balance adimensional equations, using the friction of atmospheric flow around the obstacle as the input of vorticity.

$$\frac{\partial \vec{\zeta}}{\partial t} + \vec{u}\frac{\partial \vec{\zeta}}{\partial x} + \vec{v}\frac{\partial \vec{\zeta}}{\partial y} = \frac{1}{\mathrm{Re}}\nabla^2\vec{\zeta} \qquad (1) \qquad \nabla^2\psi = \zeta \qquad (2)$$

Three simulations are made corresponding to the three wind speeds 2, 4 and 10 $\mathrm{m\,s^{-1}}$, respectively (Figure 1), taking as a diffusion coefficient AH, the one calculated by Chopra (1973) for the Canary Islands.

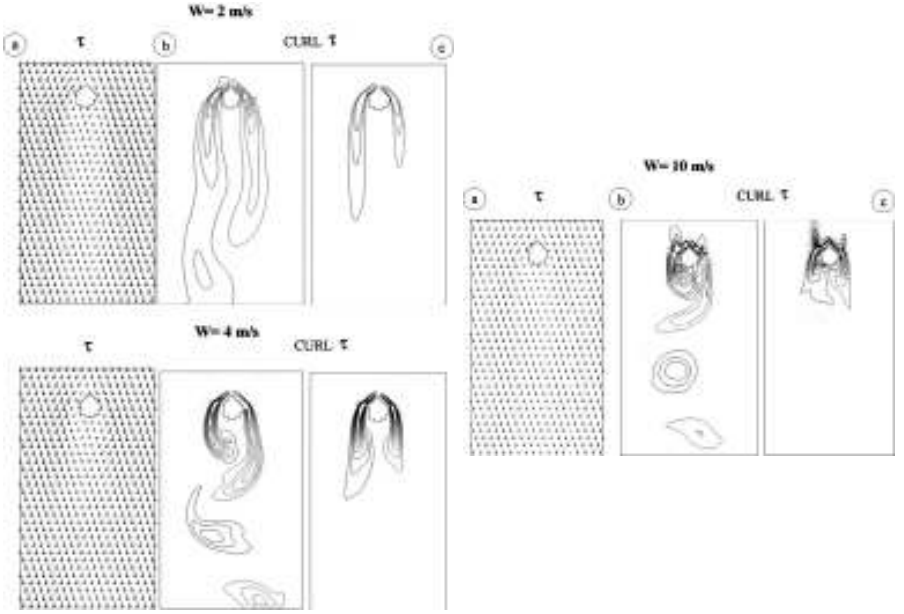

Figure 1 Representation of the wind fields 2, 4 and 10 $\mathrm{m\,s^{-1}}$. a) represents the vector speed; b) the behaviour of the lines of isovorticity; c) the average wind field. The left lines of isovorticity indicate positive vorticity, the right ones negative vorticity.

2.2 Wind curl

This term will be used to force the ocean–atmosphere model. It can be calculated with the following equations:

$$\tau_X = \frac{1}{\tau_0} C_D \rho_a u |\vec{w}|, \ \tau_Y = \frac{1}{\tau_0} C_D \rho_a v |\vec{w}| \ , \ curl\vec{\tau} = \frac{\partial \tau_Y}{\partial x} - \frac{\partial \tau_X}{\partial y} \tag{3}$$

2.3 Ocean–atmosphere model

The flow perturbation caused by the island and the influence of the atmospheric forcing is calculated through the numerical integration of the adimensional equation of the quasi-geostrophic approximation for an homogenous flow:

$$\frac{\partial \zeta_0'}{\partial t'} + J(p_0', \zeta_0') = \left(\frac{\tau_0 L}{\rho U^2 D} curl\tau' \right) - \frac{r}{2}\zeta_0' + \frac{1}{\mathrm{Re}} \nabla^2 \zeta_0' \ , \ \zeta_0' = \frac{\partial^2 p_0'}{\partial x'^2} + \frac{\partial^2 p_0'}{\partial y'^2} = \nabla^2 p_0' \tag{4}$$

Several simulations were performed:

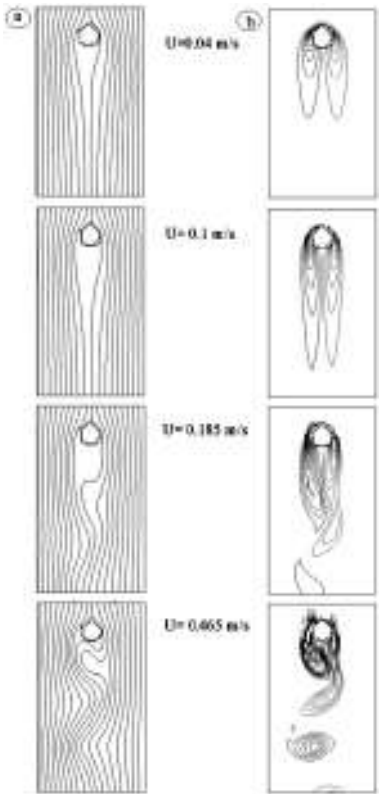

Figure 2 Streamlines (a) and isovorticity lines (b) for the flow at a certain time for different speeds (Reynolds number) of the impinging oceanic flow. The left lines of isovorticity indicate positive vorticity, the right ones negative vorticity.

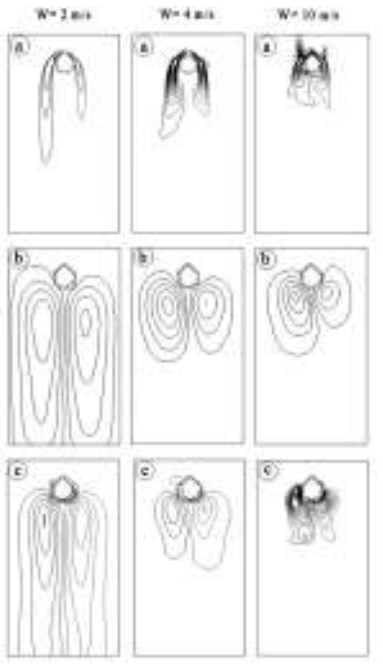

Figure 3 Behaviour of the streamlines (b) and lines of isovorticity (c), at a certain time, for increasing incident wind velocities. The left lines of isovorticity indicate positive vorticity, the right ones negative vorticity.

Case 0: Reference oceanic model without atmospheric forcing (Figure 2). A Von Kármán-like eddy street develops downstream of the island for Re > 60.

Case 1: Just wind without advection (Figure 3). Results shows that when solely atmospheric forcing is considered, eddies of opposite sign are not sequentially spun off by the island. Only two stationary eddies of opposite sign are generated at the island wake. The atmospheric forcing is then not capable of generating an eddy street without the topographic effect.

Case 2: Wind plus advection and slip-condition (non topographic forcing) (Figure 4). When the oceanic flow free slips around the island non vorticity is generated by the island (non topographic forcing) and the oceanic flow rapidly advects the only source of vorticity added by the wind at the island wake. This vorticity advection prevents oceanic eddy generation. Therefore vorticity generated by the island as a result of the friction of the oceanic flow (topographic forcing) is necessary for the eddy generation.

Figure 4 Behaviour of the lines of isovorticity, at a certain time, case 2, for a current speed of 0.04 ms^{-1} (Re=20), 0.1 ms^{-1} (Re=60), 0.185 ms^{-1} (Re=100) and 0.465 ms^{-1} (Re=250). The left lines of isovorticity indicate positive vorticity and the right ones negative vorticity.

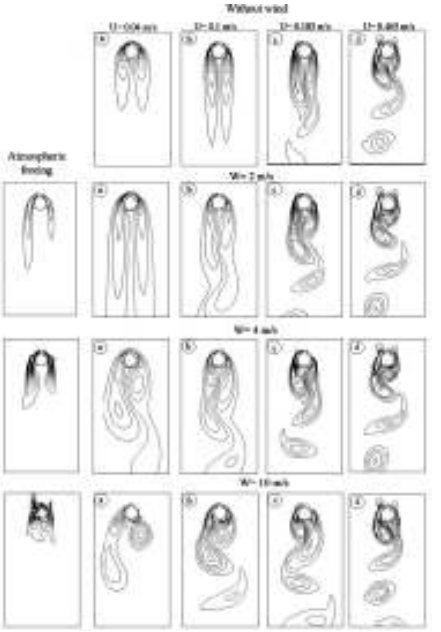

Figure 5 Lines of isovorticity, at a certain time, for increasing incident oceanic flow velocities, a) 0.04 ms^{-1} (Re=20); b) 0.1 ms^{-1} (Re=60); c) 0.185 ms^{-1} (Re=100); d) 0.465 ms^{-1} (Re=250) in case 3. The left lines of isovorticity indicate positive vorticity and the right ones negative vorticity.

Case 3: Atmospheric forcing plus topographic effect (Figure 5). Wind at the island wake acts as an additional source of vorticity promoting the generation of an eddy street to lower intensity of the impinging oceanic flow. Therefore, the atmospheric forcing acts as trigger mechanism for oceanic eddies generation at low Re of the oceanic flow (Re <20).

3. Summary

3.1 Atmospheric model

a) For weak wind intensities (W=2 ms^{-1}) atmospheric eddies of opposite sign are sequentially spun off by the island, increasing its detachment frequency for wind intensities between moderate (W=4 ms^{-1}) and strong (W=10 ms^{-1}).

3.2 Ocean–atmosphere model

a) For wind speed in the medium-strong range and incident oceanic flow slow (low Reynolds number): Atmospheric forcing is a necessary mechanism for oceanic eddy street generation.

b) For very intense current speed (high Reynolds number): Atmospheric vorticity input is quickly advected by the oceanic flow therefore not contributing on the oceanic eddy generation.

c) For only input of atmospheric vorticity: Only two stationary eddies are generated at the island wake.

4. Conclusion

The main mechanism responsible for the development of an oceanic eddy street is the topographic perturbation of the oceanic flow by the island. The atmospheric forcing at the island's wake acts as an additional source of vorticity promoting the generation of an eddy street at lower intensities of the impinging oceanic flow. However atmospheric forcing is not capable of generating an eddy street without the topographic forcing.

Acknowledgments

This work has been supported by the EC "Wind Energy Assessment Studies and Wind Engineering" (WINDENG) Training Network (contract no. HPRN–CT–2002–00215) and by the Spanish government through project RODA (CTM2004–06842–CO3–03).

References

Barton, E.D., G. Basterretxea, P. Flament, E.G. Mitchelson-Jacob, B. Jones, J. Arístegui and F. Herrera (2000). Lee region of Gran Canaria. Journal of Geophysical Research, Vol. 105, no. C7, 17173–17193.

Chopra, K.P. (1973). Atmospheric and oceanic flow problems introduced by islands. Adv. Geophys., 16, 297–421.

Flament, P. (1994). Wind-driven oceanic processes in the lee of the island of Hawaii. Annales Geophysicae, 12 (II), C268.

Lumpkin, C.F. (1998). Eddies and currents of the Hawaiian Islands. PhD Thesis, University of Hawaiian at Manoa, Honolulu, 281 pp.

Navarro-Pérez, E. and E.D. Barton (2001). Seasonal and interannual variability of the Canary Current. An interdisciplinary view of the ocean. J.L. Pelegrí, I. Alonso and J. Arístegui (Eds.) Scientia Marina, 65 (suppl.1), 205–213.

Patzer, W.C. (1969). Eddies in Hawaiian Waters. Report No. HIG 69–8. Institute of Geophysics, University of Hawaii, 51 pp.

On operational three dimensional hydrodynamic model validation

Jun She*, Per Berg, Jacob L. Høyer, Jesper Larsen and Jacob W. Nielsen

Danish Meteorological Institute, Copenhagen, Denmark

Abstract

Comprehensive validation and calibration of three-dimensional (3D) hydrodynamic models is essential in making quality assured operational simulations and process studies. Some key issues in model validation such as quality and uncertainty of observations, and validation indexes and methods are discussed in this paper. Examples of 3D ocean model validation are given using a DMI (Danish Meteorological Institute) 3D operational ocean model.

Keywords: Hydrodynamic modelling, validation, Baltic Sea, North Sea.

1. Introduction

The direct definition of model validation is to compare model values with observations in given spatial-temporal locations, so that a model−observation difference is obtained. The purpose of the model validation, however, is to reach a certain kind of quality evaluation of the model, based on this model−observation difference. Such a quality evaluation is essential in operational oceanography, ocean research and designing future research priorities. In operational oceanography, the quality of the operational products can only be obtained by model validations. In ocean climate research and process studies, the quality of the model used is essential for final conclusions made. In order to identify research priorities for modelling study, the model error sources have to be analysed in detail, and the most significant error sources are normally key areas for further improvement.

However, most of the 3D hydrodynamic models have not been regularly and widely validated due to lack of observation data and/or proper evaluation methods. The general idea of 3D hydrodynamic model validation is that

- the representativeness of the model−observation comparison should be estimated
- the model−observation comparison should be as representative as possible for a given purpose.

The representativeness of the model validation is related to the observation data quality, the uncertainty in using local observations to compare with box-averaged model values and spatial-temporal-parameter representativeness in terms of interested region, period and phenomenon.

The above validation related issues will be discussed in the following sections and relevant examples will be given by using the DMI operational 3D ocean model BSHcmod in the Baltic−North Sea region.

* Corresponding author, email: js@dmi.dk

2. Quality and uncertainties in measurements

When a model gridded value is compared with a local measured value, the model–observation difference is composed of three parts: model error, instrument error and sampling error of the observation. The model error is the difference between the model value and true box-averaged value. The instrument error is the difference between the local measurement and the local truth, which is related to different platforms. The sampling error is the standard deviation of the measured parameter in the averaged box.

Table 1 gives an example of sea surface temperature (SST) observation quality varying with platforms. All the observations used are from 2001 in the Baltic–North Sea. The bias and standard deviation are calculated by comparing the *in situ* SST observations with satellite (OISAF products). This table shows the diversity of the quality of *in situ* SST. It is shown that towed profiler and TSG (thermosalinograph) data have smallest deviation from satellite SST while the Ferrybox data have the largest difference from the satellite, which may be related to the instrument error. Details of this study can be found in Høyer and She (2004).

Table 1 Bias and standard deviation of *in situ* observations vs. satellite night SST (the satellite data have been corrected to bulk SST).

	Towed profiler	TSG	Fixed stations	CTD cast	VOS	Ferrybox
Bias (°C)	–0.03	–0.04	–0.15	–0.15	0.09	–0.13
Std. dev. (°C)	0.28	0.45	0.59	0.61	0.67	0.76
Data pairs	543	45	2832	99	5634	44

For the model validation, raw data have to be carefully quality controlled (QC). Based on several years of data from 23 buoys in the Baltic–North Sea, an investigation (Johansen *et al.*, 2005) shows that a heavy QC work is required. Due to bad and/or missing data, the percentage of the data gap is 20%, 30% and 17% for T, S and currents, respectively. The unstable density profiles make up 18.6% of the total observed profiles.

Sampling error can be a significant part in the model–observation difference in certain regions (Figure 1, based on 2001 satellite night data for SST and *in situ* measurements for sea surface salinity, SSS). For Baltic SST, the sampling error ranges from 0.12°C for the 4 km grid and 0.24°C for the 12 km grid. The sampling error is larger in April–June than other months. For SSS, the sampling error in open Baltic–North Sea waters is less than 0.1 psu. However, transition waters (Norwegian Trench, Skagerrak, Kattegat and Danish Straits) have a large sampling error between 0.3–1psu.

3. Examples of model validation in Baltic–North Sea

Here we use DMI BSHcmod as an example of model validation in the Baltic and North Sea. For this region, a hydrodynamic operational model may benefit our storm surge forecast, currents products for navigation, pollutant drift prediction, sea ice and SST products (for air–sea interaction, fishery, recreational activities, etc.) as well as Baltic–North Sea water exchange and stratification, which are very important for the ecosystem

status. Hence the model validation in this region should focus on forecasting water level, ice, SST, currents (especially in transition waters) and thermohaline stratification.

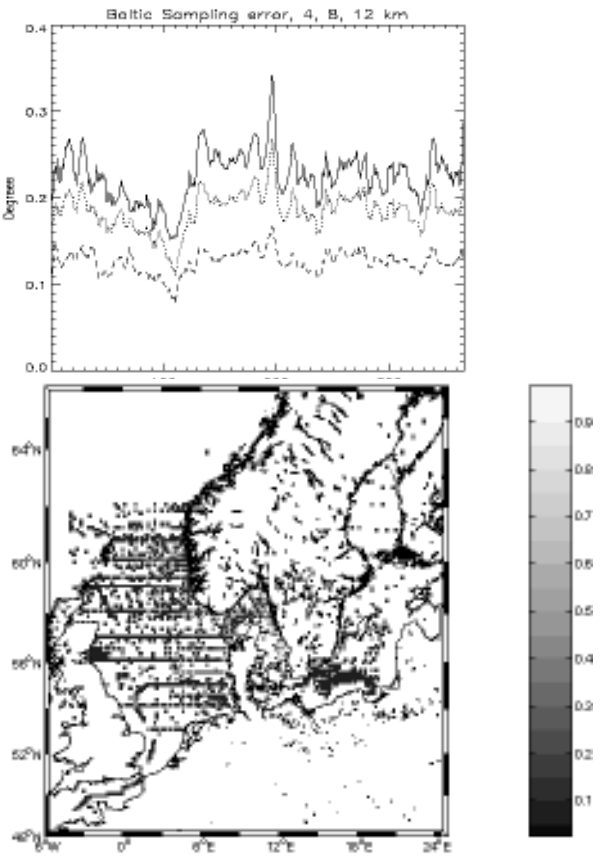

Figure 1 Top: averaged SST sampling error in the Baltic Sea for different hourly grid boxes in 4×4 km (dashed line), 8×8 km (dotted line) and 12×12 km (solid line); Bottom: SSS sampling error (in psu) distribution in hourly 6×6 nm grid box.

The most widely validated parameters for 3D hydrodynamic models are water level and SST, both due to the amount of observations available and the model quality of the two parameters. It is not a surprise that the water level and SST forecast should have the highest forecast skill among the hydrodynamic parameters because a large part of the predictability of a 3D hydrodynamic models is inherited from the weather forecast. However, both water level and SST validations are in many cases limited to a local area.

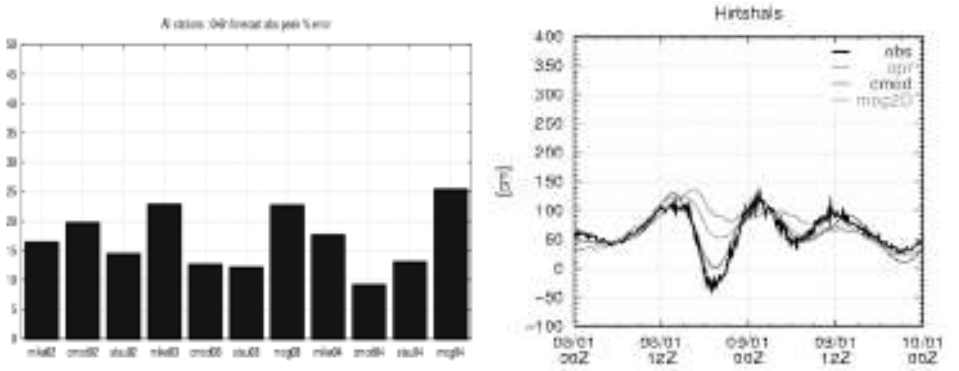

Figure 2 Left: yearly averaged peak errors (%) in different models for 18 Danish stations; Right: predicted and observed water levels in a storm in Jan. 08, 2005 in NW Jutland coast tidal gauge station Hirtshals (the highest line represents MIKE21).

3.1 Water level

Most storm surge forecasts for the Baltic–North Sea are made using 2D models due to their high quality and low computational cost. It is widely accepted that 3D hydrodynamic models do not provide better storm surge forecasts due to the extra error in vertical turbulence mixing. In this section, the quality of storm surge forecasts is calculated by comparing observed and predicted high waters for each calendar year between 2002–2004 for the BSHcmod and three 2D storm surge models: MIKE21 (DMI operational surge model), Staumod (a 2D version of the BSHcmod) and MOG2D (a finite element model). Figure 2 (left) shows that the 3D BSHcmod gives best prediction on peak errors (14%). The spatial distribution of the model errors was also investigated for a storm case on 8 January 2005. In comparing with all three 2D models, the most significant improvement of the 3D model is for the NW Jutland coast (Figure 2, right). This region is the most difficult for storm surge forecasts, because the water level here can be impacted by waves from several directions (southwards, northwards, etc.).

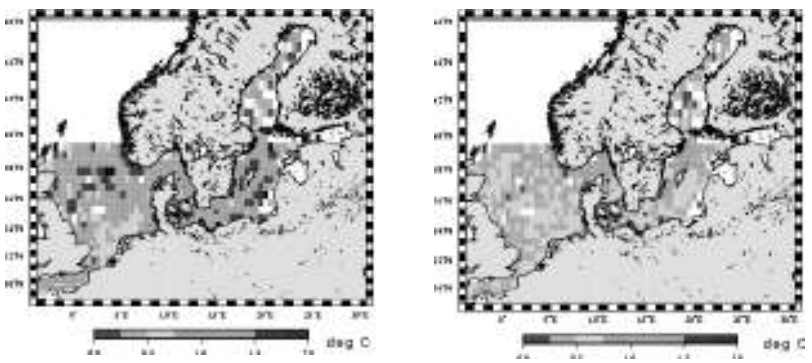

Figure 3 Spatial distribution of the BSHcmod SST RMS by comparing model and independent *in situ* observations in 2001. Left: without data assimilation; Right: after assimilating SAF satellite night SST.

3.2 SST

A validation study on the BSHcmod SST performance was made by comparing the model SST data in 2001 with ~200000 *in situ* observations from GTS, buoys and CTD casts. The results show that the model SST has a positive bias of 0.78°C and an RMS error of 1.2°C, which suggests that the 2 m air temperature and heat flux formula should be examined in order to remove this bias. Figure 3 (left) shows a large inhomogenuity of the model RMS error. The largest RMS error (1.5°C) is found in the northern North Sea, Norwegian Trench and Baltic proper. With data assimilation, the RMS error was reduced by 0.66°C and also becomes more evenly distributed.

3.3 Stratification

An efficient way to examine a hydrodynamic model's capability of reproducing real stratification is a basin-scale model–data comparison on the mixed-layer depth (MLD) and pycnocline depth. This, of course, has the drawback that in some cases, such depths are not available. Due to lack of observations, ICES' 51 years T/S profile data (1951–2000) are used to generate the mixed-layer and pycnocline depths, where the MLD is defined as the depth with a temperature difference larger than 0.5°C from the SST, while the pycnocline depth is defined as the depth with the maximum Brunt–Vaisala frequency. The model results are based on the BSHcmod simulations in 2001–2003.

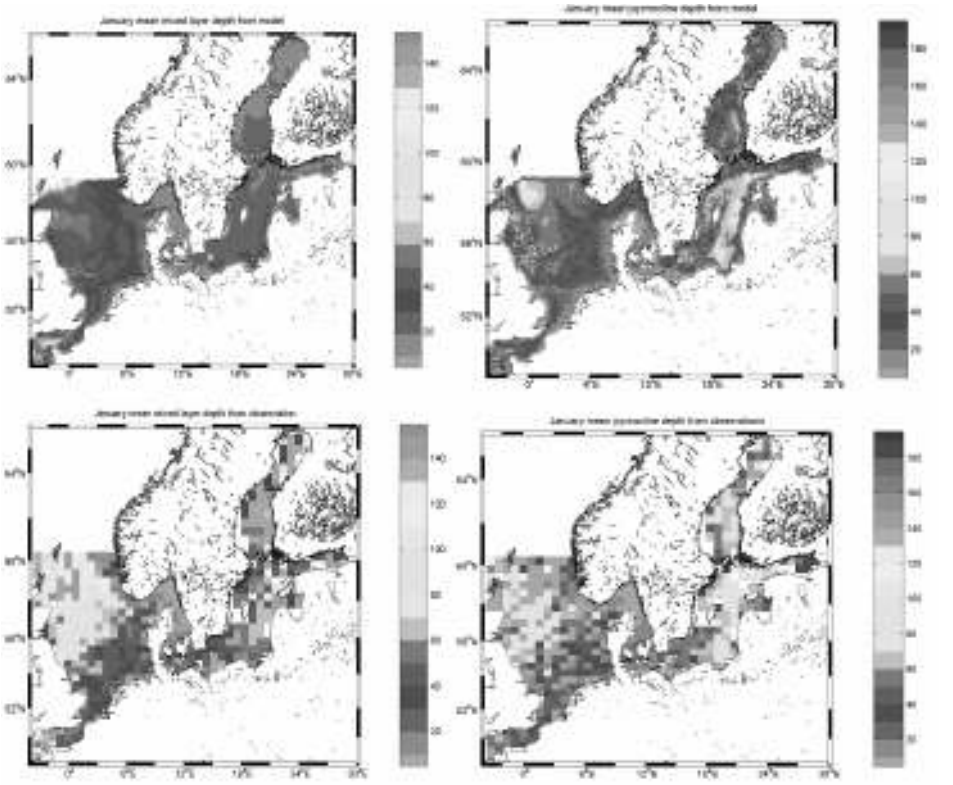

Figure 4 Modelled (upper panel) and observed (lower panel) mean mix-layer depth and pycnocline depth in January (m).

Figure 4 and Figure 5 show the simulated and observation–derived mixed-layer and pycnocline depths in January and July, respectively. The model gives correct patterns but the model performance varies with areas. In January, the model underestimates MLD in the middle and northern North Sea and mid-Baltic but overestimates in the transition waters and northern Baltic Sea; the situation is similar for the pycnocline depth in the North Sea and transition waters; the model performs quite well in the central Baltic Sea. In July, the model performs well in simulating MLD but has a large pycnocline depth error.

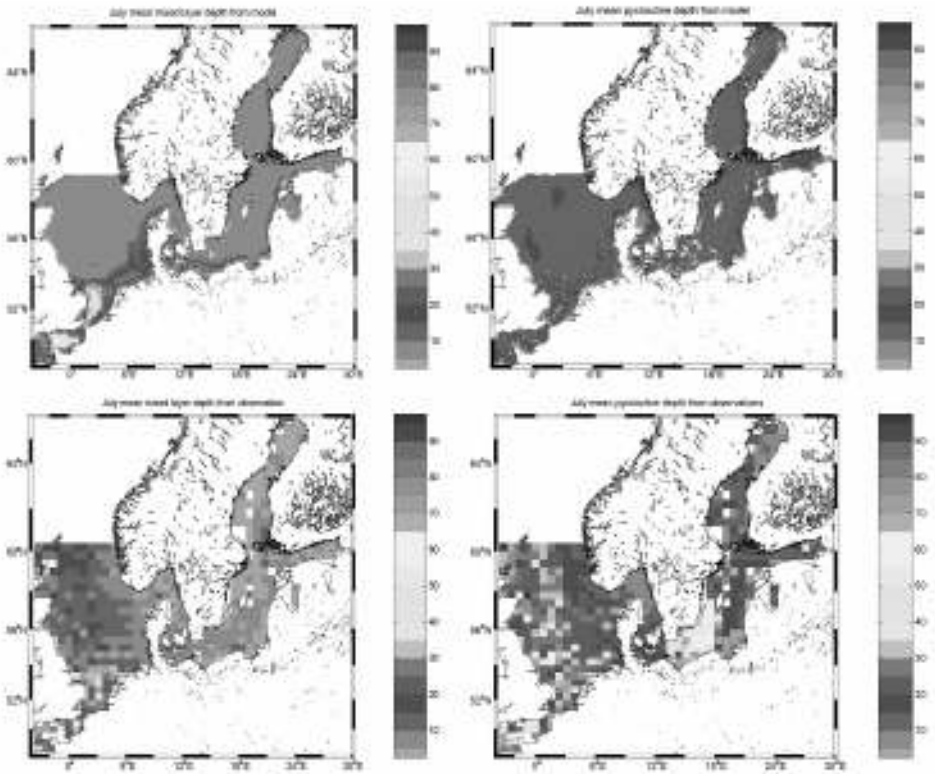

Figure 5 Modelled (upper panel) and observed (lower panel) mean mixed layer depth and pycnocline depth in July (m).

Based on above validation studies, ongoing and future research priorities for the DMI BSHcmod have been made, e.g. improvements on lateral boundary conditions, stratification, especially in transition waters, bathymetry in transition waters, mass balance between Baltic and North Sea and surface heat fluxes (atmosphere–ocean coupling), etc.

Acknowledgements

The DMI operational 3D ocean model BSHcmod was originally provided by German Bundesamt für Seeschifffahrt und Hydrographie (BSH, Kleine, 1994). The authors appreciate help from ICES for providing T/S data and Kristine S. Madsen in DMI for plotting some of the figures.

References

Høyer, J.L. and J. She (2004). Validation of satellite SST products for the North Sea–Baltic Sea region. Technical Report 04–11, Danish Meteorological Institute.

Johansen, G., P. Berg, V. Huess, J.W. Nielsen and M.H. Ribergaard (2005). NOVANA-programmet 2004–2009 Det Marine Modelkompleks Delydelse 4.1: Analyse af den naturlige variabilitet – data rapport, Danmarks Meteorologiske Institut.

Kleine, E. (1994). Das operationelle Modell des BSH feur Nordsee und Ostsee, Konzeption und Uebersicht. Bundesamt fur Seeschifffart und Hydrographie, Technical Report, 126 S.

Validation of a one year simulation of the Baltic Sea with optimised boundary conditions, improved bathymetry and data assimilation

Per Pemberton*

Swedish Meteorological and Hydrological Institute, Sweden

Abstract

Today's observational network is neither sufficient nor optimal for a cost-effective basin scale operational system. As a part of the FP5 EU project ODON, a state-of-the-art ocean model has been used to construct a high resolution data set. With a number of improvements in some identified key areas of the model an optimised data set was obtained. The data set forms the basis for further studies of optimal design methods for observational systems. The results are validated against a comprehensive set of *in situ* observations of salinity and temperature.

Keywords: High resolution modelling, Baltic Sea

1. Introduction

Existing observing systems in European seas are often the result of historical and local monitoring needs. An observing system suited to basin scale forecasting and monitoring that is cost effective requires a system analysis approach. This issue is dealt with in the FP5 EU project ODON (Optimum Design of Observational Networks). The overall objective of ODON is to develop optimal design methods for observing systems and demonstrate the methods on the Baltic/North Sea thermal saline observing networks. To compensate for the lack of "real" observations, a high resolution modelling effort is made where state-of-the-art models are optimised and a one year (2001) simulation is carried out. The outcome, named the Proxy Ocean, is used in a series of sampling strategy studies and observing system simulation experiments from which a future observational network can be designed. This paper explains the modelling and validation of the Baltic Sea Proxy Ocean.

2. Ocean model

Several European institutes run operational models covering the Baltic Sea. These models have different spatial resolution, model physics and computational capabilities. To generate the Baltic Sea Proxy Ocean the model system HIROMB (Funkquist and Kleine, 2000) was chosen. HIROMB was suitable because it has the required resolution, 1 nm (nautical mile), and it is parallelised to run on shared or distributed memory machines (Wilhelmsson, 2002) which make it suitable for long hindcast simulations.

HIROMB is a 3D baroclinic ocean model that runs operationally twice a day at SMHI. The model has a nested grid configuration with a coarser grid (12 nm) covering the

* Corresponding author, email: Per.Pemberton@smhi.se

North Sea and the Baltic Sea and finer grids (3 and 1 nm) covering the Baltic Sea, see Figure 1. The model's main forcing is the 22 km resolution atmospheric model HIRLAM (Gustafsson, 1993). River runoff is fed by either climatology values or the hydrological model HBV (Bergström, 1992) and the open western boundary is coupled to a North East Atlantic storm surge model.

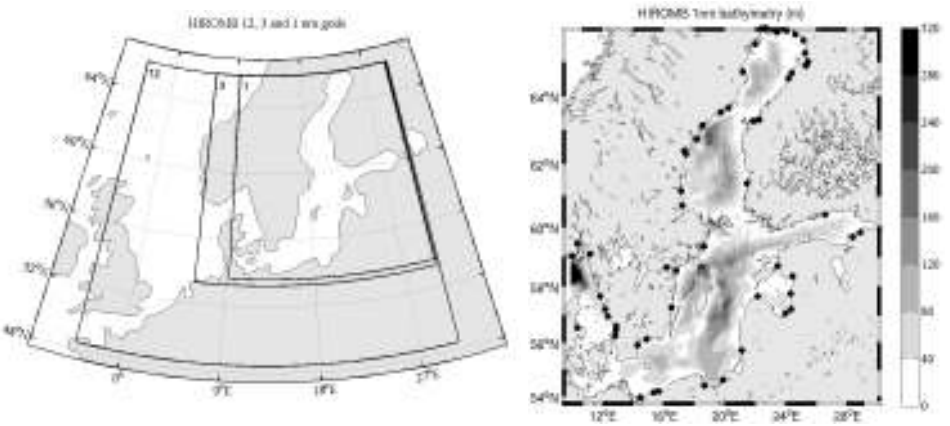

Figure 1 Left: Model domain with the North Sea and Baltic Sea 12, 3 and 1 nm grid configuration. Right: Model bathymetry (m) with rivers marked as black circles.

3. Improved model

The Baltic Sea is a great challenge for ocean modelling. The system is characterised by a complex bathymetry with a lot of fresh water discharge from numerous rivers, see Figure 1. Within the system sharp horizontal and vertical gradients exist for both the temperature and the salinity distribution. Typical features are eddies, river plumes and fronts with length scales ranging from a few to hundreds of kilometres. Numerical modelling of such a system often suffers from numerical diffusion related to the model resolution and incorrect parametrisation of physical processes.

During the last few years HIROMB has been upgraded in various projects. Recently implemented features are an improved turbulence parametrisation and a data assimilation scheme. With focus on the salinity and temperature distributions some key areas were prioritised to further improve the model. These key areas were the bathymetry, river runoff and atmospheric forcing.

3.1 Optimised bathymetry, river runoff and atmospheric forcing

When salt water is transported from the North Sea to the Baltic Sea it runs through the deep trenches of the Danish Straits. These trenches, with a maximum depth of 20–50 m, are not well resolved in a 1 nm grid as they are only a few hundred metres wide. To resolve the passages a high resolution 200 m depth database was used to parametrise depth cells around the critical depth of 25 m. Grid cells with depths of more than 25 m were set to their maximum depth and grid cells lower than 25 to their minimum depth, while cells with depths below 5 m were averaged over the grid cell. Other areas of the model's bathymetry (Gulf of Finland and Polish Coastal Waters) were also optimised by

using available high resolution data. The effect of the new bathymetry on bottom salinity can be seen in Figure 2.

The river runoff influences not only the estuary region but also has a remote effect. To account for the daily river discharge, data from the hydrological model HBV and *in situ* measurements were used to improve the river runoff. In Figure 2 this effect can be seen for the surface salinity in the central Baltic Sea.

The atmospheric forcing was optimised by using data from the Danish Meteorological Institute's HIRLAM model. This model has a 7.5 km horizontal resolution and is forced by SST (sea surface temperature) derived from satellites.

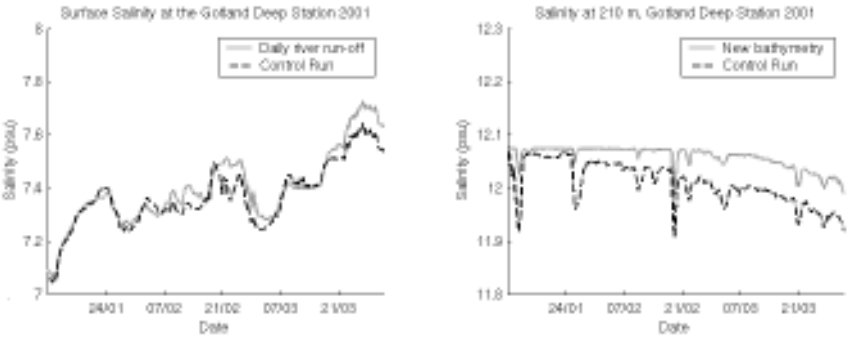

Figure 2 Left: Effects of daily river runoff on sea surface salinity; Right: new bathymetry on bottom salinity in the central Baltic Sea (20 03 E, 57 20 N).

3.2 Data assimilation

The implemented data assimilation scheme is the Method of Successive Corrections formulated by Daley (1991). The assimilation scheme uses isotropic spatial correlation length scales ranging from 10–60 nm depending on the distance to the closest coast line. Assimilated data were from an analysed SST/ice product based on data from satellites (Radarsat and NOAA), voluntary observation ships, icebreakers, buoys, coastal stations and T/S (temperature and salinity) profiles from monitoring cruises. Updates of SST were made 2–3 times a week and monthly for T/S profiles. The assimilation scheme is expected to improve the vertical stratification that is slowly deteriorated by numerical diffusion and to correct the heat flux in the surface layer.

4. Validation results

Validation was carried out by comparing quality controlled *in situ* data with model results from two year-long simulations, the Proxy Ocean run and a control run (a run without any optimisations). The time interval of the model output was 6 hours. The *in situ* data consisted of almost 240000 surface and subsurface observations from various platforms such as ferryboxes, buoys, TSG (TermoSalinoGraph) and GTS (Global Telecommunication System).

The annual RMSE (Root Mean Square Error) and bias was reduced by 32% and 22% respectively for the Proxy Ocean SST compared to the control run. Monthly RMSE and bias distributions, shown in Figure 3, imply that the SST performance of the model has been improved for months with relatively high bias, reducing the RMSE considerably for

the period April–June. During the winter months only minor improvements of the RMSE are seen, possibly a result of the poor NOAA satellite coverage in wintertime.

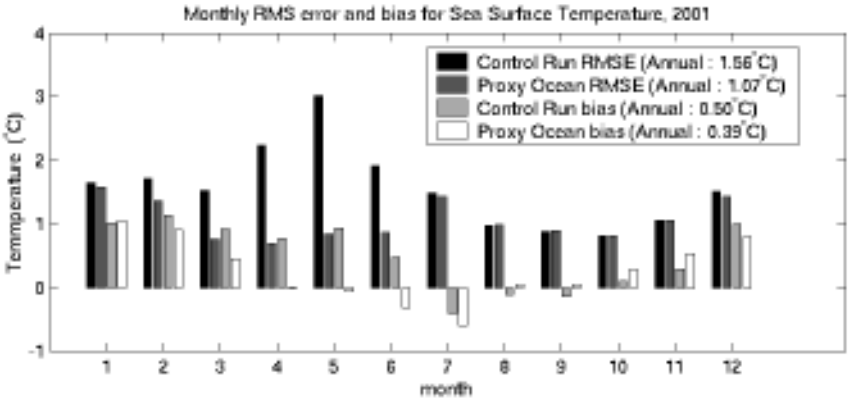

Figure 3 Root mean square error and bias compared to the *in situ* data for the Proxy Ocean and the control run. Annual values are shown in the caption legend.

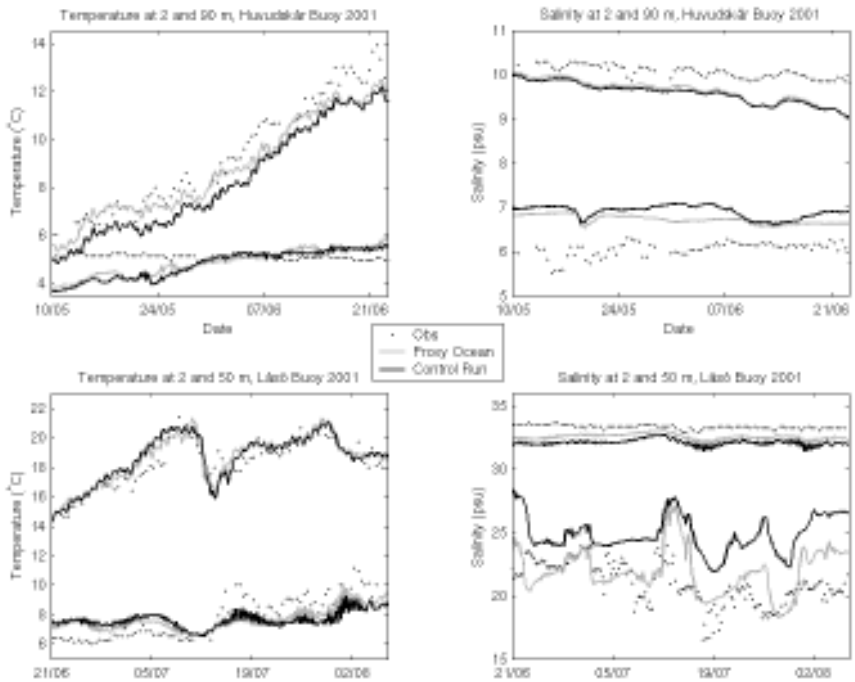

Figure 4 Surface and bottom temperature (left) and salinity (right) in the Baltic Sea at 19 11 E 58 56 N (upper panel) and in Kattegat at 11 32 E 57 12 N (lower panel). See caption legend for details.

In Figure 4 the surface and bottom salinity and temperature are compared with buoy data from two locations, one in the central Baltic Sea (Huvudskär) and one in Kattegat (Läsö). The Proxy Ocean has an overall better agreement with the observations. Surface salinity

at Läsö and SST at Huvudskär partly show a really good agreement with the *in situ* data, whereas the other cases seem to show only a minor improvement in the bias.

5. Conclusions

A high resolution modelling effort has been demonstrated where the model system HIROMB has been optimised to achieve a high quality data set. The result shows that the model improvements have given better model results. However, for certain areas and times the improvements were relatively small and imply that further improvements are still needed. Future work will be concentrated towards finding a better assimilation scheme with statistically derived anisotropic correlation length scales and error representation.

Acknowledgements

The work was supported by the EU FP5 project ODON (Contract No. EVK3−2002−00082).

References

Bergström, S. (1992). The HBV model its structure and application. SMHI report RH no. 4, available from SMHI, S−60176 Norrköping, Sweden.

Daley, R. (1991). Atmospheric Data Analysis, Cambridge Atmospheric and Space Science Series, Cambridge University Press, Cambridge.

Funkquist, L. and E. Kleine (2000). An introduction to HIROMB, an operational baroclinic model for the Baltic Sea. SMHI reports, Oceanography, available from SMHI, S−60176 Norrköping, Sweden.

Gustafsson, N. (ed.) (1993). The HIRLAM 2 Final Report, HIRLAM Tech. report 9, available from SMHI, S−60176 Norrköping, Sweden.

Wilhelmsson, T. (2002). Parallelization of the HIROMB Ocean Model, Licentiate Thesis, Department of Numerical Analysis, Royal Institute of Technology, Stockholm, Sweden.

Extended ice forecast modelling for the Baltic Sea

Lars Axell*

Swedish Meteorological and Hydrological Institute, Norrköping, Sweden

Abstract

To make year-round navigation easier in the Baltic Sea, it is desirable to include information about the degree of ice ridging in ice forecasts. This paper describes the implementation of ridging equations in the operational ice ocean model HIROMB. Some results are presented and discussed.

Keywords: Ice forecasts, ice modelling, ice ridging, ridge density, ridge height, Baltic Sea.

1. Introduction

Year-round navigation is very important for the countries surrounding the Baltic Sea, because of its positive effects on national economies and coastal communities. However, this is only possible with the help of icebreakers and reliable ice information.

The major obstacle for navigation in ice-infested waters is the presence of ice ridges. Whereas the level ice thickness is usually less than one metre in the Baltic Sea, ridge formations may be up to 30 m thick (keel depth plus sail height). It is therefore desirable to include information about the degree of ridging in operational ice charts as well as in ice forecasts. The accomplishment of this is one of the aims of the IRIS (2005) project. From the modelling point of view, the goal of this project is to include ridge density D (number of ridges per km), ridge sail height H (the part of the ridge visible above the surrounding level ice), and ridged ice thickness h_r (ridged ice volume normalised by the horizontal area) in the ice forecast models used operationally by the Swedish and Finnish Ice Services.

The purpose of this short paper is to describe the implementation of ridging equations in the ice ocean model HIROMB (High-Resolution Operational Model of the Baltic) that is run at SMHI (Swedish Meteorological and Hydrological Institute), which is used by the Swedish Ice Service. HIROMB is a fully baroclinic, thermodynamic three-dimensional model for the ocean. In the current set-up it has three nested grids with 12-nm (nautical miles) resolution in the North Sea, and up to 1-nm resolution in the Kattegat and the Baltic Sea.

* Corresponding author, email: Lars.Axell@smhi.se

2. Ridging equations

Before the IRIS project began, the ice model in HIROMB only solved prognostic equations for ice concentration C and total ice thickness h, according to[1]

$$\frac{\partial C}{\partial t} + \nabla \cdot (\bar{u} C) = R \tag{1}$$

$$\frac{\partial (Ch)}{\partial t} + \nabla \cdot (\bar{u} Ch) = 0 \tag{2}$$

where u is the ice drift. The ridging function R in equation (1) is intended to keep C from exceeding unity (100%) while at the same time keeping track of how much ridging takes place; see below. In equation (2), h is defined as the total ice thickness in the part of the grid cell in which there is ice, and Ch is thus the mean total thickness (cubic metres of ice per square metre) over the whole grid cell. The following ridging-related equations in this paper (except equation (4)) are due to Lensu (2003; 2004, personal communication).

A prognostic equation for ridge density D was added to the model according to

$$\frac{\partial (CD)}{\partial t} + \nabla \cdot (\bar{u} CD) = \frac{\beta R}{\varphi} \tag{3}$$

where the ridge structural function φ is described further below. β in (3) is the fraction of deformation events that is due to ridging, the remaining part (1−β) being due to rafting. The tuning function β was parametrised as

$$\beta = \begin{cases} \frac{1}{2}\left[1 + \sin\left(\frac{\pi h_l}{2h_l'}\right)\right] ; (h_l < 2h_l') \\ 1 \ ; (h_l \geq 2h_l') \end{cases} \tag{4}$$

where $h_l' = 0.1$ m and h_l is the level ice thickness (see below). The ridging function R encountered in equations (1) and (3) above was parametrised as

$$R = \begin{cases} \nabla \cdot \underline{u} \ ; (\nabla \cdot \underline{u} < 0 \text{and C} \geq 1.0) \\ 0; \text{otherwise} \end{cases} \tag{5}$$

which effectively keeps C from exceeding 1.0.

The ridge structural function φ encountered in equation (3) was implemented as

$$\varphi = \left\{ \begin{array}{c} -\frac{315}{315CD + 1000} ; p = 1 \\ -\frac{315p(1 - 0.081\sqrt{CDH})}{315CDp + 1000} ; \text{otherwise} \end{array} \right\} \tag{6}$$

1 Thermodynamic effects are included in the model, but excluded in this paper for brevity

where H is the ridge sail height (see below) and the clustering variable p is given by

$$p = \min[1.24\exp(-0.16\sqrt{CDH}), 1.0] \tag{7}$$

The ridge sail height H is calculated with the prognostic equation

$$\frac{\partial(CDH)}{\partial t} + \nabla \cdot (\bar{u}CDH) = \alpha_0 \langle H \mid h_l \rangle + (\alpha - \alpha_0)H \tag{8}$$

The expression within brackets (< >) in equation (8) is the mean ridge sail height formed from level ice thickness h_l, and is given by

$$\langle H \mid h_l \rangle = 3\sqrt{h_l} \tag{9}$$

Further, α in equation (8) is related to the ridging function as $\alpha = \frac{R}{C\varphi}$ (10)

and α_0 in equation (8) is given by $\alpha_0 = -\frac{3.17R}{p}$ (11)

Finally, one extra prognostic equation has been added in the ridging module, to account for level ice thickness h_l:

$$\frac{\partial(Ch_l)}{\partial t} + \nabla \cdot (\bar{u}Ch_l) = Ch_lR \tag{12}$$

As $R < 0$ whenever ridging occurs, the term on the right-hand side of (12) is negative. The net effect is to subtract the effect of mechanical growth of ice, which thus affects the total ice thickness h but not level ice thickness h_l which only increases and decreases due to thermodynamical processes not discussed here. The ridged ice thickness h_r is here approximated as the deformed ice thickness, which is the difference between total and level ice thickness:

$$h_r = h - h_l \tag{13}$$

3. Results and discussion

To test the ridging equations, HIROMB was run with 3-nm resolution in the Baltic Sea with data assimilation (Method of Successive Corrections; Daly, 1991) for the spring of 2005. Figure 1 shows some results from a 48-hour forecast forced by the operational atmospheric model HIRLAM. The figure shows the situation after a southwestern wind burst, which pushed the ice to the northeast towards the Finnish coast. During the process, the ridged ice thickness increased locally up to about 30 cm, the ridge density increased up to about 4 ridges per km, and the ridge height increased up to about 1.5 m. Longer-term simulations (whole seasons, not shown) indicate that the ridging equations produce very realistic results, in terms of location of new ridges as well as in terms of ridge density and ridge sail height.

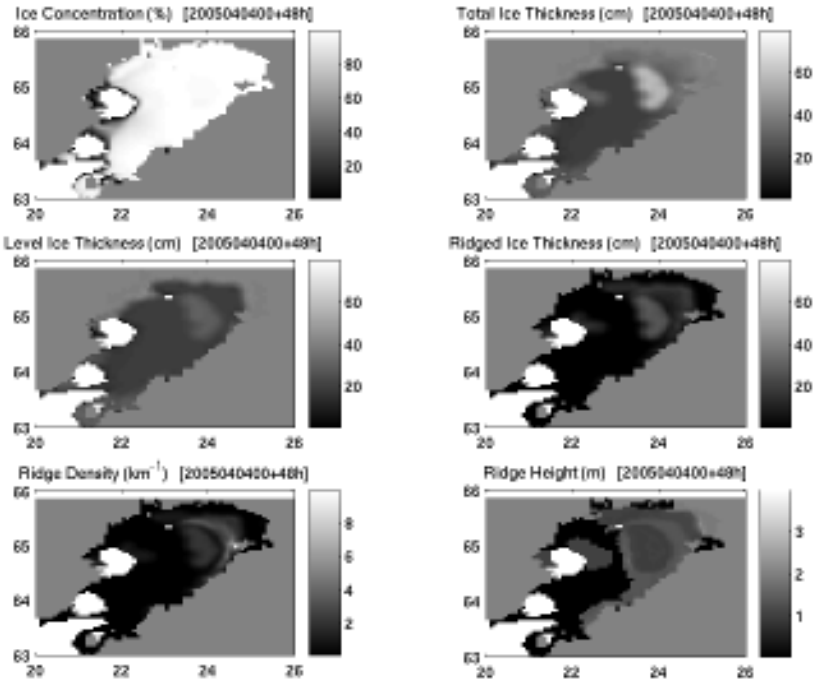

Figure 1 Example of model output (Bothnian Bay) from a 48-hour forecast started at 00 UTC on April 4, 2005. A southwestern wind burst has generated lots of new ridges off the coast of Finland.

Today only qualitative large-scale information about ice ridges is available on operational ice charts. Although uncertain, this information is today used quantitatively in the data assimilation system for HIROMB. A challenge for the future is to improve this information using analysed SAR images.

Acknowledgements

This work was sponsored by the European Commission, contract EVK3−CT−2002−00083.

References

Daley, R. (1991). Atmospheric Data Analysis, Cambridge Atmospheric and Space Science Series, Cambridge University Press, Cambridge.

IRIS (2005). Ice Ridging Information for Decision Making in Shipping Operations, see www.tkk.fi/Units/Ship/Research/Iris/Public/.

Kleine, E. and S. Sklyar (1995). Mathematical Features of Hibler's Model of Large-Scale Sea-Ice Dynamics, Deutsche Hydrographische Zeitschrift, vol. 47, no. 3, 179–230.

Lensu, M. (2003). The evolution of ridged ice fields, Dissertation for the degree of Doctor of Philosophy, Helsinki University of Technology, Ship Laboratory, Finland.

Multivariate data assimilation in the Mercator North Atlantic and Mediterranean high resolution model

Jean-Michel Lellouche*[1], Mounir Benkiran[2] and Eric Greiner[2]

[1]*CERFACS / Mercator-Ocean, Ramonville Saint Agne, France*
[2]*CLS / Mercator-Ocean, Ramonville Saint Agne, France*

Abstract

A new assimilation system based on the Reduced-Order Optimal Interpolation algorithm using 1D vertical multivariate EOFs has been implemented in the Mercator North Atlantic and Mediterranean High Resolution model. This new multivariate prototype, called PSY2v2, gives a very advanced description of the mesoscale patterns. Some assimilation diagnostics and a comparison with the previous high resolution univariate prototype, called PSY2v1, are presented.

Keywords: Multivariate data assimilation, EOFs, North Atlantic, Mediterranean Sea, high resolution

1. Introduction

The Mercator Ocean Monitoring and Forecasting System is routinely operated in real-time in Toulouse by the Mercator project since early 2001, and has been regularly upgraded through three prototypes of increasing complexity (PSY1, PSY2 and soon PSY3), expanding the geographical coverage from regional to global, improving models and assimilation schemes.

In this contribution, we focus on the North Atlantic and Mediterranean High Resolution Prototype PSY2v2. The ocean model is based on OPA-8.1 (Madec *et al.*, 1998), a general circulation model developed at LODYC (IPSL Paris), and is designed to simulate the Atlantic and Mediterranean oceans with a very high horizontal resolution (5−7 km). The assimilation system is based on the Reduced-Order Optimal Interpolation algorithm and uses 1D vertical multivariate EOFs to extract statistically-coherent information from the observations (Benkiran *et al.*, 2005). The PSY2v2 prototype assimilates, in a fully multivariate way, conjointly altimeter data (JASON1, ENVISAT and GFO), Reynolds SST and temperature and salinity vertical profiles provided by the CORIOLIS centre. The previous high resolution prototype PSY2v1 assimilates only the Sea Level Anomaly (SLA) from satellite measurements along tracks with a univariate mode. The 2D increments of SLA are then converted into 3D increments of U, V, S, T and TKE using an algorithm based on the "lifting-lowering" method (Cooper and Haines, 1996).

After a brief presentation of the multivariate/multidata assimilation algorithm, some results obtained with the PSY2v2 prototype will be presented.

* Corresponding author, email: jean-michel.lellouche@mercator-ocean.fr

2. The assimilation method

PSY2v2 assimilates SLA altimeter data, SST and *in situ* observations (temperature and salinity profiles) and works as follows:

1. The differences between SLA, T and S observations and model forecast are computed at appropriate time and data locations for a full week's model integration.
2. These misfits are projected in a 2D reduced space using a fully multivariate OI:
   - The estimation state vector is composed of the vertical profiles of temperature and salinity and the barotropic stream function.
   - EOFs of the estimation state vector are computed once at each point of the model grid from hindcast simulations.
   - The OI gain is computed for each of the EOFs independently (EOFs orthogonality) for a given number of dominant EOFs (order reduction up to 20 modes).
3. The model state is updated by the sum of the contribution of each selected EOF to the gain multiplied by the innovation vector.
4. The baroclinic velocity increments, which are not in the estimation state vector, are computed assuming geostrophy.
5. A new model state analysis is updated using the innovation vector computed above.
6. Starting from this new ocean state, the model runs for the next week of prediction, using the atmospheric forcing fields provided by the ECMWF.

3. The PSY2v2 results

This section presents some results obtained with the multivariate multidata prototype PSY2v2. After a spin up to real time of two and a half years (from January 2003 to June 2005), PSY2v2 is running in real time mode since the beginning of June 2005 and provides analyses and 2-weeks forecasts. This simulation has been initialised by Reynaud climatology in the Atlantic and Medatlas2 in the Mediterranean Sea.

3.1 Assimilation diagnostics

Figure 1a shows the number of temperature profiles that entered into the system versus time and depth. This number becomes particularly important in the second half of the year (~500 profiles). Figure 1b shows the variations of the mean value of the misfits (differences between the observation and model forecast), which is weak during the whole year. The RMS value of the misfit is plotted in Figure 1c and proves to be close to zero, with a maximum at the thermocline depth.

Satellite altimetry are used weekly to constrain the geostrophic currents, here in 2004. The data number exhibits the data availability in real-time. The misfits (i.e. correction to apply to the model) reach 8 cm, and represents 75% of the data variability (Figure 2).

3.2 Mediterranean Water Outflow (MOW) representation

One of the main problems with univariate prototypes is the representation of Mediterranean waters, mainly its vertical position near 1000 m. Figure 3 shows the salinity at 1000 m for April 2004 from PSY2v1 and PSY2v2 simulations.

For PSY2v1, the MOW is maintained by the relaxation bellow 500 m to Reynaud climatology in the Gulf of Cadix, which is no longer the case for PSY2v2. Figure 3 shows salty water which corresponds to the characteristics of Mediterranean waters (salinity close to 36.5 psu), with meddy formations and better propagation in the PSY2v2 case, showing impact of T/S vertical profiles assimilation.

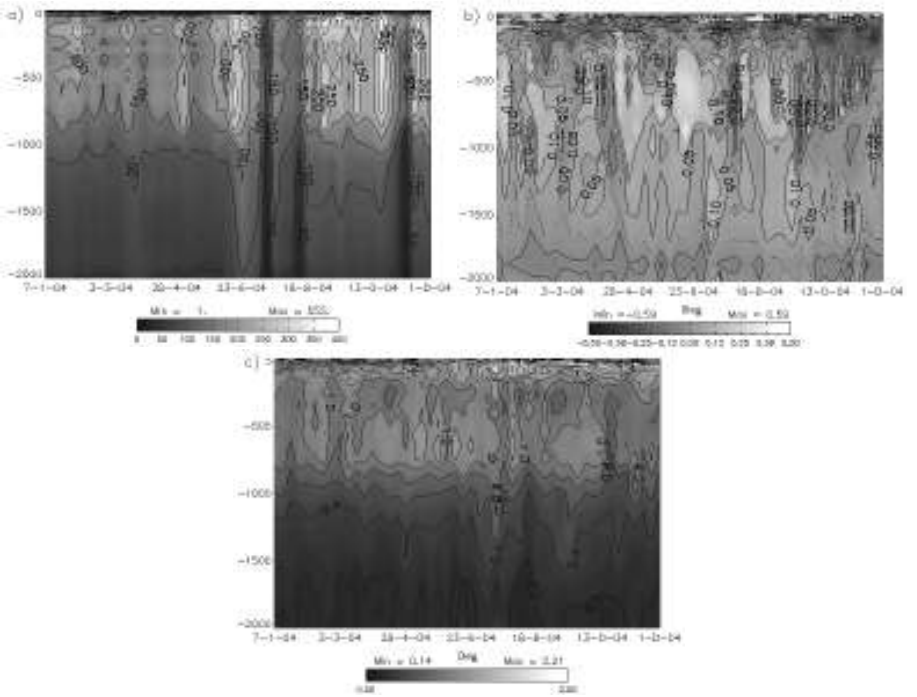

Figure 1 Assimilation diagnostics with respect to the vertical temperature profiles over 2004 (depth in metres). a) Number of temperature data; b) Mean misfit between observations and model forecast; c) RMS of the misfit.

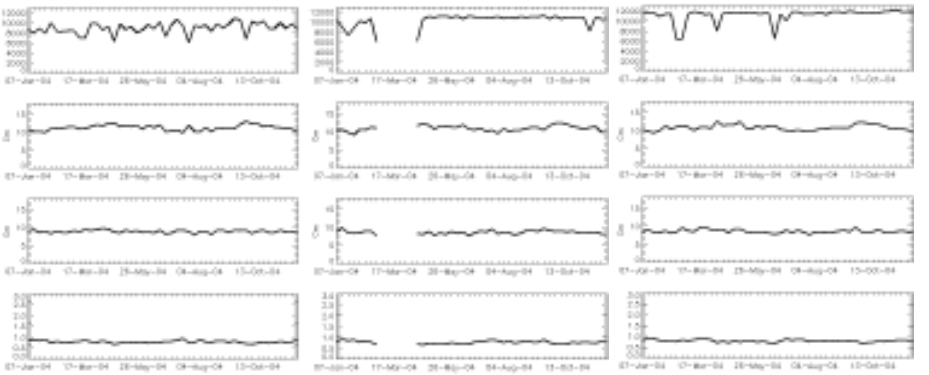

Figure 2 Assimilation diagnostics with respect to the SLA for the three satellites JASON1 (left), ENVISAT (centre) and GFO (right). From top to bottom: Data number, RMS data, RMS misfit and ratio (RMS misfit / RMS data).

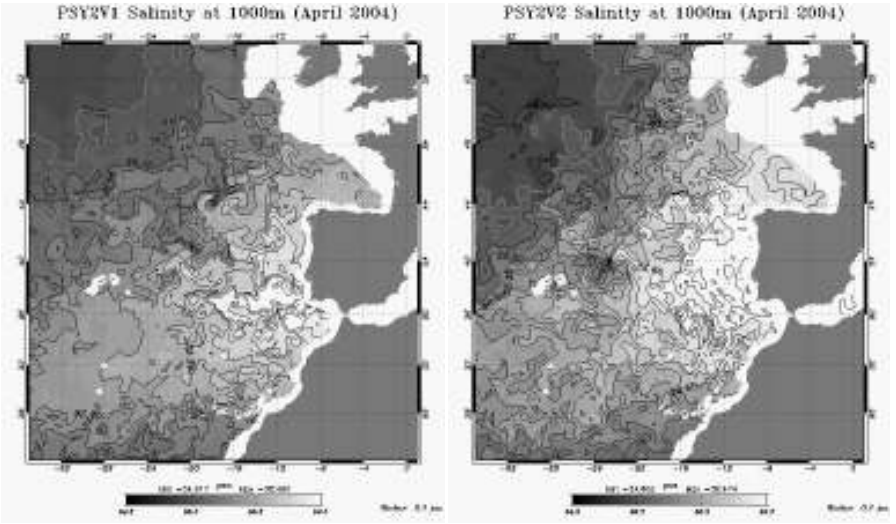

Figure 3 Salinity at 1000 m in April 2004 for PSY2v1 (left) and PSY2v2 (right) simulations.

4. Conclusion

This paper describes the new Mercator fully multivariate high resolution prototype. This new prototype has a very good statistical comportment and allows, among other things, better representation of water masses, for example, the Mediterranean Water Outflow, with a very advanced description of the mesoscale patterns. A more comprehensive validation of PSY2v2 prototype is in progress and we plan to provide analyses and forecasts in a operational mode on the Web from the beginning of September 2005.

Acknowledgements

The authors thank the PALM team for their help in the use of the PALM coupler (Piacentini *et al.*, 2003) which provides a general structure for a modular implementation of a data assimilation system and simplifies changes in the data assimilation algorithm.

References

Benkiran, M., E. Greiner and E. Dombrowsky (2005). Multivariate and multidata assimilation in the Mercator project, submitted to Journal of Marine Systems.

Cooper, M. and K. Haines (1996). Data assimilation with water property conservation, J. Geophys. Res, 101, 1059–1077.

Crosnier, L., N. Verbrugge, J.M. Lellouche, M. Benkiran and E. Greiner (2005). Validation in the two high resolution Mercator forecast systems in the North Atlantic Ocean. This volume page 598.

Madec, G., P. Delecluse, M. Imbard and C. Levy (1998). OPA8.1 ocean general circulation model reference manual, Notes du pôle de modélisation IPSL, 91 pp.

Piacentini A., S. Buis, D. Declat, and the PALM group (2003). PALM: A computational Framework for assembling high performance computing applications, Concurrency and Computat., 00, 1–7.

GMES-Oriented Projects

Towards operational sea ice monitoring services in the Arctic

Stein Sandven*[1] and Ola M. Johannessen[1,2]

[1]*Nansen Environmental and Remote Sensing Center, Bergen, Norway*
[2]*Mohn-Sverdrup Center for Global Ocean Studies and Operational Oceanography, Bergen, Norway*

Abstract

Improved monitoring systems are needed to provide consistent and long-term data on the ice–ocean circulation in the Arctic Ocean including the Fram Strait and Nordic Seas. The monitoring systems should have a central role in detection and verification of climate variability and trends. Monitoring and forecasting of the environmental conditions on a daily to seasonal scale is also needed to support all types of marine operations to secure sustainable and safe development in high latitudes. Ice monitoring and forecasting is of particular importance in the Arctic because of growing activities due to oil and gas exploration, ship transportation and other human activities. The International Polar Year 2007–2008 will focus on opportunities and challenges in the Arctic (www.ipy.org). One of the major challenges is to develop environmental monitoring systems. This paper gives an overview of recent developments in sea ice monitoring and modelling, contributing to building operational services for the Arctic.

Keywords: sea ice, Arctic, monitoring, forecasting, IPY, satellites

1. Introduction

The presence of sea ice together with harsh climate and weather conditions in the Arctic imposes strong limitations on maritime activities in these areas. Monitoring and forecasting of sea ice, weather and ocean variables are therefore of high priority to support safe and cost-effective maritime operations in ice-covered areas.

The Arctic region has over the last 2–3 decades warmed more than other regions of the world. In the same period the sea ice cover has decreased by ~10% whereas the ice thickness has decreased up to 40% during summer. Other observed changes include a warming of the Atlantic water in the Arctic Ocean, increased precipitation in the Arctic regions and higher river discharge into the Arctic Ocean. During the last decades changes detected include a significant freshening of the deep North Atlantic Ocean, warming in the deep water of the Nordic Seas and a decrease of deep overflow in the Faeroe Bank Channel. The recent changes in the Arctic environment have been investigated in books (i.e. Bobylev *et al.*, 2003), papers (i.e. Johannessen *et al.*, 1999; 2004) and in review reports (i.e. ACIA, 2004; Sandven *et al.*, 2005).

Improved monitoring systems are needed to provide consistent and long-term data on the ice–ocean circulation in the Arctic Ocean including the Fram Strait and Nordic Seas. Monitoring systems should play a central role in detection and verification of climate

* Corresponding author, email: stein.sandven@nersc.no

variability and trends. Monitoring and forecasting of the atmosphere, sea ice and ocean conditions on a daily to seasonal time scale is also needed to support all types of marine operations. Offshore operations in ice-covered seas need specific ice information which is more detailed than the standard ice charts produced by the national ice services. Search and rescue organisations dedicated to the mitigation of loss of life or property due to accidents in Arctic waters need ice information to support their operations. Coastguards and the military need ice information for planning and implementation of their operations. Marine engineers need ice information for the design of safe structures and vessels which can operate in ice conditions.

Satellite earth observation data plays an increasingly important role in monitoring sea ice, and implementation of new satellite sensors makes it possible to observe more sea ice parameters on a regular basis. Operational monitoring services offer a wider range of products, and access to these products are facilitated through extensive use of the internet. Sea ice modelling and forecasting systems, where satellite data are assimilated into coupled ice–ocean models, are under development. Several modelling systems are used to produce ice forecasts in pre-operational mode. In this paper, the development sea ice monitoring and forecasting services are reviewed against a background of the increased need for these services in the Arctic seas.

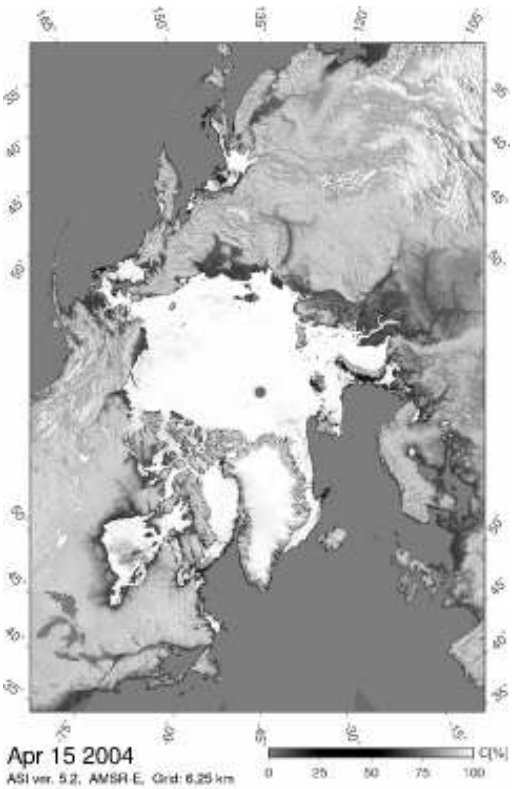

Figure 1 Example of Arctic ice concentration maps produced daily from passive microwave satellite data (AMSR-E). Courtesy: Georg Heygster, University of Bremen.

2. Monitoring sea ice on the global and regional scale

2.1 Ice extent and concentration

Sea ice monitoring on a global scale by using satellite data has been carried out operationally for more than 2 decades. Starting with NASA's Nimbus-7 in 1978, passive microwave observations have provided a continuous and unique data set to monitor seasonal, interannual and long-term variability of sea ice extent. Monthly mean areas of total and multiyear ice have been produced by the Nansen Environmental and Remote Sensing Center to study the trends in ice area in the Arctic since 1978. The time series of passive microwave data show that the total ice area has reduced by 3–4% per decade, while the multiyear ice area has reduced by 7% per decade (Johannessen *et al.*, 1999; 2004). Maps of ice concentration and extent are produced by several service providers such as the National Snow and Ice Data Center (http://nsidc.org/cryosphere/glance/), the EUMETSAT Ocean and Sea Ice Satellite Application Facility (OSI-SAF) (http://saf.met.no), and the Technical University of Denmark (www.seaice.dk). Since 2003, daily maps of ice concentration using AMSR-E passive microwave data from the EOS/Aqua satellite are produced by the Institute of Environmental Physics, University of Bremen (www.seaice.de). The AMSR-E product has an improved resolution of about 6 km for the hemispheric maps, and about 3 km for regional maps. This product is based on the ASI (ARTIST Sea Ice) algorithm (Kaleschke *et al.*, 2001). It uses the 89 GHz data of AMSR-E with a spatial resolution of 5×5 km. Examples of large scale ice concentration maps from AMSR-E data are shown in Figure 1.

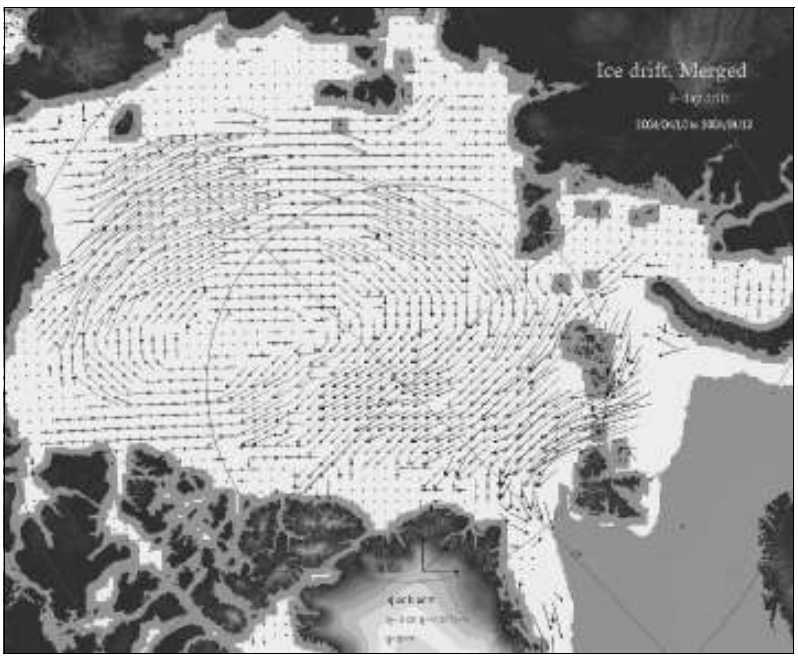

Figure 2 Example of ice drift maps produced by Ifremer merging polarisation of scatterometer satellite data over three days. Courtesy of Robert Ezraty, Ifremer.

Ice drift

Since 1990 the International Arctic Buoy programme (IABP) has operated a network of ice buoys measuring atmospheric variables and buoy position used to estimate ice drift. Usually 15–20 buoys are operating simultaneously, most of them in the central Arctic basin (http://iabp.apl.washington.edu/). The data are transmitted via ARGOS. Synoptic ice drift is derived from scatterometer and passive microwave data, providing a valuable supplement to the drifting buoy measurements. Since 1999, Ifremer has been producing ice drift from SeaWinds scatterometer data and SSM/I passive microwave data every day from October to April (Ezraty and Piollé, 2003). An example of an ice drift product is shown in Figure 2.

ENVISAT ASAR Global Monitoring Mode (GMM) offers a unique opportunity to observe and monitor the whole Arctic and Antarctic sea ice cover regularly with medium-resolution (1–2 km) radar images independent of cloud and light conditions. This capability has not been available from any other space system so far, and ESA started to deliver GMM data in April 2004. GMM is a default mode which provides extensive SAR coverage over the polar regions. The first stage in the product development from the GM data is the geolocation, radiometric correction and mosaic composition of radar images. Ice drift vectors can them be generated (Figure 3). The possibility of retrieving other sea ice parameters from the GM data such as ice classification and polynya mapping is under investigation.

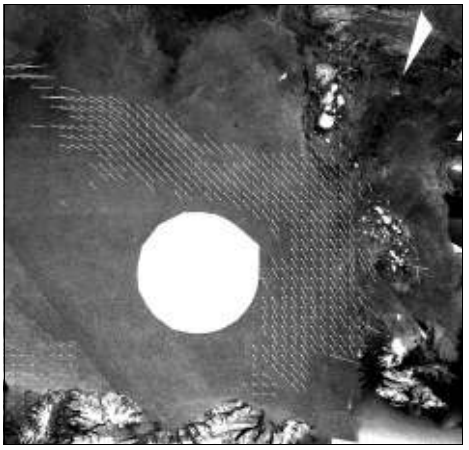

Figure 3 Example of ASAR Global Monitoring Mode mosaic and derived ice drift vectors produced by Vexcel UK.

Ice thickness

Ice thickness in the Arctic has been measured by various *in situ* methods including surveys by aircraft, helicopters and submarines for several decades, but none of these have provided synoptic mapping of ice thickness. A method for ice thickness retrieval from radar altimeter data has been developed by Laxon *et al.* (2003) based on ERS altimeter data which have been obtained up to 81.5°N since 1992. The method is based on separation of the signals from sea ice floes and open water or thin ice in leads, and

then calculation of freeboard which is translated into thickness based on climatological estimates of snow cover and ice density. CryoSat, scheduled for launch in October 2005, will carry a beam-limited altimeter providing data coverage of sea ice up to 88°N, allowing nearly complete coverage of the Arctic sea ice. The main ice thickness product from CryoSat will be monthly mean estimates with a resolution of 100 km.

3. Monitoring on the regional and local scale

3.1 Detailed mapping of ice parameters by SAR

Synthetic Aperture Radar (SAR) has been used as the main data source for regional ice mapping in Canada, Greenland, and the Baltic Sea for more than a decade. Other regions such as the Norwegian and Russian sectors of the Arctic have recently started to use SAR for ice monitoring on a limited scale. The first examples of high-resolution ice maps from ENVISAT ASAR wideswath images were tested in the Svalbard area during the winter and spring of 2003. One wideswath scene of 400×400 km can cover most of the Svalbard archipelago. An example of an ASAR scene and the corresponding high resolution ice chart produced by met.no is shown in Figure 4. The monitoring of sea ice in the Svalbard area by ASAR continued in 2004. From 2005 RADARSAT SAR are produced to monitor larger parts of the Norwegian marine and sea ice areas.

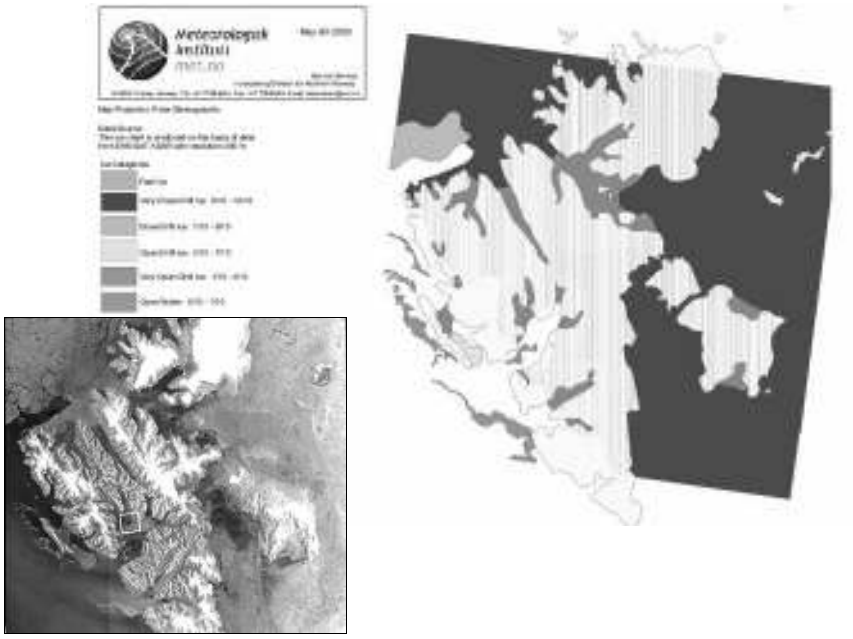

Figure 4 Left (inset): ENVISAT ASAR image of the Svalbard archipelago from 5 May 2003, where the small white rectangle indicates a validation area where ice observations from ship and helicopter were obtained. Right: Ice map produced by met.no from a ASAR image from 7 May 2003 showing five ice concentration categories and fast ice. Courtesy of Helge Tangen, met.no.

In the Northern Sea Route, use of SAR data have been demonstrated on many occasions since ERS was launched in 1991 (Johannessen *et al.*, 2000; 2005). In the winter of 2004

regular SAR acquisition in the Kara Sea was obtained for the first time, using ENVISAT ASAR wideswath images to map the sailing routes approximately once a week. An example of a weekly SAR mosaic for the Kara Sea region is shown in Figure 5. The SAR images provide additional information of importance for ice navigation which is not included in the standard ice charts, such as ice pressure information, multiyear ice floes, shear zones, cracks, and deformed ice versus level ice. This information is particularly useful for icebreakers and other ice-going vessels which need to go though the ice. The geolocated SAR images are transferred to the vessels using email transmitted via Inmarsat or Iridium. Onboard the ships, the SAR image is analysed by the captain in combination with sea charts, weather information and *in situ* ice observations. There is an ongoing development to include satellite images in ECDIS systems (Electronic Charting and Information System) which are used by many ships today. An overview of the development of SAR ice monitoring is given in a the book "Polar Seas Oceanography, Remote Sensing of Sea ice in the Northern Sea Route: Studies and Applications" (Eds. Johannessen *et al.*) Praxis Springer (in press 2005).

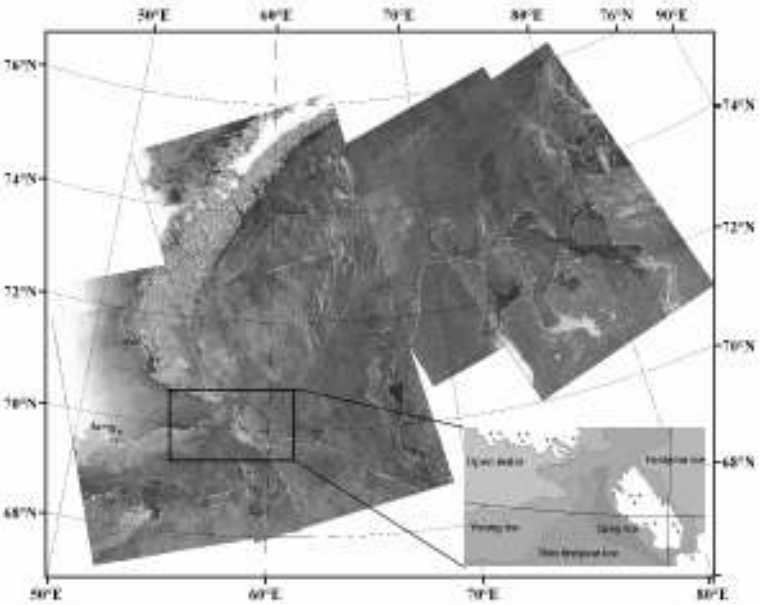

Figure 5 Example of ENVISAT ASAR mosaic produced by NERSC based on wideswath images covering the Kara Sea region on 27–28 February 2005. A subset of the image mosaic has been analysed for ice type classification, shown in the inserted ice chart.

Ice area flux in the Fram Strait derived from a sequence of ASAR images has started to be produced as a contribution to the seasonal and long-term monitoring of the Arctic sea ice. NERSC has been producing ice area flux profiles across 79 N as shown in Figure 6. The ice area flux data will be used together with thickness data from moorings for estimation of volume fluxes. The time interval between the images is presently 3 days. Time series of ice flux through the Fram Strait is a key climate parameter. Monitoring by SAR requires regular acquisition and production of ASAR wideswath data from ENVISAT and later from other SAR missions, such as RADARSAT-2.

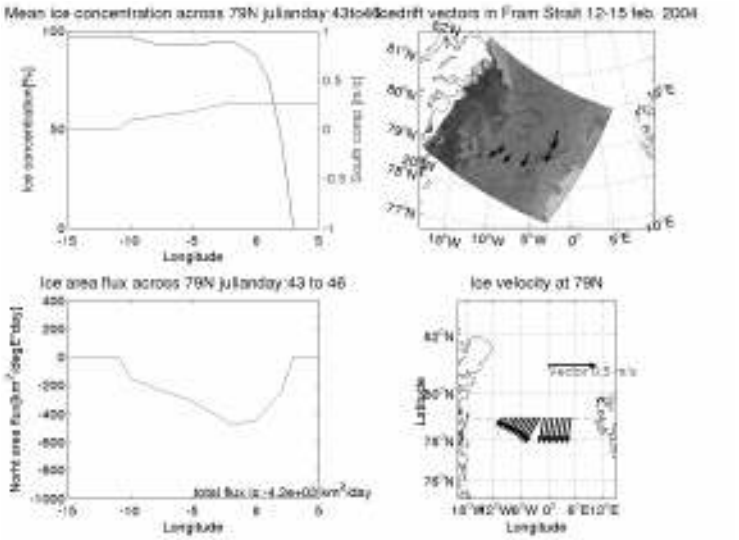

Figure 6 Upper left: Profiles of ice concentration from SSMI data and north component of ice drift retrieved form ice tracking in the two SAR images from February 22 and 25, 2004 (upper right). Lower left: Ice area flux for the three day period; lower right: Interpolated ice drift vectors across 79 N.

4. Modelling and forecasting systems

Ice modelling is required to produce ice forecasts up to typically 5 days to support marine operations in or near sea ice areas. Most operators need forecasting in addition to NRT monitoring, because planning of operations needs an estimate of the predicted ice situation a few days ahead.

Development and validation of ice modelling requires good data sets, and many of them are derived from satellites. For example, the 25 years of ice extent and ice concentration from passive microwave data is one of the main data sets for validation of ice models. Presently, ice concentration from passive microwave data are assimilated into the TOPAZ modelling system for the Arctic (Lisaeter *et al.*, 2003). Because sea ice is driven by both the atmosphere and the ocean, it is common to run coupled ice–ocean models forced by atmospheric fields. Especially short-term forecasting (up to 5 days) is forced by the predicted atmospheric fields. Furthermore, ice modelling is also used to simulate longer periods from seasons to years, as part of climate models which are normally fully coupled atmosphere–ice–ocean models. The predicted reduction in Arctic ice extent and thickness during this century is based on several climate model simulations. Ice models are also used to produce hindcast data sets, because models require careful comparison with other data obtained in hindcast, for example from monitoring moorings or from specific experiments.

The TOPAZ ice–ocean modelling and data assimilation system has been developed by NERSC through the EU-funded projects DIADEM and TOPAZ over the last 6–8 years (Bertino *et al.*, 2004). The system is presently run operationally at NERSC as a demonstration of 10-day forecasting of the Atlantic ocean, the Nordic Seas and the Arctic

Ocean. The ice model uses the Elastic Visco Plastic rheology by Hunke and Dukowicz (1997), coupled to the HYCOM ocean model. The estimated parameters include ice extent, concentration, thickness, drift as well as all the main oceanographical parameters. ECMWF forcing fields are used, with assimilation of weekly sea level height from satellite altimeter and weekly ice concentration from SSM/I data.

NERSC is developing a high-resolution (4 km) ice–ocean model for the Barents and Kara Seas, which nests within the TOPAZ system on the boundaries. ECMWF forcing fields are used as well as assimilation of weekly sea level height from satellite altimeter and weekly ice concentration from SSM/I data. The estimated parameters are ice extent, concentration, thickness, drift as well as all the main oceanographical parameters. Examples of the model output are shown in Figure 7.

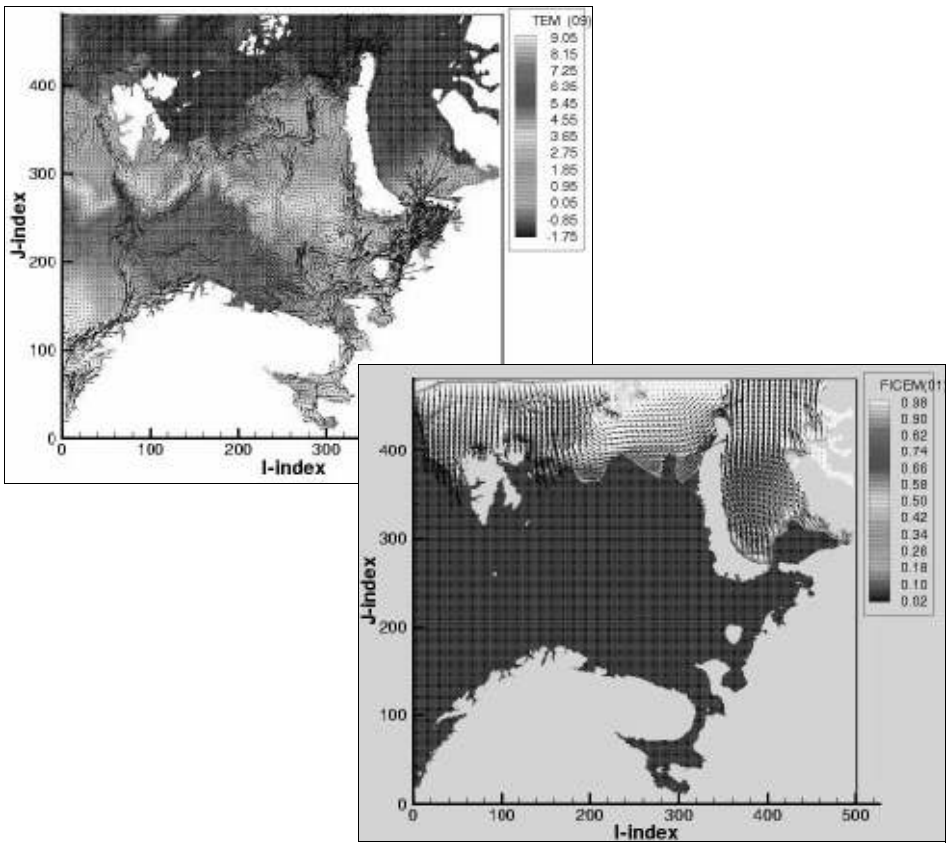

Figure 7 Example of model output from the Barents Sea coupled ice–ocean model at NERSC. Top: sea surface temperature and surface currents; Bottom: ice thickness and ice drift. The numbers along the axes indicate grid cell numbers of the model.

5. Conclusion

Timely information on sea ice and other met–ocean conditions is essential for all types of marine operations in Polar regions. The growing activities in the Arctic waters

represent a significantly higher degree of risk to shipping than most other waters. The presence of ice fields, wind and waves, icing of vessels and darkness in the winter requires adequate monitoring and forecasting services. In addition to safe and cost-effective ship transport and offshore operations, the risk of oil spill and other pollution requires specific met–ocean information. The presence of sea ice makes clean-up techniques normally employed in more temperate climates useless in ice-covered areas. The safety and efficiency of sea transportation, off-shore operations, fisheries and other marine activities have been the motivation to establish operational sea ice monitoring and forecasting services in many countries in addition to the weather services. These services are usually limited to national areas of interest and leave large parts of the Arctic without daily monitoring and forecasting services. The prospective of increased shipping, offshore operations and other human activities has created a need to establish operational monitoring and forecasting services in the Arctic. The first step towards establishing an Arctic GOOS has been taken by EuroGOOS (Sandven *et al.*, 2005).

Acknowledgements

The examples of sea ice monitoring products presented in the figures are provided by Georg Heygster, University of Bremen; Robert Ezraty, Ifremer; Kim Partington, Vexcel UK; and Helge Tangen, met.no. The ENVISAT ASAR data are provided by ESA through the GMES project ICEMON.

References

ACIA (2004). Impacts of a warming Arctic: Arctic Climate Impact Assessment, November, 2004 (http://amap.no/acia/).

Bertino, L., Lisæter, Sagen, Counillon, Winther, Stette, Natvik, G. Evensen, Morel, Brankart, Testut, Birol, Brasseur, Verron, Schartau, Schröter, Dombrowsky, Burillo, Gilles Larnicol, Schaeffer and Weller (2004). Towards an Operational Prediction system for the North Atlantic and European coastal Zones — TOPAZ Final report, NERSC Technical Report, 251.

Bobylev, L.P., K.Ya. Kondratyev and O.M. Johannessen (eds.), Arctic Environment Variability in the Context of Global Change Springer–Praxis Publishing, 470 pp.

Ezraty R. and J.F. Piollé (2003). Sea Ice drift in the Arctic, User's manuals, www.ifremer.fr/cersat.

Hunke, E.C. and J.K. Dukowicz (1997). An elastic–viscous–plastic model for sea ice dynamics. J. Phys. Oceanogr., 27, 1849–1867.

Johannessen, O.M., E.V. Shalina and M.W. Miles (1999). Satellite Evidence for an Arctic Sea Ice cover in Transformation. Science, 286, 1937–1939.

Johannessen, O.M., A.M. Volkov, L.P. Bobylev, V.D. Grischenko, S. Sandven, L.H. Pettersson, V.V. Melentyev, V. Asmus, O.E. Milekhin, V.A. Krovotyntsev, V.G. Smirnov, V.Yu. Alexandrov, G. Duchossois, V. Kozlov, G. Kohlhammer and G. Solaas (2000). ICEWATCH — Real-time sea ice monitoring of the Northern Sea Route using satellite radar (a Cooperative Earth Observation Project between the Russian and European Space Agencies). Earth Observation and Remote Sensing, Vol. 16, No. 2, 257–268.

Johannessen, O.M., M.W. Miles, L. Bengtsson, L.P. Bobylev and S.I. Kuzmina (2003). Arctic climate change, In Arctic Environment Variability in the Context of Global Change (eds. Bobylev, L.P., K.Ya. Kondratyev and O.M. Johannessen), Springer–Praxis Publishing, 470 pp.

Johannessen, O.M., L. Bengtsson, M.W. Miles, S.I. Kuzmina, V.A. Semenov, G.V. Alekseev, A.P. Nagurnyi, V.F. Zakharov, L.P. Bobylev, L.H. Pettersson, K. Hasselmann and H.P. Cattle (2004a). Arctic climate change: observed and modeled temperature and sea–ice variability. Tellus, Series A: Vol.56A, no.4, July 2004.

Johannessen O.M., V.Yu. Alexandrov, I.Ye. Frolov, S. Sandven, M. Miles, L.P. Bobylev, L.H. Pettersson, V.G. Smirnov and E.U. Mironov (2005a). Polar Seas Oceanography, Remote Sensing of Sea ice in the Northern Sea Route: Studies and Applications. Praxis Springer, in press.

Kaleschke, L. *et al.* Canadian Journal of Remote Sensing, vol. 27, no. 5, 502–516.

Laxon, S., N. Peacock and D. Smith (2003). High interannual variability of sea ice thickness in the Arctic region. Nature, Vol. 245, pp. 947–950.

Lisæter, K.A., J. Rosanova and G. Evensen (2003). "Assimilation of ice concentration into a coupled ice–ocean model, using the Ensemble Kalman Filter", Ocean Dynamics, 53: 368–388.

Sandven, S. (2005). The Arctic Ocean and the Need for an Arctic GOOS, EuroGOOS Publication no. 22, EuroGOOS Office, 31–33.

European FerryBox project: From on-line oceanographic measurements to environmental information

W. Petersen*[1], F. Colijn[1], J. Dunning[2], D.J. Hydes[3], S. Kaitala[4], H. Kontoyiannis[5], A. Lavín[6], I. Lips[7], J. Howarth[8], H. Ridderinkhof[9], K. Pfeiffer[10] and K. Sørensen[11]

[1]*GKSS Research Centre, Geesthacht, Germany*
[2]*CTG, London, United Kingdom*
[3]*NOC, Southampton, United Kingdom*
[4]*FIMR, Helsinki, Finland*
[5]*HCMR, Athens, Greece*
[6]*IEO, Santander, Spain*
[7]*EMI, Tallinn, Estonia*
[8]*POL, Liverpool, United Kingdom*
[9]*NIOZ, Texel, Netherlands*
[10]*Hydromod, Hamburg, Germany*
[11]*NIVA, Oslo, Norway*

Abstract

In the European FerryBox project eleven partners on nine routes are cooperating to develop and test operational oceanographic systems on ferries and ships of opportunity (FerryBoxes). The objectives are

1. to show how FerryBoxes can be used for autonomous measurements of environmental parameters
2. to quantify environmental variability of selected parameters on a European-wide scale
3. to improve the quality of numerical models by assimilation of FerryBox data
4. to demonstrate the reliability of such systems for monitoring the marine environment at all times of the year
5. to recommend to the European marine community how future FerryBoxes can be constructed, installed and operated.

The project encompasses the oligotrophic eastern Mediterranean to hypertrophic Northern European estuaries and shows the technical realisation and experiences after nearly two years of operation in the different areas. Examples of different applications of FerryBox data to marine environmental issues (e.g. eutrophication) and combination with other data (e.g. "conventional monitoring", remote sensing and hydrodynamic models) demonstrate that FerryBoxes are a suitable tool that can complement existing monitoring in coastal and shelf areas and provide deeper insight into marine processes.

Keywords: FerryBox, *in situ* monitoring, eutrophication, chlorophyll *a* fluorescence, phytoplankton blooms, remote sensing

* Corresponding author, email: Wilhelm.Petersen@gkss.de

1. Introduction

The lack of reliable monitoring systems that provide continuous observations of the marine environment in the coastal areas and shelf seas of Europe with an adequate data quality is a serious hindrance to understanding marine systems. Currently operational monitoring is mainly carried out by manual sampling and analysis during ship cruises. Autonomous measuring systems on buoys allow measurement of standard oceanographic parameters (temperature, salinity, currents) and in some cases other parameters, e.g. turbidity, oxygen and chlorophyll fluorescence. However, existing observations mostly lack the spatial coverage and temporal resolution required to determine the state of the marine environment and changes within it. Furthermore the automatic systems on buoys etc. are affected by biofouling and the operational costs are high due to ship costs needed for servicing.

To overcome these problems, the use of "ships of opportunity" (SoO) has been promoted by EuroGOOS (Flemming *et al.*, 2002). There are many routes for ferries and other SoOs which run frequently-repeated routes. The "Continuous Plankton Recorder" (CPR, Reid *et al.*, 1998) has followed the idea of using scientific equipment on such ships for continuous recording of biological data. Over the last 60 years it has produced an impressive data set on plankton abundance with time (e.g.Vezzulli and Reid, 2003). As a measuring platform, ferries on regular routes offer a cheap and reliable possibility to obtain regular observations on near surface water parameters. Applying such a FerryBox system on ferryboats or ships-of-opportunity has several advantages:

1. the system is protected against harsh environments, e.g. waves and currents
2. bio-fouling can be more easily prevented (in-line sensors)
3. no energy restrictions (in contrast to buoys)
4. easier maintenance when the ferry comes back "to your doorstep"
5. lower running costs since the operational costs of the ship do not need to be calculated
6. instead of point measurements (buoys) transects yield much more information.

Recently, sophisticated systems have been implemented on ferries which allow precise measurements of temperature, salinity and chlorophyll (e.g. Harashima and Kunugi, 2000; Rantajärvi *et al.*, 1998; Ridderinkhof *et al.*, 1999; Swertz *et al.*, 1999; Hydes *et al.*, 2003; Petersen *et al.*, 2003). In another EU project (CAVASSOO) a pCO_2 observing system has been established on SoOs.

2. EU FerryBox project

Within the GOOS (Global Ocean Observing System) and EuroGOOS framework the concept is being extended to develop automatic measuring systems for biological-oceanographic parameters. The EU FerryBox project is developing and testing water quality monitoring systems on "ships of opportunity". Nine ferry routes are used in order to compare different systems and environments (Figure 1). The project encompasses the oligotrophic eastern Mediterranean Sea to hypertrophic Northern European estuaries. The aims and objectives of the project are:

- to show how FerryBoxes can be used for automatic measurements of environmental parameters
- to quantify environmental variability on a European-wide scale addressing eutrophication, sediment transport and transport of water masses
- to improve the quality of numerical models by assimilation of FerryBox data
- to demonstrate the reliability of such systems for monitoring the marine environment at all times of the year
- to recommend to the European marine community how future FerryBoxes can be operated.

The project is organised in different workpackages:

1. Operation and metrology of the nine FerryBox systems
2. Data management including provision of quality controlled data sets of all ferries for an international database (BOCD)
3. Scientific analysis of FerryBox data regarding eutrophication, transport of sediments and water masses
4. Application of FerryBox for models (including data assimilation) and for validation of remote sensing data
5. Exploitation and dissemination of FerryBox data and experiences to the public as well as to marine and environmental agencies and the marine and climate science community.

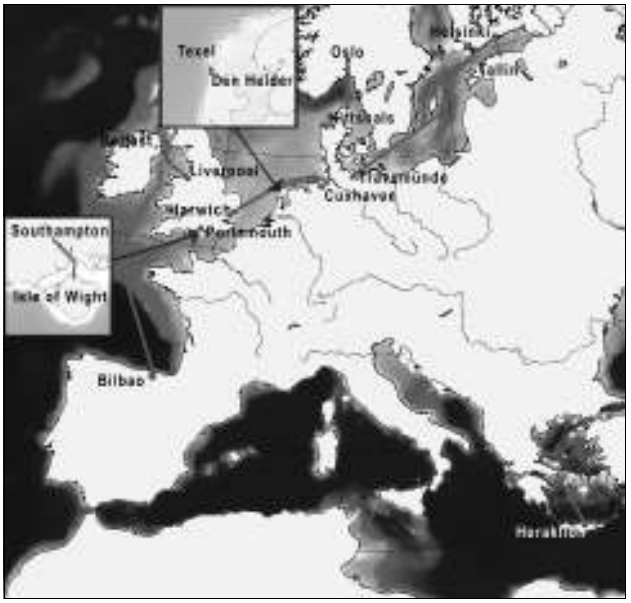

Figure 1 Ferry tracks involved in the EU FerryBox project.

The routes and the tasks on the different ferries are summarised in Table 1. Within the project the partners agreed to measure four core parameters (water temperature, salinity,

turbidity and chlorophyll *a* fluorescence) on all ferries. In addition, specific additional sensors and analysers are installed on certain lines. All FerryBox systems were in operation by the end of 2003, including the first FerryBox in the Baltic Sea (Alg@line) which started operation in 1993 (Rantajärvi 2003):

Table 1 Overview of the FerryBox routes and main tasks.

Area	Route	Main study items and tasks	Observed Parameter
1.Baltic Sea	A: Helsinki−Travemünde B: Helsinki−Tallinn	Eutrophication, algal blooms, sampling strategy	T, S, Turb, chl *a* fluorescence, pCO_2 (route A), automatically collected water samples (nutrients, chlorophyll *a* & phytoplankton)
2. Skagerrak	Oslo−Hirtshals	Validation of satellite data, combination *in situ* and remote sensing data	T, S, Turb, chl *a* fluorescence, PAR, automatically collected water samples (nutrients, phytoplankton)
3. Southern North Sea	Cuxhaven−Harwich	Nutrient input, eutrophication, algae classification, ground truth remote sensing	T, S, Turb, chl *a* fluorescence, nutrients (NO_3, NH_4, o-PO_4, SiO_2), algae groups, automatically collected water samples (nutrients, phytoplankton)
4. Wadden Sea	Den Helder−Texel	Water currents, sediment transport	T, S, Turb, chl *a* fluorescence, ADCP (water current, sediment transport)
5. Irish Sea	Birkenhead−Belfast	Transport and mixing on western Scottish shelf, algae growth, model validation	T, S, Turb, chl *a* fluorescence
6. Solent (UK) estuary	Southampton−Isle of Wight	Transport from river to sea, estuarine eutrophication	T, S, Turb, chl *a* fluorescence
7. English Channel, Bay of Biscay	Portsmouth−Bilbao	Water mass exchange shelf−ocean, range of plankton environments	T, S, Turb, chl *a* fluorescence, pCO_2, manually collected water samples (nutrients, chlorophyll, oxygen)
8. Mediterranean Sea	Athens−Heraklion (Crete)	Nutrient gradients, upwelling, data assimilation with buoy systems	T, S, Turb, chl *a* fluorescence

This paper gives examples of the reliability of the FerryBox systems in use, applications of FerryBox data for environmental problems (eutrophication, algal blooms) and the relevance of such systems for monitoring the quality of coastal waters.

3. Material and methods

As an example the setup of the German FerryBox system in the North Sea is shown in Figure 2. Water is pumped into the ship from an inlet in front of the ship's cooling water intake. A debubbling unit removes air bubbles, which may enter the system during heavy

seas. At the same time coarse sand particles which may be introduced in shallow harbours and which settle and tend to block the tubes are removed. Coupled to the debubbler is an internal water loop in which the seawater is circulated with a constant velocity of about 1 ms^{-1} passing the different sensors. A small part of the water is filtered by a ribbon-type filter for automatic nutrient analysis. For reliable unmanned operation the system is supervised by an industrial programmable logic control which can shut off the system in case of very severe errors and operates automatic cleaning cycles in harbour controlled by GPS. An industrial version (4H-Jena, Germany) of this system has been installed on the Greek ferry in the Mediterranean Sea. Data acquisition, data storage and data transfer to shore is controlled by an industrial standard PC. Data are automatically transferred to shore in the harbour and the system can be remotely operated by GSM (mobile phone).

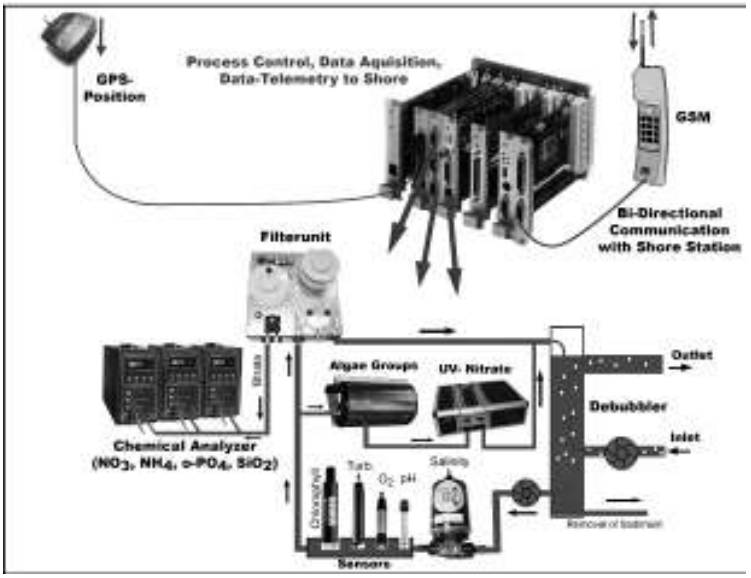

Figure 2 Schematic drawing of the German FerryBox system in the North Sea.

Biofouling is prevented by cleaning the sensors with tap water and rinsing with acidified water. Problems are sometimes caused due to clogging of the water inlet in the ship interface by debris or fish. Since all flow rates are supervised by the system in such cases an automatic pressure back-flushing cycle is initiated which clears the inlet. Water samples are automatically collected at predefined positions and stored in a refrigerator for subsequent analysis in the lab (nutrients, phytoplankton).

The FerryBox systems of the other partners are similar, however, without an automatic cleaning system. In these cases the cleaning of the system has to be carried out manually during maintenance, normally on a weekly basis. On routes 2 and 7, satellite communications systems are used to transfer the data to shore in real time for display on webpages (e.g. www.noc.soton.ac.uk/ops for route 7). On route 2, two-way communication is used to control an automatic water sampling system.

4. Results

4.1 Time series along a transect

To show that the system is able to describe the temporal evolution of water quality parameters, data of a single transect and a time series along this transect are presented in Figure 3 and Figure 4.

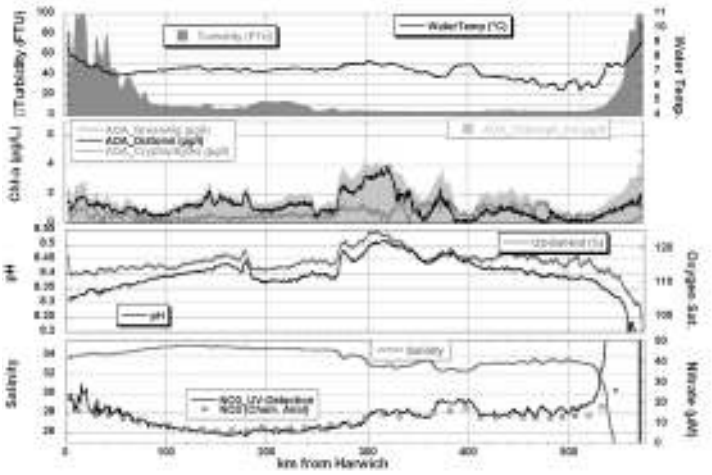

Figure 3 Route of the ferry and data measured along one transect in the Southern North Sea (Harwich to Cuxhaven) on 5 April 2005.

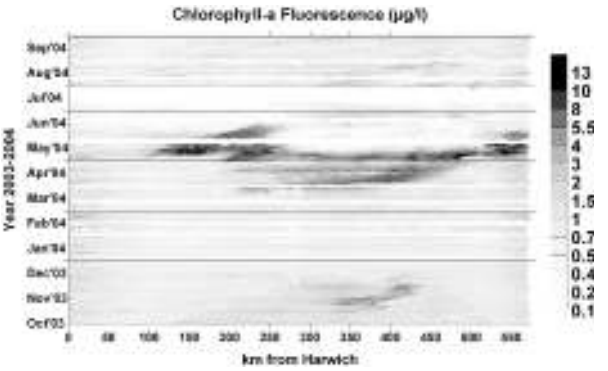

Figure 4 Algal dynamic along the transect in the Southern North Sea (Harwich to Cuxhaven) from October 2003 to September 2004.

The data of the different parameters during one crossing (Figure 4) show distinguishable sections along the transect. At the English coast and in the Elbe estuary there are higher values of temperature and turbidity. In the Southern Bight the salinity increases up to 35.2. Two algal spring blooms can be observed in the Southern Bight and along the Dutch and German coast. These blooms are also reflected by the increased oxygen and pH values at these locations. The nitrate concentrations are generally very low with higher values only in coastal regions and the Elbe estuary due to high nitrate input from

the rivers. The task of summarising all this data for the two years of the FerryBox project data set is being undertaken in the project and is reported by Hydes *et al.* (2005).

The question of whether the system can describe the dynamic characteristics of biological phenomena is illustrated on the basis of the chlorophyll concentration as obtained from fluorescence measurements in Figure 4. An unusual late fall bloom in November 2003 was detected along the Dutch coast. The first spring blooms started in late March 2004 again along the Dutch coast, spreading out into the German Bight at the end of April and beginning of May. In May a strong bloom in the English Channel also occurred. Later on at the end of June the algae concentration remained low.

4.2 Reliability and availability of FerryBox data

For all Ferryboxes, availability of reliable data related to the number of cruises will be estimated on a monthly basis. As an example the availability of the FerryBox data in the North Sea in 2004 is shown in Figure 5.

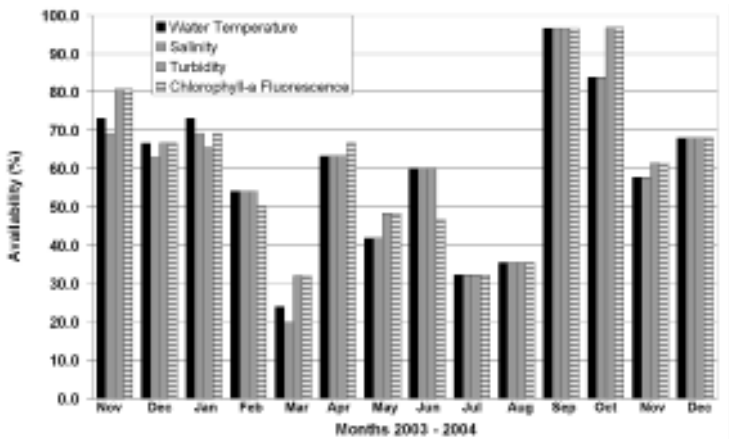

Figure 5 Availability of reliable data for the four core variables related to number of cruises per month (FerryBox data in the Southern North Sea from November 2003 until December 2004).

The availability of the four core parameters is in most cases greater than 50%. Major causes for data gaps were problems with the water supply (problems with the pumps in March 2004) and a broken debubbler in the summer months.

4.3 Remote sensing

How remote sensing data benefits from FerryBox data and vice versa is shown in the occurrence of a red-tide bloom (*Myrionecta rubra*) in the German Bight in August 2004 (Figure 6).

From 28 July until 5 August in the south-eastern part of the German Bight the chlorophyll fluorescence increased up to 35 $\mu g l^{-1}$. The extremely high oxygen super saturation (up to 200%) as well as very high pH values up to 8.65 indicate an algal bloom with high productivity. The higher water temperature is also noticable at the same position as the chlorophyll maximum occurs.

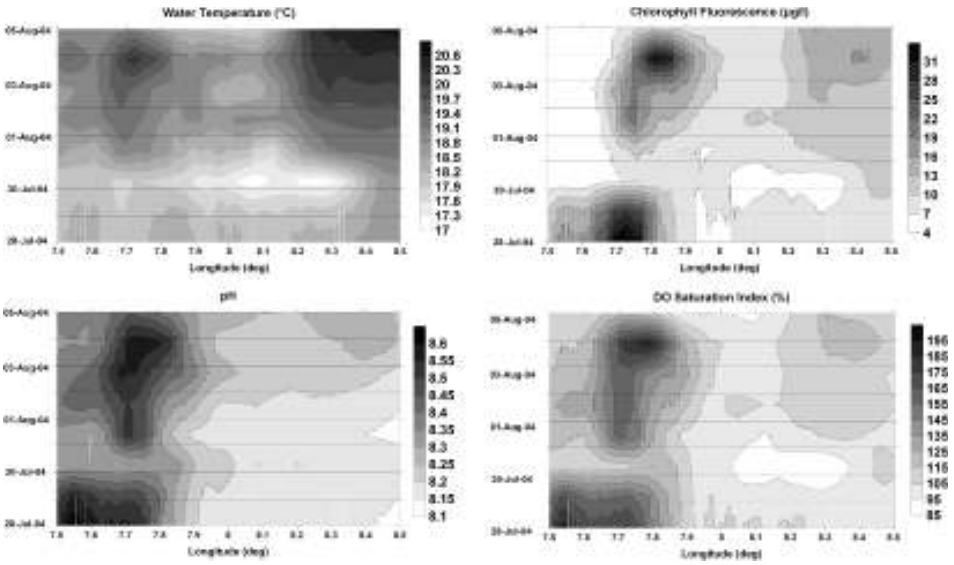

Figure 6 German Bight: contour plots of the development of water temperature, chlorophyll fluorescence, pH and DO saturation index along the transect in August 2004.

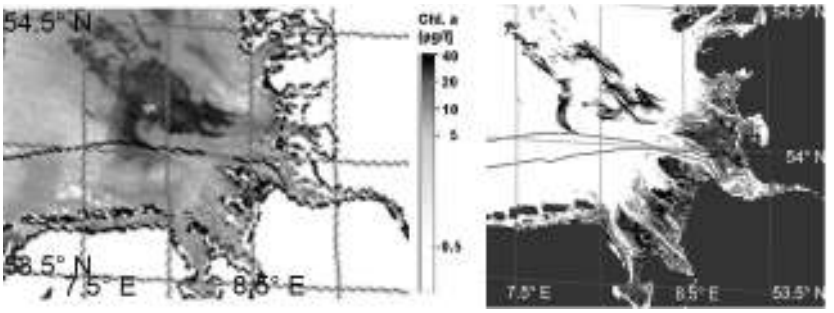

Figure 7 Algal bloom in the German Bight on 3 August 2004: Remote sensing images (MERIS) left: calculated algal concentration for coastal waters (1.2 km spatial resolution), Right: red tide index (300 m spatial resolution) Black lines indicate the tracks of the ferry.

On the remote sensing images from 3 August (Figure 7) this algal bloom is clearly visible and the red-tide index indicates a red tide bloom. By collecting water samples, this bloom was identified as a bloom of the planktonic, phototrophic ciliate *Myrionecta rubra* which is well known for its extremely high rate of primary production (Crawford, 1989). The species contains an endosymbiont of cryptomonad identity which is responsible for the primary production associated with red-water. The moderate chlorophyll fluorescence signal in comparison with the high pH and extremely high concentration of DO may be explained by the low fluorescence yield of this ciliate and/or that this species is only concentrated at the surface whereas the FerryBox collects water from a probably more or less mixed water column of about 5 m.

This red-tide is an example of an episodic short term event (duration less than two weeks) which can only be observed by high frequency monitoring such as FerryBoxes.

In combination with remote sensing the spatial distribution can also be estimated. Similar intense blooms have been monitored by the route 7 FerryBox in the English Channel (Kelly-Gerreyn *et al.*, 2005).

5. Discussion and conclusion

The FerryBox system is a new operational tool using ferries and other SoOs as carrier platforms for automated monitoring equipment. The experiences within this EU project demonstrate that such systems can cost-effectively deliver reliable high frequency data improving conventional monitoring strategies.

The examples shown here together with the other papers concerning FerryBox data in this volume demonstrate the applicability of the FerryBox system for better understanding and assessment of the ecosystem and the underlying biogeochemical processes in the marine environment. The timing of events along the track of the Harwich Cuxhaven ferry relative to data buoys in the Thames estuary has been investigated using hydrodynamic models (Wehde *et al.*, 2005). By combination with hydrodynamic transport models as well as with remote sensing images the 'one-dimensional' view along a transect of the ferry can be enlarged to a more spatial view. Special events like strong short-term algae blooms, which are only detected occasionally by standard monitoring methods, can be studied in detail and related to variations in influencing factors such as temperature, wind and nutrient load. This information can be used for further development of ecosystem models. Techniques to assimilate FerryBox data into numerical models may be used to improve reliable forecasts.

After completion of the 'FerryBox' project monitoring groups will be provided with recommendations as to how future integrated marine monitoring systems can benefit from the enhanced coverage and information density of FerryBox systems.

Acknowledgements

This work was supported within the Fifth Framework Programme "Energy, Environment and Sustainable Development", Contract no. EVK2−CT−2002−00144. Satellite data were provided by ESA (MERIS on ENVISAT) and analysed by the GKSS−RS−group within the approved project 'Validation of MERIS products under a regional point of view' (ESA−AOID 647). We thank H. Krasemann for assisting with evaluation of remote sensing data.

References

Crawford, D.W. (1989). *Mesodinium rubrum*: the phytoplankter that wasn't. Marine Ecology Progress Series 58, 161−174.

Flemming, N.C., S. Vallerga, N. Pinardi, H.W.A. Behrens, G. Manzella, D. Prandle and J.H. Stel (2002). Operational Oceanography: implementation at the European and regional seas. Proc. Second International Conference on EuroGOOS, Elsevier Oceanography Series Publication series 17.

Harashima, A. and M. Kunugi (2000). Comprehensive Report on Marine Environmental Monitoring and Related Studies Using Ferry Boats. CGER−Report, National

institute for Environmental Studies, Environmental Agency of Japan, CGER–M007–2000, ISSN 1341–4356.

Hydes, D.J., H. Wehde, W. Petersen, S. Kaitala, V. Fleming, K. Sørensen, J. Magnusson, I. Lips and U. Lips (2005). A comparison of eutrophication processes and effects in different European marine areas based on the results of the EU FP-5 FerryBox Project. This volume, page 101.

Hydes, D.J., A. Yool, J.M. Campbell, N.A. Crisp, J. Dodgson, B. Dupee, M. Edwards, S.E. Hartman, B.A. Kelly-Gerreyn, A.M. Lavin, C.M. González-Pola and P. Miller (2003). Use of a Ferrybox system to look at shelf sea and ocean margin process. in: H. Dahlin, N.C. Flemming, K. Nittis and S.E. Petersson: Building the European Capacity in Operational Oceanography, Proc. Third International Conference on EuroGOOS, Elsevier Oceanography Series Publication series 19, 297–303.

Kelly-Gerreyn, B.A., D.J. Hydes, L.J. Fernand, A.M. Jégou, P. Lazure and I. Puillat (2005). Linking French Atlantic rivers to low salinity intrusions in the western English Channel: highly resolved monitoring from the EU FerryBox project. This volume, page 432.

Petersen, W., M. Petschatnikov, F. Schroeder and F. Colijn (2003). FerryBox Systems for Monitoring Coastal Waters. in: H. Dahlin, N.C. Flemming, K. Nittis and S.E. Petersson: Building the European Capacity in Operational Oceanography, Proc. Third International Conference on EuroGOOS, Elsevier Oceanography Series Publication series 19, 325–333.

Rantajärvi, E., R. Olsonen, S. Hällfors, J.H. Leppänen and M. Raateoja (1998). Effect of sampling frequency on the detection of natural variability in phytoplankton. Experiences based on unattended high-frequency measurements on board ferries in the Baltic Sea. ICES J. Mar. Sci. 55; pp. 697–704.

Rantajärvi, E. (2003). Alg@line in 2003: 10 years of innovative plankton monitoring and research and operational information service in the Baltic Sea. Meri-Report series of the Finnish Institute of Marine Research No 48. 55 pp.

Reid, P.C., M. Edwards, H.G. Hunt and A.J. Warner (1998). Phytoplankton change in the North Atlantic. Nature, London. 391. 546.

Ridderinkhof, H., H. van Haren, F. Eijgenraam and T. Hillebrand (2002). Ferry observations on temperature, salinity and currents in the Marsdiep tidal inlet between the North Sea and Wadden Sea. In. N.C. Flemming, S. Vallerga, N. Pinardi, H.W.A. Behrens, G. Manzella, D. Prandle, J.H. Stel, Operational Oceanography: implementation at the European and regional seas. Proc. Second International Conference on EuroGOOS, Elsevier Oceanography Series Publication series 17, 139–147.

Swertz, O.C., F. Colijn, H.W. Hofstraat and B.A. Althuis (1999). Temperature, salinity and fluorescence in the Southern North Sea: high resolution data sampled from a ferry. Environmental Management, 23(4): 527–538.

Vezzulli, L. and P.C. Reid (2003). The CPR survey (1948–1997): a gridded database browser of plankton abundance in the North Sea. Progress in Oceanography 58: 327–336.

Wehde, H., F. Schroeder, F. Colijn, U. Callies, S. Reinke, W. Petersen, C. Schrum, A. Plüß and D. Mills (2005). FerryBox observations in the Southern North Sea — Application of numerical models for improving the significance of the FerryBox data. This volume page 169.

Optimal Design of Observational Networks (ODON) and operational forecasting

Jun She*

Danish Meteorological Institute, Denmark

Abstract

ODON is a fundamental research project aiming to develop quantitative and practical methods for assessing gaps and redundancies in the existing observing networks and design optimal (cost-effective) monitoring strategies for future observing networks. It is supported by the European Commission Fifth Framework Programme for a 3-year period (2003–2005). This paper introduces the overall ideas, current status (progress made) and implications for the future European ocean observing systems of ODON.

Keywords: Observing system, optimal design, Baltic Sea, North Sea.

1. What is ODON?

ODON is fundamental research aiming to develop quantitative and practical methods for assessing the gaps and redundancies in existing observing networks and design optimal (cost-effective) monitoring strategies for future observing networks. A statistical optimal design method (a combination of characteristic scale analysis, sampling error analysis, information analysis and optimal control theory), Observing System Simulation Experiments (OSSEs) via data assimilation and cost-benefit analysis will be used to achieve the goals. The method developed will be applied to assess and design the spatial–temporal sampling strategies for a water temperature and salinity observing system in the North Sea and Baltic Sea.

Supported by the European Commission Fifth Framework Programme (FP5 contract No. EVK3–2002–00082), ODON is a part of the EC FP5 Operational Forecasting Cluster. The consortium consists of five major marine research institutions in Northern Europe (DMI, BSH, POL, MUMM and SMHI). The project is coordinated by the Danish Meteorological Institute (DMI). Further details may be found in the ODON website www.noos.cc/odon.

2. Major progress so far

2.1 Historical database

A database in the Baltic–North Sea during 2001 was established for the optimal design study, which includes:

- Satellite SST products: SAF (based on NOAA AVHRR 14 and 16), NOAA AVHRR satellite 12 from BSH
- *In situ* SST: ships of opportunity, buoys, ferrybox, monitoring/research cruises

* Corresponding author, email: js@dmi.dk

- CTD profiles: buoys, monitoring cruises, research cruises, undulating profilers
- Water level: tidal gauge stations
- Waves: buoys
- Bathymetry: 1 nm
- River run-off: daily, major rivers in Baltic–North Sea
- Lateral boundary conditions from operational ocean models
- Weather forcing at 7.5 km resolution: generated by using the gridded SST products as input to HIRLAM.

2.2 Development of methods for mixing satellite and *in situ* SST

Multi-level quality control method, spatial–temporal covariance models and multi-platform optimal spatial–temporal interpolation programs have been developed. A high resolution (10 km, twice daily) gridded SST product has been generated.

2.3 Use of buoy data to reduce satellite SST measurement error

Reducing satellite measurement error has been identified as a major task in both the GHRSST and Medspiration projects (via an approach known as Single Sensor Error Statistics — SSES). ODON has developed a different approach to using buoy data to reduce the satellite measurement error, which has been proved efficient. A case study has been made. In a 200×200 km area covering a buoy station, the satellite measurement error can be reduced by about 20% by applying a buoy correction. The results have been reported at the CORPAR conference 2004 in Paris.

The implication of this result is that a rational SST observing network should be a mixing of satellite and a sparse buoy array. This will be a guideline for designing an optimal SST observing network in the next step (see Høyer and She, 2005).

2.4 Optimising of ocean models (state-of-the-art) for ODON purposes

- COHERENS (for North Sea, 1 nm resolution, parallelisation) (Luyten *et al.*, 2005)
- HIROMB (for Baltic Sea, 1 nm resolution, parallelised, improvements made in bathymetry and vertical mixing)
- Since the HIROMB model originates from BSHcmod and the latter is running as an operational model at DMI, the BSHcmod is used as an alternative model in assessing the quality of the ocean model and the data assimilation schemes, which are of fundamental importance for explaining ODON OSSE results. Vertical mixing is improved by increasing the number of vertical layers in order to reduce the numerical diffusion; a comprehensive model validation has been performed for BSHcmod in the Baltic–North Sea scale (Gästgifvars *et al.*, 2005).

2.5 A portable parallel version of COHERENS

A portable parallel version of the European community 3D ocean model COHERENS has been debugged and tested on different platforms, including Manchester CSAR supercomputer, POL Linux Cluster and DEC Alpha at MUMM. The code has been re-written in F90.

2.6 High resolution modelling for North Sea and Baltic Sea

- A one-year model ocean in the North Sea with 1 nm resolution has been generated using the parallelised COHERENS model. The results have been compared with a coarse resolution (4 nm resolution) COHERENS run. Preliminary results shown improvements in the English Straits and simulation of eddy activities.
- A similar proxy ocean has also been generated in the Baltic Sea by using HIROMB, with assimilated SST (Pemberton, 2005).

2.7 Implementing and testing data assimilation schemes in operational ocean models

- An OI assimilation method and a simplified Kalman Filter method have been implemented in HIROMB, COHERENS and DMI−BSHcmod to assimilate SST observations, respectively
- A multivariate OI scheme has been implemented and tested in HIROMB
- An Ensemble Kalman Filter scheme has been implemented and tested in POLCOM, COHERENS and DMI−BSHcmod method for assimilating 3D T/S profile data.

The above work provides a solid technical basis for using 3D T/S data assimilation in Baltic−North Sea operational forecasts. This is a notable contribution from ODON to regional sea operational forecast. For example, a one-year SST assimilation made in DMI BSHcmod showed that the SST model RMS error was reduced by around 40%.

2.8 Sampling strategy design

SST observing network assessment and design

The existing satellite and *in situ* SST observing networks have been evaluated on their data quality, effective coverage, error in reconstructing the SST gridded fields (by Optimal Interpolation and data assimilation) and their impacts on weather prediction. Two kinds of Observing System Experiments were used in assessing the *ad hoc* designed SST observing networks: one is the atmospheric model (HIRLAM) sensitivity to high resolution SST based on existing observing networks and the other is SST assimilation experiments using BSHcmod (as mentioned above). A number of *ad hoc* designed SST observational networks are used in the two types of OSEs to test the relative importance of satellite and *in situ* observations, as well as to identify the most important challenges in SST observing networks. The following conclusions have been reached:

- **Cost-effectiveness of technology**: currently *in situ* SST is mainly measured by ships of opportunity (GTS), buoys, ferryboxes and national monitoring cruises (CTD cast, undulated profilers and TSG). The most cost-effective *in situ* SST measurement platform is the ferrybox, however, sometimes the quality of ferrybox observations is not as high as buoys and CTD casts. Satellites are a major cost-effective instrument for SST observations.
- **Data quality**: For night-only data, OI SAF SST has an error (std. deviation from *in situ* SST) of 0.58°C while the BSH product has an error of 0.68°C. Day-time satellite SST is in general 0.1°C worse in quality than the night-time SST. The *in situ* SST also shows different qualities, with national monitoring cruises and buoys having the highest quality.

- **Effective coverage**: in 2001, over 200000 *in situ* SST (hourly averaged box) observations were made, where 80% were from GTS. However, the effective coverage of the *in situ* SST is negligible in comparison with satellite SST. In 2001, SAF and BSH SST had an effective coverage of about 20% for night-only data but 30% for day+night data.
- **Product quality**: by assimilating SST data into a 3D ocean model, the average RMS error is reduced to 0.66°C from 1.2°C without assimilation.
- **Relative importance of *in situ* SST**: in the Observing System Experiments (OSEs), the improvement is negligible by including *in situ* SST together with satellite SST in the assimilation. It was found that the major contribution of *in situ* SST is when it is used in correcting satellite SST, which can improve the satellite SST quality by 15–30%.
- **Gaps and redundancy**: for the basin scale SST hourly field products in 6 nm resolution, existing satellite–*in situ* SST observing networks in the Baltic–North Sea is sufficient. There is a big redundancy between different infrared satellite sensors: results vary little between OSEs by assimilating NOAA AVHHR 12 only and that by assimilating 3 satellites 12, 14 and 16.
- **Recommendations for further optimisation**: high quality *in situ* SST data (e.g. measured by buoys) should be available for the Baltic Sea. 3–5 buoys are sufficient to cover the entire Baltic Sea for this purpose. This will improve the quality of the SST field product by 15–30%. Current observing networks are not sufficient in monitoring local small scale phenomena, such as upwelling. Cost-effective *in situ* measurement at coastal stations (e.g. combined with tidal gauge stations) should be made available.

***Ad hoc* sampling design study for Baltic–North Sea T/ S observing networks**

Ad hoc designed Baltic–North Sea T/S observing networks have been identified based on existing observing networks and physical process analysis.

Cost estimation of existing observing networks

A method of cost estimation of observing networks has been developed and applied on existing Baltic–North Sea T/S observing networks. Results show that for surface temperature and salinity measurements, ferryboxes are the most cost-effective way to make observations; for T/S profiles, undulated profilers are the most cost-effective.

Assessment of existing T/S profile observing networks

ODON has developed a method for assessing and designing observing networks by combining observations and models. It shows the gaps and redundancies, and how to effectively fill the gaps. This is the basis for evaluating and further improving the GMES marine component.

One-dimensional sampling design for profile observations

The method was developed for designing a cost-effective cruise sampling strategy, e.g. temporal sampling frequencies and location of stations.

Two and three dimensional sampling design for profile observations

A Monte-Carlo method has been used to determine optimal locations for a given number of sampling stations. The optimal solution gives the maximum effective coverage. This method has been used in 2D and 3D sampling designs for profile observations. Another method (Empirical Orthogonal Teleconnection — EOT) has also been tested as an optimal design method. However, the results are not that encouraging due to the 'tail effect' of the correlations.

3. Possible implications of ODON work for GMES

ODON has only been done for the Baltic–North Sea T/S parameters. It should be estimated for entire European T/S observing networks and for biochemical parameters. Similar optimal design work should be done for biochemical parameters, especially to answer the question "what is a harmonised pan-European monitoring network based on existing national monitoring cruises?"

Based on the above extended pan-EU ODON work, an observing network assessment and design system can be built up. This is actually a GMES Marine Observation Decision Supporting (MODS) system (for mixed satellite–*in situ*). The MODS system will have the following two functions:

1. For any given (or proposed) observing network, the system will be able to tell how large an area in space and time the observing network can effectively cover, as well as the quality assessment of the final products.
2. For a new given observation task with a certain amount of resources, the system will be able to give recommendations for optimal sampling locations and strategies (based on cost-benefit analysis).

The MODS system should be set up for pan-European regional seas for all key parameters. However, this will be a completely new project. Part of the work may be included in a proposed IP (ECOOP — European COastal/shelf sea OPerational forecasting and monitoring system) for the 4th call of the FP6 programme.

References

Gästgifvars, M., K. Myrberg, S. Müller-Navarra, A. Jönsson and V. Huess (2005). Evaluation of the operational sea level forecast systems — the Gulf of Finland case. This volume page 507.

Høyer, J.L. and J. She (2005). A new method to reduce noise on satellite sea surface temperature observations. This volume page 441.

Luyten, P., I. Andreu-Burillo, A. Norro, S. Ponsar and R. Proctor (2005). A new version of the European public domain code COHERENS. This volume page 474.

Pemberton, P. (2005). Validation of a one year simulation of the Baltic Sea with optimised boundary conditions, improved bathymetry and data assimilation. This volume page 526.

Regional Systems 3

The Forecasting Ocean Assimilation Model (FOAM) system

Adrian Hines*, Mike Bell, David Acreman, Rosa Barciela, Matt Martin, Alistair Sellar, John Stark and David Storkey

Met Office, UK

Abstract

The FOAM system provides daily analyses and short-range forecasts of the three dimensional structure of the open ocean and sea−ice properties. The key components of the FOAM system are a numerical ocean model, driven by 6-hourly surface fluxes from the Met Office NWP system, and a data assimilation scheme that makes use of a range of real-time data. The FOAM system runs within the Met Office's operational suite, benefiting from full operational resilience. The system can also be run in hindcast mode from 1997 onwards.

Keywords: operational ocean forecasting, ocean data assimilation, ocean modelling

1. Introduction

The Forecasting Ocean Assimilation Model (FOAM) system has been developed over the last decade to provide real-time analyses and short range forecasts of properties of the deep ocean in support of a range of applications. The system is an integral part of the Met Office's operational suite, taking 6-hourly surface forcing from the NWP models, and providing daily operational forecasts with lead times up to six days ahead.

The core of the system is the numerical ocean model, a z-coordinate, primitive equation model based on the same code as the ocean component of the Hadley Centre coupled climate models (Gordon *et al.*, 2000). A nested model system has been developed that allows a range of model configurations to be run from a 1° global model (run operationally since 1997) to high resolution regional models. Analyses are produced through assimilation of a range of data using a method developed from the Analysis Correction scheme (Lorenc *et al.*, 1991). Other components of the operational system include an observation processing and quality control system, a verification system shared with the NWP models, and an automatic post-processing and product dissemination system. These components can also be run in hindcast mode, with 6-hourly surface forcing and observations available back to 1997. Figure 1 illustrates the structure of the operational and hindcast system.

The system was originally developed in support of defence requirements, and has more recently been applied to a wider range of applications including ship routing, cable repairs and provision of data to regional models.

This paper describes the current status of the operational FOAM system and highlights the areas in which development effort is currently focused.

* Corresponding author, email: adrian.hines@metoffice.gov.uk

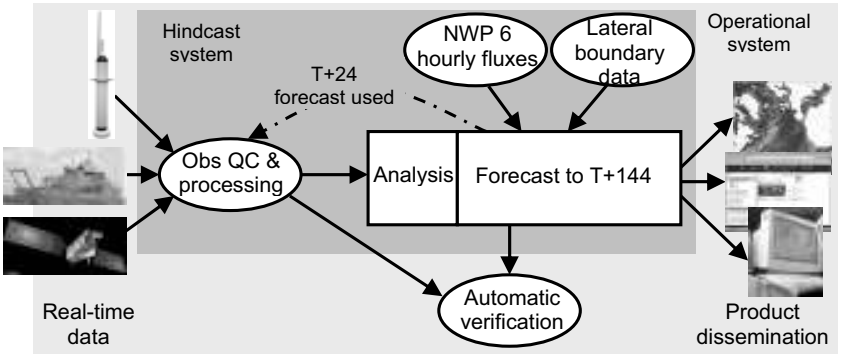

Figure 1 Schematic illustration of the structure of the FOAM system.

2. Operational FOAM system

The operational FOAM system consists of 3 hierarchies of nested models, each driven by boundary data from the Global 1º model. Models covering the North Atlantic are nested down to 1/9º; in the Indian Ocean down to 1/3º; and in the Antarctic down to ¼º (Figure 2). All model configurations have 20 vertical levels, and are run daily, with full operational support. 6-hourly surface forcing is taken from the Met Office's global NWP model runs.

The system has been designed to allow rapid relocation in response to operational requirements. The inclusion of the Global FOAM configuration provides the capability to generate boundary data for hierarchies of nested model configurations for any region globally; development of new nested model configurations and implementation of daily operational production for new regions can be established on timescales of a few weeks.

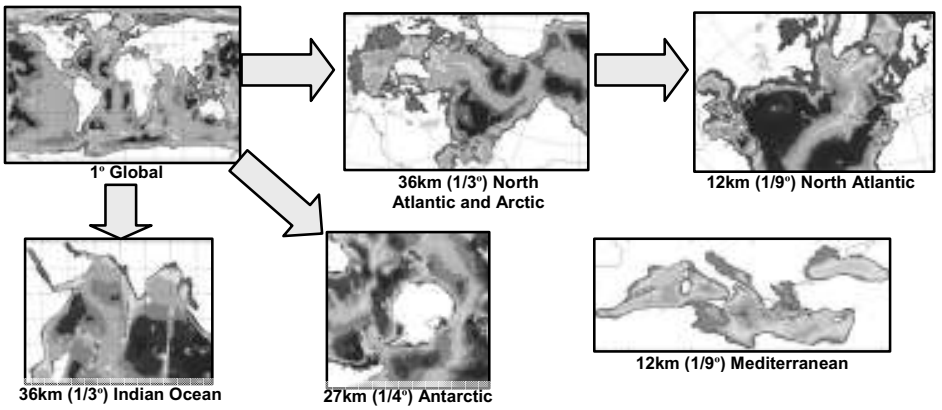

Figure 2 Schematic illustration of the operational FOAM configurations.

Output from the system is disseminated to operational customers via dedicated, secure communications links, with direct delivery onto local visualisation systems. Data is also made available to a wider range of users through the Live Access Server (www.nerc-essc.ac.uk/godiva) at the Environmental Systems Science Centre (ESSC) as part of the GODIVA Project (www.godiva-grid.org).

3. Observations and data assimilation

The FOAM data assimilation scheme has been developed from the Analysis Correction scheme used in the Met Office NWP system until 1999. The scheme deals efficiently with multiple observation types and with large numbers of observations. The FOAM implementation of the scheme includes numerous significant developments, most notably: a technique for timely assimilation of observations; a two-component background error covariance model; a bias correction scheme for controlling biases in the tropics; and a scheme to correct for bias in satellite SST observations. Developments to the scheme are described in detail in Martin *et al.* (2002) and Bell *et al.* (2003).

The operational FOAM system assimilates a range of observations: temperature and salinity profiles including Argo data; satellite altimeter sea surface height data; satellite and *in situ* sea surface temperature (SST) data; and gridded fields of sea−ice concentration data. Observations are extracted and processed daily, immediately prior to the analysis step, ensuring maximum availability of the real-time data.

Temperature profile data received in real-time over the Global Telecommunications System (GTS) have been assimilated since the original implementation of the FOAM system in 1997. Following the increase in availability of salinity profile data that has arisen from the growth of the Argo programme, the system was upgraded in 2003 to implement the assimilation of salinity profile data. The Argo salinity profiles have been demonstrated to have a significant impact on the FOAM products, and are seen to be particularly effective at preventing drifts in the deep ocean salinity fields.

Quality control of profile data has proven to be an important consideration, in particular when assimilating salinity profile data. Since 2003 the operational FOAM system has employed the sophisticated automated quality control system developed as part of the ENACT project (www.lodyc.jussieu.fr/ENACT/index.html). This system provides an extensive range of quality control checks including background checks, buddy checks, stability checks and track checks. Full details of the quality control system are given in Ingleby and Huddleston (2005).

Satellite altimeter sea surface height data produced twice weekly by CLS are assimilated using the scheme of Cooper and Haines (1996). Data from Envisat, Geosat Follow-On and Jason-1 are assimilated in to all configurations except the Global model.

SST data currently assimilated in the operational models comprises *in situ* observations received over the GTS and low resolution (2.5º) AVHRR data provided by NOAA. Work recently undertaken to assess the impact of Medspiration multi-sensor satellite SST data (www.medspiration.org) on the operational system has demonstrated a beneficial impact, resulting in a reduced bias in the FOAM SST compared to *in situ* observations. Operational use of GODAE High Resolution SST (www.ghrsst-pp.org) data is a priority for development of the operational system.

During the course of investigations of the impact of Medspiration data the FOAM data assimilation scheme was applied to the generation of a high resolution (1/20º) global SST analysis product (Figure 3). This analysis product is based on persistence, using the analysis from the previous day as the background field. This analysis product, the Ocean Surface Temperature and Ice Analysis (OSTIA), is now being developed in its own right.

Prototype OSTIA analysis products are available from http://ghrsst-pp.metoffice.com/pages/latest_analysis/ostia.html. Operational production of OSTIA is expected to commence in 2006.

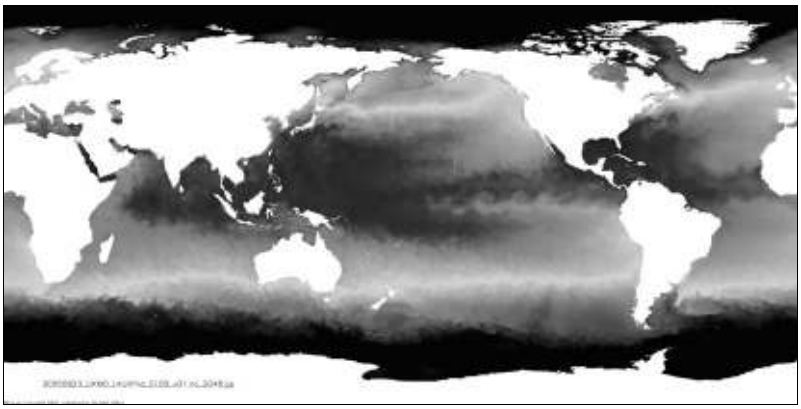

Figure 3 Prototype OSTIA 1/20º global SST analysis product for 23 August 2005.

The assimilation of sea−ice concentration data within the operational FOAM system is currently based on a simple nudging scheme applied to a gridded sea−ice concentration product received from the Canadian Met Center (CMC). Work has recently been completed to adapt the existing data assimilation scheme used for other observation types to the assimilation of sea−ice concentration data derived from SSMI observations (Kaleschke *et al.*, 2001). The scheme proved effective with root-mean-square sea−ice concentration errors constrained to below 10%. An extension to the scheme to assimilate ice drift data derived from SSMI and QuikSCAT has also been developed, and has been shown to reduce the error in the model sea−ice velocity fields by approximately 50%.

4. Ocean and sea−ice model developments

Recent developments to the FOAM ocean model have sought to improve the utility of outputs for customers in response to discussions with end users. An improved mixed layer depth diagnostic designed to better meet the needs of customers will be implemented in the operational models in October 2005. This diagnostic is based upon the optimal definition of Kara *et al.* (2000), and provides a measure with much greater temporal consistency than the Kraus-Turner mixing depth that is currently produced (Figure 4). A detailed assessment of the performance of the FOAM vertical mixing scheme, and the mixed layer depth diagnostic in particular, has recently been completed (Acreman, 2005).

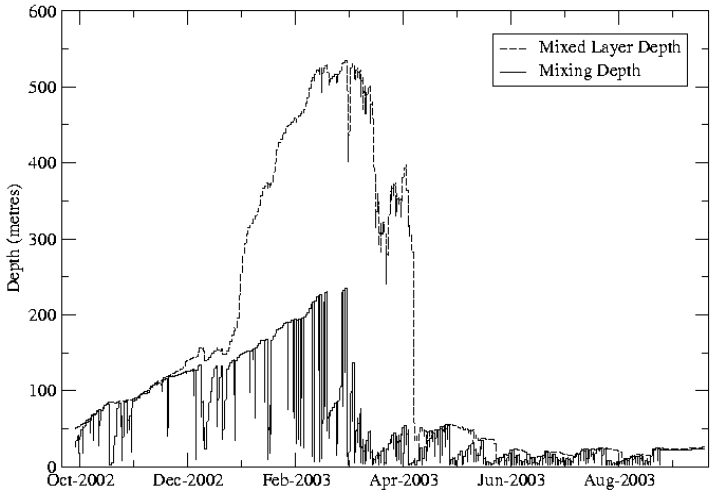

Figure 4 Time evolution of Kraus-Turner mixing depth (solid line) and diagnostic mixed layer depth (dotted line).

Other recent work has explored the impact of improved sea−ice dynamics and thermodynamics on the FOAM system. The current sea−ice model uses single layer thermodynamics and simple ice advection, and has been seen to produce sea−ice simulations in which the ice drifts too rapidly, particularly in regions of strong ocean currents. Trials have been carried out using the Elastic-Viscous-Plastic (EVP) ice rheology (Hunke and Dukowicz, 1997) in combination with multiple category thermodynamics. The improved dynamics and thermodynamics are sent to improve simulations of the ice extent, with the most significant improvements in regions where the current scheme performs poorly (Figure 5).

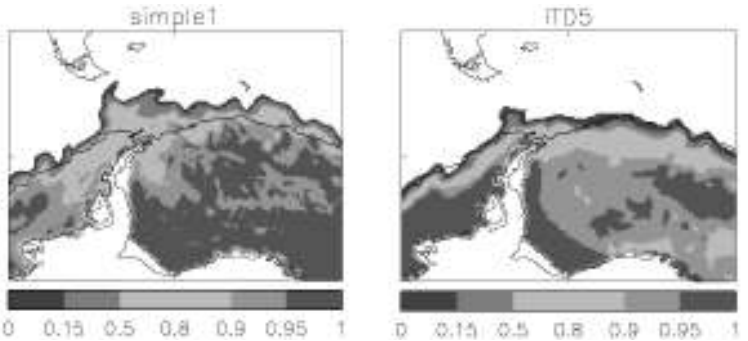

Figure 5 FOAM sea−ice concentration fields in the Drake passage for simple ice advection (left panel) and for the EVP and ITD ice model (right panel). The black line is an ice edge analysis.

Current development work includes the development of ecosystem modelling capability through the coupling of FOAM and the Hadley Centre Ocean Carbon Cycle (HadOCC) model (Palmer and Totterdell, 2001). HadOCC is a four Compartment Nutrient-Phytoplankton-Zooplankton-Detritus (NPZD) ecosystem model and has been successfully

coupled to FOAM in a range of resolutions from the 1º global to the 1/9º North Atlantic models (Figure 6). Techniques for assimilation of satellite ocean colour data in to the FOAM−HadOCC system are being developed by the National Oceanography Centre, Southampton (NOCS) with funding from the Centre for Air−Sea Interaction and Fluxes (www.pml.ac.uk/casix/). The assimilation scheme will be applied in 10-year hindcast runs and the capability to provide simulations of ocean carbon parameters will be assessed.

Much development effort is currently focused on transitioning the FOAM system to use the Nucleus for European Modelling of the Ocean (NEMO) framework. This framework includes an ocean and sea−ice model based on the OPA code and will provide the core of the next generation Met Office ocean forecasting system. This system will be configurable for both FOAM applications for the deep ocean, and for Shelf Seas applications for coastal regions. Initial work is aimed at establishing basic FOAM functionality using the NEMO framework, with subsequent refinement towards standards required for operational implementation planned for completion in 2008.

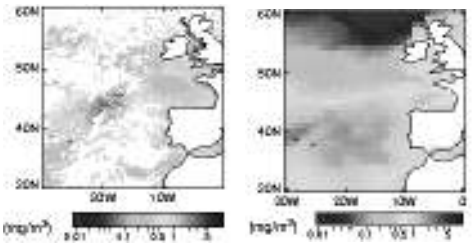

Figure 6 surface chlorophyll for a week in March 2000 from SeaWifs data (left panel) and from 1º FOAM−HadOCC (right panel).

5. National and international coordination

The team developing the FOAM system at the Met Office work within the National Centre for Ocean Forecasting (NCOF). Established in 2005, NCOF is a partnership between UK marine research institutes aimed at coordinating research and building strong collaboration between partners.

FOAM is also involved in European and international collaboration through participation in the Mersea Integrated Project (Mersea IP, www.mersea.eu.org) and the Global Ocean Data Assimilation Experiment (GODAE, www.bom.gov.au/bmrc/ocean/GODAE/). The transition of the FOAM system to the NEMO framework is supported by the Mersea IP and is in part motivated by the increased ease of collaboration with European partners.

References

Acreman, D. (2005). The impact of improved vertical resolution and model tuning on mixed layer models. National Centre for Ocean Forecasting, Technical Note 2.

Bell, M.J., A. Hines and M.J. Martin (2003). Variational assimilation evolving individual observations and their error estimates. Met Office Ocean Applications Technical Note 32.

Cooper, M. and K. Haines (1996). Altimetric assimilation with water property conservation. J. Geophys. Res., 101, C1, 1059–1077.

Gordon, C., C. Cooper, C.A. Senior, H. Banks, J.M. Gregory, T.C. Johns, J.F.B. Mitchell and R.A. Wood (2000). The simulation of SST, sea ice extents and ocean heat transports in a version of the Hadley Centre coupled model without flux adjustments. Clim. Dyn., 16, 147–168.

Hunke, E.C. and J.K. Dukowicz (1997). An elastic-viscous-plastic model for sea–ice dynamics. J. Phys. Oceanogr., 27, 1849–1867.

Ingleby, B. and M. Huddleston (2005). Quality control of ocean profiles — historical and real-time data. Submitted to J. Mar. Sys.

Kaleschke, L., C. Lüpkes, T. Vihma, J. Harrpaintner, A. Bochert and G. Heygster (2001). SSM/I sea ice remote sensing for mesoscale ocean–atmosphere interaction analysis. Can. J. Remote Sensing, 27, 5, 526–537.

Kara, A.B., P.A. Rochford and H.E. Hurlburt (2000). An optimal definition for ocean mixed layer depth. J. Geophys. Res., 105 (C7):16803–16822.

Lorenc, A.C., R.S. Bell, and B. MacPherson (1991). The Meteorological Office analysis correction data assimilation scheme. Quart. J. Roy. Meteor. Soc., 117, 59–89.

Martin, M.J., M.J. Bell and A. Hines (2002). Estimation of three-dimensional error covariance statistics for an ocean assimilation system. Met Office Ocean Application Technical Note 30.

Palmer, J.R. and I.J. Totterdell (2001). Production and export in a global ocean ecosystem model. Deep-Sea Research Part I, 48, 1169–1198.

MeDir-OP, A Mediterranean directory for operational oceanography developed within the MAMA project

A. Drago*[1], S. Vallerga[2], G. Manzella[3], J. Font[4] and the MAMA Consortium: T. Aarup, A. Abdelbaki, A. Abuissa, H. Awad, M.B. Awad, S. Besiktepe, M. Capari, A. Carlier, B. Cermelj, C. Casazza, P. Drakopoulos, N.C. Flemming, I. Gertman, G. Georgiou, A. Harzallah, G. Herrouin, A. Ibrahim, N. Kabbara, Z. Kljajic, J.L. Lopez-Jurado, P. Magni, A. Mahmoud Al-Sheikh, C. Maillard, V. Malacic, M. Morovic, K. Nittis, D.S. Rosen, A. Ribotti, A. Selenica, I. Salihoglu, C. Sammari, D. Sauzade, C. Silvestri, M. Snoussi, R. Sorgente, C. Tziavos, G. Umgiesser, M. Vargas, B. Vucijak, M. Zavatarelli and G. Zodiatis

[1]*IOI-Malta Operational Centre, University of Malta*
[2]*Consiglio Nazionale delle Ricerche, Istituto per l'Ambiente Marino e Costiero, Italy*
[3]*Ente per le Nuove Technologie, l'Energia e l'Ambiente (ENEA), Italy*
[4]*Consejo Superior de Investigaciones Cientificas (CSIC), Spain*

Abstract

The Mediterranean network to Assess and upgrade the Monitoring and forecasting Activity (MAMA), a 3-year thematic network project shared by leading marine research institutions from all the Mediterranean countries, has contributed to strengthening the institutional and scientific platform for the establishment of operational oceanography in the region.

A key task in the MAMA project consisted in the stocktaking of activities and identification of current capabilities in operational oceanography on a country basis with a focus on availability of technological infrastructures, human resources and funding, applications and product needs. The information was collected by:

1. Country Profiles on the operations of institutes/agencies/organisations dealing with marine monitoring; national structures supporting such activities and marine affairs in general; relevance of marine sectors in the economic activities of each country
2. a structured questionnaire targeting a comprehensive inventory on the routine marine monitoring activities in the Mediterranean.

The Mediterranean Directory on Operational Oceanography (MeDir-OP) presents this information through the use of a user-friendly internet-based graphical interface allowing easy viewing of the metadata according to a number of categories. Specific information sets are collated into searchable mini-databases.

MeDir-OP provides the basis for assessing the needs and potentials for operational oceanography in the region. It serves as an essential step to identifying gaps in infrastructures, to underpin further research and technological developments specific to the region, and to designing an observing system that meets the needs of end-users.

Keywords Metadatabase, operational oceanography, directory, web interface

* Corresponding author, email: aldo.drago@um.edu.mt

1. Introduction

In 2002, the World Summit on Sustainable Development in Johannesburg (UN, 2002) recognised the very large role that the sea plays in supporting economies and society at large, and reached agreement on the urgent need to take further actions to achieve the sustainable development of oceans and coasts. The principles of the United Nations Conference on Environment and Development in Rio 1992, that established the Global Ocean Observing System (GOOS), were reaffirmed. In many parts of the world marine resources bear a key element to prospering economies, and a multitude of economic activities and consequent pressures on natural resources occur primarily in the coastal zone. This has brought coastal states to an incumbent situation where further development needs to be strictly rationalised to curb potential negative impacts on such resources, and to secure the various derived coastal and marine uses in the future.

This has led to more stringent regional commitments that coastal states have gradually come to face in fulfilling obligations to policies (such as in fisheries, bathing water quality, etc.), improving the management of marine resources, and in seeking a sustained development of the coastal zone.

Operational ocean monitoring and forecasting networks at global, regional and national scales, as defined in the GOOS (IOC, 1998), are needed to assist coastal states in meeting the requisites for the sound management of the marine resources. The challenge is to shape the marine forecasting systems in the regions upon state-of-the-art 21st century science and technology, adapted to the specificity of the regions, taking into account the more demanding needs of an evolving knowledge-driven society, the greater reliance of future regional economic growth on the marine sector, and targeting the benefit of different users in all the riparian countries. It is moreover necessary to build frameworks for partnerships between nations, to combine and integrate resources and infrastructures, and to promote a harmonious implementation based on the principles of co-development, co-ownership and sharing of benefits (Drago *et al.*, 2004).

GOOS Regional Alliances (GRAs) have been set up worldwide to co-ordinate the efforts of states towards the implementation of GOOS. They have different capacities, resources and levels of activity, but all seek to establish a global sustained system of observations to predict the state of the marine environment, to fulfil commitments to international agreements and to seek practical benefits for a variety of end-users and for the public good in general.

One of the key roles that GRAs are called to exercise consists in the pooling of information on operational marine monitoring activities in the regions. This role is reiterated in the Implementation Strategy for the Coastal Module of GOOS (UNESCO, 2005), and is pursued as a main goal in GRAND (GOOS Regional Alliance Networking Development) which is an EU-funded Specific Support Action that plans to carry out a significant inventory task in the GOOS regions (Vallerga *et al.*, 2005). Such inventories of existing operational observation programmes constitute a pre-requisite to the harmonious planning and optimal design of regional ocean observing, modelling and forecasting systems composed of integrated national components, and targeting the exploitation of results by a wide range of end-users.

In the Mediterranean, the thematic network project Mediterranean network to Assess and upgrade Monitoring and forecasting Activity in the region (MAMA) was conducted from 2002 to 2005 by MedGOOS, the GOOS Regional Alliance in the region. This project brought together a consortium made up of major marine institutions from all the Mediterranean countries, and staged a joint effort between countries to strengthen scientific links and build momentum towards ocean forecasting in the region. The aims of MAMA were centred on the trans-national pooling of scientific and technological resources through the sharing of experiences and the transfer of expertise, to bring capacities relevant to operational oceanography in the region to comparable levels, and to provide an integrated effort towards the planning and design of the initial ocean observing and forecasting system in the Mediterranean (Vallerga *et al.*, 2002; Drago *et al.*, 2003). This project has enabled MedGOOS to prove its role in providing guidance to the Mediterranean states and stimulate the necessary awareness, capacity building and pre-operational R&D to support operational oceanography in the region.

One of the specific objectives of MAMA was to identify the gaps in the monitoring systems in the region and in the capability to measure, model and forecast the ecosystem; and to integrate the knowledge base derived from relevant national and international RTD projects and programmes. To this end a major effort was conducted to gather information at country level on the present assets in the Mediterranean to monitor, assess and forecast the state of the coastal waters. The main focus was on existing initiatives in relation to ocean forecasting, current activities of marine research institutions involved in operational oceanography, availability of technological infrastructures, equipment, human resources and funding.

This activity culminated in the development of a Mediterranean Directory for Operational oceanography (MeDir-OP) as a main deliverable of MAMA. MeDir-OP resides on the MAMA website (www.mama-net.org). The underlying metadatabase can be accessed from http://capemalta.net/mama/wp1interface/dbase/.

2. Survey on the current status of ocean monitoring activities

The effort conducted in the MAMA project for the identification and stocktaking of the present capability in the Mediterranean for operational oceanography was run in parallel with an awareness campaign staged in each country, and a process of consultation with key stakeholders including public authorities responsible for marine affairs, marine research institutions, marine service providers and end-users in general. Information on marine agencies, institutes and centres that make marine observations and acquire ocean and coastal data in operational mode, and details on their monitoring activities were collected by a dedicated survey.

The collection of information was mainly done by two separate activities:

1. Country Profiles on the current capabilities in pre-operational ocean observations and forecasting
2. an inventory on the ongoing marine monitoring activities compiled by major marine-related institutes/centres on a country basis.

The Country Profiles are structured in three main sections:

Section A — Profile of relevant institutions

Section B — Profile of the national organisational structure in marine affairs and research

Section C — Relevance of the marine sector to the economy.

The profiles provide an overview on:

- the operations of institutes/agencies/organisations dealing with the monitoring, assessment and forecasting of the state of the ocean and coastal areas
- the national structure for the support and conduct of marine monitoring and research activities
- the key public administration/authorities responsible for marine affairs, environmental policy formulation and implementation
- the relevance of the maritime sector in the economic activities of each country. More specifically this activity has provided detailed information on:
  - key institutions dealing with the monitoring of the marine environment or underpinning research for operational oceanography
  - providers and potential users of marine services.

The Survey on Marine Monitoring Activities in the Mediterranean has enabled a comprehensive inventory on the existing marine monitoring activities in the Mediterranean, and the current related applications, serving as a first step towards identifying gaps in infrastructures, to underpin further research and technological developments specific to the region, and to design the initial observing system that meets the needs of end-users.

The metadata was collected by means of an on-line entry sheet in the form of a questionnaire structured in two parts:

- The first part aiming to identify in each country the current demand, requirements and practice for applications that make use of routine marine observations. The requested information enabled an assessment on the type and extent of current operational activities in ocean/coastal monitoring that address the needs of existing or candidate customers, including research. It also furnished a picture of the extended potential benefits that can be derived and developed from existing activities. The information included details on:
  - the main recipients
  - the key customer-based deliverables including descriptions of products and services provided
  - the monitoring activities including the main parameters measured, type of analysis, processing and assessments made to apply measurements to user needs.
- A second part focusing on the technical details of marine monitoring and observing sites, platforms and devices. It identifies the current practices in the observation and monitoring of the marine environment, including details on platforms, instruments, sensors, maintenance, telecom systems, data storage, exchange codes and formats, etc.

3. MeDir-OP, a regional directory for operational oceanography

The metadata derived from the surveys described above provided a large variety of information with many cross-linkages between categories. The synthesis and analysis was made by compiling information on specific themes and mainly by developing a metadatabase focusing on two broad fields, namely:

- institutes engaged in operational oceanography or undertaking related research
- routine marine monitoring activities.

This metadatabase forms the backbone of MeDir-OP.

The directory can be viewed by means of an internet-based, user-friendly graphical interface that was developed to furnish visual classified representations of the underlying metadata in the form of clickable layered maps. The maps group locations and descriptions of the main ocean/coastal monitoring programmes, location of key institutes underpinning operational oceanography, positions of buoys and country descriptions of related resources.

The institutions covered in MeDir-OP are key centres and agencies in the Mediterranean that deal with the monitoring of the marine environment or underpin research for operational oceanography, oceanographic data management centres, and providers of operational marine services.

Information is also provided on end-users of marine data, on the key public administrative units responsible for conducting marine affairs, and managers of environmental issues on a national and regional scale as well as general descriptions of national maritime economies with highlights on the relevance of the sea as an economic resource through the ranking of key classes of maritime activities.

At an equally prominent level MeDir-OP gives information on routine marine monitoring activities including the type of observing platforms, instrumentation, measured parameters, method of measurement, data processing and analysis, dissemination of related products, and other relevant details.

Furthermore MeDir-OP complements the Mediterranean directory (MeDir) with individual experts and scientists involved in marine research initiatives in the region. The MeDir database is a joint initiative of the MedGOOS Secretariat in Malta and the IOC/IODE Secretariat in Paris.

4. Structure of MeDir-OP

The information in the directory is presented by means of a web interface composed of a Control Panel, a Map Area and a Summary Box (Figure 1). The Control Panel provides a handle to the first level selection of metadata categories and sub-maps. It also gives access pointers to two metadata mini-databases and to MAMA-Net for on-line access to selected operational data services.

The Map Area is an interactive window consisting of a series of maps with pointers to spatial information and several pull-down menus for easy selection of metadata requests.

The Summary Box is the area where the results from a request are presented in a concise form. Detailed metadata descriptions appear in pop-up windows.

Figure 1 Main components of the MeDir-OP web interface window.

The directory map structure consists of three main sets.

4.1 MAP 1: Country profiles

This first map gives information on a country basis of:

1. **Institutes/Entities** — listing institute/entity names in each country with marine-related activities, each classified according to one of five types: marine centres related to ocean observations/forecasting, oceanographic data centres, general marine research centres, national marine environmental agencies, and other marine-related entities.
2. **Research and monitoring programmes** — listing research programmes/projects conducted in the country, shown in the form of a table indicating name of research programme and responsible institute. This section lists also the ocean modelling archives in a country.
3. **Marine affairs** — giving a choice between: Ministries/Authorities/Agencies and Coordinating Bodies. In both cases the information is given in the form of a table with name of entity and brief description of the entity.
4. **Marine sector economy** — giving a choice between a general description and the economic relevance of marine resources/activities in each country.

4.2 MAP 2: Marine Institutes/entities related to operational oceanography

This section consists of a set of four maps, one map for each of four categories of institutes/entities according to the following classification:

1. Marine Institutes/Entities targeting ocean observations/forecasts
2. Oceanographic Data Centres
3. National Environmental Agencies
4. Other marine-related entities.

The user is allowed to choose between these four categories and work on the relevant map according to the chosen category. For each category, map entries are indicated by points positioned on the geographic location of the institute/entity. Once a map is chosen, clicking on a point gives the name of the entity and other information: contacts; mission; institute type; activity type; sectors/field of activity; human resources; and a list of research and monitoring activities.

4.3 MAP 3: Research and monitoring programmes

This consists of a map showing geographic locations of research and monitoring activities. For each activity the name of the programme appears by moving the pointer over the location of the particular programme, and the corresponding information is given upon choosing from a list menu: name of programme, responsible entity and contacts; objectives; geographical area; key variables measured; platforms used; period of operation; source of funding.

Figure 2 Map showing locations of main monitoring stations in the Mediterranean Sea.

The activities are categorised into several subsections as follows:

1. Trend monitoring dealing with observations for detecting trends, identifying and assessing environmental changes, and including traditional monitoring activities
2. Ships of Opportunity for observations made from voluntary ships
3. Sea Level Observations covering measurements made mainly by coastal systems and sea level gauge networks
4. Marine Buoys, Wave Observations and Moorings which include real time monitoring with measurements made by automated systems and long term observations by other moored instruments

5. Hydrographic surveys and other programmes referring mainly to observations from regular marine surveys.

In addition, a searchable database was prepared and forms an integral part of the MeDir-OP. This on-line database serves to search, track, and categorise:

- marine institutions with activities related to operational oceanography
- projects and platforms for routine ocean/coastal observations.

Search sessions can be conducted at first level through the entry of a keyword, or more specifically at a higher level by choosing map category, country, institute type or geographical area.

5. Concluding remarks

The survey conducted within the MAMA project has provided a first comprehensive picture of the existing institutional set-ups, infra-structural assets and the human and funding resources deployed in operational oceanography in the Mediterranean region. Besides compiling a detailed inventory with descriptions of more than 120 routine ocean and coastal monitoring activities, this effort has in addition started to map the frame-works within which marine affairs are conducted in the riparian countries, and has prepared a first reference to the major marine-related economic activities that can benefit from operational observations and forecasting.

The exercise has served to put into practice a methodology for this kind of inventorying, and established a basis for acquiring, compiling, analysing and synthesising metadata relevant to operational oceanography. Partners have been empowered to repeat and update similar assessments at national scale.

The benefits of such inventorying efforts are multiple. This kind of mapping allows quasi-quantitative comparisons between countries and between regions; it prepares the way to the identification of additional resources in operational oceanography that are needed in countries to fully benefit from the basin-wide ocean observing system planned for GOOS; it is moreover the precursor to the effective design of an initial observation and forecasting system, based on combined and complementary national contributions and a co-ordinated upgrading of capabilities in all partner countries.

The Mediterranean Directory for Operational Oceanography embraces the bulk of the collected metadata and provides a web-based resource for the use of this information in planning and management. The MedGOOS Secretariat at the IOI-Malta Operational Centre within the University of Malta, in collaboration with the MedGOOS partners, aims to maintain and regularly update this metadatabase.

Some enhancements and further developments are planned mainly to better represent the socio-economic dimensions on top of the scientific and technology-related components. In a comprehensive approach to marine resource management and sustainability the inter-dependence between ecological considerations and socio-economic impacts/ forcings needs to be addressed (Kullenberg, 2004). To this end it is necessary to merge observational parameters with socio-economic variables that represent the multi-purpose interests of the various stakeholders, and enable an integrated ecological-economic approach that quantifies the socio-economic impacts of changes in the coastal systems.

In the specific case of operational oceanography, integrated assessments can provide a handle to adapt ocean observation and forecasting systems for maximal social and economic benefits; to enable monitoring and prognoses of the impacts of operational oceanographic activities on national and regional economies, on security and on public services in general; and furthermore to elaborate adequate levels of investment in such systems commensurate to returns and to social priorities and needs. This can only be achieved by destricating the complex interactions between the social, ecological and technological counterparts. It surely cannot be done without the backbone of relevant data and information.

Acknowledgements

MAMA was funded by the EC FP5 Energy, Environment and Sustainable Development, coordinated by Fondazione Onlus — International Marine Centre (IMC, Oristano, Italy) and co-coordinated by the IOI–Malta Operational Centre, University of Malta (MedGOOS Secretariat, Malta).

References

Drago, A., M. Scerri and J. Borg (2003). MAMA — A Regional Network for Ocean Forecasting in the Mediterranean, in 'Proceedings of the Sixth International Conference on the Mediterranean Coastal Environment', MEDCOAST 2003, Volume 3, pp.2201–2210.

Drago, A., S. Vallerga and the MAMA Consortium (2004). MedGOOS — Building a strong regional partnership for operational oceanography in the Mediterranean, in 'Proceedings of the 37th CIIESM Congress' Barcelona 7–11 June 2004, pp.

IOC (1998). The Global Ocean Observing System 1998, Paris, UNESCO, 190pp.

Kullenberg, G., (2004). Ocean governance implementation: Reflections on motivations, principles, roles of sciences, socio-economy and social systems, In: 'A Gateway to Sustainable Development', Proceedings of the 30th International Conference Pacem in Maribus, A year after Johannesburg. Ocean Governance and Sustainable Development: Ocean and Coasts — a Glimpse into the future, 27–30 October, Kiev, Ukraine, pp. 64–89.

UNESCO/IOC (2005). An Implementation Strategy for the Coastal module of the Global Ocean Observing System, Paris, 113pp, (submitted as draft in the GOOS Report Series).

Vallerga, S., A. Drago and the MAMA Consortium (2002). MAMA — Towards a new paradigm for ocean monitoring in the Mediterranean, In: 'Building the European Capacity in Operational Oceanography', Proceedings of the 3rd International Conference on EuroGOOS, 3–6 December, Athens, pp. 46–56.

Vallerga S. and A. Drago (2005). Linking the coastal zone to GOOS. This volume page 262.

UNITED NATIONS PUBLICATION (2002). Report of the World Summit on Sustainable Development, Johannesburg, South Africa, 26 September–4 August 2002, A/CONF.199/20.

POSEIDON II: A second generation monitoring and forecasting system for the Eastern Mediterranean Sea

K. Nittis*[1], L. Perivoliotis[1], D. Ballas[1], G. Korres[1], T. Soukissian[1], A. Papadopoulos[1], A. Mallios[1], G. Triantafyllou[1], A. Pollani[1], V. Zervakis[2], D. Georgopoulos[1], V. Papathanassiou[1] and G. Chronis[1]

[1]*Hellenic Centre for Marine Research, Institute of Oceanography, Anavyssos, Greece*
[2]*University of Aegean, Department of Marine Sciences, Mytilene, Greece*

Abstract

Based on a network of oceanographic buoys and a set of atmosphere and ocean numerical models the POSEIDON system has operated since 1999 in the Aegean Sea, demonstrating the feasibility of regional sea monitoring and short term forecasting. A major upgrade of the system is currently underway. The existing network will be extended with additional buoys for the Ionian and NW Levantine Seas, while its observing capacity will be increased with new sensors for biochemical observations in the euphotic zone and physical observations in the deep layers (2000 m). The observing component of the system will also be enriched with remote sensing products (SLA, Ocean Color, SST, precipitation) while operational data from other existing platforms (FerryBox, VOS, XBT, etc.) will be integrated through a unified information management system. The forecasting system upgrade includes increased resolution using nesting techniques, assimilation methods for all numerical models and a non-hydrostatic version for the meteorological model. Finally, an ecological model will extend the forecasting capacity towards ecosystem predictions at basin scale. The project will be coordinated with relevant national and EU efforts for the European seas in the framework of GMES and GEOSS.

Keywords: Regional systems, buoys, multi-sensor moorings, numerical modelling, Eastern Mediterranean

1. Introduction

The POSEIDON-I project (1997–2000) developed and implemented an integrated real-time monitoring and forecasting system for marine environmental conditions in the Aegean Sea, establishing the basis of operational oceanography in Greece (Soukissian *et al.*, 2002). The main observing component of the system is the network of 11 SeaWatch oceanographic buoys that collect meteorological, wave and upper layer (50 m) oceanographic data. The forecasting component includes a limited area atmospheric model based on the Eta system, a general circulation ocean model based on POM, and an offshore wave model based on WAM. The system provides operational short-term (72 hours) forecasts of meteorological and oceanic conditions on a daily basis using a downscaling approach. A buoyant pollutant model is also ready to provide dispersion

* Corresponding author, email: knittis@ath.hcmr.gr

forecasts of oil-spills or other pollutants in case of accidents in the Aegean Sea or the Eastern Mediterranean.

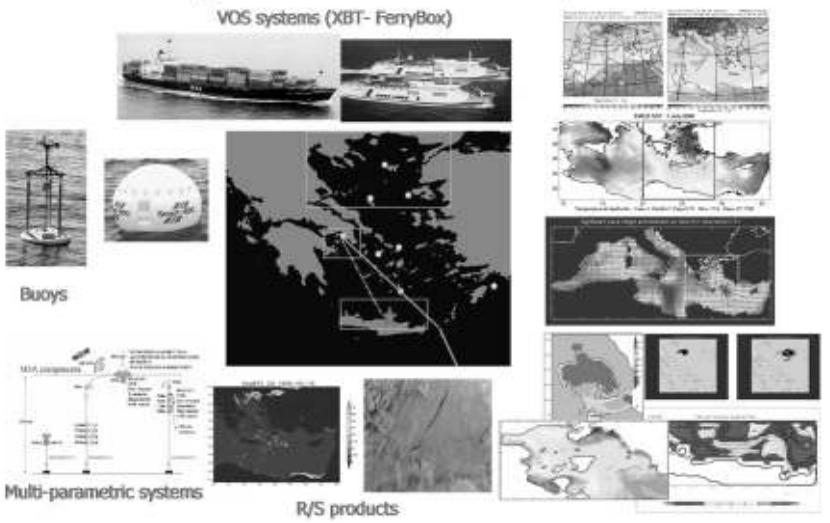

Figure 1 Components of the Aegean Sea monitoring and forecasting system.

The system implemented by POSEIDON-I has been gradually enriched during the years (2000–2005) through various national and EC funded projects (see Nittis *et al.*, 2005). The MFSPP (EC/FP4) and MFSTEP (EC/FP5) projects developed:

- a prototype multi-parametric buoy system (M3A) for deep physical (0–500 m) and bio-chemical (0–100 m) measurements in the south Aegean Sea
- a VOS/XBT line for collection of temperature profiles in the Eastern Mediterranean and the Aegean Seas
- high resolution operational forecasting models for the shelf areas of the Aegean Sea
- pre-operational 1-D and 3-D ecological models for the south Aegean Sea ecosystem (Nittis *et al.*, 2003; Triantafyllou *et al.*, 2003).

The FerryBox (EC/FP5) project developed and operates a VOS/Ferryboat line in the Aegean Sea for collection of surface physical and biochemical parameters. In the same project a new data assimilation scheme based on SEEK/SFEK filters for the exploitation of operational data by the POSEIDON ocean forecasting model has been developed. The Athens2004 project (funded by the Organizing Committee of the Olympic Games) developed a coastal sea monitoring and forecasting system to support the sailing games of the summer 2004 Olympics. The system was based on a network of 3 oceanographic buoys and a set of very high-resolution (500 m) numerical models nested into the basin-scale model for short term (3–24 h) forecasts of waves and currents in the Saronikos Gulf.

The Mersea_S1 (EC/FP5) and the ROSES (ESA/GSE) projects developed components of an integrated oil-spill detection and forecasting service focused on illicit vessel discharges, including operational dissemination of results to the end-user. Finally, the ESPEN (national/GSRT) project currently upgrades the wave forecasting in the Aegean

Sea and extends the wave monitoring network with four new-technology wave buoys. As a result of the above efforts, the Aegean Sea can today be considered a prototype "regional sea observatory" for the European Seas (Figure 1).

A major upgrade of the POSEIDON system, which is the main component of the Aegean Sea Observatory, is currently underway. It is carried out through the POSEIDON-II project (2005−2007) funded by the EFTA/EEA and the Hellenic Ministry of National Economy with a total budget of 9.8 M€. The activities of the project and the main components of the new system are presented in the following sections.

2. The upgraded observing system

2.1 SeaWatch buoy network upgrade

The eleven (11) SeaWatch buoys of POSEIDON-I are being upgraded to improve their functionality, increase the quality of collected data and extend their lifetime. This upgrade includes (see also Ballas *et al.*, 2005):

- a new central processing unit with a more modular software and additional / new type communication ports
- new communication systems; an Iridium modem will be added to the standard Inmarsat-C and GSM/GPRS systems
- new floaters, internal cabling, solar panels and navigation lights
- re-arrangement of batteries for increased safety
- a wind power generator for additional energy
- new wind speed / direction, upper layer CTDs and current speed/direction sensors
- an inductive modem controller for communication with underwater sensors attached to inductive cable
- an acoustic modem for communication and data transfer between the surface buoy and deep sensors / platforms.

2.2 New open-sea buoys and oceanographic sensors

Five (5) new buoys able to operate in open sea conditions (>2000 m depth) will complement the existing network. The new buoys, as well as the upgraded SeaWatch platforms, will be equipped with an inductive cable able to host sensors at any depth between 0 and 2000 m. Furthermore, all new sensors will be able to communicate through inductive modems either as stand alone systems or as packages of multiple sensors through an intermediate data logger. In this way the new buoy network will be flexible and modular in terms of sampling depths and sensor types.

With these additional buoys the POSEIDON network, that currently covers only the Aegean Sea, will be extended towards the Ionian and the North-West Levantine Seas. This will improve the tracking and forecasting of rapid meteorological changes associated with the passage of synoptic weather systems over Greece. It will also improve wave forecasting by providing boundary conditions able to describe the influence of large scale patterns on the Aegean Sea wave regime.

Furthermore, these buoys will be used to study the exchanges between the Aegean and the adjacent seas, mainly in the deep layers where important changes of hydrological properties associated with the thermohaline circulation variability have been observed during the previous two decades (Theocharis *et al.*, 2002). Equipped with T/S sensors down to 2000 m depth, the new buoys will be able to monitor the outflow of the Aegean Deep Water (ADW) as well as the inflow of the Transitional Mediterranean Water (TMW) and Levantine Intermediate Water (LIW).

Two of the buoys will be equipped with optical and chemical sensors (fluorometers, dissolved oxygen, PAR, turbidity, spectral radiometers, nutrients) for monitoring of biochemical variability in the upper 100 m as well as with T/S sensors for monitoring the main thermocline variability (0–500 m) in the area. They will also host a more complete set of meteorological instruments including precipitation, relative humidity, short and long wave radiation sensors. They will follow the sampling strategy of the M3A system (Mediterranean Moored Multi-sensor Array) developed for the needs of the Mediterranean Forecasting System through the MFSPP and MFSTEP projects (Nittis *et al.*, 2003). One of them will replace the prototype E1-M3A system in the oligotrophic Cretan Sea while the second will be deployed in the mesotrophic North Aegean. The data collected from these 2 Eulerian Observatories will be used for the calibration / validation of the Eastern Mediterranean Sea ecosystem model as well as process studies planed for the needs of the EurOCEANS (FP6 NoE project, www.eur-oceans.org). Their data will be distributed through the OceanSITES global network of moored time series stations (www.oceansites.org).

Finally, a set of underwater Acoustic Rain Gauges (ARG, Nystuen, 2001) will be installed on two of the new POSEIDON buoys. The data from these novel devices will be combined with surface precipitation observations from surface buoy sensors and independent weather radars as well as with satellite rainfall estimates (passive microwave sensors) to better improve weather and flood forecasting in the Eastern Mediterranean Sea region.

2.3 The deep-sea platform

A bottom platform able to host a variety of sensors (compatible with the water column sensors of the POSEIDON buoys) and able to operate at 2000 m depth or more, will be developed during the project. The platform will have energy autonomy for at least six months and will be able to transmit data to the surface buoys through underwater acoustic modems. Apart from monitoring deep sea properties, the platform will be used to detect abrupt sea level changes as a pilot component of a Tsunami warning system. For this reason the platform will use the hardware and software specifications developed for the NOAA DART system of the Pacific Ocean.

3. The new forecasting system

The project is upgrading and extending the three main components of the POSEIDON numerical forecasting system: the weather, wind–waves and general circulation models. This upgrade includes increased resolution, improved parametrisations, new down-scaling methods and assimilation techniques for all three models.

The non-hydrostatic version of the Eta mode will be used for the new POSEIDON-II weather forecasting system. This will allow a further increase of the horizontal resolution (currently 10 km, target 7 km) to better resolve and comply with the complicated topographic formations and complex coastline (Papadopoulos *et al.*, 2002). The upgrade includes improved parametrisation schemes for resolving the atmospheric processes with scales smaller than the model grid structure, as well as new techniques for assimilating surface observations obtained from the POSEIDON buoys, satellites and synoptic meteorological stations. A specific task of the project will be the operational retrieval of precipitation fields from satellite multi-channel passive microwave sensors (i.e. SSM/I, AMSR, TMI). These products will be used for operational assimilation into the daily forecasting cycle of the weather model after being cross-calibrated with data from the ARG sensors and weather radars.

The hydrodynamic model of POSEIDON is based on a 1/20° resolution implementation of POM in the Aegean Sea nested into a 1/10° resolution model of the Eastern Mediterranean (Nittis *et al.*, 2005). It will be replaced by a 1/30° version of POM for the Aegean, nested into a 1/8° Mediterranean Sea model. Both models have 24 sigma levels and will use the same assimilation scheme based on the SEEK filter approach and 50−60 multivariate EOF modes (see Korres *et al.*, 2005). A variational initialisation scheme will be used for optimal model downscaling; it will be able to use input from different large scale models, such as those developed by the MFSTEP and MERSEA projects.

Finally, the WAM-cycle4 and DAUT wind wave models (Soukissian *et al.*, 2001), currently used for operational forecasting in the Mediterranean and Aegean Seas respectively, will be upgraded following a benchmarking of three different wave models: WAM, SWAN and WAVEWATCH. The models will use the same atmospheric forcing for a specific data-rich hindcasting period and their performance will be evaluated against *in situ* (POSEIDON buoys) and remote sensing (ENVISAT) observations.

Apart from the above upgrades, the POSEIDON forecasting system will be extended towards environmental predictions using an ecosystem model developed for the Eastern Mediterranean Sea. Based on the ERSEM code this model has already been tested at subbasin (Aegean−Levantine), shelf and coastal areas of the Eastern Mediterranean (Triantafyllou *et al.*, 2003). It will be coupled to the hydrodynamic forecasting model and will use assimilation of remote sensing (ocean colour) data following the SEEK filter approach. In order to facilitate dissemination of modelling and data products to scientific users a Live Access Server will be developed during POSEIDON-II. Furthermore, general public products for the web and displaying on mobile telephones will be upgraded while new interactive web tools will be developed for easier access to the operational oil spill service.

4. Conclusions

In 1997 the POSEIDON-I project established the basis of Operational Oceanography in Greece and implemented one of Europe's most complete regional monitoring and forecasting systems. The system has been fully operational since 1999 and has managed to establish a big community of end-users and to attract the interest and funding of governmental customers. The POSEIDON-II project will carry out a major upgrade and extension of the system, building on the experience of recent research projects and

integrating new products from the marine technology industry. The project also includes new research components, such as ecosystem data assimilation — a combination of ARGs with precipitation remote sensing — and deep platforms, which will eventually be transformed to operational products during its lifetime. The multi-platform and multi-model Aegean Sea Observatory that has been developed through POSEIDON-I and consequent EC and national research projects will be extended towards the Eastern Mediterranean Sea and its components will be enriched and further integrated. These efforts are coordinated with other GMES initiatives mainly through the ROSES and MARCOAST projects of ESA/GSE and the MERSEA project of EC/DG Research. By the end of 2007 POSEIDON-II will deliver an integrated ocean monitoring and forecasting system for the Eastern Mediterranean Sea, in time for the operational phase of GMES.

Acknowledgements

The POSEIDON-I (1997–2000) and POSEIDON-II (2005–2007) projects were/are co-funded by EFTA/EEA and the Hellenic Ministry of National Economy.

References

Ballas, D., A. Mallios and P. Pagonis (2005). A technical overview of the POSEIDON II system. This volume page 69.

Korres, G., K. Nittis, I. Hoteit and G. Triantafyllou (2005). A data assimilation tool for the Aegean Sea hydrodynamic model. This volume page 611.

Nittis, K., C. Tziavos, I. Thanos, P. Drakopoulos, V. Cardin, M. Gacic, G. Petihakis and R. Basana (2003). The Mediterranean Moored Multi-sensor Array (M3A): System Development and Initial Results, Annales Geophysicae, 21(1), 75–88.

Nittis, K., L. Perivoliotis, G. Korres, C. Tziavos and I. Thanos (2005). Operational monitoring and forecasting for marine environmental applications in the Aegean Sea. Environmental Modelling and Software, in press.

Nystuen, J.A. (2001). Listening to Raindrops from Underwater: An Acoustic Disdrometer, J. Atmos. and Oceanic Tech., 18, 1640–1657.

Papadopoulos, A., G. Kallos, P. Katsafados and S. Nickovic (2002). The Poseidon weather forecasting system: An overview. The Global Atmosphere and Ocean Systems, 8, 2–3, 219–237.

Soukissian, T., L. Perivoliotis, A. Prospathopoulos and A. Papadopoulos (2001). Performance of three numerical wave models on the Aegean Sea. First results. 11th International Offshore and Polar Engineering Conference, Stavanger, Norway, 17–22 June, III, 40–45.

Soukissian, T., G. Chronis, K. Nittis and C. Diamanti (2002). Advancement of Operational Oceanography in Greece: the case of the POSEIDON system. The Global Atmosphere Ocean System, Vol. 8, No. 2–3, 119–133.

Triantafyllou, G., G. Petihakis and J.I. Allen (2003). Assessing the performance of the Cretan Sea ecosystem model with the use of high frequency M3A buoy data set. Annales Geophysicae, Vol.21, pp 365–375.

Theocharis, A., B. Klein, K. Nittis and W. Roether (2002). Evolution and status of the eastern Mediterranean Transient (1997–99), Journal of Mar. Syst., 33/34, 91–116.

An operational oceanographic forecasting and observing system for the Eastern Mediterranean Levantine basin: The Cyprus coastal ocean forecasting and observing system

George Zodiatis*, Robin Lardner, Daniel R. Hayes and Georgios Georgiou

Oceanography Centre, University of Cyprus, Nicosia, Cyprus

Abstract

The Cyprus coastal ocean forecasting and observing system (CYCOFOS) consists of several operational modules: high-resolution coastal–ocean forecasts in the NE Levantine, offshore and near-coastal wave forecasts for the Mediterranean, Levantine and Cyprus basins, satellite remote sensing for the Eastern Mediterranean, coastal remote monitoring stations, an ocean observatory, and an oil spill prediction model. All these operational modules provide the following over the internet: daily ocean forecasts for the NE Levantine Basin for the next five days, weekly ocean forecasts for the next 10 days, a three-hourly offshore and near-coast sea state forecast for the Mediterranean, Levantine and Cyprus basins for the next 60 hours, daily single remote sensing SST images with 1 km resolution for the Eastern Mediterranean and the Levantine basin, hourly *in situ* sea level and water temperature at certain coastal remote stations, and half-hourly temperature and salinity at various depths from the ocean observatory in the SE Levantine Basin. Moreover, CYCOFOS provides daily and weekly forecasting data to end users, necessary for operational applications of the MEDSLIK (Mediterranean oil spill model).

The ongoing development and improvement of CYCOFOS include the operational posting of six-hourly ocean forecasts, upgrading of the ocean observatory, expansion of the coastal remote observing stations, and processing in near real time of remote sensing images related to harmful algal blooms.

Keywords: Eastern Mediterranean, ocean forecasting, ocean observation network, wave forecasting, operational oceanography

1. Introduction

The development of operational ocean monitoring and forecasting systems on global, regional, sub-regional and local scales will support, among others, a better management of the marine environment and will assist the end users in their decisions for protecting and reducing the environmental problems that may arise from the various economic activities in the marine sector.

The Cyprus coastal ocean forecasting and observing system (CYCOFOS) was developed within the broad frame of GOOS (Global Ocean Observing System) and its regional components of EuroGOOS (European GOOS) and MedGOOS (Mediterranean GOOS),

* Corresponding author, email: gzodiac@ucy.ac.cy

to promote the operational oceanographic forecast and monitoring on local and sub-regional scales in the Eastern Mediterranean Levantine Basin. The CYCOFOS has been operational since early 2002 and consists of several forecasting, observing and end user modules. CYCOFOS has been described previously (Zodiatis *et al.*, 2002, 2003a,b), but has been enriched and improved in recent years. CYCOFOS data can be accessed at www.ucy.ac.cy/cyocean. Recently CYCOFOS joined the Mediterranean Operational Oceanography Network (MOON), aimed at sustaining the operational forecasts in the Mediterranean, in collaboration with other basin, sub-basin and coastal forecasting systems.

The development and continuous improvement of the CYCOFOS modules is carried out following the objectives of several European Union projects, including the Mediterranean forecasting system — both pilot project and towards environmental predictions (MFSPP and MFSTEP), the Mediterranean network to access and upgrade monitoring and forecast activities in the region (MAMA), the European sea level service research infrastructure (ESEAS-RI), the Mediterranean network of global sea level observing system (MedGLOSS) and the Marine environment and security in the European areas (MERSEA-Strand 1 and MERSEA-IP). The purpose of this paper is to discuss the current status of CYCOFOS.

2. Description

2.1 Forecasting

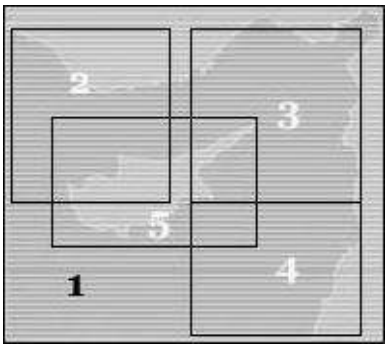

Figure 1 New, high-resolution (1.5 km) CYCOM domain. Users can click on any region to display more detailed images.

Operational ocean forecasts of the Levantine Basin (Figure 1) are carried out by CYCOM — the Cyprus Coastal Ocean Model (Zodiatis *et al.*, 2003c). CYCOM is based on the Princeton Ocean Model (POM) and is forced and initialised from lower resolution oceanic model forecasts and high frequency atmospheric forecasts. In the past, the MFS basin model has been implemented as the parent model, along with ECMWF forecasts. This mode of operation now allows 10-day forecasts to be completed every week (along with 7-day hindcasts) with a resolution of 2.5 km. Currently, a higher resolution ocean forecast (1.5 km) is produced in which the parent model has been changed to the ALERMO model (www.oc.phys.uoa.gr/), which is in turn nested within the MFS basin model (Figure 2). In addition, the SKIRON (Kallos and SKIRON group, 1998) high-

frequency (hourly) meteorological forecasts are used (http://forecast.uoa.gr/). This allows a 5-day high resolution ocean forecast to be repeated daily. A variational interpolation method, Variational Initialisation and FOrcing Platform (VIFOP, Auclair, 2000a,b), has been implemented in order to more accurately downscale the ALERMO model fields to the CYCOM grid. In particular, spurious gravity waves due to interaction of the interpolated current field and the high resolution land mask are minimised. It should also be noted that the MFS basin model now includes temperature (XBT) and conductivity–temperature (CTD) profiles into its assimilation scheme, as well as satellite-based sea level anomalies, while the satellite sea surface temperatures are used for correction of the surface heat fluxes. In the near future, six-hourly forecast fields will be posted on the CYCOFOS web page, rather than just daily averages. The CYCOFOS forecasting products will continue to be available for the end users of the Mediterranean oil spill model, MEDSLIK. Use of the six-hourly current fields will certainly improve the accuracy of MEDSLIK predictions, as well as other derived applications.

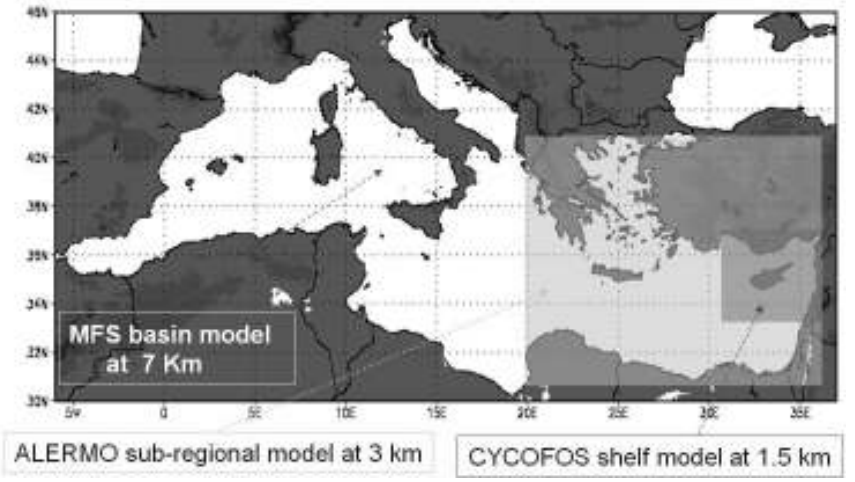

Figure 2 CYCOFOS model hierarchy. Basin model of 7 km resolution is produced by the Mediterranean Forecasting System — Toward Environmental Prediction (MFSTEP). The regional model, ALERMO, of 3 km resolution is nested within the MFSTEP model. CYCOM is nested within the ALERMO model.

Wave forecasts of the entire Mediterranean and Levantine basins are produced by a WAM model (WAMDI group, 1988). The new extended Levantine wave domain is nested within the Mediterranean wave forecast (Figure 3). The wave forecast is produced every day for the coming 60 hours. Wave height, direction, and the SKIRON wind velocity are available every three hours. The high-frequency SKIRON forecasts provide hourly forcing, rather than the previously used six-hourly ECMWF winds. An even higher resolution wave forecast (Figure 2) based on SWAN (Holthuijsen *et al.*, 1997) has been implemented for simulating waves at the near-coast sea areas around Cyprus.

Figure 3 The Cyprus Wave Model forecasts wave height and direction for the entire Mediterranean. Nested within that model is the wave forecast for the Levantine basin (inset 1). Nested within the WAM is a high-resolution SWAN model (inset 2).

2.2 Observing

In CYCOFOS, near real time observations consist of two types; periodic short field campaigns and near real time continuous measurements at fixed locations in the Levantine basin. Bi-monthly or monthly XBT short cruises are carried out in the Levantine basin within the framework of the MFSTEP project, in the region south of Cyprus. The data collected from these cruises together with similar data from other parts of the Mediterranean are assimilated into the parent MFS model.

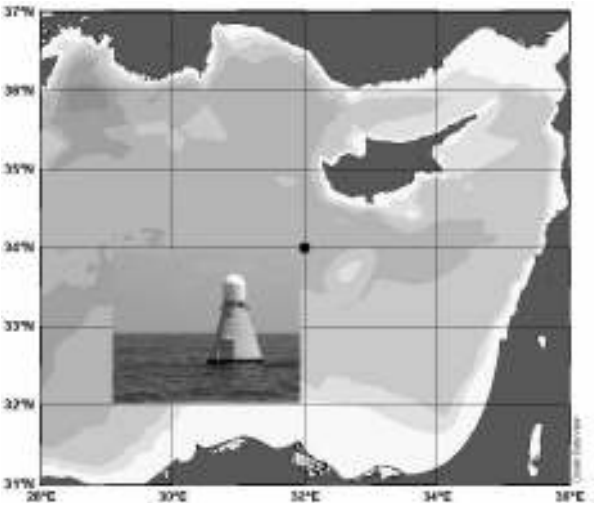

Figure 4 Location and photograph of the CYCOFOS MedGOOS-3 Ocean Observatory.

An ocean observatory has been added to CYCOFOS which measures conductivity and temperature at five levels in the open, deep Levantine basin (Figure 4). It is called the MedGOOS-3 Ocean Observatory, and was deployed by Harris Maritime Communication Services, who own and maintain the system. The sensors used are SBE-37 MicroCAT C-T recorders which communicate with the surface using an inductive modem. The deepest sensor also measures pressure. The data are collected every 30 minutes, and retrieved every 24 hours with satellite communication. They are processed and posted on the CYCOFOS web site daily. There are plans to extend the observing depth of this system beyond the current water depths with additional CT sensors. Data on buoy attitude (heave, pitch, roll) will be used to calculate wave height and direction in near real time. Finally, all observatory data will be uploaded every one or two hours rather than every 24 hours.

The existing coastal sea level, water temperature, and air pressure MedGLOSS station continues to operate, as it has since 2001 (Zodiatis *et al.*, 2002; 2003a,b). Future similar coastal stations are planned. The satellite ground receiving station also described in Zodiatis *et al.* (2002, 2003a,b) has been operating successfully since 2001. It collects images of SST from NOAA AVHRR satellites. Cloud cover is generally not extensive or persistent in the Eastern Mediterranean, so SST images are collected almost daily. Recently, SST images of the Eastern Mediterranean have been posted on the CYCOFOS web page (Figure 5), rather than just the Levantine SST images as previously. Images are currently being produced for the Levantine basin depicting frontal zones based on SST, and these will be posted on the internet too. Also, the capability of producing images of ocean colour to visualise algal blooms will be achieved and made available in the near future.

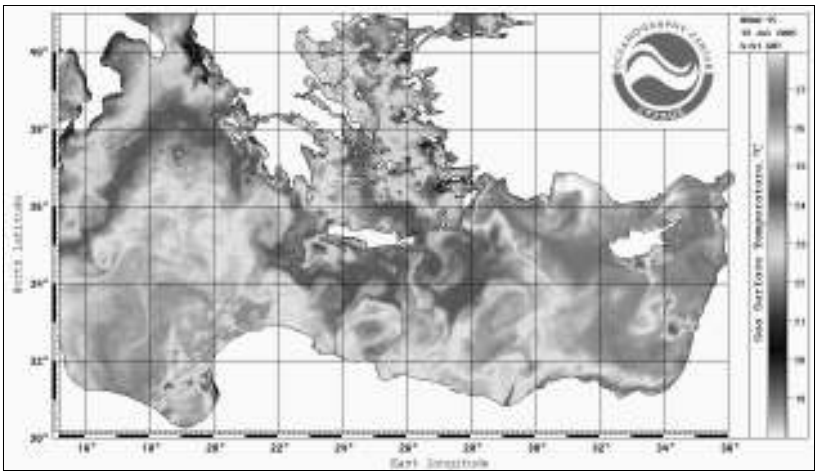

Figure 5 AVHRR image of the Eastern Mediterranean captured and processed with the CYCOFOS receiving station and processing system.

3. Conclusions

CYCOFOS, in close collaboration with other partners in EU promoting the operational oceanography in Europe and the Mediterranean, may contribute to the GMES precursor

services, particularly on sub-regional and local scales. CYCOFOS is a well-rounded system consisting of both prediction and observational components. Most components are fully operational; they produce results every day and provide them to the general public via the internet (www.ucy.ac.cy/cyocean). The components are periodically improved by providing higher resolution and more frequent oceanic forecasts, near-coastal wave forecasts, more open sea temperature, conductivity, and wave observations from the existing observatory, more coastal sea level/temperature stations, and satellite images of algal blooms and frontal zones. The ongoing developments will increase our knowledge of the Eastern Mediterranean Levantine and the adjacent coastal sea areas, thereby increasing the end users' ability to manage, protect, and enjoy it safely.

Acknowledgements

The new developments and improvements of the CYCOFOS modules have been carried out in the framework of European Union and other related international projects including MFSTEP and MERSEA-strand 1. The authors acknowledge the support of: the European Commission's Marine Science and Technology Programme, contract MAS3–CT98–0171 of the European Commission's Programme Energy, Environment and Sustainable Development, contracts EVR1–CT–2001–20010, EVK3–CT–2002–0089 and EVK3–CT–2002–00075, the CIESM providing the equipment for the Cyprus MedGLOSS station, the MFS, ALERMO and SKIRON forecasting systems providing access to their forecasting products, Prof. Nadia Pinardi, coordinator of MFSTEP project and of the MFS system, Prof. George Kallos coordinator of SKIRON system, Prof. Alex Lascaratos coordinator of ALERMO system and his scientific team from the University of Athens, Dr. Sarantis Sofianos and Dr. Nicos Skliris. We are also grateful to Dr. Dov Rosen, coordinator of MedGLOSS and his scientific team from IOLR, Dr. Isaac Gertman, Lazar Raskin and Irena Lunin for their valuable support and all CYCOFOS collaborators: Prof. Skevos Paraskeva, Dr. Vladimir Fomin, Dmitry Soloviev, Tommy Eleftheriou, Sotiris Savva, Marinos Ioannou, Marios Papaioannou, Iacovos Kostantinou and Andreas Kasenides for their contributions and to the system's modules and the system's operation, and Dr. Andrew Clark of MCS, USA for support of the CYCOFOS MedGOOS 3 Ocean Observatory.

References

Auclair, F., P. Marsaleix, and C. Estournel (2000a). Truncation errors in coastal modelling: evaluation and reduction by an inverse method. J. Atmos. Oceanic Tech., 17, 1348–1367.

Auclair, F., S. Casitas and P. Marsaleix (2000b). Application of an inverse method to coastal modelling. J. Atmos. Oceanic Tech., 17, 1368–1391.

Holthuijsen, L.H., N. Booij and R. Padilla-Hernandez (1997). A curvi-linear, third-generation coastal wave model, Conf. Coastal Dynamics '97, Plymouth, 128–136.

Kallos, G. and the SKIRON group (1998). The SKIRON forecasting system: VOL. I: Preprocessing ISBN 960–8468–15–9; VOL. II: Model description ISBN 960–8468–16–7; VOL. III: Numerical techniques ISBN 960–8468–17–5; VOL. IV: Parallelization ISBN 960–8468–18–3; VOL. V: Postprocessing ISBN 960–8468–19–1; VOL. VI: Procedures 960–8468–20–5.

WAMDI Group (1988). The WAM model — a third generation ocean wave prediction model. J. Phys. Oceanogr., 18, 1775–1810.

Zodiatis, G., R. Lardner, G. Georgiou, E. Demirov and N. Pinardi (2002). Cyprus coastal ocean forecasting and observing system, in Building the European Capacity in Operational Oceanography, Proceedings of 3rd EuroGOOS Conference, Elsevier Oceanography Series, 36–45.

Zodiatis, G., L. Lardner, E. Demirov, G. Georgiou, G. Manzella and N. Pinardi (2003a). "An Operational European Global Ocean Observing System for the Eastern Mediterranean Levantine Basin: The Cyprus Coastal Ocean Forecasting and Observing System", Journal of Marine Technology Society, v.37, no.3, 115–123.

Zodiatis, G., R. Lardner, G. Georgiou, E. Demirov, N. Pinardi and G. Manzella (2003b). The Cyprus coastal ocean forecasting and observing system, a key component in the growing network of European ocean observing systems, Sea Technology, v.44, n.10, 10–15.

Zodiatis G., R. Lardner, A. Lascaratos, G. Georgiou, G. Korres and M. Syrimis (2003c). High resolution nested model for the Cyprus, NE Levantine Basin, eastern Mediterranean Sea: implementation and climatological runs, Annales Geophysicae, 21, 221–236.

Validation in the two high resolution MERCATOR forecast systems in the North Atlantic Ocean

L. Crosnier*, N. Verbrugge, J.-M. Lellouche, M. Benkiran and E. Greiner

GIP MERCATOR, Ramonville St Agne, France

Abstract

MERCATOR has developed a high resolution (1/15°) forecast system with a new multivariate data assimilation scheme. This new system is compared to the previous monovariate MERCATOR high resolution system (1/15°) and to independent observations. Comparisons are made over the North Atlantic Ocean.

Keywords: MERCATOR, data assimilation, North Atlantic, Mediterranean Sea, MERSEA project.

1. Introduction

MERCATOR has developed a new high resolution (1/15°) forecast system using an optimal interpolation multivariate assimilation scheme (Benkiran *et al.*, 2005) with assimilation of the sea surface temperature, Sea Level Anomaly (SLA) as well as temperature and salinity vertical profiles from the Coriolis database. A detailed description of the new assimilation scheme can be found in Lellouche *et al.* (2005, this issue). This new system is compared to the previous monovariate MERCATOR high resolution system (1/15°) with assimilation of SLA only. In this paper, the new MERCATOR system is called MERCATOR2, and the older one is called MERCATOR1.

2. Validation in the North Atlantic Ocean

2.1 Impact of temperature and salinity vertical profiles assimilation on representation of water masses

This section compares the water masses in the MERCATOR 1 and 2 systems with the ones in various vertical WOCE sections (WOCE CD-ROM, 2002).

A WOCE zonal salinity section at 26°N (Figure 1) shows the Subtropical Underwater (STUW) salinity, with salinity characteristics ranging from 36.6 to 36.9 psu, centred at 200 m depth in the western Atlantic basin from 80 to 50°W. The same salinity section in the MERCATOR1 system does not display the STUW salinity characteristics, whereas the MERCATOR2 system does (Figure 1). Hence it is shown that assimilation of salinity vertical profiles in the MERCATOR2 system allows better representation of the STUW salinity characteristics, although STUW are less salty in the MERCATOR2 system than in the WOCE observations. This might be due to a lack of salinity vertical profiles to be assimilated in this region, or to an annual variation of the STUW salinity characteristics

* Corresponding author, email: laurence.crosnier@mercator-ocean.fr

between the time of the WOCE cruises (1992) and the time when we looked at the MERCATOR2 system (2003).

A WOCE meridional salinity section at 9°W (not shown) in the Gulf of Cadiz displays the salty Mediterranean Water Outflow (MOW) at 1100 m depths. In the MERCATOR1 system where the MOW is slightly too shallow compared to observations, the MOW is maintained by the relaxation below 500 m to the Reynaud *et al.* (1998) climatology in the Gulf of Cadiz. This is no longer the case in the MERCATOR2 system where no relaxation is applied and where assimilation of the climatology only occurs at depths below 1400 m at this latitude. The MERCATOR2 system represents well the MOW salinity characteristics thanks only to assimilation of salinity vertical profiles.

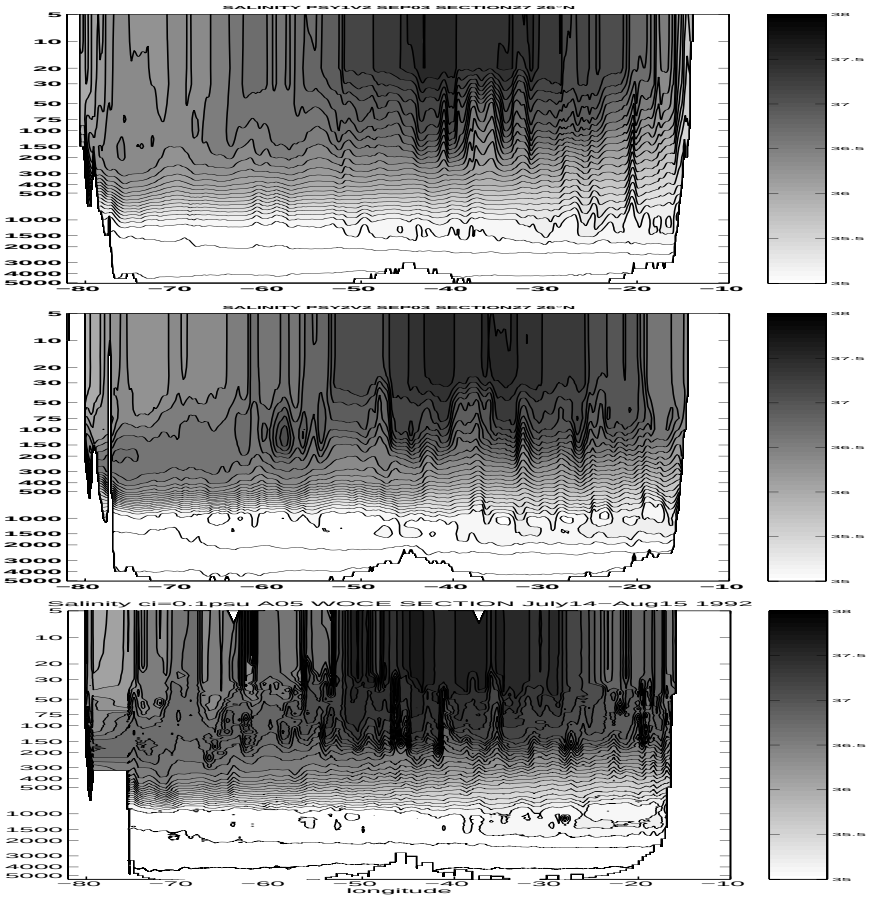

Figure 1 Zonal salinity (psu) section across latitude 26°N in the North Atlantic as a function of longitude and log10(depth) Top: in MERCATOR1 in September 2003; Middle: in MERCATOR2 in September 2003; Bottom: in the WOCE A05 synoptic section (Jul.−Aug. 1992).

2.2 The Mixed Layer Depth in the POMME area

This section gives an overview of the physical and biological processes taking place in the POMME area (16−22°W and 38−45°N), and then considers whether those processes

are well represented in the two MERCATOR systems. The POMME project investigates the processes of subduction and mode water formation at the mesoscale, as well as the coupling between the subduction dynamical processes and the Carbon cycle biological processes (Memery *et al.*, 2005). The region selected (Black square on Figure 2) presents subduction of the 11−12°C NorthEast Atlantic Mode Water. The POMME area is, according to the climatology (Boyer-Montegut *et al.*, 2004), a transition zone between deep late winter Mixed Layers (ML) in the North and shallower winter ML in the South. The POMME1 cruise during February−March 2001, with meridional sections at 20°W and 15.20°W, shows ML with depth ranging from 20 to 250 m (G. Reverdin, personal communication) with ML deeper in the northern than in the southern POMME area. The deep northern part is associated with a rather biologically productive area, when the south one is more oligotrophic (Levy *et al.*, 2005b). Moreover, as subduction and the spring bloom both occurs at the end of the winter, it is important to understand the timing of these two processes: subduction drives the biogeochemical characteristics of the water masses before they are incorporated into the main thermocline (Levy *et al.*, 2005b).

The MERCATOR1 and 2 systems (Figure 2), averaged over the winter 2004 (Jan−Feb−Mar) show a Mixed Layer Depth (MLD) deeper in the northern than in the southern POMME area, in agreement with Reverdin (personal communication) and the Boyer-Montegut *et al.* (2004) climatology.

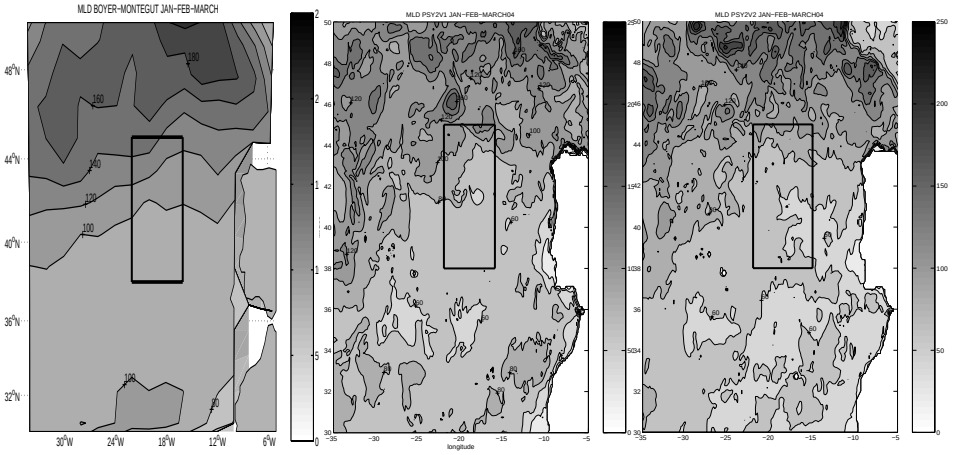

Figure 2 Winter Mixed Layer Depth (metres), Left: in the Boyer-Montegut (2004) climatology, Middle: in the MERCATOR1 system (winter 2004), Right: in the MERCATOR2 system (winter 2004).

In the high resolution CLIPPER simulation (Treguier *et al.*, 2003), the MLD seasonal cycle is well represented, with nevertheless overestimated amplitude by up to 100 m in March (Levy *et al.*, 2005a). A hovmuller diagram (Figure 3) shows that the seasonal cycle phase is also well represented in the MERCATOR1 and 2 systems, with amplitudes ranging from 40 m in the South to a maximum of 180 m in the northern part for MERCATOR1, and 20 m in the South along with maximum values of 260 m in the northern part for MERCATOR2. Following Reverdin (personal communication), MERCATOR2 MLD agrees better with observations. Figure 3 suggests that the

MERCATOR2 system displays more MLD fine-scale structures of importance for the biological activity, than the MERCATOR1 system. Although the 2 systems have the same horizontal and vertical resolution, this suggests that assimilation of temperature and salinity vertical profiles in the MERCATOR2 system enhances the development of MLD fine scale structures.

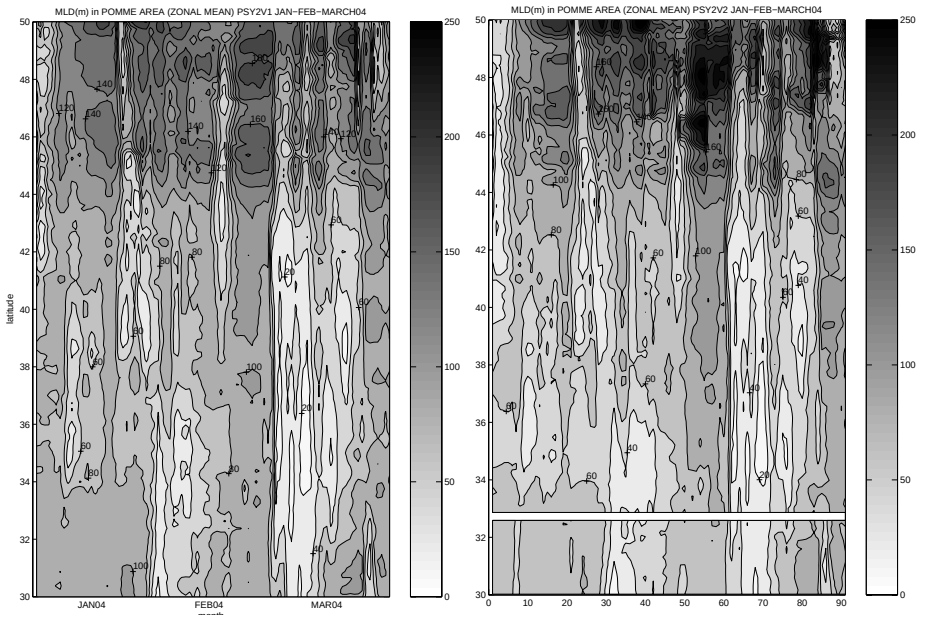

Figure 3 Hovmuller diagram (time as a function of latitude) of the Winter (JFM2004) Mixed Layer Depth (m). Left: in the MERCATOR1 system; Right: in the MERCATOR2 system.

2.3 Sea Surface Temperature and generation of the loop current eddies in the Gulf of Mexico

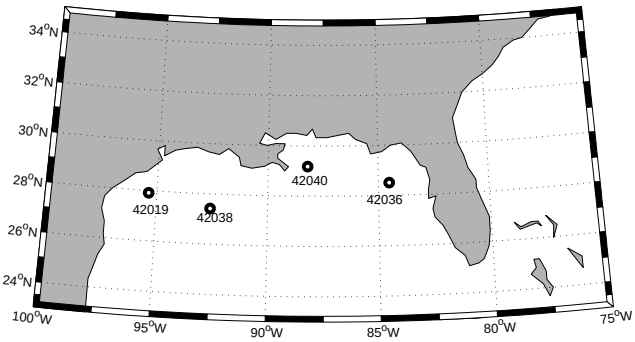

Figure 4 Location of the four moored buoys (with buoy numbers) in the Gulf of Mexico.

Sea surface temperature (SST) in the MERCATOR2 system is compared to independent observations (i.e. not assimilated) (Figure 5) at 4 buoy locations (Figure 4) for the period 15 June−19 October 2004. The MERCATOR2 SST temporal variability agrees very

well with observations, although the model shows a 0.5–1°C bias with observations, maybe because the model SST is a 3 m depth temperature, whereas the observed SST is a 0.6 m depth temperature.

The generation and evolution of the loop current eddies in the Gulf of Mexico is represented in a very realistic way by the MERCATOR2 system. Indeed, a comparison of the MERCATOR2 SLA with chlorophyll *a* concentration (independent data, i.e. not assimilated) in the Gulf of Mexico, during a cycle of 6 weeks from July to September 2004, shows very good agreement between the model and the observations (Figure 6). The loop current eddy is characterised by very low chlorophyll *a* concentration. From week1 to week6 (from top to bottom, Figure 6), we can follow the generation, the detachment and then the westward translation of the eddy, which happen in the model in phase with observations. Such eddies are generated by the instability of the Yucatan current, which is realistically represented in the MERCATOR2 system (not shown). The Yucatan current maximum velocity is 130 $cm s^{-1}$ at the end of summer 2003, in agreement with observations from Candela *et al.* (2003). Two deep countercurrents on the Yucatan and Cuban side observed by Candela *et al.* (2003) are also present in the MERCATOR2 system. In the western part of the Gulf of Mexico, we notice several patches with a very low chlorophyll *a* concentration (Figure 6, left column), associated with small scale eddies in the MERCATOR2 sea level anomaly (Figure 6, right column). Those structures are coming from a former loop current eddy which disintegrated into smaller scale eddies when colliding with the Mexican continental plateau.

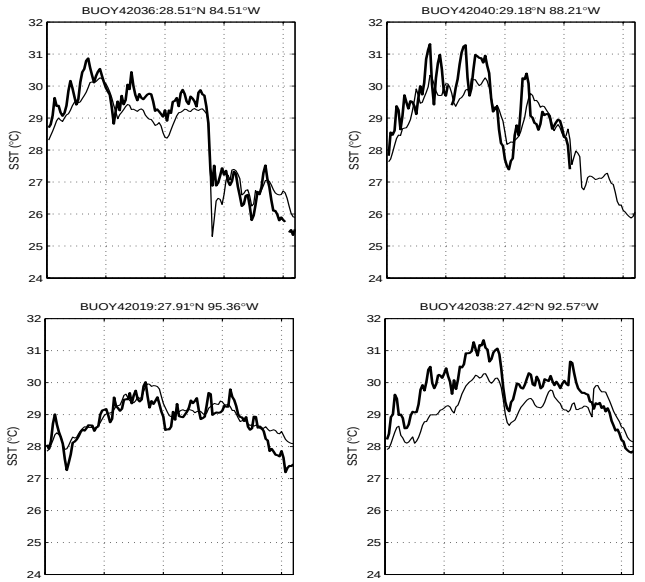

Figure 5 Moored buoys sea surface temperature (°C) (at 0.6 m depth) (Bold black curve) in the Gulf of Mexico from 15 June to 19 October 2004. The lighter curve shows the MERCATOR2 3 m depth temperature (°C) at the closest location and for the same time period.

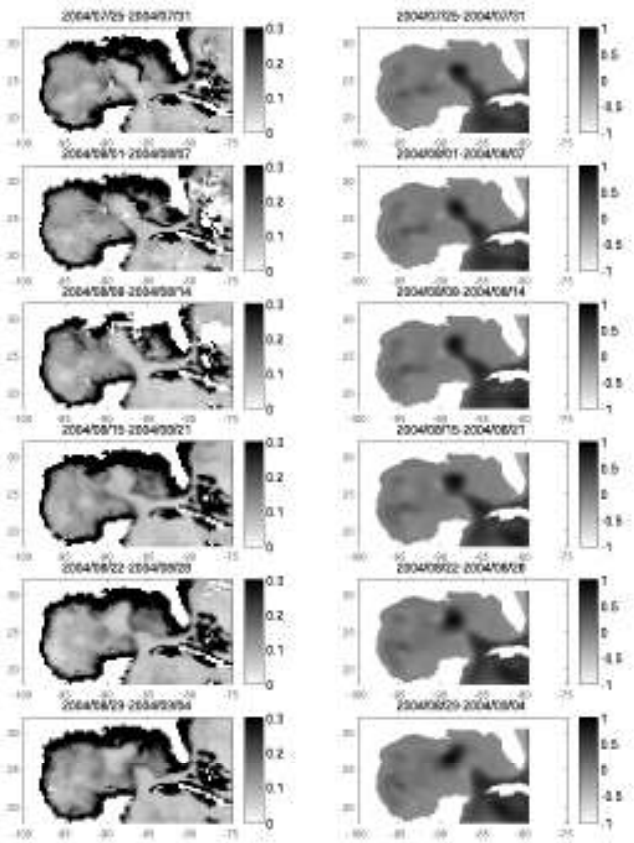

Figure 6 Weekly mean chlorophyll *a* concentration from MODIS-CATSAT (left column) and weekly mean sea level anomaly (m) from MERCATOR2 (right column) during 6 weeks. The first week (top panels) is from 25–31 July 2004 and the last week (lower panels) is from 29 August–4 September 2004.

3. Conclusion

This paper compares two MERCATOR systems at the same horizontal (1/15°) and vertical (43 levels) resolution in the North Atlantic, one with a new multivariate data assimilation scheme (MERCATOR2) and one with the previous monovariate scheme (MERCATOR1). The new scheme with assimilation of temperature and salinity vertical profiles allows better representation of water masses like mode waters and the Mediterranean Water Outflow. In the POMME area (16–22°W and 38–45°N), the mixed layer depth and its seasonal cycle are well represented in the two MERCATOR systems. MERCATOR2 seems to display more temporal and spatial mixed layer fine scale structures of interest for the biological processes. In the Gulf of Mexico, MERCATOR2 is successful at representing realistic loop current eddy shedding. In conclusion, we have investigated various regions in the North Atlantic that show that MERCATOR2 generally performs better than MERCATOR1. A more comprehensive validation of the new MERCATOR2 system is in progress.

Acknowledgements

The authors thank MODIS-CATSAT for providing their chlorophyll *a* data. Sea surface temperature moored buoys data are from the National Data Buoy Centre (http://ndbc.noaa.gov).

References

Benkiran, M., E. Greiner and E. Dombrowsky (2005). Multivariate and multidata assimilation in the Mercator project, submitted to Journal of Marine Systems.

Boyer-Montegut, C., G. Madec, A.S. Fisher, A. Lazar and D. Ludicone (2004). Mixed layer depth over the global ocean: An examination of profile data and a profile-based climatology, J. Geophys. Res., Vol 109, C12003, doi:10.1029/2004JC002378, 2004.

Candela, J., S. Tanahara, M. Crepon and B. Barnier (2003). Yucatan channel flow: observations versus CLIPPER ATL6 and MERCATOR PAM models, Journal of Geophysical Research, 108(C12), 3385.

Lellouche, J.M., M. Benkiran and E. Greiner (2005). Multivariate data assimilation in the Mercator North Atlantic and Mediterranean Sea high resolution model. This volume page 535.

Levy, M., Y. Lehahn, J.M. Andre, L. Memery, H. Loisel and E. Heifetz (2005a). Production regimes in the NorthEast Atlantic: a study based on Seawifs chlorophyll and OGCM mixed layer depth, submitted.

Levy, M., M. Gavart, L. Memery, G. Caniaux and A. Paci (2005b). A 4D-mesoscale map of the spring bloom in the northeast Atlantic (POMME experiment): results of a prognostic model, J. Geophys. Res., Vol 110, C7, C07S21 10.1029/2004JC002588.

Memery, L., G. Reverdin and J. Paillet (2005). The POMME Program (Programme Ocean Multidisciplinaire Meso Echelle). Subduction, thermocline ventilation, and biogeochemical tracer distribution in the North-East Atlantic Ocean: Impact of mesoscale dynamics, EOS, submitted.

Reynaud, T., P. Legrand, H. Mercier and B. Barnier (1998). A new analysis of hydrographic data in the Atlantic and its application to an inverse modeling study, International WOCE newsletter, 32, 29–31.

Treguier, A.M., O. Boebel, B. Barnier and G. Madec (2003). Agulhas eddy fluxes in a 1/6° Atlantic model, Deep Sea res. II, 50, 251–280.

World Ocean Circulation Experiment (WOCE) (2002). Global data Version 3.0, 2002, CD ROM.

Nowcasting/Forecasting subsystem of the circulation in the Black Sea nearshore regions

A. Kubryakov*[1], A. Grigoriev[2], A. Kordzadze[3], G. Korotaev[1], S. Stefanescu[4], D. Trukhchev[5] and V. Fomin[6]

[1]*Marine Hydrophysical Institute, Ukraine*
[2]*State Oceanographic Institute, Russia*
[3]*Institute of Geophysics, Georgia*
[4]*National Meteorological Administration, Romania*
[5]*Institute of Oceanology, Bulgaria*
[6]*Marine Branch of Hydrometeorological Institute, Ukraine*

Abstract

As part of the Nowcasting/Forecasting System of the Black Sea circulation a set of high-resolution models is implemented for the six nearshore regions of the Black Sea. The models are nested in a basin scale (5 km grid resolution) model with satellite altimetry data assimilation and forcing by the wind obtained from NCEP reanalysis data and climatological heat and salt fluxes. While there is some internal variability evident in the results, it is clear that, due to the relatively small domains, the results are strongly influenced by the imposed lateral boundary conditions. The main improvement is in the simulation over the narrow shelf region, which is not adequately resolved by the coarser grid model. Comparisons with satellite images and direct current measurements over the shelf and slope show reasonable agreement despite the limitations of the climatological forcing.

Keywords: numerical modelling, regional oceanography, nested grid technique.

1. Introduction

The health and well-being of 162 million people are affected by the environmental degradation in the Black Sea. Therefore, adequate prediction of the environmental variability in the Black Sea is needed to identify, analyse and determine the costs of solutions for better management of the marine environment for sustainable development of the resources. Furthermore, the environmental management of the Black Sea and the related scientific and technological developments require a system aimed towards an operational and forecasting system aware of end user needs. A nowcasting/forecasting system of the circulation is considered a necessary operational tool, useful as an aid to decision-making in case of events affecting marine operations or the marine environment. In this regard, the Black Sea Global Ocean Observing System (Black Sea GOOS, 2002) has promoted the Nowcasting/Forecasting System of the Black Sea, in order to implement the operational oceanography in the region. The first phase in the realisation of this goal is the development of the Nowcasting/Forecasting System of the Black Sea Circulation in the framework of the ARENA project (A Regional capacity building and Networking

* Corresponding author, email: akubr@alpha.mhi.iuf.net

programme to upgrade monitoring and forecasting Activity in the Black Sea basin) funded by the European Union, in order to demonstrate that a near real time oceanographic forecast in the Black Sea is possible.

The scientific rationale of the ARENA project is based on the hypothesis that both hydrodynamical and ecosystem fluctuations in the coastal/shelf areas of the Black Sea are closely connected to the open sea large-scale general circulation. The project includes the implementation of advanced modelling and remote sensing data assimilation tools.

The simplified scheme of the Nowcasting/Forecasting System of the Black Sea Circulation is shown in Figure 1.

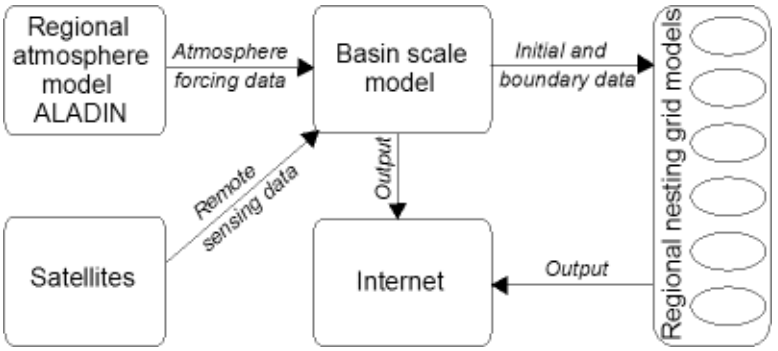

Figure 1 The scheme of the Nowcasting/Forecasting System of the Black Sea Circulation.

This paper describes the Nowcasting/Forecasting System of the Black Sea Nearshore Circulation which represents a set of high-resolution models implemented for the six coastal regions of the Black Sea.

2. Design of the system

The requirement for the high resolution models, aimed at the description of circulation in coastal areas, is that they should be capable of resolving scales associated with mesoscale phenomena, such as fronts and eddies. Their temporal scales are usually of the order of weeks, while their length scales are of the order of the local internal Rossby radius of deformation, which for the coastal and shelf zones of the Black Sea is of the order of about 5–10 km (Blatov *et al.*, 1984). However, using the necessary high resolution in global models has not been obviously possible until now, despite major progress in computer technologies. The high resolution can be used only in compact regional models. Thus the problem of the setting of boundary conditions on the open boundaries arises. Therefore, nesting high-resolution, limited-area nearshore models within a coarse-grid model covering all basins of the sea is the only viable approach to capturing the details of hydrodynamic phenomena that originate in the nearshore regions, but may be of great importance to the coarsely resolved all-basin scale. In a nested grid model, the nearshore component is hydrodynamically driven by the basin scale model.

The basin scale model (BSM) (Dorofeyev *et al.*, 2003) and all regional models are three-dimensional. The BSM is based on a fixed Cartesian grid while the nested models use

different grids for horizontal and vertical directions that allow large final scales. The numerical schemes are also different.

Two regional models — for the Burgas Bay (Ibraev *et al.*, 1996) and for the Georgian nearshore zone (Kordzadze *et al.*, 2003) are domestic models in z-coordinates. The other regional models represent the version of the Princeton Ocean Model for the Kalamita Bay (Kubryakov, 2004) near the western Crimea, for the Romanian nearshore zone (Stefanescu *et al.*, 2004; Kubryakov, 2004), for the North-Western Shelf zone (Fomin, 2005) and Russian nearshore zone (Kubryakov, 2004; Kubryakov *et al.*, 2005) of the Black Sea. The nesting method that has been used is a passive, off-line, one way interaction, where the nesting provides information to be passed along the open boundaries from the basin scale model coarse grid to the regional high-resolution grid models. An integral constraint is applied so that the net mass flux across the open boundaries is identical to the net flux in the basin scale model.

The BSM is used to initialise regional models, which receive boundary fields at the requested time frequency. The downscaling will bring the BSM 5-km resolution fields down to 0.5–1 km resolution for the shelf areas. The initialisation of the regional models crucially depends upon the BSM dynamical fields. This is contrary to most coastal forecasting systems that started with the observations tuned to the coastal areas leaving the remote effects as a secondary aspect of the general circulation on the shelf. The Black Sea shelf area is narrow in most regions and the general circulation can determine a large portion of the coastal hydrodynamics variability.

The areas for which regional models are developed are shown on Figure 2. The choice of these areas is due to the presence of intensive navigation, fisheries and other kinds of commercial operation of water areas, that is the high anthropogenic impact. At the same time there are complex water dynamics caused by a sharp bottom slope, a complicated coastline configuration, influence of the external border of the Rim Current and other factors, in particular river discharges.

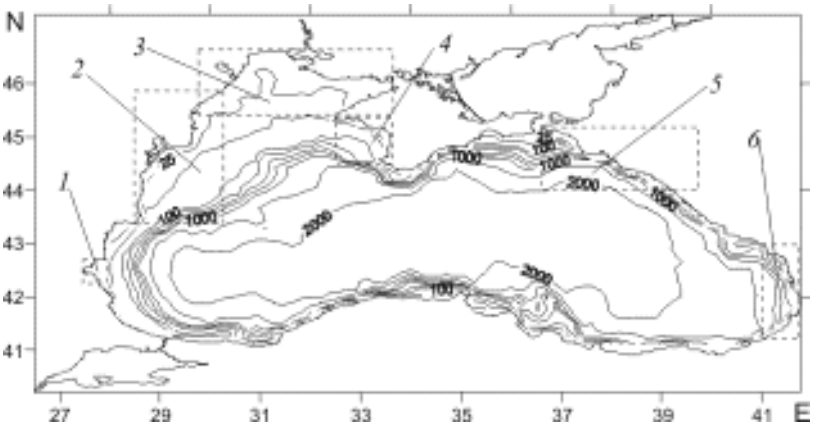

Figure 2 Areas for which regional models are developed: 1–Burgas Bay, Bulgaria; 2–Romanian coastal zone; 3–North-Western Shelf zone; 4–Kalamita Bay, Crimea; 5–Russian coastal zone; 6–Georgian coastal zone.

3. Some parameters of models and results

Some parameters of the models used are presented in Table 1.

Table 1 Models used.

Model	Type	Vertical coordinates	Grid size	Number of grid points	Time step (baroclinic mode/ barotropic mode)
Basin scale model	MHI-model with remote sensing data assimilation	Fixed levels in the vertical z-direction	~4900 m	237×131×35	600 s
North-Western Shelf Zone regional model	POM-model	Terrain following σ-coordinates	~1500 m	100×76×10	300 s / 10 s
Romanian Coastal Zone regional model	POM-model	Terrain following σ-coordinates	~1200 m	117×217×20	180 s / 4 s
Kalamita Bay regional model	POM-model	Terrain following σ-coordinates	~600 m	145×137×20	60 s / 1.5 s
Russian Coastal Zone regional model	POM-model	Terrain following σ-coordinates	~1200 m	305×105×25	120 s / 3 s
Georgian Coastal Zone regional model	Domestic model	Fixed levels in the vertical z-direction	1000 m	216×347×32	1800 s
Burgas Bay regional model	Domestic model	Fixed levels in the vertical z-direction	500 m	78×88×50	600 s

Numerical simulations have been carried out under 6-hourly NCEP wind and climatological surface heat and salt fluxes forcing. The simulations aim to assess the effectiveness of the nesting techniques and the skill of the system to reproduce known features of the Black Sea coastal circulation phenomenology, in view of the pre-operational use of the modelling system.

For numerical experiments we chose the period 7–14 June, 2003, when the sky was cloud-free for the entire sea, as we planned to compare results with the satellite SST images.

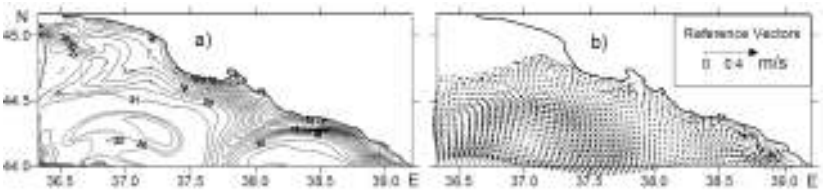

Figure 3 a) Surface temperature; b) Current velocities at 200 m depth, calculated from the regional model.

The results of the simulation of all regional models show good conformity with the satellite SST fields and with available representations of circulation in examined areas. For example, the fields of SST and current velocities, obtained from the Russian regional model, are presented in Figure 3. The anticyclonic eddy in the southern part of the water area is distinctly shown on this figure. In the current field at 200 m depth, except for this eddy, the presence of anticyclonic eddies of smaller scales at the northern border and in the southeast of area is also observed. In the most southeastern corner a cyclonic eddy is observed.

The satellite image of SST for the same time is presented in Figure 4.

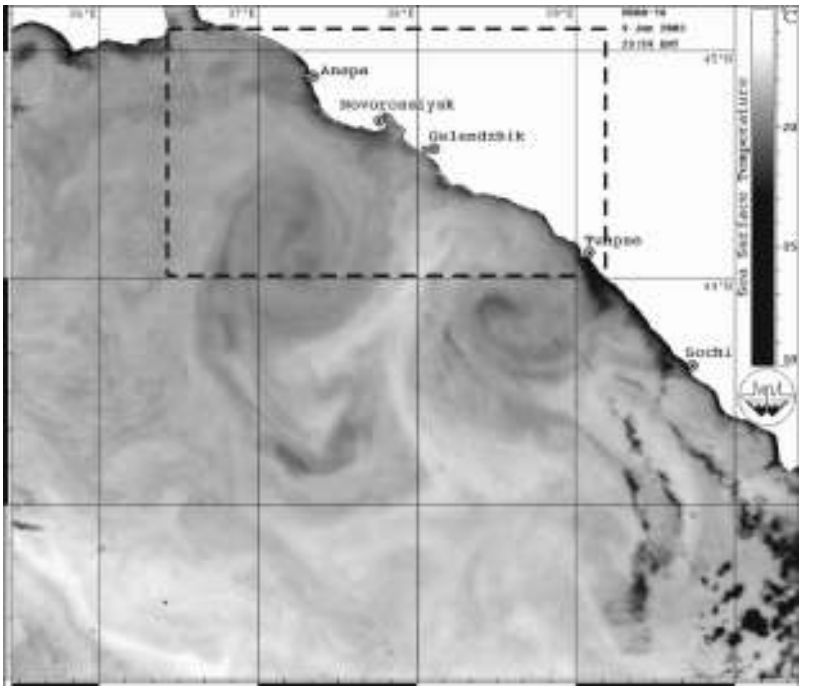

Figure 4 The SST image, obtained from the NOAA-16 satellite. The simulation region is marked by the dashed rectangle.

The anticyclonic eddy, which is in the northern half, is within the limits of simulation area and clearly visible. Moreover, southeast of it a mushroom dynamic formation can be observed, which branches with opposite vorticity just in the southeast corner of the examined area. It is necessary to note that, looking through a continuous series of satellite images for the entire simulation period, it is possible to observe distinct along-shore water transport in a northeast direction.

The received conformity of results of modelling calculations to remote sensing data, in spite of the fact that we used the climatological atmospheric forcing, gives hope for a satisfactory realisation of monitoring of hydrophysical fields in the Black Sea coastal regions on the basis of use of the developed set of nested grid regional models.

Acknowledgements

The authors would like to acknowledge, with many thanks, all the Black Sea GOOS partners whose contribution made this study possible. This work was supported by the European Union Project EVK3−CT−2002−80011−ARENA.

References

Black Sea GOOS: Strategic Science and Implementation Plan for the Black Sea Global Ocean Observing System. Ankara, 2002. pp. 81.

Blatov, A.S., N.P. Bulgakov, V.A. Ivanov *et al.* (1984). Variability of the Black Sea Hydrophysical fields. Leningrad, Gidrometeoizdat, pp. 238.

Dorofeyev, V.L., G.K. Korotaev and C.J. Koblinsky (2003). The Black Sea circulation model using assimilation of satellite altimetry. In: Oceanography of the Eastern Mediterranean and Black Sea. Ed. Yilmaz A., Erdemli−Icel, Turkey, IMS METU. pp.362−368.

Fomin, V.V. (2005). The Black Sea North-Western Shelf Circulation Model. (Printed).

Ibraev, R.A. and D.I. Trukhchev (1996). Seasonal variability of the Black Sea climatic circulation (In Russian). Doklady Akademii Nauk, V 350, N 4, Oct., p. 541−543.

Kordzadze, A.A., K.A. Bilashvili and D.I. Demetrashvili (2003). Numerical modeling of hydrological regime in the Black Sea with taking into account of water exchange with the Mediterranean Sea. Proceeding of the "Second International Conference on Oceanography of the Mediterranean and Black sea: Similarities and Differences of Two Interconnnected Basins" 14−18 October, 2002. Ankara, Turkey, p.335−343.

Kubryakov, A.I. (2004). Application of nested grid technology at the development of the monitoring system of hydrophysical fields in the Black Sea coastal areas (In Russian). Ecological safety of coastal and shelf zones and complex use of shelf resources. Issue 11, NAS of the Ukraine. Eds.: Korotaev G. K., Kubryakov A. I., Sevastopol, pp. 31−50.

Kubryakov, A.I., A.V. Grigor'ev and S. Stefanescu (2005). Modelling of the synoptic dynamics of waters in the coastal regions of the Black Sea. (In Russian). Fluxes and Structures in Fluids. International conference. Moscow, pp. 254−256.

Stefanescu, S., E. Cordoneanu and A. Kubryakov (2004). Ocean wave and circulation modeling at NIMH Romania. Romanian Journal of Meteorology, Vol. 6, No.1−2, 75−88.

A data assimilation tool for the Aegean Sea hydrodynamic model

G. Korres*[1], K. Nittis[1], I. Hoteit[2] and G. Triantafyllou[1]

[1]*Hellenic Center for Marine Research, Anavyssos, Greece*
[2]*Scripps Institution of Oceanography, USA*

Abstract

This paper presents the implementation and validation of a data assimilation system for the Aegean Sea hydrodynamics that has been developed as part of the Poseidon operational system. The assimilation scheme is based on the Singular Evolutive Extended Kalman (SEEK) filter which operates with low-rank error covariance matrices as a way of reducing the computational burden. This system was validated for a 6-month period (January–June 2004) during which weekly satellite SLA, SST data and daily Ferrybox SSS data were jointly assimilated into the model.

Keywords: Aegean Sea, data assimilation, POM model, SEEK filter.

1. Introduction

Numerical modelling has advanced to the stage where operational ocean forecasting systems (mainly with asynchronous ocean–atmosphere coupling) are now run on a routine basis even at the global scale, predicting an ever-increasing number of physical properties. Simultaneously, a growing amount of observations are becoming available in real or near-real time. Besides these advances, the ocean forecasting in shelf and coastal areas and the data assimilation problem especially in these areas where numerical models are run with increased resolution is still under active research, at least within the oceanographic community.

Greece is a maritime country with over 18000 km of coastline and 2000 islands, and relies heavily on the surrounding sea environment since most of its marine resources (tourism, fisheries, marine trade) are of major economic importance. Accurate forecasting of the sea state is of vital importance for the safety of human life in the sea and for a wide field of marine applications. Moreover, the growing concern over an accidental spill in the oil transport routes in the Eastern Aegean Sea is a motivating factor for improving currents and waves forecasts.

The model initialisation problem is of central importance for all short-range near-real time forecast systems. This is addressed through the use of data assimilation methods which efficiently provide an estimate of the state of a dynamical system by combining both the information from a numerical model and from the observations. Assimilation techniques can be classified into two principal categories: sequential methods based on the statistical estimation theory and variational methods based on the optimal control theory (Wunsch, 1995). The Kalman filter is a sequential technique which provides the optimal estimate of the state of a linear system. It has been extended (EKF), by a lineari-

* Corresponding author, email: gkorres@ncmr.gr

sation of the system, in order to handle non-linear dynamics (Jazwinski, 1970). However, the prohibitive computational cost of the EK filter makes its brute-force implementation unfeasible. The SEEK filter is a simplified EK filter in which computational cost reduction is achieved by approximating the EK filter error covariance matrices by singular low-rank matrices. In this way a finite number of directions are selected in the state-space and the model state is then corrected with the new observations in order to intermittently bring back the system to its most probable trajectory. These directions evolve in time to follow changes in the system dynamics.

This paper aims to describe the development of an assimilation system based on the SEEK filter for the Aegean Sea hydrodynamic model. It first briefly presents the components of our assimilation system — the Aegean Sea numerical model and the assimilation scheme — before showing and discussing assimilation results.

2. The assimilation system

2.1 The Aegean Sea numerical model

The Aegean Sea model is based on the Princeton Ocean model and is part of the Poseidon system (Soukisian *et al.*, 2002). The computational grid covers the geographical area 20°E–29°E and 30°N–41°N with a resolution of 1/20°. The model is forced with hourly surface fluxes of momentum, heat and water provided by the ETA high resolution (1/10°) regional atmospheric model (Papadopoulos *et al.*, 2002) issuing forecasts for 72 hours ahead. Boundary conditions at the western and eastern open boundaries of this model are provided by a large scale model covering the whole Eastern Mediterranean Sea with a resolution of 1/10°. A detailed description of the modelling system and a preliminary evaluation of its forecasting skill are provided by Nittis *et al.* (2001).

2.2 The SEEK filter

Assume an ensemble of system states that describe the probability distribution of a given system is available. An EOF (Empirical Orthogonal Function) decomposition of the ensemble usually provides those few dominant directions that describe the spreading of the ensemble. The SEEK filter uses these dominant directions to construct its correction subspace at the initial time and then evolves them in time according to the EK filter equations.

Let the filter's error covariance matrix P_i^a be factorised as $L_i U_i L_i^T$. The SEEK filter operates in two stages:

Forecast stage: The model is integrated forward to obtain the forecast state X^f at time t_i starting from the analysis state X^a available at time t_{i-1}:

$$X^f(t_i) = M(t_{i-1}, t_i) X^a(t_{i-1}) \tag{1}$$

where $M(t_{i-1},t_i)$ is the model transition operator.

Correction stage: The analysis state at time t_i is estimated as:

$$X^a(t_i) = X^f(t_i) + K_i[Y_i^o - H_k X^f(t_i)] \quad (2)$$

where the Kalman gain matrix K_i is given by $K_i = L_i U_i L_i^T \boldsymbol{H}_i^T R_i^{-1}$ (3)

and $U_i^{-1} = \rho U_{i-1}^{-1} + L_i^T \boldsymbol{H}_i^T R_i^{-1} \boldsymbol{H}_i L_i \; 0<\rho<1$ (4)

In (2), Y_i^o is the observations vector and H_i is the observational operator which projects the model state onto the locations of the observations. In (3), $\boldsymbol{H}_i$ is the gradient of H_i and R_i is the observations error covariance matrix. The latter is usually taken as a diagonal matrix by assuming that the observations are spatially uncorrelated. Note that in cases of a linear observational operator, $\boldsymbol{H}_i$=H_i. The filter's correction basis L_i evolves in time according to:

$$L_i = \boldsymbol{M}(t_{i-1}, t_i) L_{i-1} \quad (5)$$

where $\boldsymbol{M}(t_{i-1}, t_i)$ is the gradient of $M(t_{i-1}, t_i)$ evaluated at $X^a(t_{i-1})$. The factor ρ appearing in (4) is a forgetting factor which stands for the increment of uncertainty during the model integration in order to attenuate the impact of model errors. Practically, with $\rho<1$ recent data are exponentially more weighted than old data.

Semi-evolutive SEEK filter

In order to further reduce the computational burden of the SEEK filter, the evolution of the correction basis was only performed for the first dominant EOFs while the rest of the modes were kept invariant. This idea was first proposed by Hoteit *et al.* (2002) who found that this approximation has a rather limited impact on the filter's performance, especially when the dynamical system evolves through a stable regime.

Localisation of the filter gain

The SEEK filter is usually initialised by an error covariance matrix which is approximated using a finite set of state vectors extracted from a long enough model simulation. Correlations resumed by the last EOFs, which remain invariant in the present study, might often therefore be noisy especially in strongly variable high resolution systems. In order to deal with this problem a strategy is to retain the short-range correlations structure which is the most reliable and to filter out long-range correlations. This can be done through a Schur product (an element-by-element multiplication) of the error covariance matrix with a correlation function γ as suggested by Houtekamer and Mitchell (2000). In this approach, the gain K_i of the original Kalman filter is reformulated as:

$$K_i = (\gamma \circ P_i^f) H^T [H(\gamma \circ P_i^f) H^T + R]^{-1} \quad (6)$$

where the notation $\gamma \circ P_i^f$ denotes the Schur product of the covariance matrix P_i^f with the localisation function γ.

3. Results and discussion

The model has been first spun-up from climatology for a 3-year period (1999–2001) forced with the ETA atmospheric model 24-hour forecasts. A 2-year run of the model (2002–2003) was then performed in order to estimate the multivariate EOFs needed for the SEEK filter algorithm. Finally, an additional integration of 6 months (January–June 2004) initialised from the previous experiment constitutes the "free-run" of the model.

The time window chosen for the assimilation experiment extends from January–June 2004 during which SST, SLA and Ferrybox SSS data products are available. The SLA data are merged T/P and ERS altimetric data on a weekly basis provided by the AVISO project and mapped on a 1/3° Mercator grid. The mean SSH added to these SLA maps is derived from a long run (2000–2003) of the Aegean Sea model. The SST data consist of weekly composite AVHRR observations on a 1/8° grid provided by the MFSTEP EU project. Finally the SSS data are available on a daily basis along the ferry route from Piraeus to Heraklion. However due to ferrybox malfunctioning, these data were often sparse during the study period. The overall availability of all observational data during the time window selected is shown in Figure 1.

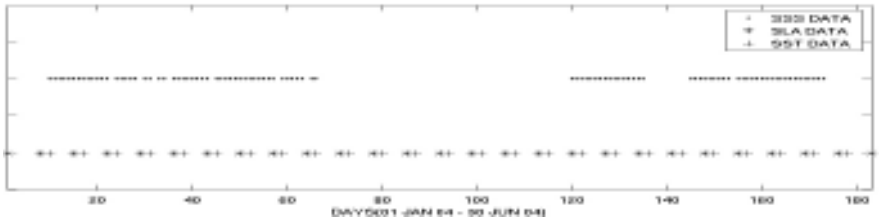

Figure 1 Time distribution of assimilated observational data.

In the assimilation runs, the rank of the filter's covariance matrices was set to 60. The first 10 modes are evolved according to the system's dynamics while the rest of the modes are kept invariant. For the localisation of the filter gain, we have defined a radius of influence of 150 km outside of which the correlations are set to zero. The assimilation system assumes an accuracy of 2.5 cm on the SLA data, 0.5°C on SST data and 0.08 psu on SSS data.

Table 1 RMS error (free run, forecast and analysis fields of the SEEK filter) on SSH, SST and SSS averaged over Jan.–Jun. 2004.

	Free run	Forecast	Analysis
SSH	5.17 cm	4.20 cm	3.32 cm
SST	0.932°C	0.766°C	0.486°C
SSS	0.330 psu	0.094 psu	0.068 psu

An evaluation of the behaviour of the assimilation system is shown in Table 1 in terms of the RMS misfits between observational data and model estimates for the free-run and the forecast and analysed fields as estimated by the filter. Regarding SSH, the filter analysis is almost 2 cm more accurate on average than the free-run. The filter also improves the estimation of the model SST by 50%. The most significant improvement was obtained

on the estimation of the SSS, probably because of the daily availability of these data. Overall, the assimilation system was able to fit the data within the specified observational errors.

Time series of the RMS misfits for SSH, SST and SSS are presented in Figure 2. The forecast and analysis SSH misfits with respect to the observations generally follow the free-run errors but reduced by more than 20% and 35% respectively. Regarding SST (Figure 2b), the model free-run significantly deviated from the observations toward the end of the assimilation window due to the model's inability to correctly describe a strong warming event occurring in the Aegean Sea. The filter greatly enhances the behaviour of the model and efficiently stabilises the RMS error of both SST forecast and analysis during the warming period.

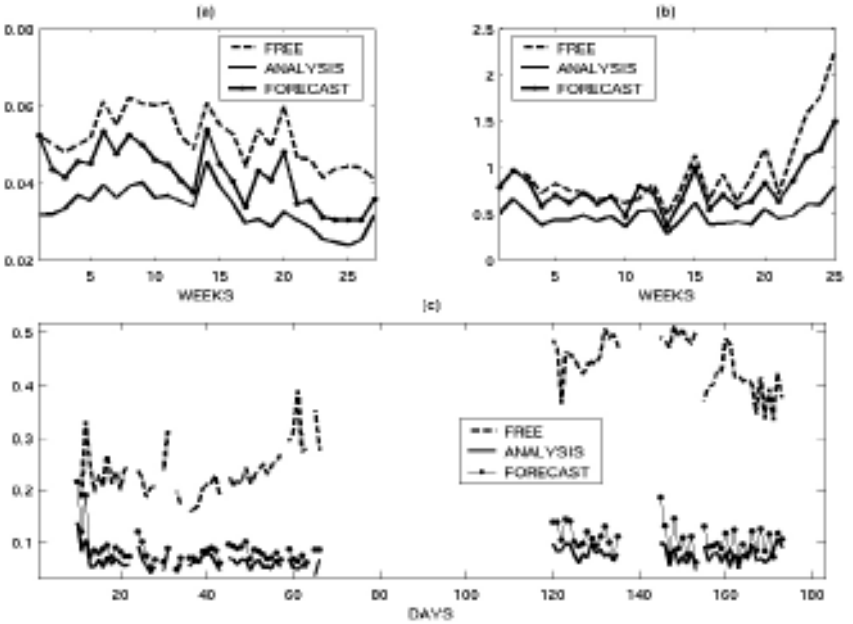

Figure 2 a) RMS misfits (in metres) — time series between the model SSH (free run, analysis and forecast of the assimilation system) and the altimetric data; b) RMS misfits (in °C) — time series between the model SST (free run, analysis and forecast of the assimilation system), and the AVHRR SST data; c) RMS misfits (in psu) — time series between the model SSS (free run, analysis and forecast of the assimilation system) and the ferrybox SSS data.

The spatial distribution of the average RMS errors for SSH and SST as obtained from the model free-run and the assimilation system are shown in Figure 3 and Figure 4, respectively. Regarding the SSH error it can be seen that the model was unable to reproduce several mesoscale features (Rhodes cyclonic gyre, Mersha Matruh cyclone) mainly occurring within the Levantine basin south of Crete. The assimilation system significantly improved this picture while correctly introducing the Mersha–Matruh anticyclone and relocating the Rhodes gyre. The system, however, still needs improvements especially in areas like the Cretan Sea where the error reduction was practically insignificant. The model free-run error for SST shows maxima in the area close to Dardanelles

(almost 3°C) and along the Black Sea waters route within the North Aegean, and secondary maxima along the Asia Minor route within the Aegean Sea. Both areas of high errors are probably related to the highly specified nonlinear open boundaries. The assimilation system is very skilful and drastically reduces the SST RMS error all over the modelling area by approximately 50%.

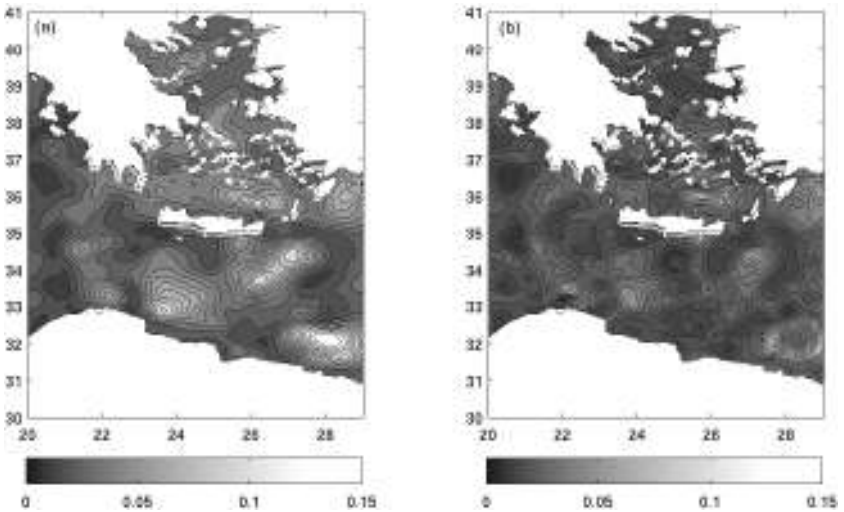

Figure 3 Distribution of the average RMS misfits (in metres) between altimetric data and a) the model free run SSH, and b) the assimilation system analysis SSH.

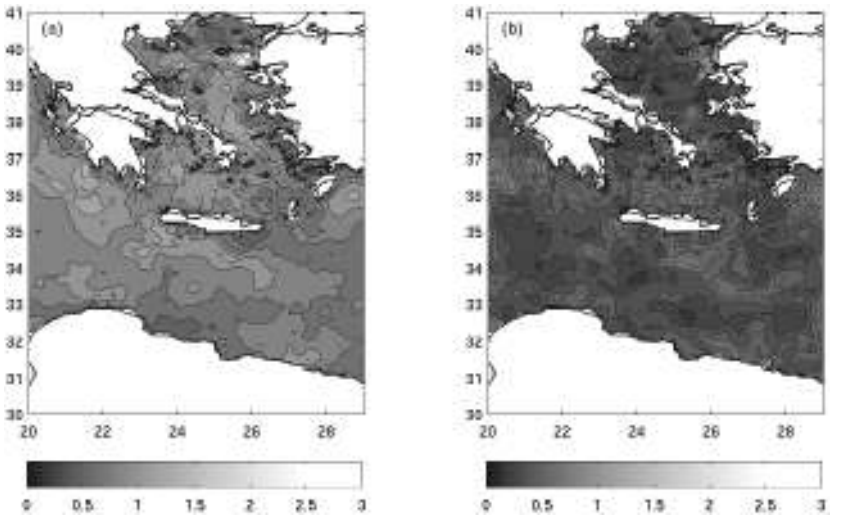

Figure 4 Distribution of the average RMS misfits (in °C) between AVHRR SST data and a) the model free run SST, and b) the assimilation system analysis SST.

Overall the results obtained so far with the assimilation system are very encouraging, but clearly call for further improvements in the model parametrisations (Dardanelles outflow) and the assimilation scheme. As for the latter we believe that the assimilation

system should be extended to the coarse resolution Eastern Mediterranean model which controls a large part of the errors present in the southern sector of the Aegean Sea model. Finally the definition of a realistic SSH climatology needed to convert SLA data to absolute signals remains open for near future studies.

Acknowledgements

This work has been supported by the FerryBox EU project. SST AVHRR data were provided by the MFSTEP project. The SLA products were supplied by the CLS Space Oceanography Division, Toulouse, France with financial support from the CEO programme (Center for Earth Observation) and Midi-Pyrénées regional council.

References

Hoteit, I., D.T. Pham and J. Blum (2002). A simplified reduced Kalman filtering and application to altimetric data assimilation in the Tropical Pacific. J. Mar. Sys. 36, 101–127.

Houtekamer, P. and H. Mitchell (2001). A sequential Ensemble Kalman Filter for Atmospheric Data Assimilation. Mon. Weather Rev., 123–137.

Jazwinski, A.H. (1970). Stochastic processes and filtering theory. Academic Press, New York, 376 pp.

Nittis, N., V. Zervakis, L. Perivoliotis, A. Papadopoulos and G. Chronis (2001). Operational monitoring and forecasting in the Aegean Sea: system limitations and forecasting skill evaluation. Mar. Pol. Bul., 43, 154–163.

Papadopoulos, A., G. Kallos, P. Katsafados and S. Nickovic (2002). The Poseidon weather forecasting system: an overview. Glob. Atmos. Ocean Sys. 8, 218–237.

Soukissian, T., G. Chronis, K. Nittis and C. Diamanti (2002). Advancement of operational oceanography in Greece: the case of the POSEIDON system. Global Atmos. Ocean Sys. 8, 119–133.

Wunsch, C., The Ocean Circulation Inverse Problem, Cambridge University Press, 437 pp., 1996.

Marine services at DMI

Erik Buch*

Danish Meteorological Institute, Denmark

Abstract

In 1998, the Danish Meteorological Institute (DMI) formed a division for Operational Oceanography, and on 1 January 2005 the division was upgraded to DMI's Centre for Marine Forecasting. This Centre is today engaged and responsible for the operational production of forecasts of water levels, currents, waves, temperature, salinity and sea ice distribution in the North Atlantic and North Sea−Baltic Sea region with special focus on Danish Waters. Additionally operational production of wave forecasts in the Mediterranean Sea as well as drift of sea ice in Greenland Waters are part of the daily routines.

DMI's Centre for Marine Forecasting is actively engaged in international operational oceanographic coordination work within EuroGOOS, NOOS and BOOS, and is a partner in EU-funded projects such as PAPA, ODON, MERSEA and MOEN.

1. Introduction

The Centre for Marine Forecasting has the duty to:

- forecast the ocean conditions for the Domestic Danish Waters, Baltic Sea, North Sea and for the North Atlantic with special focus on Greenland Waters
- disseminate general information and advice on issues related to the marine environment and climate.

The primary tasks of the Centre are to:

- issue storm surge warnings for the Danish Waters
- forecast waves for the North Atlantic area including the Baltic Sea, North Sea and Mediterranean Sea
- forecast current, temperature, salinity and sea ice for the North Atlantic and North Sea−Baltic Sea area
- forecast ice drift for the Greenland Waters
- forecast drift of oil and floating objects
- advise on oceanographic conditions in Danish and Greenland waters
- produce and study scenarios of variability of the marine climate in the North Atlantic.

Ocean forecast animations are displayed routinely on ocean.dmi.dk. Case studies, verification studies, and general information about the division are also published on this web page.

The centre is also engaged in climate-related oceanographic monitoring and research in the North Atlantic region with special focus on the variability of ocean circulation, deep

* Corresponding author, email: ebu@dmi.dk

water formation, and the impact of marine environmental changes on fish recruitment in West Greenland Waters.

DMI's Centre for Marine Forecasting is actively engaged in international operational oceanographic coordination work within EuroGOOS, NOOS and BOOS. The division participates in a number of scientific research projects funded by the Danish Research Council, the Nordic Council of Ministers, and the EU. Most of the projects are related to operational ocean forecasting with partners primarily from the Baltic Sea and North Sea countries. The second group of research projects is concerned with ocean climate research with partners primarily from the Nordic countries.

2. Developing an operational Marine Forecasting System (MFS)

A major long-term goal for DMI's Centre for Marine Forecasting is to build up a sustainable marine forecasting system by strengthening the internal research capacity and international cooperation. A strategy on how to develop such a system and maintain its sustainability has matured during recent years' research and development in operational oceanography (She, 2003). A state-of-the-art MFS should include at least three components: models, observations and a networked development group. These components must be developed in a harmonised way. DMI has adopted the following strategy in developing the MFS:

- Priority area: The inner Danish waters, Baltic–North Sea, and waters around Greenland and Faroe Islands. A large forecasting area (Baltic–North Sea–North Atlantic) is required, in order to improve lateral boundary conditions and weather forcing via atmospheric–ocean coupling. To achieve this, multi-layer nested model areas are used.
- Modelling system: a future MFS consists of fully coupled models, as shown in Figure 1. This system will be developed stepwise. Following the success of NWP (HIRLAM), the surface physical forecast (e.g. storm surge, waves) has been successfully implemented, with a reasonable forecasting quality. For the 3D marine physical structure, data assimilation is essential to reach acceptable forecasting quality. The arrows in Figure 1 describe coupling relations: solid lines represent active interfaces in the present DMI operational set up while dashed lines are still in research phase. HIRLAM forces all models, but there is no feed-back at present. Providing a high quality forecast on waves, sea ice and marine physical structure, the ecosystem modelling, costal zone modelling and sediment transport modelling may be added into MFS with the required quality.
- Observations: DMI operates tide gauge stations in Danish waters. International cooperation is a major way for operational agencies to obtain real-time observations
- International cooperation: Through active involvement in international cooperation, DMI contributes to BOOS (see Table 2 for acronyms), NOOS and EuroGOOS in international coordination, exchanges of best practice in operational model development, exchanges of forecasts and observations, and carries out fundamental research on designing a cost-effective observing system. In return, DMI has obtained a 3D ocean model (including a sea ice model and a drift module), as well as real-time observations of water level, waves, and 3D temperature, salinity and currents.

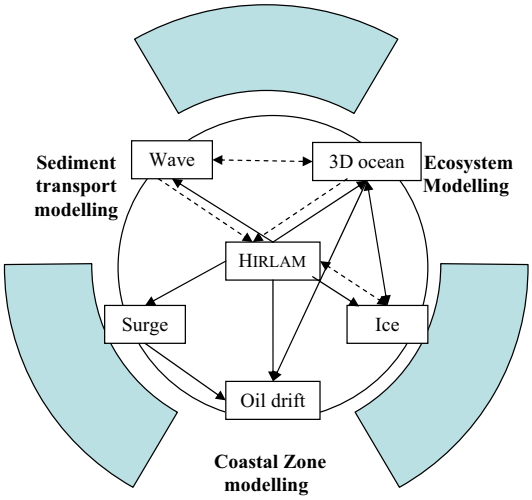

Figure 1 Operational Marine Forecasting System. Solid arrows describe existing coupling relations, dashed arrows represent coupling yet to be developed.

- Research and development strategy: DMI will select, test and calibrate models suitable for its operational use, set up the models to run operationally, carry out on-line validation and/or off-line regular validation, and address research topics raised from validation and problem-solving style research.
- Sustainability strategy: DMI will perform an enhanced active marketing effort.

In the following sections we briefly introduce the DMI MFS development during recent years, including newly-developed forecasting capacity, validation system and results, and research work to solve problems raised in the operational validation.

3. Forecasting capacity

During the existence of the Centre for Marine Forecasting an operational forecasting capacity has been built up for storm surge, 3D ocean forecast, wave forecast, oil-drift and ice forecast.

3.1 Storm surge

The Danish coasts — especially the North Sea coast and primarily throughout the winter — are exposed to storm surges due to the passing of strong atmospheric low pressure systems, and some very severe flooding events have been experienced over the years. There is therefore a high alertness in Denmark regarding storm surge warning. A detailed network of Tide Gauges (more than 40) is operated by DMI, the Danish Coastal Authority and the Royal Danish Administration of Navigation and Hydrography and a number of local authorities.

The storm surge forecasting is the responsibility of DMI's Centre for Marine Forecasting. Prognoses are made using the MIKE 21 model developed by DHI-Water and environments. The model has 4 nesting levels with 9, 3, 1 and 1/3 nm resolution respectively, with the 2 highest resolution domains found in the inner Danish waters and

the Wadden Sea on the west coast of Jutland. An additional separate high resolution set-up covers the Limfjord. The model is forced with DMI's own meteorological model HIRLAM with 54-hour forecasts produced every 6 hours.

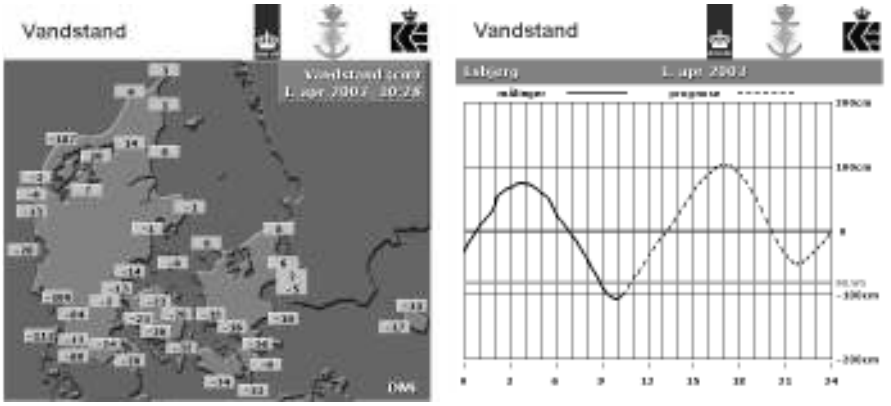

Figure 2 Data from the Danish tide gauge network are displayed in real-time on the internet (www.dmi.dk/dmi/index/danmark/vandstand.htm). Real-time in this context means that data are updated every 10 minutes and if data for a particular station is not updated within 30 minutes because of instrument- or communication failure, a "?" is shown instead of a data value. The forecast for all the observations sites are shown on the same web site — clicking on the station of interest shows a curve of the most recent observations and a prognosis for the next 24 hours.

In 2004–2005 a project has been initiated to implement a new storm surge model for the North Sea–Baltic Sea area based on the finite element methodology. The model was implemented to be semi-operational from September 2004 and is planned to be fully operational from September 2005.

At the initiative of the Centre for Marine Forecasting, responsible institutes in all the countries surrounding the North Sea exchange storm surge forecasts for the North Sea. This forms a broader and more sound basis of judgement for the forecaster on duty and constitutes the basis for the establishment of a North Sea Storm Surge Ensemble Prediction System.

3.2 3D ocean forecast

A 3D ocean model BSHcmod (obtained from Bundesamt für Seeschifffahrt in Hamburg) has been set up and runs operationally. It provides twice daily 54 h forecasts on 3D water temperature, salinity, currents, water level and ice coverage in the Baltic–North Sea system. The model has a resolution of 6 nautical miles (nm) in the Baltic–North Sea, and 1 nm in the inner Danish waters and the German Bight (Figure 3). The model has flooding-drying and two-way nesting facilities, and is forced by the HIRLAM hourly forecast, climatological T/S lateral boundary conditions, and real-time river run-off.

Some changes to the operational setup are underway:

- Higher vertical resolution
- Improved horizontal and vertical mixing schemes
- Better topography

- Dynamic lateral boundary conditions
- Data assimilation.

The circulation in the North Atlantic is operationally forecasted by operational running of the HYCOM model set up with two nesting levels with a horizontal resolutions of ½° and 1/10° respectively.

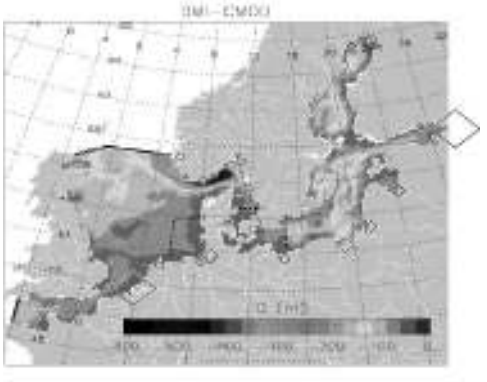

Figure 3 CMOD model domain and bathymetry. The dotted black line indicates the grid boundaries. Diamonds represent fresh water input through rivers.

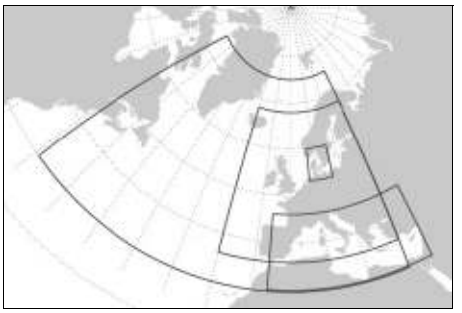

Figure 4 DMI–WAM nested model domains.

3.3 Wave forecast

During 2001–2002, the existing DMI 3rd generation WAM model was extended to cover the North Atlantic and Mediterranean Sea (Figure 4). Table 1 shows DMI–WAM set-up parameters.

Table 1 DMI–WAM set up.

Model	North Atlantic	Danish Waters	Baltic–North Sea	Mediterranean
Spatial resolution	1/2°	1/30°	1/6°	1/6°
Time step	4 min.	4 min.	4 min.	2 min.
Frequencies	25	25	25	25
Direction resolution	30°	30°	30°	30°
Forcing model	HIRLAM T15	HIRLAM S05	HIRLAM T15/S05	HIRLAM T15
Forcing model resol.	15 km	5 km	5/15 km	15 km
Longitude	69W–30E	7E–16E	20W–30E	6W–46E
Latitude	30N–75N	53N–60N	36N–68N	30.5N–46N
Open boundaries	JONSWAP	Nested	Nested	Closed basin
Forecast range	54 h	54 h	54 h	54 h
Schedule	4×daily	4×daily	4×daily	4×daily
Output time step	1 h	1 h	1h	1 h

3.4 Ice forecast

DMI's Centre for Marine Forecasting has for some years produced ice forecast in the Cape Farewell area in Greenland. A similar service has been established for the Baltic–North Sea, through a Hibler type thermodynamic ice model coupled with the DMI 3D ocean model. The model calculates the ice concentration and ice thickness. Comparison with Finnish ice charts of the Bothnian Bay have shown good agreement.

3.5 Drift of oil and floating objects

DMI's Centre for Marine Forecasting manage the oil preparedness on behalf of Mærsk Oil and Gas in the North Sea. This includes the ability to predict at any time the drift of oil and floating objects. This task is performed by utilising a special drift module coupled to the above mentioned operational 3D-model. The drift module calculates the drift, spreading, evaporation and sinking of oil, and includes a backtracking facility.

The system is available for use in many other connections such as search and rescue operations, and drift of biological material such as fish eggs and larvae.

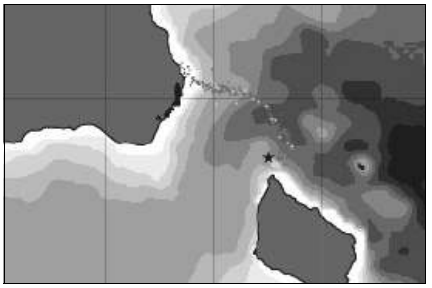

Figure 5 Simulation of the oil drift released from the sunken ship Fu San Hai north of the island of Bornholm in 2003.

4. International cooperation

Aiming to build up an advanced MFS, DMI is actively involved in international research and development activities. DMI chairs the BOOS organisation, coordinates two EU-funded projects (PAPA and ODON), plays a leading role in the EU-funded projects MERSEA and MOEN, hosts the BOOS and NOOS websites, and is leading the NOOS water level forecast and observation exchange project. Successful cooperation has been carried out with BSH, UK Met. Office, met.no and SMHI in sharing best practice. Detailed cooperation has focused on developing and/or sharing 3D ocean model code, lateral boundary conditions, wave-current interaction, bathymetry optimisation and oil drift prediction.

Table 2 Acronyms.

PAPA	Programme for a bAltic network to assess and upgrade an oPerational observing and forecAsting System in the region	www.boos.org/PAPA/
ODON	Optimal Design of Observational Networks	www.noos.cc/ODON/
BOOS	Baltic Operational Oceanographic System	www.boos.org/
NOOS	North Sea Operational Oceanographic System	www.noos.cc/
MERSEA	Marine EnviRonment and Security for the European Area	www.mersea.eu.org/

5. Verification

Major MFS related research activities at DMI's Centre for Marine Forecasting have been to validate the operational 3D ocean model, wave model and surge model, to identify research priorities based on the validation and to carry out relevant research and development.

5.1 3D ocean modelling

An on-line system has been set up to validate the model forecast against near real-time buoy measurements. Preliminary validation results (not shown) show a root mean square error of 0.5–1°C for SST prediction in costal waters, and a reasonable thermal stratification.

Salinity and related transport in transition waters (Skagerrak) remain to be improved. A series of research topics have been raised to resolve problems found in the validation work (e.g. initialisation and data assimilation; sensitivity of Baltic–North Sea exchange to the bathymetry and model resolution in Danish Straits; horizontal diffusion, Skagerrak circulation/salinity pattern, and estuary effects; lateral boundary condition optimisation etc.). These topics form the priority area for on-going and near future research activities in 3D ocean modelling.

5.2 Wave modelling

Quarterly verification reports have been issued since November 2001 (Nielsen *et al.*, 2002). About 32 wave buoys in the Baltic–North Sea, NE Atlantic and Mediterranean Sea have been used in the verification. The results showed that significant wave height and mean wave directions are well predicted. DMI–WAM still has some problems in predicting the peak period. The reason for these errors remain to be studied. Research topics are coupling with time-varying surface current, feed-back to Hirlam through surface roughness, and further resolution increase.

5.3 Storm surge modelling

The storm surge warning system is verified in annual reports with standard and peak error statistics. In addition to DMI sea level predictions, forecasts from other countries surrounding the North Sea are freely available to all participating institutes through ftp boxes. This informal networking project paves the way for a sea level forecast intercomparison study and ensemble forecasting.

Reference

She J. (2003). Sustainability analysis in marine research, monitoring and forecasting systems. In Building the European Capacity in operational Oceanography, Proceedings of the Third International Conference on EuroGOOS, Ed. H. Dahlin, N.C.Flemming, K.Nittis, S.E.Petersson. Elsevier Oceanography Series no. 69.

Nielsen J.W., J.B. Jørgensen and J. She (2002). Verification of wave forecasts: DMI–WAM Nov–Dec 2001. Tech. Rep. 02–18, Danish Meteorological Institute, 2002.

ANIMATE: Quality control of data from multi-disciplinary moorings in the Northeast Atlantic

J. Karstensen*[1], M. Edwards[2], A. Körtzinger[1], R. Lampitt[2], O. Llinas[3], T. Müller[1], U. Send[1], T. Steinhoff[1] and M. Villagarcia[3]

[1]*Leibniz-Institut für Meereswissenschaften, Kiel, Germany*
[2]*National Oceanography Centre, Southampton, UK*
[3]*Instituto Canario de Ciencias Marinas, Telde, Spain*

Abstract

This paper describes the processing of data from three multidisciplinary moorings in the Northeast Atlantic. The data comprises physical data (temperature, conductivity/salinity) as well as biogeochemical data (pCO2, nitrate, chlorophyll fluorescence) which is collected with a number of different instruments. The quality control process is different depending on the instruments as well as the accessibility as real-time and delayed mode data. Specific procedures are described that help to improve the quality of the data.

Keywords: Operational oceanography, multidisciplinary data, quality control, mooring

1. Introduction

Three mooring sites have been established in the Northeast Atlantic — the ANIMATE network (Figure 1, left). The sites are equipped with sensors that deliver subsurface temperature, salinity, pressure, and biogeochemical data in near real time and delayed mode to the MERSEA system. A typical ANIMATE mooring comprises (depth given in brackets): 1 – Telemetry head buoy, 2 – Nitrate sensor (~40 m), 3 – Chlorophyll/ backscatter (~40 m), 4 – SAMI pCO2 (~40 m), 5 – ADCP (0 m to ~800 m), 6 – MicroCat (approx. 10 – 15 sensors, 10 – 1400 m), 7 – Sediment trap (~1000 m above bottom).

The sensor data need quality control procedures to ensure the highest possible quantified and reproducible quality of the data. The procedures applied to real time and delayed mode data are described here. Data reports have been produced containing further details (Karstensen, 2005; Villagarcia, 2005; Lampitt, 2005).

2. Data and quality control

2.1 Physical data

The following physical data is collected (sensor in brackets): temperature, conductivity, pressure (SBE-37 MicroCat), and velocity (RD Instruments ADCP). MicroCat data calibration comprises pre- and post-calibration casts by mounting the MicroCat sensors on a CTD rosette and later comparing the CTD with the MicroCat data. Data from profile stops of longer than 5 minutes (which accounts for different sensor response times) is useful for comparison. The stops should be in a region with low vertical gradients in

* Corresponding author, email: jkarstensen@ifm-geomar.de

temperature and conductivity. The resulting correction for the MicroCat can be a linear bias correction. For pressure sensors the deck readings are used to determine biases.

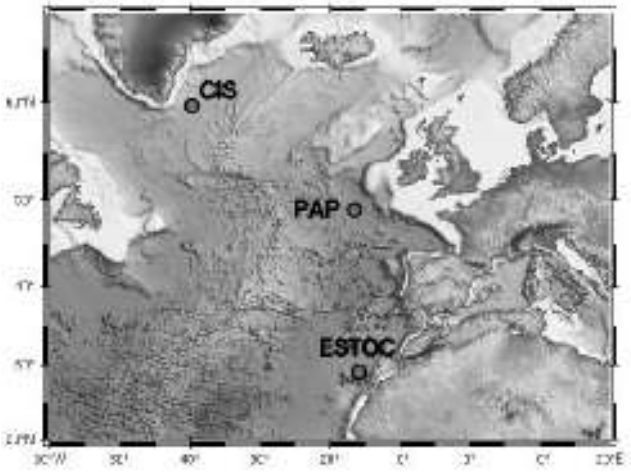

Figure 1 Left: The three ANIMATE mooring sites — CIS Central Irminger Sea, PAP Porcupine Abyssal Plain, ESTOC Estacion Europea de Series Temporales del Ocean, Islas Canarias.

For the ADCP velocity data a correction for the local magnetic deviation is made. No correction for the salinity-dependent variability in transducer sound speed is made as the effect is typically very small. The instrument depth as a function of time, and thus the real depth-cell depth, is derived from the acoustic intensity maximum associated with the ocean/atmosphere interface as well as from neighbouring MicroCat records.

Accuracies expected from the calibration procedures are: temperature (0.002°C), conductivity (0.003 $mS\,cm^{-1}$), pressure (5 dbar), and velocity (standard deviation order 0.1 $cm\,s^{-1}$).

One of the most critical parameters for density and multidisciplinary data is the exact knowledge of instrument depth. To determine the dynamically induced depth variability of instruments it is recommended to equip at least the upper and lower dynamically active part of the mooring with pressure sensors. With the aid of a dynamical mooring program the instantaneous depth of instruments can be derived.

2.2 Biogeochemical data

A common quality control procedure for all biogeochemical data (pCO2, nitrate, chlorophyll) is the acquisition of bottle samples. Typically, it is recommended that the samples are analysed independently in two different laboratories to ensure higher accuracy and to detect biases from the analysis techniques.

pCO2 data is recorded with a SAMI instrument. Bottle samples are analysed for dissolved inorganic carbon (DIC) and alkalinity (TA) from which pCO2 is calculated. In addition, pCO2 data measured by VOS lines or other research vessels passing close to the mooring site are used. Internal blank corrections are made to correct for ageing of the optical parts of the SAMI. Before and after each deployment, a plausibility check is carried out by storing the SAMI for one night in seawater that is in equilibrium with the

atmosphere. The expected accuracy is 10 μatm. It should be pointed out that very accurate samples in DIC and TA are needed. Ideally, casts needs to be done before and 1 or 2 days after deployment with a minimum of 10 m vertical resolution and duplicate samples at nominal SAMI depth.

Nutrient Data (nitrate and nitrite) is recorded with NAS-2E and NAS-3X instruments. A laboratory calibration with nitrate and nitrate standards versus skalar laboratory analyses is made. A pre- and post-deployment check of onboard standard bags against skalar analyses is carried out. During deployment, two standard calibrations on a weekly basis are programmed. We expect an accuracy of approx. 0.3 $\mu mol\,l^{-1}$ (sensitivity of approx. 0.05 $\mu mol\,l^{-1}$). As an additional comment, the standards should be chosen according to the expected extreme values at the mooring site.

The chlorophyll *a* and backscatter data is recorded with a HydroScat-2 instrument (HobiLabs). Beside pre- and post-deployment calibration casts, a laboratory calibration with acetone extracted chlorophyll (commercial and from cultures of various phytoplankton species) is made. The expected accuracy is approx. $0.1\mu g\,l^{-1}$.

2.3 Real-time data

Currently only part of the physical (temperature, salinity, pressure) and biogeochemcial (pCO2) data is transmitted in real time. The real time data quality control process is based on a number of steps. First, data corrupted during the transmission is excluded by use of a Cyclical Redundancy Check (CRC) on the length of the message. Then a gross range check based on World Ocean Atlas 1998 is done for temperature and salinity data only. Pressure data is compared and checked against the nominal depth of the instruments. An additional check is done against previous data from the respective site. Finally, a quality control marker is set based on the above procedure. Not yet implemented in the quality control process of real-time data is a correction based on the recent individual sensors bias estimates (e.g. from the most recent calibration cast).

Acknowledgements

Funding by the European Union under contracts EVR1–CT–2001–40014 (FP5 ANIMATE), SIP3–CT–2003–502885 (FP6 MERSEA IP), 511176–2 (FP6 CarboOcean) is acknowledged.

References

Karstensen, J. (2005). ANIMATE calibration of physical data, 48 pp. Available on request.

Lampitt, R. and M. Edwards (2005). ANIMATE: of biogeochemical data — chlorophyll *a* and backscatter, 53 pp. Available on request.

Villagarcia, M. (2005). ANIMATE: calibration of biogeochemical data — nitrate, 17 pp. Available on request.

ANIMATE: Meteorological data from an open-ocean buoy off the Canary Islands

J. Karstensen*[1], M. Bergenthal[2], E. Kopiske[2], G. Meinecke[2] and U. Send[1,3]

[1]*Leibniz-Institut für Meereswissenschaften (IFM-GEOMAR), Kiel, Germany*
[2]*MARUM, Bremen, Germany*
[3]*Scripps Institute for Oceanography, La Jolla, USA*

Abstract

Collecting meteorological data at open ocean locations is a challenging task but critical for high quality weather forecasting. This paper presents about 360 days of measurements (air/sea surface temperature, air pressure, humidity, wind speed and direction) collected from a number of meteorological sensors mounted on an open ocean-buoy. The buoy is moored off the Canary Islands within the EU FP project ANIMATE. Data is recorded every 2 hours and sent to shore via satellite. Reanalysis products show considerable biases in all variables compared to the buoy data.

Keywords: Operational oceanography, meteorology, air/sea exchange, moorings, time series

1. Introduction

The ESTOC/DOLAN mooring location is at 29°11.0'N/015°55.0'W, about 50 nm north of Gran Canaria in deep waters (~3600 m) (Figure 1, left). The surface buoy is equipped with telemetry and a meteorological package (wind speed, direction, air temperature, humidity, air pressure). The subsurface part is equipped with MicroCats (8), ADCP (at 150 m; upward looking), and biogeochemical sensors. Part of the data is sent to shore in near real time. The meteorological sensors are all from Vaisala Oyj, Helsinki, Finland. The following sensors are used (with height given in parenthesis): PTU200 air temperature (1.5 m), air pressure (1.0 m), relative humidity (1.5 m), and WS425 ultrasonic wind sensor (2.4 m). Buoy positioning comes from GPS. There is a PNI Cooperation (TCM2) pitch, roll, heading sensor.

This paper compares about 360 days of buoy data with reanalysis products from the National Centre of Environmental Prediction (NCEP). It is known that the NCEP reanalysis shows apparent biases to buoy measurements (e.g. Smith *et al.*, 2001).

2. Air/sea interface data: Observation vs. NCEP reanalysis output

2.1 Air temperature

Air temperature was sampled every second hour (12 values per day). About 366 days of data were acquired between April 2003 and May 2005 (Figure 2a, left). A short-circuit in the power supply through seawater leakage was the reason for the data gap during one deployment period (February 2004 to March 2005).

* Corresponding author, email: jkarstensen@ifm-geomar.de

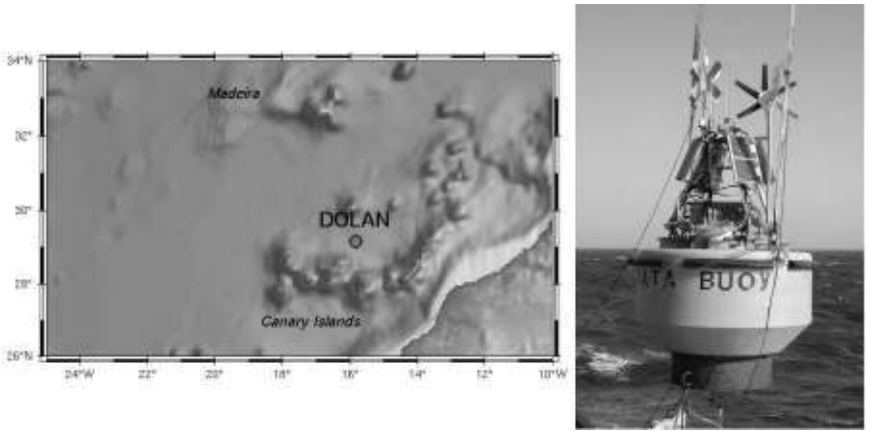

Figure 1 Left: The ESTOC/DOLAN buoy location. Right: The head buoy with the meteorological sensors before launch.

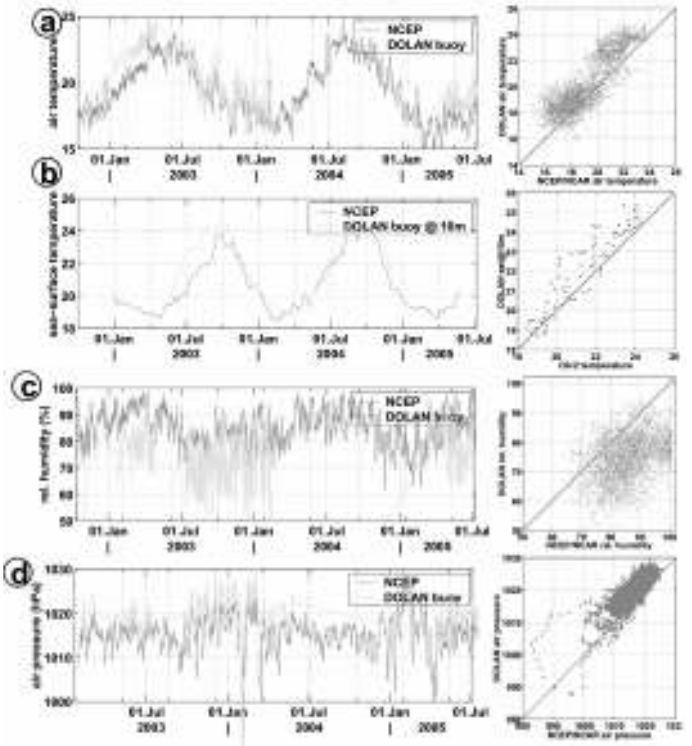

Figure 2 Time series (left) and direct comparison between observations and NCEP model data (right). (a) Air temperature; (b) sea surface temperature; (c) humidity; (d) air pressure.

In comparison with the NCEP/NCAR reanalysis the DOLAN buoy data is of the order of 1.8K higher (Figure 2a, right).

2.2 Sea-surface temperature (SST)

Sea surface temperature was measured with a MicroCat at about 10 m depth. In comparison to NOAA optimum interpolation SSTv2 data, weekly averaged buoy 'SST' (10 m depth) is of the order of 1 K higher in temperature than NOAA SST. As the measurements come from 10 m depth it would be expected for the NOAA SST to be higher, if different at all.

2.3 Humidity

The ESTOC/DOLAN relative humidity data is about 10% lower than the relative humidity derived from specific humidity and saturation as a function of Tair of the NCEP reanalysis. Such disagreement would be consistent with an underestimate of the air temperature as for the NCEP air temperatures. Note however, that humidity as well as air/sea surface temperature difference is a key parameter for sensible and latent heat flux calculations in numerical modelling.

2.4 Air pressure

The air pressure sensor data and NCEP reanalysis agree well in terms of variability. However, the ESTOC/DOLAN buoy air pressure is about 5 hPa higher than the NCEP data. It is unclear if this bias is a sensor problem or a 'real' bias. This will be tested during the next servicing of the buoy.

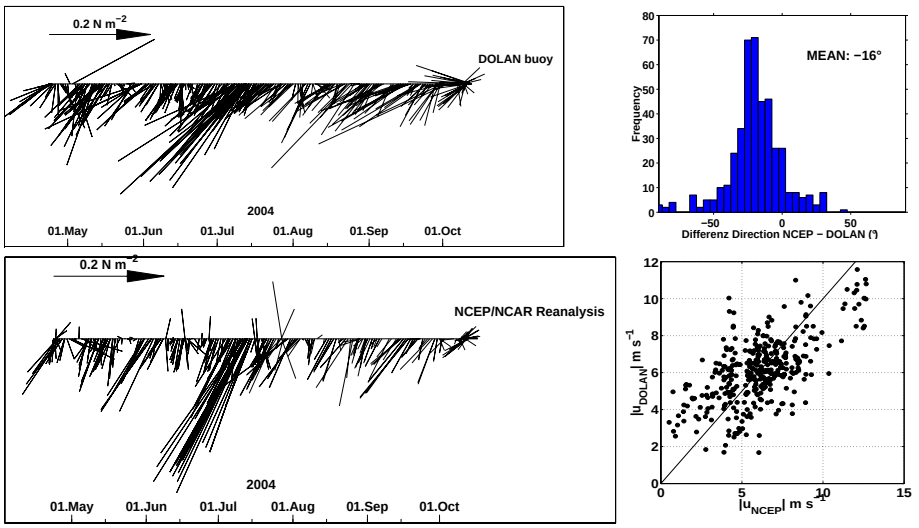

Figure 3 Left: Wind stress derived from Smith (1980) using observational data (upper) and NCEP reanalysis (lower). Right: Difference in wind direction (upper) and wind speed (lower).

2.5 Wind speed and direction

Figure 3 shows wind stress time series as well as a speed and direction comparison between observational data and NCEP reanalysis. Data from the wind sensor is converted into horizontal wind components (east/north) considering pitch/roll/heading information.

In general, DOLAN wind (stress) data (Figure 3 left upper) shows what is expected for a Northeast Trade wind region. Qualitatively the observational data agrees reasonably well with the NCEP/NCAR reanalysis (compare Figure 3 left upper and lower). This is also true comparing the wind speed (right, lower). There is however, a bias of about 15° in wind direction (Figure 3 right, upper). It is not clear if this is a model or observational (or both) problem.

3. Conclusion

- A comparison of about 1 year of meteorological data from the ESTOC/DOLAN open ocean buoy with output from the reanalysis (NCEP/NCAR) revealed apparent systematic deviations (biases) in: air temperature (observations ~1.8°C higher), sea-surface temperature (observations ~1°C higher), pressure (observations ~5hPa higher), relative humidity (observations ~10% lower), wind speed (similar), and wind direction (observations 10° to the right). Except for the wind measurements, all instruments have been calibrated against the NIST standard.
- Such biases in the NCEP/NCAR data will seriously alter bulk parametrised air/sea heat flux estimates. As a result, the buoyancy forcing at the ocean surface is questionable which is also true for prognostics of operational ocean models based on the reanalysis data. Lower SST and air temperature in the NCEP/NCAR reanalysis may compensate in part when using bulk flux estimates.
- As the telemetry allows access to the DOLAN buoy data within a few hours, the data could be incorporated into the global network of meteorological observations.
- The observational data would be even more valuable if additional sensors for short- and long-wave radiation are added.
- It would be of interest to compare the observations with the European Centre of Medium range weather forecasts (ECMWF) but accessibility to the data set is complicated.

Acknowledgements

Financial support from BMBF in the framework of DOLAN (Operationelle Datenübertragung im Ozean und Laterales Akustisches Netzwerk in der Tiefsee) and from the European Union (FP5 ANIMATE EVR1−CT−2001−40014; FP6 MERSEA SIP3−CT−2003−502885) is acknowledged. NCEP Reanalysis and NOAA Optimum Interpolation (OI) SST V2 data was provided by the NOAA−CIRES Climate Diagnostics Center, Boulder, Colorado, USA, from their Web site at www.cdc.noaa.gov/.

References

Smith, S.D. (1988). Coefficients for sea surface wind stress, heat flux, and wind profiles as a function of wind speed and temperature, J. Geophys. Res., 93(C12), 15467−15472.

Smith, S.R., D.M. Legler and K.V. Verzone (2001). Quantifying uncertainties in NCEP reanalysis using high-quality research vessel observations. Journal of Climate, 14, 4062−4072.

The assessment of temperature and salinity sampling strategies in the Mediterranean Forecasting System

Fabio Raicich*

CNR, Istituto di Scienze Marine, Trieste, Italy

Abstract

This paper has the objective of assessing and comparing the usefulness of sampling strategies involving the collection of temperature and salinity profiles in the Mediterranean Sea. This task is accomplished by twin experiments, studying the data impact in a Mediterranean GCM. Idealised, although realistic, sampling strategies involving data collected along Volunteer Observing Ship (VOS) tracks are compared and the relative impacts of the individual tracks are assessed. Tracks crossing regions with fronts and notable mesoscale variability, such as the western Mediterranean and the northwestern Ionian Sea, exhibit the largest impacts. Real sampling strategies involving VOS tracks and profiling floats turn out to be almost as effective as the idealised strategies.

Keywords: Mediterranean Sea, operational forecasting, observing system simulation experiments

1. Introduction

The objective of the Mediterranean Forecasting System (MFS) is to explore, model and quantify the potential predictability of the marine ecosystem variability (Pinardi and Flemming, 1998), which requires, among other elements, a suitable observational system. The time and space coverage provided by the oceanographic data sets is generally limited. Its optimisation is a desirable task, although difficult to achieve due to financial and logistic constraints.

The MFS includes a programme of temperature and salinity (TS) data collection along Volunteer Observing Ship (VOS) tracks and by profiling floats. Such data are assimilated into a Mediterranean GCM for forecasting purposes (Demirov *et al.*, 2003).

Following a previous exploratory study (Raicich and Rampazzo, 2003), the present work has the objective of assessing and comparing the usefulness of different sampling strategies involving the collection of TS profiles. The assessment of each sampling strategy is obtained by studying the impact of TS data assimilation into the Mediterranean GCM by means of Observing System Simulation Experiment (OSSE) techniques.

2. Data and methods

The OSSEs of this work consist of identical twin experiments, where data extracted from one model run are assimilated into another run with different initial conditions.

* Corresponding author, email: fabio.raicich@ts.ismar.cnr.it

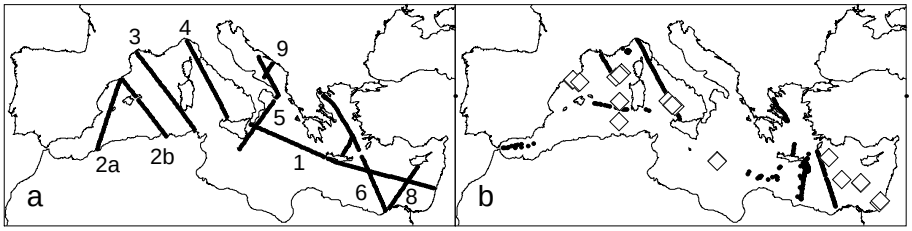

Figure 1 a) Idealised VOS track network. b) Real distribution of profiles from VOS (dots) and profiling floats (diamonds) for week 7 in summer.

The convergence of the second run towards the first one, defined as the 'truth', is measured to quantify the effectiveness of data assimilation in driving the model with 'wrong' initial conditions towards the truth. Each twin experiment includes the following simulations: a) control run, which represents the 'true' ocean and provides the synthetic TS data to be used in the assimilation; b) assimilation run, with different initial conditions from the control run and including the assimilation of TS data extracted from the control run; c) free run, initialised as the assimilation run but without data assimilation. All runs are driven by the same external forcing.

The Mediterranean GCM used for the simulations is GFDL MOM-1, with 1/8°×1/8° horizontal resolution and 31 vertical levels, forced by ECMWF 6-hourly operational analyses. Multivariate data assimilation is performed by means of the optimal interpolation of SOFA (De Mey and Benkiran, 2002).

The OSSEs are based on a sequence of two 7-day assimilation cycles. In the first cycle TS profiles are assimilated using bivariate TS EOFs. In the second cycle sea-level anomaly assimilation is performed by means of trivariate EOFs for T, S and the barotropic streamfunction, with the aim of providing the model with an external dynamic control. OSSEs are made in 'summer' and 'winter' configurations, according to the initial state of the ocean, with initialisation on 1 September 1999 and 1 February 2000, respectively. Free and assimilation runs are initialised exactly one year earlier.

The convergence of the assimilation run towards the control is measured by means of the standard deviation of the difference between the two runs, here denoted as the 'error'. The convergence of the free run towards the control run shows how effectively the GCM is driven towards the 'truth' due to the atmospheric forcing and the SLA assimilation control, and is used for reference. Errors are computed for the western and eastern Mediterranean basins, and three layers, namely the surface layer (L1), from 5 to 260 m depth, the intermediate layer (L2), from 260 to 420 m, and the deep layer (L3), from 420 m to the bottom.

3. Results and concluding remarks

The impact of VOS TS profiles is studied for sampling strategies based upon the VOS track network (Figure 1a) adopted in the MFS VOS programme (Manzella *et al.*, 2003). In the idealised configuration ('ideal-VOS'), used here as a reference, all tracks are covered weekly except 2a and 7 (odd weeks) and 2b and 8 (even weeks). To assess the

impact of a particular track, this is removed from the complete set and the error reduction loss relative to 'ideal-VOS' is evaluated.

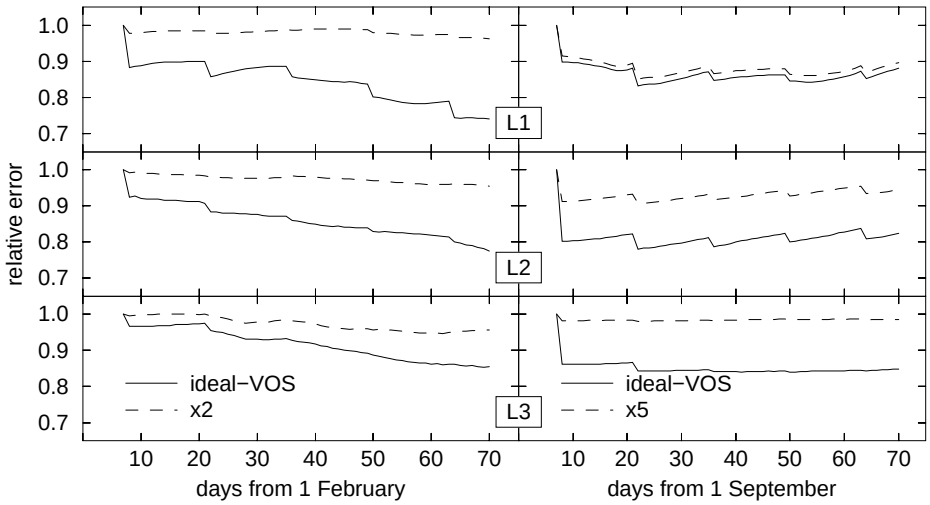

Figure 2 Left panels: Winter salinity relative errors in the western Mediterranean using 'ideal-VOS' (solid lines) and 'x2' (dashed). Right panels: Summer temperature relative errors in the eastern Mediterranean with 'all VOS' (solid lines) and 'x5' (dashed). L1, L2 and L3 indicate the surface, intermediate and deep layer, respectively.

Figure 2 displays examples of relative (assimilation over free run) errors obtained in OSSEs with 'ideal-VOS', and strategies where selected tracks are removed. In the western Mediterranean track 2 exhibits the largest impact, as its removal ('x2') results in almost no improvement in the assimilation with respect to the free run. The track length is important since it allows a more extensive sampling, but it is not the only critical element. In fact, in the eastern basin the largest impact is associated with track 5 ('x5'), particularly in the intermediate and deep layers, rather than track 1, which is much longer. An inspection of the basin circulation reveals that tracks 2 and 5 sample regions with notable mesoscale variability and fronts between water masses, namely the western Mediterranean and the northwestern Ionian, respectively.

The frequency of track coverage used in these experiments is notably higher than in practice. A more realistic assessment is performed using sampling strategies actually adopted in autumn 2004 and winter 2005. In such experiments TS data are extracted from the control run at the times and positions of the real profiles. Figure 1b shows an example of real data distribution. Comparisons of data impacts with 'ideal-VOS' and real sampling strategies are shown in Figure 3. Two cases are shown, corresponding to the assimilation of TS data collected by MFS VOS only ('VOS') and from all available VOS and profiling floats ('VOS+floats'). Although 'ideal-VOS' is generally the most effective strategy in the first 50 days, both 'VOS' and 'VOS+floats' become similar or better than 'ideal-VOS' afterwards. Moreover, the addition of floats enhances the spatial coverage, including areas not crossed by VOS, and allows a continuous data collection.

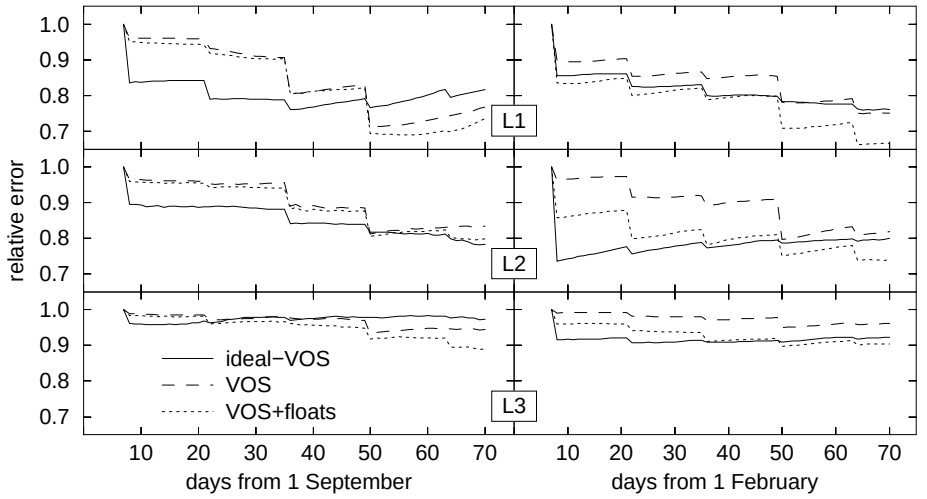

Figure 3 Left panels: Summer salinity relative errors in the western Mediterranean. Right panels: Winter temperature relative errors in the eastern Mediterranean. 'ideal-VOS' sampling strategy (solid lines), 'VOS' (dashed) and 'VOS+floats' (dotted). L1, L2 and L3 indicate the surface, intermediate and deep layer, respectively.

Acknowledgements

This work was partly funded by EC Contract EVK3−CT−2002−00075, 'Mediterranean Forecasting System Toward Environmental Predictions'. Times and positions of real data profiles are taken from the Coriolis Data Centre through www.ifremer.fr/mfstep/.

References

De Mey, P. and M. Benkiran (2002). A multivariate reduced-order optimal interpolation method and its application to the Mediterranean basin-scale circulation, In: Ocean Forecasting Conceptual Basis and Applications, Pinardi, N., and J. Woods (eds.), Springer-Verlag, 281−306.

Demirov, E., N. Pinardi, C. Fratianni, M. Tonani, L. Giacomelli and P. De Mey (2003). Assimilation scheme of Mediterranean Forecasting System: Operational implementation, Ann. Geophys., 21, 189−204.

Manzella, G.M.R., E. Scoccimarro, N. Pinardi and M. Tonani (2003). Improved near-real time management procedures for the Mediterranean ocean Forecasting System — Voluntary Observing Ship program, Ann. Geophys., 21, 49−62.

Pinardi, N. and N.C. Flemming (eds.) (1998). The Mediterranean Forecasting System Science Plan, EuroGOOS Publication No. 11, Southampton Oceanography Centre, Southampton, UK, 52 pp.

Raicich, F. and A. Rampazzo (2003). Observing System Simulation Experiments for the assessment of temperature sampling strategies in the Mediterranean Sea, Ann. Geophys., 21, 151−165.

Sea surface temperature forecasts of the Central Mediterranean Sea: Sensitivity to atmospheric forcing — preliminary results

S. Natale*[1], R. Sorgente[1], S. Gaberšek[1,2], A. Ribotti[1] and A. Olita[1]

[1]*IMC-Centro Marino Internazionale, Torregrande (OR), Italy*
[2]*On sabbatical leave from University of Ljubljana, Dept. of Mathematics and Physics, Slovenia*

Abstract

The Sea Surface Temperature (SST) over the Central Mediterranean Sea predicted by a Near Real Time regional scale forecasting system has been evaluated in order to assess the predictability. The regional ocean circulation model has been forced at the surface by either low or high-resolution atmospheric forcings, both spatially and temporally. The simulated SST has been compared with satellite measurements and found to be in good agreement. No substantial advantages are found in using the high-resolution atmospheric forcing.

Keywords: Atmospheric forcing, ocean forecasting, SST, Central Mediterranean Sea

1. Introduction

The Sea Surface Temperature (SST) is one of the main parameters for evaluating the ability of numerical models to reproduce ocean conditions. It is deeply influenced by marine circulation structures and atmospheric forcings (AF) used as surface boundary conditions. Efforts have been made to refine ocean simulations through increasing temporal and spatial resolution of the AF (e.g. Herbaut *et al.*, 1997) and to evaluate performances of high-resolution (HR) AFs with respect to low-resolution (LR) AFs; for example Castellari *et al.* (2000) compared ocean simulations obtained with monthly and 12-hourly AFs, finding evidence for an improved capability to simulate the water mass formation processes. In this paper we focus on SST forecasting skill, during a transition from a 6-hourly to 1-hourly AF, with the satellite data used as a reference.

2. Methods

The physical model used to simulate the ocean circulation at a regional scale over the Central Mediterranean region is the Sicily Channel Regional Model (SCRM) developed during the MFSTEP project framework. It is based on the Princeton Ocean Model — POM (Blumberg and Mellor, 1987), a three-dimensional, free surface ocean model using the Boussinesq approximation and the hydrostatic equilibrium condition. The domain extends from 9°E to 17°E and from 31°N to 39.5°N with a horizontal resolution of 1/32° (~3.5 km). There are 258×274 mesh points with 24 sigma levels; the external time step is 4 s and the internal time step is 120 s. The SCRM is driven through initial and lateral boundary conditions by a coarse resolution model across a one-way nesting of

* Corresponding author, email: s.natale@imc-it.org

temperature, salinity and velocity daily mean fields from the coarse weekly forecast. SCRM is forced at the surface by a forecast of atmospheric fields, using an interactive air–sea coupling algorithm based on bulk formulae for the computations of the momentum, heat and fresh water fluxes at the air–sea interface.

The SCRM Near Real Time forecast system performs a 5 day ocean forecast in slave mode (i.e. re-initialised once a week from the coarse resolution model). The forecast starts at 00:00 UTC each Wednesday. The AFs used for the surface boundary conditions are LR (0.5°, 6-hourly) from the European Centre for Medium-Range Weather Forecasts-ECMWF, and HR (0.1°, 1-hourly) from the Skiron modelling system (Kallos *et al.*, 2005).

The analysed period ranges from 22 September 2004 to 27 March 2005. Daily mean SST satellite data from an AVHRR/3 sensor on the NOAA-16 satellite, quality checked and interpolated onto a 1/16° grid, have been used as a reference. For each forecast, a basin average and a root mean square error (rmse) of daily SST were calculated with respect to the satellite data.

3. Results

A time series of the basin-averaged computed and satellite derived daily mean SST is shown in Figure 1. It is characterised by a negative trend from the beginning of integration (September 2004) to January 2005 due to the progressive heat losses and evaporative cooling across the air–sea interface and currents.

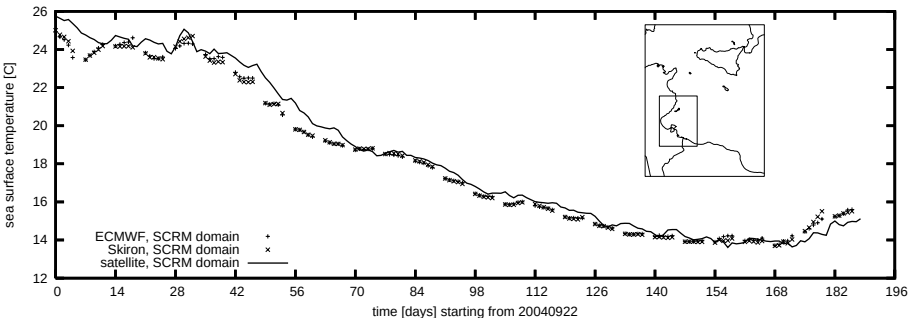

Figure 1 Basin-averaged SST from 22 September 2004 to 27 March 2005. The lack of temporal continuity in the SCRM data is due to a 2-day gap in each weekly forecast. Inset: SCRM domain and Gabes Gulf region.

The heat losses at the surface were maximal in the period November 2004–January 2005 (not shown). The maximum daily mean value of satellite SST is observed at the end of September 2004 (~25°C), while the minimum is reached at the end of January 2005 (~14°C). From February 2005 the heat gain occurs and the SST trend reverses. Regardless of the AF, the simulated daily mean SST values are in good agreement with satellite measurements, but the simulated SST series were colder than the satellite SST during the study period (–0.3°C on average), except at the end of the study period (January and February 2005) when the simulated SST presents higher values with respect to the satellite data (+0.2°C on average).

Figure 2 shows the time series of basin mean rmse of forecast obtained with both AFs with respect to the satellite data. Trends are very similar, and the two rmse usually differ less than 0.1°C; this difference is smaller than the uncertainty of satellite measurements (usually ~0.3°C), so to the extent of predicting the SST the two AFs have the same skill. The general behaviour of rmse is to decrease in time, from ~2.5°C in September 2004 to ~1°C in March 2005; this is probably related to the variability of vertical mixing depth due to seasonal effects, such as different wind intensities and variations in circulation patterns, e.g. the upwelling region south of Sicily induced by the Atlantic Ionian Stream (AIS, Robinson *et al.*, 1999).

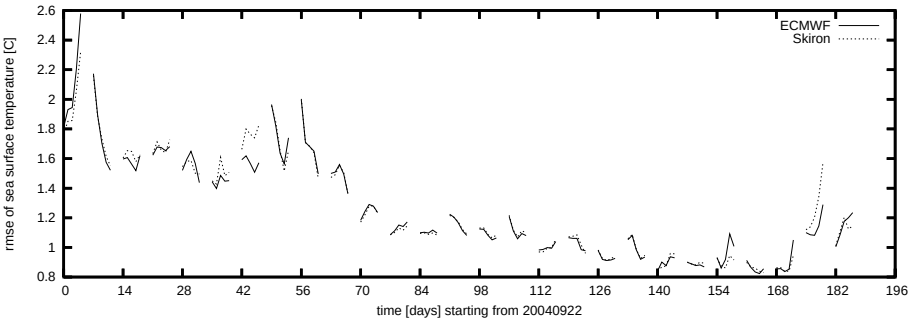

Figure 2 Basin-averaged root mean square error of SST from 22 September 2004 to 27 March 2005.

It appears that the SST forecast is not sensitive to the choice of AF. The spatially averaged surface kinetic energy available at every internal time step exhibits a higher variability (calculated for each 5-day forecast) using the HR AF, which can be up to 50% greater during the autumn–winter period (Figure 3) compared to the variability obtained with LR AF.

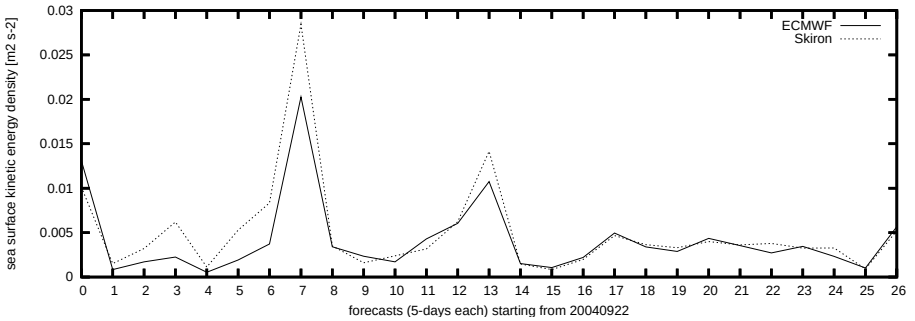

Figure 3 Standard deviation of spatially averaged surface kinetic energy for each 5-day forecast.

4. Conclusion

The LR and HR AFs have the same skill to forecast sea surface temperature, but no substantial advantages are found in using the high-resolution atmospheric forcing with the ocean model running in a slave mode.

However, the HR AF appears to be more dynamical than the LR, and often produces important differences in mesoscale surface circulation patterns. This is very important for an application such as the oil-spill modelling. A future goal will be to test these different surface currents against experimental data from current gauges.

Acknowledgements

Satellite daily SST are produced by ISAC–CNR (Italy) in the framework of the MFSTEP project. For atmospheric forcings we thank IASA (Greece) for Skiron data, and ECMWF (UK). Thanks also to INGV (Italy) for the ocean coarse model and for coordination of the MFSTEP project.

This work has been realised in the framework of the EC MFSTEP project (EVK3–2001–00174), EC ARENA project (EVK3–2002–00516) and the EU Marie Curie host fellowship: ODASS project (HPMD–CT–2001–00075).

References

Blumberg A.F. and G. Mellor (1987). A description of a three-dimensional coastal ocean circulation model, Three-dimensional Coastal Ocean Models, Coastal Estuarine Science, N.S. Heaps Ed., Americ. Geophys. Union, 1–16.

Castellari, S., N. Pinardi and K. Leaman (2000). Simulation of water mass formation process in the Mediterranean Sea: Influence of the time frequency of the atmospheric forcing, Journal of Geophysical Research, 105(C10), 24157–24181.

Herbaut C., F. Martel and M. Crépon (1997). A sensitivity study of the general circulation of the Western Mediterranean Sea. Part II: the response to atmospheric forcing. Journal of Physical Oceanography, 27, 2126–2145.

Kallos G., I. Pytharoulis and P. Katsafados (2005). Limited area weather forecasting for the MFSTEP activities: sensitivity and performance analysis. This volume, page 43.

Robinson A.R., J. Sellschopp, A. Warn-Varnas, L.A. Anderson and P.F.J. Lermusiaux (1999). The Atlantic Ionian Stream, J. Marine System, 20, 129–156.

EU Models 2

Marine Environment and Security for the European Area: lessons learned from MERSEA Strand-1

J.A. Johannessen[1], P.-Y. Le Traon[2], I. Robinson[3], K. Nittis[4], M. Bell[5], N. Pinardi[6], P. Bahurel[7], B. Furevik[1] and the MERSEA Strand-1 Consortium

[1]*Nansen Environmental and Remote Sensing Center, Bergen, Norway*
[2]*CLS, Toulouse, France*
[3]*National Oceanography Centre, Southampton, UK*
[4]*Hellenic Centre for Marine Research, Institute of Oceanography, Anavyssos, Greece*
[5]*Met Office, UK*
[6]*INGV, Bologne, Italy*
[7]*MERCATOR, Toulouse, France*

Abstract

In response to the joint European Commission and European Space Agency initiative to establish by 2008 a system for Global Monitoring for Environment and Security (GMES) the MERSEA Strand-1 project was executed to demonstrate the capacity of present monitoring systems. By integration of existing spaceborne observations with data from *in situ* measurement networks and ocean models, daily mean products and forecasts from four core data assimilation systems were generated and distributed through an OPeNDAP server from 1 June 2003 to 31 May 2004. Moreover, downscaling to high resolution models was used for specific applications to (harmful) algal bloom, eutrophication and oil spill monitoring. The lessons learned from this project are reported here.

Keywords: GMES, integrated monitoring system, MERSEA Strand-1

1. Introduction

The MERSEA Strand-1 (www.nersc.no/~mersea) project kicked-off in January 2003 for a duration of 18 months (Johannessen *et al.*, 2003). At the termination in July 2004 four core data assimilation systems including MERCATOR, FOAM, TOPAZ and MFS had been delivering marine products for the Atlantic Ocean and Mediterranean on a routine basis for almost a year. Assessment of the quality and consistency of these outputs was conducted based on internal metrics. Moreover, they supplied relevant marine information including boundary conditions for nested regional-to-local models. These models (including MIPOM, OD3D, BOOS, NORWECOM, POSEIDON, CYCOFOS and POLCOMS/ERSEM) were, in turn, used for specific applications to and monitoring of (harmful) algal bloom, eutrophication and oil spill. The MERSEA Integrated Project, which is funded until 2008, will continue to advance the European capacity for monitoring of the marine environment and security (Desaubies *et al.*, 2005)

* Corresponding author, email: johnny.johannessen@nersc.no

2. MERSEA Strand-1 objectives and approach

The MERSEA Strand-1 project was directly related to the GMES Action Plan (initial period 2001–2003). Through integration of existing spaceborne observations with data from *in situ* monitoring networks and ocean modelling and data assimilation system the specific objectives were to:

- deliver information products (physical, chemical and biological) needed by users concerned with European marine environment and security policies
- report on the problems met and lessons learnt in supplying this information
- contribute to improve knowledge, methods and tools required for monitoring, information production and delivery to users occupied with marine environmental monitoring, management and security.

The four core data assimilation systems were forced with atmospheric data from numerical weather prediction models and assimilated satellite-derived sea-level anomaly (SLA), sea surface temperature (SST), sea ice fields and ocean colour measurements (only tested). In addition profiling data from the Argo floats measuring temperature and salinity in the upper 2000 m were both used for model validation as well as data assimilation (FOAM system only). Regular XBT observations from VOS were also used for validation. The nested models used for targeted application demonstrations also relied on the atmospheric forcing field and specification of 3D current fields from the core data assimilation systems.

In context of the so-called GMES diamond (see Figure 1) the MERSEA Strand-1 project essentially examined the individual functionalities and integration of the *in situ* observing system, the spaceborne observing system, the data integration, information and management handling and the corresponding demonstration services. Through combined research, development and forecasting services the diamond was gradually more shaped and tailored towards marine monitoring for environment and security. As already mentioned, further shaping is presently taking place within the MERSEA Integrated Project (Desaubies *et al.*, 2005).

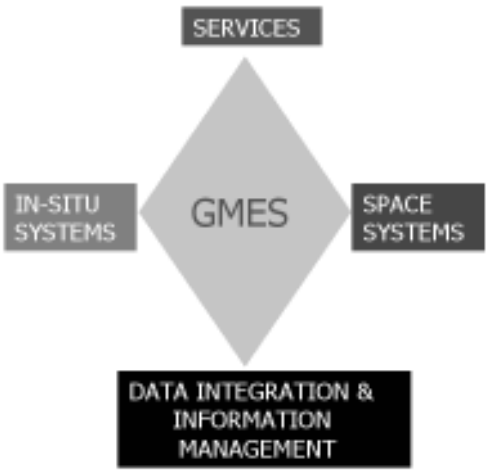

Figure 1 The relevance of the MERSEA Strand-1 approach in the context of the GMES diamond.

Table 1 Summary of the approach, activities and achievements.

Approach	Scientific and technical activities	Key achievements
Adapting the 4 basin scale integrated monitoring systems to the needs of real time experiments and hindcast application demonstration studies.	Regular production of 3D oceanographic fields for the Atlantic Ocean and Mediterranean.	A 12-month database containing products from real-time experiments. Freely available by ftp from server.
Integrated examination of observation capabilities, data exchange methods and monitoring capacity.	Sampling characteristics, accuracy, data delivery and validation. Deficiencies in global, regional and local scale measurement systems. Technical and non-technical obstacles.	Observational Requirements for input to European Ocean Forecasting System Models. Management Challenges for a European Ocean Forecasting System. Demonstration of the effective use of observational data in support of operational ocean forecasting.
Generation of Internal Metrics for intercomparison and assessment of the 4 integrated monitoring systems.	MERSEA Strand-1 information and product management system. Impact of: vertical coordinate system, horizontal and vertical resolutions, length of spin-up, mixing parametrisation, assimilation methods, SLA fields, mean sea surface height, relaxation, bulk formulae, ice model.	Internal Metrics for the Data assimilation product intercomparison. Web-server. Strengths and weaknesses of the integrated system.
Selection of 11 application demonstration services related to HAB, eutrophication and oil spill.	HAB and eutrophication monitoring; what is mature and what needs more research. Oil spill drift simulation; what is acceptable and what needs more research.	Web site for service demonstrations. End-user analyses and evaluation of strength and weaknesses of the services.
These can be further explored at http://www.imr.no/english/activities/cooperation_projects/merseastrand/ http://moncoze.met.no/ http://www.fimr.fi/en/itamerikanta/bsds/2033.html http://www.poseidon.ncmr.gr/mersea/ http://env1.ncmr.gr/oilSpill/ http://ocean.dmi.dk/DMI-MERSEA/MERSEA_WP5_DMI.htm http://www.ucy.ac.cy/cyocean/New/wp5mersea1/		

3. Achievements

The information production as well as the downscaling and nesting solutions achieved during the MERSEA Strand-1 project clearly demonstrated how operational oceanography based on modelling and data assimilation at global-to-basin-to-regional scales establishes the backbone for provision of services tailored to GMES (see www.mersea.eu.org/html/information/overview/LAS). The major outcome and results of these application demonstration services were made available at the web demonstrator

sites arranged according to HAB, eutrophication and accidental and/or deliberate oil spills. Table 1 provides an overview of the approach, the main activities, and the key achievements.

Inter-comparison and assessments of the output products from the core data assimilation system were routinely carried out for the North Atlantic and Mediterranean using internal metrics. The methodology is described in the MERSEA Strand-1 report (MERSEA, 2004) and further highlighted by Crosnier and Le Provost, 2005.

Sorted into four classes the inter-comparison allowed testing of the consistency and quality of the information products delivered by the core assimilation systems. The four classes included:

Class 1: 2D fields of wind stress (τ_x,τ_y), total net heat fluxes including relaxation terms, surface freshwater flux (E-P-R) including relaxation terms, barotropic stream function, mixed layer depth, sea surface height, 3D fields of temperature, salinity and velocity, and mean Sea Surface Height (MSSH).

Class 2: Temperature, salinity and velocity fields along high resolution sections and at mooring locations.

Class 3: Integrated quantities such as daily volume transport through a given section, meridional heat transport, and overturning stream function.

Class 4: Statistics in the model and observation space to assess data assimilation method performances and forecast skill.

Class 1 to 3 diagnostics were provided for the daily mean best estimated fields on a daily basis as well as for the T0+6 day forecast from 1 June 2003 to 31 May 2004. The Class 4 inter-comparison was not completed due to difficulties with its complete definition and lack of time.

In addition, the outcome of the application demonstration experiments for HAB, eutrophication and oil spills were reported in the MERSEA Strand-1 report (MERSEA, 2004) and more comprehensively in individual reports and papers including Hackett (2004), Nittis *et al.* (2004) and Stipa *et al.* (2003). A common important finding from these application studies is the improved surface transport estimates and particle trajectories obtained when the upper layer baroclinic motion from the model systems are combined with the direct wind induced surface drift.

The reliability and utilisation of the information products depend not only upon the performance of the models and assimilation tools, but also on the availability and quality of the observing systems, telecommunication networks, data processing and distribution, data access, rapid information integration and flow tailored to the specific needs of the different services. In general these systems are more mature for ocean physics, while they are still at the research level for pollution and ecosystem simulations (Blackford *et al.*, 2004). Moreover, as the coastal systems reach finer spatial resolution the need for validation becomes more constrained by lack of data. Resulting from the experience achieved during the execution of MERSEA Strand-1 the key challenges for sustainable integrated ocean forecasting systems were identified to include:

Altimetry. A high inclination altimeter mission (post-ENVISAT) after 2007 is needed to complement Jason-2 (planned launch in 2008) and to constrain the open ocean currents and their mesoscale variability.

Radiometry. High quality and high resolution SST measurements are needed beyond 2007. In agreement with the GHRSST-PP this implies the need to maintain at least one sensor in orbit having measurement stability and accuracy equivalent to that of the ATSR/AATSR series of sensors.

Spectrometry. 2–3 spectrometers are needed to minimise the limiting effects of cloud cover impact, and thus ensure better conditions for near-real time data for validation of or assimilation into marine biochemical models.

Argo, VOS and Ferryboxes: The deployment of Argo profiling floats should be sustained, while the use of VOS and Ferryboxes through European coastal and shelf seas should be extended.

Observatories: The development and operation of integrated observatories at selected tie-points along the European coastal and regional seas is an essential approach to secure routine and sustained *in situ* monitoring for environment (physical, biogeochemical) and security (oil spills, red tides, toxic algal blooms).

HF radars: The number of operating short and long range HF radar systems should increase (today 3 systems are operating) and be implemented at selected observatories.

Biogeochemical sensor development: There is a developing need to be able to measure pigments, nutrients, dissolved gases and other biogeochemical properties in the sea at fine spatial and temporal resolution.

River discharges: There is an urgent requirement for a routine monitoring system of river discharges (volume and nutrients) into coastal seas.

Skill Assessment: There is a need for systematic examinations of the performances of forecasting models which quantify their dependence on the availability, timeliness and quality of measured ocean data from satellites and *in situ* systems.

Downscaling: The regional high resolution forecasting systems improve with systematic and reliable information on the open boundaries from global and basin scale systems.

Coastal Models: Coastal models are far from being developed and operated at the adequate resolution for applications to pollution monitoring from offshore installations, ships and land sources.

Ecosystem modelling: There is a strong need to develop and advance the maturity of ecosystem modelling.

System integration: The optimum performance of the marine GMES will only be achieved when there is an effective two-way integration between the local-to-regional scale observations and models and the basin scale forecasting system.

Education and training: A new curriculum in operational oceanography at universities around Europe is urgently needed to meet the gradual demand for adequate and timely analyses of the large amount of new quality controlled information products.

User involvement: Effective two-way communication and involvement of the users should become mandatory as it is through them that the whole enterprise for European Ocean Forecasting can be justified.

4. Summary

The MERSEA Strand-1 project initiated a series of multidisciplinary tasks regarding the assessment of the current capacity for marine GMES in Europe. In finalising the project a number of valuable achievements and findings have been accomplished regarding the shape and functionalities of the four corners of the GMES diamond. In line with these achievements, specific recommendations of cost-effective and sustainable solutions to obstacles encountered for the development and implementation of a fully operational oceanography system beneficial to GMES have been delivered (MERSEA Strand-1, 2004).

The initial execution of the MERSEA Integrated Project has capitalised on many of these achievements and recommendations thus allowing for an efficient jump-start of this large four year project funded by the EC. In parallel, ESA-initiated GMES Service Element (GSE) activities and projects have also benefited from the key outcome of MERSEA Strand-1, notably the ROSES and MARCOAST projects. The same is true for the Roadmap project that targeted the satellite payload need in the context of operational oceanography, in particular focusing on radar altimetry, infrared radiometer and colour spectrometer as considered for Sentinel 3. All in all these projects and findings are also importantly forming the platform for the consolidated European view and contribution to the Global Ocean Data Assimilation Experiment (GODAE), in its full operational phase through 2006. They have also significantly contributed in pushing the consensus view on operational oceanography within EuroGOOS.

In summary, from the execution of MERSEA Strand-1 until 2008 with the completion of the MERSEA Integrated Project we have achieved and will continue to achieve a gradual accumulation of expertise and knowledge to design, implement and operate an operational European ocean forecasting system of systems. This is extremely timely and will be entirely in phase with the full execution of GMES in 2008.

Acknowledgement

The MERSEA STRAND-1 project was supported by the European Commission through contract no. EVK3−CT−2002−00089. In addition to the authors the consortium included scientific and technical staff from Ifremer, Météo-France, and LEGOS (France), DMI (Denmark), DFMR (Cyprus), Met.no and IMR (Norway), POL, PML and CEFAS (UK), DLR (Germany) and FIMR (Finland).

References

Blackford, J.C., J.I. Allen and F.G. Gilbert (2004). ERSEM-2003 a generic ecosystem model, submitted to Journal of Marine System.

Crosnier, L. and C. Le Provost (2005). Inter-Comparing Five Forecast Operational Systems in the North Atlantic and Mediterranean basins: The MERSEA Strand-1 Methodology, Journal of Marine Systems (submitted).

Hackett, B. (2004). The impact of global ocean model forcing data on oil spill fate prediction: a comparative study of the "Prestige" accident, Report No. 13 Norwegian Meteorological Institute, Oslo, Norway, 26 pp.

Johannessen, J.A., P.-Y. Le Traon, I. Robinson, K. Nittis, M. Bell, N. Pinardi, P. Bahurel and B. Furevik (2003). Marine EnviRonment and Security for the European Area, MERSEA Strand-1, Building the European Capacity in Operational Oceanography, Proceedings of the Third International Conference on EuroGOOS, 3–6 December 2002, Athens, Greece, Eds. H. Dahlin, N.C. Flemming, K. Nittis, S.E. Petersson, Elsevier Oceanography Series, 69.

MERSEA Strand-1 Final Report (2004). Marine EnviRonment and Security for the European Area (MERSEA) Strand-1, 5th Framework Programme, Contract No. EVK3–CT–2002–00089, available upon request from NERSC.

Nittis, K., L. Perivoliotis, G. Korres, C. Tziavos and I. Thanos (2004). Operational monitoring and forecasting for marine environmental applications in the Aegean Sea, Environmental Modelling and Software.

Stipa, T., M. Skogen, I. Hansen, A. Eriksen, I. Hense, A. Kiiltomäki, H. Søiland and A. Westerlund (2003). Short-term effects of nutrient reductions in the North Sea and the Baltic Sea as seen by an ensemble of numerical models, Meri 49, 43–70.

SAM2: The Second Generation of MERCATOR Assimilation System

Benoît Tranchant*[1], Charles-Emmanuel Testut[1], Nicolas Ferry[1] and Pierre Brasseur[2]

[1]*Mercator-Océan, France*
[2]*LEGI, France*

Abstract

The French MERCATOR project is developing several operational ocean forecasting systems to take part in the Global Ocean Data Assimilation Experiment (GODAE). Prototype systems are designed to simulate

1. the Atlantic and Mediterranean Sea (from 1/3° to 1/15°)
2. the global ocean circulation (from 2° to 1/4°).

The first generation of the multivariate assimilation scheme referred to as SAM1v2 is based on the SOFA reduced order interpolation scheme (developed at LEGOS, Toulouse). It uses a vertical/horizontal separation of error statistics, and an order reduction in the vertical in terms of multivariate Empirical Orthogonal Functions (EOFs) of temperature, salinity, and the barotropic stream function. This scheme has been implemented in the operational system and provides routine weekly analyses and forecasts. The new generation of a fully multivariate assimilation system referred to as SAM2v1 is being developed from the SEEK (Singular Evolutive Extended Kalman) algorithm (developed at LEGI, Grenoble). This scheme is a Reduced Order Kalman Filter using a 3D multivariate modal decomposition of the forecast error covariance as well as an adaptive scheme to specify parameters of the forecast error. The use of the SEEK filter and its 3D modal representation for the error statistic is intended to overcome some of the limitations of SAM1v2 in highly inhomogeneous, anisotropic, and non-separable regions of the world ocean such as shallow areas, as well as in the surface layer. As in the previous system, it allows assimilation of vertical profiles and SST in addition to altimetric data (JASON, ERS-2 and GFO), but in larger quantities at a lower cost. Recent results will be presented and discussed for hindcast experiments.

Keywords: Data assimilation, operational oceanography, SEEK

1. Introduction

During the last few years, a large number of data assimilation schemes for very large dimension ocean systems have been developed (e.g. Verron, 1992; Blayo *et al.*, 1997; De Mey, 1997; Fukumori, 2001; Evensen, 2003; Brusdal *et al.*, 2003; Weaver *et al.*, 2003). This recent evolution contributed to the development of operational forecasting systems operating at regional and global scales at a national level (e.g. MERCATOR in France, FOAM in the United Kingdom, MFS in Italy, TOPAZ in Norway, ECCO in US and

* Corresponding author, email: benoit.tranchant@mercator-ocean.fr

BLUElink in Australia). Moreover, the coordination between these efforts started to be organised internationally through the Global Ocean Data Assimilation Experiment (GODAE, Smith, 2005). The Mercator Ocean Monitoring and Forecasting System has been routinely operated in real-time in Toulouse by the Mercator Project since early 2001. It has been regularly upgraded through several prototypes of increasing complexity, expanding the geographical coverage from regional to global, improving models and assimilation schemes.

In this contribution, we focus on the new data assimilation system SAM2. This assimilation system is based on a Singular Extended Evolutive Kalman (SEEK) filter (Pham *et al.*, 1998) and uses error statistics built from 3D multivariate EOFs. This scheme allows the assimilation of a large number of data in a fully multivariate way, conjointly altimeter data (JASON1, ENVISAT and GFO), Reynolds SST and temperature and salinity vertical profiles provided by the CORIOLIS centre.

After a brief presentation of the SAM2 scheme, we will present results showing the impact of the truncation error from hindcast experiments.

2. SAM2: a reduced order Kalman filter

Mercator is developing a suite of assimilation tools (called "SAM" for Système d'Assimilation MERCATOR) of increasing complexity, from sub-optimal sequential schemes to variational methods. The first release, SAM1 has been elaborated from an optimal interpolation scheme based originally on the SOFA code (De Mey and Benkiran, 2002; Benkiran *et al.*, 2005). See also Bahurel *et al.* (2005).

SAM2 is the second release which can be considered as a Singular Extended Evolutive Kalman (SEEK) filter (Pham *et al.*, 1998) analysis method. Indeed, some limitations due to the concept of separability (separation between horizontal and vertical correlations) led to development of a more advanced assimilation system. As in the SAM1 scheme, SAM2 is a reduced order Kalman filter, but the main difference comes from the error sub-space. In SAM2, the background error covariance matrix is approximated by a singular low-rank matrix. Unlike the SAM1 scheme for which the inversion of the innovation covariances matrix is performed in the observational space, the inversion is done in the modal space for the SAM2 scheme. Indeed, the error statistics of the SEEK filter are represented in a sub-space spanned by a small number of dominant error directions. The formulation of the assimilation algorithm relies on a singular low-rank matrix, which makes the calculations tractable even with state vectors of very large dimension (>106, Brasseur *et al.*, 2005). Several strategies can be adopted to initialise the vectors of the reduced basis. A method involving the computation of empirical orthogonal functions (EOFs) obtained from prior simulations (without assimilation) has been applied in the majority of case studies; this approach leads to corrections of the model trajectory that are multivariate and dynamically consistent. In addition, considering the size of several ocean configurations we use, unlike the original SEEK filter, SAM2 does not yet make it possible for the statistics of error to evolve according to model dynamics. However, some form of evolutivity of the background error is taken into account by considering different error sub-spaces for the four seasons. In addition, an adaptive scheme of the background variance error is being developed which will allow its better fit at each analysis step.

From a computational point of view, and to minimise the computational requirements, the analysis kernel in SAM2 has been massively parallelised and integrated in a generic platform hosting the SAM1 and SAM2 kernel families (Brasseur *et al.*, 2005). This platform is driven by the PALM software (Piacentini *et al.*, 2003) which makes the coupling between the model codes and the assimilation schemes more effective.

3. Hindcast experiment in 2003

3.1 Ocean model

The ocean model is based on the rigid-lid version of OPA-8.1 (Madec *et al.*, 1998), a general circulation model developed at LOCEAN laboratory (Paris), and is designed to simulate the North Atlantic and Tropics (20°S−70°N) with an intermediate resolution of 1/3° and 43 vertical levels distributed from 12 m at the surface to 200 m at the bottom (Benkiran *et al.*, 2005). Surface forcing consists of daily fields of wind stress, evaporation, precipitation, non-solar and solar heat fluxes provided by the European Centre for Medium-Range Weather Forecast (ECMWF) analysis and forecasts. To describe the coupling between atmosphere and ocean, a retroaction term (-40 Wm^{-2}) based on the difference between the model Sea Surface Temperature (SST) and the daily Reynolds SST is added to the net heat fluxes. The main river outflows are represented by an input of fresh water at the river mouth given by the climatological monthly database from UNESCO (Vörömarsty *et al.*, 1996).

3.2 Input data

Input data include *in situ* as well as remotely sensed observations which are used for several applications: forcing, data assimilation, model verification and validation. Data are assimilated over a 7-day time window with the FGAT technique (First Guess at Appropriate Time), which means that innovation is computed at the observation time. Along track altimeter data from three satellites (JASON1, ENVISAT and GFO) are assimilated every week (~40000 SLA measurements), Reynolds SST (2° resolution at analysis day: ~7000 data) and temperature and salinity vertical profiles (~300−500) provided by the CORIOLIS centre.

3.3 Background error covariances

The background error covariance is represented by means of a set of 3D error modes (3D EOFs of model variability) in the control space. The control state vector includes the temperature, salinity and barotropic height model variables. Nevertheless the correction modifies the whole model state with a geostrophic adjustment at each analysis step. In this hindcast experiment, we used seasonal 3D EOFs computed from a multivariate SEEK analysis (1993−1998) where only surface data (SST, SLA) were assimilated, see Testut *et al.* (2003).

3.4 Impact of the error sub-space

Several experiments have been realised over the year 2003. To validate the method with independent *in situ* temperature, an assimilation skill is illustrated in Figure 1. It shows the vertical distribution of the misfit variance computed between non-assimilated temperature profiles and the climatology, the control run and the hindcast experiments

with 21 and 71 modes. Only the assimilation with the larger amount of modes improves the temperature field at all depths, whereas a significant reduction of the error in the thermocline takes place for the two hindcast experiments.

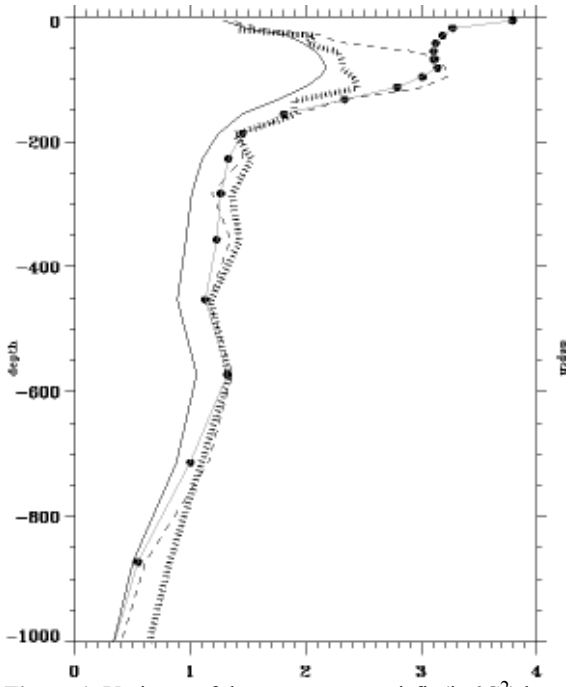

Figure 1 Variance of the temperature misfit (in $°C^2$) between *in situ* data and: (i) the climatology (big dots), (ii) the control run (dashed line) (iii) the assimilation simulation with 71 modes (solid line) and 21 modes (barred line) down to 1000 metre depth during 2003 over the North Atlantic.

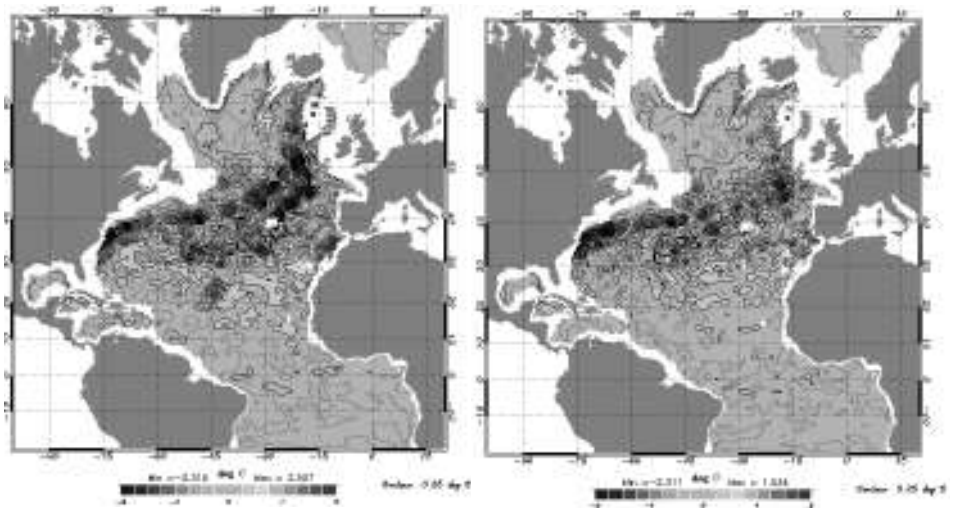

Figure 2 Difference between the annual mean of temperature (2003) and the climatology at 300 metre depth: (left) 21 modes used, (right) 71 modes used.

Figure 2 shows the difference between the annual mean of the temperature field at 1000 metre depth and the corresponding climatology for two different experiments, with 21 modes and 71 modes. The impact of the size of the sub-error space is clearly seen, the assimilation experiment with 71 modes has reduced the bias with the climatology, mainly in the region of the Mediterranean outflow and in the North Atlantic Current (NAC).

4. Conclusion

This paper has described the new Mercator reduced order scheme SAM2 and presented results from hindcast experiments. The assimilation scheme uses 3D EOFs for the error statistics representation which is intended to overcome some of the limitations of the previous OI scheme in anisotropic and non separable regions. Nevertheless, we point out the importance of the choice of the sub-error space by varying the number of modes. In addition, different techniques can be used to compute the multivariate error covariance estimates. For example, EOFs of model states extracted from a prior model simulation or from hindcast experiments, and EOFs of the system tendencies occurring over several assimilation cycles are being investigated. Another example is that these techniques may differ according to the OGCM geographical domain (regional versus global configurations). These different studies should lead to interesting results on the structure of the model forecast error covariances. An adaptative scheme of the background variance error is also being developed. In addition, the using of a generic platform with the PALM software (Piacentini *et al.*, 2003) and a massively parallel analysis kernel provides a technological capacity to extend the dimension of the error sub-space up to several hundred modes (typically 200 with the MERCATOR prototype configurations).

Acknowledgements

The authors thank the PALM team for their help in the use of the PALM coupler (Piacentini *et al.*, 2003) which provides a general structure for a modular implementation of a data assimilation system and makes the changes easier in the data assimilation algorithm.

References

Bahurel, P., E. Dombrowsky and the Mercator project team (2005). Mercator Ocean Monitoring and Forecasting System, a contribution to GMES. This volume page 449.

Benkiran, M., E. Greiner, and E. Dombrowsky (2005). Multivariate and multidata assimilation in the Mercator project, J. Marine System special issue, in revision.

Blayo, E., T. Mailly, B. Barnier, P. Brasseur, C. Le Provost, J.M. Molines and J. Verron, (1997). Complementarity of ERS-1 and TOPEX/Poseidon altimeter data in estimating the ocean circulation: Assimilation into a model of the North Atlantic, J. Geophys. Res., 102(C8), 18573–18584.

Brasseur, P., P. Bahurel, L. Bertino, F. Birol, J.M. Brankart, N. Ferry, S. Losa, E. Remy, J. Schröter, S. Skachko, C.E. Testut, B. Tranchant, P.J. Van Leeuwen and J. Verron (2005). Data assimilation in operational ocean forecasting systems: The MERCATOR and MERSEA developments, submitted to Q. J. R. Met. Soc., (June 2005).

Brusdal, K., J.M. Brankart, G. Halberstadt, G. Evensen, P. Brasseur, P.J. Van Leeuwen, E. Dombrowsky and J. Verron (2003). A demonstration of ensemble-based assimilation methods with a layered OGCM from the perspective of operational ocean forecasting systems. J. Mar. Systems, 40–41, 253–289.

De Mey, P. (1997). Data assimilation at the oceanic mesoscale: a review, J. Met. Soc. Japan, Special issue on "Data assimilation in meteorology and oceanography: Theory and Practice", 75, 415–425.

De Mey, P. and M. Benkiran (2002). A multivariate reduced-order optimal interpolation method and its application to the Mediterranean basin-scale circulation. In: Ocean Forecasting: Conceptual basis and applications, N. Pinardi, Ed., Springer-Verlag Heidelberg, 472 pp.

Fukumori, I. (2001). Data assimilation by models. In: Satellite Altimetry and Earth Sciences, a Handbook of Techniques and Applications (Fu L. and A. Cazenave Eds), Academic Press, 237–265.

Madec, G., P. Delecluse, M. Imbard and C. Levy (1998). OPA8.1 ocean general circulation model reference manual, Notes du pôle de modélisation IPSL, 91 pp.

Piacentini, A., S. Buis, D. Declat and the PALM group (2003). PALM: A computational Framework for assembling high performance computing applications, Concurrency and Computat., 00, 1–7.

Pham, D., J. Verron and C. Roubaud (1998). A singular evolutive extended Kalman filter for data assimilation in oceanography, J. Mar. Syst., 16, 323–340.

Smith, N. (2005). Perspectives from the Global Ocean Data Assimilation Experiment, In: GODAE, an Integrated View of Oceanography: Ocean Weather Forecasting in the 21st Century (J. Verron and E. Chassignet Eds.), Kluwer Academic Press, in press.

Testut, C.E., P. Brasseur, J.M. Brankart and J. Verron (2003). Assimilation of sea surface temperature and altimetric observations during 1992–1993 into an eddy-permitting primitive equation model of the North Atlantic Ocean, J. Mar. Syst., 40–41, 291–316.

Verron, J. (1992). Nudging altimeter data into a quasi-geostrophic ocean models, J. Geophy. Res., 97(C5), 7497.

Vörömarsty, C.J., B. Fekete, B.A. Tucker, River Discharge Database, Version 1.0 (RivDISv1.0), Volumes 0 through 6., A contribution to IHP-V Theme. Technical Documents in Hydrology Series. UNESCO, Paris.

Weaver, A., J. Vialard and L.T. Anderson (2003). Three- and Four-Dimensional Variational Assimilation with a General Circulation Model of the Tropical Pacific Ocean;, Part I: Formulation, Internal Diagnostics, and Consistency Checks, Mon. Wea. Rev., 131, 1360–1378.

An operational data assimilation system for the Baltic Sea

Lennart Funkquist*

Swedish Meteorological and Hydrological Institute, Norrköping, Sweden

Abstract

An Optimal Interpolation (OI) scheme for assimilation of surface parameters and T/S profiles has been developed and tested for daily use in SMHI's operational ocean model HIROMB (HIgh Resolution Operational Model for the Baltic).

Keywords: Data assimilation, optimal interpolation, ocean modelling

1. Introduction

Though data assimilation has been used for decades in operational meteorology and the use of data assimilation in ocean models has undergone significant progress during the last ten years, its implementation in operational ocean models has not yet reached the same level as in meteorology. One reason for this is of course the limited number of real-time observations.

For a couple of years, SMHI as a partner in the EU-funded project ODON (Optimal Design of Observational Network) has been engaged in development of data assimilation methods. The successive correction method has already been implemented in the operational version of HIROMB and optimal interpolation has been used in observing system experiments as part of the ODON project.

2. Assimilation scheme

Well-established assimilation schemes for three-dimensional fields have been examined and valued. For the 3D T/S assimilation in HIROMB, a multivariate optimum interpolation (OI) scheme has been chosen as a first candidate. The reason for this is its good performance in view of available data and amount of work needed to implement the scheme. The scheme is also used for 2D assimilation of sea surface temperature, while the method of successive correction is used for sea ice parameters.

Although the OI scheme may appear simpler compared to more theoretically advanced schemes like those based on variational methods and EnKF (Ensemble Kalman Filter), it requires specified values on a number of crucial parameters such as correlation length scales and estimates on observational errors.

The OI method may be written in a simple form as the equation

$$Analysis = Forecast + K(Observation - H\{Forecast\})$$

where K interpolates the difference between observations and model data and H interpolates from model to observation space. In condensed form the equation may also be written as

* Corresponding author, email: Lennart.Funkquist@smhi.se

$A = F + K(O - HF)$, with $K = P^f H^T (HP^f H^T + R)^{-1}$

P^f is the forecast error covariance matrix, R the observation error covariance matrix and $O-HF$ is the innovation vector. K is also called a "Gain" matrix and controls the relative weight between O and F.

It is assumed that the forecast or background error is uncorrelated with the observation error, which is almost the case. But if forecast data has been used together with satellite data to create a blended product which is what is assimilated in the model, then the above assumption does not hold any longer.

Normally the OI is done in the following order after the variance of the forecast and observation error has been estimated and a first quality check has been done.

1. Compute innovation $\Rightarrow (y - Hx_f)$
2. Perform quality control on observations
3. Construct innovation matrix $\Rightarrow M = (HP^f H^T + R)$
4. Invert the innovation matrix M
5. Correct the model state.

3. Correlation length scales

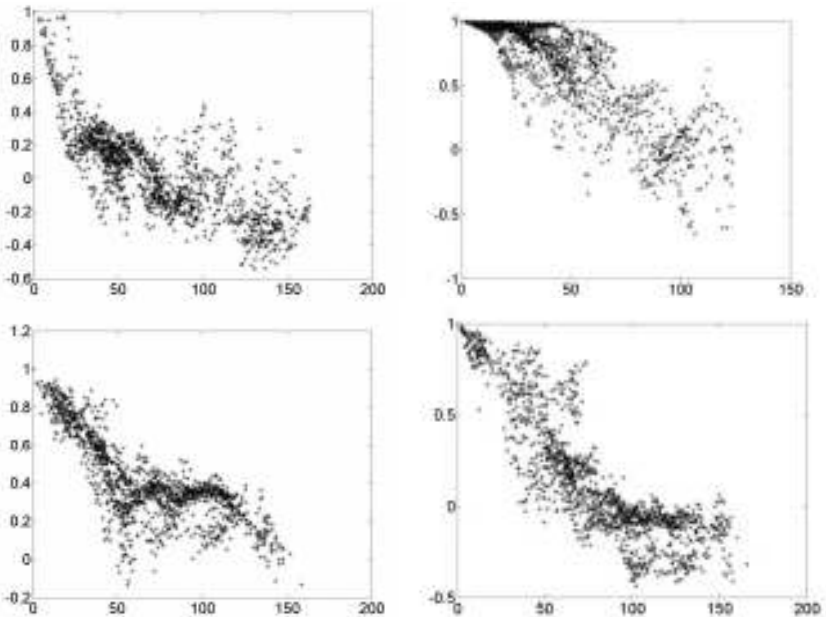

Figure 1 SST correlations between four arbitrarily-chosen points in a sub-area in the NW Baltic Proper and neighbouring gridpoints. The x axis is the distance in km and the y axis is the correlation coefficient.

The estimation of the correlation length scale for SST has been based on the innovation vector, i.e. the difference between the background and the observation fields. The method of only using observations normally results in too large length scales. All data

presented here is from the ODON year 2001 and the sparseness of satellite data restricts the value of the computed length scales. However, it has been possible to get a qualitative picture of the whole region which may then form the basis for constructing the error covariance matrix. There is a clear seasonal cycle with the largest length scale during winter. At areas with frequent upwelling much smaller length scales are observed. Generally the shape of the covariance matrix has a more elliptic shape close to the coast while it is more Gaussian-like offshore. Figure 1 shows an example from the NW Baltic Proper where four different points have been correlated with other points in a chosen rectangle of the size of 200×200 km. If a value on the correlation of 0.5 is chosen as a limit, the upper left panel which is a near-coastal point seems to have a typical length scale of 20 km while others show scales up to 50 km.

The purpose of the investigation where one example is shown in Figure 1 is to create a space-dependent and seasonally varying correlation length scale. To better include the near-coastal effect, the correlation length scale is limited by a factor which decreases when approaching the coast. An example of a factor matrix is shown in Figure 2 (right).

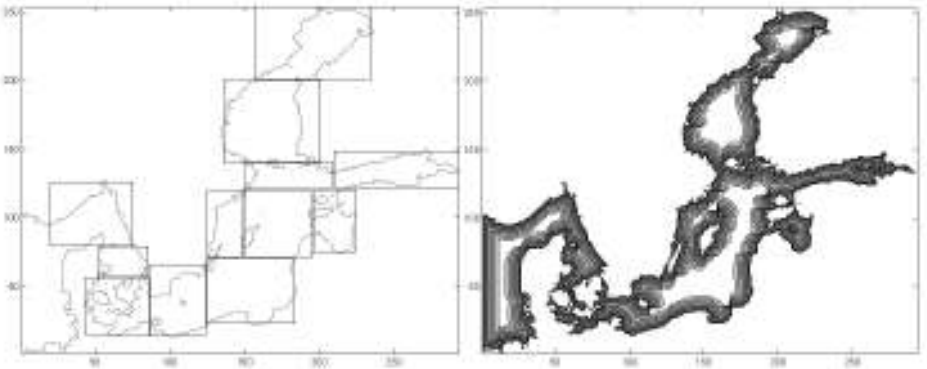

Figure 2 Left: An example of a division of the area into thirteen overlapping boxes; Right: Gradual decrease of length scale when approaching the coast.

4. Assimilation of temperature

Experiments limited to assimilating temperature in the Baltic Sea have been performed for the ODON year 2001. Using satellite data normally results in a redundant data set. However, it can be mapped into a much smaller one that contains almost the same information. This results in what is normally called “super-observations”. The reason for doing this is to decrease the dimension of the innovation matrix which has to be inverted. To further decrease the computational work the area has been divided into overlapping boxes as shown in Figure 2 (left) and the boxes overlap with the maximum length scale.

4.1 Sea surface temperature

As a result of assimilation of SST an example for the SW Baltic is shown in Figure 3. The model was run with no assimilation for several months resulting in higher temperature (upper left) compared to the subjective analysis (lower left). After one assimilation the temperature has decreased up to one degree. The five super-observations are marked as circles in Figure 3.

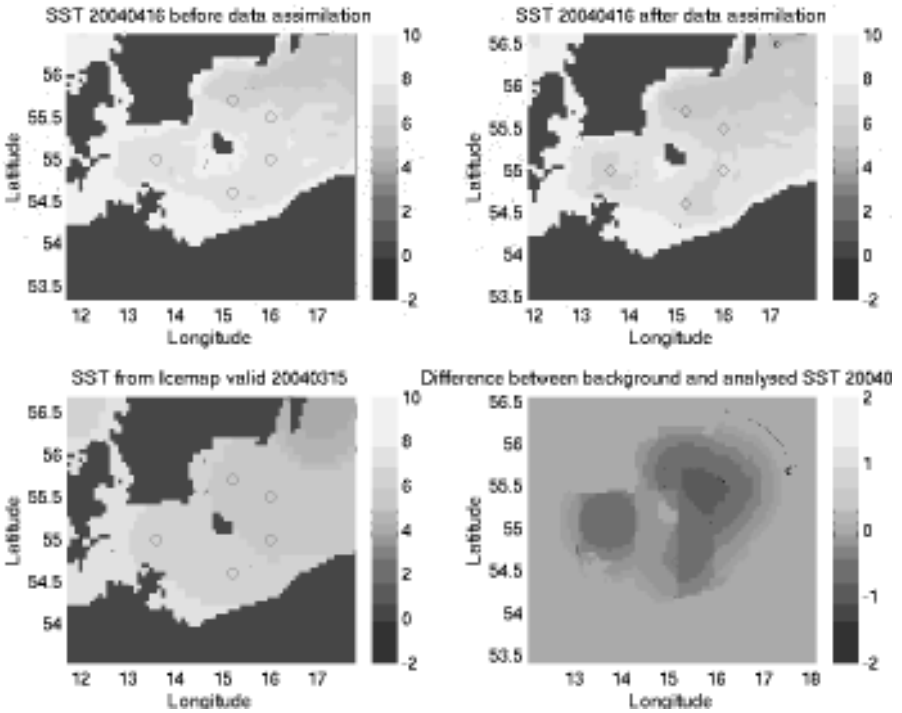

Figure 3 Results from assimilation of SST in SW Baltic. The upper figures show SST before and after assimilation. Super-observations are marked as circles. The lower left figure shows a subjective analysis of SST from *in situ* and satellite data averaged over three days. The lower right shows the difference between the background and analysed field.

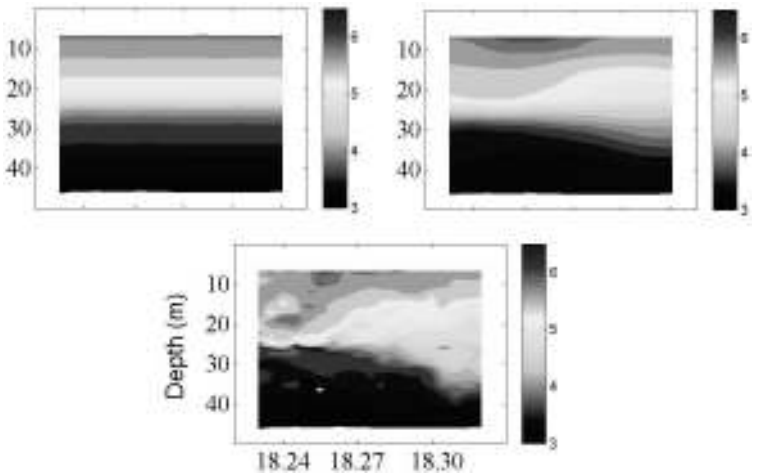

Figure 4 Assimilation of temperature in a near-coastal section in the NW Baltic Proper. Top left panel shows climatology, here used as the background field. Top right panel shows the result of the assimilation using 10 observations. The observed temperature from CTD measurements are shown in the lower panel. Longitude values are on the x-axis.

4.2 Assimilation of vertical temperature profiles

Figure 4 shows an example of assimilation of temperature profiles in a near-coastal section in the NW Baltic Proper. For this particular case, the vertical length scale was set everywhere to 5 m, but should be a function of the temperature gradient. The lower figure with the observations clearly shows the variable horizontal length scale, which for temperature is shortest in the thermocline region and largest in deeper water.

5. Conclusions

The development of an OI scheme has been shown to improve both the SST and the development of the thermocline. However, much work remains to further improve the variable correlation length scale in the horizontal as well as in the vertical. Proper values of the horizontal length scales seem to lie between 20 and 50 km, while the vertical may vary from only a few metres up to 50 m in the deepest parts.

The analysis scheme is still under development and will be extended to also include salinity, resulting in a 3D multivariate scheme.

Acknowledgements

This work has been financed by the EU Framework V programme ODON.

Assimilation of sea surface temperature and sea ice concentration in a coupled sea ice and ocean model

Jon Albretsen and Ingunn Burud*

Norwegian Meteorological Institute

Abstract

Derived sea surface temperature (SST) and sea ice concentration (SIC) from satellite observations are assimilated into a coupled sea ice–ocean model covering the Nordic seas and the Arctic Ocean. The SST data are assimilated using a simple heat flux nudging method, while the temperature below the sea surface is changed through the vertical diffusion scheme only. The SIC data are assimilated through nudging of the ice production rates. Model disruptions are avoided by having sufficiently long assimilation windows and fairly weak nudging coefficients.

The model system has been run operationally for more than three years as a monitoring and forecasting system for the Nordic seas and the Arctic Ocean. The assimilation of SST and SIC is shown to be effective in the sense that it clearly improves the forecast with only a slight increase in the processing and computational costs. The operational run is compared with control simulations, which are run in parallel without any data assimilation, and with SST observations. Comparison with CTD-observations from research vessels, moored and drifting buoys and *in situ* temperature profiles also shows a positive impact from assimilating remotely sensed SST.

Keywords: Assimilation, operational, sea surface temperature, sea ice concentration, Arctic Ocean, Nordic seas

1. Introduction

The Norwegian Meteorological Institute (met.no) has a mandated responsibility for monitoring and forecasting ocean and sea ice conditions in the Nordic seas and the Arctic. To meet this responsibility, met.no processes, by routine, available observations to produce maps of sea surface temperature (SST) and sea ice concentration (SIC), as well as running numerical forecast models for ocean circulation and sea ice. This paper shows how these newly developed operational SST and sea ice observation products are assimilated into the models with the aim of improving the forecasts. Given that the forecasts need to be produced daily in the operational system, it is important that the assimilation scheme requires a minimum of extra computer capacity. The approach was then a simple assimilation scheme where heat flux and ice production rates are nudged according to the SST and SIC observations. Although there are several weaknesses in using these simple nudging schemes, it will be shown that when observations are reliable and the data density is sufficiently high, there is a positive impact, and the error is reduced.

* Corresponding author, email: ingunn.burud@met.no

2. The ocean forecast model

The operational model system consists of an ocean model, a sea ice model and the coupling between them. The atmospheric forcing is provided from the operational model at the European Centre for Medium-Range Weather Forecasts (ECMWF). The models run on a polar stereographic grid that extends from about 50°N in the North Atlantic and includes the Arctic Ocean. The horizontal grid spacing is 20 km. The bathymetry used is interpolated to the model grid using an enhanced version of the ETOPO-5 database from the National Geophysical Data Centre (NGDC).

The ocean model is met.no's operational model MI-POM (met.no's version of POM) (Engedahl, 1995). This is a version of the sigma coordinate model POM (Princeton Ocean Model) (Blumberg and Mellor, 1987). At the open boundary towards the south, a flow relaxation scheme applies climatological data. The model is also relaxed towards climatological salinity and temperature at depths greater than about 1000 m. Also implemented is fresh and brackish run-off from rivers and/or estuaries. Tidal forcing is not applied to this model.

MI-POM is coupled to a state-of-art dynamic-thermodynamic sea ice model, MI-IM (met.no's Ice Model) (Røed and Debernard, 2004). MI-IM is based on the elastic-viscous-plastic dynamics of Hunke and Dukowicz (1997) and the thermodynamics of Mellor and Kantha (1989). Every model hour, the sea surface state and the sea ice state are exchanged between the models. MI-IM receives sea surface variables such as temperature, salinity and currents from MI-POM. SIC and sea ice velocities are sent to MI-POM to be used in the momentum stress calculations. A net heat flux is also calculated in MI-IM both in ice-covered and ice-free regions, and this flux is used as a surface boundary condition for temperature in MI-POM. The heat flux is calculated using a "skin-to-bulk" parametrisation since the upper temperature level in MI-POM is below the sea surface, i.e. between the two first sigma levels. The short wave radiation absorbed above the upper temperature grid point is added to the net heat flux, while the remainder is attenuated according to a tabulated function (Jerlov, 1976).

3. Satellite data

The OSI-SAF produces twice daily maps of SST on a 10 km grid. From each satellite pass, a 1.5 km resolution SST product is derived, and a 10 km resolution composite is produced by accumulating the high-resolution data over 12 hour periods. At high latitudes, the 1.5 km high-resolution products are calculated from AVHRR data from the polar orbiting NOAA satellite passes. The high latitude OSI-SAF SST is routinely validated against *in situ* observations from drifting buoys. Validation shows that the product error has an overall standard deviation below 0.5ºC when cloud cover is below 10%.

An automatic analysis system that derives SIC from SSM/I on a daily basis is also implemented at met.no. The analysis is produced on the same 10 km grid as the SST product (current OSI-SAF SIC analyses are global, but they were not used in these experiments). The automatic OSI-SAF sea ice analysis is validated against navigational ice analysis and weekly overview ice charts issued by the ice centres in Denmark and Norway (DMI and met.no), and the SIC values are defined as "good" when the average deviation is

below 10%, and "acceptable" when the same deviation is between 10% and 30%. Data comparison for the first four months of 2002 showed that the SIC product had an accuracy of 10% in 85–90% of the cases. While the SIC seemed to be underestimated off the Greenland East coast, the estimates were more correct off the Greenland West coast. More information on OSI-SAF SST and SIC products and validation can be found at http://saf.met.no.

4. Assimilation schemes

In the met.no operational suite, each daily run produces a 10 day forecast from noon UTC, which is the model's analysis time. Every run has a 30 hour assimilation window, also called hindcast period. All the latest OSI-SAF data are then used to assimilate the SST and SIC analysis into the ocean and sea ice models, respectively. Note that the final SST analysis, which is assimilated into the model, consists of the last five days' 12 h OSI-SAF SST composites successively overlaid on a digitised, smooth SST map produced weekly by met.no's Ice Mapping Service.

A heat flux nudging method is used to force the ocean model toward the SST analysis. The heat flux used as the surface boundary condition for temperature in the vertical diffusion equation can be expressed mathematically as $F_h = \alpha F_c + (1-\alpha)F_i$, where $F_c = -k_T(T_a - T_m)$. Here, α is a weight factor between 0 and 1, F_c is the heat flux correction and F_i is the net heat flux calculated in the model. F_i is the sum of short and long wave radiation and turbulent heat fluxes and is calculated from atmospheric variables and SST that is updated in the sea ice model by the ocean model. F_c is the difference between the analysed SST, here denoted T_a, and the SST in the model itself, denoted T_m, multiplied with a flux coefficient or the "nudging" factor k_T. The value of k_T and the thickness of the upper vertical sigma layer decide how fast the model temperature approaches T_a. Larger values of α are chosen if the SST analysis is more reliable, dependent on the spatial coverage of the satellite data and the quality indices. In the operational runs, the value α=0.9 is chosen. During the prognosis period, α=0.9, i.e. only the heat flux from the sea ice model, F_i, is used as surface boundary condition for temperature in the ocean model.

The sea ice model receives an updated field with the OSI-SAF SIC valid at 12 hours before model analysis time. A nudging scheme is then executed for the first 18 hours of the hindcast period. The nudging of the model values towards the data consists in melting or freezing of ice, which in the model translates into modifying the ice production rates. An assimilation production rate, W_{assim}, representing the difference between the sea ice concentration from the analysed data and from the model itself at each grid point can be expressed as $W_{assim} = K(C_a - C_m)$, where K is a tuning factor determined empirically. The factor K determines how fast the model SIC approaches the data, and the chosen value of K corresponds to a timescale of approximately 27 hours. C_a and C_m are the analysed and model SIC, respectively. When the model overestimates the SIC, ($C_a - C_m < 0$), all the net ice melt in the ice covered portion of a unit is exploited to decrease the ice fraction, i.e. lateral melt. The ice production rates at the atmosphere–ice interface and ice–ocean interface are then expressed as $W_{ai} = \alpha W_{ai}$ and $W_{io} = \alpha W_{io} + (1-\alpha)W_{assim}$, respectively. The weight α is a value between 0 and 1. During the forecast period, α = 1, i.e. the only production rates utilised are those from the sea ice model.

Similarly, when the model underestimates the SIC ($C_a - C_m > 0$), the production rate at the atmosphere–ocean interface is modified so that $W_{ao} = \alpha W_{ao} + (1-\alpha) W_{assim}$.

5. Impact of the data assimilation

The model system has been run operationally for more than three years, but the data used to study the impact of the assimilation were extracted during three months from December 2002 to February 2003. Two model runs in forecast mode within this period, one with assimilation and one without, have been compared with OSI-SAF values, both SST and SIC, to calculate the prognosis error.

The root mean square error (rmse) between the forecast model values and the OSI-SAF data was calculated for each 12/24 hour SST/SIC composite and averaged over the three month period. Nudging the model toward the observed SST appears, as expected, to lower mean rmse throughout the whole forecast period compared to the run without assimilation (Figure 1, left). The rmse in the run without any SST assimilation is about 0.5ºC larger than for the assimilated run, and it increases slightly due to errors in the numerical weather prediction of the heat flux prognosis. A similar improvement is obtained from the nudging of the SIC (Figure 1, right). As the sea ice model is known to freeze too much ice during winter time the significant high rmse in the no assimilation run can be attributed to the poor thermodynamic parametrisations in the model.

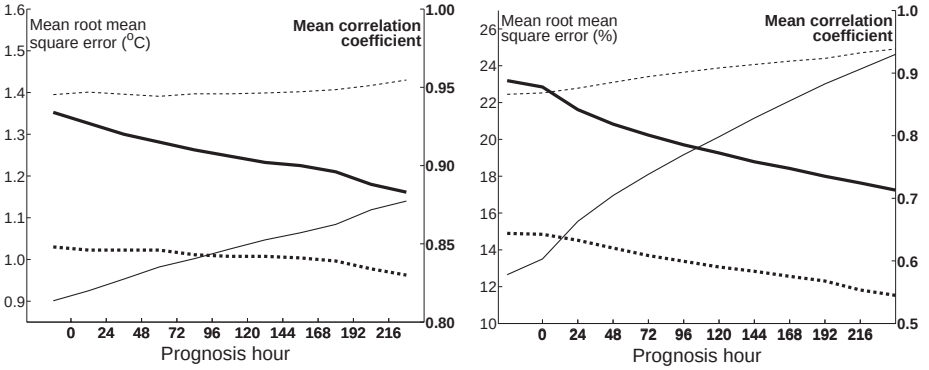

Figure 1 Left: Mean root mean square error and mean correlation coefficient (bold line and bold dotted line with scale to the right) of model SST taken over all OSI-SAF values over all 12 hour composites during a three month period. Right: Mean root mean square error and mean correlation coefficient (bold line and bold dotted line) of model SIC taken over all OSI-SAF values over all 24 h composites during a three month period. The solid and the dashed line present the rmse for the run with and without assimilation, respectively, and the means are taken for each prognosis hour.

While the root mean square error indicates how far model values are from observed values, the correlation coefficient is less sensitive about the absolute model error. The correlation coefficient is designed to detect similarities in the variability of the observed and modelled values. The mean correlation coefficient is taken over all composites for each prognosis hour and shown in Figure 1 (bold lines). The correlation coefficient is, as expected, highest in the run with assimilation of both SST and SIC with maximum mean correlation coefficients of 0.93 for the SST and 0.89 for the SIC. Their minima, seen at

the end of the forecast period, are 0.88 for the SST and 0.71 for the SIC. The mean correlation coefficients in the run without assimilation are close to constant during the forecast period with 0.84 for the SST and 0.6 for the SIC. This shows that the model adjusts toward the observed state through the assimilation period and remembers some of this information during the forward integration in the forecast period.

Several buoys, both moored and drifting, operate in the area and send near real time SST observations through the GTS (Global Telecommunication System). Around 100 measurements were available every 6th hour during the three months from December 2002 to February 2003. The rmse increases here from about 1.2 to 1.4ºC during the forecast period (not shown). Compared with the errors relative to the OSI-SAF observations, the rmse against buoy observations is about 0.3ºC higher for both runs. The relationship between the two model runs is however similar.

Observation errors are not accounted for in the assimilation or the validation, and it is also assumed that the SST in the model represents the same vertical level as for the SST observations. Assumptions like this could affect the quantitative error estimates, but the relative difference between the model runs should be representative. Since model SST does not exactly represent the surface, it has also been compared with CTD measurements. The upper temperature value has been extracted from more than 400 CTD profiles off the Norwegian coast. The observation depth varies from 1 to 5 metres, which is a better representation of the model SST than the surface measurements from OSI-SAF and the buoys. The rmse is lower than for the other rmse estimates (OSI-SAF SST and SST from drifting and moored buoys). The minimum rmse in the runs with assimilation is about 0.77ºC, and it increases to about 0.85ºC for the 10-day forecast.

The Ocean Weather Station 'Mike', located at 65ºN 2ºE, measures temperature profiles approximately once a week. These data have been compared with corresponding temperature profile data from the runs with and without assimilation (not shown). The error in temperature in the run with assimilation has its smallest values near the surface, and the error increases with depth. Along the surface the difference is reduced from 3–4°C to approximately 1.0ºC in this period, and at 100 m depth the difference is reduced by 1.0ºC. In the run without assimilation the error is more or less constant with depth and time with values near 4.0ºC.

6. Conclusions

Remotely sensed observations of sea surface temperature and sea ice concentration have been assimilated into an operational sea ice and ocean model. The OSI-SAF SST and SIC data are shown to have small observation errors. The assimilation schemes used, based on nudging, do not explicitly utilise information on the error characteristics of the model and the observations, and therefore are dependent on observations with small errors and good spatial coverage. The main strength of these assimilation schemes is their low processing and computational costs.

The nudging schemes used are monovariate assimilation methods, where other model variables are changed according to the physics in the model. Correcting only SST in an ocean model will usually only give minor changes in the interior density field. The assimilation of SST is shown to give positive impacts on the SST forecast, and this

positive impact diminishes, but is maintained throughout the ten-day forecast period. The positive impacts are shown to propagate downward when comparing model analysis with *in situ* temperature profiles. Also, the sea ice model adjusts toward observations through the sea ice assimilation period and remembers some of the information during the forecast period.

In order to improve the results a more advanced (multivariate) assimilation scheme is required. The SEIK (Singular Evolutive Interpolated Kalman) filter is therefore currently being implemented at met.no with the purpose of improving the assimilation, still keeping the computational costs sufficiently low to perform daily forecasts.

Acknowledgements

The authors are grateful to Bruce Hackett, Lars Petter Røed and Steinar Eastwood, all at the Norwegian Meteorological Institute, for valuable discussions and information during the work. Thanks also to Knut Barthel, Geophysical Institute, University of Bergen, for making the data from Station Mike available, and Øyvin Strand, Institute of Marine Research, for making the CTD-data from different research vessels available. This work has been part of the projects MONCOZE (Monitoring the Norwegian Coastal Zone Environment) and UNISOF (Use of New *In Situ* Observations on Ocean Forecasting), supported by the Norwegian Research Council under contract no. 143559/431 and 152880/120, respectively.

References

Blumberg, A.F. and G.L. Mellor (1987). A description of a three-dimensional coastal ocean circulation model, In: Three Dimensional Coastal Ocean Models Vol. 4, N. Heaps (Ed.), American Geophysical Union, Washington D.C., 1–16.

Engedahl, H. (1995). Implementation of the Princeton Ocean Model (POM/ECOM-3D) at the Norwegian Meteorological Institute (DNMI). Research Report 5, Norwegian Meteorological Institute, P.O. Box 43 Blindern, 0313 Oslo, Norway.

Hunke, E.C. and J.K. Dukowicz (1997). An elastic-viscous-plastic model for sea ice dynamics, J. Phys. Oceanography, 27, 1849–1867.

Jerlov, N.G. (1976). Marine Optics, vol. 14, Elsevier Sci. Pub. Co., Amsterdam.

Mellor, G.L. and L. Kantha (1989). An ice–ocean coupled model, J. Geophysical. Res., 94, 10,937–10,954.

Røed, L.P. and J. Debernard (2004). Description of an integrated flux and sea–ice model suitable for coupling to an ocean and atmosphere model, met.no report no. 4, Norwegian Meteorological Institute, P.O. Box 43 Blindern, 0313 Oslo, Norway.

GSE programme benefits to Baltic Sea ice navigation

Ari Seina*, Pentti Malkki and Hannu Grönvall

Finnish Institute of Marine Research, Finland

Abstract

Efficient winter navigation in the Baltic Sea is an important factor for the functioning of the European transport system. Safe, reliable and frequent sea transport connecting the Baltic Sea ports and Western Europe all year round is essential for shippers when they choose between transport solutions by sea or on land. A transport system, where the cargo is delayed for days every winter due to ice, is a heavy drawback for industries that are dependent on "just in time" deliveries, therefore better and more effective ice information is needed.

ICEMON was a 20-month (2003–2004) ESA GSE project with objectives to establish the integrated, European, operational, high latitude meteorological, ice and ocean information services available to users through a single interface/contact point. The future service will be implemented through a network of existing service providers, who already deliver operational services. A suite of new monitoring products based on satellite data and model forecasting products will be developed and implemented by 2008. Polar View, the continuation project of ICEMON, will focus on lowering barriers in services identified in ICEMON.

Keywords: GMES, GSE, ESA, ice monitoring, Baltic Sea

1. Introduction

GMES (Global Monitoring for Environment and Security) is a joint programme launched by the European Commission and European Space Agency (ESA). GMES objectives are to establish European capacity for provision and use of operational information for GMES, production and dissemination of information in support of EU policies for environmental and security, and start a permanent dialogue between stakeholders and in particular between providers of services and users. ESA is responsible for building up operational services; the GMES Service Element (GSE). ICEMON and Polar View were ice-related projects in the first stage of GSE in 2003–2004.

ICEMON was coordinated by met.no, Norway, and 18 partners and two associated projects from 8 countries participated. These were Conrolware from Belgium, CIS from Canada, FIMR, VTT and SMA from Finland, Ifremer from France, AWI from Germany, met.no, NERSC, KSPT, KSAT, NP and DNV from Norway, SMHI from Sweden, and Vexcel and ULC from UK. EuroClim and IRIS projects were associated partners. Partners represented service providers, system developers and core users. ICEMON identified the four most important policy sectors where ice monitoring is needed: marine safety, climate change, environmental issues and resource administration.

* Corresponding author, email: Ari.Seina@fimr.fi

A number of demonstrations were conducted during the project. Demonstrations concentrated on the Fram Strait and Svalbard areas in the European Arctic, the Kara Sea in the Northern Sea Route, and the Baltic Sea, and included for example high-resolution ice thickness charts and medium resolution ice forecasts in the Baltic Sea, high resolution ice charts in the Svalbard area, SAR images to vessels in the Kara Sea area, and medium resolution ice charts and ice drift charts in the Arctic. Most of the products supported safety at sea and also climate issues. Demonstrations were published on the project web pages (www.icemon.org) (See also Sandven, 2005).

2. Baltic Sea requirements

2.1 Marine transportation

The Baltic Sea freezes annually, and its ice season lasts from weeks in the south up to seven months in the north. The maximum annual ice extent occurs between January and March, when ice covers an average of 218000 km^2.

Ice ridges and brash ice barriers are the most significant obstructions to navigation. Powerful, ice-strengthened vessels can break through thick level ice, but they are not capable of navigating through ridges and heavy brash ice barriers without icebreaker assistance. Ice dynamics cause high pressure in the ice field and can be dangerous to vessels, and may cause time delays up to several days. Under normal conditions the sailing time from the ice-edge to the northernmost ports of the Baltic Sea is one day (400 nautical miles), but under severe conditions it can extend to one week (Gronvall *et al.*, 2002).

The two most heavily navigated waterways in the world, where seasonal sea ice plays an important role in navigation, are the Gulf of St. Lawrence in Canada and the Baltic Sea in Europe. In the Gulf of St. Lawrence some 180 million tons of goods are transported annually. The total cargo turnover in the Baltic Sea is about 700 million tons, some 40% of which occurs during winter.

In Finland almost 90% of foreign trade is transported by sea. The annual turnover in 2004 was 95 million tons. During the winter months there are more than 25000 port-calls in Finnish harbours with transport of about 40 million tons of goods. The winter marine transportation is worth about 28 billion Euro. It should also be noted that about 90% of marine transportation has tight timetables.

Marine transportation has increased worldwide. In the Baltic Sea, the number of vessels that sailed in the Gulf of Finland in 2001 was 38000 (port calls); in 2015 this is expected to rise to 53000. Russian oil export is growing rapidly. About 76 million tons of oil was transported through Gulf of Finland in 2002; in 2005 it will be more than 100 million tons, and by 2015 this is expected to grow to at least 200 million tons.

Winter navigation is made possible by the use of icebreakers, ice-strengthened vessels and by restricting navigation. Navigation is restricted by closing half of the harbours for the winter, and icebreakers only assist vessels suitable for ice navigation.

During the last ten years the marine traffic has increased in Finland by 34%, and the trend is expected to continue: by 2015 it is expected to grow into 130–150 million tons a year. In the same period, however, the number of icebreakers has not increased. The

smoothness of traffic has been possible due to better ice monitoring, where the use of EO data has become more and more important. Icebreakers need detailed ice information for route planning. Considerable savings in ice navigation could be achieved by optimising the use of satellite-based operational ice monitoring.

National ice services are responsible for collecting, analysing and distributing sea ice data. The input data consists of ground truth, visual and/or digital air-borne data, and space-borne data from various satellites. All these data are collected by the ice services using various means of communication.

The value of an ice chart is determined by its accuracy and validity. The real-time aspect is important as the ice conditions change over time. Ice charts issued on a daily basis are the most important and widely used ice information products from the Baltic Sea ice services.

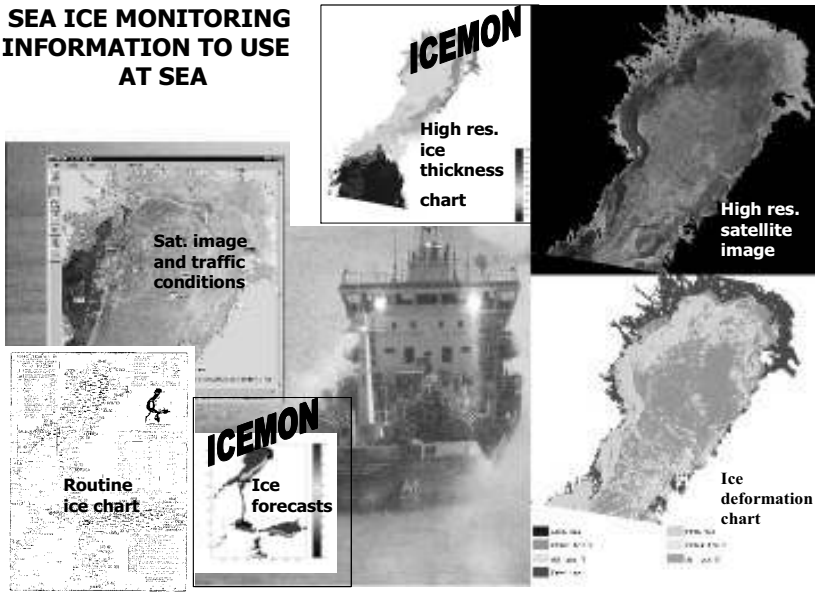

Figure 1 Set of ice information available to users at sea from the Finnish Ice Service. High-resolution ice thickness charts and ice forecasts were ICEMON products and services.

2.2 Product and service requirements

In ICEMON many challenges were found which must be solved — better cooperation with service providers is needed, acquisition of EO data is not coordinated among the service providers, EO data policy and price policy is a barrier for operational data users, heterogeneous data formats are a barrier for efficient exchange of data, *in situ* data are not easily available, products and quality of products are heterogeneous, there is an inefficient distribution of products from providers to users, access to databanks is not streamlined, and new expanded and integrated services should be considered. In future there are requirements that EO data should be used more effectively in ice monitoring, and there should be a better information distribution system between providers and users (Seina, 2004).

User requirements for the Baltic Sea are:

1. Products must meet user requirements. Products must contain the most usable information in a clear and understandable format.
2. Products must be of good quality. At the moment there are nine ice services in the Baltic Sea publishing products with variable quality. The quality of output products cannot be better than input data, thus quality is highly dependent on use of EO data. With more extensive use of EO data, and especially high-resolution data, quality of output products could be made better.
3. Coverage must be according to user needs. Users on land need coarse, wide.scale ice information, while users at sea need information for a relatively small area.
4. Resolution of products must be at the user's scale. Ships need information in ship's scale. Today routine ice charts have at best a 1 km scale, when ships require information over a 100–400 m scale.
5. Time-lines must be user friendly, and information available when users need it. There are basically two kind of requirements: near real-time (1–6 h) and off-line. Near real time users should have a 24 h service. Forecasts should cover a useful period: for users on land from days to a week ahead; for users at sea 25–54 h is most suitable.
6. There should be one or few contact points, where users can download the information of their choice. Today the customer must contact each service individually.
7. The distribution system must be reliable and meet user requirements. File sizes must be adequate for use under poor communication systems for users at sea.

3. ICEMON in the Baltic Sea

3.1 Products and services in the Baltic Sea

During the ICEMON project in the Baltic Sea two types of products were delivered: high-resolution ice thickness charts and ice forecasts (see Figure 1).

SAR data were used to produce more accurate ice thickness charts than those provided by ice services. The charts were operationally produced after a SAR image was received, using the latest available routine ice chart as initial data on which local modifications were made based on SAR statistics. This product is available when RADARSAT SAR images are available and can be delivered to users in near real time. The charts were produced in 500 m resolution, and delivered in near real-time to Finnish and Swedish icebreakers, Finnish ice service, Finnish and Swedish Maritime Administration, a selective number of ships, and also published on the project's web pages.

The forecasts of sea–ice motion, concentration and ridging in the Baltic Sea for the next 54 hours were produced by FIMR (Finland) and SMHI (Sweden). SMHI in Sweden provided ice forecasts using the HIROMB model. Two advanced models are used in FIMR: the multi-category sea–ice model (HELMI), which included separate classes for un-deformed and deformed ice types, and the IRIS sea–ice model where ridge characteristics were calculated according statistical principles. Both model outputs were in a one nautical mile resolution, providing information on a daily basis for ice-edge, ice concentration, mean level thickness, ridged ice thickness, ridge density and ridge height in +12 h, +24 h, +48 h, and +54 h intervals. BIRIS and HELMI models, covering the Baltic Sea,

were run on a daily basis and forecasts were made available through the ICEMON web pages. The HELMI model was run operationally and the IRIS model semi-operationally.

3.2 Cost-benefit analysis

The ICEMON project was from a cost-benefit point of view a sound investment, since society as a whole will gain economic benefits higher than the cost of investments. Additionally, a large number of intangible benefits were identified as having a positive impact on society (Holt Andersen *et al.*, 2004).

The ICEMON Service Portfolio consisted of a number of near real-time and off-line products. NRT products in particular were aimed at operational users to improve transport navigation and offshore operations in ice covered areas as well as the quality of environmental monitoring in the Arctic. Off-line products were mainly to improve risk assessments of maritime constructions and operations leading to improved safety at sea and they also serve as an important input for understanding global change issues.

The main innovative aspects of the ICEMON Service Portfolio compared with existing ice services and products were: a) high-resolution products, b) cost-effective production line, c) one-stop-shopping facility for all ice products, and d) product format and delivery optimised for customer use.

Of the six market segments identified in the ICEMON project, ice navigation and sea transport, off-shore and ship design, and environmental monitoring were considered to be the most promising segments in terms of market growth and demand for ICEMON services.

Three main drivers affecting the future demand for ice services have been identified: ship traffic, oil exploitation and environmental concerns leading to an increased level of regulation.

Cost savings due to reduced sailing time for ships *en route* in the Baltic Sea during the ice season were the main direct benefits of ICEMON services and account for the majority of all measured monetary benefits (63%). Cost avoidance due to the reduced risk of major oil spills in both the Baltic Sea, the Barents Sea and along the NSR made up the second largest area of benefits (21%). Offshore operations such as design and logistics were also an important area and are likely to have been underestimated in the analysis.

The realisation of the identified benefits, both tangible and intangible, does not come automatically. The market uptake, e.g. the timing and the level of user acceptance will be the single most important challenge facing the successful implementation of the findings in ICEMON. That is, the degree to which ICEMON will manage to become part of existing and emerging ice information service chains and thereby realise the potential benefits. Some areas of potential benefits are more risky in terms of realisation than others. The positive news is that the bulk of the identified monetary benefits are associated with rather well-established segments, e.g. ice navigation in the Baltic Sea, while the more risky areas are associated with offshore operations accounting for a conservative estimate of 14% of total identified monetary benefits. In any case a well-planned service provision strategy to be implemented in due course will be critical to ensure benefits are fully explored.

4. Conclusions

Globalisation has increased marine transportation worldwide. In the Baltic Sea marine transportation has been increased by about 33% during the last ten years, and a similar trend is expected to continue. With increasing marine transportation in the Baltic Sea, user requirements for better quality and quantity in sea ice information have increased.

During the ICEMON project more user-friendly high-resolution products were demonstrated. In the near future this kind of product must become fully operational, and in particular new products with user scales must be developed. There is a need for one system or systems with one or very few contact points, where users at sea could download all information needed. This could mean radical changes in national ice service operations. However, new services must be as sustainable as the present services. This means that they must be available — readily accessible when users need them, and they must be available now and also in the future. They must be reliable — consistently meeting user-defined quality and standards. They also must be affordable — the service benefit must justify the costs.

A cost benefit analysis showed that it is worth investing in the new system, and the benefits could be large. The ICEMON project was from a cost-benefit point of view a sound investment, since society as a whole will gain economic benefits higher than the cost of investments. Additionally, a large number of intangible benefits were identified as having a positive impact on society.

In the first stage of the GSE Programme, the sea ice related projects Northern View and ICEMON already started to cooperate. In 2005 these projects have been merged into the Polar View project. Polar View aims to build up a fully operational system by 2008, where users constantly validate products and services; there are multi-year contracts with users; the number of user is expected to grow radically; central activities also include user training; there will be a network for development and delivery especially to R&D projects which could upgrade new products and services into operational level; marketing will be coordinated; and licensing and procurement agreements could be made more effective.

References

Gronvall, H. and A. Seina (2002). Satellite data use in Finnish winter navigation, in Flemming, N.C., S. Vallerga, N. Pinardi, H.W.A. Behrens, G. Manzella, D. Prandle, and J.H. Stel (eds.) Operational Oceanography: Implementation at the European and regional scales, Elsevier pp. 429–436.

Holt Andersen, B. and N. Schumacher (2004). Cost Benefit Analysis of ICEMON Service Analysis — deliverable C2, Stage 1 Version 2, Service Consolidation Actions on the Earthwatch GMES Service Element.

Sandven, S. (2005). Towards operational services in the Arctic. This volume page 541.

Seina, A. (2004). Strategic Plan — deliverable S1, Stage 1 Version 2, Service Consolidation Actions on the Earthwatch GMES Service Element.

Dynamical modelling of underwater visibility

S. Loyer*[1], F. Jourdin[2], P. Le Hir[3] and P. Lazure[3]

[1]*ATLANTIDE, Technopole Brest Iroise, France*
[2]*EPSHOM/CMO, Brest, France*
[3]*IFREMER/DYNECO, Centre de Brest, France*

Abstract

Among the various missions assigned to the SHOM and responding to the French Navy and public administration requests (involved in environmental affairs), one of the recent objectives is to ensure better knowledge of the continental maritime area. Among coastal projects, the one dealt with in this study consists of evaluating the optical properties of shelf waters. This project called "Turbidity" focuses more particularly on turbidity processes having an impact on submarine visibility. One of the topics of this project includes a modelling approach. The modelling theme, presented here, involves development of simulation tools coupling hydrodynamics, biological and sedimentary influences. An optical model completes this tool, in order to convert the turbidity parameters in terms of submarine visibility. The actual configuration of the model simulates the turbid waters above the French Atlantic continental shelf. Consistent with the observations, the model presents encouraging results. It reproduces reasonably well the main algal and mineral seasonal structures. Concerning the optical module, it is based on empirical laws coming from literature and is limited to a monochromatic approach; however, *in situ* measurement cruises are planned in order to be suited to the specific characteristics of the study areas. The difficulty of this feasibility study is based on the fact that neither *in situ* measurements nor model estimations are directly linked to the visibility parameters and that biological and sedimentary transport models are not able to reproduce the whole nature and multitude of particles and molecules influencing the optical properties. All this makes the visibility distances difficult to assess.

Keywords: 3D model, hydro-sedimentary and biological model coupling, suspended particulate matter, optical properties, French Atlantic continental shelf.

1. Introduction

Antisubmarine warfare, mine warfare and special operations require the prediction of underwater visibility for aircraft observers, divers and cameras using ambient (natural) light or lamps. Visibility ranges can be assessed using *in situ* measurements, satellite remote sensing of ocean colour and modelling. The latter allows conceptualisation of advances in this research field. The parameters which modify coastal ocean colours are numerous: phytoplankton pigments, mineral particles, their size distribution and index of refraction, dissolved organic matter, and others. These biogenic and mineral fractions of suspended particles are then responsible for the absorption and scattering of visible light.

* Corresponding author, email: sloyer@shom.fr

The goal of this feasibility study is to perfect an analytical model that combines hydrodynamics, biology and hydrosedimentary processes in coastal areas. We attempt a first application of numerical modelling over the shelf of the bay of Biscay. Observations and model validation are the complementary components of this study.

2. Methodology

Observations are based on satellite data and *in situ* measurements. Processing algorithms of remote sensing data have been developed and validated in the Bay of Biscay (Gohin *et al.*, 2002; Gohin *et al.*, in press; Froidefond *et al.*, 2002). They are based on empirical laws coming from studies combining SeaWiFS data with *in situ* measurements. Hence, satellite data sets provide two products: surface concentrations of chlorophyll *a* and surface concentrations of suspended particulate matter. Ocean colour sensors provide a unique means for observing the phytoplankton and suspended particles' distribution over the continental shelf.

In situ measurements are obtained during the Bio-Modycot cruises carried out by the French Hydrographic and Oceanographic Service. Since 2004, optical sensors (transmissometer, absorption meter, gelbstoff and light scattering turbidimeter) were added to the vertical CTD profiles. The aim is to provide (1) a description of the turbidity structures at different seasons, (2) correlations between hydrological, chemical, optical and turbidity parameters and (3) a dataset to calibrate and validate the model in this area.

The model is a coupling of a three dimensional hydrodynamical model with a biological and an hydro-sedimentary model. This model simulates the evolution of the main turbidity components at a scale of the whole Bay of Biscay shelf. Our study is limited to two turbidity components: the living and detrital biological particles, and the mineral particles carried out by the river plumes or stirred up from the sediment. This model is coupled to an optical module which converts the particles' concentrations to underwater visibility range.

3. Model description

The objective of the coupled bio-physical model is to determine how the forcing of meteorology, hydrodynamics and human activities influence the distribution and the abundance of turbidity in the continental margin.

3.1 Physical frame

This study is based on the MARS3D hydrodynamical model (IFREMER Brest, Lazure and Jegou, 1998). The Bay of Biscay exhibits complex hydrodynamical features with strong density gradients. Hence, these physical processes need three dimensional modelling. The temperature, salinity and current evolution over the French Atlantic shelf are computed with respect to tides, freshwater inputs and wind-induced advection and diffusion. The model uses a rectangular Cartesian grid with a homogeneous mesh size (25 km²). Ten vertical layers are used with sigma coordinates and a refinement step near the surface. The western boundary is closed to the continental slope at a depth of 200 m. The model is forced by the tide at its open offshore boundaries and by wind fields at the surface. At the upper boundary, heat transfer at the ocean surface interface is calculated using climatological values for air temperature, cloudiness and specific humidity.

3.2 Hydro-sedimentary frame

The hydro-sedimentary model is based on the SiAM3D model developed at Ifremer Brest (Cugier and Le Hir, 2001). It consists of a pelagic part, which simulates the distribution of mineral suspension particles, and a sediment part. In the pelagic part, all state variables are transported by advection and diffusion. The state variables are composed of two classes of particles size. Fine mineral particles differ from larger ones by their sedimentation rate. Sedimentary layers are created by the deposit of mineral particles. The sedimentary model is a vertical uni-dimensional model with several layers. Only the surface layer is in relation with the water column. The number of layers and thickness of the surface layer fluctuate with erosion and deposit processes according to bottom currents and swell and to sedimentation rates of particles. The dissolved component (T, S, nutrients) is contained in sediment interstitial water. Diffusion processes in interstitial water and at the interface with the water column are taken into account.

3.3 Biological frame

Biological dynamics are implemented into this three dimensional physical frame where all state variables are transported by advection and diffusion. The physical and biological models are linked through the diffusion coefficient, the transport, the temperature and the heat fluxes (light).

The biological scheme is a simplified representation of the pelagic ecosystem. The model is conceptualised for a shelf sea including the shallow sea features characterised by the replenishment of the mixed layer with nutrients from the underlying layers. Cycling of three elements is modelised: nitrogen, phosphorus and silicon. It takes into account two classes of algal size, the microphytoplankton and a small class more representative of the nanophytoplankton group. This algal biomass is subjected to loss by mortality and by zooplankton grazing. This organic particulate matter is represented by the detrital material component. The benthic compartment of the sediment simulates the storage of organic matter and its regeneration through the superficial layer of the sediment. The growth rate of the algal biomass is a function of temperature, photosynthetic available radiation and nutrient concentrations.

The biological model allows simulation of the seasonal development of algal biomass and algal blooms linked to the nutrient river loads. Therefore it is the biological component of the turbidity.

3.4 Optical frame

Underwater visual detection of objects is subject to contrast perception. A small or distant feature contrasts with its environment through observation of its relative difference of luminosity. Blackwell (1946) found that there is a reasonably constant limiting contrast for human beings. This limiting contrast can be either positive or negative depending on whether the target is brighter or darker than its background. When the target moves away from the observer, contrast reduces as light attenuates in the medium with the distance. When the contrast reaches the limit, the target can no longer be distinguished from the background by a human observer. The distance reached in this way defines the visibility range.

Thus underwater visibility depends on external lighting conditions, inherent optical properties (absorption and scattering) of the aquatic medium, spectral reflectivity of the target and human eye sensitivity. Sun or lamps carried by diver are the sources of light considered here. The effect of bioluminescence is ignored. Littoral waters, where bottom reflectivity impacts on water column light field, are not taken into account. The effect of fluorescence is also ignored.

Under such hypotheses, visibility ranges are computed in three stages (Figure 1, central box). First, inherent optical properties of turbid waters are assessed through a spectral absorption and scattering model for different kinds of in-water particles. Second, a diffuse light attenuation law defines irradiance profiles with depth. Third, an equation of contrast reduction with the distance from target to observer allows assessment of visibility range. It depends on the inherent contrast of the object, beam and diffuse attenuation coefficients, and views the angle from the horizontal (see Preisendorfer, 1986). If a black target is used, the inherent contrast is always negative unity. Therefore, the visibility range of a black target is used here as a standard product owing to its simplicity.

Photopic parameters, perceived by the human eye, are approximated with reasonably good accuracy by monochromatic parameters at a light wavelength of 530 nm (Zaneveld and Pegau, 2003).

Using Monte Carlo modelling of the radiative transfert equation, Kirk (2003) found a non-linear relationship between the vertical averaged diffuse attenuation coefficient and the inherent optical properties of water. The equation is valid even for relatively high scattering coastal waters (scattering reaching 30 times absorption). However diffuse attenuation depends also on the sun height, sea state, nebulosity and vertical inhomogeneity of waters in the well-illuminated zone. Those effects of second order cannot be assessed easily so that standard products here are for overcast sky (which is also valid for clear sky when the sun is high enough above the horizon — 45° at least), flat surface and homogeneous waters in the illuminated zone.

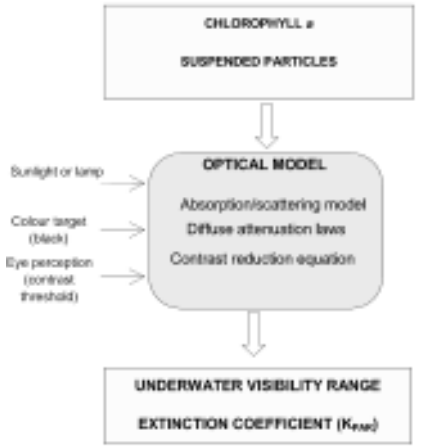

Figure 1 Schematic diagram of the optical model.

Absorption and scattering coefficients for pure water are derived from laboratory experiments of Smith and Baker (1981) and Morel (1974) respectively. Absorption rate due to dissolved organic matter is derived from Bricaud *et al.* (1998) assuming a constant concentration which is probably not satisfactory in areas influenced by fresh water inputs. Absorption and scattering rates due to variations in non-algal particle concentration derive from Babin *et al.* (2003a and 2003b respectively), and are based on data collected in European coastal waters (COASTlOOC data). On the same basis, the absorption rate due to algal particle concentration is derived from Bricaud *et al.* (2003). Following the Beer-Lambert law, the sum of all these parts gives the whole absorption and scattering coefficients for turbid water. Finally the beam attenuation coefficient is the sum of the absorption and scattering coefficients. Thus all optical parameters having given values, so visibility ranges can be computed.

4. Results

4.1 The turbid features

Spatial distribution of simulated chlorophyll *a* (Chl) and suspended particulate matter (SPM) are compared with those estimated by colour remote sensing images. In winter, strong storms lead to resuspension of sediment in the surface layer. This phenomenon, associated with large river outflows, gives high SPM loads over a large part of the continental shelf. The model result of SPM concentrations reproduces fairly well these high values and the extension of such phenomena. Due to the decrease of wind stress and strong swell, the spring situation is marked by the decrease of SPM concentrations in the surface layer. The turbidity is limited to coastal estuary areas.

In winter, turbid water reduces light penetration. With vertical mixing and low temperatures, this limits the phytoplankton development and so Chl concentrations remain low. From mid-spring to the beginning of summer, the increase of solar irradiance and nutrient loads by the two main rivers favour spring algal blooms. The freshwater inputs induce a nitrate gradient from river mouths to offshore waters. Therefore, productivity can be significant, even in turbid waters. The simulated surface concentrations of Chl shows a range from low offshore values to larger shelf values (between 2 and 5$\mu g l^{-1}$); nearly all the biomass is located in the mixed-surface layer.

Simulated spatial distribution of Chl and SPM surface concentrations have been compared with *in situ* measurements through their logarithmic values. The results are shown in Figure 2 and show discrepancies between modelled and measured values in terms of order of magnitude. This first quantitative comparison with *in situ* data displays underestimation or overestimation of the model results. Total suspended particulate matter (both mineral and biogenic) are compared in spring and summer situations.

Simulated estimates of Chl decrease too strongly in offshore waters in spring, and coastal water turbidity rates are overestimated from the end of spring to the end of summer. This discrepancy with *in situ* data is due to an overestimation of the erosion flux of mineral matter in coastal areas influenced by tidal currents.

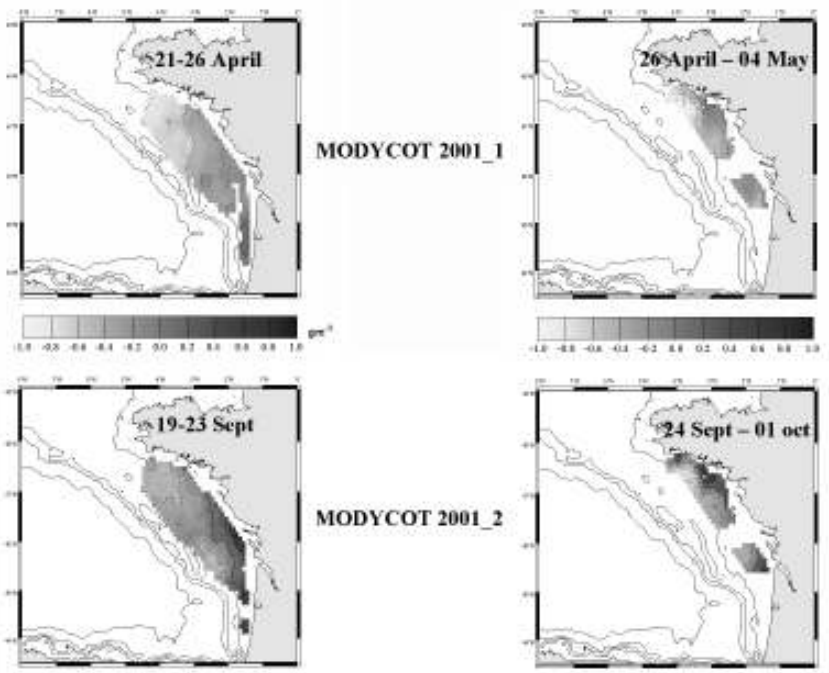

Figure 2 Distribution of differences between simulated and *in situ* measurements of total suspended particulate matter.

4.2 Optical products

Figure 3 is an example of operational products for a whole area of naval operations. It displays synoptical views of the turbid features in terms of underwater visibility ranges. The visibility range for an observer looking downward is deduced from the Duntley and Preisendorfer formulation (Preisendorfer, 1986). The range is inversely proportional to the beam and diffuse attenuation coefficients. Products are the monthly composites that represent the winter and summer situations.

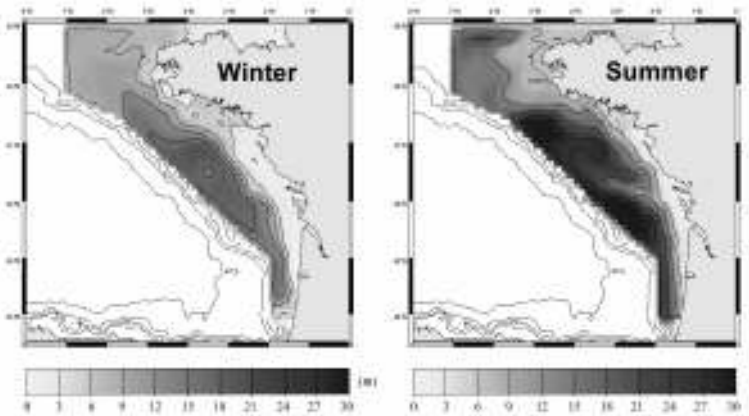

Figure 3 Monthly composites of the vertical downwelling visibility range.

In the less turbid offshore waters, from winter to summer, the vertical downwelling visibility increases from 15 metres depth to more than 25 metres depth. Along the coastal strip, visibility ranges do not vary much with the season in comparison with offshore waters. In the coastal area, concentrations of SPM remain high enough to induce a beam attenuation coefficient lower than 1 m^{-1}. Therefore, the vertical visibility remains lower than 4 metres of range throughout the year in this area. In the formulation used, mineral SPM concentration highly influences the value of the beam attenuation coefficient, and spatial distribution of low visibility (<2 m) is related to mineral SPM distribution. Therefore, the overestimation of simulated SPM concentrations during summer could lead to a likely underestimation of the vertical visibility.

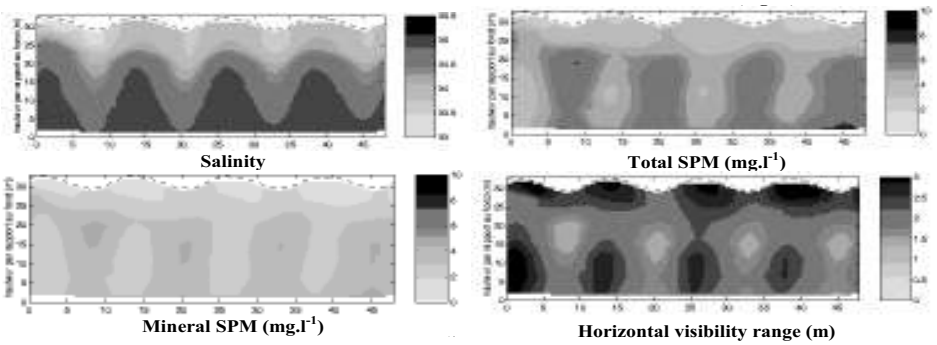

Figure 4 Simulated vertical evolution of salinity, mineral and total suspended particulate matter concentrations and horizontal visibility range (14–15 July 1998).

Figure 4 is an example of a product suited to a tactical use. It displays the evolution of vertical profiles at a fixed point over a period of two days. The point is located in front of the Loire estuary (cf. Figure 3) during a typical summer situation. Vertical profiles of mineral SPM, total SPM and horizontal visibility are displayed. Visibility ranges are also deduced from the Duntley and Preisendorfer formulation with a view angle of $\pi/2$. Model results are recorded hourly, and tidal effects are reproduced.

Surface water carries mineral SPM concentrations of about 1 mgl^{-1}. This value varies from 1 to 5 mgl^{-1} under the thermocline. Salinity profiles alternate between the two following situations: a two layer stratification and a nearly constant gradient from surface to bottom. Therefore, the isohaline 34.5 varies between 10 and 25 metres depth. The evolution of the vertical profiles follows the horizontal variation of the halocline, as the fixed point is in or out of the river plume (and its associated turbid structures). Therefore, it is difficult to observe the sole resuspension of SPM subjected to tidal stirring. Total SPM concentrations show the major role of the biogenic compartment during summer. Surface water has total SPM concentrations of about 3 mgl^{-1}. They vary from 5 to 7 mgl^{-1} under the thermocline. The increase of SPM is associated with detrital particles. These particles correspond to biological degradation processes that mainly occur in bottom layers.

5. Future prospects

This work provides an outline of the modelling of underwater visibility. Future research efforts will focus on qualitative and quantitative improvements of the model. Qualitative improvements will be additional physical processes, biological species and an optical parameter in the model. Concerning the optical parameter, CDOM (coloured dissolved organic matter) is the parameter whose dynamics need to be assessed for its impact on light absorption. Nevertheless, there is a great lack of data and knowledge to add this parameter to the model. Concerning the biological species, those impacting most on optical properties, such as coccolithophorids, should be modelled specifically. Attention should be paid also to flocculation processes. Quantitative improvements will include realistic meteorological forcings deduced from 2D nowcast spatial fields (instead of geographically invariant values) of nebulosity, wind and waves. The use of assimilation methods as a tool to improve accuracy and objectivity of the results is not yet envisaged because the error budgets on model equations, data and forcings are not known with enough confidence.

A big effort must also be made to validate the empirical laws of the optical model in the study area. Furthermore developments of the optical model will be used to derive products from ship *in situ* data (transmissometers, absorption meters) and satellite remote sensing of ocean colour.

References

Babin, M., D. Stramski, G.M. Ferrari, H. Claustre, A. Bricaud, G. Obolensky and N. Hoepffner (2003a). Variations in the light absorption coefficients of phytoplankton, nonalgal particles, and dissolved organic matter in coastal waters around Europe, J. of Geoph. Res., vol. 108(C7), pp. 3211–3231.

Babin, M., A. Morel, V. Fournier-Sicre, F. Fell, and D. Stramski (2003b). Light scattering properties of marine particles in coastal and open waters as related to the particle mass concentration, Limnol. Oceanogr., vol. 48(2), pp. 843–859.

Blackwell, H.R. (1946). Contrast thresholds of the human eye, J. Opt. Soc. Am., vol. 36, pp. 624–643.

Bricaud, A., M. Babin, A. Morel, and H. Claustre (2003). Variability in the chlorophyll-specific absorption coefficients of natural phytoplankton: analysis and parametrization, J. Geophys. Res., vol. 100(C7), pp. 13321–13332.

Bricaud, A., A. Morel, M. Babin, K. Allali, and H. Claustre (1998). Variations of light absorption by suspended particles with chlorophyll a concentration in oceanic (case 1) waters: analysis and implications for bio-opticals models, J. of Geoph. Res., vol. 103(C13), pp. 31033–31044.

Cugier, P. and P. Le Hir (2001). Modélisation 3D des matières en suspension en baie de Seine orientale (Manche, France). C.R. Acad. Sci., 331, pp. 287–294.

Kirk, J.T.O. (2003). The vertical attenuation of irradiance as a function of the optical properties of the water, Limnol. Oceanogr., vol. 48 (1), pp. 9–17.

Lazure, P. and A.M. Jegou (1998). 3D modeling of seasonal evolution of Loire and Gironde plumes on Biscay Bay continental shelf, Oceanol. Acta, vol. 21(2), pp.165–177.

Morel, A. (1974). Optical properties of pure water and pure sea water, in: Optical Aspects of Oceanography, N.G. Jerlov and E.S. Nielsen Eds. New York, Academic Press, pp. 1–24.

Preisendorfer, R.W. (1986). Secchi disk science: Visual optics of natural waters, Limnol. Oceanogr., vol. 31(5), pp. 909–926.

Smith, R.C. and K.S. Baker (1981). Optical properties of the clearest natural waters (200–800 nm), Applied Optics, vol. 20 (2), pp. 177–184.

Zaneveld, J.R. and W.S. Pegau (2003). Robust underwater visibility parameter, Optics Express, vol. 11(23), pp. 1–13.

The impact of long period assimilation of ENVISAT ASAR directional wave spectra on wave forecasts

Lotfi Aouf*[1], Jean-Michel Lefèvre[1], Danièle Hauser[2] and Bertrand Chapron[3]

[1]*Météo France, Division Marine et Océanographie, France*
[2]*CETP/IPSL/CNRS, Université de Versailles Saint-Quentin, France*
[3]*Ifremer, Laboratoire d'Océanographie Spatiale, France*

Abstract

The assimilation of directional ASAR wave spectra in the WAM wave model over a long period is performed for two different wavelengths cut off at 200 and 240 metres. The assimilation period is from 1−21 February 2004. A quality control on ASAR wave spectra is applied in a procedure prior to assimilation. Threshold values are considered to remove corrupted data. The results showed that the assimilation works correctly and the estimate of mean wave parameters is significantly improved. The impact of the assimilation for long periods stays effective for more than three days after the end of the assimilation. Statistical analysis in comparison with Jason-1 altimeter data exhibits a positive impact in terms of root mean square error of significant wave height. Preliminary results on combined assimilation of RA2 and ASAR data are also discussed.

Keywords: ASAR wave spectra, assimilation, impact, analysis, forecast

1. Introduction

Better wave forecasting is an essential need for several activities at sea, such as off-shore activities, ship navigation and coastal surveys. The main efforts of the wave community are focused on using satellite observations to constrain wave models to the true sea state. The spectral characteristics of waves are now available continuously from imaging radar ASAR of the satellite ENVISAT, but limited to the specific range of wavelength (long waves). At Météo-France, the assimilation of directional wave spectra (ASAR level 2 wave products) has already started, and currently consists on the one hand of improving the assimilation system, and on the other hand validating ASAR data and assimilation results with independent wave observations in preparation for operational use. Our previous studies found that the use of spectral information induces a better estimate of wave parameters (wave height, period and direction), in particular for swell (Aouf *et al.* 2004).

The goal of this study is to evaluate the impact of using ASAR directional wave spectra for a long period. In addition, the choice of wavelength cut-off for ASAR wave spectra and its impact on the assimilation is analysed.

2. Assimilation system and ASAR data

The assimilation system consists of using the partitioning principle and an optimal interpolation on mean wave parameters (energy and components of wave number) of the

* Corresponding author, email: lotfi.aouf@meteo.fr

dominant wave trains (Aouf *et al.*, 2005). The partitioning procedure decomposes the wave spectrum in several dominant wave trains and each one is characterised by its mean parameters (energy, direction and frequency). In this study, the wave model WAM is used for a global scale with a resolution in latitude and longitude of 1×1 degrees, and the wave spectrum is discretised in 36 directions by a step of 10 degrees and 24 frequencies (from 0.044 to 0.39 Hz). The ASAR level 2 wave products implemented by the European Space Agency (ESA) provide the directional wave spectra, and wind speed at the ocean surface. The intercomparison between model and ASAR wave parameters indicates that the wave model WAM underestimates low frequency wave height and mean wave period. To remove corrupted data from the analysis process, quality controls depending on the retrieved ASAR wind speed, the ratio of signal to noise and the normalised variance of image, are used prior to assimilation. Only ASAR data satisfying the three threshold ranges of 3–16 $m s^{-1}$ for ASAR wind speed, 1–1.6 for normalised variance of image and 3–200 for ratio of signal to noise, are kept in the optimal interpolation procedure. 44067 ASAR wave spectra were then selected for the assimilation procedure.

The assimilation of ASAR wave spectra was performed for 1–21 February 2004. The numerical experiment consisted of first running the wave model WAM, driven by analysed ECMWF wind fields, for one week to get a well-developed sea. Thereafter, the ASAR directional wave spectra are assimilated for different dates with a step of three hours (assimilation window). Two cases of wavelengths cut off at 200 and 240 metres are investigated. For weak low frequency wave heights (less than 1 m), the ASAR wave spectra are not included in the analysis. The assimilation parameters, which are the correlation length, the distance of influence of the observations and the cross-assignment threshold value, are considered as 250 km, 600 km and 2, respectively.

In the following, runs A and B indicate the assimilation of ASAR wave spectra with wavelengths cut off at 200 and 240 metres, respectively. However, runs C and D stand for the baseline run with no assimilation and run with assimilation of altimeter RA2 wave height only (altimeter case), respectively.

3. Results

3.1 Assimilation impact

First the impact based on a comparison between model outputs with and without assimilation is analysed. This indicates how large the difference is on wave parameters induced by the assimilation. The assimilation skill with respect to the no assimilation case is examined. The impact of the assimilation on significant wave height and mean wave period is significant and respectively reaches more than 1.5 metres and 5 seconds on 4 February 2004 at 0:00 (UTC), illustrated in Figure 1a and b.

To analyse the contribution of spectral characteristics of waves information, a comparison between assimilation impacts on significant wave height for runs A and D, which is the case of assimilation of RA2 altimeter wave height, is performed. Figure 2a and b show the assimilation skill with respect to the no assimilation case for significant wave height after a 1-day forecast. This clearly indicates that when using ASAR wave spectra the impact stays significant and effective longer.

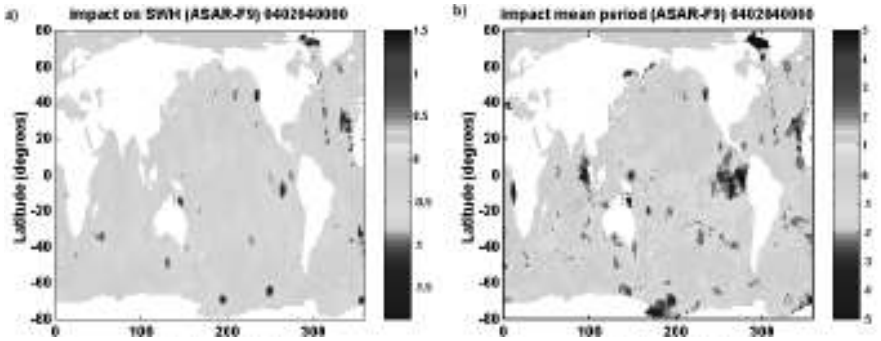

Figure 1 Difference of wave parameters between runs with and without assimilation of ASAR wave spectra on 4 February 2004 at 0:00 (UTC). (a) Significant wave height (m); (b) mean wave period (s).

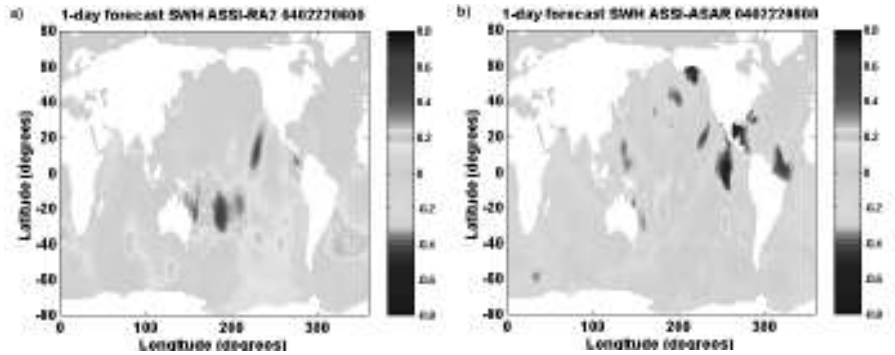

Figure 2 Difference of significant wave heights between runs with and without assimilation on 22 February 2004 at 06:00 (1-day forecast). (a) with RA2 wave height only; (b) with ASAR wave spectra (cut-off of 200 m).

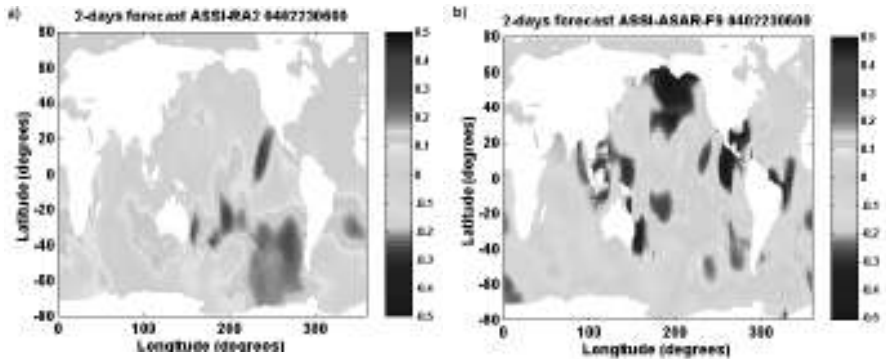

Figure 3 Difference of low frequency wave heights (H_{12}) between runs with and without assimilation on 23 February 2004 at 06:00 (UTC). (a) RA2 wave height only; (b) Run A (ASAR wave spectra).

The maximum impact for run A is estimated at 0.8 metres, while for run D it decreases to 0.5 metres. This tendency is more pronounced for the low frequency wave height after a 2-day forecast, as illustrated in Figure 3a and b. The most affected ocean areas are mainly located in the northern and southern parts of the Indian ocean, the north Pacific and the inter-tropical region of the Atlantic ocean.

3.2 Statistical analysis at crossover locations

This section investigates the assimilation skill with respect to independent observations. The model results are compared with independent wave data such as altimeter Jason-1; this concerns only significant wave height. A statistical analysis is performed at crossover locations between Jason-1 and ASAR orbit tracks. The procedure uses a maximum space lag between Jason-1 and ASAR orbit tracks of 120 km and a time window of 3 hours. The time lag range is from −1.5 to +1.5 hours. We collected 1147 and 866 crossover points for runs A and B, respectively. They are mainly located in high latitude ocean areas. Table 1 clearly shows that the assimilation of ASAR wave spectra reduces well the root mean square (RMS) error to 0.55 and 0.57 metres for wavelengths cut off at 200 and 240 metres, respectively. In addition, the mean bias is also significantly reduced for runs A and B. The assimilation index (see appendix) of significant wave height for runs A and B are estimated at 12.4 and 16.4%, respectively.

Table 1 statistical analysis in comparison with significant wave height of altimeter Jason-1.

	Cut-off of 240 m		Cut-off of 200 m	
	MB (m)	**RMSE (m)**	**MB (m)**	**RMSE (m)**
ASSI/ASAR/JASON	–0.22	0.57	–0.18	0.55
NOASSI/JASON	–0.40	0.68	–0.35	0.63
Selected crossovers	866		1147	

3.3 Combined assimilation of RA2 and ASAR data

To improve both the wind sea and swell parts of the sea state, the assimilation conjointly of RA2 altimeter wave height and ASAR wave spectra is implemented and performed. In this test case, the wavelength cut-off is considered as 240 metres for the ASAR wave spectra. The results are compared to Jason-1 significant wave height at crossover locations between Jason-1 and Envisat orbit tracks. The statistical analysis is performed for 3245 collected crossover points. This clearly shows that the RMS error for significant wave height is significantly reduced to 0.4 metres, as illustrated in Table 2. The corresponding assimilation index increases to 22% in comparison with the assimilation of ASAR wave spectra. In other respects, the impact on low frequency wave height with respect to the no assimilation case stays effective and it is still estimated at 0.5 metres after a 3-day forecast, as illustrated in Figure 4. The affected areas are mainly located in the northern and southern parts of the Pacific Ocean and in the intertropical ocean regions.

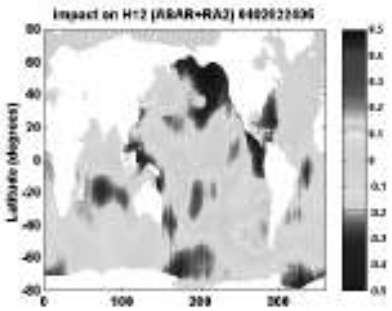

Figure 4 The impact (in metres) of combined assimilation of RA2 wave height and ASAR wave spectra on low frequency wave height (H_{12}) after a 3-day forecast (on 24 February 2004 at 06:00 UTC).

Table 2 Statistical analysis for combined assimilation (AI see appendix).

	MB (m)	RMS (m)	AI (%)
ASAR+RA2/JASON	–0.21	0.40	22
NOASSI/JASON	–0.09	0.53	-
Selected crossovers		3245	

4. Conclusions

The assimilation of ASAR wave spectra for long periods works correctly and the estimate of mean wave parameters is significantly improved. The filtering procedure seems to work efficiently and has removed 16% as spurious data of the total number of wave spectra. The optimistic wavelength cut-off of 200 metres included more ASAR wave spectra in the analysis process in comparison with the case of wavelength cut-off of 240 metres. It has been shown that the impact of the assimilation of ASAR wave spectra stays longer in comparison with the case of the assimilation of RA2 wave height only. In other respects, the comparison with significant wave height from altimeter Jason-1 has indicated a positive impact in terms of RMS error and assimilation index for both wavelengths' cut-off. Promising results on combined assimilation of RA2 altimeter wave height and ASAR wave spectra showed that the assimilation index of significant wave height in comparison with Jason-1 data is significantly increased and the impact stays effective after 3 days of forecast. This clearly suggests the complementary use of such wave observations. In the context of future works, further assimilation tests and validation of results with buoy data are needed before using the assimilation system for operational applications.

Acknowledgements

The authors would like to thank the French Space Agency (CNES) for their financial support.

Appendix

The low frequency swell wave height (H_{12}) is defined as the wave height computed on a limited part in frequency of the wave spectrum. This can be obtained from the following relation:

$$H_{12} = 4\sqrt{\int_{f_1}^{f_{12}} E(f)df}$$

where $E(f)$ is the density of wave energy, while f_1 and f_{12} are respectively the first value in the frequency interval of the wave spectrum (f_1=0.044 Hz) and the upper limited frequency (f_{12}=0.08 Hz).

The assimilation index describes the skill of the assimilation scheme. This parameter indicates the percentage of correction on the root mean square error of wave parameters:

$$AI = \frac{RMSN - RMSA}{RMSN} \times 100\,(\%)$$

where *RMSN* is the root mean square error of wave parameters for the run with assimilation, while *RMSA* is the root mean square error of wave parameters for the run with no assimilation. The closer to 100% the index value is, the closer to the observations the analysed wave parameters are, thus giving a better assimilation skill. On the contrary a negative index value means that the assimilation deteriorates the first-guess.

References

Aouf, L., J-M. Lefèvre, D. Hauser and B. Chapron (2004). Validation and assimilation of ENVISAT-ASAR directional wave spectra in wave model WAM, Proceedings of ISOPE Conference, Toulon (France).

Aouf, L., J-M. Lefèvre and D. Hauser (2005). Assimilation of directional wave spectra in the wave model WAM: an impact study from synthetic observations in preparation to the SWIMSAT satellite mission, submitted to Jour. of Atmos. and Oceanic Tech.

Iberia–Biscay–Ireland regional operational oceanographic system (IBIROOS) physical modelling — State-of-the-art and plans

Dominique Obaton*[1], Enrique Alvarez Fanjul[2], Marcos Garcia Sotillo[2], Manuel Ruiz-Villarreal[3], Pedro Montero[4], Paulo Chambel Leitao[5], Rodrigo Fernandes[6], Yann-Hervé De Roeck[7] and Marcel Cure[8]

[1]*Mercator-Océan, France*
[2]*Puertos del Estado, Spain*
[3]*IEO, Spain*
[4]*MeteoGalicia, Spain*
[5]*Hidromod, Portugal*
[6]*IST/MARETEC, Portugal*
[7]*IFREMER, France*
[8]*Irish Marine Institute, Ireland*

Abstract

The IBIROOS system is the Southwestern European shelf contribution to the EuroGOOS sustained system, with a studied area extending from Northern Ireland to the Gulf of Cadix. The system will be built considering observations, data, modelling and applications and data and results will be gathered and shared between involved teams from Ireland, France, Spain and Portugal. This paper presents the objectives planned for the IBIROOS modelling team to be reached by 2010.

Keywords: IBI-roos, hydrodynamic modelling, regional model, coastal model, downscaling, validation

1. Introduction

Coastal Europe is mostly covered by regional EuroGOOS sustained systems such as BOOS (for the Baltic sea), NOOS (for the Northwest shelf including North Sea and the shelf around Great Britain), MedGOOS and Black Sea GOOS. Up until now, the Biscayan and Iberian shelves were not covered by any regional –OOS, a missing area in this patchwork European distribution. Because these shelves are strongly linked, from a dynamical and a biological point of view, to the Irish shelf, it makes sense to study the whole area extending from Ireland down to Morocco. It is therefore important to gather people working in this area with observations, data, modelling and applications from different countries to create first a task team (TT) and then the IBIROOS: Iberia–Biscay–Ireland operational oceanographic sustained system. The objective of such a system is to improve exchanges and share knowledge between scientists. This paper deals with the physical modelling part of the IBIROOS system and describes existing physical modelling in the area and plans made for the near future up to 2010.

* Corresponding author, email: dobaton@mercator-ocean.fr

2. Existing modelling systems in the IBI region

Six modelling systems/models cover and describe the IBI area. Their scale varies from basin to regional and coastal. Some local models also exist embedded in coastal ones. Apart from that, there is little downscaling between models. Two of them are Spanish (ESEOO and IEO/MeteoGalicia), one is Portuguese (IST/Maretec), one is Irish (IMI) and two are French (MERCATOR and IFREMER). The common point between these systems/models is to be or become operational.

The operational MERCATOR basin scale system (Figure 1) covers the North Atlantic and the Mediterranean Sea at a 1/15° horizontal resolution and assimilates satellite data. It uses OPA code with a rigid lid and z coordinate on the vertical. Sponge layers are used both at the North and South open boundaries.

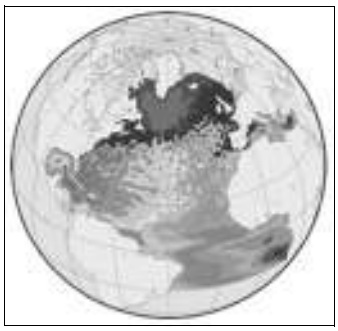

Figure 1 The MERCATOR North Atlantic operational system.

Figure 2 The ESEOO regional system of the Atlantic margin.

The Spanish operational oceanographic system ESEOO runs a pre-operational regional system (Figure 2) which covers the Biscayan and Iberian shelves with a 1/20° horizontal resolution. The model used is POLCOMS with a free surface and S-coordinate on the vertical. General circulation from the FOAM model as well as tides is considered at open boundaries.

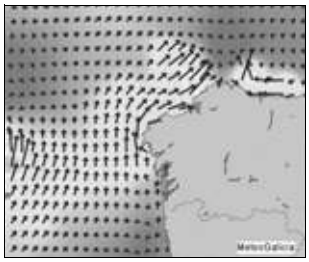

Figure 3 The MeteoGalicia and IEO Galician coastal model. This is a tidal operational model.

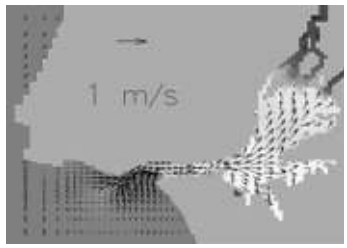

Figure 4 The IST/MARETEC operational model of the Tagus estuary.

MeteoGalicia and IEO run an operational tidal coastal model of the Galician coast at 1 km resolution. The model used is MOHID with a free surface and S-coordinate on the

vertical. Tides and climatological temperature and salinity fields are used at open boundaries.

IST/MARETEC also uses MOHID to run their local model of the Tagus estuary. This operational model has a 300 m horizontal resolution and uses tides, river fluxes and climatological forcings at its boundaries.

IFREMER runs a barotropic tidal operational coastal system off the English Channel and the Northern part of the gulf of Biscay (Figure 5) within a 3 km horizontal resolution. The code used is MARS with a free surface and tides and pressure at open boundaries. A local model of the Iroise sea–Western Brittany (800 m horizontal resolution) is nested in this coastal system and the smaller model of the Bay of Brest (150 m horizontal resolution) is itself embedded in the local model of the Iroise Sea. Tides and barotropic processes are both used at open boundaries of these 2 local models.

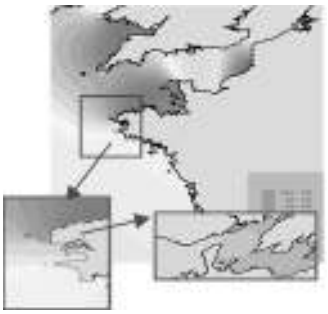

Figure 5 The IFREMER tidal operational coastal system of the English Channel and the North of the gulf of Biscay and the 2 local models nested in one another and in the coastal model.

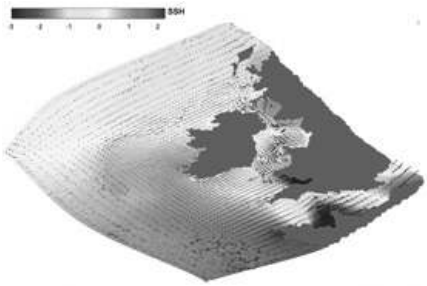

Figure 6 The IMI coastal model of the Irish shelf.

The Irish Marine Institute (IMI) runs a coastal model covering the whole Irish shelf (Figure 6) at 1 km horizontal resolution. The code used is ROMS with a free surface and σ-coordinate on the vertical.

3. Modelling system in the IBI region: plan for 2010

Open to the Atlantic Ocean, the IBI region is strongly influenced and driven by open sea circulation and the shelf coastal areas have to deal with the slope/shelf interaction which is still not well understood and described. A complete validation of models and systems in this region will also find their limits and see where they need be improved.

Accordingly, 2 objectives have been defined to improve these operational systems and models:

- Downscaling from global (MERSEA) to regional, coastal and local scales considering each individual system/model as it exists now and some more that could be easily added to the final system of systems/models obtained.
- Validation of the different systems/models and intercomparison between them.

Validation will benefit from a monitoring network over the area scheduled by the IBIROOS observation team.

To reach these objectives the IBIROOS modelling team plans to run a complete operational system including a regional system nested in MERSEA, 5 coastal systems/models nested in the regional one and covering all the IBI coasts and 5 local spot models embedded in coastal systems/models (Figure 7). The main idea is to link these systems/models through downscaling which itself will be improved to give confident results. Careful validation and intercomparison of this system of systems/models will be done for the slope current flowing from South to North along the shelf of the IBI area.

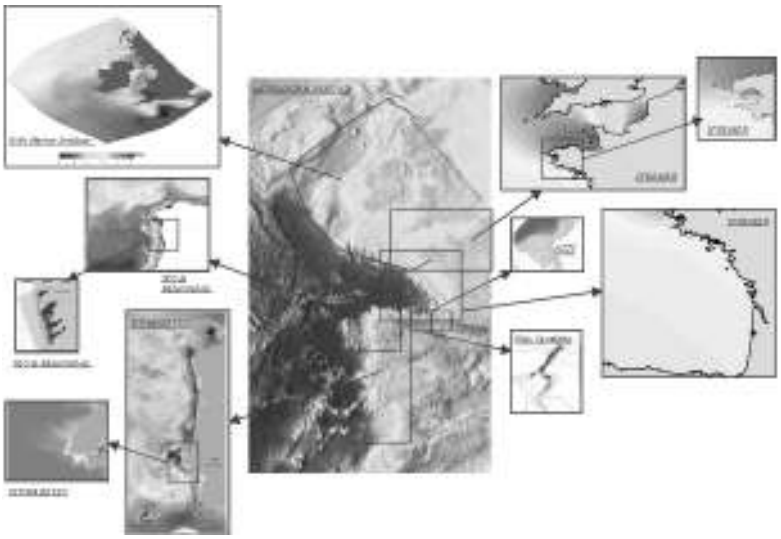

Figure 7 The IBIROOS modelling and assimilation system planned for 2010, from regional to coastal and local scales.

This system of systems and models will include:

1. a regional system:
   - From Northern Ireland to the Gulf of Cadix run by MERCATOR and ESEOO-2 (OPA code including tides, ~2.5 km resolution, assimilation of satellite and *in situ* data)
2. some coastal systems or models:
   - Iberian shelf coastal model run by IST/MARETEC (MOHID code, 2 km resolution)
   - Galician coastal model run by IEO (MOHID code, 1 km resolution)
   - Gulf of Biscay system run by IFREMER (MARS code, σ-coordinate, 1 km resolution, assimilation of satellite and *in situ* data)
   - English Channel model run by IFREMER (MARS code, 1 km resolution)
   - Irish shelf model run by IMI (ROMS code, 1 km resolution).
3. some local models:

- Tagus estuary model run by IST/MARETEC (MOHID code, 300 m resolution). Nested in the Iberian shelf model.
- Rias de Vigo model run by the University de Vigo and MeteoGalicia (MOHID code, 150 m resolution). Nested in the Galician coastal model.
- Cantabrian Bay model run by the University de Cantabria (H2D/H3D code, 50 m resolution). Nested in the regional model.
- Bilbao Bay model run by AZTI (100 m resolution). Nested in the regional model.
- Iroise Sea model run by IFREMER (MARS code, 300 m resolution). Nested in the English Channel model.

Validation and intercomparison will be made easier by the use of common files and gridded data formats defined by the IBIROOS data team. This will also contribute to tightening links between the teams.

This improved system of systems and models will give more realistic answers to different applications: direct applications such as accident pollution, sea level, storm surge, algal bloom or those which need a biological model coupled to the hydrodynamical one such as water quality, eutrophication, larvae transport and bacterial contamination.

4. Conclusion

The plans of the IBIROOS modelling team are to have an operational system of systems and models composed of different scales systems/models from regional to coastal and local scales linked together through a downscaling strategy. The regional system will itself be nested in the MERSEA global system. Validation and intercomparison will be made in this complex system and special attention will be put on the slope current along the IBI region.

References

Pouliquen, S, A. Lavin *et al.* (2006). IBI-ROOS: Iberia–Biscay–Ireland Regional Operational Oceanographic System plan, 2006–2010. In preparation.

The European Seafloor Observatory Network Implementation Model (ESONIM)

G.D. Nolan*[1], M. Gillooly, N. O'Neill, I.G. Priede, O. Pfannkuche, P. Linke, G. Waterworth, J.-F. Rolin, P. Hall, P. Lee and C. O'Rourke

[1]*Marine Institute, Galway, Ireland*

Abstract

The scientific justification for a European Seafloor Observatory Network has been made by the ESONET consortium. The authors now propose to develop a comprehensive implementation model for such a network. The European Seafloor Observatory Network Implementation Model (ESONIM) will bring together technical, legal and financial experts to design the optimum implementation plan for a cabled seafloor observatory in European waters. The consortium will consider the detailed technical specification of sub-sea cabling, scientific nodes and shore station infrastructure required for the network. The indicative capital expenditure required to establish a cabled seafloor observatory is thought to be in the region of €40m. Estimates of annual running costs are in the region of €1.5m to €3m. The ESONIM partners will examine various mechanisms by which an observatory can be financed and maintained by closely examining instruments such as public private partnerships, national capital expenditure programmes and stakeholder financial participation in the proposed network. Furthermore the consortium will examine the legal framework within which such a cabled seafloor observatory needs to operate.

This paper aims to inform the wider operational oceanographic community on progress regarding the practical implementation of real-time systems on Europe's seabed to complement the existing network of surface and water column measurements that are now made routinely.

1. Background to ESONIM

ESONIM is a Specific Support Action (SSA) that builds on the EU FP5 ESONET (European Seafloor Observatory Network) project to contribute to the realisation of the seabed observatory component of the EU Global Monitoring for Environment and Security (GMES) initiative and Global Earth Observation (GEO) programme.

ESONIM will produce a practical, flexible business plan to establish a seafloor observatory based on the ESONET Porcupine site. The business plan will include the technical specifications of the observatory components; the observatory architecture that will deliver the best technical solution; a ten year cashflow forecast, capital and operating expenditure and projected revenue; and draft contracts and partnership agreements that will address the share of financial risk and insurance liability between the private and public sector partners (PPPs) in the observatory. While based on the Porcupine site the plan will be implementable at any or all of the other ESONET sites.

* Corresponding author, email: Glenn.Nolan@marine.ie

2. Partners and specialities

The Irish Marine Institute acts as project co-ordinator and is Ireland's marine agency responsible for marine research, technology, development and innovation. CSA Group Ltd. are geoscience professionals providing technical and project management.

The IFM GEOMAR research institute envelopes all scientific expertise for operational oceanography while IFREMER is France's lead marine agency with expertise in underwater technology and systems. Alcatel (ASN) is a world leader in engineering design, implementation and maintenance of underwater telecommunication cable systems. Oceanlab at the University of Aberdeen is a unique facility designed for development, testing and servicing of deep ocean autonomous vehicles and other instrumentation. Goodbody Corporate Finance (GCF) is one of Ireland's leading corporate finance houses. Philip Lee Solicitors are specialist legal experts in European law with an emphasis on public procurement, competition law and construction law. University of Göteborg are a world authority on free-vehicle benthic lander technology and on design, development and use of deep-sea landers, lander sensors and oceanographic instrumentation.

3. ESONIM project structure

The project structure is shown below. Both a steering committee and an advisory group will provide guidance to the four task team chairs in Technology, Science, Legal and Commercial work packages. Individual partners are then assigned specific programmes of work dependant on their expertise.

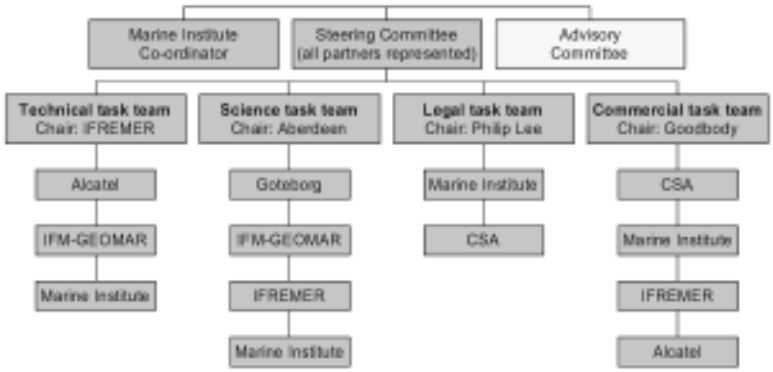

Figure 1 ESONIM organisation.

4. Work package descriptions

WP1 will define the ESONIM project's management structure and reporting procedures. WP2 aims to provide the over-arching specification of user needs and justification for the establishment of a European seafloor observatory network. WP3 will identify the most appropriate technical design and engineering solution for a cabled seafloor observatory. The opportunities for industry involvement in the design, manufacture, deployment and operation of the system will be addressed in this work package. WP4 will produce a 10 year cash-flow forecast for a cabled seafloor observatory within the

European Seafloor Observatory Network (ESONET). WP5 will clarify the overall legal context and framework for the implementation of a cabled seafloor observatory. WP6 will analyse and integrate the results of WP2–5 to develop a technical and financial project appraisal for a test case seafloor observatory that meets the criteria established by lending institutions. WP7 will disseminate the information and knowledge gained within ESONIM to the widest possible audience using multiple communication methods.

5. Workshops

An invited international workshop (circa 20 international experts) on cabled seafloor observatory technologies will be organised in January/February 2006.

The ongoing deliverables from ESONIM will be disseminated via oral and poster presentations at key international workshops and conferences such as Oceanology 2006 and EurOCEAN 2006.

There will be a Final ESONIM Workshop (by invitation) that will include stakeholder, investor and end user participants. The economic viability and actions for sustainable operation of the model cabled seafloor observatory will be presented to an audience that will include targeted public and private sector investors.

6. Website

ESONIM will establish a project website to be hosted on the existing ESONET website www.abdn.ac.uk/ecosystem/esonet/ and establish links to related projects/websites.

ESONIM is funded as a Specific Support Action of the European Commission FP6 programme in Global Change and Ecosystems.

Variations in phytoplankton speciation and growth due to hydrodynamic and chemical drivers between coastal and open ocean waters: use of data from a "FerryBox" ship of opportunity

M.A. Qurban*[1], D.J. Hydes[1], B.A. Kelly-Gerreyn[1], P. Holligan[1] and P. Miller[2]

[1]*National Oceanography Centre, Southampton, UK*
[2]*RSDAS-Plymouth Marine Laboratory, Plymouth, UK*

Abstract

Near-continuous observations of upper layer temperature, conductivity, and chlorophyll fluorescence have been made (except in January) between Portsmouth (UK) and Bilbao (Spain) since April 2002 as part of the EU–FP5 project "FerryBox". Different upper water conditions over the shelf, slope and deep waters along the route can be detected and studied — from eutrophic harbour waters to the southern Bay of Biscay which is oligotrophic in summer. Regular sampling on board the ferry provides information on concentrations of nutrients and plankton biomass and speciation. Phytoplankton species are determined by both HPLC analysis and microscopy. This enables the progress of the blooms of plankton to not only be followed in terms of the drivers such as concentrations of nutrients but also the types of plankton present during different stages of the growth and decay cycle.

Keywords: Ship of opportunity, FerryBox, sustained observations, Bay of Biscay, plankton blooms, chlorophyll fluorescence, metrology

1. Introduction

Progress in understanding the way the earth's biogeochemical systems function is limited by a lack of data. This is particularly true for studies at the shelf break (Wollast and Chou, 2001). An important feature of the shelf break is its variability, so extending our understanding needs tools to observe the system in its different states. This requires establishing data collecting systems that sample both for a duration and at a frequency that allows the magnitude of events and controlling processes to be defined. A cost effective way of enabling better temporal coverage is by placing autonomous instruments on commercial vessels running regularly repeated routes (Hydes *et al.*, 2003).

The system described here is aimed at providing an un-aliased view of changes in hydrographic and biogeochemical conditions along a section crossing from the northwest European Shelf to adjacent deep north Atlantic waters. The key scientific target of this work is the precise determination of plankton production along the track in relation to physical forcing and the supply of nutrients. This can be examined with respect to both natural and anthropogenic sources of nutrients. Because the phytoplankton are the dominant plant in the ocean, they make up the first trophic level of the pelagic food chain (Miller, 2004). Chlorophyll *a* is the main light-harvesting pigment in all species of

* Corresponding author, email: mqurban@noc.soton.ac.uk

phytoplankton and its relative abundance enables estimates of the phytoplankton biomass (Raymont, 1980; Kirk, 1994; Miller, 2004). Accessory pigments provide information regarding the phytoplankton community. HPLC analysis of the chlorophylls and carotenoids present in a seawater sample can reveal the taxonomic composition of phytoplankton populations.

2. Methods

Since 2002, a "FerryBox" has operated on the P&O "Pride of Bilbao". It runs all year round, twice a week, between Portsmouth (UK) and Bilbao (Spain). Sensors measure temperature, chlorophyll-fluorescence, conductivity, and oxygen. Data are logged at 1 Hz in the engine room. Data are transferred every 5 minutes to an Orbcomm satellite communicator on the bridge and sent back to NOC where they enter an SQL database.

The Portsmouth–Bilbao route crosses a number of very different hydrographic regions, see Figure 1.

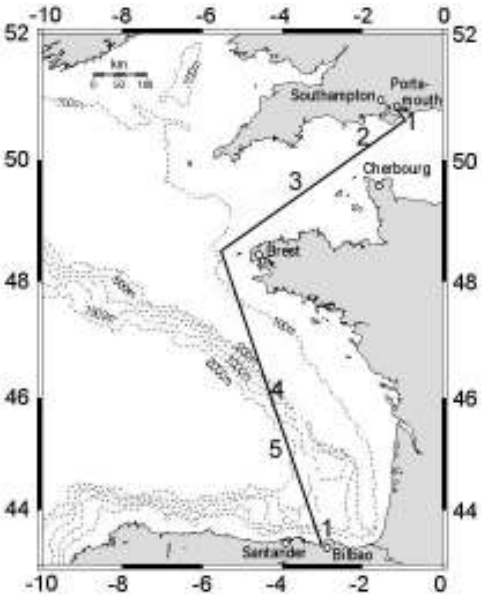

Figure 1 Route of the P&O "Pride of Bilbao" between Portsmouth and Bilbao. The main hydrographic regions (numbered) are (1) Hypernutrified harbours; (2) Central English Channel — well mixed; (3) Western Channel — seasonally stratified; (4) Shelf break with up-welling events; (5) Deep ocean water — seasonally oligotrophic.

Water samples are taken each month to calibrate the system and extend the range of measurements. These are salinity, chlorophyll (Acetone extracted and HPLC pigments), nutrients (nitrate, phosphate and silicate), phytoplankton cell number and species. Duplicate water samples for chlorophyll *a* analysis were collected between Portsmouth and Bilbao every hour, filtered and stored immediately in acetone at −30°C. The chlorophyll *a* concentration was determined spectrophotometrically relative to a chlorophyll *a* standard solution (Sigma Chemical Co.) in 90% acetone following the method of Jeffrey

and Humphrey (1975). Filtered samples for HPLC pigment measurements were collected between Bilbao and Portsmouth and stored immediately at −30°C at sea and then −80°C on shore. The determination of pigments followed the method described by Barlow *et al.* (1993).

3. Results

Figure 2 shows a posted dot plot of all the data for chlorophyll fluorescence collected as a continuous record on the ferry during 2003 and 2004. Gaps in the data are due to ship refit (January−February 2003 and 2004) and a breakdown in the logging system in the heat of the engine room in late summer. Chlorophyll *a* fluorescence varied spatially and temporally (between <1 and >100 mg Chl m^{-3}) in 2003. Chlorophyll fluorescence was generally high in March−May and extended from across the shelf break and shelf 45°N into the English Channel 51.7°N. From May onwards, chlorophyll fluorescence drops sharply and the lowest values were observed in the summer along the Bay of Biscay (from 44°N to 48°N). In 2004 the duration of the spring bloom was longer. The peak in July 2003 was due to an exceptional bloom of *Karenia mikimotoi*. In 2003 an autumn bloom was observed at the shelf break and corresponded to an increase in concentrations of nutrients.

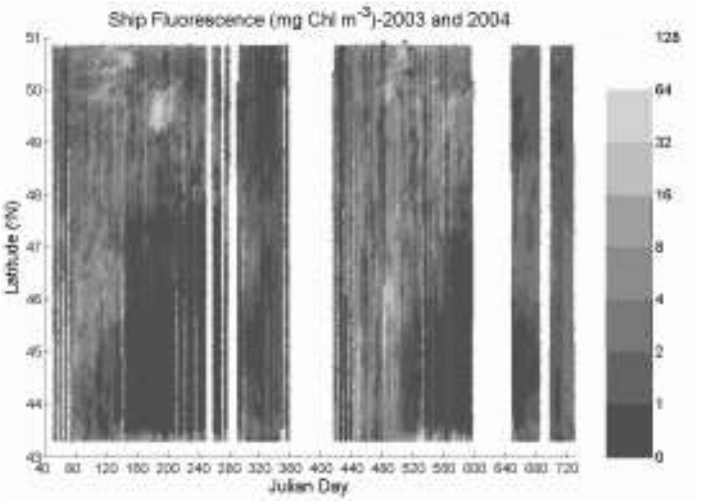

Figure 2 Dot plot of five-minute averaged data between Portsmouth (UK) and Bilbao (Spain) from FerryBox MiniPack sensors for fluorescence for 2003 and 2004.

Horizontal sea surface distributions of chlorophyll estimated from weekly composite satellite data (SeaWiFS) have been compared for data extracted at positions corresponding to the route of the ferry in 2003 and 2004. They confirm the longer duration of the bloom in 2004 relative to 2003.

The distribution of chlorophyll differs from that of fluorescence due to changes in the dominant type of organism and their photo-physiological state. These variations have been discussed in Qurban *et al.* (2004). A consistent pattern of phytoplankton pigments was present in the study area during 2003 and 2004. The distribution of HPLC chloro-

phyll *a* matches the distribution of chlorophyll *a* determined directly by the fluorescence of filtered samples for 2003 and 2004. In addition three pigments appear to be useful as primary taxonomic markers — fucoxanthin, 19'-hexanoyloxyfucoxanthin and peridinin. They indicate the presence of diatoms, prymnesiophytes and dinoflagellates respectively. Levels of fucoxanthin and 19'-hexanoyloxyfucoxanthin increased concomitantly with chlorophyll *a* as the bloom developed. Fucoxanthin pigment increased from March to May and decreased in June. It extended from 45°N to the English Channel 51.7°N across the shelf break and shelf. A concentration maximum of 17μg l^{-1} of fucoxanthin was observed in July 2003. Microscope analysis of preserved samples indicated that this intense bloom was *Karenia mikimotoi*, formally known as *Gyrodinium aureolum*. Peridinin pigment is an indictor of the presence of dinoflagellates. Peridinin reached maximum concentrations in the summer of both years. The highest concentrations of peridinin were measured in association with the bloom of *Karenia mikimotoi* in 2003.

4. Conclusions

The measurement of a continuous record of fluorescence from a FerryBox system is a relatively simple technique. The data presented here shows that it provides valuable information on the variation in bloom intensity and location in different years. The more complex collection and analysis of pigment samples is proving effective in identifying the different organisms present and greatly reduces the amount of labour intensive microscopic analysis required for monitoring the evolution of plankton populations. We are now in the process of relating these changes to changes in hydrographic conditions between 2003 and 2004.

Acknowledgements

The help of P&O Ferries Ltd. in making this work possible is greatly appreciated. It was supported by the EU FP project "FerryBox" (EVK2–CT–2002–00144), the NERC–UK "BICEPS" project at NOC and a Saudi Arabian government studentship to M.A. Qurban.

References

Barlow, R.G., R.F.C. Mantoura, M.A. Gough, and T.W. Fileman (1993). Pigment signatures of the phytoplankton composition in the northeast Atlantic during the 1990 spring bloom. Deep-Sea Research II, 40, 459–477.

Hydes, D.J., C.P. Bargeron, B.A. Kelly-Gerreyn, H. Wehde, W. Petersen, S. Kaitala, V. Fleming, K. Sørensen, J. Magnusson, I. Lips and U. Lips (2005). Comparison of eutrophication processes and effects in different European marine areas based on the results of the EU FP-5 FerryBox Project. This volume page 101.

Hydes, D.J., A. Yool, S.E. Hartman, B.A. Kelly-Gerreyn, J. Dodgson, J.M. Campbell, N.A. Crisp, M. Edwards, B. Dupee, A.M. Lavin and C.M. González-Pola (2003). Use of a FerryBox system to look at shelf sea and ocean margin process pp 297–303 In Building the European Capacity in Operational Oceanography, (H. Dahlin, N.C. Flemming, K. Nittis & S.E. Petersson, eds) EuroGOOS Publication 19. Elsevier Oceanography Series, 69. Elsevier Amsterdam.

Jeffrey, S.W. and G.F. Humphrey (1975). New spectrophotometric equation for determining chlorophylls a, b, c1, and c2 in higher plants, algae and natural phytoplankton, Biochem. Physiol. Pflanz. 167, 191–194.

Kirk J. T. (1994). Light & photosynthesis in aquatic ecosystems. Cambridge University Press, Cambridge.

Miller, C.B. (2004) Biological Oceanography. Blackwell.

Qurban, M.A., D.J. Hydes, A.M. Lavin, C.M. González-Pola, B.A. Kelly-Gerreyn and P. Miller (2004). Sustained “Ferry-Box” Ship of Opportunity observations of physical and biogeochemical conditions across the Bay of Biscay ICES Annual Science Conference Vigo Spain 2004, paper no. CM 2004/N:09 19pp CD ROM publication.

Raymont, J.E. (1980). Plankton and Productivity in the Oceans. Pergamon Press, Oxford.

Wollast, R. and L. Chou (2001). Ocean Margin EXchange in the Northern Gulf of Biscay: OMEX I. An Introduction. Deep-Sea Research II 48, 2971–2978.

A Ka-band altimetry payload as a candidate for the next decade operational altimetry system

N. Steunou*[1], P. Vincent[2], E. Thouvenot[1], E. Caubet[3] and J. Verron[4]

[1]*Centre National d'Etudes Spatiales, Toulouse, France*
[2]*IFREMER, Paris, France*
[3]*Alcatel Space Industries, Toulouse, France*
[4]*LEGI, Grenoble, France*

Abstract

In partnership with scientific laboratories and industry, and for several years, CNES has studied the feasibility of a high-resolution ocean topography mission based on a new class of wide-band Ka-band altimeter in preparation for the post-ENVISAT mission to complement the OSTM/Jason-2 mission. A preliminary definition study of a coupled altimeter-radiometer instrument has been performed in 2001−2003 with the support of Alcatel Space.

This paper gives the current status and objectives of the mission and instrument description and expected performances.

Keywords: Mesoscale circulation, altimeter, radiometer

1. Introduction

In the framework of the European GMES programme, altimetry is a key technique to providing ocean users with the dynamic data to contribute to the development of operational ocean applications.

2. Mission objectives

The science objectives of the AltiKa mission are detailed in Verron *et al.* (2001) and in Remy *et al.* (1999). The main objectives are described in the following subsections.

2.1 Central objective: Pre-operational demonstration

The central objective is related to the ocean mesoscale circulation and the data assimilation in a global ocean model. At least 2 satellites are needed to measure mesoscale variations of the ocean.

To answer the needs in terms of time−space sampling of the ocean for operational purposes, the AltiKa payload could be deployed on three identical satellites flying in the same orbit plane with a 120 degrees lag in terms of position on the orbit, as a complement to Jason-like reference missions. The main characteristics of the orbit are a high inclination (coverage of oceans and Antarctica), a ground track repetitivity between 15 and 35 days, and an altitude range between 700 and 900 km.

* Corresponding author, email: nathalie.steunou@cnes.fr

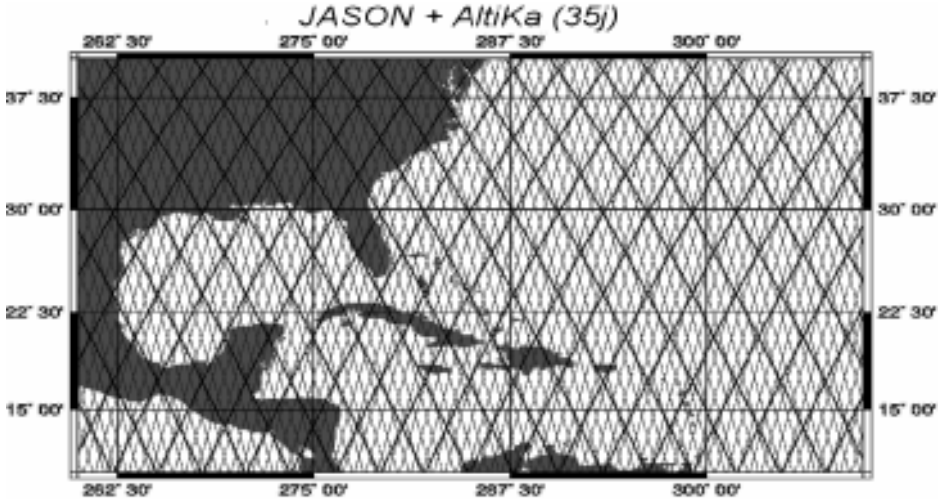

Figure 1 Example of combined sampling of JASON-2 (10 days) and AltiKa3 with a sun-synchronous orbit of the ERS / ENVISAT type (800 km, 98.6 degrees).

2.2 Research objectives

Several research objectives are associated with the mission:

- Continental ice studies: Penetration depth is much reduced in Ka-band, 0.1 to 0.3 m (versus 2 to 10 m in Ku-band).
- Sea-state analysis and forecast
- Low rain detection and characterisation
- Coastal/inland water altimetry.

  The altimeter tracking mode has been optimised in order to better improve its behaviour in coastal regions and near inland water areas. Two tracking modes will be available. First of all, the conventional tracking loop will be implemented, with a first order loop for gain and a second order loop for range. Secondly, DORIS navigator messages, completed with an on-board stored Digital Elevation Model, will be used to estimate the range to track. Moreover, an additional high data rate mode will allow download of I and Q samples for speckle and echo analysis in coastal regions at the PRF rate.
- Feasibility of an additional mode is being studied, which consists of working in SAR mode to improve the spatial resolution over sea ice surfaces. Open water and ice masses can be discriminated by analysis of the shape of the return echoes, and then differences in altitude between the two surfaces can be used to measure the "freeboard" of floating sea ice and thus derive its total thickness.

3. Payload description

3.1 Main characteristics

The main characteristics of the AltiKa altimeter/radiometer are given in Table 1 below.

Table 1 Altimeter / radiometer main characteristics.

Parameter	Value
Altimeter band	35.75 GHz ± 250 MHz
Pulse bandwidth	500 MHz
Pulse duration	110 μs
Altimeter Pulse repetition frequency	4 kHz
Echo averaging (altimeter)	25 ms
Spectrum analyser (altimeter)	128 points
Altimeter Link budget	11 dB (sigma naught = 6.5 dB)
Antenna diameter	1000 mm
Focal length	700 mm
Offset	100 mm
Radiometer band	23.8 GHz ± 200 MHz 36.8 GHz ± 200 MHz
Radiometric resolution	<0.5 K
Radiometric accuracy	<3 K
Radiometer averaging	200 ms
Mass (altimeter+radiometer)	33 kg
Power consumption (altimeter+radiometer)	<76 W

The AltiKa main instrument consists of a Ka-band altimeter and a dual-frequency radiometer embedded in the altimeter. It also includes an accurate orbitography system, DORIS, and a Laser retro-reflector array.

The altimeter is a single frequency instrument, as ionospheric effects can be negligible in Ka frequency most of the time. The bandwidth is enhanced compared to Ku-band altimeters: 500 MHz, thus improving the vertical resolution (0.3 m instead of 0.5 m).

The radiometer is of the total power type and is based on direct detection. Altimeter and radiometer share the same antenna.

The AltiKa altimeter/radiometer is based on proven concepts and already developed subsystems, as it inherits a lot from Siral (mission CRYOSAT) and Poseidon-3 (mission JASON-2).

The instrument can be accommodated either on a micro-satellite or as a passenger on an opportunity mission.

3.2 Status

A preliminary definition phase of the instrument has been conducted with the support of Alcatel Space from November 2001 to June 2003. At the present time, a delta phase B is beginning, with an expected phase C/D in the end of 2005. An opportunity to embark AltiKa on OCEANSAT-3 in the frame of a cooperation with ISRO (Indian Space Research Organisation) is being discussed. This mission would thus be a demonstration

of the Ka-band altimetry as a complement to JASON mission. The launch of OCEANSAT-3 is planned in mid 2009.

3.3 Performances

The enhanced bandwidth and the possibility to double the number of independent echoes per second due to the shorter decorrelation time of sea echoes in Ka band contribute to an improvement of the radar performances compared to conventional Ku-band altimeters. For instance, the noise on the 1 second range measurement will be less than 2 cm for a significant waveheight of 2 metres, thus about 40% of improvement versus Ku-band performance.

Moreover, a new experimental mode will be implemented, consisting of coupling of the altimeter with DORIS navigator. This leads to a maximum acquisition duration less than 200 ms and, by using in addition an optimised on-board Digital Elevation Model, an improved behaviour of the tracking in transitions from land to water and over continental waters.

4. Conclusion

The characteristics and performances of the AltiKa payload make it a good candidate for a future participation in a sustained altimetric system answering research and operational requirements of an ocean observing component within the GMES programme and the Global Earth Observation System of Systems (GEOSS).

References

Caubet, E., L. Phalippou and E. Thouvenot (2002). Design status of a combined Ka-band altimeter/radiometer. OPTRO 2002.

Caubet, E., N. Steunou and M. Meerman (2003). Phase B and breadboard results of the Ka-band altimeter for future micro-satellite altimetry missions. IGARSS'03.

Rémy, F., B. Legresy and P. Vincent (1999). New scientific opportunities from Ka-band altimetry, IGARSS'99.

Verron, J., P. Bahurel and P. Vincent (2001). AltiKa: Etude de la circulation océanique mésoéchelle par altimétrie en bande Ka sur microsatellite, Research proposal to CNES.

Vincent, P., E. Thouvenot, N. Steunou *et al.* (2002). ALTIKA3: A high resolution Ocean Topography Mission. IGARSS'02.

Marine overlays on topography for Annex II valuation and exploitation — MOTIIVE

Keiran Millard*[1] and Roger Longhorn[2]

[1]*HR Wallingford, UK*
[2]*IDG Ltd., UK*

Abstract

The objective of MOTIIVE is to examine the cost benefit of using non-proprietary data standards. MOTIIVE addresses the harmonisation requirements between the INSPIRE core data component "elevation" (terrestrial, bathymetric and coastal) and INSPIRE marine thematic data for "sea regions", "oceanic spatial features" and "coastal zone management areas". The proposal stresses analysis of the cost-benefit implied by strong harmonisation between "core" and "thematic" INSPIRE data, while fulfilling the infrastructure requirements of the GMES "Ocean and Marine Applications" theme, already being determined by GMES Service Element (GSE) pilot projects. The aims of the project are to produce application instances of a series of OpenGIS specifications and use this to support a fully qualified business case for creating a formal OGC Working Group for Marine Data.

Keywords: INSPIRE, GML, ISO–TC211, marine data exchange, cost-benefit

1. GMES and INSPIRE

Following several years of preparatory work (1998–2001), in June 2001, the European Commission (EC) and European Space Agency (ESA) embarked on a joint initiative called GMES — Global Monitoring for Environment and Security, with the objective "to support Europe's goals regarding sustainable development and global governance by providing timely and quality data, information and knowledge". GMES has three main themes: meeting Europe's environmental obligations, supporting sustainable development, and contributing to the security of citizens in Europe and globally. GMES is meant to contribute to key European Union (EU) policies in a number of areas spanning environment, sustainable development, and common foreign and security policy.

In regard to data needs, GMES focuses on six primary themes — Land Cover and Vegetation, Water Resources, Ocean and Marine Applications, Atmosphere, Risk Management, and Security. In the Initial Period, ESA funded a series of GMES Service Element (GSE) pilot projects aimed at delivering actual information services, under the aegis of the ESA Earthwatch programme. These projects are being conducted in three phases, Phase 1 of which ended (for most) at the end of 2003. (Two new GSE projects have been launched in 2004 focused on Humanitarian Aid and Atmospheric Chemistry).

In parallel with the GMES Service Element projects funded by ESA during the Implementation Phase, the EC funded or co-funded 18 projects dealing with all thematic areas, plus three cross-cutting assessment studies. Five of these 18 projects were focused

* Corresponding author, email: k.millard@hrwallingford.co.uk

directly on marine or coastal themes: DISMAR — Data Integration System for Marine Pollution and Water Quality; ESONET — European Sea Floor Observatory Network; EUROSION — Information for Coastal Erosion Mitigation (funded by DG Environment); MERSEA — Marine environment and security in the European Area; OCEANIDES — Harmonised monitoring, reporting and assessment of illegal marine oil discharges. There are also marine elements to some of the other more horizontal projects focusing on earth observation for risk management, monitoring and security.

In the GMES Initial Period Final Report (2001–2003) of 10 February 2004, the GMES Steering Committee (current "owner" of the joint GMES initiative), concluded that further important issues that needed addressing in the Implementation Period included: "the explicit GMES data policies which will optimise the use of services, information and data; and how services, information and data can best be made readily accessible in the most efficient and effective way to the widest possible range of users and applications". These are issues that INSPIRE is addressing today, albeit without an EU-wide legal framework to support the work, such as is enjoyed by GMES itself.

The findings of the final GSE co-location meeting held in October 2003 stated that "GMES is about all available data-sets and each service plans to use the most appropriate combination of measurement sources. It is hoped that initiatives such as INSPIRE will help ensure adequate access terms and supply of *in situ* data". The EU Communication "Establishing a GMES capacity by 2008 — Action Plan (2004–2008)" also "… emphasises the need to maintain coherence between various data sources and information initiatives at Community level. For the selected services, GMES will contribute to the development of the European Spatial Data Infrastructure in compliance with INSPIRE." The communication also states that the GMES initiative expects INSPIRE to provide the underpinning spatial information infrastructure to support the GMES priority themes. Thus, INSPIRE must provide adequate infrastructure to ensure harmonisation between not only the INSPIRE "core" data sets, and INSPIRE "thematic" data sets, but also for the thematic data elements of GMES, including coastal, marine and ocean themes.

The cost of implementing this infrastructure — including data capture and "publishing" to those who need it under varying accessibility regimes — is significant, estimated at more than 200 million Euro per year across the EU. It is still unclear as to how this cost can be met or reduced by realignment of planned work and better harmonisation of current data collection work at local, national and regional levels. Thus, the ability of GMES services to take full advantage of the planned INSPIRE framework is key — and still to be fully investigated or tested.

2. The Role of MOTIIVE

The EC's INSPIRE initiative proposed harmonised 'Annex 1' core spatial data will underpin the harmonisation of 'Annex 2' thematic data. The existence of Open GIS Consortium (OGC) and International Organization for Standardisation (ISO) TC 211 non-proprietary spatial data standards and interoperability tools is expected to help foster data integration at lower cost than previously experienced when using multiple data sources in integrated data projects. A key objective of this proposal is to examine this expectation for a selected set of core and thematic data, while fully documenting the processes, procedures, barriers and resource requirements involved in creating, then

using, non-proprietary spatial data geographic information standards and new interoperability tools to aid such data harmonisation. The cost-benefit analysis included in MOTIIVE explores the implications of harmonisation across core and thematic data areas as well as within thematic data groups.

The MOTIIVE proposal stresses the importance of the cost-benefit aspect of data harmonisation raised in the call document relating to the FP6–SPACE–GMES work plan. MOTIIVE do not feel that the existing cost-benefit analysis contained in the latest INSPIRE documentation can be improved upon by looking at only core INSPIRE data elements, especially in regard to GMES thematic data which relies on only one or at most two such data groups, e.g. elevation or ortho-imagery. Rather, a more comprehensive analysis is required that focuses on estimated costs and forecast benefits appertaining to ready access to the wide range of spatial data intrinsic to the INSPIRE core data sets, INSPIRE thematic data sets and GMES thematic data and information service needs. The goal of the cost-benefit element of the MOTIIVE proposal is to re-examine and re-validate the methodology(ies) used in the prior INSPIRE impact analysis study(ies) and related cost-benefit studies, from the specific viewpoint of cost-benefit to GMES services as well as harmonisation of INSPIRE core and thematic data sets.

This work will be supported by monitoring and learning from the harmonisation activities enacted in other parts of the project, between the selected INSPIRE core data group (elevation) and thematic groups (sea regions, oceanic spatial features and coastal zone management areas), specifically in relation to how such harmonisation will impact on the GMES services being developed in the Implementation Phase of GMES, which will begin at approximately the same time as the MOTIIVE work, i.e. 2005–2006.

3. Measurable objectives of MOTIIVE

Several partners in the MOTIIVE project are members of Phase I GSE pilot projects, including COASTWATCH and ROSES. As the name implies, COASTWATCH focuses on satisfying European and global information needs of the marine and coastal research, policy monitoring and management communities, especially in relation to the EC's Water Framework Directive, now being enacted in law in all EU Member States. The GMES services being developed in COASTWATCH will also support eventual monitoring of the EC's ICZM Recommendation regarding indicators for coastal health and environmental sustainability. MOTIIVE partners are also represented on the GSE ROSES (Real-time Ocean Services for Environment and Security) project that focuses on marine environment protection and marine safety respectively. Thus, MOTIIVE partners have learned much — and contributed much — to understanding the data and information needs behind the services that COASTWATCH and ROSES must deliver in meeting the overall GMES service objectives.

Accordingly, the aims of MOTIIVE are:

- Provide a documented methodology for implementing and monitoring data harmonisation activities between INSPIRE 'Annex I' (core–elevation) and 'Annex II' (thematic–marine/coastal) datasets. This follows the steps required in the Open GIS Consortium (OGC) Reference Model for interoperability, application of ISO 19xxx

series of spatial standards and CEN/TC 287 standards profiles for ISO 19xxx, with associated Feature Type Catalogues and marine ontologies.

- Using the open standards and tools developed in early stages of the project, demonstrate this methodology applied to the data integration requirements of those GMES (Global Monitoring for Environment and Security) Service Element (GSE) pilot projects. These projects have a marine/coastal focus and in which MOTIIVE partners already participate, underpinned by INSPIRE core (elevation) and thematic data.
- Provide a cost-benefit assessment for using OGC interoperability specifications to harmonise INSPIRE Annex I (elevation) and Annex II (marine, coastal management) spatial data. This assessment includes analysis of two existing marine information services created without using open source standards (proprietary code, no GML schema, no agreed ontology, no standard feature catalogues, etc.) and one or two 'post-standardisation' marine information services created using the tools developed in the early stages of the project.
- Building on the pre-standardisation work of the EC MarineXML project (Millard *et al.*, 2005), establish a marine data standards registry under the auspices of the Intergovernmental Oceanographic Commission (IOC and International Hydrographic Organization (IHO).
- Produce a fully qualified business case for the establishment of an official OGC Working Group on Marine Data, based on marine data related deliverables from the project, i.e. a marine ontology, a UML marine data model, review and recommendation of marine terminology thesauri, OGC feature type catalogue and GML application schema.

References

Millard *et al.* (2005). Using XML Technology for Marine Data Exchange. A Position Paper of the MarineXML Initiative. Download from www.marineXML.net.

Evaluating the assimilation of continuous Cloud-to-Ground lightning in mesoscale models

Anastasios Papadopoulos*[1], Themis G. Chronis[2] and Emmanouil N. Anagnostou[2]

[1]*Hellenic Centre for Marine Research, Institute of Oceanography, Greece*
[2]*Department of Civil and Environmental Engineering, University of Connecticut, USA*

Abstract

This paper evaluates a technique developed for assimilating regional lightning measurements into a meteorological model. The goal is to exploit how useful Cloud-to-Ground (CG) lightning information can be for improving the convective precipitation forecasting. The main concept of the technique is that utilising real-time location, timing and flash rate data retrieved from a long-range lightning detection network, a regional/ mesoscale meteorological model is informed about the deep moist convection spatio-temporal development and intensity. This information is then used to nudge the model-generated humidity profiles to empirical profiles as a function of the observed lightning intensity. The performance of the technique was verified on the basis of three major thunderstorm activities which occurred in different warm-season environments: the Mediterranean basin, Continental US and Central–West Africa. The results show that the assimilation of lightning data can significantly improve the model's prediction accuracy of convective precipitation demonstrating consistent performance in all three convective regimes.

Keywords: Convective precipitation forecasting, lightning, mesoscale modelling

1. Introduction

Convective events produce very intense rainfall, which can lead to river floods, flash floods, and soil erosion among other problems. These problems are most acute in urban and coastal areas where run-off production is quickest and human population living in flood prone areas most common. In most situations convective systems are responsible for the heaviest and most damaging spring to early autumn rainfall and flood events in the Mediterranean region. However, the prediction of rainfall structures and variability are not yet good enough to enable accurate flood forecasting from such systems. An aspect that has shown convincing signs of improving numerical weather prediction is data assimilation on the basis of satellite and continuous lightning observations (e.g. Alexander *et al.*, 1999; Chang *et al.*, 2001). Recently, a technique was developed to amend the initialisation data inadequacies and the limitations in formulating sub-grid scale processes using continuous lightning observations. In this study, Papadopoulos *et al.* (2005) showed that nudging model humidity profiles to an empirical profile related to flash rates, leads to more realistic model soundings and consequential improvements in convective precipitation forecasts. The definition of those empirical humidity profiles can be made either experimentally or through cloud resolving model simulations.

* Corresponding author, email: tpapa@ath.hcmr.gr

Papadopoulos *et al.* (2005) determined them empirically from atmospheric sounding data (through trial and error analysis) on the basis of maximising the assimilation impact on quantitative precipitation forecasting accuracy. In this study we verify the technique performance based on major thunderstorm activities that occurred in different warm-season environments, i.e. the Mediterranean basin, continental USA and Central–West Africa.

2. The assimilation technique

The assimilation technique has been implemented into the POSEIDON weather forecasting system, which is based on the SKIRON/Eta model (Papadopoulos *et al.*, 2002). The assimilation scheme makes direct use of lightning data to indicate areas of convection in the model's domain. Based on that information the model humidity profiles are nudged relative to the observed flash rates. The adjusted humidity profiles are then used, on the basis of the model's convective parametrisation scheme, to compute heating rate profiles that are more compatible with the local scale convective environment. The technique starts by projecting the flash rate data on the model's spatio-temporal grid structure. Convective areas are then delineated from grid points with a flash rate exceeding a certain threshold (in Papadopoulos *et al.* the threshold was set to 2 and 10 flashes/15 min over sea and land, respectively) and compared to model simulations.

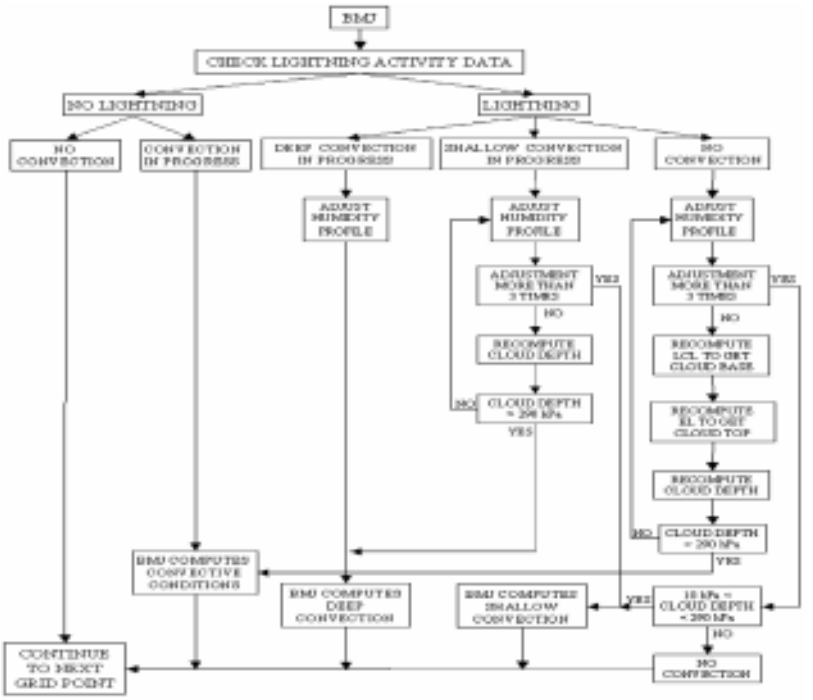

Figure 1 Flow chart of the assimilation technique (adapted from Papadopoulos *et al.*, 2005).

Four possible scenarios are considered. The first scenario concerns model grid cells where lightning observations indicate that there is no significant electrical activity. In this case the model's convective scheme is allowed to carry on, as it would normally do without nudging. The other three scenarios are associated with grid cells where flash rate data are above the threshold denoting convection. These scenarios are then classified as deep, shallow or no-convection, according to the model output. Subsequently a nudging technique is applied into the model convective parametrisation scheme following the decision-making procedure shown in Figure 1. A detailed description of this procedure is given in the work of Papadopoulos *et al.* (2005).

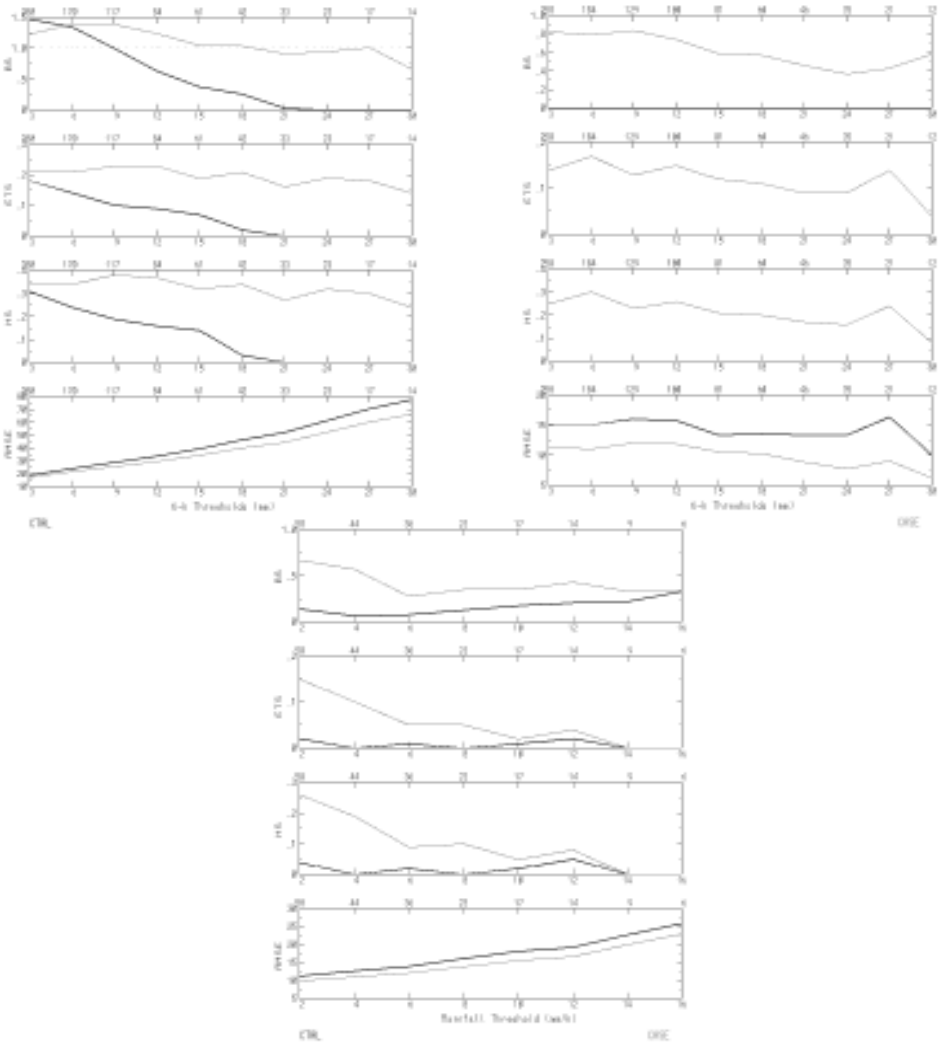

Figure 2 Statistical values of skill and error calculated from the CTRL (black) and CASE (grey) experiments for the entire storm period against (left) 6 hourly ECMWF rain gauge data in Europe; (centre) TRMM PR-calibrated instantaneous SSM/I rain rates; (right) hourly rain gauge-calibrated WSR-88D radar rain data.See text for details.

3. Numerical experiments

To investigate the sensitivity of precipitation forecasts two experiments were performed: a control run in which no lightning data were assimilated (hereafter named CTRL) and a run where lightning data were continuously assimilated for the entire storm period (CASE). For the numerical experiments the POSEIDON weather forecasting system was used, incorporating data from the ZEUS regional network of ground-based receivers (covering Europe and Africa) and from the US National Lightning Detection Network. The assessment was performed using 6-hourly rain accumulation measurements as reference, available from the European Centre for Medium-range Weather Forecasts (ECMWF) rain gauge network in Europe, and gridded rainfall fields derived from Tropical Rainfall Measurement Mission (TRMM)-calibrated Special Sensor Microwave/ Imager (SSM/I) rain rates over Africa and from a mosaic of hourly rain gauge-calibrated WSR-88D radar rain observations in USA.

Using the contingency table approach (Wilks, 1995) the forecast skill was measured by evaluating the bias score (BS), the equitable threat score (ETS), the Heidke skill score (HSS) and the root mean square error (RMSE) for varying threshold values of rainfall accumulation. Combining these statistical criteria a comprehensive evaluation of the impact of assimilation on model performance can be achieved. For example, a greater ETS would represent a significant model improvement only if it is accompanied by a BS with a value closer to one and a lowering RMS. The statistical values calculated from the CTRL and CASE experiments for three storm cases (one in each continent) are presented in Figure 2. The results indicate that assimilation of CG lightning data considerably improves the model's convective precipitation forecasts. It is important to note that assimilation has a greater impact on the prediction of higher rainfall amounts.

4. Conclusions

The performance of the technique was originally verified in the Papadopoulos *et al.* (2005) study on the basis of three major thunderstorms that occurred in the Mediterranean region in the warm seasons of 2002 and 2003. In this study we further evaluated the technique on the basis of storms that occurred in three different continents: Europe, Central–West Africa, and continental USA. The statistical evaluation denotes that the regional lightning assimilation can help improve the model's efficiency to simulate convective precipitation, and that this improvement is consistent across different continental regimes. Consequently, the definition of the empirical humidity profiles can have a global applicability.

However, a known limitation of this technique is the weak physical basis for the selection of the empirical humidity profiles. Those profiles were derived from initial atmospheric soundings through trial and error adjustments using the model performance as sole criterion. Consequently, the establishment of a stronger physical basis for determining the humidity profiles (e.g. using outputs from electrified cloud resolving models) is mandated for further improving the accuracy of the forecasts. Further improvements are also expected by nudging both humidity and temperature profiles and assimilating latent heating profiles derived on the basis of rain rates retrieved from combined remotely sensed observations.

Acknowledgements

This study was supported by the X-FLOOD Marie Curie project funded by the EU.

References

Alexander, G.D., J.A. Weinman, V.M. Karyampudi, W.S. Olson and A.C.L. Lee (1999). The effect of assimilating rain rates derived from satellites and lightning on forecasts of the 1993 Superstorm. Mon. Wea. Rev., 127, 1433–1457.

Chang, D.-E., J.A. Weinman, C.A. Morales and W.S. Olson (2001). The effect of spaceborne microwave and ground-based continuous lightning measurements on forecasts of the 1998 Groundhog Day Storm. Mon. Wea. Rev., 129, 1809–1833.

Papadopoulos, A., T.G. Chronis and E.N. Anagnostou (2005). Improving Convective Precipitation Forecasting Through Assimilation of Regional Lightning Measurements in a Mesoscale Model. Mon. Wea. Rev., 133, 1961–1977.

Papadopoulos, A., G. Kallos, P. Katsafados and S. Nickovic (2002). The Poseidon weather forecasting system: An overview. GAOS, 8, 219–237.

Wilks, D.S. (1995). Statistical Methods in the Atmospheric Sciences: An Introduction. Academic Press, 467 pp.

Data assimilation in numerical wave models

G. Galanis[1,2], G. Emmanouil[1] and G. Kallos*[1]

[1]*Institute of Accelerating Systems and Applications, University of Athens, School of Physics, Atmospheric Modeling and Weather Forecasting Group, Greece*
[2]*Greek Naval Academy, Section of Mathematics, Greece*

Abstract

This paper presents the results of the operational utilisation of remote sensing data (Envisat Significant Wave Height and Spectra) assimilated in the WAM model (cycle 4). Different assimilation methods have been employed and validated in order to study the benefits of such a procedure in operational wave forecasting.

Keywords: Numerical wave prediction, wave height and spectral assimilation, WAM

1. Numerical wave forecasting model and assimilation methods used

Nowadays, high quality wave forecasts are necessary in order to handle several sections of sea and ocean activities like ship traffic, aquaculture, tourism and offshore exploration, in an appropriate way. An increasing number of operational forecasting centres and research institutes are currently using numerical wave models for regional or global forecasts. A recent development is the use of wave models that are based on the solution of the spectral equation of wave energy. In the present study, one of the most commonly used models of the previous type, WAM (cycle 4), is employed.

WAM is a third generation wave model which solves the wave transport equation explicitly without any presumptions on the shape of the wave spectrum. It represents the physics of the wave evolution in accordance with our knowledge for the full set of degrees of freedom of a 2d wave spectrum.

The resulting forecasts are mainly dependent on the initial atmospheric and wave conditions, the quality of the atmospheric forecast used, as well as local domain characteristics which may lead to possible biases. In order to improve the short and long-term specification of wave conditions in both offshore and coastal waters, as well as to get more accurate and reliable global long term wave statistics, different assimilation techniques are applied. The main sources of data used as input to the assimilation algorithms for the correction of wave forecasts are buoy measurements and satellite records (altimeter and scatterometer).

Two different assimilation methods have been employed in this work:

1.1 Assimilation of significant wave height

The module used has been developed by Norwegian Meteorological Institute (DNMI, see Breivik, 1994). The analysis scheme is based on a modification of the traditional

* Corresponding author, email: kallos@mg.uoa.gr, cc ggalanis@mg.uoa.gr

successive correction methods (Cressmann, 1959). It is analogous to the statistical interpolation (Hollingsworth, 1987). The method is based on the following two iterative equations for Significant Wave Height (*SWH*):

$$SWH_i^A(k+1) = SWH_i^A(k) + \sum_{j=1}^{N} a_{ij}(SWH_j^O - SWH_j^A(k)) \quad (1)$$

$$SWH_x^A(k+1) = SWH_x^A(k) + \sum_{j=1}^{N} a_{xj}(SWH_j^O - SWH_j^A(k)) \quad (2)$$

where $a_{ij} = \frac{(m_{ij} + d_{ij})}{M_j}$, $a_{xj} = \frac{m_{xj}}{M_j}$

Subscripts i, j refer to observation points, x to grid points, superscripts O, P, T and A to observed, first guess, true and analysed value, N is the number of observations and k an iteration counter. m_{ij} and d_{ij} are model error and observation error covariances respectively, M_j is a function of m_{ij} and d_{ij} chosen so that the above equation converges.

1.2 Assimilation of wave spectrum

This scheme is the latest development obtained in the framework of the EU ENVIWAVE project (www.oceanor.no/projects/enviwave/index.htm). It is based on an Optimal Interpolation Scheme (Aarnes, 2003). The matrix equation used is:

$$(R + HBH^T)w_a = y - Hx_b,\ x_a = x_b + BH^T w_a \quad (3)$$

where R is the observation covariance matrix, B the model covariance matrix, H the observation operator, y the observations, x_b model's first guess and x_a the analysed data.

2. Results and statistics

The Atmospheric Modeling and Weather Forecasting Group group at the University of Athens covers several different areas operationally, starting from the global scale, to open oceans (Indian), closed seas (Mediterranean and Aegean Sea) and down to small gulfs (Saronic Gulf).

This paper presents the results from a detailed study for the Mediterranean Sea and Indian Ocean. The testing period was 50 days during November–December 2004. The assimilation window for these tests was 12 hours and the input data were satellite measurements from Envisat (altimeter-RA2 and scatterometer-ASAR instrument).

Table 1 presents some general statistical results for both domains. In the Mediterranean Sea, there is a high correlation between altimeter data and initial WAM outputs without any assimilation scheme activated. This fact combined with the local characteristics of the Mediterranean area (wind sea dominated closed basin), leads to restricted assimilation influence.

Table 1 Bias and standard deviation between WAM (with and without assimilation) and satellite measurements of significant wave height in metres.

	RA2 vs. model				ASAR vs. model	
	Mediterranean Sea		Indian Ocean		Indian Ocean	
	RA2-WAM	RA2-(WAM+assim)	RA2-WAM	RA2-(WAM+assim)	ASAR-WAM	ASAR-(WAM+assim)
Bias	–0.37	–0.39	0.12	–0.11	0.04	0.60
St.deviation	0.49	0.50	0.67	0.43	0.15	0.38

For the Indian Ocean, the assimilation of altimeter data leads to the reduction of the model output's deviation, as well as to the elimination of high differences between WAM and satellite records. On the other hand, the assimilation of spectra measurements leads to increased bias compared to that of the altimeter, but the deviation (RMSE) remains at the same level (Table 1).

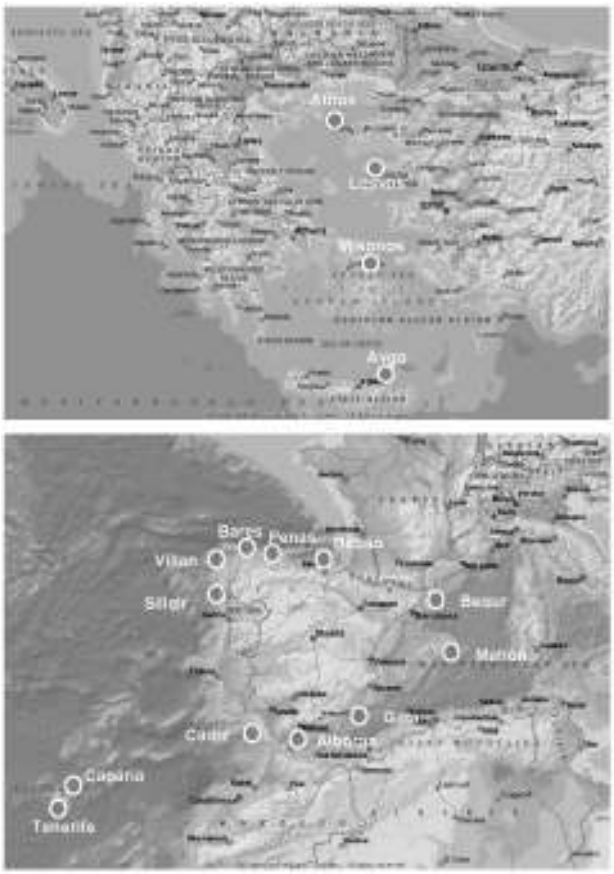

Figure 1 Top: Location of the Greek buoys; Bottom: Location of the Spanish buoys.

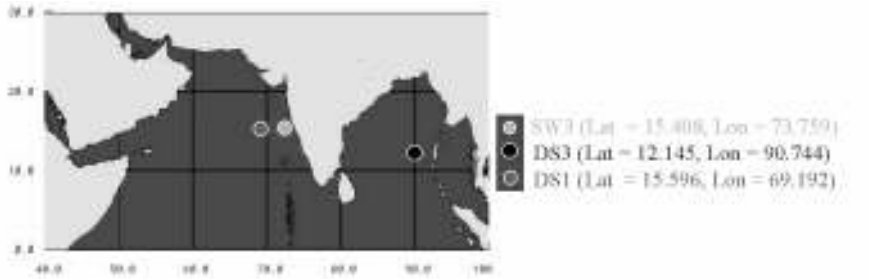

Figure 2 Location of Indian buoys.

The evaluation of the model results against the available buoy measurements (Table 2 and Table 3) leads to the conclusion that the initial forecast (without any assimilation) of the wave model in the Mediterranean Sea has a high accuracy, in contrast with the one for the Indian Ocean where increased differences between model and buoy measurements have emerged. In this case the use of both assimilation systems significantly improves the final forecasting output.

Table 2 Swh bias and absolute bias between WAM vs. buoy measurements, without assimilation (in m).

	24 hour forecast		48 hour forecast		72 hour forecast	
Buoys	**WH bias**	**WH abs. bias**	**WH bias**	**WH abs. bias**	**WH bias**	**WH abs. bias**
Athos	0.17	0.24	0.18	0.25	0.20	0.31
Avgo	–0.07	0.18	–0.06	0.16	–0.11	0.16
Mykonos	0.13	0.47	0.19	0.43	0.27	0.42
Lesvos	0.23	0.26	0.25	0.27	0.27	0.30
Aegean	**0.12**	**0.28**	**0.14**	**0.28**	**0.16**	**0.30**
Alboran	0.02	0.22	0.04	0.20	0.05	0.18
Gata	0.13	0.23	0.13	0.24	0.13	0.25
Begur	0.12	0.29	0.11	0.29	0.10	0.34
Mahon	0.24	0.34	0.23	0.32	0.24	0.35
Spain/Med	**0.13**	**0.27**	**0.13**	**0.27**	**0.13**	**0.28**
Tenerife	–0.75	0.81	–0.85	0.85	–0.91	0.91
Canaria	–0.68	0.81	–0.76	0.81	–0.83	0.85
Bares	–0.15	0.48	–0.21	0.45	–0.21	0.47
Bilbao	–0.19	0.47	–0.24	0.42	–0.26	0.42
Gadiz	–0.22	0.49	–0.33	0.50	–0.33	0.51
Sileiro	–0.18	0.49	–0.25	0.47	–0.27	0.51
Vilano	–0.27	0.60	–0.31	0.59	–0.36	0.58
Spain/Atlantic	**–0.35**	**0.59**	**–0.42**	**0.59**	**–0.45**	**0.61**

Table 3 Bias and root mean square error (RMSE) for SWH between WAM (with and without assimilation) and buoy measurements for the Indian Ocean (in m).

	NoAssim vs. buoy			AssimRA2 vs. buoy			AssimSpectra vs. buoy		
Buoy	**SW3**	**DS3**	**DS1**	**SW3**	**DS3**	**DS1**	**SW3**	**DS3**	**DS1**
Bias	0.51	0.44	0.50	0.41	0.15	0.51	0.53	0.26	0.51
RMSE	0.60	1.14	0.60	0.44	0.30	0.54	0.55	0.34	0.54

3. Conclusions

Both assimilation modules used (altimeter and scatterometer) significantly improve the wave forecast.

In the Indian Ocean, the wide number of available observation data combined with the fact that this is a swell dominated area (Aouf *et al.*, 2005), leads to an increased assimilation impact and therefore to better forecasting results.

In the Mediterranean Sea, the influence of assimilation seems to be restricted mainly due to lack of a sufficient number of observation data, high correlation of satellite records with model outputs and local characteristics of the Mediterranean basin. Despite this, the assimilated results are of a very satisfactory level.

Acknowledgments

This work is supported by the EnviWave project (EVG−2001−00017). SINTEF and DNMI are acknowledged for their cooperation during this project concerning data filtering and assimilation algorithms.

References

Aarnes, J.E. (2003). Iterative methods for data assimilation and an application to ocean state modeling, SINTEF Applied Mathematics, December 2003.

Aouf, L., J.-M. Lefèvre, D. Hauser and B. Chapron (2005). The impact of long period assimilation of ENVISAT ASAR directional wave spectra on wave forecasts. This volume page 682.

Breivik, L.-A. and M. Reistad (1994). Assimilation of ERS-1 Altimeter Wave Heights in an Operational Numerical Wave Model, Weather and Forecasting, Vol. 9, No. 3.

Cressman, G.P. (1959). An Operational Objective Analysis System. Mon. Wea. Rev., 87, 367−374.

Hollingsworth, A. (1987). Objective analysis for numerical weather prediction. J. Meteor. Soc. Japan, 65, 11−60.

Janssen, P.A.E.M., P. Lionello, M. Reistad and A. Hollingsworth (1987). A study of the feasibility of using sea and wind information from the ERS-1 satellite, part 2: Use of scatterometer and altimeter data in wave modelling and assimilation. ECMWF report to ESA, Reading.

Sea surface temperature assimilation in a high resolution model of the North Sea

S. Ponsar*[1], I. Andreu-Burillo[2] and P. Luyten[1]

[1]*Management Unit of the North Sea Mathematical Models (MUMM), Brussels, Belgium*
[2]*Proudman Oceanographic Laboratory (POL), Liverpool, United Kingdom*

Abstract

This paper presents a three-dimensional numerical study of the effect of satellite sea surface temperature assimilation on previsions of the temperature field in the North Sea. The results are compared with *in situ* temperature profiles. Model predictions are improved when sea surface temperature data are assimilated.

Keywords: Data assimilation, numerical modelling, sea surface temperature, North Sea.

1. Introduction

The three-dimensional hydrodynamic component of the model COHERENS has been recently developed in parallel to allow high resolution simulations of the North Sea. The effect of assimilating satellite sea surface temperature data on the previsions of the temperature field is examined through a sea surface temperature (SST) assimilation scheme. A series of simulations with a spatial resolution of 4 nautical miles (~7 km) has been conducted for the year 2001.

2. Model description

The basic equations of momentum, continuity, temperature and salinity, written in spherical polar coordinates are discretised on an Arakawa-C grid with 20 s-levels in the vertical. For further details concerning the parallelised version of COHERENS, see Luyten *et al.* (2005).

The main sources of error on the model results are thought to be due to uncertainties in the initial conditions, unresolved physical processes, and errors in the parametrisation of the air-sea interaction. One way of improving the results is to introduce data assimilation.

3. Data assimilation scheme description

The data assimilation scheme was proposed by Annan and Hargreaves (1999). It is a one-dimensional simplification of the Kalman filter. At the analysis step, the model state vector is computed as

$$x^a_{n+1} = x^f_{n+1} + K_{n+1}(x^0_{n+1} - Hx^f_{n+1}) \quad (1)$$

* Corresponding author, email: s.ponsar@mumm.ac.be

where x^a_{n+1} is the analysed state vector at time step n+1,
x^f_{n+1} is the forecast state vector, x^0_{n+1} is the observations vector,
K_{n+1} is the Kalman gain, and H is a matrix which interpolates model variables to observed variables.

To compute the Kalman gain matrix (which is dependent on the model and observation error covariances), the following assumptions are imposed (at the assimilation step): the horizontal correlations between horizontal temperature gradients and density-driven flows are assumed to be sufficiently small so that they can be ignored, the temperature in the mixed layer is adjusted independently of the turbulent kinetic energy and the regions above and below the thermocline are supposed to be well mixed but mixing through the thermocline is assumed to be negligible. Therefore, the expression of the increase of the model error covariance between two analysis steps reduces to

$$d = k\frac{d\tau}{dh} \tag{2}$$

with k a constant adjusted depending on the experiments, $d\tau$ the time interval between two assimilations and dh the depth of the upper mixed layer.

4. Results

Simulations were performed with a spatial resolution of 4 nautical miles for the year 2001 on the North Sea domain extending from 4° W to 10° E and from 48.5° N to 60° N. Meteorological data have a temporal resolution of one hour. Tidal harmonics and daily inflow/outflow conditions at the boundaries of the domain are derived from simulations with the POLCOMS model covering a larger area. Two series of simulations were performed: a first series of hydrodynamic simulations without data assimilation, and a second series with assimilation of SAF satellite temperature data. The SAF products have been validated (climatology check) and tested to remove erroneous data and data contaminated by cloudy pixels (Hoyer and She, 2004). We only assimilate night time data (standard deviation of 0.64°C) because the mean SST differences from day to night amount to 1.5°C and are still larger in summer. Of course, the satellite data are not uniformly distributed in space and time (depending on the cloud cover at the time of the measurement). At points where no satellite data are available, no assimilation is performed.

The model error covariance is computed at each assimilation step using a value for k equivalent to a model variance of $(1/4°C)^2$ per day for a thermocline at 20 metres depth. This value has been chosen because it gives the results which are the closest to the observations (for more details, see Annan and Hargreaves (1999) who determined this value through simulations for the North Sea). The results presented in this article are preliminary results of a study which is not yet fully completed. We present the horizontal distribution of the temperature at the sea surface as well as at the sea bed in winter (January) and summer conditions (August). Moreover, the root mean square discrepancy between the temperature profiles modelled with and without data assimilation has been computed.

Finally, a one-dimensional comparison of the modelled temperature profiles to observations is presented.

Figure 1 shows the horizontal distribution of temperature at the sea surface on 15 August 2001 without (Figure 1 left) and with (Figure 1 right) data assimilation. This temperature distribution can be compared to the same sea surface temperature distribution on 15 January 2001 in absence of assimilation (Figure 2 left) and including data assimilation (Figure 2 right). The temperature distribution at the sea bed on 15 August 2001 is given in Figure 3 for both cases.

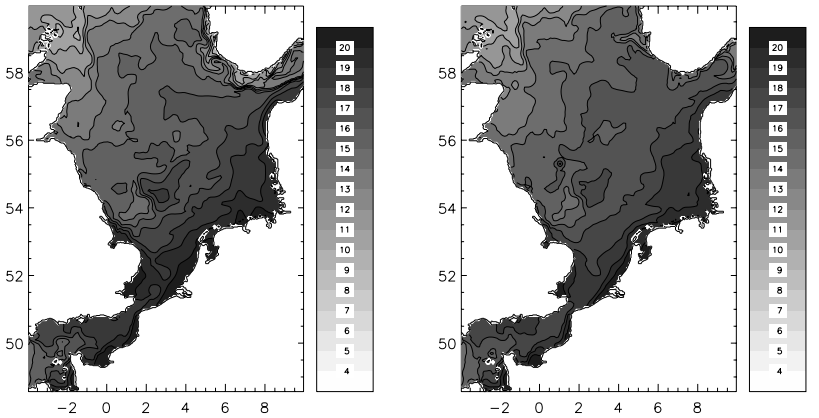

Figure 1 Horizontal distribution of modelled temperature (°C) at the sea surface on 15 August 2001. Left: without data assimilation; Right: with data assimilation.

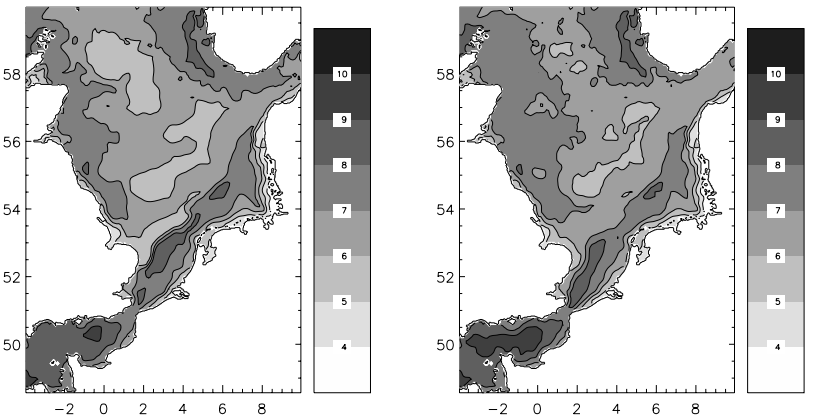

Figure 2 Horizontal distribution of modelled temperature (°C) at the sea surface on 15 January 2001. Left: without data assimilation; Right: with data assimilation.

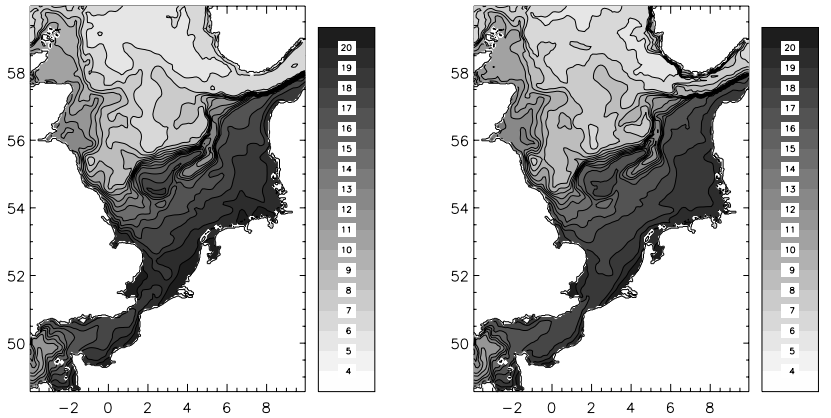

Figure 3 Horizontal distribution of modelled temperature (°C) at the sea bed on 15 August 2001. Left: without data assimilation; Right: with data assimilation.

Figure 4 shows that assimilation decreases the temperature in winter (at the sea bed and at the sea surface) and increases the summer temperature (sea bed and sea surface).

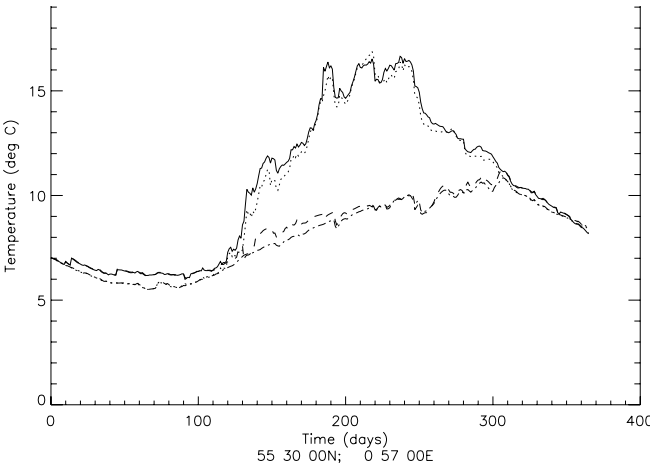

Figure 4 Time series of modelled temperature at the CS North Sea station, (55°31'N, 0°54'E): sea surface with data assimilation (continuous line), sea surface without data assimilation (dotted line), sea bed with data assimilation (dashed line), sea bed without data assimilation (dotted-dashed).

The root mean square (rms) discrepancy between temperature modelled without and with data assimilation has been computed for each month. The averaged values at the sea surface for January 2001 and August 2001 are respectively shown on Figure 5 left and centre. Figure 5 (right) represents the rms values for August 2001 at the sea bed. The maps show a seasonal signal in the rms temperature discrepancy.

Finally, the modelled temperature profiles were compared with observations. Neglecting the horizontal correlations, the Annan scheme reduces to a one-dimensional problem, so that the first tests presented here are based on a vertical one-dimensional model.

Thermistor chain data from the North Sea project, 1989, have been used to estimate the quality of the temperature profiles modelled without and with data assimilation at the North Sea station CS (55°31'N, 0°54'E). The assimilated surface temperature is located at 10 metres depth. The accuracy of the NSP data is within 0.1°C rms error. The profiles are extracted for 15 June 1989.

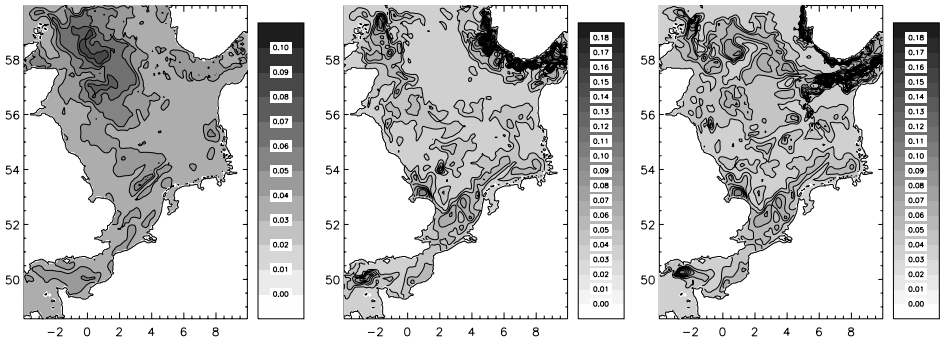

Figure 5 a) Horizontal distribution of rms discrepancy (°C) between temperature modelled without and with data assimilation. Left: at the sea surface for January 2001; Centre: at the sea surface for August 2001; Right: at the sea bed for August 2001.

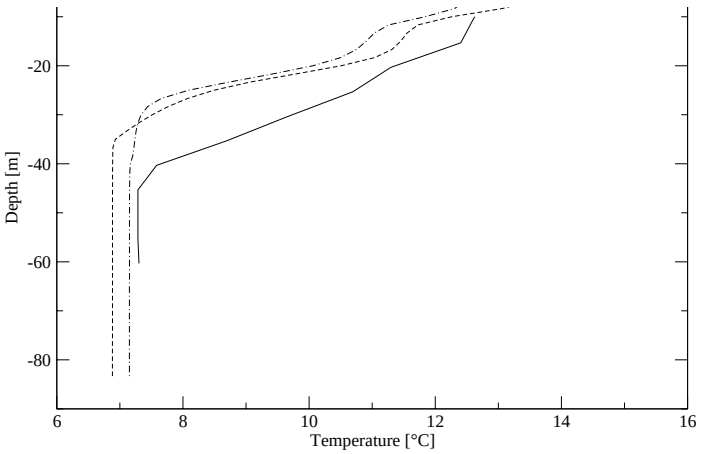

Figure 6 Vertical profiles of temperature modelled without assimilation (dashed line), with assimilation (dotted-dashed line), and observed temperature (North Sea Project data) (continuous line), (15 June 1989, CS North Sea Station).

Figure 6 indicates a better agreement between the observations and the surface temperature modelled when data assimilation is taken into account. However, the Annan scheme is not completely adapted to correct the temperature below the thermocline.

Full validation of the results for the year 2001 and for the whole North Sea domain studied is ongoing. It is based on a comparison of the modelled temperature without assimilation and with assimilation of satellite surface data to *in situ* temperature profiles.

5. Conclusions

In this study, we have examined the effect of the assimilation of satellite SST data on high resolution (4 nautical miles) modelled temperature profiles for the North Sea. One of the great advantages of the Annan scheme is its low computational cost. The model slightly underestimates the winter temperature and slightly overestimates the summer temperature; these anomalies are corrected by the assimilation scheme. Results show a seasonal signal in the rms discrepancy between temperature modelled without and with data assimilation. Moreover, there is a better agreement with the observations for the surface temperature modelled with data assimilation. However, the Annan scheme is not completely adapted to correct the temperature below the thermocline. To take this correction into account, a next step in this study is to implement and test the Ensemble Kalman Filter assimilation scheme (Evensen, 2003).

Acknowledgements

This work has been supported by the European Commission under the Fifth Framework Programme under the ODON project (Optimal Design of Observational Networks), Contract No. EVK3−CT−2002−00082.

References

Annan, J.D. and J.C. Hargreaves (1999). Sea surface temperature assimilation for a three-dimensional baroclinic model of shelf seas, Continental Shelf Research, 19, 1507−1520.

Evensen, G. (2003). The Ensemble Kalman Filter: theoretical formulation and practical implementation, Ocean Dynamics, 53, 343−367.

Hoyer, J.L. and J. She (2004). Validation of satellite SST products for the North Sea−Baltic Sea region, Danish Meteorological Institute, Technical report.

Luyten, P., I. Andreu-Burillo, A. Norro, S. Ponsar and R. Proctor (2005). A new version of the European public domain code COHERENS. This volume page 474.

Luyten, P.J., J.E. Jones, R. Proctor, A. Tabor and K. Wild-Allen (1999). COHERENS-A coupled hydrodynamical-ecological model for regional and shelf seas, user documentation, MUMM Report 911 pp. Available on CD-ROM at www.mumm.ac.be/coherens.

Evaluation of the Ensemble Kalman Filter in ecosystem state forecasting

Ricardo Torres*[1], Icarus Allen[1] and Francisco Figueiras[2]

[1]*Plymouth Marine Laboratory, UK*
[2]*Instituto de Investigaciones Marinas, Spain*

Abstract

An evaluation of the Ensemble Kalman filter for ecosystem state forecasting has been carried out. The system consists of a 1D coupled physical–biological model ERSEM–GOTM implemented inside an estuarine system affected by upwelling (Ria de Vigo, Spain). The Square Root Ensemble Kalman Filter has been used in the sequential assimilation of chlorophyll, nitrate, ammonia, silicate and phosphorous. Comparison of model runs with and without assimilation show an improvement on the assimilated variables and a large effect on all the other pelagic estate variables. Comparison of model results and functional group biomass observations show that the assimilation of chlorophyll reduces the bias on most of the functional groups at the same time as it corrects the model variance with respect to observations.

Keywords: Data assimilation, ecosystem model, Ria de Vigo

1. Introduction

In the last two decades there has been a noticeable increase in the occurrence of "Harmful Algal Blooms" (Glibert and Pitcher, 2001). HABs may develop rapidly with a marked increase in the local population of microscopic and macroscopic algae that can cause harm in a multitude of ways, from health risks through the food chain to fouling of fishing gear, and smearing beaches causing economic losses.

Warning systems of such rapidly evolving events are required to prevent both environmental and health disasters. Coupled hydrodynamic–ecosystem models are an important tool for reproducing the major qualitative aspects of the ecosystem and addressing issues like coastal zone management, eutrophication and harmful algal blooms (Gentien *et al.*, 2003).

A combination of ecosystem modelling and data assimilation techniques provides the necessary tools for prediction of such events and helps to mitigate their noxious consequences. This is tested with the 1D coupled physical–biological model ERSEM–GOTM (Allen *et al.*, 2004).

2. Model system components

2.1 European Regional Seas Ecosystem Model

The Functional Group Model (FGM) ERSEM divides the ecosystem into aggregated groups representing basic functional roles (production, consumption and decomposition)

* Corresponding author, email: rito@pml.ac.uk

for both the pelagic and benthic systems. These are subdivided into size classes to create a foodweb with five phytoplankton groups, three zooplankton and one bacteria group including a dissolved and particulate detritus pool (Blackford *et al.*, 2004).

Physiological processes and population dynamics are described by fluxes of carbon or nutrients between functional groups. For any phytoplankton group the dynamics are described as:

*Change of carbon = (Assimilation − Excretion − Respiration − Lysis − Sedimentation)*C − Grazing*

ERSEM features include de-coupled Carbon-Nutrient dynamics following a Droop type quota model which allows for luxury storage; a simple relaxation scheme simulates phytoplankton photoacclimatation; and a benthic module describes the recycling of nutrients in a layered benthic substrate and the exchange of nutrients with the pelagic system.

2.2 Data assimilation

Data assimilation is a technique that combines model output and observations simultaneously to control the evolution of a model. They allow the creation of "optimal initial conditions" to improve the system's predictability (Figure 1).

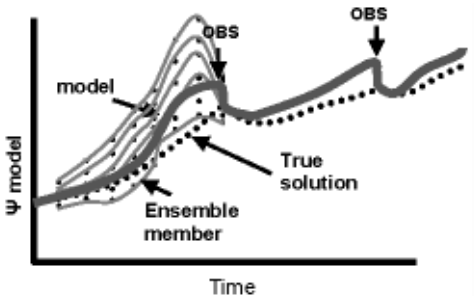

Figure 1 Schematic of data assimilation.

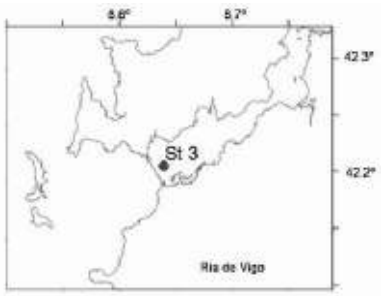

Figure 2 Coastline of the Ria de Vigo, Spain and location of 1D model setup (St 3).

The Ensemble Kalman Filter (EnKF) (Evensen, 2004) predicts the model error evolution through a Monte Carlo method. Gaussian errors are assigned to the initial conditions and model dynamics, generating an ensemble of model states which are integrated forward in time. When observations are available, an analysis scheme is used to update the ensemble members. In this case, the analysis scheme used is the Square Root Ensemble Kalman Filter (EnKFSQR) (Evensen, 2004). The updated state is a linear combination of the forecasted ensemble members mediated by the observations, and minimises the error variance of the analysed estimate.

These functions are multivariate statistical functions and the cross-correlations between the different variables in the model are included. Thus, a change in one of the model variables will update the other variables. The final solution is the mean of the ensemble.

2.3 1D model implementation

The 1D coupled model ERSEM−GOTM was implemented in the estuary like Ria de Vigo (42º15'N, 8º50'W, NW Spain, St 3, Figure 2). Seasonal upwelling (May−October) and downwelling (November−March) takes place over the shelf and inside the Ria.

Short time events (2–4 days) of upwelling–downwelling pulses are common throughout the year.

The 40 m water column is partially mixed during the winter months (Figure 3) and stratified in a two layer structure during the summer months. The evolution of the water column structure is largely controlled by cold shelf water advection at the bottom during upwelling pulses (See for example periods in July and August in Figure 3).

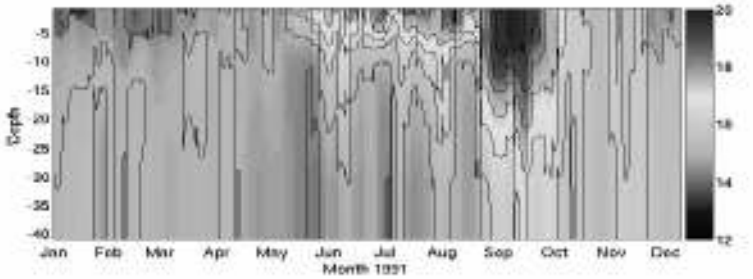

Figure 3 Time evolution of the temperature structure during 1991 simulation, °C.

To "realistically" reproduce the water column structure, temperature and salinity profiles have been assimilated every ~4 days into the model using a relaxation scheme (Buchard *et al.*, 1999).

3. Results

A square root algorithm of the EnKF (EnKFSQR) has been implemented in the 1D model. This differs from the standard EnKF in that no perturbation of measurements is needed (Evensen, 2004). Chlorophyll, nitrate, ammonia, silicate and phosphate have been assimilated at three depths (surface, depth of thermocline and bottom) every four days. Initial condition and model errors were set to 20% while measurement errors were kept at 5%. Assimilation of all variables has been sequentially implemented together with a log transformation model. This restricts variable values to positive ones. Errors in the forcing have been introduced through perturbations of the sea surface irradiance and the light attenuation coefficient amounting to a 20% error.

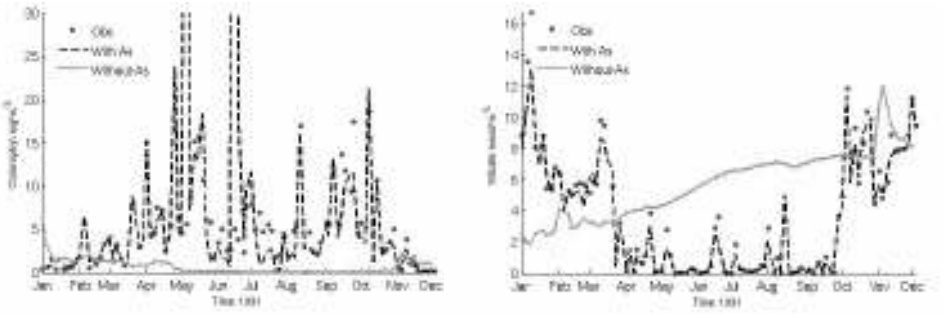

Figure 4 Time evolution of assimilated variables from model and observations at the surface. Left: chlorophyll; Right: nitrate. Model data include simulation with and without assimilation.

The assimilated variables are all well reproduced by the model and represent a dramatic improvement on the free run (as shown by the example from surface values in Figure 4). The absence of a parametrisation of nutrient advection due to upwelling and downwelling dynamics is responsible for the divergence of the free run with respect to the data. It is worth noting the rapid and extreme changes that take place inside the Ria de Vigo, e.g. chlorophyll levels can change by the order of 15 mg m^{-3} in 3 days (3 days being the minimum sampling interval of the data series).

Non-assimilated variables are also transformed during assimilation (Figure 5). The improvement on diatom biomass is particularly important as they represent the largest biomass compartment in the planktonic ecosystem of the Ria de Vigo (46% of the year integrated biomass). Bacteria biomass is also improved with respect to the free run even though they are not directly related to the observed chlorophyll values used in the assimilation. The partitioning of the chlorophyll among the model variables is done according to the internal dynamics of the model ensembles.

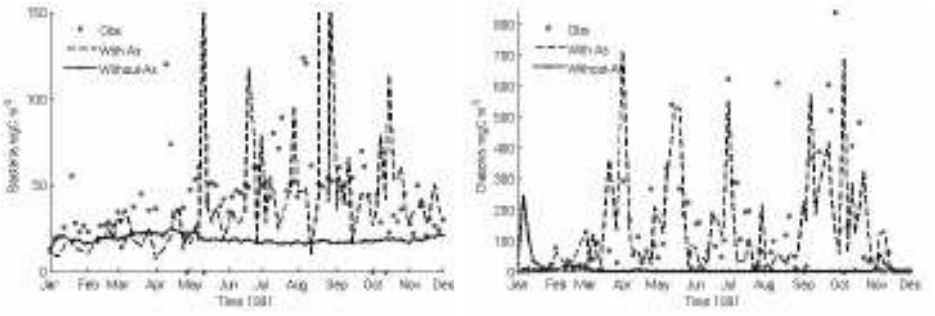

Figure 5 Time evolution of non assimilated variables from model and observations at the surface. Left: Bacteria; Right: Diatoms. Model run without assimilation is shown as a continuous line.

Figure 6 provides a summary of the impact of assimilation on all measured variables. On the Y axis, the ratio of observation to model standard deviations represents the agreement in variability between the two datasets (model vs. observations) while the R^2 for linear correlation is on the X axis. It is clear from Figure 6 (left), that all assimilated variables improve in the assimilation run, both correcting the time evolution (R^2) and the overall variance. The improvement on the non-assimilated variables is less consistent. The discrepancy in the variance is improved on all variables but only the diatoms show a significant improvement in the linear correlation. Nonetheless, most variables corrected their mean bias, in particular diatoms, dinoflagellates, picoplankton and bacteria.

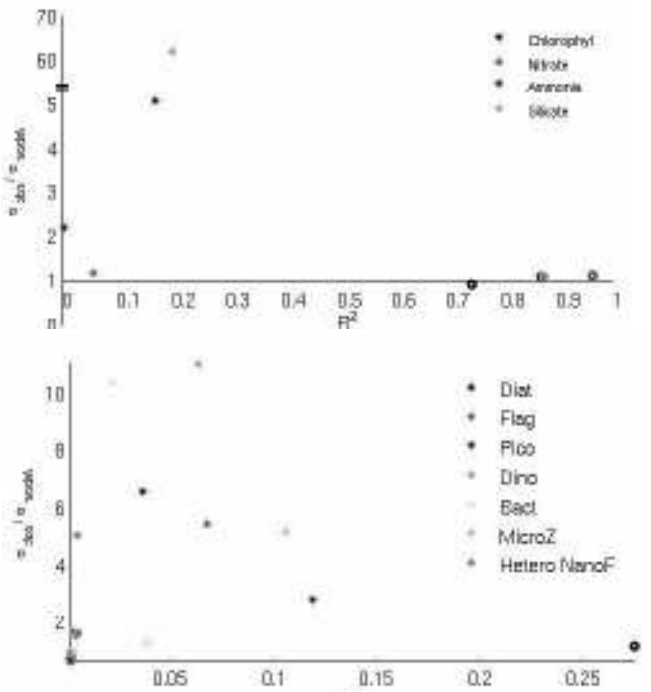

Figure 6 Model skill summary. Left: assimilated variables; Right: non assimilated variables (diatoms, flagellates, picoplankton, dinoflagellates, bacteria, microzooplankton and heterotrophic nanoflagellates). Asterisks correspond to model runs without assimilation while solid circles correspond to the model runs with assimilation. In all cases the difference in variance between model and observations is reduced.

4. Conclusions

The comparison of model simulations with observed data indicate that the EnKF can be used to update aspects of the model state variable fields. Assimilation of the major nutrients and chlorophyll tightly constrains the model evolution and improves the overall model representation of the ecosystem. The assimilation of chlorophyll as a proxy for phytoplankton biomass shows good promise for constraining the model error propagation in parts of the ecosystem, in particular total phytoplankton biomass. This is particularly true considering the shortcomings of the model with respect to the physical environment, in particular the lack of active advection of the nutrients in relation to upwelling/downwelling processes. Improvement of non-assimilated variables correctly reproduces 61% of the biomass which is a dramatic improvement on the run without assimilation. Overall, the study shows potential application of these methodologies to the forecasting of phytoplankton succession including HABs.

Acknowledgements

This work was partly funded by the HABILE project contract no. EVK3–CT2001–00063. Isabel Andreu-Burillo provided many interesting discussions and suggestions.

References

Allen, J., J. Siddorn, J. Blackford and F. Gilbert (2004). Turbulence as a control on the microbial loop in a temperate seasonally stratified marine ecosystem, Journal of Sea Research, 52, 1–20.

Blackford, J.C., J.I. Allen and F.J. Gilbert (2004). Ecosystem dynamics at six contrasting sites: A generic modelling study, Journal of Marine Systems, 52, 191–215.

Burchard, H., K. Bolding and M.R. Villarreal (1999). GOTM, a general ocean turbulence model. Theory, applications and test cases, Tech. Rep. EUR 18745 EN, European Commission.

Evensen, G. (2004). Sampling strategies and square root analysis schemes for the EnKF. Ocean Dynamics, 54, 539–560.

Gentien, P., G. Pitcher, A. Cembella and P. Glibert (Eds.) (2003). GEOHAB, Global Ecology and Oceanography of Harmful Algal Blooms, Implementation Plan, SCOR and IOC, Baltimore and Paris.

Glibert, P. and G. Pitcher (Eds.) (2001). GEOHAB, Global Ecology and Oceanography of Harmful Algal Blooms, Science Plan, SCOR and IOC, Baltimore and Paris.

Water circulation between the North Atlantic and the Arctic Ocean

A. Vyazilova*

Dept. of Oceanology, Faculty of Geography Moscow State University, Russia

1. Introduction

The interaction between the North Atlantic Ocean and the Arctic basin includes a warm ocean flux from the Atlantic to the Arctic region, and a cold flux from the Arctic basin to the North Atlantic Ocean. The Greenland Sea basin plays an important role in water exchange between the Arctic and Atlantic oceans. A lot of attention has been given to this problem by many scientists (see for example Mamaev, 2000; Nikiforov and Shpaiher, 1980; Treshnikov and Baranov, 1972; Aagaard and Coachman, 1968a,b; Delworth *et al.*, 1997; Hay, 1993). The exchange through the Dutch, Fram and Faeroe–Shetland Straits is of special importance in this context. The purpose of this research is to obtain characteristics of thermohaline structure and the ocean circulation in this region based on observed data and model results.

The analysis included the creation of section maps for temperature and salinity along 60º N in the North Atlantic, and through the Dutch, Fram and Faeroe–Shetland Straits based on observed data from the World Ocean Database 2001/NODC/NOAA/USA (Conkright *et al.*, 2002), cruise ships and NOAA satellites. The Ocean Circulation Model was developed at the Institute of Numerical Mathematics RAS (Dianskiy *et al.*, 2002; Moshonkin *et al.*, 2004).

1.1 Analysis of comparison models and observed data

TS-diagrams, sections of salinity and temperature, and velocity were produced, using measured and model data, for four regions (Figure 1). Sections and diagrams of each region were analysed.

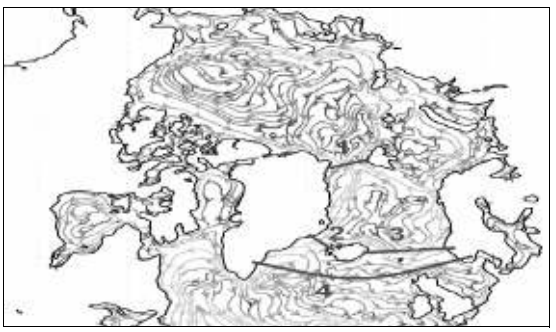

Figure 1 Chosen sections for research and comparison 1–Fram Strait; 2–Dutch Strait; 3–Section between Norway and Iceland; 4–60ºN.

* Corresponding author, email: nev51_99@rambler.ru

1.2 Analysis of TS-diagrams

TS-diagrams were made of observed and model data. The model reproduces water mass characteristics in the same range, but water from the East Greenland current (mostly surface water) is represented as colder and fresher in comparison with observed data. As shown in Figure 2, the model represents main water masses at 60º N (including surface water, Iceland Intermediate water, Labrador Sea water, Iceland–Shetland overflow water, Denmark Strait overflow water, Eastern basin water of the Atlantic ocean, and Norwegian Sea waters). Surface water is warmer (>7ºC) for observed data, in comparison with model data (>4ºC). The model has a slightly lower temperature in comparison probably due to salinity.

The average temperature difference is about 1ºC, but in deep water the temperatures are closer. In the surface layer (above 500 m) salinity differs by 0.20‰, but is similar in other layers.

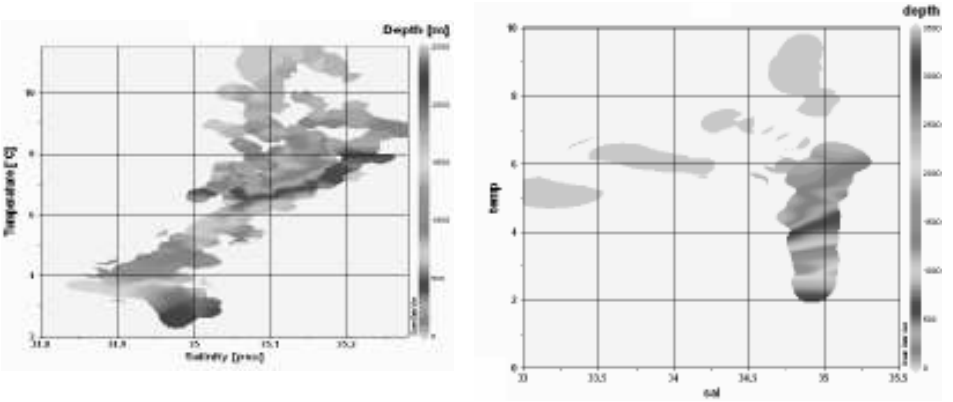

Figure 2 TS-diagram in the section of 60º N. Left: observed data; Right: model result.

1.3 Analysis of temperature sections in Fram Strait

At the coast of Greenland the temperature is about 1ºC (observed data) and about –1.5ºC (model data); this is related to the East-Greenland current (Figure 3). Accordingly the model's data surface temperature rises to +5ºC and this layer spreads to 200 m, but observed data has a maximum surface temperature of 3.5ºC.

At 1500 m depth the model temperature falls to –1.5ºC, while the mean observed temperature at this depth is –0.5ºC. The model and observed data prove distribution of the same elements in the Fram Strait: cold East-Greenland current, warm West-Spitsbergen current, deep water masses.

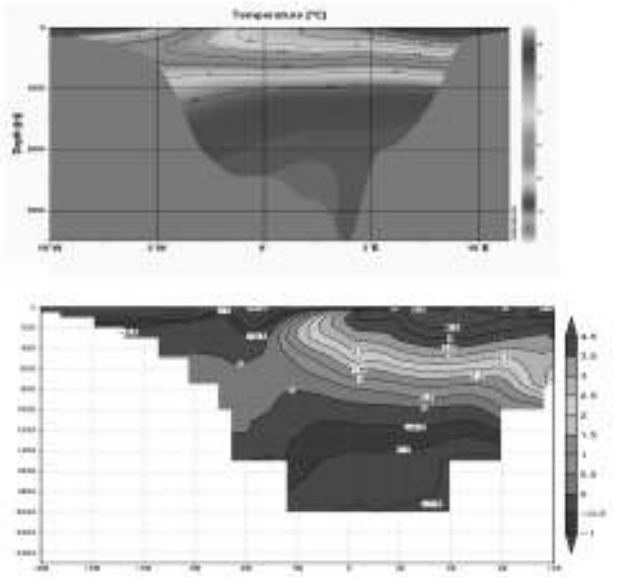

Figure 3 Fram Strait, 79ºN, temperature. Top: Observed data; Bottom: Model result.

1.4 Analysis of salinity section between Norway and Iceland, 64ºN

Mean salinity in the section between Norway and Iceland, represented by model data, is spread evenly in the whole basin and is 34.8‰, represented by observed data 34.9‰. However, an appreciable rise of salinity is noticed at the west and east borders, where salinity increases to 35.1‰ (observed) and 35.4‰ (model) as shown in Figure 4.

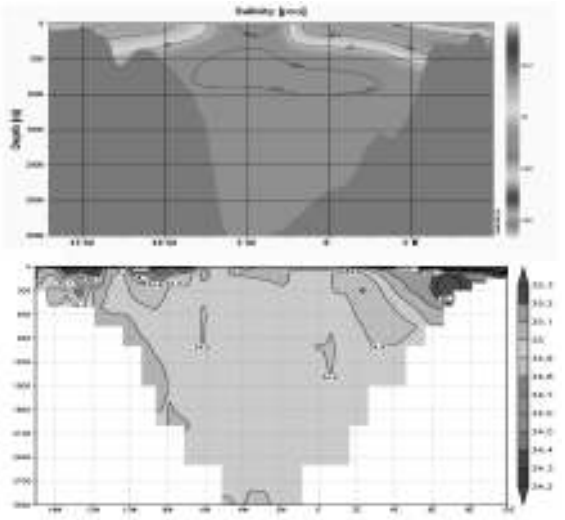

Figure 4 Section between Norway and Iceland, 64ºN, salinity. Top: Observed data; Bottom: model result.

1.5 Analysis of speed sections

According to observed and modelled maps of velocity (Figure 5) large currents are isolated in the upper layer of 800 m — the East-Greenland current, currents in the basin Irminger, and branches of the North Atlantic stream. The model does not notice zero surface at the section of 60ºN, which is represented by observed data (r/v "Ak. M. Keldysh", Aug. 2002), but for both figures we can see alternation of speeds (streams to the south and to the north).

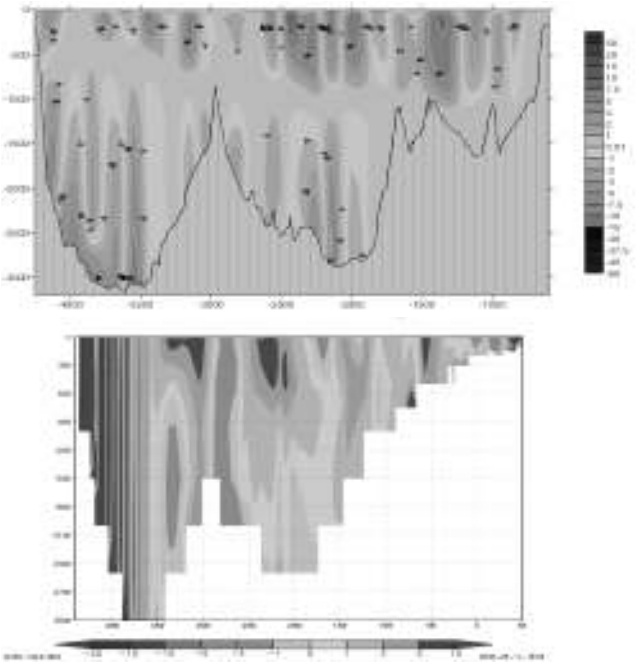

Figure 5 Current speed at the section of 60º N, Left: model result; Right: r/v "Ak. M. Keldysh", August 2002.

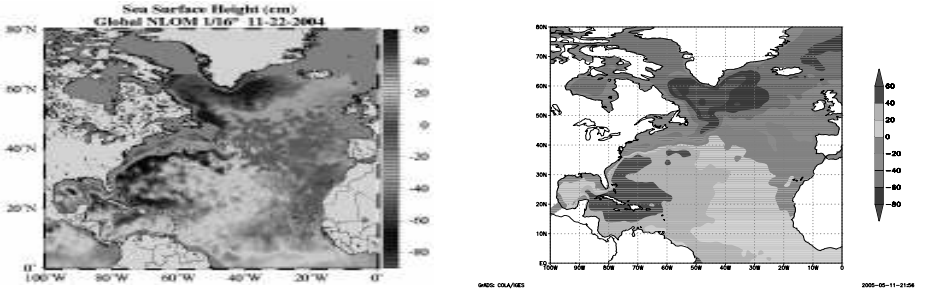

Figure 6 Sea level in the North Atlantic, November. Left: NOAA satellite data: Right: model data.

1.6 Analysis of sea level

The mean sea level for November (in cm) is represented in Figure 6. The main characteristics of the model distribution correspond to the relief of the sea level, known by

observed data — a subtropical maximum and sub-arctic minimum, situated in the west part of North Atlantic Ocean.

2. Conclusions

The model representation corresponds to the relief of sea level on the satellite illustration. It reproduces the main features — the subtropical maximum of sea level (up to 60 cm) and subarctic minimum (down to –80 cm), and a significant fall in sea level in the Gulf stream region.

Water masses are situated in the same regions and the same depths for both model data and observed data. Water masses have similar temperature and salinity. Current speeds qualitatively and somewhere numerically coincide. The mean model and observed current speeds are about $8-10\ \mathrm{cm\,s^{-1}}$ in the upper layer.

The model reproduces the horizontal cell structure of currents, but the plane with zero speeds between upper and deep layers is not represented.

References

Aagaard, K. and L.K. Coachman (1968a). The East Greenland Current north of Denmark Strait, Part I. Arctic, Vol.21, 181–200.

Aagaard, K. and L.K. Coachman (1968b). The East Greenland Current north of Denmark Strait, Part II. Arctic, Vol.21, 267–290.

Conkright, M.E., R.A. Locarnini, H.E. Garcia, T.D. O'Brien and T.P. Boyer (2002). World Ocean Atlas 2001: Objective analysis, Data Statistics, and Figures. CD–ROM Documentation. US Department of Commerce. NODC, 17 p. CD–ROMs WOA01.

Delworth, T.L., S. Manabe and R.J. Stoufer (1997). Multidecadal climate variability in the Greenland Sea and surrounding regions: a coupled model simulation, Geophysical Research Letters, Vol.24, No.3 (February 1), pp.257–260.

Dianskiy N.A., A.V. Bagno and V.B. Zalesniy (2002). Sigma-model of global ocean circulation and its reaction to variations of wind strain. Physics of Atmosphere and Ocean. Vol.38, No.4, pp.537–556.

Hay, W.W. (1993). The Role of Polar Deep Water Formation in Global Climate Change, Annual Review of Earth and Planetary Sciences, May 1993, Vol. 21, pp. 227–254.

Mamaev, O.I. (2000). Physical oceanography, Selected proceedings. Moscow: VNIRO, 2000, 364 p.

Moshonkin, S.N., N.A.C.H. Dianskiy, D.A. Eydinov and A.V.A. Bagno (2004). Modelling of circulation between North Atlantic and the Arctic Ocean, Oceanology, Vol.44, No.6, pp.811–825.

Nikiforov, E.G. and A.O. Shpaiher (1980). Regularities in Formation of Large-Scale Hydrological Regime in the Arctic Ocean (in Russian). Leningrad: Gidrometeoizdat, 248p.

Treshnikov, A.F. and G.I. Baranov (1972). Structure of arctic water circulation. Leningrad: Hydrometeoizdat, 160 p.

Operational forecast system of ocean upper layer in the North Atlantic

E. Nesterov* and I. Rozinkina

Hydrometeorological Research Centre of Russia

Abstract

An operational system of short-term (5 days) forecasts of sea surface temperature (SST) and mixed layer depth (MLD) in the North Atlantic has been developed. The information maintenance of the system is based on the use of operational cyclic databases. The system includes an integral model of the ocean active layer (OAL), and adjustment of the OAL model to the SST objective analysis and to the products of the global atmosphere spectral model.

Keywords: North Atlantic, mixed layer, integral model, sea surface temperature, atmosphere model, forecast.

1. Introduction

The thermal structure of the ocean active layer concerns the major parameters of the ocean, including characteristics such as sea surface temperature, mixed layer depth, and a vertical gradient of temperature in the seasonal thermocline. The diagnosis and forecast of these characteristics represents the scientific and practical interest for fishery, underwater navigation and other kinds of activity connected to use of sea resources.

The Hydrometeorological Research Centre of Russia (HRCR) is developing an operational system of short-term (5 days) forecasts of SST and MLD in the North Atlantic. The information maintenance of the system is based on the use of HRCR operational cyclic databases. The system includes an integral model of the ocean active layer, adjustment of the OAL model to the SST objective analysis and to the products of the global atmosphere spectral model. The grid resolution of the forecast is 1.25°. In particular, the following parameters have been used for the OAL model: 1) latent and sensible heat fluxes; 2) radiation balance; 3) zonal and meridional components of wind in the boundary layer of the atmosphere.

2. Products of the global spectral atmosphere model

The global spectral atmosphere model has configuration T85L31 (85 spherical harmonics, a 1.25° step on horizontal coordinates, and a 31 level vertical resolution — in an atmospheric boundary layer there are 7–8 levels). Forecasts are issued twice daily on the initial data for 00 and 12 hours; with a maximal forecast time of 240 h. Output products are written in cyclic databases at latitude–longitude grids with a 2.5° step (the standard for users) and 1.25° (Gauss grid). The contents of the database are updated periodically.

* Corresponding author, email: nesterov@mecom.ru

The products are transmitted via the Global Telecommunication System (GTS) and ftp server over the internet in GRIB code (resolution 2.5° via GTS and ftp in free access; resolution 1.25° via ftp in limited access). The model products include air temperature, sea level pressure, specific humidity, zonal and meridional components of wind speed, radiation heat fluxes, precipitation, cloudiness, latent heat flux, sensible heat flux, surface stress, surface albedo, and surface roughness.

The model parametrisation takes into account the major small-scale physical processes: radiation–cloud interaction, turbulence in a boundary layer and in the free atmosphere, penetrating convection, and land-surface processes. Some parameters are calculated in different blocks, i.e. different parts of the atmosphere model.

The meteorological parameters describing atmospheric influences on the ocean surface are calculated in the block of physical parametrisations. Turbulent heat fluxes and wind stress are calculated in the block of vertical diffusion describing a vertical turbulent exchange in atmosphere, including a boundary layer. Calculations are carried out on the basis of relations following from the Monin-Obukhov similarity theory.

Empirical dependencies for steady and unstable stratification are used as the universal dimensionless functions which are included in formulae. Above the ocean the roughness parameter is determined by the Charnock formula.

The short-wave and long-wave radiation fluxes are determined in the radiation block of the atmosphere model. Interaction of radiation with cloudiness and with active gases (H_2O, CO_2, O_3) and also with aerosol impurity is taken into account. Spatial distribution of gases and impurity is set on the climatic data. Albedo depends on the type and condition of the underlying surface (water objects, snow cover and its thickness, landscape type). Calculations of radiation fluxes are conducted in view of the daily course of the sun.

For an estimation of the quality of the forecast fluxes they are compared to data from an independent source — NCEP/NCAR reanalysis is carried out (Resnyansky *et al.*, 2005). Comparison is carried out for space-averaged values, for monthly average geographic distributions, and also for concrete synoptic situations developing in time.

Estimating discrepancies between different sources of the data for a 10-year interval of 1981–1992, it is possible to conclude that for time-averaged fields deviations of the HRCR fluxes from NCEP1 data in 2003, as a whole, are stacked in an uncertainty range of flux estimations (except for radiation fluxes mainly in the equator-tropical zone).

From the analysis of concrete situations it follows that HRCR forecast fields of surface fluxes on the whole agree with NCEP/NCAR reanalysis. In particular, in the mature cyclonic systems a distinct similarity of the displacement of a zone of the maximal sensible and latent heat fluxes as well as wind stress connected to a cyclone is traced.

Numerical experiments on calculation of atmospheric boundary layer characteristics (wind, air temperature, turbulent fluxes) have been carried out. In particular, SST most of all influences air temperature, latent and sensible heat fluxes, and also, occasionally, trajectories of movement of atmosphere synoptic systems.

Experiments of the forecast of latent and sensible heat fluxes for various synoptic situations have been carried out. The greatest interest represents the forecast of heat fluxes for a case when, for example, the North Atlantic is crossed by an intensive cyclone. Figure 1

presents forecast fields of sea level pressure and a sensible heat over 24 hours with initial date taken from the forecast on 4 October 2002. From the figure it can be seen that the maximal values of a sensible heat flux (more than 100 Wtm^{-2}) are predicted in zones where there will be a northern stream and the greatest difference between temperatures of water and air.

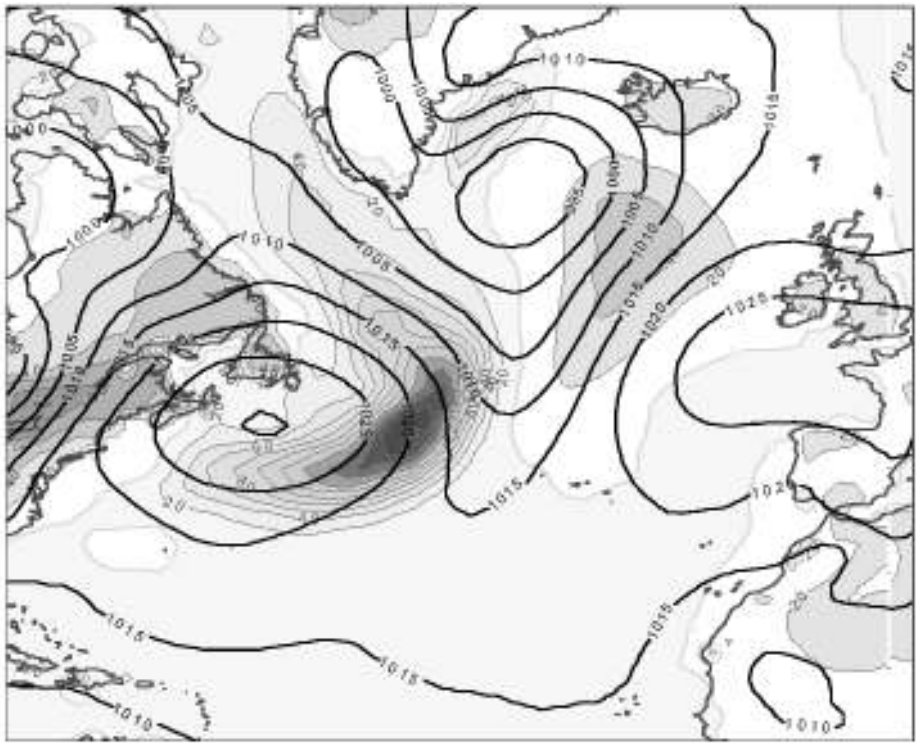

Figure 1 North Atlantic forecast on 5 October 2002 of sea level pressure (hPa) and sensible heat flux (Wtm^{-2}).

The data received for atmospheric influences are suitable for use in numerical experiments with models of the ocean general circulation, for study of mechanisms of formation of large-scale thermal anomalies, and for analysis of integrated fluxes of heat and salt in the ocean.

The second use of the operational information on fluxes is in systems for diagnosis and forecast of ocean parameters. Construction of such systems is impossible without information on the surface fluxes, being a product of meteorological forecast systems. Improvement of the quality of this information for use in such applications can be achieved by eliminating regular errors, or improvement of the HRCR forecast system regarding calculation of surface fluxes.

3. Ocean active layer model

The OAL model takes into account heat exchange of ocean with atmosphere, vertical turbulent mixing and heat advection by drift currents. In the model the two-layer structure of an active layer consisting of mixed layer and seasonal thermocline is considered. For both layers the equation of heat conduction is written on the border between layers with the condition of achievement of critical value of the Richardson number. Heat advection by drift currents is calculated with Ekman equations using wind stress components. Model testing in the various synoptic situations including strong storm influence and intensive warming up at a weak wind has preliminarily been executed.

Forecasting of OAL parameters is carried out in four stages:

1. reading from cyclic databases of forecast fields (forecast up to 24, 48, 72, 96 and 120 hours)
2. reading from a database of results of SST objective analysis
3. adjustment of OAL model with the SST objective analysis and forecasts of atmospheric characteristics
4. integration of OAL model and the forecast for 24, 48, 72, 96 and 120 hours of SST and MLD fields.

The assessment of system products including an estimation of surface fluxes, SST and MLD fields in various synoptic situations is carried out.

References

Resnyansky, Yu.D., A.A. Zelenko, E.S. Nesterov and I.A. Rozinkina. (2005). Assessment of ocean surface fluxes calculated by operational forecast system of Russian Hydrometeorological Centre. — Meteorologiya i gidrologiya, 2005, No.4, p.85–101.

Coastal Zone

Wave monitoring and wind input as key issues in operational wave forecasting systems

I. Gertman*[1], A. Murashkovsky[1], V. Levin[2], G. Kallos[3] and D.S. Rosen[1]

[1]*Israel Oceanographic and Limnological Research (IOLR)*
[2]*Hydrographic Office, Israel Navy*
[3]*University of Athens, Greece*

Abstract

The state-of-the-art wave forecasting models are capable of calculating sea state with great accuracy, limited mostly by a wind input term. The performance of the Mediterranean WAM-based operational wave forecasting system deployed at IOLR is estimated by comparing hindcasted and observed significant wave height time series on the Israeli shelf for 2003–2005. Wind fields (10 m above sea surface) of two different meteorological models are evaluated. Both models underestimate wind speed which could be improved by implementing a multiplication factor of about 1.2–1.5.

Keywords: Wave forecast, wave observations, meteorological models, system performance assessment.

1. Introduction

Oceanic wave forecasting systems have made significant progress. Two of the most commonly used wave models (WAM, WAMDI Group, 1988 and Wave Watch III, Tolman, 1992) forced by global atmospheric models are capable of predicting the sea state quite accurately, reaching biases of 5 cm (Cavaleri and Bertotti, 2005). The situation in closed and semi-closed basins is more complicated as wave forecasting systems tend to underestimate wave height especially during severe storms (Murashkovsky and Gertman, 2004; Cavaleri and Bertotti, 2005). Thus, in closed and semi-closed wave forecasting systems, wind input tuning and sea state monitoring are of utmost importance. In such a basin wind measurements (mostly coastal) are significantly affected by orography and are therefore less effective for open sea wind input tuning. As pointed out by Cavaleri *et al.* (1996), wave observations combined with sophisticated wave models could be used as an indirect, but fully reliable tool for wind field evaluation, because wave observations even at a single point reflect the integral result of wind influence on a large sea area, in contrast to a point wind observation (particularly on the coastline), which represents a limited area.

In this paper, performance of the wave forecasting system developed at IOLR is assessed for the period 2003–2005. The system uses the wind input from two different atmospheric models — The Atmospheric Modeling and Weather Forecasting Group model, Athens University (SKIRON Model: http://forecast.uoa.gr) and The Unified Global Numerical Weather Prediction model, UK Met Office (Unified Model: http://

* Corresponding author, email: isaac@ocean.org.il

www.metoffice.com). The assessment tools are the WAM model implemented for the entire Mediterranean and ground truth wave measurements.

2. System description

The wave forecasting system was deployed at IOLR at 1997 (Gertman *et al.*, 2000). For the current study the system is based on WAM cycle 4 FORTRAN90 code, provided by Prof. H. Günter (GKSS Research Center). In addition to the base third generation model features implemented in initial FORTRAN77 code (Komen *et al.*, 1994), the code includes the garden sprinkler effect elimination (Booij and Holthuijsen, 1987) and fully implicit integration of the source functions and a much less restrictive growth limiter, as given in Hersbach and Janssen (1999). The model output parameters are: significant wave height, mean wave direction and frequency, swell wave height and direction. The model runs on a coarse space grid with a resolution of 1/2° for the entire Mediterranean Sea as well as on a fine grid with resolution 1/8° for the Eastern Mediterranean from longitude 22°E eastward. On both grids directional wave spectra are calculated using 25 frequencies between 0.042 Hz and 0.42 Hz; and 24 directions (every 15 degrees).

All the comparisons in the study are performed against ground truth measurements from Hadera GLOSS station number 80 (Figure 1).

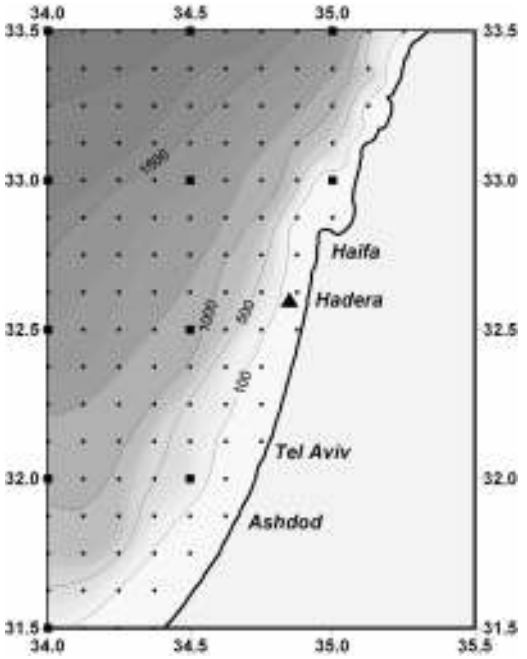

Figure 1 WAM fine grid (1/8°×1/8°) embedded in coarse grid (1/2°×1/2°) near the Israeli coast and position of the Hadera wave station.

The wave gauge is positioned 2.1 km out to sea, at 27 m depth and provides near-real time data on significant and maximum wave height and direction, as well as hourly averaged wind and wind gusts.

In the current study two atmospheric models wind field datasets were used. The first one, used in day-by-day operational forecasts, is a 10 m above sea surface wind produced by the SKIRON model. The model resolution is 0.2º×0.2º (~22×22 km), and it produces daily forecasts at 12 GMT, for every 3 hours, with a forecasting period of 72 hours. The second dataset, used in delayed mode, is a 10 m above sea surface wind produced by the Unified Model. It is a coupled global model with 0.833°×0.556° (~92×62 km) horizontal resolution. The model runs twice a day (at 00 and 12 GMT) for +144 h period for every 6 hours.

3. Forecasting system general performance evaluation

To estimate the system performance, wave fields were hindcasted with wind fields from both the atmospheric models without any correction applied and with forecast index less than 24 hours. The hindcast periods were limited by continuous datasets availability. The SKIRON Model driven hindcast was run for a period spanning from December 2003 to March 2005, and the Unified Model driven hindcast for a period spanning from October 2004 to March 2005. Time series were extracted at the Hadera station coordinates from the hindcasted significant wave height fields. The synchronous hindcasted and observed time series were used to build two-dimensional histograms (Figure 2) of the observed and hindcasted significant wave heights and to calculate two statistical parameters, which were used for the system evaluation. The first one is the slope of the scatter best-fit line K which quantifies an average correspondence of wave energy between real and modelled wave fields. The second one is the correlation coefficient R, between the modelled and observed time series, which quantifies scattering of the points around the best-fit line or in other terms; it represents a time matching between real and modelled wave height changes. Following Signell *et al.* (2005) the average energetic error of the hindcast at the point of wave observation is defined as $E = 100(K–1)$.

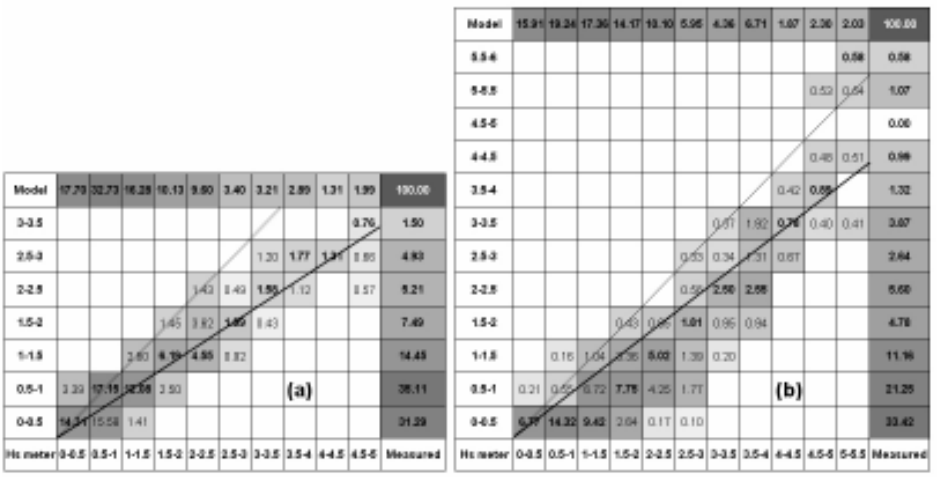

Figure 2 Scatter histograms of hindcasted versus observed significant wave height at Hadera coordinates for (a) Unified Model driven system, years 2004–2005 and (b) Skiron Model driven system, years 2003–2005. Dashed line denotes perfect fit. Solid line denotes best fit. Numbers in filled cells are percentages of total number of compared couples.

Scatter histograms (Figure 2) as well as slopes of the best fits (Table 1) indicate that implementation of wind fields from both meteorological models resulted in a significant underestimation of the wave height. The low resolution Unified Model has an energetic error of –34% versus –24% for the Skiron Model. It means that the high resolution model produced energetically a more realistic wind speed. The same results were achieved for the Adriatic Sea (Signel *et al.*, 2005; Cavaleri and Bertotti, 2005). In those investigations a weak modelled wind speed was attributed to the negative effects produced by closed-basin orography which is better described by a higher resolution model. This conclusion does not cause any objections for the relatively small Adriatic Sea bordered by complicated orography (Cavaleri *et al.*, 1996). Moreover, Cavaleri and Bertotti (2005), basing on comparison between modelled and satellite measured wind speeds, showed that there is a significant reduction of modelled wind underestimation on the Southern coast of the Eastern Mediterranean, i.e. for regions having wind basically flowing from the sea to the coast, the modelled wind is closer to the real wind. Based on those investigations, the average modelled wave underestimation of 24−34% is unexpected for the Eastern Mediterranean coast, where most of the high sea cases are characterised by western and south-western winds which generally generate wave fields without fetch limitation.

Table 1 Statistical parameters of comparisons between hindcasted and observed significant wave height at Hadera coordinates.

Atmospheric model	Slope	Energetic Error (%)	Correlation Coeff.
Unified Model (uncorrected)	0.66	–34	0.93
Skiron Model (uncorrected)	0.76	–24	0.92
Unified Model (multiplied by 1.5)	0.94	–6	0.93
Skiron Model (multiplied by 1.2)	0.94	–6	0.92
Skiron Model (WW III correction)	0.96	–4	0.90

In terms of the correlation coefficient R, both models demonstrated good performance (Table 1), allowing the assumption that the timing of wave and wind models is quite satisfactory. Thus most effort should be invested in decreasing the energetic error.

Because only the energy of the wave fields is needed to be increased, it is possible to try to implement the simplest method of input wind field increase, by multiplying it by a constant value. The next section presents such a method, applied for both the models.

4. Modelled wind input enhancing

The simplest method of wind input enhancing, in order to avoid wave underestimation without affecting wind field's timing, is the introduction of a multiplication factor. An iterative derivation of such a multiplicator was carried out by minimising the value of $|K–1|$. The multiplicator's starting value was 1.1 and was increased by 0.1 step, until the value of $|K–1|$ started to increase. The minimum of this value was produced by using a multiplication factor of 1.2 for the SKIRON model and of 1.5 for the Unified Model (Table 1). The resulting scatter histograms of system performance, using these factors for both models, are shown in Figure 3. Indeed, along with energy error decrease, the correlation coefficient for wave fields remained unchanged, in spite of non-linear wind-

wave parametrisation within the WAM model (Table 1). For the SKIRON model, sea surface temperature fields were available allowing implementation of another method of wind enhancement, based on physical considerations. This method was introduced by Tolman (1999) where the wind input field is improved by introducing a correction term, which depends on air–sea temperature difference. The wind correction coefficient is calculated using the formula

$$U_{\text{effective}} = U \cdot \sqrt{\frac{1 + C_1 + C_2}{c_0}}, \text{ where}$$

$C_1 = c_1 \tanh[\max\{0, f_1 \cdot (ST - ST_0)\}]$, $C_2 = c_2 \tanh[\max\{0, f_2 \cdot (ST - ST_0)\}]$,

$U_{\text{effective}}$ is improved wind speed, U is the wind speed from the model, ST is the bulk stability parameter derived from air–sea temperature difference and wind speed, and c_0, c_1, c_2, f_1, and f_2 are constants.

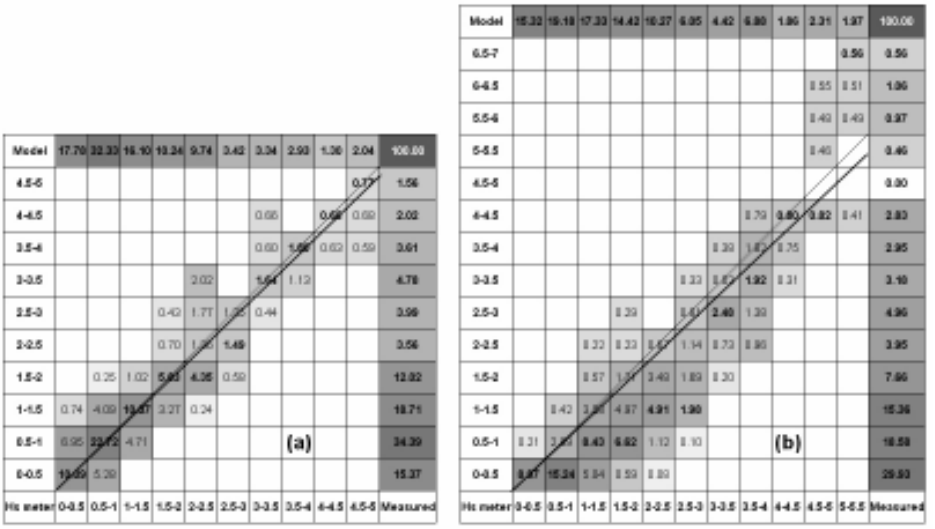

Figure 3 (a) System performance with 10 m SKIRON model wind input multiplied by 1.2 (b) System performance with 10 m Unified model wind input multiplied by 1.5 The legend is the same as in Figure 2.

The results of system performance versus ground truth data using Tolman's (1999) correction are shown in Figure 4. There is clearly no doubt that this method also results in a significant decrease of the energetic error; however it also decreases the correlation parameter (Table 1).

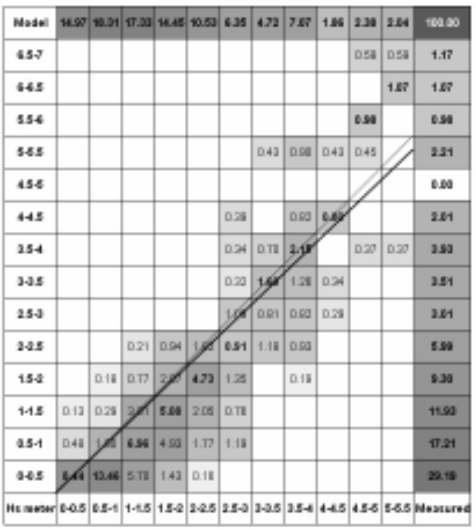

Figure 4 System performance with 10 m Skiron model wind input enhanced by Tolman's (1999) correction method.

5. Conclusions

The use of modern meteorological models in wave forecasting systems ensure good correlation between observed and calculated wind wave fields. However those systems underestimate energies of wave fields, mostly during severe weather conditions. This underestimation occurs even at the Eastern Mediterranean coast, where wave fields usually have almost unlimited fetch. Thus, continuous observation of wave fields and their comparison to model results appears to be a crucial part of the wave forecasting system.

Comparison of two meteorological models with different resolutions (Unified Model and SKIRON model) revealed that a higher-resolution model performs better in terms of energetic error.

A significant decrease of the energetic error of modelled wave fields is achieved by multiplying wind speed input by a constant factor. This factor appeared to be larger for the coarser-resolution model (1.2 for the 22 km resolution SKIRON Model vs. 1.5 for the 70 km resolution Unified Model). Implementation of the multiplication factor does not lead to any change in correlation between modelled and observed wave fields.

Experiments with another method of input wind field improvement, based on physical considerations (Tolman, 1999) revealed a decrease in the energetic error similar to the wind multiplication factor implementation. However the Tolman (1999) correction also decreased the correlation between modelled and observed wave fields.

Future development of the wave forecasting system by implementation of a higher-resolution meteorological model is expected to improve the overall system performance.

References

Booij, N. and L.H. Holthuijsen (1987). Propagation of ocean waves in discrete spectral wave models. J. Comp. Phys., 68, 307–326.

Cavaleri, L., L. Bertotti, L. Pedulli, S. Tibaldi and E. Tosi (1996). Wind evaluation in the Adriatic Sea. In: L. Cavaleri (ed), Wind and Waves in the Northern Adriatic Sea, Societa Italiana di Fisica, pp 51–66.

Cavaleri, L. and L. Bertotti (2005). Accuracy of modelled wind and wave fields in enclosed seas. Tellus, 56A, 167–175.

Gertman, I., D.S. Rosen, S. Kariel and L. Raskin (2000). Comparison of Two Years of Wind and Wave Hindcasts via WAM based Operational Forecasting System versus Field and other Models Data. Preprints 6th International Workshop on Wave Hindcasting and Forecasting, November 6–10, 2000, Monterey, California, pp. 91–98.

Hersbach, H. and P.A.E.M. Janssen (1999). Improvement of the Short-Fetch Behavior in the Wave Ocean Model (WAM). Journal of Atmospheric and Oceanic Technology, Volume: 16/7, 884–892.

Komen, G.J., L. Cavaleri, M. Donelan, K. Hasselmann, S. Hasselmann and P.A.E.M. Janssen (1994). Dynamics and Modelling of Ocean Waves. Cambridge University Press, 532 pp.

Murashkovsky, A. and I. Gertman (2004). Correction of modeled sea surface wind in order to improve wave forecast. 37th CIESM Congress Proceedings, Volume 37, 127.

Tolman, H.L. (1999). User Manual and system documentation of Wavewatch-III, ver 1.18. OMB Contribution No 166.

WAMDI group (1988). The WAM model — a third generation ocean wave prediction model. J. Phys. Oceanogr., 18, 1775–1810.

Storm surge monitoring with HF radar

Lucy R. Wyatt*[1,2], J. Jim Green[1,2], A. Middleditch[1,2] and Mike Moorhead[3]

[1]*Sheffield Centre for Earth Observation Science, Department of Applied Mathematics, University of Sheffield, UK*
[2]*Seaview Sensing Ltd., UK*
[3]*Neptune Radar Ltd., UK*

Abstract

The Pisces HF radar system was undertaking wave, current and wind measurements in the Celtic Sea during a strong storm event in October 2004. The data were being collected during a trial being carried out to assess the feasibility of including such systems in the UK wave monitoring network, WAVENET. This paper reports on aspects of this trial focusing in particular on the exploitation of the combined wave, surface current and wind direction measurement capability for storm surge monitoring.

Keywords: HF radar, storm surge, wave, current, wind, spring tide

1. Introduction

Storm surges are caused mainly by the action of wind on the surface of the sea. Barometric pressure is a secondary factor. When combined with high tides, a storm surge can significantly raise the mean water level. The strong winds that create surges also generate large waves. Although HF radars do not measure sea level or provide surge forecasts, they can measure waves, currents and winds operationally and hence such systems provide valuable data for monitoring and for surge model development and thus forecasts.

On Thursday 28 October 2004 the UK Guardian newspaper reported on storms that pounded Britain the previous night. Amongst other things they referred to an Irish Ferries vessel that had arrived at Pembroke dock in west Wales at about 2.30 p.m., but the captain decided conditions were too risky to dock. They also reported that UK Met Office had said the winds were expected to peak during the night and were not remarkable, but, combined with high seas, they were a potential danger.

During that night the Pisces HF radar system was in operation collecting current, wave and wind data over the Celtic Sea and displaying the results on a web site normally within 10 minutes of the end of the data collection period. This was part of trials to assess the feasibility of including HF radar systems in the wave monitoring system, WAVENET, set up by the UK Department for Environment, Food and Rural Affairs (DEFRA).

The trials have been funded by DEFRA and managed by the UK Met Office. Neptune Radar Ltd. installed and operated their Pisces HF radar system to deliver wave measurements in real time. The first trial, November 2001 to May 2002, involved a single radar system that provides only a limited range of wave, current and wind parameters but

* Corresponding author, email: l.wyatt@sheffield.ac.uk

demonstrated the feasibility of round the clock real time data delivery (Moorhead *et al.*, 2002, Wyatt *et al.*, 2003). During the period December 2003 to June 2005 Neptune Radar provided data from a second radar enabling measurements of the directional spectrum and derived parameters, surface current speed and direction and wind direction. Radar backscatter power spectra from both sites were sent every hour via a telephone line and ftp to a server at the University of Sheffield. During the second half of the measurement period, management of the metocean processing and web site was carried out by Seaview Sensing Ltd. who have licensed the software from the University.

Extensive validation of the radar data has been carried out using data from a directional waverider deployed in the radar coverage region and also with products from the Met Office wave model. This paper will report on aspects of this trial focusing in particular on the exploitation of the combined wave, surface current and wind direction measurement capability for storm surge monitoring. Further information on the availability and accuracy of these measurements can be found in various publications (e.g. Wyatt *et al.*, 2005a, 2005b).

2. Storm data

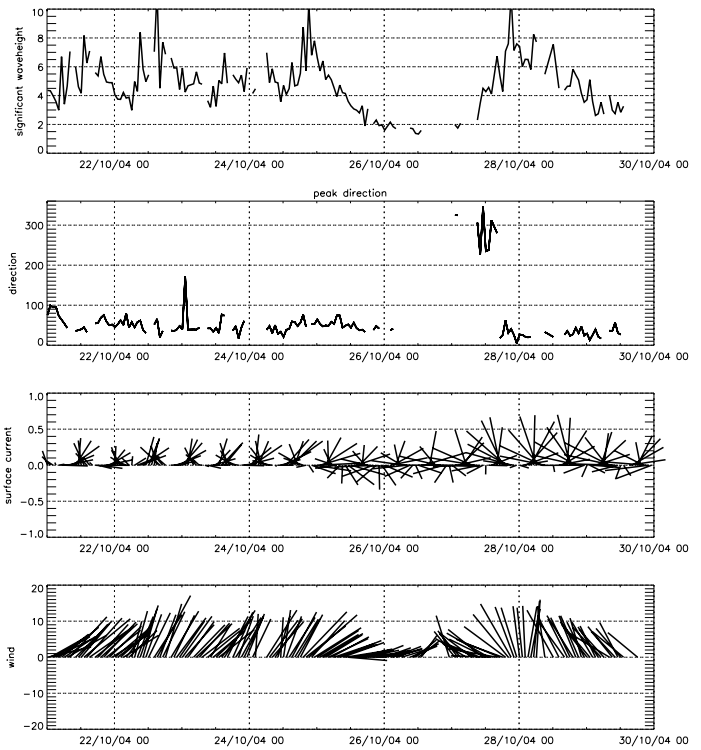

Figure 1 Data before and during the headline storm event. Top panel show significant waveheight, second panel, peak wave direction, third panel surface current and bottom panel, wind direction, all measured by the radar at a location 60 km from each radar.

The storm event is shown towards the end of the timeseries in Figure 1. Significant waveheights greater than 6 m and onshore winds, combined with spring tides peaking at 4–5 a.m. on 28 October provided the potential for a flooding event on the Welsh coast. The ferry was held up at 2:30 p.m. on 27 October. Figure 2 shows wave, current and wind measurements at this time. The ferry was presumably experiencing difficulty as a result of the strong winds and high waves crossing the entrance to Milford Haven at this time.

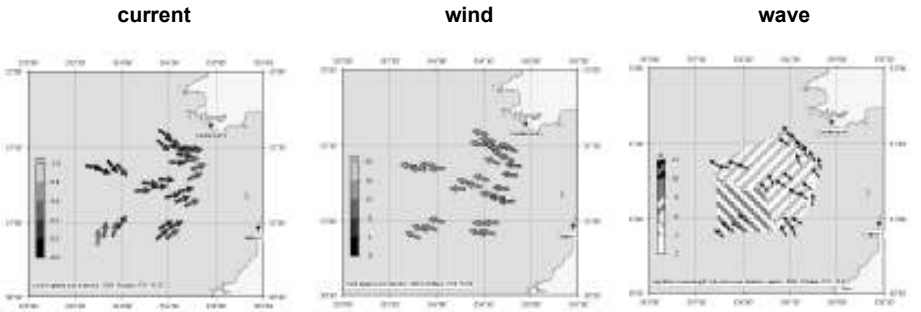

Figure 2 Current, wind and wave maps at the time the ferry was experiencing difficulties.

Figure 3 shows wave, wind and current measurements at 1, 5 and 7 a.m. the following morning. Winds and waves have changed direction and are now towards the Welsh coast. At 5 a.m. the maximum range for waves is reduced due to either propagation losses due to high seas or to increased noise at this time. A variation in maximum range of wave measurement with waveheight, time of day and season of the year has to be expected with HF radar systems. There is also a variation for current measurement but it is much smaller and the maximum range is longer. Although the highest waves shown here are at 1 a.m., the more serious conditions occur later. At 5 a.m. waves, winds and currents are all directed onshore and the current speeds associated with the peak of the spring tide are high. These data confirm the need for the Met Office storm surge warning. By 7 a.m., although waveheights were larger the tide had turned and currents were no longer directed onshore indicating that flooding danger was much reduced.

The earlier storms seen in Figure 1 did not coincide with the spring tide and were thus less dangerous. The wave buoy was operational and measured similar wave parameters during this period but does not provide wind and surface current data. UK Met Office wave model data were available for this period but only six-hourly (thus missing the key periods mentioned in the Guardian report) and providing only depth averaged currents. The advantage of real-time simultaneous monitoring, as provided by HF radar, of all the main contributing factors to a surge is clear. The Met Office do provide storm surge forecasts on a more regular basis but these data were not available for this work. There are a few gaps in the radar wave data occurring mainly in periods of low seas when the backscattered radar signal is not sufficient for accurate measurement at the radar frequencies used with Pisces.

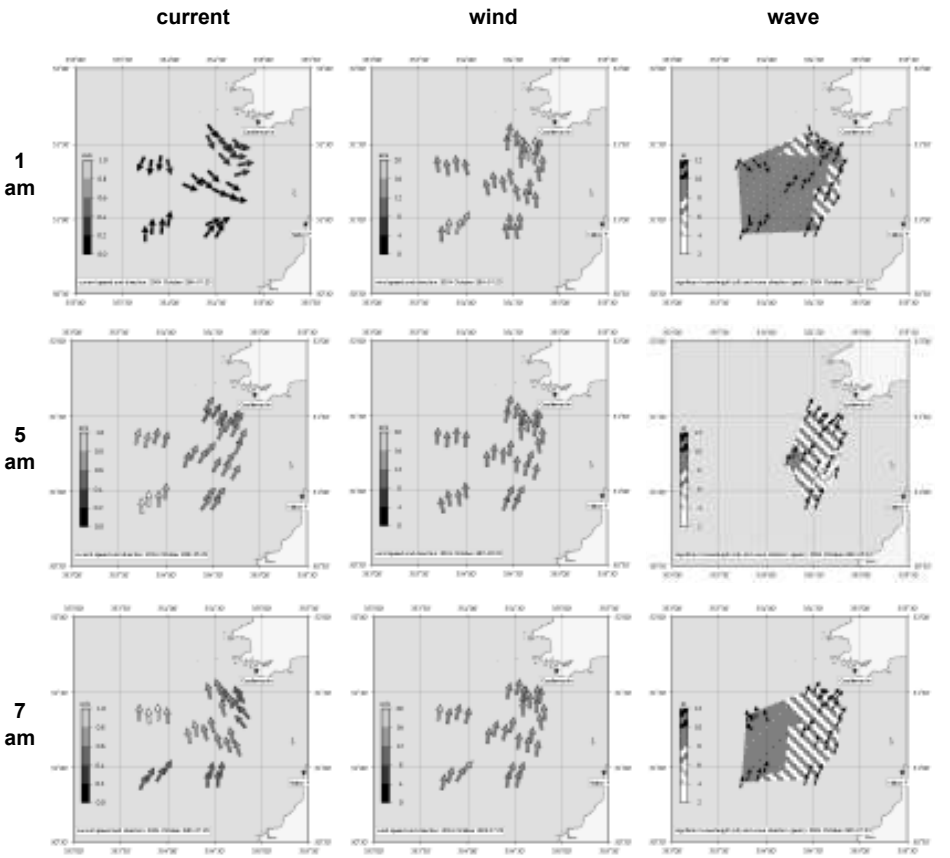

Figure 3 Current, wind and wave maps before and near the peak of the spring tide.

3. Summary and conclusions

We have demonstrated 18 months of operational measurement with Pisces of waves, currents and winds presented on a website within 10 minutes of data collection. Recovery from system faults is not reliant on weather windows and ship time availability (unlike the case with wave buoys in general and the one deployed in this trial in particular). Accuracy of wave, current and wind measurements has been assessed (Wyatt *et al.*, 2005a). Future operational systems (with Pisces or WERA) will have real time download capabilities from website and/or via ftp.

The results presented here demonstrate the value of HF radar for monitoring storm surge events and for providing data for further development of storm surge models. This has only been a qualitative study and has not taken into account the detailed spatial and temporal evolution of the event that has been measured with this radar system with a view to perhaps, with the assistance of models, identifying locations along the coast more exposed to the dangerous wave, wind and tide conditions that would enable more targeted warnings to be issued.

Acknowledgements

The Pisces radar systems were managed and data supplied by Neptune Radar Ltd. The Wavenet HF radar project was managed by UK Met Office and funded by DEFRA.

Wave Model data was provided by Martin Holt, UK Met Office and wavebuoy data was provided by Cefas.

4. References

Moorhead, M.D., L.R. Wyatt, W.J. Penketh, L.A. Binks, J.J. Green (2002). WAVENET: Trials report of the Pisces Oceanographic HF radar. Prepared for DEFRA, 31/10/2002.

Wyatt, L.R., J.J. Green, L.A. Binks, M. Moorhead and M. Holt (2003). Performance of the Pisces HF radar during the DEFRA trial. Building the European Capacity in Operational Oceanography, Proceedings of the 3rd International Conference on EuroGOOS, Ed. Dahlin *et al.* 161–167.

Wyatt, L.R., J.J. Green, A. Middleditch, M.D. Moorhead, J. Howarth, M. Holt and S. Keogh (2005a). Operational wave, current and wind measurements with the Pisces HF radar. Submitted to IEEE Journal of Oceanic Engineering.

Wyatt, L.R., J.J. Green, A. Middleditch and M.D. Moorhead (2005b). HF Radar and the UK Wave Monitoring Network, WAVENET. Proceedings of IEEE Oceans'05 Europe, Brest, France, June 20–23, 2005 (CD).

Mangrove as indicator of coastal changes, Wadi El-Gemal area, Red Sea, Egypt

Suzan E. A. Kholeif* and Mona Kh. Khalil

National Institute of Oceanography and Fisheries, Alexandria, Egypt

Abstract

Although mangroves have long graced the Red Sea coastline, they have vanished in many locations. In recent decades the mangrove forests of the Wadi El-Gemal area have been affected by many detrimental changes in extent, density, actual forest quality and composition. Palynological analysis of recent sediments and core samples revealed a low to common influence of the main mangrove pollen Avicennia marina in 10–20 cm core sediments (~2–12%) while it is rare or lacking in recent bottom sediments (~0–1%). The mangrove pollen is replaced by herbaceous plants such as *Chenopodiaceae*, *Amaranthaceae* and *Poaceae* of the Wadi El-Gemal area. The geochemical analysis of the studied sediments recognised that heavy metals have a negative impact on the mangal of Wadi El-Gemal, and result from the influence of terrigenous sediment input. Coastal changes, large waves, low catchments of runoff and the strong monsoon as well as anthropogenic impacts are increasing the threatened mangrove communities of Wadi El-Gemal area.

Keywords: Mangrove, palynology, coastal changes, Red Sea, Wadi El-Gemal

1. Introduction

Mangroves are marine tidal plants and include trees, shrubs, ferns and palms. These plants have adapted to muddy, shifting, saline environments for fresh water draining from surface developments or seeping from ground water, nutrients, oxygen and sunlight. Mangroves often prefer to colonise shorelines around the mid-tide mark where regular tidal inundation and exposure may occur. Tidal flooding affects plant communities by its influence on soil salinity, seed dispersal and by reducing seedling establishment (Clarke and Myerscough, 1993).

Recently, with the progressive development in the tourist industry in Egypt, mangroves have been in significant danger. The tourist projects along the Red Sea coastal zone, the new coastal road and coastal changes affect the density and health of mangroves.

Wadi El-Gemal lies at latitude 24°40' N and longitude 35°05' E on the southern side of the city of Marsa Alam along the Egyptian Red Sea coast. It is a protectorate (about 380 km²) created by Prime Ministerial Decree # 143 of 2003 and is considered a part of the largest watershed in Egypt's southern Red Sea region.

This work aims to give an overview of the vegetation picture, coastal changes, pollution and anthropogenic disturbance as well as predictable future impacts on mangroves in Wadi El-Gemal on the Red Sea coast.

* Corresponding author, email: suzan_kholeif@yahoo.com

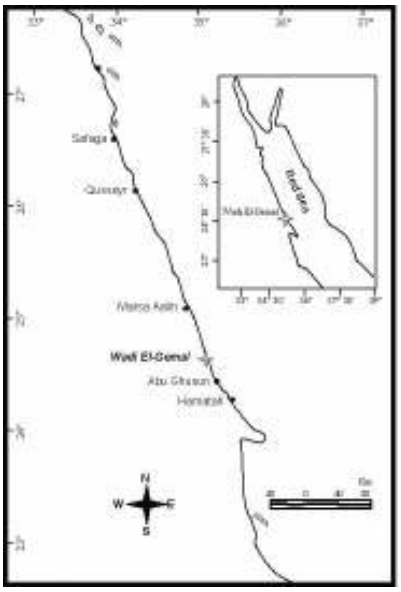

Figure 1 Location of the area studied.

2. Material and methods

Ten surface sediment samples were collected along three transects (I, II & III: 70 m apart) running seaward in the intertidal zone, covered all mangrove area and two samples (D_1 and D_2) from the main drainages of Wadi El-Gemal area. Two short cores were also taken (20 and 10 cm) from different localities of mangrove area. The sediment samples were studied for every 2 cm interval.

For separation of pollen grains, 25 grams of each dry sample was processed using a standard palynological technique (HCl, HF). Two slides of each sample were examined under a light microscope. The first 300 palynomorphs were counted for statistical purposes.

All samples were analysed following Folk (1974) to determine the grain size parameters, Walkley and Black (1934) to determine the organic carbon contents, Herrin *et al.* (1957) and Black (1965) for the carbonate contents determination. Total phosphorus was extracted by the method of Aspila, (1976). The total metals concentrations were measured by flame atomic absorption spectrophotometer.

3. Physical parameters of sea water

The investigated samples and their related data were gathered during the winter season (January, 2004). The surface water temperature ranged between 22.9ºC and 25.0ºC. The Red Sea is one of the world's most saline water bodies. The mean salinity varied from 40.0‰ to 41.6‰. The dissolved oxygen of the surface water varied between 7.2 mgL^{-1} and 9.6 mgL^{-1}. The pH value of surface water ranged between 8.3 and 8.5. The lower salinity and lower pH were recorded in drainage water samples (D_1 and D_2).

4. Results and discussion

4.1 Palynological results

The unique biological characteristic of mangrove ecosystems (mangal) can be used as indicators of coastal changes due to the assumption that ecosystem structure and plant zonation are uniform (Bacon, 1994; Blasco *et al.*, 1996). Mangrove vegetation is one of the most suitable ecosystems for which palynology can help in tracing history and evolution.

The mangroves in the Wadi El-Gemal area are represented by one species Avicennia marina. The pollen analysis in mangrove grab sediments transects I, II & III reveals an absent to rare (~0−1%) amount of measured pollen in the intertidal zone and the upper few centimetres of core samples. The pollen grains of Avicennia marina which represent the mangrove plant in the studied area is far below expected. This species is missing in recent grab sediments while it is common in the core samples from 5−18 cm depths (core 1) and 2−10 cm depth (core 2). Its percentage increases downwards and reaches up to 12%. The low percentage of Avicennia indicates the prevalence of a drier period with a lowstand sea level (Carratini, 1992; Clarke and Myerscough, 1993; Kholeif and Ibrahim, 2003).

The high pollen grain percentage was recognised by allochthonous herbaceous families; *Chenopodiaceae*, *Amaranthacea* and *Poaceae*. These genera are common vegetation in the area (Figure 2 and Figure 3). They have an appreciable percentage ranging from 22 to 36% of the total pollen count (core 2) and from 7 up to ~40% (core 1). The widespread occurrence of these families supports the prevailing drier climate, rare rainfall and increased salinity (El-Moslimany, 1986).

Other allochthonous pollen grains are common but they do not exceed 6% (Figure 2 and Figure 3) and are represented by *Compositae*, *Plantaginaceae*, *Polypodiaceae*, *Lycopodiaceae*, *Capparaceae*, *Caryophyllaceae*, *Acacia*, *Palmae*, *Scrophulariaceae*, *Meliaceae*, *Tamaricaceae* and *Bisaccate* pollen.

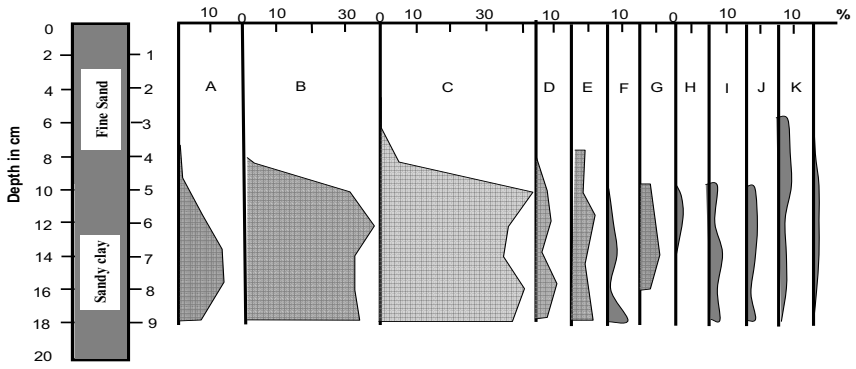

Figure 2 Pollen diagram (core 1) showing the progressive vanishing of mangrove pollen and replacement by herbaceous plants in the Wadi El Gemal area, Red Sea coast. A – *Avicenniaceae*; B – *Chenopodiaceae*/*Amaranthaceae*; C – *Poaceae*; D – *Compositae*; E – *Capparaceae*; F – *Palmae*; G – *Tamaricaceae*; H – *Caryophyllaceae*; I – *Meliaceae*; J – Spores; K – *Araucariacare*.

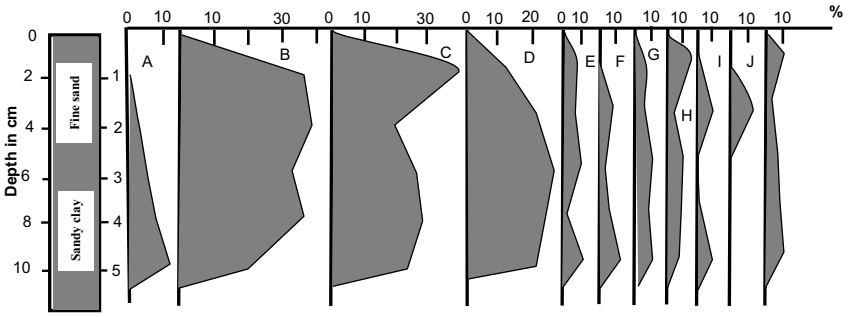

Figure 3 Pollen diagram (core 2), showing the progressive vanishing of mangrove pollen and replacement by herbaceous plants in the Wadi El Gemal area, Red Sea coast. A – *Avicenniaceae*; B – *Chenopodiaceae*/*Amaranthaceae*; C – *Poaceae*; D – *Compositae*; E – *Palmae*; F – *Tamaricaceae*; G – *Geraniaceae*; H – *Plantaginaceae*; I – *Scrophulariaceae*; J – *Lamiaceae*; K – Spores.

4.2 Particle size

The grain size analysis data (Table 2) shows that the surface sediments are composed of fine (2−3 φ) to medium (1−2 φ) sand. The sediments have been derived from two principal sources; igneous, metamorphic and sedimentary rocks and skeletal carbonates. Surface sediments are missing for mud, due to mechanical sorting by tidal current and waves, as well as the steep slope of the bottom which helps washing of the fine fraction by current and torrent water which has high energy capable of moving even coarser fractions.

The studied core sediments of the mangrove area are finer than those of the grab samples. This is consistent with the data of Rifaat and El-Mamoney (2001).

4.3 Geochemical results

Organic Carbon (OC wt %)

The organic carbon content of bottom sediments ranges from 5.6% to 0.1%. It decreases seaward (Table 2). In core 1 and 2 the OC increase downward. It ranges from 0.1% to 4.2% (Table 3). Presumably, this reflects an active history of the wadi resulting in a high rate of mud sedimentation laden with plant detritus.

Total carbonate

The total carbonate ($CaCO_3$%) in the grab sediments increased gradually from 5.8% to 77.9% seaward (Table 2), reflects the influence of marine conditions. The decrease of $CaCO_3$ in the lower interval of core 1 and core 2 (Table 3) may reflect limited marine conditions.

Phosphorus (TP)

The concentration of total phosphorus in surface sediments generally decreases seaward (Table 1), which suggests that it is basically derived from the basement rocks through wadis to the sea (Mansour *et al.*, 1997). The highest value of TP observed at the top of cores 1 and 2 reflects the influence of fresh precipitated material.

Table 1 Factor analysis of the observed variables in the studied sediments.

Variables	Factor 1	Factor 2
Mean (φ)	0.89	
Total Organic Carbon (TOC)		0.86
Total Carbonate ($CaCO_3$)	–0.96	
Total Phosphorous (TP)	0.75	
Zn	0.97	
Pb		0.85
Cu	0.80	0.56
Fe	0.91	

Metals

The metals analyses reveal that concentration of zinc (Zn), copper (Cu), lead (Pb) and iron (Fe) in grab and core sediments show nearly the same levels and lie within normal range (Table 2). The origin of these metals is attributed to the influence of terrigenous sediment input. High levels of Cu content were noticed in subsurface sediments of the two cores (Table 3). This increase coincides with the increase of OC content.

Factor analysis: Two factors explain 78% of the total variance for the study area (Table 1). Factor 1 represents derivation of metals and phosphorus from land source (terrigenous fragments) with fine sediment particles. Factor 2 is a strictly organic factor, showing marked positive loading of Pb.

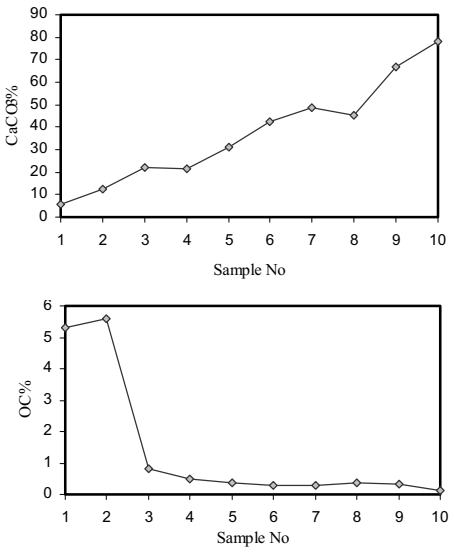

Figure 4 Total carbonate ($CaCO_3$%) and Total Organic Carbon (OC wt %) in the studied grab sediment samples.

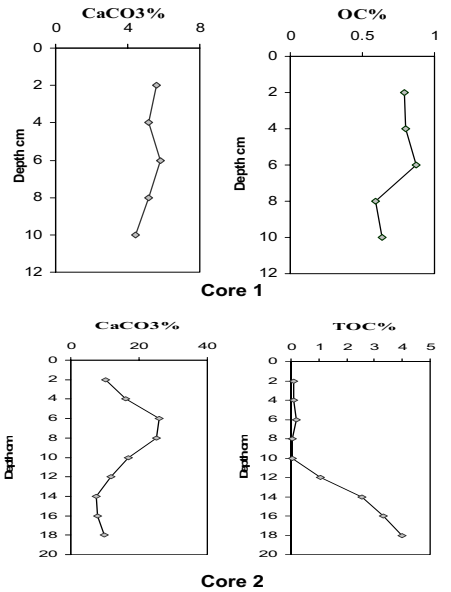

Figure 5 Total carbonate ($CaCO_3$%) and Total Organic Carbon (OC wt %) in the studied subsurface samples (core 1 and core 2).

Table 2 Data of the studied grab sediment samples of the Wadi El-Gemal area; D_1 and D_2 refer to the drainages 1 and 2 samples; TOC=Total Organic Carbon, $CaCO_3$%=Total carbonate, TP=Total Phosphorous, Mean (φ)=mean grain size.

Sample No	Depth m	Mean (φ)	TOC %	$CaCO_3$ %	TP ppm	Zn ppm	Pb ppm	Cu ppm	Fe ppm
1	0		5.31	5.84	534	26.7	n.d.	14.8	6133
2	0.25	2.09	5.61	12.44	737	41.4	29	10	7287
3	0.32	2.23	0.8	21.86	749	37.9	8.3	7.8	7031
4	0.37	3.09	0.49	21.27	975	42.7	3	5.8	7161
5	0.42	1.71	0.38	31.29	687	18	3	3.2	5795
6	0.51	2.89	0.29	42.36	722	26.7	20.2	2.5	6470
7	0.63	1.92	0.3	48.63	597	22.8	8.8	1.9	5884
8	0.7	2.35	0.35	45.16	1053	37.6	n.d.	5.7	7265
9	0.82	0.08	0.32	66.82	297	5.5	n.d.	n.d.	1386
10	0.94	1.47	0.13	77.9	326	2.1	n.d.	3.3	1398
D_1	0.2	1.09	0.39	54.62	306	11.8	n.d.	1.3	3890
D_2	0.27	1.31	0.12	26.34	430	23.7	n.d.	6.3	6061

Table 3 Data of the studied subsurface samples (core 1 and core 2); TOC=Total organic Carbon, $CaCO_3$%=Total carbonate, TP= Total Phosphorous, Mean (φ)=mean grain size.

	TOC%	CaCO3%	TP ppm	Zn ppm	Pb ppm	Cu ppm	Fe ppm
	0.11	10.08	1053	48.9	5.9	7.7	7576
	0.1	15.97	1043	49.3	8.6	7.4	7342
	0.17	25.87	512	30.8	n.d.	8	6403
	0.07	24.93	445	33.5	15.5	4.7	6724
core 1	0.07	16.68	598	40.7	n.d.	12	7133
	1.067	11.73	887	43.54	n.d.	9.4	7391
	2.57	7.49	746	42.9	n.d.	18.44	7476
	3.3	7.96	623	49.4	n.d.	21.18	7608
	4	9.61	623	43.6	24	14.8	7564
	0.79	5.6	1031	55.7	22.1	18.4	7210
	0.8	5.13	809	52.9	n.d.	16	7593
core 2	0.87	5.84	739	67.7	n.d.	22.6	7486
	0.59	5.13	814	69.1	2.9	20.3	7284
	0.64	4.43	663	58	3	20.8	7633

5. Organic compound

5.1 Oil pollution

The analysis of aliphatic hydrocarbons in mangrove roots reveals the very low concentration of C^{12} and C^{40} which might indicate the negligible fresh petroleum inputs.

5.2 Chlorinated organic compound

Chlorinated organic compounds analysis indicated that there are no adverse effect DDTs (Dichlorodiphenyltrichloroethane) in the marine organisms in the studied area, while the total PCBs (Polychlorinated biphenyl) has an adverse effect on the community of the bottom organisms in this area which reaches up to 90%.

6. Conclusion

The deterioration of mangrove plants is due to several reasons, the most significant one in the studied area being the high energy of coastal current, large waves and sloping of the intertidal area which withdraws the fine sediments offshore. Mangrove vegetation generally achieves greatest size and species diversity on fine-grained, semi-fluid saline, poorly drained and anoxic soils with abundant organic matter. The loss of this sediment causes deterioration to mangroves, consequently the adjacent coral reefs will be under threat.

Anthropogenic influence and camel and goat browsing are the next reason, while poor pollen production and rapid decay may also be considered. Also, we can not ignore the impact of the coastal road, the role of a drier climate, high PCBs, increased salinity and a weak fresh water supply.

Acknowledgement

We thank Dr. Azza Khaled, National Institute of Oceanography and Fisheries (NIOF) for her help in the organic hydrocarbon analysis.

References

Aspila, K.I., H. Agemian and A.S.Y. Chau (1976). A semi-automated method for the determination of inorganic, organic and total phosphate in sediments, Analyst, 101:187–197.

Bacon, P.R. (1994). Template for Evaluation of Impacts of Sea-Level Rise on Caribbean Coastal Wetlands. Ecological Engineering, 3(2): 171–186.

Black, C.A. (1965). "Methods of soil analysis" part 2, "Chemical and Microbiological properties", American Society of Agronomy Inc., Madison, Wisconsin., 1965.

Blasco, F. (1984). Mangrove evolution and palynology. In: S.C. Snedaker and J.G. Snedaker, 1984 (eds.), The mangrove ecosystem: research methods, UNESCO, Paris, Part I, 36–48.

Blasco, F., P. Saenger and E. Janodet (1996). Mangroves as indicators of coastal change. Catena, 27(3/4): 167–178.

Caratini, C. (1992). Mangrove pollen in marine Quaternary sediments: marker of regional climatic evolution and global eustatic sea level changes. In: K.P. Singh and J.S. Singh (eds.), Tropical Ecosystems: Ecology and Management, 349–357.

Clarke, P.J. and P.J. Myerscough (1993). The Intertidal Distribution of the Gray Mangrove (Avicennia-Marina) in Southeastern Australia–the Effects of Physical Conditions, Interspecific Competition, and Predation on Propagule Establishment and Survival. Australian Journal of Ecology, 18(3): 307–315.

El-Moslimany, A. (1986). Ecology and Late Quaternary history of the Kurdo-Zagrosian Oak forest near Lake Zeribar, Kurdistan (western Iran). Vegetatio 68: 55–63.

Folk, K.L. (1974). Petrography of sedimentary rocks. University Texas, Hemphill, Austin, Texas, 182 p.

Herrin *et al.* (1957). Carbonate-carbon by titration technique in principle of chemical sedimentology, Berner, R.A. 1971, McGraw-Hill-Book Company, 593–594.

Kholeif, S.E. and M.I.A. Ibrahim (2003). Microfauna and microflora of the intertidal flat environment in the northern coast of Qatar peninsula, Arabian Gulf. Egyptian Journal of Paleontology, Egypt, 3: 161–177.

Mansour, A.M., A.H. Nawar and A.M. Mohamed (1997). Recent intertidal sediments and negative impact of human activities, Red Sea coast, Egypt. Egyptian Journal of Geology, 41/2A: 239–272.

Rifaat, A.E. and M.H. El-Mamoney (2001). The textural, geochemical and mineralogical characteristics of mangrove sediments, south of Quseir City, Red Sea, Egypt. J.KAU: Marine Science, vol.12, Special Issue, 141–148 (1421 A.H./2001 A.D.)

Walkely, A. and T.A. Black (1934). An examination of the Degthareff method for determination soil organic matter and a proposed modification of the chromic acid, titration methods. Soil Science, 37: 29–38.

Forecasting circulation in the Cilician Basin of the Levantine Sea

Emin Özsoy* and Adil Sözer

Institute Marine Sciences, Middle East Technical University, Turkey

Abstract

The Cilician Basin/Shelf Model has been adapted for studying the shelf circulation in the Cilician Basin–Gulf of the İskenderun region of the Levantine Basin in the eastern Mediterranean between the Turkish Mediterranean coast, Syria and the island of Cyprus. The model initial conditions and open boundary conditions are supplied by the ALERMO regional model of the Levantine Sea, while interactive surface flux boundary conditions are specified by an atmospheric boundary layer sub-model using calculated water properties and surface atmospheric variables supplied by the Skiron atmospheric model, within the nested modelling approach of the MFSTEP (Mediterranean Forecasting System: Towards Environmental Predictions) project. Sensitivity tests are performed for alternative surface boundary conditions. Model performance for shelf/ meso-scale forecasts is demonstrated.

Keywords: Shelf, coast, circulation, Cilician Basin, Levantine Sea

1. Introduction

The Cilician Basin coastal system occupies the northeastern part of the eastern Mediterranean Levantine Basin between Cyprus and Turkey, and includes the wide, shallow continental shelf areas of the Mersin and İskenderun bays (Figure 1).

The continental shelf adjoining the Mersin and İskenderun bays is one of the widest in the entire Levantine Sea (excluding the Nile Cone) where the coastal bathymetry is often very steep. The Taurus and Amanos mountain ranges bound the Cilician Basin respectively in the north and east, lined with narrow 'riviera' coastal plains except in the vast delta plains of the Seyhan and Ceyhan Rivers northwest of İskenderun Bay.

The regional climate is typical of the eastern Mediterranean, with hot, humid summers and rainy, mild winters, and short transitional seasons. Northerly winds dominate the winter (November to March), and a sea-breeze system with southwesterly winds in the summer (April to October). Weather systems steered by steep mountain ranges but intercepted by valleys along the northern shore, such as at the Göksu river valley and Gulf of İskenderun, often develop local gale force winds in winter (Reiter, 1975; Özsoy, 1981).

Eddies and meanders, wind-driven currents, topographic/continental shelf waves, and inertial/internal oscillations add significant variability to the basic cyclonic circulation exemplified by the satellite SST (Figure 2a), the bifurcating mid-basin jet and the Asia-Minor current along the Turkish coast, interspersed with quasi-permanent anticyclonic eddies in the Eastern Mediterranean (Wüst, 1961; The POEM Group, 1992; Özsoy *et al.*,

* Corresponding author, email: ozsoy@ims.metu.edu.tr

1993). Focusing on the Cilician Basin with the nested model simulations (Figure 2b) described in the sequel, produces similar features to those observed via satellite.

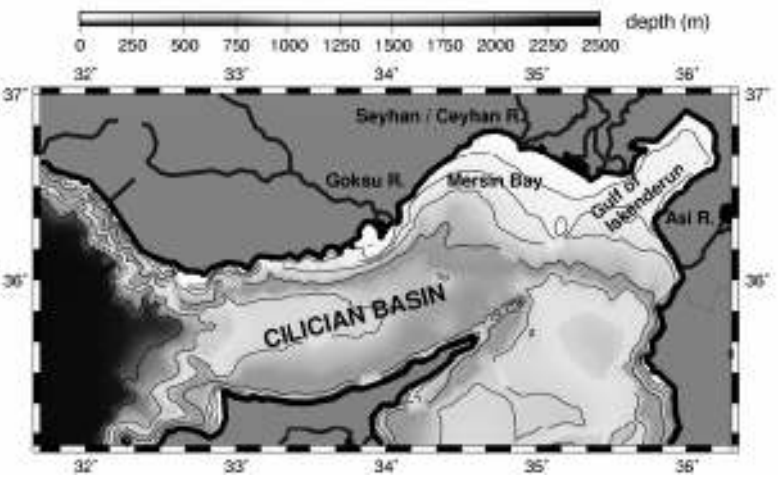

Figure 1 Layout of the Cilician Basin showing the topography, with important rivers and bays.

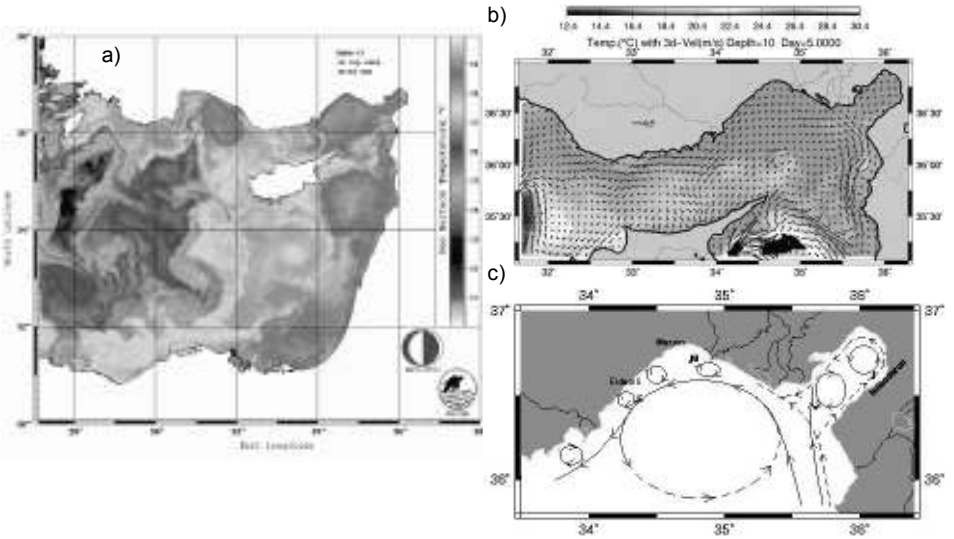

Figure 2 (a) Eddies, jets and gyres in the Levantine Basin of the Eastern Mediterranean Sea shown in a satellite-derived sea surface temperature field for 28 September 2004; (b) Cilician Basin model 5 day forecast of 10 m currents and temperature on 27 September 2004; (c) schematic surface circulation in the Mersin Bay and the Gulf of İskenderun area (continuous line: summer, dashed line: winter) suggested by Collins and Banner (1979).

The classic picture of surface circulation in the Gulf of İskenderun after Collins and Banner (1979) aided by satellite imagery and unpublished observations of IMS–METU in the region are schematised in Figure 2c. Two main types of circulation were observed within the İskenderun Bay: in summer two eddies, rotating in opposite directions, driven

by surface currents entering west of the Bay were inferred, while in winter it was presumed that the currents following the eastern coast could enter east of the Bay. Less saline and cooler waters were observed in the inner part of the bay. Direct current measurements carried out in winter 1992 indicated several high frequency oscillations in addition to an oscillation of about an eight-day period with current speeds in the range of $5-25\ \mathrm{cm\,s^{-1}}$.

The Cilician Basin coastal system is presently experiencing significant environmental stress as a result of explosive increases in population, industrial, agricultural and tourism activities. Waste from industries (steel, paper, fertiliser, etc.) and untreated or primary-treated municipal waste from the major towns of Mersin, Adana, İskenderun and Antakya are potential sources of marine pollution. Civilian and military marine transport linked to the harbours of Mersin, İskenderun and Taşucu, oil storage and pipeline terminals at Yumurtalık, Ceyhan and Dörtyol (including the recently completed Baku–Tblisi–Ceyhan pipeline transporting oil and gas from the Caspian Sea) are additional activities with potential impact on the environment.

The perennial rivers Göksu, Lamas, Tarsus, Seyhan, Ceyhan and Asi plus some smaller rivers account for a total fresh water flux of $27\mathrm{km^3/yr}$ ($870\ \mathrm{m\,s^{-1}}$), accounting for about half the river discharge along the Turkish Mediterranean–Aegean coasts, and are much greater than the present discharge of the Nile in the Eastern Mediterranean (estimated to be $540\ \mathrm{m^3\,s^{-1}}$, Pinardi *et al.*, 2005). Following the almost 90% reduction in the discharge of the River Nile in the 1960s, Turkish rivers concentrated in the Cilician Basin presently seem to be the main fresh water and nutrient sources for the entire Levantine Basin of the oligotrophic eastern Mediterranean. Because of the significant inputs of these rivers, the Cilician Basin has all the characteristics of the ROFI (regions of freshwater influence) but in the oligotrophic environment typical of the Eastern Mediterranean Sea.

2. Cilician Basin/Shelf circulation modelling

The Cilician Basin/Shelf model domain with 303×150 grid points covers an area of 409×201 km centred at 36.0245°N 33.9725°E shown in Figure 1, with a uniform nominal horizontal grid resolution of 1.35 km in both directions, and a vertical resolution of 28 sigma levels. The external and internal integration time steps were Δt_e=2 s and Δt_i=40 s respectively, and model constants were: horizontal mixing coefficients $A_m=A_h=200\ \mathrm{m^2\,s^{-1}}$, and initial vertical mixing coefficients $K_m=K_h=K_s=2\times10^{-4}\ \mathrm{m^2\,s^{-1}}$ respectively for momentum, heat, salt and bottom roughness parameters z_0=0.01, $C_{b,min}$=0.0025.

The fine scale model bathymetry was generated from contour data of UNESCO bathymetric maps of Mediterranean, making limited use of the US Navy DBDB1 gridded bathymetry to fill areas shallower than 50 m where contour data were missing. The model bathymetry was then filtered with a selective filter that smooths only the steep slope areas so that the r-value $r=\Delta H/(2H)$ (where H is the depth) between adjacent grid points remains below r=0.2. Large differences were detected in some areas between the coarse grid ALERMO and the fine grid model bathymetries (Figure 3).

The bathymetry at about 10 rows of grids at open boundary sections were taken to be exactly the same as the coarse model, regardless of the fine topography created, in order

to conserve volume fluxes and transport properties between the coarse and fine grid models, and gradually melded into the interior fine topography. Coarse grid model data were then interpolated to the Cilician Basin/Shelf model grid using weighted averaging with different horizontal and vertical scales.

Open boundary conditions tested for nested domains in the Mediterranean Forecasting System MFS (e.g. papers in De Mey *et al.*, 2003 special volume for MFS), namely the specification of barotropic flow velocity with a radiation component on the normal component (Flather b.c.), baroclinic velocity components and temperature/salinity with advective conditions during outflow have been adopted in the present model.

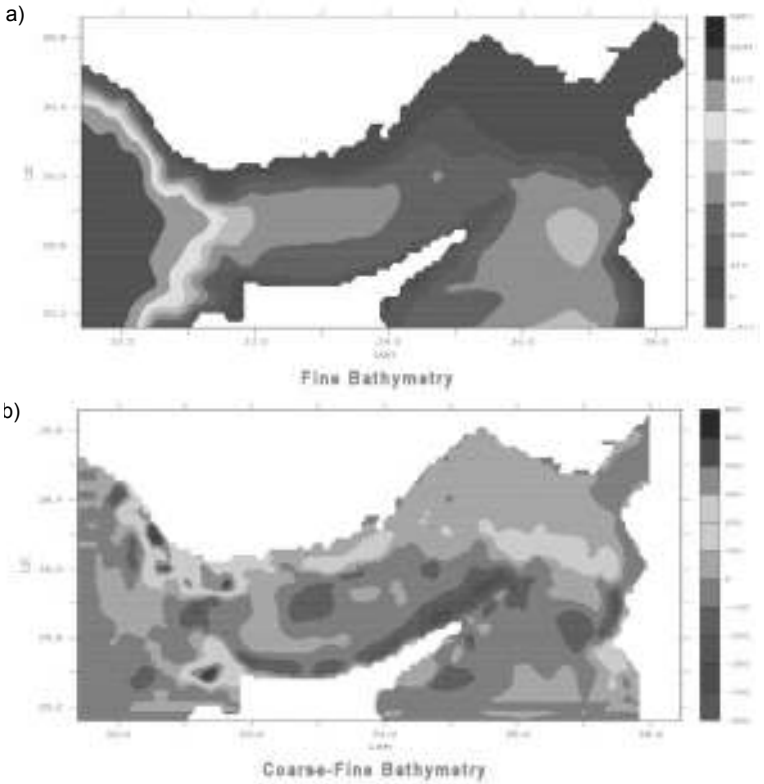

Figure 3 Model bathymetry (depth in m) of (a) the fine grid Cilician Basin/Shelf Model, and (b) the difference between coarse and fine grid bathymetry data sets with coarse grid data interpolated and the difference calculated on the fine grid.

Instantaneous momentum, heat and salt flux boundary conditions at the sea surface,

$$\rho K_m\left(\frac{du}{dz}\right) = T_x,\ \rho K_m\left(\frac{dv}{dz}\right) = T_y,\ \rho c_p K_h\left(\frac{dT}{dz}\right) = Q_h,\ \rho K_s\left(\frac{dS}{dz}\right) = S(E-P)$$

are specified for wind stress components T_x, T_y, net heat flux Q_h and salt flux $Q_s = S(E-P)$ with surface salinity S and net water flux at the surface (evaporation minus precipitation E–P), where the fluxes are specified through either an ABL or bulk formulae.

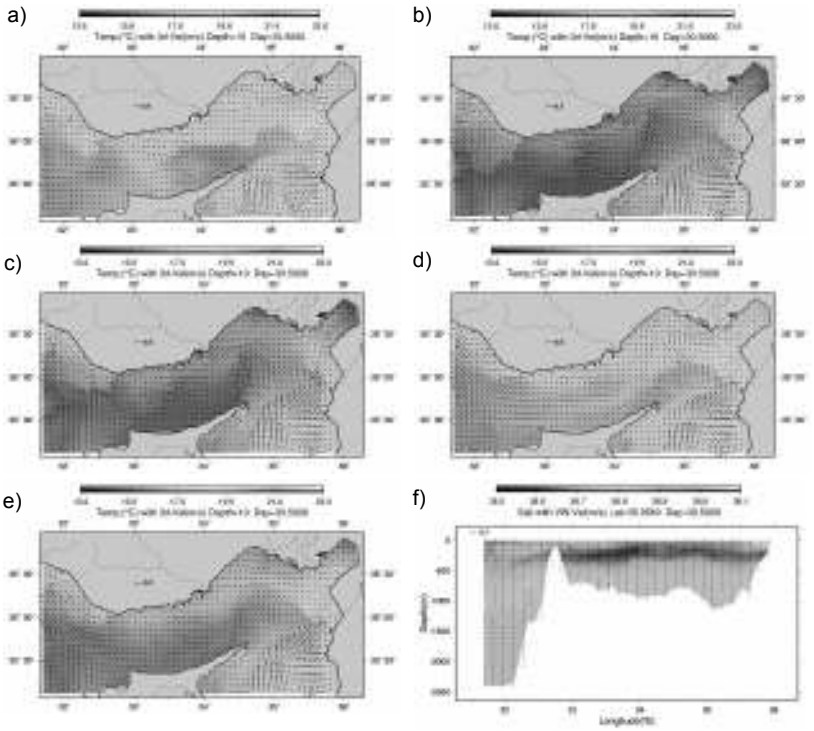

Figure 4 (a) Currents and temperature at 10 m depth for run A, (b) run B, (c) run C, (d) run D, (e) run E and (f) west–east salinity section along 36°N on 31 January 2003 after a one-month run.

Sensitivity to surface fluxes was tested making runs with identical initial and lateral but with alternative surface boundary conditions for the January 2003 validation period (in all cases ALERMO open boundary and initial conditions were used):

Run A: no surface fluxes applied.

Run B: non-interactive surface heat and salt fluxes computed with the Monin-Obukhov ABL sub-model based on iterative flux calculations of Launiainen and Vihma (1990) and Vihma (1995) and used by Ibrayev *et al.* (2004), from SKIRON surface variables, SST and short wave radiation.

Run C: surface heat and salt fluxes interactively calculated by the ABL sub-model from SKIRON surface atmospheric variables and model SST.

Run D: surface heat and salt fluxes including short and long wave radiation calculated by bulk formulae after Bignami *et al.* (1995), Castellari *et al.* (1998), Korres and Lascaratos (2003), from SKIRON surface atmospheric variables and model SST.

Run E: Same as Run C except for penetrative radiation.

Temperatures at 10 m after a one month run with continuous forcing in January 2003 compared in Figure 4 for the above cases show little difference between cases B and C, (i.e. the non-interactive and bulk fluxes), but much weaker cooling in case C using interactive fluxes. Penetrative radiation case E results in higher temperatures. Other compar-

isons between fields show significant changes especially up to a depth of 100 m, but even at greater depths, as a function of the surface fluxes specification.

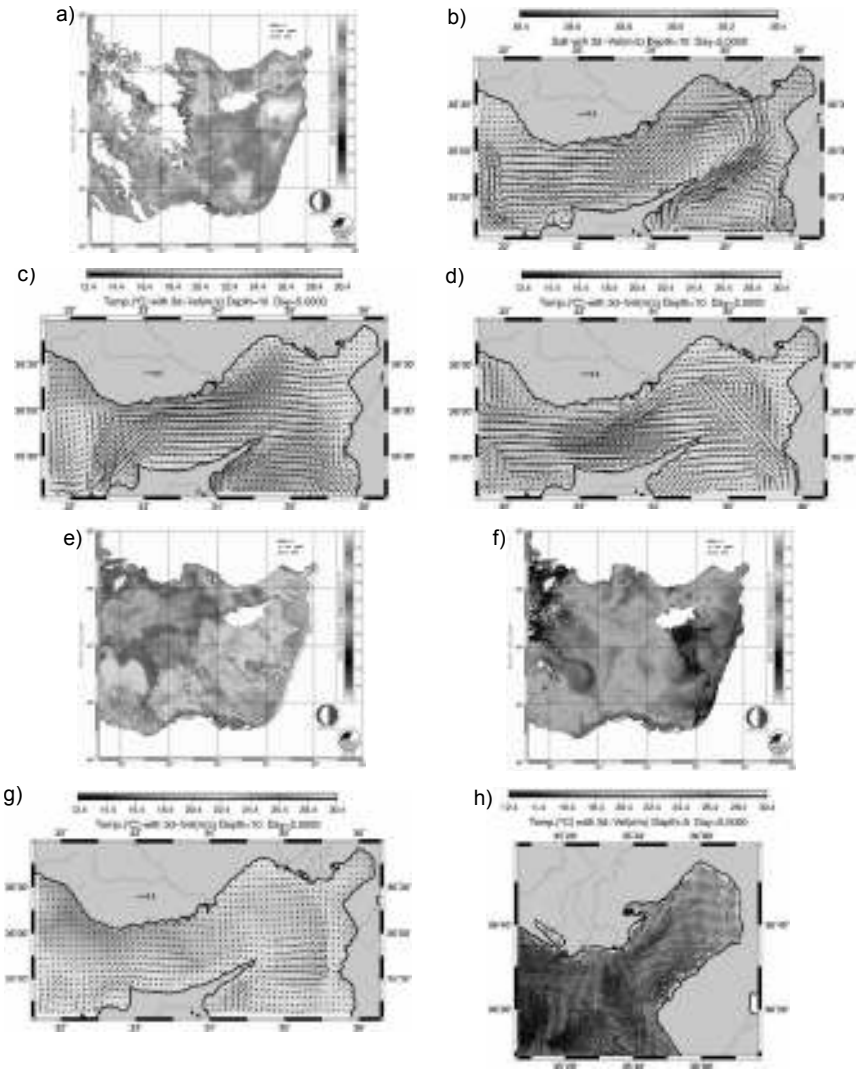

Figure 5 (a) Satellite SST image on 11 November 2004; (b) forecast currents and temperature at 10 m depth for a 5 day forecast on 8 November 2004 12:00 UTC; (c) same for 22 November 2004 and (d) 6 December 2004; (e) SST image on 11 January 2005; (f) SST image on 17 June 2005; (g) currents and temperature at 10 m depth for 21 June 2005 (h) currents and temperature at 5 m depth in İskenderun Bay on 8 September 2005.

3. Operational forecasts

An intensive data collection and assimilation effort was made during the 6 month Target Operational Period beginning in September 2004, producing weekly forecasts of 5 days

for the entire series of nested MFSTEP model domains. Examples of forecasts are provided here. In the September–November 2004 period, the persistent anticyclonic eddy east of Cyprus (Figure 2a and Figure 2b) moved north (Figure 5a) and created persistent jet flows (Figure 5b) following the 'tip' of Cyprus, impinging on the Gulf of İskenderun, and feeding the Asia Minor current flowing west along the northern continental slope. In mid-November a sudden change in direction of surface currents due to wind and remote forcing (Figure 5c) was followed by a temporary switch in currents in December and January to flow along the Syrian coast (Figure 5d and Figure 5e). The flow through the Cilician Basin was observed to have a significant barotropic component with current speeds reaching up to 0.3 ms^{-1} at 500 m depth. In June 2005 an upwelling event developed simultaneously south of Cyprus and along the Turkish coast in the western Cilician Basin (Figure 5f), which was well reproduced in the model (Figure 5g).

Shelf scale motions are displayed by focusing on specific regions. The meso-scale circulations developed in İskenderun Bay are exemplified in Figure 5h. In this example, the flow along the shelf slope bypasses the bay across its southwest opening, while a branch circulates anticyclonically in the bay, as suggested earlier in Figure 2b. Other types of circulation entering the bay on the surface with a return flow at deeper layers were also detected. However unsteady effects resulting from weekly initialisation cycles affected the results, and should be remedied by implementation of continuous forecasts.

Acknowledgements

This work was supported by the MFSTEP project (contract no. EVK–CT–2002–00075, 2003–2006) under FP5 of the Commission of the European Community, with Dr. Nadia Pinardi as the coordinator. We thank Dr. Şükrü Beşiktepe and the Institute of Marine Sciences of METU for their support, and Hasan Örek for the satellite data processing.

References

Bignami, F., S. Marullo, R. Santoleri and M.E. Schiano (1995). Longwave Radiation Budget in the Mediterranean Sea, J. Geophys. Res. 100 (C2), 2501–2514.

Castellari, S., N. Pinardi and K. Leaman (1998). A Model Study of Air–Sea Interactions in the Mediterranean Sea, J. of Marine Systems, 18, 89–114.

Collins, M.B. and F.T. Banner (1979). Secchi disk depths, suspensions and circulation in Northeastern Mediterranean Sea. Marine Geology, 31, M39–M46.

De Mey, P., A. Lascaratos, G. Manzella and N. Pinardi (Guest Editors) (2003). Mediterranean Forecasting System Pilot Project — Parts I and II, Annales Geophysicae Special Issue, 21(1) 436 pp.

Ibrayev, R.A., E. Özsoy, C. Schrum and H.I. Sur (2004). Seasonal Variability of the Caspian Sea — Three-Dimensional Circulation and Air–Sea Interaction, unpublished.

Korres, G. and A. Lascaratos (2003). A one-way nested eddy resolving model of the Aegean and Levantine basins: Implementation and Climatological Runs, Annales Geophysicae, 21, 205–220.

Launiainen, J. and T. Vihma (1990). Derivation of turbulent surface fluxes — an iterative flux-profile method allowing arbitrary observing heights, Environmental Software, 5(3), 113–124.

Özsoy, E. (1981). On the Atmospheric Factors Affecting the Levantine Sea, European Center for Medium Range Weather Forecasts, Reading, U.K., Technical Report No. 25, 30p.

Özsoy, E., A. Hecht, Ü. Ünlüata, S. Brenner, H.I. Sur, J. Bishop, M.A. Latif, Z. Rozentraub and T. Oguz (1993). A Synthesis of the Levantine Basin Circulation and Hydrography, 1985–1990, Deep-Sea Res., 40 1075–1119.

Pinardi, N., E. Arneri, A. Crise, M. Ravaioli and M. Zavatarelli (2005). The physical, sedimentary and ecological structure and variability of shelf areas in the Mediterranean Sea, The Sea, Vol. 14.

Reiter, E.R. (1979). Handbook for Forecasters in the Mediterranean; Weather Phenomena of the Mediterranean Basin; Part 1: General Description of the Meteorological Processes, Tech. Pap. 5–75, 344 pp., Environmental Prediction Research Facility, Naval Postgraduate School, Monterey, California.

The POEM Group (A. Robinson, P. Malanotte-Rizzoli, A. Hecht, A. Michelato, W. Roether, A. Theocharis, Ü. Ünlüata, N. Pinardi, A. Artegiani, J. Bishop, S. Brenner, S. Christianidis, M. Gacic, D. Georgopoulos, M. Golnaraghi, M. Hausmann, H.-G. Junghaus, A. Lascaratos, M.A. Latif, W.G. Leslie, T. Oguz, E. Özsoy, E. Papageorgiou, E. Paschini, Z. Rosentroub, E. Sansone, P. Scarazzato, R. Schlitzer, G.-C. Spezie, G. Zodiatis, L. Athanassiadou, M. Gerges and M. Osman) (1992). General Circulation of the Eastern Mediterranean, Earth Sci. Rev., 32, 285–309.

Vihma, T. (1995). Atmosphere–Surface Interactions over Polar Oceans and Heterogeneous Surfaces, Finnish Marine Research, 264, 3–41.

Sensitivity of Skagerrak dynamics to freshwater discharges: insight from a numerical model

Jon Albretsen*[1] and Lars Petter Røed[1,2]

[1]*Norwegian Meteorological Institute (met.no), Oslo, Norway*
[2]*Department of Geosciences, University of Oslo, Norway*

Abstract

This paper considers the relative importance of the various freshwater discharges to the Skagerrak/northern North Sea and its impact on the dynamics. The freshwater discharges are lumped into three sources, namely the Baltic, the UK and European continental rivers and the Norwegian and Swedish rivers. These discharges not only sustain the large scale cyclonic circulation in the area, but are also of crucial importance for the formation and subsistence of fronts, which in turn preserves the rich mesoscale activity in the area. Four sensitivity experiments and one control experiment, using a contemporary terrain-following ocean model covering the North Sea, Skagerrak and Kattegat, are performed. The experiments isolate the sources from the three regions above and compare the results with a control experiment which includes all of the freshwater sources. The main conclusion is that the inflow of brackish water from the Baltic through the Kattegat is the dominant source for the freshwater content along the southern Norwegian coast up to about 60°N.

Keywords: Numerical ocean model, freshwater from rivers, sensitivity experiments

1. Introduction

The Skagerrak, located between Norway, Denmark and Sweden, is the main body of water connecting the North Sea to the Baltic Sea, and is the birthplace of the Norwegian Coastal Current (NCC). The Baltic Sea is a large body of water containing low salinity water of about 8 psu, and is believed to be a major source of freshwater content for the water masses in the NCC as it flows first along the south-eastern coast of Norway and then continues northward along the south-western Norwegian coast. The Skagerrak is relatively deep compared to its adjacent seas with an average depth of about 210 m. Its main topographic feature is the Norwegian Trench located in the northern and central parts which cuts in from the Norwegian Sea and reaches depths of about 700 m in the inner part (Figure 1, left). As revealed by the right-hand panel of Figure 1, the dominating circulation pattern in the area is cyclonic confirming observations (Rodhe, 1987) as well as earlier model studies (e.g. Røed and Fossum, 2004; Melsom, 2005). Saline water of Atlantic origin enters north of Jutland, where it mixes with fresher water that flows northward along the west coast of Denmark containing freshwater from the UK and European rivers. The inflow continues eastward and is then mixed with fresh-water due to the inflow of low salinity water of Baltic origin through the Kattegat. As it turns northward along the Swedish coast and then south-westward along the Norwegian

* Corresponding author, email: jon.albretsen@met.no

coast it is further mixed with freshwater from the many Norwegian and Swedish rivers discharging their water masses into the area. The volume flux of the circulation is about 0.5−1 Sv (Rhode, 1987; Rydberg *et al.*, 1996; Røed and Fossum, 2004). The freshwater input results in a strong haline stratification in the upper layers of Skagerrak. The salinity ranges from 20−25 psu in the south-east corner of the Skagerrak to more than 35 psu in the deep water with the largest gradients across the front delineating the NCC from the inflowing water of Atlantic origin. As a result the area is rich in mesoscale activity (eddies, meanders, filaments and current jets) of temporal scales of several days to weeks and spatial scales associated with the Rossby deformation radius (typically of the order of 10 km in these sub-polar areas). As indicated both by Melsom (2005) and Fossum (2005) the sustenance of the mesoscale activity depends on the continued existence of a haline dominated density front, possibly combined with a large current shear.

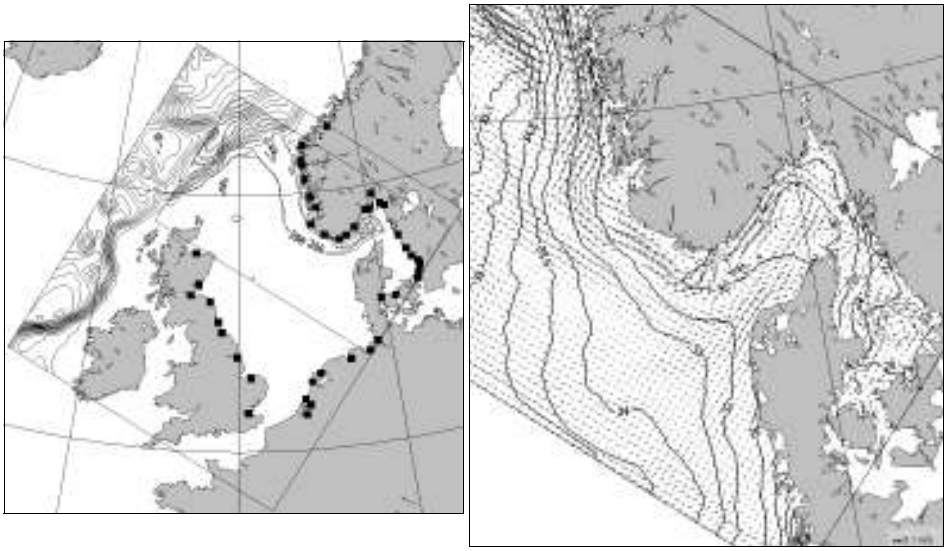

Figure 1 Left: the area covered by the coarse mesh grid (20 km grid size) which also conveniently displays the bathymetry of the area of interest. Bottom contours are shown every 200 m. Right: the area of the inset nested fine mesh grid of 4 km grid size, and the main pattern in surface currents and salinity. The current and salinity values (5 m depth) shown are annual means (1998) from the control experiment. Only every 3rd arrow is shown (i.e. 12 km between each arrow) scaled according to the arrow in the lower right hand corner (0.1 $m s^{-1}$). Contours give sea surface salinity in psu with a variable contour interval. The black squares in the left panel show the positions where freshwater discharges into the model area. These positions encompass all the major rivers within the model domain in addition to the Baltic inflow to the Kattegat through the Belts and Øresund.

2. The model ocean

The ocean model is the Norwegian Meteorological Institute's (met.no) version of the terrain-following σ-coordinate ocean model developed at Princeton University (Blumberg and Mellor, 1987; Engedahl, 1995a). It is part of the met.no ocean prediction system as described in Røed and Fossum (2004). Only a brief description is therefore offered here. In the present configuration the atmospheric forcing is via a surface flux

model, including salinity fluxes, coupled to the ocean model (Røed and Debernard, 2004). All atmospheric input is from the operational model at the European Centre for Medium-Range Weather Forecasts (ECMWF).

As described in Røed and Fossum (2004), the system is run on a fine mesh polar stereographic grid with grid size 4 km nested into a coarser mesh grid with 20 km grid size. The computational domain is given in Figure 1 (left). At all open boundaries the Flow Relaxation Scheme is applied (Martinsen and Engedahl, 1987; Engedahl, 1995b), with input from met.no's climatological data archive (Engedahl *et al.*, 1997). The bathymetry used is an improved version of the ETOPO-5 database from the National Geophysical Data Centre (NGDC). Tidal forcing at lateral boundaries is included in all model experiments.

The river discharges are implemented as point sources at the coast with a specified volume flux, salinity and temperature (Figure 1, left). As such the addition of water has a direct impact on the barotropic flow through the continuity equation, while the addition of freshwater directly affects the baroclinic flow through the conservation equations for heat and salt. As a rule, the freshwater is mixed over the entire water column according to a linear vertical distribution with maximum flux at the surface and zero flux at the bottom. The discharge data are monthly climatological means from the largest rivers. The amount of freshwater is represented well over time, but the timing and amplitude of the peaks and troughs in discharge is probably incorrect.

The inflow of the brackish water of Baltic origin into the Kattegat through the Belts and Øresund channel is also represented as a discharge with a constant salinity of 18 psu. The climatological volume fluxes representing this inflow are originally fluxes representing the total river runoff into the Baltic Sea. The actual in- and outflow of water from the Baltic Sea is then replaced by a net outflow. It should be noted that the Baltic inflow may be, and has been, parametrised in many different ways.

3. Model sensitivity experiments

Five model experiments with different amounts of freshwater input were performed and are summarised in Table 1. The first (Control) is a reference experiment, and the remaining four are compared with the Control. All experiments are run for the two years 1997 and 1998. Only the latter year is used in the analysis to exclude model spin-up effects.

Table 1 Summary of the five experiments.

Exp. No.	Name	Description
0	Control	Includes all rivers and Baltic inflow
1	EXP1	No freshwater inflow
2	EXP2	UK, Belgian, Dutch and German rivers only
3	EXP3	Norwegian and Swedish rivers only
4	EXP4	Baltic inflow only

Monthly mean anomalies for each month of the year 1998 are computed for each of the experiments EXP1–4 with Control as reference, and include salinity, temperature,

currents, freshwater height, and volume fluxes through various vertical sections. Included here is only the freshwater height F (Gustafsson and Stigebrandt, 1996) given by

$$F = \frac{1}{S_{\text{ref}}} \int_{-D}^{0} (S_{\text{ref}} - S) H(S_{\text{ref}} - S) dz$$

where $H(\Psi)$ is the Heaviside function, S_{ref} is a reference salinity corresponding to the salinity below the freshwater-influenced upper layers, here equal to 35 psu, and $S=S(z)$ is the salinity profile. Note that only positive contributions to F are included in the integral. Since the density of the Skagerrak and Kattegat water is essentially determined by its salinity, the amount of freshwater in a vertical column is a measure of the total buoyancy. Hence the freshwater height illustrates the effect of stratification on the baroclinic dynamics. The monthly mean freshwater height is derived from the mean salinity by using the Control as a reference.

4. Results

The freshwater height anomalies for the month of April are depicted in Figure 2 for the four experiments EXP1–4, respectively. Two striking results are evident in these images. First the near-shore freshwater height anomaly along the west coast of Denmark seen in EXP1, EXP2, and EXP3 are completely removed in EXP2 (upper right panel). This is a strong indication that the freshwater along the west coast of Denmark is completely dominated by the UK and European continental river discharges. Next the freshwater height anomaly in EXP4 (lower right panel) is significantly lower than in the three other experiments, except along the west coast of Denmark and the area around 60°N along the west coast of Norway. This shows that most of the Skagerrak and the Kattegat is dominated by the freshwater content supplied by the Baltic inflow, in particular the central to eastern parts.

Shutting off all river discharges (EXP1) clearly reduces the freshwater height in the area, most notably along the coasts (Figure 2, upper left panel). In particular this is evident in the central and eastern part of the domain as well as in Kattegat where the anomalies are reduced by more than 4–5 m in certain areas with a maximum of 5.5 m north of Skagen. The inclusion of the UK and European continental rivers (EXP2) not only completely removes the anomaly along the west coast of Denmark, but as revealed by Figure 2 (upper right panel) also impacts the anomaly in remaining area. In fact the maximum freshwater height anomaly is reduced by about 1 m, a reduction of about 20%. Next including Norwegian and Swedish rivers only (EXP3), also reduces the maximum anomalies with about the same amount, but the maximum effect is along the Norwegian coast all the way up to the northern boundary of the domain.

Shutting off all river discharges, but including the Baltic inflow (EXP4), has the most dramatic impact on the freshwater height anomalies in the central parts of Skagerrak and in Kattegat. Here the reduction in the maximum anomaly (north of Skagen) is more than 60%. It is interesting to note, however, that the impact on the anomaly around 60°N along the west coast of Norway is only 1 m, that is, as for the UK and European conti-

nental rivers (EXP2). The largest impact in this area is obtained when the Norwegian and Swedish river discharges are included (EXP3).

Finally, it is worth mentioning that the above results are further underscored by a similar analysis of the other variables like salinity, currents, temperature, and volume fluxes (not shown). For instance in the NCC area which is rich in mesoscale activity, the current anomalies are relatively large in all experiments. This is most probably due to local variations in instability patterns and growth of mesoscale motion due to local variations in the frontogenesis.

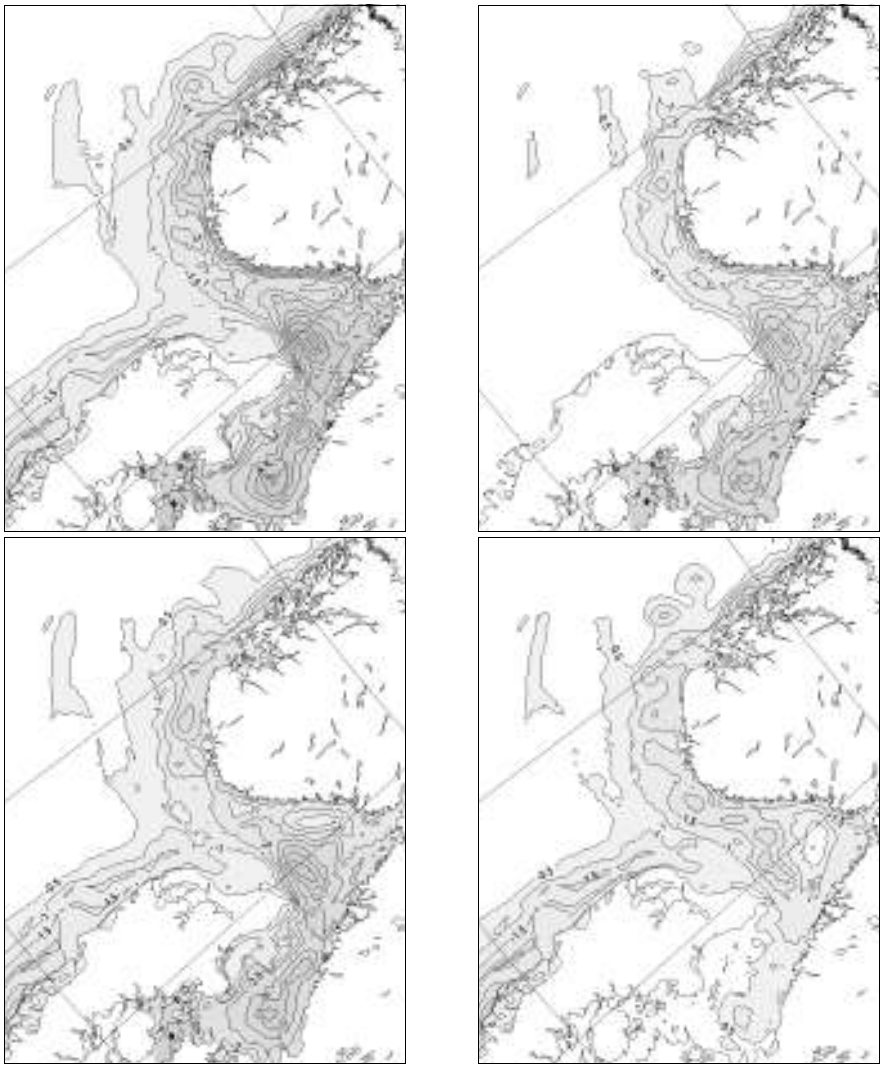

Figure 2 Mean freshwater height anomalies (Control−EXP) for April in metres. Upper left: freshwater height anomaly for EXP1, upper right: EXP2. Lower left: EXP3 lower right: EXP4. The contour interval is 0.5 m.

5. Conclusions

It is found that most dominant freshwater source feeding the Norwegian Coastal Current (NCC) is the freshwater content in the Baltic inflow to the Skagerrak through the Kattegat. In fact it accounts for more than 60% of the freshwater height in the water columns. The NCC area is an area rich in mesoscale activities. To sustain this activity it is of utmost importance that the frontogenesis along the density front delineating the saline inflowing water of Atlantic origin and the fresher waters of the NCC is upheld. This result therefore strongly supports the idea that to obtain a realistic mesoscale activity in the NCC area the single most important process to parametrise correctly is the Baltic inflow. Several improved and promising parametrisations of the Baltic are explored and will be reported elsewhere.

Acknowledgements

This work is part of the MONCOZE (Monitoring the Norwegian Coastal Zone Environment) project, and is funded in part by the Research Council of Norway under grant no. 143559/431, and the Norwegian Meteorological Institute.

References

Blumberg, A.F. and G.L. Mellor (1987). A description of a three-dimensional coastal ocean circulation model, In: Three Dimensional Coastal Ocean Models Vol. 4, N. Heaps (Ed.), American Geophysical Union, Washington D.C., 1–16.

Engedahl, H. (1995a). Implementation of the Princeton Ocean Model (POM/ECOM-3D) at the Norwegian Meteorological Institute (DNMI). Research Report 5, Norwegian Meteorological Institute, P.O. Box 43 Blindern, 0313 Oslo, Norway.

Engedahl, H. (1995b). Use of the flow relaxation scheme in a three-dimensional baroclinic ocean model with realistic topography. Tellus, 47(A), 365–382.

Engedahl, H., G. Eriksrød, C. Ulstad and B. Ådlandsvik (1997). Climatological oceanographic archives covering the Nordic Seas and the Arctic Ocean with adjacent waters. Research Report No. 59, Norwegian Meteorological Institute, P.O. Box 43 Blindern, 0313 Oslo, Norway. ISSN 0332–9879.

Fossum, I. (2005). Ocean eddies off southern Norway. Series of dissertations submitted to the Faculty of Mathematics and Natural Sciences, University of Oslo No. 435, Department of Geosciences, University of Oslo, P.O. Box 1022 Blindern, 0316 Oslo, Norway. ISSN 1501–7710.

Gustafsson, B. and A. Stigebrandt (1996). Dynamics of the freshwater-influenced surface layers in the Skagerrak, Journal of Sea Research, 35 (1–3), 39–53.

Martinsen, E.A. and H. Engedahl (1987). Implementation and testing of a lateral boundary scheme as an open boundary condition in a barotropic ocean model, Coastal Engineering, 11, 603–627.

Melsom, A. (2005). Mesoscale activity in the North Sea as seen in ensemble simulations, Ocean Dynamics (in press).

Rodhe, J. (1987). The large-scale circulation in the Skagerrak, interpretation of some observations, Tellus, 39A, 245–253.

Røed, L. P. and I. Fossum (2004). Mean and eddy motion in the Skagerrak northern North Sea: insight from a numerical model. Ocean Dynamics, 54, 197–220.

Røed, L.P. and J. Debernard (2004). Description of an integrated flux and sea−ice model suitable for coupling to an ocean and atmosphere model. Met.no Report No. 4/2004, Norwegian Meteorological Institute, P.O. Box 43 Blindern, 0313 Oslo, Norway, 51p.

Rydberg, L., J. Haamer, and O. Liungman (1996). Fluxes of water and nutrients within and into the Skagerrak, Journal of Sea Research, 35, 23−38.

The Litto3D project

L. Louvart* and C. Grateau

SHOM, Brest, France

Abstract

In 2003 the French Institut Géographique National (IGN) and Service Hydrographique et Océanographique de la Marine (SHOM) were tasked by the Prime Minister to combine efforts to produce together a seamless, modern, precise topographic and bathymetric model, possibly including the tides, of the entire French coasts. The area envisaged should extend from the 10-metre contour line inland to a distance of 10 kilometres seaward, or 6 nautical miles from the coastal baselines. This project was created to meet the more than one hundred requirements expressed by coastal managers concerned with the protection and exploitation of the littoral and by users of geo-referenced data, and should become the core of all future integrated coastal management projects.

The preliminary study conducted in the Golfe du Morbihan, Southern Brittany, has already proved that France should be spared the strenuous geodetic problems met elsewhere. Thanks to the Napoleonic tradition of keeping common geodetic references inland and at sea, the historical database "Histolitt" could be assembled fairly quickly, showing the gaps in poorly surveyed areas that could be filled efficiently by modern technology (laser bathymetry and topography, MBES, RTK, aerial orthophotos, permanent digital tide gauges), allowing metric accuracy on the plane and decimetric precision of heights and depths (Figure 1).

A first lidar survey has already been planned for summer 2005 in the Golfe du Morbihan to conduct further tests and generate a precise Digital Terrain Model (DTM) at different resolutions (2×2 m and 4×4 m). The survey strategy comprises three different approaches, depending on the bathymetric interest, the near shore seabed complexity and the Rapid Environment Assessment military program requirements.

1. Many needs on Littoral

Coastal management is an essential objective to satisfy many needs: public maritime delimitation, littoral protection (e.g. change of coastline due to erosion, fauna and flora protection), risk prevention (e.g. floods, pollution, safety at sea, natural disasters), regional development (ports, tourism and industry), concern for mineral and living resources, research and scientific studies, military needs (e.g. inshore patrol, search and rescue, amphibious operation, mine warfare). More than a hundred applications have been registered.

The large concentration of people and coastal housing justifies a specific cartography of this area. The population density at the seaside is two and a half times greater than inland. Littoral actors need a very good description of the coast: dense everywhere, precise, low cost, rapid, open to everybody and fully shared. Apart from the fact that areas of interest do not match, there is no difference between civil and military needs.

* Corresponding author, email: laurent.louvart@shom.fr

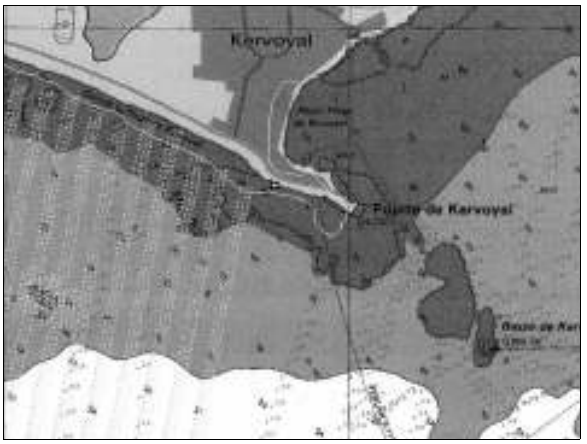

Figure 1 Printed sea charts depths (dark grey) with bathymetric survey sheets (medium grey and light grey).

2. Present cartographic deficiencies

Sea charts and nautical documents are not fully suited to these needs as they are mainly dedicated to seamen. The information is condensed around the navigation routes and ports. Moreover, for legibility, information is less dense than in bathymetric surveys (Figure 1). Access to these plotting sheets is not easy and many people have no idea that hydrographic services have much more information digitally than is printed on charts. Consequently, some people lose time and money digitising charts and get very poor (and even false) results if they use only charted information to describe and model coastal phenomena.

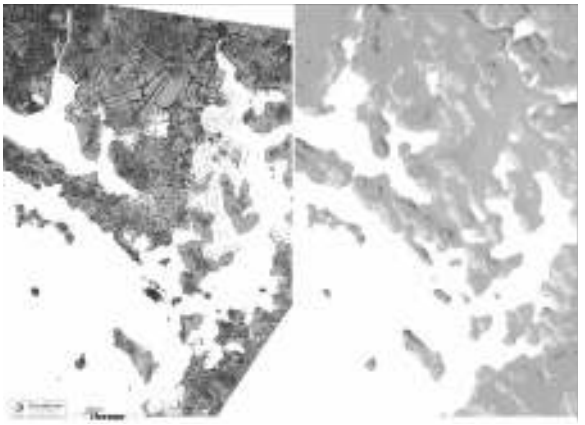

Figure 2 Left: a lidar topographic model (showing relief and some coverage of vegetation and buildings, cell size = 2 m, σZ: 15 cm). Right: an IGN BDAlti™ DTM derived from photogrammetric restitution (relief, without any vegetation or buildings informations, cell size = 50 m, σZ = 2 m). Shading is used to highlight the texture of the relief and exaggerates the differences between flat and step areas.

On land, height information usually comes from digitised chart contours (1:25 000 at most) and photogrammetric interpretation. There is a good density but accuracy is not sufficient to describe precisely the coast and to match with depths (Figure 2).

The intertidal area is not very well described as it is very difficult to make surveys in very shallow waters (not enough water, too many rocks and breakers) and to get good photogrammetric restitution (especially for wet and flat areas). That is the reason why, in many places, there is no data at all and no continuity between sea and land (Figure 3).

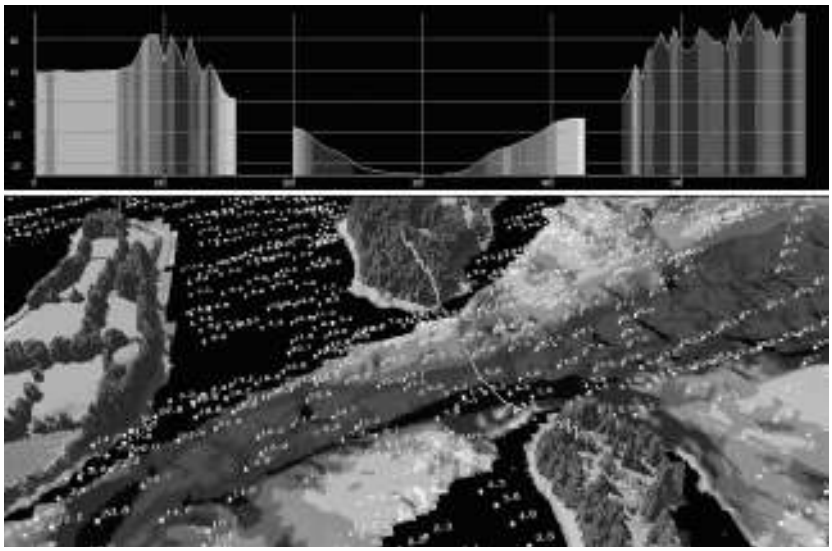

Figure 3 Fusion of lidar heights, multibeam survey and old vertical sound depths. The cross section shows a large gap between data (black hole ~50 m wide).

3. European recommendation and French response

Erika (December 1999) and Prestige (November 2002) disasters have emphasised the lack of coastal information: for instance it was quite impossible to estimate environmental damages due to pollution and to take the best decisions (which beach to protect or to evacuate, which port of refuge to choose, etc.) as the coastal relief and the nearby currents were not known exactly. On 30 May 2002, the European Parliament made a recommendation aimed at European members to start the inventory of the littoral and to carry out an integrated coastal management. On 29 April 2003, CNIG (Conseil National d'Information Géographique) and CIMER (Comité Interministeriel de la MER) took their turn and recommended that SHOM and IGN prepare this inventory, achieving together an altimetric continuous model for metropolitan coast and over seas French subdivisions. On this model, all the different thematic layers will be based and will constitute what is called RGL (Littoral Geographic Reference).

4. Preliminaries

During a preliminary study (March 2003), SHOM and IGN have evaluated the different issues to solve before getting a seamless database with continuous relief between water

and land. In addition to the previous observations (§2), it also appears that there is no difficulty in merging information as SHOM and IGN data can in most cases share the same geodetic reference level: there are known correspondences between sea chart datum (LAT) and land datum.

These first results have been reported to CIMER who encouraged SHOM and IGN to keep going (14 September 2004). The enlargement of SHOM and IGN's original attributions have been justified. Within their present responsibilities, SHOM and IGN have all the necessary skills to contribute to this project: bathymetric, geodetic and cartographic expertise. Notably, a French tide model has been implemented with a precision compatible with Litto3D requirements.

The very first and easy stage is to promote and provide existing digital information through a new product called Histolitt (2006). Thus, a part of littoral requirements will soon be satisfied.

The commercial policy is not yet defined as these data belong to SHOM, IGN and other organisations. Many agreements must be reached before these data can be made available to everybody.

5. Demonstrator in the Golfe du Morbihan

For the same period, SHOM and IGN must show that it is possible to achieve together a continuous altimetric model in a small area, combining different and new acquisition means.

A laser airborne system provides an accurate, rapid, safe and cost effective method of surveying coastal areas. This system has been used by governments and commercial organisations over the last decade to conduct surveys for nautical charting, coastal zone management, etc. It seems particularly suited to filling the gap between former sea charts and Litto3D (Figure 3 – cross-section).

The objectives of the laser demonstrator are:

- To know the performances and the limits of airborne laser survey
- To compare and merge MBES (multibeam echo sounder) and laser data
- To be up to the highest hydrographic and cartographic standards
- To lay down standards to Litto3D partners: data acquisition methods and qualification rules.

The Golfe du Morbihan offers a huge variety of relief and thematic. It is a good spot to achieve a demonstrator as it concentrates all difficulties: 0–50 m depths, turbidity, currents, wide inter-tidal area, flat sandy beaches and rocky coastlines that are most representatives of the French littoral. This is also a highly frequented boating spot in summer and SHOM ought to refresh nautical documents there.

Another point is the demonstrator for the navy. For a well known landing area, SHOM will try to get a very precise description of the seabed and to elaborate some very specific products, dedicated to amphibious operation. If the demonstrator is convincing, a navy military concept will be set up and could be replicated to military areas of real interest.

This survey took place in summer 2005.

5.1 Survey objectives

There are two different areas to be surveyed: a global survey of the whole gulf and a landing spot.

Small scale survey of the whole gulf: each depth will individually fulfil the S44 order 1 requirements (absolute accuracy: vertical = 50 cm and horizontal = 5 m) and the area will be incompletely surveyed, as shallow waters will not be exhaustively detected. The spatial resolution will be 1 measure every 4×4 m laser spot spacing and there will be 20% overlapping between tracks. Data processing will be done in batch mode.

Large scale survey of a landing beach area (Figure 4) in respect to S44 order 1 (absolute accuracy: vertical = 25 cm and horizontal = 2 m) with a full exploration of the seabed (all cubic obstructions detected). This survey will be split into two separate surveys:

- A first flight, lengthwise along the beach, will be made in order to determine the best landing route (1 measure per 4×4 m cell size). Data processing will be achieved in near real time (some hours).
- A second flight, perpendicular to the beach and in accordance with the best landing way previously determined, will be done with a spatial resolution of 1 measure per 2×2 m laser spot spacing with a 60% overlapping tracks. Data will be processed in very short time (few hours). In the landing area, 2 cubic targets will be dumped at 5 and 10 metres deep, and must be detected.

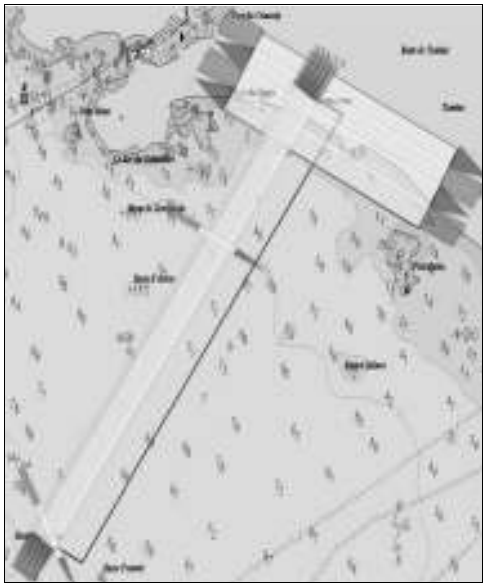

Figure 4 Flight plan for a laser bathymetric and altitude survey of the landing beach.

The industrial team in charge is committed to survey the whole coverage but not to sound the bottom everywhere, as it is too dependent on turbidity and hazardous meteorological conditions.

5.2 Survey equipment

There will be a laser bathymeter (SHOALS 1000-T) boarded on a twin-engine aircraft (CESNA 404) (Figure 5). This laser works with a near infrared (1064 nm) and a green (532 nm) light. There are two distinct working modes:

- Hydrographic and topographic mode at 1 kHz frequency
- Topographic mode at 10 kHz frequency.

Figure 5 Aircraft equipped for laser surveys and inside racks.

The aircraft will be located through at least 3 different ways:

- Real time DGPS: For navigation and data pre-processing, OMNISTAR differential corrections will be used; in case of loss of signal, inertial central data will be used too.
- Batch stage KGPS: For data post-processing, both raw GPS data and inertial central data will be computed in L1/L2 mode to get a Kinematic GPS location.
- Real time GPS-RTK: ground stations will provide differential corrections through GSM antenna. This third way is too uncertain for real time navigation as there are some risks (data communications losses) but it will be used for post-processing and quality assurance.

5.3 Survey strategy

Many strategies are possible, but only a few are optimal. In water it depends on tide and turbidity for laser water penetration. On land it depends on tide. In all cases it depends on weather conditions, best being high-pressure conditions with no rain and light wind (<15 knots): the best weather period seems to be summer. July and August must be avoided, as there are too many navigators in the gulf.

The progress survey state of the gulf is typical of a multi-captors Litto3D survey. There is already a land laser survey of the gulf so the strategy is to make sure that there is small but existing overlapping between this land survey and the new one, to be able to create seamless products: high water rather than low water.

There are already MBES surveys in navigation channels, the deepest waters of the gulf, so the strategy is to cover the unsurveyed areas rather than to penetrate deep water again: topographic laser mode in low water and bathymetric laser mode in high water at springs.

Turbidity is the conjunction of 3 factors: chlorophyll content, organic materials content and suspended sediments in water. The best period for chlorophyll and organic materials

are summer and winter. The optimal period for sediments is the less turbulent current periods: slacks at neaps.

Costs must be taken into account too. The strategy must minimise operational risks with an acquisition duration of 2 weeks. The general strategy will be:

- Bathymetric surveys will be made during slacks of high water at springs: turbidity is not optimal but rather good at slacks, deep depths can not be reached but there are some MBES surveys to fill in the gap.
- Topographic surveys will be made during slacks of low water.
- Flights will take place night and day in order to get best laser measurements (no sun interference) or waste of slacks.

5.4 Flight tactics

Flight tracks are oriented perpendicular to tide propagation into the gulf and will follow the slacks. There is a tidal model of the gulf with 143 tide harmonics every 200 m. It will be used to get predicted tide information all along the tracks and to follow the tide with the aircraft in real time (Figure 6). As a hydrographical rule, 10% of the tracks will be perpendicular to regular survey tracks to enable error detection and S44 qualification.

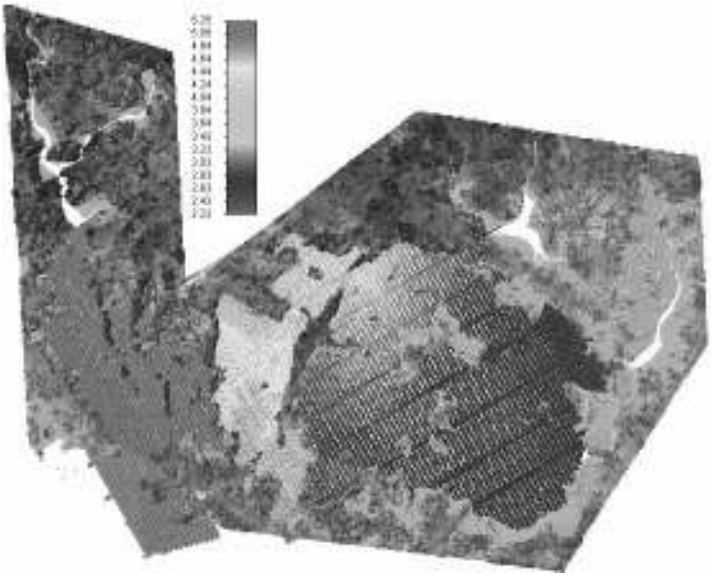

Figure 6 Evolution of tide height along flight tracks (heights in metres).

5.5 Quality assurance

Laser calibration (static and on the fly), GPS (Ground Control Point and levelling) and tide monitoring (SHOM) are carried out all along the survey.

Every day, environmental information, geometric calibration measures and laser data are downloaded to a ground control system (GCS). GCS involves a signal processor to discriminate sea or land surface and sea bottom from the different signals. It contains automatic algorithms that calculate the exact location of laser signal from GPS and

inertial central attitude data: X, Y, Z and a confidence interval is given for each measure. Doubtful signals are underlined and submitted for human control (Figure 7). Some video camera information will be helpful to eliminate artefacts in signals: birds, boats, shore breaking, etc. At the end of the process, data will be provided into XYZ format and related to RGF93 datum.

The same tide model used for flight planning is reused to reduce laser data into depths. In the first stage, depths will be relative to lowest astronomical tides (LAT), then to chart datum (CD) and eventually to land survey datum (IGN69). The tide model makes this possible as it contains difference models between these vertical references (Figure 7).

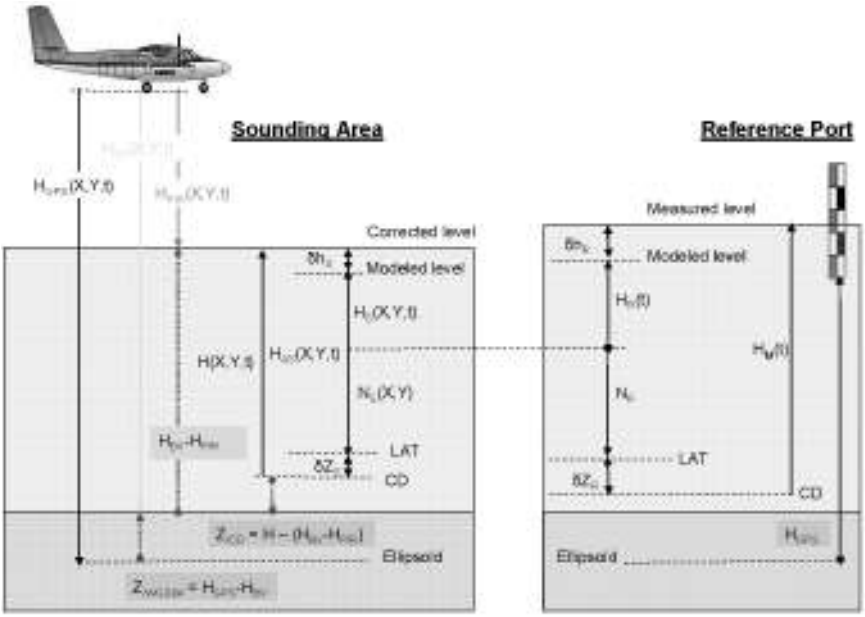

Figure 7 Propagation of tide observations at depth sounding area throughout model application.

In Figure 7, $\frac{\delta z_S(X, Y)}{\delta z_R} = \frac{N_S(X, Y)}{N_R}$ and $\delta h_S = \delta h_R$

Laser data will be compared to land surveys (laser and GPS levelling) and MBES surveys. Data will be merged in accordance with the different accuracy and uncertainty of these different surveys. Many methods could be applied: GIS methods or geo-statistical criteria (CUBE algorithms for instance).

5.6 Products

First of all, if any hazards are found out during the laser survey, they will be automatically reported to SHOM and brought to the attention of mariners.

The results acquired within this demonstrator give SHOM and IGN a good idea of the feasibility, costs and real interest of laser. Results should be extrapolated quite easily to other metropolitan parts, within the Litto3D project. The basic products are usually:

- Raw laser data

- GPS and inertial central data
- Calibration data
- Seamless numerical models (2×2 m) with uncertainty information on nodes
- Mosaic of digital images (day surveys only)
- Charts
- Final report included procedures and operations description.

Validated data will be stored in bathymetric SHOM and IGN databases for general public use. The first customers of these data are likely to be the different littoral agents of the Golfe du Morbihan and SHOM cartographers. As soon as these basic products have been produced, many modern and accurate by-products can be created (Figure 8).

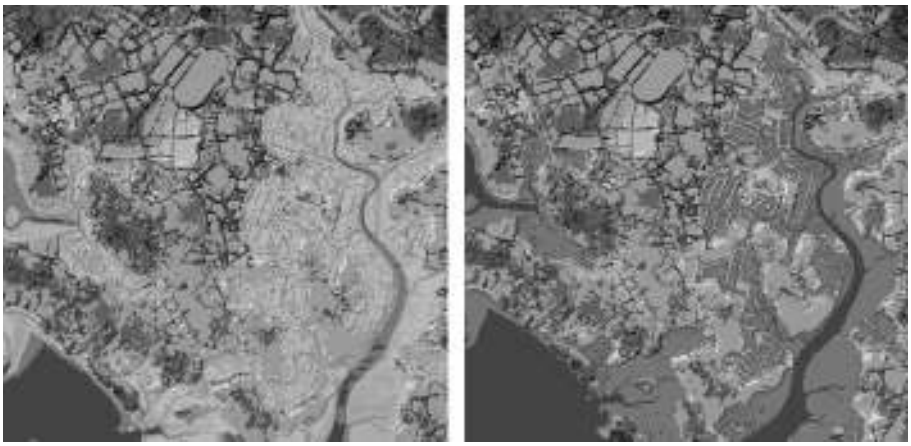

Figure 8 Sea flood simulation. The same DTM overlapping 2 different sea surfaces: low water (left) and high water (right). Some terrestrial parts become flooded, while others parts are quite unaffected.

6. Conception issues and production plan

The replication of this demonstrator all along the metropolitan coast and French subdivisions demands new knowledge, mainly in the laser survey domain. SHOM and IGN are not the only organisms concerned with the Litto3D project. This project also has a big impact on French industry and on the research field. Subcontracting and cooperation are essential to constitute Litto3D products and services. In addition to public investment, European funding possibilities must be investigated as this initiative is spreading in Europe.

At the moment, there are still many open issues that SHOM and IGN should resolve during the conception phase:

- Data acquisition: Should a national and independent laser captor be purchased or rented? Should the complete mastery be acquired or do we remain project manager?
- What are the geographic priorities?

- The demonstrator for Golfe du Morbihan costs 500 k€. A first estimation of the whole project costs gives 25 million euros for 10 years. Who is ready to fund a part of this project? State-government, Region, Inter-Region?
- What does the commercial policy look like? Public data must be reused according to the European law (17 November 2003) and the French ordnance in progress.
- Updating the product: It is quite hard to evaluate as it depends both on environmental factors (e.g. variability and anthropogenic features) and technological possibilities.

A new near real time monitoring network in the Gulf of Manfredonia – Southern Adriatic Sea

F. Fiesoletti[1], A. Specchiulli[1], F. Spagnoli*[1] and G. Zappalà[2]

[1]*CNR–ISMAR, Coastal and Lagoon Ecosystem Department, Lesina, Italy*
[2]*CNR–IAMC, Coastal Marine Environment Institute, Messina, Italy*

Abstract

Starting at the end of 2002, a monitoring network was set up in the Gulf of Manfredonia to assess in near real time the ecological conditions of coastal waters, integrating real time oceanographic and atmospheric observations performed by a multiparametric marine platform with bimonthly oceanographic observations carried out by a coastal vessel.

Correct and continuous data were acquired by *in situ* temperature sensors (at five fixed depths), air pressure and wind direction sensors from August 2004 to April 2005, and by air temperature, solar radiation and wind speed sensors from December 2004 to April 2005.

Early data obtained with the bimonthly monitoring in the Gulf of Manfredonia showed that this area is subject to high seasonal variations and both biochemical and hydrological characteristics of the Gulf are influenced by coastal morphology, continental inputs and Western Southward Adriatic Current effects.

Keywords: coastal monitoring network, real time automatic observations, marine ecosystem, oceanographic instrumentations, data quality check, sensor calibration.

1. Introduction

Coastal areas are complex systems characterised by various processes with variable space and time scales; a continuous and high frequency monitoring of all oceanographic and meteorological variables gives information on the near real time status of the marine ecosystem and enables estimation of possible perturbations due to natural or anthropogenic events. Furthermore, a (near) real time observation system could allow better management and a sustainable exploitation of marine environment.

The PITAGEM project (Integrated methodologies for the study of marine trophic processes and deployment and management of oceanographic platform for marine monitoring), coordinated by ISMAR–CNR of Lesina in collaboration with the IAMC–CNR of Messina, aims to set up and manage an automatic integrated monitoring network in the Gulf of Manfredonia (Southern Adriatic Sea) to assess in near real time the ecological conditions of coastal waters.

A long-term monitoring experiment based both on vessel and platform measurements in the Gulf of Manfredonia (Figure 1) is described in this paper; the main results are summarised in Sections 4 and some comments on future perspective are given.

* Corresponding author, email: federico.spagnoli@fg.ismar.cnr.it

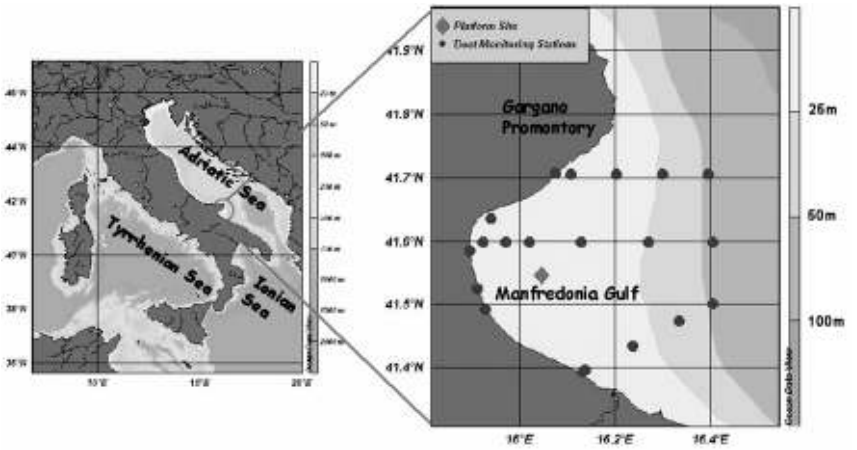

Figure 1 Study area: the Gulf of Manfredonia. Vessel monitoring stations and the platform site are marked with dots and a diamond respectively. Tints show depth in metres.

2. Study area

The Gulf of Manfredonia is a shallow area located in the western part of the South Adriatic Sea, just south of the protected area and tourist resort of the Gargano Promontory (Figure 1). In the Gulf of Manfredonia a cyclonic gyre is often observed, but it may reverse depending on wind direction: cyclonic and anticyclonic gyres are respectively generated by N–NW and S–SE winds (Signell, pers. comm.). The offshore area of the Gulf is influenced by the Southward coastal current flowing along the Western coast of the Adriatic basin (Artegiani *et al.*, 1997–part II). In this context, open waters clearly show oligotrophic characteristics (Vilicic *et al.*, 1989), while the high nutrient supply into the Gulf depends on hydrodynamic conditions of the Southern Adriatic Sea and on continental inputs.

3. The monitoring network in the Gulf of Manfredonia

The integrated monitoring network of the PITAGEM project consists of observations performed by a coastal oceanographic platform developed by CNR–IAMC (Zappalà *et al.*, 2003) and a coastal vessel. The data acquired were filtered by an automatic quality control procedure detecting values outside predefined ranges of natural variability and checking for spikes. Validated data were transferred to a database and published on the Internet through the web page for CNR–IAMC in Messina.

3.1 The platform monitoring system

The platform was deployed in October 2002 in the Gulf of Manfredonia (Figure 1); after a first test period, it was upgraded with a mixed wind and solar power supply system and some minor software modifications were performed. The platform was equipped with:

- a meteorological station measuring air temperature, pressure, solar radiation, wind speed and direction

- A system pumping water samples from 5 depths (1.8 m, 3.8 m, 7.8 m, 11.5 m, 13.8 m) into a chamber where a multiparametric probe measured conductivity, temperature, dissolved oxygen, fluorescence and turbidity; N and P measurements were performed on the same water using an automatic colorimetric nutrient analyser
- 5 *in situ* temperature sensors at the same water sampling depths.

Data acquired by platform instrumentations were automatically transmitted in near real time, via SMS coded e-mail, to the processing centre in Messina.

3.2 The vessel monitoring system

The vessel, formerly in use for CNR–IAMC in Messina, was adapted to the PITAGEM monitoring programme and equipped with:

- a keel-mounted (0.5 m depth) pumping system feeding a chamber with a multiparametric probe for automatic, horizontal, continuous profiles of temperature, salinity, dissolved oxygen, pH, *in vivo* fluorescence, and turbidity along the coastline
- a multiparametric probe, equipped with a rosette water sampler, measuring vertical profiles of temperature, salinity, pH, dissolved oxygen and fluorescence in a grid of fixed stations (Figure 1). Sub-surface and bottom water samples were collected for nutrients, chlorophyll *a* and suspended solids analyses.

4. Results and conclusions

Continuous values of sea water *in situ* temperature were acquired by platform sensors at 5 depths from August 2004 to April 2005. Temperature data at different depths describe the mid-summer, autumn, winter and early spring cycle due to seasonal heating and cooling. Figure 2 shows an example of *in situ* sea water temperature acquired by platform sensors at 5 depths in August 2004 with the water column stratification state in summer. The onset of stratification starts at the beginning of August with the thermocline between approximately 8–11 m depth. During the third week of August the thermocline sinks to between 12–14 m depth; the water column became homogenous and well mixed by the end of August. A sinusoidal trend due to thermal excursion between night and day is shown (Figure 2), especially in sub-surface layers that feel the effect of air temperature cooling and heating.

The results of the monitoring activities operational phase (October 2002–April 2005) showed that platform and vessel monitoring systems need consistent and periodic sensor maintenance and re-calibration to guarantee correct and reliable multiparametric observations.

The PITAGEM project finished at the end of December 2004; future developments should lead to the creation of bigger integrated monitoring networks to be used by Research Institutes and Private/Public Enterprises.

Six cruises (from spring 2002 to autumn 2004) were performed in the Gulf of Manfredonia obtaining continuous, horizontal tracking and vertical profiles of bio-chemical parameters. Figure 3 shows an example of early data indicating thermohaline stratification and bottom waters riches in oxygen and with high fluorescence values during late spring 2002.

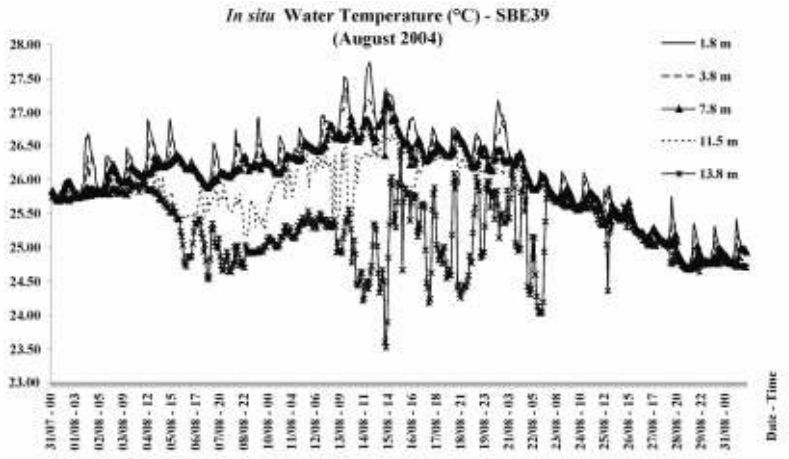

Figure 2 An example of *in situ* sea water temperature acquired by platform sensors at 5 depths (1.8 m, 3.8 m, 7.8 m, 11.5 m, 13.8 m) in August 2004 showing water column stratification and the thermocline presence in summer.

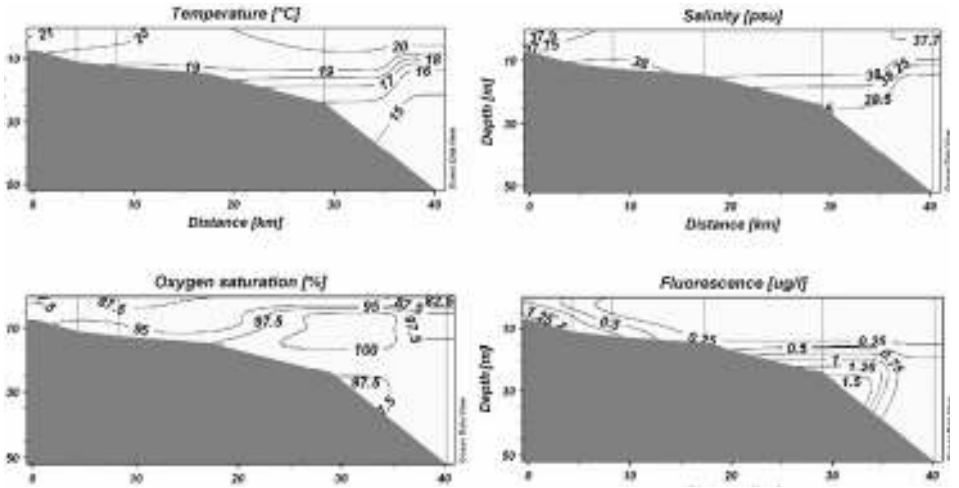

Figure 3 An example of physico-bio-chemical water column stratification in spring 2002.

Acknowledgements

The work was carried out in the framework of the PITAGEM project which is part of CLUSTER 10 funded by MIUR. The authors would like to thank G. Casolino, P. Schiavone for their great help in the monitoring activities, Dr.ssa G. Bartholini directly involved in PITAGEM project and Dr. A. Bergamasco for the data bank.

References

Artegiani, A., D. Bregant, E. Paschini, N. Pinardi, F. Raicich and A. Russo (1997). The Adriatic Sea general circulation. Part I: air–sea interactions and water mass structure, Journal of physical Oceanography, 27: 1492–1514.

Artegiani, A., D. Bregant, E. Paschini, N. Pinardi, F. Raicich and A. Russo (1997). The Adriatic Sea general circulation. Part II: Baroclinic circulation structure, Journal of physical Oceanography, 27: 1515–1532.

Vilicic, D., Z. Vucak, A. Skrivanic and Z. Grzetic (1989). Phytoplankton blooms in oligotrophic open South Adriatic waters, Marine Chemistry, 28: 89–107.

Zappalà, G., G. Caruso, F. Azzaro and E. Crisafi (2003). Integrated Environment Monitoring from Coastal Platforms. Proceedings of the Sixth International Conference on the Mediterranean Coastal Environment, MEDCOAST 03, Ravenna (Italy), 7–11 October 2003: 2007–2018.

Evaluation of wave and current models from EPEL-GNB 2003 observations

F. Girard-Becq*[1], B. Seillé[1], M. Benoit[2], F. Bazou[2] and F. Ardhuin[3]

[1]*ACTIMAR, Brest, France*
[2]*Laboratoire National d'Hydraulique et Environnement (LNHE), Chatou, France*
[3]*Service Hydrographique et Océanographique de la Marine (SHOM), Brest, France*

Abstract

In the framework of the EPEL programme, SHOM (Service Hydrographique et Oceanographique de la Marine) conducted an extensive met−ocean data acquisition campaign in the Normand−Breton Gulf in February and March 2003. This data set in a tidal-dominated environment was designed to enhance existing test-beds for sea-state models, with the objective to help choose the components of an operational system for forecasting met−ocean conditions up to the shoreline.

Two bi-dimensional hydrodynamical models, namely TELEMAC-2D (Galland *et al.*, 1991) and MARS-2D (developed at Ifremer in France) and three spectral wave models, namely WAVEWATCH III (Tolman 1991), TOMAWAC (Benoit *et al.*, 1996), and SWAN (Booij *et al.*, 1999) have been selected for the comparison. The computational area covers the entire Channel (from 5°15'W to the Dover Straits) and includes a finer model fitting in the triangle St-Malo−Chausey−Granville which corresponds to the EPEL−GNB area. The wave models are forced with one of the two hydrodynamical models, in order to consider the effects of currents and water level variations induced on the waves. The wave model parameters are calibrated by running a selection of storm events. At the end of the whole computation, the models are evaluated from the buoy and satellite observations of the EPEL campaign.

Keywords: Spectral waves, sea-state, tide, tidal currents, wave−current interaction, modelling

1. Introduction

An extensive field experiment has been conducted, in February−March 2003, by SHOM to measure waves, currents and water levels. The aim is to analyse (unsteady) tidal effects on wave propagation and to examine the performances of several spectral wave models under these specific conditions. Section 2 describes the data acquisition campaign. Two hydrodynamical models, presented in section 3, are set up to model the tidal flow dynamics and sea surface elevation fields. Spectral wave modelling is presented in section 4.

2. Data acquisition campaign

The EPEL 2003 experiment took place in the western part of La Manche, between Saint-Malo, Chausey and Granville, an area known as the "Golfe Normand−Breton" (GNB).

* Corresponding author, email: girard@actimar.fr

Instruments were moored in 20−50 m water depths (Figure 1). In that area, the highest tidal range is about 13 m, with mean neap tide currents up to 2 $m s^{-1}$.

The instrumentation used included two directional (DW1 and DW4) and two non-directional Datawell waverider buoys (DW2 and DW3), an AWAC ADCP, and three Aquadopp current meters. Additional surface current was available from a 47 MHz VHF radar (Cochin *et al.*, 2005). Data from the UK Met. Office Channel and Greenwich Lightships were also used. Tidal modulation of wave heights is clearly observed in the EPEL area, more particularly at DW4 (see Figure 3).

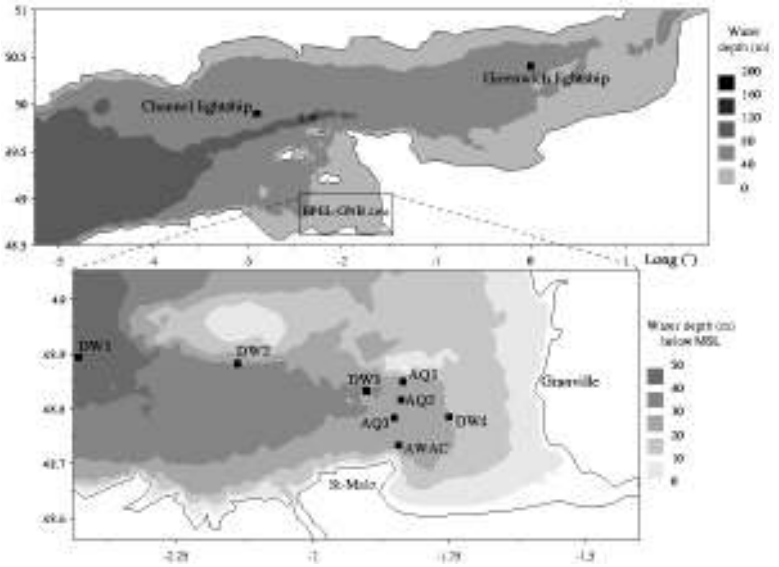

Figure 1 Presentation of the EPEL experiment area and measurement positions.

3. Tidal flow modelling

The two bi-dimensional (2D) hydro-dynamical models MARS2D and TELEMAC2D were compared. The computational area covers the entire Channel, as presented in Figure 1. Three nested finite difference grids are used for MARS-2D to reach a spatial resolution of 300 m in the EPEL area. TELEMAC-2D is based on an unstructured spatial meshing and uses two grids to reach the same resolution in the EPEL area. Both models are forced with the same tidal conditions at the boundaries.

Currents from MARS-2D were first calibrated and validated with historical data, by fitting (K2, M2, N2, S2) ellipses and reducing the phase mismatch. In the EPEL-GNB area, simulated current velocities were compared to VHF radar measurement to tune the Strickler coefficient for bottom friction (Figure 2). A better fitting of measurement is obtained for Ux components, rather than for Uy components which are very weak. Similar work on TELEMAC-2D is now under way.

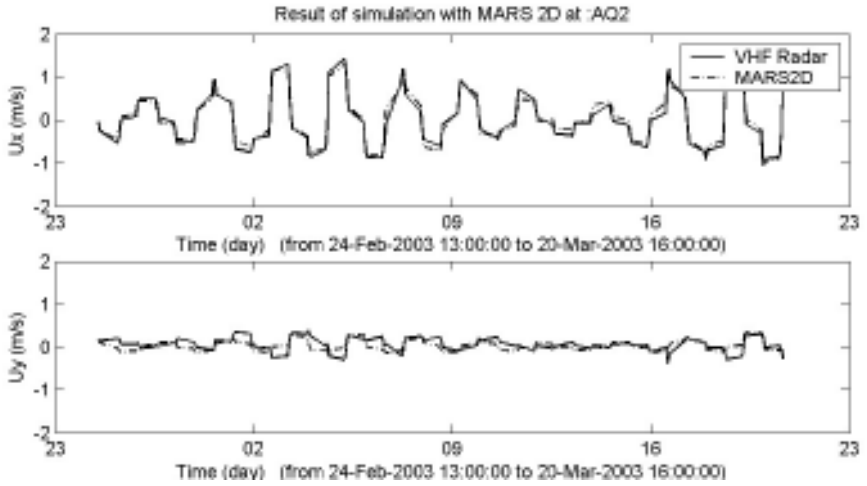

Figure 2 Comparison between simulations with MARS-2D and measurement at AQ2 position.

4. Wave modelling

Three spectral wave models have been implemented and are currently under validation: TOMAWAC (Benoit *et al.*, 1996), SWAN (Booij *et al.*, 1999) and WAVEWATCH III (Tolman, 1991). To reach a spatial resolution of 1 km in the EPEL−GNB area, each wave model uses two nested grids. SWAN and WAVEWATCH use the same finite difference grids. As TOMAWAC is based on an unstructured spatial meshing, islands and the shallowest regions can be more precisely represented and sensible results are obtained right from the coarser grid. All models use the same spectral grid (36 directions and 31 frequencies on a logarithmic scale from 0.04 to 0.7 Hz).

Wave boundary conditions for La Manche are extracted from the wave atlas built with TOMAWAC oceanic modelling forced by NOAA/NCEP reanalysed winds (Benoit and Lafon, 2004). Aladin wind fields, computed by Météo-France on a spatial grid of 0.1° with a time step of 3 hours are used as atmosphere forcing of the wave models. A correction has been applied to the wind fields in order to fit QuikScat measurements during the campaign. The wind fields were also validated from UKMO wind data and SAR measurements.

The influence of currents and sea surface elevation variations on spectral wave modelling is currently analysed by introducing the MARS-2D outputs into the wave models. Preliminary results are presented in Figure 3 at the locations of the directional buoys DW1 and DW4. Figure 3 clearly shows that the models reproduce some tidal modulations of the wave heights (particularly at DW4). However, large discrepancies are observed between the different models and work is ongoing to find the sources of these differences.

5. Preliminary conclusions and future work

A careful validation and calibration of forcing fields (winds, currents, open boundary conditions) was performed to reduce potential sources of errors. To understand the

discrepancies observed in the wave models outputs, additional wave simulations, all using the same physics, are planned in order to identify the separate effects of source term parametrisations and numerical schemes.

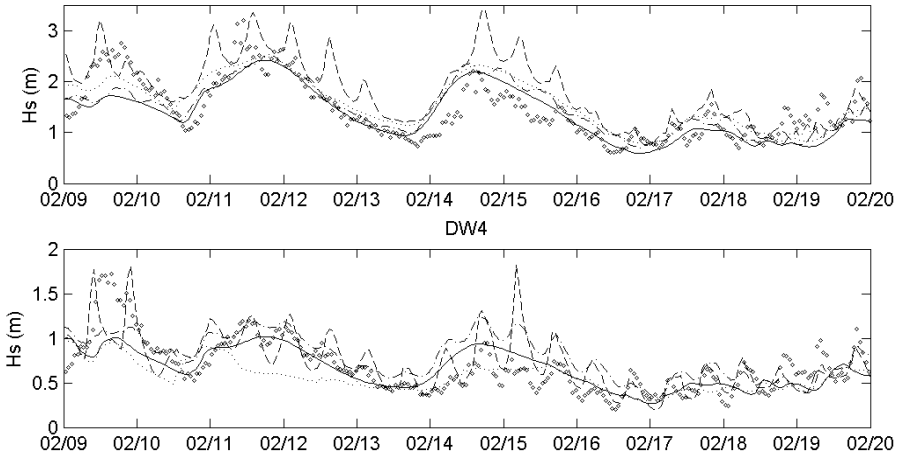

Figure 3 Tidal influence on wave propagation. Diamonds: measurements, continuous/dotted lines: TOMAWAC/SWAN without tidal effect, Dot-dashed/dashed lines: TOMAWAC/SWAN with tidal effects.

Acknowledgements

The dedication of the crew of r/v "Laplace" and personnel from CETMEF and SHOM was a key to the success of the field measurements.

References

Benoit, M., F. Marcos and F. Becq (1996). Development of a third generation shallow-water wave model with unstructured spatial meshing. Proc. 25th Int. Conf. on Coastal Eng., ASCE, Orlando (Florida, USA), 465–478.

Benoit, M. and F. Lafon (2004). A nearshore wave atlas along the coasts of France based on the numerical modelling of wave climate over 25 years. Proc. 29th Int. Conf. on Coastal Eng., Lisbon (Portugal).

Booij N., R.C. Ris and L.H. Holthuijsen (1999). A third generation wave model for coastal regions. Part I: Model description and validation. J. Geophys. Res., 104 (C4), 7649–7666.

Cochin, V., P. Forget, B. Seille and G. Mercier (2005). Sea Surface Currents and Wind Direction by VHF Radar: Results and Validation, Oceans 05 Europe, 21–23 June 2005.

Galland, J.C., N. Goutal and J.-M. Hervouet (1991). TELEMAC: A new numerical model for solving shallow water equations, Adv. Water Resources, 14(3) 138–148.

Tolman, H.L. (1991). A third generation model for wind waves on slowly varying, unsteady and inhomogeneous depths and currents. J. Phys. Oceanogr., 21, 782–797.

Ocean wave forecast modelling at the Met Office

M.W. Holt*, G.H. Fullerton, J.-G. Li, M.E. McCulloch and A. Saulter

Met Office, Exeter, UK

Abstract

The Met Office routinely runs a suite of spectral wave models to provide global and regional forecasts of sea state. For the NW European shelf seas the model additionally accounts for the time-varying effect of currents on the waves. Nearshore wave forecasts are produced for selected sites, in collaboration with HR Wallingford. Forecasts from the wave models are used in a range of applications, including coastal flood forecasting, offshore operations, and by forecasters providing input to GMDSS. Model predictions of long period swell are used for vessel response forecasting for cable laying and offshore heavy lift operations, both in the North Sea and worldwide.

Predictions from the global wave model are compared with along-track observations of wave height and wind speed from the ENVISAT altimeter, and the modelled wave energy spectrum is compared with ENVISAT ASAR observations and with moored buoy data, for selected ranges of wave period.

Global wave model forecasts are routinely validated against moored buoy observations, and the Met Office participates in a monthly exchange of verification data with other modelling centres. Regional wave model forecasts are validated in detail against observations from the UK WAVENET moored buoy network, and have been compared with HF radar observations in a pre-operational trial and with data from the Channel Coast Observatory.

Keywords: Sea state forecasts, wave forecasts, nearshore waves, extreme waves

1. Introduction

The Met Office routinely runs a suite of spectral wave models to provide global and regional forecasts of the sea state. Nearshore wave forecasts are produced for selected sites, in collaboration with HR Wallingford. In this paper we briefly describe the wave models run at the Met Office, summarise our validation of model output against satellite and WAVENET buoy observations, and briefly discuss current applications.

2. The ocean wave forecast model

The Met Office performs operational wave forecasting using a 2nd generation spectral wave model, based on the work of Golding (1983). The operational wave forecast suite runs models at three different spatial resolutions:

- The 60 km Global wave model, covering the entire world ocean surface from north to south ice edges, runs twice daily with a forecast range of 5 days.

* Corresponding author, email: martin.holt@metoffice.gov.uk

- The 35 km resolution European wave model, covering the European continental shelf, the Mediterranean, the Baltic and the Black Sea, also runs twice daily with a forecast range of 2 days.
- The 12 km UK Waters wave model, covering the North-West European continental shelf, including the English Channel, the North Sea and the Irish Sea, is run four times daily with a forecast range of 2 days.

The wave models evolve the ocean wave energy spectrum as a function of frequency, direction, location and time. The present operational models are configured with 16 equally spaced directions and 13 frequency bins, scaled logarithmically between 0.04 Hz and 0.324 Hz, giving a spread of wave periods from approximately 25 to 3 seconds, corresponding to deep-water wavelengths of 975 to 15 metres. For the Global and European models, forcing is supplied by hourly 10 m winds from the Met Office global atmosphere model, and for the UK Waters model winds from the Met Office UK mesoscale atmosphere model are used. All wave models include the effects of bottom friction, refraction and wave shoaling. The UK Waters wave model additionally includes the effects of time-varying currents produced from the operational storm surge model. Long running comparisons with wave models from other operational centres, such as the third generation models of ECMWF and NCEP, have shown the Met Office wave model significant wave heights to be similar in performance when validated against buoy data, Bidlot *et al.* (2002).

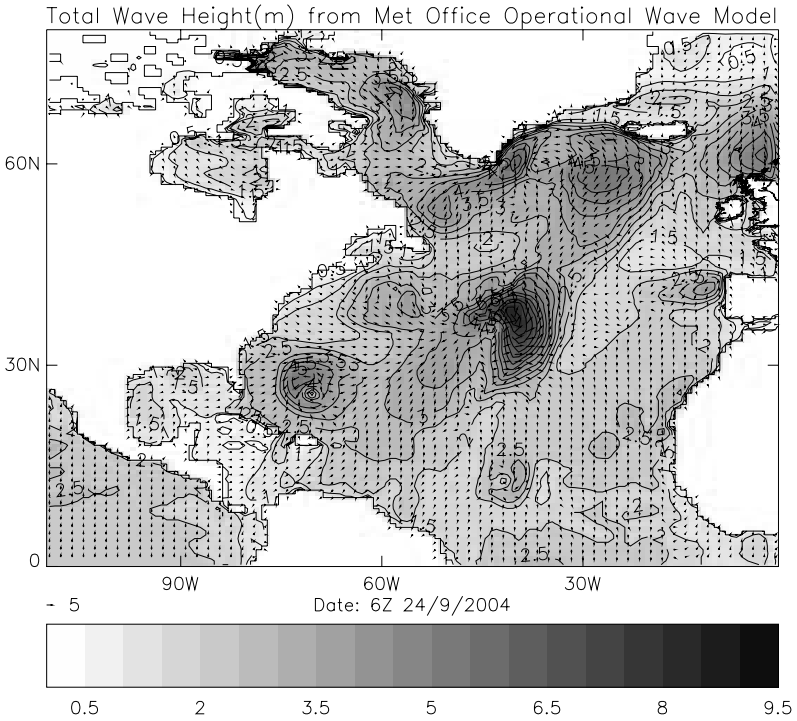

Figure 1 Significant wave height from the Met Office global wave model at 6 a.m. on 24 September 2004, showing waves under hurricanes Jeanne, Karl and Lisa.

3. Validation of the wave model

3.1 Validation: ENVISAT

The global wave model is validated with buoy and satellite observations. Figure 2 shows the significant wave height scatter plot of the wave model against ENVISAT altimeter data for March 2005 which covered nearly the whole global ocean surface. The wave model and altimeter data are well correlated with very close mean (model 2.78 m; observed 2.72 m) and standard deviation (model 1.21 m observed 1.26 m) values. The overall SWH difference rms value is 0.652 m, which is comparable to other wave models as showed by Bidlot *et al.* (2002).

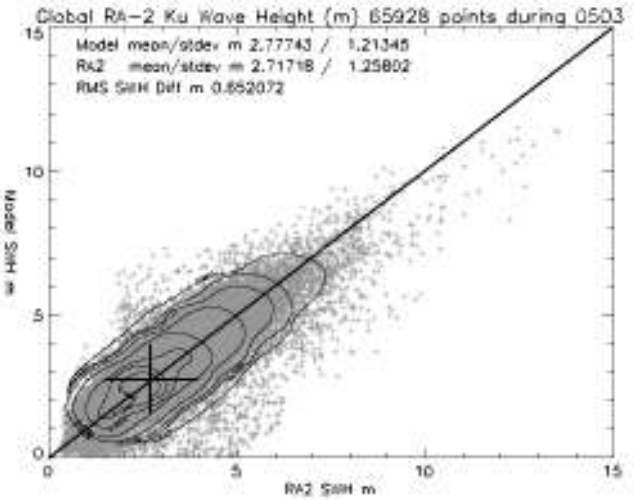

Figure 2 Comparison between wave heights forecast by the global model and ENVISAT altimeter during March 2005.

Directional wave spectra retrieved from ENVISAT ASAR images are valuable observations but they are difficult to evaluate since they are the only 2−D global spectra available. Comparison of ENVISAT ASAR level 2 wave spectra with our wave model indicates that the total energy is in good agreement but swell energy in the ASAR spectra is larger than our modelled swell energy.

3.2 Validation: WAVENET buoys

We have developed a capability to compare hourly wave height data from WAVENET buoys with co-located wave model forecasts, and demonstrated this with 7 storm case studies off the UK coast, chosen because wave heights of around 4 m were observed. For these cases, forecasts of the highest storm-induced wave height made 36 hours before the events had an average error of 0.4 m, and the forecast time of occurrence of the highest waves was in error by some 4 hours. However, for the forecasts made only 12 hours before the events these errors reduced to 0.2 m in wave height, and 2 hours in predicted time of occurrence.

Wave model output has also been compared with observations from the Channel Coast Observatory (Bradbury *et al.*, 2004), and the PISCES dual HF Radar in the Celtic Sea (Wyatt *et al.*, 2003).

4. Applications

Analyses and forecasts of the sea-state are used by shipping, off-shore installations, and coastal defence networks. In addition several private companies take global wave model daily forecast data from the Data Products Delivery System (www.metoffice.gov.uk/research/ncof/wave/dpds.html) for use in their own provision of forecast and ship routeing services.

Working with HR Wallingford (www.hrwallingford.co.uk/home/index.html), the Met Office has developed operational systems for forecasting nearshore waves and associated parameters. The present technique couples Met Office regional wave models to the TELURAY ray-tracing model in order to represent changes to the wave field resulting from refraction. Wave forecasts for the nearshore zone are also applied to models describing surf wave breaking and coastal structure overtopping to provide a forecast tailored to user's needs. Wave refraction and breaking provide two major controls on wave energy in the coastal zone.

References

Bidlot, J.R., D.J. Holmes, P.A. Wittman, R. Lalbeharry and H.S. Chen (2002). Inter-comparisons of the performance of operational ocean wave forecasting systems with buoy data, Weather and Forecasting, 17:287–310, 2002.

Bradbury, A.P., T.E. Mason and M.W. Holt (2004). Comparison of the performance of the Met Office UK — Waters wave model with a network of shallow water moored buoy data. Proceedings of the 8th International Workshop on Wave Hindcasting and Forecasting, Hawaii, 2004.

Golding, B.W. (1983). A wave prediction system for real time sea state forecasting. Q.J. Roy. Met Soc., 109, 393–310.

Li, J.G. and M. Holt (2004). Comparison of the Met Office global spectral wave model with ENVISAT satellite and buoy observations. Proceedings of 2004 ESA Envisat & ERS Symposium, Salzburg, Austria 6–10 Sept. 2004, 9pp.

McCulloch, M.E. and M. Holt (2005). Comparison of Met Office wave model output with WAVENET data. Met Office Operational Oceanography Internal note.

Wyatt L.R., J.J. Green, L.A. Binks, M. Moorhead and M. Holt (2003). Performance of the Pisces HF radar during the DEFRA trial, Building the European Capacity in Operational Oceanography, Proceedings of the 3rd International Conference on EuroGOOS, Ed. Dahlin *et al.*, 161–167.

Assessment of the reanalysed wind field accuracy for wave modelling purposes in the Black Sea region

Izrail Davidan[1], Nikolay Valchev*[2], Zdravko Belberov[2] and Nadezhda Valcheva[2]

[1]*St. Petersburg Branch of State Oceanographic Institute, Russian Federation*
[2]*Institute of Oceanology – Bulgarian Academy of Sciences, Bulgaria*

Abstract

The paper addresses a crucial issue for wave modelling — reliability of input wind fields. It considers outputs obtained for the Black Sea through a couple of regional atmospheric models both forced with the major reanalysis (ECMWF and NCEP/NCAR) data. The simulated wind speed time series for one of severest storms in the Black Sea during the last 50 years are derived and compared with meteorological stations records. Subsequently, scatter plots and error statistics, estimated for a 10-year period, are reviewed. Furthermore, indirect evaluation of the wind data feasibility is performed taking into account the accuracy of the modelled significant wave height. Three of the wave models widely used in operational practise — WAM (cycles 3 and 4), Tolman's WAVEWATCH-3 and Davidan's new spectral-parametric model — are adopted.

Keywords: input wind fields, global atmospheric reanalysis, RAM, wave models

1. Introduction

The importance of the wind waves is marked as they define the sea state and represent the surface dividing the ocean and atmosphere — the two most important subsystems — regulating the climate dynamics. They affect many human activities related to navigation, gas and oil industry, and hydro-technical design. Moreover, the waves are one of the main factors determining human and environmental security in the coastal zone. Therefore, wind waves are of strategic geophysical significance and their observation and forecasting are relatively well-developed.

Availability of realistic input information on spatial and temporal distribution of atmospheric pressure or wind speed significantly affects the accuracy of model results for wind wave parameters. In recent years a number of studies (Cardone *et al.*, 1995; Günther *et al.*, 1998) have arrived at the conclusion that the wind fields derived from global models either in operational mode or by reanalysis tend to underestimate the observed measurements. This is valid in particular for storm events and for regions where wind measurements are irregular or scarce. Due to the specific geographic features of the Black Sea, long-term observations in deep water are rare and regular records are only available for coastal meteorological stations. Therefore, a number of regional atmospheric models are tested to increase the feasibility of input wind fields, which will then be applied for wave modelling.

* Corresponding author, email: valchev@io-bas.bg

2. The models

The outputs of two RAMs are used: REMO, designed in the MPI, and the model worked out in the St. Petersburg branch of SOI. While REMO is a hydrostatic circulation model that calculates three-dimensional atmospheric fields of many meteorological parameters utilising the NCEP/NCAR global wind field reanalysis (Feser *et al.*, 2001), the SPB–SOI model is principally dedicated to estimating this input information for wave modelling purposes (Davidan, 1995) but based on the global pressure reanalysis as the more reliable.

WAM and WW3 are third generation wave models, which solve the wave transport equation explicitly without any assumptions on the shape of the wave spectrum. They are comprehensively described in relevant publications (Komen *et al.*, 1994; Tolman, 1999). SPM is an improved second generation model. It parametrises feasibly weak non-linear wave interactions considering the stages of wave growth and dissipation and accounts for wave-induced stresses in the boundary layer (Davidan, 1996). In this study the latest version of the model, elaborated in 2001, is employed.

3. Numeric experiments

The models are implemented on the Black Sea grid, which is extended from 27.0°E to 42.0°E and from 41.0°N to 47.0°N.

3.1 Wind fields

Wind fields used in the present study are derived by application of the above-mentioned RAMs. The REMO has been driven by the global NCEP wind reanalysis and applied at a spatial resolution of about 50 km. These wind data are believed to be homogeneous enough for wave modelling. Wind fields are also derived by using the SPB–SOI model driven with both NCEP and ECMWF reanalysis of atmospheric pressure with a spatial resolution of 0.5°×0.5°. The output wind fields have been stored every hour. Besides, information on the atmospheric pressure field drawn from synoptic maps is used for the extreme storms.

3.2 Wave models set-up

WAMC4 is forced with the REMO/NCEP wind fields in a spherical grid at 5' spatial resolution. WAMC3, WW3 and SPM are implemented using the SPB–SOI model result with the same wind field spatial resolution. Integrated parameters and total sea and swell spectra output are obtained every 3 hours.

The wave models employed use frequency-directional spectrum with 25 frequencies and 24 directional bands with 15º resolution. Propagation and integration of source term time steps are set up at 300 s and 900 s, respectively. The models are run for deep water.

4. Computed versus measured wind speed analysis

The first comparison between the RAMs' output concerns the extreme storm event that occurred during 16–22 February, 1979. The model results are evaluated against the wind speed measurements from the meteo station Kaliakra. The storm itself was distinguished by a powerful and continued NE inrush of cold air masses.

During the developed storm stage wind speed reached 24 ms^{-1} twice. The three observed peaks are caught by model results obtained using information from synoptic maps and the differences do not exceed 1–3 ms^{-1}. In the Davidan/ERA and Davidan/NCEP series the first peak is not apparent and the computed speed is 5–6 ms^{-1} lower compared to measurements (see Figure 1). The second and third peaks cannot be well discerned, but the quality of simulation is high with slight overestimation (Davidan/ERA) or underestimation (Davidan/NCEP) of observations. The best agreement is achieved precisely for the series mentioned. As for the REMO/NCEP, the degree of underestimation is higher (about 6 ms^{-1}), valid for the entire phase of the developed storm.

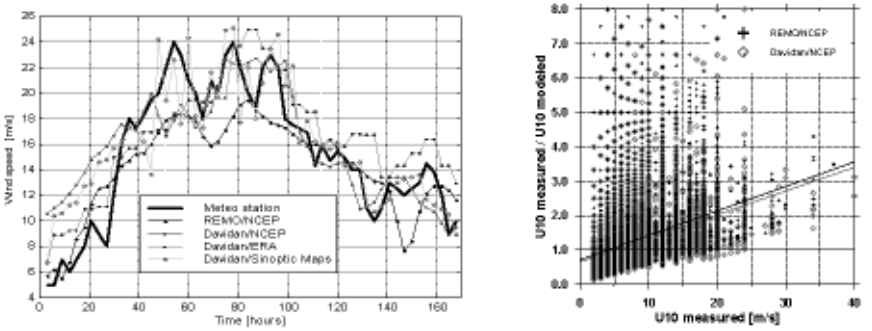

Figure 1 Quality of input wind fields: RAM outputs for the deep water grid point closest to Kaliakra for storm event (left); ratio U10 mes/U10 mod for different wind speeds for 1972–1981 (right).

Estimated error statistics indicate that wind speeds simulated with the SPB–SOI model deviate less, in particular using NCEP reanalysis (bias 0.13 ms^{-1}) and synoptic map (RMSE 2.66 ms^{-1}) data, while via ECMWF reanalysis the errors are higher: bias –0.86 ms^{-1}, RMSE 3.30 ms^{-1}. The same statistics for the REMO series are the highest assessed and read 1.87 ms^{-1} and 3.36 ms^{-1}, respectively.

Another direct evaluation that indicates advantages of using certain reanalysis products is comparison over a longer period. In the present case there are 10 years (1972–1981) of wind speed gauging for the same meteo station. Only results derived from the NCEP input data are considered. Overestimation of measured values is noted at speeds less than 5 ms^{-1}. Further, the opposite tendency takes place: the higher the speed the larger the deviation. Nevertheless, the errors associated with speeds less than 15 ms^{-1} are still acceptable, for example, bias is about 2–3 ms^{-1} and for range 5–10 ms^{-1} the picture is even better. The SPB–SOI model performs more precisely whereas results for REMO winds indicate a larger rate of underestimation. This can be seen in Figure 2, which represents the ratio U10 mes/U10 mod for different wind speeds. There, the regression line relevant for SPB–SOI simulations tends more to the ideal one.

It is important to note that estimated RMSE for REMO winds is 3.83 ms^{-1} and 3.7 ms^{-1} for the SPB–SOI. These values are about 1.5–2 times greater than those simulated with similar models basing on ECMWF reanalysis for the North and the Baltic Sea. The main reason for this is the deficiency of assimilated data for the Black Sea open areas.

5. Assessment of the wave model accuracy

An underestimation of measured H_S in most of the cases could be pointed out with respect to WAMC4 simulations driven with the REMO wind fields. They are compared against the directional buoy data set obtained in the north-eastern part of the Black Sea. As a number of publications prove that WAMC4 performs excellently evaluated with both wave measurements and other wave models outcomes, the main reason for the results in this case is attributed to the limited quality of Black Sea wind fields, calculated with REMO.

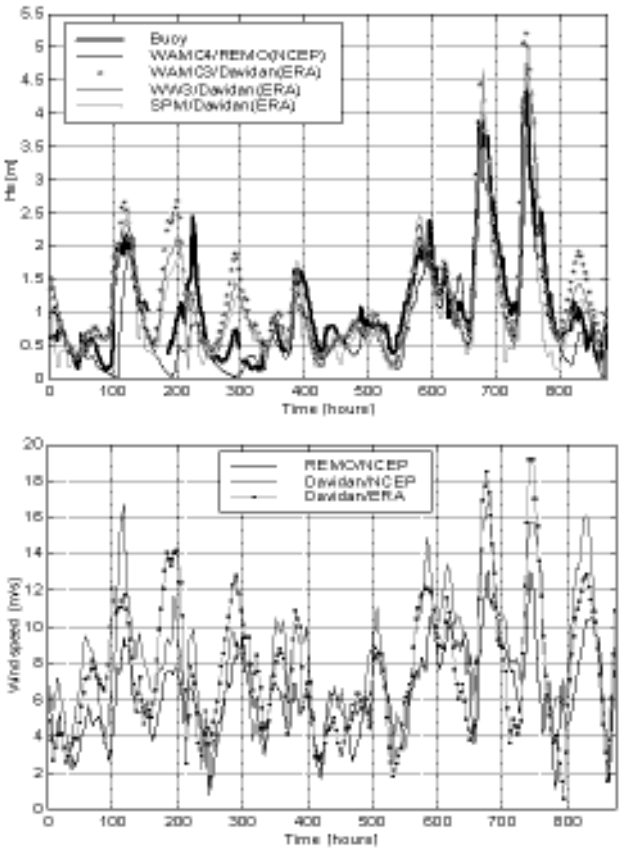

Figure 2 Wave model accuracy: simulated vs. buoy H_S (top) in the light of the input wind fields feasibility (bottom) for the period 1 Jan–6 Feb 1997.

When wave models are run with input wind fields coming from the SPB–SOI model a better reconstruction of the H_S field and an improved series agreement is achieved. A number of examples for high wind speed simulations are demonstrated in Figure 2 (bottom). During the second part of the period all wave models reach proper performance although differences in input wind speed still exist. Therefore, wave models could be regarded as filters that smooth out the wind field discrepancies.

6. Concluding remarks

Identified errors are more due to atmospheric models input than to the wave models themselves. Reanalysis of wind fields underestimates the wind speed significantly, whilst the reanalysis of atmospheric pressure proved to be a more reliable source of input information for wave modelling. In the present study the SPB–SOI RAM performance is better than the REMO one. In this respect, the issue arises of how far the products of certain RAMs could be extended given the lack of data to be assimilated and verified. Considering excellent results, the use of quality synoptic maps is a suitable alternative to attain reliable information for extreme storms. This confirms the convenience of using the reanalysis of atmospheric pressure rather than the wind speed.

With respect to wave modelling, WW3 simulates best H_s especially for values grater than 1.5 m; WAM tends to overestimate some of the peaks but as a whole the quality of simulations is close to those with WW3, particularly in the range 1.5–3.0 m. SPM achieves quite reasonable outcomes and being less computer time consuming makes it a suitable option for operational use in the Black Sea region.

Acknowledgements

This study is a contribution to the EC FP5 ARENA project. Part of it was performed within the EC FP5 HIPOCAS project that provided the REMO wind fields. Thanks are expressed to R. Kos'yan, SBSIO-Gelendzhik for making the wave buoy data set available.

References

Cardone, V.J., H.C. Graben, R.E. Jensen, D.A.T. Cox, T. Resio and V.R. Swail (1995). In search of the true surface wind field in SWADE IOP-1, The Global atmosphere and ocean system, 3(2–3), 107–150.

Davidan, I.N. (Ed.) (1995). Problems in investigation and numerical modelling of wind waves, Gidrometeoizdat, St. Petersburg, 472 (in Russian).

Davidan, I.N. (1996). New results on wind wave growth, Met. and Hydr., 4, 65–72 (in Russian).

Komen, G.J., L. Cavaleri, M. Donelan, K. Hasselmann, S. Hasselmann and P.A.E.M. Janseen (1994). Dynamics and Modelling of Ocean Waves, Cambridge University Press, UK.

Feser, F., R. Weisse and H. von Storch (2001). Multi-decadal atmospheric modeling for Europe yields multipurpose data, EOS Transactions, 82, 305–310.

Tolman, H.L. (1999). User manual and system documentation of WAVEWATCH-III version 1.18, NOAA/NWS/NCEP/OMB Technical Note 166, 110.

Data, Technology and Users

Monitoring of the Norwegian coastal zone environment–the MONCOZE approach

J.A. Johannessen*[1,2], B. Hackett[3], E. Svendsen[4], H. Søiland[4], L.P. Røed[3], N. Winther[1], J. Albretsen[3], D. Danielssen[4], L. Pettersson[1], M. Skogen[4] and L. Bertino[1]

[1]*Nansen Environmental and Remote Sensing Center, Bergen, Norway*
[2]*Geophysical Institute, University of Bergen, Norway*
[3]*The Norwegian Meteorological Institute, Oslo, Norway*
[4]*Institute of Marine Research, Bergen, Norway*

Abstract

The development, implementation and operation of the MONCOZE system has documented improved capacity for routine monitoring and prediction of the physical and biochemical state of the North Sea and Skagerrak. Key activities connected to this have included data access, flow and harmonisation, model validation, nesting, assimilation, sensitivity experiments, and execution of dedicated validation field campaigns. In addition the project has designed and operated a web-based server for routine provision of information and forecasts of the marine coastal zone environment and security.

Keywords: Monitoring of coastal zone environment, ocean modelling, validation, information and forecast system

1. Introduction

The dominant inflowing water masses to the North Sea and Skagerrak are the saline Atlantic Water entering from the north and the fresh water coming from the Baltic Sea. It is essential to have the correct transport magnitudes as well as thermohaline values of these water masses in order to obtain a reliable baroclinic structure and strength of the frontal zone of the Norwegian Coastal Current (Johannessen *et al.*, 1989; Røed and Fossum, 2004; Winther and Evensen, 2005). Moreover, these water masses, their circulation pattern, nutrient loads and mixing along the frontal boundary play a dominant role for the biological activity including algae composition, growth and distribution (Skogen and Mol, 2005). Over the past two decades, the means to observe and model the NCC and its boundary to the offshore waters have gradually improved through:

- developments of *in situ* and remote sensing observational technologies
- rapid access to data
- advances in high performance computing and numerical modelling
- new methods for assimilation of heterogenic, time-dependent data
- access to analysed and forecasted atmospheric forcing fields.

Capitalising on this, the MONCOZE project has therefore implemented, tested and operated a marine coastal zone monitoring and prediction system. In so doing we have

* Corresponding author, email: johnny.johannessen@nersc.no

also been able to identify deficiencies in our ability to fully understand and describe the temporal and spatial variability of this marine environment. In particular, lack of regular near real time observations can limit proper validation of the numerical ocean models. This paper addresses the status of the implementation and testing of the MONCOZE system, and exemplifies the use of the products for information and decision support.

2. MONCOZE objectives and approach

The MONCOZE project (www.nersc.no/MONCOZE) aims at making significant contributions to three specific themes:

- Advancing the understanding and description of the mesoscale variability in the Norwegian Coastal Current and adjacent waters (see Figure 1).
- Developing and demonstrating methods to combine multiple data sources, heterogenic in time and space, for consistent and reliable analysis and estimation of algal blooms.
- Providing monitoring and warnings of extreme and potentially harmful events.

The design and operation of a web based information server (see Hackett *et al.*, this issue) have been essential in this context in order to:

- Bring together specified monitoring and forecast products (e.g. current and transport variability, plankton concentration and distribution, contaminant exposure time, and extreme events) in a consistent presentation framework.
- Facilitate timely acquisition, updating and dissemination of information and data products for users including the scientific community, value-added users, offshore industry and coastal management.

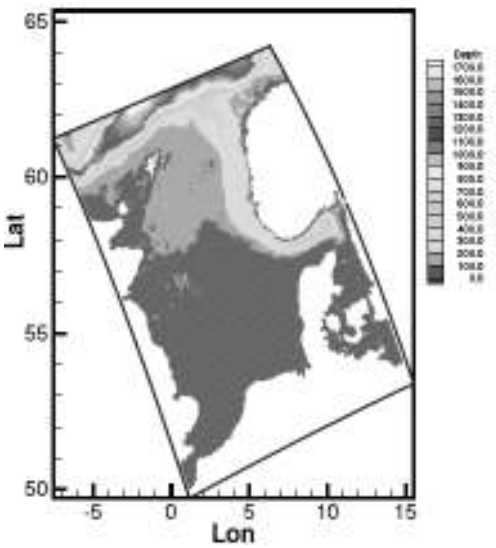

Figure 1 Coverage of the MONCOZE system. The grey scale bar represents bathymetry with an interval of 100 m from the deepest part in the northwest to waters less than 100 m in the south.

3. MONCOZE status

The approach to the monitoring and forecasting system design, testing and operation has evolved by incremental integration and optimal use of satellite observations, *in situ* measurements, atmospheric forcing fields, and regional scale and nested models (Johannessen *et al.*, 2003). The system validation, assessment and analyses of information products have been carried out both in hindcast and forecast mode.

3.1 Observations

Satellite observations provide wide area quantitative information on SST, ocean colour and surface current features. Rapid access to *in situ* measurements is essential in order to obtain complementary sub-surface observations of the currents and water masses. Such data are also highly needed for model validation. Moreover, a HF radar system adds important observations of surface current and its spatial and temporal variability.

The most distinct limitation of the observation network is the lack of fixed moorings, drifters and gliders for temporal and Lagrangian observations of the currents, water masses and biological parameters including phytoplankton. Similarly a routine real time observation network for river run-off fluxes and nutrients to the North Sea and Skagerrak is very fragmented and incomplete (see Figure 1).

Recent advances in the ability to interpret surface current fronts and eddies in SAR images (Johannessen *et al.*, 2005; Chapron *et al.*, 2005) can also now be more routinely used for model comparison and validation. The latter together with NRT access to Ferrybox data is expected to become operational shortly. In the longer term, moreover, a long range HF radar system for the Skagerrak is a very attractive contender, as is operation of gliders. However, the investment needed to purchase, operate and sustain such observation technology (bottom mounted ADCP, CTD profiling string, smart physical-biology buoys, HF radar, gliders) for the entire Norwegian coastal zone is a major challenge. It is therefore only feasible to establish, operate and incrementally expand observatories in selected local tie-point regions.

3.2 Models

Three high resolution (4 km) numerical ocean models are systematically used in MONCOZE. The HYCOM (Hybrid Coordinate Ocean Model) (Bleck, 2002; Winther and Evensen, 2005) and the MIPOM (Blumberg, 1987; Martinsen *et al.*, 1997; Albretsen and Røed, 2005) model the physical state including the time evolution of sea surface elevation, currents, salinity and temperature. In addition, the MIPOM derived physical state is used in MIPOM-BIO for studies of the primary production in the North Sea and the Skagerrak/Kattegat area. The biochemical parameters includes diatoms, flagellates, nitrate, phosphate, silicate, detritus, (N+P, SI), oxygen, and ISPM. For more detailed information of the model set-up for the MONCOZE area see Albretsen *et al.* (2004).

3.3 Validation and assessment

Regular validation of the models (in off-line mode) has played an essential role in the operation of MONCOZE. Although the time of formation and location of eddies are not always in agreement with for instance observations from satellites, it is mandatory that the models have correct forcing fields, reliable water masses, frontal locations and

strength of topographic steering. In turn, the mean and eddy kinetic energy can be realistically described (Røed and Fossum, 2004).

In the MONCOZE hindcast studies from 1998 the importance of the freshwater (see Figure 1) was tested for different combination of freshwater sources (no freshwater, only river runoff, only Baltic Sea, river runoff and Baltic Sea) and its impact on the dynamics in the Skagerrak/northern North Sea (Albretsen and Røed, 2005). The results reveal that to obtain a realistic mesoscale activity in the NCC area, the single most important process to parametrise correctly is the inflow from the Baltic Sea. In addition, there is a potential for further improvements from using near real time direct river runoff and nutrient measurements rather than climatology. This also includes the account of coast–fjord exchanges up along the west coast.

To obtain the reliable water mass distribution and stratification the salinity source of the Atlantic Water (AW) must be properly quantified and transported into the model domain. The inflow is predominantly topographically steered along the west slope of the Norwegian trench into the Skagerrak (see Figure 1). A branch of AW also enters the North Sea between Shetland and Scotland. On average the magnitudes of these transports are 1.73 Sv and 0.48 Sv respectively (Winther, in preparation). In this context, Skogen and Mol (2005) recently documented important impacts and effects on the biochemical conditions in the North Sea and Skagerrak due to the physical state and forcing.

Two experiments, using climatology and TOPAZ boundary conditions, were conducted to examine the sensitivity to the inflowing Atlantic water. TOPAZ provides sea surface elevation, horizontal currents and hydrography (temperature and salinity) at selected depths at the lateral boundaries. In comparison to section observations it appears that when the boundary conditions from TOPAZ are used the results are slightly better, although the maximum salinity is higher than the observed (35.4 versus 35.2 psu). Moreover, the seasonal variability of the inflowing Atlantic Water looks better with TOPAZ. All in all, the downscaling from the large scale Atlantic-to-Arctic coverage within TOPAZ to the finer scale North Sea and Skagerrak coverage within MONCOZE ensures reliable open boundary conditions (see Figure 1). Anomalies in the oceanic state in the North-East Atlantic can thus be properly propagated eastward into the MONCOZE domain (Bertino *et al.*, 2004).

4. Information and marine decision support systems

The MONCOZE models provide 3–D estimates of velocity, salinity, temperature, diatoms, flagellates, and nitrate (see temperature field in Figure 2). With the routine delivery of such marine environmental quantities and value added information the system provides an operational tool for prediction and assessment of the environmental state of the Norwegian Coastal Zone, including:

- current strength, frontal locations and mesoscale variability
- temperature and salinity distribution
- location and spreading of (harmful) algae
- long time series (Hovmuller observations and models).

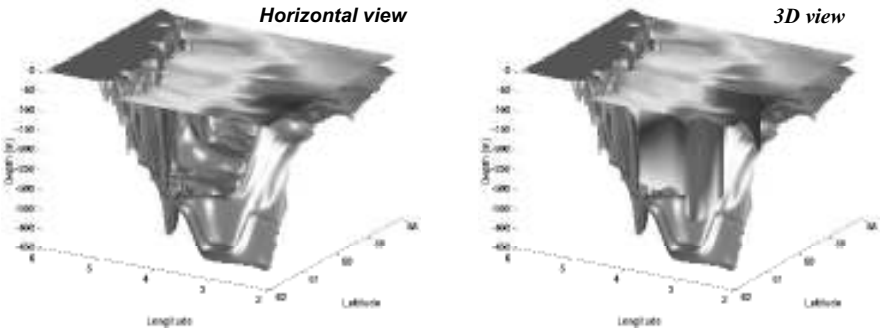

Figure 2 Selected view of the temperature field (light grey indicate cold water) provided by the MONCOZE system as seen from northwest (depicting the Norwegian Trench along the west coast of Norway). Left: horizontal temperature structure at 50 m. Right: vertical temperature structure across the Norwegian Trench displayed together with the horizontal temperature.

Figure 3 reveals how the MONCOZE system bridges four major modules; notably the satellite and *in situ* observation modules, the forcing field module, and the ocean model module. These modules provide input to an information, products, analyses and assessment module, called the MONCOZE POMS server (see also Hackett *et al.*, this issue). This server, in turn, acts as a marine information and decision support system as well as a tool for research, education and training. An example of its usefulness can be documented with regards to its functionality as a decision support system for advanced users. During a field campaign in May 2005 the planning and execution of the ship based sampling was efficiently based on analyses and comparison of the information and products at the MONCOZE server jointly with the current and hydrological fields taken from the ship. POMS is reached at http://moncoze.met.no where it is possible to log on to access the available information products.

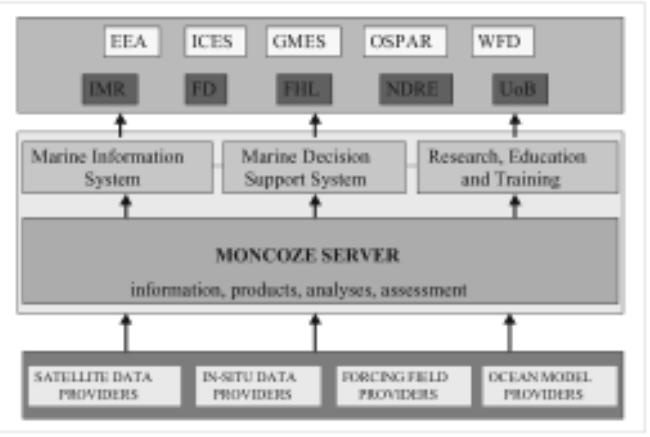

Figure 3 The structure of the MONCOZE server with its input and output functions.

The end users that have up to now been exploring the content on the server are arranged according to:

- marine environmental and resource management (predominantly IMR and FD)
- harmful algae bloom monitoring (FD and FHL)
- research (IMR, met.no and NERSC)
- education and training (UoB).

In addition NDRE has signalled interest in the system and its provision of information from the server. Moreover, the system is also highly relevant as a tool and information source for international agencies (EEA, GMES), commissions (ICES) and declarations (WFD). A few examples of such dedicated exploration according to the end users specified here include:

- analyses of seasonal and annual variability in the inflow of Atlantic Water to the North Sea and Skagerrak in the context of fish stock assessment such as horse mackerel (Iversen *et al.*, etc.)
- rapid alert and collection of *in situ* observations for determination of species and eventual toxic levels in case of abnormal algal blooms
- examination of the mesoscale variability in the NCC including shedding of eddies and their effect on biochemical conditions
- efficient and user friendly tools for interactive demonstration and visualisation of routine information products in a new study course on operational oceanography.

5. Summary

The MONCOZE project running from 2001 until the end of 2005 is currently operating a monitoring and forecasting system for the coastal zone environment confined to the North Sea and Skagerrak. The routine provision of information products is highly relevant and needed for sustainable ocean and near shore environmental monitoring, but also as a tool for advancing the understanding of the dynamics in the NCC and its frontal boundaries. It is therefore a high priority to maintain and advance the MONCOZE system. At a national level a stepwise implementation and operation of such a regional dedicated monitoring and forecasting system along the entire Norwegian coast and adjacent seas would seem very beneficial considering the significant economic importance of these regions. In addition, it would be highly timely in view of the planned implementation and operation of the joint ESA and EU initiative on Global Monitoring for Environment and Security (GMES) by 2008.

Acknowledgments

The MONCOZE project is supported over 5 years (2001–2005) by the Research Council of Norway under contract 143559/431. We would also like to express our gratitude to r/v Håkon Mosby's captain and his crew for their excellent support during the MONCOZE Cruise in May 2005.

References

Albretsen, J. and L.P. Røed (2005). Sensitivity of Skagerrak dynamics to freshwater discharges: insight from a numerical model. This volume page 771.

Albretsen, J., N. Winther, H. Søiland, L.P. Røed (2004). Models in MONCOZE, Met.no Report no. 14/2004 Oceanography, ISSN: 1503−8025 Oslo.

Bleck, R. (2002). An oceanic general circulation model framed in hybrid isopycnic−Cartesian coordinates. Ocean Modelling, 4, 55−88.

Blumberg, A. and G. Mellor (1987). A description of the three-dimensional coastal ocean circulation model. In Three-dimensional Coastal Ocean Models, edited by N. Heaps, vol. 4 of Coastal and Estuarine Sciences, American Geophysical Union.

Bertino, L., N. Winther and J.A. Johannessen (2004). Real time marine monitoring systems: Forecasting the oceans and regional seas. Hydro International, Vol. 8, No. 5.

Chapron, B., F. Collard and F. Ardhuin (2005). Direct measurements of ocean surface velocity from space: Interpretation and validation, Journal of Geophysical Research, Vol. 110, doi:10.1029/2004JC002809, pp.

Hackett, B., J. Albretsen, L.P. Røed, J.A. Johannessen and E. Svendsen (2005). The MONCOZE Pilot Ocean Monitoring System (POMS); A Tool for Marine Environmental Monitoring. This volume page 242.

Iversen, S.A., M.D. Skogen and E. Svendsen (2002). Availability of horse mackerel (*Trachurus trachurus*) in the north-eastern North Sea, predicted by the transport of Atlantic water. Fish. Oceanogr. 11:4, 245−250.

Johannessen, J.A., V. Kudryavtsev, D. Akimov, T. Eldevik, N. Winther, O.M. Johannessen and B. Chapron (2005). On Radar Imaging of Current Features; 2: Mesoscale Eddy and Current Front detection. Journal of Geophysical Research, Vol. 110, C7, doi:10.1029/2004JC002802, pp.

Johannessen, J.A., B. Hackett, E. Svendsen, H. Søiland, G. Evensen, L.P. Røed, N. Winther, J. Albretsen, M. Skogen, L. Pettersson, D. Durand and D. Obaton (2003). Monitoring the Norwegian Coastal Zone Environment (MONCOZE), Building the European Capacity in Operational Oceanography, Proceedings of the Third International Conference on EuroGOOS, 3−6 December 2002, Athens, Greece, Eds. H. Dahlin, N.C. Flemming, K. Nittis, S.E. Petersson, Elsevier Oceanography Series, 69.

Johannessen, J.A., E. Svendsen, S. Sandven, O.M. Johannessen and K. Lygre (1989). Three Dimensional Structure of Mesoscale Eddies in the Norwegian Coastal Current, Journal of Phys. Oceanography, Vol.19, No. 1, 3−19.

Martinsen, E., B. Hackett, L.P. Røed and A. Melsom (1997). Operational marine models at the Norwegian Meteorological Institute, Operational Oceanography, The challenge for European Co-operation, edited by J.H. Stel *et al.*, Elsevier.

Røed, L.P., I. Fossum (2004). Mean and eddy motion in the Skagerrak/northern North Sea: insight from a numerical model, Ocean Dynamics.

Skogen, M. and A. Moll (2005). Importance of ocean circulation in ecological modelling: An example from the North Sea, Journal of Marine Systems.

Winter, N. and G. Evensen (2005). A Hybrid Coordinate Ocean Model for shelf sea simulation, Submitted to Ocean Modelling.

Real time availability of data for operational oceanography

S. Pouliquen*

Ifremer Brest, France

Abstract

This paper presents the main characteristics of operational observing systems and the data management issues to be addressed for operational oceanography needs. It highlights the main elements that have to be put in place for operational system data availability and management.

Keywords: Data exchange, operational oceanography, data management, quality control

1. Introduction

In order to build an ocean forecast we need a model, that would be perfect if we knew exactly how the ocean behaves in space and time and could put all this knowledge into equations. But as this is not the case and since even perfect models have a limited range of predictability, we need to assimilate observations in order to call the model back to reality. While satellites provide a global view of the surface of the ocean, *in situ* systems monitor the interior. Basically, the following are needed:

- Global scale observations of the surface provided by satellites (sea surface height, sea surface temperature, ocean colour and soon sea surface salinity)
- Autonomous instruments (moorings, drifters, profiling floats, gliders, etc.) to monitor over long period of times and regular ship measurements to monitor long repeat sections
- A well-designed and robust observing system, with good communication to earth or shore to deliver data rapidly, in order to have all these data available for operational models
- Real time operational data centres
- Suitable data protocols to distribute data to operational centres in a timely way
- International cooperation to achieve global coverage, set up an adequate system and maintain it in the long term.

2. Characteristics of an observing system for operational oceanography

An observing system is useful for operational oceanography activities if it is able to provide data in a timely and sustained manner with the appropriate sampling according

* Corresponding author, email: Sylvie.Pouliquen@ifremer.fr

the applications targeted. The number of parameters used by operational oceanography applications is limited but the access to data has to be straightforward.

2.1 Timeliness

What does real time mean for operational oceanography? The main criterion is to define the delay between measurements and assimilation beyond which the measurement adds nothing to the performance of the model. There is no unique answer: this depends on the type of models, the variables that are assimilated, the forecast product and the application for which it is produced. For instance, assimilated information of deep ocean temperature and salinity will persist within an ocean global circulation model for weeks or months and so a delay of several days in supplying data can be acceptable. On the other hand, ocean mixed layers vary on more rapid timescales in response to the diurnal heating and to storms. The impact of such data will probably not persist more than 3–5 days after assimilation, so measurements are needed within a day. As a compromise, real time for operational oceanography generally means availability within 1 or 2 days from acquisition, to allow data centres to better quality-control the data.

2.2 Sustainability

The observations have to be sustained because when an emergency event happens (tanker pollution, storm event,…) only very few additional measurements can be carried out. An operational system is sustained in different ways. This regards funding of course, as they are often expensive: new funding mechanisms have to be set up coming from sources other than R&D. Not all countries are organised in such a way that a transition to operational is easy — for example it is the case between NSF or NASA and NOAA in the USA, between ESA and Eumetsat for earth observations in Europe. Systems must be sustained also in terms of the operation: this goes from deployment planning, to at-sea servicing, to data processing in the operational data centres who are committed to do such tasks.

2.3 Coverage

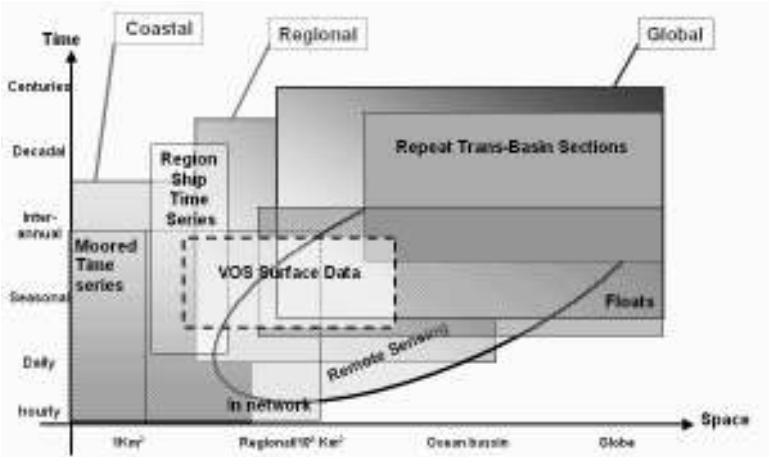

Figure 1 Platforms to use according to applications (Coastal, Regional, Global).

The observing systems to be put in place are different depending on the area and the phenomena to be sampled. We usually sort observing systems into 3 categories:

- **Global**: System designed to provide data all over the ocean (e.g altimetry, Argo for general circulation). Such a system can only be built at the international level. It is built to resolve climate scale phenomena with sufficient resolution and accuracy and provides systematic upper ocean observations of a limited number of parameters (Temperature, salinity, SSH, SST, currents) on a time scale from 1 day to 1 month.
- **Regional**: System designed to provide data in a specific area to monitor specific phenomena (e.g. TAO/TRITON/PIRATA array for El Niño detection, Arctic buoy network for ice monitoring, etc.). For satellite products it is often required to combine data from different satellites to achieve the appropriate resolution both in time and space. Collaboration with several countries (usually less than 10) is needed and the number of parameters is larger (between 10 and 20), including ocean (both physical and biochemical) and meteorological measurements. The temporal sampling is often higher rate: from hours to days.
- **Coastal**: These observing systems are usually set up at a national level to answer very specific questions such as coastal monitoring of the water quality or wind/wave/tide monitoring in harbour areas, satellite radar image acquisition, etc. There is little collaboration among countries and these data are often used exclusively by the coastal models that have led to the setting up of the system.

3. Drawbacks of data management at present

In 1998 EuroGOOS issued "The Science Base of EuroGOOS" publication where some limitations related to data exchanges were highlighted. The situation has improved but some statements are still relevant and should be seen as targeted actions within Europe.

1. Lack of international infrastructure for operational oceanographic data gathering, transmission, and products (e.g. as adopted in World Weather Watch), and consequently lack of common standards. If this is still true in general, some experiences within GODAE like the Argo programme have shown that it is possible to reach consensus on common standards (formats, real-time and delayed mode quality control, data distribution…)
2. Lack of clear right or duty to collect and transmit real-time data. Once again in the past five years we have seen the concept of "portals" emerging with the duty to serve users in real-time: Salto/DUACS for altimetry, Medspiration/GHRSST for SST, Argo and Gosud Global Data centres, JCOMMOPS are examples that exist nowadays.
3. Lack of proper design of a services infrastructure, using, for example, multiple data inputs such as wind, waves and currents, to generate predictions of oil spill movements. With the GMES initiative in Europe we have seen a demonstration of the capability to build end-to-end services for users. Some projects like Mersea, Marcoast or PolarView are consolidating the systems that will need to be sustained in the future.
4. Imbalance between monitoring (measurement) technology and capacity for post-processing data and subsequent real time use of numerical models. Once again money and man power have been input for improved data access both at national and

European level to ease access to homogeneous datasets. This is illustrated by the Coriolis project at the French level, or SeaDataNet IP that is funded by the European Union within GMES. This effort should be sustained in the future.

4. Key issues for data management activities to be solved in the near future

Data processing and distribution must be designed properly to be able to deliver the data in time for operational use. First, data have to be publicly available in real-time for forecasting activities, and within a few months for re-analysis purposes. This is an important data policy element to be solved by the funding agencies at national and international levels. Second is the organisation of the data flow among the different contributors in order to have an efficient data management network able to answer the operational needs. For a long time, data management aspects have been neglected in projects and too little funding was devoted to this activity both for *in situ* and satellite data processing. It is now clear that operational observing systems have to be processed by professional data centres that are sustained in the long term, and that distribution has to be tailored to fulfil operational user needs.

At present, there is no consensus on data management and a communication strategy for effectively integrating the wide variety of complex marine environmental measurements and observations across disciplines, institutions, and temporal and spatial scales. Data are obtained by diverse means both *in situ* (ships, drifters, floats, moorings, seafloor observatories, etc.) and satellites, and they come in very different forms, from a single variable measured at a single point to multivariate, four dimensional collections of data, that can represent from a few bytes a day to gigabytes.

Even if an observing system were to make excellent measurements in a sustained way, if the data are not easily available to the operational users, they will not be used because they will not meet the operational modeller's basic requirements: a data system for operational oceanography must provide quality controlled data, in a timely way, on a regular basis, according to procedures that are clearly documented and evolve upon common agreed decisions between user and provider.

There are three main characteristics of a data management system that will be focused on here:

1. Data access
2. Quality control procedures
3. Data format and metadata attached to the data.

4.1 Data access

Access to data often looks like a plate of spaghetti where you never know how long the path will be to reach the data you need. This is clearly not the way to distribute data to operational applications. What these users need are portals that build the connections to all the relevant datasets and provide access to these data as if it were all in a single place.

Data are acquired at coastal, regional, pan-continental, and global levels and together form the observing system needed by operational systems. The more we go from coastal to global, the less parameters we usually need. In Europe, EuroGOOS has started,

through task teams, to coordinate data exchange between coastal and regional activities. At the European level it could be possible to organise data exchange between task teams and contribute to data exchange at the global level. Such coordination would complement initiatives like ESEAS for sea level, SeaDataNet for data infrastructure, DMAC in USA, Argo or GHRSST for GODAE, etc.

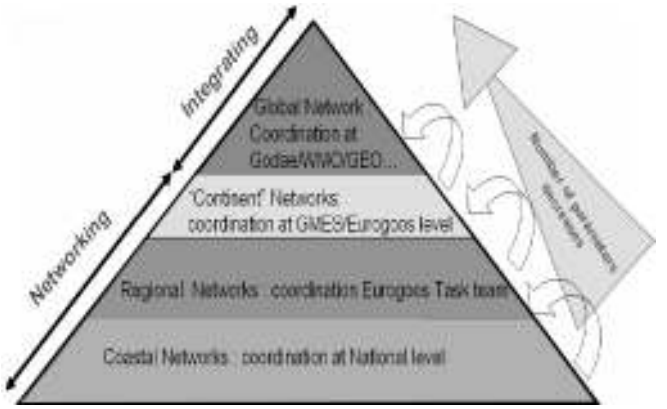

Figure 2 Global integration of observing systems.

4.2 Quality control

These procedures have to be adapted to the permitted delivery delay. In real-time most of this QC is done automatically and only outliers are rejected for *in situ*, or sensor drift is estimated against *in situ* for satellite data. In delayed mode, more scientific expertise is applied to the data and error estimations can be provided with the data.

Data quality control is a fundamental component of any ocean data assimilation system since acceptance of erroneous data can cause incorrect forecasts, but rejecting extreme data can also lead to erroneous forecasts by missing important events or anomalous but genuine features. The challenge of quality control is to check the input data against a pre-established "ground truth". But who really knows this truth when we know that the ocean varies in time and space, and also that no instrument gives an exact value of any parameter but only an estimation of the "truth" within some error bars?

As most of the data are processed by different actors, but used all together by operational models, clear documentation of the quality control procedures, a homogenisation of the quality flags, and a reliability of different actors in applying these rules are required.

4.3 Standardisation

Data must be preserved in such a manner that they will still be useful in the future when the PI that acquired the data may have moved somewhere else. They must also be distributed in a way that a user can easily merge it with other datasets relevant for his application. They must help to find the data among the network (data catalogues). That is the purpose of correctly defining data distribution formats as well as the metadata (data on the data) that need to be preserved for future processing.

Data formats have always been a nightmare both for users and data managers who both dream of the "Esperanto" of data formats. Computer technology has improved a lot in

the past decade and we are slowly moving from ASCII formats (easy to use by human eyes but not for software), to binary format (easy for software but not shareable among platforms (Windows, Unix, etc.), to self-descriptive, multiplatform formats (Netcdf, Hdf, etc.) that allow more flexibility in sharing data among a network and are read by all software that are commonly used by scientists.

One important point for metadata is to identify a common vocabulary to record most of this information. This should be easy to achieve for a specific community such as physical operational oceanography as the number of parameters is small, but it starts to be a bit more difficult when we want to address multidisciplinary datasets. To help in this area some metadata standards are emerging for the marine community with MarineXML in Europe, CF/COARDS convention in USA, and the ISO19115 norm.

5. Perspectives

Over the past decade, data exchange between partners involved in operational oceanography has improved. We now need to take necessary steps to ensure that the shared observations and products are:

- Accessible: this goal will be achieved by free access to essential data and implies incentives from funding agencies and a change in scientist behaviour
- Comparable: this implies agreement on quality control procedures both in real-time and delayed mode to provide datasets independent of the platform that sampled it
- Understandable: this will be solved by common standards for data description and distribution. Computer techniques will help to solve the syntactic part of the problem but better coordination between Europe, USA, etc. is needed to solve the semantic part of the problem.

We also have to move from primary observation to information production. This leads to major integration of data by merging different data sources coming from various instruments both *in situ* and satellite.

Finally we should not re-invent the wheel and take benefit of the expertise by other communities (meteorology, deep ocean operational oceanography…) to improve data exchange at the regional level and improve answers to monitoring and crisis management activities. At the end of the day, we will contribute to the Global Earth Observing System of Systems (GEOSS).

References

Prandle, D. and N.C. Flemming (1998). The Science Base of EuroGOOS, EuroGOOS Publication No. 6, EuroGOOS Office.

Pouliquen, S. (in press). *In Situ* observation: Operational systems and data management, 2004 Godae summer school lecture notes “An Integrated View of Oceanography: Ocean Weather Forecasting in the 21st Century”.

In situ monitoring of the ocean: present and future technology for operational oceanography

Philippe Marchand* and Gérard Loaec

Ifremer, Centre de Brest, France

Abstract

The paper reviews both present and future technologies available for the *in situ* component of operational oceanography, in the fields of global ocean, coastal, fisheries and geohazards monitoring. The global observing system for climate, made of composite existing networks, is under completion, and the related technology is mature. The present need is to increase the global coverage with proven technologies. Nevertheless, technological improvements are possible to improve the quality of data and decrease their cost, especially for Argo floats and gliders. The coastal observation module of GOOS is still in infancy with many objectives, many stakeholders, a diversity of regions of interest, and many variables to monitor including bio-geochemical ones. If the Ferrybox technology is mature, significant technical progress in platforms and sensors is expected such as coastal profilers, gliders and autonomous sensors able to provide good data for months in the biological rich coastal waters. The fishery monitoring is classically made by research vessels during repeated surveys, such as IBTS of ICES. New acoustical equipment for RVs are under development to improve both the productivity and the precision of biomass stock assessments; other innovative ways to monitor the fish biomass are considered. The technology available for geohazards monitoring looks mature for tsunami or earthquake dynamics but large technical improvements could be made to scientific packages, nodes and transmission systems.

Keywords: *In situ* monitoring, technology, global, coastal, fisheries, geohazards.

1. Introduction

An operational integrated system has to be capable of delivering products and services to end users in a routine and sustainable way. It is made of three components: the monitoring component which collects observations from *in situ* or satellite systems, the modelling component which transforms data into usable products, and a data management system.

This paper reviews both present and future technologies available for the *in situ* component of operational oceanography, in the fields of global ocean, coastal, fisheries and geohazards monitoring.

2. Global ocean monitoring

The global ocean monitoring network is made of several observing systems focused on the observation of essential climatic variables: surface temperature (T) and salinity (S), sea level, currents, T−S profiles, CO2. (GCOS−92, 2004).

* Corresponding author, email: Philippe.Marchand@ifremer.fr

According to JCOMM, 53% of the goals of the 2000–2010 implementation plan (of the ocean observing system for climate) were achieved in February 2005. The measurement technologies used in those networks are mature:

- Tide gauges transmitting observations in real time (part of GLOSS)
- Surface drifting buoys of DBCP, with several manufacturers including the latest one from Ukraine
- Ship observations with XBT and thermosalinometers; XBT multiple automatic launchers are being tested (MFSTEP)
- Tropical moored buoys of TAO, PIRATA networks: except vandalism problems, the main evolution would be to decrease the maintenance cost using dedicated vessels (such as a fast tailor-sized vessel NOR-50), (Marchand and Servain, 2003)
- Moorings of ocean sites which have to be made more reliable
- Argo profiler network with almost 1900 operational floats deployed in May 2005 (60% of the 3000 floats objective). Despite continuous improvements in float reliability/lifetime during the last years, technical progress is still possible.

2.1 From drifting floats to profiling floats

The natural equilibrium at depth of free-drifting floats can be obtained by matching the density of the floats and that of seawater. The drifting depth can be set by adjusting the mass of the float according to its buoyancy. This technique was used first around 1955 by J. Swallow and floats fitted with low frequency acoustic devices have been used for more than forty years to track movements of water masses at depth.

The first floats were acoustic drifting sources (Sofar), tracked by a network of hydrophones and later moored autonomous listening systems (1975). The availability of the Argos satellite system allowed the technique to be reversed around 1985 to develop cheaper instruments fitted with an acoustic receiver, moving in an array of emitting sources, and surfacing at the end of their life (Rafos floats, Rossby *et al.*, 1986) or every two months (Marvor multicycle floats, Ollitrault *et al.*, 1994). Woce (World Ocean Circulation Experiment) was a major experiment to improve and promote this technology.

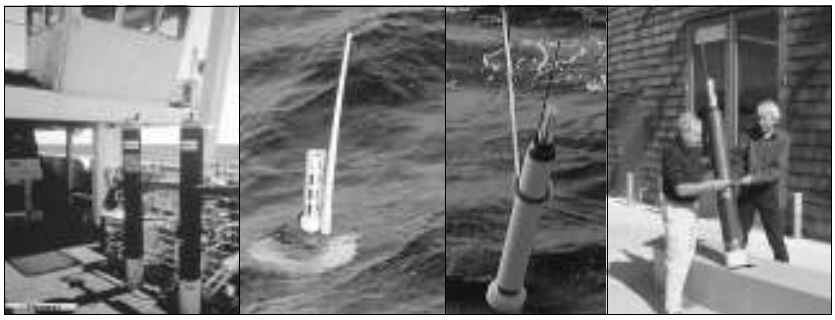

Figure 1 Floats: Marvor, Provor, Apex and Solo floats.

More recently, within the framework of Argo (Gould *et al.*, 2004), subsurface floats have been modified to carry CTD sensors (salinity, temperature) and profile between 2000

metres and the surface every 10 days (Apex, Provor, Solo/Nemo, Ninja...). 3000 operating floats should be operating in the near future which would make Argo the largest *in situ* observing array of the global ocean. The main topics are reliability, cost and facility of deployment.

The same platforms are now used to add a wide range of sensors to measure other physical, biological and chemical parameters, eventually based on Argo floats as floats of opportunity. The ALPS workshop recommended the design of a multidisciplinary float with a greater sensor payload (Rudnick and Perry, 2003).

2.2 Undersea gliders

Gliders are built on the same concept of profiling floats and can profile through the water column by modifying buoyancy. The addition of wings enables conversion of the vertical velocity into horizontal motions and steering is enabled by external rudders or by modifying the location of the masses inside the vehicle. The gliders are fitted with GPS receivers and a 2-way communication link (Iridium) is used to control trajectories and modify way-points.

The typical operating mode shows a sawtooth pattern, which gives the gliders the capacity to observe phenomena such as internal waves, fronts and coastal variability, along routes that are set before deployment or can be modified in real time by remote control. The virtual mooring mode allows expensive moorings to be avoided, as the glider is configured to remain at a given location. Some operationally significant successes were obtained with existing gliders such as Slocum, Spray and SeaGlider (Davis *et al.*, 2003). However the technology is still under development (vehicles, dedicated sensors) and should provide gliders (or fleets of gliders) that can be operated at sea for more than one year without maintenance.

Figure 2 Gliders: Slocum (Webb Research Corp), Spray (Scripps + Bluefin), Seaglider (Univ. of Washington).

2.3 Other new technologies

- **Marine mammal profilers**: Sea elephants are interesting biological profilers for the under-sampled Antarctic ocean. A French team of biologists from CNRS (Guinet) has obtained 3854 T&S profiles during the 2005 February–August period with a fleet of 10 animals diving down to 1500 m.
- **Emma**: A new expandable 6000 m temperature profiler was successfully developed and tested by Ifremer in 2003 with a 5250 m T profile. It is made of a titanium tube fitted with a CTD and an Argo data transmission system. The instrument stays (2 years max.) on the bottom and pops up after separation from a drop weight (a burning wire is activated by a clock signal). It is a small system (2.3 kg, 60 cm long) able to

give high accuracy temperature profiles (±0.004°C between 0 and 6°C; ±0.050°C beyond, Resolution: 0.001°C). The Emma concept is quite innovative and the only autonomous 6000 m profiler, but still too expensive (about 2000€). If a deep-sea T,S global network was required in the future, it would be possible to substantially decrease the cost of such expandable instruments.

3. Coastal monitoring

The coastal observation module of GOOS is still in infancy when compared to the global climatic monitoring system (GOOS, 2003). It has many objectives, many stakeholders, a diversity of regions of interest, and many variables to monitor including bio-geochemical ones:

- Physical: T, S, SL, Currents, Waves, bathymetry
- Chemical: Dissolved O_2, N−P−Si, sediment grain size/organic content
- Biological: Chl *a*, Benthic biomass, light attenuation.

Several regional monitoring networks are operated with proven technologies such as Ferrybox, Continuous Plankton Recorder (CPR) and wave monitoring buoys. Mooring buoys routinely monitoring the water quality need to progress to prevent sensor biofouling in the coastal rich waters because the sensors are generally immersed into the water. To avoid fouling problems, Ifremer has developed and proven the Marel technology (with ten years of experience at sea) for automatic monitoring of coastal waters (Répécaud *et al.*, 2005). It consists of a pumping system bringing water into a loop fitted with all kinds of sensors which are regularly chlorinated. Seawater variables are monitored on an hourly basis and maintenance is only required every three months. The concept is available for buoys, piers, tidal zone and Ferrybox.

Figure 3 Marel water quality automatic monitoring concept (buoy, pier, aquaculture, Ferrybox).

Other concepts have a good potential in coastal monitoring such as gliders or:

- Autonomous profilers of various types:
  - yo-yo system profiling up and down along a mooring line
  - bottom winch system moving up and down a sensor package at the extremity of the cable
  - coastal profiler derived from an Argo float. A “Pagode” profiler has been developed at Ifremer. It lies on the floor, profiling daily, and transmits data

through the Argos link (quickly to prevent excessive drift) before diving for a new cycle.

- HF radar is an interesting emerging technology to monitor currents and waves in a 10 to 100 miles range zone. Several applications are running and planned.
- Biofouling prevention: having autonomous sensors able to provide good data during months in the biological rich coastal waters is a big challenge. An efficient solution based on local chlorination was successfully tested during the EC Brimon project (three months without maintenance for various sensors obtained by Ifremer (Delauney *et al.*, 2005).
- Biosensor technology has a very good potential within the foreseeable future, to monitor numerous variables *in situ*, such as:
  - nitrite and nitrates (Unisense from Denmark sells a system but the sensors are not very suitable for long-term monitoring)
  - phytoplankton species determination (based on nucleic acids), HAB, fish eggs
  - pollutants (pesticides, chlorophenols)
  - heavy metals (lead, mercury, cadmium, copper).

  The application of the UE Water Framework Directive after 2009 will stimulate biosensor research because of a wide range of substances to detect at very low rate of concentration (i.e. toxic substances, TBT, polyaromatic hydrocarbons….) (Krüger and Law, 2004).

Figure 4 The Pagode coastal profiler (under development, preliminary profiles with a prototype).

4. Fishery monitoring

Research vessels, fitted with sonar and echo-sounders, perform routine cruises for biomass assessment (benthic and pelagic species). Sophisticated software permits classification of echo and sometimes a rough identification of species. Some major technical innovations are under development. (Cadiou *et al.*, 2005).

- Multibeam echosounder (MBES): Ifremer is developing an MBES with Simrad for fisheries to be installed on the RV Thalassa in 2005. It will enable a refined angular resolution (2°) in a widened across-track angular sector (60° to 90°), compared with a classical vertical sonar. Pelagic shoals will be detected in three dimensions, and detection of fish close to the bottom will be improved. The MBES data flow is equivalent to thirty monobeam vertical sounders.
- Multifrequency classification is quite a promising technique developed in the EC Simfami project. Utilising typically four frequencies enables a much better species classification to be obtained.
- Acoustic underwater observatories are a new experimental way to observe the evolution of the biomass at a fixed location for a few hundred metres around the observatory. Such equipment made of three Simrad EK60 sounders (two horizontal beams and a vertical one) was installed in 2005 along the French "Côte des Landes" for a three year experiment. Data acquisition is made hourly, and a three year time series collection will provide a better understanding of local behaviour of fish.
- Sensors on fishing gear: The GOMOS programme is developing the concept, as well as Ifremer. The idea is to fit a trawl or fishing net with autonomous sensors (i.e. CTD) to collect data profiles during the vertical movement of the gear. The data are automatically transferred by radio when the gear is onboard and are transmitted to the shore with other data such as catches. With a fishing fleet equipped with such systems, it will be possible to collect environmental data at a marginal cost.

5. Geohazard monitoring

Underwater observatories are running in some specific cases and will be developed in the future for two purposes:

1. real time monitoring of geohazards potentially dangerous for human life (i.e. seismic activity, tsunami, slope stability, turbidity currents)
2. scientific observation which does not need systematic real time transmission of data (i.e. biodiversity imaging, particle dynamics, physical oceanography, chemical and nuclear pollution).

An example of the first category is given by the Pacific Tsunami warning system made of several stations including four Dart systems in operation since 1998 with 96% data return. A Dart system consists of a seafloor pressure sensor BPR capable of detecting tsunamis as small as 1 cm and a moored surface buoy for real-time communications. An acoustic link transmits data from the BPR to the surface buoy. The data are then relayed via a GOES satellite link to ground stations, which demodulate the signals for immediate dissemination to NOAA's Tsunami Warning Centres and PMEL.

An example of the second category is the Antares cable observatory for Neutrino detection, in the South of Toulon, at a depth of 2400 m. It is made of three mooring lines (many more in the future) fitted with neutrino detectors, transmitting real time data to a junction box linked to the shore with a cable transferring energy and data in real time. A plan exists to connect a future Ligurian multipurpose observatory to the Antares cable.

Seafloor observatories are made of three subsystems:

- Scientific packages with sensors able to monitor seismology, biological, environmental and security variables
- A seafloor observatory itself based on an open architecture (such ASSEM), hardware and communication standards
- A transmission link: seafloor cable for real time communication, electric tether or acoustic link to a surface buoy for near real time.

A seafloor observatory can be deployed by cables from a vessel (i.e. Geostar) or using work class manned or unmanned submersibles.

Basic technology and first demonstrations were performed in Europe in the framework of several projects: (Alipor, Geostar, Orion, ASSEM, Esonet). A successful demonstration of the ASSEM (Array of Sensor for long-term Seabed Monitoring of geohazards) system was done in the Gulf of Corinth with several sensors (seismometer, geodetic, methane, CTD) acoustically and bidirectionally linked to the shore.

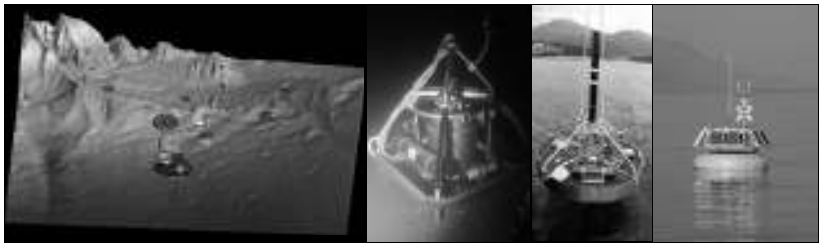

Figure 5 ASSEM (artist view of Ligurian observatory, ASSEM modules demonstration).

Conclusion

Mature networks using proven technology are running in the four *in situ* fields which have been considered: global, coastal, fisheries, and geohazard monitoring. Our vision of the technical challenges for ocean *in situ* monitoring is the following:

- Global monitoring needs to decrease the cost of data, when improving profilers.
- In coastal monitoring, technical progress will be focused on improvement and dissemination of efficient biofouling prevention techniques, development of autonomous coastal profilers, gliders and radars. The development of efficient and innovative biosensors is very challenging.
- Fisheries monitoring will progress considerably with the introduction of multibeam echo-sounders, the development of multifrequency techniques for a better classification of species, when collecting time series with fixed bottom observatories, and using fishing boats to collect both catches and environmental data in a sustained and routine way.
- Geohazard monitoring requires the development of reliable technology and big investments.

References

Cadiou, J.F., D. Choqueuse, C. Compère, L. Delauney, P. Marchand, C. Marchalot, F. Marchese, C. Scalabrin and V. Trenkel. (2005). Synthèse des développements

technologiques. Ifremer "Colloque défi golfe de Gascogne", www.ifremer.fr/gascogne/colloque2005/communications/index.htm.

Davis, R.E., C. Eriksen and C. Jones (2003). Autonomous buoyancy-driven underwater gliders. In: Technology and Applications of Autonomous Underwater Vehicles. Ed G. Griffiths, pp. 37–58. Taylor and Francis.

Delauney, L. *et al.* (2005). Biofouling prevention by local chlorination for *in situ* measuring systems. This volume page 397.

GCOS–92 (2004). Implementation plan for the global observing system for climate in support of the UNFCC.

GOOS (2003). Report no. 125: The Integrated Strategic Design Plan for the Coastal Ocean Observations Module of the Global Ocean Observing System. UNESCO.

Gould, J. and the Argo Science Team (2004). Argo Profiling Floats Bring New Era of *in situ* Ocean Observations. EoS, Transactions of the American Geophysical Union, 85 (19).

Guinet, C. Elephant Seals sounding the Southern Ocean. www.mercator-ocean.fr.

Krüger, S. and Robin J. Law (2004). Biosensors for marine applications — we all need the sea, but does the sea need biosensors? www.sciencedirect.com.

Marchand, P. and J. Servain (2003). The NOR-50: a fast research vessel for operational oceanography. Third EuroGOOS conference, Elsevier.

Ollitrault, M., G. Loaec and C. Dumortier (1994). MARVOR: a multi-cycle RAFOS float. Sea Technology.

Répécaud, M. *et al.* (2005). An automated system for high frequency monitoring of coastal waters. This volume page 404.

Rossby, T., D. Dorson and J. Fontaine (1986). The RAFOS system. J. Atmos. Oceanic. Tech., 3

Rudnick, D.L. and M.J. Perry, eds. (2003). ALPS: Autonomous and Lagrangian Platforms and Sensors. Workshop Report.

Index

Index of Authors

I

J

K

L

M

N

O

P

Q

R

S

Index of Keywords

E

F

G

H

I

K

L

M

N

O

P

List of Participants

Albretsen, Jon
Norwegian Meteorological Institute
Norway

Ali, Mahmoud
Al Azhar University-Gaza
Palestine

Allen, Icarus
Plymouth Marine Laboratory
United Kingdom

Aloisi, Roberto
Alcatel Space
France

Altalo, Mary
Science Applications International Corporation
USA

Aman, Anders
Norwegian Meteorological Institute
Norway

Ambjörn, Cecilia
SMHI
Sweden

Andreu-Burillo, Isabel
POL
United Kingdom

Aouf, Lotfi
Meteo France Division Marine et Oceanographie
France

Aoustin, Yannick
Ifremer
France

Ardhuin, Fabrice
SHOM - CMO
France

Autret, Emmanuelle
Ifremer, LPO
France

Bacher, Cédric
Ifremer
France

Bahurel, Pierre
GIP Mercator Ocean
France

Baillion, Yvan
Alcatel Space
France

Barciela-Fernandez, Rosa M
Met Office
United Kingdom

Belbeoch, Mathieu
JCOMMOPS
France

Bell, Mike
Met Office
United Kingdom

Bentamy, Abderrahim
Ifremer
France

Berniere, Lothar
Atlantide
France

Bertino, Laurent
Nansen Environmental and Remote Sensing Center
Norway

Blanc, Frédérique
CLS
France

Blouch, Pierre
Meteo France - Centre de Meteorologie Marine
France

Borst, Kees
Rijkswaterstaat RIKZ
The Netherlands

Bozzano, Roberto
CNR-ISSIA
Italy

Burt, Richard
Chelsea Technologies Group
United Kingdom

Burud, Ingunn
Norwegian Meteorological Institute
Norway

Cariou, Thierry
Station Biologique de Roscoff CNRS
France

Carval, Thierry
Ifremer
France

Chapon, Monique
Ifremer
France

Coatanoan, Christine
Ifremer
France

Colijn, Franciscus
GKSS Research Centre
Germany

Comerma, Eric
Catalonia Polytechnic University
Spain

Connolly, Niamh
Marine Board - European Science Foundation
France

Cowling, Mike
IACMST
United Kingdom

Craneguy, Philippe
Actimar
France

Crosnier, Laurence
GIP Mercator Ocean
France

Cuillandre, François
Maire de Brest
France

Dahlin, Hans
EuroGOOS
Sweden

Davis, Daniel
Monterey Bay Aquarium Research Institute
USA

de Roeck, Yann Hervé
Ifremer
France

de Vries, Hans
KNMI
The Netherlands

Degres, Yves
Micrel NKE
France

Delauney, Laurent
Ifremer
France

Derval, Corinne
Mercator-Ocean
France

Desaubies, Yves
Ifremer
France

Djavidnia, Samuel
EC - Joint Research Centre
Italy

Dorandeu, Joel
CLS
France

Dorofeyev, Viktor
Marine Hydrophysical Institute
Ukraine

Drago, Aldo
IOI-MOC, University of Malta
Malta

Driesenaar, Mathilda
TNO Defence, Security and Safety
The Netherlands

Drillet, Yann
CERFACS/Mercator Ocean
France

Dumon, Guido
AWZ - Division Coast
Belgium

Dunning, Justin
Chelsea Technologies Group
United Kingdom

Durand, Dominique
Norwegian Institute for Water Research
Norway

Dwyer, Edward
Coastal Marine Resources Centre
Ireland

Kholeif, Suzan
National Institute of Oceanography and Fisheries
Egypt

Engelke, Clemens
Alfred-Wegener-Institute for Polar and Marine Res.
Germany

Erb, William
IOC
Australia

Espino, Manuel
Catalonia Polytechnic University
Spain

Espinosa Daggenweiler, Gonzalo Eduardo
Servicio Meteorologico de la Armada de Chile
Chile

Fennell, Sheena
Marine Institute
Ireland

Ferrer, Maria Immaculada
Imedea CSIC-UIB
Spain

Fiesoletti, Federica
ISMAR-CNR
Italy

Froysa, Kristin Guld
AAnderaa Data Instruments
Norway

Fuda, Jean-Luc
Centre d'Océanologie de Marseille
France

Funkquist, Lennart
SMHI
Sweden

Furevik, Birgitte Rugaard
Norwegian Meteorological Institute
Norway

Gaillard, Fabienne
Ifremer
France

Garcia Sotillo, Marcos
Puertos del Estado
Spain

Gastgifvars, Maria
Finnish Environment Institute (SYKE)
Finland

Gerard, François
GIP Mercator Ocean
France

Gertman, Isaac
Isreal Oceanographic & Limnological Research
Israel

Girard, Françoise
Actimar
France

Gohin, Francis
Ifremer
France

Gorringe, Patrick
EuroGOOS
Sweden

Gouriou, Vincent
IRD Brest
France

Graybeal, John
Monterey Bay Aquarium Research Institute
USA

Greenwood, Naomi
CEFAS
United Kingdom

Grönvall, Hannu
Finnish Institute of Marine Research
Finland

Guevel, Guénolé
Meteo France
France

Guillou, Jacques
CNRS / IUEM UBO
France

Guymer, Trevor
IACMST
United Kingdom

Haaring, Pieter
Rijkswaterstaat RIKZ
The Netherlands

Hackett, Bruce
Norwegian Meteorological Institute
Norway

Håkansson, Bertil
SMHI
Sweden

Hansson, Martin
SMHI Oceanographic Services
Sweden

Heiberg, Hanne
Norwegian Meteorological Institute
Norway

Heygster, Georg
Institute of Environmental Physics,
University of Bremen
Germany

Hibral, Sidonie
Atlantide
France

Hoeyer, Jacob
Danish Meteorological Institute
Denmark

Holt, Martin
Met Office
United Kingdom

Hydes, David
National Oceanography Centre
United Kingdom

Iona, Athanassia
Hellenic Centre for Marine Research
Greece

Isern-Fontanet, Jordi
Institut de Ciències del Mar (CSIC)
Spain

Jimenez, Barbara
Forwind Center for Wind Research
Germany

Johannessen, Johnny
Nansen Environmental and Remote
Sensing Center
Norway

Johannessen, Ola M.
Nansen Environmental and Remote
Sensing Center
Norway

Jourdin, Frédéric
SHOM
France

Kaitala, Seppo
Finnish Institute of Marine Research
Finland

Kalantzi, Georgia
Hellenic Centre for Marine Research
Greece

Kallos, George
University of Athens
Greece

Kaminska, Magdalena
Institute of Meteorology and Water
Management
Poland

Karlson, Bengt
SMHI
Sweden

Karstensen, Johannes
Leibniz-Institut für Meereswissenschaften
Germany

Kellermann, Adolf
ICES
Denmark

Kelly-Gerreyn, Boris
National Oceanography Centre
United Kingdom

Kerkhoven, David
Rijkswaterstaat North Sea
The Netherlands

Koltermann, Peter
Bundesamt für Seeschifffahrt und Hydrographie
Germany

Kontoyiannis, Harilaos
Hellenic Centre for Marine Research
Greece

Korotayev, Gennady
Marine Hydrophysical Institute
Ukraine

Korres, Gerasimos
Hellenic Centre for Marine Research
Greece

Kõuts, Tarmo
Marine Systems Institute
Estonia

Krzyminski, Wlodzimierz
IMGW
Poland

Kubryakov, Alexander
Marine Hydrophysical Institute
Ukraine

Kyriakidis, Lysis
RDI Europe
France

Laffont, Karine
Ifremer
France

Lagrange, Alain
Ifremer
France

Lam, Frans-Peter
TNO Defence, Security and Safety
The Netherlands

Lampitt, Richard
National Oceanography Centre
United Kingdom

Lane, Andrew
National Oceanography Centre
United Kingdom

Langlais, Clothilde
LSEET
France

Larnicol, Gilles
CLS
France

Lavin, Alicia
Instituto Espanol de Oceanografia
Spain

Le Grand, Geneviève
Ifremer
France

Le Guen, Véronique
Ifremer
France

Le Traon, Pierre-Yves
CLS
France

Lee, Dong Young
Korea Ocean Research and Development Institute
South Korea

Lefevre, Jean-Michel
CNRS INSU-CNRM
France

Legrand, Jacques
Ifremer
France

Legrand, Sebastien
CEDRE
France

Lellouche, Jean-Michel
Chercheur GIP-Mercator
France

Lewis, Katy
Plymouth Marine Laboratory
United Kingdom

Lilja Bye, Bente
European Sea Level Service
Norway

Loaec, Gérard
Ifremer
France

Louazel, Stephanie
SHOM
France

Loubrieu, Francine
Ifremer
France

Loubrieu, Thomas
Ifremer Geosciences Marines
France

Louvart, Laurent
SHOM
France

Loyer, Sophie
Atlantide
France

Lux, Muriel
Noveltis
France

Luyten, Patrick
Management Unit of North Sea Mathematical Models
Belgium

Maillard, Catherine
Ifremer
France

Malone, Thomas
Ocean.us Office
USA

Marchand, Philippe
Ifremer
France

Mariette, Vincent
Actimar
France

Mathy, Pierre
European Commission
Belgium

Mattsson, Johan
Danish Adm of Navigation and Hydrography
Denmark

Meinecke, Gerrit
MARUM
Germany

Michel, Sylvain
Ifremer
France

Millard, Keiran
HR Wallingford
United Kingdom

Minster, Jean-François
CNRS
France

Montero, Pedro
Meteogalicia - Conselleria de Medio Ambiente
Spain

Moorhead, Michael
Neptune RADAR
United Kingdom

Morel, Yves
SHOM
France

Nash, Stephen
National University of Ireland, Galway
Ireland

Natale, Salvatore
Fondazione IMC
Italy

Needham, Neil
CEFAS
United Kingdom

Nesterov, Eugeny
Hydrometerorological Research Center
Russia

Nesterov, Oleksandr
Tropical Marine Science Institute
Singapore

Nittis, Kostas
Hellenic Centre for Marine Research
Greece

Nolan, Glenn
Marine Institute
Ireland

Obaton, Dominique
GIP Mercator Ocean
France

O'Kelly, Charlotte
Techworks Marine Ltd.
Ireland

Ollier, Gilles
European Commission
Belgium

Ortega, Christian
CLS - ARGOS
France

Ozer, José
Management Unit of North Sea Mathematical Models
Belgium

Pagonis, Paraskevas
Hellenic Centre for Marine Research
Greece

Papadopoulos, Anastasios
Hellenic Centre for Marine Research
Greece

Paradis, Denis
Meteo France
France

Parrilla, Gregorio
Instituto Espanol Oceanografia
Spain

Pemberton, Per
SMHI
Sweden

Perivoliotis, Leonidas
Hellenic Centre for Marine Research
Greece

Perrot, Jean-Yves
Ifremer
France

Petersen, Wilhelm
GKSS Research Centre, Institute For Coastal Research
Germany

Petersson, Siân
EuroGOOS
Sweden

Petit de la Villeon, Loïc
Ifremer
France

Philippart, Marc
Rijkswaterstaat North Sea
The Netherlands

Pinardi, Nadia
University of Bologna
Italy

Piolle, Jean-François
Ifremer
France

Piotrowicz, Stephen
NOAA/OAR
USA

Pison, Virginie
Management Unit of North Sea Mathematical Models
Belgium

Ponsar, Stéphanie
Management Unit of North Sea Mathematical Models
Belgium

Pouliquen, Sylvie
Ifremer
France

Quentel, Marie-Laure
Ifremer
France

Qurban, Mohammed
National Oceanography Centre
United Kingdom

Raicich, Fabio
CNR - Istituto di Scienze Marine
Italy

Rayner, Ralph
Fugro Global Environmental & Ocean Sciences Ltd.
United Kingdom

Rebhan, Helge
ESA - ESTEC
The Netherlands

Rendas, Maria Joao
Laboratoire I3S
France

Repecaud, Michel
Ifremer
France

Ribotti, Alberto
Fondazione IMC
Italy

Richer de Forges, Hugues
Ifremer
France

Ríos, Aida F.
CSIC-Instituto de Investigaciones Marinas
Spain

Riou, Gérard
Ifremer
France

Rolin, Jean-François
Ifremer
France

Rosen, Dov S.
Israel Oceanographic & Limnological Research
Israel

Rosmorduc, Vinca
CLS
France

Ruiz Villarreal, Manuel
Instituto Español de Oceanografía
Spain

Ryder, Peter
EuroGOOS
United Kingdom

Rzeszotarska-Wichorowska, Renata
IOPAS
Poland

Sandven, Stein
Nansen Environmental and Remote Sensing Center
Norway

Santoro, Francesca
University of Venice
Italy

Schroeder, Friedhelm
GKSS Research Centre
Germany

Seina, Ari
Finnish Institute of Marine Research
Finland

She, Jun
Danish Meterological Institute
Denmark

Siddorn, John
Met Office
United Kingdom

Skandrani, Chafils
CNRS INSU-CNRM
France

Soltwedel, Thomas
Alfred Wegener Institute
Germany

Sorensen, Kai
Norwegian Institute for Water Research
Norway

Stel, Jan H.
ICIS / NWO ALW
The Netherlands

Stepko, Waldemar
IMGW
Poland

Steunou, Nathalie
CNES
France

Stipa, Tapani
Finnish Institute of Marine Research
Finland

Svendsen, Einar
Institute of Marine Research
Norway

Sztobryn, Marzenna
IMGW
Poland

Tenore, Kenneth
Alliance for Coastal Technologies
USA

Torres, Ricardo
Plymouth Marine Laboratory
United Kingdom

Toumazou, Vincent
Mercator Ocean
France

Townend, Ian
ABP Marine Environmental Research Ltd.
United Kingdom

Tranchant, Benoît
Mercator Ocean
France

Trenaman, Neil
RD Instruments
USA

Tufte, Lars
Federal Institute of Hydrology
Germany

Turton, Jonathan
Met Office
United Kingdom

Valchev, Nikolay
Institute of Oceanology
Bulgaria

Valdivieso, Maria
GIP Mercator Ocean
France

Waldmann, Christoph
University of Bremen / Marum
Germany

Vallerga, Silvana
CNR - IAMC
Italy

Walter, Nicolas
Marine Board
France

van Ruiten, Kees
Rijkswaterstaat RIKZ
The Netherlands

Varlamov, Sergey
Meteo France
France

Wehde, Henning
GKSS Research Centre
Germany

Westbrook, Guy
Marine Institute
Ireland

Wichorowski, Marcin
Institute of Oceanology
Poland

Vincent, Patrick
Ifremer
France

Winther, Nina
Nansen Environmental and Remote Sensing Center
Norway

Violeau, Damien
EDF R&D
France

Wyatt, Lucy
University of Sheffield
United Kingdom

Vyazilov, Evgeny
RIHMI-WDC
Russia

Zappala, Giuseppe
CNR - IAMC
Italy

Zodiatis, George
Oceanography Centre, University of Cyprus
Cyprus

Australia	1
Belgium	7
Bulgaria	1
Chile	1
Cyprus	1
Denmark	4
Egypt	2
Estonia	1
Finland	5
France	86
Germany	13
Greece	9
Ireland	6
Israel	2
Italy	10
Malta	1
Norway	16
Palestine	1
Poland	6
Russia	2
Singapore	1
South Korea	1
Spain	10
Sweden	9
The Netherlands	10
Ukraine	3
United Kingdom	26
USA	7

European Commission

EUR 21697 PROCEEDINGS OF THE FOURTH INTERNATIONAL CONFERENCE PROCEEDINGS OF THE FOURTH INTERNATIONAL CONFERENCE

Luxembourg: Office for Official Publications of the European Communities

2005 — XVI, 854 pp. — 17.6 x 25 cm

ISBN 92-894-9788-2